



## FORGING SP3 ARCHITECTURES VIA SP3 C-C BOND CLEAVAGE AND 1,2- ALKYLBORATION STRATEGIES

Fei Cong

**ADVERTIMENT.** L'accés als continguts d'aquesta tesi doctoral i la seva utilització ha de respectar els drets de la persona autora. Pot ser utilitzada per a consulta o estudi personal, així com en activitats o materials d'investigació i docència en els termes establerts a l'art. 32 del Text Refós de la Llei de Propietat Intel·lectual (RDL 1/1996). Per altres utilitzacions es requereix l'autorització prèvia i expressa de la persona autora. En qualsevol cas, en la utilització dels seus continguts caldrà indicar de forma clara el nom i cognoms de la persona autora i el títol de la tesi doctoral. No s'autoritza la seva reproducció o altres formes d'explotació efectuades amb finalitats de lucre ni la seva comunicació pública des d'un lloc aliè al servei TDX. Tampoc s'autoritza la presentació del seu contingut en una finestra o marc aliè a TDX (framing). Aquesta reserva de drets afecta tant als continguts de la tesi com als seus resums i índexs.

**ADVERTENCIA.** El acceso a los contenidos de esta tesis doctoral y su utilización debe respetar los derechos de la persona autora. Puede ser utilizada para consulta o estudio personal, así como en actividades o materiales de investigación y docencia en los términos establecidos en el art. 32 del Texto Refundido de la Ley de Propiedad Intelectual (RDL 1/1996). Para otros usos se requiere la autorización previa y expresa de la persona autora. En cualquier caso, en la utilización de sus contenidos se deberá indicar de forma clara el nombre y apellidos de la persona autora y el título de la tesis doctoral. No se autoriza su reproducción u otras formas de explotación efectuadas con fines lucrativos ni su comunicación pública desde un sitio ajeno al servicio TDR. Tampoco se autoriza la presentación de su contenido en una ventana o marco ajeno a TDR (framing). Esta reserva de derechos afecta tanto al contenido de la tesis como a sus resúmenes e índices.

**WARNING.** Access to the contents of this doctoral thesis and its use must respect the rights of the author. It can be used for reference or private study, as well as research and learning activities or materials in the terms established by the 32nd article of the Spanish Consolidated Copyright Act (RDL 1/1996). Express and previous authorization of the author is required for any other uses. In any case, when using its content, full name of the author and title of the thesis must be clearly indicated. Reproduction or other forms of for profit use or public communication from outside TDX service is not allowed. Presentation of its content in a window or frame external to TDX (framing) is not authorized either. These rights affect both the content of the thesis and its abstracts and indexes.

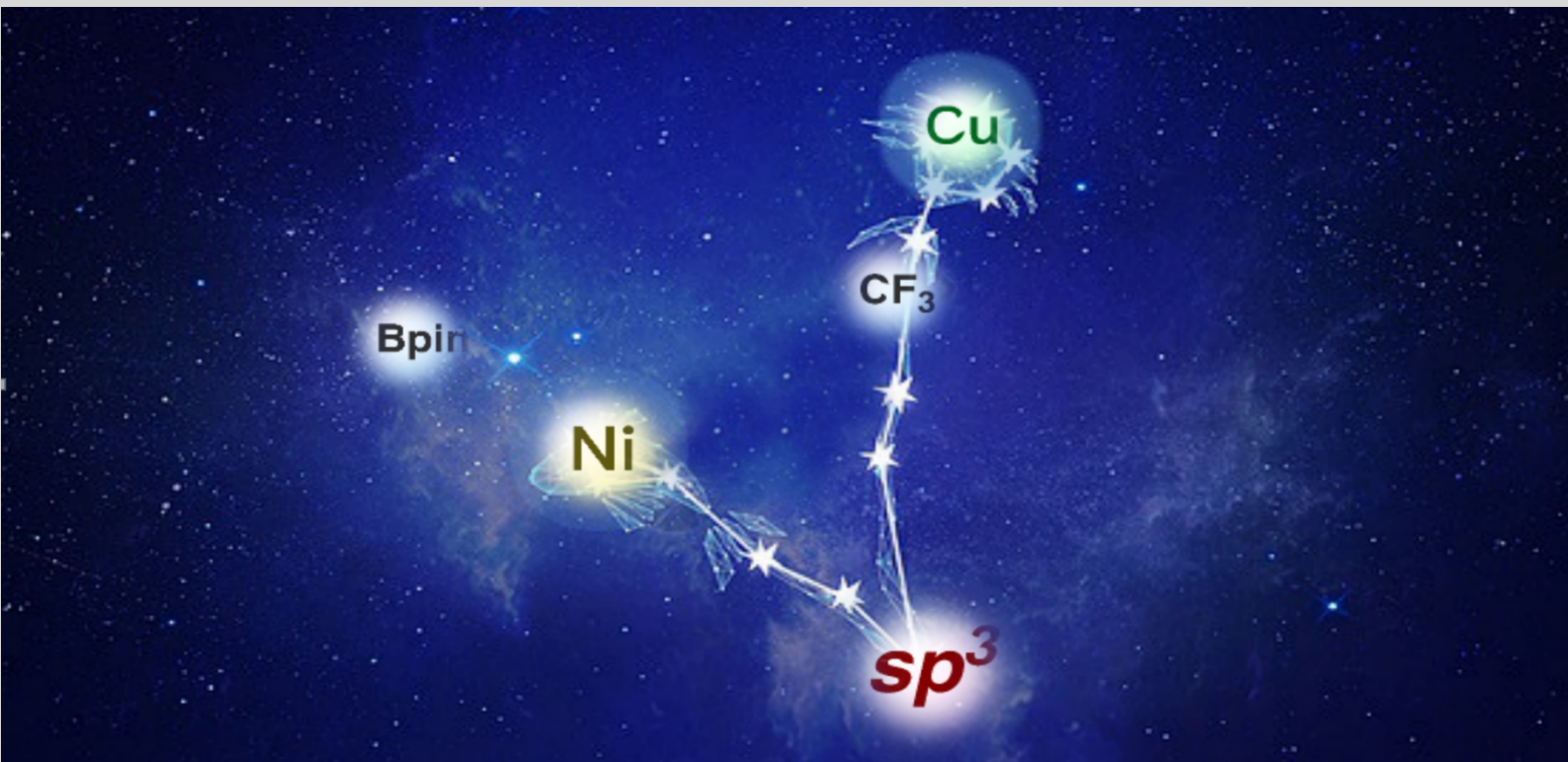


UNIVERSITAT  
ROVIRA i VIRGILI

# Forging $sp^3$ Architectures via $sp^3$ C–C Bond Cleavage and 1,2-Alkylboration Strategies

---

Fei Cong



DOCTORAL THESIS

2022





# Forging $sp^3$ Architectures via $sp^3$ C–C Bond Cleavage and 1,2-Alkylboration Strategies

Fei Cong

Doctoral Thesis

**Supervised by Prof. Ruben Martin**

Institute of Chemical Research of Catalonia (ICIQ)

Universitat Rovira i Virgili (URV)

Department of Analytical Chemistry & Organic Chemistry



Tarragona, 2022



UNIVERSITAT  
ROVIRA i VIRGILI



Prof. Ruben Martin Romo, Group Leader at the Institute of Chemical Research of Catalonia (ICIQ) and Research Professor of the Catalan Institution for Research and Advanced Studies (ICREA),

STATES that the present study, entitled “Forging  $sp^3$  Architectures via  $sp^3$  C–C Bond Cleavage and 1,2-Alkylboration Strategies”, presented by Fei Cong for the award of the degree of Doctor, has been carried out under his supervision at the Institute of Chemical Research of Catalonia (ICIQ).

Tarragona, November 18<sup>th</sup> 2022

Doctoral Thesis Supervisor

Prof. Ruben Martin Romo

## **List of Publications**

1. **Fei Cong**, Riccardo S. Mega, Jinhong Chen, Craig S. Day, Ruben Martin. Trifluoromethylation of Carbonyl and Olefin Derivatives by C( $sp^3$ )-C Bond Cleavage. *Angew. Chem. Int. Ed. Accepted*.
2. **Fei Cong**, Xin-Yang Lv, Craig S. Day, Ruben Martin. Dual Catalytic Strategy for Forging  $sp^2-sp^3$  and  $sp^3-sp^3$  Architectures via  $\beta$ -Scission of Aliphatic Alcohol Derivatives. *J. Am. Chem. Soc.* **2020**, *142*, 20594–20599. Highlighted in *Synfacts*.
3. Andreu Tortajada, Yaya Duan<sup>†</sup>, Basudev Sahoo<sup>†</sup>, **Fei Cong**<sup>†</sup>, Georgios Toupalas<sup>†</sup>, Antoine Sallustrau, Olivier Loreau, Davide Audisio, Ruben Martin. Catalytic Decarboxylation/Carboxylation Platform for Accessing Isotopically Labeled Carboxylic Acids. *ACS Catal.* **2019**, *9*, 5897–5901.





---

## Table Contents

Acknowledgements.....	6
Preface.....	9
Abbreviations & Acronyms .....	11
Abstract.....	14
Chapter 1 <i>General Introduction</i> .....	17
1.1 General Introduction .....	18
1.2 Carbon–Carbon Bond Cleavage .....	19
1.2.1 Transition-Metal-Catalyzed C–C Bond Cleavage.....	22
1.2.2 Radical-Mediated C–C Bond Cleavage.....	28
1.3 Transition-Metal-Catalyzed 1,2-Carboboration.....	47
1.3.1 Cu-Catalyzed 1,2-Alkylboration Reactions .....	49
1.3.2 Nickel-Catalyzed 1,2-Carboboration Reactions .....	52
1.4 General Aim of This Thesis.....	56
1.5 References:.....	58
Chapter 2 <i>Dual Catalytic Strategy for Forging <math>sp^2</math>–<math>sp^3</math> and <math>sp^3</math>–<math>sp^3</math> Architectures via <math>\beta</math>-Scission of Aliphatic Alcohol Derivatives</i> .....	83
2.1 General Introduction .....	85
2.1.1 $sp^3$ C–C Bond Formation via Ni-Catalyzed Reductive Coupling .....	85
2.1.2 $sp^3$ C–C Bond Formation by Nickel/Photoredox Cross-Coupling .....	90
2.1.3 Nickel-Catalyzed Cross-Coupling Using Aliphatic Alcohols as $sp^3$ -Carbon Handles .....	98
2.2 General Aim of the Project .....	105
2.3 Dual Catalytic Strategy for Forging $sp^3$ C–C Architectures via $\beta$ -Scission of Aliphatic Alcohol Derivatives .....	106
2.3.1 Optimization of the Reaction Conditions .....	106
2.3.2 Substrate Scope.....	111
2.3.3 Mechanistic Studies .....	117
2.4 Extended Research and Future outlook .....	121
2.5 Conclusion .....	122
2.6 References.....	123
2.7 Experimental Section.....	134
2.7.1 General Considerations.....	134
2.7.2 Synthesis of Starting Materials .....	135
2.7.3 General Procedure of Ni-Catalyzed Reductive Coupling.....	148
2.7.4 Mechanistic Experiments.....	172

2.7.5 X-Ray Crystallography Data.....	180
2.7.6 References of Experimental Procedures .....	189
2.7.7 NMR Spectra .....	191
Chapter 3 <i>Trifluoromethylation of Carbonyl and Olefin Derivatives by C(sp<sup>3</sup>)-C Bond Cleavage</i> .....	299
3.1 General Introduction .....	300
3.1.1 Radical Trifluoromethylation to Forge C(sp <sup>3</sup> )-CF <sub>3</sub> Bonds .....	301
3.1.2 Addition of Trifluoromethyl Group to Unsaturated Moieties for Forging C(sp <sup>3</sup> )-CF <sub>3</sub> Bonds.....	315
3.2 General Aim of the Project .....	323
3.3 Trifluoromethylation of Carbonyl and Unactivated Olefin Derivatives via sp <sup>3</sup> C-C Bond Cleavage.....	325
3.3.1 Optimization of the Reaction Conditions .....	325
3.3.2 Substrate Scope.....	337
3.3.3 Mechanistic Proposal .....	345
3.4 Extended Research and Future outlook .....	356
3.5 Conclusion .....	357
3.6 References.....	357
3.7 Experimental Section.....	367
3.7.1 General Considerations.....	367
3.7.2 Synthesis of Starting Materials .....	369
3.7.3 General Procedures for Trifluoromethylation.....	406
3.7.4 Mechanistic Experiments.....	445
3.7.5 X-Ray Crystallography Data.....	447
3.7.6 References of Experimental Procedures .....	466
3.7.7 NMR Spectra .....	468
Chapter 4 <i>Nickel-Catalyzed Regio- and Stereoselective 1,2-Alkylboration of Allenes</i> .....	650
4.1 General Introduction .....	652
4.1.1 Copper Catalyzed 1,2-Carboboration Reactions of Allenes.....	652
4.1.2 Nickel-Catalyzed Alkylboration of Unsaturated C-C Bond .....	660
4.2 General Aim of the Project .....	665
4.3 Nickel-Catalyzed Regio- and Stereoselective 1,2-Alkylboration of Allenes ..	667
4.3.1 Optimization of the Reaction Conditions .....	667
4.3.2 Substrate Scope.....	676
4.3.3 Mechanistic Proposal.....	677
4.4 Conclusion .....	678
4.5 References.....	678
4.6 Experimental Section.....	685

---

4.6.1 General Considerations .....	685
4.6.2 Synthesis of Ligands and Starting Materials .....	685
4.6.3 General Procedure of Ni-Catalyzed 1,1-Alkylboration of Allenes with $\alpha$ -Haloboranes and B <sub>2</sub> Pin <sub>2</sub> .....	690
4.6.4 General Procedure of Ni-Catalyzed 1,1-Alkylboration of Allenes with Alkyl iodines and B <sub>2</sub> Pin <sub>2</sub> .....	693
4.6.5 References of Experimental Procedures .....	695
4.6.6 NMR Spectra .....	696
Chapter 5 <i>General Conclusions</i> .....	726

---

## Acknowledgements

My four years of research at the Institute of Chemical Research of Catalonia (ICIQ) are coming to an end with soundless and stirless, and it has also been a very special time in my life. I will be reluctant to leave here. I am looking back on my four years of study with all the pains and sorrows, but I still got through it with strength. So, on all the way through.

First of all, I would like to express my most sincere gratitude to my supervisor, **Prof. Ruben Martin**. I remember when I was interviewed online. I had difficulty expressing myself in English, but you still gave me the opportunity to join the Martinis family, which made me feel really lucky. During the past four years with you, your patient support and guidance have helped me a lot to walk towards my goal step by step. At the same time, you gave me enough freedom to find projects and helped me realize each idea as much as possible. I admire your open-mindedness in scientific research, profound knowledge, hard work, and tireless pursuit of your career, which I should learn from throughout my life. In the future, I will bear in mind my supervisor's great advice, seek new ideas, respect academic ethics, and be courageous and persistent in my scientific research.

Secondly, I would like to express my highest respect to the **China Scholarship Council (CSC)** and I am very grateful for the financial support it has provided for my four-year PhD scholarship in Spain. I would not have been able to carry out the work here without the support of my motherland!

I'd also like to thank my committee members.

**Ingrid Mateu, Sergio Sopena and David Sádaba**, you are so kind and friendly to me, thank you for all your help and support and for all your efforts to keep the laboratory running smoothly for many years. I am also very grateful to the **ICIQ** Research Support Units for making the research environment comfortable and work smoother. Thanks to crystallographers **Jordi** and **Eduardo** for help with crystal structure, **Isra** and **Kerman** for help with NMR experiments, **Noemí** for help with HRMS, **Georgana** for help with EPR experiments, and **Mariona** for help with UV-VIS research.

Next, I would like to thank all the excellent partners I have worked with during our projects. **Dr. Craig. S. Day**, you are a very excellent and capable scientist. You were always there to help me and pull me forward when I was at my most difficult and helpless, and you did your best to help me make a breakthrough in the mechanism and

---

thus improve our project's level. Craig, thank you also for the events you used to organise and encourage me to join, it just opened up my heart and made me start to fit in here. We have a friendship like family, my sister, best wishes for you. **Dr. Riccardo Mega**, thank you for joining us in the CF<sub>3</sub> project. I always told you my real thoughts and my situation, and you can understand me and help me. **Dr. Andreu Tortajada**, thanks for teaching me about the <sup>13</sup>CO<sub>2</sub> project. I have learnt a lot. **Jinhong**, thank you for your help with the CF<sub>3</sub> project. You are a PhD student who approaches experiments very carefully, and I am sure you will produce more interesting research. **Xinyang**, thank you for your help with the C–C bond cleavage project at the beginning. I understand your situation and hope you will persevere with the C–C bond cleavage project and make a breakthrough.

Here, I would like to give special thanks to my friends (Craig, Riccardo, Franz, Jesús, Dmitry) who helped me revise and correct my thesis. **Dr. Franz-Lucas Haut**, I wish I had known you at the beginning of my PhD career because you really know that PhD students need to learn more than just experiments, and I actually agree with you very much. **Dr. Jesús Rodrigalvarez**, I receive a warm smile from you when I see you every time, you are really friendly, and you know my anxiety. I remember that time you asked me to join the lunch of PhD interview and it made me feel something I hadn't felt before, thank you. **PhD. Dmitry Zimin**, thank you for being my friend all the way from lab 2.7 to lab 2.4. Your Russian food (cakes and salads) completely overwhelmed me and was very tasty. I will also remember your words that this is just a point in our life, it will all pass, we should be happy and know how to enjoy life, I learned.

Now, I would like to thank all the current and past members of the Martin group. I really enjoyed working together with you all. **Dr. Daniel Janssen-Muller**, you are the most German person I have ever met and admired, and I was lucky to have you as my first tablemate. **Antonio García**, my second tablemate, I really miss the time when we hung out together. **Dr. Marino Börjesson**, although you didn't say much to me, I could feel your concern. you were the only one who suggested and told me to find someone else to work with when I was struggling to explore the project. **Dr. Jessica Giacoboni**, my big Italian sister, thank you for your most sincere care and concern for me, you were always thoughtful enough to send me home when we got home late. **Dr. José Tiago** and **Dr. Victoria Rendón**, I miss when we worked and enjoyed music together in Lab 2.7. **Dr. Raul Martin**, **Dr. Rosie Somerville** and **Dr. Jacob Davies**, thanks for all your help during my time in Lab 2.7. **Dr. Basudev Sahoo**, I enjoyed talking to you about the

---

problems in my project, and you were always patient in helping me to analyze them. **Dr. Ciro Romano, Bradley Higginson and Laura Talavera**, thank you for coming together to help me move my things into my new flat. **Bradley**, I don't know why, but it's always a pleasure to see you every time. Also thank you for sharing your knowledge. **Laura**, my Spanish friend, you really understand my fragility and really care about me. Thank you for your warm hugs. I believe I will miss your “Hola”. **Carlota Odena**, thank you for your concern for me. When I hurt my ankle, you always asked me if I was feeling better. **Adrian J. Brenes Rucinski and Julien Lyonnet**, I had a great time going to the buffet with you guys. **Adrian**, thank you for saving my phone from unfamiliar calls every time, it was also great to spend time with you in lab 2.4. **Dr. Matthew Wakeling, Dr. Roman Abrams, Dr. Santosh Gadekar and Julia**, thank you for all your help in research. **Philipp Spieß**, I remember the discussions we had about the project and the ideas, and I'm glad we're still in touch.

To the Chinese communities in our group, I would like to thank all of you for your help. **Dr. Hongfei Yin and Dr. Juzeng An**, I always enjoyed going to Lab 2.12 and talking to you guys while you were here. **Dr. Liang Xu and Dr. Shang-Zheng Sun**, thank you so much for your continued concern since you left. **Shang-Zheng**, you are really brilliant, I am also happy for you to publish more results. **Dr. Yaya Duan, Dr. Yangyang and Dr. Yiting Gu**, thank you for all your help before. **Wenjun**, thank you for organising a get-together on a Chinese festival. **Huihui**, thank you for helping me bring things from China, your independence and persistence in the project will certainly be rewarded. **Hao**, I especially thank you for the warmth and happiness you bring to Lab 2.4, and also thanks for your support.

Finally, I would like to deeply thank my parents for their hard work in raising and educating me, and they have always been with me. I can only talk to them about the bitterness in my heart and thank them for their silent support and understanding. Of course, I would also like to thank my distant friends and colleagues for their concern and support.

I would like to thank once again all those who have helped and cared for me over the past four years!

---

## Preface

The work presented in this dissertation has been carried out at the Institute of Chemical Research of Catalonia (ICIQ) during a period from October 2018 to October 2022 under the supervision of Professor Ruben Martin. The thesis contains five chapters: a general introduction, three research chapters, and the last chapter with a general conclusion of all the research work. Each research chapter includes a brief introduction and the aim of the respective topic, followed by a discussion of the experimental results, mechanistic experiments, conclusions, and experimental sections. Relevant references and their numbering are organized independently by chapters.

The first chapter is a general introduction to the background and development of C–C bond activation. In particular, it is focused on the functionalization of molecules by radical-promoted C–C bond cleavage. Another topic introduced and discussed is the development of transition-metal-catalyzed 1,2-carboboration.

The second chapter, “*Dual Catalytic Strategy for Forging  $sp^2$ – $sp^3$  and  $sp^3$ – $sp^3$  Architectures via  $\beta$ -Scission of Aliphatic Alcohol Derivatives*”, describes  $sp^3$ -arylation and  $sp^3$ -alkylation from abundant aliphatic alcohols as alkyl synthons by combining light-induced  $\beta$ -scission of alkoxy radicals with Ni catalysts. The reaction displays excellent compatibility of functional groups and a wide substrate scope under mild conditions. The synthetic utility could be further showcased in the context of the late-stage functionalization of advanced intermediates. The results of this chapter have been published in *J. Am. Chem. Soc.* **2020**, *142*, 20594–20599, in collaboration with Xin-Yang Lv and Dr. Craig S. Day.

The third chapter, “*Trifluoromethylation of Carbonyl and Olefin Derivatives by  $C(sp^3)$ –C Bond Cleavage*”, describes the conversion of structurally diverse feedstocks containing ketones, aldehydes, or alkenes to the corresponding trifluoromethylated analogues by inert  $sp^3$  C–C cleavage. The reaction proceeds under visible-light mediated copper-catalyzed or promoted conditions, which offers an operationally simple and scalable protocol to aliphatic trifluoromethylated products. Particularly, the successful construction of this conversion platform offers the possibility to be used as a vehicle to access libraries of trifluoromethylated compounds of interest in drug

---

discovery programs. The results of this chapter have been accepted in *Angew. Chem. Int. Ed.*, in collaboration with Dr. Riccardo S. Mega, Jinhong Chen and Dr. Craig S. Day.

The fourth chapter, “*Nickel-Catalyzed Regio- and Stereoselective Alkylboration of Allenes*”, describes efforts towards the development of a nickel-catalyzed regio- and stereoselective three-component coupling reactions between allenes, ambiphilic  $\alpha$ -haloboranes, and a diboron reagent to afford *Z*-multi-substituted alkenylboronates. This protocol would offer a new blueprint for preparing densely functionalized, yet synthetically versatile, 1,3-( $sp^2$ ,  $sp^3$ )-bisorganometallics compounds from simple and readily accessible precursors. The optimization of the conditions has been completed and is discussed in this chapter, and the scope of the protocol is expanded to various substrates has been shown. Further refinements and studies of this strategy are being implemented. The results of this chapter have not yet been published.



---

## Abbreviations & Acronyms

4CzIPN = 2,4,5,6-Tetra(9*H*-carbazol-9-yl)isophthalonitrile

acac = acetylacetonate

B<sub>2</sub>(nep)<sub>2</sub> = bis(nepentylglycolato)diboron

BDE = Bond dissociation energy

BTMD = 2-*tert*-Butyl-1,1,3,3-tetramethylguanidine

Bpin = 4,4,5,5-Tetramethyl-1,3,2-dioxaboronic ester

bpy = 2,2'-Bipyridine

Cat. = Catalyst

COD = 1,5-Cyclooctadiene

Cy = cyclohexyl

Conv = conversion

Cbz = benzyloxycarbonyl

dtbppy = 4,4'-Di-*tert*-butyl-2,2'-dipyridyl

DFT = Density Functional Theory

DG = Directing group

DMAP = 4-Dimethylaminopyridine

DME = Ethylene glycol dimethyl ether

DMF = *N,N*-Dimethylformamide

DEF = *N,N*-Diethylformamide

DMPU = *N,N'*-Dimethylpropyleneurea

DMSO = Dimethyl sulfoxide

DIB = (diacetoxy)iodobenzene

Bathphen = Bathophenanthroline

dtbppy = 4,4'-Di-*tert*-butyl-2,2'-dipyridyl

dcpe = 1,2-Bis(dicyclohexylphosphino)ethane

dppe = 1,2-bis(diphenylphosphino)ethane

dppf = Bis(diphenylphosphino)ferrocene

dppm = Bis(diphenylphosphino)methane

---

dr = diastereomeric ratio

equiv = Equivalent

EDA = electron donor acceptor

ET = energy transfer

ee = enantiomeric excess

er = enantiomeric ratio

FID = Flame Ionization Detector

GC = gas chromatography

h = hour(s)

HAT = hydrogen atom transfer

HE = Hantzsch Ester

IPr = 1,3-Bis(2,6-diisopropylphenyl)imidazol-2-ylidene

IPr = 1,3-Bis(2,6-diisopropylphenyl)imidazol-2-ylidene

Int = Intermediate

L = ligand

LHMDS = Lithium bis(trimethylsilyl)amide

LED = light-emitting diode

MLCT = metal-to-ligand charge transfer

Mes = mesityl

m = meta

NHC = *N*-heterocyclic carbene

NHPI = *N*-(acyloxy)phthalimides

NMP = *N*-Methyl-2-pyrrolidone

NCRs = Nitrogen-centered radicals

NMR = Nuclear Magnetic Resonance

nep = Neopentyl glycolate

o = ortho

OA = oxidative addition

OPhth = *N*-phthalimide ethers

p = para

---

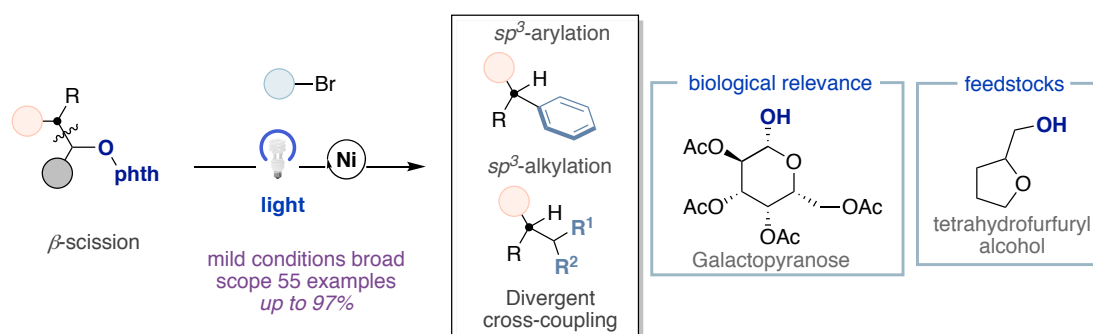
PC = Photocatalyst  
PET = photoinduced electron transfer  
PCET = proton-coupled electron transfer  
PT = proton transfer  
Piv = pivalate  
PMP = para-methoxyphenyl  
phen = 1,10-phenanthroline  
ppm = parts per million  
rt (RT) = Room temperature  
SCE = Saturated calomel electrode  
SET = Single electron transfer  
SM = starting material  
Ts = Tosyl  
TBS = Tert-butyldimethylsilyl  
TBDPS = tert-butyldiphenylsilyl  
TEMPO = 2,2,6,6-Tetramethyl-1-piperidinyloxy  
THF = Tetrahydrofuran  
TMEDA = Tetrametiletilendiamina T = temperature  
THF = tetrahydrofuran  
TMS = tetramethylsilane  
TBADT = Tetra-n-butylammonium decatungstate  
TMG = 1,1,3,3-Tetramethylguanidine  
TBPB = *tert*-Butyl peroxybenzoate  
*t*Bu-terpy = 4,4',4''-Tri-*tert*-Butyl-2,2':6',2''-terpyridine  
*t* = *tert*  
UV = Ultraviolet  
VCP = vinylcyclopropane

## Abstract

With the increasing demand for  $sp^3$  architectures in drug development, new methods to construct  $sp^3$ -carbon linkages have attracted significant attention from medicinal chemists. Metal-catalyzed cross-coupling reactions have offered innovative solutions to synthesize structurally diverse  $sp^3$ -carbon scaffolds, and increasing interest in the catalytic cleavage of abundant C–C bonds has emerged as a promising area for remodeling skeletal frameworks. Other approaches to build up  $sp^3$  architectures have been pursued within the context of multicomponent reactions, which can simultaneously introduce different residues across some unsaturated systems, which have become a powerful tool for the formation of a new  $sp^3$  C–C bond.

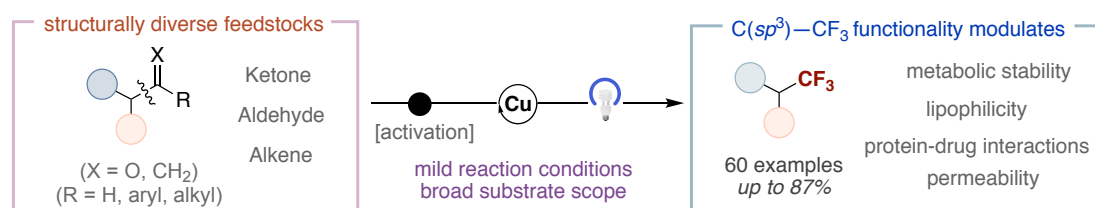
In line with the Martin group's interest in activating inert bonds and Ni-catalyzed 1,2-difunctionalization reactions, my doctoral studies have focused on exploring methodologies for  $sp^3$  C–C bond formation via C–C bond cleavage and Ni-catalyzed 1,2-carboration.

The initial research chapter focuses on the development of a dual catalytic strategy for forging  $sp^2$ – $sp^3$  and  $sp^3$ – $sp^3$  architectures via  $\beta$ -scission of aliphatic alcohol derivatives. Conditions were developed involving  $\beta$ -scission of aliphatic alcohol derivatives with a range of aryl- and alkyl halides under nickel catalysis and mild photocatalytic conditions. Employing naturally abundant and commercially available aliphatic alcohols as building blocks, this methodology successfully offers an unconventional manifold for enabling  $sp^3$ -arylation and  $sp^3$ -alkylation events with excellent chemoselectivity and a broad application profile. The applicability of this reaction was further expanded within the context of late-stage functionalization of saccharide derivatives and advanced intermediates. In particular,  $sp^3$ -carbon synthons derived from  $\beta$ -scission of alkoxy radicals hold great synthetic potential as a general and flexible C–C bond-forming protocol.



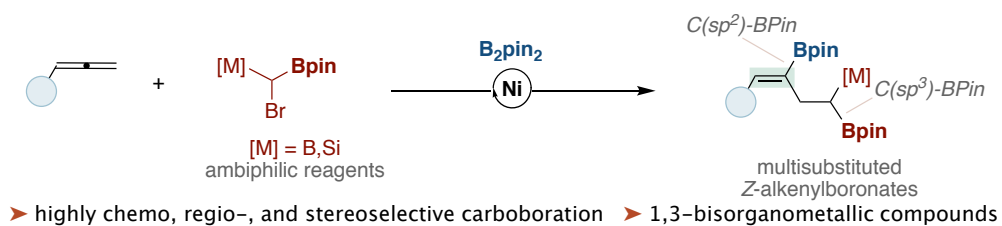
**Scheme 1.** Dual catalytic strategy for forging  $sp^2-sp^3$  and  $sp^3-sp^3$  architectures via  $\beta$ -scission of aliphatic alcohol derivatives.

The next research chapter is in line with our initial findings in C–C bond cleavage events. Following our interest in such a topic, we then developed an efficient protocol for the conversion of structurally diverse feedstocks containing ketones, aldehydes, or alkenes to the corresponding trifluoromethylated analogues by aromatization-driven  $sp^3$  C–C cleavage. This technology offers an unconventional manifold for enabling trifluoromethylation events with excellent chemoselectivity and a broad application profile under mild conditions. Notably, we provide multiple transformation platforms to undergo trifluoromethylation, which might provide access to a library of trifluoromethylated compounds in drug discovery, and would be of considerable value to the chemical industry and academia.



**Scheme 2.** Trifluoromethylation of structurally diverse feedstocks by C( $sp^3$ )–C bond cleavage.

Prompted by a recent disclosure from our group that dealt with a catalytic 1,1-difunctionalization of unactivated olefins en route to  $sp^3$  bis-organometallic B, B(Si)-reagents, we aimed to expand our studies toward the 1,2-alkylboration of unsaturated systems with  $sp^3$  mono-organometallic reagents, which is discussed in the last research chapter. We anticipated that through 1,2-alkylboration of allenes, we could access multisubstituted 1,3-( $sp^2$ ,  $sp^3$ )-bisorganometallic alkenes. However, forming a new  $sp^3$  C–C bond while controlling the chemo-, regio- and stereoselective alkylboration of allenes is highly challenging due to competing side reactions. After considerable optimization, reaction conditions with high selectivity have been obtained and further studies are ongoing to expand the substrate scope and synthetic applications.



**Scheme 3.** Nickel-catalyzed regio- and stereoselective alkylboration of allenes with  $\alpha$ -haloboranes.

In conclusion, we have developed new methods for the synthesis of  $sp^3$  architectures via C–C bond cleavage and Ni-catalyzed 1,2-carboboration strategies. All the above transformations are characterized by their broad scope, mild conditions and exquisite site-selectivity, thus offering a complementary new blueprint for preparing densely functionalized, yet synthetically versatile,  $sp^3$  C–C bonds from simple and readily accessible precursors.

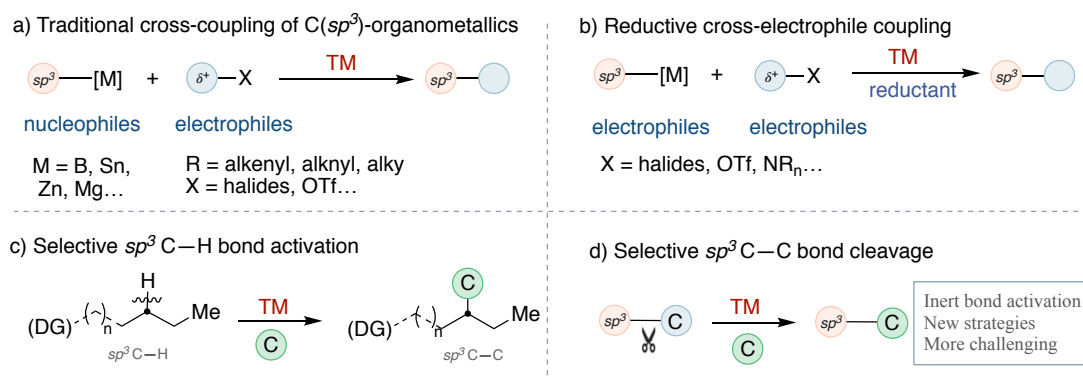
---

# **Chapter 1**

## ***General Introduction***

## 1.1 General Introduction

The development of new catalytic methods to increase the complexity of organic molecular structures has been one of the central goals of organic synthesis. In recent years, medicinal chemists have noted that compounds with a higher fraction of  $sp^3$ -carbon atoms improve significantly physicochemical and pharmacokinetic profiles in clinical candidates, thus challenging chemists to come up with new catalytic techniques aiming at forging  $sp^3$ -architectures.<sup>1</sup> Beyond any reasonable doubt, transition-metal-catalyzed cross-coupling reactions have offered innovative solutions for the construction of  $sp^3$ - $sp^3$  linkages.<sup>2</sup> These reactions provide substantial advantages when compared to standard  $S_N1$  or  $S_N2$  substitution processes of alkyl electrophiles, such as improved selectivity and milder reaction conditions<sup>3</sup> (Scheme 1.1, *pathway a* & *pathway b*).



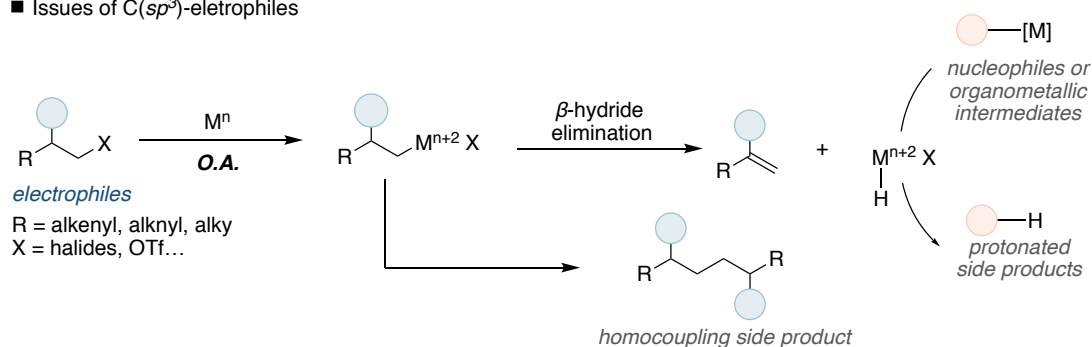
**Scheme 1.1** Forging  $sp^3$  architectures via metal-catalyzed cross-coupling reactions.

The importance of transition-metal-catalyzed reactions was recognized by the 2010 Nobel Prize in Chemistry,<sup>4</sup> which was awarded to Prof. Richard F. Heck, Ei-ichi Negishi and Akira Suzuki for their pioneering contributions in Pd-catalyzed cross-coupling reactions for the formation of C-C bonds. Despite the advances realized, the coupling of  $sp^3$ -hybridized carbon fragments still remains challenging due to (a) the low coordination of  $sp^3$  centers to transition metals,<sup>5</sup> (b) the slow oxidative addition of  $sp^3$  electrophiles to low-valent catalysts and (c) the lower propensity for triggering  $sp^3$ - $sp^3$  bond-reductive elimination at metal centers, thus leaving ample room for side reactions via competitive homocoupling,  $\beta$ -hydride elimination or hydrogen atom transfer events (Scheme 1.2).<sup>6</sup> In most instances, the means to enable  $sp^3$  C-C bond-formation requires the utilization of alkyl organometallics,<sup>7</sup> organic halides,<sup>8</sup> or



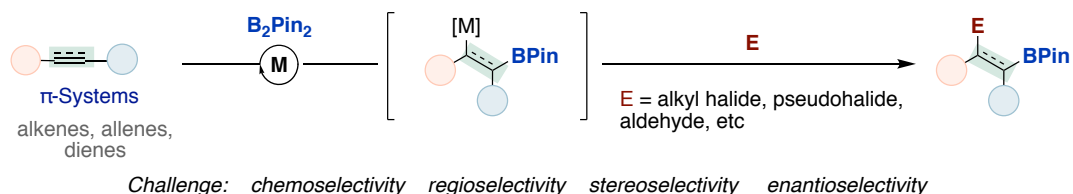
C–O/C–N electrophiles,<sup>9,10</sup> which have seen broad adoption in the cross-coupling arena (Scheme 1.1, *pathway a & b*). Although considerable progress has been made in the area of  $sp^3$  C–H functionalization (Scheme 1.1, *pathway c*),<sup>11</sup> transition-metal-catalyzed C–C bond cleavage<sup>12</sup> has comparatively received much less attention (Scheme 1.1, *pathway d*). Given the prevalence of  $sp^3$  C–C bonds in organic molecules, the ability to forge new  $sp^3$  architectures from the latter might offer flexibility in synthetic design for both academic and industrial laboratories.

■ Issues of C( $sp^3$ )-electrophiles



**Scheme 1.2** The issues of the coupling of  $sp^3$ -hybridized carbon fragments.

On the other hand, multicomponent reactions hold great promise for rapidly and reliably build up  $sp^3$  architectures by forming C–C and/or C–X bonds across  $\pi$ -systems<sup>13</sup> such as alkenes, alkynes, allenes or dienes. Among these endeavors, borylative 1,2-difunctionalization is rapidly emerging as a powerful method to simultaneously introduce  $sp^3$  C–C bonds and C( $sp^2/sp^3$ )–B bonds that can later on be functionalized by conventional cross-coupling reactions giving the flexibility that organoboranes offer for downstream applications (Scheme 1.3).<sup>14,15,16</sup>



**Scheme 1.3** Transition-metal-catalyzed 1,2-carboboration reactions.

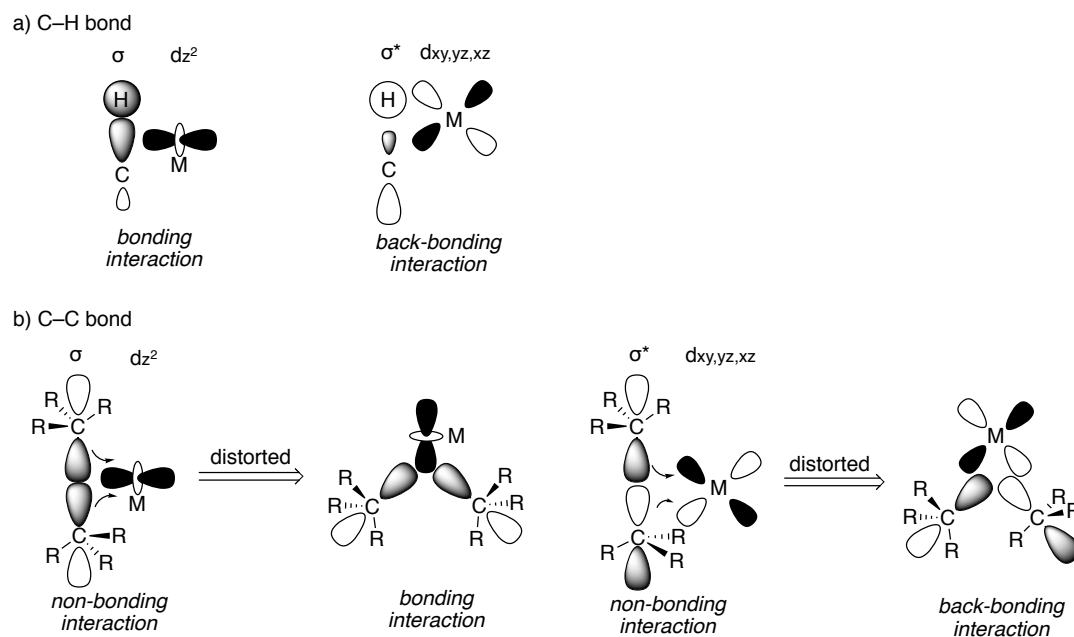
## 1.2 Carbon–Carbon Bond Cleavage

The development of novel methods for C–C bond cleavage provides a synthetic applicability for a large number of cheap and readily available raw materials.<sup>12,17</sup> Key

---

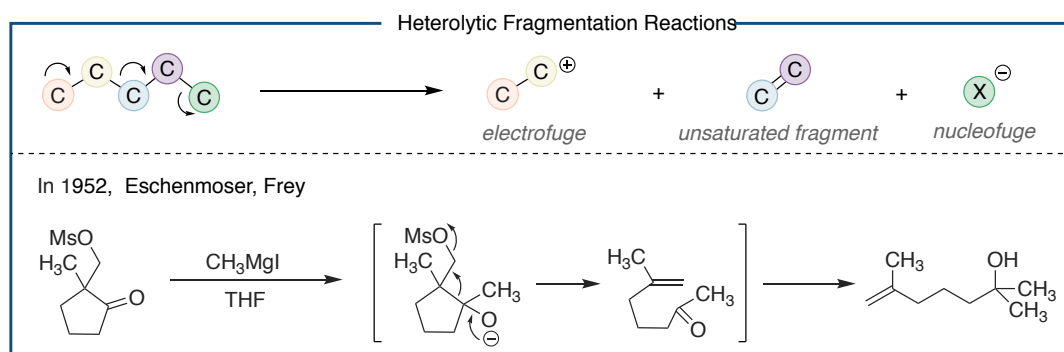
applications of these techniques can be found in the valorization of petroleum-derived products,<sup>18</sup> lignocellulose, or the degradation/recycling of industrially-relevant polymers.<sup>19</sup> Given the prevalence of C–C linkages in organic molecules, the ability to utilize these scaffolds as a manifold for molecular diversity might offer new innovative solutions for forging  $sp^3$  architectures without relying on prefunctionalized reagents.<sup>20</sup>

Although considerable progress has been made in the area of C–H functionalization, there are significantly fewer methodologies that enable catalytic C–C bond activation.<sup>21,22</sup> A clear distinction between the two can be seen by comparing their bond dissociation energies: BDE (C–H)  $\approx$  100–110 kcal/mol vs BDE (C–C)  $\approx$  105 kcal/mol.<sup>23</sup> Although these values suggest C–C bonds to be weaker than C–H bonds, there are kinetic considerations when activating C–C bonds as these are generally more sterically hindered than C–H bonds and therefore harder to activate.<sup>24</sup> Indeed, C–C bonds are less polarized and have less favorable orbital directionality than C–H bonds when they interact with a transition metal.<sup>12b, 25</sup> In addition, the C–H bond is oriented perpendicular to the metal orbital, and the hydrogen orbital's spherical shape allows for significant overlap with the metal orbital (Scheme 1.4, *top*).<sup>24</sup> Moreover, the highly oriented  $\sigma$ -bond orbitals of the C–C bond are not able to overlap well with the d-orbitals of the transition metal unless the C–C bond is distorted by the influence of the transition metal (Scheme 1.4, *bottom*). Lastly, the transition-metal catalyst should distinguish between minor differences in sterics or electronics among various C–C bonds.<sup>26</sup> Indeed, direct C–C bond activation of unstrained compounds normally requires directing groups to facilitate the functionalization via proximity effects,<sup>17a</sup> thus reinforcing the notion that the site-selective functionalization of C–C bonds still represents a considerable challenge and a worthwhile endeavor for chemical invention.



**Scheme 1.4** a) Interaction of metal orbitals with a C–H bond, b) Interaction of metal orbitals with a C–C bond.

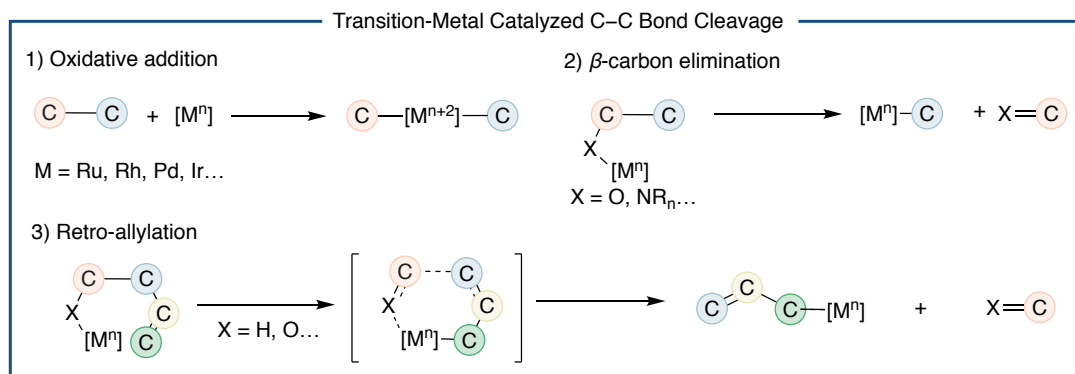
Most relevant C–C bond cleavage reactions occurs frequently in the petroleum industry during the steam cracking of crude oil at high temperatures and pressures<sup>18b</sup> (Scheme 1.5, *top*).<sup>27</sup> The first reaction of C–C bond cleavage can be traced back to the 1950s, where Eschenmoser and Frey disclosed the archetypal C–C fragmentation reaction (Scheme 1.5, *bottom*).<sup>28</sup>



**Scheme 1.5** Historical C–C bond-functionalization reactions.

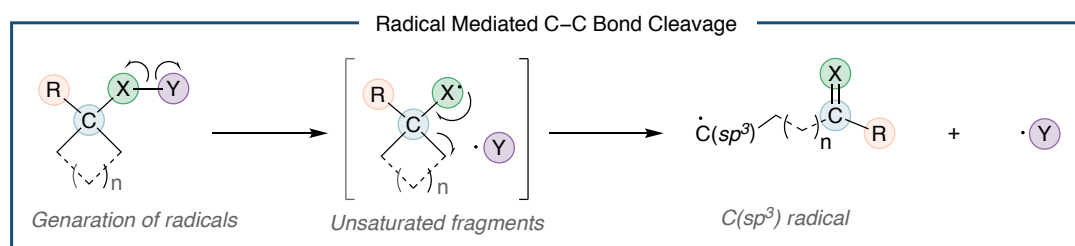
During the past decades, transition-metal-catalyzed C–C bond-functionalizations have been focused on the utilization of strained rings,<sup>12d</sup> sigmatropic rearrangements,<sup>29</sup> Beckmann rearrangements<sup>30</sup> and retro-aldol reactions<sup>31</sup> among others. In general, there are three different types of C–C bond-functionalization mediated by metal catalysts

(Scheme 1.6): (a) direct oxidative addition to low valent ruthenium, rhodium, palladium and iridium complexes,<sup>12a, 17a,g, 26b, 32</sup> a process typically driven by strain release, chelation assistance or decarbonylation events; (b)  $\beta$ -carbon elimination by formation of a strong C–X bond;<sup>17c, 21</sup> (c) retro-allylation<sup>33</sup> that results in the formation of allyl metal species via six-membered transition states. However, the above-mentioned pathways usually have some limitations such as the need to introduce chelating or coordinating groups, relatively harsh reaction conditions and/or low selectivity profiles.



**Scheme 1.6** Transition-metal-catalyzed strategies for C–C bond cleavage.

Radical-type reactions rank among the most promising ways to enable C–C bond-functionalization. This area has gained considerable momentum giving the multiple number of techniques that allows to harness the potential of open-shell intermediates. In addition, radical-mediated C–C bond cleavage<sup>34</sup> reactions often occur under mild conditions, offering a technique that might rapidly and reliably assemble complex structures in late-stage diversification (Scheme 1.7).

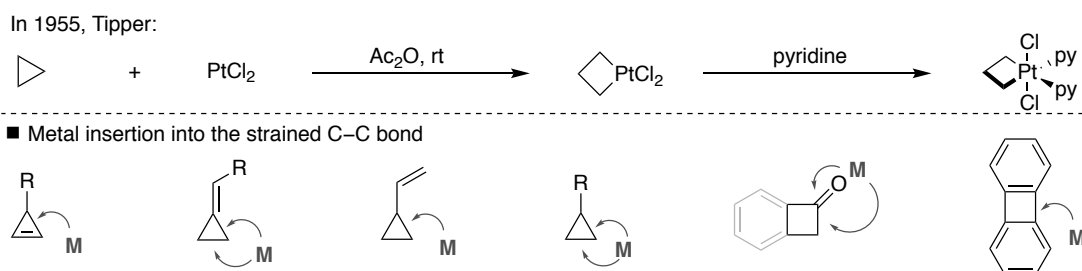


**Scheme 1.7** Radical mediated strategies for the activation of C–C bonds.

## 1.2.1 Transition-Metal-Catalyzed C–C Bond Cleavage

Metal-catalyzed C–C bond cleavage reactions have relied predominantly on small

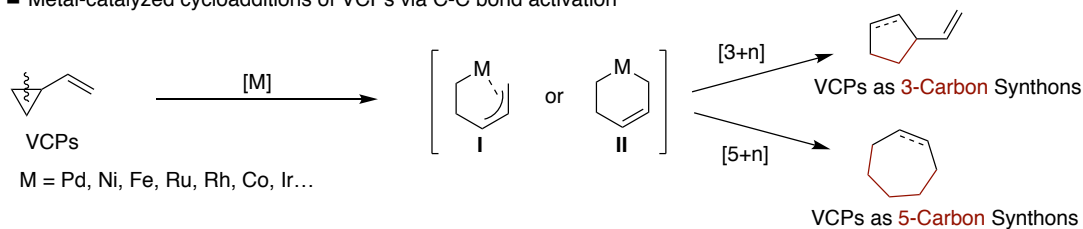
rings, using strain-release as a driving force. In 1955, Tipper reported the first example about the oxidative addition of C–C bonds to Pt complexes, resulting in the formation of a platinum cyclobutane adduct (Scheme 1.8, *top*),<sup>35</sup> the formation of compensate the thermodynamic disadvantage of C–C bond activation by affording stable ring expanded metallacyclic complexes (Scheme 1.8, *bottom*).<sup>36</sup>



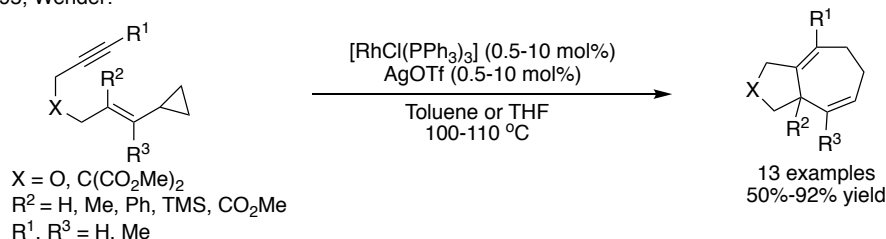
**Scheme 1.8** Small ring system used in C–C bond activation models and common sites for metal insertion.

Activation of cyclopropene,<sup>37</sup> alkylidenecyclopropane<sup>38</sup> and allylcyclopropane<sup>17g</sup> possessing rather high strain energies of 39 ~ 55 kcal/ mol<sup>36b</sup> is relatively easy to achieve, offering a great potential for the synthesis of more complex molecules. For example, Tang and coworkers summarized a series of transition-metal-catalyzed cycloaddition reactions that selectively functionalize C–C bonds in vinylcyclopropanes (VCP).<sup>39</sup> These VCPs can undergo oxidative addition to produce metallacycle **I** or **II**, which then undergo some cycloaddition reactions (Scheme 1.9, *top*).<sup>40</sup> In 1995, Wender reported a Rh(I)-catalyzed intramolecular [5 + 2] cycloadditions of VCPs with alkynes (Scheme 1.9, *bottom*),<sup>41</sup> which disclosed a conceptually novel approach for the synthesis of fused 5,7-bicyclic cycloheptadienes.

■ Metal-catalyzed cycloadditions of VCPs via C-C bond activation



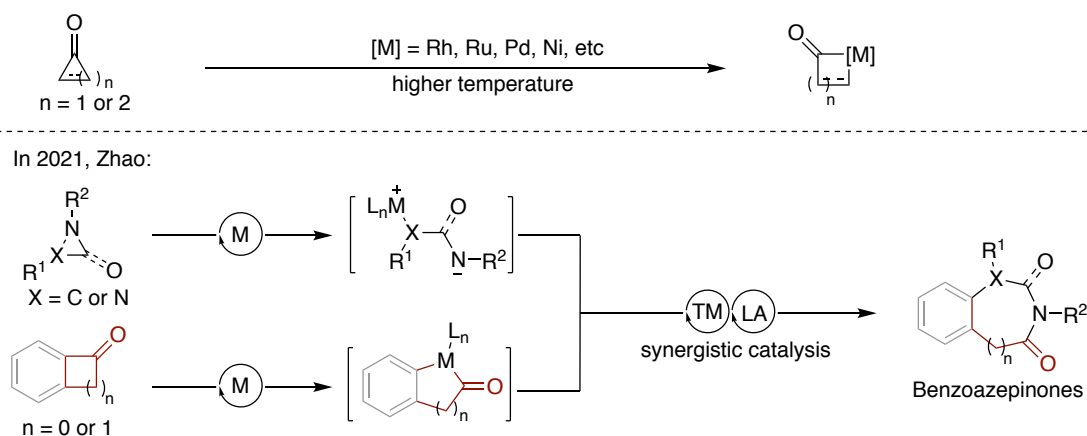
In 1995, Wender:



**Scheme 1.9** C–C Bond cleavage of VCPs.

The C–C bonds adjacent to highly strained ketones are typically highly reactive as stable acyl-metal bonds can be generated by strain release. Indeed, numerous strategies have been designed along these lines<sup>42</sup> by using strained cyclopropanones,<sup>36a, 43</sup> cyclobutanones,<sup>44</sup> cyclobutenones,<sup>45</sup> or cyclobutenediones<sup>46</sup> (Scheme 1.10, *top*). For example, Zhao reported an interesting ring expansion that combines two different strained molecules where cyclobutanones and three-membered azaheterocycles are coupled to form structurally different N-heterocycles (Scheme 1.10, *bottom*).<sup>47</sup>

■ Transition metal-catalyzed ring opening:

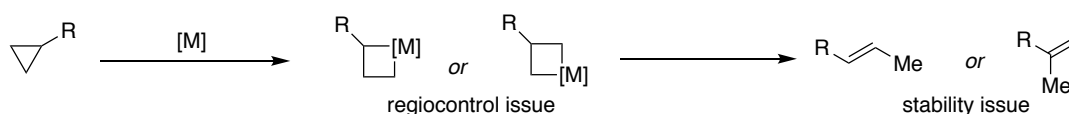


**Scheme 1.10** Transition-metal-catalyzed ring opening of cyclo-ketones.

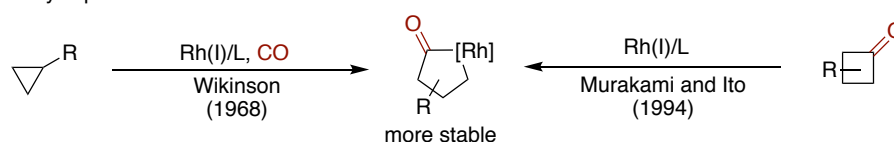
Although metal-catalyzed oxidative addition of non-activated cyclopropanes is well known, it has rarely been used in catalysis beyond reduction and simple isomerization.<sup>48</sup> Fundamental challenges of metallocyclobutane stability and C–C oxidative addition regioselectivity would hamper the development of these reactions into viable catalytic

methodologies. The latter originates from the presence of multiple, yet electronically identical, C–C bonds present in simple cyclopropanes (Scheme 1.11, A). The instability of the resulting metallocyclobutanes could be alleviated in a subsequent reaction in the presence of CO en route to stable metallocyclopentanones.<sup>49, 50</sup> Additionally, Rh(I) catalysts could be inserted into the  $\alpha$ -C–C bond of cyclobutanone (Scheme 1.11, B).<sup>51</sup> Later on, Sophie Rousseaux and John Bower highlighted the importance of directed metal insertion for C–C bond activation in heterosubstituted cyclopropanes such as cyclopropanols and cyclopropylamines containing directing groups (Scheme 1.11, C).<sup>52</sup>

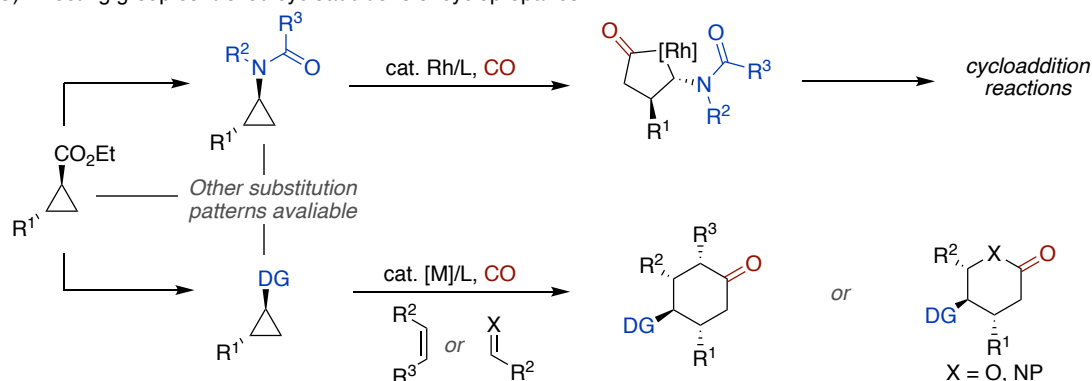
A) Issues:



B) Rhodacyclopentanones via C–C bond activation:



C) Directing group controlled cycloadditions of cyclopropanes:

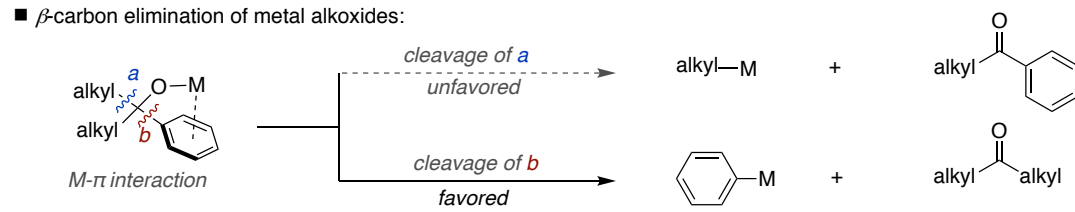


**Scheme 1.11** Metal-catalyzed activation of non-activated cyclopropanes.

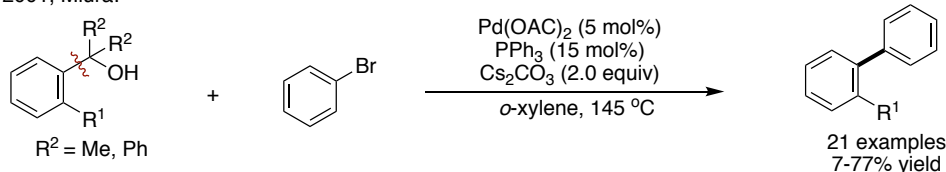
In contrast to the wealth of strategies to promote C–C activation in small rings, the functionalization of unstrained C–C single bonds has received much less attention.<sup>12a,12b, 17c, 53</sup> Recent advances in transition-metal-catalyzed unstrained C–C bond functionalization by  $\beta$ -carbon elimination have been gradually explored and studied.<sup>54</sup> Notably,  $\beta$ -carbon elimination of alcohols requires an interaction between the  $\sigma$ -bond orbital of the  $\beta$ -carbon bond and the metal orbital. From a site-selective perspective with unsymmetrical alcohols,  $\beta$ -carbon elimination is typically more facile with aryl substituents due to the presence of  $\pi$ -orbitals that interact with the metal d orbital, thus facilitating C–C bond cleavage (Scheme 1.12, top).<sup>55</sup> In 2001, Miura reported the first cross-coupling reaction proceeding via  $C(sp^2)$ – $C(sp^3)$  bond cleavage

of unstrained tertiary benzyl alcohols that utilize Pd catalysts and aryl bromides, resulting in the corresponding biaryl motifs (Scheme 1.12, *bottom*).<sup>56, 25</sup>

■  $\beta$ -carbon elimination of metal alkoxides:



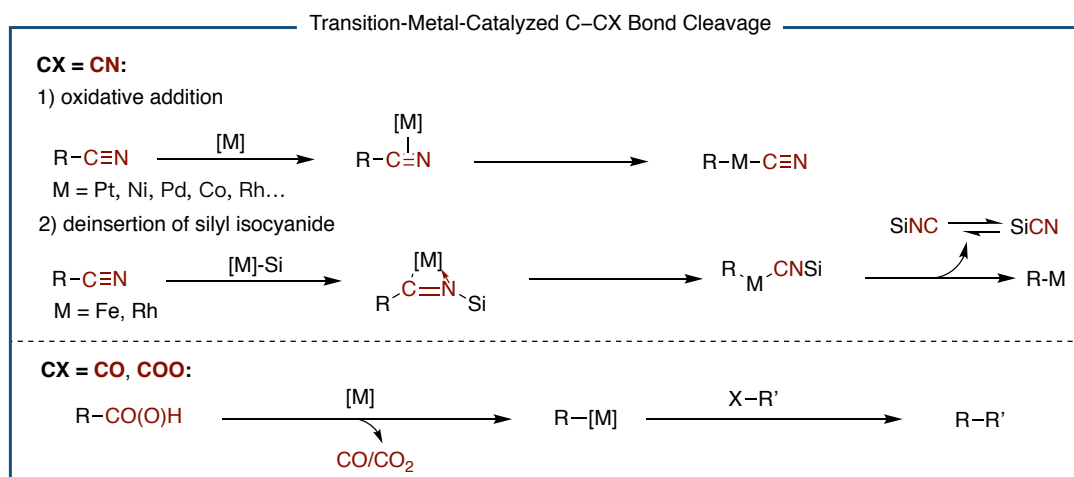
In 2001, Miura:



**Scheme 1.12** Transition-metal-catalyzed  $\beta$ -carbon elimination of unstrained alcohols.

Transition metal-catalyzed C–CX bond cleavage (CX = CN, CO, COO) also offers innovative opportunities within the realm of C–C bond-functionalization.<sup>57, 58, 59</sup> A number of metals such as Pd,<sup>60</sup> Ni,<sup>58a</sup> Rh,<sup>61</sup> Cu,<sup>62</sup> among others,<sup>63</sup> have been used to activate C–CN bonds. Two pathways are commonly accepted for enabling C–CN bond activation: (a) oxidative addition to low-valent transition metals,<sup>58a, 60, 61</sup> (b) silyl isocyanide deinsertion with Fe or Rh complexes (Scheme 1.13, *top*).<sup>64</sup> On the other hand, the presence of carbonyl groups such as aldehydes or acid chlorides might facilitate the establishment of decarbonylative reactions, thus offering "traceless handles" for method development (Scheme 1.13, *bottom*).<sup>58</sup> Alternatively, decarboxylation of simple and abundant carboxylic acids offer intermediates containing carbon-metal bonds by neat CO<sub>2</sub> extrusion.<sup>59</sup>

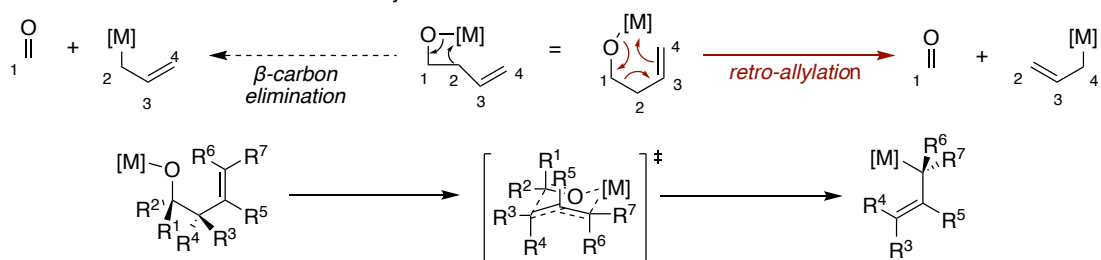




**Scheme 1.13** Two major mechanisms for C–CX (CX = CN, CO, COO) bond activation.

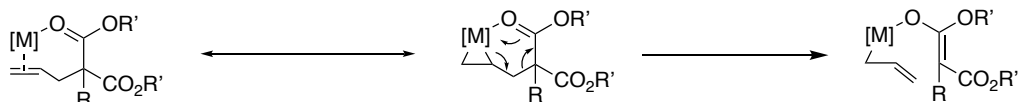
Retroallylation and deallylation reactions of allylic compounds have also been explored in the context of C–C bond cleavage as a means to generate stereo-defined allyl metal compounds via six-membered chair-like transition states<sup>33, 65</sup> (Scheme 1.14, *top*).<sup>66, 67</sup> Alternatively, deallylation constitutes a type of C–C  $\sigma$ -bond cleavage that involves the generation of carbanions by oxidative addition to low-valent metals<sup>68</sup> or via addition/elimination cascade<sup>69</sup> (Scheme 1.14, *bottom*). In this vein, Keisuke Nogi and Hideki Yorimitsu summarized the prospect of retro-allylation and deallylation via C–C bond cleavage.<sup>65</sup>

■ Mechanism of metal-mediated Retro-allylation:

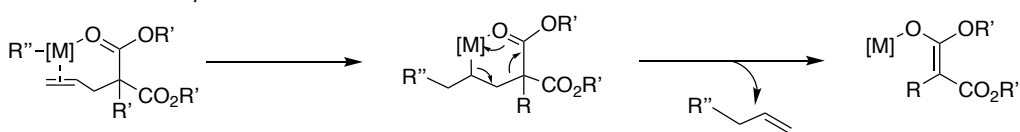


■ Two modes of Deallylation:

a) Oxidative addition to low-valent metal



b) Cascade of addition/β-elimination



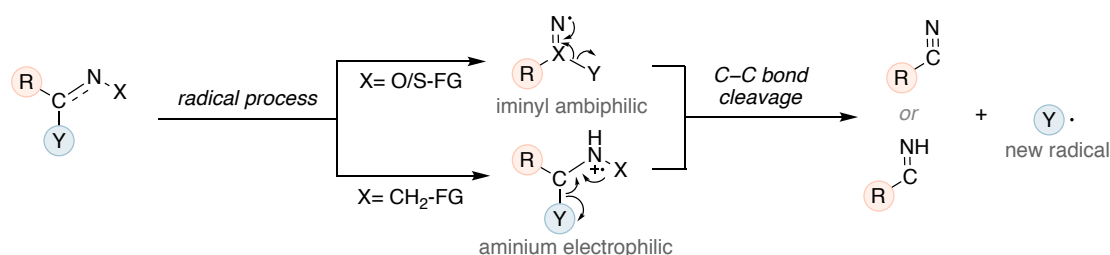
**Scheme 1.14** Retro-allylation and deallylation of allylic compounds.

## 1.2.2 Radical-Mediated C–C Bond Cleavage

An innovative solution in modern chemistry is free radical chemistry which offers an alternative pathway to traditional two electron processes.<sup>70</sup> As free radical species can be generated under mild conditions, selective C–C bond cleavage by free radical processes has also emerged as an attractive strategy for construction of new C–C and C-heteroatom bonds.<sup>71</sup> Radical-mediated C–C bond cleavage is commonly driven by interaction of metal complexes or organic dyes with organic substrates via single electron transfer (SET) events which induces the formation of open-shell species. These processes often have unique selectivity, operate under mild reaction conditions, and excellent functional group tolerance. Typically, formation of alkyl radicals via C–C bond cleavage is usually triggered by N-, O-, or C-centered radical intermediates<sup>71</sup> whereas carbon radical migration reactions are driven by strain-elimination cleavage.<sup>71d</sup>

Nitrogen-centered radicals (NCRs), such as iminyl, amide and amine radicals, are an important and versatile class of radical intermediates that have been widely used in various C–N bond formation reactions (Scheme 1.15).<sup>72</sup> Recently, the C–C bond cleavage mediated by nitrogen-centered radicals under mild conditions has attracted a lot of attention in the synthetic community, offering a new pathway to generate open-

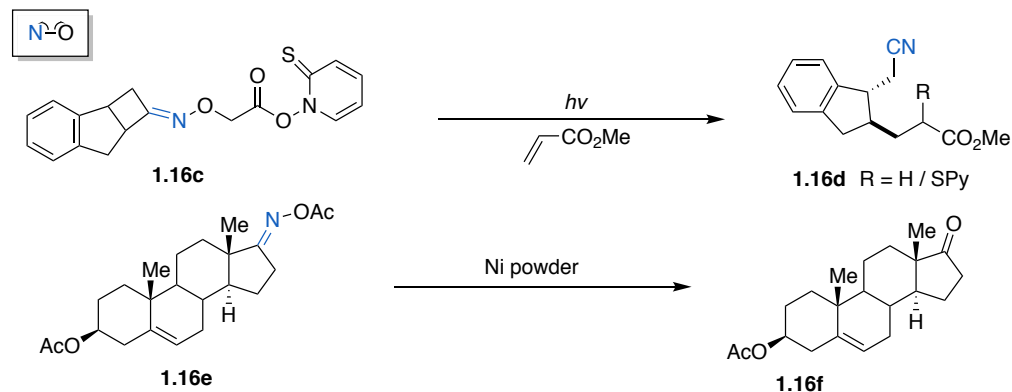
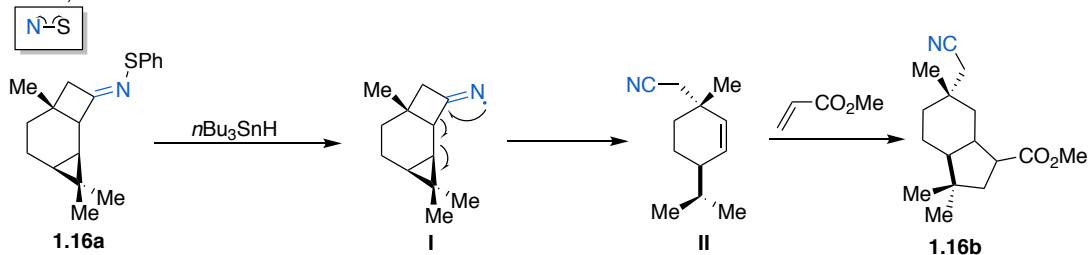
shell intermediates by extruding an unsaturated imine or nitrile surrogate.



**Scheme 1.15** C–C bonds cleavage from nitrogen-centered radicals (NCRs).

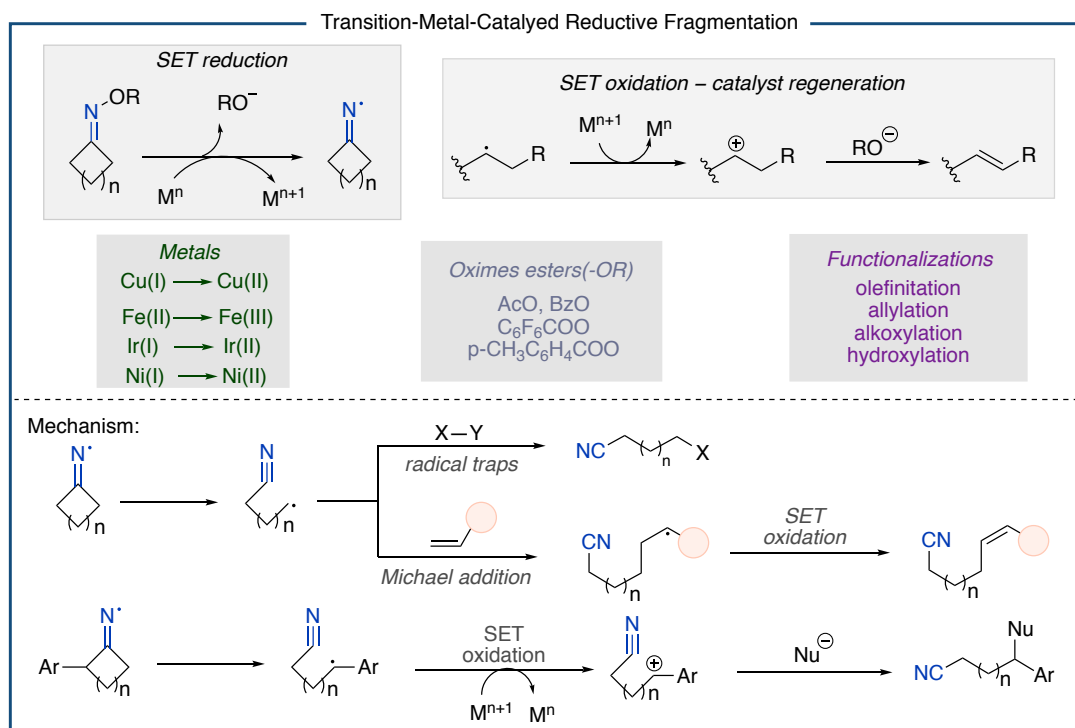
Iminyl radicals typically require addition of oxime derivatives to promote homolysis, because of their weak N–O bond (BDE = 50 kcal/mol).<sup>73</sup> Homolysis of the N–O bond producing iminyl radicals have been primarily accomplished through SET reduction or SET oxidation.<sup>72f</sup> In the 1990s, Zard reported that stannyl radicals initiates the formation of iminyl radicals (I) through homolysis of N–S bonds in sulphenylimines (Scheme 1.16, top).<sup>74</sup> However, this reaction requires the use of toxic reagents such as  $Bu_3SnH/AIBN$ , which may act as hydrogen atom donors resulting in undesirable pathways, hence preventing the desired functionalization. This drawback was addressed later on with a method based on O-carboxymethyl oxime derivatives (**1.16c**),<sup>75</sup> which was a modification of the Barton's decarboxylation. The authors demonstrated that iminyl radicals can be produced by photolytic homolysis, with the resulting alkyl radical generated after  $\beta$ -fragmentation trapped by an electrophilic olefin (**1.16d**). Subsequently, Zard discovered other methods to reduce oxime acetates (**1.16e**) by utilizing Ni powder (Scheme 1.16).<sup>76</sup>

In 1990s, Zard:



**Scheme 1.16** Groundbreaking studies for the generation of iminyl radicals.

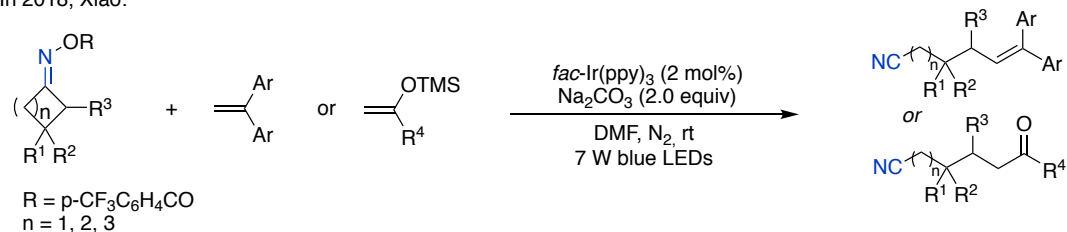
Prompted by the studies of Zard, there has been a significant increase in the use of transition metals such as Fe, Cu, Ir and Ni to reduce oxime esters and to generate iminyl radicals.<sup>77</sup> Comparing with the two-electron oxidative process of precious metals, these transition-metal-catalyzed fragmentation processes mainly undergo SET pathway to afford the targeted radical intermediates (Scheme 1.17).



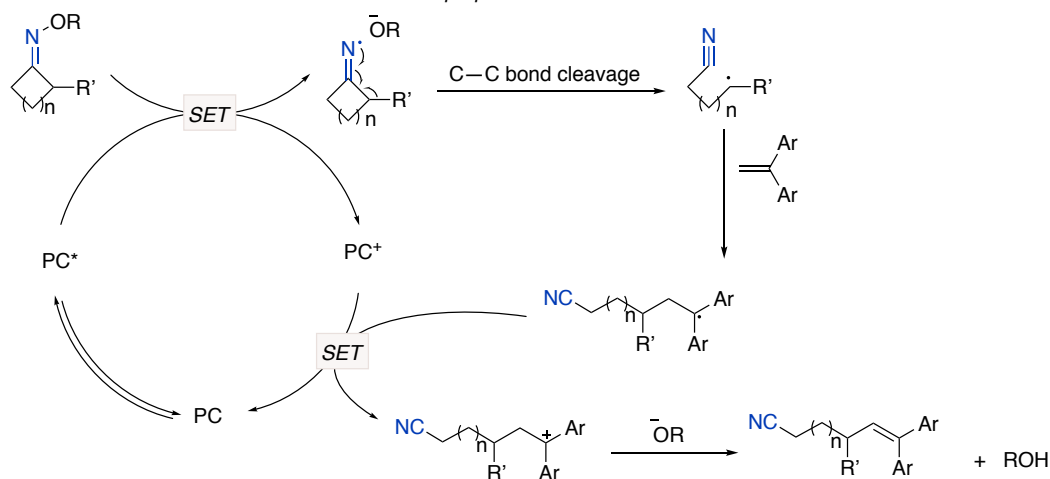
**Scheme 1.17** Transition-metal-catalyzed homolysis of N–O bond by SET.

In recent years, photoredox catalysis have emerged as a powerful tool for rapidly and reliably generate open-shell intermediates,<sup>78,79</sup> including the formation of nitrogen-centered radicals.<sup>72e</sup> Xiao and others discovered a number of transformations based on photoinduced reductive fragmentation of O-acyl oxime derivatives.<sup>80</sup> For example, in 2018, the authors reported that oxime esters undergo visible light-driven iminyl radical-mediated C–C bond cleavage leading to a radical addition cascade reaction with various unsaturated systems (Scheme 1.18).<sup>80a</sup>

In 2018, Xiao:



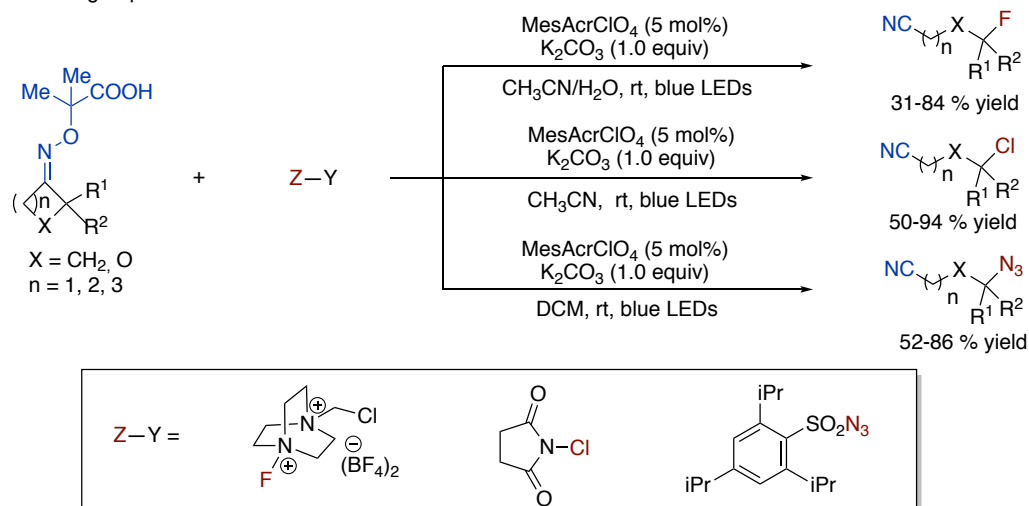
proposed mechanism



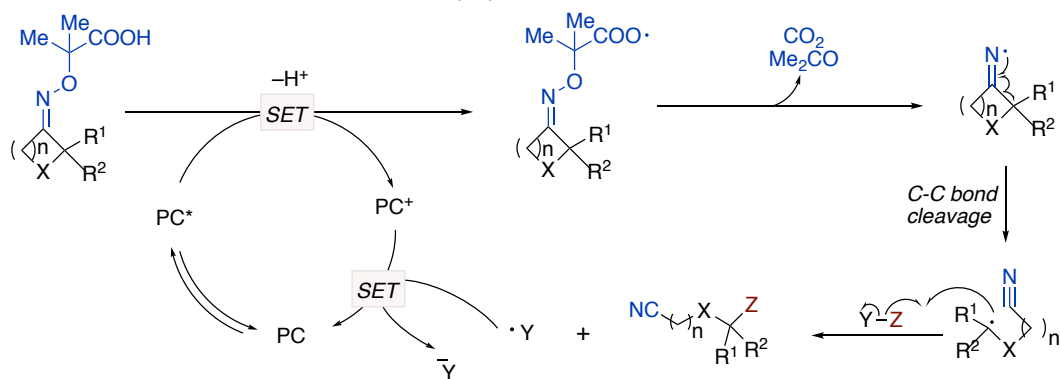
**Scheme 1.18** Visible light-driven iminyl radical-mediated C–C bond cleavage.

Prompted by Zard's early discoveries,<sup>75</sup> Leonori reported an approach using carboxylic acids containing oximes as precursors to generate iminyl radicals. Upon an oxidative SET mechanism, carboxylates undergo bis- $\beta$ -cleavage releasing carbon dioxide and acetone (Scheme 1.19).<sup>81</sup> Subsequently, Leonori combined visible-light photo-oxidation and nickel catalysis to achieve cross-coupling of aryl/alkyl bromides or alkynes and to further expand the functionalization of unactivated  $sp^3$ -hybridized carbons (Scheme 1.20)<sup>82</sup>, demonstrating the potential of this dual-catalytic system for the formation of C–C bonds.

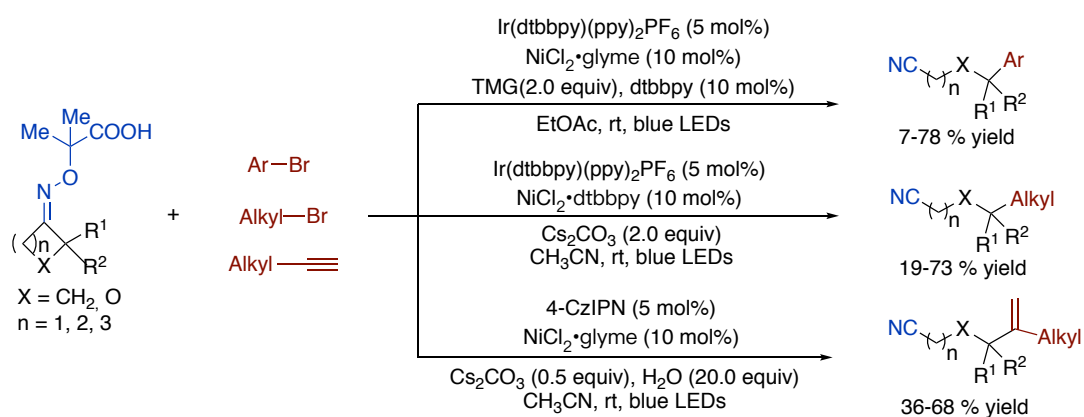
The Leonori group:



proposed mechanism



**Scheme 1.19** Visible light-induced ring-opening functionalization of  $\alpha$ -imino-oxy acids.

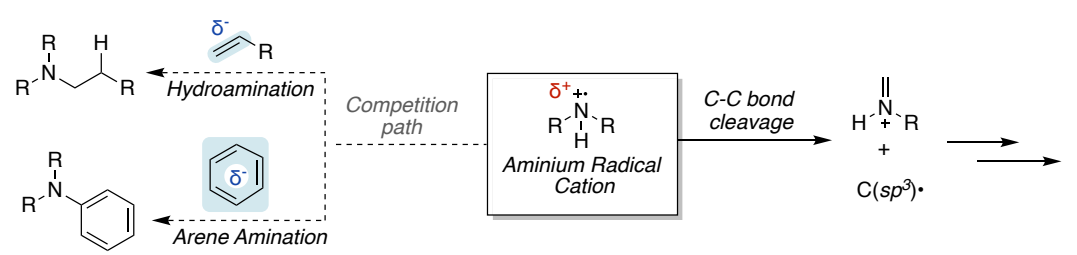


**Scheme 1.20** Dual photoredox/nickel-catalyzed ring-opening arylations, vinylations, and alkylations of  $\alpha$ -imino-oxy acids.

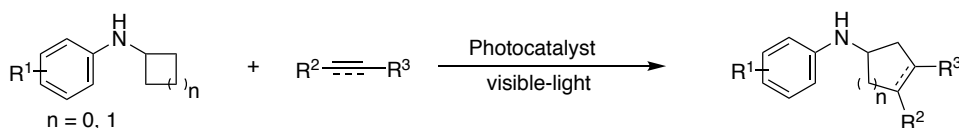
In general, amines have often been used as sacrificial reducing agents in visible-light photoredox processes. To improve its atomic economy, chemists started to further study the different role of amines, which can act as both reductants and reactive intermediates.

For example, amine radicals might be converted into carbon-centered radicals through irreversible C–C bond cleavage,<sup>83</sup> thus setting the basis for designing future reactions.

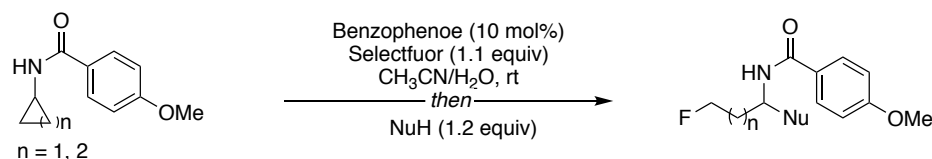
Recently, a series of strategies have been designed for enabling C–C bond-functionalization via in situ generated on secondary amine-derived radical cations.<sup>84</sup> While these species might react with electron-rich fractions such as alkenes, alkynes and aromatic rings forming C(*sp*<sup>2</sup>/*sp*<sup>3</sup>)–N bonds (Scheme 1.21, *top*), Zeng reported that aminium radical cations produced from cyclopropylamine or cyclobutylamine substrates undergo irreversible ring opening induced by photocatalytic SET oxidation, enabling intermolecular [n + 2] (n=3, 4) cyclization reactions with alkenes, alkynes (Scheme 1.21, *bottom*).<sup>85</sup> In 2020, Waser reported a ring-opening method to accomplish oxidative difunctionalization of *N*-cyclopropyl and *N*-cyclobutyl amides using Selectfluor as fluorine source and benzophenone as photocatalyst (Scheme 1.21, *bottom*).<sup>86</sup>



In 2019, Zeng group:



In 2020, Waser group:



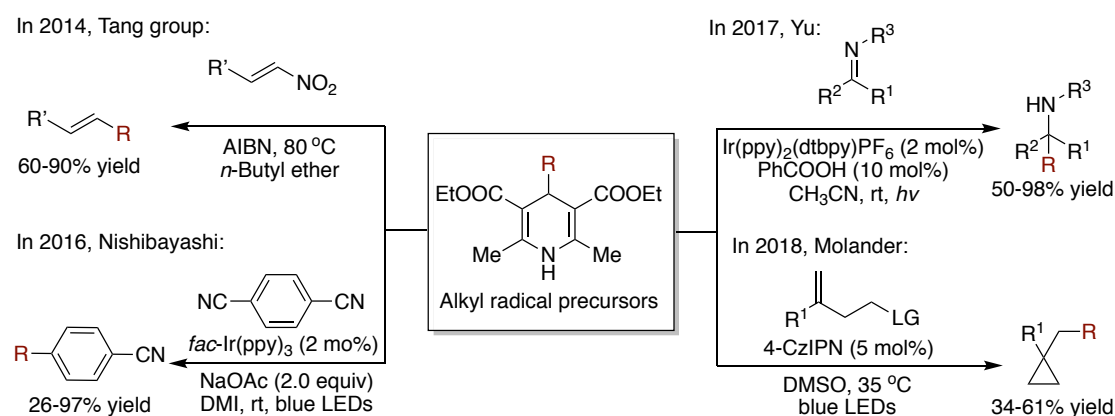
**Scheme 1.21** Secondary aminium radical cation-mediated C–C bond cleavage.

Other strategies based on aminium radical cations are the utilization of backbones susceptible to dearomatization, thus offering a thermodynamic driving force for effecting C–C bond-cleavage.<sup>87</sup> The most representative and well-known are the alkyl-substituted Hantzsch esters (4-Alkyl-1,4-dihydropyridines (DHPs)), which are easy to prepare from various aldehydes.<sup>88</sup> Mechanistic studies suggest that DHP can undergo different pathways of single-electron transfer under light conditions. For example, (a) in the presence of a photocatalyst single-electron oxidation of secondary amines

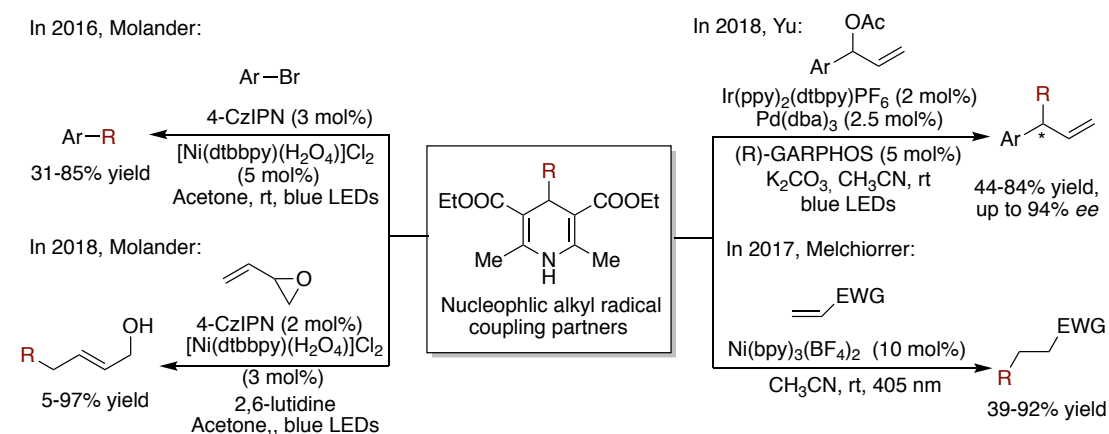


generates an amine radical, followed by C–C bond cleavage at the 4-position of the dihydropyridine ring,<sup>89</sup> or (b) in the absence of a photocatalyst, the excited alkyl-DHP is a powerful reductant ( $[E_{red}^*(\text{Bn-DHP}^*/\text{Bn-DHP}^+)] = 2.0 \text{ V vs. Ag/Ag}^+$  in  $\text{CH}_3\text{CN}$ ), capable of reducing other reagents via single electron transfer pathway while undergoing homolytic cleavage to generate the targeted  $\text{C}(sp^3)$ -centered radicals.<sup>90</sup>

In 2014, Tang disclosed the first example of using alkyl-substituted Hantzsch esters as alkylating reagents.<sup>90</sup> Subsequently, Nishibayashi,<sup>91</sup> Yu,<sup>92</sup> Molander,<sup>93</sup> Melchiorre,<sup>94</sup> and others<sup>95</sup> have contributed to the adoption of Hantzsch esters as a source of alkyl radicals under photoredox catalysis (Scheme 1.22). Notably, the Molander group has made important efforts to develop dual Ni/photoredox catalytic cross-coupling reactions by using 4-alkyl-1,4-dihydropyridines as nucleophilic coupling partners, and photoinduced metal-catalyzed cross-coupling reactions (Scheme 1.23).<sup>92, 93, 94, 96</sup>

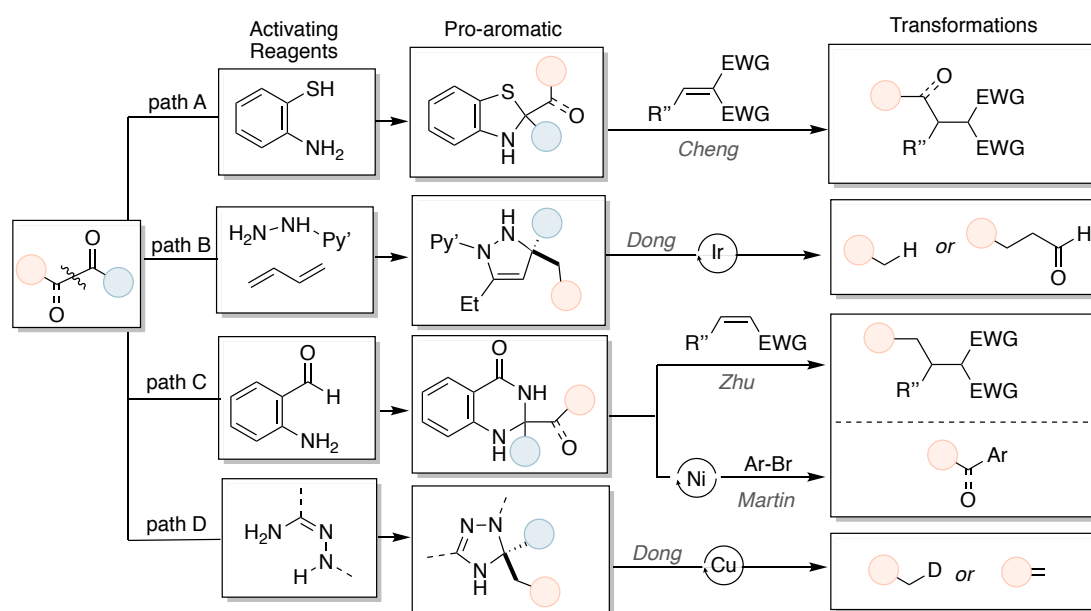


**Scheme 1.22** Radical addition reactions of DHPs as alkyl radical precursors.



**Scheme 1.23** Dual metal/photo-redox catalytic cross-coupling reactions of DHPs as alkyl radical precursors.

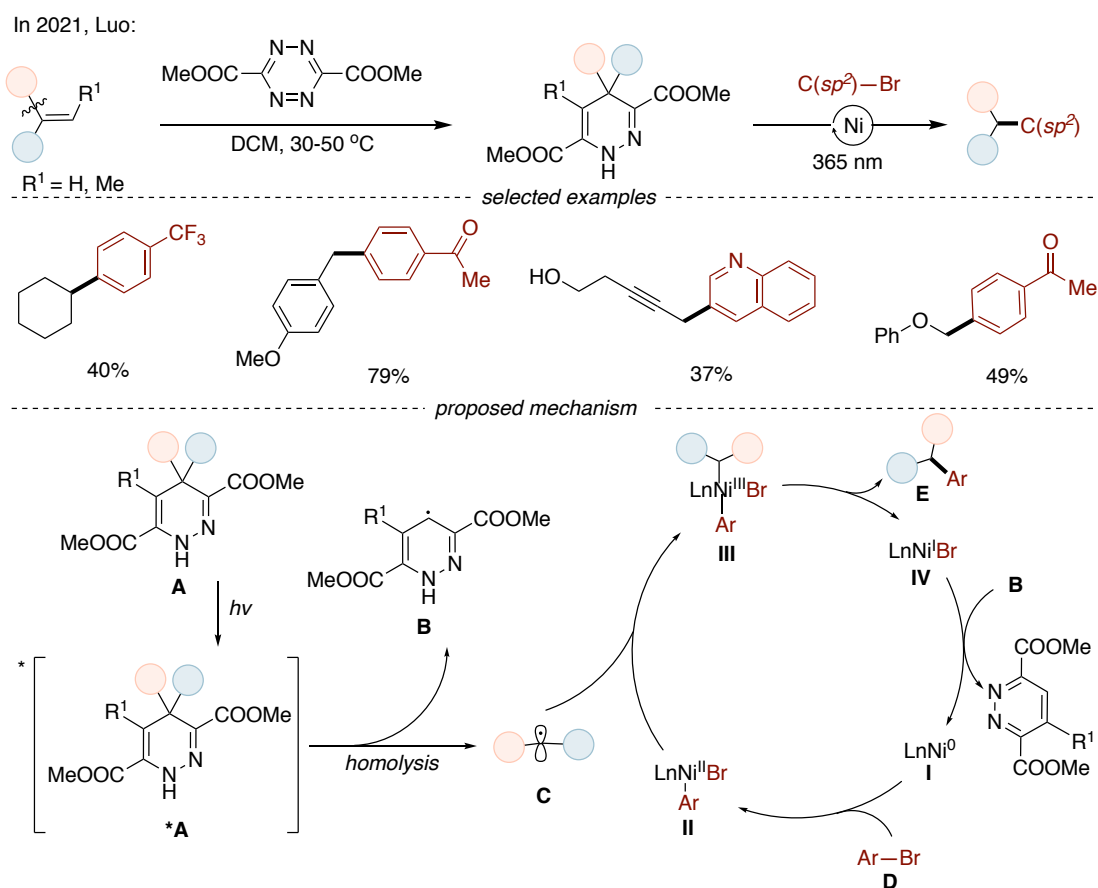
In recent years, a series of disclosures have been reported for the generation of open-shell intermediates via the intermediacy of pro-aromatic compounds<sup>87</sup> (Scheme 1.24). Examples include (A) 2-substituted benzothiazolines which can be used as reagents for reductive radical acylation, alkylation, alkenylation, and alkynylation of electron-poor alkenes.<sup>97</sup> (B) Dihydropyrazole intermediates, prepared *in situ* from a ketone, a 1,3-diene and substituted hydrazine, which subsequently undergo C–C bond cleavage to form alkyl radical species.<sup>98</sup> (C) 2,2-Disubstituted dihydroquinazolinones, which can be easily prepared from ketones and *ortho*-carbamoylaniline in one step.<sup>99</sup> Based on this strategy, our group developed a nickel-catalyzed arylation and alkylation using these pro-aromatic precursors as adaptative C(*sp*<sup>3</sup>) handles.<sup>99b</sup> (D) Guangbin Dong's discovery on pro-aromatic intermediates (D-PAI) derived from ketones have also been reported in the context of Cu-mediated olefination and deuteration.<sup>100</sup>



**Scheme 1.24** Different decarbonylative reagents via dearomatic C–C bond cleavage.

Alternatively, Luo's group disclosed an intriguing Ni-catalyzed dealkenylative cross-coupling enabled by the formation of 4-alkyl-1,4-dihydropyridazine, which can be obtained by the Hetero-Diels–Alder reaction of alkene and tetrazine (Scheme 1.25).<sup>101</sup> Authors proposed that the radical precursor (A) can be excited at 390 nm to produce the excited state A\* that generates the alkyl radical C and 1,4-dihydropyridazine B by homolysis. Subsequently, C can be intercepted by the aryl-Ni<sup>II</sup>(Ln)-Br intermediate (II) to produce the aryl-Ni<sup>III</sup>(Ln)Br-alkyl intermediate (III), thus resulting in the product E and Ni<sup>I</sup>(Ln)Br intermediate (IV) by reductive elimination. B reacts with IV to obtain

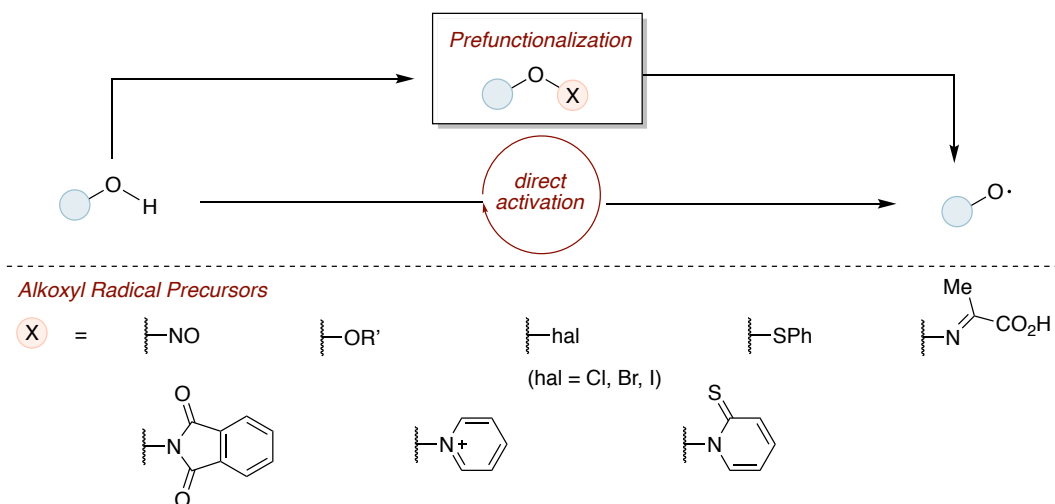
$\text{Ni}^0$  (Ln) (**I**), which reacts with the aryl bromide **D** to form the aryl- $\text{Ni}^{\text{II}}$ (Ln)-Br intermediate (**II**) by oxidative addition.



**Scheme 1.25** Dealkenylative Ni-catalyzed cross-coupling enabled by 4-alkyl-1,4-dihydropyridazine and photoexcitation.

Alkoxy radicals are useful reactive intermediates which also have been used in a wide range of synthetic reactions. Along with *N*-centered radicals, *O*-centered radicals have a high potential for initiating  $\beta$ C–C bond cleavage.<sup>102</sup> However, alkoxy radicals are particularly high-energetic species when compared to other heteroatom-centered radicals due to the lack of stabilization of oxygen-centered radicals, which is associated with mesomeric effects and spin-density delocalization. This results in facile  $\beta$ -scission of alkoxy radicals, a reaction dictated by (a) the thermodynamic stability of the generated alkyl radical; (b) a favorable relief of ring strain (strain release),<sup>103,104</sup> Currently, there are two main ways to generate alkoxy radicals (Scheme 1.26). The indirect method avoids direct homolysis of alkanol O–H bonds with high bond dissociation free energies. Thus, chemists have developed different strategies to obtain alkoxy radicals by building weak oxygen-heteroatom bonds, such as nitrite esters,<sup>105</sup>

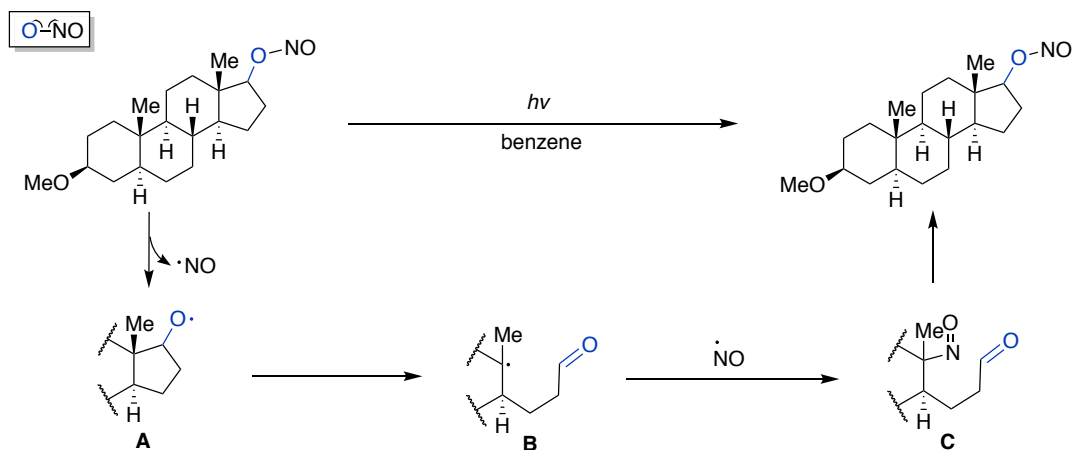
peroxides,<sup>106</sup> hypohalites,<sup>107</sup> sulfenates,<sup>108</sup> *N*-alkoxy-pyridine-2-thiones,<sup>109</sup> and *N*-alkoxyphthalimides for enabling such a transformation.<sup>110</sup> The second method is selective and direct homolysis of O–H bonds.



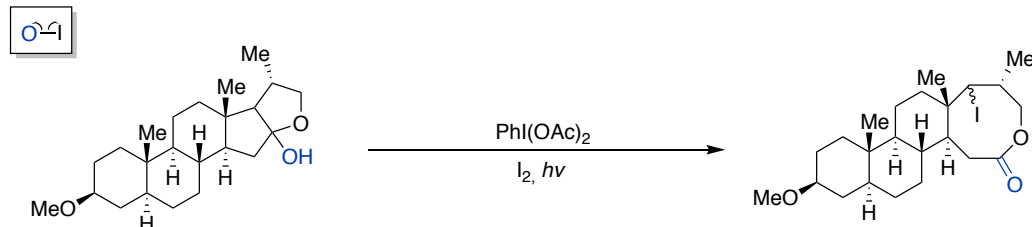
**Scheme 1.26** Different ways to generate alkoxy radicals.

In 1961, Barton devised a strategy for producing alkoxy radicals by using weak O–NO bonding precursors (BDE O–NO = 37 Kcal/mol<sup>-1</sup>). The proposed mechanism is based on photolytic homolysis of nitrite to nitric oxide and  $\beta$ -fragmentation of an alkoxy radical **A** (Scheme 1.27, *top*).<sup>111</sup> After cyclization, the tertiary alkyl radical **B** captures nitric oxide to produce the nitroso aldehyde **C**. Suarez's group devised a method for deconstructing steroidal lactols using iodobenzene diacetate (IBDA) and iodine a few years later (Scheme 1.27, *bottom*).<sup>112</sup> Suarez's reagent (DIB) can form weak O–I bond *in situ*, which then could be homolyzed by visible light to produce alkoxy radicals.<sup>113</sup>

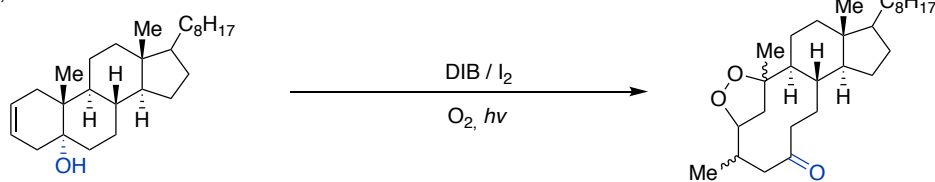
In 1961, Barton:



In 1986, Soares:

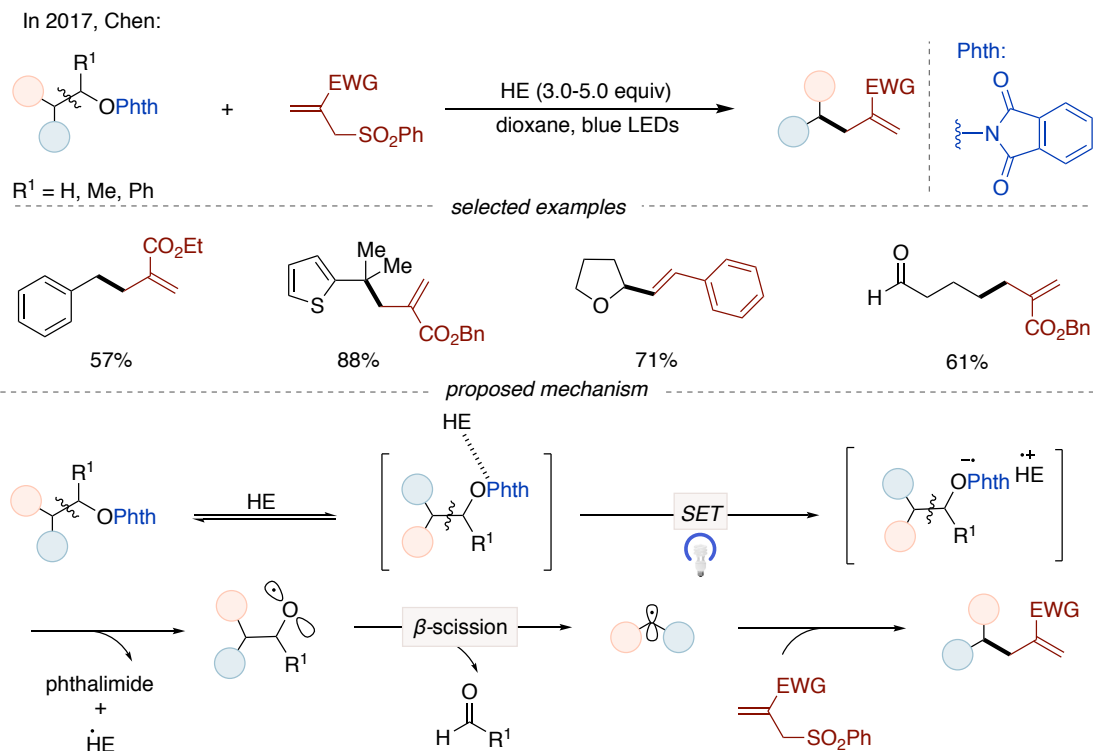


In 1994, Soares:



**Scheme 1.27** Early discovery of alkoxy radicals generated.

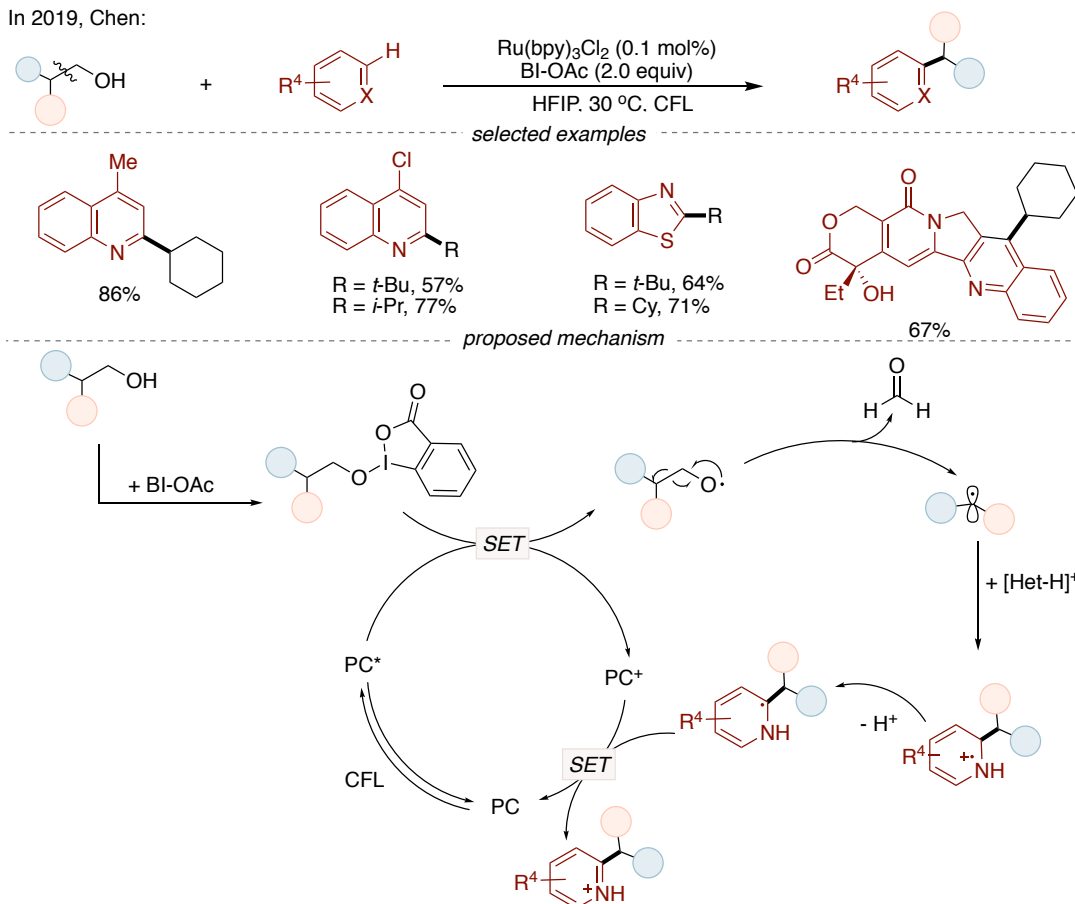
In 2017, Chen reported a novel approach to promote an allylation/alkenylation of N-alkoxyphthalimides derived from aliphatic alcohols via  $\beta$ -scission of alkoxy radicals under photoinduced single electron transfer of donor-acceptor complexes (EDA) (Scheme 1.28).<sup>110c</sup> Formation of the EDA complex between Hantzsch ester and N-alkoxyphthalimide was critical, setting the basis for a single electron transfer that results in alkoxy radical intermediate prior to  $\beta$ -scission.



**Scheme 1.28**  $\beta$ -scission of alkoxy radicals generated from EDA complex.

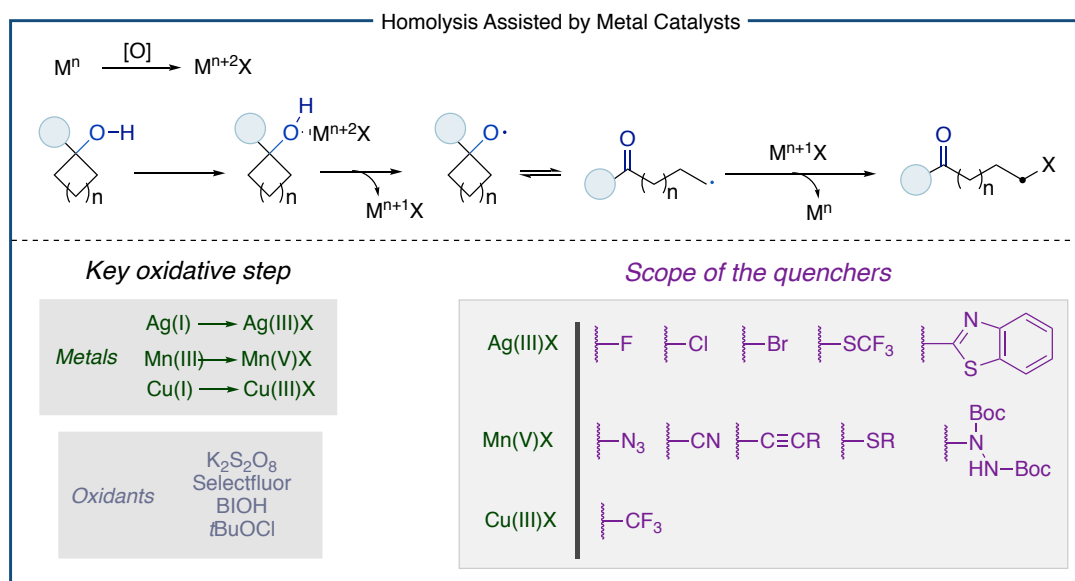
In 2019, Chen disclosed an alternate pathway consisting of the formation of alkoxybenziodoxolones (BI-OR) using 1-acetoxy-1,2-benziodoxol-3(1*H*)-one (BI-OAc).<sup>114</sup> Under photoredox conditions, reduction of BI-OR leads to the formation of an alkoxy radical that sets the basis for a  $\beta$ -scission prior to reaction with a heterocycle via Minisci-type process (Scheme 1.29).

In 2019, Chen:



**Scheme 1.29** Alkoxy radicals generated from BI-OR under photoredox catalysis.

Giving the high bond dissociation energy of O–H bonds, chemists have designed strategies for easily generating alkoxy radicals.<sup>115</sup> In 1960, Schaafsma discovered that  $\text{Cu}^{\text{II}}$ - and  $\text{Fe}^{\text{III}}$ - can facilitate one-electron oxidation of cyclopropanol, resulting in a ring-opened alkyl radical intermediate.<sup>116</sup> In 1972, Rocek discovered that  $\text{Mn}^{\text{III}}$ ,  $\text{V}^{\text{V}}$ , and  $\text{Ce}^{\text{IV}}$  are suitable for one-electron oxidation of cyclobutanols.<sup>117</sup> In the following decades, a series of strategies have combined the utilization of sub-stoichiometric amounts of  $\text{Ag}^{\text{I}}$ ,  $\text{Mn}^{\text{III}}$ , or  $\text{Cu}^{\text{I}}$  and oxidants to promote the homolysis of cycloalkanols and produce alkoxy radicals (Scheme 1.30, *bottom*).<sup>118</sup> Under oxidative conditions,  $\text{M}^{\text{n}}$ -X species are converted to the corresponding  $\text{M}^{\text{n}+2}$ -X species, setting the scene for a single-electron transfer (SET) prior to formation of an alkoxy radical (Scheme 1.30, *top*).<sup>102b</sup>

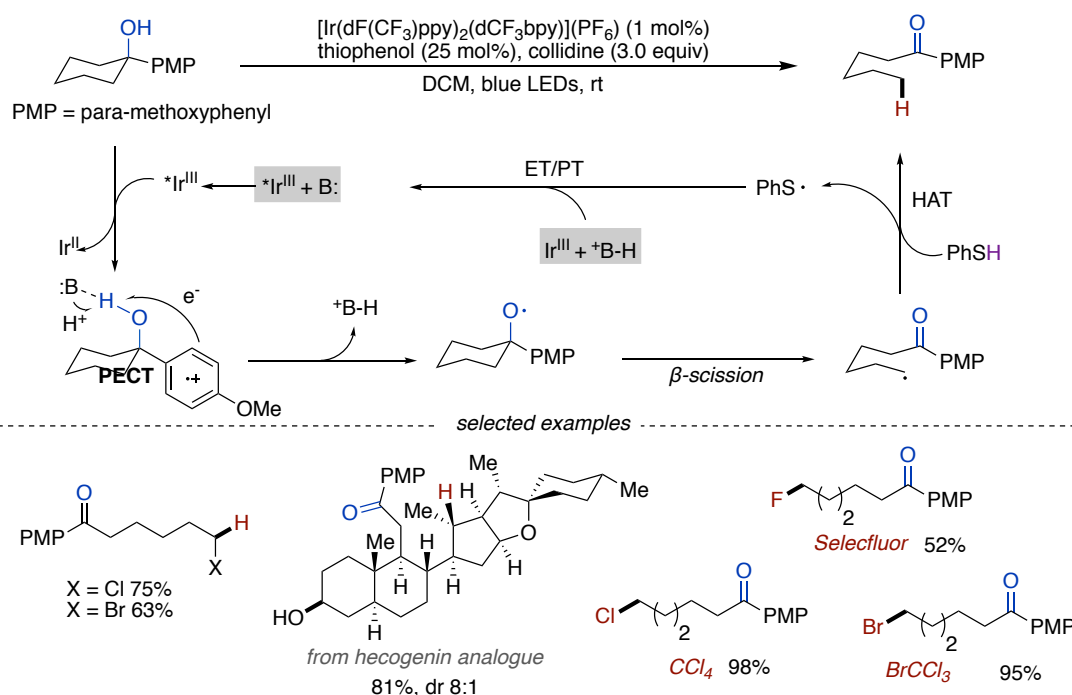


**Scheme 1.30** Homolysis of O–H bonds by metals.

Recently, PCET became a competitive pathway for generating alkoxy radicals under visible-light excitation via *in situ* generation of hydrogen bonding complexes between alcohols and bases.<sup>102d, 102e</sup> Baciocchi reported the presence of PCET events between hydroxyl groups of alcohols and adjacent aromatic radical cations.<sup>119</sup> In 2016, Knowles reported the first proton-coupled electron transfer (PCET) activation of unstrained cycloalkanols under mild reaction conditions to achieve the hydrogenation of a broad scope of natural alcohol derivatives (Scheme 1.31).<sup>120</sup> Furthermore, Knowles described that PCET might lead to homolytic activation of O–H bonds in secondary cycloalkanols. They disclosed a catalytic amount of tetrabutylphosphonium dimethyl phosphate can be used to directly activate O–H bonds of free alcohols by PCET and avoid the use of substrate-based aromatic groups (Scheme 1.32).<sup>121</sup>

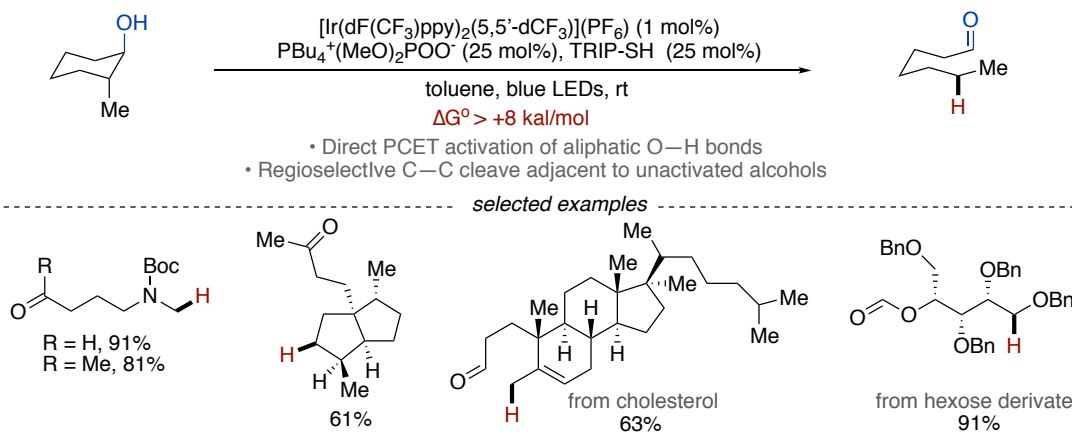


In 2016, Knowles:



**Scheme 1.31** Proton-coupled electron transfer (PCET) activation of un-strained cycloalkanols.

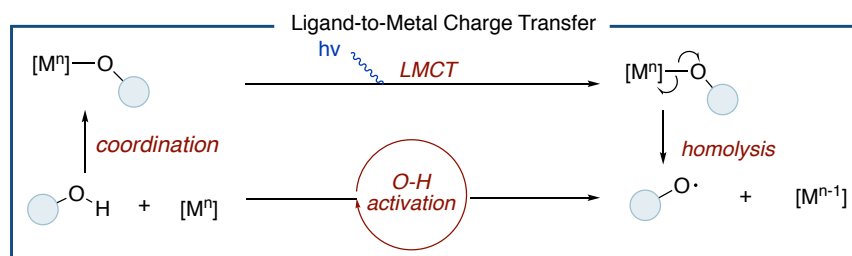
In 2019, Knowles:



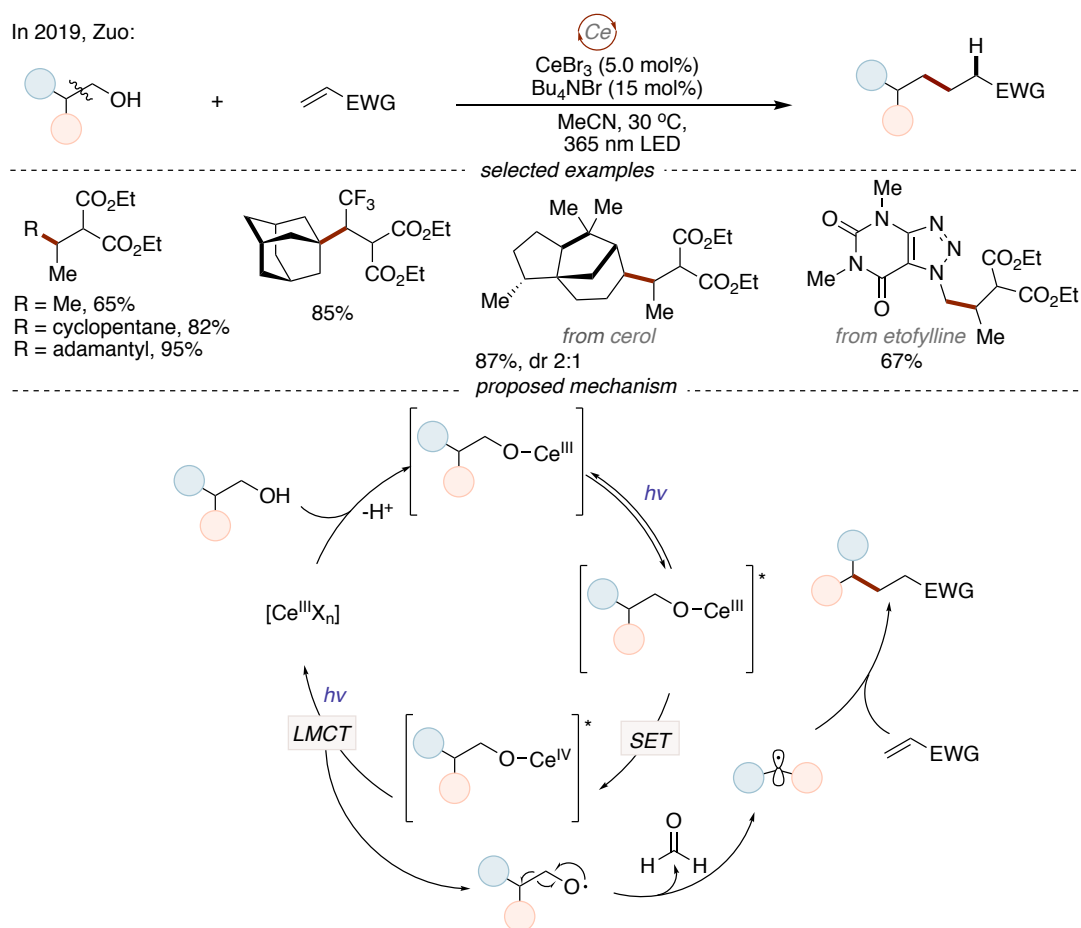
**Scheme 1.32** Deconstruction/hydrogenation of secondary cyclic alcohols by PCET.

Alternative methods for the generation of open-shell intermediates have been described via photoinduced ligand-to-metal charge transfer (LMCT) which undergoes a formal reduction of the metal, causing a directly selective homolysis of a metal-ligand bond, only allowing the coordinated R—OM<sup>n</sup> (M = Ce, Fe) bond to be oxidized and avoiding an over-oxidation (Scheme 1.33).<sup>122-125</sup> For example, in 2019 Zuo described a Ce-catalyzed dehydroxymethylative functionalization through  $\beta$ -scission of alkoxy radicals generated by ligand-to-metal charge transfer of photoexcited Ce(IV) alkoxide

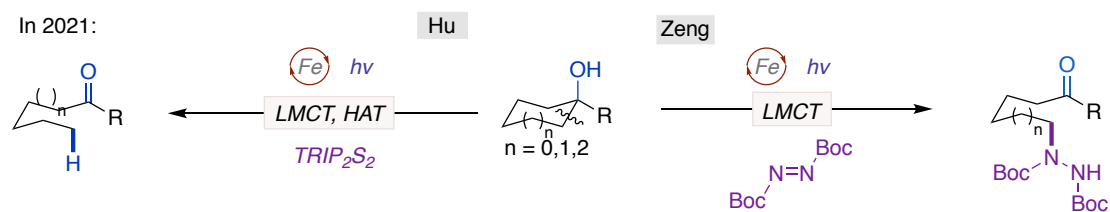
(Scheme 1.34).<sup>126</sup> Recently, Zeng found that readily available iron catalysts [Fe(*Ot*-Bu)<sub>3</sub> or Fe(acac)<sub>3</sub>/*t*-BuONa] can allow the generation of alkoxy radicals by LMCT of iron alkoxide to achieve the amination of cyclic alcohols as well (Scheme 1.35, *right*).<sup>127</sup> Hu also reported an iron-catalyzed deconstructive hydrogenation of cycloalkanols via LMCT (Scheme 1.35, *left*).<sup>128</sup>



**Scheme 1.33** LMCT as a platform to generate alkoxy radicals.



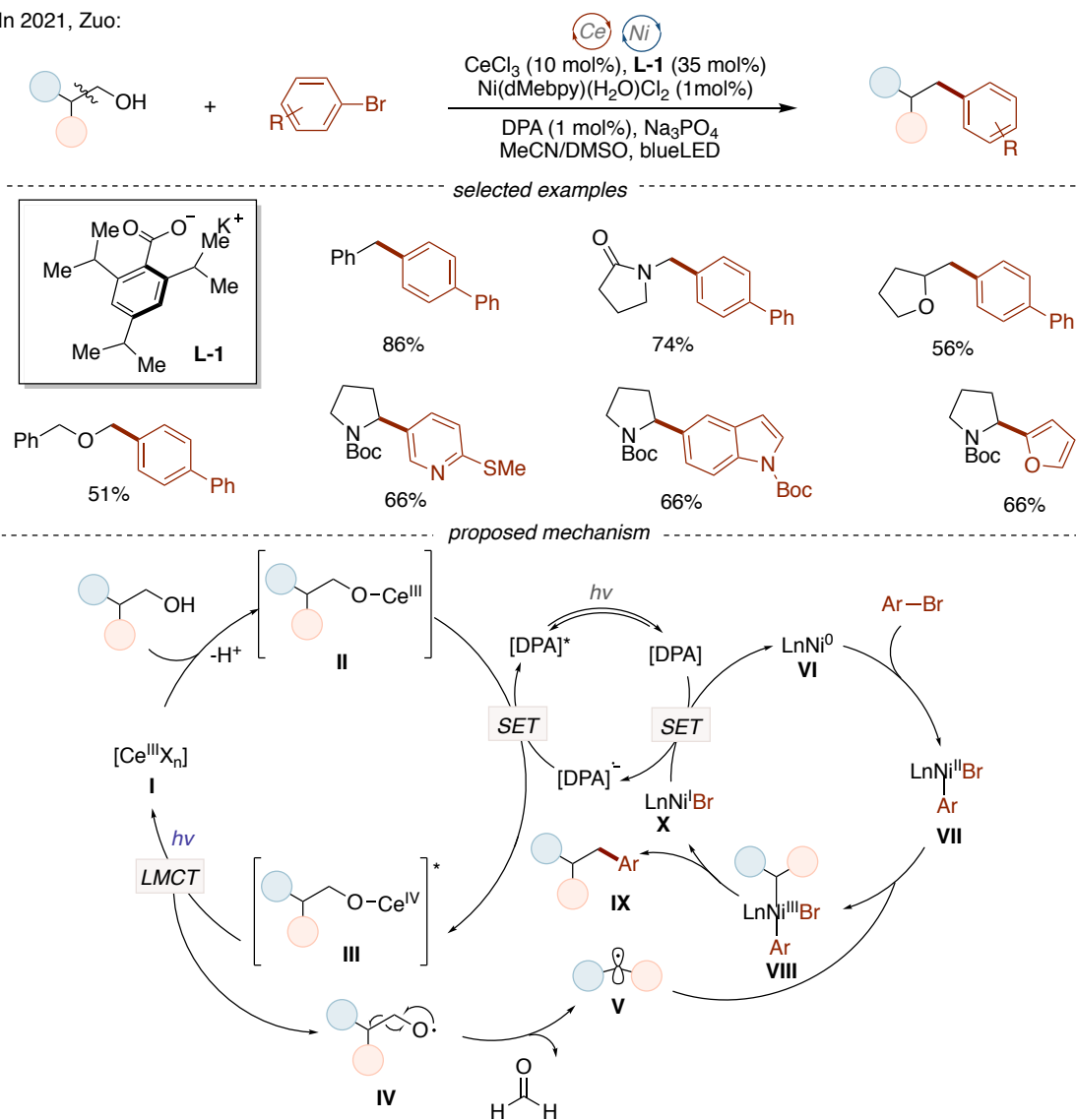
**Scheme 1.34** C–C bond cleavage by using a Ce<sup>III</sup> photocatalyst.



**Scheme 1.35** alkoxy radical generation from cycloalkanols via LMCT of Fe–OR.

Zuo later on reported a synergistic nickel-catalyzed cross-coupling via dehydroxymethylarylation (Scheme 1.36).<sup>129</sup> The authors used the specific modulation of benzoate ligands to optimize experiments by an automated high-throughput experimental platform to achieve a wide range of transformations of alcohols and aryl halides. The authors proposed that a cerium<sup>III</sup> benzoate complex (**I**) undergoes photoinduced electron transfer with **DPA** to produce a photoactive Ce<sup>IV</sup> alcohol salt species (**II**). The homogeneous cleavage of the Ce–O bond via LMCT leads to the production of cerium<sup>III</sup> benzoate and alkoxy radicals (**IV**), which undergo  $\beta$ -scission to form alkyl radicals (**V**). Meanwhile, the low-valent nickel complex (**VI**) undergoes an oxidative addition with aryl bromides to form aryl-Ni<sup>II</sup> complex (**VII**) which can intercept the alkyl radical (**V**) to form the aryl-Ni<sup>III</sup>-alkyl intermediate (**VIII**), setting the basis for a rapid reductive elimination to generate the dehydroxymethylated arylated product (**IX**). The authors suggested that the reduction of Ni<sup>I</sup> (**X**) by the radical anion of **DPA** and the excitation of the latter play a critical role in the reaction.

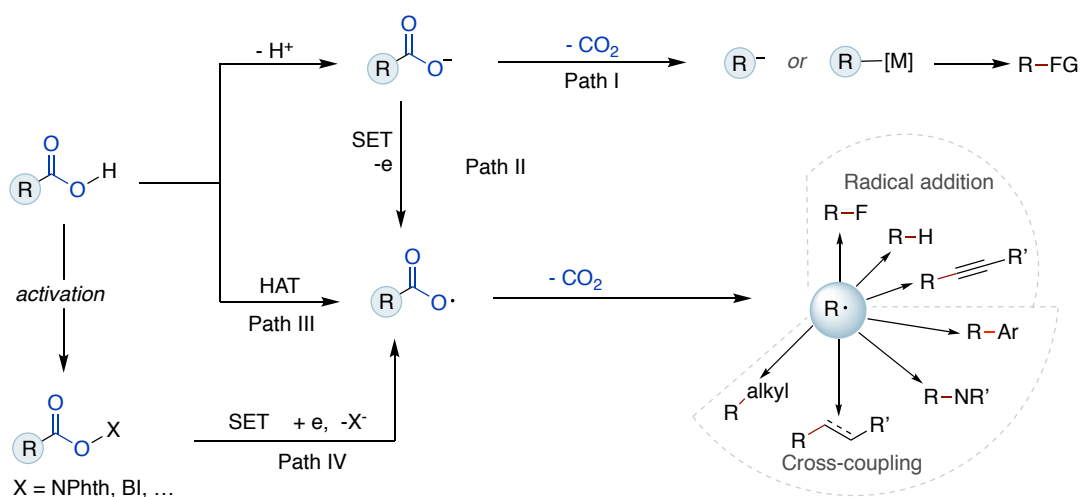
In 2021, Zuo:



**Scheme 1.36** Nickel-catalyzed dehydroxymethylarylation via LMCT.

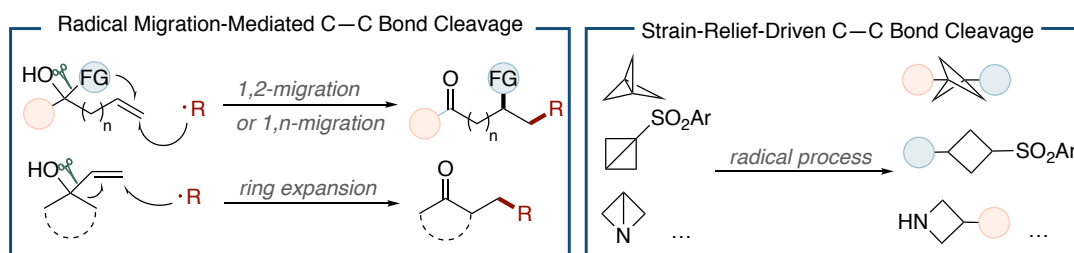
Radical-mediated decarboxylation functionalization studies have been explored for decades,<sup>130, 131</sup> especially the use of aliphatic carboxylic acids as naturally abundant materials (Scheme 1.37). Traditionally, these reactions operate by (a) ligation of the metal center followed by heterolytic cleavage with release of CO<sub>2</sub>, resulting in the formation of a carbanion or metal-stabilized carbanion (pathway I);<sup>130</sup> (b) single electron oxidation prior to decarboxylation (pathway II)<sup>131e,f</sup> or by hydrogen atom transfer (HAT) (pathway III)<sup>132</sup> resulting in the extrusion of CO<sub>2</sub> and the formation of carbon radicals.<sup>131</sup> Traditional decarboxylation procedures need high temperatures or powerful oxidants, while transition-metal-catalyzed or photocatalyzed direct radical decarboxylation from alkyl carboxylic acids can release CO<sub>2</sub> to afford alkyl radicals under mild conditions. Doyle, MacMillan, and colleagues disclosed a seminal

metallaphotoredox scenario for directed decarboxylation of  $\alpha$ -amino acids with aryl halides;<sup>133</sup> (c) Decarboxylation could also be initiated via SET manifolds from carboxylic acid derivatives (pathway VI). Examples can be found in the work of Baran,<sup>134</sup> Overman,<sup>135</sup> and others<sup>136</sup> by transforming the carboxylic acid into the relatively stable N-(acyloxy)phthalimides prior to reduction in the presence of a Ni catalyst<sup>134</sup> or excited photocatalyst.<sup>131e,f</sup>



**Scheme 1.37** Radical-mediated decarboxylative functionalization.

In addition to the methods described above, radical migration-mediated C–C bond cleavage<sup>137</sup> (Scheme 1.38, *left*) or strain-release-driven C–C bond cleavage of [1.1.1] propellane derivatives<sup>138</sup> (Scheme 1.38, *right*) have also been developed, but these protocols are outside the scope of this introduction.

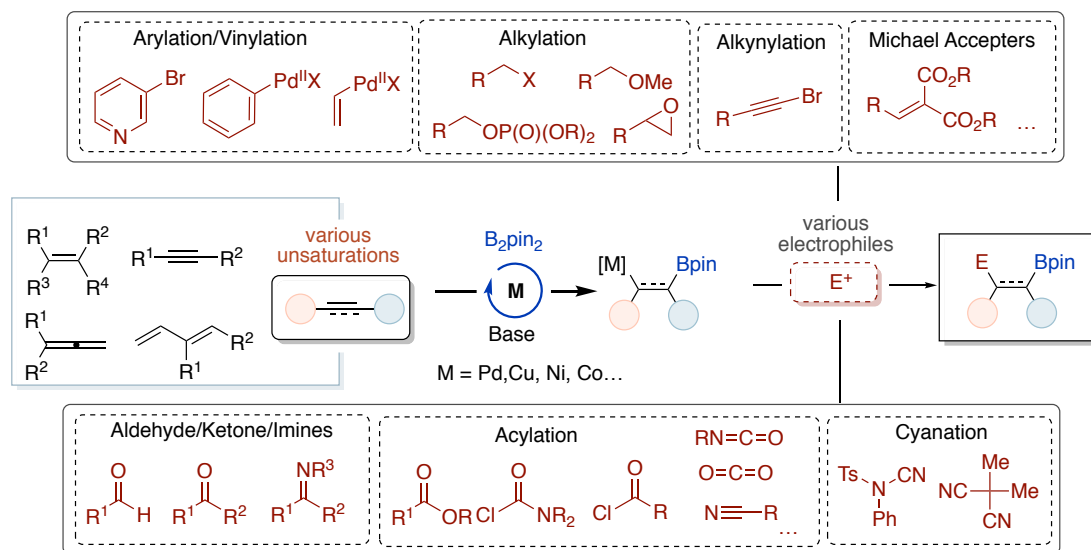


**Scheme 1.38** Radical-mediated migration and strain-relief-driven strategies for C–C bond cleavage.

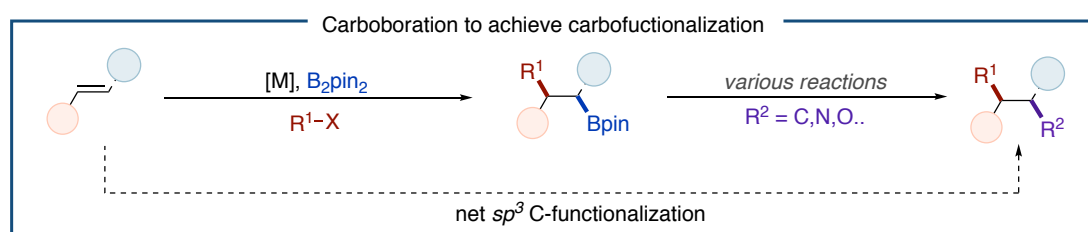
### 1.3 Transition-Metal-Catalyzed 1,2-Carboration

Over the past years, transition-metal-catalyzed 1,2-carboration of  $\pi$ -systems<sup>139, 140</sup> has evolved as a powerful tool for the rapid synthesis of diverse organoborates.<sup>141</sup> 1,2-

Carboration forges a new  $C(sp^2/sp^3)-C$  bond and a new  $C(sp^2/sp^3)-B$  bond by simultaneously inserting a boron and carbon moiety across an unsaturated system. These kinds of reactions can proceed with different transition metals such as copper,<sup>140, 142, 143</sup> palladium,<sup>143, 144</sup> and nickel<sup>145</sup> and offer the possibility of establishing regio- and stereoselective 1,2-carboration events. In particular, the utilization of alkenes,<sup>140c, 140e, 140f</sup> alkynes,<sup>146</sup> dienes or<sup>147</sup> allenes<sup>148</sup> with more than 20 different electrophiles offers the rapid and reliable assembly of chemical libraries (Scheme 1.39). Among them, 1,2-carboration reactions of alkenes have emerged as a tool for constructing complex molecules from simple and available olefin feedstocks. In particular, the final  $C(sp^3)-B$  bonds can be used as linchpins for further transformations, thus enabling a series of  $C(sp^3)-C$  bond-forming reactions (Scheme 1.40).<sup>141</sup> Among the different protocols that are currently available, the utilization of copper-catalyzed 1,2-borylalkylation ranks among the most versatile and powerful technique to forge C–C and C–B bonds in a simultaneous, yet site-selective, manner.



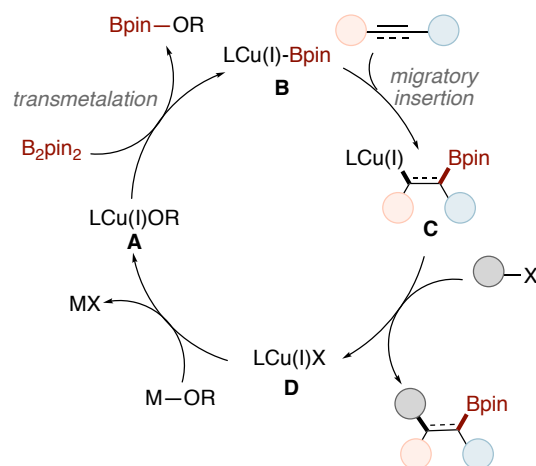
**Scheme 1.39** Transition-metal-catalyzed 1,2-carboration of  $\pi$ -systems.



**Scheme 1.40** Carbofunctionalization based on 1,2-carboration.

### 1.3.1 Cu-Catalyzed 1,2-Alkylboration Reactions

Recently, our improved knowledge in ligand design has allowed the utilization of modular phosphines and *N*-heterocyclic carbenes (NHC) in the context of Cu-catalyzed reactions to forge C(*sp*<sup>3</sup>)-C linkages. These ligands have shown to be particularly important to stabilize alkyl-Cu intermediates and thus circumvent side reactions, while also greatly expanding the possibilities for bond-forming reactions. Among these, Cu-catalyzed alkylboration of unsaturated bonds with alkyl halides has received significant attention.<sup>148</sup> Specifically, organocopper intermediates<sup>139b, 149</sup> can be obtained *in situ* by addition of Cu-B(OR)<sub>2</sub> species to alkynes, alkenes or allenes. The mechanism of these reactions is proposed to operate via the formation of a copper alkoxide (**A**) that react with a diboron reagent en route to a borylcopper species (**B**) (Scheme 1.41). Then, migratory insertion with the unsaturated C-C bond forms an organocopper intermediate (**C**) which reacts with an alkyl halide by SET or S<sub>N</sub>2 to afford the alkylboration product and a copper halide (**D**) that regenerates the catalytically active species **A** in the presence of an alkoxide base.

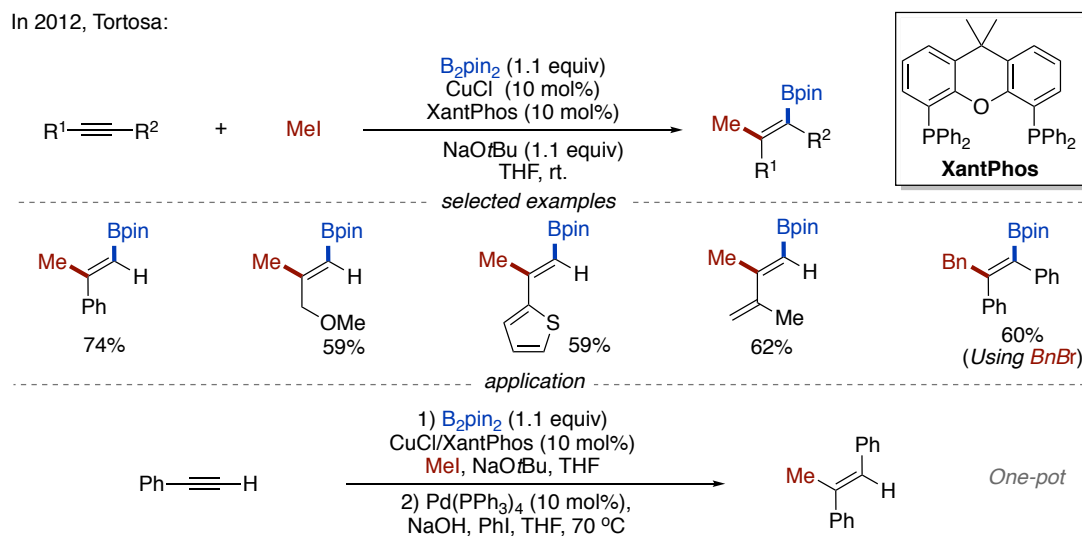


**Scheme 1.41** Cu-catalyzed alkylboration of  $\pi$ -systems.

In 2012, Tortosa developed the first Cu-catalyzed alkylboration of alkynes using Xantphos as a ligand (Scheme 1.42).<sup>142b</sup> The reaction proceeded with high regioselectivity and syn-stereoselectivity to form the corresponding methylbored products. Although a wide range of alkynes were successfully used, only a small number of alkylating reagents such as methyl iodide, benzyl bromide and allyl iodide were compatible as electrophilic coupling partners. In addition, the authors successfully

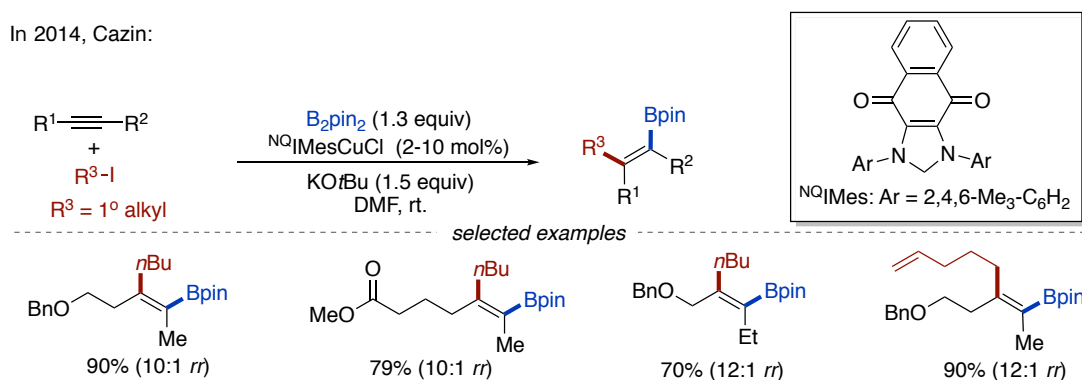
implemented a one-pot methylation/Suzuki-Miyaura coupling, allowing rapid access to highly functionalized alkenes.

In 2012, Tortosa:



In 2014, Cazin reported a comparable approach that used IMesCuCl as catalyst and alkyl halides as electrophiles to achieve alkylborylation of internal alkynes (Scheme 1.43).<sup>150</sup> The use of the N-heterocyclic carbene ligand allowed the reaction to be carried out in air with a 2 mol% low catalyst loading.

In 2014, Cazin:

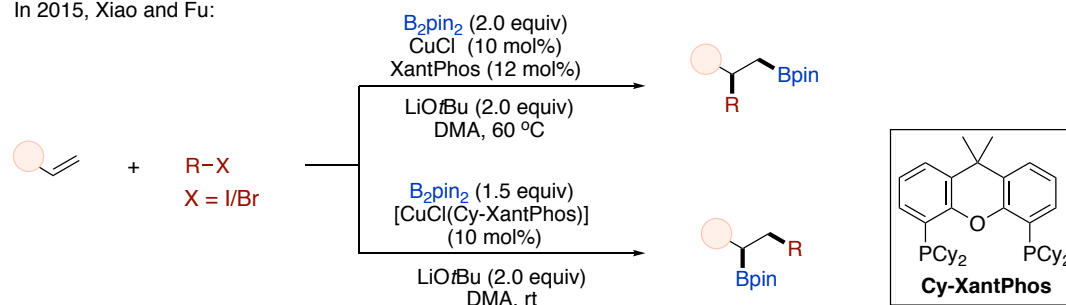


In 2015, Xiao and Fu devised a novel approach of a copper-catalyzed regioselective alkylboration of unactivated alkenes with bis(pinacolato)diboron and alkyl halides using Xantphos or Cy-Xantphos (Scheme 1.44).<sup>151</sup> The authors discovered a weak coordination effect by introducing a heteroatom into the unactivated alkene, probably allowing to promote the insertion of a [Cu-Bpin] intermediate to the C–C double bond. Regiodivergence was also discovered based on the ligand's steric bulk, in which bulky



Cy-Xantphos results in internal borylated products. On the contrary, the less bulky Xantphos ligand promote migratory insertion with the alkene substituents away from the Bpin group, resulting in terminal borylated products.

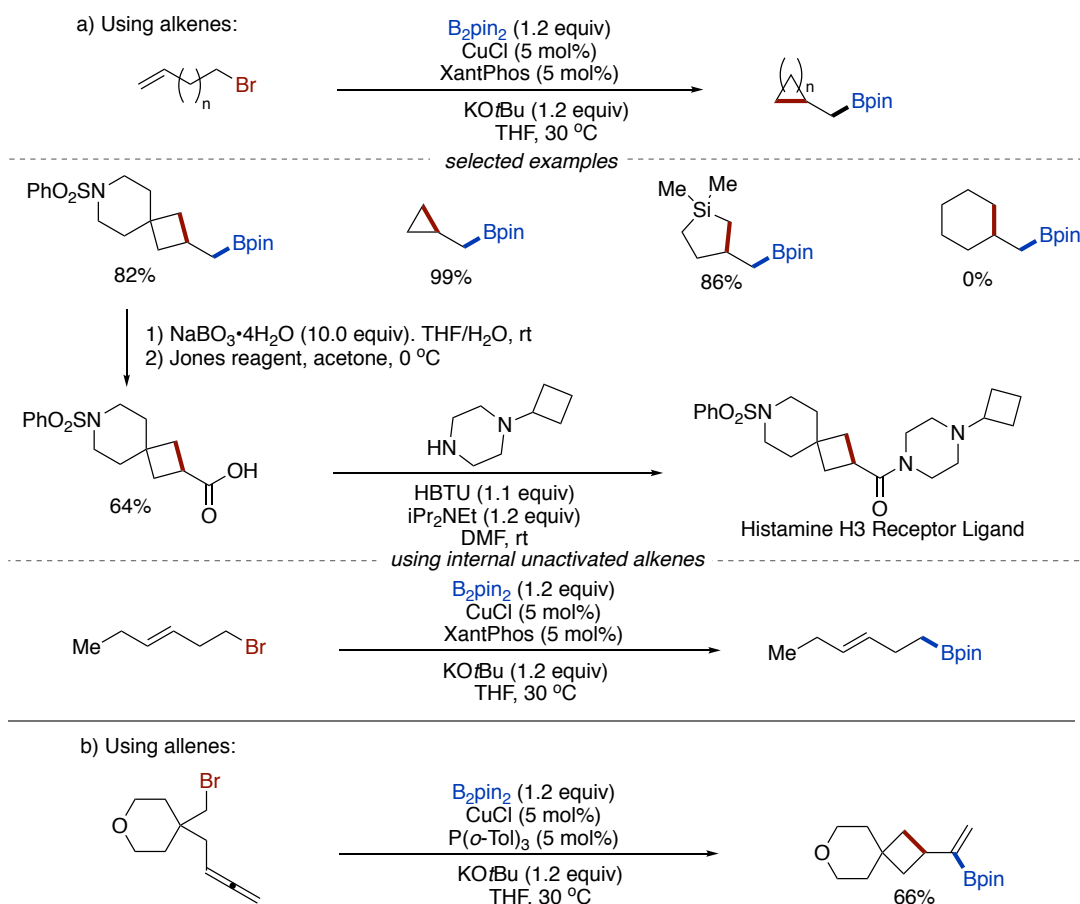
In 2015, Xiao and Fu:



**Scheme 1.44** Ligand-controlled regioselective Alkylboration of alkenes.

At the same time, intramolecular borylalkylation procedures were developed by Ito<sup>152</sup> (Scheme 1.45 *a*). Notably, spirocyclic boronates could be produced, interesting intermediates towards the synthesis of histamine H3 receptor. However, internal unactivated olefins remain some of the most difficult systems for borylcupration events. This challenge was tackled by Ito in a copper(I)-catalyzed intramolecular 2,3-alkylboration of terminal allenenes with an alkyl halide (Scheme 1.45 *b*).<sup>153</sup> The authors proposed that facile isomerization of the allylcopper(I) intermediates allowed the alkenylboronates bearing a four-membered ring structure to be kinetically generated with high regio- and diastereoselectivities.

In 2015, Ito:



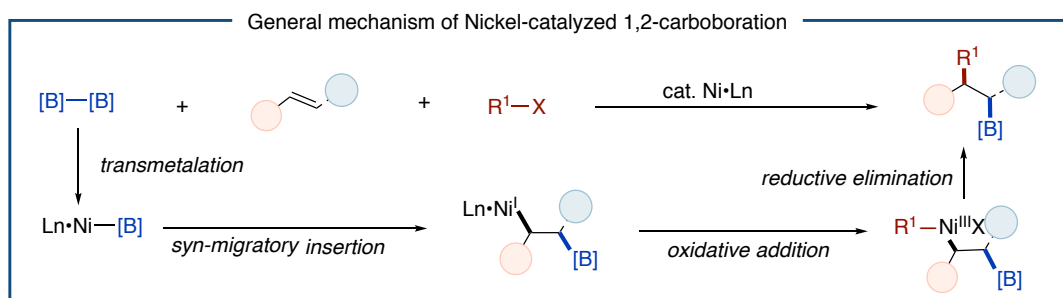
**Scheme 1.45** Intramolecular alkylation of alkenes or allenes.

In addition to traditional alkylation reagents, strategies for generating diastereoselective cyclobutanes, cyclopentanes and cyclohexanes using methanesulfonates or phosphate-based retention groups in intramolecular alkylation have also been reported.<sup>140b, 154</sup> Nevertheless, both intermolecular and intramolecular 1,2-carboration of  $\pi$ -systems reactions remain a great challenge for transition metal-catalyzed 1,2-alkylboronation to construct  $sp^3$  carbon-centered molecules.

### 1.3.2 Nickel-Catalyzed 1,2-Carboration Reactions

In comparison with palladium catalysts, the relatively low cost, earth-abundant, and fundamental reactivity of nickel catalysts have received considerable attention as a new manifold to build up molecular complexity.<sup>155</sup> In addition, nickel catalysts have exhibited high reactivity and selectivity for the formation of  $sp^3$ -hybridized centers.<sup>156</sup> From a mechanistic perspective, Ni catalysts undergo transmetalation with  $B_2pin_2$  to

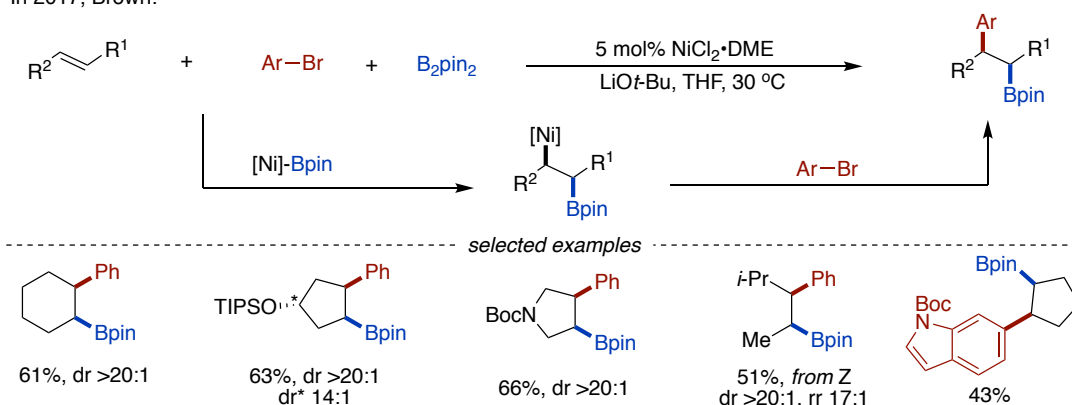
form a Ni(I)–B complex, which promotes syn-migratory insertion into a double bond to form alkyl–Ni(I) species. A final reductive elimination with an appropriate electrophile results in the targeted C–C bond via the intermediacy of alkyl–Ni(III) species (Scheme 1.46). Unlike Cu catalysts, the transient alkyl–Ni intermediates produced after migratory insertion of nickel–boron species into double bonds might be susceptible for  $\beta$ -hydride elimination and migratory insertion, setting the basis for establishing a new rationale for obtaining otherwise inaccessible compounds.<sup>157</sup>



**Scheme 1.46** Nickel-catalyzed 1,2-carboration of alkenes.

In 2017, Brown reported the first Ni-catalyzed three-component 1,2-arylboration reaction of unactivated alkenes. (Scheme 1.47).<sup>145</sup> A wide range of 1,2-disubstituted alkenes which included cyclic alkenes could be employed with excellent yields. The main alkyl–Ni(I) intermediate is proposed to be more resistant to  $\beta$ -hydride elimination than an alkyl–Pd (II) species. As a result, a directing group was not required to mitigate  $\beta$ -hydride elimination.

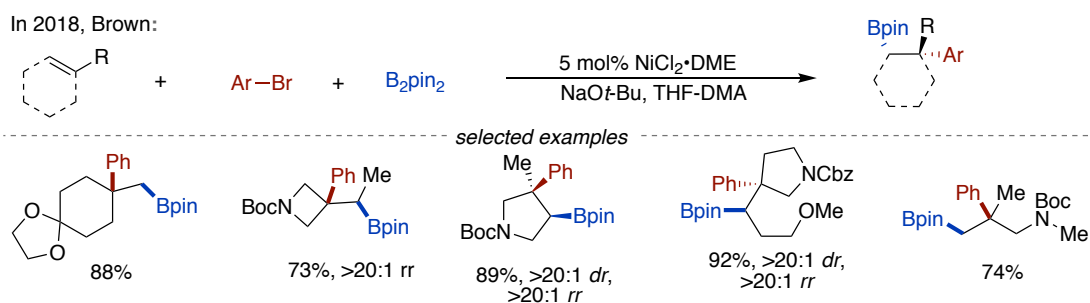
In 2017, Brown:



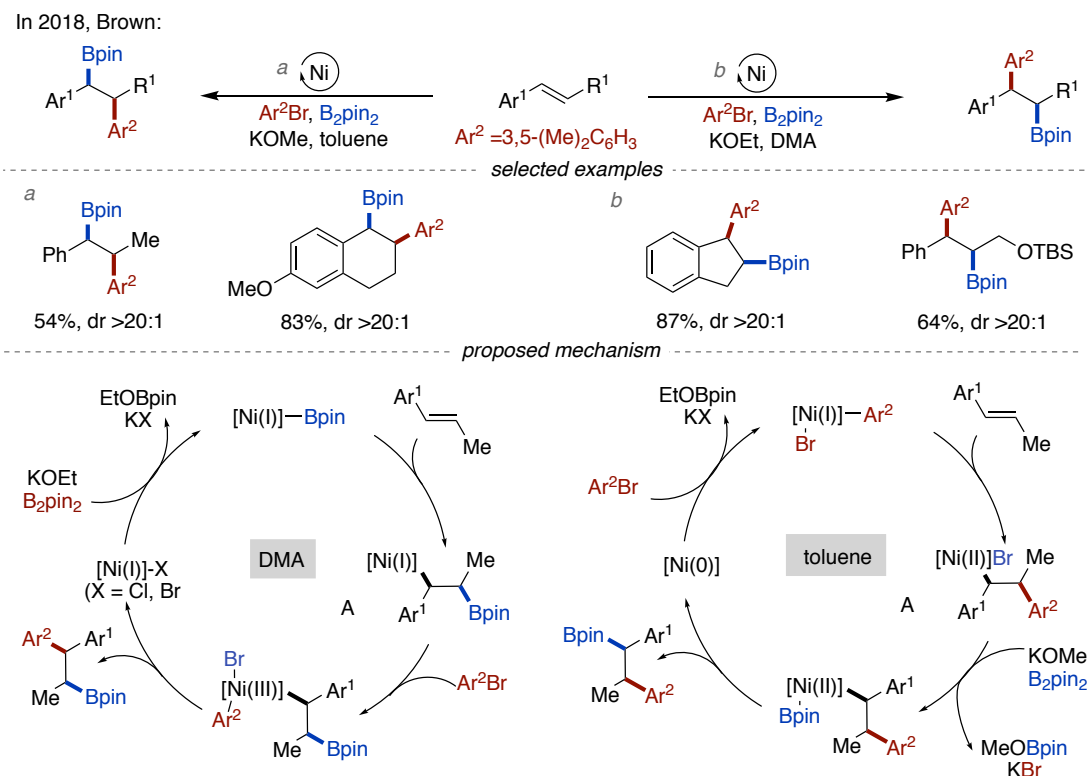
**Scheme 1.47** Ni-catalyzed 1,2-arylboration reaction of unactivated alkenes.

Later on, Brown applied nickel catalysis to create more difficult and challenging boron-substituted quaternary carbons or diarylquaternary carbons via arylation of

various trisubstituted alkenes (Scheme 1.48).<sup>158</sup> The authors suggested that DMA acts as a weakly coordinating ligand, stabilizing the alkylnickel(I) intermediate and inhibiting  $\beta$ -hydride elimination. Interestingly, the utilization of 1,2-disubstituted olefins results in a solvent-dependent regiodivergent and diastereoselective arylation without directing groups (Scheme 1.49 *top*). The authors proposed that the utilization of DMA results in the formation of a [Ni]-Bpin (Scheme 1.49 *bottom*). The phenyl-[Ni]-complex is formed by oxidative addition of ArBr followed by reductive elimination to form the product. In the case of reactions using toluene, migratory insertion is thought to occur from ArNi<sup>II</sup>Br complex which determines the regioselectivity. Then the benzyl-[Ni]-complex undergoes transmetalation with B<sub>2</sub>pin<sub>2</sub>, which is followed by reductive elimination to form the desired product.

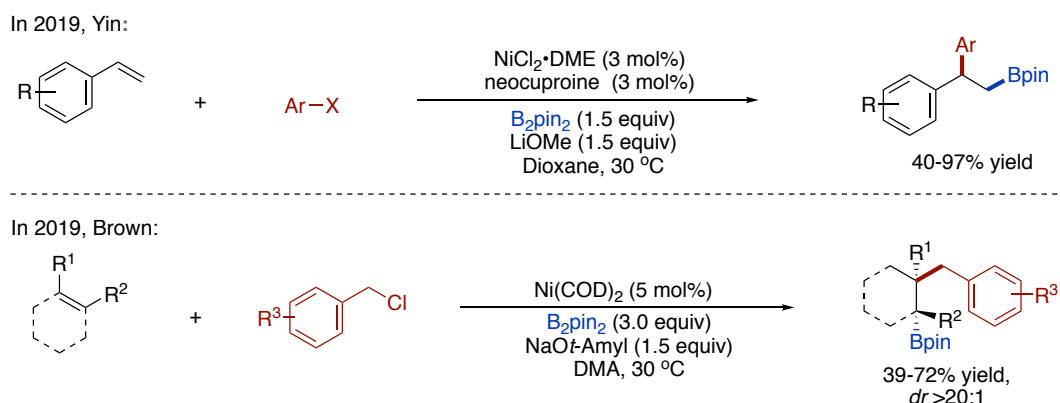


**Scheme 1.48** Ni-catalyzed arylation of various trisubstituted alkenes.



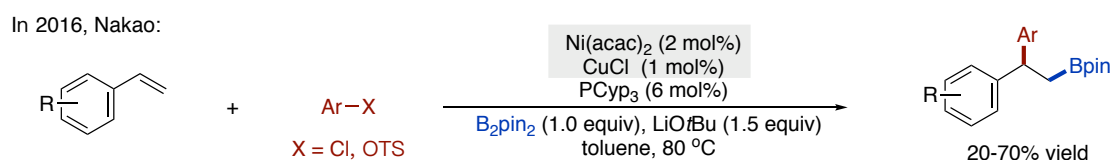
**Scheme 1.49** Solvent-dependent regiodivergent and diastereoselective arylboration.

In 2019, Yin reported a Ni-catalyzed 1,2-arylboration of vinyl arenes with a variety of aryl halides as suitable electrophiles (Scheme 1.50, *top*).<sup>159</sup> Given that nickel catalysis has been used to form C(*sp*<sup>3</sup>)-C(*sp*<sup>3</sup>) bonds by reductive elimination of dialkyl-[Ni] complexes, Brown tried to use benzyl chlorides as a source of *sp*<sup>3</sup>-architectures and succeeded in achieving the stereoselective controlled benzylation of unactivated alkenes (Scheme 1.50, *bottom*).<sup>160</sup>



**Scheme 1.50** Other Nickel-catalyzed methods for 1,2-carboboration of alkenes.

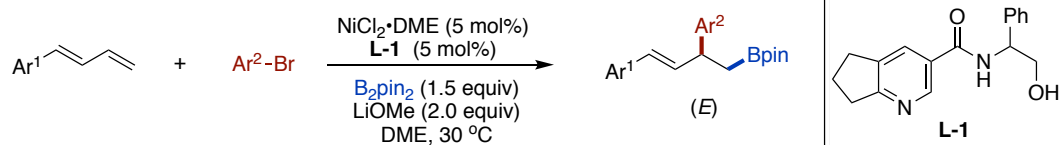
In 2016, Nakao discovered a novel catalytic system (Scheme 1.51) using a Ni/Cu cooperative catalysis to achieve the 1,2-arylboration of vinyl arenes<sup>161</sup> with aryl chlorides and tosylates, which were never used before in carboboration reactions.



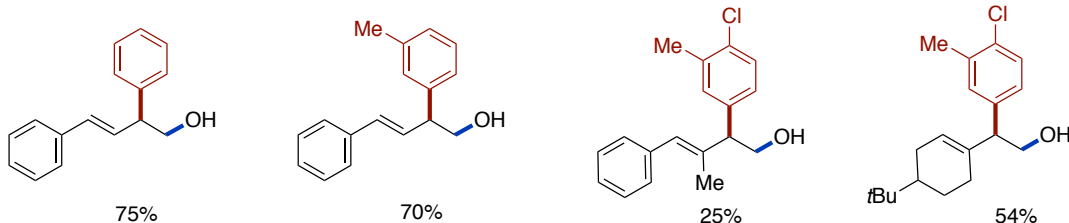
**Scheme 1.51** Ni/Cu cooperative catalyzed 1,2-arylboration of vinyl arenes.

Recently, the arylboration of conjugated dienes using nickel complexes as a catalyst was described by Yin (Scheme 1.52).<sup>162</sup> The authors used 1-arylbutadienes as substrates which showed excellent 1,2-regioselectivity and (*E*)-stereoselectivity. During their study the authors found that pyridylcarboamide-based ligands could modify the regioselectivity of the arylboration event.

In 2021, Yin:



selected examples



Note: the boron-containing products were converted to their corresponding alcohols by *in situ* oxidation of  $\text{H}_2\text{O}_2$ .

### Scheme 1.52 Ni-catalyzed arylation of conjugated dienes.

Taken together, the available nickel-catalyzed 1,2-carboborylation portfolio of  $\pi$ -systems is mainly limited to the use of electrophilic reagents such as aryl halides and benzylic halides. In addition, the development of nickel-catalyzed 1,2-alkylborylation as a platform to build up more complicated  $sp^3$  architectures remained challenging at the beginning of this doctoral thesis.

## 1.4 General Aim of This Thesis

In the past decades, transition-metal-catalysed cross-coupling processes have proven to be an effective way for forming C–C bonds in the field of modern organic chemical synthesis. While considerable success has been realized when forging  $sp^3$  C–C bonds by transition metal-catalysis, there is still ample room for further improvements. For example, while the majority of cross-coupling reactions focus on the activation of C–H bonds or carbon-heteroatom bonds, general strategies based on the functionalization of particularly strong C–C bonds still remain elusive. On the other hand, despite the advances realized in 1,2-carboboration of  $\pi$ -systems, transition metal-catalyzed construction of  $\text{C}(sp^3)\text{--C}(sp^3)$  bonds with alkyl halides as the source of  $sp^3$ -carbon centers is still challenging. These limitations are related to the reactivity of metal-boryl species and/or the instability of alkyl-metal species.

Driven by the inherent interest of Martin's group in developing metal-catalyzed coupling reactions strategies for the construction of  $sp^3$  architectures, this thesis aims at utilizing abundant and readily available feedstocks as a new manifold for forging C–C bonds via the utilization of Cu or Ni catalysts. To this end, the following objectives

---

will be pursued:

- ★ To study the merger of nickel and photoredox catalysis as a vehicle to enable the cross-coupling reaction of aliphatic alcohols and organic halides via  $sp^3$  C–C cleavage.
- ★ To explore a general and efficient protocol for the C( $sp^3$ )-trifluoromethylation of aliphatic carbonyl or alkene precursors via inert  $sp^3$  C–C bond cleavage.
- ★ To develop a nickel catalyzed 1,2-alkylboration of allenes as a tool to synthesize a variety of alkenes which will be powerful intermediates for further functionalization.

---

## 1.5 References:

1. (a) Talele, T. T. Opportunities for tapping into three-dimensional chemical space through a quaternary carbon; *J. Med. Chem.* **2020**, *63*, 13291. (b) Lovering, F.; Bikker, J.; Humblet, C. Escape from flatland: increasing saturation as an approach to improving clinical success. *J. Med. Chem.* **2009**, *52*, 6752. (c) Giordanetto, F.; Jin, C.; Willmore, L.; Feher, M.; Shaw, D. E. Fragment hits: What do they look like and how do they bind? *J. Med. Chem.* **2019**, *62*, 3381. (d) Meyers, J.; Carter, M.; Mok, N. Y.; Brown, N. On the origin of three-dimensionality in drug-like molecules. *Future Med. Chem.* **2016**, *8*, 1753.
2. For selected references, see: (a) Campeau, L.; Hazari, N. Cross-coupling and related reactions: connecting past success to the development of new reactions for the future. *Organometallics.* **2019**, *38*, 3. (b) Choi, J.; Fu, G. C. Transition metal-catalyzed alkyl-alkyl bond formation: Another dimension in cross-coupling chemistry. *Science* **2017**, *356*, 152. (c) Kaga, A.; Chiba, S. Engaging radicals in transition metal-catalyzed cross-coupling with alkyl electrophiles: recent advances. *ACS Catal.* **2017**, *7*, 4697. (d) Gu, J.; Wang, X.; Xue, W.; Gong, H.; Nickel-catalyzed reductive coupling of alkyl halides with other electrophiles: concept and mechanistic considerations. *Org.Chem. Front.* **2015**, *2*, 1411.
3. (a) Hartshorn, S. R. Aliphatic nucleophilic substitution; Cambridge University Press: London, 1973. (b) Anslyn, E. V.; Dougherty, D. A. Substitutions at aliphatic centers and thermal isomerizations/rearrangements. Modern Physical Organic Chemistry; University Science Books: Sausalito, CA, 2006; Chapter 11. (c) Fu, G. C. Transition-metal catalysis of nucleophilic substitution reactions: a radical alternative to S<sub>N</sub>1 and S<sub>N</sub>2 processes. *ACS Cent. Sci.* **2017**, *3*, 692.
4. The Nobel Prize in Chemistry 2010 - Richard F. Heck, Ei-ichi Negishi and Akira Suzuki. [https://www.nobelprize.org/nobel\\_prizes/chemistry/laureates/2010/press.pdf](https://www.nobelprize.org/nobel_prizes/chemistry/laureates/2010/press.pdf). (Accessed: 10th April 2018)
5. (a) A. C. Frisch, M. Beller, Catalysts for cross-coupling reactions with non-activated alkyl halides. *Angew. Chem. Int. Ed.* **2005**, *44*, 674. (b) Iwasaki, T.; Kambe, N. Coupling reactions between sp<sup>3</sup>-carbon centers. *Comprehensive Organic Synthesis*, **2014**, *3*, 337.
6. Rilatt, I.; Jackson, R. F. W. Kinetic studies on the stability and reactivity of α-amino alkylzinc iodides derived from amino Acids. *J. Org. Chem.* **2008**, *73*, 8694.



- 
7. Jana, R.; Pathak, T. P.; Sigman, M. S. Advances in transition metal (Pd, Ni, Fe)-catalyzed cross-coupling reactions using alkyl-organometallics as reaction partners. *Chem. Rev.* **2011**, *111*, 1417.
  8. (a) Weix, J.D. Methods and mechanisms for cross-electrophile coupling of  $Csp^2$  halides with Alkyl Electrophiles. *Acc. Chem. Res.* **2015**, *48*, 1767. (b) Hu, X. Nickel-catalyzed cross-coupling of non-activated alkyl halides: a mechanistic perspective. *Chem. Sci.* **2011**, *2*, 1867.
  9. For selected reviews on C–O cleavage: (a) Zeng, H.; Qiu, Z.; Dominguez-Huerta, A.; Hearne, Z.; Chen, Z.; Li, C. J. An Adventure in sustainable cross-coupling of phenols and derivatives via carbon–oxygen bond cleavage. *ACS Catal.* **2017**, *7*, 510. (b) Zarate, C.; Van Gemmeren, M.; Somerville, R. J.; Martin, R. Phenol derivatives: Modern electrophiles in cross-coupling Reactions. *Adv. Organomet. Chem.* **2016**, *66*, 143. (c) Tobisu, M.; Chatani, N. Cross-couplings using aryl ethers via C–O bond activation enabled by nickel catalysts. *Acc. Chem. Res.* **2015**, *48*, 1717. (d) Tollefson, E. J.; Hanna, L. E.; Jarvo, E. R. Stereospecific nickel-catalyzed cross-coupling reactions of benzylic ethers and esters. *Acc. Chem. Res.* **2015**, *48*, 2344.
  10. For selected reviews: (a) Kong, Duanyang.; Moon, P. J.; Lundgren, R. J. Radical coupling from alkyl amines. *Nature Catalysis* **2019**, *2*, 473. (b) Correia, J. T. M.; Fernandes, V. A.; Matsuo, B. T.; Delgado, J. A. C.; de Souza, W. C., Paixão, W. Photoinduced deaminative strategies: Katritzky salts as alkyl radical precursors. *Chem. Commun.* **2020**, *56*, 503. For selected examples of catalytic deamination of alkyl amines: (c) Plunkett, S.; Basch, C. H.; Santana, S. O.; Watson, M. P. *J. Am. Chem. Soc.* **2019**, *141*, 2257. (d) R. Martin-Montero, V. R. Yatham, H. Yin, R. Martin, Ni-catalyzed reductive deaminative arylation at  $sp^3$  carbon centers. *Org. Lett.* **2019**, *21*, 2947.
  11. For selected reviews: (a) Davies, H. M. L.; Morton, D. Recent advances in C–H functionalization. *J. Org. Chem.* **2016**, *81*, 343. (b) Chen, Z.; Rong, M-Y.; Nie, J.; Zhu, X-F.; Shi, B-F.; Ma, J-A. Catalytic alkylation of unactivated  $C(sp^3)$ –H bonds for  $C(sp^3)$ – $C(sp^3)$  bond formation. *Chem.Soc.Rev.* **2019**, *48*, 4921. (c) Campos, K. R. Direct  $sp^3$  C–H bond activation adjacent to nitrogen in heterocycles. *Chem. Soc. Rev.* **2007**, *36*, 1069. (d) Zhang, F-L, Hong, K.; Li, T-J.; Park, H.; Yu, J-Q. Functionalization of  $C(sp^3)$ –H bonds using a transient directing group. *Science* **2016**, *351*, 252.
  12. For authoritative reviews on C–C cleavage aided by transition metal complexes,

- 
- see:(a) Ruhland, K. Transition-metal-mediated cleavage and activation of C–C single bonds. *Eur. J. Org. Chem.* **2012**, 2012, 2683. (b) Murakami, M.; Ishida, N. Potential of metal-catalyzed C–C single bond cleavage for organic synthesis. *J. Am. Chem. Soc.* **2016**, 138, 13759. (c) Chen, P.; Billet, B.; Tsukamoto, T.; Dong, G. “Cut and Sew” transformations via transition-metal-catalyzed carbon–carbon bond activation. *ACS Catal.* **2017**, 7, 1340. (d) Fumagalli, G.; Stanton, S.; Bower, J. F. Recent methodologies that exploit C–C single-bond cleavage of strained ring systems by transition metal complexes. *Chem. Rev.* **2017**, 117, 9404. (e) Wang, B.; Perea, M. A.; Sarpong, R. Transition metal-mediated C–C single bond cleavage: making the cut in total synthesis. *Angew. Chem., Int. Ed.* **2020**, 59, 18898. (f) Chen, F.; Wang, C.; Jiao, N. Recent advances in transition-metal-catalyzed functionalization of unstrained carbon–carbon bonds. *Chem. Rev.* **2014**, 114, 8613.
13. For selected reviews: (a) Beller, M.; Seayad, J.; Tillack, A.; Jiao, H. Catalytic Markovnikov and anti-Markovnikov functionalization of alkenes and alkynes: recent developments and trends. *Angew. Chem., Int. Ed.* **2004**, 43, 3368. (b) Zhang, J.-S.; Liu, L.; Chen, T.; Han, L.-B. Transition-metal-catalyzed three-component difunctionalizations of alkenes. *Chem.-Asian J.* **2018**, 13, 2277. (c) Giri, R.; Kc, S. Strategies toward dicarbofunctionalization of unactivated olefins by combined Heck carbometalation and cross-coupling. *J. Org. Chem.* **2018**, 83, 3013. (d) Wickham, L. M.; Giri, R. Transition metal (Ni, Cu, Pd)-catalyzed alkene dicarbofunctionalization reactions. *Acc. Chem. Res.* **2021**, 54, 3415. (e) Yin, G.; Mu, X.; Liu, G. Palladium(II)-catalyzed oxidative difunctionalization of alkenes: bond forming at a high-valent palladium center. *Acc. Chem. Res.* **2016**, 49, 2413.
14. For selected reviews: (a) Suginome, M. Catalytic carboborations. *Chem. Rec.* **2010**, 10, 348. (b) Zhen Liu, Z.; Gao, Y.; Zeng, T.; Engle, K. M. Transition-metal-catalyzed 1,2-carboboration of alkenes: strategies, mechanisms, and stereocontrol. *Isr. J. Chem.* **2020**, 60, 219. (c) Shimizu, Y.; Kanai, M.; *Tetrahedron Lett.* **2014**, 55, 3727..
15. (a) Pelter, K.; Smith, A.; Brown, H. C. Borane Reagents.: Best synthetic methods. Academic Press, New York **1988**. (b) Boronic Acids: Preparation and applications in organic synthesis medicine and materials (Ed.: D. G. Hall), Wiley-VCH, Weinheim, **2011**.
16. (a) Miyaura, N.; Suzuki, A. Palladium-catalyzed cross-coupling reactions of organoboron compounds. *Chem. Rev.* **1995**, 95, 2457. (b) Sanford, C.; Aggarwal, V.

- 
- K. Stereospecific functionalizations and transformations of secondary and tertiary boronic esters. *Chem. Commun.* **2017**, 53, 5481.
17. (a) Rybtchinski, B.; Milstein, D. Metal insertion into C–C bonds in solution. *Angew. Chem., Int. Ed.* **1999**, 38, 870. (b) Souillart, L.; Cramer, N. Catalytic C–C bond activations via oxidative addition to transition metals. *Chem. Rev.* **2015**, 115, 9410. (c) O'Reilly, M. E., Dutta, S.; Veige, A. S.  $\beta$ -Alkyl elimination: fundamental principles and some applications. *Chem. Rev.* **2016**, 116, 8105. (c) Dong, G. C–C bond activation. Springer: Berlin, **2014**, Topics in Current Chemistry 346. (d) Dermenci, A.; Coe, J. W.; Dong, G. Direct activation of relatively unstrained carbon–carbon bonds in homogeneous systems. *Org. Chem. Front.* **2014**, 1, 567. (e) Jones, W. D. The fall of the C–C bond. *Nature*. **1993**, 364, 676. (f) Murakami, M.; Matsuda, T. Metal-catalysed cleavage of carbon–carbon bonds. *Chem. Commun.* **2011**, 47, 1100. (g) Jun, C-H. Transition metal-catalyzed carbon–carbon bond activation. *Chem. Soc. Rev.* **2004**, 33, 610. (h) Murakami, M.; Amii, H.; Ito, Y. Selective activation of carbon–carbon bonds next to a carbonyl group. *Nature* **1994**, 370, 540.
18. (a) Negi, H.; Verma, P.; Singh, R. K. A comprehensive review on the applications of functionalized chitosan in petroleum industry. *Carbohydrate Polymers.* **2021**, 266, 118125. (b) Matar, S.; Hatch, L. F. Crude oil processing and production of hydrocarbon intermediates. *In Chemistry of Petrochemical Processes*, **2001**, 49, 110.
19. (a) Zakzeski, J.; Bruijninx, P. C. A.; Jongerius, A. L.; Weckhuysen, B. M. The Catalytic valorization of lignin for the production of renewable chemicals. *Chem. Rev.* **2010**, 110, 3552. (b) Gallezot, P. Process options for converting renewable feedstocks to bioproducts. *Green Chem.*, **2007**, 9, 295. (c) Jambeck, J. R.; Geyer, R.; Wilcox, C.; Siegler, T. R.; Perryman, M.; Andrady, A.; Narayan, R.; Law, K. L. Plastic Waste Inputs from Land into the Ocean. *Science* **2015**, 347, 768–771.
20. (a) Trost, B. The Atom Economy—a search for synthetic efficiency. *Science* **1991**, 254, 1471. (b) Trost, B. M. Atom economy—a challenge for organic synthesis: homogeneous catalysis leads the way. *Angew. Chem., Int. Ed.* **1995**, 34, 259.
21. Miura, M.; Satoh, T. Catalytic processes involving  $\beta$ -carbon elimination. in palladium in organic synthesis; Springer: Berlin, Heidelberg, **2005**; pp 1–20.
22. Halpern, J. Determination and significance of transition-metal-alkyl bond dissociation energies. *Acc. Chem. Res.* **1982**, 15, 238.
23. Blanksby, S. J.; Ellison, G. B. Bond dissociation energies of organic molecules. *Acc.*

---

*Chem. Res.* **2003**, *36*, 255.

24. (a) Neufeldt, S. R.; Sanford, M. S. Controlling site selectivity in palladium-catalyzed C–H bond functionalization. *Acc. Chem. Res.* **2012**, *45*, 936. (b) Park, Y. J.; Park, J-W.; Jun, C-H. Metal-organic cooperative catalysis in C–H and C–C bond activation and its concurrent recovery. *Acc. Chem. Res.* **2008**, *41*, 2, 222. (c) Nairoukh, Z.; Cormier, M.; Marek, I. Merging C–H and C–C bond cleavage in organic synthesis. *Nat. Rev. Chem.* **2017**, *1*, 0035.
25. Lutz, M. D. R.; Morandi, B. . Metal-catalyzed carbon–carbon bond cleavage of unstrained alcohols. *Chem. Rev.* **2021**, *121*, 300.
26. (a) Murakami, M.; Ito, Y. cleavage of carbon–carbon single bonds by transition metals. In activation of unreactive bonds and organic synthesis; Springer: Heidelberg, **1999**; *18*, 97. (b) Murakami, M. Cleavage of carbon-carbon single bonds by transition metals, Wiley-VCH Verlag GmbH & Co. KGaA: Weinheim, Germany, **2015**.
27. (a) Weyerstahl, P.; Marschall, H. 5.4-Fragmentation reactions. *comprehensive organic synthesis.* **1991**, *6*, 1041. (b) Drahl, M. A.; Manpadi, M.; Williams, L. J. C–C fragmentation: origins and recent applications. *Angew Chem Int Ed.* **2013**, *52*, 11222.
28. Eschenmoser, A.; Frey, A. Über die Spaltung des Mesylesters von 2-Methyl-2-oxymethyl-cyclopentanon mit Basen. *Helv.Chim.Acta.* **1952**, *35*, 1660.
29. Spangler, C. W. Thermal [1,j] sigmatropic rearrangements. *Chem. Rev.* **1976**, *76*, 187.
30. Kaur, K.; Srivastava, S. Beckmann rearrangement catalysis: a review of recent advances. *New J. Chem.* **2020**, *44*, 18530.
31. Zhang, S-Lin.; Yu Z-L. C–C activation by Retro-Aldol reaction of two  $\beta$ -hydroxy carbonyl compounds: synergy with Pd-catalyzed cross-coupling to access mono- $\alpha$ -arylated ketones and esters. *J. Org. Chem.* **2016**, *81*, 57.
32. (a) Kondo, T.; Mitsudo, T. Ruthenium-catalyzed reconstructive synthesis of functional organic molecules via cleavage of carbon–carbon bonds. *Chem. Lett.* **2005**, *34*, 1462. (b) Song, F.; Gou, T.; Wang, B.-Q.; Shi, Z.-J. Catalytic activations of unstrained C–C bond involving organometallic intermediates. *Chem. Soc. Rev.* **2018**, *47*, 7078 (c) Kondo, T. Ruthenium- and Rhodium-catalyzed strain-driven cleavage and reconstruction of the C–C Bond. *Eur. J. Org. Chem.* **2016**, *2016*, 1232.
33. Yorimitsu, H. Retro-Allylation and Deallylation. In cleavage of carbon–carbon

- 
- single bonds by transition metals; Murakami, M., Ed.; Wiley-VCH Verlag GmbH & Co. KGaA: Weinheim, Germany, 2015; pp 165–192.
34. (a) Yu, X-Y.; Chen, J-R.; Xiao, W-J. Visible light-driven radical-mediated C–C bond cleavage/functionalization in organic synthesis. *Chem. Rev.* **2021**, *121*, 1, 506. (b) Morcillo, S. P. Radical-promoted C–C bond cleavage: A deconstructive approach for selective functionalization. *Angew. Chem. Int. Ed.* **2019**, *58*, 14044. (c) Sivaguru, P.; Wang, Z.; Zanoni, G.; Bi, X. Cleavage of carbon–carbon bonds by radical reactions. *Chem. Soc. Rev.*, **2019**, *48*, 2615.
35. Tipper, C. F. H. Some reactions of cyclopropane, and a comparison with the lower olefins. Part II. some platinum-cyclopropane complexes. *J. Chem. Soc.* **1955**, 713.
36. (a) Johnson, W. T. G.; Borden, W. T. Why are methylenecyclo-propane and 1-methylcyclopropene more “strained” than methyl-cyclopropane? *J. Am. Chem. Soc.* **1997**, *119*, 5930. (b) Bach, R. D.; Dmitrenko, O. Strain energy of small ring hydrocarbons. influence of C–H bond dissociation energies. *J. Am. Chem. Soc.* **2004**, *126*, 4444.
37. Vicente, R. C–C Bond cleavages of cyclopropenes: operating for selective ring-opening reactions. *Chem. Rev.* **2021**, *121*, 162.
38. (a) Brandi, A.; Cicchi, S.; Cordero, F. M.; Goti, A. Progress in the synthesis and transformations of alkylidenecyclopropanes and alkylidenecyclobutanes. *Chem. Rev.* **2014**, *114*, 15, 7317. (b) Nakamura, I.; Yamamoto, Y. Transition metal-catalyzed reactions of methylenecyclopropanes. *Adv. Synth. Catal.* **2002**, *344*, 111.
39. Wang, J.; Blaszczyk, S. A.; Li, X.; Tang, W. Transition metal-catalyzed selective carbon–carbon bond cleavage of vinylcyclopropanes in cycloaddition reactions. *Chem. Rev.* **2021**, *121*, 110.
40. (a) Pellissier, H. Recent developments in the [5 + 2] cyclo-addition. *Adv. Synth. Catal.* **2011**, *353*, 189. (b) Ylijoki, K. E. O.; Stryker, J. M. [5 + 2] Cycloaddition reactions in organic and natural product synthesis. *Chem. Rev.* **2013**, *113*, 2244. (c) Li, Q.; Jiang, G.-J.; Jiao, L.; Yu, Z.-X. Reaction of  $\alpha$ -Ene- vinylcyclopropanes: Type II intramolecular [5 + 2] cycloaddition or [3 + 2] cycloaddition? *Org. Lett.* **2010**, *12*, 1332.
41. Wender, P. A.; Takahashi, H.; Witulski, B. Transition metal catalyzed [5 + 2] cycloadditions of vinylcyclopropanes and alkynes: A homolog of the Diels-Alder reaction for the synthesis of seven-membered rings. *J. Am. Chem. Soc.* **1995**, *117*, 4720.

- 
42. (a) Xia, Y.; Lu, G.; Liu, P.; Dong, G. Catalytic activation of carbon–carbon bonds in cyclopentanones. *Nature* **2016**, *539*, 546. (b) Deng, L.; Dong, G. Carbon–carbon bond activation of ketones. *Trends in Chemistry*, **2020**, *2*, 183. (c) Xue, Y.; Dong, G. Deconstructive synthesis of bridged and fused rings via transition-metal-catalyzed “Cut-and-Sew” reactions of benzocyclobutenones and cyclobutanones. *Acc. Chem. Res.* **2022**, *55*, 2341.
43. (a) Potts, K. T.; Baum, J. S. Chemistry of cyclopropanones. *Chem. Rev.* **1974**, *74*, 189. (b) Krebs, A. W. New reactions of alkylidenephosphanes and their preparative uses. Part II. alkylidenephosphanes and halogen compounds. *Angew. Chem. Int. Ed.* **1965**, *77*, 10. (c) Eicher, T.; Weber, J. L. Structure and reactivity of cyclopropanones and triafulvenes. In cyclic compounds, Springer: Berlin, Heidelberg, **1975**, pp 1–109.
44. (a) Murakami, M.; Amii, H.; Shigeto, K.; Ito, Y. Breaking of the C–C bond of cyclobutanones by rhodium (I) and its extension to catalytic synthetic reactions. *J. Am. Chem. Soc.* **1996**, *118*, 8285. (b) Murakami, M.; Takahashi, K.; Amii, H.; Ito, Y. Rhodium(I)-catalyzed successive double cleavage of carbon–carbon bonds of strained spiro cyclobutanones. *J. Am. Chem. Soc.* **1997**, *119*, 9307. (c) Deng, L.; Jin, L.; Dong, G. Fused-ring formation via an intramolecular “Cut-and-Sew” reaction between cyclobutanones and alkynes. *Angew. Chem. Int. Ed.* **2018**, *57*, 2702.
45. (a) Liebeskind, L. S. Unexpected formation of novel butenolides by thermolysis of o-carboranyl substituted cyclobutenones. *Tetrahedron* **1989**, *45*, 3053. (b) Liebeskind, L. S.; Baysdon, S. L.; South, M. S.; Iyer, S.; Leeds, J. P. The development of an organotransition metal synthesis of quinones. *Tetrahedron* **1985**, *41*, 5839. (c) Liebeskind, L. S.; Leeds, J. P.; Baysdon, S. L.; Iyer, S. Convergent, high-yield, regioselective synthesis of substituted benzoquinones from maleoylcobalt complexes and alkynes. *J. Am. Chem. Soc.* **1984**, *106*, 6451.
46. (a) Huffman, M. A.; Liebeskind, L. S.; Pennington, W. T. Synthesis of metallacyclopentenones by insertion of rhodium into cyclobutenones. *Organometallics* **1990**, *9*, 2194. (b) Huffman, M. A.; Liebeskind, L. S.; Pennington, W. T. Reaction of cyclobutenones with low-valent metal reagents to form  $\eta^4$ - and  $\eta^2$ -vinylketene complexes. Reaction of  $\eta^4$ -vinylketene complexes with alkynes to form phenols. *Organometallics* **1992**, *11*, 255.
47. Li, R.; Li, B.; Zhang, H.; Ju, C-W.; Qin, Y.; Xue, X-S.; Zhao, D. A ring expansion strategy towards diverse azaheterocycles. *Nature Chemistry*, **2021**, *12*, 1006.

- 
48. Bart, S. C.; Chirik, P. J. Selective, catalytic carbon–carbon bond activation and functionalization promoted by late transition metal catalysts. *J. Am. Chem. Soc.* **2003**, *125*, 886.
49. Roundhill, D. M.; Lawson, D. N.; Wilkinson, G. New complexes derived from the interaction of dicarbonylchlororhodium(I) and tris(triphenylphosphine)chlororhodium(I) with cyclopropane, butadiene, and perfluorobutadiene. *J. Am. Chem. Soc.* **1968**, 845.
50. Shaw, M. H. Bower, J. F. Synthesis and applications of Rhodacyclopentanones derived from C–C bond activation. *Chem. Commun.* **2016**, *52*, 10817.
51. Murakami, M.; Amii, H.; Shigeto, K.; Ito, Y. Breaking of the C–C bond of cyclobutanones by Rhodium(I) and its extension to catalytic synthetic reactions. *J. Am. Chem. Soc.* **1996**, *118*, 8285.
52. (a) Shaw, M. H.; Melikhova, E. Y.; Kloer, D. P.; Whittingham, W. G.; Bower, J. F. Directing group Enhanced carbonylative ring expansions of amino-substituted cyclopropanes: Rhodium-catalyzed multicomponent synthesis of N-heterobicyclic enones. *J. Am. Chem. Soc.* **2013**, *135*, 4992. (b) Mills, L. R.; Zhou, C.; Fung, E.; Rousseaux, S. A. L. Ni-Catalyzed  $\beta$ -alkylation of cyclopropanol-derived homoenolates. *Org. Lett.* **2019**, *21*, 8805. (c) Sokolova, O. O. Bower, J. F. Selective carbon–carbon bond cleavage of cyclopropylamine derivatives. *Chem. Rev.* **2021**, *121*, 80. (d) Shaw, M. H.; McCreanor, N. G.; Whittingham, W. G. Bower, J. F. Reversible C–C bond activation enables stereocontrol in Rh-catalyzed carbonylative cycloadditions of aminocyclopropanes. *J. Am. Chem. Soc.* **2015**, *137*, 463.
53. Long, Y.; Zhou, W.; Lia, Q.; Zhou, Xi. Transition metal-catalyzed arylation of unstrained C–C single bonds. *Org. Biomol. Chem.*, **2021**, *19*, 9809.
54. (a) Miura, M.; Satoh, T. Topics in organometallic chemistry, Springer, **2005**, *14*, 1. (b) Yorimitsu, H.; Oshima, K. Catalytic processes involving  $\beta$ -Carbon Elimination. *Bull. Chem. Soc. Jpn.* 2009, *82*, 778. M. Murakami, M. Makino, S. Ashida, T. Matsuda, Construction of carbon frameworks through  $\beta$ -carbon elimination mediated by transition metals. *Bull. Chem. Soc. Jpn.* **2006**, *79*, 1315. (c) Zhu, Jun.; Xue, Yi.; Zhang, R.; Ratchford, B. L. Dong, G. Catalytic activation of unstrained C(Aryl)–C(Alkyl) bonds in 2,2'-methylenediphenols. *J. Am. Chem. Soc.* **2022**, *144*, 3242.
55. (a) Zhao, P.; Incarvito, C. D.; Hartwig, J. F. Direct observation of  $\beta$ -aryl

- 
- eliminations from Rh (I) alkoxides. *J. Am. Chem. Soc.* **2006**, *128*, 3124. (b) Zhao, P.; Hartwig, J. F. Insertions of ketones and nitriles into organorhodium(I) complexes and  $\beta$ -hydrocarbyl eliminations from Rhodium(I) alkoxo and iminyl complexes. *Organometallics* **2008**, *27*, 4749. (c) Ishida, N.; Sawano, S.; Masuda, Y.; Murakami, M. Rhodium-catalyzed ring opening of benzocyclobutenols with site-selectivity complementary to thermal ring opening. *J. Am. Chem. Soc.* **2012**, *134*, 17502. (d) Li, Y.; Lin, Z. Theoretical studies of ring-opening reactions of phenylcyclobutabenzenol and its reactions with alkynes catalyzed by Rhodium complexes. *J. Org. Chem.* **2013**, *78*, 11357. (e) Ding, L.; Ishida, N.; Murakami, M.; Morokuma, K.  $sp^3$ - $sp^2$  vs  $sp^3$ - $sp^3$  C–C site selectivity in Rh-catalyzed ring opening of benzocyclobutenol: a DFT study. *J. Am. Chem. Soc.* **2014**, *136*, 169.
56. Terao, Y.; Wakui, H.; Satoh, T.; Miura, M.; Nomura, M. Palladium-catalyzed arylative carbon–carbon bond cleavage of  $\alpha,\alpha$ -disubstituted arylmethanols. *J. Am. Chem. Soc.* **2001**, *123*, 10407.
57. Van Tamelen, E. E.; Rudler, H.; Bjorklund, C. Transition metal promoted reductive decyanation of alkyl nitriles. *J. Am. Chem. Soc.* **1971**, *93*, 7113.
58. (a) Blum, J.; Oppenheimer, E.; Bergmann, E. D. Decarbonylation of aromatic carbonyl compounds catalyzed by rhodium complexes. *J. Am. Chem. Soc.* **1967**, *89*, 2338. (b) Tsuji, J.; Ohno, K. Organic syntheses by means of noble metal compounds. Carbonylation and decarbonylation reactions catalyzed by palladium. *J. Am. Chem. Soc.* **1968**, *901*, 94. (c) O'Connor, J. M.; Ma, J. Metal-catalyzed decarbonylation of primary aldehydes at room temperature. *J. Org. Chem.* **1992**, *57*, 5075.
59. (a) Gooßen, L. J.; Rodriguez, N.; Gooßen, K. Carboxylic acids as substrates in homogeneous catalysis. *Angew. Chem., Int. Ed.* **2008**, *47*, 3100. (b) Gooßen, L. J.; Gooßen, K.; Rodriguez, N.; Blanchot, M.; Linder, C.; Zimmermann, B. New catalytic transformations of carboxylic acids. *Pure Appl. Chem.* **2008**, *80*, 1725. (c) Gooßen, L. J.; Collet, F.; Gooßen, K. Decarboxylative coupling reactions. *Isr. J. Chem.* **2010**, *50*, 617. (d) Rodriguez, N.; Goossen, L. Decarboxylative coupling reactions: a modern strategy for C–C-bond formation. *J. Chem. Soc. Rev.* **2011**, *40*, 5030.
60. Zheng, S.; Yu, C.; Shen, Z. Ethyl cyanoacetate: a new cyanating agent for the palladium-catalyzed cyanation of aryl halides. *Org. Lett.* **2012**, *14*, 3644
61. Liu, N.; Wang, Z.-X. Nickel-catalyzed cross-coupling of arene- or



- 
- heteroarene carbonitriles with aryl- or heteroarylmanganese reagents through C–CN bond activation. *Adv. Synth. Catal.* **2012**, *354*, 1641.
62. (a) Lu, T.; Zhuang, X.; Li, Y.; Chen, S. C–C bond cleavage of acetonitrile by a dinuclear copper (II) Cryptate. *J. Am. Chem. Soc.* **2004**, *126*, 4760. (b) Marlin, D. S.; Olmstead, M. M.; Mascharak, P. K. Heterolytic cleavage of the C–C bond of acetonitrile with simple monomeric Cu<sup>II</sup> complexes: Melding old copper chemistry with new reactivity. *Angew. Chem., Int. Ed.* **2001**, *40*, 4752.
63. (a) Churchill, D.; Shin, J. H.; Hascall, T.; Hahn, J. M.; Bridgewater, B. M.; Parkin, G. The Ansa effect in permethylmolybdenocene chemistry: a [Me<sub>2</sub>Si] Ansa bridge promotes intermolecular C–H and C–C bond activation. *Organometallics* **1999**, *18*, 2403. (b) Tanabe, T.; Evans, M. E.; Brennessel, W. W.; Jones, W. D. C–H and C–CN bond activation of acetonitrile and succinonitrile by [Tp’Rh(PR<sub>3</sub>)]. *Organometallics* **2011**, *30*, 834.
64. 1(a) Nakazawa, H.; Kamata, K.; Itazaki, M. Catalytic C–C bond cleavage and C–Si bond formation in the reaction of RCN with Et<sub>3</sub>SiH promoted by an iron complex. *Chem. Commun.* **2005**, *31*, 4004. (b) Itazaki, M.; Nakazawa, H. Iron-catalyzed silylcyanation of aldehydes and ketones with silyl cyanide prepared from silane and acetonitrile. *Chem. Lett.* **2005**, *34*, 1054. (c) Nakazawa, H.; Itazaki, M.; Kamata, K.; Ueda, K. Iron-complex-catalyzed C–C Bond cleavage of organonitriles: catalytic metathesis reaction between H–Si and R–CN bonds to afford R–H and Si–CN bonds. *Chem.–Asian J.* **2007**, *2*, 882. (d) Taw, F. L.; White, P. S.; Bergman, R. G.; Brookhart, M. Carbon–Carbon bond activation of R–CN (R = Me, Ar, iPr, *t*Bu) using a cationic Rh(III) complex. *J. Am. Chem. Soc.* **2002**, *124*, 4192. (e) Taw, F. L.; Mueller, A. H.; Bergman, R. G.; Brookhart, M. A mechanistic investigation of the carbon–carbon bond cleavage of aryl and alkyl cyanides using a cationic Rh (III) silyl complex. *J. Am. Chem. Soc.* **2003**, *125*, 9808.
65. Nogi, K.; Yorimitsu, Hideki. Carbon–Carbon bond cleavage at allylic positions: retro-allylation and deallylation. *Chem. Rev.* **2021**, *121*, 345.
66. (a) Jones, W. D. In C–C Bond Activation; Dong, G., Ed.; Springer:Berlin, 2014; Topics in Current Chemistry 346, pp 1–31. (b) Nakao, Y. Cleavage of Carbon–Carbon single bonds by transition metals. *Bull. Chem. Soc. Jpn.* **2012**, *85*, 731. (c) Najera, C.; Sansano, J. M. Asymmetric intramolecular carbocyanation of alkenes by C–C bond activation. *Angew. Chem., Int. Ed.* **2009**, *48*, 2452.
67. (a) Yorimitsu, H.; Oshima, K. Selective reactions based on retro-allylation of

- 
- homoallyl alcohols. *J. Synth. Org. Chem., Jpn.* **2008**, *66*, 332. (b) Yorimitsu, H.; Oshima, K. Metal-mediated retro-allylation of homoallyl alcohols for highly selective organic synthesis. *Bull. Chem. Soc. Jpn.* **2009**, *82*, 778.
68. Nilsson, Y. I. M.; Andersson, P. G.; Backvall, J-E. Example of thermodynamic control in palladium-catalyzed allylic alkylation. evidence for palladium-assisted allylic C–C bond cleavage. *J. Am. Chem. Soc.* **1993**, *115*, 6609.
69. (a) Necas, D.; Tursky, M.; Kotora, M. Catalytic deallylation of allyl- and diallylmalonates. *J. Am. Chem. Soc.* **2004**, *126*, 10222. (b) Nicas, D.; Tursky, M.; Tislerova, I.; Kotora, M. Nickel-catalyzed cyclization of  $\alpha,\omega$ -dienes: formation vs. cleavage of C–C bonds. *New J. Chem.* **2006**, *30*, 671. (c) Tursky, M.; Necas, D.; Drabina, P.; Sedlak, M.; Kotora, M. Rhodium-catalyzed deallylation of allylmalonates and related compounds. *Organometallics* **2006**, *25*, 901.
70. (a) Xie, J.; Jin, H.; A. Hashmi, S. K. The recent achievements of redox-neutral radical C–C cross-coupling enabled by visible-light. *Chem. Soc. Rev.*, **2017**, *46*, 5193. (b) Studer, A.; Curran, D. P. Catalysis of radical reactions: a radical chemistry perspective. *Angew. Chem., Int. Ed.*, **2016**, *55*, 58. (c) Plesniak, M. P.; Huang, H-M.; Procter, D. J. Radical cascade reactions triggered by single electron transfer. *Nat. Rev. Chem.*, **2017**, *1*, 0077.
71. For selected reviews on radical-mediated C–C bond cleavage: (a) Yu, X.; Chen, J.; Xiao, W.; Visible light-driven radical-mediated C–C bond cleavage/functionalization in organic synthesis. *Chem. Rev.* **2021**, *121*, 506 (b) Morcillo, S. P. Radical-promoted C–C bond cleavage: A deconstructive approach for selective functionalization. *Angew. Chem., Int. Ed.* **2019**, *58*, 14044. (c) Sivaguru, P.; Wang, Z.; Zaroni, G.; Bi, X. Cleavage of carbon–carbon bonds by radical reactions. *Chem.Soc.Rev.*, **2019**, *48*, 2615. (d) Wu, X.; Zhu, C. Recent advances in radical-mediated C–C bond fragmentation of non-strained molecules. *Chin. J. Chem.* **2018**, *37*, 171.
72. For selected reviews: (a) Zard, S. Z. Recent progress in the generation and use of nitrogen-centred radicals. *Chem. Soc. Rev.* **2008**, *37*, 1603. (b) Chen, J.-R.; Hu, X-Q.; Lu, L-Q.; Xiao, W-J. Visible light photoredox-controlled reactions of N-radicals and radical ions. *Chem. Soc. Rev.* **2016**, *45*, 2044. (c) Xiong, T.; Zhang, Q. New amination strategies based on nitrogen-centered radical chemistry. *Chem. Soc. Rev.* **2016**, *45*, 3069. (d) Nguyen, L. Q.; Knowles, R. R. Catalytic C–N bond-forming reactions enabled by proton-coupled electron transfer activation of amide N-H

- 
- bonds. *ACS Catal.* **2016**, *6*, 2894. (e) Davies, J.; Morcillo, S. P.; Douglas, J. J.; Leonori, D. Hydroxylamine derivatives as nitrogen-radical precursors in visible-light photochemistry. *Chem. - Eur. J.* **2018**, *24*, 12154. (f) Zhao, Y.; Xia, W. Recent advances in radical-based C–N bond formation via photo-/electrochemistry. *Chem. Soc. Rev.* **2018**, *47*, 2591
73. (a) Beckmann, E. To know the isonitroso compounds. *Ber. Dtsch. Chem. Ges.* **1886**, *19*, 988. (b) Szwarc, M. The determination of bond dissociation energies by pyrolytic methods. *Chem. Rev.* **1950**, *47*, 75.
74. Boivin, J.; Fouquet, E.; Zard, S. Z. Ring opening induced by iminyl radicals derived from cyclobutanones: new aspects of tin hydride cleavage of S-phenyl sulfenylimines. *J. Am. Chem. Soc.* **1991**, *113*, 1055.
75. Boivin, J.; Fouquet, E.; Zard, S. Z. A new and synthetically useful source of iminyl radicals. *Tetrahedron Lett.* **1991**, *32*, 4299.
76. Boivin, J.; Schiano, A-M.; Zard, S. Z. *Tetrahedron Lett.* **1992**, *33*, 849.
77. For selected references: (a) Yang, H-B.; Selander, N. Divergent iron-catalyzed coupling of O-Acyloximes with silyl enol ethers. *Chem. Eur. J.* **2017**, *23*, 1779. (b) Zhao, B.; Shi, Z. Copper-catalyzed intermolecular Heck-Like coupling of cyclobutanone oximes initiated by selective C–C bond cleavage. *Angew. Chem. Int. Ed.* **2017**, *56*, 12727. (c) Wang, P.; Zhao, B.; Yuan, Y.; Shi, Z. Radical-induced ring-opening and reconstruction of cyclobutanone oxime esters. *Chem. Commun.* **2019**, *55*, 1971. (d) Zhao, J-F.; Duan, X-H.; Gu, Y.-R.; Gao, P.; Guo, L-N. Iron-catalyzed decarboxylative olefination of cycloketone oxime esters with  $\alpha$ ,  $\beta$ -unsaturated carboxylic acids via C–C bond cleavage. *Org. Lett.* **2018**, *20*, 4614. (e) D. Ding, C. Wang, *ACS Catal.* **2018**, *8*, 11324 – 11329.
78. (a) Shaw, M. H.; Twilton, J.; MacMillan, D. W. C. Photoredox catalysis in organic chemistry. *J. Org. Chem.* **2016**, *81*, 6898. (b) Prier, C. K.; Rankic, D. A. MacMillan, D. W. C. Visible light photoredox catalysis with transition metal complexes: Applications in organic synthesis. *Chem. Rev.* **2013**, *113*, 5322.
79. Wang, P.; Zhao, Q.; Xiao, W-J.; Chen, J. Recent advances in visible-light photoredox-catalyzed nitrogen radical cyclization. *Green Synthesis and Catalysis.* **2020**, *1*, 42.
80. (a) Yu, X-Y.; Chen, J-R.; Wang, P. Z.; Yang, M-N.; Liang, D.; Xiao, W-J. A visible-light-driven iminyl radical-mediated C–C single bond cleavage/radical addition cascade of oxime esters. *Angew. Chem. Int. Ed.* **2018**, *57*, 738.

- 
81. Dauncey, E. M.; Morcillo, S. P.; Douglas, J. J.; Sheikh, N. S.; Leonori, D. Photoinduced remote functionalisations by iminyl radical promoted C–C and C–H bond cleavage cascades. *Angew. Chem., Int. Ed.* **2018**, *57*, 744.
82. Dauncey, E. M.; Dighe, S. U.; Douglas, J. J.; Leonori, D. A dual photoredox-nickel strategy for remote functionalization via iminyl radicals: radical ringopening-arylation, -vinylation and -alkylation cascades. *Chem. Sci.* **2019**, *10*, 7728.
83. Maity, S.; Zheng, N. A Photo touch on amines: New synthetic adventures of nitrogen radical cations. *Synlett* **2012**, *23*, 1851.
84. Morris, S. A.; Wang, J.; Zheng, N. The prowess of photogenerated amine radical cations in cascade reactions: From carbocycles to heterocycles. *Acc. Chem. Res.* **2016**, *49*, 1957.
85. Wang, J.; Zheng, N. The cleavage of a C–C Bond in cyclobutylanilines by visible-light photoredox catalysis: development of a [4 + 2] annulation method. *Angew. Chem., Int. Ed.* **2015**, *54*, 11424.
86. Wang M-M.; Waser, J. Oxidative fluorination of cyclopropylamides through organic photoredox catalysis. *Angew. Chem., Int. Ed.* **2020**, *59*, 16420.
87. A. Bhunia, A. Studer. Recent advances in radical chemistry proceeding through pro-aromatic radicals. *Chem* **2021**, *7*, 2060.
88. (a) Wang, P.; Chen, J.; Xiao, W. Hantzsch esters: an emerging versatile class of reagents in photoredox catalyzed organic synthesis. *Org. Biomol. Chem.* **2019**, *17*, 6936. (b) Milligan, J. A.; Phelan, J. P.; Badir, S. O.; Molander, G. A. Hantzsch esters as multifunctional reagents in visible-light photo-redox catalysis. *Angew. Chem., Int. Ed.* **2019**, *58*, 6152. (c) Wang, P-Z.; Chen, J-R.; Xiao, W-J. Hantzsch esters: an emerging versatile class of reagents in photoredox catalyzed organic synthesis. *Org. Biomol. Chem.* **2019**, *17*, 6936.
89. (a) Li, G.; Wu, L.; Lv, G.; Liu, H.; Fu, Q.; Zhang, X.; Tang, Z. Alkyl transfer from C–C cleavage: Replacing the nitro group of nitro-olefins. *Chem. Commun.* **2014**, *50*, 6246. (b) Chen, W.; Liu, Z.; Tian, J.; Li, J.; Ma, J.; Cheng, X.; Li, G. Building congested ketone: Substituted hantzsch ester and nitrile as alkylation reagents in photoredox catalysis. *J. Am. Chem. Soc.* **2016**, *138*, 12312.
90. van Leeuwen, T.; Buzzetti, L.; Perego, L. A.; Melchiorre, P. A redox-active nickel complex that acts as an electron mediator in photochemical giese reactions. *Angew. Chem., Int. Ed.* **2019**, *58*, 4953.
91. (a) Nakajima, K.; Nojima, S.; Sakata, K.; Nishibayashi, Y. Visible-light-mediated

- 
- aromatic substitution reactions of cyanoarenes with 4-Alkyl-1,4-dihydropyridines through double carbon-carbon bond cleavage. *ChemCatChem* **2016**, *8*, 1028. (b) Nakajima, K.; Nojima, S.; Nishibayashi, Y. Nickel- and photoredox-catalyzed cross-coupling reactions of aryl halides with 4-Alkyl-1,4-dihydropyridines as formal nucleophilic alkylation reagents. *Angew. Chem., Int. Ed.* **2016**, *55*, 14106. (c) Nakajima, K.; Guo, X.; Nishibayashi, Y. Cross-coupling reactions of alkenyl halides with 4-benzyl-1,4-dihydropyridines associated with E to Z isomerization under nickel and photoredox-catalysis. *Chem. - Asian J.* **2018**, *13*, 3653.
92. Zhang, H-H.; Zhao, J-J.; Yu, S. Enantioselective allylic Alkylation with 4-alkyl-1,4-dihydropyridines enabled by photoredox/palladium cocatalysis. *J. Am. Chem. Soc.* **2018**, *140*, 16914.
93. (a) Gutierrez-Bonet, Á.; Tellis, J.C.; Matsui, J. K.; Vara, B. A.; Molander, G. A. 1,4-Dihydropyridines as alkyl radical precursors: Introducing the aldehyde feedstock to nickel/photoredox dual catalysis. *ACS Catal.* **2016**, *6*, 8004. (b) Dumoulin, A.; Matsui, J. K.; Gutierrez-Bonet, A.; Molander, G. A. Synthesis of non-classical arylated C-saccharides through nickel/ photoredox dual catalysis. *Angew. Chem., Int. Ed.* **2018**, *57*, 6614. (c) Gutiérrez-Bonet, Á.; Remeur, C.; Matsui, J. K.; Molander, G. A. Late-Stage C–H alkylation of heterocycles and 1,4-quinones via oxidative homolysis of 1,4-Dihydropyridines. *J. Am. Chem. Soc.* **2017**, *139*, 12251. (d) Phelan, J. P.; Lang, S. B.; Sim, J.; Berritt, S.; Peat, A. J.; Billings, K.; Fan, L.; Molander, G. A. Open-air alkylation reactions in photoredox-catalyzed DNA Encoded Library Synthesis. *J. Am. Chem. Soc.* **2019**, *141*, 3723.
94. (a) Verrier, C.; Alandini, N.; Pezzetta, C.; Moliterno, M.; Buzzetti, L.; Hepburn, H. B.; Vega-Peñaloza, A.; Silvi, M.; Melchiorre, P. Direct stereoselective installation of alkyl fragments at the  $\beta$ -carbon of enals via excited iminium ion catalysis. *ACS Catal.* **2018**, *8*, 1062. (b) Goti, G.; Bieszczad, B.; Vega-Penalzoza, A.; Melchiorre, P. Stereocontrolled Synthesis of 1,4-dicarbonyl compounds by photo-chemical organocatalytic acyl radical addition to enals. *Angew. Chem., Int. Ed.* **2019**, *58*, 1213.
95. (a) Wang, X.; Li, H.; Qiu, G.; Wu, J. Substituted Hantzsch esters as radical reservoirs with the insertion of sulfur dioxide under photoredox catalysis. *Chem. Commun.* **2019**, *55*, 2062. (b) Song, Z-Y.; Zhang, C-L.; Ye, S. Visible light promoted coupling of alkynyl bromides and Hantzsch esters for the synthesis of internal alkynes. *Org. Biomol. Chem.* **2019**, *17*, 181.
96. (a) Badir, S. O.; Dumoulin, A.; Matsui, J. K.; Molander, G. A. Synthesis of reversed

- 
- C-Acyl glycosides through Ni/Photoredox dual catalysis. *Angew. Chem., Int. Ed.* **2018**, *57*, 6610. (b) Gandolfo, E.; Tang, X.; Raha Roy, S.; Melchiorre, P. Photochemical asymmetric Nickel-catalyzed acyl cross-coupling. *Angew. Chem., Int. Ed.* **2019**, *58*, 16854. (c) Alandini, N.; Buzzetti, L.; Favi, G.; Schulte, T.; Candish, L.; Collins, K.; Melchiorre, P. Amide synthesis by nickel/photoredox-catalyzed direct carbamoylation of (hetero)aryl bromides. *Angew. Chem. Int. Ed.* **2020**, *59*, 5248.
97. Chen, J.; Huang, W.; Li, Y.; Cheng, X. Visible-light-induced difluoropropargylation reaction with benzothiazoline as a reductant. *Adv. Synth. Catal.* **2018**, *360*, 1466.
98. Xu, Y.; Qi, X.; Zheng, P.; Berti, C. C.; Liu, P.; Dong, G. Deacylative transformations of ketones via aromatization-promoted C–C bond activation. *Nature* **2019**, *567*, 373.
99. (a) Li, L.; Fang, L.; Wu, W.; Zhu, J. Visible-light-mediated intermolecular radical conjugate addition for the construction of vicinal quaternary carbon centers. *Org. Lett.* **2020**, *22*, 5401. (b) Lv, X. Y.; Abrams, R.; Martin, R. Dihydroquinazolinones as adaptative C(sp<sup>3</sup>) handles in arylations and alkylations via dual catalytic C–C bond-functionalization. *Nat. Commun.* **2022**, *13*, 2394. (c) Lee, S-C.; Li, L-Y.; Tsai, Z-N.; Lee, Y-H.; Tsao, Y-T.; Huang, P-G.; Cheng, C-K.; Lin, H-B.; Chen, T-W.; Yang, C-H.; Chiu, C-C. Liao, H-H. Aromatization as an impetus to harness ketones for metallaphotoredox-catalyzed benzylation/benzoylation of (hetero)arenes. *Org. Lett.* **2022**, *24*, 85.
100. (a) Zhou, X.; Xu, Y.; Dong, G. Deacylation-aided C–H alkylative annulation through C–C cleavage of unstrained ketones. *Nature Catal.* **2021**, *4*, 703. (b) Zhou, X.; Xu, Y.; Dong, G. Olefination via Cu-mediated dehydroacylation of unstrained ketones. *J. Am. Chem. Soc.* **2021**, *143*, 20042.
101. Chen, S.; Zhu, Qi.; Cao, Y.; Li, C.; Guo, Y.; Kong, L.; Che, J.; Guo, Z.; Chen, H.; Zhang, N.; Fang, X.; Lu, J.; Luo, T. Dealkenyative Ni-catalyzed cross-coupling enabled by tetrazine and photoexcitation. *J. Am. Chem. Soc.* **2021**, *143*, 14046.
102. For selected review articles on alkoxy radicals (a) Gray, P.; Williams, A. The thermochemistry and reactivity of alkoxy radicals. *Chem. Rev.* **1959**, *59*, 239. (b) Murakami, Masahiro.; Ishida, Naoki.  $\beta$ -Scission of alkoxy radicals in synthetic transformations. *Chem. Lett.* **2017**, *46*, 1692. (c) Wu, X.; Zhu, C. Recent advances in alkoxy radical-promoted C–C and C–H bond functionalization starting from free alcohols. *Chem. Commun.* **2019**, *55*, 9747. (d) Guo, J.; Hu, A.; Zuo, Z. Photocatalytic alkoxy radical-mediated transformations. *Tet. Lett.* **2018**, *59*, 2103. (e) Jia, K.; Chen,

- 
- Y. Visible-light-induced alkoxy radical generation for inert chemical bond cleavage/functionalization. *Chem. Commun.* **2018**, *54*, 6105. (f) Tsui, E.; Wang, H.; Knowles, R. R. Catalytic generation of alkoxy radicals from unfunctionalized alcohols. *Chem. Sci.* **2020**, *11*, 11124. (g) Chang, L.; An, Qing.; Duan, L.; Feng, K.; Zuo, Z. Alkoxy radicals see the light: New paradigms of photochemical synthesis. *Chem. Rev.* **2022**, *122*, 2429.
103. (a) Warren, J. J.; Tronic, T. A.; Mayer, J. M. Thermochemistry of proton-coupled electron transfer reagents and its implications. *Chem. Rev.* **2010**, *110*, 6961. (b) Blanksby, S. J.; Ellison, G. B. Bond dissociation energies of organic molecules. *Acc. Chem. Res.*, **2003**, *36*, 255.
104. (a) Hudlicky, M. *Oxidations in Organic Chemistry*; American Chemical Society: Washington, DC, **1990**. (b) Parmeggiani, C.; Cardona, F. Transition metal based catalysts in the aerobic oxidation of alcohols. *Green Chem.* **2012**, *14*, 547.
105. J. M. Surzur, M. P. Bertrand and R. Nouguier, *Tetrahedron Lett.*, **1969**, *48*, 4197.
106. (a) Kundu, R.; Ball, Z. T. Copper-catalyzed remote sp<sup>3</sup> C–H chlorination of alkyl hydroperoxides. *Org. Lett.*, **2010**, *12*, 2460; (b) Guan, H.; Sun, S. Mao, Y.; Chen, L; Lu, R.; Huang, J.; Liu, L. *Angew. Chem., Int. Ed.*, **2018**, *57*, 11413.
107. (a) Walling, C.; Bristol, D. Delta-chloro alcohols and tetrahydrofurans from primary and secondary alkyl hypochlorites. *J. Org. Chem.*, **1972**, *37*, 3514. (b) Walling, C.; McGuinness, J. A. Positive halogen compounds. XVI. Comparison of alkoxy radicals from different sources and the role of halogen atoms in hypohalite reactions. *J. Am. Chem. Soc.* **1969**, *91*, 2053. (d) Heusler, K.; Kalvoda, J. Intramolecular free-radical reactions. *Angew. Chem., Int. Ed.* **1964**, *3*, 525.
108. (a) Beckwith, A. L. J.; Hay, B. P.; Williams, G. M. Generation of alkoxy radicals from O-alkyl benzenesulphenates. *J. Chem. Soc., Chem. Commun.* **1989**, 1202; (b) Pasto, D. J.; Cottard, F. Demonstration of the synthetic utility of the generation of alkoxy radicals by the photo-induced homolytic dissociation of alkyl 4-nitrobenzenesulfenates. *Tetrahedron Lett.* **1994**, *35*, 4303.
109. Beckwith, A. L. J.; Hay, B. P. Generation of alkoxy radicals from N-alkoxy-pyridinethiones. *J. Am. Chem. Soc.* **1988**, *110*, 4415.
110. (a) Kim, S. T.; Lee, A.; Song, Y. Facile generation of alkoxy radicals from N-alkoxyphthalimides. *Synlett*, **1998**, 471. (b) Zlotorzynska, M.; Zhai, H.; Sammis, G. M. Chemoselective oxygen-centered radical cyclizations onto silyl enol ethers. *Org.*

- 
- Lett.* **2008**, *10*, 5083. (b) Zhang, J.; Li, Y.; Zhang, F.; Hu, C.; Chen, Y. Generation of alkoxy radicals by photoredox catalysis enables selective C(sp<sup>3</sup>)-H functionalization under mild reaction conditions. *Angew. Chem., Int. Ed.* **2016**, *55*, 1872. (c) Zhang, J.; Li, Y.; Xu, R.; Chen, Y. Donor-Acceptor complex enables alkoxy radical generation for metal-free C(sp<sup>3</sup>)-C(sp<sup>3</sup>) cleavage and allylation/alkenylation. *Angew Chem Int Ed.* **2017**, *56*, 12619.
111. Robinson, C. H.; Gnoj, O.; Mitchell, A.; Wayne, R.; Townley, E.; Kabasakalian, P.; Oliveto, E. P.; Barton, D. H. R. The photolysis of organic nitrites. II. Synthesis of steroidal hydroxamic acids. *J. Am. Chem. Soc.* **1961**, *83*, 1771.
112. Freire, R.; Marrero, J. J.; Rodriguez, M. S.; Suarez, E. Synthesis of medium-sized lactones: Iodosobenzene diacetate an efficient reagent for  $\beta$ -fragmentation of alkoxy-radicals. *Tetrahedron Lett.* **1986**, *27*, 383.
113. Boto, A.; Betancor, C.; PrangØ, T.; Suarez, E. Fragmentation of alkoxy radicals: tandem.  $\beta$ -fragmentation-cycloperoxyiodination reaction. *J. Org. Chem.* **1994**, *59*, 4393.
114. Li, G-X.; Hu, X.; He, G.; Chen, G. Photoredox-mediated remote C(sp<sup>3</sup>)-H heteroarylation of free alcohols. *Chem. Sci.* **2019**, *688*, 3791.
115. Huynh, M. H. V.; Meyer, T. J. Proton-coupled electron transfer. *Chem. Rev.* **2007**, *107*, 5004.
116. (a) Schaafsma, S. E.; Steinberg, H.; Boer, T. J. Generation of  $\beta$ -keto radicals from cyclopropanol derivatives by the use of manganese (III) 2-pyridinecarboxylate as an oxidant and their reactions with olefins. *Recl. Trav. Chim. Pays-Bas* **1966**, *85*, 73. (b) Schaafsma, S. E.; Jorritsma, R.; Steinberg, H.; de Boer, T. J. Reaction of tertiary cyclopropyl silyl ethers with diethylaminosulfur trifluoride: the effects of substituents on the cleavage of the cyclopropane ring. *Tetrahedron Lett.* **1973**, *14*, 827.
117. Meyer, K.; Rocek, J. One-electron vs. two-electron oxidations. Cerium (IV) and cyclobutanol. *J. Am. Chem. Soc.* **1972**, *94*, 1209.
118. (a) Chiba, S.; Cao, Z.; El Bialy, S. A. A.; Narasaka, K. Generation of  $\beta$ -keto radicals from cyclopropanols catalyzed by AgNO<sub>3</sub>. *Chem. Lett.* **2006**, *35*, 18. (b) Zhao, H.; Fan, X.; Yu, J.; Zhu, C. Silver-catalyzed ring-opening strategy for the synthesis of  $\beta$ - and  $\alpha$ -fluorinated ketones. *J. Am. Chem. Soc.* **2015**, *137*, 3490. (c) Ren, R.; Zhao, H.; Huan, L.; Zhu, C. Manganese-catalyzed oxidative azidation of cyclobutanols: Regiospecific synthesis of alkyl azides by C-C bond cleavage.



- 
- Angew. Chem. Int. Ed.* **2015**, *54*, 12692. (d) Ren, S.; Feng, C.; Loh, T-P. Iron- or silver-catalyzed oxidative fluorination of cyclopropanols for the synthesis of  $\beta$ -fluoroketones. *Org. Biomol. Chem.* **2015**, *13*, 5105. (e) Kananovich, D. G.; Konik, Y. A.; Zubrytski, D. M.; Jarvinga, I.; Lopp, M. Simple access to  $\beta$ -trifluoromethyl-substituted ketones via copper-catalyzed ring-opening trifluoromethylation of substituted cyclopropanols. *Chem. Commun.* **2015**, *51*, 8349. (f) Wang, Y-F. Chiba, S. Mn(III)-mediated reactions of cyclopropanols with vinyl azides: synthesis of pyridine and 2-azabicyclo [3.3. 1] non-2-en-1-ol derivatives. *J. Am. Chem. Soc.* **2009**, *131*, 12570.
119. (a) Baciocchi, E.; Bietti, M.; Steenken, S. Base-catalyzed C–H deprotonation of 4-methoxybenzyl alcohol radical cations in water: evidence for a carbon-to-oxygen 1,2-H-shift mechanism. *J. Am. Chem. Soc.* **1997**, *119*, 4078. (b) Baciocchi, E.; Bietti, M.; Lanzalunga, O.; Steenken, S. Oxygen acidity of 1-aryllkanol radical cations. 4-methoxycumyloxyl radical as -C(Me)<sub>2</sub>-O–to-nucleus electron-transfer intermediate in the reaction of 4-methoxycumyl alcohol radical cation with OH. *J. Am. Chem. Soc.* **1998**, *120*, 11516. (c) Baciocchi, E.; Bietti, M.; Lanzalunga, O. Mechanistic aspects of  $\beta$ -bond-cleavage reactions of aromatic radical cations. *Acc. Chem. Res.* **2000**, *33*, 243.
120. Yayla, H. G.; Wang, H.; Tarantino, K. T.; Orbe, H. S.; Knowles, R. R. Catalytic ring-opening of cyclic alcohols enabled by PCET activation of strong O–H bonds. *J. Am. Chem. Soc.* **2016**, *138*, 10794.
121. Ota, E.; Wang, H.; Frye, N. L.; Knowles, R. R. A redox strategy for light-driven, out-of-equilibrium isomerizations and application to catalytic C–C bond cleavage reactions. *J. Am. Chem. Soc.* **2019**, *141*, 1457.
122. (a) Zhao, R.; Shi, L. A renaissance of ligand-to-metal charge transfer by cerium photocatalysis. *Org. Chem. Front.* **2018**, *5*, 3018. (b) Juliá, F. Ligand-to-Metal Charge Transfer (LMCT) photochemistry at 3d-metal complexes: An emerging tool for sustainable organic synthesis. *ChemCatChem* **2022**, doi.org/10.1002/cctc.202200916.
123. (a) Griesbeck, A. G.; Hoffmann, N.; Warzecha, K. Photoinduced-electron-transfer chemistry: from studies on PET processes to applications in natural product synthesis. *Acc. Chem. Res.* **2007**, *40*, 128. (b) Oelgemöllera, M.; Griesbeck, A.G. Photoinduced electron transfer chemistry of phthalimides: an efficient tool for C–C-bond formation. *Journal of Photochemistry and Photobiology C: Photochemistry*

- 
- Reviews*. **2002**, *3*, 109. (c) Mattay, J. Photoinduced electron transfer in organic synthesis. *Synthesis* **1989**; *1989*, 233.
124. (a) Hammes-Schiffer, S. Introduction: Proton-coupled electron transfer. *Chem. Rev.* **2010**, *110*, 6937. (b) Hoffmann, N. Proton-coupled electron transfer in photoredox catalytic reactions. *Eur. J. Org. Chem.* **2017**, *2017*, 1982. (c)
125. (a) Guo, J-J.; Hu, A.; Chen, Y.; Sun, J.; Tang, H.; Zuo, Z. Photocatalytic C–C bond cleavage and amination of cycloalkanols by cerium (III) chloride complex. *Angew. Chem. Int. Ed.* **2016**, *55*, 15319. (b) Hu, A.; Chen, Y.; Guo, J-J.; Yu, An, N. Q.; Zuo, Z. Cerium-catalyzed formal cycloaddition of cycloalkanols with alkenes through dual photoexcitation. *J. Am. Chem. Soc.* **2018**, *140*, 13580. (c) Zhao, R.; Shi, L.; A renaissance of ligand-to-metal charge transfer by cerium photocatalysis. *Org. Chem. Front.* **2018**, *5*, 3018. (d) Yin, H. Carroll, P. J.; Anna, J. M.; Schelter, E. J. Luminescent Ce (III) complexes as stoichiometric and catalytic photoreductants for halogen atom abstraction reactions. *J. Am. Chem. Soc.* **2015**, *137*, 9234. (e) Yin, H.; Carroll, P. J.; Manor, B. C.; Anna, J. M.; Schelter, E. J. Cerium photosensitizers: structure–function relationships and applications in photocatalytic aryl coupling reactions. *J. Am. Chem. Soc.* **2016**, *138*, 5984. (f) Hu, A.; Guo, J-J.; Pan, H.; Zuo, Z. *Science* **2018**, *361*, 668. (g) Li, Z.; Wang, X.; Xia, S.; Jin, J. Ligand-accelerated iron photocatalysis enabling decarboxylative alkylation of heteroarenes. *Org. Lett.* **2019**, *21*, 4259.
126. Zhang, K.; Chang, L.; An, Q.; Wang, X.; Zuo, Z. Dehydroxymethylation of alcohols enabled by cerium photocatalysis. *J. Am. Chem. Soc.* **2019**, *141*, 10556.
127. Xue, T.; Zhang, Z.; Zeng, R. Photoinduced ligand-to-metal charge transfer (LMCT) of Fe alkoxide enabled C–C bond cleavage and amination of unstrained cyclic alcohols. *Org. Lett.* **2022**, *24*, 977.
128. Liu, W.; Wu, Q.; Wang, M.; Huang, Yahao.; Hu, P. Iron-catalyzed C–C single-bond cleavage of alcohols. *Org. Lett.* **2021**, *23*, 8413.
129. Chen, Y.; Wang, X.; He, X.; An, Q.; Zuo, Z. Photocatalytic dehydroxymethylative arylation by synergistic cerium and nickel catalysis. *J. Am. Chem. Soc.* **2021**, *143*, 4896.
130. (a) Gooßen, L. J.; Rodriguez, N.; Gooßen, K. Carboxylic acids as substrates in homogeneous catalysis. *Angew. Chem. Int. Ed.* **2008**, *47*, 3100. (b) Uemura, S.; Tanaka, M.; Okano, M.; Hamana, M. Decarboxylative ipso halogenation of mercury (II) pyridinecarboxylates. Facile formation of 3-iodo- and 3-bromopyridines. *J. Org.*

- 
- Chem.* **1983**, *48*, 3297. (c) McKillop, A.; Bromley, D.; Taylor, E. C. Thallium in organic synthesis. VI. Synthesis of primary aliphatic bromides. *J. Org. Chem.* **1969**, *34*, 1172.
131. For selected reviews on Decarboxylation: (a) Rodriguez, N.; Goossen, L. J. Decarboxylative coupling reactions: a modern strategy for C–C-bond formation. *Chem. Soc. Rev.* **2011**, *40*, 5030. (b) Zeng, Z.; Feceu, A.; Sivendran, N.; Gooßen, L. J. Decarboxylation-initiated intermolecular carbon-heteroatom bond formation. *Adv. Synth. Catal.* **2021**, *363*, 2678. (c) Weaver, J. D.; Recio, A.; Grenning, A. J. J.; Tunge, A. Transition metal-catalyzed decarboxylative allylation and benzylation reactions. *Chem. Rev.* **2011**, *111*, 1846. (d) Konev, M. O.; Jarvo, E. R. Decarboxylative alkyl–alkyl cross-coupling reactions. *Angew. Chem. Int. Ed.* **2016**, *55*, 11340. (e) Xuan, J.; Zhang, Z-G. Xiao, W-J. Visible-light-induced decarboxylative functionalization of carboxylic acids and their derivatives. *Angew. Chem. Int. Ed.* **2015**, *54*, 15632. (f) Jin, Y.; Fu, H. Visible-light photoredox decarboxylative couplings. *Asian J. Org. Chem.* **2017**, *6*, 368.
132. (a) Na, C. G.; Ravelli, D.; Alexanian, E. J. Direct decarboxylative functionalization of carboxylic acids via O–H hydrogen atom transfer. *J. Am. Chem. Soc.* **2020**, *142*, 44. (b) Mao, R.; Bera, S.; Turla, A. C. Hu, X. Copper-catalyzed intermolecular functionalization of unactivated C(sp<sup>3</sup>)–H bonds and aliphatic carboxylic acids. *J. Am. Chem. Soc.* **2021**, *143*, 14667.
133. Zuo, Z-W.; Ahneman, D. T.; Chu, L-L.; J. Terrett, A.; Doyle, A. G. MacMillan, D. W. C. *Science* **2014**, *345*, 437.
134. (a) Qin, T.; Cornella, J.; Li, C. L.; Malins, R.; Edwards, J. T.; Kawamura, S. Maxwell, B. D.; Eastgate, M. D.; Baran, P. S. *Science* **2016**, *352*, 801. (b) Cornella, J.; Edwards, J. T.; Qin, T.; Kawamura, S.; Wang, J.; Pan, C-M.; Gianatassio, R. M.; Schmidt, A.; Eastgate, M. D. Baran, P. S. Practical Ni-catalyzed aryl–alkyl cross-coupling of secondary redox-active esters. *J. Am. Chem. Soc.* **2016**, *138*, 2174.
135. (a) Schnermann, M. J.; Overman, L. E. A concise synthesis of (–)-aplyviolene facilitated by a strategic tertiary radical conjugate addition. *Angew. Chem. Int. Ed.* **2012**, *51*, 9576. (b) Lackner, G. L.; Quasdorf, K. W.; Overman, L. E. Direct construction of quaternary carbons from tertiary alcohols via photoredox-catalyzed fragmentation of tert-alkyl N-phthalimidoyl lxalates. *J. Am. Chem. Soc.* **2013**, *135*, 15342.
136. (a) Patra, T.; Mukherjee, S.; Ma, J.; Strieth-Kalthoff, F.; Glorius, Frank.

- 
- Visible-light-photosensitized aryl and alkyl decarboxylative functionalization reactions. *Angew. Chem. Int. Ed.* **2019**, *131*, 10624. (b) Yang, J.; Zhang, J.; Qi, L. Hu, C. Chen, Y. Visible-light-induced chemoselective reductive decarboxylative alkylation under biomolecule-compatible conditions. *Chem. Commun.* **2015**, *51*, 5275. (c) Huihui, K. M.; Caputo, M. J. A.; Melchor, Z.; Olivares, A. M.; Spiewak, A. M.; Johnson, K. A.; DiBenedetto, T. A.; Kim, S.; Ackerman, L. K.; Weix, G. D. Decarboxylative cross-electrophile coupling of N-hydroxyphthalimide esters with aryl iodides. *J. J. Am. Chem. Soc.* **2016**, *138*, 5016. (d) Yi, X.; Mao, R.; Lavrencic, L.; Hu, X. Photocatalytic decarboxylative coupling of aliphatic N-hydroxyphthalimide esters with polyfluoroaryl nucleophiles. *Angew. Chem. Int. Ed.* **2021**, *60*, 23557.
137. (a) Wu, X.; Wu, S.; Zhu, C. Radical-mediated difunctionalization of unactivated alkenes through distal migration of functional groups. *Tetrahedron Lett.* **2018**, *59*, 1328. (b) Zeng, Y.; Ni, C.; Hu, J. Recent advances in the one-step synthesis of distally fluorinated ketones. *Chem. - Eur. J.* **2016**, *22*, 3210. (c) Weng, W-Z.; Zhang, B. Recent advances in the synthesis of  $\beta$ -functionalized ketones by radical-mediated 1,2-rearrangement of allylic alcohols. *Chem. - Eur. J.* **2018**, *24*, 10934. (d) Chen, Z-M.; Zhang, X-M.; Tu, Y-Q. Radical aryl migration reactions and synthetic applications. *Chem. Soc. Rev.* **2015**, *44*, 5220. (e) Li, W.; Xu, W.; Xie, J.; Yu, S.; Zhu, C. Distal radical migration strategy: an emerging synthetic means. *Chem. Soc. Rev.* **2018**, *47*, 654.
138. (a) Zheng, Y.; Tice, C. M.; Singh, S. B. The Use of spirocyclic scaffolds in drug discovery. *Bioorg. Med. Chem. Lett.* **2014**, *24*, 3673. (b) Walczak, M.; Krainz, A. A.; Wipf, T. P. Ring-strain-enabled reaction discovery: New heterocycles from bicycle [1.1.0] butanes. *Acc. Chem. Res.* **2015**, *48*, 1149. (c) Gianatassio, R.; Lopchuk, J. M.; Wang, J.; Pan, C-M.; Malins, L. R.; Prieto, L.; Brandt, T. A.; Collins, M. R.; Gallego, G. M.; Sach, N. W.; Spangler, J. E.; Zhu, H.; Zhu, J.; Baran, P. S. Strain-Release Amination. Strain-release amination. *Science* **2016**, *351*, 241. (d) Anderson, J. M. Measom, N. D.; Murphy, J. A.; Poole, D. L. Bridge functionalisation of bicycle [1.1.1] pentane derivatives. *Angew. Chem. Int. Ed.* **2021**, *60*, 24754.
139. For selected reviews: (a) Suginome, M. Catalytic carboborations. *Chem. Rec.* **2010**, *10*, 348. (b) Shimizu, Y.; Kanai, M. Recent progress in copper-catalyzed difunctionalization of unactivated carbon-carbon multiple bonds. *Tetrahedron Lett.*

- 
- 2014**, *55*, 3727. (c) Semba, K.; Fujihara, T.; Terao, J.; Tsuji, Y. Copper-catalyzed borylative transformations of non-polar carbon–carbon unsaturated compounds employing borylcopper as an active catalyst species. *Tetrahedron* **2015**, *71*, 2183. (d) Neeve, E. C.; Geier, S. J.; Mkhaliid, I. A. I.; Westcott, S. A.; Marder, T. B. Diboron compounds: From structural curiosity to synthetic workhorse. *Chem. Rev.* **2016**, *116*, 9091. (e) Hemming, D.; Fritzemeier, R.; Westcott, S. A.; Santos, W. L.; Steel, P. G. Copper-boryl mediated organic synthesis. *Chem. Soc. Rev.* **2018**, *47*, 7477. (f) Lazreg, F.; Nahra, F.; Cazin, C. S. J. Coord. Copper–NHC complexes in catalysis. *Chem. Rev.* **2015**, *48*, 293. (g) Radomkit, S.; Liu, Z.; Closs, A.; Mikus, M. S.; Hoveyda, A. H. Practical, efficient, and broadly applicable synthesis of readily differentiable vicinal diboronate compounds by catalytic three-component reactions. *Tetrahedron* **2017**, *73*, 5011. (h) Cuenca, A. B.; Shishido, R.; Ito, H.; Fernandez, E. *Chem.Soc.Rev.* **2017**, *46*, 415. (i) Liu, Z.; Gao, Y.; Zeng, T.; Engle K. M. *Isr. Transition-metal-catalyzed 1,2-carboboration of alkenes: Strategies, mechanisms, and stereocontrol. Isr. J. Chem.* **2020**, *60*, 219
140. For selected researchs: (a) Ito, H.; Kosaka, Y.; Nonoyama, K.; Sasaki, Y.; Sawamura, M. Synthesis of optically active boron–silicon bifunctional cyclopropane derivatives through enantioselective copper(I)-catalyzed reaction of allylic carbonates with a diboron derivative. *Angew. Chem., Int. Ed.* **2008**, *47*, 7424. (b) Ito, H.; Toyoda, T.; Sawamura, M. Stereospecific synthesis of cyclobutylboronates through copper(I)-catalyzed Reaction of homoallylic sulfonates and a diboron derivative. *J. Am. Chem. Soc.* **2010**, *132*, 5990. (c) Kubota, K.; Yamamoto, E.; Ito, H. Copper(I)-catalyzed borylative exo-cyclization of alkenyl halides containing unactivated double bond. *J. Am. Chem. Soc.* **2013**, *135*, 2635. (d) Yoshida, H.; Kageyuki, I.; Takaki, K. Copper-catalyzed three-component carboboration of alkynes and alkenes. *Org. Lett.* **2013**, *15*, 952. (e) Kageyuki, I.; Yoshida, H.; Takaki, K. Three-component carboboration of alkenes under copper catalysis. *Synthesis* **2014**, *46*, 1924. (f) Su, W.; Gong, T.-J.; Lu, X.; Xu, M.-Y.; Yu, C.-G.; Xu, Z.-Y.; Yu, H.-Z.; Xiao, B.; Fu, Y. Ligand-controlled regiodivergent copper-catalyzed alkylboration of alkenes. *Angew. Chem., Int. Ed.* **2015**, *54*, 12957. (g) Kageyuki, I.; Osaka, I.; Takaki, K.; Yoshida, H. Copper-catalyzed B (dan)-installing carboboration of alkenes. *Org. Lett.* **2017**, *19*, 830.
141. Akira Suzuki, Organoborates in new synthetic reactions. *Acc. Chem. Res.* **1982**, *15*, 6, 178.

- 
142. (a) Y. Okuno, M. Yamashita, K. Nozaki, Borylcyanocuprate in a one-pot carboboration by a sequential reaction with an electron-deficient alkyne and an organic carbon electrophile. *Angew. Chem. Int. Ed.* **2011**, *50*, 920. (b) R. Alfaro, A. Parra, J. Alemun, J. L. García Ruano, M. Tortosa, Copper (I)-catalyzed formal carboboration of alkynes: synthesis of tri- and tetrasubstituted vinylboronates. *J. Am. Chem. Soc.* **2012**, *134*, 15165. (c) Y. Zhou, W. You, K. B. Smith, M. K. Brown, Copper-catalyzed cross-coupling of boronic esters with aryl iodides and application to the carboboration of alkynes and allenes. *Angew. Chem. Int. Ed.* **2014**, *53*, 3475.
143. For copper-palladium-cocatalyzed carboboration reaction, see: (a) Semba, K.; Nakao, Y. Arylboration of alkenes by cooperative palladium/copper catalysis. *J. Am. Chem. Soc.* **2014**, *136*, 7567. (b) Jia, T.; Cao, P.; Wang, B.; Lou, Y.; Yin, X.; Wang, M.; Liao, J. A Cu/Pd cooperative catalysis for enantioselective allylboration of alkenes. *J. Am. Chem. Soc.* **2015**, *137*, 13760.
144. (a) Yang, K.; Song, Q. Palladium-catalyzed arylboration of bicyclic alkenes. *J. Org. Chem.* **2016**, *81*, 1000. (b) Yang, K.; Song, Q. Pd-catalyzed regioselective arylboration of vinylarenes. *Org. Lett.* **2016**, *18*, 5460. (c) Liu, Z.; Ni, H.-Q.; Zeng, T.; Engle, K. M. Catalytic carbo- and aminoboration of alkenyl carbonyl compounds via five- and six-membered palladacycles. *J. Am. Chem. Soc.* **2018**, *140*, 3223. (d) Liu, Z.; Li, X.; Zeng, T.; Engle, K. M. Directed, palladium(II)-catalyzed enantioselective anti- carboboration of alkenyl carbonyl compounds. *ACS Catal.* **2019**, *9*, 3260.
145. (a) Logan, K. M.; Sardini, S. R.; White, S. D.; Brown, M. K. Nickel-catalyzed stereoselective arylboration of unactivated alkenes. *J. Am. Chem. Soc.* **2018**, *140*, 159.
146. (a) Alfaro, R.; Parra, A.; Alemun, J.; Tortosa, M. New methods in organic synthesis through copper-catalyzed borylation reactions: Stereoselective synthesis of 1, 4-diols and vinylboronates. *Synlett* **2013**, *24*, 804. (b) Nakagawa, N.; Hatakeyama, Takuji.; Nakamura, Masaharu. Iron-catalyzed diboration and carboboration of alkynes. *Chem. Eur. J.* **2015**, *21*, 4257. (c) Cade, I.; A. Ingleson, M. J. Syn-1,2-carboboration of alkynes with borenium cations. *Chem. Eur. J.* **2014**, *20*, 12874. (c) Li, Z.; Sun, J. Copper-catalyzed 1,1-boroalkylation of terminal alkynes: Access to alkenylboronates via a three-component reaction. *Org. Lett.* **2021**, *23*, 3706.
147. (a) Li, X.; Meng, F.; Torker, S.; Shi, Y.; Hoveyda, A. H. Catalytic

- 
- enantioselective conjugate additions of (pin)B-substituted allylcopper Compounds generated in situ from butadiene or isoprene. *Angew. Chem., Int. Ed.* **2016**, *55*, 9997.
- (b) Sardini, S. R.; Brown, M. K. Catalyst controlled regiodivergent arylboration of dienes. *J. Am. Chem. Soc.* **2017**, *139*, 9823.
148. (a) Pulis, A. P.; Yeung, K.; Procter, D. J. Enantioselective copper catalysed, direct functionalisation of allenes via allyl copper intermediates. *Chem. Sci.* **2017**, *8*, 5240. (b) Liu, Y.; Bandini, M. Nickel catalyzed functionalization of allenes. *Chin. J. Chem.* **2019**, *37*, 431.
149. (a) Fujihara, T.; Semba, K.; Terao, J.; Tsuji, Y. Regioselective transformation of alkynes catalyzed by a copper hydride or boryl copper species, *Catal. Sci. Technol.* **2014**, *4*, 1699. (b) Suess, A. M. Lalic, G. Copper-catalyzed hydrofunctionalization of alkynes. *Synlett*, **2016**, *27*, 116. (c) A. J. Jordan, G. Lalic and J. P. Sadighi, *Chem. Rev.*, 2016, *116*, 8318–8372; (d) Chen, J.; Guo, J.; Lu, Z. Recent advances in hydrometallation of alkenes and alkynes via the first row transition metal catalysis. *Chin. J. Chem.* **2018**, *36*, 1075.
150. Bidal, Y. D.; Lazreg, F.; Cazin, C. S. J. Copper-catalyzed regioselective formation of Tri-and tetrasubstituted vinylboronates in air. *ACS Catal.* **2014**, *4*, 1564.
151. Su, W.; Gong, T.-J.; Zhang, Q.; Zhang, Q.; Xiao, B.; Fu, Y. Ligand-controlled regiodivergent copper-catalyzed alkylboration of unactivated terminal alkynes. *ACS Catal.* **2016**, *6*, 6417.
152. Iwamoto, H.; Akiyama, S.; Hayama, K.; Ito, H. Copper (I)-catalyzed stereo- and chemoselective borylative radical cyclization of alkyl halides bearing an alkene moiety. *Org. Lett.* **2017**, *19*, 2614.
153. Ozawa, Y.; Iwamoto, H.; Ito, H. Copper(I)-catalysed regio- and diastereoselective intramolecular alkylboration of terminal allenes via allylcopper (i) isomerization. *Chem. Commun.* **2018**, *54*, 4991.
154. (a) Ito, H.; Toyoda, T.; Sawamura, M. Stereospecific synthesis of cyclobutylboronates through copper(I)-catalyzed reaction of homoallylic sulfonates and a diboron derivative. *J. Am. Chem. Soc.* **2010**, *132*, 5990. (b) Zhong, C.; Kunii, S.; Kosaka, Y.; Sawamura, M.; Ito, H. Enantioselective synthesis of trans-aryl- and heteroaryl-substituted cyclopropylboronates by copper(I)-catalyzed reactions of allylic phosphates with a diboron derivative. *J. Am. Chem. Soc.* **2010**, *132*, 11440.
155. (a) Tasker, S. Z.; Standley, E. A.; Jamison, T. F. Recent advances in homogeneous nickel catalysis. *Nature* **2014**, *509*, 299. (b) Ananikov, V. P. *ACS*

- 
- Catal.* **2015**, *5*, 1964.
156. Diccianni, J.; Lin, Qiao.; Diao, T. Mechanisms of nickel-catalyzed coupling reactions and applications in alkene functionalization. *Acc. Chem. Res.* **2020**, *53*, 906.
157. Sommer, H.; Hernandez, F. J.; Martin, Ruben.; Marek, I. Walking metals for remote functionalization. *ACS Cent. Sci.* **2018**, *4*, 153.
158. Sardini, S. R.; Lambright, A. L.; Trammel, G. L.; Omer, H. M.; Liu, P. Brown, M. K. Ni-catalyzed arylboration of unactivated alkenes: scope and mechanistic studies. *J. Am. Chem. Soc.* **2019**, *141*, 9391.
159. Wang, W.; Ding, C.; Pang, H.; Yin, G. Nickel-catalyzed 1,2-arylboration of vinylarenes. *Org. Lett.* **2019**, *21*, 3968.
160. Chen, L-A.; Lear, A. R.; Gao, P.; Brown, M. K. *Angew. Chem., Int. Ed.* **2019**, *131*, 11072.
161. Semba, K.; Ohtagaki, Y.; Nakao, Y. Arylboration of 1-arylalkenes by cooperative nickel/copper catalysis. *Org. Lett.* **2016**, *18*, 3956.
162. Li, H.; Long, J.; Li, Y.; Wang, W.; Pang, H.; Yin, G. Nickel-catalyzed regioselective arylboration of conjugated dienes. *Eur. J. Org. Chem.* **2021**, *2021*, 1424.



---

## Chapter 2

### *Dual Catalytic Strategy for Forging $sp^2-sp^3$ and $sp^3-sp^3$ Architectures via $\beta$ -Scission of Aliphatic Alcohol Derivatives*



---

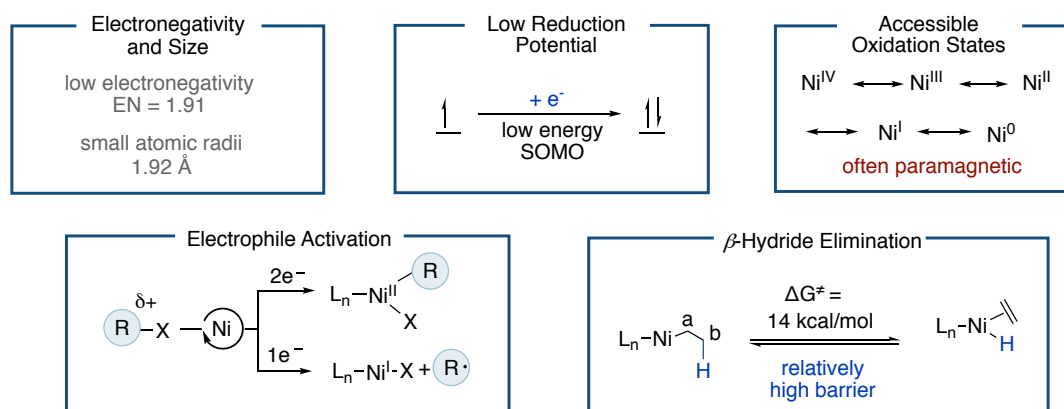
## 2.1 General Introduction

Transition-metal-catalyzed cross-coupling reactions have offered a series of innovative strategies to forge C–C bonds in the field of synthetic organic chemistry.<sup>1</sup> Not surprisingly, these techniques have received considerable echo in both academic and industrial laboratories. Conventional transition-metal-catalyzed C–C bond-forming reactions rely on the combination of an electrophile and a nucleophilic reagent, typically stoichiometric organometallic reagents such as Grignard or organozinc reagents.<sup>2</sup> Unfortunately, the latter are oftentimes particularly sensitive, require a previous synthetic procedure for their preparation and in most instances specialized techniques are mandatory for their execution, thus limiting the application profile that these platforms might have for building up  $sp^3$  carbon architectures.<sup>3</sup> In recent years, cross-electrophile coupling reactions have become a powerful alternative to nucleophilic regimes, and have attracted considerable attention due to the ready availability of electrophilic partners and the exceptional mild conditions that are used for forging  $sp^3$  architectures.<sup>3, 4-6</sup> Among different transition metals, Ni catalysts have offered interesting solutions in the field of cross-electrophile reactions and reductive coupling events.<sup>3-7</sup> The popularity of Ni is partially ascribed to its low electronegativity and reduction potentials, making it particularly suited for promoting facile oxidative addition and single-electron transfer processes, giving access to multiple oxidation states and therefore ample opportunities to forge  $sp^3$  architectures via multiple catalytic manifolds.<sup>7-10</sup> Despite the advances realized, these most of these transformations require prefunctionalization at the targeted  $sp^3$  site, and therefore considerable attention should be devoted to the development of techniques that harness the potential of  $sp^3$  C–H<sup>11</sup> or C–C linkages<sup>12</sup> as adaptive nucleophilic handles.

### 2.1.1 $sp^3$ C–C Bond Formation via Ni-Catalyzed Reductive Coupling

Despite the considerable progress in Pd-catalyzed cross-coupling reactions, the means to forge  $sp^3$  architectures in these endeavors have been hindered,<sup>13</sup> at least at some extent, by the propensity of alkyl-Pd complexes towards parasitic  $\beta$ -hydride elimination pathways.<sup>13a,b, 14</sup> These observations prompted the utilization of Ni catalysts for these purposes due to its low tendency for promoting  $\beta$ -hydride elimination (Scheme 2.1).<sup>7, 15, 16</sup> In addition to a series of elegant disclosures that demonstrated the ability of

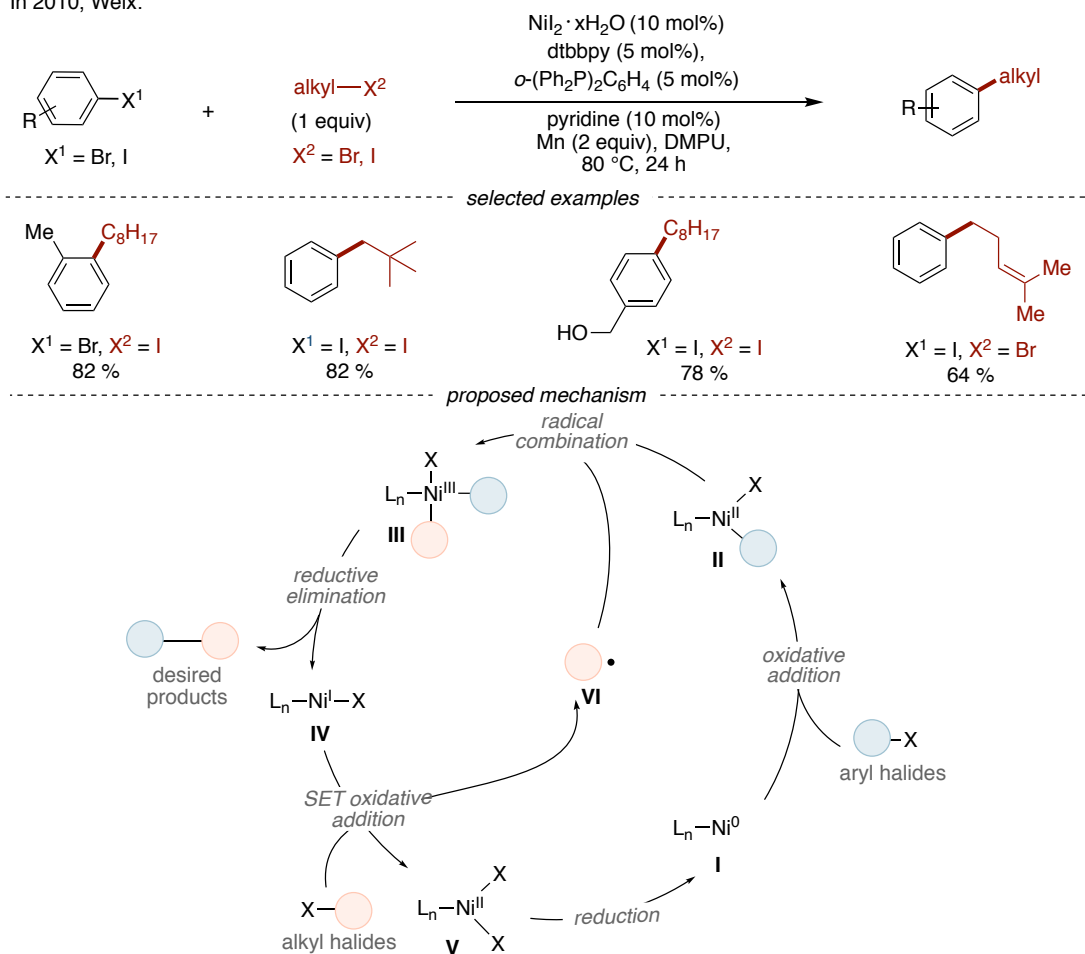
classical nucleophilic/electrophilic regimes for forging  $sp^3$  architectures, we have witnessed tremendous progress in the area of Ni-catalyzed reductive couplings<sup>17</sup> that make use of simple, yet readily available, starting materials such as carboxylic acids, amines, alcohols or unactivated olefins, thus offering innovative pathways for rapidly and reliably access molecular complexity, even in the context of late-stage functionalization.



**Scheme 2.1** General characteristics of nickel catalysts.

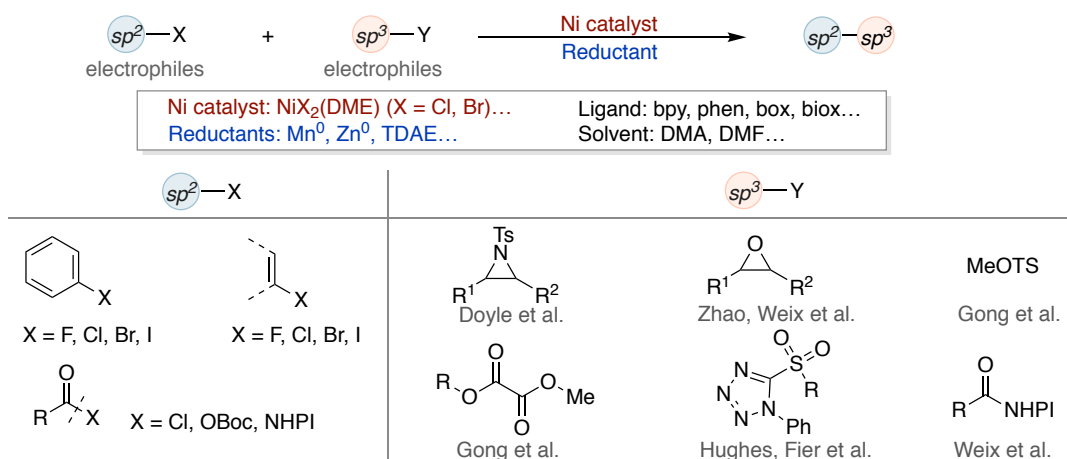
Initial progress in the field of Ni-catalyzed cross-electrophile couplings was focused on the utilization of metallic reductants such as Mn or Zn, providing the source of electrons that is required to effect turnover when coupling two different electrophiles.<sup>2c, 3, 7</sup> In 2010, Weix developed a Ni/Mn  $C(sp^2)$ – $C(sp^3)$  selective cross-coupling of aryl iodides with alkyl iodides (Scheme 2.2, *top*).<sup>6</sup> Both a bipyridyl and a phosphine ligand were used to produce high cross-selectivities. The authors ruled out the intermediacy of organomanganese reagents by the successful utilization of TDAE in lieu of Mn;<sup>18</sup> careful, however, must be taken when generalizing this as the utilization of a different reductant doesn't necessarily rule out whether the presence of Mn causes a mechanistic switch. Still, the authors suggested a mechanism (Scheme 2.2, *bottom*) consisting of oxidative addition to  $Ni^0$  complex (**I**) and interception of the corresponding  $Ni(II)$  with an alkyl radical en route to a  $Ni(III)$  intermediate (**III**). A final reductive elimination delivers the product and generates a  $Ni(I)$  halide complex (**IV**) that can subsequently react with the alkyl halide to promote the formation of the alkyl radical **VI** and a  $Ni(II)$  (**V**) that ultimately is reduced to the propagating  $Ni^0$  (**I**).

In 2010, Weix:



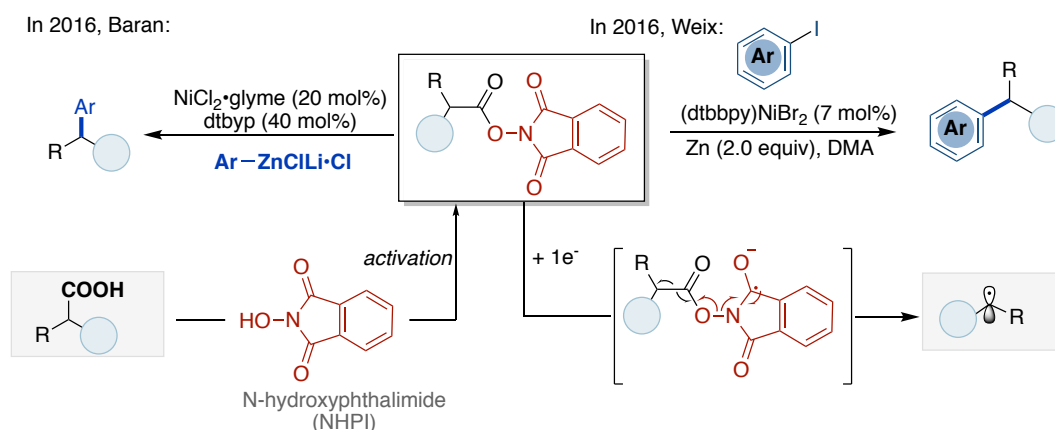
**Scheme 2.2** Ni-catalyzed reductive cross-coupling of aryl halides with alkyl halides.

Following the seminal work of Weix, many research groups provided a series of alternative procedures within the area of nickel-catalyzed reductive cross-coupling reactions.<sup>4b</sup> Indeed, a variety of different  $sp^3$  electrophiles<sup>19</sup> have been used with success, including epoxides,<sup>20</sup> aziridines,<sup>21</sup> alkyl sulfones,<sup>22</sup> phosphates,<sup>23</sup> N-hydroxyphthalimide (NHPI) esters,<sup>24</sup> Katritzky salts<sup>9,10</sup> or oxalates<sup>25</sup> among others (Scheme 2.3).<sup>19</sup>



**Scheme 2.3** Typical  $C(sp^3)$  electrophiles for the reductive cross-coupling.

In 2016, Baran<sup>26</sup> and Weix<sup>24</sup> independently reported the formation of  $sp^3$  C–C bonds via Ni-catalyzed decarboxylative cross-coupling events (Scheme 2.4). The authors utilized alkyl carboxylic acids as convenient, stable and available "workhorse" building blocks for alkyl fragments via the formation of NHPI esters that are susceptible to single-electron transfer en route to alkyl radical intermediates. Baran disclosed Ni-catalyzed decarboxylative cross-coupling of arylzinc reagents and NHPI esters (Scheme 2.4, left), whereas Weix and co-workers made use of NHPI esters with Zn as reductant (Scheme 2.4, right). Later on, the scope of these transformations was expanded to alkylation,<sup>27</sup> acylation<sup>28</sup> and enantioselective vinylation.<sup>29</sup>



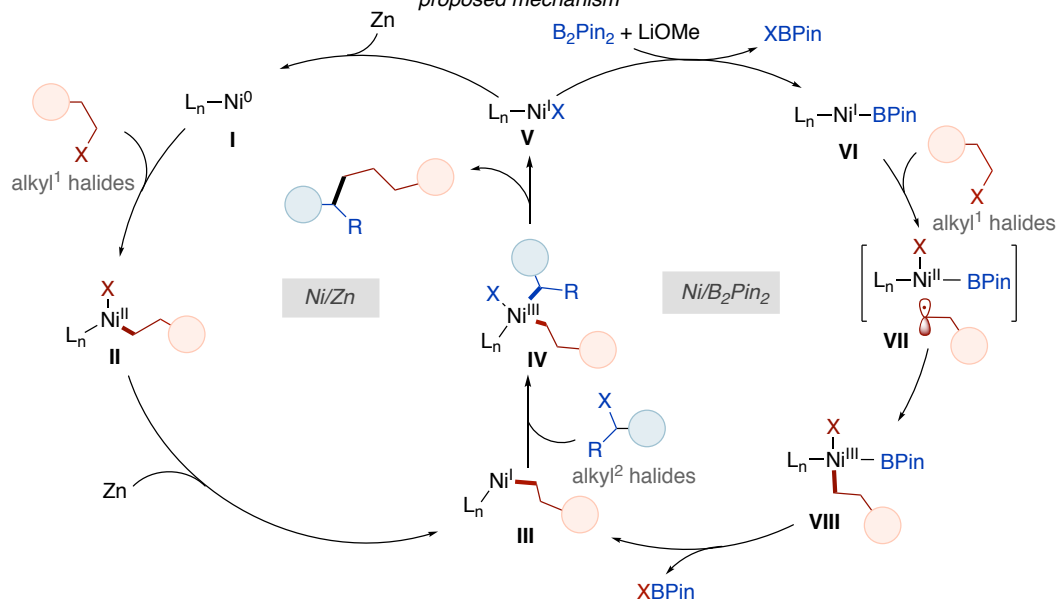
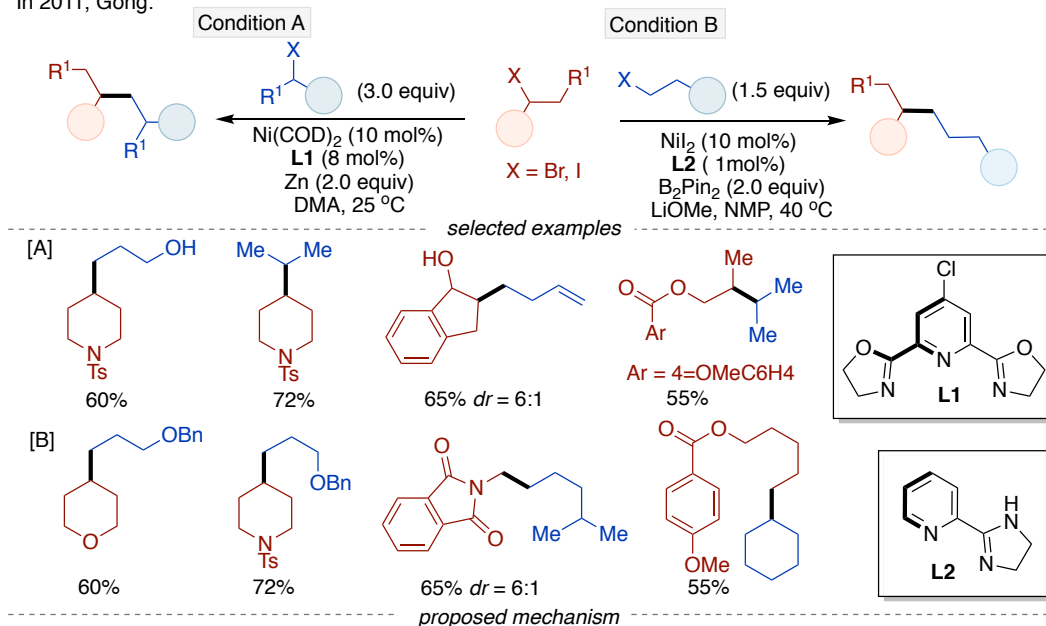
**Scheme 2.4** Ni-catalyzed decarboxylative coupling of NHPI esters.

Historically, transition-metal-catalyzed cross-coupling reactions to forge  $C(sp^3)-C(sp^3)$  bonds<sup>30</sup> can be traced back to the early work of Kharasch in the 1950s.<sup>31</sup> Indeed, the vast majority of approaches to tackle this problem involved the reductive

---

homocoupling of alkyl halides.<sup>32</sup> It was not until 2011 that Gong reported the first nickel-catalyzed cross-reduction coupling of two different alkyl halides (Scheme 2.5, *top left*).<sup>33</sup> They found that high selectivity and high yields could be obtained by using excess amounts of primary alkyl bromide with Zn as the reductant. In addition, the authors found that replacing Zn by B<sub>2</sub>Pin<sub>2</sub> improved the chemoselectivity (Scheme 2.5, *top right*).<sup>34</sup> The authors noted that the formation of Ni-Bpin complexes may be the key factor to differentiate the coupled alkyl partners and produce cross-coupling products with greater selectivity. In addition, control experiments ruled out the intermediacy of organoboron reagents. In the Ni/B<sub>2</sub>Pin<sub>2</sub> system, the reaction was proposed to first undergo SET of Ni<sup>I</sup>-Bpin (**VI**) to the alkyl halide, followed by radical recombination to form an alkyl-Ni<sup>III</sup> intermediate (**VII**) and reductive elimination to deliver the targeted product (Scheme 2.5, *bottom*).

In 2011, Gong:



**Scheme 2.5**  $\text{C}(sp^3)\text{-C}(sp^3)$  bond formation via Ni-catalyzed reductive coupling with either Zn or  $\text{B}_2\text{pin}_2$  as reductants.

## 2.1.2 $sp^3$ C–C Bond Formation by Nickel/Photoredox Cross-Coupling

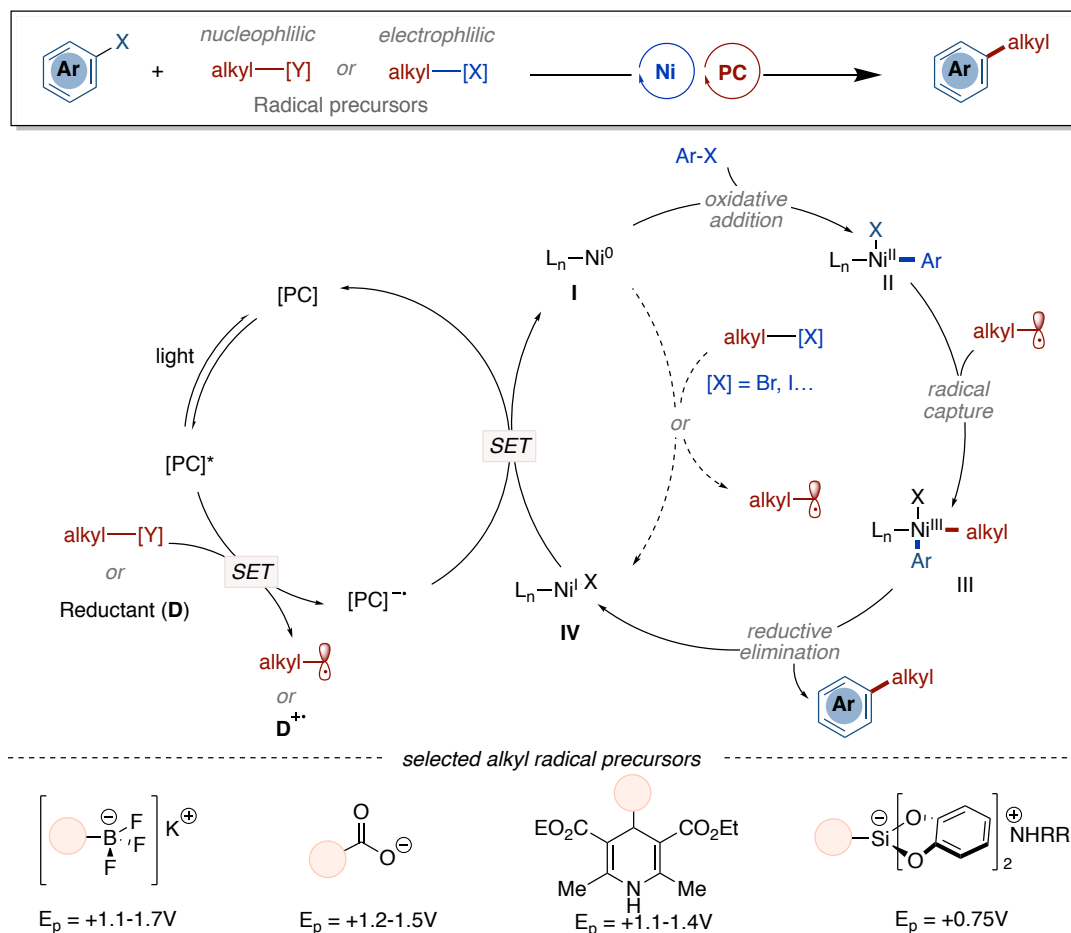
Photoredox catalysis have offered new opportunities in synthetic organic endeavors to promote reactions via distinctive mechanistic manifolds.<sup>35</sup> In the absence of stoichiometric strong oxidants or high-energy light irradiation, the utilization of photoinduced SET and ET increases the possibilities for establishing high-valence and excited-state catalysis. In addition, the combination of nickel and photoredox dual



---

catalysis has shown to be a flexible platform for the creation of novel, highly realizable synthetic methods due to the proclivity of photoredox manifolds to generate open-shell intermediates and the flexibility for bond-formation associated to the field of Ni catalysts.<sup>5d,36</sup>

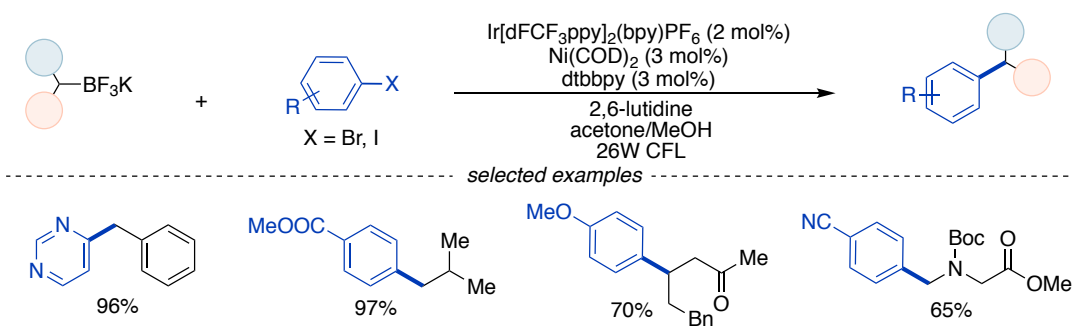
As shown in Scheme 2.6, a canonical nickel/photoredox dual catalytic system is initiated by oxidative addition of an aryl electrophile to Ni<sup>0</sup>. Subsequently, interception of the in situ generated Ni<sup>II</sup> intermediate(**II**) with an alkyl radical obtained via a photoinduced event<sup>37</sup> leads to the targeted product via reductive elimination and a Ni<sup>I</sup>LnX intermediate (**IV**) that is subjected to a final single-electron transfer to recover back the propagating Ni<sup>0</sup> species.<sup>38</sup> The corresponding alkyl radicals can be obtained from a series of different precursors including simple carboxylic acids,<sup>39</sup> electrophilic C(*sp*<sup>3</sup>) reagents,<sup>40, 41</sup> organoboron reagents,<sup>42</sup> organosilanes<sup>43</sup> or aldehydes<sup>41</sup> among many others.<sup>41</sup> In addition, alkyl radicals can also be obtained via hydrogen atom transfer (HAT) processes or C–C bond cleavage. Additionally, amines and silanes are commonly used as reductants to quench the excited state of the photocatalyst in nickel/photoredox dual catalytic systems instead of the common heterogeneous reductants (eg, Zn, Mn) in traditional reductive coupling reactions.<sup>5d, 35c, 35d, 44</sup>



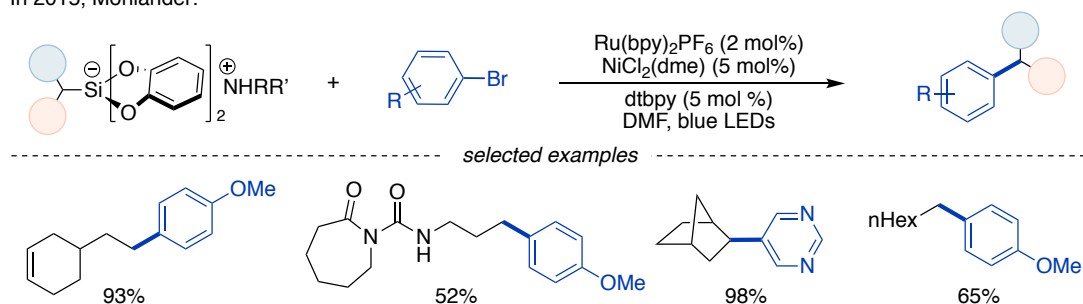
**Scheme 2.6** General Ni/photoredox dual catalytic cycle.

In 2014, Molander described a nickel/photoredox catalyzed cross-coupling using alkylboronate nucleophiles.<sup>45</sup> The report details the use of benzyl trifluoroborate salts as benzyl radical precursors in combination with aryl bromides for  $C(sp^2)-C(sp^3)$  bond-formation (Scheme 2.7, *top*), thus circumventing the traditionally sluggish transmetallation step of boronic acids in Suzuki-Miyaura couplings. Subsequently, Molander further explored the use of a series of alkyl bis(catecholate) silicates as radical precursors for reaction with aryl bromides under nickel/photocatalyst conditions (Scheme 2.7, *bottom*).<sup>46</sup>

In 2014, Monlander:



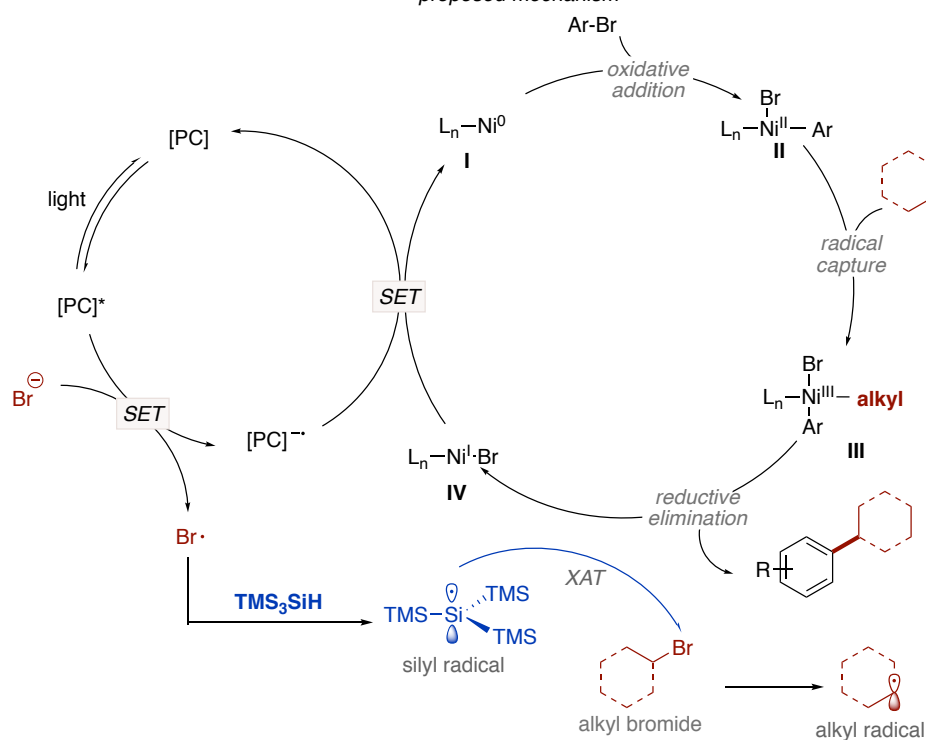
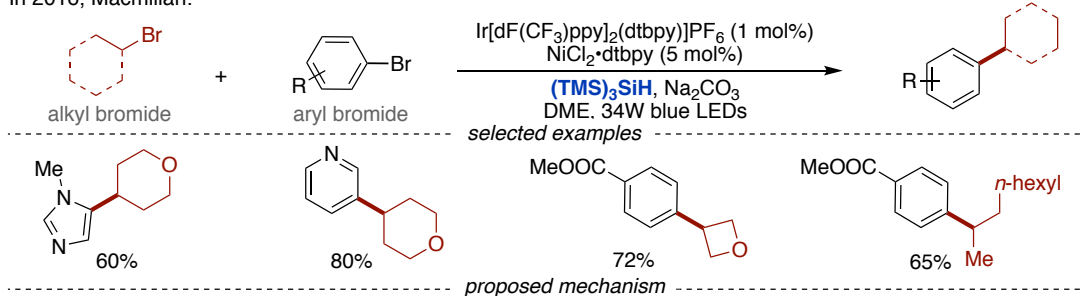
In 2015, Monlander:



**Scheme 2.7** Dual catalyzed C(*sp*<sup>2</sup>)-C(*sp*<sup>3</sup>) cross-coupling using alkyl trifluoroborates or alkyl bis(catechol) silicates.

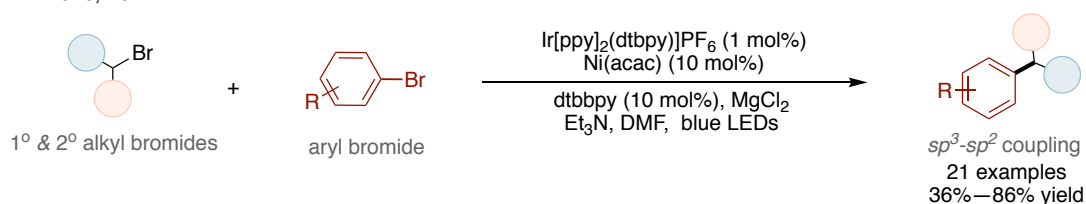
In 2016, MacMillan disclosed a metallaphotoredox scenario for the reductive cross-coupling of aryl bromides and alkyl bromides without the use of metal reductants (Scheme 2.8).<sup>47</sup> The reaction proceeded via the intermediacy of bromine radicals that can abstract the hydrogen atom of tris(trimethylsilyl)silane to create a stable silyl radical intermediate by HAT. Subsequently, an alkyl radical is generated via halogen atom abstraction (XAT) which generate a Ni<sup>III</sup> intermediate (**III**) prior to reductive elimination. Turnover is achieved by final single-electron transfer to the Ni<sup>I</sup> species (**IV**), thus recovering back the propagating Ni<sup>0</sup>Ln (**I**). It is worth noting that Lei independently reported an otherwise similar endeavor by using Et<sub>3</sub>N as reducing agent, both quenching the excited-state of the photocatalyst and serving as a XAT reagent to promote the formation of alkyl radicals (Scheme 2.9).<sup>48</sup>

In 2016, Macmillan:



**Scheme 2.8** Silyl-radical-mediated cross-electrophile coupling.

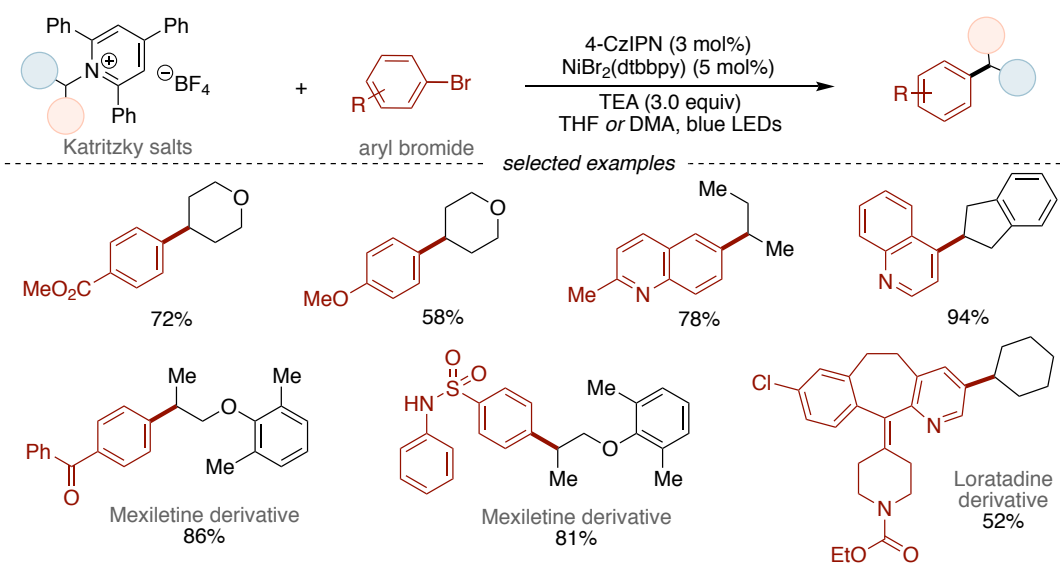
In 2016, Lei:



**Scheme 2.9** Nickel catalyzed reductive coupling with  $\text{EtN}_3$  as XAT reagent.

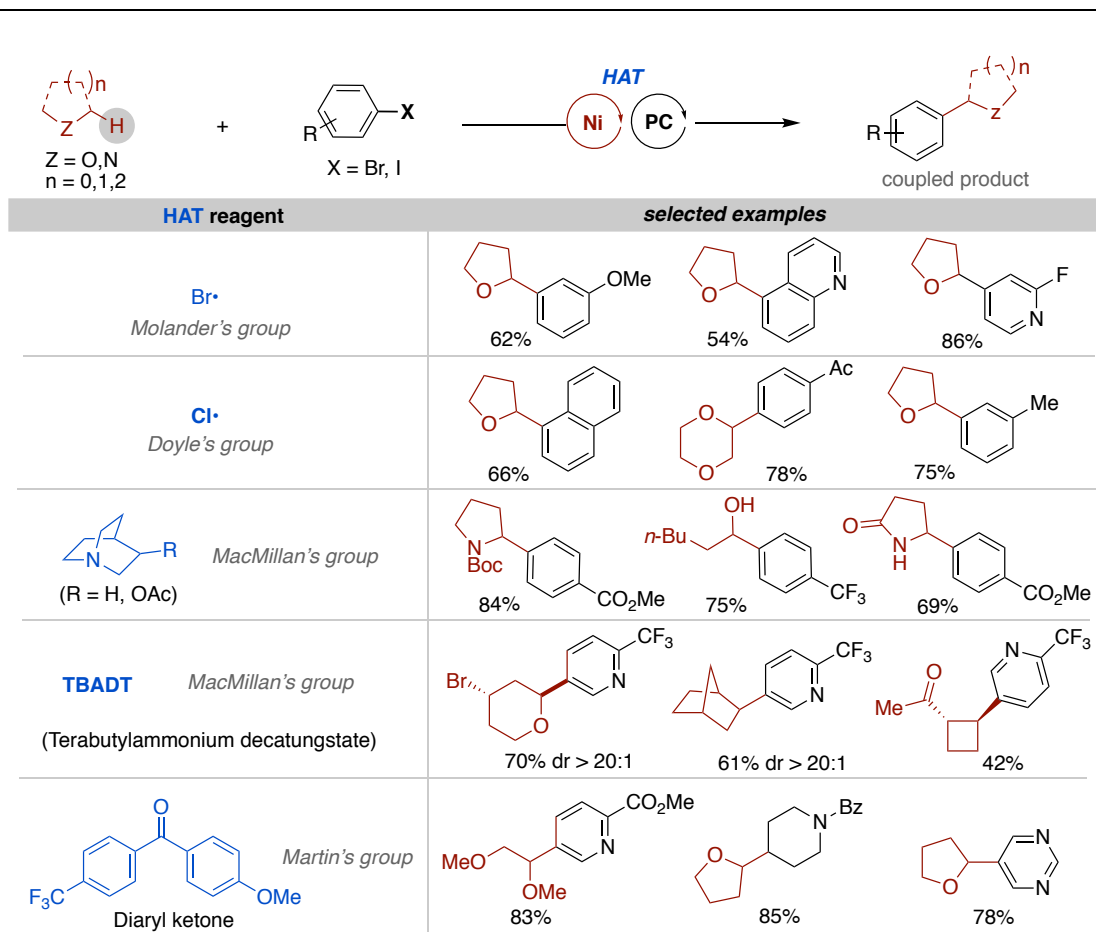
In addition, Katritzky salts<sup>10</sup> were identified as nucleophilic handles in metallaphotoredox catalysis (Scheme 2.10).<sup>49</sup> Mechanistically, Katritzky salts are susceptible to single-electron transfer from the excited state of the photocatalyst or  $\text{Ni}^0\text{Ln}$  complexes to form the corresponding alkyl radical intermediate.

In 2019, Monlander:



### Scheme 2.10 Ni/photoredox-catalyzed cross-coupling with Katritzky salts.

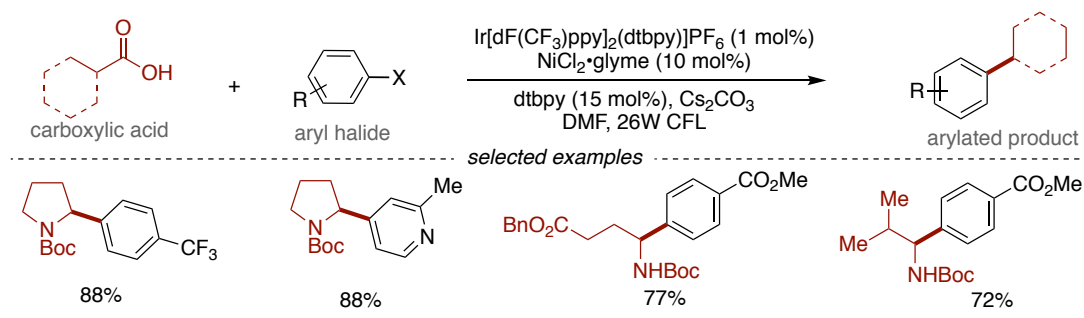
In 2016, Molander<sup>50</sup> and Doyle<sup>51</sup> independently reported that metallaphotoredox scenarios could be initiated by hydrogen atom abstraction (HAT) with simple ethereal solvents via the intermediacy of either bromine or chlorine radicals. Alternative HAT agents such as pyrrolidine derivatives,<sup>52</sup> and polyoxometalate photocatalyst tetrabutylammonium decatungstate (TBADT)<sup>53</sup> have been recently described. In addition, our research group also contributed to this field by proposing the utilization of simple, yet modular, diaryl ketones as triplet photocatalysts in lieu of the commonly utilized Ir or Ru photocatalysts with the advantage of avoiding the need for additional HAT reagents<sup>54</sup> (Scheme 2.11).<sup>55</sup>



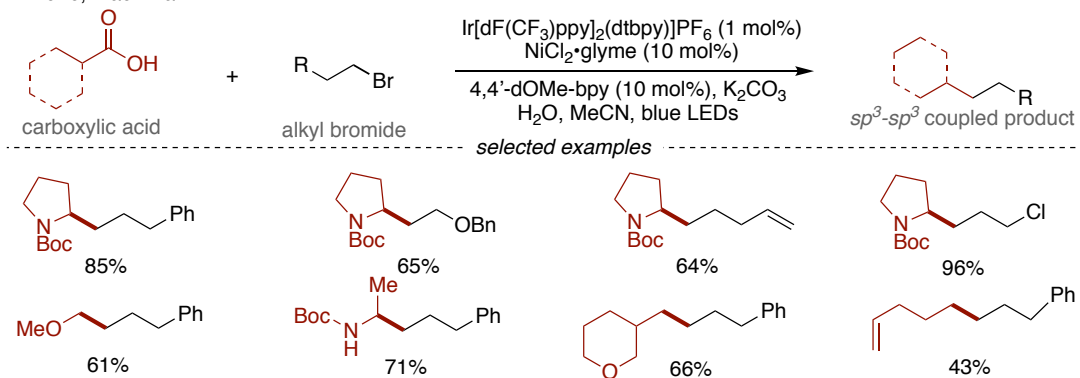
**Scheme 2.11** Alkyl-aryl dual cross-coupling mediated by HAT.

MacMillan and Doyle reported that abundant carboxylic acids are suitable candidates for generating alkyl radicals within a metallaphotoredox event in the context of  $sp^2$ – $sp^3$  bond-forming reactions (Scheme. 2.12, *top*).<sup>56</sup> Later on, the authors further expanded this technique to accommodate alkyl bromides as electrophilic partners (Scheme. 2.12, *bottom*).<sup>57</sup>

In 2014, MacMillan and Doyle:



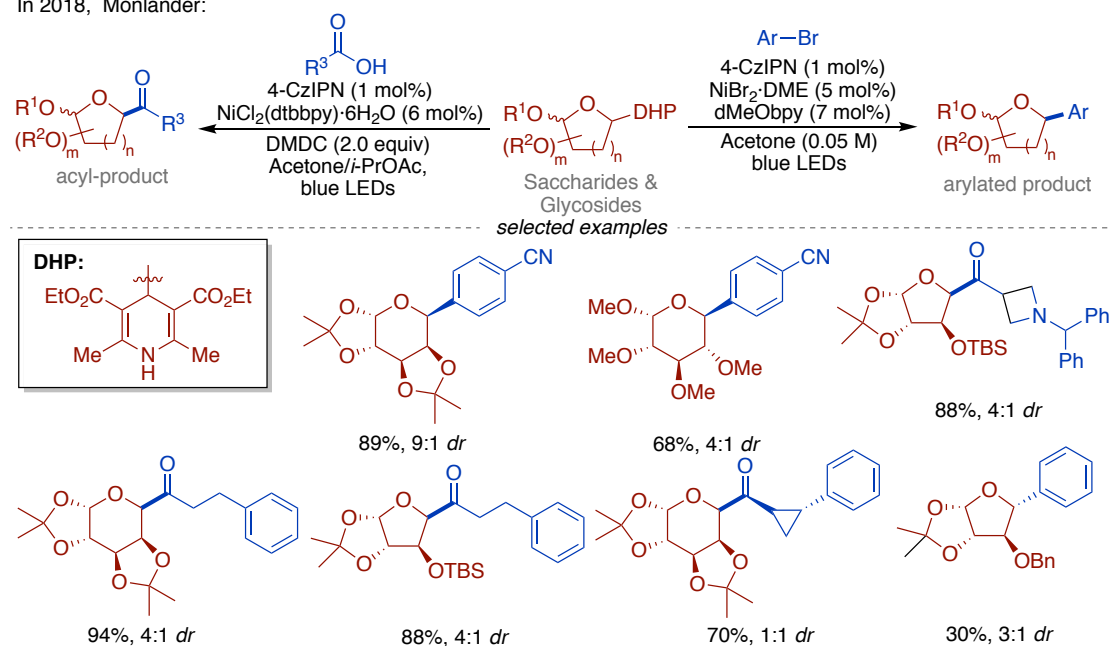
In 2016, MacMillan:



**Scheme 2.12** Ni/photoredox-catalyzed  $sp^3$  C–C decarboxylation cross-coupling.

The utilization of C–C bond-cleavage as a manifold for generating alkyl radicals within the context of metallaphotoredox catalysis was demonstrated by Molander when utilizing alkyl-substituted Hantzsch esters (4-Alkyl-1,4-dihydropyridines (DHPs))<sup>59</sup> in combination with aryl halides<sup>60</sup> (Scheme 2.13, *right*) or acyl halides in situ<sup>61</sup> (Scheme 2.13, *left*). Specifically, an oxidative SET sets the basis for C–C bond-cleavage to release alkyl radicals, with aromatization being the thermodynamic driving force that ultimately generates simple pyridine derivatives.<sup>59</sup>

In 2018, Monlander:



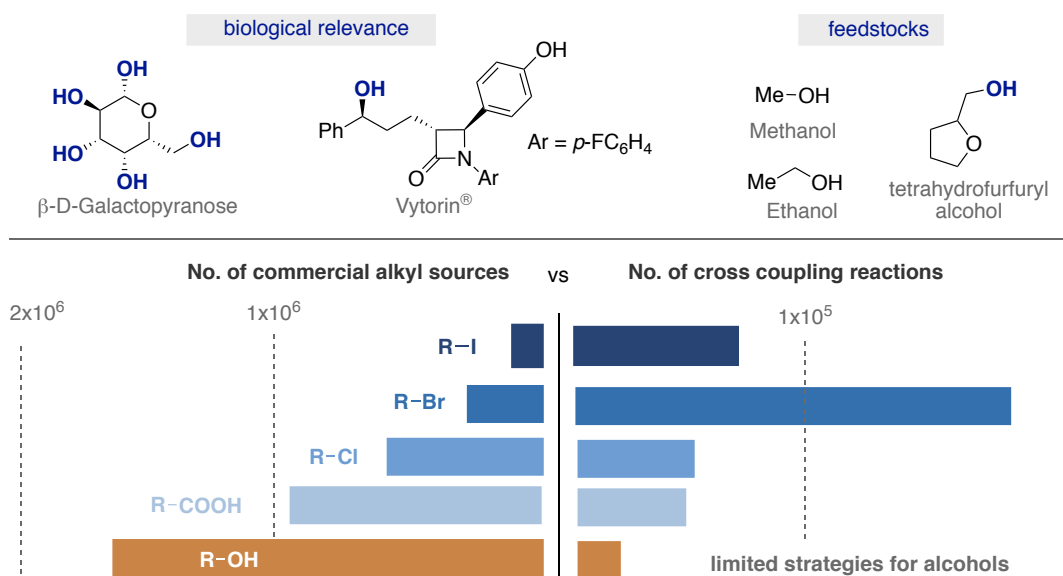
**Scheme 2.13** Ni/photoredox-catalyzed cross-coupling with alkyl DHP derived from saccharide analogues.

### 2.1.3 Nickel-Catalyzed Cross-Coupling Using Aliphatic Alcohols as $sp^3$ -Carbon Handles

Aliphatic alcohols rank among the most widespread and naturally abundant organic compounds<sup>62</sup> (Scheme 2.14, *top*). Although aliphatic alcohols have been used as a vehicle to produce oxygen-centered nucleophiles under basic conditions,<sup>63</sup> their utilization as  $sp^3$  carbon handles is not commonly practiced as one might initially anticipate and certainly less common than the utilization of carboxylic acids and alkyl halides (Scheme 2.14, *bottom*).<sup>64,65</sup>

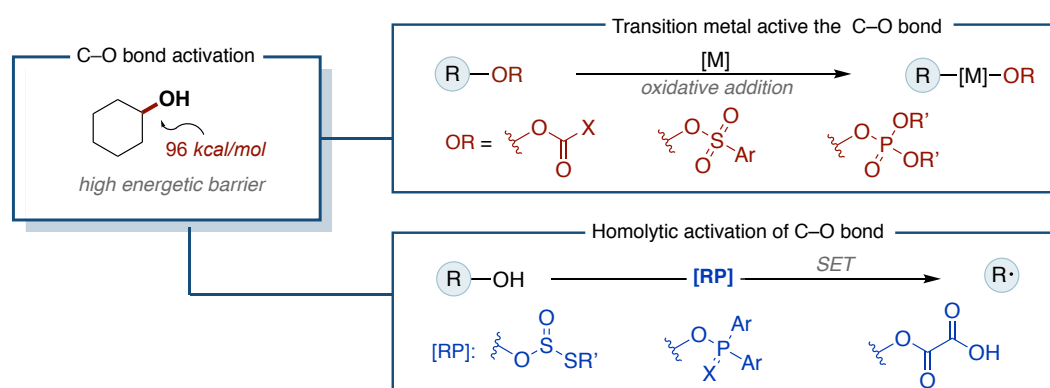


■ Aliphatic alcohol motifs as  $sp^3$ -counterparts



**Scheme 2.14** Aliphatic alcohol motifs as  $sp^3$ -counterparts.

One of the fundamental challenges involved in the utilization of aliphatic alcohols as  $sp^3$  nucleophilic handles is the high bond dissociation energy to undergo  $sp^3$  C–OH cleavage (BDE)  $\approx$  96 kcal/mol).<sup>66</sup> However, this challenge has been alleviated by the conversion of alcohols into their activated congeners such as esters,<sup>25b</sup> sulfonates,<sup>22</sup> phosphates,<sup>67</sup> and ethers,<sup>68</sup> making these susceptible for activation via oxidative addition with transition metals or via single-electron transfer when utilizing xanthates,<sup>69</sup> phosphites,<sup>65c</sup> and oxalates<sup>70</sup> (Scheme. 2.15).

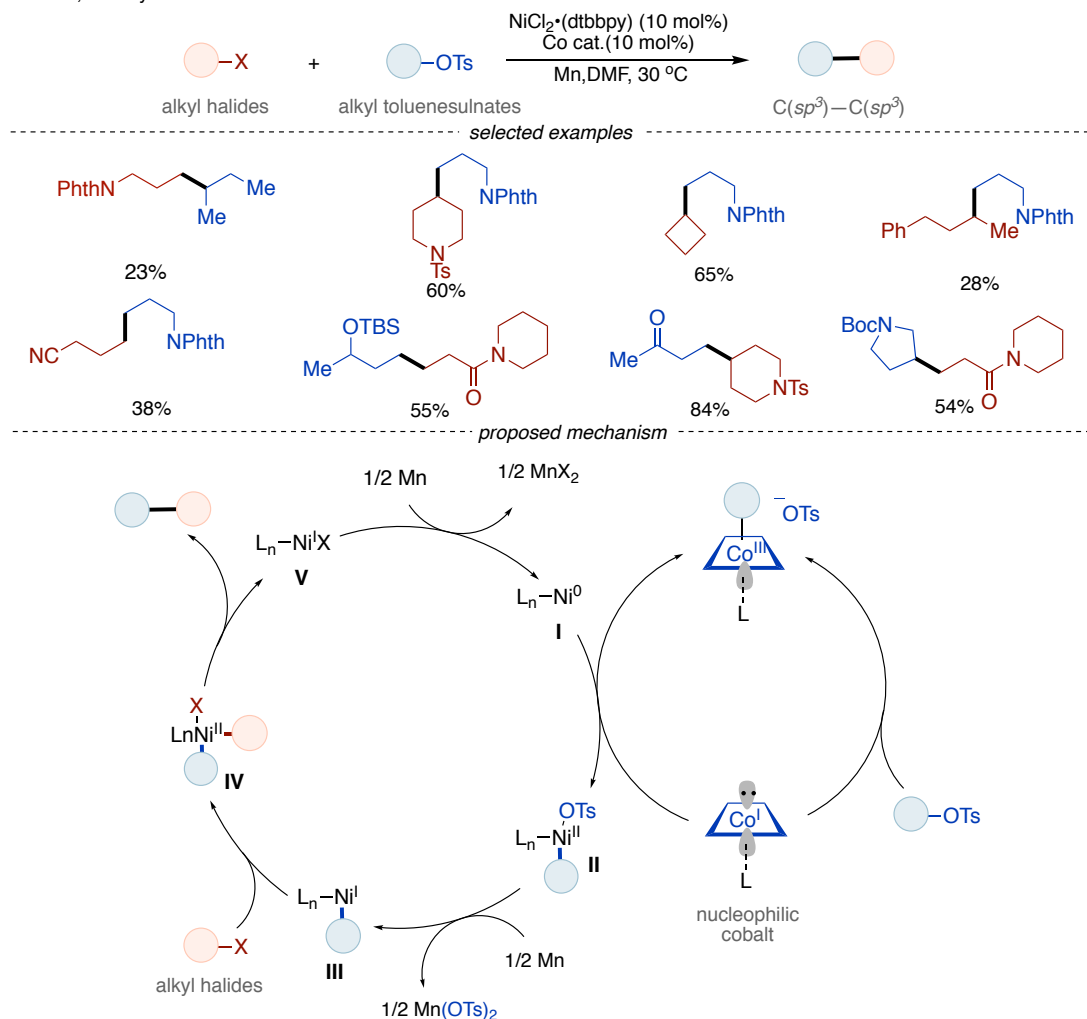


**Scheme 2.15** The mode of  $C(sp^3)$ –O bond cleavage.

Komeyama successfully achieved the Co-catalyzed reductive cross-coupling between alkyl *p*-toluenesulfonate as an activated  $sp^3$  C–O electrophile and alkyl halides<sup>71</sup> (Scheme 2.16). The authors proposed a mechanism consisting of nucleophilic

cobalt(I) species that are interfaced with a Ni-catalyzed endeavor in the presence of Mn as the terminal reductant.

In 2019, Komeyama:

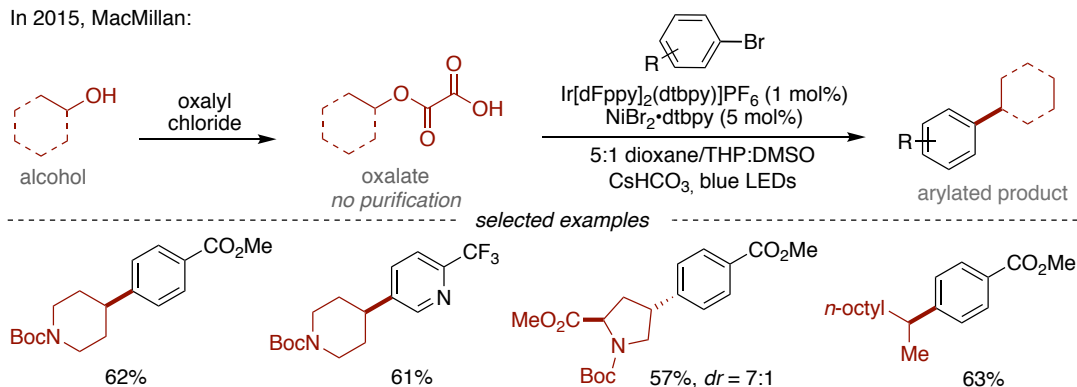


**Scheme 2.16** Dual Ni/Co catalyzed reductive cross-coupling with alkyl toluenesulfonate.

Inspired by the pioneering work of Barton<sup>72</sup> when utilizing xanthates or oxalates as radical precursors, MacMillan and Overman reported a technique that harnesses the potential of oxalates as nucleophilic handles for  $\text{C}(\text{sp}^3)\text{-C}(\text{sp}^2)$  bond-forming reactions by utilizing a photoredox scenario.<sup>73</sup> Upon single-electron oxidation, oxalates generate two molecules of  $\text{CO}_2$  and alkyl radicals that can be intercepted with an appropriate electron acceptor (Scheme 2.17). In addition, Molander employed benzyl xanthates as radical precursors<sup>74</sup> in a formal deoxygenative  $\text{C}(\text{sp}^3)$ -arylation protocol (Scheme 2.18). In 2021, Diao described a cross-coupling technique to generate  $\text{sp}^3$  C-aryl and heteroaryl glycosides from glycosyl esters and aryl bromides.<sup>75</sup> The authors used

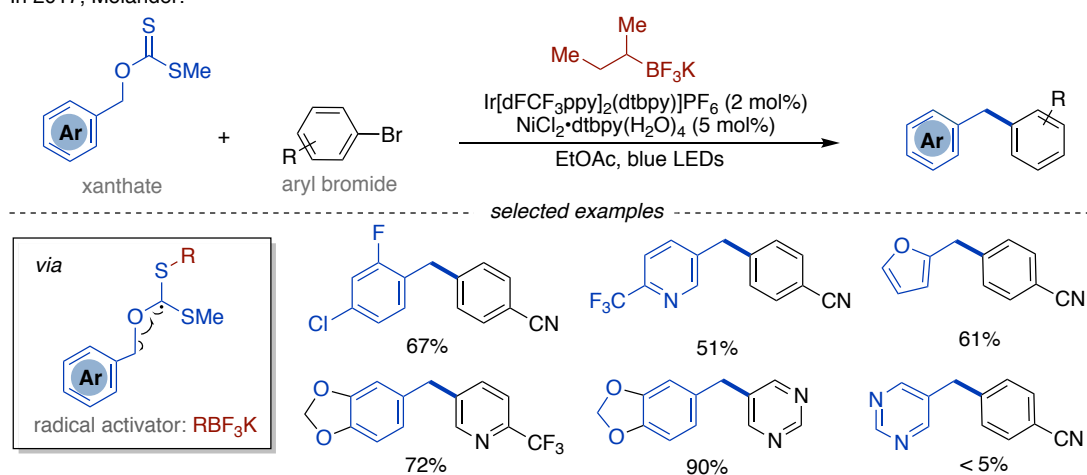
dihydropyridine (DHP) as the activating group followed by C–O bond homolytic cleavage to produce glycosyl radicals (Scheme 2.19).

In 2015, MacMillan:



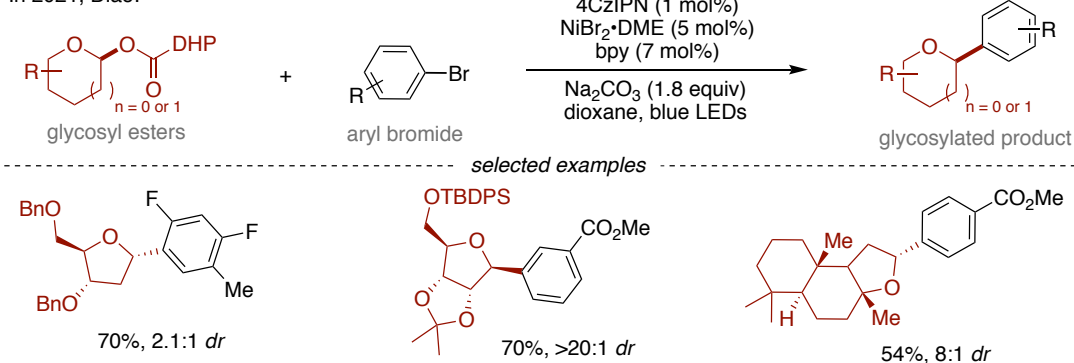
**Scheme 2.17** Dual-catalytic cross-coupling reactions using oxalates as radical precursors.

In 2017, Molander:



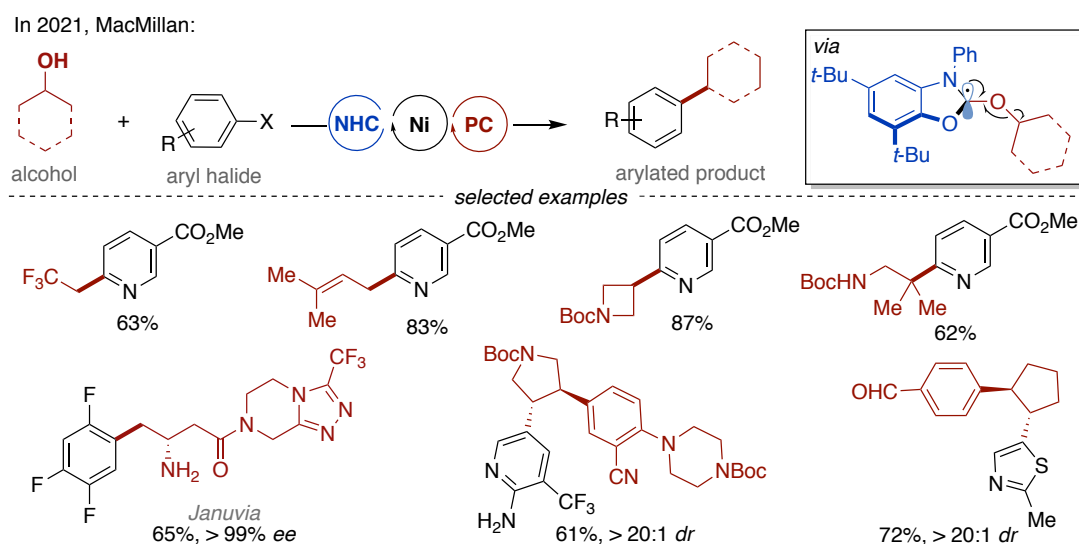
**Scheme 2.18** Dual-catalytic cross-coupling reactions using xanthates as radical precursors.

In 2021, Diao:



**Scheme 2.19** Dual-catalytic cross-coupling reactions using DHP as radical precursors.

In 2021, MacMillan developed a strategy for the direct deoxygenative cross-coupling of  $sp^3$ -hybridized alcohols (Scheme 2.20).<sup>76</sup> The authors made use of a *N*-heterocyclic carbene salt to activate the aliphatic alcohol prior to single-electron transfer en route to the corresponding alkyl radical that can finally be interfaced within the context of a Ni-catalyzed endeavor.

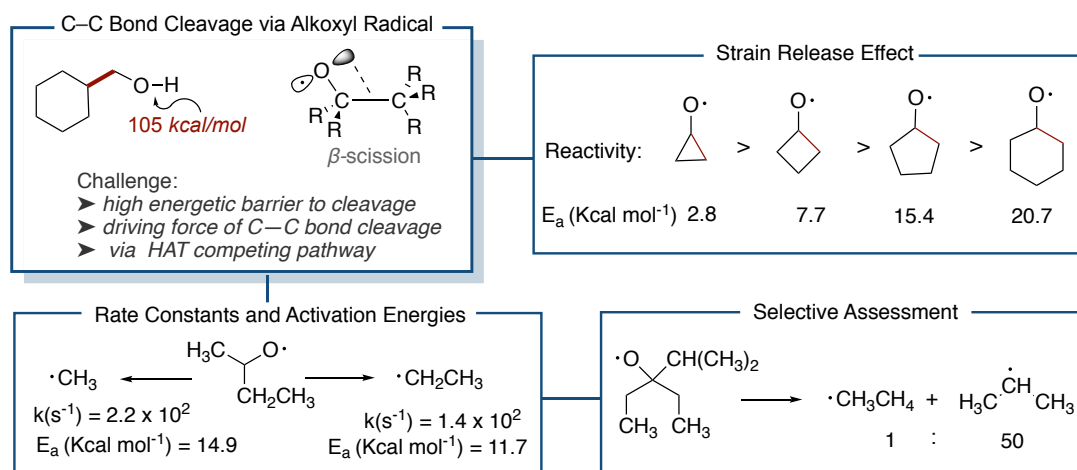


**Scheme 2.20** Alcohol deoxygenative cross-coupling via NHC-mediated C–O bond homolytic cleavage.

An alternative route to using aliphatic alcohols as nucleophilic  $sp^3$  handles is to promote C–C bond-cleavage via  $\beta$ -scission, which includes the following: (a)  $\beta$ -carbon elimination from metal alkoxides;<sup>77</sup> (b)  $\beta$ -scission of in situ generated alkoxy radicals.<sup>78</sup> Typically,  $\beta$ -carbon elimination of metal alkoxides occurs in ring-opening reactions of strained cyclic alcohols; indeed, linear aliphatic alcohols are not suited as coupling partners in these reactions. This is probably due to the observation that the energy of the  $\sigma$  orbital of the C–C bond is too low to match the vacant d orbital of the metal and that the energy of the antibonding orbital of the C–C bond is too high to interact with the filled orbital of the metal.<sup>78a</sup> On the other hand, linear alcohols are more exposed to steric considerations, making the  $\beta$ -scission particularly uphill.<sup>78a</sup> Alternatively, the  $\beta$ -scission of alkoxy radicals can be carried out without the need for ring strain. However, the O–H bond in aliphatic alcohols has a higher BDE  $\sim$  106 kcal/mol, the alkoxy radical requires a significant driving force to functionalizing the C–C bond,<sup>78g</sup> and the electrophilic alkoxy radical might be susceptible to promote hydrogen atom abstraction at electron-rich  $sp^3$  C–H centers, thus preventing the

corresponding  $\beta$ -scission.<sup>78g</sup>

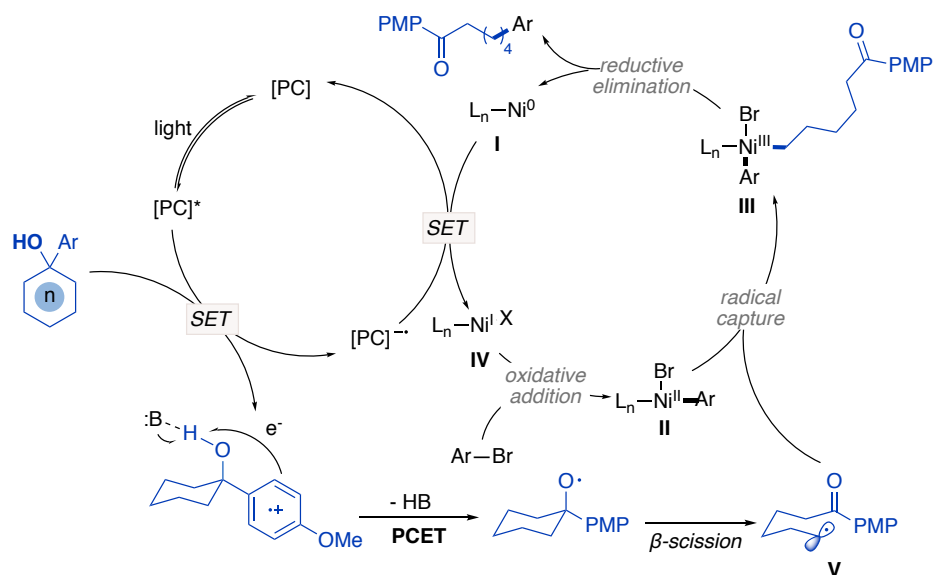
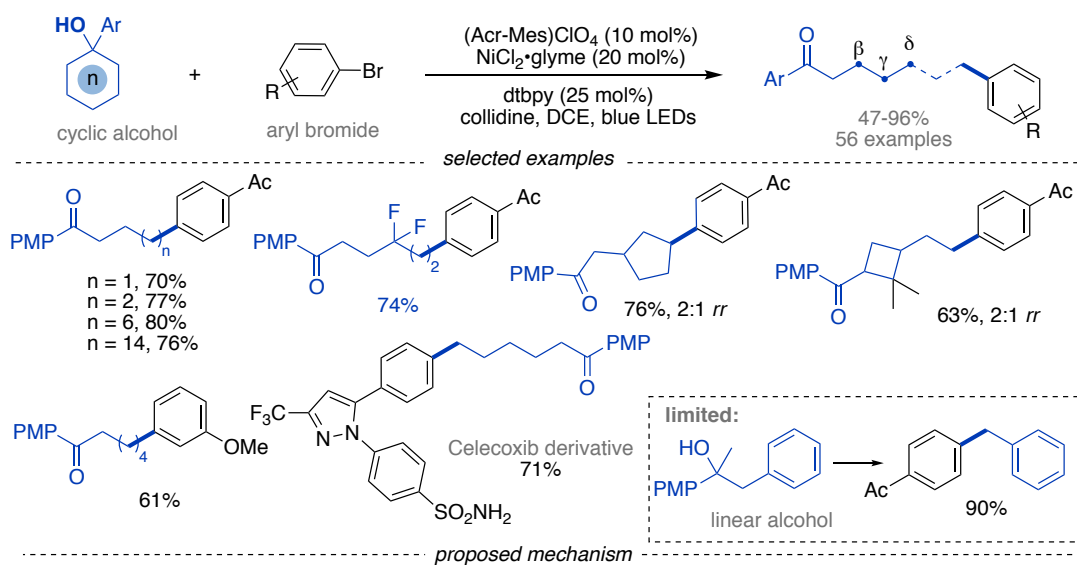
$\beta$ -scission of cyclic alkoxy radicals is controlled by strain release, with a favorable reaction for particularly strained cyclopropyl rings (Scheme 2.21). Secondly, the thermodynamic stability of the alkyl radicals generated by  $\beta$ -scission largely dictates the chemoselectivity, and the C–C bond energy is affected by the different substituents adjacent to the  $\beta$ -position of the alcohol.<sup>79</sup>



**Scheme 2.21** The mode of  $\text{C}(sp^3)\text{--C}(sp^3)$  bond cleavage via alkoxy radical.

In contrast, the use of unactivated aliphatic alcohols as  $sp^3$  synthons via  $\beta$ -scission remains a challenging task due to the lack of a thermodynamic driving force. During the implementation of this chapter at Martin's laboratories, Rueping developed a nickel/photocatalytic ring-opening arylation from cyclic benzyl alcohols<sup>80</sup> (Scheme 2.22). It is worth noting, however, that this strategy is limited to a specific set of alcohols and similar to the PCET event described by Knowles.<sup>81</sup>

In 2019, Rueping:

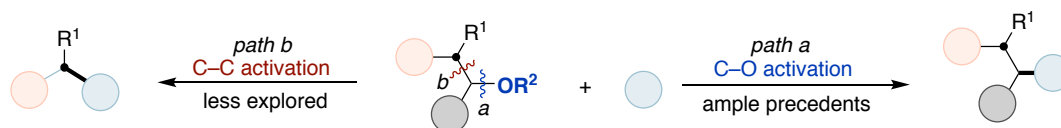


**Scheme 2.22** Ni/photo catalyzed ring-opening arylation from cyclic benzyl alcohols.

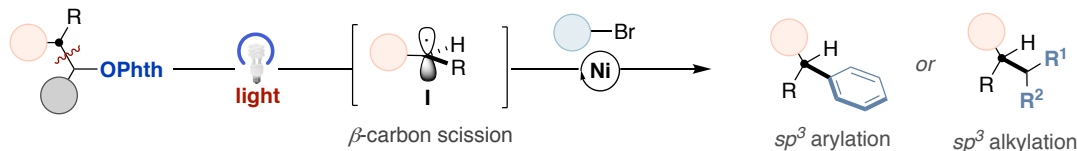
## 2.2 General Aim of the Project

We wondered whether we could harness the potential of aliphatic alcohols – readily available precursors that are particularly prevalent in a myriad of biologically-relevant molecules – as adaptive  $sp^3$  nucleophilic handles for forging  $sp^3$  architectures via  $\beta$ -scission events. Specifically, we aimed at designing a generic platform for that could be applied across a wide number of alcohols and organic halides, thus becoming a powerful strategy for medicinal chemists when attempting late-stage diversification in clinical candidates. Taking into consideration the work of Baran and Chen on the utilization of NHPI esters, we anticipated that the ease at which these precursors generate alkyl radicals might be interfaced with a Ni-catalyzed event for generating an array of  $sp^3$  C–C bond-forming reactions (Scheme 2.23).

- Two different pathways to using aliphatic alcohols as alkyl synthons



- **this chapter:** dual strategy for forging  $sp^3$  bonds via  $\beta$ -scission of alcohols

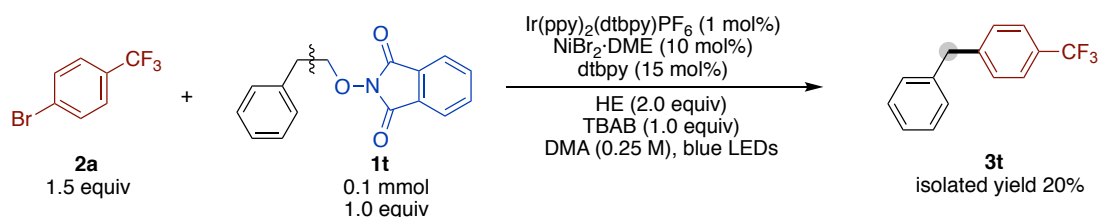


**Scheme 2.23** Aliphatic alcohol motifs as adaptive  $sp^3$  nucleophilic handles.

## 2.3 Dual Catalytic Strategy for Forging $sp^3$ C–C Architectures via $\beta$ -Scission of Aliphatic Alcohol Derivatives

### 2.3.1 Optimization of the Reaction Conditions

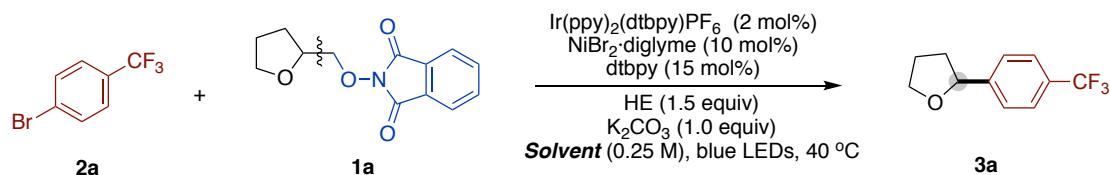
We chose 2-phenethoxyisoindoline-1,3-dione (**1t**) as starting precursor, as  $\beta$ -scission would generate a stable benzyl radical prior to the targeted C–C bond-forming reaction (Scheme 2.24). We found that the utilization of 1-bromo-4-(trifluoromethyl) benzene (**2a**), Ir(ppy)<sub>2</sub>(dtbpy)PF<sub>6</sub> as photocatalyst, NiBr<sub>2</sub>·DME as nickel source, dtbpy as ligand, Hantzsch Ester (HE) as reductant, and TBAB in DMA under blue LEDs irradiation delivered 20% of **3t**. Under these conditions, a large amount of trifluoromethylbenzene and significant amounts of 4,4'-bis(trifluoromethyl)-1,1'-biphenyl were observed in the crude mixtures. It is worth noting, however, that the utilization of TMEDA or (iPr)<sub>2</sub>NEt as reductants did not lead to the targeted products, thus reinforcing the notion that HE might not merely be a reductant.



**Scheme 2.24** Initial test for reactivity.

Our optimization began by evaluating the reaction of **1a** – readily available from simple tetrahydrofurfuryl alcohol – with 4-trifluoromethylbromobenzene **2a** (Table 2.1). When utilizing polar aprotic solvents such as DMA, NMP and DMF, good yields were obtained, likely due to their ability to coordinate metal centers. While THF also performed relatively well, the utilization of aprotic solvents that are favorable for radical-type reactions<sup>82</sup> such as acetonitrile, and acetone gave lower yields. Similarly, non-polar solvents such as toluene led to poor yields.



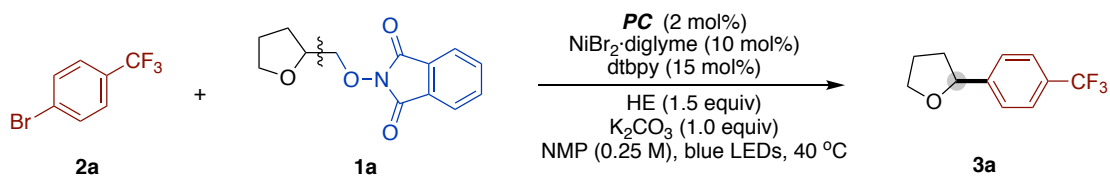


Entry	Solvent	<b>3a</b> Yield (%) <sup>b</sup>
1	DMA	54
2	DMF	73
<b>3</b>	<b>NMP</b>	<b>87</b>
4	DMSO	8
5	THF	61
6	CH <sub>3</sub> CN	6
7	Acetone	5
8	PhMe	3
9	NMP (0.5M)	76
10	NMP (0.15M)	85

Conditions: <sup>a</sup> **2a** (0.10 mmol), **1a** (0.15 mmol), NiBr<sub>2</sub>·diglyme (10 mol%), dtbpy (15 mol%), Ir(ppy)<sub>2</sub>(dtbpy)PF<sub>6</sub> (2 mol%), HE (0.15 mmol), K<sub>2</sub>CO<sub>3</sub> (0.10 mmol), in **solvent** (0.25 M) at 40 °C under irradiation of blue LEDs with a fan for 18 hours. <sup>b</sup> <sup>19</sup>F NMR yields using 1-fluoro-3-nitrobenzene as internal standard. HE = Diethyl 1,4-dihydro-2,6-dimethyl-3,5-pyridinedicarboxylate.

**Table 2.1** Screening of solvents.<sup>a</sup>

Next, we focused our attention on the utilization of photoredox catalysts with different redox potentials such as [Ir(ppy)<sub>2</sub>(dtbbpy)]PF<sub>6</sub> ( $E_{1/2}[\text{Ir}^{\text{II}}/\text{Ir}^{\text{III}}] = -1.51$  V vs. SCE in MeCN), Ir(dFCF<sub>3</sub>ppy)<sub>2</sub>(dtbpy)PF<sub>6</sub> ( $E_{1/2}[\text{Ir}^{\text{II}}/\text{Ir}^{\text{III}}] = -1.37$  V vs. SCE in MeCN), [Ru(bpy)<sub>3</sub>]Cl<sub>2</sub> ( $E_{1/2}[\text{Ru}^{\text{I}}/\text{Ru}^{\text{II}}] = -1.36$  V vs. SCE in MeCN), 4-CzIPN  $E_{1/2}[\text{PC}^{-1}/\text{PC}] = -1.24$  V vs. SCE in MeCN) and MesAcrClO<sub>4</sub> ( $E_{1/2}[\text{PC}^{-1}/\text{PC}] = -0.57$  V vs. SCE in MeCN). As shown in Table 2.2, the utilization of iridium-based photocatalysts gave rise to **3a** in excellent yields. Similar yields were obtained with 4-CzIPN, so this photocatalyst was used in subsequent optimization due to its availability. Note, however, that a non-negligible 63% yield was found in the absence of photocatalyst (entry 6), indirectly pointing at the possibility that the Hantzsch ester (HE) might generate an electron donor-acceptor (EDA) complex with **1a**.

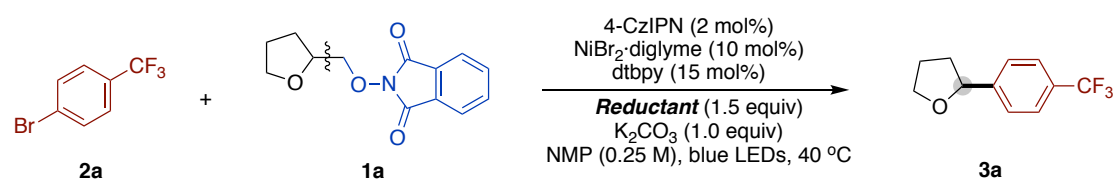


Entry	PC	<b>3a</b> Yield (%) <sup>b</sup>
1	[Ir(ppy) <sub>2</sub> (dtbpy)]PF <sub>6</sub>	87
2	Ir(dFCF <sub>3</sub> ppy) <sub>2</sub> (dtbpy)PF <sub>6</sub>	84
3	[Ru(bpy) <sub>3</sub> ]Cl <sub>2</sub>	<b>51</b>
<b>4</b>	<b>4-CzIPN</b>	<b>84</b>
5	MesAcrClO <sub>4</sub>	54
6	no PC	63

Conditions: <sup>a</sup> **2a** (0.10 mmol), **1a** (0.15 mmol), NiBr<sub>2</sub>·diglyme (10 mol%), dtbpy (15 mol%), **PC** (2 mol%), HE (0.15 mmol), K<sub>2</sub>CO<sub>3</sub> (0.10 mmol), in NMP (0.25 M) at 40 °C under irradiation of blue LEDs with a fan for 18 hours. <sup>b</sup> <sup>19</sup>F NMR yields using 1-fluoro-3-nitrobenzene as internal standard.

**Table 2.2** Screening of photocatalysts.<sup>a</sup>

Interestingly, a significant decrease in yield was found when utilizing (iPr)<sub>2</sub>NEt or Et<sub>3</sub>N instead of HE, whereas no reaction was observed for TMEDA (Table 2.3). This result indicates a non-effective quenching of the photoexcited state or the lack of EDA complex with the substrate. It is worth noting that the utilization of other substituted HE did not have a significant effect on reactivity (entry 5).

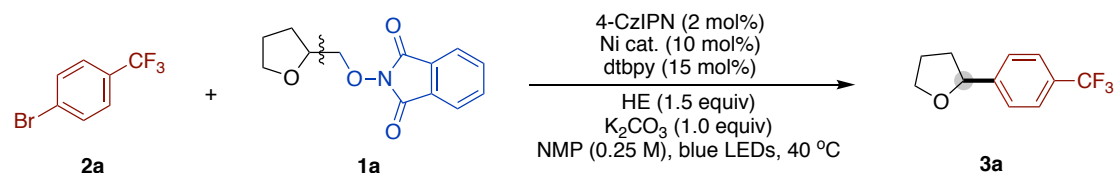


Entry	Reductant	<b>3a</b> Yield (%) <sup>b</sup>
<b>1</b>	<b>HE</b>	<b>84</b>
2	TMEDA	0
3	(iPr) <sub>2</sub> NEt	6
4	Et <sub>3</sub> N	42
5	4-Ph-HE <sup>c</sup>	80
6	no HE	0

Conditions: <sup>a</sup> **2a** (0.10 mmol), **1a** (0.15 mmol), NiBr<sub>2</sub>·diglyme (10 mol%), dtbpy (15 mol%), 4-CzIPN (2 mol%), **reductant** (0.15 mmol), K<sub>2</sub>CO<sub>3</sub> (0.10 mmol), in NMP (0.25 M) at 40 °C under irradiation of blue LEDs with a fan for 18 hours. <sup>b</sup> <sup>19</sup>F NMR yields using 1-fluoro-3-nitrobenzene as internal standard. <sup>c</sup> 4-Ph-HE = Diethyl 2,6-dimethyl-4-phenyl-1,4-dihydropyridine-3,5-dicarboxylate.

**Table 2.3** Screening of reductants.<sup>a</sup>

Next, we turned our attention to studying the influence of the nickel pre-catalysts (Table 2.4). NiBr<sub>2</sub>·diglyme still proved to be optimal, as other nickel catalysts such as NiCl<sub>2</sub>·DME, Ni(COD)<sub>2</sub> and NiI<sub>2</sub> led to moderate yields (entries 3-4, entry 6). Decreasing and increasing the loading of NiBr<sub>2</sub>·diglyme didn't promote the yield (entries 9-10). As expected, no product was generated in the absence of nickel precatalysts (entry 11).

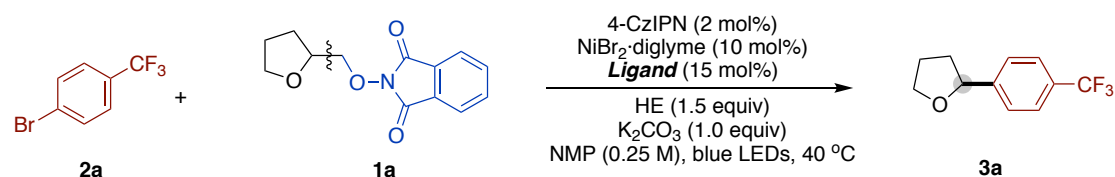


Entry	Ni cat.	<b>3a</b> Yield (%) <sup>b</sup>
1	<b>NiBr<sub>2</sub>·diglyme</b>	<b>84</b>
2	NiBr <sub>2</sub> ·glyme	75
3	NiCl <sub>2</sub> ·DME	58
4	Ni(COD) <sub>2</sub>	51
5	NiBr <sub>2</sub>	67
6	NiI <sub>2</sub>	46
7	Ni(acac) <sub>2</sub>	0
8	NiBr <sub>2</sub> (TBAB) <sub>4</sub>	40
9	NiBr <sub>2</sub> ·diglyme (5 mol%)	61
10	NiBr <sub>2</sub> ·diglyme (15 mol%)	78
11	no Ni cat.	0

Conditions: <sup>a</sup> **2a** (0.10 mmol), **1a** (0.15 mmol), **Ni cat.** (10 mol%), dtbpy (15 mol%), 4-CzIPN (2 mol%), HE (0.15 mmol), K<sub>2</sub>CO<sub>3</sub> (0.10 mmol), in NMP (0.25 M) at 40 °C under irradiation of blue LEDs with a fan for 18 hours. <sup>b</sup> <sup>19</sup>F NMR yields using 1-fluoro-3-nitrobenzene as internal standard.

**Table 2.4** Screening of nickel pre-catalysts.<sup>a</sup>

Taking into consideration that the ligands might modulate the properties of the metal atom, we set out to investigate their effect on the reaction outcome (Table 2.5). Among all ligands examined, we found that 4,4'-dibutyl-bipyridine (dtbpy) afforded the best results (entry 1) when compared to similar bipyridyl backbones containing different electron properties (entries 1-5). Bipyridines possessing a 6-methyl group inhibited the reaction (entry 4, entry 7) whereas the utilization of 1,10-phenanthroline ligands (**L8**) resulted in lower yields. In addition, tridentate ligands such as **L6** or phosphorus ligands delivered traces, if any, of the targeted **3a**.



Entry	Ligand	<b>3a</b> Yield (%) <sup>b</sup>
1	<b>dtbpy (L1)</b>	<b>84</b>
2	<b>L2</b>	74
3	<b>L3</b>	8
4	<b>L4</b>	2
5	<b>L5</b>	61
6	<b>L6</b>	16
7	<b>L7</b>	5
8	<b>L8</b>	37
9	<b>PPh<sub>3</sub></b>	0
10	No Ligand	0

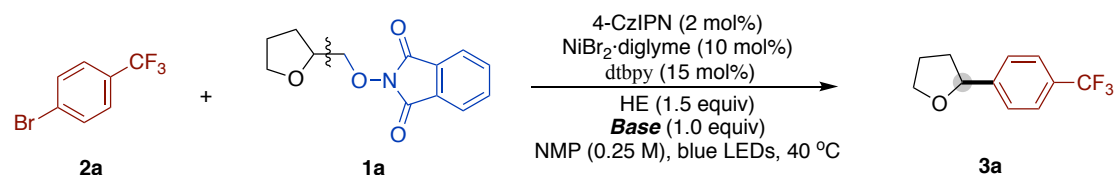
**L1** (R<sup>1</sup> = H; R<sup>2</sup> = *t*-Bu)  
**L2** (R<sup>1</sup> = H; R<sup>2</sup> = OMe)  
**L3** (R<sup>1</sup> = H; R<sup>2</sup> = COOMe)  
**L4** (R<sup>1</sup> = Me; R<sup>2</sup> = OMe)  
**L5**

**L6**  
**L7**  
**L8**

Conditions: <sup>a</sup> **2a** (0.10 mmol), **1a** (0.15 mmol), NiBr<sub>2</sub>·diglyme (10 mol%), **Ligand** (15 mol%), 4-CzIPN (2 mol%), HE (0.15 mmol), K<sub>2</sub>CO<sub>3</sub> (0.10 mmol), in NMP (0.25 M) at 40 °C under irradiation of blue LEDs with a fan for 18 hours. <sup>b</sup> <sup>19</sup>F NMR yields using 1-fluoro-3-nitrobenzene as internal standard.

**Table 2.5** Screening of ligands.<sup>a</sup>

Next, we assessed the role exerted by the base (Table 2.6). As shown, the utilization of carbonate bases provided better results than stronger KOtBu. We hypothesized that the carbonate base interacts with HE, facilitating the formation of EDA complexes prior to homolytic cleavage. This observation was supported by UV-visible absorption experiments.

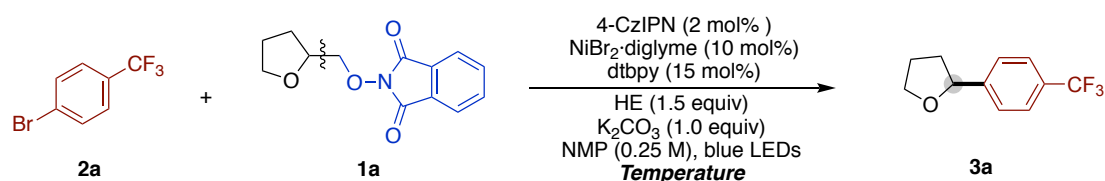


Entry	Base	<b>3a</b> Yield (%) <sup>b</sup>
1	K <sub>2</sub> CO <sub>3</sub>	84
2	Na <sub>2</sub> CO <sub>3</sub>	82
3	CS <sub>2</sub> CO <sub>3</sub>	83
4	K <sub>3</sub> PO <sub>4</sub>	72
5	K <sub>2</sub> HPO <sub>4</sub>	57
6	KOtBu	51
7	No base	70

Conditions: <sup>a</sup> **2a** (0.10 mmol), **1a** (0.15 mmol), NiBr<sub>2</sub>·diglyme (10 mol%), dtbpy (15 mol%), 4-CzIPN (2 mol%), HE (0.15 mmol), **base** (0.10 mmol), in NMP (0.25 M) at 40 °C under irradiation of blue LEDs with a fan for 18 hours. <sup>b</sup> <sup>19</sup>F NMR yields using 1-fluoro-3-nitrobenzene as internal standard.

**Table 2.6** Screening of bases.<sup>a</sup>

Finally, we turned our attention to study the influence of the reaction temperature. As shown in table 2.7, the reaction was better performed at 40 °C (entry 1) whereas no product formation was observed in the absence of light irradiation (entry 5).



Entry	Temperature	<b>3a</b> Yield (%) <sup>b</sup>
1	40 °C	84
2	35 °C	78
3	25 °C	69
4	10 °C	43
5	no light, 40 °C	0

---

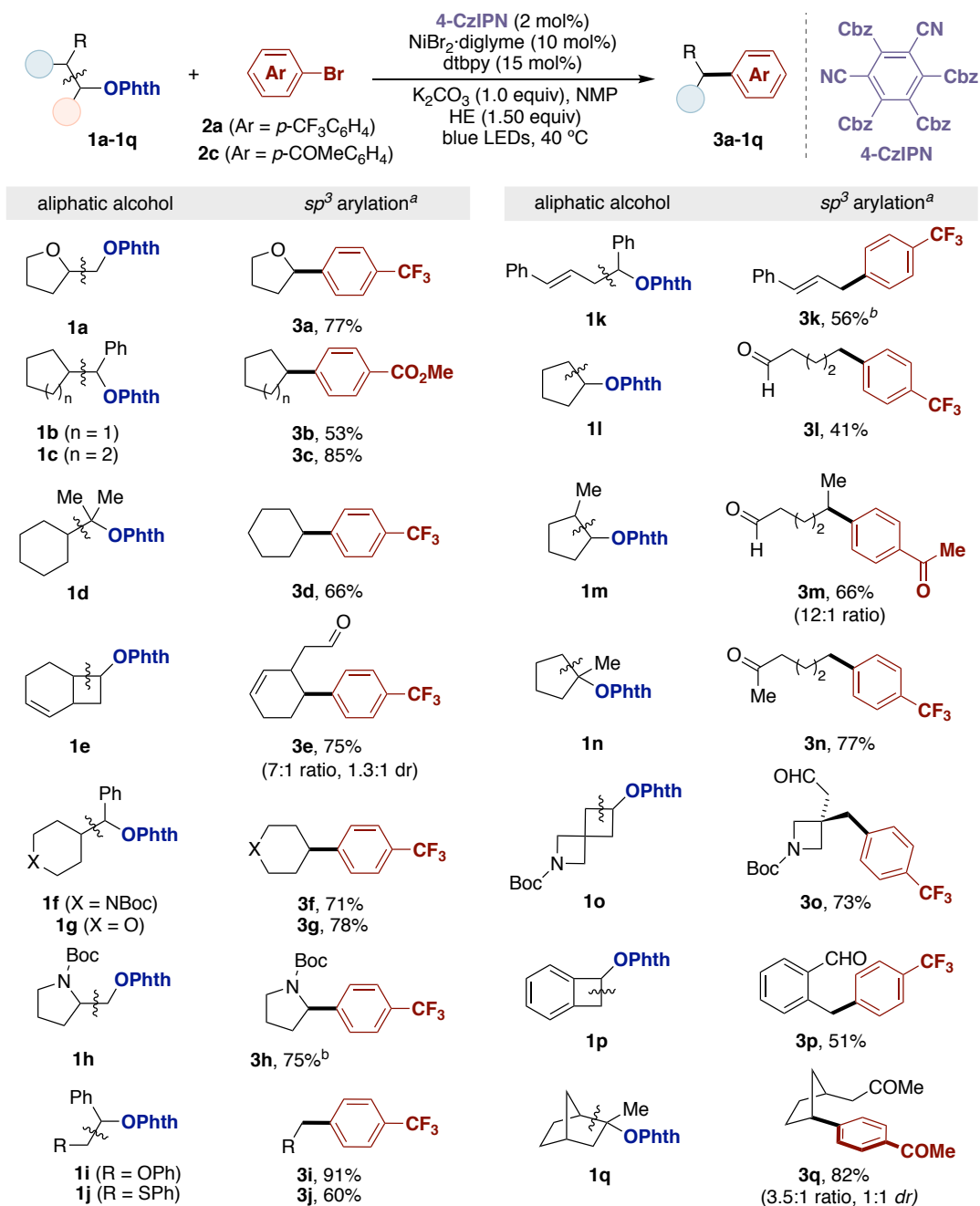
Conditions: <sup>a</sup> **2a** (0.10 mmol), **1a** (0.15 mmol), NiBr<sub>2</sub>·diglyme (10 mol%), dtbpy (15 mol%), 4-CzIPN (2 mol%), HE (0.15 mmol), K<sub>2</sub>CO<sub>3</sub> (0.10 mmol), in NMP (0.25 M) under irradiation of blue LEDs with a fan for 18 hours. <sup>b</sup> <sup>19</sup>F NMR yields using 1-fluoro-3-nitrobenzene as internal standard.

**Table 2.7** Screening of reaction temperature.<sup>a</sup>

## 2.3.2 Substrate Scope

### 2.3.2.1 Scope of Alcohol derived N-alkoxyphthalimides

With the optimal reaction conditions in hand, we began to explore the scope of the *N*-alkoxyphthalimides derived from aliphatic alcohols (Scheme 2.25). As shown, *N*-alkoxyphthalimides from linear primary, secondary and tertiary alcohols were all accommodated under our optimized reaction conditions (**3a-3w**). Different functional groups adjacent to the reactive hydroxyl groups such as allyl (**3k**), NHBoc (**3h**), ether (**3i**), and sulfur-containing groups (**3j**) were also tolerated. Importantly, alkenes remained intact and did not undergo isomerization (**3e**). Gratifyingly, cyclic alcohols with various ring sizes, such as those with spirocyclic or bridged motifs, could be used as substrates to generate aliphatic carbonyl compounds through ring-opening arylation (**3e**, **3l-3q**). The tolerance with carbonyl groups is not surprising given that formaldehyde, acetaldehyde, benzaldehyde and acetone are all obtained from the  $\beta$ -scission of alkoxy radicals. Notably,  $\beta$ -scission occurred preferentially at the more substituted carbon, an indication that the reaction is dictated by the stability of the resulting open shell intermediate.<sup>70</sup>

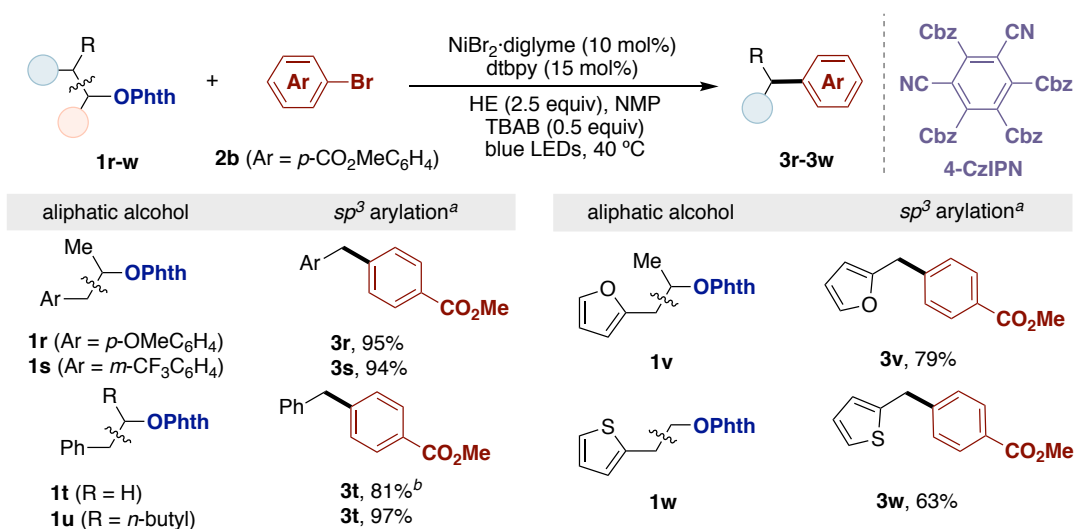


Conditions: <sup>a</sup> aryl halide (1.0 equiv, 0.20 mmol), *N*-phthalimide ethers **1** (1.5 equiv, 0.30 mmol), NiBr<sub>2</sub>·diglyme (10 mol%), dtbpy (15 mol%), 4-CzIPN (2 mol%), HE (1.5 equiv, 0.30 mmol), K<sub>2</sub>CO<sub>3</sub> (1.0 equiv, 0.20 mmol) in NMP (0.25 M) at 40 °C for 18 h; Isolated yields, average of at least two independent runs. <sup>b</sup> Using HE (2.0 equiv), *N*-phthalimide ethers **1** (2.0 equiv).

### Scheme 2.25 Scope of alcohol derived *N*-alkoxyphthalimides.

Substrates containing more reactive benzylic sites could be employed in our protocol without photocatalyst 4-CzIPN (Scheme 2.6, **3r-3w**). In these cases, it is necessary to increase the amount of HE and add TBAB as additive. Both electron-deficient and electron-rich substrates (**1r**, **1s**), including the utilization of furan and thiophene (**3v**,

**3w**), are suitable substrates in this reaction.

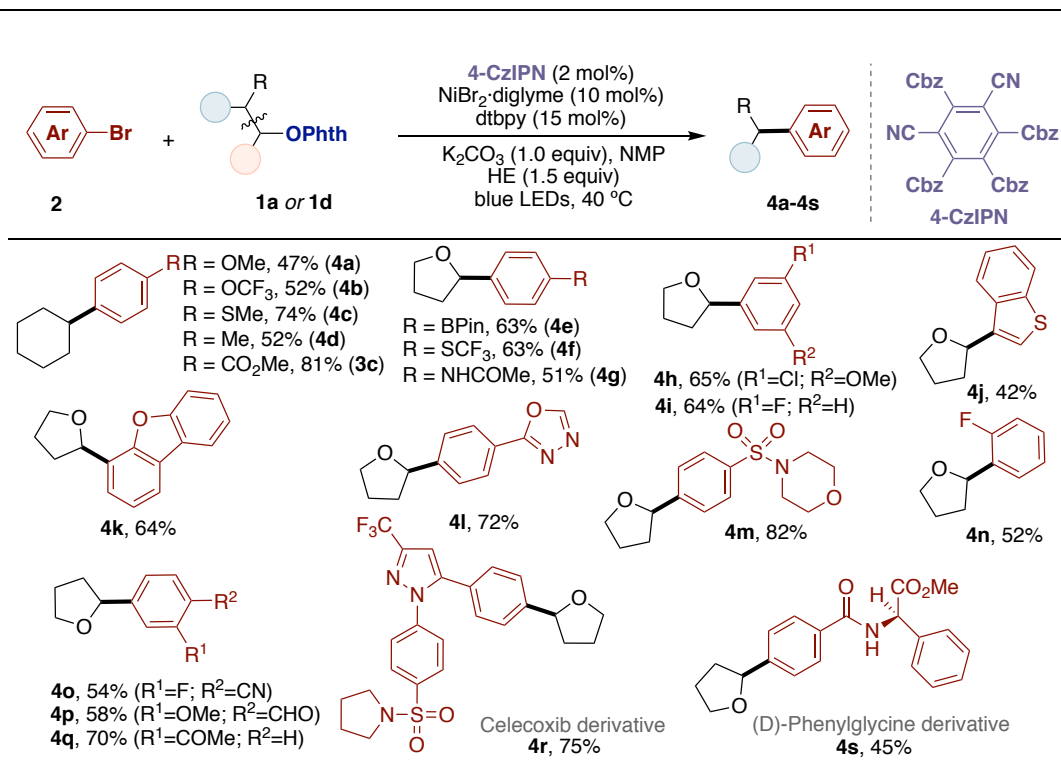


Conditions: <sup>a</sup> aryl halide (0.20 mmol), *N*-phthalimide ethers **1** (0.30 mmol), NiBr<sub>2</sub>·diglyme (10 mol%), dtbpy (15 mol%), HE (0.50 mmol), TBAB (0.10 mmol) in NMP (0.25 M) at 40 °C for 18 h; Isolated yields, average of at least two independent runs. <sup>b</sup> Using 4-Ph-HE (2.50 equiv).

**Scheme 2.26** Scope of phenethyl-alcohol derived *N*-alkoxyphthalimides.

### 2.3.2.2 Scope of Aryl Bromides and Alkyl Bromides

Next, we turned our attention to the scope of the aryl bromides (Scheme 2.27). The targeted *sp*<sup>3</sup>-arylated products were achieved in good yields regardless of the electronic and steric environment of the aryl bromides, even in the presence of *ortho*-substituents (**4q**). It is noteworthy that electron-deficient aryl bromides usually provide better yields. In addition, the method tolerated the presence of boronic esters (**4e**) and aryl halides (**4h**, **4i**, **4n**, **4q**), thus offering opportunities for further functionalization via cross-coupling reactions. In addition, the protocol accommodated the presence of ketones (**4p**), nitriles (**4n**), sulfonamides (**4m**, **4r**), amides (**4g**, **4s**), esters (**3c**, **4s**), aldehydes (**4o**) or heterocycles containing sulfur, oxygen, or even nitrogen atoms (**4g**, **4k**, **4l**, **4r**). In addition, we were able to apply our protocol to advanced synthetic intermediates such as celecoxib derivative (**4r**) and (D)-phenylglycine (**4s**), demonstrating the potential of this method in medicinal chemistry settings.

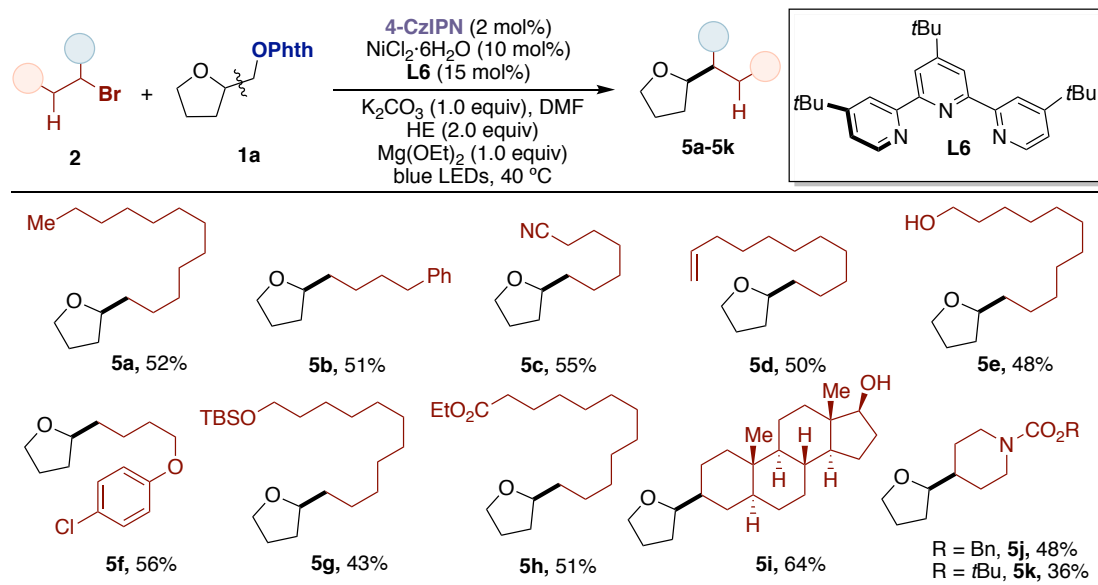


Conditions: <sup>a</sup> aryl halide (0.20 mmol), *N*-phthalimide ethers **1a** or **1d** (0.30 mmol), NiBr<sub>2</sub>·diglyme (10 mol%), dtbpy (15 mol%), 4-CzIPN (2 mol%), HE (0.3 mmol), K<sub>2</sub>CO<sub>3</sub> (0.2 mmol) in NMP (0.25 M) at 40 °C for 18 h; Isolated yields, average of at least two independent runs.

### Scheme 2.27 Scope of aryl bromides.<sup>a</sup>

Next, we focused our attention on the utilization of unactivated alkyl halides as counterparts in order to forge *sp*<sup>3</sup>–*sp*<sup>3</sup> architectures. We anticipated that this transformation would be more problematic than utilizing aryl halides, as (a) Ni-alkyl species undergo facile  $\beta$ -hydride elimination and are significantly less stable than their corresponding Ni-aryl counterparts and (b) the recombination of electron-rich alkyl radicals with more electron-rich Ni-alkyl species might be considered a mismatch case scenario, leaving ample room for parasitic side-reactions. Gratifyingly, this transformation could be achieved by using NiCl<sub>2</sub>·6H<sub>2</sub>O/L6 in DMF in combination with Mg(OEt)<sub>2</sub> as additive. The successful utilization of **L1** is tentatively attributed to the ability of tridentate ligands to stabilize the corresponding Ni-alkyl species while preventing decomposition pathways arising from  $\beta$ -hydride elimination. A wide variety of unactivated primary and secondary alkyl bromides possessing different functional groups such as nitriles (**5c**), alkenes (**5d**), free alcohols (**5e**, **5i**), aryl chlorides (**5f**), silyl groups (**5g**), esters (**5h**), and carbamates (**5j**, **5k**) could all be coupled under our optimized conditions (Scheme 2.28).



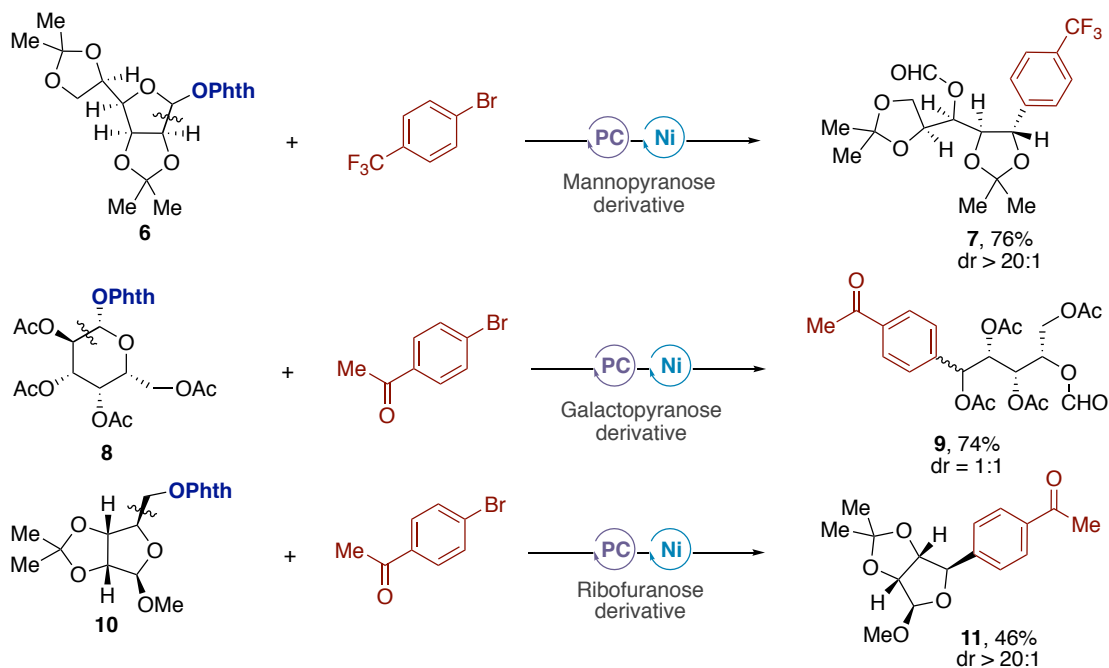


Conditions: <sup>a</sup> **1a** (0.40 mmol), alkyl bromide (0.20 mmol), NiCl<sub>2</sub>·6H<sub>2</sub>O (10 mol%), **L6** (15 mol%), HE (0.40 mmol), K<sub>2</sub>CO<sub>3</sub> (0.20 mmol), Mg(OEt)<sub>2</sub> (0.20 mmol) in DMF (0.125 M) at 40 °C for 20 h; Isolated yields, average of two independent runs.

**Scheme 2.28** Scope of alkyl bromides.<sup>a</sup>

### 2.3.2.3 Functionalization of Saccharides via $\beta$ -Scission

In order to assess the potential applicability of this reaction, we turned our attention to the utilization of our protocol for densely functionalized saccharides (Scheme 2.29). Gratifyingly, various saccharide derivatives of mannofuranose, galactopyranose, and ribofuranoside (**7**, **9**, **11**) could all be functionalized with equal ease. In contrast to existing approaches that focus on the functionalization of C–O bonds, our strategy provides an entry point for enabling a C–C bond cleavage of saccharides followed by a further C–C bond-forming event. We believe these results might offer an opportunity for medicinal chemists in the context of late-stage diversification of advanced intermediates.

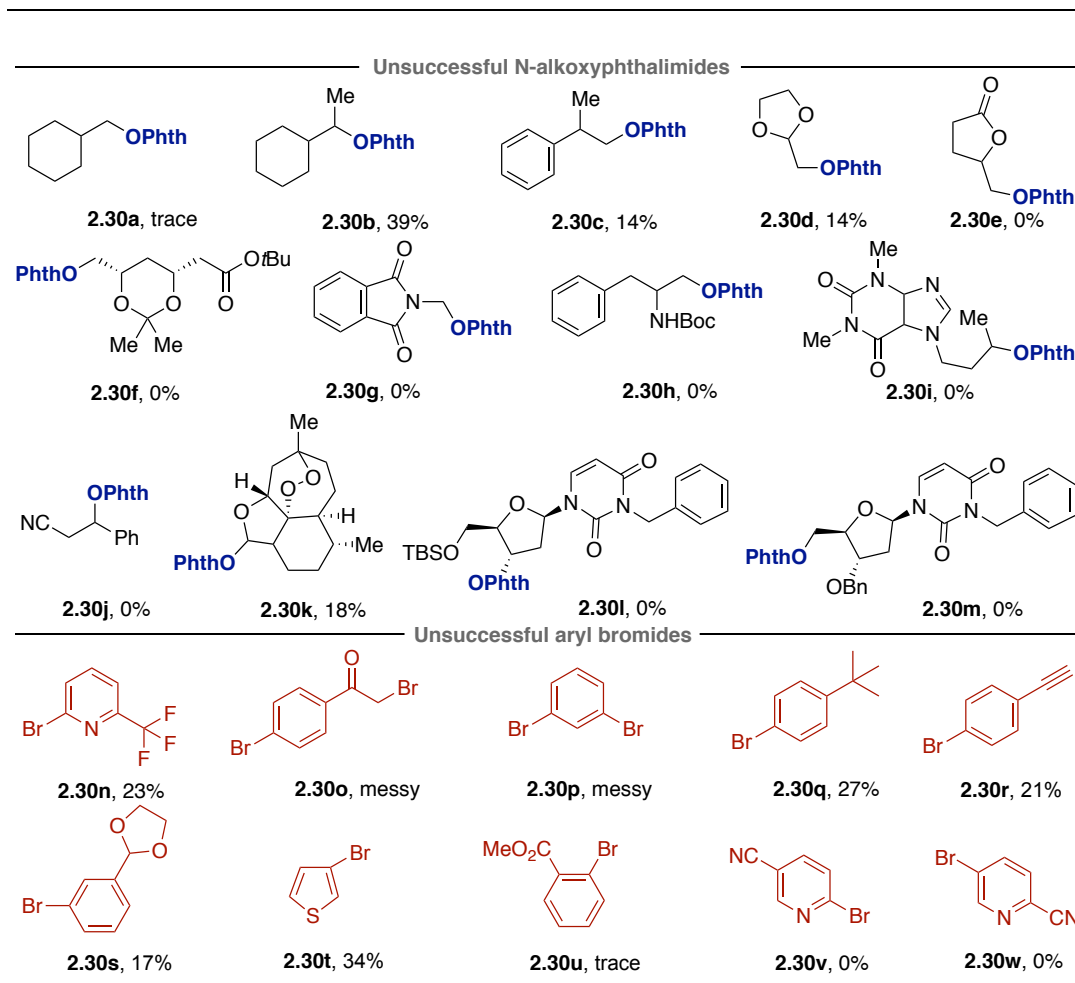


**Scheme 2.29** Functionalization of saccharides via  $\beta$ -scission.

### 2.3.2.4 Unsuccessful Substrates

Unfortunately, there were still some substrates that did not give the desired reactivity, or resulted in low yields of the targeted products (**2.30a-2.30m**) (Scheme 2.30, *top*). Nevertheless, we could gather important information when utilizing these substrates, such as (a) substituents adjacent to the alkoxy group can have a significant impact on the  $\beta$ -scission; (b) although substrates possessing an oxygen (**2.30d**, **2.30e**, **2.30f**, **2.30l**, **2.30m**) or nitrogen atom (**2.30g**, **2.30h**) adjacent to the alkoxy group might result in a more stable alkyl radical, these compounds resulted in the formation of aldehydes via  $\alpha$ -hydrogen elimination of the alkoxy radical (**2.30f**, **2.30m**); (c) competing HAT processes with the solvent comes into play when electron-deficient alkoxy radicals are formed (**2.30d**, **2.30e**, **2.30g**, **2.30j**). However, this HAT process also showed us the possibility that this technology might provide the basis for the establishment of a C–H functionalization event.

A series of aryl bromides were not suitable substrates in our  $\beta$ -scission event (**2.30n-2.30w**) (Scheme 2.30, *bottom*). For example, heteroaryl bromides (**2.30n**, **2.30v**, **2.30w**) possessing nitrogens with a lone pair likely failed due to competitive binding of the nitrogen atom to the Ni catalyst. In addition, very electron-rich aryl halides or polybrominated compounds provided low yields of the targeted products (**2.30o-q**).



**Scheme 2.30** Unsuccessful substrates.

## 2.3.3 Mechanistic Studies

### 2.3.3.1 UV/Vis Absorption Spectra

To support our initial hypothesis that an electron donor-acceptor complex was formed by the interaction of N-alkoxyphthalimide and Hantzsch ester, we compared the UV/Vis absorption spectra between HE and **1a** (Figure 2.1). As shown, the spectra for both HE and **1a** have absorption tails that extend to 450 nm. The addition of  $K_2CO_3$  resulted in a significant bathochromic shift attributed to the formation of the HE-anion that ultimately leads to the formation of the EDA complex. Furthermore, an association constant ( $K_{EDA}$ ) of  $2.8 M^{-1}$  was determined indicating significant formation of the corresponding EDA-complex (See mechanistic experiments for detail).

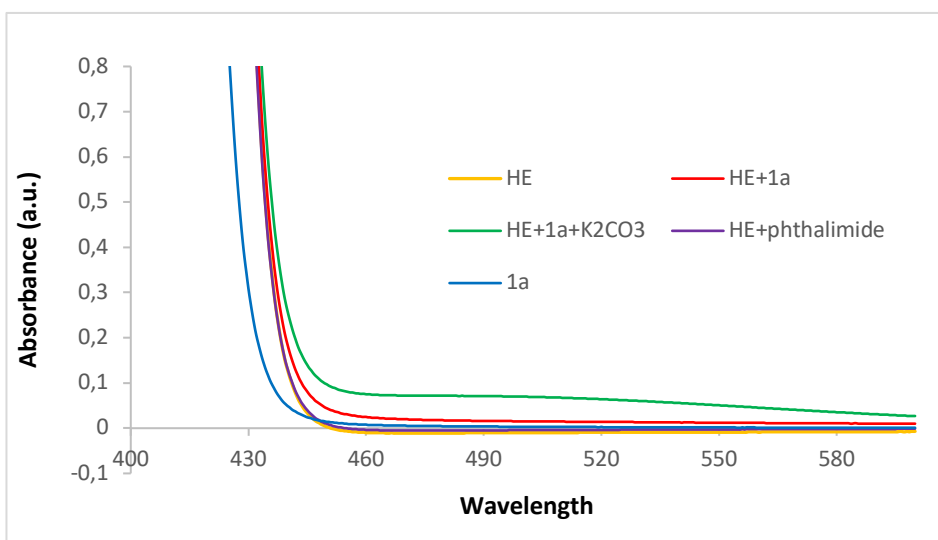
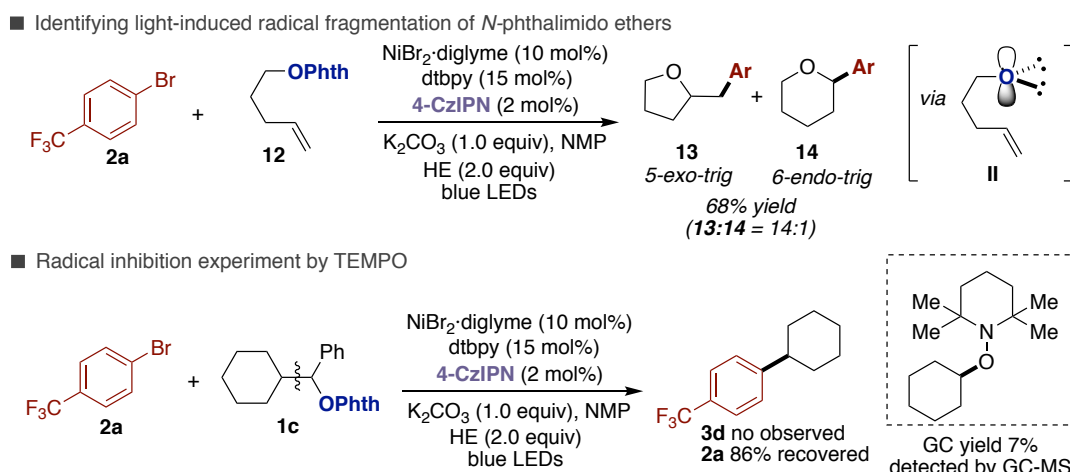


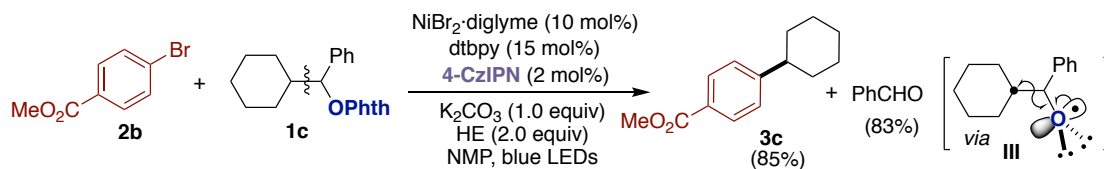
**Figure 2.1.** UV/Vis Spectra the interaction between Hantzsch ester and N-alkoxyphthalimide **1a** in NMP.

### 2.3.3.2 Radical Clock Experiments

The radical fragmentation generated during the reaction was further supported by radical clock experiments with N-alkoxyphthalimide **12** that forms the ring-closed coupling products **13** and **14** on the basis of a 5-*exo*-trig or 6-*endo*-dig cyclization from an in situ generated oxygen-centered radical intermediate **II** (Scheme 2.31, *top*). Furthermore, under standard catalytic conditions with added spin-trapping reagent TEMPO, loss of catalytic activity was observed with significant starting material remaining (86%) and the formation of 7% yield of cyclohexyl-TEMPO adduct (Scheme 2.31, *bottom*). Additionally, 83% of benzaldehyde was found when **1c** was reacted with methyl 4-bromobenzoate (Scheme 2.32), suggesting the intervention of species **III** prior to  $\beta$ -scission en route to alkyl radical intermediates.



**Scheme 2.31** Radical trapping experiments with radical probes.

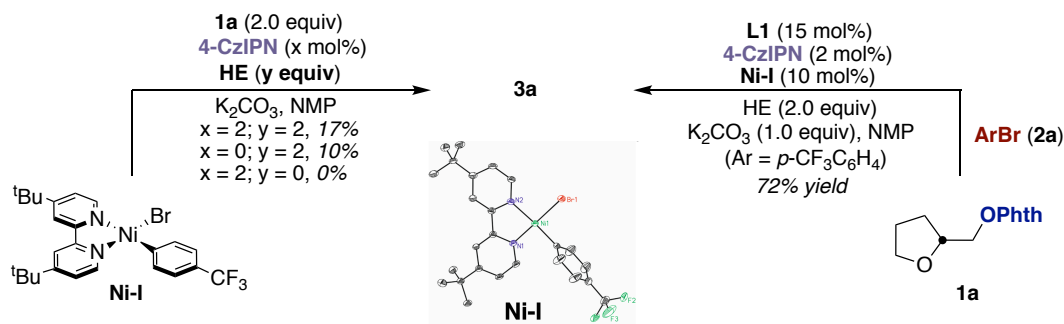


**Scheme 2.32** Indirect evidence for a carbon  $\beta$ -scission.

### 2.3.3.3 Stoichiometric Experiments of Oxidative Addition Complex Ni I

Stoichiometric experiments with the isolated oxidative addition complex (dtbbpy)Ni(Aryl)(Br) **I** and **1a** revealed that photocatalyst 4-CzIPN was not required to generate **3a** and that it could only be generated in the presence of HE (Scheme 2.33). These findings are consistent with our initial findings that a photocatalyst was not entirely required (Table 2.2. Entry 6), and that an EDA complex might be formed upon exposure of HE and **1a**. Importantly, however, the addition of 4-CzIPN improved the yield of these stoichiometric experiments, suggesting that its presence assists in the generation of the alkyl radical and fragmentation of the EDA complex. Consistent with **I** being an on-cycle intermediate, its utilization in catalytic amounts led to **3a** in 72% yield. In addition, stoichiometric Ni-**I** had a significant impact on the absorption of EDA complexes between HE and **1a** (See mechanistic experiments for detail).

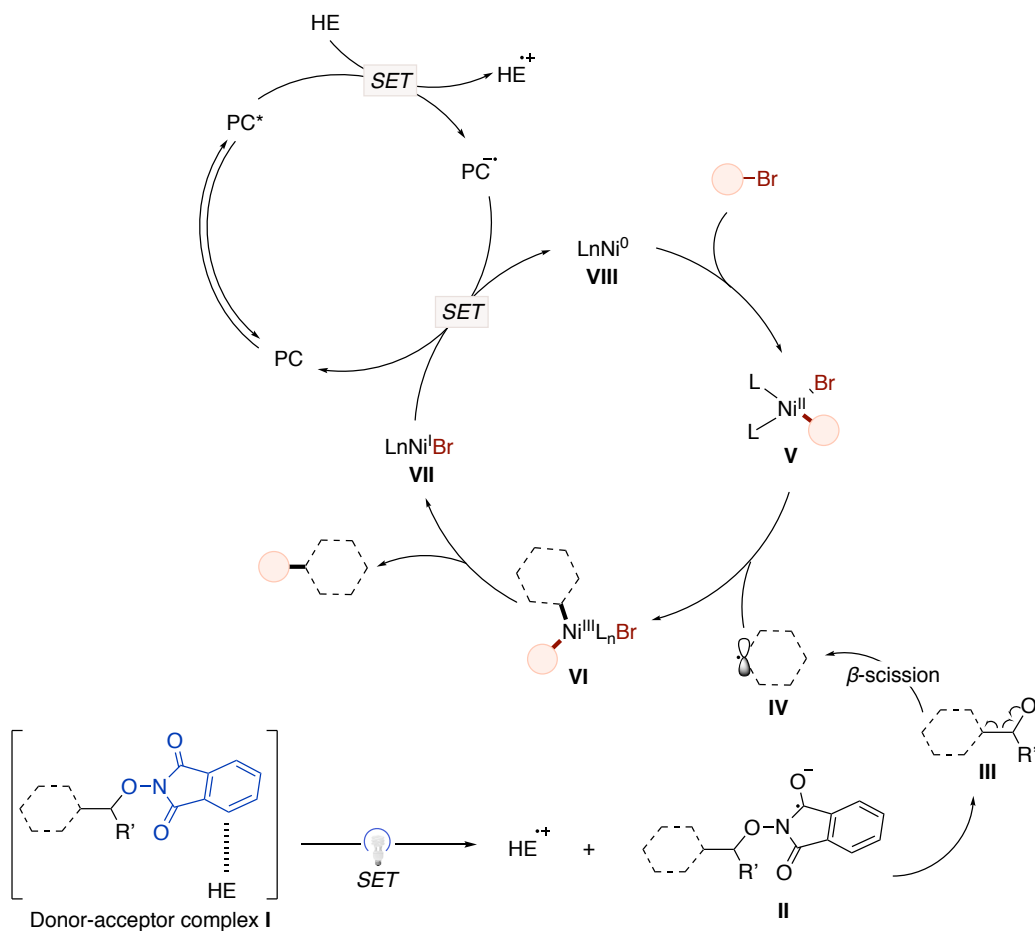
■ Experiments with well-defined oxidative addition species Ni-I



**Scheme 2.33** Stoichiometric experiments of oxidative addition complex Ni-I.

### 2.3.3.4 Mechanistic Proposal

Taken together, we propose that an electron donor-acceptor complex (**I**) between Hantzsch esters and *N*-alkoxyphthalimides is initially formed, which undergoes visible-light-induced electron transfer to give a *N*-alkoxyphthalimide radical anion (**II**) and HE<sup>•+</sup>. Collapse of **II** to eliminate phthalimide gives the alkoxy radical (**III**) which then undergoes  $\beta$ -scission to afford the aldehyde by-product and alkyl radical (**IV**). The latter can be intercepted by a Ni<sup>II</sup>-aryl/alkyl bromide intermediate (**V**), which upon reductive elimination from aryl-Ni<sup>III</sup>-alkyl species (**VI**) affords the desired cross-coupling product and Ni<sup>I</sup> (**VII**). At the same time, the ground-state of 4-CzIPN is promoted to the excited state of 4-CzIPN\* which oxidizes the HE, thus forming the reduced photocatalyst that ultimately promotes a SET reduction to recover back the propagating Ni<sup>0</sup> intermediates (**VIII**) within the catalytic cycle (Scheme 2.34).



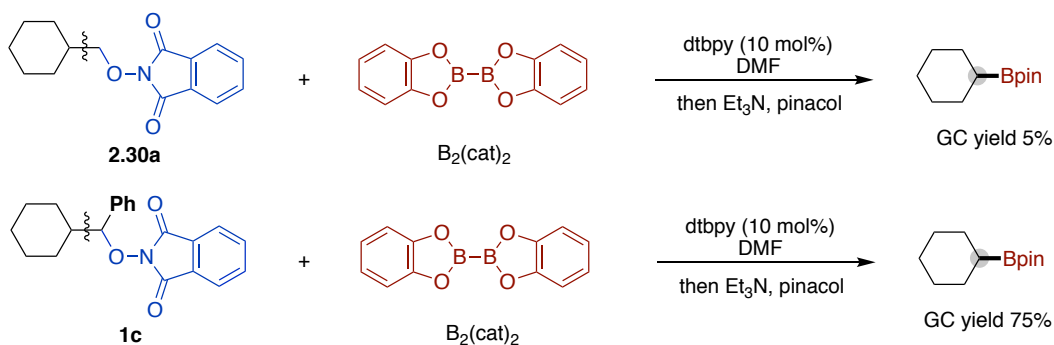
**Scheme 2.34** Proposed mechanism of the reaction.

## 2.4 Extended Research and Future outlook

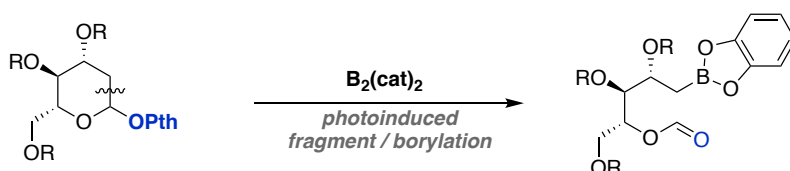
During the final stages of the project, we concluded that the formation of donor-acceptor (EDA) complexes could be applied to other reaction systems by using *N*-alkoxyphthalimides as electron acceptors. A close look into the literature data revealed that borylation reactions can be carried out under metal catalyst-free conditions by photoinduced electron transfer (PET) reactions using electron donor-acceptor (EDA) complexes formed between substrates and B<sub>2</sub>(cat)<sub>2</sub>. Therefore, we speculated that *N*-alkoxyphthalimides can form EDA complexes with B<sub>2</sub>(cat)<sub>2</sub> to initiate fragmentation borylation under similar conditions. We started our study by investigating the reaction of 1c with B<sub>2</sub>(cat)<sub>2</sub>, observing decent reactivity (Scheme 2.35, *top*). Unfortunately, during the process of this study, the Aggarwal group reported a similar method, and therefore this reaction was no longer pursued in our group (Scheme 2.35, *bottom*).<sup>83</sup> In the future, we will explore the possibility of enabling cascade-type reactions of 1,5-

hydrogen shifts<sup>78g</sup> as vehicles for triggering remote functionalization at distal positions within an alkyl side-chain.

■ Our extended research:



■ Similar method by the Aggarwal group:



**Scheme 2.35** Extended research on fragmentation borylation.

## 2.5 Conclusion

In summary, we have developed a catalytic manifold that utilizes dual nickel and photoredox catalysis as a vehicle to promote C–C bond-cleavage via  $\beta$ -scission events. The reaction operates under mild conditions, showcases excellent functional group compatibility and a wide substrate scope, including the utilization of saccharide derivatives. The methodology was amenable to a variety of linear, cyclic, and bridged alcohols which constitute a significant step forward in the functionalization of aliphatic alcohols in the context of medicinal chemistry programs.



---

## 2.6 References

1. (a) Netherton, M. R.; Fu, G. C. Nickel-catalyzed cross-couplings of unactivated alkyl halides and pseudohalides with organometallic compounds. *Adv. Synth. Catal.* **2004**, *346*, 1525. (b) Phapale, V. B.; Cardenas, D. J. Nickel-catalysed Negishi cross-coupling reactions: scope and mechanisms. *Chem. Soc. Rev.* **2009**, *38*, 1598. (c) Jana, R.; Pathak, T. P.; Sigman, M. S. Advances in transition metal (Pd, Ni, Fe)-catalyzed cross-coupling reactions using alkyl-organometallics as reaction partners. *Chem. Rev.* **2011**, *111*, 1417. (d) Meijere, A. D.; Bräse, S.; Oestreich, M. Metal-catalyzed cross-coupling reactions and more; Wiley-VCH: Weinheim, Germany, **2014**. (e) Chen, Z.; Rong, M.-Y.; Nie, J.; Zhu, X.-F.; Shi, B.-F.; Ma, J.-A. Catalytic alkylation of unactivated C(sp<sup>3</sup>)-H bonds for C(sp<sup>3</sup>)-C(sp<sup>3</sup>) bond formation. *Chem. Soc. Rev.* **2019**, *48*, 4921.
2. (a) Shi, W.; Liu, C.; Lei, A. Transition-metal catalyzed oxidative cross-coupling reactions to form C-C bonds involving organometallic reagents as nucleophiles. *Chem. Soc. Rev.* **2011**, *40*, 2761. (b) Handbook of functionalized organometallics (Ed.: P. Knöchel) Wiley-VCH, Weinheim (Germany), **2005**. (c) The manipulation of air-sensitive compounds, 2nd ed. (Eds.: D. F. Shriver, M. A. Drezdson), Wiley, New York (USA), **1986**.
3. (a) Choi, J.; Fu, G. C. Transition metal-catalyzed alkyl-alkyl bond formation: another dimension in cross-coupling chemistry. *Science* **2017**, *356*, 152. (b) Rudolph, A.; Lautens, M. Secondary alkyl halides in transition-metal-catalyzed cross-coupling reactions. *Angew. Chem. Int. Ed.* **2009**, *48*, 2656.
4. Selected reviews on cross-electrophile coupling: (a) Gu, J.; Wang, X.; Xue, W.; Gong, H. Nickel-catalyzed reductive coupling of alkyl halides with other electrophiles: Concept and mechanistic considerations. *Org. Chem. Front.* **2015**, *3*, 1411. (b) Knappke, C. E. I.; Grupe, S.; Gärtner, D.; Corpet, M.; Gosmini, C.; Jacobi von Wangelin, A. Reductive cross-coupling reactions between two electrophiles. *Chem. - Eur. J.* **2014**, *20*, 6828. (c) Weix, J. D. Methods and mechanisms for cross-electrophile coupling of Csp<sup>2</sup> halides with alkyl electrophiles. *Acc. Chem. Res.* **2015**, *48*, 1767. (d) Moragas, T.; Correa, A.; Martin, R. Metal-catalyzed reductive coupling reactions of organic halides with carbonyl-type compounds. *Chem. - Eur. J.* **2014**, *20*, 8242.

- 
5. Selected reviews on  $sp^3$  C–C bond formation: (a) Luh, T. Y.; Leung, M. K.; Wong, K. T. Transition metal-catalyzed activation of aliphatic C–X bonds in carbon–carbon bond formation. *Chem. Rev.* **2000**, *100*, 3187. (b) Kambe, N.; Iwasakia, T.; Terao, J. Pd-catalyzed cross-coupling reactions of alkyl halides. *Chem. Soc. Rev.*, **2011**, *40*, 4937. (c) Frisch, A. C.; Beller, M. Catalysts for cross-coupling reactions with non-activated alkyl halides. *Angew. Chem., Int. Ed.*, **2005**, *44*, 674. (d) Molander, G.; Milligan, J. A.; Phelan, J. P.; Badir, S. O. Recent advances in alkyl carbon-carbon bond formation by nickel/photoredox cross-coupling. *Angew. Chem. Int. Ed.*, **2019**, *58*, 6152. (e) Hu, X. Nickel-catalyzed cross-coupling of non-activated alkyl halides: A mechanistic perspective. *Chem. Sci.* **2011**, *2*, 1867.
  6. Everson, D. A.; Shrestha, Ruja; Weix, D. J. Nickel-catalyzed reductive cross-coupling of aryl halides with alkyl halides. *J. Am. Chem. Soc.* **2010**, *132*, 920.
  7. (a) Diccianni, J. B.; Diao, T. Mechanisms of nickel-catalyzed cross-coupling reactions. *Trends Chem.* **2019**, *1*, 830. (b) Diccianni, J. B.; Lin, Q.; Diao, T. Mechanisms of nickel-catalyzed coupling reactions and applications in alkene functionalization. *Acc. Chem. Res.* **2020**, *53*, 906.
  8. For selected reviews on C–O cleavage: (a) Zeng, H.; Qiu, Z.; Dominguez-Huerta, A.; Hearne, Z.; Chen, Z.; Li, C. J. An Adventure in sustainable cross-coupling of phenols and derivatives via carbon–oxygen bond cleavage. *ACS Catal.* **2017**, *7*, 510. (b) Zarate, C.; Van Gemmeren, M.; Somerville, R. J.; Martin, R. Phenol derivatives: Modern electrophiles in cross-coupling reactions. *Adv. Organomet. Chem.* **2016**, *66*, 143. (c) Tobisu, M.; Chatani, N. Cross-couplings using aryl ethers via C–O bond activation enabled by nickel catalysts. *Acc. Chem. Res.* **2015**, *48*, 1717. (d) Tollefson, E. J.; Hanna, L. E.; Jarvo, E. R. Stereospecific nickel-catalyzed cross-coupling reactions of benzylic ethers and esters. *Acc. Chem. Res.* **2015**, *48*, 2344.
  9. For selected reviews on C–N cleavage: (a) Kong, Duanyang.; Moon, P. J.; Lundgren, R. J. Radical coupling from alkyl amines. *Nature Catalysis* **2019**, *2*, 473. (b) Correia, J. T. M.; Fernandes, V. A.; Matsuo, B. T.; Delgado, J. A. C.; de Souza, W. C., Paixão, W. Photoinduced deaminative strategies: Katritzky salts as alkyl radical precursors. *Chem. Commun.* **2020**, *56*, 503.
  10. For selected examples of catalytic deamination of alkyl amines: (a) Plunkett, S.; Basch, C. H.; Santana, S. O.; Watson, M. P. Harnessing alkylpyridinium salts as electrophiles in deaminative alkyl–alkyl cross-couplings. *J. Am. Chem. Soc.* **2019**,

- 
- 141, 2257. (d) R. Martin-Montero, V. R. Yatham, H. Yin, R. Martin, Ni-catalyzed reductive deaminative arylation at  $sp^3$  carbon centers. *Org. Lett.* **2019**, *21*, 29471.
- (e) Basch, C. H.; Liao, J.; Watson, M. P. Harnessing Alkyl amines as electrophiles for nickel-catalyzed cross Couplings via C–N bond activation. *J. Am. Chem. Soc.* **2017**, *139*, 5313.
11. For selected reviews on  $sp^3$  C–H bond-functionalization: (a) Chu, J. C. K.; Rovis, T. Complementary strategies for directed C( $sp^3$ )–H functionalization: A comparison of transition-metal-catalyzed activation, hydrogen atom transfer and carbene/nitrene transfer. *Angew. Chem. Int. Ed.* **2018**, *57*, 62. (b) He, J.; Wasa, M.; Chan, K. S. L.; Shao, Q.; Yu, J-Q. Palladium-catalyzed transformations of alkyl C – H bonds. *Chem. Rev.* **2017**, *117*, 8754. (c) Wang, B.; Qiu, D.; Zhang, Y.; Wang, J. Recent advances in C( $sp^3$ )–H bond functionalization via metal-carbene insertions. *Beilstein J. Org. Chem.* **2016**, *12*, 796. (d) Davies, H. M. L.; Morton, D. Recent advances in C–H functionalization. *J. Org. Chem.* **2016**, *81*, 343.
12. For selected reviews on  $sp^3$  C–C bond-cleavage: (a) Morcillo, S. P. Radical-promoted C–C bond cleavage: A deconstructive approach for selective functionalization. *Angew. Chem., Int. Ed.* **2019**, *58*, 14044. (b) Nairoukh, Z.; Cormier, M.; Marek, I. Merging C–H and C–C bond cleavage in organic synthesis. *Nat. Rev. Chem.* **2017**, *1*, 0035. (c) Souillart, L.; Cramer, N. Catalytic C–C bond activations via oxidative addition to transition metals. *Chem. Rev.* **2015**, *115*, 9410. (d) Fumagalli, G.; Stanton, S.; Bower, J. F. Recent methodologies that exploit C–C single-bond cleavage of strained ring systems by transition metal complexes. *Chem. Rev.* **2017**, *117*, 9404.
13. Selected references on Pd-catalyzed cross-couplings:(a) Johansson Seechurn, C. C. C.; Kitching, M. O.; Colacot, T. J.; Snieckus, V. Palladium-catalyzed cross-coupling: A historical contextual perspective to the 2010 Nobel Prize. *Angew. Chem., Int. Ed.* **2012**, *51*, 5062. (b) De Meijere, A.; Diederich, F. Metal-catalyzed cross-coupling reactions; Wiley-VCH: Weinheim, **2004**. (c) Krasovskiy, A.; Duplais, C.; Lipshutz, B. H. Stereoselective Negishi-like Couplings Between Alkenyl and Alkyl Halides in Water at Room Temperature. *Org. Lett.* **2010**, *12*, 4742.
14. Xu, H. W.; Hu, C. T.; Wang, X.; Diao, T. Structural characterization of  $\beta$ -Agostic bonds in Pd-catalyzed polymerization. *Organometallics* **2017**, *36*, 4099.
15. (a) Tamaru, Y. (ed.) Modern Organonickel Chemistry (Wiley-VCH, 2005). (b) Lin, C-Y.; Power, P. P. Complexes of Ni(I): A “Rare” oxidation state of growing

- 
- importance. *Chem. Soc. Rev.* **2017**, *46*, 5347. (c) Zheng, B.; Tang, F.; Luo, J.; Schultz, J. W.; Rath, N. P.; Mirica, L. M. Organometallic nickel(III) complexes relevant to cross-coupling and carbon–heteroatom bond formation reactions. *J. Am. Chem. Soc.* **2014**, *136*, 6499.
16. (a) Leatherman, M. D.; Svejda, S. A.; Johnson, L. K.; Brookhart, M. Mechanistic studies of nickel(II) alkyl agostic cations and alkyl ethylene complexes: investigations of chain propagation and isomerization in (a-Diimine)Ni(II)-catalyzed ethylene polymerization. *J. Am. Chem. Soc.* **2003**, *125*, 3068. (b) Xu, H.W.; White, P. B.; Hu, C. T.; Diao, T. Structure and isotope Effects of The  $\beta$ -H Agostic (a-Diimine)nickel cation as A polymerization intermediate. *Angew. Chem. Int. Ed.* **2017**, *56*, 1535.
17. Tasker, S. Z.; Standley, E. A.; Jamison, T. F. Recent advances in homogeneous nickel catalysis. *Nature* **2014**, *509*, 299.
18. Biswas, S.; Weix, D. J. Mechanism and selectivity in nickel catalyzed cross-electrophile coupling of aryl halides with alkyl halides. *J. Am. Chem. Soc.* **2013**, *135*, 16192.
19. Everson, D.A.; Weix, D.J. Cross- electrophile coupling: principles of reactivity and selectivity. *J. Org. Chem.* **2014**, *79*, 4793.
20. (a) Zhao, Y.; Weix, D. J. Enantioselective cross-coupling of meso-epoxides with aryl halides. *J. Am. Chem. Soc.* **2015**, *137*, 3237. (b) Zhao, Y.; Weix, D. J. Nickel-catalyzed regiodivergent opening of epoxides with aryl halides: Co-catalysis controls regioselectivity. *J. Am. Chem. Soc.* **2014**, *136*, 481.
21. Woods, B. P.; Orlandi, M.; Huang, C.-Y.; Sigman, M. S.; Doyle, A. G. Nickel-catalyzed enantioselective reductive cross-coupling of styrenyl aziridines. *J. Am. Chem. Soc.* **2017**, *139*, 5688.
22. Wang, J.; Zhao, J.; Gong, H. Nickel-catalyzed methylation of aryl halides/tosylates with methyl tosylate. *Chem. Commun.* **2017**, *53*, 10180.
23. (a) Ackerman, L.K.G.; Anka-Lufford, L. L.; Naodovic, M.; Weix, D. J. Cobalt co-catalysis for cross-electrophile coupling: diarylmethanes from benzyl mesylates and aryl halides. *Chem. Sci.* **2015**, *6*, 1115. (b) Hughes, J. M. E.; Fier, P. S. Desulfonylative arylation of redox-active alkyl sulfones with aryl bromides. *Org. Lett.* **2019**, *21*, 5650.
24. Huihui, K. M. M.; Caputo, J. A.; Melchor, Z.; Olivares, A. M.; Spiewak, A. M.; Johnson, K. A.; DiBenedetto, T. A.; Kim, S.; Ackerman, L. K. G.; Weix, D. J.

- 
- Decarboxylative cross-electrophile coupling of N-hydroxyphthalimide esters with aryl iodides. *J. Am. Chem. Soc.* **2016**, *138*, 5016.
25. (a) Gao, M.; Sun, D.; Gong, H. Ni-catalyzed reductive C–O bond arylation of oxalates derived from  $\alpha$ -hydroxy esters with aryl halides. *Org. Lett.* **2019**, *21*, 1645. (b) Ye, Y.; Chen, H.; Sessler, J. L.; Gong, H. Zn-mediated fragmentation of tertiary alkyl oxalates enabling formation of alkylated and arylated quaternary carbon centers. *J. Am. Chem. Soc.* **2019**, *141*, 820.
26. Cornella, J.; Edwards, J.; Qin, T.; Kawamura, S.; Wang, J.; Pan, C.-M.; Gianatassio, R.; Schmidt, M.; Eastgate, M. D.; Baran, P. S. Practical Ni-catalyzed aryl–alkyl cross-coupling of secondary redox-active esters. *J. Am. Chem. Soc.* **2016**, *138*, 2174.
27. Huang, L.; Olivares, A. M.; Weix, D. J. Reductive decarboxylative alkynylation of N-hydroxyphthalimide esters with bromoalkynes. *Angew. Chem. Int. Ed.* **2017**, *56*, 11901.
28. Wang, J.; Cary, B. P.; Beyer, P.; Gellman, S. H.; Weix, D. J. Ketones from Nickel-catalyzed decarboxylative, Non-symmetric cross-electrophile coupling of carboxylic acid esters. *Angew. Chem. Int. Ed.* **2019**, *58*, 12081.
29. Suzuki, N.; Hofstra, J. L.; Poremba, K. E.; Reisman, S. E. Nickel-catalyzed enantioselective cross-coupling of N-hydroxyphthalimide esters with vinyl bromides. *Org. Lett.* **2017**, *19*, 2150.
30. (a) Lide, D. R. Handbook of Chemistry and Physics. CRC Press, **2003**. (b) Bajo, S.; Laidlaw, G.; Kennedy, A. R.; Stephen Sproules, O. O.; Nelson, D. J.; Oxidative addition of aryl electrophiles to a prototypical nickel(0) complex: mechanism and structure/reactivity relationships. *Organometallics* **2017**, *36*, 1662.
31. Kharasch, M. S.; Hambling, J. K.; Rudy, T. P. Reactions of atoms and free radicals in solution. XL. Reaction of grignard reagents with 1-bromooctane in the presence of cobaltous bromide. *J. Org. Chem.* 1959, *24*, 303.
32. (a) Qin, T.; Cornella, J.; Li, Chao.; Malins, L. R.; Edwards, J. T.; Kawamura, S.; Maxwell, B. D.; Eastgate, M. D.; Baran, P. S. A general alkyl–alkyl cross-coupling enabled by redox-active esters and alkylzinc reagents. *Science* **2016**, *352*, 6287.
33. Yu, X.; Yang, T.; Wang, S.; Xu, H.; Gong, H. Nickel-catalyzed reductive cross-coupling of unactivated alkyl halides. *Org. Lett.* **2011**, *14*, 2138.
34. Xu, H.; Zhao, C.; Qian, Q.; Deng, W.; Gong, H. Nickel-catalyzed cross-coupling of unactivated alkyl halides using bis(pinacolato)diboron as reductant. *Chem. Sci.* **2013**, *4*, 4022.

- 
35. (a) Luo, J.; Zhang J. Donor–acceptor fluorophores for visible-light-promoted organic synthesis: Photoredox/Ni dual catalytic C(sp<sup>3</sup>)–C(sp<sup>2</sup>) cross-coupling *ACS Catal.* **2016**, *6*, 873. (b) N.A. Romero, D. A. Nicewicz, Organic photoredox catalysis. *Chem. Rev.* **2016**, *116*, 10075. (c) Shaw, M. H.; Twilton, J.; MacMillan, D. W. C. Photoredox catalysis in organic chemistry. *J. Org. Chem.* **2016**, *81*, 6898. (d) Prier, C. K.; Rankic, D.A.; MacMillan, D.W.C. Metallaphotoredox: The merger of photoredox and transition metal catalysis. *Chem. Rev.* **2013**, *113*, 5322.
36. Chan, A.Y.; Perry, I. B.; Bissonnette, N. B.; Buksh, B. F.; Edwards, G.A.; Frye, L. I.; Garry, O. L.; Lavagnino, M.; N. Li, B. X.; Liang, Y.; Mao, E.; Millet, A.; Oakley, J. V.; Reed, N. L.; Sakai, H. A.; Seath, C. P.; MacMillan, D. W. C. *Chem. Rev.* **2022**, *122*, 1485.
37. Yan, M.; Lo, J. C.; Edwards, J. T.; Baran, P. S. Radicals: Reactive intermediates with translational potential. *J. Am. Chem. Soc.* **2016**, *138*, 12692.
38. Gutierrez, O.; Tellis, J. C.; Primer, D. N.; Molander, G. A.; Kozlowski, M. C. Nickel-catalyzed cross-coupling of photoredox-generated radicals: Uncovering a general manifold for stereo-convergence in nickel-catalyzed cross-couplings. *J. Am. Chem. Soc.* **2015**, *137*, 4896.
39. (a) Zuo, Z.; MacMillan, D. W. C. Decarboxylative arylation of  $\alpha$ -amino acids via photoredox catalysis: A one-step conversion of biomass to drug pharmacophore. *J. Am. Chem. Soc.* **2014**, *136*, 5257. (b) Chu, L.; Ohta, C.; Zuo, Z.; MacMillan, D. W. C. Carboxylic acids as a traceless activation group for conjugate additions. *J. Am. Chem. Soc.* **2014**, *136*, 10886. (c) Ventre, S.; Petronijevic, F. R.; MacMillan, D. W. C. Decarboxylative fluorination of aliphatic carboxylic acids via photoredox catalysis. *J. Am. Chem. Soc.* **2015**, *137*, 5654.
40. Kaga, A.; Chiba, Shunsuke. Engaging radicals in transition metal-catalyzed cross-coupling with alkyl electrophiles: Recent advances. *ACS Catal.* **2017**, *7*, 4697.
41. Matsui, J. K.; Lang, S. B.; Heitz, D. R.; Molander, G. A. Photoredox-mediated routes to radicals: The value of catalytic radical generation in synthetic methods development. *ACS Catal.* **2017**, *7*, 2563.
42. (a) Molander, G. A.; Ellis, N. Organotrifluoroborates: Protected boronic acids that expand the versatility of the Suzuki coupling reaction. *Acc. Chem. Res.* **2007**, *40*, 275. (b) El Khatib, M.; Serafim, R. A. M.; Molander, G. A.  $\alpha$ -Arylation/heteroarylation of chiral  $\alpha$ -aminomethyltrifluoroborates by synergistic iridium photoredox/nickel cross-coupling catalysis. *Angew. Chem., Int. Ed.* **2016**, *55*, 254.

- 
- (c) Tellis, J. C.; Amani, J.; Molander, G. A. Single-electron transmetalation: photoredox/nickel dual catalytic cross-coupling of secondary alkyl  $\beta$ -trifluoroboratoketones and -esters with aryl bromides. *Org. Lett.* **2016**, *18*, 2994. (d) Lima, F.; Kabeshov, M. A.; Tran, D. N.; Battilocchio, C.; Sedelmeier, J.; Sedelmeier, G.; Schenkel, B.; Ley, S. V. Visible light activation of boronic esters enables efficient photoredox C(sp<sup>2</sup>)-C(sp<sup>3</sup>) cross-couplings in flow. *Angew. Chem., Int. Ed.* **2016**, *55*, 14085.
43. (a) Chatgililoglu, C. Organosilanes in radical chemistry. John Wiley & Sons, Ltd, **2004**. (b) Levéque, C.; Chenneberg, L.; Corce, V.; Ollivier, C.; Fensterbank, L. Organic photoredox catalysis for the oxidation of silicates: applications in radical synthesis and dual catalysis. *Chem. Commun.* **2016**, *52*, 9877. (c) Corce, V.; Chamoreau, L.-M.; Derat, E.; Goddard, J.-P.; Ollivier, C.; Fensterbank, L. Silicates as latent alkyl radical precursors: visible-light photocatalytic oxidation of hypervalent bis-catecholato silicon compounds. *Angew. Chem., Int. Ed.* **2015**, *54*, 11414. (d) Levéque, C.; Chenneberg, L.; Corce, V.; Goddard, J.-P.; Ollivier, C.; Fensterbank, L. Primary alkyl bis-catecholato silicates in dual photoredox/nickel catalysis: aryl-and heteroaryl-alkyl cross coupling reactions. *Org. Chem. Front.* **2016**, *3*, 462.
44. (a) Twilton, J.; Le, C.; Zhang, P.; Shaw, M. H.; Evans, R. W.; MacMillan, D. W. C. The merger of transition metal and photocatalysis. *Nat. Rev. Chem.* **2017**, *1*, 0052.
45. Tellis, J. C.; Primer, D. N.; Molander, G. A. Single-electron transmetalation in organoboron cross-coupling by photoredox/nickel dual catalysis. *Science* **2014**, *345*, 433.
46. Jouffroy, M.; Primer, D. N.; Molander, G. A. Base-free photoredox/nickel dual-catalytic cross-coupling of ammonium alkylsilicates. *J. Am. Chem. Soc.*, **2016**, *138*, 475.
47. Zhang, P.; Le, C. C.; MacMillan, D. W. C. Silyl radical activation of alkyl Halides in metallaphotoredox catalysis: A unique pathway for cross-electrophile coupling. *J. Am. Chem. Soc.* **2016**, *138*, 8084
48. Duan, Z.; Li, W.; Lei, A. Nickel-catalyzed reductive cross-coupling of aryl bromides with alkyl bromides: Et<sub>3</sub>N as the terminal reductant. *Org. Lett.* **2016**, *18*, 4012.

- 
49. Yi, J.; Badir, S. O.; Kammer, L. M.; Ribagorda, M.; Molander, G. A. Deaminative reductive arylation enabled by nickel/photoredox dual catalysis. *Org. Lett.*, **2019**, *21*, 3346.
50. Heitz, D. R.; Tellis, J. C.; Molander, G. A. Photochemical nickel-catalyzed C–H arylation: synthetic scope and mechanistic investigations. *J. Am. Chem. Soc.* **2016**, *138*, 12715.
51. Shields, B. J.; Doyle, A. G. Direct C(sp<sup>3</sup>)–H cross coupling enabled by catalytic generation of chlorine radicals. *J. Am. Chem. Soc.* **2016**, *138*, 12719.
52. Shaw, M. H.; Shurtleff, V. W.; Terrett, J. A.; Cuthbertson, J. D.; MacMillan, D. W. Native functionality in triple catalytic cross-coupling: sp<sup>3</sup> C–H bonds as latent nucleophiles. *Science* **2016**, *352*, 1304.
53. Perry, I. B.; Brewer, T. F.; Sarver, P. J.; Schultz, D.; Rocco, M.; MacMillan, D. W. C. Direct arylation of strong aliphatic C–H bonds. *Nature* **2018**, *560*, 70.
54. Shen, Y.; Gu, Y.; Martin, R. Sp<sup>3</sup> C–H arylation and alkylation enabled by the synergy of triplet excited ketones and nickel catalysts. *J. Am. Chem. Soc.* **2018**, *140*, 12200.
55. Qin, Q.; Jiang, H.; Hu, Z.; Ren, D.; Yu, S. Functionalization of C–H bonds by photoredox catalysis. *Chem. Rec.* **2017**, *17*, 754.
56. Zuo, Z.; Ahneman, D. T.; Chu, L.; Terrett, J. A.; Doyle, A. G.; MacMillan, D. W. C. Merging photoredox with nickel catalysis: Coupling of  $\alpha$ -carboxyl sp<sup>3</sup>-carbons with aryl halides. *Science* **2014**, *345*, 437.
57. Johnston, C. P.; Smith, R. T.; Allmendinger, S.; MacMillan, D. W. C. Metallaphotoredox-catalysed sp<sup>3</sup>–sp<sup>3</sup> cross-coupling of carboxylic acids with alkyl halides. *Nature* **2016**, *536*, 322.
58. Bhunia, A.; Studer, A. Recent advances in radical chemistry proceeding through pro-aromatic radicals. *Chem* **2021**, *7*, 2060.
59. Wang, P.; Chen, J.; Xiao, W. Hantzsch esters: an emerging versatile class of reagents in photoredox catalyzed organic synthesis. *Org. Biomol. Chem.* **2019**, *17*, 6936.
60. Dumoulin, A.; Matsui, J. K.; Gutierrez-Bonet, A.; Molander, G. A. Synthesis of non-classical arylated C-saccharides through nickel/photoredox dual catalysis. *Angew. Chem. Int. Ed.* **2018**, *57*, 6614.
61. Dumoulin, A.; Matsui, J. K.; Gutierrez-Bonet, A.; Molander, G. A. Synthesis of reversed C-acyl glycosides through Ni/photoredox dual catalysis. *Angew. Chem. Int. Ed.* **2018**, *57*, 6614.



- 
62. Henkel, T.; Brunne, R. M.; Müller, H.; Reichel, F. Statistical investigation into the structural complementarity of natural products and synthetic compounds. *Angew. Chem., Int. Ed.* **1999**, *38*, 643.
63. (a) Ertl, P.; Schuhmann, T. A Systematic cheminformatics analysis of functional groups occurring in natural products. *J. Nat. Prod.* **2019**, *82*, 1258. (b) Ertl, P. An algorithm to identify functional groups in organic molecules. *J. Cheminformatics* **2017**, *9*, 36.
64. (a) Suga, T.; Ukaji, Y. Nickel-catalyzed cross-electrophile coupling between benzyl alcohols and aryl halides assisted by Titanium Co-reductant. *Org. Lett.* **2018**, *20*, 7846. (b) Ertl, P.; Schuhmann, T. A systematic cheminformatics analysis of functional groups occurring in natural products. *J. Nat. Prod.* **2019**, *82*, 1258. (c) Jia, X-G.; Guo, P.; Duan, J.; Shu, X-Z. Dual nickel and Lewis acid catalysis for cross-electrophile coupling: the allylation of aryl halides with allylic alcohols. *Chem. Sci.* **2018**, *9*, 640. (d). Guo, P.; Wang, Ke.; Jin, W-J.; Xie, H.; Qi, L.; Liu, X-Y.; Shu, X-Z. Dynamic kinetic cross-electrophile arylation of benzyl alcohols by nickel catalysis. *J. Am. Chem. Soc.* **2021**, *143*, 513.
65. (a) Li, Z.; Sun, W.; Wang, X.; Li, L.; Zhang, Y.; Li, C. Electrochemically enabled, nickel-catalyzed dehydroxylative cross-coupling of alcohols with aryl halides. *J. Am. Chem. Soc.* **2021**, *143*, 3536. (b). Barton, D. H. R.; McCombie, S. W. A new method for the deoxygenation of secondary alcohols. *J. Chem. Soc., Perkin Trans. I.* **1975**, *16*, 1574. (c) Zhang, L.; Koreeda, M. Radical deoxygenation of hydroxyl groups via phosphites. *J. Am. Chem. Soc.* **2004**, *126*, 13190. (d) Vara, B. A., Patel, N. R. & Molander, G. A. O-Benzyl xanthate esters under Ni/Photoredox dual catalysis: Selective radical generation and  $Csp^3 - Csp^2$ . *ACS Catal.* **2017**, *7*, 3955.
66. Pedley, J. B.; Naylor, R. D.; Kirby, S. P. In *Thermochemical Data of Organic Compounds*, 2nd ed.; Chapman and Hall: New York, **1986**.
67. (a) Levia, S. M.; Lia, Q.; Röthelia A. R.; Jacobsenand, E. N. Catalytic activation of glycosyl phosphates for stereoselective coupling reactions. *PNAS* **2019**, *116*, 35. (b) Tros, B. M.; Czabaniuk, L. C. Benzylic phosphates as electrophiles in the palladium-catalyzed asymmetric benzylation of azlactones. *J. Am. Chem. Soc.* **2012**, *134*, 5778.
68. Cornella, J.; Zarate, C.; Martin, R. Metal-catalyzed activation of ethers via C–O bond cleavage: a new strategy for molecular diversity. *Chem. Soc. Rev.*, **2014**, *43*, 8081.

- 
69. Quiclet-Sire, B.; Zard, S. Z. Some aspects of the radical chemistry of xanthates. *Chimia* **2012**, *66*, 404.
70. Nawrat, C. C.; Jamison, C. R.; Slutskyy, Y.; MacMillan, D. W. C.; Overman, L. E. Oxalates as activating groups for alcohols in visible light photoredox catalysis: Formation of quaternary centers by redox-neutral fragment coupling. *J. Am. Chem. Soc.* **2015**, *137*, 11270.
71. Komeyama, K.; Michiyuki, T.; Osaka, I. Nickel/Cobalt-catalyzed C(sp<sup>3</sup>)-C(sp<sup>3</sup>) cross-coupling of alkyl halides with alkyl tosylates. *ACS Catal.* **2019**, *9*, 9285.
72. Barton, D. H. R.; Crich, D. The invention of new radical chain reactions. Part 9. further radical chemistry of thiohydroxamic esters; Formation of carbon-carbon bonds. *J. Chem. Soc., Perkin Trans.* **1986**, *1*, 1603.
73. Zhang, X.; MacMillan, D. W. C. Alcohols as latent coupling fragments for metallaphotoredox catalysis: sp<sup>3</sup>-sp<sup>2</sup> cross-coupling of oxalates with aryl halides. *J. Am. Chem. Soc.* **2016**, *138*, 13862.
74. Vara, B. A.; Patel, N. R.; Molander, G. A. O-Benzyl xanthate esters under Ni/Photoredox dual catalysis: Selective radical generation and Csp<sup>3</sup>-Csp<sup>2</sup> cross-coupling. *ACS Catal.* **2017**, *7*, 3955.
75. (a) Wei, Y.; Ben-zvi, B.; Diao, T. Diastereoselective synthesis of aryl C-glycosides from glycosyl esters via C-O bond homolysis. *Angew. Chem. Int. Ed.* **2021**, *60*, 9433. (b) Wei, Y.; Lam, J.; Diao, T. Synthesis of C-acyl furanosides via the cross-coupling of glycosyl esters with carboxylic acids. *Chem. Sci.* **2021**, *12*, 11414.
76. Dong, Z.; MacMillan, D. W. C. Metallaphotoredox-enabled deoxygenative arylation of alcohols. *Nature* **2021**, *598*, 451.
77. (a) Yorimitsu, H.; Oshima, K. Catalytic processes involving  $\beta$ -Carbon Elimination. *Bull. Chem. Soc. Jpn.* **2009**, *82*, 778. (b) Murakami, M.; Makino, M.; Ashida, S.; Matsuda, T. Construction of carbon frameworks through  $\beta$ -carbon elimination mediated by transition metals. *Bull. Chem. Soc. Jpn.* **2006**, *79*, 1315. (c) Zhu, Jun.; Xue, Yi.; Zhang, R.; Ratchford, B. L. Dong, G. Catalytic activation of unstrained C(Aryl)-C(Alkyl) bonds in 2,2'-methylenediphenols. *J. Am. Chem. Soc.* **2022**, *144*, 3242. (d) Zhao, P.; Incarvito, C. D.; Hartwig, J. F. Direct observation of  $\beta$ -aryl eliminations from Rh (I) alkoxides. *J. Am. Chem. Soc.* **2006**, *128*, 3124. (e) Zhao, P.; Hartwig, J. F. Insertions of ketones and nitriles into organorhodium(I) complexes and  $\beta$ -hydrocarbyl eliminations from Rhodium(I) alkoxo and iminyl complexes. *Organometallics* **2008**, *27*, 4749.

- 
78. For selected review articles on alkoxy radicals (a) Gray, P.; Williams, A. The thermochemistry and reactivity of alkoxy radicals. *Chem. Rev.* **1959**, *59*, 239. (b) Murakami, Masahiro.; Ishida, Naoki.  $\beta$ -Scission of alkoxy radicals in synthetic transformations. *Chem. Lett.* **2017**, *46*, 1692. (c) Wu, X.; Zhu, C. Recent advances in alkoxy radical-promoted C–C and C–H bond functionalization starting from free alcohols. *Chem. Commun.* **2019**, *55*, 9747. (d) Guo, J.; Hu, A.; Zuo, Z. Photocatalytic alkoxy radical-mediated transformations. *Tet. Lett.* **2018**, *59*, 2103. (e) Jia, K.; Chen, Y. Visible-light-induced alkoxy radical generation for inert chemical bond cleavage/functionalization. *Chem. Commun.* **2018**, *54*, 6105. (f) Tsui, E.; Wang, H.; Knowles, R. R. Catalytic generation of alkoxy radicals from unfunctionalized alcohols. *Chem. Sci.* **2020**, *11*, 11124. (g) Chang, L.; An, Qing.; Duan, L.; Feng, K.; Zuo, Z. Alkoxy radicals see the light: New paradigms of photochemical synthesis. *Chem. Rev.* **2022**, *122*, 2429.
79. Wilsey, S.; Dowd, P.; Houk, K. N. Effect of alkyl substituents and ring size on alkoxy radical cleavage reactions. *J. Org. Chem.* **1999**, *64*, 8801.
80. Huang, L.; Ji, T.; Rueping, M. Remote nickel-catalyzed cross-coupling arylation via proton-coupled electron transfer-enabled C–C bond cleavage. *J. Am. Chem. Soc.* **2020**, *142*, 3532.
81. Yayla, H. G.; Wang, H.; Tarantino, K. T.; Orbe, H. S.; Knowles, R. R. Catalytic ring-opening of cyclic alcohols enabled by PCET activation of strong O–H bonds. *J. Am. Chem. Soc.* **2016**, *138*, 10794.
82. (a) Litwinienko, G. A. L.; Beckwith, J.; Ingold, K. U. The frequently overlooked importance of solvent in free radical syntheses. *Chem. Soc. Rev.*, **2011**, *40*, 2157. (b) Tsentalovich, Y. P.; Kulik, L. V.; Gritsan, N. P.; Yurkovskaya, A. V. Solvent effect on the rate of  $\beta$ -scission of the tert-butoxy radical. *J. Phys. Chem. A.* **1998**, *102*, 7975. (c) Akisaka, R.; Ohga, Y.; Abe, M. Dynamic solvent effects in radical–radical coupling reactions: an almost bottleable localised singlet diradical. *Phys. Chem. Chem. Phys.* **2020**, *22*, 27949.
83. Shu, C.; Madhavachary, R.; Noble, A.; Aggarwal, V. K. Photoinduced fragmentation borylation of cyclic alcohols and hemiacetals. *Org. Lett.* **2020**, *22*, 7213.

---

## 2.7 Experimental Section

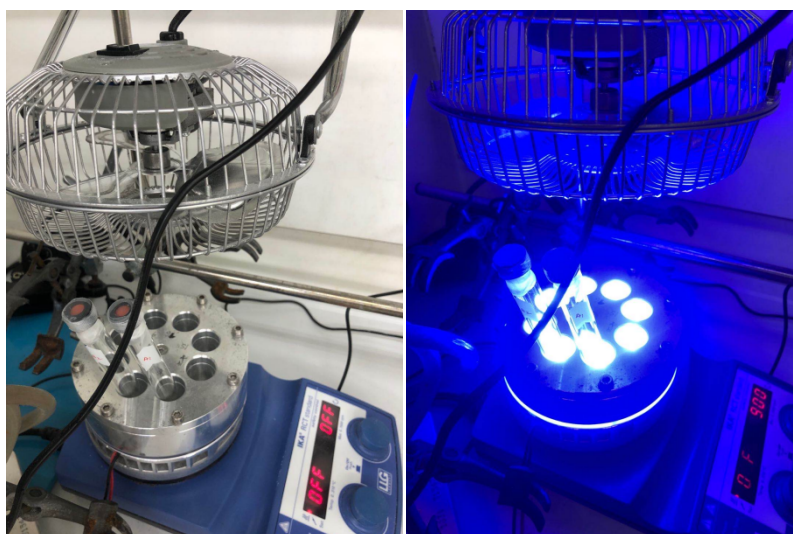
### 2.7.1 General Considerations

**Analytical methods.**  $^1\text{H}$  and  $^{13}\text{C}$  NMR spectra were recorded on Bruker 300 MHz, Bruker 400 MHz and Bruker 500 MHz at 20 °C. All  $^1\text{H}$  NMR spectra are reported in parts per million (ppm) downfield of TMS and were calibrated using the residual solvent peak of  $\text{CHCl}_3$  (7.26 ppm), unless otherwise indicated. All  $^{13}\text{C}$  NMR spectra are reported in ppm relative to TMS, were calibrated using the signal of residual  $\text{CHCl}_3$  (77.16 ppm),  $^{19}\text{F}$  NMR was obtained with  $^1\text{H}$  decoupling unless otherwise indicated. Coupling constants,  $J$  are reported in Hertz. Melting points were measured using open glass capillaries in a Büchi B540 apparatus. Infrared spectra (FT-IR) measurements were carried out on a Bruker Optics FT-IR Alpha spectrometer equipped with a DTGS detector, KBr beamsplitter at  $4\text{ cm}^{-1}$  resolution using a one bounce ATR accessory with diamond windows. Mass spectra were recorded on a Waters LCT Premier spectrometer or in a MicroTOF Focus, Bruker Daltonics spectrometer. UV/Vis absorption spectra were recorded using a Agilent Technologies Cary 300 UV/Vis spectrophotometer and UV-1800PC spectrophotometer in quartz cuvettes with a path length of 1.0 cm. Bulk electrolysis was conducted on a PARSTAT 2273 potentiometer using a 3-electrode cell configuration at room temperature, The same electrodes were used as for CV experiments, namely a glassy carbon working electrode, platinum flag counter electrode and Ag/AgCl (KCl sat.) reference electrode. Flash chromatography was performed with EM Science silica gel 60 (230-400 mesh). Thin layer chromatography was used to monitor reaction progress and analysed fractions from column chromatography. To this purpose TLC Silica gel 60 F<sub>254</sub> aluminium sheets from Merck were used and visualization was achieved using UV irradiation and/or staining with Potassium Permanganate or Cerium Molybdate solution. The yields reported refer to isolated yields and represent an average of at least two independent runs. The procedures described in this section are representative. Thus, the yields may differ slightly from those given in the tables of the manuscript.

**Reagents.** Commercially available materials were used as received without further purification.  $\text{NiBr}_2 \cdot \text{diglyme}$  (97% purity) were purchased from Aldrich. 4,4'-Di-*tert*-butyl-2,2'-bipyridine (97% purity) was purchased from Aldrich. Hantzsch ester (97%

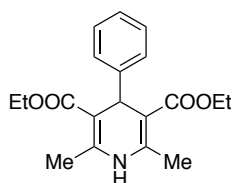
purity) was purchased from Fluorochem. Anhydrous  $K_2CO_3$  was purchased from Aldrich (99% purity). Tetrabutylammonium bromide was dried at 120 °C under reduced pressure, purchased from Aldrich. Anhydrous 1-Methyl-2-pyrrolidinone (NMP, 99.5% purity) was purchased from Across.

Arylation reactions were performed with 451 nm LEDs (OSRAM Oslon® SSL 80 royal-blue LEDs), which were installed at the bottom of a custom-made 8 flat-bottom Schlenk tubes holder (the distance between the flat-bottom Schlenk tube and the light source was measured to be ~7 mm), equipped with a fan cooling system (the thermostat was set at 35-40 °C) and a magnetic stirrer (~ 900 rpm).



## 2.7.2 Synthesis of Starting Materials

### Synthesis of Hantzsch Ester Analogues

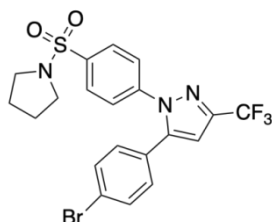


### Diethyl 2,6-dimethyl-4-phenyl-1,4-dihydropyridine-3,5-dicarboxylate (4-Ph-HE)

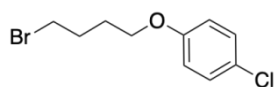
In accordance to the reported procedure<sup>[1]</sup>, ethyl-3-aminocrotonate (1.0 equiv) and ethylene glycol (2.5 M) were added to a flask under nitrogen atmospheres. Next, ethyl acetoacetate (1.0 equiv) was added followed by the corresponding aldehyde (1.0 equiv) and tetrabutylammonium hydrogen sulfate (12 mol%). The resultant solution was heated at 80 °C for 4 hours, then cooled and diluted with ethyl acetate. The solution was added to a solution of brine and separated using ethyl acetate (3 x 50 mL). The organic layers were combined, dried ( $MgSO_4$ ) and concentrated. The crude material

was purified by flash column chromatography to furnish the desired product.  $^1\text{H}$  NMR (400 MHz,  $\text{CDCl}_3$ )  $\delta$  7.29–7.27 (m, 2H), 7.22–7.18 (m, 2H), 7.14–7.09 (m, 1H), 5.61 (s, 1H), 4.98 (s, 1H), 4.08 (q,  $J = 8.2$  Hz, 4H), 2.32 (s, 6H), 1.21 (t,  $J = 7.7$  Hz, 6H) ppm.  $^{13}\text{C}$  NMR (101 MHz,  $\text{CDCl}_3$ )  $\delta$  167.6, 147.7, 143.7, 128.0, 127.8, 126.0, 104.2, 59.7, 39.6, 19.6, 14.2 ppm. Spectral data was in agreement with the literature<sup>[1]</sup>.

### Synthesis of Organic Halides



**5-(4-bromophenyl)-1-(4-(pyrrolidin-1-ylsulfonyl)phenyl)-3-(trifluoromethyl)-1H-pyrazole (2d)** To a mixture of 4-(5-(4-bromophenyl)-3-(trifluoromethyl)-1H-pyrazol-1-yl)benzenesulfonamide (2.0 mmol) and butane-1,4-diol (3.0 mmol) in toluene (3 mL) was added  $\text{Tf}_2\text{O}$  (20 mol%). The mixture was then sealed and stirred at 120 °C until the reaction was completed as judged by TLC. After quenching with sat. aq.  $\text{NaHCO}_3$ , the reaction mixture was extracted three times with EtOAc, dried over  $\text{Na}_2\text{SO}_4$ , and concentrated in vacuo. The residue was purified by flash chromatography with Hexane / EtOAc (3:1) as the eluent to give the product as a white solid. (650 mg, 65 % yield).  $^{19}\text{F}$  NMR (376 MHz,  $\text{CDCl}_3$ )  $\delta$  -62.18 ppm.  $^1\text{H}$  NMR (400 MHz,  $\text{CDCl}_3$ )  $\delta$  7.84 (d,  $J = 8.7$  Hz, 2H), 7.49 (dd,  $J = 15.8, 8.7$  Hz, 4H), 7.09 (d,  $J = 8.6$  Hz, 2H), 6.78 (s, 1H), 3.26 – 3.20 (m, 4H), 1.81 – 1.74 (m, 4H) ppm.  $^{13}\text{C}$  NMR (101 MHz,  $\text{CDCl}_3$ )  $\delta$  144.3 (q,  $J = 38.8$  Hz), 144.0, 142.1, 137.2, 132.4, 130.3, 128.6, 127.5, 125.7, 124.2, 121.0 (q,  $J = 269.1$  Hz), 106.6 (d,  $J = 1.9$  Hz), 48.1, 25.3 ppm. IR (neat): 3181, 3087, 2973, 2876, 1593, 1492, 1469, 1446, 1401, 1345, 1269, 1231, 1156, 1135, 1091, 1013, 973, 912, 837, 806, 769, 751, 712, 624, 580, 532, 491, 449. Mp: 128 °C. HRMS *calcd.* for  $(\text{C}_{20}\text{H}_{17}\text{BrF}_3\text{N}_3\text{NaO}_2\text{S})$   $[\text{M}+\text{Na}]^+$ : 522.0075, *found* 522.0069.

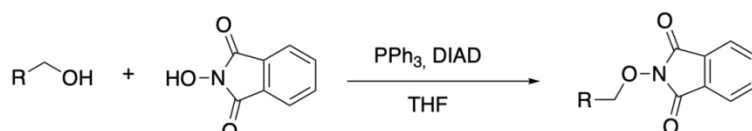


**1-(4-bromobutoxy)-4-chlorobenzene (2e)** To a solution of 4-chlorophenol (1.0 g, 7.8 mmol, 1.0 equiv) in acetone (40 mL, 0.2 M) were added  $\text{K}_2\text{CO}_3$  (2.2 g, 16.0 mmol, 2.0 equiv) and 1,4-dibromobutane (1.9 mL, 16.0 mmol, 2.0 equiv). The resulting solution was heated at reflux for 12 h, then cooled to room temperature, filtered through celite, eluted with acetone and concentrated under reduced pressure. The residue was purified

by flash chromatography with Hexane / EtOAc (50:1) to afford the product as a liquid (1.59 g, 78% yield).  $^1\text{H NMR}$  (400 MHz,  $\text{CDCl}_3$ )  $\delta$  7.25 – 7.20 (m, 2H), 6.85 – 6.78 (m, 2H), 3.96 (t,  $J = 6.1$  Hz, 2H), 3.48 (t,  $J = 6.6$  Hz, 2H), 2.10 – 2.02 (m, 2H), 1.98 – 1.90 (m, 2H) ppm.  $^{13}\text{C NMR}$  (101 MHz,  $\text{CDCl}_3$ )  $\delta$  157.6, 129.4, 125.7, 115.8, 67.3, 33.5, 29.5, 28.0 ppm. Spectral data was in agreement with the literature<sup>[2]</sup>.

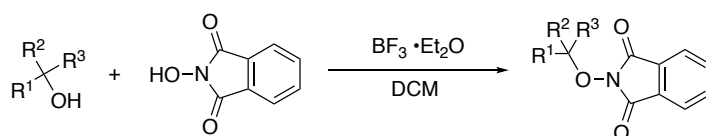
## Synthesis of N-Alkoxyphthalimides

### Method A



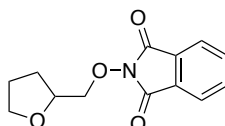
To a solution of the corresponding aliphatic alcohol (10.0 mmol), PPh<sub>3</sub> (3.15 g, 12.0 mmol), and N-hydroxyphthalimide (1.96 g, 12.0 mmol) in THF (30 mL) was added diisopropyl azodicarboxylate (2.4 mL, 12.0 mmol) over 10 min at room temperature. The resulting mixture was stirred for 3-24 h, taken up in EtOAc (20 mL), and washed with saturated NaHCO<sub>3</sub> (3 x 20 mL) and brine (2 x 30 mL). The organic layers were dried over anhydrous Na<sub>2</sub>SO<sub>4</sub>, concentrated in vacuo, and subjected to flash chromatography to afford the targeted N-alkoxyphthalimides.

### Method B

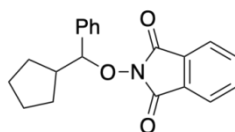


Following a literature procedure,<sup>[3]</sup> to a solution of the corresponding tertiary alcohol (20 mmol) and N-hydroxyphthalimide (6.53 g, 40 mmol) in 70 mL wet DCM, BF<sub>3</sub>·Et<sub>2</sub>O (13.5 mL, 50 mmol) was added dropwise by syringe at 0 °C. The reaction mixture was stirred for 1.5-2.0 h at room temperature. To the resulting mixture, DCM (10 mL) and saturated Na<sub>2</sub>CO<sub>3</sub> solution in H<sub>2</sub>O (50 mL) was added. The aqueous layer was extracted with DCM (20 mL x 3), the combined organic layers were dried over anhydrous Na<sub>2</sub>SO<sub>4</sub>, concentrated in vacuo, and subjected to flash chromatography to afford the targeted N-alkoxyphthalimides.

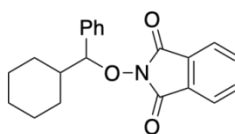
*Note:* Further purification of the product can be performed by recrystallization in DCM/hexanes or Et<sub>2</sub>O/hexanes if necessary.



**2-((tetrahydrofuran-2-yl)methoxy)isoindoline-1,3-dione (1a)** Following Method A, the utilization of (tetrahydrofuran-2-yl)methanol (1.00 g, 9.8 mmol) afforded the title compound as a white solid (1.79 g, 74% yield) by using Hexane/EtOAc (4:1) as eluent.  $^1\text{H NMR}$  (400 MHz,  $\text{CDCl}_3$ )  $\delta$  7.83 (dd,  $J = 5.4, 3.0$  Hz, 2H), 7.75 (dd,  $J = 5.4, 3.0$  Hz, 2H), 4.32 – 4.23 (m, 2H), 4.17 (dd,  $J = 10.1, 4.0$  Hz, 1H), 3.89 – 3.84 (m, 1H), 3.80 – 3.76 (m, 1H), 2.12 – 2.06 (m, 1H), 1.98 – 1.85 (m, 2H), 1.81 – 1.74 (m, 1H) ppm.  $^{13}\text{C NMR}$  (101 MHz,  $\text{CDCl}_3$ )  $\delta$  163.5, 134.5, 129.1, 123.6, 80.0, 76.4, 68.7, 28.3, 25.5 ppm. Spectral data was in agreement with the literature<sup>[4]</sup>.

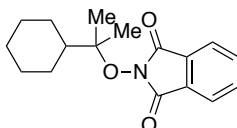


**2-(cyclopentyl(phenyl)methoxy)isoindoline-1,3-dione (1b)** Following Method A, the utilization of cyclopentyl(phenyl)methanol (0.44 g, 3.0 mmol) afforded the title compound as a white solid (0.72 g, 74% yield) by using Hexane/EtOAc (5:1) as eluent.  $^1\text{H NMR}$  (400 MHz,  $\text{CDCl}_3$ )  $\delta$  7.70 – 7.61 (m, 4H), 7.47 – 7.37 (m, 2H), 7.32 – 7.21 (m, 3H), 5.09 (d,  $J = 9.8$  Hz, 1H), 2.64 – 2.41 (m, 1H), 2.13 (m, 1H), 1.91 (m, 1H), 1.83 – 1.70 (m, 1H), 1.63 (m, 2H), 1.48 (m, 1H), 1.37 (m, 1H), 1.10 (m, 1H) ppm.  $^{13}\text{C NMR}$  (101 MHz,  $\text{CDCl}_3$ )  $\delta$  163.8, 138.3, 134.2, 128.99, 128.97, 128.6, 128.2, 123.3, 93.8, 44.6, 30.38, 29.9, 25.8, 25.2 ppm. **IR (neat):** 3032, 2957, 2869, 1790, 1727, 1610, 1467, 1454, 1372, 1186, 1130, 1081, 1130, 1081, 1014, 973, 908, 875, 784, 758, 730, 697, 648, 599, 518. **Mp:** 57 °C. **HRMS *calcd.* for (C<sub>20</sub>H<sub>19</sub>NNaO<sub>3</sub>) [M+Na]<sup>+</sup>: 344.1263, found 344.1256.**

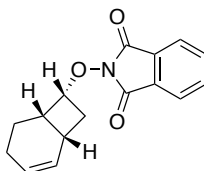


**2-(cyclohexyl(phenyl)methoxy)isoindoline-1,3-dione (1c)** Following Method A, the utilization of cyclohexyl(phenyl)methanol (0.80 g, 4.0mmol) afforded the title compound as a white solid (1.08 g, 80 % yield) by using Hexane/EtOAc (5:1) as eluent.  $^1\text{H NMR}$  (400 MHz,  $\text{CDCl}_3$ )  $\delta$  7.69-7.62 (m, 4H), 7.41 – 7.38 (m, 2H), 7.31 – 7.26 (m, 3H), 5.09 (d,  $J = 8.7$  Hz, 1H), 2.36 – 2.34 (m, 1H), 2.05 – 1.98 (m, 1H), 1.86 – 1.79 (m, 1H), 1.66 – 1.64 (m, 2H), 1.38 – 1.26 (m, 3H), 1.24 – 1.16 (m, 2H), 0.89 – 0.88 (m, 1H) ppm.  $^{13}\text{C NMR}$  (101 MHz,  $\text{CDCl}_3$ )  $\delta$  163.8, 137.4, 134.2, 129.0, 128.8, 128.7, 128.1, 123.3, 93.6, 42.4, 29.9, 29.1, 26.4, 25.9, 25.7 ppm. Spectral data was in agreement with the literature<sup>[5]</sup>.

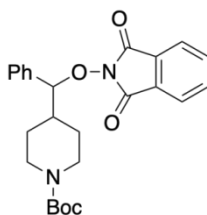




**2-((2-cyclohexylpropan-2-yl)oxy)isoindoline-1,3-dione (1d)** Following Method B, the utilization of 2-cyclohexylpropan-2-ol (1.00 g, 7.0 mmol) afforded the title compound as a white solid (0.46 g, 23% yield) by using Hexane/EtOAc (7:1) as eluent. **<sup>1</sup>H NMR (400 MHz, CDCl<sub>3</sub>)** δ 7.83 (dd, *J* = 5.5, 3.0 Hz, 2H), 7.75 (dd, *J* = 5.5, 3.0 Hz, 2H), 2.05 – 2.02 (m, 2H), 1.82 (dt, *J* = 12.6, 3.0 Hz, 2H), 1.72 – 1.64 (m, 2H), 1.32 – 1.09 (m, 11H) ppm. **<sup>13</sup>C NMR (101 MHz, CDCl<sub>3</sub>)** δ 166.1, 134.5, 129.5, 123.5, 91.4, 46.9, 28.0, 26.8, 26.6, 22.9 ppm. **IR (neat):** 2989, 2935, 2854, 1788, 1728, 1465, 1369, 1346, 1317, 1260, 1186, 1142, 1101, 1076, 1029, 968, 875, 86, 699, 636, 521. **Mp:** 68 °C. **HRMS *calcd.* for (C<sub>17</sub>H<sub>21</sub>NNaO<sub>3</sub>) [M+Na]<sup>+</sup>: 310.1419, *found* 310.1416.**

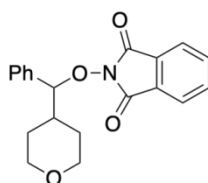


**2-(((1R,6S,7R)-bicyclo[4.2.0]oct-2-en-7-yl)oxy)isoindoline-1,3-dione (1e)** Following Method A, the utilization of (±)-*Bicyclo[4.2.0]oct-2-en-7-ol* (1.00 g, 8.0 mmol) afforded the title compound as a white solid (1.84 g, 85% yield) by using Hexane/EtOAc (5:1) as eluent. **<sup>1</sup>H NMR (400 MHz, CDCl<sub>3</sub>)** δ 7.83 (dd, *J* = 5.5, 3.0 Hz, 2H), 7.74 (dd, *J* = 5.4, 3.1 Hz, 2H), 5.82 – 5.68 (m, 2H), 4.66 (q, *J* = 7.4 Hz, 1H), 2.94 (tt, *J* = 7.6, 3.6 Hz, 1H), 2.63 (t, *J* = 9.3 Hz, 1H), 2.50 (m, 1H), 2.13 – 2.01 (m, 3H), 1.74 (m, 1H), 1.45 (m, 1H) ppm. **<sup>13</sup>C NMR (101 MHz, CDCl<sub>3</sub>)** δ 164.1, 134.6, 130.0, 129.1, 127.1, 123.6, 82.2, 40.0, 34.9, 24.2, 21.4, 20.9 ppm. **IR (neat):** 3020, 2919, 2839, 1784, 1735, 1609, 1466, 1358, 1243, 1158, 1082, 1012, 985, 955, 877, 792, 702, 519. **Mp:** 87 °C. **HRMS *calcd.* for (C<sub>16</sub>H<sub>15</sub>NNaO<sub>3</sub>) [M+Na]<sup>+</sup>: 292.0950, *found* 292.0945.**



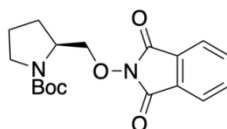
**tert-butyl 4-(((1,3-dioxoisindolin-2-yl)oxy)(phenyl)methyl)piperidine-1-carboxylate (1f)** Following Method A, the utilization of *tert*-butyl 4-(hydroxy(phenyl)methyl)piperidine-1-carboxylate (1.00 g, 3.4 mmol) afforded the title

compound as a white solid (0.83 g, 56% yield) by using Hexane/EtOAc (4:1) as eluent. **<sup>1</sup>H NMR (400 MHz, CDCl<sub>3</sub>)** δ 7.71 – 7.60 (m, 4H), 7.45 – 7.37 (m, 2H), 7.30 (m, 3H), 5.08 (d, *J* = 8.9 Hz, 1H), 4.19 (d, *J* = 13.2 Hz, 1H), 4.03 (d, *J* = 12.4 Hz, 1H), 2.77 (t, *J* = 12.1 Hz, 1H), 2.64 (t, *J* = 11.3 Hz, 1H), 2.31 (d, *J* = 13.5 Hz, 1H), 2.14 (m, 1H), 1.45 (s, 9H), 1.35 – 1.07 (m, 3H) ppm. **<sup>13</sup>C NMR (101 MHz, CDCl<sub>3</sub>)** δ 163.7, 154.9, 136.7, 134.4, 129.2, 128.9, 128.6, 128.3, 123.4, 92.7, 79.5, 43.57 (d, *J* = 16.2 Hz), 41.1, 29.2, 28.6, 28.3 ppm. **IR (neat):** 2959, 2923, 1792, 1730, 1674, 1468, 1451, 1423, 1364, 1229, 1164, 1125, 1065, 977, 924, 876, 762, 700, 519. **Mp:** 192 °C. **HRMS calcd. for (C<sub>25</sub>H<sub>28</sub>N<sub>2</sub>NaO<sub>5</sub>) [M+Na]<sup>+</sup>: 459.1896, found 459.1890.**



**2-(phenyl(tetrahydro-2H-pyran-4-yl)methoxy)isoindoline-1,3-dione (1g)**

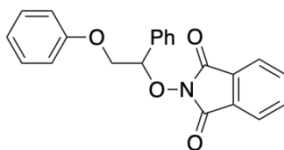
Following Method A, the utilization of phenyl(tetrahydro-2H-pyran-4-yl)methanol (1.0 g, 5.2 mmol) afforded the title compound as a white solid (1.16 g, 66% yield) by using Hexane/EtOAc (4:1) as eluent. **<sup>1</sup>H NMR (400 MHz, CDCl<sub>3</sub>)** δ 7.70 – 7.48 (m, 4H), 7.39 – 7.29 (m, 2H), 7.28 – 7.18 (m, 3H), 5.09 (d, *J* = 8.7 Hz, 1H), 4.06 (dd, *J* = 11.5, 3.4 Hz, 1H), 3.88 (ddd, *J* = 11.4, 4.2, 1.7 Hz, 1H), 3.44 (td, *J* = 12.0, 2.1 Hz, 1H), 3.33 (td, *J* = 11.8, 2.3 Hz, 1H), 2.28 – 2.20 (m, 2H), 1.81 (m, 1H), 1.36 – 1.25 (m, 1H), 1.14–1.08 (m, 1H) ppm. **<sup>13</sup>C NMR (101 MHz, CDCl<sub>3</sub>)** δ 163.7, 136.6, 134.3, 129.2, 128.9, 128.6, 128.3, 123.4, 92.9, 67.66, 67.60, 40.1, 30.2, 29.1 ppm. **IR (neat):** 3280, 2953, 2856, 1783, 1721, 1469, 1456, 1374, 1244, 1184, 1149, 1126, 1095, 1015, 991, 974, 872, 786, 753, 694, 518. **Mp:** 138 °C. **HRMS calcd. for (C<sub>20</sub>H<sub>19</sub>NNaO<sub>4</sub>) [M+Na]<sup>+</sup>: 360.1212, found 360.1206.**



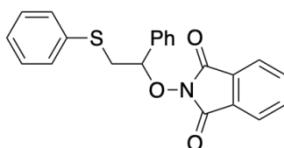
**tert-butyl (S)-2-(((1,3-dioxoisoindolin-2-yl)oxy)methyl)pyrrolidine-1-carboxylate**

**(1h)** Following Method A, the utilization of *tert*-butyl (S)-2-(hydroxymethyl)pyrrolidine-1-carboxylate (0.42 g, 2.0 mmol) afforded the title compound as a white solid (0.43 g, 62% yield) by using Hexane/EtOAc (2:1) as eluent. **<sup>1</sup>H NMR (400 MHz, CDCl<sub>3</sub>)** δ 8.83 – 7.66 (m, 4H), 4.39 – 4.23 (dd, *J* = 8.3, 35.8 Hz, 1H), 4.14 – 4.06 (br, 1H), 4.05 – 3.90 (dt, *J* = 35.8, 8.3 Hz, 1H), 3.40 – 3.25 (m, 2H),

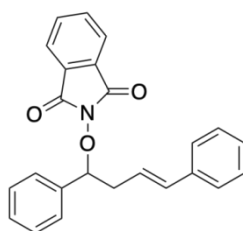
2.31 – 2.22 (m, 1H), 2.13 – 1.79 (m, 3H), 1.37 (s, 9H) ppm.  $^{13}\text{C}$  NMR (101 MHz,  $\text{CDCl}_3$ )  $\delta$  163.4, 154.3, 134.6, 128.9, 123.5, 79.8, 78.30, 54.9, 55.2, 47.0, 46.4, 29.0, 28.4, 22.9 21.8 ppm. Spectral data was in agreement with the literature<sup>[6]</sup>



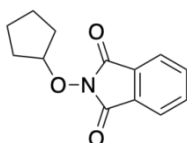
**2-(2-phenoxy-1-phenylethoxy)isoindoline-1,3-dione (1i)** Following Method A, the utilization of 2-phenoxy-1-phenylethan-1-ol (1.00 g, 4.7 mmol) afforded the title compound as a white solid (1.37 g, 82% yield) by using Hexane/EtOAc (5:1) as eluent.  $^1\text{H}$  NMR (400 MHz,  $\text{CDCl}_3$ )  $\delta$  7.42 – 7.40 (m, 2H), 7.35 – 7.33 (m, 2H), 7.30 – 7.20 (m, 2H), 7.11 – 7.02 (m, 3H), 6.96 – 6.84 (m, 2H), 6.59 (t,  $J = 7.4$  Hz, 1H), 6.50–6.41 (m, 2H), 5.46 – 5.44 (m, 1H), 4.28 (dd,  $J = 10.9, 7.4$  Hz, 1H), 3.96 (dd,  $J = 10.9, 3.7$  Hz, 1H) ppm.  $^{13}\text{C}$  NMR (101 MHz,  $\text{CDCl}_3$ )  $\delta$  163.7, 158.3, 135.1, 134.5, 129.7, 129.6, 129.0, 128.7, 128.2, 123.6, 121.4, 114.8, 86.7, 70.4 ppm. IR (neat): 3065, 2919, 1794, 1730, 1598, 1495, 1454, 1376, 1291, 1226, 1191, 1171, 1126, 1080, 1039, 1014, 974, 907, 877, 848, 767, 724, 701, 649, 590, 520. Mp: 121 °C. HRMS *calcd.* for ( $\text{C}_{22}\text{H}_{17}\text{NNaO}_4$ ) [ $\text{M}+\text{Na}$ ] $^+$ : 382.1055, *found* 382.1050.



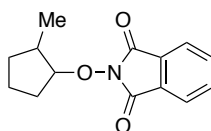
**2-(1-phenyl-2-(phenylthio)ethoxy)isoindoline-1,3-dione (1j)** Following Method A, the utilization of 1-phenyl-2-(phenylthio)ethan-1-ol (1.15 g, 5.0 mmol) afforded the title compound as a white solid (1.70 g, 90% yield) by using Hexane/EtOAc (5:1) as eluent.  $^1\text{H}$  NMR (400 MHz,  $\text{CDCl}_3$ )  $\delta$  7.48 (dd,  $J = 5.5, 3.0$  Hz, 2H), 7.43 (dd,  $J = 5.6, 3.0$  Hz, 2H), 7.21 (dd,  $J = 6.6, 3.0$  Hz, 2H), 7.13 – 7.05 (m, 5H), 7.05 – 6.98 (m, 2H), 6.97 – 6.91 (m, 1H), 5.29 – 5.08 (m, 1H), 3.46 (dd,  $J = 13.7, 6.3$  Hz, 1H), 3.17 (dd,  $J = 13.7, 7.5$  Hz, 1H) ppm.  $^{13}\text{C}$  NMR (101 MHz,  $\text{CDCl}_3$ )  $\delta$  163.6, 136.5, 135.3, 134.5, 130.3, 129.6, 129.1, 128.9, 128.5, 128.3, 126.7, 123.5, 87.5, 38.5 ppm. IR (neat): 3060, 2930, 1789, 1730, 1586, 1481, 1466, 1455, 1439, 1425, 1375, 1355, 1221, 1188, 961, 921, 778, 733, 696, 626, 518. Mp: 99 °C. HRMS *calcd.* for ( $\text{C}_{22}\text{H}_{17}\text{NNaO}_3\text{S}$ ) [ $\text{M}+\text{Na}$ ] $^+$ : 398.0827, *found* 398.0827.



**(E)-2-((1,4-diphenylbut-3-en-1-yl)oxy)isoindoline-1,3-dione (1k)** Following Method A, the utilization of (E)-1,4-diphenylbut-3-en-1-ol (1.0 g, 4.5 mmol) afforded the title compound as a white solid (1.56 g, 95% yield) by using Hexane/EtOAc (5:1) as eluent. **<sup>1</sup>H NMR (400 MHz, CDCl<sub>3</sub>)** δ 7.73 (dd, *J* = 5.6, 3.0 Hz, 2H), 7.70 – 7.64 (m, 2H), 7.51 (dd, *J* = 7.8, 1.7 Hz, 2H), 7.41 – 7.22 (m, 7H), 7.24 – 7.10 (m, 1H), 6.50 (d, *J* = 15.9 Hz, 1H), 6.18 (dt, *J* = 15.8, 7.1 Hz, 1H), 5.47 (t, *J* = 7.0 Hz, 1H), 3.10 (m, 1H), 2.98 – 2.69 (m, 1H) ppm. **<sup>13</sup>C NMR (101 MHz, CDCl<sub>3</sub>)** δ 163.8, 137.8, 137.4, 134.4, 133.1, 129.3, 128.9, 128.6, 128.5, 128.2, 127.3, 126.3, 124.7, 123.5, 88.6, 38.7 ppm. **IR (neat):** 3059, 3028, 2935, 1788, 1725, 1608, 1494, 1466, 1455, 1367, 1244, 1186, 1117, 1080, 1014, 971, 875, 761, 695, 571, 517. **Mp:** 61 °C. **HRMS *calcd.* for (C<sub>24</sub>H<sub>19</sub>NNaO<sub>3</sub>) [M+Na]<sup>+</sup>: 392.1263, *found* 392.1257.**

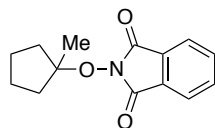


**2-(Cyclopentyloxy)isoindoline-1,3-dione (1l)** Following Method A, the utilization of cyclopentanol (0.86 g, 10.0 mmol) afforded the title compound as a white solid (1.90 g, 82% yield) by using Hexane/EtOAc (4:1) as eluent. **<sup>1</sup>H NMR (400 MHz, CDCl<sub>3</sub>)** δ 7.82 (dd, *J* = 5.5, 3.0 Hz, 2H), 7.74 (dd, *J* = 5.5, 3.0 Hz, 2H), 4.94 – 4.88 (m, 1H), 2.02 – 1.90 (m, 4H), 1.79 – 1.72 (m, 2H), 1.64 – 1.59 (m, 2H) ppm. **<sup>13</sup>C NMR (101 MHz, CDCl<sub>3</sub>)** δ 164.5, 134.5, 129.2, 123.6, 90.5, 31.7, 23.7 ppm. Spectral data was in agreement with the literature<sup>[4]</sup>.

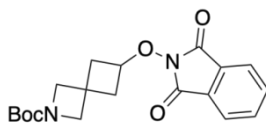


**2-((2-methylcyclopentyl)oxy)isoindoline-1,3-dione (1m)** Following Method A, 2-methylcyclopentanol (0.30 g, 3.0 mmol) afforded the title compound as a white solid (0.50 g, 68% yield) by using Hexane/EtOAc (4:1) as eluent. **<sup>1</sup>H NMR (400 MHz, CDCl<sub>3</sub>)** δ 7.82 (dd, *J* = 5.5, 3.6 Hz, 2H), 7.73 (dd, *J* = 5.4, 3.4 Hz, 2H), 4.63 (dt, *J* = 4.6, 2.4 Hz, 0.75H), 4.45 (dt, *J* = 5.9, 3.1 Hz, 0.25H), 2.16 – 1.50 (m, 7H), 1.26 (d, *J* =

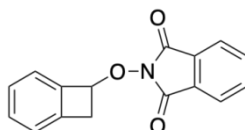
7.0 Hz, 2.3H), 1.01 (d,  $J = 7.1$  Hz, 0.8H) ppm.  $^{13}\text{C}$  NMR (101 MHz,  $\text{CDCl}_3$ )  $\delta$  164.4, 134.5, 134.4, 129.2, 123.5, 123.4, 96.3, 92.2, 39.3, 38.8, 32.2, 31.1, 30.5, 22.6, 22.1, 18.8, 13.6 ppm. IR (neat): 2959, 2876, 1781, 1725, 1607, 1464, 1371, 1184, 1158, 1123, 1080, 1012, 970, 877, 782, 696, 517. Mp: 60 °C. HRMS *calcd.* for ( $\text{C}_{14}\text{H}_{15}\text{NNaO}_3$ )  $[\text{M}+\text{Na}]^+$ : 268.0950, *found* 268.0944.



**2-((1-methylcyclopentyl)oxy)isoindoline-1,3-dione (1n)** Following Method B, the utilization of 1-methylcyclopentanol (1.00 g, 10.0 mmol) afforded the title compound as a white solid (1.30 g, 54% yield) by using Hexane/EtOAc (4:1) as eluent.  $^1\text{H}$  NMR (400 MHz,  $\text{CDCl}_3$ )  $\delta$  7.8 – 7.8 (m, 2H), 7.7 – 7.7 (m, 2H), 2.15 – 1.98 (m, 4H), 1.72 – 1.55 (m, 4H), 1.46 (s, 3H) ppm.  $^{13}\text{C}$  NMR (101 MHz,  $\text{CDCl}_3$ )  $\delta$  166.0, 134.5, 129.5, 123.5, 98.0, 38.1, 24.6, 24.4 ppm. Spectral data was in agreement with the literature<sup>[7]</sup>.

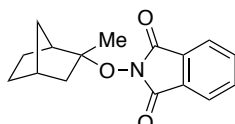


**tert-butyl 6-((1,3-dioxoisindolin-2-yl)oxy)-2-azaspiro[3.3]heptane-2-carboxylate (1o)** Following Method A, the utilization of *tert*-butyl 6-hydroxy-2-azaspiro[3.3]heptane-2-carboxylate (1.00 g, 4.5 mmol) afforded the title compound as a white solid (0.68 g, 40% yield) by using Hexane/EtOAc (3:1) as eluent.  $^1\text{H}$  NMR (400 MHz,  $\text{CDCl}_3$ )  $\delta$  7.84 (dd,  $J = 5.6, 3.0$  Hz, 2H), 7.78 – 7.74 (dd,  $J = 5.6, 3.0$  Hz, 2H), 4.72 (t,  $J = 6.7$  Hz, 1H), 3.98 (s, 2H), 3.88 (s, 2H), 2.65 – 2.47 (m, 4H), 1.43 (s, 9H) ppm.  $^{13}\text{C}$  NMR (101 MHz,  $\text{CDCl}_3$ )  $\delta$  164.0, 156.2, 134.7, 129.0, 123.7, 79.6, 60.9 (d,  $J = 48.5$  Hz), 39.8, 30.4, 28.5 ppm. IR (neat): 2968, 2937, 2876, 1790, 1729, 1683, 1469, 1451, 1397, 1363, 1319, 1256, 1174, 1137, 1110, 1078, 1029, 961, 928, 876, 775, 711, 693, 520. Mp: 149 °C. HRMS *calcd.* for ( $\text{C}_{19}\text{H}_{22}\text{N}_2\text{NaO}_5$ )  $[\text{M}+\text{Na}]^+$ : 381.1426, *found* 381.1421.

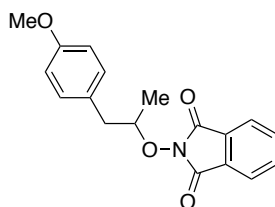


**2-(bicyclo[4.2.0]octa-1,3,5-trien-7-yloxy)isoindoline-1,3-dione (1p)** Following General Procedure A, the utilization of bicyclo[4.2.0]octa-1,3,5-trien-7-ol (0.48 g, 4.0 mmol) afforded the title compound as a white solid (0.45 g, 42% yield) by using

Hexane/EtOAc (5:1) as eluent. **<sup>1</sup>H NMR (400 MHz, CDCl<sub>3</sub>)** δ 7.60 (dd, *J* = 5.5, 3.1 Hz, 2H), 7.50 (dd, *J* = 5.5, 3.1 Hz, 2H), 7.12 – 7.05 (m, 2H), 7.03 – 6.97 (m, 1H), 6.90 (d, *J* = 7.3 Hz, 1H), 5.55 (t, *J* = 3.2 Hz, 1H), 3.36 (d, *J* = 3.2 Hz, 2H) ppm. **<sup>13</sup>C NMR (101 MHz, CDCl<sub>3</sub>)** δ 164.3, 142.6, 142.5, 134.6, 130.7, 129.1, 127.6, 124.1, 123.7, 123.3, 83.4, 38.9 ppm. **IR (neat):** 1790, 1726, 1462, 1374, 1183, 1125, 1076, 1027, 980, 962, 876, 748, 698. **Mp:** 141 °C. **HRMS *calcd.* for (C<sub>16</sub>H<sub>11</sub>NNaO<sub>3</sub>) [M+Na]<sup>+</sup>: 288.0637, *found* 288.0630.**

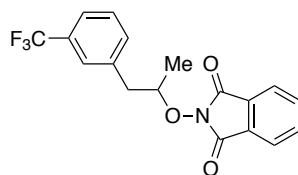


**2-((2-methylbicyclo[2.2.1]heptan-2-yl)oxy)isoindoline-1,3-dione (1q)** Following Method A, the utilization of 2-methylbicyclo[2.2.1]heptan-2-ol (1.20 g, 9.5 mmol) afforded the title compound as a white solid (1.44 g, 56% yield) by using Hexane/EtOAc (5:1) as eluent. **<sup>1</sup>H NMR (400 MHz, CDCl<sub>3</sub>)** δ 8.00 – 7.96 (m, 2H), 7.90 (m, 2H), 2.55 (d, *J* = 4.1 Hz, 1H), 2.52 – 2.43 (m, 2H), 2.29 – 2.17 (m, 1H), 1.75 – 1.37 (m, 8H), 1.26 (m, 1H) ppm. **<sup>13</sup>C NMR (101 MHz, CDCl<sub>3</sub>)** δ 166.1, 134.5, 129.5, 123.5, 96.3, 46.5, 45.1, 37.8, 36.9, 28.1, 24.1, 21.7 ppm. **IR (neat):** 2955, 2869, 1785, 1735, 1610, 1466, 1437, 1351, 1312, 1185, 1108, 1079, 1068, 962, 875, 790, 704, 519. **Mp:** 89 °C. **HRMS *calcd.* for (C<sub>16</sub>H<sub>17</sub>NNaO<sub>3</sub>) [M+Na]<sup>+</sup>: 294.1106, *found* 294.1101.**

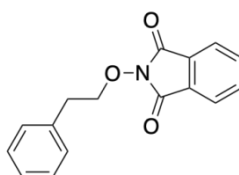


**2-((1-(4-methoxyphenyl)propan-2-yl)oxy)isoindoline-1,3-dione (1r)** Following Method A, the utilization of 1-(4-methoxyphenyl)propan-2-ol (1.20 g, 7.0 mmol) afforded the title compound as a white solid (1.20 g, 55% yield) by using Hexane/EtOAc (4:1) as eluent. **<sup>1</sup>H NMR (400 MHz, CDCl<sub>3</sub>)** δ 7.82 (dd, *J* = 5.4, 3.1 Hz, 2H), 7.74 (dd, *J* = 5.5, 3.1 Hz, 2H), 7.17 (d, *J* = 8.7 Hz, 2H), 6.81 (d, *J* = 8.7 Hz, 2H), 4.63 (dq, *J* = 6.0, 1.5 Hz, 1H), 3.76 (s, 3H), 3.16 (dd, *J* = 13.9, 5.6 Hz, 1H), 2.83 (dd, *J* = 13.9, 7.8 Hz, 1H), 1.31 (d, *J* = 6.2 Hz, 3H) ppm. **<sup>13</sup>C NMR (101 MHz, CDCl<sub>3</sub>)** δ 164.4, 158.4, 134.5, 130.4, 129.3, 129.1, 123.6, 113.9, 84.9, 55.3, 40.6, 18.4 ppm. **IR (neat):** 3035, 2994, 2933, 2838, 1725, 1509, 1465, 1385, 1354, 1245, 1177, 1147, 1115, 1082, 1042, 1015, 975, 878, 800, 759, 600, 519. **Mp:** 83 °C. **HRMS *calcd.* for**

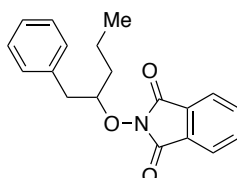
(C<sub>19</sub>H<sub>17</sub>NNaO<sub>4</sub>) [M+Na]<sup>+</sup>: 334.1055, *found* 334.1050.



**2-((1-(3-(trifluoromethyl)phenyl)propan-2-yl)oxy)isoindoline-1,3-dione (1s)** Following Method A, the utilization of 1-(3-(trifluoromethyl)phenyl)propan-2-ol (1.63 g, 8.0 mmol) afforded the title compound as a white solid (2.13 g, 76% yield) by using Hexane/EtOAc (5:1) as eluent. <sup>19</sup>F NMR (376 MHz, CDCl<sub>3</sub>) δ -62.68 ppm. <sup>1</sup>H NMR (400 MHz, CDCl<sub>3</sub>) δ 7.80 (dd, *J* = 5.5, 3.0 Hz, 2H), 7.73 (dd, *J* = 5.5, 3.0 Hz, 2H), 7.59 – 7.35 (m, 4H), 4.69 (q, *J* = 6.4 Hz, 1H), 3.23 (dd, *J* = 14.3, 6.3 Hz, 1H), 2.99 (dd, *J* = 14.3, 6.7 Hz, 1H), 1.34 (d, *J* = 6.3 Hz, 3H) ppm. <sup>13</sup>C NMR (75 MHz, CDCl<sub>3</sub>) δ 164.3, 138.2, 134.9, 134.6, 132.9, 130.8 (q, *J*<sub>C,F</sub> = 32.0 Hz), 128.9, 126.1 (q, *J*<sub>C,F</sub> = 3.8 Hz), 124.1, 123.6, 123.5 (q, *J*<sub>C,F</sub> = 3.8 Hz), 84.1, 41.2, 18.5 ppm. IR (neat): 2981, 1786, 1740, 1727, 1609, 1466, 1453, 1344, 1203, 1107, 1068, 976, 904, 877, 796, 699, 665, 520. Mp: 89 °C. HRMS *calcd.* for (C<sub>18</sub>H<sub>14</sub>F<sub>3</sub>NNaO<sub>3</sub>) [M+Na]<sup>+</sup>: 372.0823, *found* 372.0818.

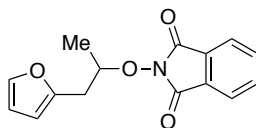


**2-phenethoxyisoindoline-1,3-dione (1t)** Following Method A, the utilization of 2-phenylethan-1-ol (1.00 g, 8.2 mmol) afforded the title compound as a white solid (1.60 g, 87% yield) by using Hexane/EtOAc (5:1) as eluent. <sup>1</sup>H NMR (400 MHz, CDCl<sub>3</sub>) δ 7.83 (dd, *J* = 5.5, 3.0 Hz, 2H), 7.75 (dd, *J* = 5.4, 3.1 Hz, 2H), 7.30 (d, *J* = 4.6 Hz, 4H), 7.24 – 7.19 (m, 1H), 4.44 (t, *J* = 7.4 Hz, 2H), 3.16 (t, *J* = 7.4 Hz, 2H) ppm. <sup>13</sup>C NMR (101 MHz, CDCl<sub>3</sub>) δ 163.7, 136.9, 134.6, 129.1, 129.0, 128.7, 126.8, 123.7, 78.7, 34.8 ppm. Spectral data was in agreement with the literature<sup>[8]</sup>

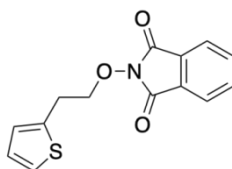


**2-((1-phenylpentan-2-yl)oxy)isoindoline-1,3-dione (1u)** Following Method A, the utilization of 1-phenylpentan-2-ol (0.49 g, 3.0 mmol) afforded the title compound as a white solid (0.73 g, 79% yield) by using Hexane/EtOAc (5:1) as eluent. <sup>1</sup>H NMR (400 MHz, CDCl<sub>3</sub>) δ 7.80 (dd, *J* = 5.5, 3.0 Hz, 2H), 7.72 (dd, *J* = 5.4, 3.1 Hz, 2H), 7.23 (d, *J* = 4.8 Hz, 4H), 7.18 – 7.11 (m, 1H), 4.62 – 4.47 (m, 1H), 3.11 (dd, *J* = 14.2, 5.9 Hz,

1H), 2.96 (dd,  $J = 14.2, 7.1$  Hz, 1H), 1.74 – 1.49 (m, 4H), 1.04 – 0.81 (m, 3H) ppm.  $^{13}\text{C}$  NMR (101 MHz,  $\text{CDCl}_3$ )  $\delta$  164.4, 137.5, 134.5, 129.3, 129.1, 128.5, 126.4, 123.5, 88.3, 39.7, 34.6, 18.6, 14.1 ppm. IR (neat): 2961, 2936, 2875, 1786, 1722, 1600, 1495, 1467, 1455, 1369, 1291, 1184, 1144, 1120, 1081, 975, 940, 877, 756, 696, 619, 517. Mp: 45 °C. HRMS *calcd.* for  $(\text{C}_{19}\text{H}_{19}\text{NNaO}_3)$   $[\text{M}+\text{Na}]^+$ : 332.1263, *found* 332.1257.

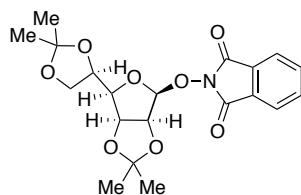


**2-((1-(furan-2-yl)propan-2-yl)oxy)isoindoline-1,3-dione (1v)** Following Method A, the utilization of 1-(furan-2-yl)propan-2-ol (0,76 g, 6.0 mmol) afforded the title compound as a white solid (1.20 g, 73% yield) by using Hexane/EtOAc (5:1) as eluent.  $^1\text{H}$  NMR (400 MHz,  $\text{CDCl}_3$ )  $\delta$  7.83 (dd,  $J = 5.5, 3.0$  Hz, 2H), 7.74 (dd,  $J = 5.4, 3.1$  Hz, 2H), 7.34 – 7.08 (m, 1H), 6.26 (dd,  $J = 3.1, 1.9$  Hz, 1H), 6.24 – 6.14 (m, 1H), 4.69 (dt,  $J = 7.3, 6.3$  Hz, 1H), 3.22 (dd,  $J = 15.2, 5.6$  Hz, 1H), 2.95 (dd,  $J = 15.2, 7.4$  Hz, 1H), 1.38 (d,  $J = 6.3$  Hz, 3H) ppm.  $^{13}\text{C}$  NMR (101 MHz,  $\text{CDCl}_3$ )  $\delta$  164.3, 151.3, 141.6, 134.6, 129.1, 123.6, 110.4, 107.3, 82.7, 34.0, 18.8 ppm. IR (neat): 3033, 2998, 1786, 1728, 1615, 1468, 1390, 1158, 1125, 997, 951, 905, 878, 850, 828, 784, 695, 519. Mp: 45 °C. HRMS *calcd.* for  $(\text{C}_{15}\text{H}_{13}\text{NNaO}_4)$   $[\text{M}+\text{Na}]^+$ : 294.0742, *found* 294.0737.



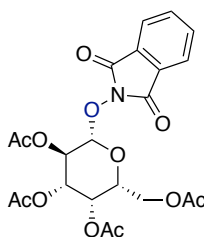
**2-(2-(thiophen-2-yl)ethoxy)isoindoline-1,3-dione (1w)** Following Method A, the utilization of 2-(thiophen-2-yl)ethan-1-ol (1.03 g, 8.0 mmol) afforded the title compound as a light yellow solid (1.5 g, 69% yield) by using Hexane/EtOAc (5:1) as eluent.  $^1\text{H}$  NMR (400 MHz,  $\text{CDCl}_3$ )  $\delta$  7.84 (dd,  $J = 5.5, 3.1$  Hz, 2H), 7.75 (dd,  $J = 5.5, 3.1$  Hz, 2H), 7.15 (dd,  $J = 5.1, 1.2$  Hz, 1H), 7.04 – 6.84 (m, 2H), 4.45 (t,  $J = 7.2$  Hz, 2H), 3.36 (td,  $J = 7.2, 0.8$  Hz, 2H) ppm.  $^{13}\text{C}$  NMR (101 MHz,  $\text{CDCl}_3$ )  $\delta$  163.7, 138.8, 134.6, 129.0, 127.1, 125.9, 124.2, 123.7, 78.3, 29.1 ppm. IR (neat): 3100, 2969, 2895, 2857, 1784, 1723, 1610, 1466, 1399, 1376, 1239, 1185, 1157, 1080, 1017, 997, 951, 905, 878, 850, 828, 784, 695, 519. Mp: 51 °C. HRMS *calcd.* for  $(\text{C}_{14}\text{H}_{11}\text{NNaO}_3\text{S})$   $[\text{M}+\text{Na}]^+$ : 296.0357, *found* 296.0352.





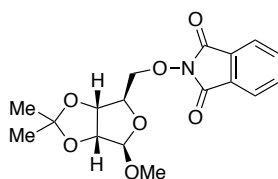
**2-(((3*aS*,4*S*,6*R*,6*aS*)-6-((*R*)-2,2-dimethyl-1,3-dioxolan-4-yl)-2,2-dimethyltetrahydrofuro[3,4-*d*][1,3]dioxol-4-yl)oxy)isoindoline-1,3-dione (6)**

Following General Procedure A, (3*aS*,4*S*,6*R*,6*aS*)-6-((*R*)-2,2-dimethyl-1,3-dioxolan-4-yl)-2,2-dimethyltetrahydrofuro[3,4-*d*][1,3]dioxol-4-ol (1.00 g, 3.6 mmol) afforded the title compound as a white solid (1.00 g, 68% yield) by using Hexane/EtOAc (2:1) as eluent. <sup>1</sup>H NMR (400 MHz, CDCl<sub>3</sub>) δ 7.80 (dd, *J* = 5.4, 3.1 Hz, 2H), 7.72 (dd, *J* = 5.5, 3.1 Hz, 2H), 5.38 (d, *J* = 4.6 Hz, 1H), 5.00 – 4.78 (m, 3H), 4.16 (dd, *J* = 9.1, 6.1 Hz, 1H), 4.00 (m, 2H), 1.61 (s, 3H), 1.42 (s, 3H), 1.40 (s, 3H), 1.38 (s, 3H) ppm. <sup>13</sup>C NMR (101 MHz, CDCl<sub>3</sub>) δ 163.1, 134.4, 129.0, 123.5, 115.6, 109.5, 104.9, 80.7, 80.2, 78.6, 73.4, 67.0, 27.3, 25.6, 25.3, 25.3 ppm. Spectral data was in agreement with the literature<sup>[9]</sup>.



**(2*R*,3*S*,4*S*,5*R*,6*S*)-2-(acetoxymethyl)-6-((1,3-dioxoisindolin-2-yl)oxy)tetrahydro-2*H*-pyran-3,4,5-triyl triacetate (8)** Following the general procedure, but adding 36 mL of 1 M NaOH (water) to a solution of 1.85 g of 1-bromo-2,3,4,6-tetra-*O*-acetyl-β-D-galactopyranose (4.5 mmol), 3.68 g *N*-hydroxyphthalimide (22.6 mmol) and 1.52 g tetrabutylammonium hydrogensulfate (4.5 mmol) in 36 mL of CH<sub>2</sub>Cl<sub>2</sub>. The reaction was stirred for 4 h at room temperature, and then 40 mL of CH<sub>2</sub>Cl<sub>2</sub> was added to the reaction mixture. Then, the organic phase was washed 6 times with water and twice with brine (20 mL each), then dried with Na<sub>2</sub>SO<sub>4</sub>, and the mixture was concentrated in vacuum, affording the title compound as a white solid (0.99 g, 45% yield) by using Hexane/EtOAc (1:1) as eluent. <sup>1</sup>H NMR (400 MHz, CDCl<sub>3</sub>) δ 7.86 (dd, *J* = 5.5, 3.1 Hz, 2H), 7.78 (dd, *J* = 5.5, 3.1 Hz, 2H), 5.31 – 5.28 (m, 2H), 5.26 – 5.21 (m, 1H), 5.13 – 5.09 (m, 1H), 4.33 (dd, *J* = 12.4, 4.9 Hz, 1H), 4.14 (dd, *J* = 12.3, 2.7 Hz, 1H), 3.77 (m, 1H), 2.19 (s, 3H), 2.10 – 1.99 (m, 9H) ppm. <sup>13</sup>C NMR (101 MHz, CDCl<sub>3</sub>) δ <sup>13</sup>C NMR (126 MHz, CDCl<sub>3</sub>) δ 170.7, 170.2, 169.6, 169.4, 162.7, 134.9, 128.9, 123.9, 105.2, 72.6, 72.5, 69.7, 68.3, 61.9, 20.8, 20.8, 20.7, 20.6 ppm. Spectral data was in agreement

with the literature<sup>[10]</sup>.



**2-(((3aR,4R,6R,6aR)-6-methoxy-2,2-dimethyltetrahydrofuro[3,4-d][1,3]dioxol-4-yl)methoxy)isoindoline-1,3-dione (10)** Following Method A, the utilization of ((3aR,4R,6R,6aR)-6-methoxy-2,2-dimethyltetrahydrofuro[3,4-d][1,3]dioxol-4-yl)methanol (1.20 g, 5.9 mmol) afforded the title compound as a white solid (1.37 g, 67% yield) by using Hexane/EtOAc (2:1) as eluent. <sup>1</sup>H NMR (400 MHz, CDCl<sub>3</sub>) δ 7.84 (dd, *J* = 5.4, 3.1 Hz, 2H), 7.75 (dd, *J* = 5.5, 3.1 Hz, 2H), 4.98 (s, 1H), 4.92 (dd, *J* = 6.0, 1.0 Hz, 1H), 4.62 (d, *J* = 5.9 Hz, 1H), 4.55 (ddd, *J* = 7.5, 6.1, 1.1 Hz, 1H), 4.28 (dd, *J* = 9.7, 6.2 Hz, 1H), 4.16 (dd, *J* = 9.6, 7.8 Hz, 1H), 3.33 (s, 3H), 1.49 (s, 3H), 1.34 (s, 3H) ppm. <sup>13</sup>C NMR (101 MHz, CDCl<sub>3</sub>) δ 163.6, 134.9, 129.2, 123.9, 113.0, 109.8, 85.3, 83.6, 82.3, 78.7, 55.4, 26.7, 25.3, 22.2 ppm. IR (neat): 2984, 2938, 1791, 1729, 1468, 1373, 1239, 1187, 1160, 1089, 1048, 1019, 996, 967, 868, 786, 700, 517. Mp: 35 °C. HRMS *calcd.* for (C<sub>17</sub>H<sub>19</sub>NNaO<sub>7</sub>) [M+Na]<sup>+</sup>: 372.1059, *found* 372.1054.

## 2.7.3 General Procedure of Ni-Catalyzed Reductive Coupling

### Ni-Catalyzed Reductive Coupling with Aryl Bromides

**General procedure A:** An oven-dried 8 mL screw-cap test tube containing a stirring bar was charged with 4-CzIPN (3.2 mg, 2 mol%), 4,4'-Di-*tert*-butyl-2,2'-bipyridine (8.0 mg, 15 mol%), Hantzsch ester (HE) (1.5-2.0 equiv) and N-alkoxyphthalimides (1.5 - 2.0 equiv). The test tube was introduced in an argon-filled glovebox where NiBr<sub>2</sub>·diglyme (7.0 mg, 10 mol%) and K<sub>2</sub>CO<sub>3</sub> (28.0 mg, 1.0 equiv) were subsequently added followed by addition of NMP (0.8 mL, 0.25 M). Then the tube was brought out, and aryl bromide (0.20 mmol) (if aryl bromide is liquid, it can be added to the reaction mixture last; if solid, it should be weighed out in the glovebox) was added to the reaction mixture. PTFE tape was used to ensure the tightness of the reaction system, and then the tube was stirred at 35-40 °C under irradiation of blue LEDs with a fan for 18-24 h. After the reaction was finished, the reaction mixture was extracted with ethyl acetate/Et<sub>2</sub>O and water/brine (3 times). Then, the organic layers were combined, dried over MgSO<sub>4</sub> and concentrated under vacuum. The product was purified by flash

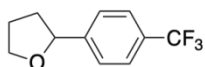
---

chromatography column on silica gel.

**General procedure B:** An oven-dried 8 mL screw-cap test tube containing a stirring bar was charged with 4,4'-Di-*tert*-butyl-2,2'-bipyridine (8.0 mg, 15 mol%), Hantzsch ester (HE) (126.7 mg, 2.5 equiv) and N-alkoxyphthalimides (0.30 mmol, 1.5 equiv). The test tube was introduced in an argon-filled glovebox where NiBr<sub>2</sub>·diglyme (7.0 mg, 10 mol%) and TBAB (32.2 mg, 0.5 equiv) were subsequently added followed by addition of NMP (0.8 mL, 0.25 M). Then the tube was brought out, and aryl bromide (0.20 mmol) (if aryl bromide is liquid, it can be added to the reaction mixture last; if solid, it should be weight out in the glovebox) was added to the reaction mixture. PTFE tape was used to ensure the tightness of the reaction system, and then the tube was stirred at 35-40 °C under irradiation of blue LEDs with a fan for 18-24 h. After the reaction was finished, the reaction mixture was extracted with ethyl acetate/Et<sub>2</sub>O and water/brine (3 times). Then, the organic layers were combined, dried over MgSO<sub>4</sub> and concentrated under vacuum. The product was purified by flash chromatography column on silica gel.

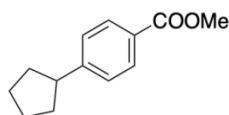
#### Ni-Catalyzed Reductive Coupling with Unactivated Alkyl Bromides

**General procedure C:** An oven-dried 8 mL screw-cap test tube containing a stirring bar was charged with 4-CzIPN (3.2 mg, 2 mol%), NiCl<sub>2</sub>·6H<sub>2</sub>O (4.8 mg, 10 mol% ), 4,4"-di-*tert*-butyl-4'-(4-(*tert*-butyl)phenyl)-2,2':6',2"-terpyridine (14.3 mg, 15 mol%), Hantzsch ester (HE) (101.3 mg, 2.0 equiv) and N-alkoxyphthalimides (0.40 mmol, 2.0 equiv). The test tube was introduced in an argon-filled glovebox where K<sub>2</sub>CO<sub>3</sub> (28.0 mg, 1.0 equiv) and Mg(OEt)<sub>2</sub> (23.0 mg, 1.0 equiv) were subsequently added followed by addition of DMF (1.6 mL, 0.125 M). Then the tube was brought out, and alkyl bromide (0.20 mmol) (if aryl bromide is liquid, it can be added to the reaction mixture last; if solid, it should be weight out in the glovebox) was added to the reaction mixture. PTFE tape was used to ensure the tightness of the reaction system, and then the tube was stirred at 35-40 °C under irradiation of blue LEDs with a fan for 18-24 h. After the reaction was finished, the reaction mixture was extracted with ethyl acetate/Et<sub>2</sub>O and water/brine (3 times). Then, the organic layers were combined, dried over MgSO<sub>4</sub> and concentrated under vacuum. The product was purified by flash chromatography column on silica gel.

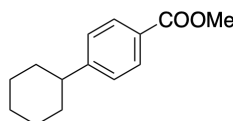


**2-(4-(trifluoromethyl)phenyl)tetrahydrofuran (3a)** Following General Procedure A, 1-bromo-4-(trifluoromethyl)benzene (**2a**) (44.8 mg, 0.20 mmol) and 2-((tetrahydrofuran-2-yl)methoxy)isoindoline-1,3-dione (**1a**) (74.1 mg, 0.30 mmol) were

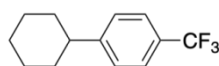
used, affording the title compound as a colourless liquid (33.3 mg, 77% yield) by using Hexane/EtOAc (100:1) as eluent.  $^{19}\text{F}$  NMR (376 MHz,  $\text{CDCl}_3$ )  $\delta$  -62.50 ppm.  $^1\text{H}$  NMR (500 MHz,  $\text{CDCl}_3$ )  $\delta$  7.59 (d,  $J$  = 8.5 Hz, 2H), 7.45 (d,  $J$  = 8.5 Hz, 2H), 4.94 (t,  $J$  = 7.5 Hz, 1H), 4.10 (dt,  $J$  = 8.0, 7.0 Hz, 1H), 3.96 (dt,  $J$  = 8.0, 7.0 Hz, 1H), 2.39 – 2.33 (m, 1H), 2.03 – 1.98 (m, 2H), 1.80 – 1.73 (m, 1H) ppm.  $^{13}\text{C}$  NMR (126 MHz,  $\text{CDCl}_3$ )  $\delta$  147.9, 129.3 (q,  $J_{\text{C,F}}$  = 32.3 Hz), 125.8, 125.3 (q,  $J_{\text{C,F}}$  = 3.8 Hz), 124.4 (q,  $J_{\text{C,F}}$  = 272.3 Hz), 80.0, 68.9, 34.8, 26.0 ppm. Spectral data was in agreement with the literature<sup>[11]</sup>.



**Methyl 4-cyclopentylbenzoate (3b)** Following General Procedure A, Methyl 4-bromobenzoate (**2b**) (42.8 mg, 0.20 mmol) and 2-(cyclopentyl(phenyl)methoxy)isoindoline-1,3-dione (**1b**) (96.3 mg, 0.30 mmol) were used, affording the title compound as a colourless liquid (21.6 mg, 53% yield) by using Hexane/EtOAc (50:1) as eluent.  $^1\text{H}$  NMR (400 MHz,  $\text{CDCl}_3$ )  $\delta$  7.95 (d,  $J$  = 8.5 Hz, 2H), 7.29 (d,  $J$  = 8.5 Hz, 2H), 3.89 (s, 3H), 3.04 (q,  $J$  = 8.5 Hz, 1H), 2.08 (m, 2H), 1.82 – 1.59 (m, 6H) ppm.  $^{13}\text{C}$  NMR (101 MHz,  $\text{CDCl}_3$ )  $\delta$  167.1, 152.1, 129.5, 127.6, 127.0, 51.8, 45.9, 34.4, 25.5 ppm. Spectral data was in agreement with the literature<sup>[12]</sup>.

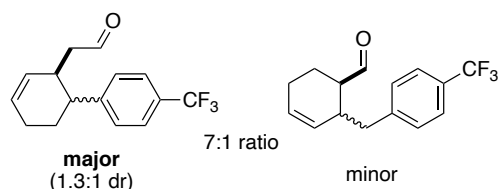


**Methyl 4-cyclohexylbenzoate (3c)** Following General Procedure A, Methyl 4-bromobenzoate (**2b**) (42.8 mg, 0.20 mmol) and 2-(cyclohexyl(phenyl)methoxy)isoindoline-1,3-dione (**1c**) (100.5 mg, 0.30 mmol) were used, affording the title compound as a colourless liquid (37.0 mg, 85% yield) by using Hexane/EtOAc (50:1) as eluent.  $^1\text{H}$  NMR (400 MHz,  $\text{CDCl}_3$ )  $\delta$  7.97 (d,  $J$  = 8.0 Hz, 2H), 7.28 (d,  $J$  = 8.0 Hz, 2H), 3.90 (s, 3H), 2.58-2.54 (m, 1H), 1.87 (m, 4H), 1.77 (d,  $J$  = 12.5 Hz, 1 H), 1.48 – 1.31 (m, 4H), 1.29 – 1.25 (m, 1H) ppm.  $^{13}\text{C}$  NMR (101 MHz,  $\text{CDCl}_3$ )  $\delta$  167.3, 153.6, 129.8, 127.9, 127.0, 52.0, 44.8, 34.3, 26.9, 26.2 ppm. Spectral data was in agreement with the literature<sup>[13]</sup>.



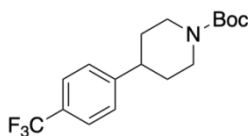
**1-cyclohexyl-4-(trifluoromethyl)benzene (3d)** Following General Procedure A, 1-bromo-4-(trifluoromethyl)benzene (**2a**) (44.8 mg, 0.20 mmol) and 2-((2-cyclohexylpropan-2-yl)oxy)isoindoline-1,3-dione (**1d**) (86.1 mg, 0.30 mmol) were used, affording the title compound as a colourless liquid (30.1 mg, 66% yield) by using

Hexane/EtOAc (100:1) as eluent.  $^{19}\text{F}$  NMR (376 MHz,  $\text{CDCl}_3$ )  $\delta$  -62.37 ppm.  $^1\text{H}$  NMR (400 MHz,  $\text{CDCl}_3$ )  $\delta$  7.56 (d,  $J = 8.1$  Hz, 2H), 7.32 (d,  $J = 8.1$  Hz, 2H), 2.65 – 2.48 (m, 1H), 1.91 – 1.76 (m, 5H), 1.51 – 1.23 (m, 5H) ppm.  $^{13}\text{C}$  NMR (126 MHz,  $\text{CDCl}_3$ )  $\delta$  152.1, 128.2 (q,  $J_{\text{C,F}} = 32.0$  Hz), 127.2, 125.3 (q,  $J_{\text{C,F}} = 3.8$  Hz), 124.5 (q,  $J_{\text{C,F}} = 269.9$  Hz), 44.6, 34.3, 26.8, 26.1 ppm. Spectral data was in agreement with the literature<sup>[14]</sup>.



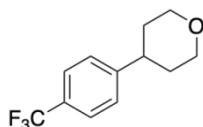
**2-(4'-(trifluoromethyl)-1,2,5,6-tetrahydro-[1,1'-biphenyl]-2-yl)acetaldehyde (3e)**

Following General Procedure A, 1-bromo-4-(trifluoromethyl)benzene (**2a**) (44.8 mg, 0.20 mmol) and 2-(bicyclo[4.2.0]oct-2-en-7-yloxy)isoindoline-1,3-dione (**1e**) (80.7 mg, 0.30 mmol) were used, affording the title compound as a liquid (40.2 mg, 75% yield, 7:1 regioisomeric ratio, with 1.3:1 dr for the major isomer) by using Hexane/EtOAc (20:1) as eluent, with the regioselectivities being determined by NMR analysis.  $^{19}\text{F}$  NMR (376 MHz,  $\text{CDCl}_3$ )  $\delta$  -62.47, -62.50 ppm.  $^1\text{H}$  NMR (400 MHz,  $\text{CDCl}_3$ )  $\delta$  9.64 (d,  $J = 1.6$  Hz,  $0.09\text{H}_{\text{minor}}$ ), 9.63 (dd,  $J = 2.6, 1.3$  Hz,  $0.62\text{H}_{\text{major}}$ ), 7.60 – 7.48 (m,  $2\text{H}_{\text{major+minor}}$ ), 7.31 (d,  $J = 8.0$  Hz,  $2\text{H}_{\text{major+minor}}$ ), 5.83 (m,  $0.79\text{H}_{\text{major}}$ ), 5.71 (m,  $0.23\text{H}_{\text{minor}}$ ), 5.68 – 5.63 (m,  $0.68\text{H}_{\text{major1+major2}}$ ), 5.54 (m,  $0.12\text{H}_{\text{minor1+minor2}}$ ), 2.99 – 2.77 (m,  $1\text{H}_{\text{major+minor}}$ ), 2.55 (m,  $1\text{H}_{\text{major+minor}}$ ), 2.38 (m,  $1\text{H}_{\text{major+minor}}$ ), 2.27 (m,  $1\text{H}_{\text{major+minor}}$ ), 2.23 – 2.03 (m,  $2\text{H}_{\text{major+minor}}$ ), 1.86 (m,  $2\text{H}_{\text{major+minor}}$ ) ppm  $^{13}\text{C}$  NMR (101 MHz,  $\text{CDCl}_3$ )  $\delta$  204.0, 202.0, 149.4, 129.9, 129.5, 129.4, 129.4, 129.2, 128.9, 128.6, 128.4, 128.3, 128.3, 128.2, 127.7, 125.6, 125.9 (q,  $J_{\text{C,F}} = 3.7$  Hz), 123.4, 50.9, 48.0, 46.5, 46.3, 40.9, 38.7, 38.2, 37.1, 36.1, 30.7, 25.8, 25.7, 23.7, 21.2 ppm. IR (neat): 3025, 2924, 2726, 1722, 1619, 1421, 1322, 1161, 1109, 1067, 1017, 837, 719, 685, 605. HRMS *calcd.* for ( $\text{C}_{15}\text{H}_{15}\text{F}_3\text{NaO}$ )  $[\text{M}+\text{Na}]^+$ : 291.0973, *found* 291.0968.

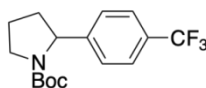


**tert-butyl 4-(4-(trifluoromethyl)phenyl)piperidine-1-carboxylate (3f)** Following General Procedure A, 1-bromo-4-(trifluoromethyl)benzene (**2a**) (44.8 mg, 0.20 mmol) and *tert*-butyl 4-(((1,3-dioxisoindolin-2-yl)oxy)(phenyl)methyl)piperidine-1-carboxylate (**1f**) (114.1 mg, 0.30 mmol) were used, affording the title compound as a liquid (46.8 mg, 71% yield) by using Hexane/EtOAc (20:1) as eluent.  $^{19}\text{F}$  NMR (376

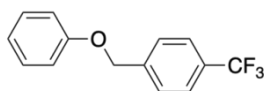
**MHz, CDCl<sub>3</sub>**)  $\delta$  -62.48 ppm. **<sup>1</sup>H NMR (400 MHz, CDCl<sub>3</sub>)**  $\delta$  7.56 (d,  $J$  = 8.2 Hz, 2H), 7.31 (d,  $J$  = 8.1 Hz, 2H), 4.26 (d,  $J$  = 13.1 Hz, 2H), 2.81 (t,  $J$  = 13.9 Hz, 2H), 2.71 (tt,  $J$  = 12.2, 3.5 Hz, 1H), 1.82 (d,  $J$  = 13.3 Hz, 2H), 1.66 – 1.58 (m, 2H), 1.48 (s, 9H) ppm. **<sup>13</sup>C NMR (101 MHz, CDCl<sub>3</sub>)**  $\delta$  154.9, 149.8 (q,  $J_{C,F}$  = 1.4 Hz), 128.8 (q,  $J_{C,F}$  = 32.4 Hz), 127.2, 125.5 (q,  $J_{C,F}$  = 4.0 Hz), 124.3 (q,  $J_{C,F}$  = 271.8 Hz), 79.7, 44.3 (br), 42.7, 33.0, 28.6 ppm. Spectral data was in agreement with the literature<sup>[15]</sup>.



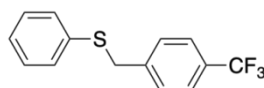
**4-(4-(trifluoromethyl)phenyl)tetrahydro-2H-pyran (3g)** Following General Procedure A, 1-bromo-4-(trifluoromethyl)benzene (**2a**) (44.8 mg, 0.20 mmol) and 2-(phenyl(tetrahydro-2H-pyran-4-yl)methoxy)isoindoline-1,3-dione (**1g**) (101.1 mg, 0.30 mmol) were used, affording the title compound as a liquid (35.9 mg, 78% yield) by using Hexane/EtOAc (20:1) as eluent. **<sup>19</sup>F NMR (376 MHz, CDCl<sub>3</sub>)**  $\delta$  -62.47 ppm. **<sup>1</sup>H NMR (400 MHz, CDCl<sub>3</sub>)**  $\delta$  7.57 (d,  $J$  = 7.9 Hz, 2H), 7.34 (d,  $J$  = 8.0 Hz, 2H), 4.16 – 4.04 (m, 2H), 3.54 (td,  $J$  = 11.6, 2.5 Hz, 2H), 2.83 (tt,  $J$  = 11.6, 4.3 Hz, 1H), 1.92 – 1.72 (m, 4H) ppm. **<sup>13</sup>C NMR (101 MHz, CDCl<sub>3</sub>)**  $\delta$  149.9, 128.8 (q,  $J_{C,F}$  = 31.5 Hz), 127.2, 125.6 (q,  $J_{C,F}$  = 3.8 Hz), 124.4 (q,  $J_{C,F}$  = 272.2 Hz), 68.3, 41.6, 33.7 ppm. Spectral data was in agreement with the literature<sup>[16]</sup>.



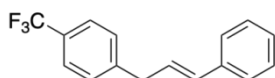
**tert-butyl 2-(4-(trifluoromethyl)phenyl)pyrrolidine-1-carboxylate (3h)** Following General Procedure A, 1-bromo-4-(trifluoromethyl)benzene (**2a**) (44.8 mg, 0.20 mmol), Hantzsch ester (HE) (101.3 mg, 0.40 mmol) and *tert*-butyl 2-(((1,3-dioxoisindolin-2-yl)oxy)methyl)pyrrolidine-1-carboxylate (**1h**) (138.5 mg, 0.40 mmol) were used, affording the title compound as a liquid (47.3 mg, 75% yield) by using Hexane/EtOAc (20:1) as eluent. mixture of rotamers (1.7:1). **<sup>19</sup>F NMR (376 MHz, CDCl<sub>3</sub>)**  $\delta$  -62.39, -62.46 ppm. **<sup>1</sup>H NMR (400 MHz, CDCl<sub>3</sub>)**  $\delta$  7.55 (d,  $J$  = 8.1 Hz, 2H), 7.28 (d,  $J$  = 8.1 Hz, 2H), 5.01 – 4.75 (m, 1H), 3.69 – 3.47 (m, 2H), 2.42 – 2.25 (m, 1H), 1.95 – 1.74 (m, 3H), 1.45 (s, 3H), 1.18 (m, 6H) ppm. **<sup>13</sup>C NMR (101 MHz, CDCl<sub>3</sub>)**  $\delta$  154.5, 149.4, 148.3, 129.0 (q,  $J_{C,F}$  = 32.3 Hz, s), 125.9, 125.7, 124.3 (q,  $J_{C,F}$  = 340.2 Hz, s), 115.6, 79.6, 61.1, 60.6, 47.5, 47.2, 36.0, 34.8, 28.5, 28.2, 23.6, 23.3 ppm. Spectral data was in agreement with the literature<sup>[17]</sup>.



**1-(phenoxyethyl)-4-(trifluoromethyl)benzene (3i)** Following General Procedure A, 1-bromo-4-(trifluoromethyl)benzene (**2a**) (44.8 mg, 0.20 mmol) and 2-(2-phenoxy-1-phenylethoxy)isoindoline-1,3-dione (**1i**) (107.7 mg, 0.03 mmol) were used, affording the title compound as a liquid (45.9 mg, 91% yield) by using Hexane/EtOAc (100:1) as eluent.  $^{19}\text{F}$  NMR (376 MHz,  $\text{CDCl}_3$ )  $\delta$  -62.63 ppm.  $^1\text{H}$  NMR (500 MHz,  $\text{CDCl}_3$ )  $\delta$  7.63 (d,  $J$  = 8.1 Hz, 2H), 7.54 (d,  $J$  = 8.1 Hz, 2H), 7.30 (t,  $J$  = 8.0 Hz, 2H), 6.94 – 7.01 (m, 3H), 5.11 (s, 2H) ppm.  $^{13}\text{C}$  NMR (126 MHz,  $\text{CDCl}_3$ )  $\delta$  158.5, 141.3, 130.2 (q,  $J_{\text{C,F}}$  = 32 Hz), 129.7, 127.4, 125.5 (q,  $J_{\text{C,F}}$  = 4 Hz), 124.2 (q,  $J_{\text{C,F}}$  = 272 Hz), 120.2, 114.9, 69.1 ppm. Spectral data was in agreement with the literature<sup>[18]</sup>.

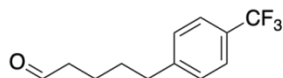


**Phenyl(4-(trifluoromethyl)benzyl)sulfane (3j)** Following General Procedure A, 1-bromo-4-(trifluoromethyl)benzene (**2a**) (44.8 mg, 0.20 mmol) and 2-(1-phenyl-2-(phenylthio)ethoxy)isoindoline-1,3-dione (**1j**) (112.5 mg, 0.30 mmol) were used, affording the title compound as a liquid (32.2 mg, 60% yield) by using Hexane/EtOAc (100:1) as eluent.  $^{19}\text{F}$  NMR (376 MHz,  $\text{CDCl}_3$ )  $\delta$  -62.56 ppm.  $^1\text{H}$  NMR (500 MHz,  $\text{CDCl}_3$ )  $\delta$  7.55–7.53 (m, 2H), 7.40 – 7.37 (m, 2H), 7.33 – 7.21 (m, 5H), 4.14 (s, 2H) ppm.  $^{13}\text{C}$  NMR (126 MHz,  $\text{CDCl}_3$ )  $\delta$  141.9, 135.4, 130.5, 129.5 (q,  $J_{\text{C,F}}$  = 32 Hz), 129.1, 129.0, 127.0, 125.5 (q,  $J_{\text{C,F}}$  = 4 Hz), 124.2 (q,  $J_{\text{C,F}}$  = 271 Hz), 38.9 ppm. Spectral data was in agreement with the literature<sup>[19]</sup>.

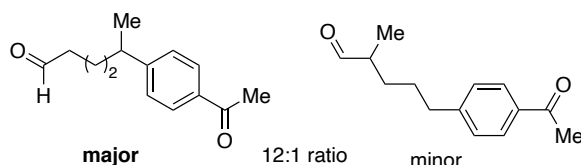


**(E)-2-((1,4-diphenylbut-3-en-1-yl)oxy)isoindoline-1,3-dione (3k)** Following General Procedure A, 1-bromo-4-(trifluoromethyl)benzene (**2a**) (44.8 mg, 0.20 mmol), Hantzsch ester (HE) (101.3 mg, 0.40 mmol) and 1-cinnamyl-4-(trifluoromethyl)benzene (**1k**) (147.6 mg, 0.40 mmol) were used, affording the title compound as a liquid (29.4 mg, 56% yield) by using Hexane/EtOAc (20:1) as eluent.  $^{19}\text{F}$  NMR (376 MHz,  $\text{CDCl}_3$ )  $\delta$  -62.41 ppm.  $^1\text{H}$  NMR (400 MHz,  $\text{CDCl}_3$ )  $\delta$  7.54 (d,  $J$  = 8.0 Hz, 2H), 7.36 – 7.18 (m, 7H), 6.46 (d,  $J$  = 16.0 Hz, 1H), 6.30 (dt,  $J$  = 16.0, 6.8 Hz, 1H), 3.58 (d,  $J$  = 6.8 Hz, 2H) ppm.  $^{13}\text{C}$  NMR (101 MHz,  $\text{CDCl}_3$ )  $\delta$  144.4, 137.2, 132.0, 129.1, 128.8 (q,  $J_{\text{C,F}}$  = 32.1 Hz), 128.7, 128.0, 127.5, 126.3, 125.5 (q,  $J_{\text{C,F}}$  = 3.8 Hz),

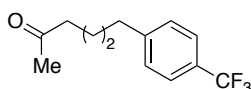
124.5(q,  $J_{C,F} = 271.6$  Hz), 39.2 ppm. Spectral data was in agreement with the literature<sup>[20]</sup>.



**5-(4-(trifluoromethyl)phenyl)pentanal (3l)** Following General Procedure A, 1-bromo-4-(trifluoromethyl)benzene (**2a**) (44.8 mg, 0.20 mmol) and 2-(cyclopentyloxy)isoindoline-1,3-dione (**1l**) (69.3 mg, 0.30 mmol) were used, affording the title compound as a liquid (18.9 mg, 41% yield) by using Hexane/EtOAc (20:1) as eluent.  $^{19}\text{F}$  NMR (376 MHz,  $\text{CDCl}_3$ )  $\delta$  -62.50 ppm.  $^1\text{H}$  NMR (400 MHz,  $\text{CDCl}_3$ )  $\delta$  9.76 (s, 1H), 7.53 (d,  $J = 8.1$  Hz, 2H), 7.28 (d,  $J = 8.0$  Hz, 2H), 2.70 (m, 2H), 2.56 – 2.41 (m, 2H), 1.71 – 1.64 (m, 4H) ppm.  $^{13}\text{C}$  NMR (101 MHz,  $\text{CDCl}_3$ )  $\delta$  202.2, 146.1, 128.8, 128.4 (q,  $J_{C,F} = 32.3$  Hz), 125.4 (q,  $J_{C,F} = 3.8$  Hz), 124.4 (q,  $J_{C,F} = 271.8$  Hz), 43.7, 35.6, 30.6, 21.7 ppm. IR (neat): 2940, 2865, 1734, 1618, 1418, 1325, 1163, 1120, 1067, 1019. HRMS *calcd.* for ( $\text{C}_{12}\text{H}_{12}\text{F}_3\text{O}$ ) [ $\text{M}-\text{H}$ ] $^-$ : 229.0840, *found* 229.0602.

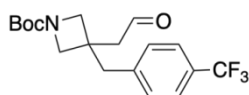


**5-(4-acetylphenyl)hexanal (3m)** Following General Procedure A, 1-(4-bromophenyl)ethan-1-one (**2c**) (39.6 mg, 0.20 mmol), Hantzsch ester (HE) (101.3 mg, 0.40 mmol) and 2-((2-methylcyclopentyl)oxy)isoindoline-1,3-dione (**1m**) (98.0 mg, 0.40 mmol) were used, affording the title compound as a liquid (24.4 mg, 60% yield, 12:1 regioisomeric ratio) by using Hexane/EtOAc (20:1) as eluent, with the regioselectivities being determined by NMR analysis  $^1\text{H}$  NMR (400 MHz,  $\text{CDCl}_3$ )  $\delta$  9.69 (q,  $J = 1.4$  Hz, 0.8H<sub>major</sub>), 9.59 (dd,  $J = 2.1, 1.0$  Hz, 0.07H<sub>minor</sub>), 7.89 – 7.87 (m, 2H<sub>major+minor</sub>), 7.26 (d,  $J = 8.1$  Hz, 2H<sub>major+minor</sub>), 2.76 (q,  $J = 7.0$  Hz, 0.93H<sub>major</sub>), 2.69 (d,  $J = 7.3$  Hz, 0.09H<sub>minor</sub>), 2.57 (s, 3H<sub>major+minor</sub>), 2.41 – 2.35 (m, 2H<sub>major+minor</sub>), 1.66 – 1.53 (m, 3H<sub>major+minor</sub>), 1.52 – 1.43 (m, 1H<sub>major+minor</sub>), 1.26 (dd,  $J = 7.0, 0.9$  Hz, 3H<sub>major</sub>), 1.09 (dd,  $J = 7.1, 1.0$  Hz, 0.26H<sub>minor</sub>) ppm.  $^{13}\text{C}$  NMR (101 MHz,  $\text{CDCl}_3$ )  $\delta$  204.8, 202.3, 197.8, 152.8, 147.8, 135.5, 135.3, 46.2, 43.8, 40.1, 37.5, 35.9, 30.0, 28.4, 26.6, 22.1, 20.2, 13.4 ppm. IR (neat): 2938, 2863, 1737, 1715, 1618, 1417, 1360, 1322, 1160, 1110, 1066, 1018, 846, 819, 733, 592. HRMS *calcd.* for ( $\text{C}_{14}\text{H}_{18}\text{NaO}_2$ ) [ $\text{M}+\text{Na}$ ] $^+$ : 241.1204, *found* 241.1199.

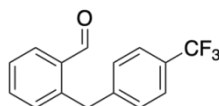




**6-(4-(trifluoromethyl)phenyl)hexan-2-one (3n)** Following General Procedure A, 1-bromo-4-(trifluoromethyl)benzene (**2a**) (44.8 mg, 0.20 mmol) and 2-((1-methylcyclopentyl)oxy)isoindoline-1,3-dione (**1n**) (73.5 mg, 0.30 mmol) were used, affording the title compound as a liquid (37.6 mg, 77% yield) by using Hexane/EtOAc (20:1) as eluent.  $^{19}\text{F}$  NMR (376 MHz,  $\text{CDCl}_3$ )  $\delta$  -62.39 ppm.  $^1\text{H}$  NMR (500 MHz,  $\text{CDCl}_3$ )  $\delta$  7.52 (d,  $J$  = 8.0 Hz, 2H), 7.27 (d,  $J$  = 8.1 Hz, 2H), 2.67 (t,  $J$  = 6.8 Hz, 2H), 2.45 (t,  $J$  = 6.7 Hz, 2H), 2.12 (s, 3H), 1.65 – 1.59 (m, 4H) ppm.  $^{13}\text{C}$  NMR (126 MHz,  $\text{CDCl}_3$ )  $\delta$  208.8, 146.4, 128.8, 128.3 (q,  $J_{\text{C,F}}$  = 32.3 Hz), 125.3 (q,  $J_{\text{C,F}}$  = 3.8 Hz), 124.5 (q,  $J_{\text{C,F}}$  = 271.8 Hz), 43.5, 35.7, 30.7, 30.0, 23.4 ppm. IR (neat): 2938, 2863, 1736, 1714, 1617, 1417, 1359, 1322, 1160, 1109, 1065, 1018, 845, 819, 732, 591. HRMS *calcd.* for ( $\text{C}_{13}\text{H}_{15}\text{F}_3\text{NaO}$ ) [ $\text{M}+\text{Na}$ ] $^+$ : 267.0973, *found* 267.0967.

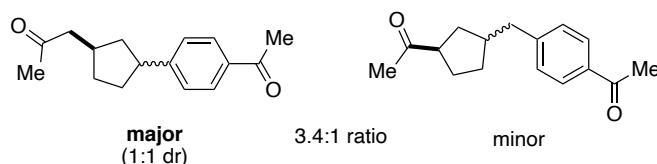


**tert-butyl 3-(2-oxoethyl)-3-(4-(trifluoromethyl)benzyl)azetidino-1-carboxylate (3o)** Following General Procedure A, 1-bromo-4-(trifluoromethyl)benzene (**2a**) (44.8 mg, 0.20 mmol) and *tert*-butyl 6-((1,3-dioxoisindolin-2-yl)oxy)-2-azaspiro[3.3]heptane-2-carboxylate (**1o**) (107.4 mg, 0.30 mmol) were used, affording the title compound as a liquid (52.1 mg, 73% yield) by using Hexane/EtOAc (2:1) as eluent.  $^{19}\text{F}$  NMR (376 MHz,  $\text{CDCl}_3$ )  $\delta$  -62.64 ppm.  $^1\text{H}$  NMR (400 MHz,  $\text{CDCl}_3$ )  $\delta$   $^1\text{H}$  NMR (500 MHz, Chloroform-*d*)  $\delta$  9.76 (s, 1H), 7.56 (d,  $J$  = 8.0 Hz, 2H), 7.21 (d,  $J$  = 8.0 Hz, 2H), 3.96 (d,  $J$  = 8.8 Hz, 2H), 3.71 (d,  $J$  = 8.8 Hz, 2H), 3.12 (s, 2H), 2.70 (s, 2H), 1.43 (s, 9H) ppm.  $^{13}\text{C}$  NMR (126 MHz,  $\text{CDCl}_3$ )  $\delta$  200.1, 156.4, 141.5, 129.9, 129.4 (q,  $J_{\text{C,F}}$  = 32.6 Hz), 125.7 (q,  $J_{\text{C,F}}$  = 3.8 Hz), 124.2 (d,  $J_{\text{C,F}}$  = 271.9 Hz), 79.9, 59.3, 52.8, 49.8, 42.3, 35.5, 28.4 ppm. IR (neat): 3023, 2918, 2837, 1720, 1610, 1435, 1417, 1312, 1277, 1180, 1104, 1019, 851, 770, 706, 665. HRMS *calcd.* for ( $\text{C}_{18}\text{H}_{22}\text{F}_3\text{NNaO}_3$ ) [ $\text{M}+\text{Na}$ ] $^+$ : 380.1449, *found* 380.1450.

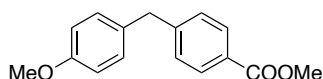


**2-(4-(trifluoromethyl)benzyl)benzaldehyde (3p)** Following General Procedure A, 1-bromo-4-(trifluoromethyl)benzene (**2a**) (44.8 mg, 0.20 mmol), Hantzsch ester (HE) (101.3 mg, 0.40 mmol) and 2-(bicyclo[4.2.0]octa-1,3,5-trien-7-yloxy)isoindoline-1,3-dione (**1p**) (106.0 mg, 0.40 mmol) were used, affording the title compound as a liquid

(27.0 mg, 51% yield) by using Hexane/EtOAc (20:1) as eluent.  $^{19}\text{F}$  NMR (376 MHz,  $\text{CDCl}_3$ )  $\delta$  -62.52 ppm.  $^1\text{H}$  NMR (500 MHz,  $\text{CDCl}_3$ )  $\delta$  10.16 (s, 1H), 7.85 (dd,  $J = 7.8\text{ Hz}$ ,  $J = 1.2\text{ Hz}$ , 1H), 7.58–7.45 (m, 4H), 7.26 (d,  $J = 7.2\text{ Hz}$ , 3H), 4.50 (s, 2H) ppm.  $^{13}\text{C}$  NMR (126 MHz,  $\text{CDCl}_3$ )  $\delta$  192.7, 144.5, 141.7, 134.1, 134.0, 133.8, 131.9, 129.2, 127.5, 128.7 (q,  $J_{\text{C,F}} = 32.4\text{ Hz}$ ), 125.56 (q,  $J_{\text{C,F}} = 3.8\text{ Hz}$ ), 124.38 (q,  $J_{\text{C,F}} = 271.9\text{ Hz}$ ), 38.0 ppm. Spectral data was in agreement with the literature<sup>[21]</sup>.

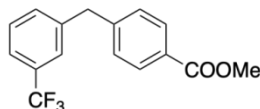


**1-(3-(4-acetylphenyl)cyclopentyl)propan-2-one (major isomer) and 1-(3-(4-acetylbenzyl)cyclopentyl)ethan-1-one (minor isomer) (3q)** Following General Procedure A, 1-(4-bromophenyl)ethan-1-one (**2c**) (39.6 mg, 0.20 mmol) and 2-((2-methylbicyclo[2.2.1]heptan-2-yl)oxy)isoindoline-1,3-dione (**1q**) (81.3 mg, 0.30 mmol) were used, affording the title compound as a liquid (40.0 mg, 82% yield, 3.4:1 regioisomeric ratio, and 1:1 dr for the major isomer) by using Hexane/EtOAc (10:1) as eluent, with regioselectivities being determined by NMR analysis.  $^1\text{H}$  NMR (400 MHz,  $\text{CDCl}_3$ )  $\delta$  7.87 (m,  $2\text{H}_{\text{major+minor}}$ ), 7.29 (m,  $1.54\text{H}_{\text{major}}$ ), 7.25 (m,  $0.45\text{H}_{\text{minor}}$ ), 3.23 – 3.07 (m,  $0.76\text{H}_{\text{major}}$ ), 3.03 – 2.95 (m,  $0.09\text{H}_{\text{minor}}$ ), 2.96 – 2.87 (m,  $0.12\text{H}_{\text{minor}}$ ), 2.69 – 2.64 (m,  $0.5\text{H}_{\text{major}}$ ), 2.57 – 2.54 (m,  $5\text{H}_{\text{major+minor}}$ ), 2.46–2.44 (m,  $0.5\text{H}_{\text{major}}$ ), 2.30 – 2.27 (m,  $0.5\text{H}_{\text{major}}$ ), 2.17 – 1.92 (m,  $5.5\text{H}_{\text{major+minor}}$ ), 1.97–1.91 (m,  $1.5\text{H}_{\text{major+minor}}$ ), 1.45 – 1.36 (m,  $0.5\text{H}_{\text{major}}$ ), 1.32 – 1.20 (m,  $1\text{H}_{\text{major+minor}}$ ) ppm.  $^{13}\text{C}$  NMR (101 MHz,  $\text{CDCl}_3$ )  $\delta$  210.6, 208.5, 197.8, 152.3, 151.8, 147.5, 147.3, 135.2, 135.2, 129.0, 129.0, 128.6, 128.6, 128.6, 127.3, 127.3, 51.9, 51.1, 50.5, 50.1, 45.7, 44.5, 42.4, 41.8, 41.6, 41.6, 41.1, 40.1, 35.6, 35.3, 34.9, 34.8, 34.2, 33.3, 33.0, 32.8, 32.0, 31.93, 30.3, 30.2, 29.3, 28.3, 27.5, 26.6 ppm. IR (neat): 2945, 2867, 1711, 1679, 1605, 1415, 1358, 1269, 1183. HRMS *calcd.* for  $(\text{C}_{16}\text{H}_{20}\text{O}_2)$   $[\text{M}+\text{Na}]^+$ : 267.1361, *found* 267.1356.

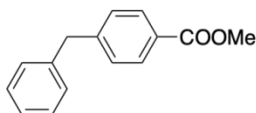


**Methyl 4-(4-methoxybenzyl)benzoate (3r)** Following General Procedure B, Methyl 4-bromobenzoate (**2b**) (42.6 mg, 0.20 mmol) and 2-((4-methoxybenzyl)oxy)isoindoline-1,3-dione (**1r**) (93.3 mg, 0.30 mmol) were used, affording the title compound as a liquid (48.6 mg, 95% yield) by using Hexane/EtOAc (5:1) as eluent.  $^1\text{H}$  NMR (400 MHz,  $\text{CDCl}_3$ )  $\delta$  7.96 (d,  $J = 8.5\text{ Hz}$ , 2H), 7.25 (d,  $J =$

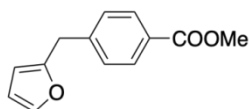
8.5 Hz, 2H), 7.10 (d,  $J = 8.5$  Hz, 2H), 6.85 (d,  $J = 8.5$  Hz, 2H), 3.98 (s, 2H), 3.90 (s, 3H), 3.79 (s, 3H) ppm.  $^{13}\text{C}$  NMR (101 MHz,  $\text{CDCl}_3$ )  $\delta$  167.1, 158.2, 147.0, 132.2, 129.9, 129.8, 128.8, 128.0, 114.0, 55.2, 51.9, 41.04 ppm. Spectral data was in agreement with the literature<sup>[22]</sup>.



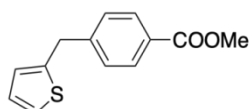
**Methyl 4-(3-(trifluoromethyl)benzyl)benzoate (3s)** Following General Procedure B, Methyl 4-bromobenzoate (**2b**) (42.6 mg, 0.20 mmol) and 2-((3-(trifluoromethyl)benzyl)oxy)isoindoline-1,3-dione (**1s**) (104.7 mg, 0.30 mmol) were used, affording the title compound as a liquid (55.3 mg, 94% yield) by using Hexane/EtOAc (20:1) as eluent.  $^{19}\text{F}$  NMR (376 MHz,  $\text{CDCl}_3$ )  $\delta$  -62.69 ppm.  $^1\text{H}$  NMR (400 MHz,  $\text{CDCl}_3$ )  $\delta$  7.98 (d,  $J = 8.4$  Hz, 2H), 7.49 (d br,  $J = 7.7$  Hz, 1H), 7.44 (s br, 1H), 7.41 (t br,  $J = 8.0$  Hz, 1H), 7.34 (d br,  $J = 7.6$  Hz, 1H), 7.25 (d,  $J = 8.4$  Hz, 2H), 4.09 (s, 2H), 3.91 (s, 3H) ppm.  $^{13}\text{C}$  NMR (101 MHz,  $\text{CDCl}_3$ )  $\delta$  167.0, 145.4, 141.1, 132.3 (q,  $J_{\text{C,F}} = 1.2$  Hz), 131.1 (q,  $J_{\text{C,F}} = 32.1$  Hz), 130.1, 129.2, 129.0, 128.6, 125.7 (q,  $J_{\text{C,F}} = 4.0$  Hz), 124.2 (q,  $J_{\text{C,F}} = 273$  Hz), 123.4 (q,  $J_{\text{C,F}} = 3.8$  Hz), 52.2, 41.7 ppm. Spectral data was in agreement with the literature<sup>[23]</sup>.



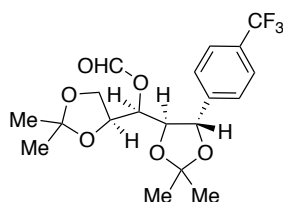
**Methyl 4-benzylbenzoate (3t)** Following General Procedure B, Methyl 4-bromobenzoate (**2b**) (42.6 mg, 0.20 mmol), 2-(benzyloxy)isoindoline-1,3-dione (**1t**) (80.1 mg, 0.30 mmol) and Diethyl 2,6-dimethyl-4-phenyl-1,4-dihydropyridine-3,5-dicarboxylate (**1t**) (164.6 mg, 0.50 mmol) were used, affording the title compound as a liquid (36.6 mg, 81% yield) by using Hexane/EtOAc (20:1) as eluent. Following General Procedure B, Methyl 4-bromobenzoate (**2b**) (42.6 mg, 0.20 mmol) and 2-((1-phenylpentyl)oxy)isoindoline-1,3-dione (**1u**) (92.7 mg, 0.30 mmol) were used, affording the title compound as a colorless oil (43.9 mg, 97% yield) by using Hexane/EtOAc (20:1) as eluent.  $^1\text{H}$  NMR (400 MHz,  $\text{CDCl}_3$ )  $\delta$  7.96 (d,  $J = 8.2$  Hz, 2H), 7.30 (t,  $J = 7.4$  Hz, 2H), 7.27 – 7.20 (m, 3H), 7.18 (d,  $J = 7.3$  Hz, 2H), 4.03 (s, 2H), 3.90 (s, 3H) ppm.  $^{13}\text{C}$  NMR (101 MHz,  $\text{CDCl}_3$ )  $\delta$  167.2, 146.6, 140.2, 129.9, 129.0, 128.7, 128.2, 126.5, 52.1, 42.0. ppm. Spectral data was in agreement with the literature<sup>[24]</sup>.



**Methyl 4-(furan-2-ylmethyl)benzoate (3v)** Following General Procedure B, Methyl 4-bromobenzoate (**2b**) (42.6 mg, 0.20 mmol) and 2-((1-(furan-2-yl)propan-2-yl)oxy)isoindoline-1,3-dione (**1v**) (81.3 mg, 0.30 mmol) were used, affording the title compound as a colourless oil (34.1 mg, 79% yield) by using Hexane/EtOAc (20:1) as eluent.  $^1\text{H NMR}$  (400 MHz,  $\text{CDCl}_3$ )  $\delta$  7.98 (d,  $J = 8.2$  Hz, 2H), 7.35 – 7.32 (m, 1H), 7.30 (d,  $J = 8.2$  Hz, 2H), 6.31 – 6.29 (m, 1H), 6.03 (d,  $J = 2.7$  Hz, 1H), 4.02 (s, 2H), 3.90 (s, 3H) ppm.  $^{13}\text{C NMR}$  (101 MHz,  $\text{CDCl}_3$ )  $\delta$  167.1, 153.7, 143.6, 141.9, 130.0, 128.8, 128.6, 110.5, 106.8, 52.2, 34.6 ppm. Spectral data was in agreement with the literature<sup>[25]</sup>.

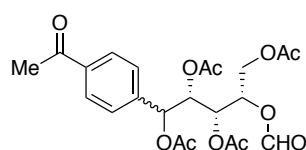


**Methyl 4-(thiophen-2-ylmethyl)benzoate (3w)** Following General Procedure B, Methyl 4-bromobenzoate (**2b**) (42.6 mg, 0.20 mmol) and 2-(2-(thiophen-2-yl)ethoxy)isoindoline-1,3-dione (**1w**) (81.9 mg, 0.30 mmol) were used, affording the title compound as a liquid (29.2 mg, 63% yield) by using Hexane/EtOAc (20:1) as eluent.  $^1\text{H NMR}$  (400 MHz,  $\text{CDCl}_3$ )  $\delta$  7.98 (d,  $J = 8.4$  Hz, 2H), 7.39 – 7.28 (m, 2H), 7.17 (dd,  $J = 5.2, 1.2$  Hz, 1H), 6.94 (dd,  $J = 5.1, 3.4$  Hz, 1H), 6.81 (dt,  $J = 3.4, 1.0$  Hz, 1H), 4.21 (s, 2H), 3.90 (s, 3H) ppm.  $^{13}\text{C NMR}$  (101 MHz,  $\text{CDCl}_3$ )  $\delta$  167.1, 145.7, 142.8, 130.0, 128.7, 128.6, 127.0, 125.6, 124.4, 52.1, 36.1 ppm. **IR (neat):** 2951, 1710, 1610, 1435, 1415, 1176, 1106, 1020, 698. **HRMS *calcd.* for (C<sub>13</sub>H<sub>12</sub>NaO<sub>2</sub>S) [M+Na]<sup>+</sup>: 255,0456, *found* 255,0457.**



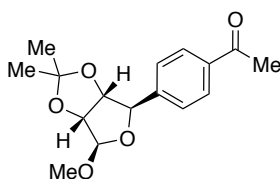
**(R)-((S)-2,2-dimethyl-1,3-dioxolan-4-yl)((4R,5S)-2,2-dimethyl-5-(4-(trifluoromethyl)phenyl)-1,3-dioxolan-4-yl)methyl formate (7)** Following General Procedure A, 1-bromo-4-(trifluoromethyl)benzene (**2a**) (44.8 mg, 0.20 mmol) and (**6**) (121.5 mg, 0.30 mmol) were used, affording the title compound as a liquid (61.4 mg, 76% yield) by using Hexane/EtOA (20:1) as eluent; dr > 20:1. Two-dimensional nuclear magnetic resonance spectroscopy (2D NMR) was used to determine the major diastereoisomer.  $^{19}\text{F NMR}$  (376 MHz,  $\text{CDCl}_3$ )  $\delta$  -62.75 ppm.  $^1\text{H NMR}$  (400 MHz,

$\text{CDCl}_3$ )  $\delta$  8.32 (s, 1H), 7.64 (d,  $J = 8.1$  Hz, 2H), 7.55 (d,  $J = 8.1$  Hz, 2H), 5.25 (dt,  $J = 5.9, 1.3$  Hz, 1H), 4.75 (d,  $J = 8.7$  Hz, 1H), 4.26 (q,  $J = 6.0$  Hz, 1H), 4.06 – 3.96 (m, 2H), 3.91 (dd,  $J = 8.9, 5.9$  Hz, 1H), 1.58 (s, 3H), 1.50 (s, 3H), 1.30 (s, 3H), 1.28 (s, 3H) ppm.  $^{13}\text{C}$  NMR (101 MHz,  $\text{CDCl}_3$ )  $\delta$  160.4, 141.4, 130.8 (q,  $J_{\text{C,F}} = 32.5$  Hz), 126.9, 125.8 (q,  $J_{\text{C,F}} = 3.7$  Hz), 124.1 (q,  $J_{\text{C,F}} = 272.2$  Hz), 110.4, 109.6, 81.7, 77.9, 75.2, 68.6, 65.9, 27.2, 26.8, 26.5, 25.3 ppm. IR (neat): 2990, 2936, 1729, 1373, 1326, 1220, 1167, 1127, 1069, 1017, 835. HRMS *calcd.* for  $(\text{C}_{19}\text{H}_{23}\text{F}_3\text{NaO}_6)$   $[\text{M}+\text{Na}]^+$ : 427.1344, *found* 427.1339.

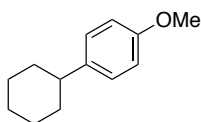


**(2*S*,3*S*,4*S*)-1-(4-acetylphenyl)-4-(formyloxy)pentane-1,2,3,5-tetraacetate (9)** Following General Procedure A, 1-(4-bromophenyl)ethan-1-one (**2c**) (39.6 mg, 0.20 mmol) and (**8**) (148.0 mg, 0.30 mmol) were used, affording the title compound as a liquid (69.0 mg, 74% yield, 1:1 diastereomeric ratio) by using Hexane/EtOAc (1:1) as eluent. *Diastereoisomer-1*:  $^1\text{H}$  NMR (400 MHz,  $\text{CDCl}_3$ )  $\delta$  7.96 (d,  $J = 0.9$  Hz, 1H), 7.91 (d,  $J = 8.3$  Hz, 2H), 7.45 (d,  $J = 8.3$  Hz, 2H), 5.67 (d,  $J = 9.4$  Hz, 1H), 5.63 (dd,  $J = 8.7, 2.1$  Hz, 1H), 5.56 (dd,  $J = 9.4, 2.1$  Hz, 1H), 5.25 (m, 1H), 4.27 (dd,  $J = 12.6, 2.7$  Hz, 1H), 4.13 (dd,  $J = 12.7, 5.8$  Hz, 1H), 2.58 (s, 3H), 2.15 (s, 3H), 2.08 (s, 3H), 2.06 (s, 3H), 1.81 (s, 3H) ppm.  $^{13}\text{C}$  NMR (101 MHz,  $\text{CDCl}_3$ )  $\delta$  197.5, 170.6, 169.7, 169.4, 169.1, 159.6, 141.4, 137.5, 128.5, 128.0, 71.4, 70.7, 67.9, 67.6, 61.9, 26.7, 21.0, 20.7, 20.7, 20.4 ppm. IR (neat): 2938, 2863, 1737, 1715, 1618, 1417, 1360, 1322, 1160, 1110, 1066, 1018, 846, 819, 733, 592. HRMS *calcd.* for  $(\text{C}_{22}\text{H}_{26}\text{NaO}_{11})$   $[\text{M}+\text{Na}]^+$ : 489,1373, *found* 489,1367.

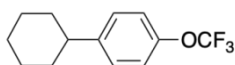
*Diastereoisomer-2*:  $^1\text{H}$  NMR (400 MHz,  $\text{CDCl}_3$ )  $\delta$  7.96 (s,  $J = 1.0$  Hz, 1H), 7.94 (d,  $J = 8.4$  Hz, 2H), 7.42 (d,  $J = 8.2$  Hz, 2H), 5.90 (d,  $J = 6.9$  Hz, 1H), 5.58 (dd,  $J = 7.0, 3.8$  Hz, 1H), 5.22 (tdd,  $J = 6.5, 3.2, 1.0$  Hz, 1H), 5.13 (dd,  $J = 6.5, 3.8$  Hz, 1H), 4.29 (dd,  $J = 12.5, 3.2$  Hz, 1H), 4.03 (dd,  $J = 12.5, 6.5$  Hz, 1H), 2.58 (s, 3H), 2.12 (s, 3H), 2.08 (s, 3H), 2.03 (s, 3H), 2.00 (s, 3H) ppm.  $^{13}\text{C}$  NMR (101 MHz,  $\text{CDCl}_3$ )  $\delta$  197.4, 170.5, 169.7, 169.7, 169.5, 159.5, 140.6, 137.7, 128.8, 127.7, 73.5, 71.2, 68.8, 68.6, 61.6, 26.7, 20.9, 20.7, 20.7, 20.5 ppm.



**1-(4-((3aR,4R,6R,6aR)-6-methoxy-2,2-dimethyltetrahydrofuro[3,4-d][1,3]dioxol-4-yl)phenyl)ethan-1-one (11)** Following General Procedure A, 1-(4-bromophenyl)ethan-1-one (**2c**) (39.6 mg, 0.20 mmol) and (**10**) (139.7 mg, 0.40 mmol) were used, affording the title compound as a liquid (26.9 mg, 46% yield) by using Hexane/EtOAc (3:1) as eluent; dr > 20:1. Two-dimensional nuclear magnetic resonance spectroscopy (2D NMR) was used to determine the major diastereoisomer. <sup>1</sup>H NMR (400 MHz, CDCl<sub>3</sub>) δ 7.94 (d, *J* = 8.5 Hz, 2H), 7.49 (d, *J* = 8.1 Hz, 2H), 5.27 (d, *J* = 2.2 Hz, 1H), 5.15 (s, 1H), 4.85 (dd, *J* = 6.0, 2.2 Hz, 1H), 4.65 (dt, *J* = 5.9, 0.7 Hz, 1H), 3.39 (s, 3H), 2.59 (s, 3H), 1.58 (d, *J* = 0.7 Hz, 3H), 1.35 (d, *J* = 0.7 Hz, 3H) ppm. <sup>13</sup>C NMR (101 MHz, CDCl<sub>3</sub>) δ 197.8, 146.0, 136.5, 128.6, 126.4, 113.2, 110.3, 88.7, 85.8, 55.7, 26.9, 26.7, 25.3 ppm. IR (neat): 2990, 2962, 2929, 2848, 1679, 1606, 1573, 1456, 1415, 1379, 1359, 1266, 1200, 1159, 1115, 1078, 1055, 1032, 1001, 963, 938, 878, 860, 824, 762, 714, 589, 570, 522. HRMS *calcd.* for (C<sub>16</sub>H<sub>20</sub>NaO<sub>5</sub>) [M+Na]<sup>+</sup>: 315.1208, *found* 315.1203.

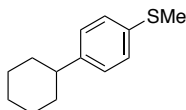


**1-cyclohexyl-4-methoxybenzene (4a)** Following General Procedure A, 1-bromo-4-methoxybenzene (37.2 mg, 0.20 mmol) and 2-((2-cyclohexylpropan-2-yl)oxy)isoindoline-1,3-dione (**1d**) (114.9 mg, 0.40 mmol), HE (101.3 mg, 0.40 mmol) were used, affording the title compound as a colourless liquid (17.8 mg, 47% yield) by using Hexane/EtOAc (50:1) as eluent. <sup>1</sup>H NMR (400 MHz, CDCl<sub>3</sub>) δ 7.13 (d, *J* = 8.7 Hz, 2H), 6.83 (d, *J* = 8.7 Hz, 2H), 3.78 (s, 3H), 2.50 – 2.39 (m, 1H), 1.92 – 1.78 (m, 4H), 1.78 – 1.68 (m, 1H), 1.44 – 1.32 (m, 4H), 1.29 – 1.22 (m, 1H) ppm. <sup>13</sup>C NMR (101 MHz, CDCl<sub>3</sub>) δ 157.8, 140.5, 127.8, 113.9, 55.5, 43.9, 34.9, 27.2, 26.4 ppm. Spectral data was in agreement with the literature<sup>[26]</sup>.

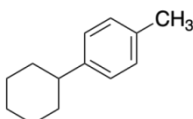


**1-cyclohexyl-4-(trifluoromethoxy)benzene (4b)** Following General Procedure A, 1-bromo-4-(trifluoromethoxy)benzene (48.0 mg, 0.20 mmol) and 2-((2-cyclohexylpropan-2-yl)oxy)isoindoline-1,3-dione (**1d**) (114.9 mg, 0.40 mmol), HE

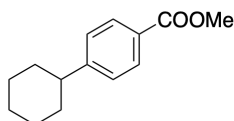
(101.3 mg, 0.40 mmol) were used, affording the title compound as a colourless liquid (25.5 mg, 52% yield) by using Hexane/EtOAc (100:1) as eluent.  $^{19}\text{F}$  NMR (376 MHz,  $\text{CDCl}_3$ )  $\delta$  -58.00.  $^1\text{H}$  NMR (400 MHz,  $\text{CDCl}_3$ )  $\delta$  7.20 (d,  $J$  = 8.8 Hz, 2H), 7.11 (d,  $J$  = 8.6 Hz, 2H), 2.50 (tt,  $J$  = 8.6, 3.2 Hz, 1H), 1.91 – 1.79 (m, 4H), 1.79 – 1.70 (m, 1H), 1.45 – 1.32 (m, 4H), 1.30 – 1.20 (m, 1H) ppm.  $^{13}\text{C}$  NMR (101 MHz,  $\text{CDCl}_3$ )  $\delta$  147.3, 146.8, 127.9, 120.8, 120.5 (q,  $J_{\text{C,F}}$  = 256.3 Hz), 43.9, 34.4, 26.8, 26.0. Spectral data was in agreement with the literature<sup>[27]</sup>.



**(4-cyclohexylphenyl)(methyl)sulfane (4c)** Following General Procedure A, (4-bromophenyl)(methyl)sulfane (40.4 mg, 0.20 mmol) and 2-((2-cyclohexylpropan-2-yl)oxy)isoindoline-1,3-dione (**1d**) (114.9 mg, 0.40 mmol), HE (101.3 mg, 0.40 mmol) were used, affording the title compound as a colourless liquid (30.3 mg, 74% yield) by using Hexane/EtOAc (50:1) as eluent.  $^1\text{H}$  NMR (400 MHz,  $\text{CDCl}_3$ )  $\delta$  7.20 (d,  $J$  = 8.3 Hz, 2H), 7.13 (d,  $J$  = 8.2 Hz, 2H), 2.47 (s, 4H), 1.84 (s, 4H), 1.77 – 1.69 (m, 1H), 1.45 – 1.31 (m, 4H), 1.27 – 1.20 (m, 1H) ppm.  $^{13}\text{C}$  NMR (101 MHz,  $\text{CDCl}_3$ )  $\delta$  145.5, 135.2, 127.6, 127.4, 44.2, 34.6, 27.0, 26.3, 16.5 ppm. Spectral data was in agreement with the literature<sup>[28]</sup>.

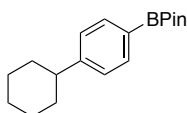


**1-cyclohexyl-4-methylbenzene (4d)** Following General Procedure A, 1-bromo-4-methylbenzene (34.0 mg, 0.20 mmol) and 2-((2-cyclohexylpropan-2-yl)oxy)isoindoline-1,3-dione (**1d**) (114.9 mg, 0.40 mmol), HE (101.3 mg, 0.40 mmol) were used, affording the title compound as a colourless liquid (18.1 mg, 52% yield) by using Hexane/EtOAc (100:1) as eluent.  $^1\text{H}$  NMR (400 MHz,  $\text{CDCl}_3$ )  $\delta$  7.14 (s, 4H), 2.49 (tt,  $J$  = 11.3, 3.6 Hz, 1H), 2.35 (s, 3H), 1.94 – 1.82 (m, 4H), 1.81 – 1.74 (m, 1H), 1.49 – 1.36 (m, 4H), 1.33 – 1.25 (m, 1H) ppm.  $^{13}\text{C}$  NMR (101 MHz,  $\text{CDCl}_3$ )  $\delta$  145.3, 135.3, 129.1, 126.8, 44.3, 34.7, 27.1, 26.3, 21.1. ppm. Spectral data was in agreement with the literature<sup>[29]</sup>.



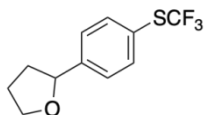
**Methyl 4-cyclohexylbenzoate (3c)** Following General Procedure A, Methyl 4-bromobenzoate (**2b**) (42.8 mg, 0.20 mmol) and 2-((2-cyclohexylpropan-2-

yl)oxy)isoindoline-1,3-dione (**1d**) (114.9 mg, 0.40 mmol) were used, affording the title compound as a colourless liquid (35.0 mg, 81% yield) by using Hexane/EtOAc (50:1) as eluent.  $^1\text{H NMR}$  (400 MHz,  $\text{CDCl}_3$ )  $\delta$  7.97 (d,  $J = 8.0$  Hz, 2H), 7.28 (d,  $J = 8.0$  Hz, 2H), 3.90 (s, 3H), 2.58 – 2.54 (m, 1H), 1.87 (m, 4H), 1.77 (d,  $J = 12.5$  Hz, 1 H), 1.48 – 1.31 (m, 4H), 1.29-1.25 (m, 1H) ppm.  $^{13}\text{C NMR}$  (101 MHz,  $\text{CDCl}_3$ )  $\delta$  167.3, 153.6, 129.8, 127.9, 127.0, 52.0, 44.8, 34.3, 26.9, 26.2 ppm. Spectral data was in agreement with the literature<sup>[13]</sup>.



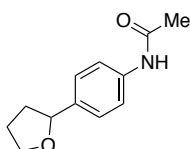
**4,4,5,5-tetramethyl-2-(4-(tetrahydrofuran-2-yl)phenyl)-1,3,2-dioxaborolane (4e)**

Following General Procedure A, 2-(4-bromophenyl)-4,4,5,5-tetramethyl-1,3,2-dioxaborolane (56.4 mg, 0.20 mmol) and 2-((tetrahydrofuran-2-yl)methoxy)isoindoline-1,3-dione (**1a**) (98.8 mg, 0.40 mmol), HE (101.3 mg, 0.40 mmol) were used, affording the title compound as a colourless liquid (34.5 mg, 63% yield) by using Hexane/EtOAc (15:1) as eluent.  $^1\text{H NMR}$  (400 MHz,  $\text{CDCl}_3$ )  $\delta$  7.78 (d,  $J = 7.8$  Hz, 2H), 7.34 (d,  $J = 7.8$  Hz, 2H), 4.92 (t,  $J = 6.9$  Hz, 1H), 4.13-4.06 (m, 1H), 3.98-3.90 (m, 1H), 2.38-2.27 (m, 1H), 2.04-1.94 (m, 2H), 1.84-1.72 (m, 1H), 1.34 (s, 12 H) ppm.  $^{13}\text{C NMR}$  (101 MHz,  $\text{CDCl}_3$ )  $\delta$  146.9, 134.9, 124.9, 83.8, 80.7, 68.8, 34.8, 26.0, 24.9 ppm. Spectral data was in agreement with the literature<sup>[30]</sup>.

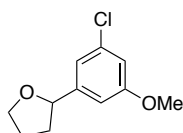


**2-(4-((trifluoromethyl)thio)phenyl)tetrahydrofuran (4f)** Following General Procedure A, (4-bromophenyl)(trifluoromethyl)sulfane (51.2 mg, 0.20 mmol) and 2-((tetrahydrofuran-2-yl)methoxy)isoindoline-1,3-dione (**1a**) (98.9 mg, 0.40 mmol), HE (101.3 mg, 0.40 mmol) were used, affording the title compound as a colourless liquid (31.3 mg, 63% yield) by using Hexane/EtOAc (20:1) as eluent.  $^{19}\text{F NMR}$  (376 MHz,  $\text{CDCl}_3$ )  $\delta$  -43.00 ppm.  $^1\text{H NMR}$  (400 MHz,  $\text{CDCl}_3$ )  $\delta$  7.61 (d,  $J = 8.2$  Hz, 2H), 7.38 (d,  $J = 8.0$  Hz, 2H), 4.92 (t,  $J = 7.2$  Hz, 1H), 4.10 (dt,  $J = 8.1, 6.9$  Hz, 1H), 3.96 (dt,  $J = 8.2, 6.9$  Hz, 1H), 2.45 – 2.26 (m, 1H), 2.18 – 1.96 (m, 2H), 1.78 (dq,  $J = 12.2, 7.7$  Hz, 1H) ppm.  $^{13}\text{C NMR}$  (101 MHz,  $\text{CDCl}_3$ )  $\delta$  147.0, 136.4, 129.79 (q,  $J_{\text{C,F}} = 308.1$  Hz), 126.8, 122.8, 80.1, 69.0, 34.8, 26.1 ppm. **IR (neat):** 1492, 1402, 1109, 1083, 1062, 1015, 923, 828, 756, 570, 530. **HRMS calcd. for (C<sub>11</sub>H<sub>11</sub>F<sub>3</sub>KOS) [M+K]<sup>+</sup>: 287.0120, found 287.0320.**

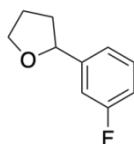




**N-(4-(tetrahydrofuran-2-yl)phenyl)acetamide (4g)** Following General Procedure A, N-(4-bromophenyl)acetamide (42.6 mg, 0.20 mmol) and 2-((tetrahydrofuran-2-yl)methoxy)isoindoline-1,3-dione (**1a**) (98.8 mg, 0.40 mmol), HE (101.3 mg, 0.40 mmol) were used, affording the title compound as a colourless liquid (21.0 mg, 51% yield) by using Hexane/EtOAc (1:1) as eluent. **<sup>1</sup>H NMR (500 MHz, CDCl<sub>3</sub>)** δ 7.49 (s, 1H), 7.44 (d, *J* = 8.5 Hz, 2H), 7.26 (d, *J* = 8.4 Hz, 2H), 4.84 (t, *J* = 7.1 Hz, 1H), 4.07 (q, *J* = 7.3, 6.8 Hz, 1H), 3.91 (q, *J* = 7.6 Hz, 1H), 2.28 (m, 1H), 2.13 (s, 3H), 2.07 – 1.91 (m, 2H), 1.77 (m, 1H) ppm. **<sup>13</sup>C NMR (126 MHz, CDCl<sub>3</sub>)** δ 168.5, 139.4, 137.0, 126.4, 120.0, 80.5, 68.7, 34.6, 26.1, 24.5 ppm. Spectral data was in agreement with the literature<sup>[30]</sup>.

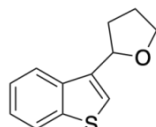


**2-(3-chloro-5-methoxyphenyl)tetrahydrofuran (4h)** Following General Procedure A, 1-bromo-3-chloro-5-methoxybenzene (44.0 mg, 0.20 mmol) and 2-((tetrahydrofuran-2-yl)methoxy)isoindoline-1,3-dione (**1a**) (98.8 mg, 0.40 mmol), HE (101.3 mg, 0.40 mmol) were used, affording the title compound as a colourless liquid (27.6 mg, 65% yield) by using Hexane/EtOAc (15:1) as eluent. **<sup>1</sup>H NMR (400 MHz, CDCl<sub>3</sub>)** δ 6.93 – 6.87 (m, 1H), 6.82 – 6.72 (m, 2H), 4.83 (t, *J* = 7.1 Hz, 1H), 4.08 (dt, *J* = 8.1, 6.8 Hz, 1H), 3.93 (dt, *J* = 8.2, 6.9 Hz, 1H), 3.79 (s, 3H), 2.37 – 2.24 (m, 1H), 2.06 – 1.89 (m, 2H), 1.82 – 1.69 (m, 1H) ppm. **<sup>13</sup>C NMR (101 MHz, CDCl<sub>3</sub>)** δ 160.4, 146.9, 134.9, 118.2, 112.9, 109.9, 80.0, 68.9, 55.6, 34.7, 26.0 ppm. **IR (neat):** 2943, 2869, 1599, 1576, 1458, 1428, 1348 1270, 1190, 1152, 1093, 1048, 925, 845, 689. **HRMS calcd. for (C<sub>11</sub>H<sub>13</sub>ClNaO<sub>2</sub>) [M+Na]<sup>+</sup>: 235.0502, found 235.0496.**

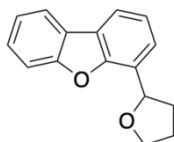


**2-(3-fluorophenyl)tetrahydrofuran (4i)** Following General Procedure A, 1-bromo-3-fluorobenzene (34.8 mg, 0.20 mmol) and 2-((tetrahydrofuran-2-yl)methoxy)isoindoline-1,3-dione (**1a**) (98.8 mg, 0.40 mmol), HE (101.3 mg, 0.40 mmol) were used, affording the title compound as a colourless liquid (21.3 mg, 64%

yield) by using Hexane/EtOAc (30:1) as eluent.  $^{19}\text{F}$  NMR (376 MHz,  $\text{CDCl}_3$ )  $\delta$  -113.47 ppm.  $^1\text{H}$  NMR (400 MHz,  $\text{CDCl}_3$ )  $\delta$  7.32 - 7.24 (m, 1H), 7.11 - 7.01 (m, 2H), 6.96 - 6.89 (m, 1H), 4.89 (t,  $J$  = 7.1 Hz, 1H), 4.14 - 4.03 (m, 1H), 3.99 - 3.88 (m, 1H), 2.40 - 2.23 (m, 1H), 2.08 - 1.94 (m, 2H), 1.85 - 1.71 (m, 1H) ppm.  $^{13}\text{C}$  NMR (101 MHz,  $\text{CDCl}_3$ )  $\delta$  163.2 (d,  $J_{\text{C,F}}$  = 245.3 Hz), 146.5 (d,  $J_{\text{C,F}}$  = 6.7 Hz), 129.9 (d,  $J_{\text{C,F}}$  = 8.3 Hz), 121.2 (d,  $J_{\text{C,F}}$  = 2.9 Hz), 113.9 (d,  $J_{\text{C,F}}$  = 21.1 Hz), 112.6 (d,  $J_{\text{C,F}}$  = 22.1 Hz), 80.1, 68.9, 34.7, 26.0 ppm. Spectral data was in agreement with the literature<sup>[31]</sup>.

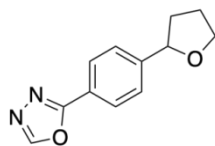


**2-(benzo[b]thiophen-3-yl)tetrahydrofuran (4j)** Following General Procedure A, 3-bromobenzo[b]thiophene (42.4 mg, 0.20 mmol) and 2-((tetrahydrofuran-2-yl)methoxy)isoindoline-1,3-dione (**1a**) (98.8 mg, 0.40 mmol), HE (101.3 mg, 0.40 mmol) were used, affording the title compound as a colourless liquid (17.2 mg, 42% yield) by using Hexane/EtOAc (15:1) as eluent.  $^1\text{H}$  NMR (400 MHz,  $\text{CDCl}_3$ )  $\delta$  7.86 - 7.84 (m, 1H), 7.81 - 7.79 (m, 1H), 7.38 - 7.34 (m, 3H), 5.27 - 5.25 (m, 1H), 4.13 (dt,  $J$  = 8.1, 6.5 Hz, 1H), 3.96 (dt,  $J$  = 8.3, 6.9 Hz, 1H), 2.48 - 2.38 (m, 1H), 2.09 - 2.00 (m, 3H) ppm.  $^{13}\text{C}$  NMR (101 MHz,  $\text{CDCl}_3$ )  $\delta$  141.2, 138.3, 137.6, 124.3, 124.0, 123.0, 122.3, 121.3, 76.8, 68.4, 32.3, 26.0 ppm. IR (neat): 3057, 2972, 2868, 1527, 1459, 1428, 1368, 1314, 1256, 1183, 1139, 1064, 1019, 907, 838, 758, 729, 646, 423. HRMS *calcd.* for ( $\text{C}_{12}\text{H}_{12}\text{NaOS}$ ) [ $\text{M}+\text{Na}$ ] $^+$ : 227.0507, *found* 227.0501.

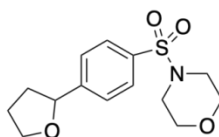


**4-(tetrahydrofuran-2-yl)dibenzo[b,d]furan (4k)** Following General Procedure A, 4-bromodibenzo[b,d]furan (49.2 mg, 0.20 mmol) and 2-((tetrahydrofuran-2-yl)methoxy)isoindoline-1,3-dione (**1a**) (98.8 mg, 0.40 mmol), HE (101.3 mg, 0.40 mmol) were used, affording the title compound as a colourless liquid (30.5 mg, 64% yield) by using Hexane/EtOAc (15:1) as eluent.  $^1\text{H}$  NMR (400 MHz,  $\text{CDCl}_3$ )  $\delta$  7.95 (d,  $J$  = 7.6 Hz, 1H), 7.86 (dd,  $J$  = 7.7, 1.1 Hz, 1H), 7.59 (d,  $J$  = 8.2 Hz, 1H), 7.53 (d,  $J$  = 7.5 Hz, 1H), 7.46 (td,  $J$  = 8.4, 7.9, 1.3 Hz, 1H), 7.37 - 7.31 (m, 2H), 5.48 (t,  $J$  = 6.9 Hz, 1H), 4.28 - 4.17 (m, 1H), 4.15 - 3.97 (m, 1H), 2.65 - 2.48 (m, 1H), 2.21 - 1.95 (m, 3H) ppm.  $^{13}\text{C}$  NMR (101 MHz,  $\text{CDCl}_3$ )  $\delta$  156.2, 153.2, 127.8, 127.1, 124.4, 124.2, 123.9, 122.8, 122.8, 120.7, 119.4, 111.8, 76.3, 68.9, 33.4, 26.3 ppm. IR (neat): 3056,

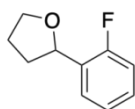
2973, 2870, 1587, 1494, 1473, 1451, 1421, 1344, 1320, 1265, 1242, 1184, 1150, 1050, 908, 842, 796, 748, 722, 615, 562. **HRMS *calcd.* for (C<sub>16</sub>H<sub>14</sub>NaO<sub>2</sub>) [M+Na]<sup>+</sup>: 261.0891, *found* 261.0887.**



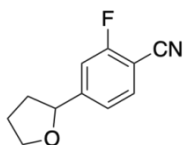
**2-(4-(tetrahydrofuran-2-yl)phenyl)-1,3,4-oxadiazole (4l)** Following General Procedure A, 2-(4-bromophenyl)-1,3,4-oxadiazole (44.8 mg, 0.20 mmol) and 2-((tetrahydrofuran-2-yl)methoxy)isoindoline-1,3-dione (**1a**) (98.8 mg, 0.40 mmol), HE (101.3 mg, 0.40 mmol) were used, affording the title compound as a colourless liquid (31 mg, 72% yield) by using Hexane/EtOAc (3:1) as eluent. **<sup>1</sup>H NMR (500 MHz, CDCl<sub>3</sub>)** δ 8.45 (s, 1H), 8.04 (d, *J* = 8.3 Hz, 2H), 7.48 (d, *J* = 8.1 Hz, 2H), 4.96 (t, *J* = 7.2 Hz, 1H), 4.23 – 4.02 (m, 1H), 3.97 (q, *J* = 7.0 Hz, 1H), 2.38 (dt, *J* = 13.3, 6.7 Hz, 1H), 2.02 (m, 2H), 1.79 (dq, *J* = 12.3, 7.8 Hz, 1H) ppm. **<sup>13</sup>C NMR (126 MHz, CDCl<sub>3</sub>)** δ 164.8, 152.6, 148.2, 127.2, 126.3, 122.3, 80.2, 69.0, 34.8, 26.1 ppm. **IR (neat):** 3126, 2978, 2871, 2245, 1733, 1617, 1587, 1557, 1515, 1497, 1460, 1418, 1105, 1062, 1017, 955, 911, 843, 728, 539. **HRMS *calcd.* for (C<sub>12</sub>H<sub>13</sub>N<sub>2</sub>O<sub>2</sub>) [M+H]<sup>+</sup>: 217.0977, *found* 217.0977.**



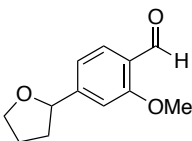
**4-((4-(tetrahydrofuran-2-yl)phenyl)sulfonyl)morpholine (4m)** Following General Procedure A, 4-((4-bromophenyl)sulfonyl)morpholine (61.0 mg, 0.20 mmol) and 2-((tetrahydrofuran-2-yl)methoxy)isoindoline-1,3-dione (**1a**) (98.8 mg, 0.40 mmol), HE (101.3 mg, 0.40 mmol) were used, affording the title compound as a solid (48.8 mg, 82% yield) by using Hexane/EtOAc (3:1) as eluent. **<sup>1</sup>H NMR (400 MHz, CDCl<sub>3</sub>)** δ 7.81 – 7.64 (m, 2H), 7.51 (d, *J* = 8.2 Hz, 2H), 4.96 (t, *J* = 7.2 Hz, 1H), 4.21 – 4.03 (m, 1H), 3.97 (q, *J* = 7.0 Hz, 1H), 3.86 – 3.67 (m, 4H), 3.11 – 2.90 (m, 4H), 2.40 (m, 1H), 2.03 (m, 2H), 1.77 (m, 1H) ppm. **<sup>13</sup>C NMR (101 MHz, CDCl<sub>3</sub>)** δ 149.5, 133.7, 128.1, 126.3, 79.9, 69.1, 66.2, 46.1, 34.8, 26.1 ppm. **IR (neat):** 2978, 2850, 1720, 1596, 1449, 1406, 1344, 1293, 1260, 1160, 1111, 1092, 1063, 1016, 938, 839, 727, 611, 585, 541, 503. **Mp:** 62 °C. **HRMS *calcd.* for (C<sub>14</sub>H<sub>19</sub>NNaO<sub>4</sub>S) [M+Na]<sup>+</sup>: 320,0932, *found* 320,0927.**



**2-(2-fluorophenyl)tetrahydrofuran (4n)** Following General Procedure A, 1-bromo-2-fluorobenzene (34.8 mg, 0.20 mmol) and 2-((tetrahydrofuran-2-yl)methoxy)isoindoline-1,3-dione (**1a**) (98.8 mg, 0.40 mmol), HE (101.3 mg, 0.40 mmol) were used, affording the title compound as a colourless liquid (17.2 mg, 52% yield) by using Hexane/EtOAc (20:1) as eluent.  $^{19}\text{F}$  NMR (376 MHz,  $\text{CDCl}_3$ )  $\delta$  -113.14 ppm.  $^1\text{H}$  NMR (400 MHz,  $\text{CDCl}_3$ )  $\delta$  7.46 (td,  $J = 7.6, 1.4$  Hz, 1H), 7.22 (m, 1H), 7.12 (td,  $J = 7.5, 0.9$  Hz, 1H), 7.01 (m, 1H), 5.15 (t,  $J = 7.1$  Hz, 1H), 4.17 – 4.06 (m, 1H), 4.00 – 3.90 (m, 1H), 2.50 – 2.34 (m, 1H), 2.00 (q,  $J = 6.8$  Hz, 2H), 1.79 (m, 1H) ppm.  $^{13}\text{C}$  NMR (101 MHz,  $\text{CDCl}_3$ )  $\delta$  159.9 (d,  $J_{\text{C,F}} = 245.5$  Hz), 130.9 (d,  $J_{\text{C,F}} = 13.4$  Hz), 128.5 (d,  $J_{\text{C,F}} = 8.1$  Hz), 126.9 (d,  $J_{\text{C,F}} = 4.7$  Hz), 124.1 (d,  $J_{\text{C,F}} = 3.5$  Hz), 115.1 (d,  $J_{\text{C,F}} = 21.3$  Hz), 75.1 (d,  $J_{\text{C,F}} = 2.7$  Hz), 68.7, 33.6 (d,  $J_{\text{C,F}} = 1.3$  Hz), 26.0 ppm. Spectral data was in agreement with the literature<sup>[32]</sup>.

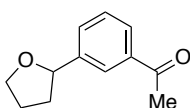


**2-fluoro-4-(tetrahydrofuran-2-yl)benzonitrile (4o)** Following General Procedure A, 4-bromo-2-fluorobenzonitrile (39.8 mg, 0.20 mmol) and 2-((tetrahydrofuran-2-yl)methoxy)isoindoline-1,3-dione (**1a**) (98.8 mg, 0.40 mmol), HE (101.3 mg, 0.40 mmol) were used, affording the title compound as a colourless liquid (20.8 mg, 54% yield) by using Hexane/EtOAc (15:1) as eluent.  $^{19}\text{F}$  NMR (471 MHz,  $\text{CDCl}_3$ )  $\delta$  -109.47 ppm.  $^1\text{H}$  NMR (500 MHz,  $\text{CDCl}_3$ )  $\delta$  7.60 (dd,  $J = 6.1, 2.2$  Hz, 1H), 7.54 (m, 1H), 7.16 (t,  $J = 8.7$  Hz, 1H), 4.86 (t,  $J = 7.2$  Hz, 1H), 4.20 – 4.00 (m, 1H), 4.02 – 3.84 (m, 1H), 2.35 (td,  $J = 12.8, 6.9$  Hz, 1H), 2.10 – 1.87 (m, 2H), 1.82 – 1.66 (m, 1H) ppm.  $^{13}\text{C}$  NMR (126 MHz,  $\text{CDCl}_3$ )  $\delta$  163.3, 161.2, 141.0, 132.4, 132.3, 130.5, 116.4, 116.3, 114.1, 101.3, 101.2, 79.1, 69.0, 34.8, 26.0 ppm. IR (neat): 3384, 3075, 2979, 2876, 2236, 1614, 1498, 1460, 1414, 1349, 1267, 1112, 1060, 910, 832, 730, 648, 627, 492. HRMS *calcd.* for ( $\text{C}_{11}\text{H}_{10}\text{FNNaO}$ ) [ $\text{M}+\text{Na}$ ] $^+$ : 214.0644, *found* 214.0639.

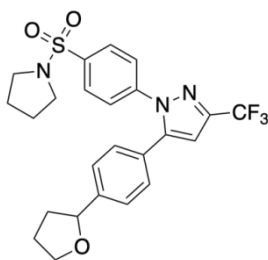


**2-methoxy-4-(tetrahydrofuran-2-yl)benzaldehyde (4p)** Following General Procedure A, 4-bromo-2-methoxybenzaldehyde (42.8 mg, 0.20 mmol) and 2-

((tetrahydrofuran-2-yl)methoxy)isoindoline-1,3-dione (**1a**) (98.8 mg, 0.40 mmol), HE (101.3 mg, 0.40 mmol) were used, affording the title compound as a colourless liquid (19.5 mg, 58% yield) by using Hexane/EtOAc (5:1) as eluent.  $^1\text{H NMR}$  (400 MHz,  $\text{CDCl}_3$ )  $\delta$  10.40 (s, 1H), 7.77 (d,  $J = 7.9$  Hz, 1H), 7.00 (s, 1H), 6.93 (d,  $J = 7.9$  Hz, 1H), 4.91 (t,  $J = 7.2$  Hz, 1H), 4.08 (d,  $J = 7.0$  Hz, 1H), 4.01 – 3.86 (m, 4H), 2.37 (m, 1H), 2.00 (m, 2H), 1.83 – 1.71 (m, 1H) ppm.  $^{13}\text{C NMR}$  (75 MHz,  $\text{CDCl}_3$ )  $\delta$  189.7, 162.2, 152.8, 128.8, 123.8, 117.9, 108.4, 80.3, 69.0, 55.7, 34.7, 26.0. ppm. IR (neat): 2943, 2865, 1736, 1670, 1574, 1493, 1461, 1415, 1395, 1361, 1249, 1196, 1157, 1113, 1062, 1028, 925, 868, 809. HRMS *calcd.* for ( $\text{C}_{12}\text{H}_{14}\text{NaO}_3$ )  $[\text{M}+\text{Na}]^+$ : 229.0841, *found* 229.0835.

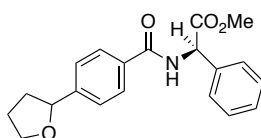


1-(3-(tetrahydrofuran-2-yl)phenyl)ethan-1-one (**4q**) Following General Procedure A, 1-(3-bromophenyl)ethan-1-one (40.0 mg, 0.20 mmol) and 2-((tetrahydrofuran-2-yl)methoxy)isoindoline-1,3-dione (**1a**) (98.8 mg, 0.40 mmol), HE (101.3 mg, 0.40 mmol) were used, affording the title compound as a colourless liquid (26.6 mg, 70% yield) by using Hexane/EtOAc (10:1 – 5:1) as eluent.  $^1\text{H NMR}$  (400 MHz,  $\text{CDCl}_3$ )  $\delta$  7.92 (s, 1H), 7.84 (d,  $J = 7.7$  Hz, 1H), 7.56 (s, 1H), 7.43 (t,  $J = 7.6$  Hz, 1H), 4.94 (t,  $J = 7.2$  Hz, 1H), 4.18 – 4.07 (m, 1H), 3.96 (q,  $J = 7.0$  Hz, 1H), 2.60 (d,  $J = 3.8$  Hz, 3H), 2.37 (m, 1H), 2.03 (m, 2H), 1.79 (m, 1H) ppm.  $^{13}\text{C NMR}$  (101 MHz,  $\text{CDCl}_3$ )  $\delta$  199.5, 144.3, 137.3, 130.5, 128.7, 127.3, 125.5, 80.3, 68.9, 34.8, 26.8, 26.1 ppm. IR (neat): 2976, 2872, 2250, 1692, 1603, 1586, 1435, 1359, 1259, 1196, 1059, 906, 797, 727, 694, 647, 589. HRMS *calcd.* for ( $\text{C}_{12}\text{H}_{15}\text{O}_2$ )  $[\text{M}+\text{H}]^+$ : 191.1072, *found* 191.1067.



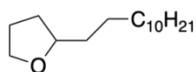
1-(4-(pyrrolidin-1-ylsulfonyl)phenyl)-5-(4-(tetrahydrofuran-2-yl)phenyl)-3-(trifluoromethyl)-1H-pyrazole (**4r**) Following General Procedure A, 5-(4-bromophenyl)-1-(4-(pyrrolidin-1-ylsulfonyl)phenyl)-3-(trifluoromethyl)-1H-pyrazole (99.8 mg, 0.20 mmol) and 2-((tetrahydrofuran-2-yl)methoxy)isoindoline-1,3-dione (**1a**) (98.8 mg, 0.40 mmol), HE (101.3 mg, 0.40 mmol) were used, affording the title

compound as a solid (73.6 mg, 75% yield) by using Hexane/EtOAc (10:1 to 2:1 ) as eluent.  $^{19}\text{F}$  NMR (376 MHz,  $\text{CDCl}_3$ )  $\delta$  -62,16 ppm.  $^1\text{H}$  NMR (400 MHz,  $\text{CDCl}_3$ )  $\delta$  7.81 (d,  $J$  = 8.5 Hz, 2H), 7.49 (s, 2H), 7.33 (d,  $J$  = 8.4 Hz, 2H), 7.17 (d,  $J$  = 8.2 Hz, 2H), 6.76 (s, 1H), 4.88 (t,  $J$  = 7.2 Hz, 1H), 4.24 – 4.00 (m, 1H), 4.03 – 3.86 (m, 1H), 3.22 (t,  $J$  = 6.7 Hz, 4H), 2.35 (m, 1H), 2.14 – 1.97 (m, 2H), 1.89 – 1.71 (m, 5H) ppm.  $^{13}\text{C}$  NMR (101 MHz,  $\text{CDCl}_3$ )  $\delta$  145.4, 145.1, 144.2 (q,  $J_{\text{C,F}}$  = 38.6 Hz), 142.5, 136.9, 128.8, 128.5, 127.3, 126.4, 125.7, 121.1 (d,  $J_{\text{C,F}}$  = 269.2 Hz), 106.4, 106.4, 80.20, 68.9, 48.0, 34.7, 26.1, 25.3 ppm. IR (neat): 2980, 2877, 2250, 1735, 1595, 1497, 1471, 1346, 1235, 1160, 113, 1096, 1060, 976, 907, 843, 770, 726, 621, 583. Mp: 45 °C. HRMS *calcd.* for ( $\text{C}_{24}\text{H}_{24}\text{F}_3\text{N}_3\text{NaO}_3\text{S}$ ) [ $\text{M}+\text{Na}$ ] $^+$ : 514.1388, *found* 514.1383.

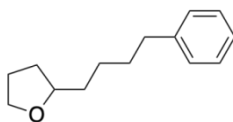


**Methyl (R)-2-phenyl-2-(4-(tetrahydrofuran-2-yl)benzamido)acetate (4s)**

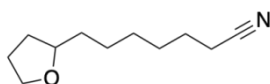
Following General Procedure A, Methyl (R)-2-(4-bromobenzamido)-2-phenylacetate (69.4 mg, 0.20 mmol) and 2-((tetrahydrofuran-2-yl)methoxy)isoindoline-1,3-dione (**1a**) (98.8 mg, 0.40 mmol), HE (101.3 mg, 0.40 mmol) were used, affording the title compound as a colourless liquid (30.5 mg, 45% yield, 1:1 dr) by using Hexane/EtOAc (2:1) as eluent.  $^1\text{H}$  NMR (400 MHz,  $\text{CDCl}_3$ )  $\delta$  7.77 (d,  $J$  = 8.4 Hz, 2H), 7.44-7.24 (m, 8H), 5.77 (d,  $J$  = 6.9 Hz, 1H), 4.90 (t,  $J$  = 7.2 Hz, 1H), 4.10-4.03 (m, 1H), 3.95-3.88 (m, 1H), 3.73 (s, 3H), 2.37-2.27 (m, 1H), 2.02-1.92 (m, 2H), 1.78-1.66 (m, 1H) ppm.  $^{13}\text{C}$  NMR (101 MHz,  $\text{CDCl}_3$ )  $\delta$  171.1, 166.4, 147.9, 136.7, 132.4, 129.1, 128.6, 127.4, 127.3, 125.7, 80.2, 68.9, 56.9, 52.9, 34.8, 26.0 ppm. Spectral data was in agreement with the literature<sup>[30]</sup>.



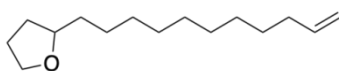
**2-dodecyltetrahydrofuran (5a)** Following General Procedure C, 1-bromododecane (49.6 mg, 0.20 mmol) and 2-((tetrahydrofuran-2-yl)methoxy)isoindoline-1,3-dione (**1a**) (98.8 mg, 0.40 mmol) were used, affording the title compound as a colourless liquid (25.0 mg, 52% yield) by using Hexane/EtOAc (30:1) as eluent.  $^1\text{H}$  NMR (300 MHz,  $\text{CDCl}_3$ )  $\delta$  3.89 – 3.62 (m, 3H), 2.02 – 1.76 (m, 3H), 1.55 – 1.14 (m, 24H), 0.87 (t,  $J$  = 6.4 Hz, 3H) ppm.  $^{13}\text{C}$  NMR (75 MHz,  $\text{CDCl}_3$ )  $\delta$  79.6, 67.7, 35.9, 32.0, 31.5, 29.9, 29.8, 29.7, 29.7, 29.7, 29.5, 26.5, 25.8, 22.8, 14.2 ppm. Spectral data was in agreement with the literature<sup>[30]</sup>.



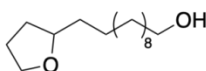
**2-(4-phenylbutyl)tetrahydrofuran (5b)** Following General Procedure C, (4-bromobutyl)benzene (42.4 mg, 0.20 mmol) and 2-((tetrahydrofuran-2-yl)methoxy)isoindoline-1,3-dione (**1a**) (98.8 mg, 0.40 mmol) were used, affording the title compound as a colourless liquid (20.6 mg, 51% yield) by using Hexane/EtOAc (30:1) as eluent.  $^1\text{H NMR}$  (400 MHz,  $\text{CDCl}_3$ )  $\delta$  7.48 – 7.41 (m, 2H), 7.37 – 7.30 (m, 3H), 4.08 – 4.78 (m, 3H), 2.83 – 2.76 (m, 2H), 2.19 – 1.97 (m, 3H), 1.88 – 1.74 (m, 3H), 1.69 – 1.50 (m, 4H) ppm.  $^{13}\text{C NMR}$  (101 MHz,  $\text{CDCl}_3$ )  $\delta$  142.8, 128.5, 128.3, 125.7, 79.4, 67.3, 36.0, 35.72, 31.7, 31.5, 26.6, 25.8 ppm. Spectral data was in agreement with the literature<sup>[30]</sup>.



**7-(tetrahydrofuran-2-yl)heptanenitrile (5c)** Following General Procedure C, 7-bromoheptanenitrile (37.8 mg, 0.20 mmol) and 2-((tetrahydrofuran-2-yl)methoxy)isoindoline-1,3-dione (**1a**) (98.8 mg, 0.40 mmol) were used, affording the title compound as a colourless liquid (19.9 mg, 55% yield) by using Hexane/EtOAc (30:1) as eluent.  $^1\text{H NMR}$  (400 MHz,  $\text{CDCl}_3$ )  $\delta$  3.89 – 3.63 (m, 3H), 2.33 (t,  $J = 7.1$  Hz, 2H), 2.04 – 1.79 (m, 3H), 1.72 – 1.60 (m, 2H), 1.59 – 1.31 (m, 7H) ppm.  $^{13}\text{C NMR}$  (101 MHz,  $\text{CDCl}_3$ )  $\delta$  119.9, 79.1, 67.7, 35.4, 31.5, 28.8, 25.8, 25.7, 25.4, 17.1 ppm. Spectral data was in agreement with the literature<sup>[30]</sup>.

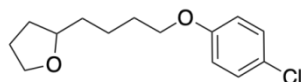


**2-(undec-10-en-1-yl)tetrahydrofuran (5d)** Following General Procedure C, 11-bromoundec-1-ene (46.4 mg, 0.20 mmol) and 2-((tetrahydrofuran-2-yl)methoxy)isoindoline-1,3-dione (**1a**) (98.8 mg, 0.40 mmol) were used, affording the title compound as a colourless liquid (22.4 mg, 50% yield) by using Hexane/EtOAc (30:1) as eluent.  $^1\text{H NMR}$  (400 MHz,  $\text{CDCl}_3$ )  $\delta$  5.87 – 5.73 (m, 1H), 5.01 – 4.88 (m, 2H), 3.88–3.65 (m, 3H), 2.06 – 1.81 (m, 5H), 1.47 – 1.26 (m, 17H) ppm.  $^{13}\text{C NMR}$  (101 MHz,  $\text{CDCl}_3$ )  $\delta$  139.4, 114.2, 79.6, 67.1, 35.9, 33.95, 31.5, 29.9, 29.7, 29.7, 29.6, 29.3, 29.1, 26.6, 25.8 ppm. Spectral data was in agreement with the literature<sup>[30]</sup>.

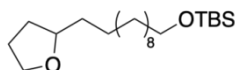


**11-(tetrahydrofuran-2-yl)undecan-1-ol (5e)** Following General Procedure C, 11-

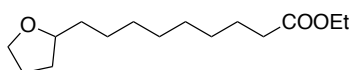
bromoundecan-1-ol (50.0 mg, 0.20 mmol) and 2-((tetrahydrofuran-2-yl)methoxy)isoindoline-1,3-dione (**1a**) (98.8 mg, 0.40 mmol) were used, affording the title compound as a colourless liquid (23.9 mg, 49% yield) by using Hexane/EtOAc (3:1) as eluent.  $^1\text{H NMR}$  (400 MHz,  $\text{CDCl}_3$ )  $\delta$  3.87 – 3.63 (m, 3H), 3.59 (t,  $J$  = 6.6 Hz, 2H), 1.99 – 1.78 (m, 3H), 1.64 – 1.52 (m, 5H) 1.37 – 1.26(m, 17H) ppm.  $^{13}\text{C NMR}$  (101 MHz,  $\text{CDCl}_3$ )  $\delta$  79.6, 67.7, 63.1, 35.8, 32.9, 31.5, 29.9, 29.7, 29.7, 29.6, 26.5, 25.9, 25.8 ppm. Spectral data was in agreement with the literature<sup>[30]</sup>.



**2-(4-(4-chlorophenoxy)butyl)tetrahydrofuran (5f)** Following General Procedure C, 1-(4-bromobutoxy)-4-chlorobenzene (52.4 mg, 0.20 mmol) and 2-((tetrahydrofuran-2-yl)methoxy)isoindoline-1,3-dione (**1a**) (98.8 mg, 0.40 mmol) were used, affording the title compound as a colourless liquid (28.5 mg, 56% yield) by using Hexane/EtOAc (3:1) as eluent.  $^1\text{H NMR}$  (400 MHz,  $\text{CDCl}_3$ )  $\delta$  7.22 – 7.18 (m, 2H), 6.82 – 6.78 (m, 2H), 3.92 (t,  $J$  = 6.0 Hz, 2H), 3.88 – 3.78 (m, 2H), 3.74 – 3.68 (m, 1H), 1.99 – 1.76 (m, 5H), 1.65 – 1.42 (m, 5H) ppm.  $^{13}\text{C NMR}$  (101 MHz,  $\text{CDCl}_3$ )  $\delta$  157.8, 129.3, 125.4, 115.8, 79.3, 68.2, 67.7, 35.5, 31.5, 29.3, 25.8, 23.0 ppm. **IR (neat):** 2941, 2864, 1597, 1580, 1491, 1472, 1389, 1285, 1241, 1169, 1091, 1037, 1005, 909, 823, 731, 666, 508. **HRMS *calcd.* for (C<sub>14</sub>H<sub>19</sub>ClNaO<sub>2</sub>) [M+Na]<sup>+</sup>: 277.0971, *found* 277.0969.**



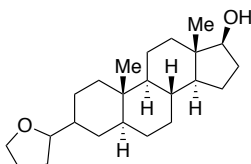
**tert-butyldimethyl((11-(tetrahydrofuran-2-yl)undecyl)oxy)silane (5g)** Following General Procedure C, ((11-bromoundecyl)oxy)(tert-butyl)dimethylsilane (72.8 mg, 0.20 mmol) and 2-((tetrahydrofuran-2-yl)methoxy)isoindoline-1,3-dione (**2a**) (98.8 mg, 0.40 mmol) were used, affording the title compound as a colourless liquid (30.6 mg, 43% yield) by using Hexane/EtOAc (3:1) as eluent.  $^1\text{H NMR}$  (400 MHz,  $\text{CDCl}_3$ )  $\delta$  3.88 – 3.82 (m, 1H), 3.78 – 3.67 (m, 2H), 3.58 (t,  $J$  = 6.6 Hz, 2H), 1.97 – 1.81 (m, 3H), 1.52 – 1.36 (m, 21H), 0.89 (s, 9H), 0.04 (s, 6H) ppm.  $^{13}\text{C NMR}$  (101 MHz,  $\text{CDCl}_3$ )  $\delta$  79.6, 67.7, 63.5, 35.9, 33.0, 31.5, 29.9, 29.8, 29.8, 29.6, 26.5, 26.1, 25.9, 25.9, 18.5, -5.1 ppm. Spectral data was in agreement with the literature<sup>[30]</sup>.



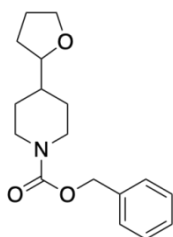
**Methyl 12-(tetrahydrofuran-2-yl)dodecanoate (5h)** Following General Procedure C, Methyl 12-bromododecanoate (58.4 mg, 0.20 mmol) and 2-((tetrahydrofuran-2-yl)methoxy)isoindoline-1,3-dione (**1a**) (98.8 mg, 0.40 mmol) were used, affording the



title compound as a colourless liquid (28.9 mg, 51% yield) by using Hexane/EtOAc (3:1) as eluent.  $^1\text{H NMR}$  (400 MHz,  $\text{CDCl}_3$ )  $\delta$  4.11 (q,  $J = 7.1$  Hz, 2H), 3.93 – 3.64 (m, 3H), 2.27 (t,  $J = 7.6$  Hz, 2H), 2.05 – 1.79 (m, 3H), 1.71 – 1.49 (m, 3H), 1.43 – 1.38 (m, 3H), 1.34 – 1.20 (m, 12H) ppm.  $^{13}\text{C NMR}$  (101 MHz,  $\text{CDCl}_3$ )  $\delta$  174.0, 79.5, 67.7, 60.2, 35.8, 34.5, 31.5, 29.7, 29.5, 29.3, 29.2, 26.5, 25.8, 25.1, 14.3 ppm. **IR (neat):** 2927, 2855, 1735, 1463, 132, 1178, 1097, 1035, 918, 732. **HRMS *calcd.* for ( $\text{C}_{15}\text{H}_{28}\text{NaO}_3$ ) [ $\text{M}+\text{Na}$ ] $^+$ : 279.1936, *found* 279.1931.**

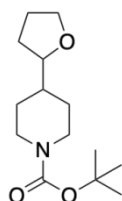


**(5S,8R,9S,10S,13S,14S)-10,13-dimethyl-3-(tetrahydrofuran-2-yl)hexadecahydro-1H-cyclopenta[a]phenanthren-17-ol (5i)** Following General Procedure C, (3R,5S,8R,9S,10S,13S,14S)-3-bromo-10,13-dimethylhexadecahydro-1H-cyclopenta[a]phenanthren-17-ol (70.8 mg, 0.20 mmol) and 2-((tetrahydrofuran-2-yl)methoxy)isoindoline-1,3-dione (**1a**) (98.8 mg, 0.40 mmol) were used, affording the title compound as a colourless liquid (88.6 mg, 64% yield, 1:1 diastereomeric ratio) by using Hexane/EtOAc (5:1) as eluent.  $^1\text{H NMR}$  (400 MHz,  $\text{CDCl}_3$ )  $\delta$  3.81 (q,  $J = 7.1$ , 6.6 Hz, 1H), 3.69 (q,  $J = 7.6$  Hz, 1H), 3.60 (t,  $J = 8.6$  Hz, 1H), 3.48 (q,  $J = 7.6$  Hz, 1H), 2.09 – 1.98 (m, 1H), 1.94 – 1.33 (m, 15H), 1.32 – 1.14 (m, 5H), 1.09 – 0.99 (m, 3H), 0.97 – 0.81 (m, 3H), 0.76 (s, 3H), 0.71 (s, 3H), 0.64 (td,  $J = 12.2$ , 4.1 Hz, 1H) ppm.  $^{13}\text{C NMR}$  (101 MHz,  $\text{CDCl}_3$ )  $\delta$  84.18, 84.15, 82.11, 82.10, 67.83, 54.88, 51.25, 46.53, 46.39, 43.44, 43.42, 43.12, 43.12, 38.39, 38.29, 36.96, 36.94, 36.27, 36.22, 35.74, 32.31, 31.83, 31.53, 30.66, 30.64, 29.31, 29.25, 29.05, 28.91, 25.97, 25.96, 25.53, 24.74, 23.51, 20.72, 12.46, 12.45, 11.27 ppm. **IR (neat):** 3253, 2921, 2850, 1713, 1446, 1322, 1121, 1051, 953, 917, 867, 731. **Mp:** 137 °C. **HRMS *calcd.* for ( $\text{C}_{23}\text{H}_{38}\text{NaO}_2$ ) [ $\text{M}+\text{Na}$ ] $^+$ : 369.2770, *found* 369.2764.**



**Benzyl 4-(tetrahydrofuran-2-yl)piperidine-1-carboxylate (5j)** Following General Procedure C, Benzyl 4-bromopiperidine-1-carboxylate (59.4 mg, 0.20 mmol) and 2-((tetrahydrofuran-2-yl)methoxy)isoindoline-1,3-dione (**1a**) (98.8 mg, 0.40 mmol) were

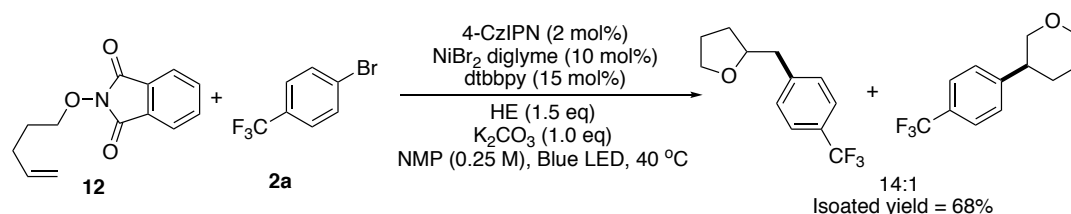
used, affording the title compound as a colourless liquid (27.8 mg, 48% yield) by using Hexane/EtOAc (3:1) as eluent.  $^1\text{H NMR}$  (400 MHz,  $\text{CDCl}_3$ )  $\delta$  7.39 – 7.28 (m, 5H), 5.12 (s, 2H), 4.21 (s, 2H), 3.81 (dt,  $J = 8.1, 6.7$  Hz, 1H), 3.76 – 3.65 (m, 1H), 3.52 (q,  $J = 7.4$  Hz, 1H), 2.75 (s, 2H), 2.18 – 1.76 (m, 4H), 1.68 – 1.43 (m, 3H), 1.21 (m, 2H) ppm.  $^{13}\text{C NMR}$  (101 MHz,  $\text{CDCl}_3$ )  $\delta$  155.3, 137.0, 128.5, 128.0, 127.9, 82.9, 67.9, 67.0, 44.08, 44.02, 41.4, 29.1, 28.2, 25.8 ppm. **IR (neat):** 2945, 2857, 1693, 1428, 1356, 1278, 1221, 1181, 1061, 1022, 920, 731, 697. **HRMS calcd. for ( $\text{C}_{17}\text{H}_{23}\text{NNaO}_3$ ) [ $\text{M}+\text{Na}$ ] $^+$ : 312.1576, found 312.1570**



**Tert-butyl 4-(tetrahydrofuran-2-yl)piperidine-1-carboxylate (5k)** Following General Procedure C, Tert-butyl 4-bromopiperidine-1-carboxylate (52.6 mg, 0.20 mmol) and 2-((tetrahydrofuran-2-yl)methoxy)isoindoline-1,3-dione (**2a**) (98.8 mg, 0.40 mmol) were used, affording the title compound as a colourless liquid (18.4 mg, 36% yield) by using Hexane/EtOAc (3:1) as eluent.  $^1\text{H NMR}$  (500 MHz,  $\text{CDCl}_3$ )  $\delta$  4.12 (d,  $J = 13.2$  Hz, 1H), 3.82 (dt,  $J = 8.1, 6.8$  Hz, 0.5H), 3.77 – 3.66 (m, 0.5H), 3.59 – 3.42 (m, 0.5H), 2.79 – 2.53 (m, 1H), 2.10 – 1.73 (m, 2H), 1.45 (s, 6H), 1.31 – 1.09 (m, 1H) ppm.  $^{13}\text{C NMR}$  (126 MHz,  $\text{CDCl}_3$ )  $\delta$  155.0, 83.1, 79.3, 67.9, 43.7(br), 41.6, 29.2, 29.1, 28.6, 28.3, 25.9 ppm. **IR (neat):** 2974, 2931, 2857, 2246, 1679, 1422, 1365, 1279, 1234, 1166, 1101, 1064, 977, 920, 868, 769, 729, 646.

## 2.7.4 Mechanistic Experiments

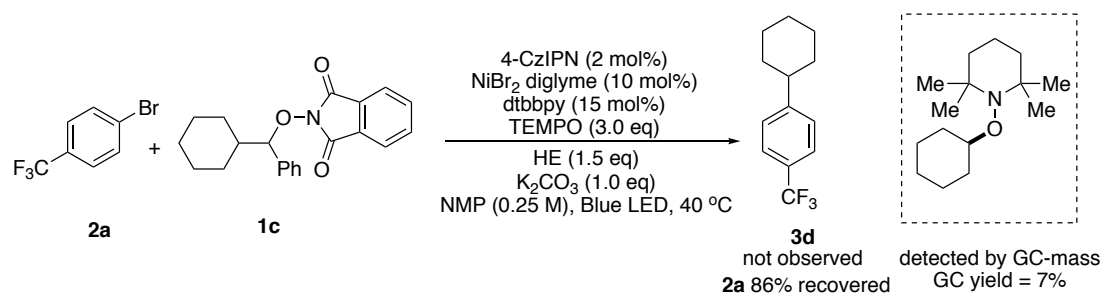
### Radical clock experiments



**2-(4-(trifluoromethyl)benzyl)tetrahydrofuran (13)** An oven-dried 8 mL screw-cap test tube containing a stirring bar was charged with 4-CzIPN (3.2 mg, 2 mol%), 4,4'-Di-*tert*-butyl-2,2'-bipyridine (8.0 mg, 15 mol%), Hantzsch ester (HE) (1.5 equiv) and 2-(pent-4-en-1-yloxy)isoindoline-1,3-dione (**12**) (69.3 mg, 0.30 mmol). The test tube

was introduced in an argon-filled glovebox where NiBr<sub>2</sub>·diglyme (7.0 mg, 10 mol%) and K<sub>2</sub>CO<sub>3</sub> (28.0 mg, 1.0 equiv) were subsequently added followed by addition of NMP (0.8 mL, 0.25 M). Then the tube was brought out, and 1-bromo-4-(trifluoromethyl)benzene (**2a**, 44.8 mg, 0.20 mmol). PTFE tape was used to ensure the tightness of the reaction system, and then the tube was stirred at 40 °C under irradiation of blue LEDs with a fan for 18-24 h. After this time, the reaction mixture was extracted with ethyl acetate and water/brine (3 times). Then, the organic layers were combined, dried over MgSO<sub>4</sub> and concentrated under vacuum. The product was purified by flash chromatography column on silica gel, affording the title compound as a colourless liquid (31.3 mg, 68% yield) by using Hexane/EtOAc (30:1) as eluent. The mixture included the 5-exo-trig adduct (**13**) and 6-endo-trig adduct (**14**) in a 14.3:1 ratio. <sup>19</sup>F NMR (376 MHz, CDCl<sub>3</sub>) δ -62.48, -62.55 ppm. <sup>1</sup>H NMR (500 MHz, CDCl<sub>3</sub>) δ 7.54 (d, *J* = 8.1 Hz, 2.1H), 7.35 (d, *J* = 8.0 Hz, 2.16H), 4.08 (p, *J* = 6.9 Hz, 1H), 4.02 – 3.95 (m, 0.15H), 3.93 – 3.84 (m, 1.0H), 3.79 – 3.68 (m, 1.0H), 3.49 – 3.37 (m, 0.07H), 2.92 (dd, *J* = 13.7, 7.0 Hz, 1.11H), 2.84 (dd, *J* = 13.7, 5.6 Hz, 1H), 2.10 – 2.04 (m, 0.04H), 2.02 – 1.92 (m, 1H), 1.88 (m, 2H), 1.80 – 1.71 (m, 0.21H), 1.65 – 1.48 (m, 1H). ppm. <sup>13</sup>C NMR (126 MHz, CDCl<sub>3</sub>) δ 143.36, 143.35, 129.68, 129.66, 128.67 (q, *J*<sub>C,F</sub> = 32.3 Hz), 127.87, 125.55 (d, *J*<sub>C,F</sub> = 4.1 Hz), 125.34 (q, *J*<sub>C,F</sub> = 3.8 Hz), 125.34 (q, *J*<sub>C,F</sub> = 3.8 Hz), 124.50 (q, *J*<sub>C,F</sub> = 271.8 Hz), 79.61, 73.43, 68.33, 68.16, 68.15, 42.94, 41.84, 31.23, 31.22, 31.22, 30.39, 25.99, 25.76, 25.75, 25.73 ppm. IR (neat): 2946, 2865, 1619, 1418, 1322, 1160, 1113, 1064, 1019, 846. HRMS *calcd.* for (C<sub>12</sub>H<sub>12</sub>F<sub>3</sub>O) [M-H]<sup>+</sup>: 229.0840, *found* 229.08436. HRMS *calcd.* for (C<sub>12</sub>H<sub>14</sub>F<sub>3</sub>O) [M+H]<sup>+</sup>: 231.0997, *found* 231.0979.

### Radical inhibition experiment



An oven-dried 8 mL screw-cap test tube containing a stirring bar was charged with 4-CzIPN (1.6 mg, 2 mol%), 4,4'-Di-*tert*-butyl-2,2'-bipyridine (4.0 mg, 15 mol%), Hantzsch ester (HE) (38.0 mg, 1.5 equiv), TEMPO (46.9 mg, 0.3 mmol, 3.0 equiv) and 2-(cyclohexyl(phenyl)methoxy)isoindoline-1,3-dione (**1c**) (50.3 mg, 1.5 equiv).

The test tube was introduced in an argon-filled glovebox where NiBr<sub>2</sub>·diglyme (3.5 mg, 10 mol%) and K<sub>2</sub>CO<sub>3</sub> (14.0 mg, 1.0 equiv) in NMP were subsequently added followed by addition of NMP (0.4 mL, 0.25 M). Then the tube was brought out, and 1-bromo-4-(trifluoromethyl)benzene (**2a**, 22.4 mg, 0.10 mmol) was added to the reaction mixture. PTFE tape was used to ensure the tightness of the reaction system, and then the tube was stirred at around 40 °C under irradiation of blue LEDs with a fan for 18 hours. After this time, the reaction mixture was analyzed by GC-mass and the corresponding TEMPO- adduct was detected by GC mass spectroscopy. Conversion and the yield of TEMPO- adduct were calculated using GC-Fid with dodecane (17.0 mg, 0.10 mmol) as internal standard.

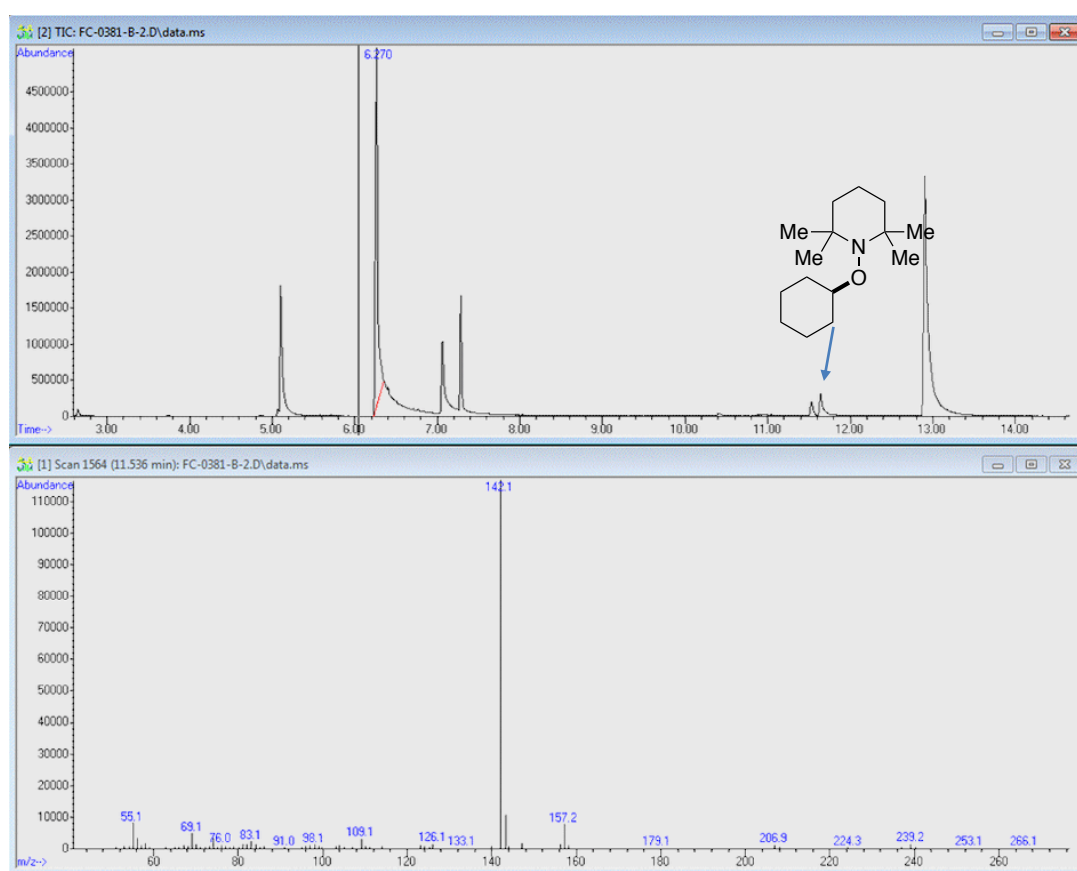
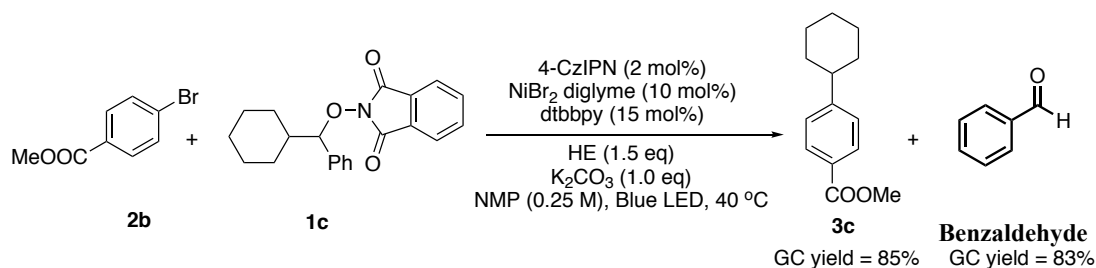


**Figure S1.** GC-mass spectra of radical inhibition reaction mixtures.

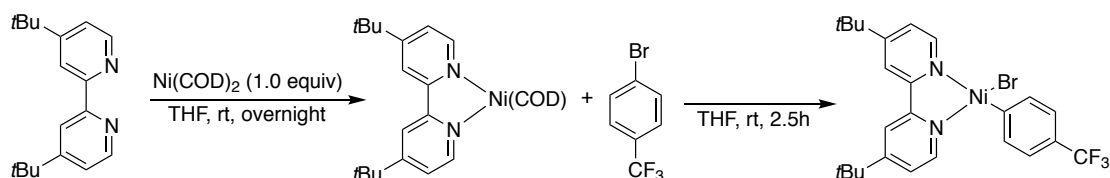
These results can be interpreted on the basis of the known behavior of TEMPO as an electron donor in EDA complexes<sup>[33-35]</sup>. Specifically, it has been speculated that TEMPO can affect the interaction between HE and alkoxyphthalimide.

### **Benzaldehyde quantitative detection experiment**



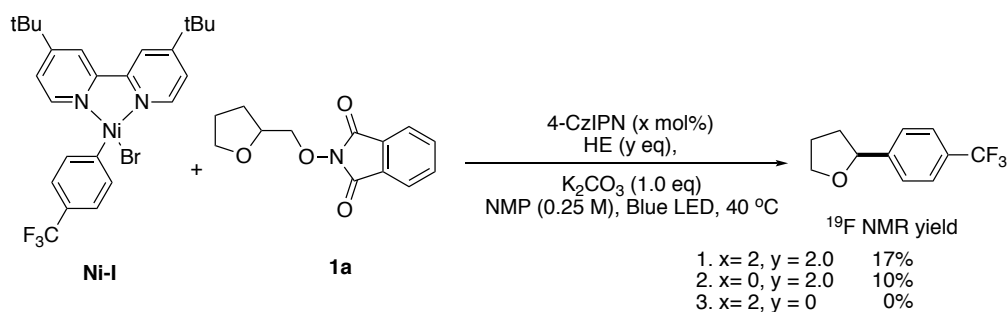
An oven-dried 8 mL screw-cap test tube containing a stirring bar was charged with 4-CzIPN (1.6 mg, 2 mol%), 4,4'-Di-*tert*-butyl-2,2'-bipyridine (4.0 mg, 15 mol%), Hantzsch ester (HE) (38.0 mg, 1.5 equiv) and 2-(cyclohexyl(phenyl)methoxy)isoindoline-1,3-dione (**1c**) (50.3 mg, 1.5 equiv). The test tube was introduced in an argon-filled glovebox where NiBr<sub>2</sub>·diglyme (3.5 mg, 10 mol%) and K<sub>2</sub>CO<sub>3</sub> (14.0 mg, 1.0 equiv) in NMP were subsequently added followed by addition of NMP (0.4 mL, 0.25 M). Then the tube was brought out, and Methyl 4-bromobenzoate (**2b**) (21.3 mg, 0.10 mmol) was added to the reaction mixture. PTFE tape was used to ensure the tightness of the reaction system, and then the tube was stirred at around 40 °C under irradiation of blue LEDs with a fan for 12 hours. The yields of **3c** and benzaldehyde were calculated using GC-Fid with dodecane (17.0 mg, 0.10 mmol) as internal standard.

### Oxidative Addition complex



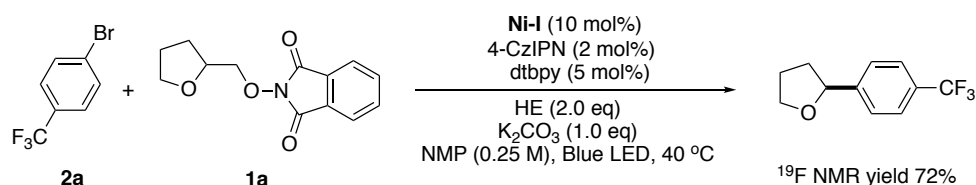
In a nitrogen filled glove box, a 100 mL round bottom flask containing a stirring bar was charged with Ni(COD)<sub>2</sub> (276 mg, 1.0 mmol, 1.0 equiv), 4,4'-di-*tert*-butyl-2,2'-bipyridine (268 mg, 1.0 mmol, 1.0 equiv) and dry THF (10 mL) giving a dark purple mixture which was stirred for 12 hours at 25 °C. 1-bromo-4-(trifluoromethyl)benzene (2.8 mL, 20 mmol, 10.0 equiv) was added and stirred for additional 2.5 h. Dry pentane (60 mL) was added to the deep red colored mixture and filtered. The resulting precipitate was washed with pentane (3 x 10 mL) and dried under vacuum to afford Ni(II) complex (**Ni-I**) as a brown solid the (504 mg, 45 % yield). The complex was stored in a nitrogen filled glove box at -35 °C. <sup>1</sup>H NMR (400 MHz, CD<sub>2</sub>Cl<sub>2</sub>) δ 9.22 (s, 1H), 7.85-7.75 (m, 4H), 7.51 (br, 1H), 7.19-7.09 (m, 4H), 1.34 (s, 18H). <sup>19</sup>F NMR (376 MHz, CD<sub>2</sub>Cl<sub>2</sub>) δ -62.02. spectral data was in agreement with the literature<sup>[36]</sup>.

### Stoichiometric reactions with Ni-I



An oven-dried 8 mL screw-cap test tube containing a stirring bar was charged with 4-CzIPN (x mol%), Hantzsch ester (HE) (y equiv) and 2-((tetrahydrofuran-2-yl)methoxy)isoindoline-1,3-dione (**1a**) (49.4 mg, 2.0 equiv). The test tube was introduced in an argon-filled glovebox where **Ni-I** (55.0 mg, 0.10 mmol, 1.0 equiv) and  $\text{K}_2\text{CO}_3$  (14.0 mg, 1.0 equiv) in NMP were subsequently added followed by addition of NMP (0.4 mL, 0.25 M). Then the tube was brought out, PTFE tape was used to ensure the tightness of the reaction system, and then the tube was stirred at around 40 °C under irradiation of blue LEDs with a fan for 18 hours. After this time, 3-fluoronitrobenzene (10.00  $\mu\text{L}$ , 0.10 mmol) as internal standard was added to the reaction mixture. Yields were determined by comparing the integration of the  $^{19}\text{F}$  NMR resonance of 2-(4-(trifluoromethyl)phenyl)tetrahydrofuran (-62.6 ppm) with that of 3-fluoronitrobenzene (-119.0 ppm).

### Catalytic competence of Ni-I



An oven-dried 8 mL screw-cap test tube containing a stirring bar was charged with 4-CzIPN (1.6 mg, 2 mol%), Hantzsch ester (HE) (50.7 mg, 2.0 equiv), 4,4'-di-*tert*-butyl-2,2'-bipyridine (1.3 mg, 5 mol%) and 2-((tetrahydrofuran-2-yl)methoxy)isoindoline-1,3-dione (**2a**) (49.4 mg, 2.0 equiv). The test tube was introduced in an argon-filled glovebox where **Ni-I** (5.5 mg, 10 mmol%) and  $\text{K}_2\text{CO}_3$  (14.0 mg, 1.0 equiv) in NMP were subsequently added followed by addition of NMP (0.4 mL, 0.25 M). Then the tube was brought out, and 1-bromo-4-(trifluoromethyl)benzene (**1a**, 22.4 mg, 0.10 mmol) was added to the reaction mixture. PTFE tape was used to ensure the tightness of the reaction system, and then the tube was stirred at around 40 °C under irradiation of blue LEDs with a fan for 18 hours. After this time, 3-fluoronitrobenzene (10.00  $\mu\text{L}$ , 0.10 mmol) as internal standard was added to the reaction mixture. Yields were determined

by comparing the integration of the  $^{19}\text{F}$  NMR resonance of 2-(4-(trifluoromethyl)phenyl)tetrahydrofuran (-62.6 ppm) with that of 3-Fluoronitrobenzene (-119.0 ppm).

### UV/Vis Absorption Spectra

The UV/Vis absorption spectra of NMP solutions of Hantzsch ester (0.023 M), N-alkoxyphthalimide **1a** (0.05 M), a mixture of HE (0.023 M) and **1a** (0.023 M), a mixture of HE (0.023 M) and phthalimide (0.023 M) and a mixture of HE (0.023 M), **1a** (0.023 M) and  $\text{K}_2\text{CO}_3$  (0.023 M) were recorded in 1 cm path quartz cuvettes using a UV-1800PC spectrophotometer. As shown, the spectra for both HE and **1a** have absorption tails that extend to 450 nm. The addition of  $\text{K}_2\text{CO}_3$  results in a significant bathochromic shift attributed to the formation of the HE-anion that ultimately leads to the formation of the EDA complex.

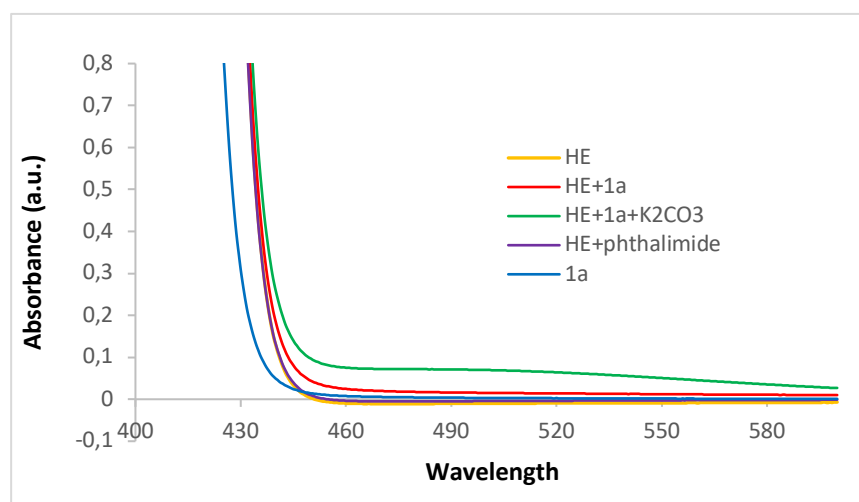


**Figure S2.** The interaction between Hantzsch ester and N-alkoxyphthalimide **1a** in NMP.

### Determination of the Association Constant ( $K_{\text{EDA}}$ )

The association constant of the EDA complex formed between N-alkoxyphthalimide derivative **1a** and Hantzsch ester was determined by spectroscopic means in NMP employing the Benesi-Hildebrand methodology<sup>[37]</sup>. We measured the absorption of solutions with constant concentration of N-alkoxyphthalimides **1a** and HE (0.02 M) at 440 nm, and added an excess of Hantzsch ester to increase the donor/acceptor ratios. All the absorption spectra were recorded in 1 cm path quartz cuvettes using a UV-1800PC spectrophotometer. A straight line was obtained when the reciprocal of the

absorbance ( $A$ ) was plotted against the reciprocal of the concentration of the partner in excess (Table S2). The association constant ( $K_{EDA}$ ) was calculated by dividing the intercept by the slope:  $2.9 \text{ M}^{-1}$  for the N-alkoxyphthalimide **1a**/Hantzsch ester.

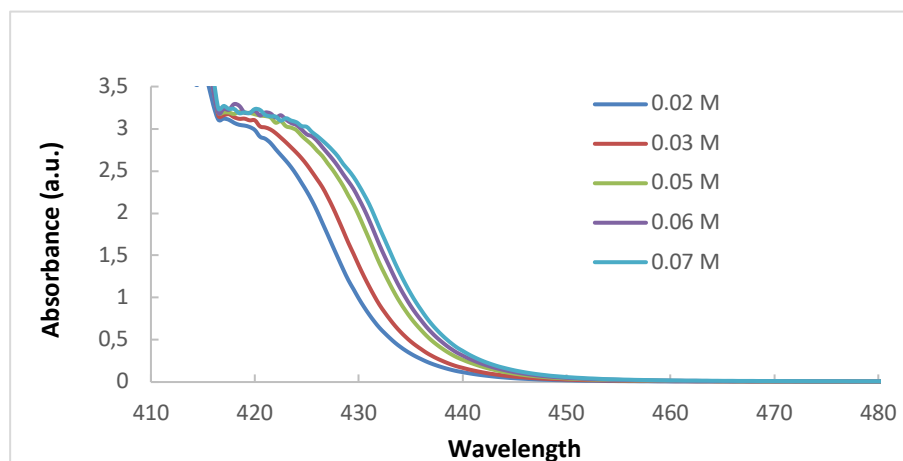


**Figure S3.** UV-vis. data from varying the concentration of Hantzsch ester in the presence of **1a**.

[HE] (M)	1/[HE] ( $\text{M}^{-1}$ )	Abs <sub>SEDA</sub>	1/(Abs <sub>SEDA</sub> -A <sub>0</sub> )
0.02	50	0.117	8.547
0.03	33.3	0.168	5.952
0.05	20	0.264	3.787
0.06	16.7	0.314	3.185
0.07	14.3	0.369	2.710

**Table S2:** Data obtained by UV/vis absorption spectra for EDA complexes in NMP.



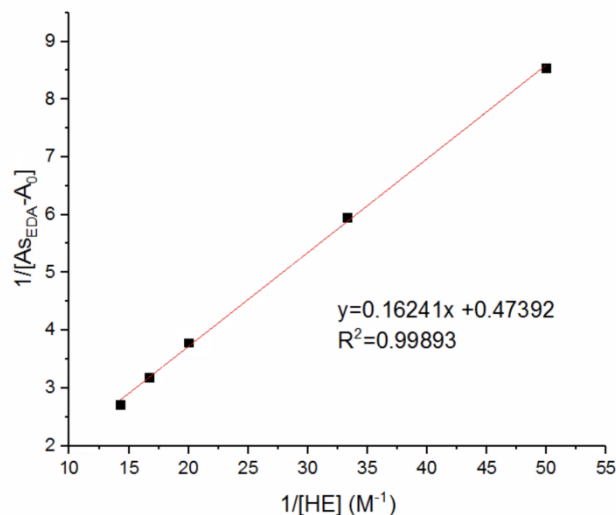


**Figure S4.** Hildebrand-Benesi plots for the EDA complexes generated in NMP upon association of the N-alkoxyphthalimide **1a** and Hantzsch ester.

#### **Influence of Ni-I on the absorption of EDA complexes**

The UV/Vis absorption spectra of NMP solutions of **Ni-I** (0.02 M), a mixture of HE (0.02 M) and **1a** (0.02 M) and a mixture of HE (0.02 M), Ni(II)complex (0.02 M) and **1a** (0.02 M) were recorded in 1 cm path quartz cuvettes using a Agilent Technologies Cary 300 UV/Vis spectrophotometer. As shown in Figure S5, **Ni-I** has a significant impact on the absorption of EDA complexes between HE and **1a**.

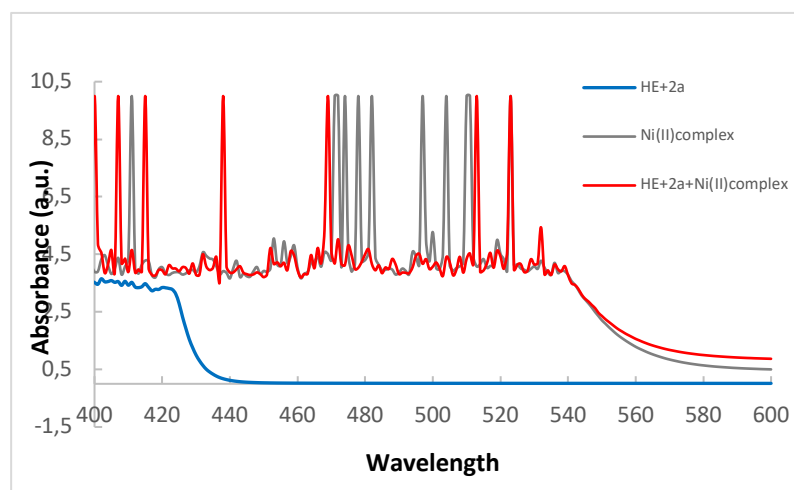
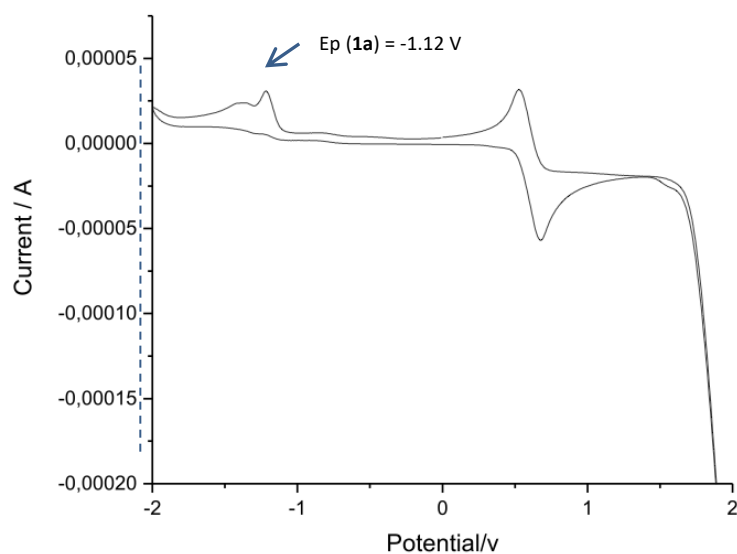


**Figure S5.** The interaction between Ni(II)complex and EDA complexes in NMP.

#### **Cyclic voltammetry data**

Cyclic voltammetry was performed on a CH Instruments Electrochemical Analyzer. A 0.01 M NMP solution of the N-alkoxyphthalimide **1a** was prepared with 0.1 M

tetrabutylammonium hexafluorophosphate as the supporting electrolyte and the solution was sparged with N<sub>2</sub> for 10 minutes. The cyclic voltammogram was obtained using a glassy carbon working electrode, platinum flag counter electrode and Ag/AgCl (KCl sat.) reference electrode. Data was collected with a scan rate of 25 mV/s. A ferrocene solution was used as an internal standard to determine the precise potential scale<sup>[38]</sup>.



Ep (**1a**) = -1.12 V vs. Ag/ AgCl in NMP, Ep (**1a**) = -1.74 V vs. Fc/ Fc<sup>+</sup> in NMP

**Figure S6.** Cyclic voltammogram of N-alkoxyphthalimide derivative **1a**.

## 2.7.5 X-Ray Crystallography Data

### X-ray diffraction of Ni-I

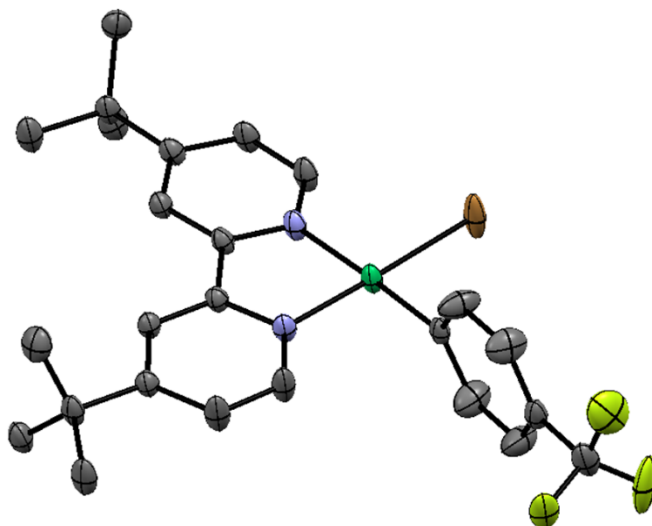


**Figure S8.** ORTEP Diagram (dtbbpy)Ni(*p*-trifluoromethylphenyl)(Br) Ni-I.

CCSD deposition number **2038983**

**Table S3. Crystallographic Data.**

	Ni-I
<b>Formula</b>	C <sub>28.50</sub> H <sub>32</sub> Br F <sub>3</sub> N <sub>2</sub> Ni
<b>Formula weight</b>	598.18
<b>T (K)</b>	100(2)
<b>Wavelength (Å)</b>	0.71073
<b>Crystal system</b>	triclinic
<b>Space group</b>	P -1
<b><i>a</i> (Å)</b>	9.3470(6)
<b><i>b</i> (Å)</b>	12.1428(8)
<b><i>c</i> (Å)</b>	13.0223(7)
<b><i>a</i> (deg)</b>	100.693(5)
<b><i>b</i> (deg)</b>	96.050(5)
<b><i>g</i> (deg)</b>	108.457(6)
<b><i>V</i> (Å<sup>3</sup>)</b>	1356.12(15)
<b><i>Z</i></b>	2
<b>Density (calc.) (Mg/m<sup>3</sup>)</b>	1.465
<b>μ (mm<sup>-1</sup>)</b>	2.229
<b>F(000)</b>	614
<b>Crystal size (mm<sup>3</sup>)</b>	0.100 x 0.050 x 0.050
<b>Theta range for data collection</b>	2.334 to 29.694

<b>(deg)</b>	
<b>Index ranges</b>	-10<=h<=12, -16<=k<=16, -17<=l<=17
<b>Reflections collected</b>	14644
<b>Independent reflections</b>	14644[R(int) = ?]
<b>Completeness to theta</b>	90.4% 29.694°
<b>Absorption correction</b>	Multi-scan
<b>Max. and min. transmission</b>	1.00 and 0.87
<b>Refinement method</b>	Full-matrix least-squares on F2
<b>Data / restraints / parameters</b>	14644/ 97/ 376
<b>Goodness-of-fit on F2</b>	1.025
<b>Final R indices [I&gt;2sigma(I)]</b>	R1 = 0.0767, wR2 = 0.2000
<b>R indices (all data)</b>	R1 = 0.1009, wR2 = 0.2129
<b>Largest diff. peak and hole</b>	1.875 and 0.794 e.Å <sup>-3</sup>

**Table S4. Bond lengths [Å] and angles [°] for Ni-I.**

Bond lengths----

C1	N1	1.340(7)
C1	C2	1.388(8)
Ni1	C19	1.879(5)
Ni1	N1	1.914(5)
Ni1	N2	1.971(5)
Ni1	Br1	2.2876(9)
N1	C5	1.359(7)
C2	C3	1.392(8)
N2	C6	1.346(7)
N2	C10	1.347(7)

---

F1	C25	1.34(3)
F2	C25	1.22(2)
F3	C25	1.452(18)
F1'	C25	1.33(4)
F2'	C25	1.437(17)
F3'	C25	1.273(15)
C3	C4	1.407(7)
C3	C11	1.514(8)
C4	C5	1.380(7)
C5	C6	1.473(7)
C6	C7	1.397(7)
C7	C8	1.396(7)
C8	C9	1.388(8)
C8	C15	1.520(8)
C9	C10	1.384(8)
C11	C14	1.531(9)
C11	C12	1.537(8)
C11	C13	1.540(8)
C15	C16	1.528(9)
C15	C17	1.535(8)
C15	C18	1.541(9)
C19	C24	1.374(9)
C19	C20	1.384(9)
C20	C21	1.384(9)
C21	C22	1.355(10)
C22	C23	1.380(10)
C22	C25	1.494(8)
C23	C24	1.388(9)
C1A	C2A	1.3900
C1A	C6A	1.3900
C1A	C7A	1.510(7)
C2A	C3A	1.3900
C3A	C4A	1.3900
C4A	C5A	1.3900

---

C5A C6A 1.3900

Angles-----

N1	C1	C2	123.0(5)
C19	Ni1	N1	93.9(2)
C19	Ni1	N2	176.1(2)
N1	Ni1	N2	82.48(19)
C19	Ni1	Br1	86.62(16)
N1	Ni1	Br1	178.00(16)
N2	Ni1	Br1	96.99(14)
C1	N1	C5	117.7(5)
C1	N1	Ni1	127.1(4)
C5	N1	Ni1	115.2(3)
C1	C2	C3	120.4(5)
C6	N2	C10	117.6(5)
C6	N2	Ni1	114.3(4)
C10	N2	Ni1	128.0(4)
C2	C3	C4	115.9(5)
C2	C3	C11	123.6(5)
C4	C3	C11	120.5(5)
C5	C4	C3	121.1(5)
N1	C5	C4	121.8(5)
N1	C5	C6	114.1(5)
C4	C5	C6	124.0(5)
N2	C6	C7	122.4(5)
N2	C6	C5	113.3(5)
C7	C6	C5	124.3(5)
C8	C7	C6	120.3(5)
C9	C8	C7	116.2(5)
C9	C8	C15	120.1(5)
C7	C8	C15	123.7(5)
C10	C9	C8	121.0(5)
N2	C10	C9	122.5(5)
C3	C11	C14	108.0(5)

---

C3	C11	C12	111.5(5)
C14	C11	C12	108.8(5)
C3	C11	C13	109.6(5)
C14	C11	C13	110.6(5)
C12	C11	C13	108.5(5)
C8	C15	C16	109.3(5)
C8	C15	C17	112.8(5)
C16	C15	C17	109.1(5)
C8	C15	C18	108.7(5)
C16	C15	C18	108.9(5)
C17	C15	C18	107.9(5)
C24	C19	C20	116.6(5)
C24	C19	Ni1	121.7(5)
C20	C19	Ni1	121.7(4)
C21	C20	C19	123.0(6)
C22	C21	C20	119.3(6)
C21	C22	C23	119.2(6)
C21	C22	C25	120.2(6)
C23	C22	C25	120.6(6)
C22	C23	C24	120.9(6)
C19	C24	C23	120.9(6)
F3'	C25	F1'	110(2)
F2	C25	F1	113(2)
F3'	C25	F2'	102.5(10)
F1'	C25	F2'	100.8(17)
F2	C25	F3	104.3(11)
F1	C25	F3	99.8(17)
F2	C25	C22	119.4(11)
F3'	C25	C22	115.8(9)
F1'	C25	C22	118(3)
F1	C25	C22	109(3)
F2'	C25	C22	107.8(9)
F3	C25	C22	108.9(9)
C2A	C1A	C6A	120.0

---

C2A	C1A	C7A	120.6(10)
C6A	C1A	C7A	119.4(10)
C1A	C2A	C3A	120.0
C4A	C3A	C2A	120.0
C3A	C4A	C5A	120.0
C6A	C5A	C4A	120.0
C5A	C6A	C1A	120.0

---

**Table S5. Torsion angles [°] for Ni-I.**

---

C2	C1	N1	C5	-2.4(10)
C2	C1	N1	Ni1	175.1(5)
N1	C1	C2	C3	0.4(11)
C1	C2	C3	C4	1.2(9)
C1	C2	C3	C11	-178.7(6)
C2	C3	C4	C5	-1.0(8)
C11	C3	C4	C5	178.9(5)
C1	N1	C5	C4	2.6(8)
Ni1	N1	C5	C4	-175.2(4)
C1	N1	C5	C6	-175.7(5)
Ni1	N1	C5	C6	6.6(6)
C3	C4	C5	N1	-0.9(8)
C3	C4	C5	C6	177.1(5)
C10	N2	C6	C7	-1.7(9)
Ni1	N2	C6	C7	176.0(4)
C10	N2	C6	C5	177.9(5)
Ni1	N2	C6	C5	-4.4(6)
N1	C5	C6	N2	-1.3(7)
C4	C5	C6	N2	-179.5(5)
N1	C5	C6	C7	178.3(5)
C4	C5	C6	C7	0.1(9)
N2	C6	C7	C8	1.2(9)
C5	C6	C7	C8	-178.4(5)
C6	C7	C8	C9	-0.9(8)



---

C6	C7	C8	C15	-179.7(5)
C7	C8	C9	C10	1.3(9)
C15	C8	C9	C10	-179.9(6)
C6	N2	C10	C9	2.1(9)
Ni1	N2	C10	C9	-175.3(5)
C8	C9	C10	N2	-1.9(10)
C2	C3	C11	C14	116.9(7)
C4	C3	C11	C14	-63.0(7)
C2	C3	C11	C12	-2.5(9)
C4	C3	C11	C12	177.5(5)
C2	C3	C11	C13	-122.6(6)
C4	C3	C11	C13	57.5(7)
C9	C8	C15	C16	57.4(7)
C7	C8	C15	C16	-123.8(6)
C9	C8	C15	C17	178.9(6)
C7	C8	C15	C17	-2.3(8)
C9	C8	C15	C18	-61.4(7)
C7	C8	C15	C18	117.4(6)
N1	Ni1	C19	C24	-88.1(6)
Br1	Ni1	C19	C24	89.9(5)
N1	Ni1	C19	C20	90.3(6)
Br1	Ni1	C19	C20	-91.7(5)
C24	C19	C20	C21	2.2(11)
Ni1	C19	C20	C21	-176.3(6)
C19	C20	C21	C22	-1.0(12)
C20	C21	C22	C23	-0.4(11)
C20	C21	C22	C25	179.0(7)
C21	C22	C23	C24	0.5(11)
C25	C22	C23	C24	-179.0(7)
C20	C19	C24	C23	-2.1(11)
Ni1	C19	C24	C23	176.4(6)
C22	C23	C24	C19	0.8(12)
C21	C22	C25	F2	48.4(14)
C23	C22	C25	F2	-132.1(13)

---

C21	C22	C25	F3'	140.7(10)
C23	C22	C25	F3'	-39.9(12)
C21	C22	C25	F1'	-86.4(16)
C23	C22	C25	F1'	93.1(16)
C21	C22	C25	F1	-83.8(15)
C23	C22	C25	F1	95.6(15)
C21	C22	C25	F2'	26.6(11)
C23	C22	C25	F2'	-154.0(10)
C21	C22	C25	F3	168.0(9)
C23	C22	C25	F3	-12.6(11)
C6A	C1A	C2A	C3A	0.0
C7A	C1A	C2A	C3A	-178.3(15)
C1A	C2A	C3A	C4A	0.0
C2A	C3A	C4A	C5A	0.0
C3A	C4A	C5A	C6A	0.0
C4A	C5A	C6A	C1A	0.0
C2A	C1A	C6A	C5A	0.0
C7A	C1A	C6A	C5A	178.3(15)

-----  
Symetry operations

- 
- 1 'x, y, z'
  - 2 '-x, -y, -z'

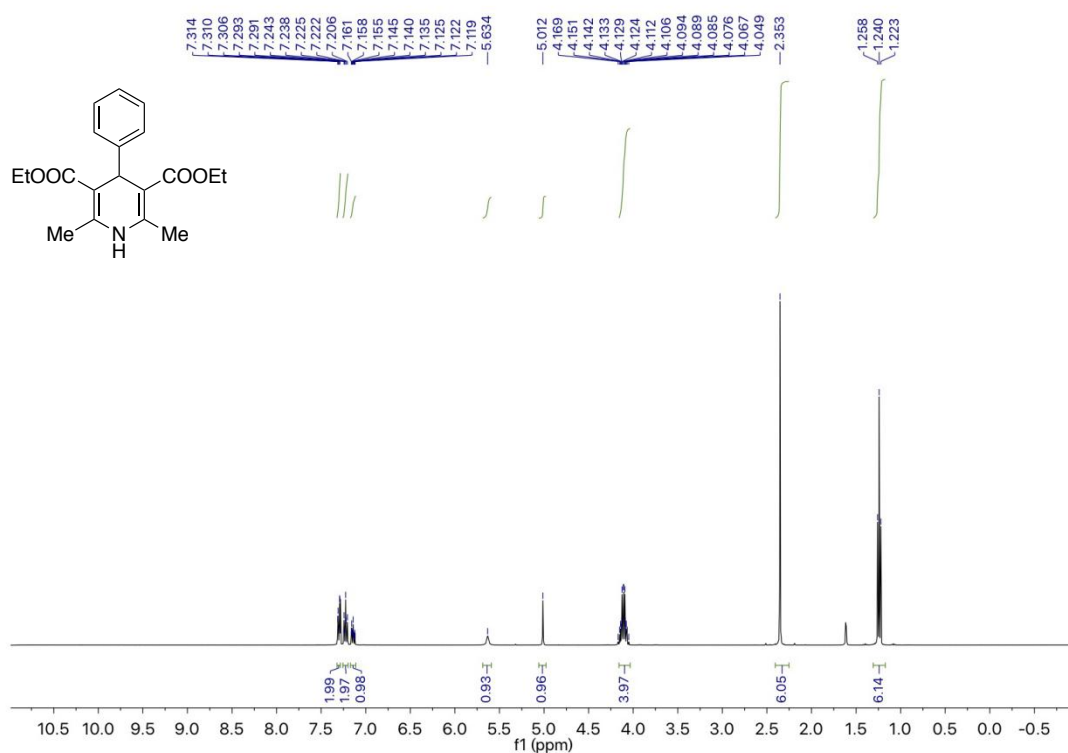
---

## 2.7.6 References of Experimental Procedures

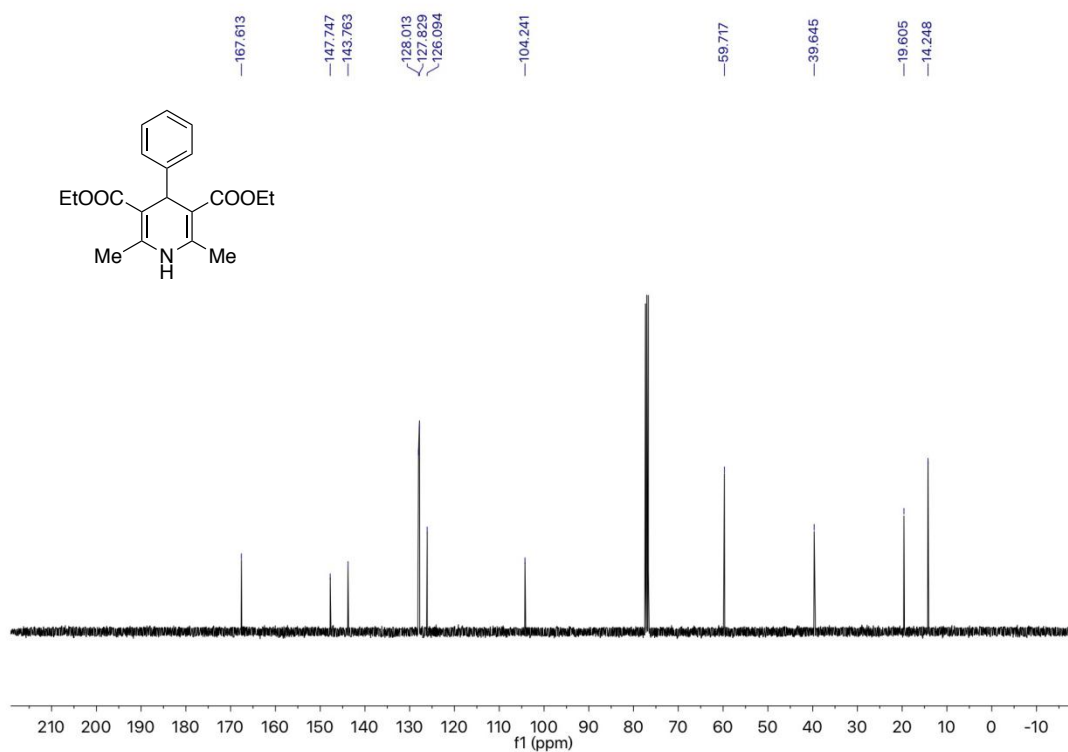
1. Gutierrez-Bonet, A.; Tellis, J. C.; Matsui, J. K.; Vara, B. A.; Molander, G. A. *ACS Catal.* **2016**, *6*, 8004-8008.
2. Serrano, E.; Martin, R. *Angew. Chem., Int. Ed.* **2016**, *55*, 11207-11211.
3. Kang, T.; Kim, H.; Kim, J. G.; Chang, S. *Chem. Commun.* **2014**, *50*, 12073-12075.
4. Zhang, J.; Li, Y.; Xu, R.; Chen, Y. *Angew. Chem., Int. Ed.* **2017**, *56*, 12619-12623.
5. Ren, Z.; Schulz, J. E.; Dong, G. *Org. Lett.* **2015**, *17*, 2696-2699.
6. Kumar, T. P.; Radhika, L.; Haribabu, K.; Kumar, V. N. *Tetrahedron: Asymmetry.* **2014**, *25*, 1555-1560.
7. Tan, E.; Zanini, M.; Echavarren, A. M. *Angew. Chem., Int. Ed.* **2020**, *59*, 10470-10473.
8. Alanine, A.; Bourson, A.; Buttelmann, B.; Gill, R.; Heitz, M.P.e; Mutel, V.; Pinard, E.; Trube, G.; Wyler, R. *Bioorganic & Medicinal Chemistry Letters.* **2003**, *13*, 3155-3159.
9. Tronchet, J. M. J.; Zosimo-Landolfo, G.; Galland-Barrera, G.; Dolatshahi, N. *Carbohydrate Research.* **1990**, *204*, 145-56.
10. Schade, Dennis; Kotthaus, Juerke; Klein, Nikola; Kotthaus, Joscha; Clement, Bernd, *Organic & Biomolecular Chemistry*, 9(14), 5249-5259; 2011.
11. Heitz, D. R.; Tellis, J. C.; Molander, G. A. *J. Am. Chem. Soc.* **2016**, *138*, 12715-12718.
12. Liu, Z.; Dong, N.; Xu, M.; Sun, Z.; Tu, T. *J. Org. Chem.* **2013**, *78*, 7436-7444.
13. Primer, D. N.; Karakaya, Idris.; Tellis, J. C.; Molander, G. A. *J. Am. Chem. Soc.* **2015**, *137*, 2195-2198.
14. Liu, D.; Li, Y.; Qi, X.; Liu, C.; Lan, Y.; Lei, A. *Org. Lett.* **2015**, *17*, 998-1001.
15. Corley, E. G.; Conrad, K.; Murry, J. A.; Savarin, C.; Holko, J.; Boice, G. *J. Org. Chem.* **2004**, *69*, 5120-5122.
16. Zhang, P.; Le, Chi.; MacMillan, D. W. C. *J. Am. Chem. Soc.* **2016**, *138*, 8084-8087.
17. Si, X.; Zhang, L.; Hashmi, A. S. K. *Org. Lett.* **2019**, *21*, 6329-6332.
18. Pratt, D. A.; Heer, M. I. d.; Mulder, P.; Ingold, K. U. *J. Am. Chem. Soc.* **2001**, *123*, 5518-5526.
19. Pan, X.; Curran, D. P. *Org. Lett.* **2014**, *16*, 10, 2728-2731.
20. Tsukamoto, H.; Uchiyama, T.; Suzuki, T.; Kondo, Y. *Org. Biomol. Chem.* **2008**, *6*, 3005-3013.

- 
21. Wem, F.; Li, Z. *Advanced Synthesis & Catalysis*. **2020**, *362*, 133-138.
  22. McDaniel, S. W.C.; Keyari, M.; Rider, K. C.; Natale, N. R.; Diaz, P. *Tetrahedron Lett.* **2011**, *52*, 5656-5658.
  23. Schafer, G.; Bode, J. W. *Angew. Chem. Int. Ed.* **2011**, *50*, 10913–10916.
  24. Maity, P.; Shacklady-McAtee, D. M.; Yap, G. P. A.; Sirianni, E. R.; Watson, M. P. *J. Am. Chem. Soc.* **2013**, *135*, 280-285.
  25. Ronson, T. O.; Carney, J. R.; Whitwood, A. C.; Taylora, R. J. K.; Fairlamb, J. S. *Chemical Communications*. **2015**, *51*, 3466-3469.
  26. Ghorai, S. K.; Jin, M.; Hatakeyama, T.; Nakamura, M. *Org. Lett.* **2012**, *14*, 1066–1069.
  27. Zhang, Q. W.; Brusoe, A. T.; Mascitti, V.; Hesp, K. D.; Blakemore, D. C.; Kohrt, J. T.; Hartwig, J. F. *Angew. Chem. Int. Ed.* **2016**, *55*, 9758-9762.
  28. Wang, J.; Qin, T.; Chen, T. G.; Wimmer, L.; Edwards, J. T.; Cornella, J.; Vokits, B.; Shaw, S. A.; Baran, P. S. *Angew. Chem. Int. Ed.* **2016**, *55*, 9676-9679.
  29. Perry, I. B.; Brewer, F.; Sarver, P. J.; Schultz, D. M.; Dirococo, D. A.; MacMillan, D. W. C. *Nature*. **2018**, *560*, 70-75.
  30. Shen, Y.; Gu, Y.; Martin, R. *J. Am. Chem. Soc.* **2018**, *140*, 12200–12209.
  31. Minuti, L.; Barattucci, A.; Bonaccorsi, P. M.; Di Gioia, M. L.; Leggio, A.; Siciliano, C.; Temperini, A. *Org. Lett.* **2013**, *15*, 3906-3909.
  32. Rodrigo, S. K.; Guan, H. *J. Org. Chem.* **2012**, *77*, 8303-8309.
  33. Nakatsuji, S. I. et al. *Chem. Commun.*, **1997**, 275-276.
  34. Nakatsuji, S. I. et al. *J. Mater. Chem.* **1999**, *9*, 1747-1754.
  35. Arceo, E.; Jurberg, I. D.; Ivarez-Fernandez, A.; Melchiorre, P. *Nature Chemistry*. **2013**, *5*, 750–756.
  36. Guo, L.; Tu, H.; Zhu, S.; Chu, L. *Org. Lett.* **2019**, *21*, 4771–4776.
  37. Benesi, H. A.; Hildebrand, J. H. *J. Am. Chem. Soc.* **1949**, *71*, 2703-2707.
  38. An oxidation potential of 0.62 V was measured for ferrocene solution in NMP. This provided a conversion factor of -0.62 V to convert between Ag/AgCl and Fc/Fc<sup>+</sup> reference electrodes.

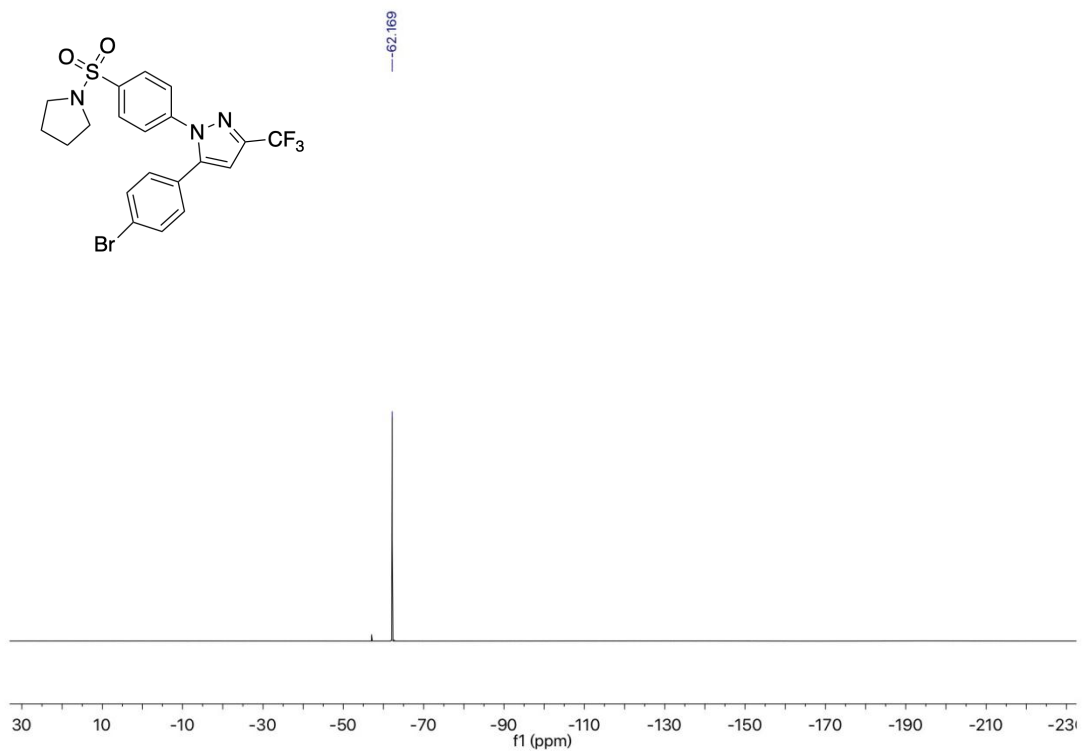
## 2.7.7 NMR Spectra



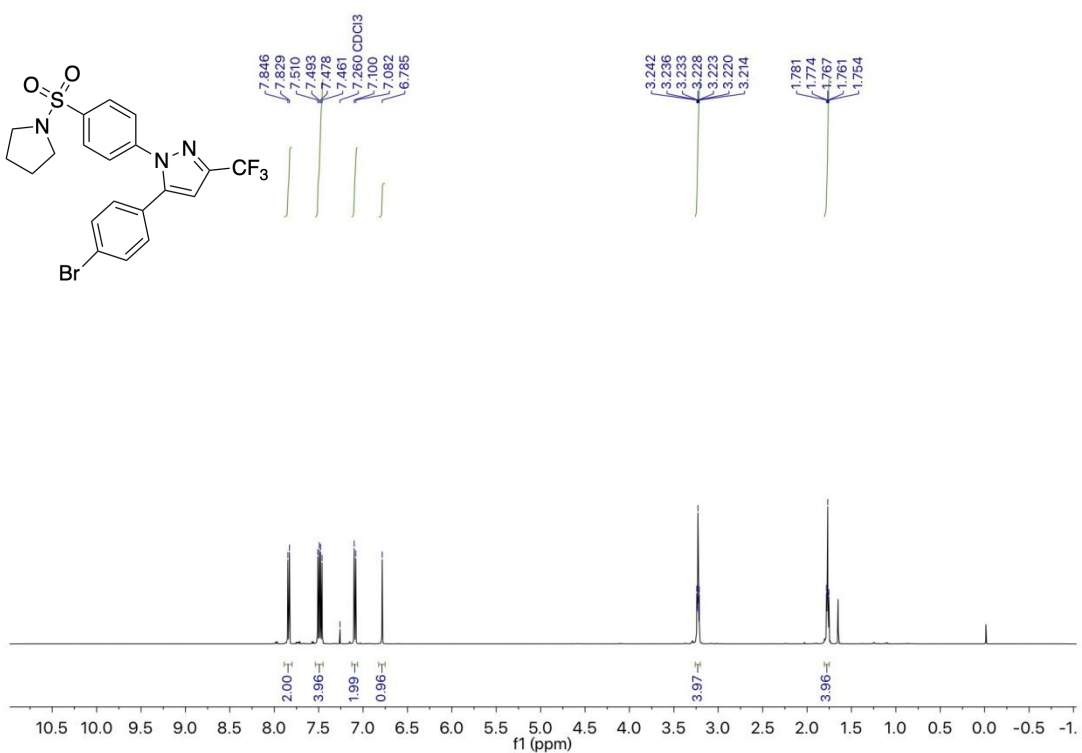
<sup>1</sup>H NMR spectrum (400 MHz, CDCl<sub>3</sub>) of Ph-HE



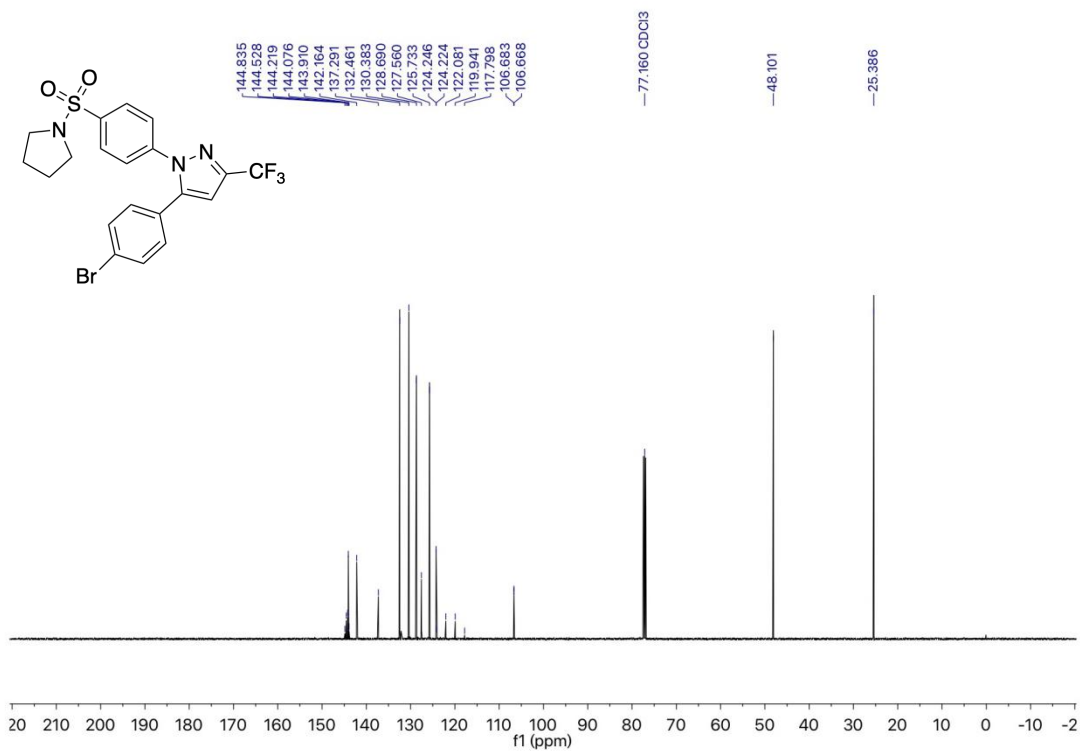
<sup>13</sup>C NMR spectrum (101 MHz, CDCl<sub>3</sub>) of Ph-HE



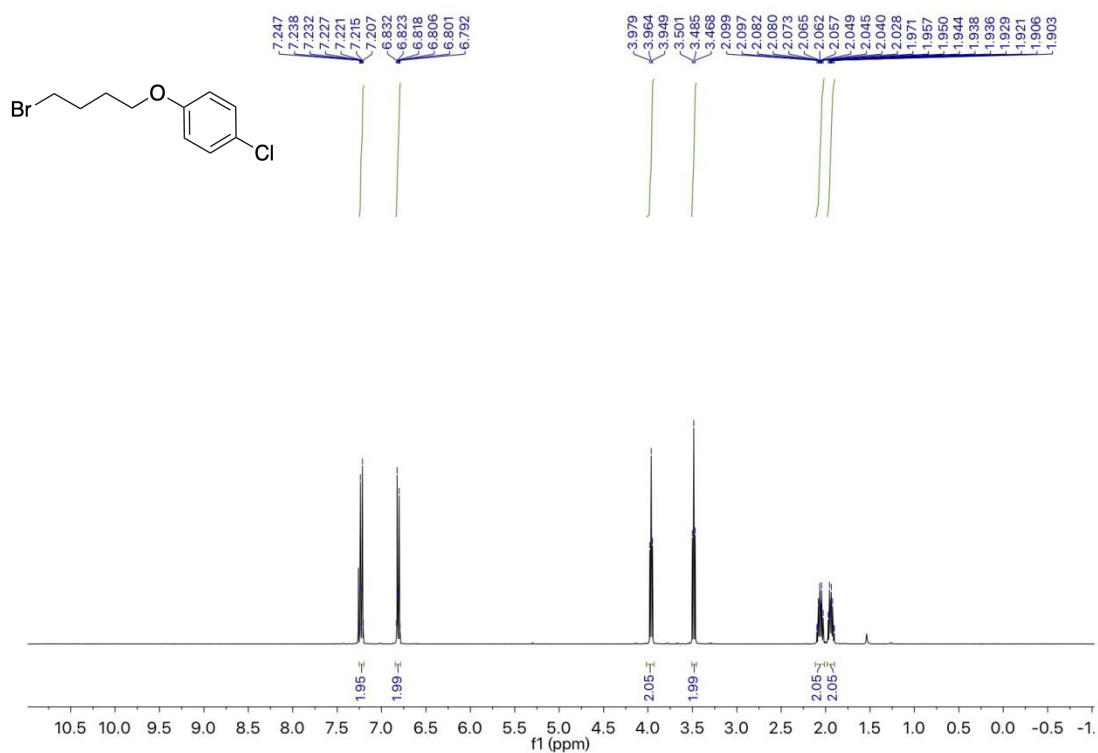
$^{19}\text{F}$  NMR spectrum (375 MHz,  $\text{CDCl}_3$ ) of **2d**



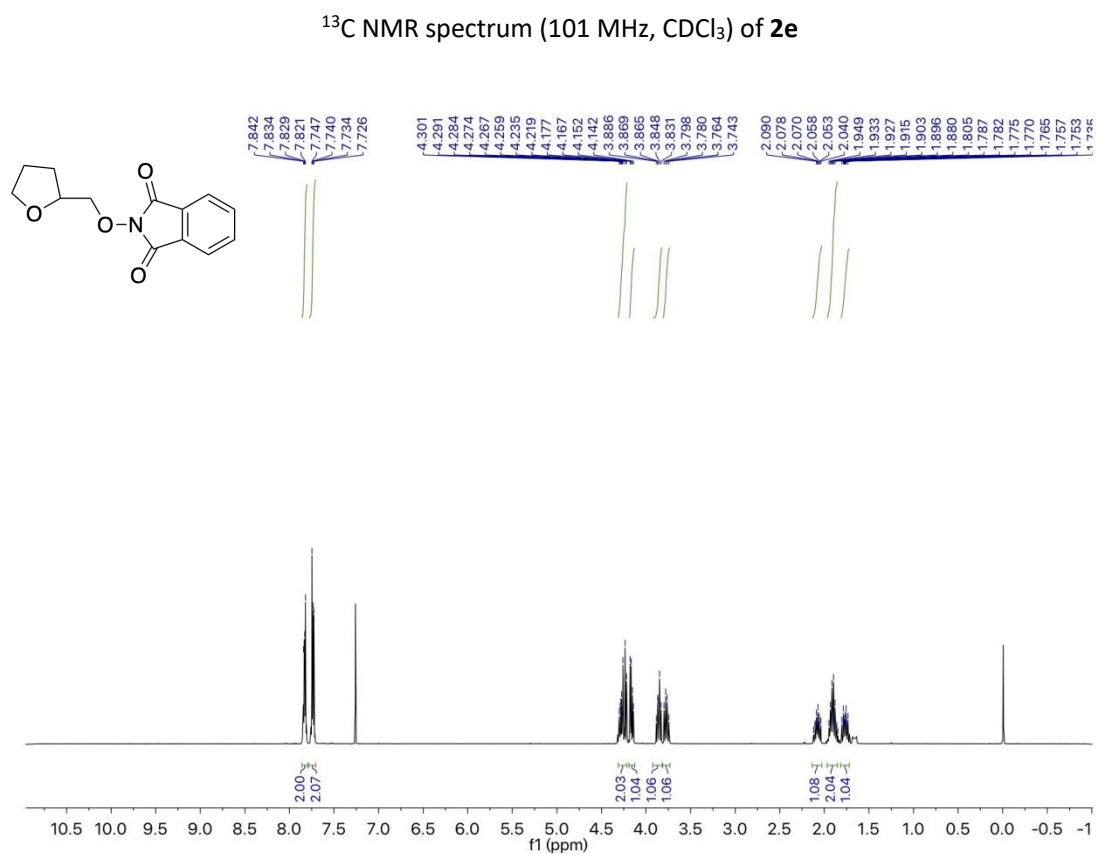
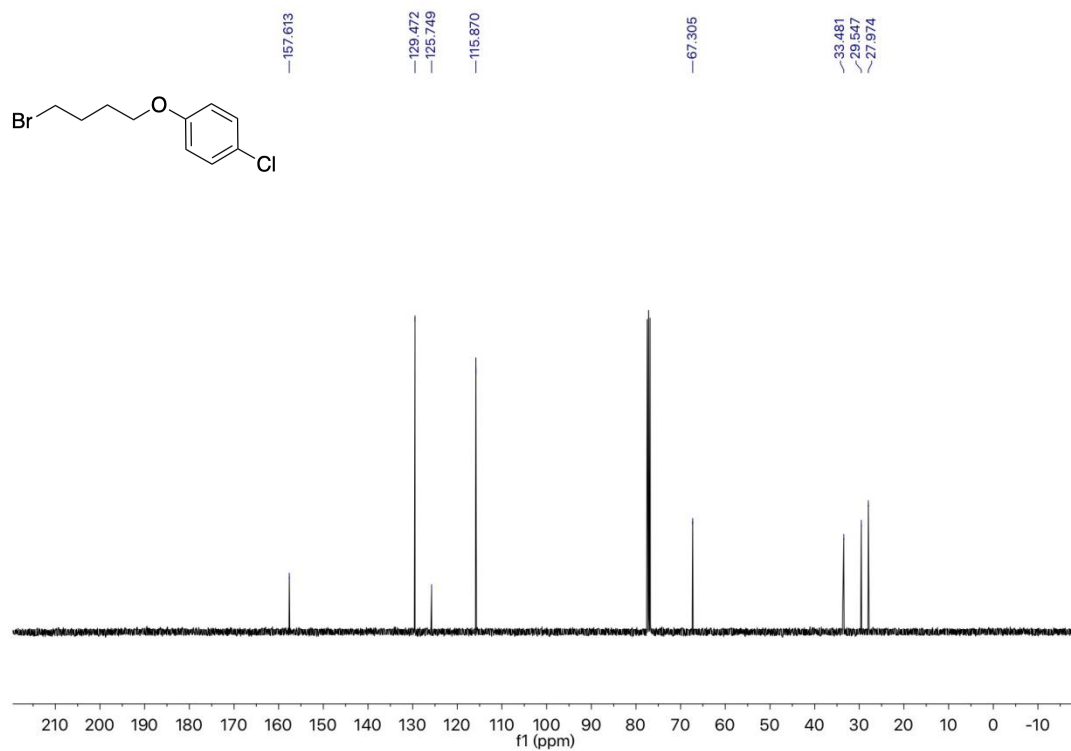
$^1\text{H}$  NMR spectrum (400 MHz,  $\text{CDCl}_3$ ) of **2d**



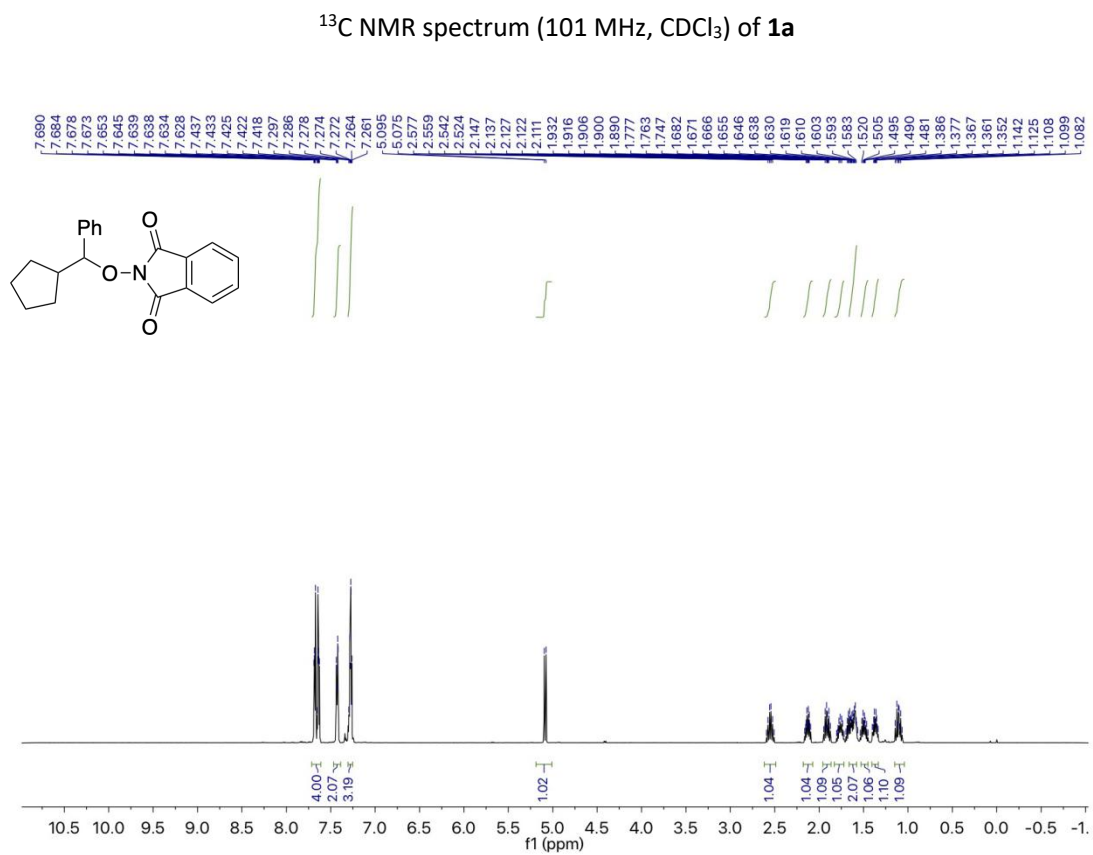
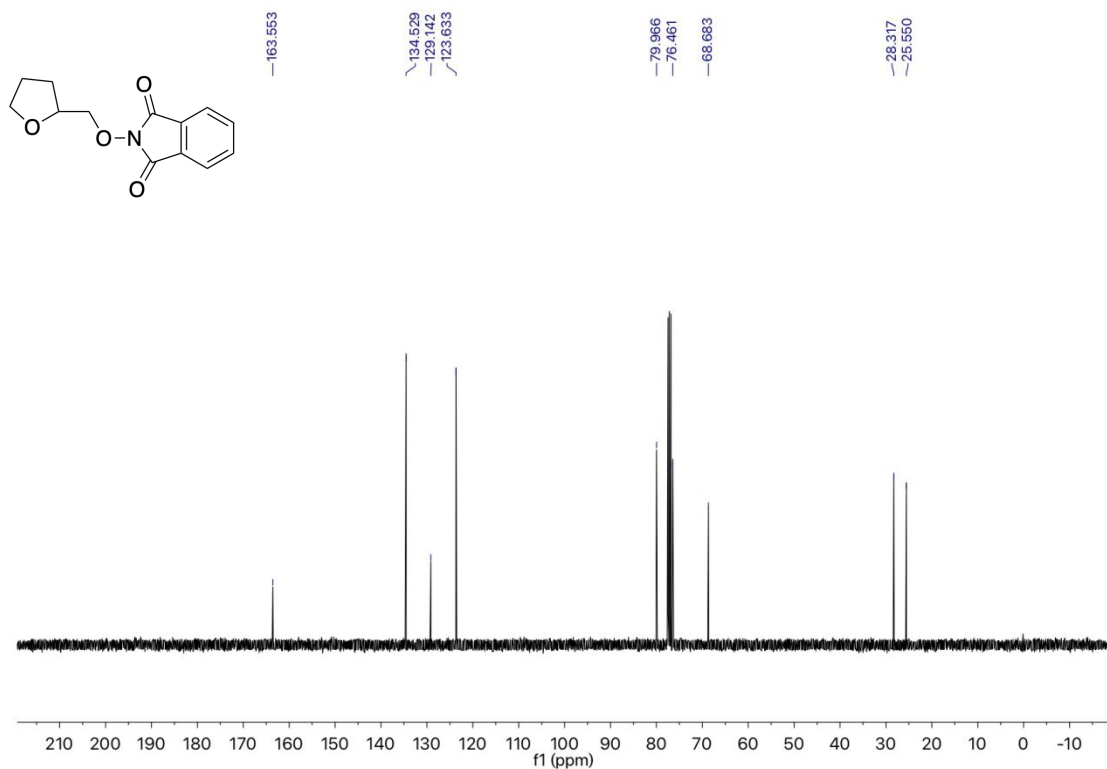
<sup>13</sup>C NMR spectrum (101 MHz, CDCl<sub>3</sub>) of **2d**



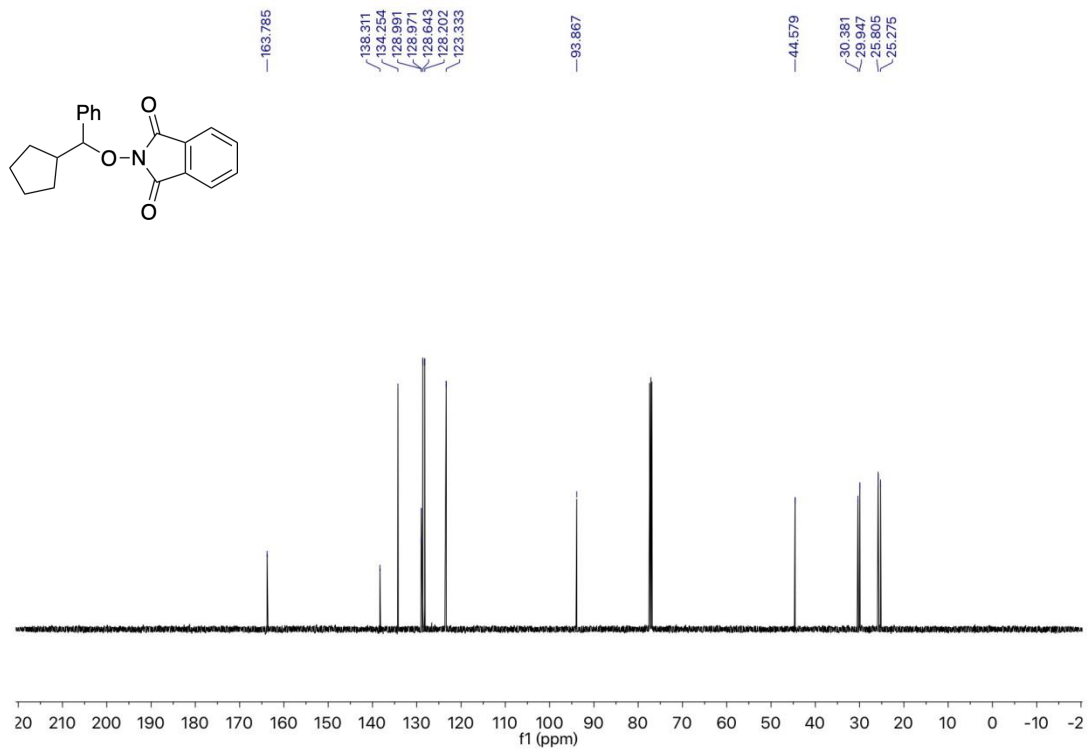
<sup>1</sup>H NMR spectrum (400 MHz, CDCl<sub>3</sub>) of **2e**



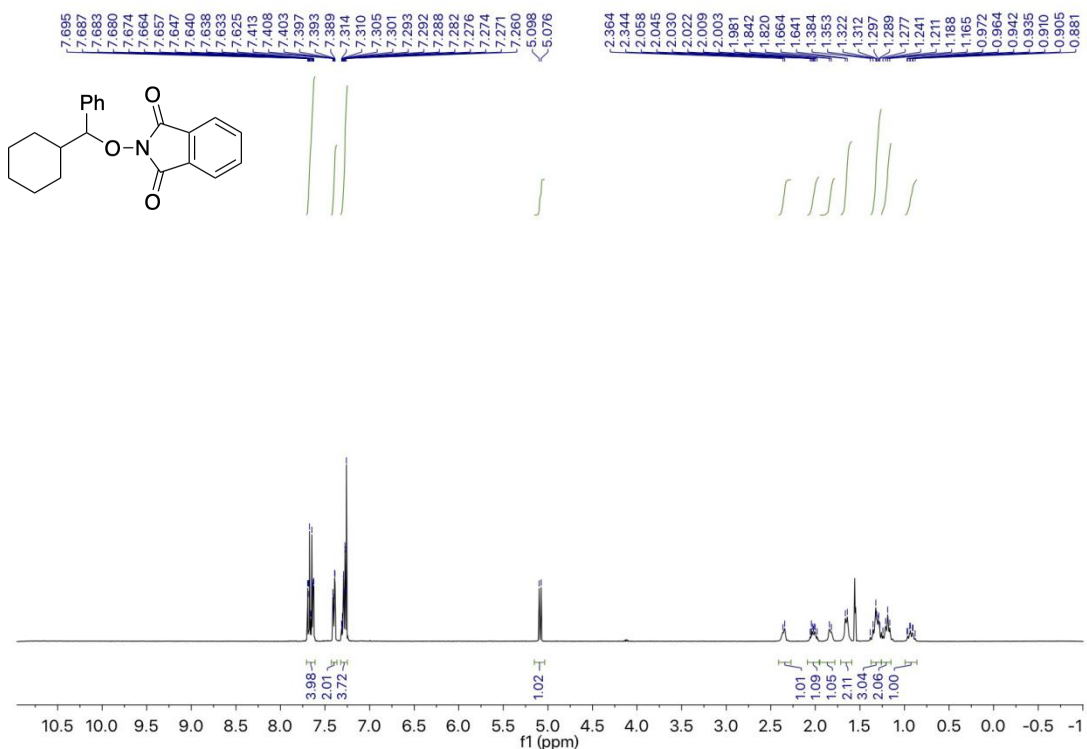




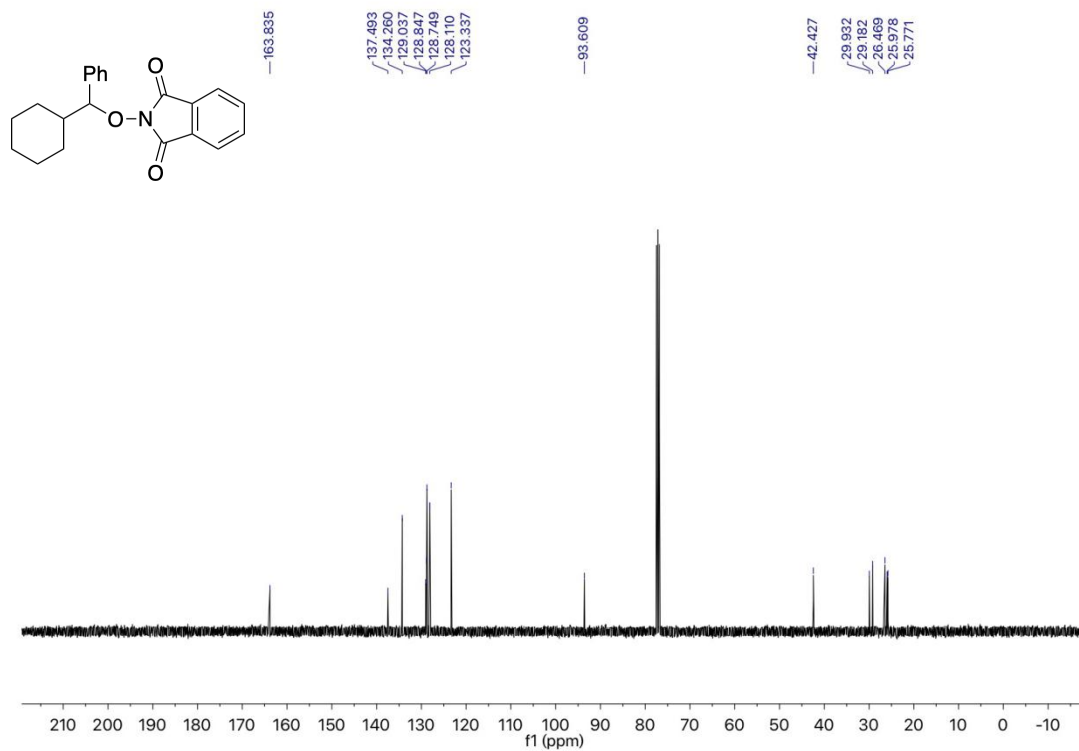
$^1\text{H}$  NMR spectrum (400 MHz,  $\text{CDCl}_3$ ) of **1b**



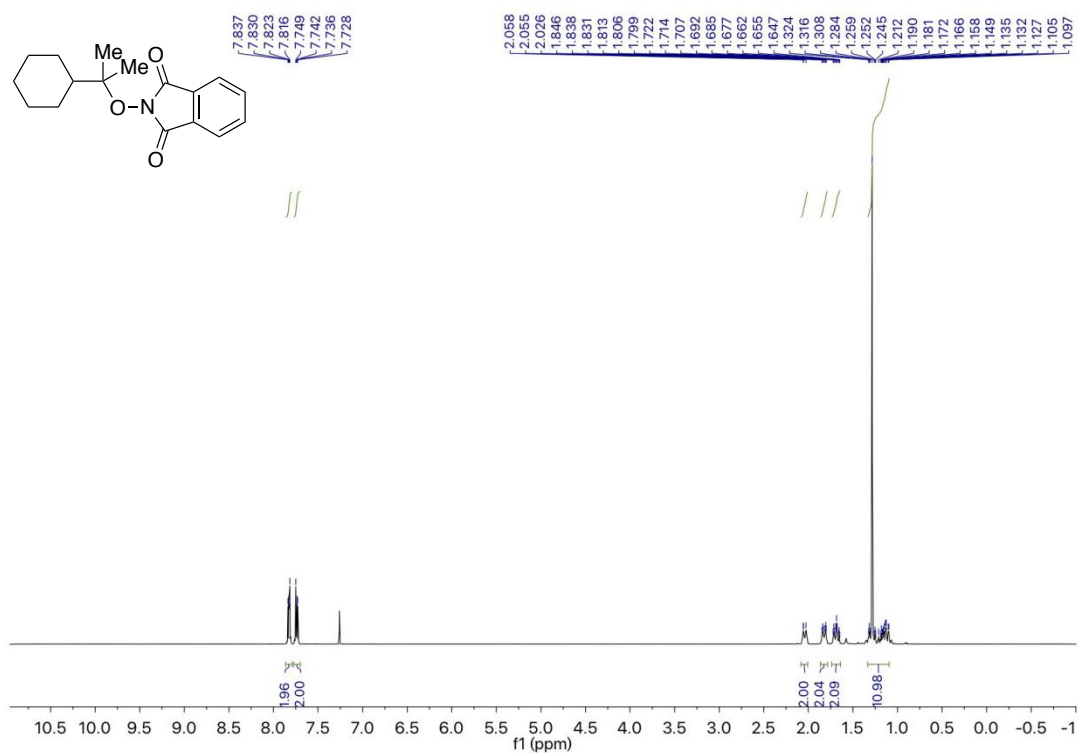
$^{13}\text{C}$  NMR spectrum (101 MHz,  $\text{CDCl}_3$ ) of **1b**



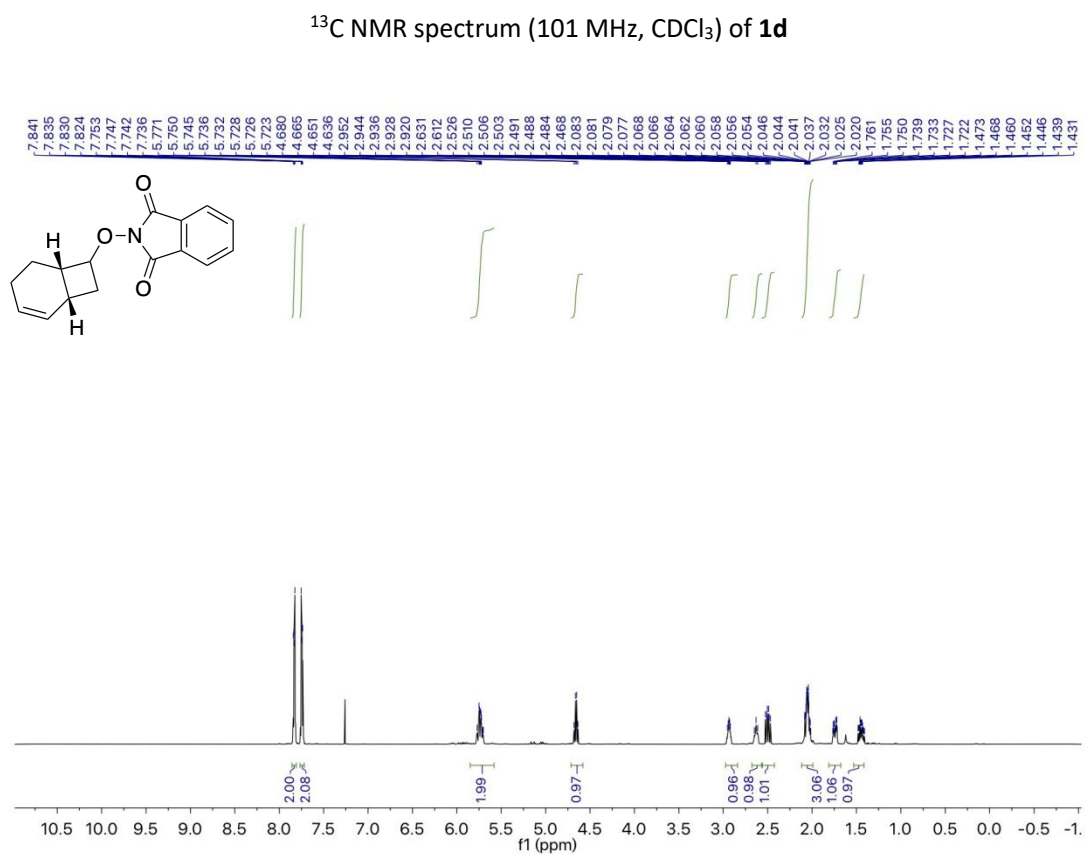
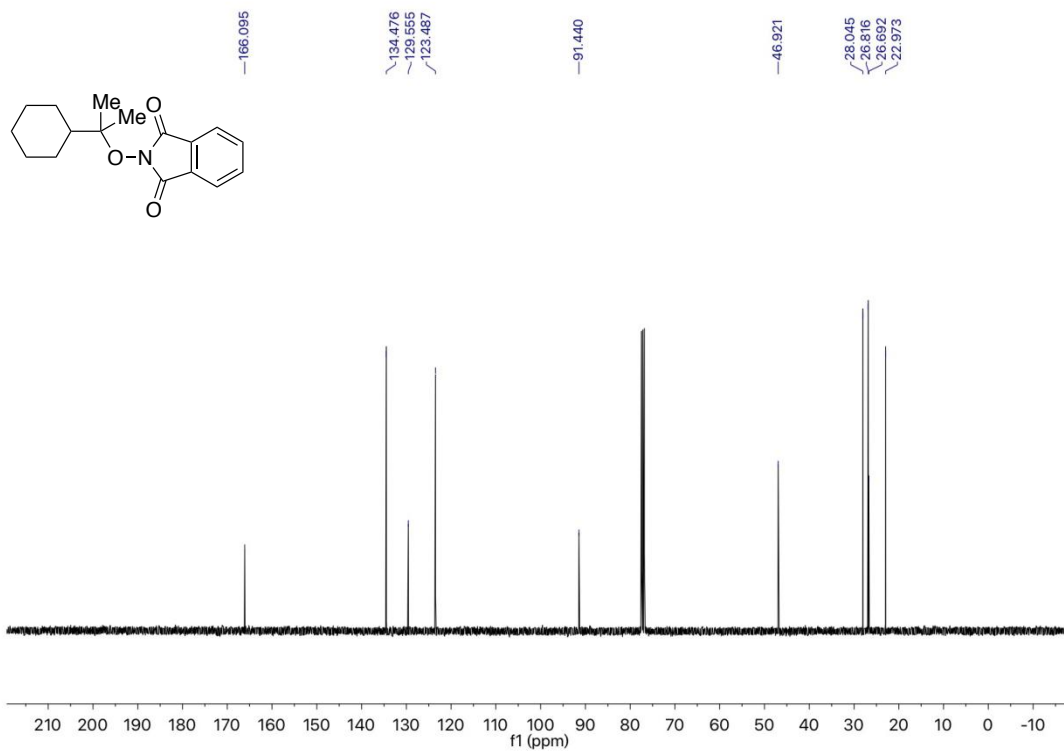
$^1\text{H}$  NMR spectrum (400 MHz,  $\text{CDCl}_3$ ) of **1c**

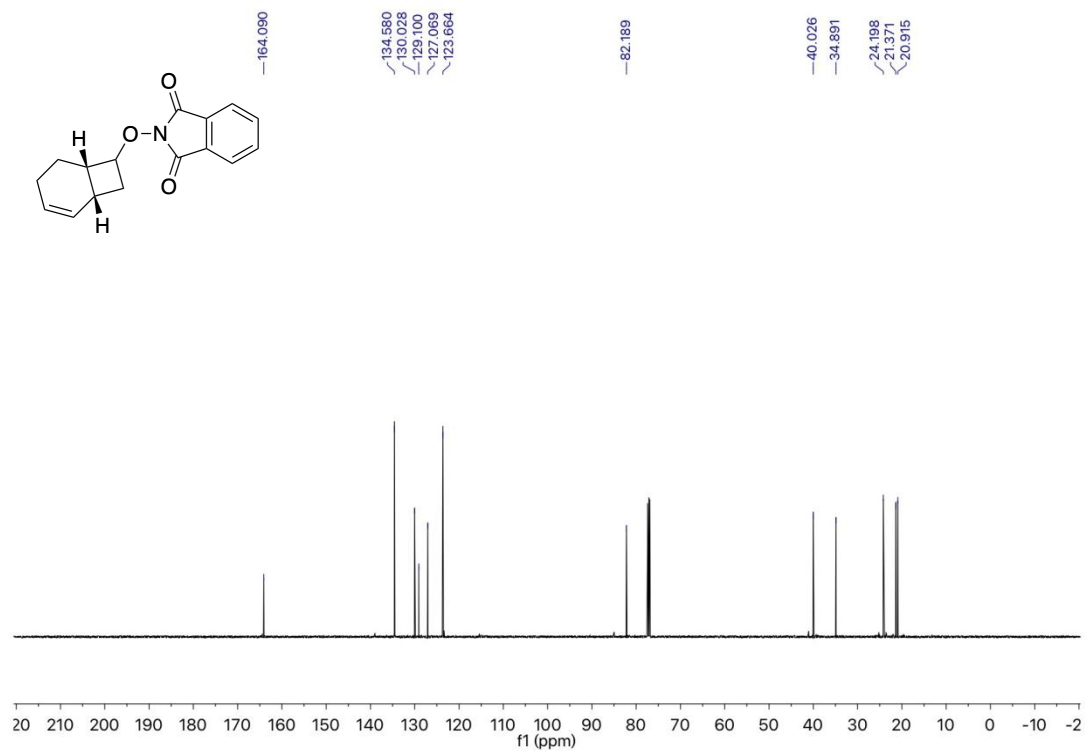


$^{13}\text{C}$  NMR spectrum (101 MHz,  $\text{CDCl}_3$ ) of **1c**

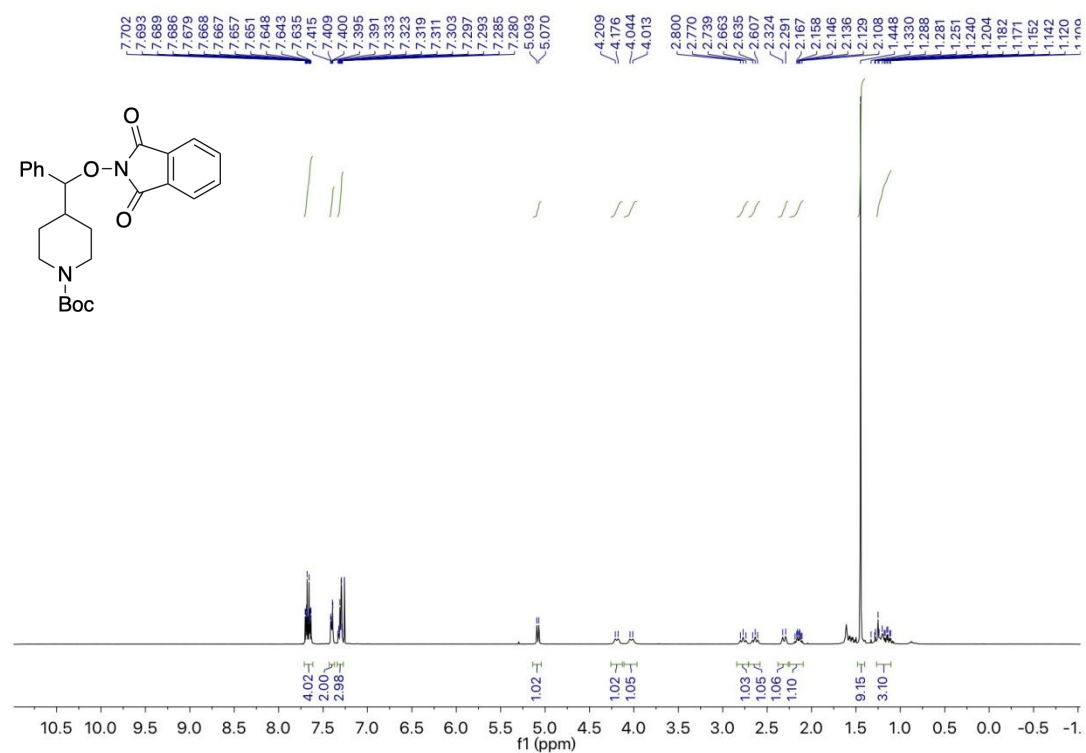


$^1\text{H}$  NMR spectrum (400 MHz,  $\text{CDCl}_3$ ) of **1d**

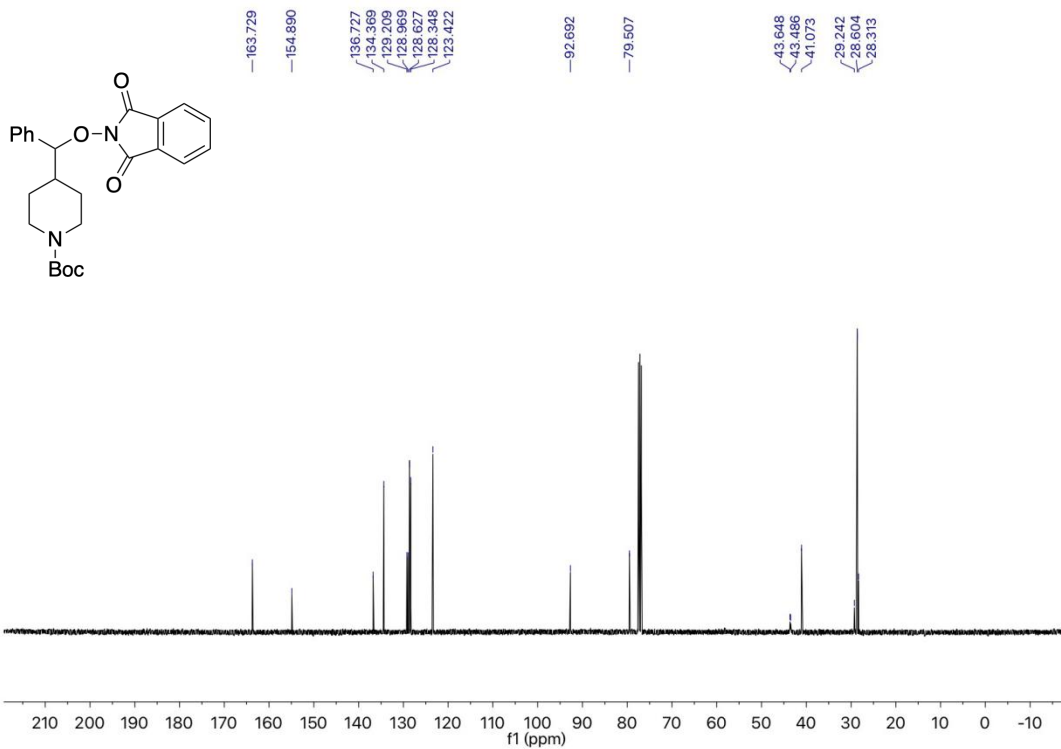




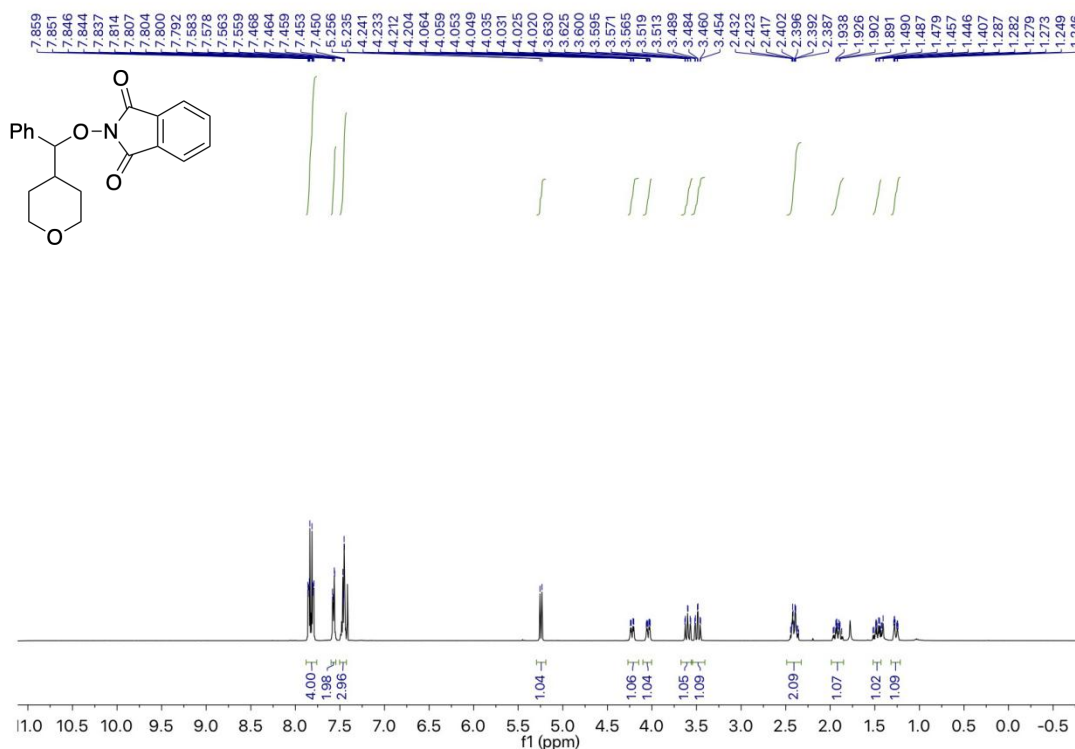
**<sup>13</sup>C NMR spectrum (101 MHz, CDCl<sub>3</sub>) of **1e****



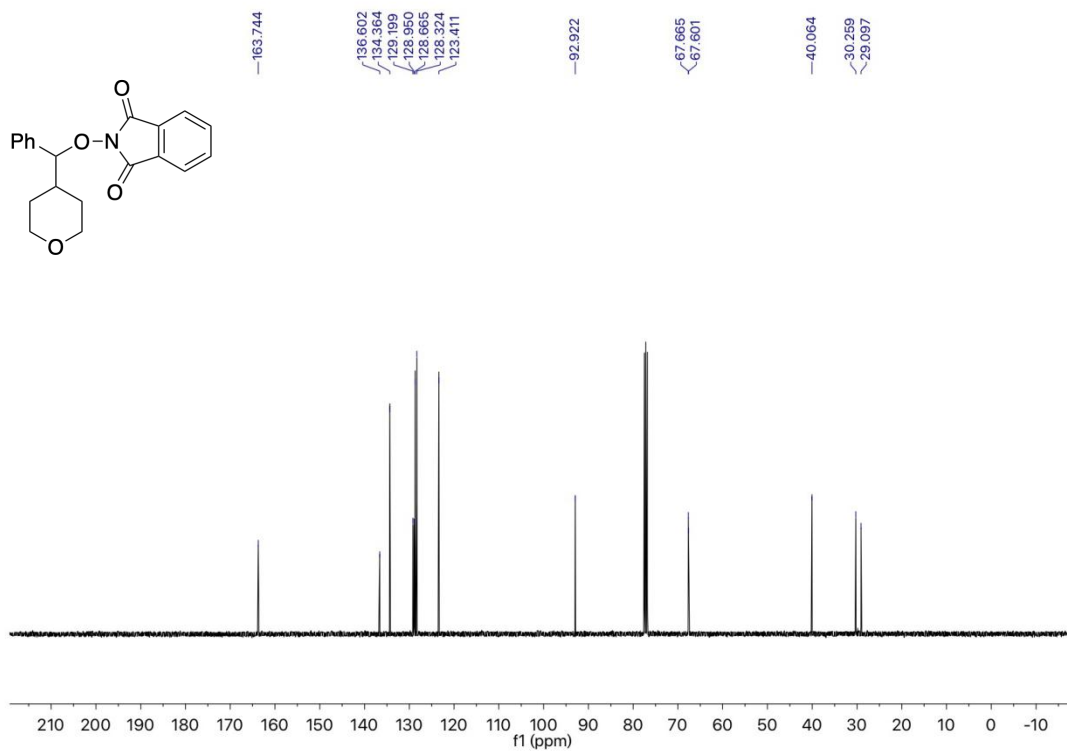
**<sup>1</sup>H NMR spectrum (400 MHz, CDCl<sub>3</sub>) of **1f****



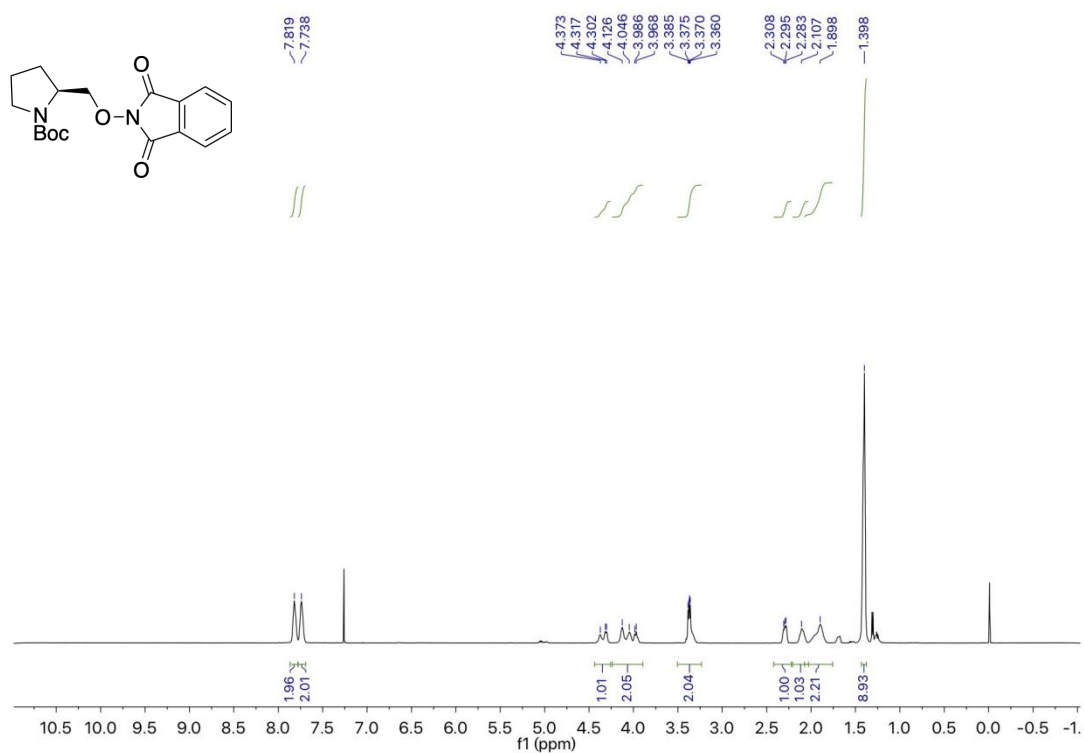
$^{13}\text{C}$  NMR spectrum (101 MHz,  $\text{CDCl}_3$ ) of **1f**



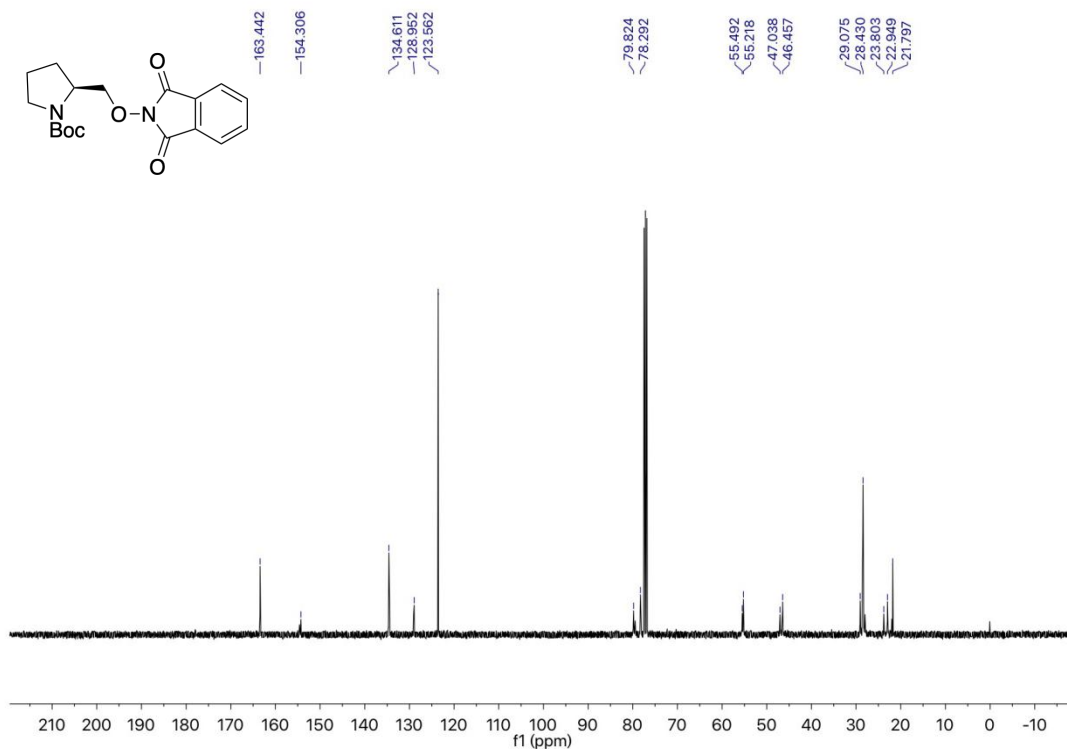
$^1\text{H}$  NMR spectrum (400 MHz,  $\text{CDCl}_3$ ) of **1g**



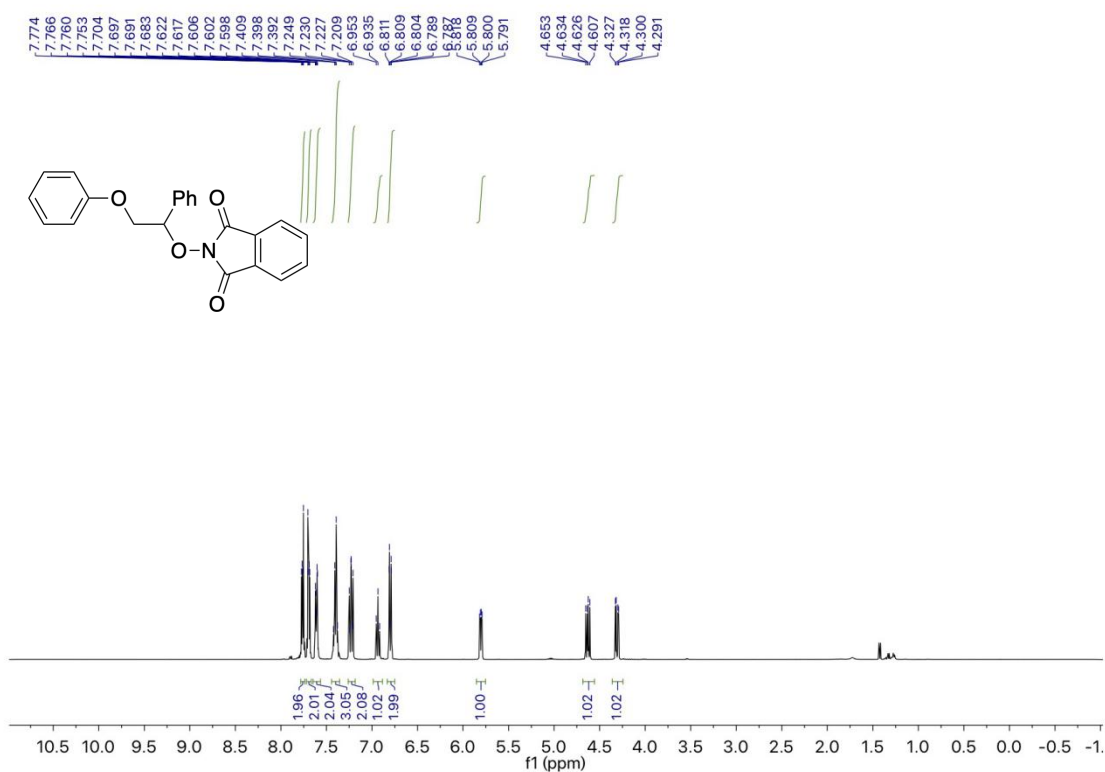
$^{13}\text{C}$  NMR spectrum (101 MHz,  $\text{CDCl}_3$ ) of **1g**



$^1\text{H}$  NMR spectrum (400 MHz,  $\text{CDCl}_3$ ) of **1h**

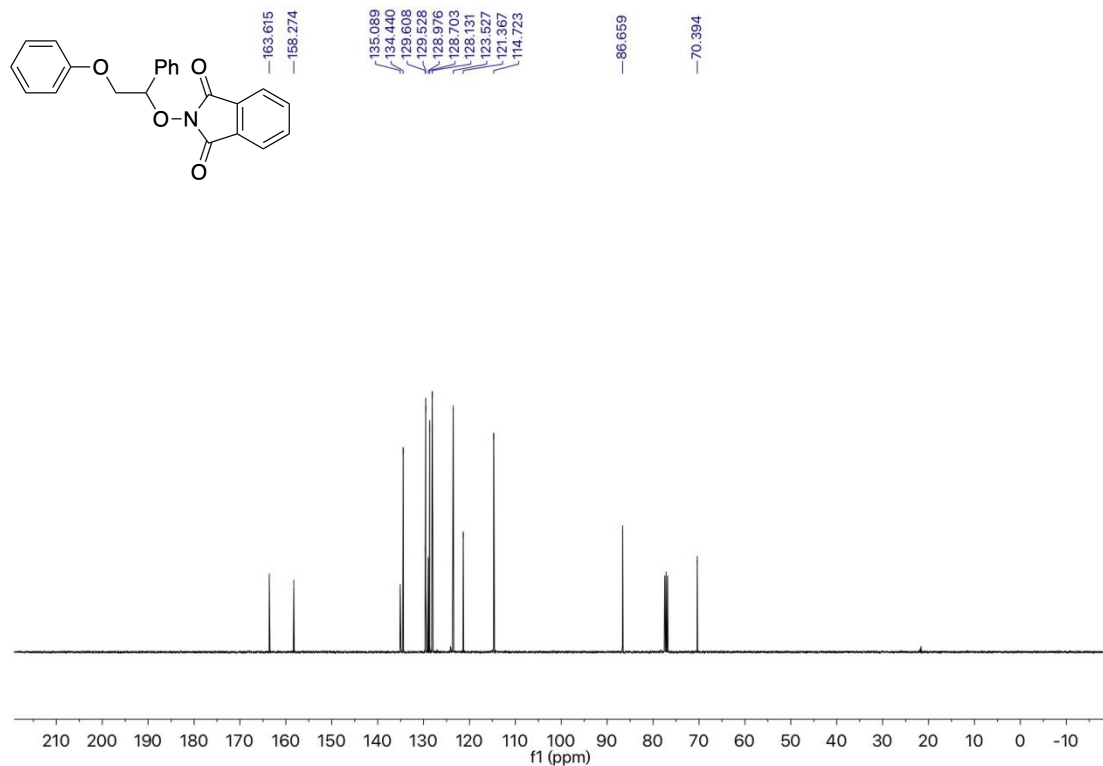


<sup>13</sup>C NMR spectrum (101 MHz, CDCl<sub>3</sub>) of **1h**

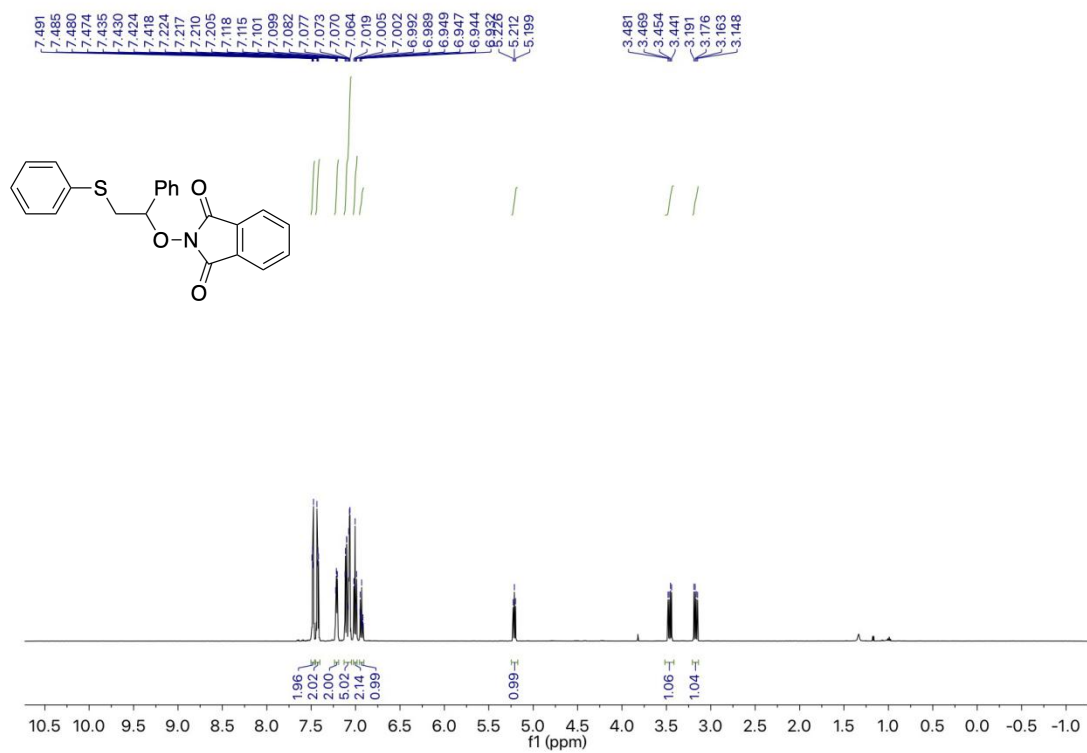


<sup>1</sup>H NMR spectrum (400 MHz, CDCl<sub>3</sub>) of **1i**

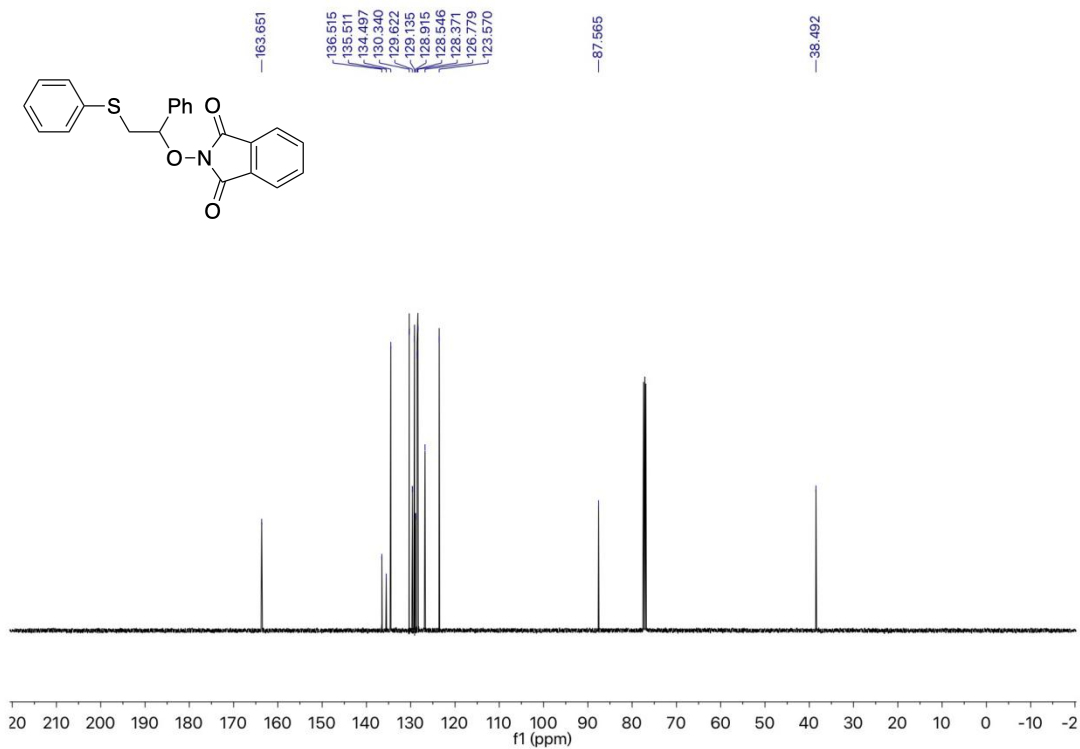




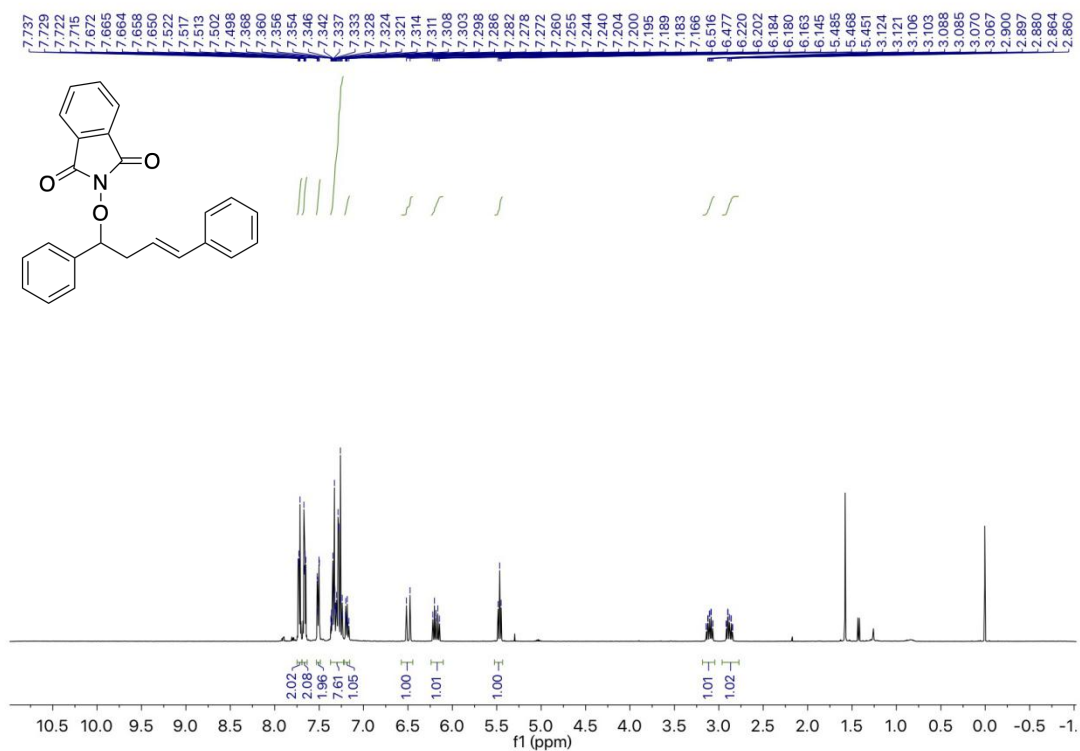
$^{13}\text{C}$  NMR spectrum (101 MHz,  $\text{CDCl}_3$ ) of **1i**



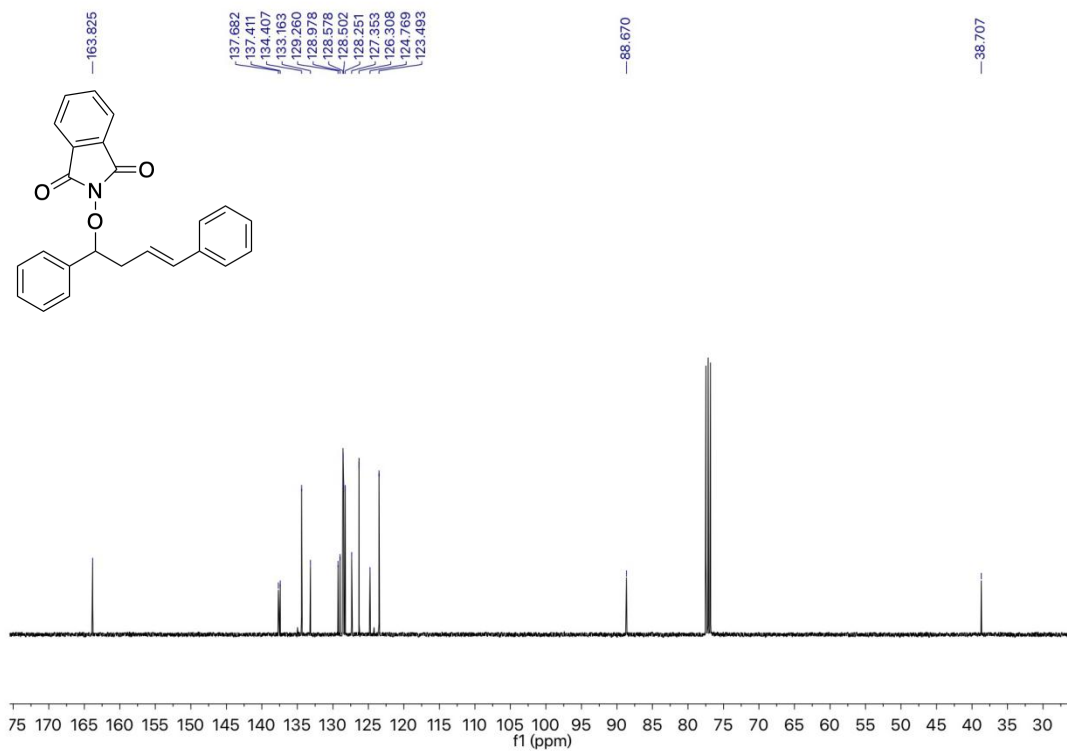
$^1\text{H}$  NMR spectrum (400 MHz,  $\text{CDCl}_3$ ) of **1j**



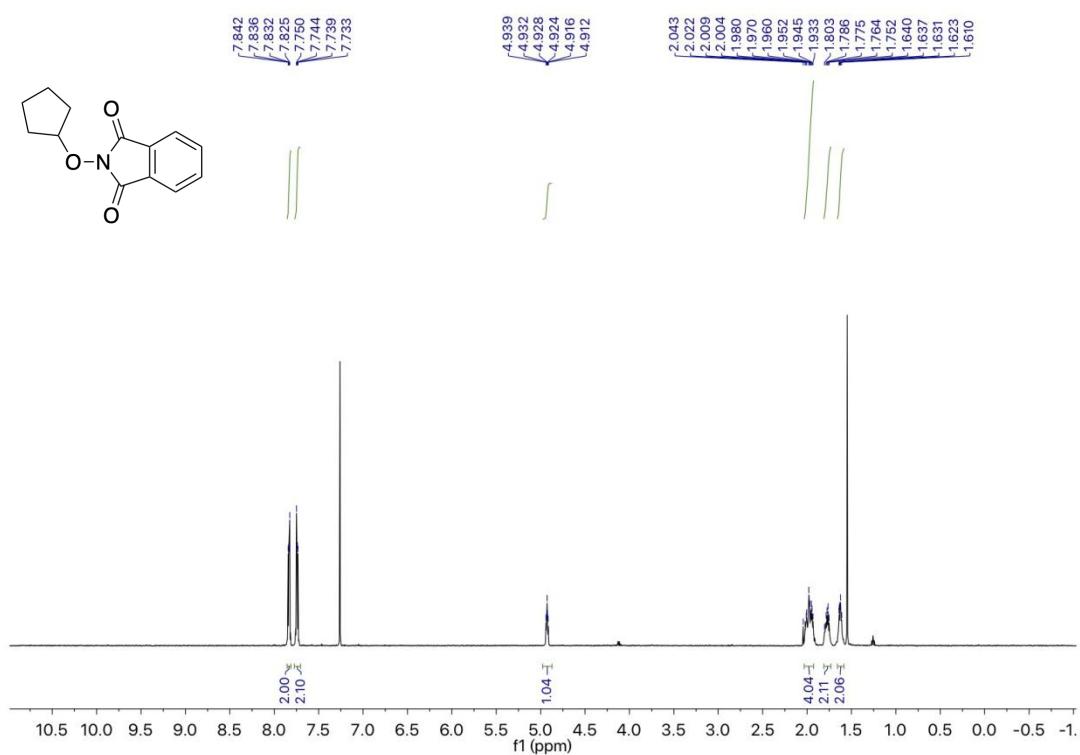
<sup>13</sup>C NMR spectrum (101 MHz, CDCl<sub>3</sub>) of **1j**



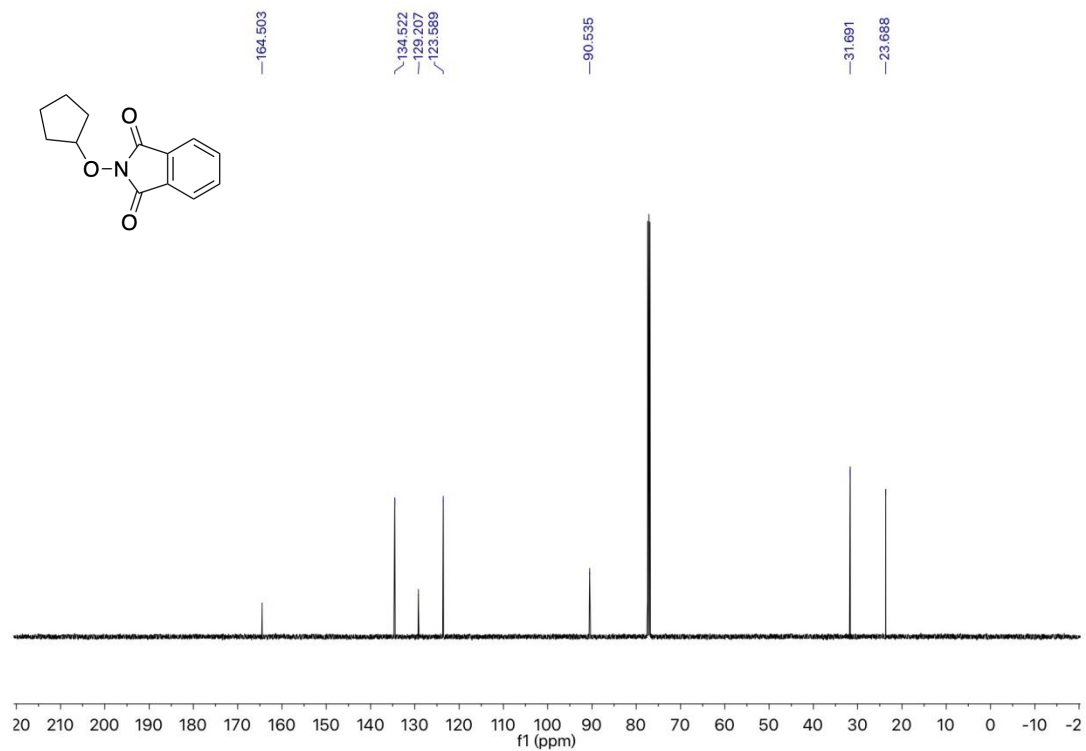
<sup>1</sup>H NMR spectrum (400 MHz, CDCl<sub>3</sub>) of **1k**



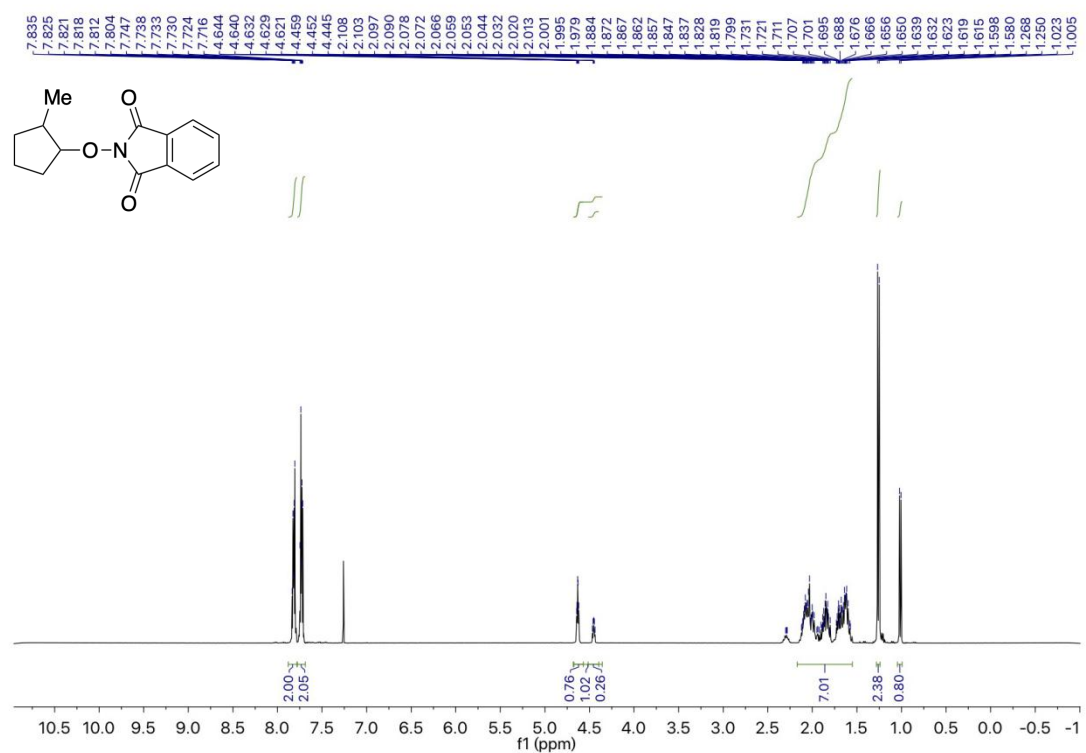
$^{13}\text{C}$  NMR spectrum (101 MHz,  $\text{CDCl}_3$ ) of **1k**



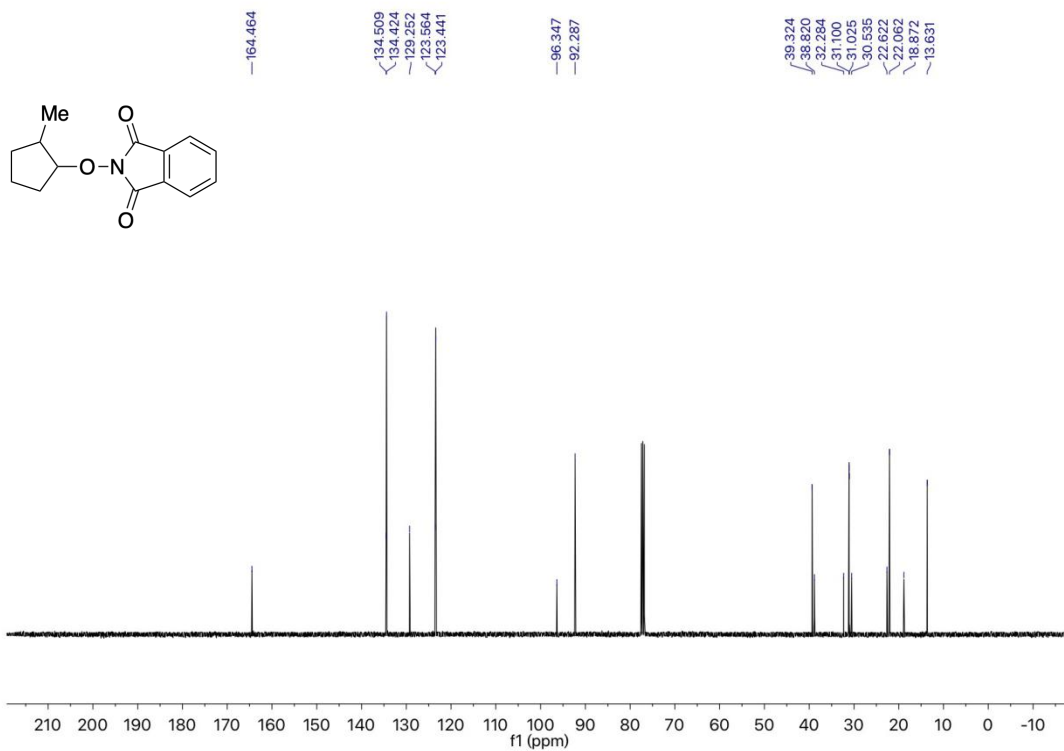
$^1\text{H}$  NMR spectrum (400 MHz,  $\text{CDCl}_3$ ) of **1l**



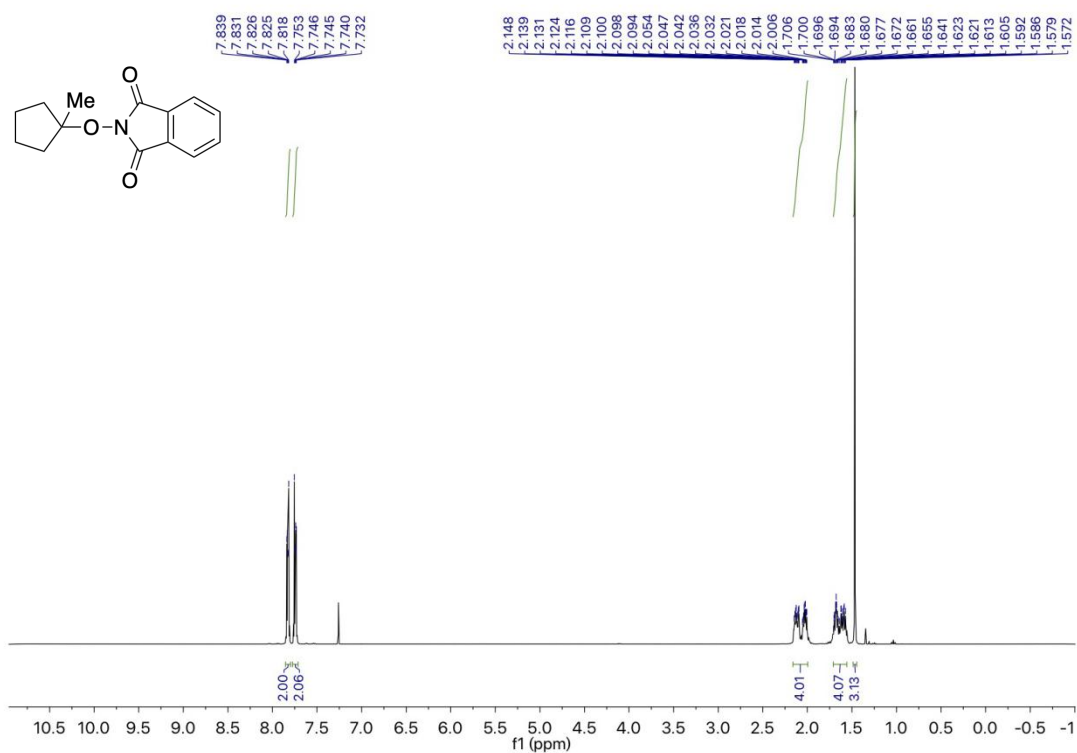
<sup>13</sup>C NMR spectrum (101 MHz, CDCl<sub>3</sub>) of **1l**



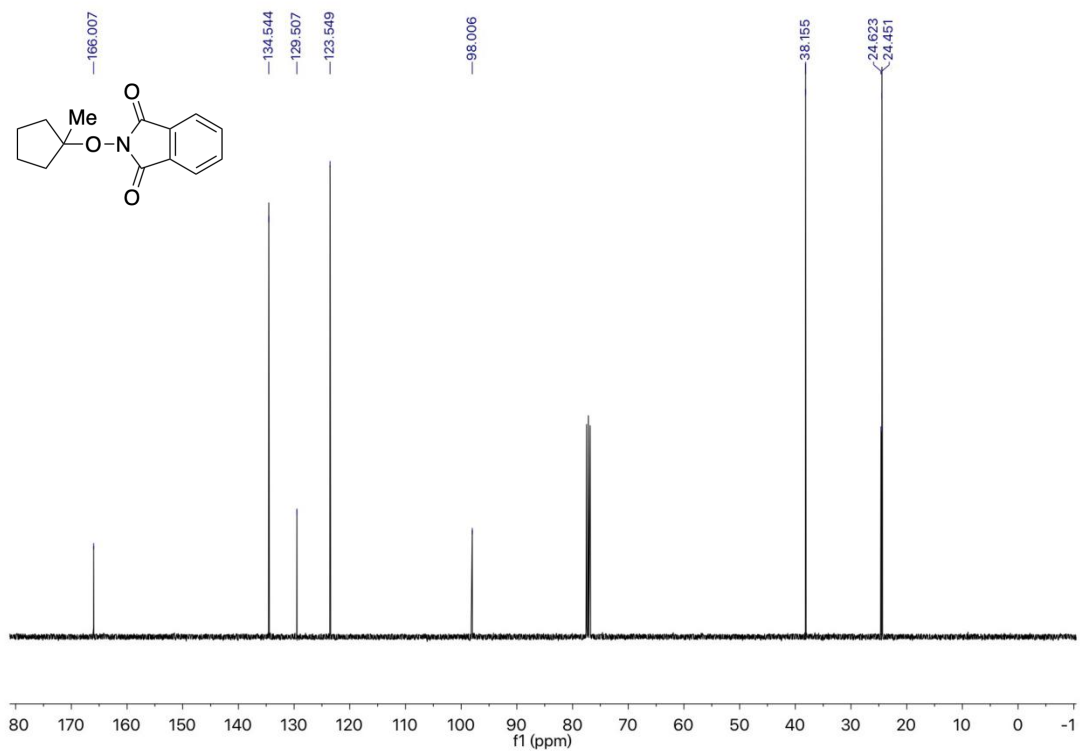
<sup>1</sup>H NMR spectrum (400 MHz, CDCl<sub>3</sub>) of **1m**



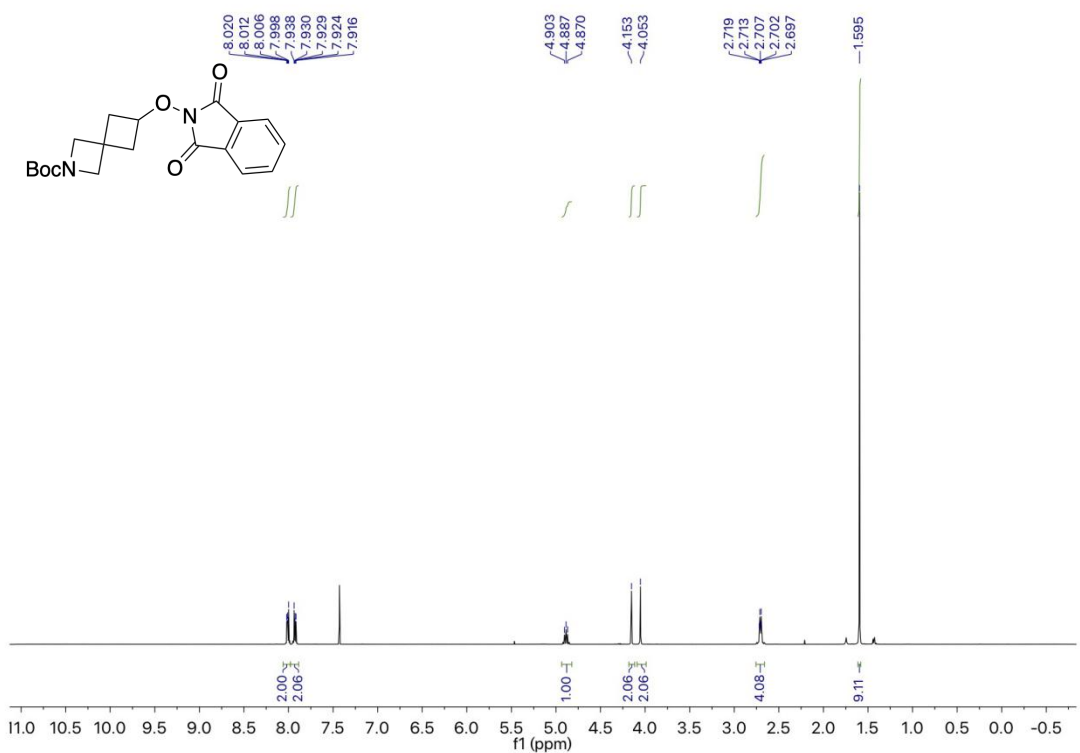
<sup>13</sup>C NMR spectrum (101 MHz, CDCl<sub>3</sub>) of **1m**



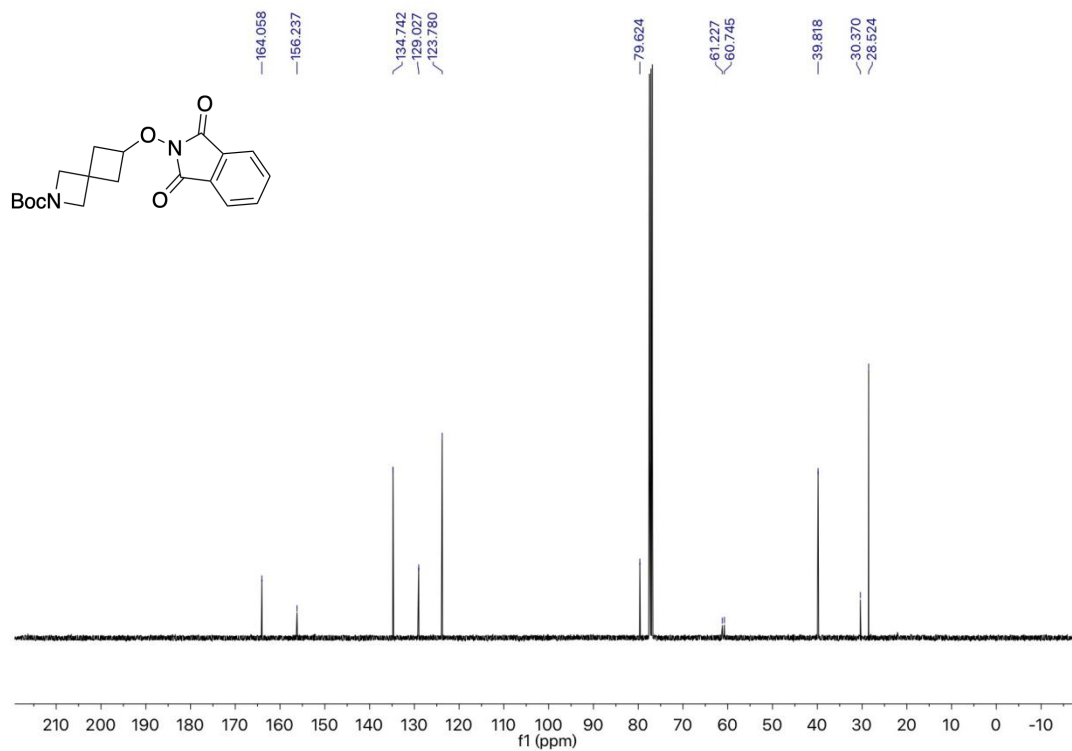
<sup>1</sup>H NMR spectrum (400 MHz, CDCl<sub>3</sub>) of **1n**



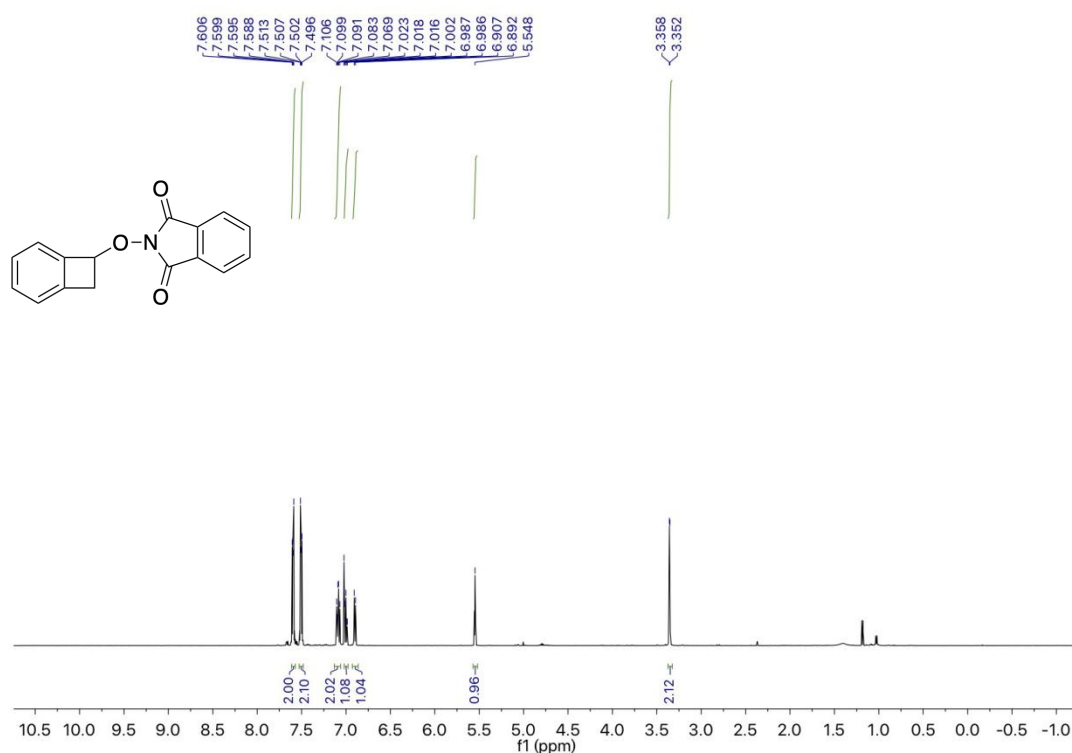
$^{13}\text{C}$  NMR spectrum (101 MHz,  $\text{CDCl}_3$ ) of **1n**



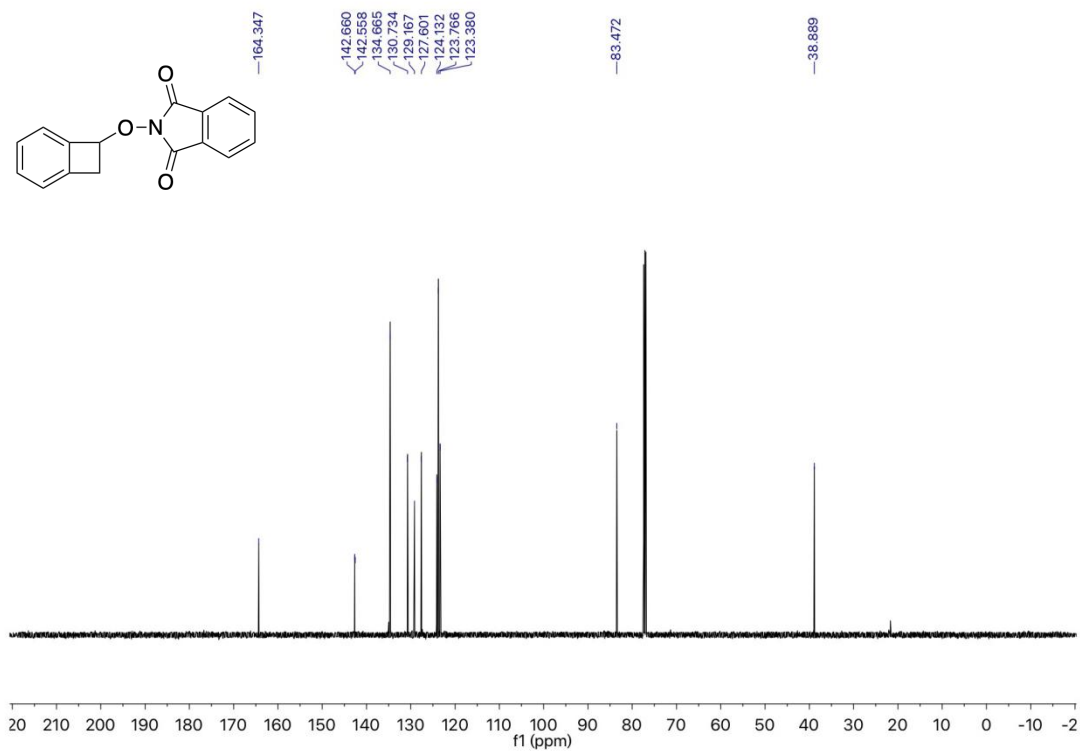
$^1\text{H}$  NMR spectrum (400 MHz,  $\text{CDCl}_3$ ) of **1o**



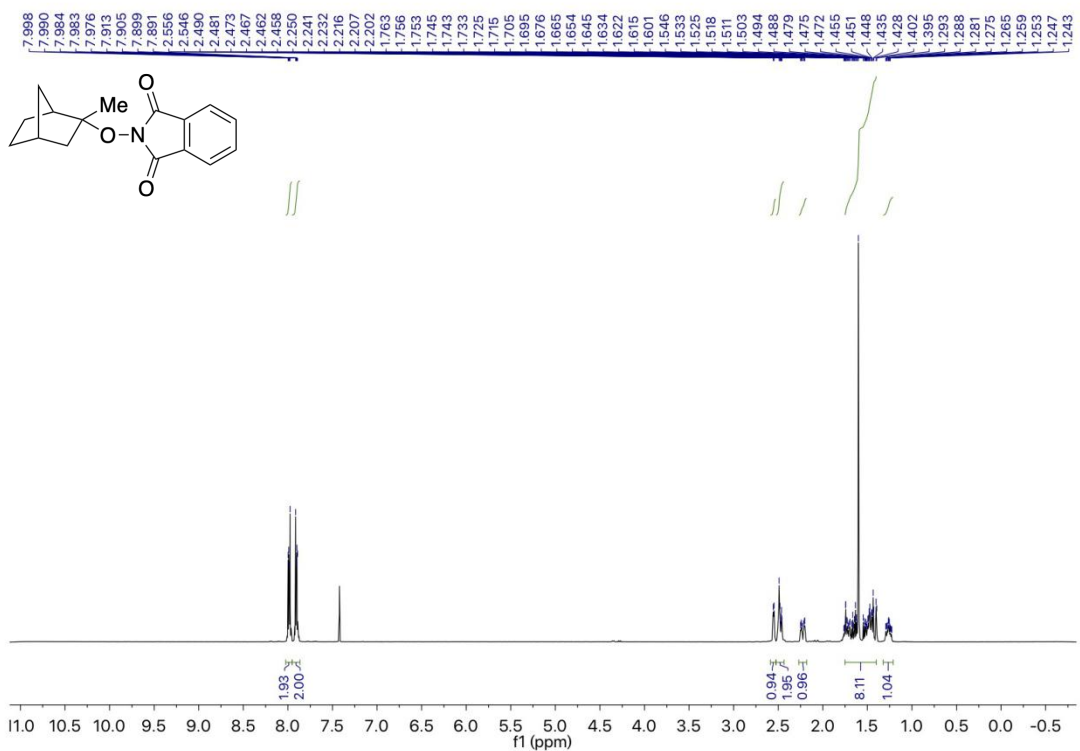
$^{13}\text{C}$  NMR spectrum (101 MHz,  $\text{CDCl}_3$ ) of **1o**



$^1\text{H}$  NMR spectrum (400 MHz,  $\text{CDCl}_3$ ) of **1p**

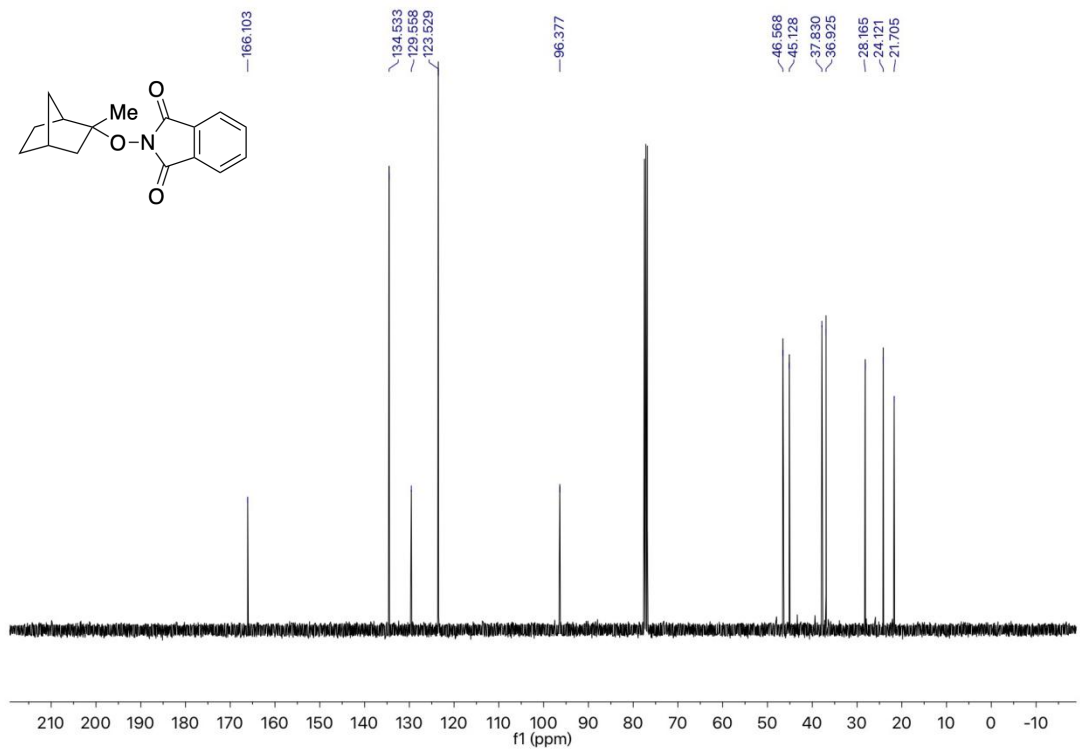


<sup>13</sup>C NMR spectrum (101 MHz, CDCl<sub>3</sub>) of **1p**

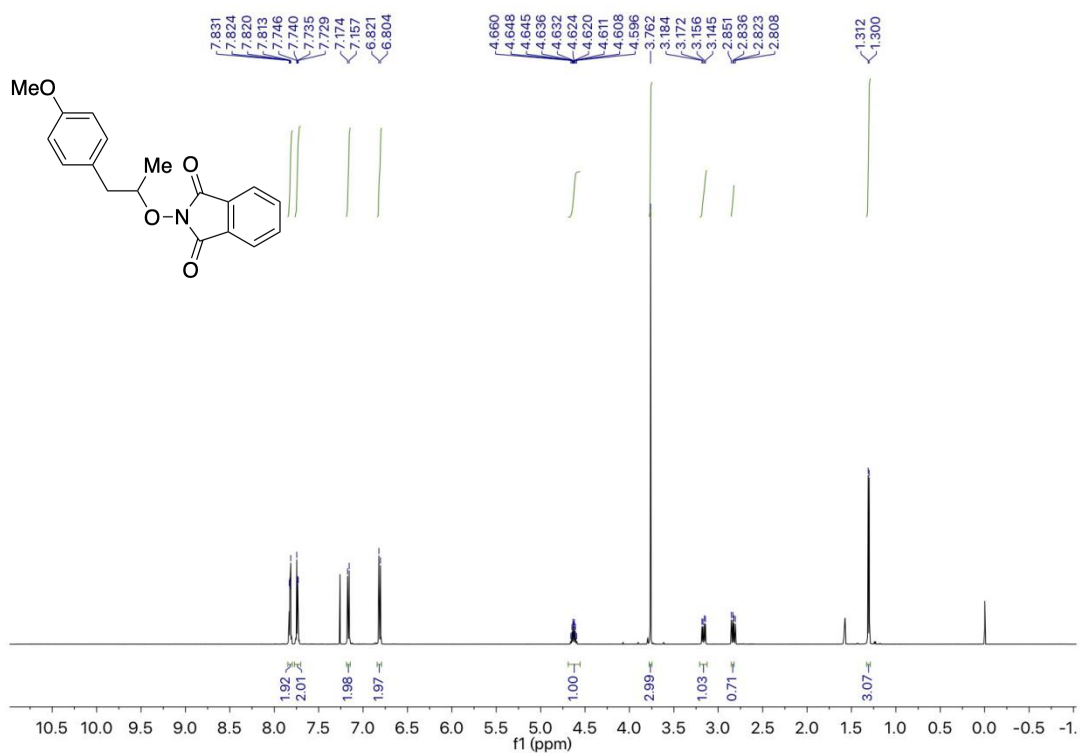


<sup>1</sup>H NMR spectrum (400 MHz, CDCl<sub>3</sub>) of **1q**

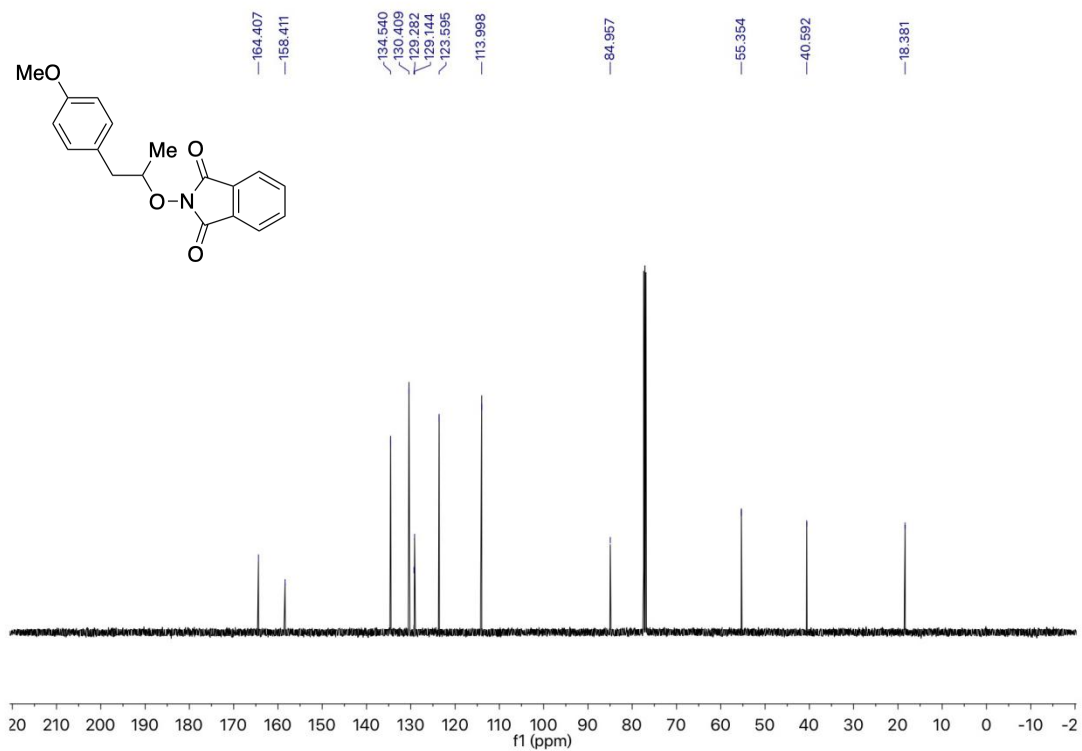




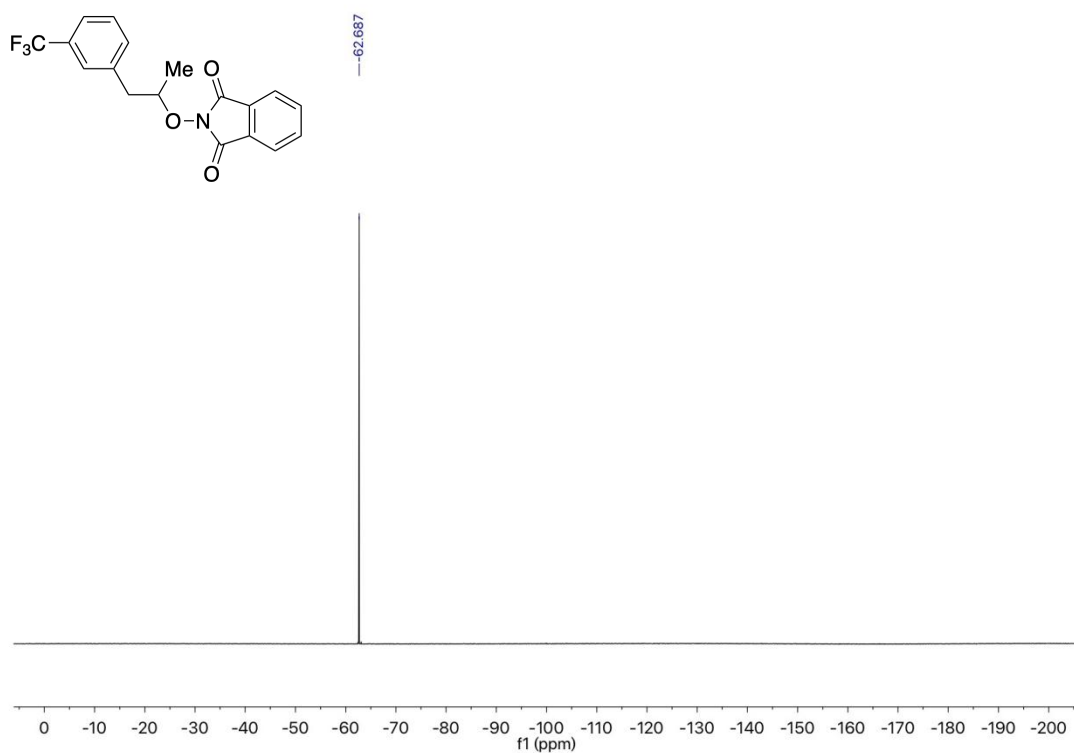
<sup>13</sup>C NMR spectrum (101 MHz, CDCl<sub>3</sub>) of **1q**



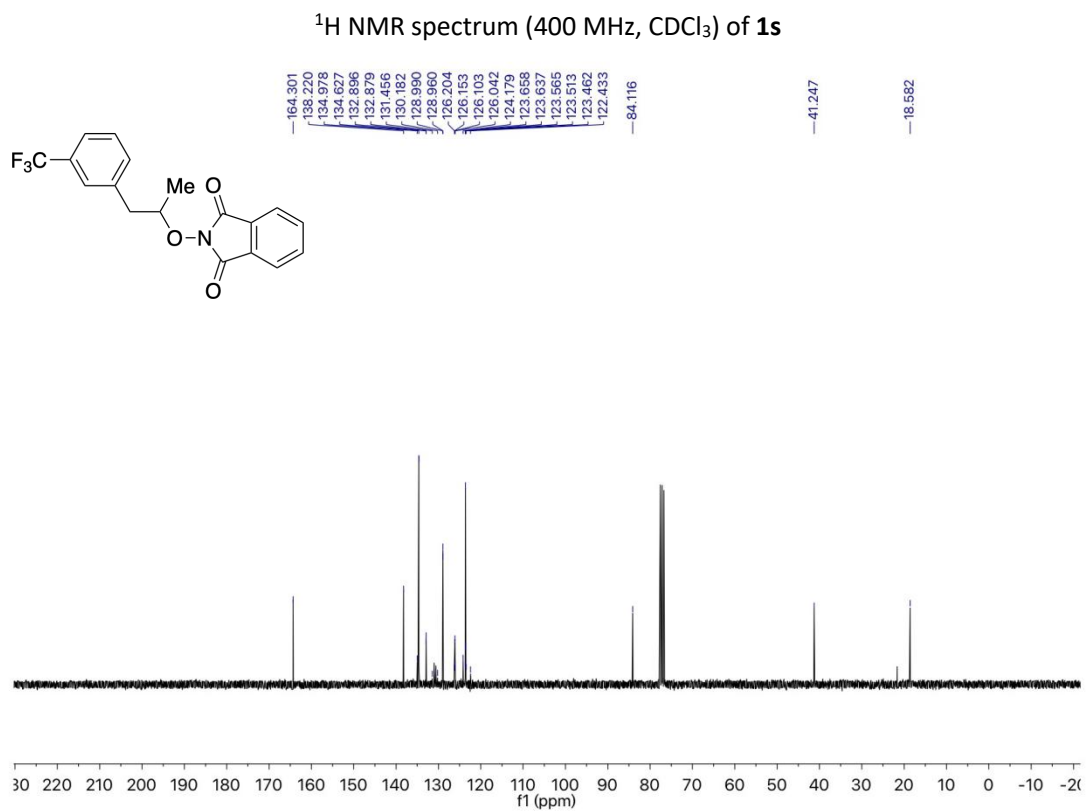
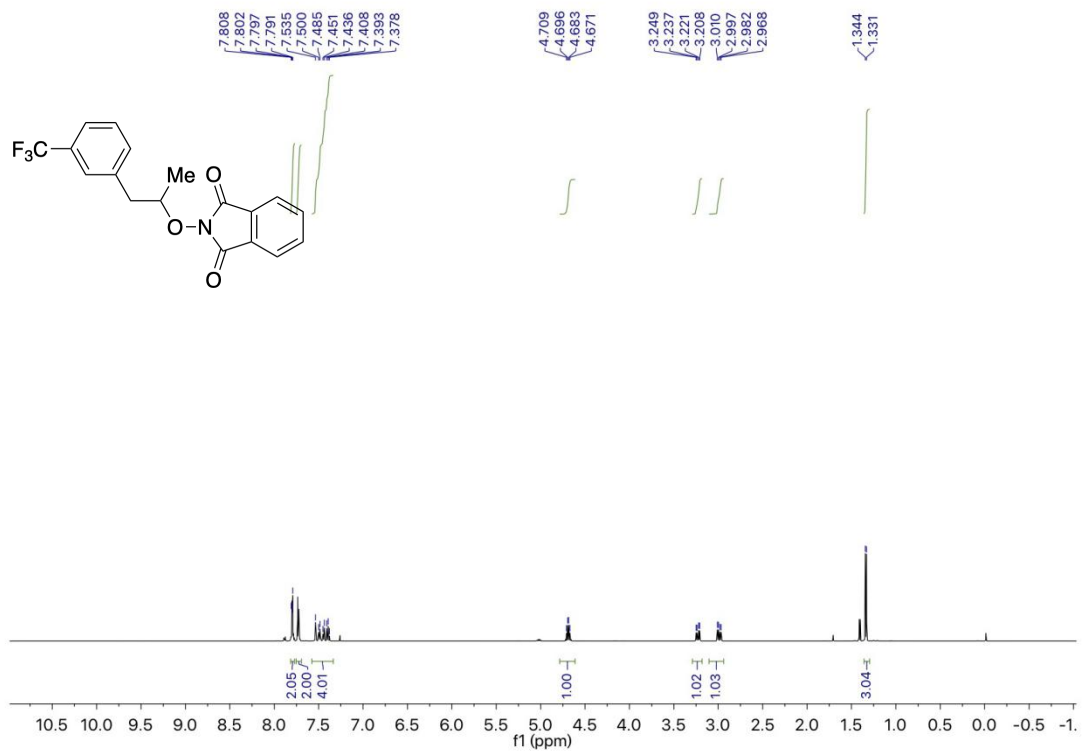
<sup>1</sup>H NMR spectrum (400 MHz, CDCl<sub>3</sub>) of **1r**

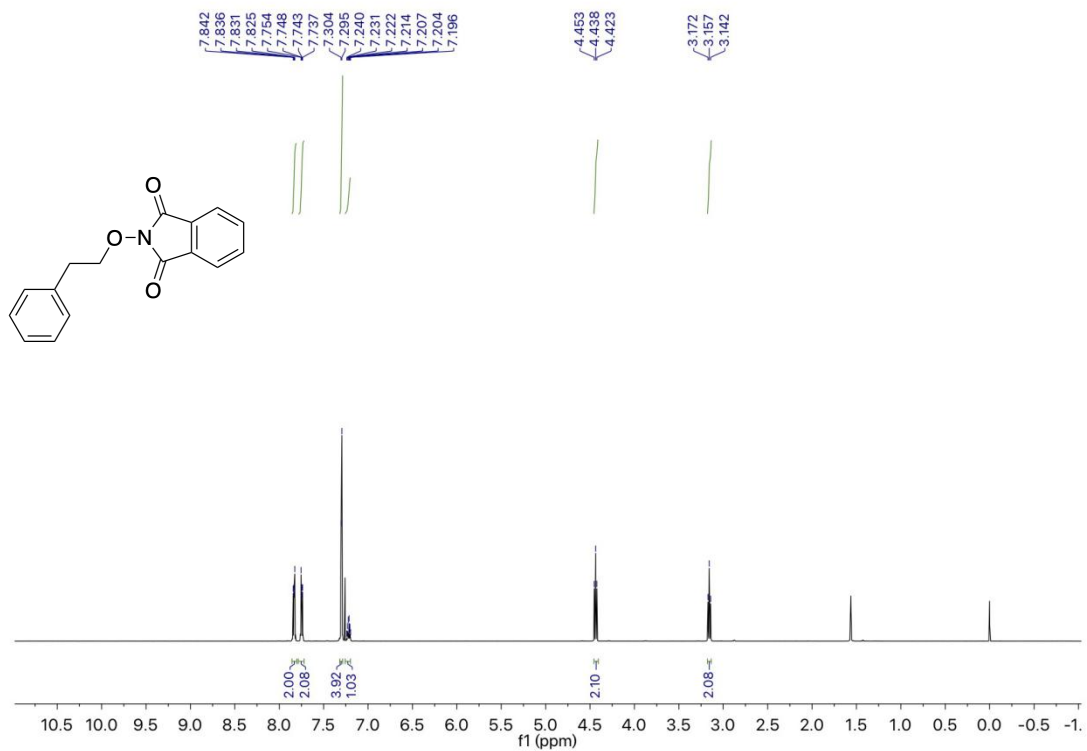


<sup>13</sup>C NMR spectrum (101 MHz, CDCl<sub>3</sub>) of **1r**

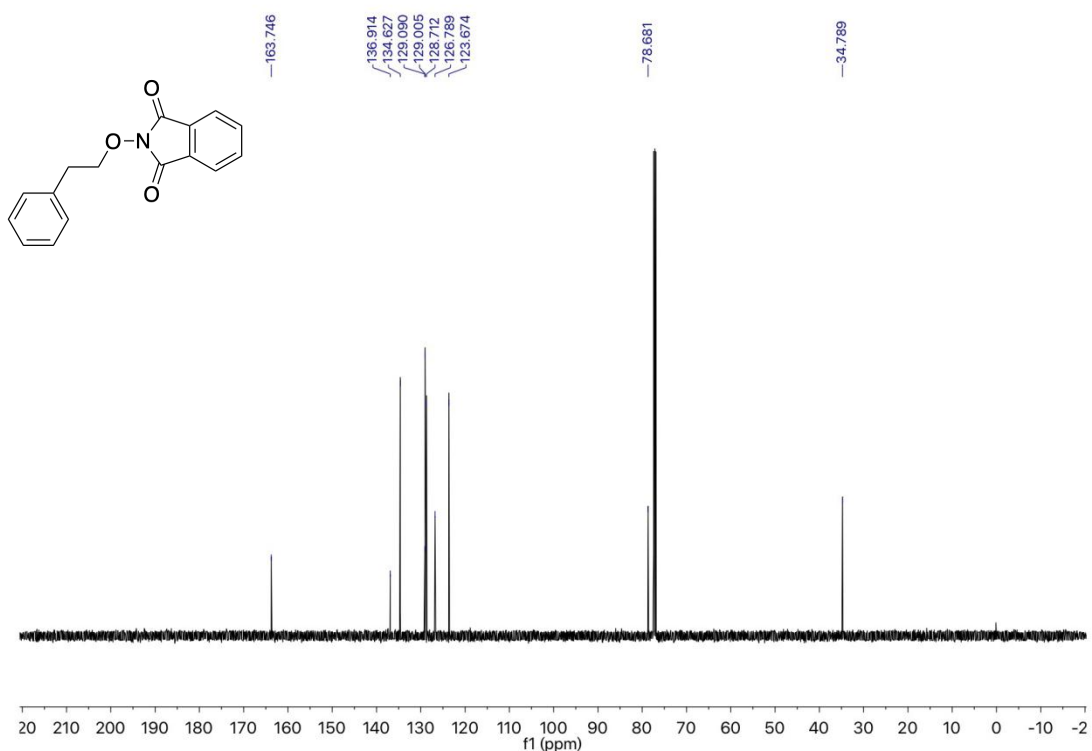


<sup>19</sup>F NMR spectrum (375 MHz, CDCl<sub>3</sub>) of **1s**

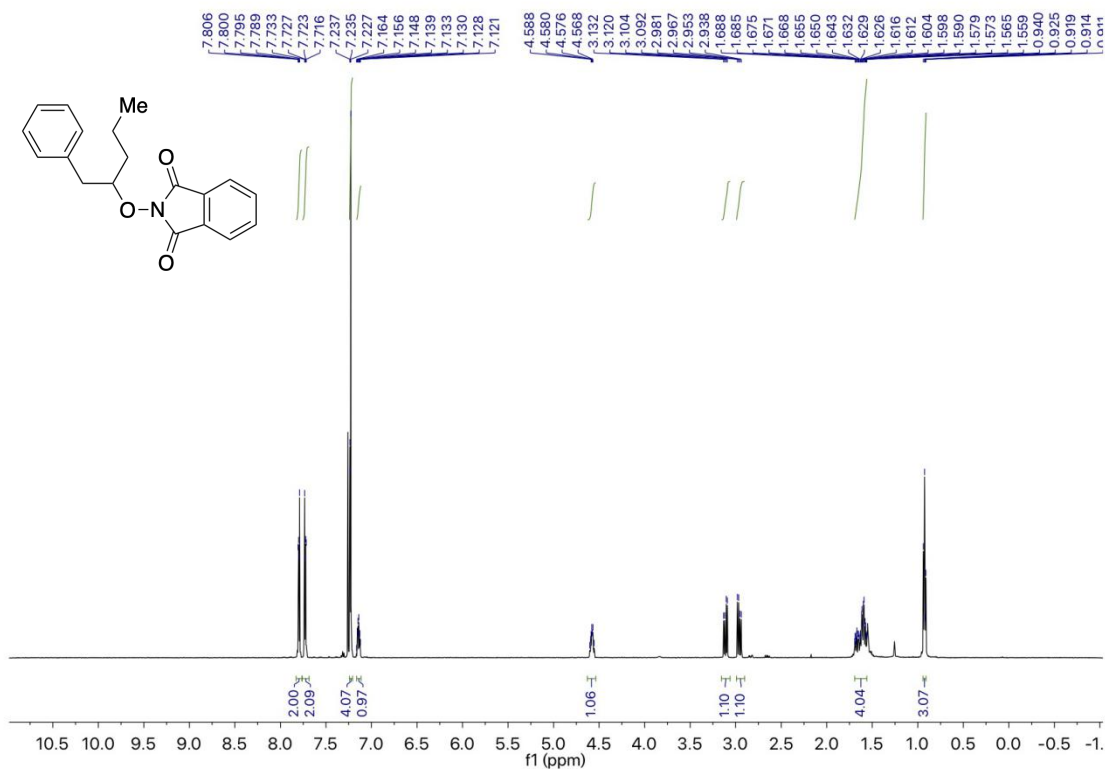




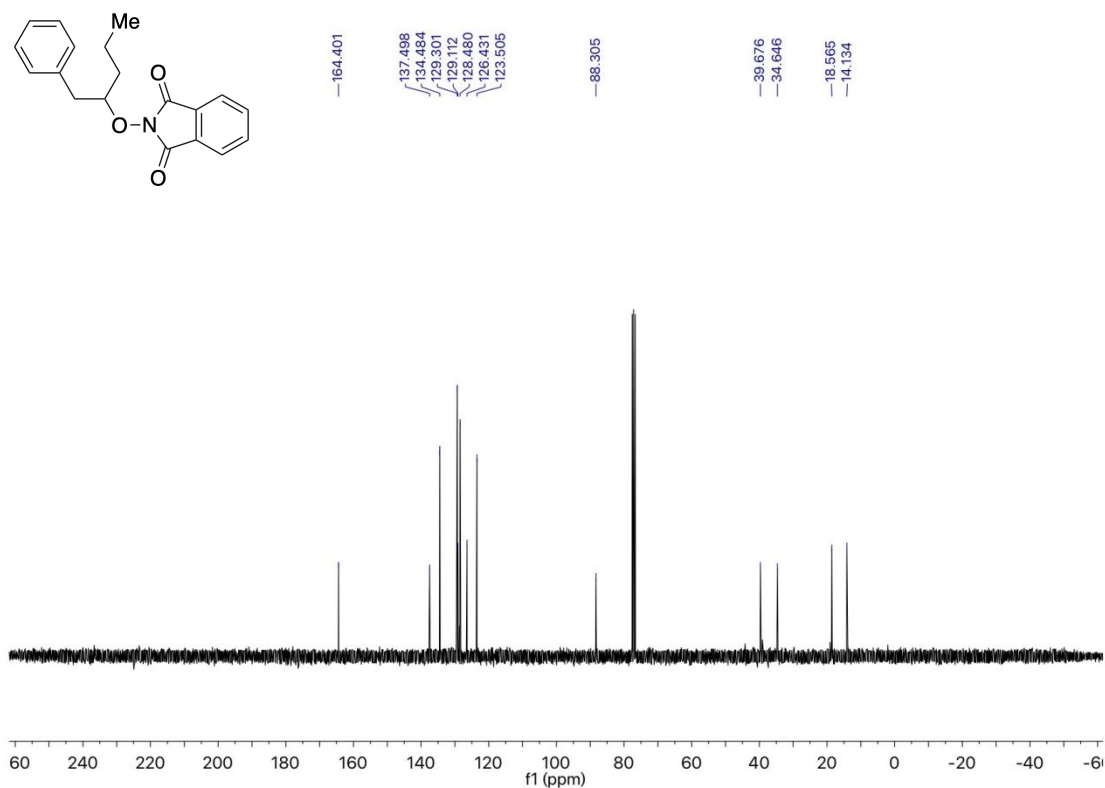
<sup>1</sup>H NMR spectrum (400 MHz, CDCl<sub>3</sub>) of **1t**



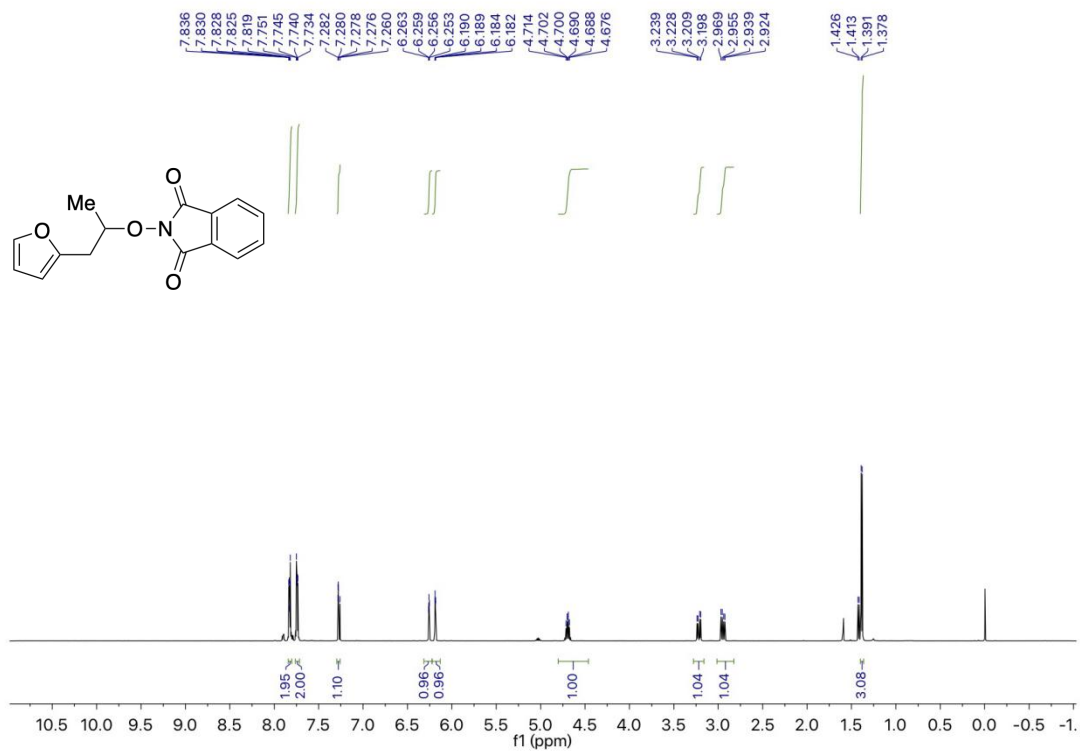
<sup>13</sup>C NMR spectrum (101 MHz, CDCl<sub>3</sub>) of **1t**



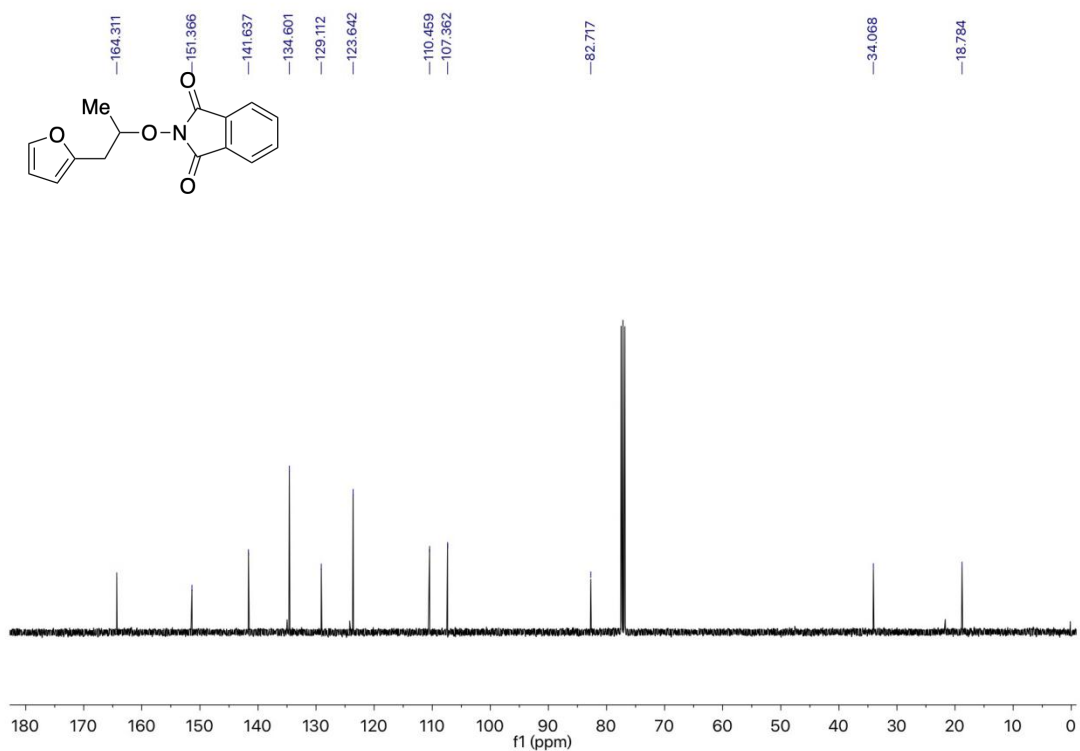
<sup>1</sup>H NMR spectrum (400 MHz, CDCl<sub>3</sub>) of **1u**



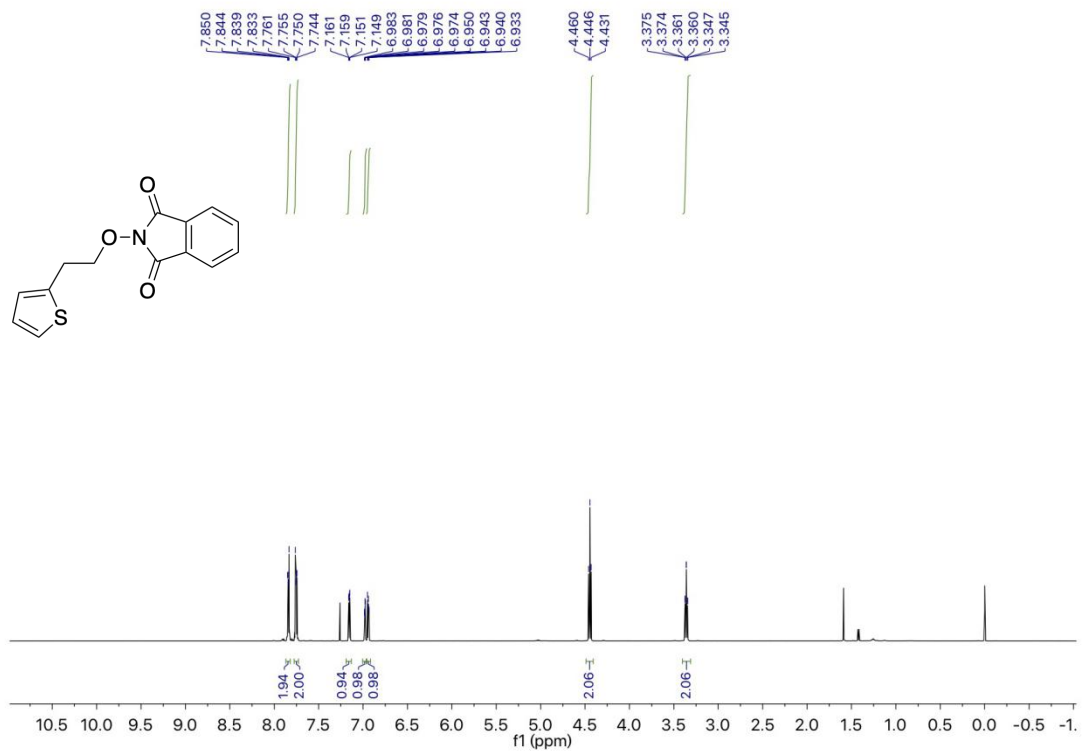
<sup>13</sup>C NMR spectrum (101 MHz, CDCl<sub>3</sub>) of **1u**



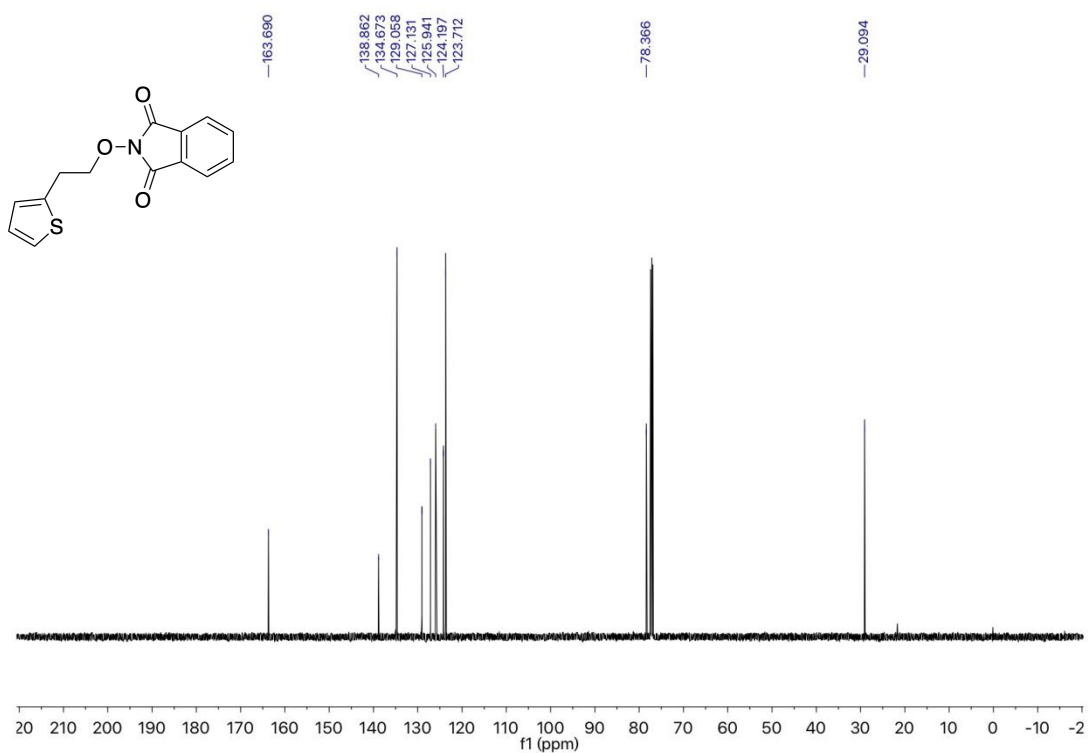
**<sup>1</sup>H NMR spectrum (400 MHz, CDCl<sub>3</sub>) of **1v****



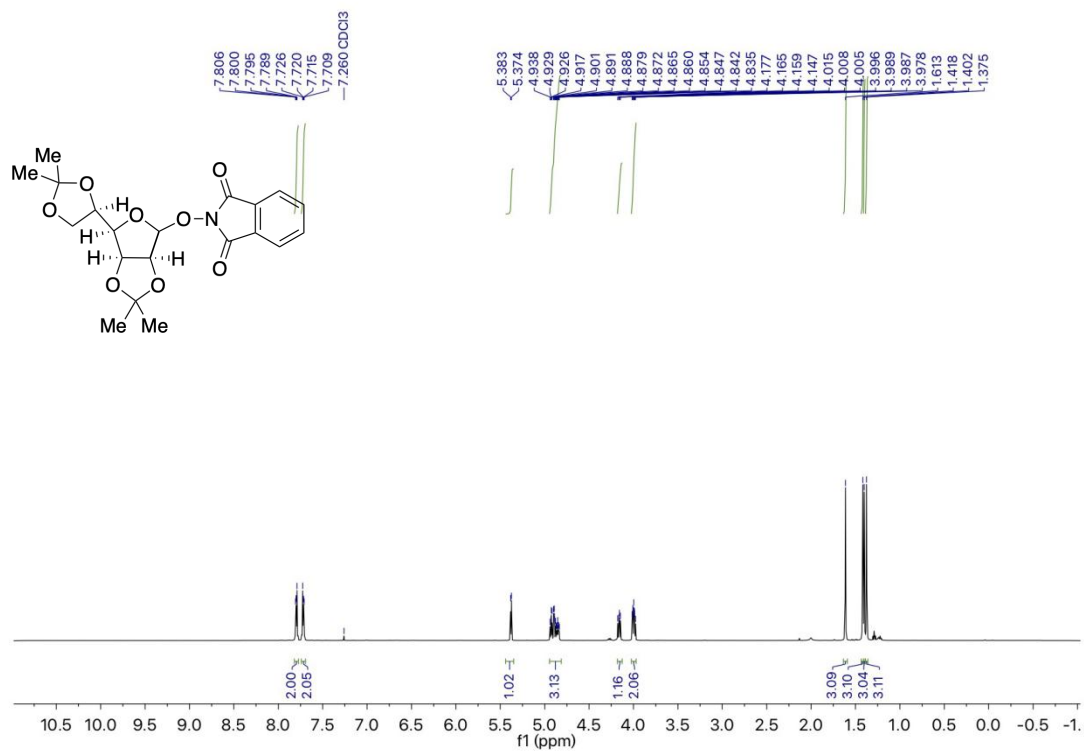
**<sup>13</sup>C NMR spectrum (101 MHz, CDCl<sub>3</sub>) of **1v****



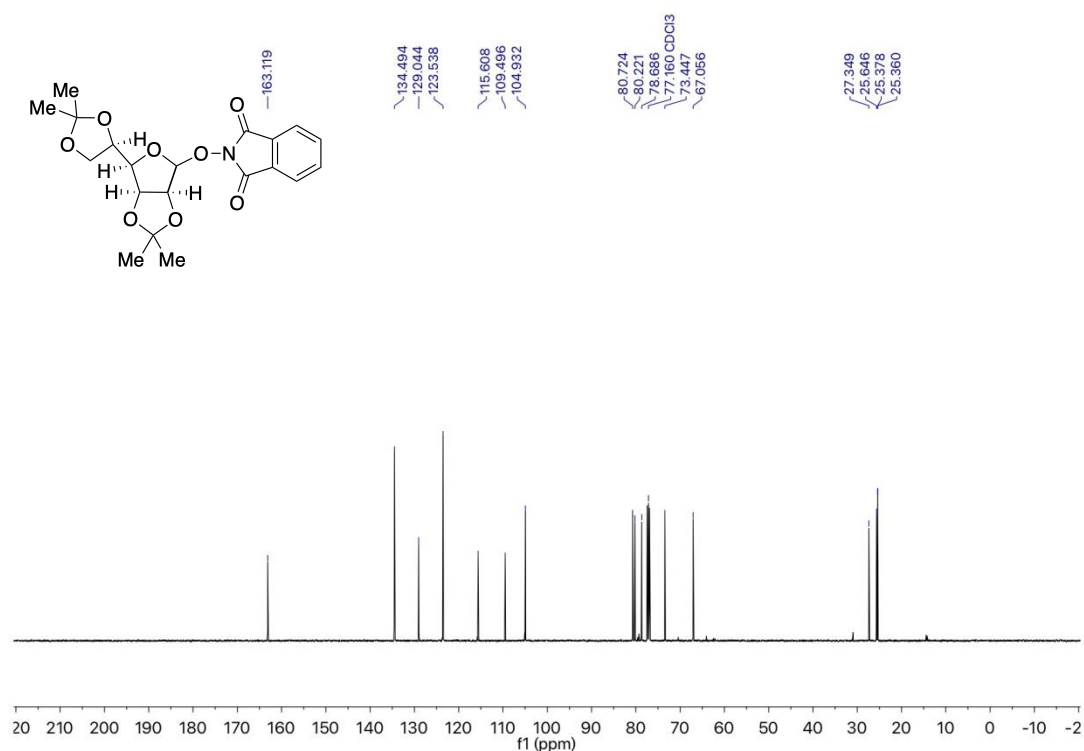
**<sup>1</sup>H NMR spectrum (400 MHz, CDCl<sub>3</sub>) of **1w****



**<sup>13</sup>C NMR spectrum (101 MHz, CDCl<sub>3</sub>) of **1w****

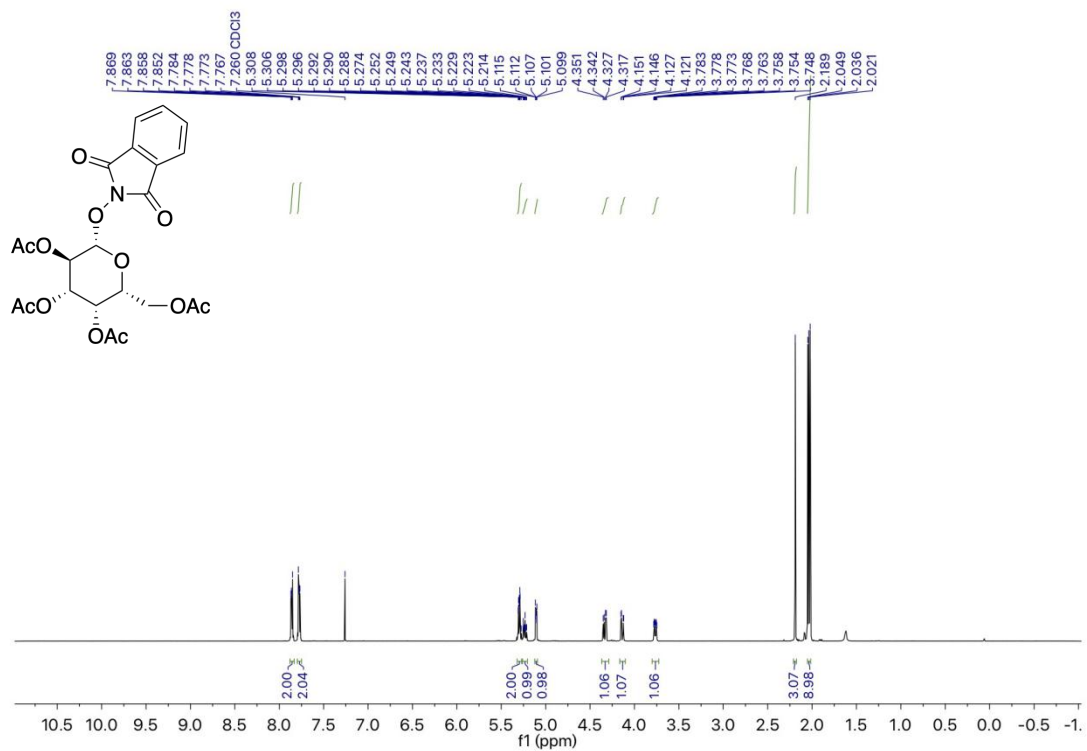


**<sup>1</sup>H NMR spectrum (400 MHz, CDCl<sub>3</sub>) of 6**

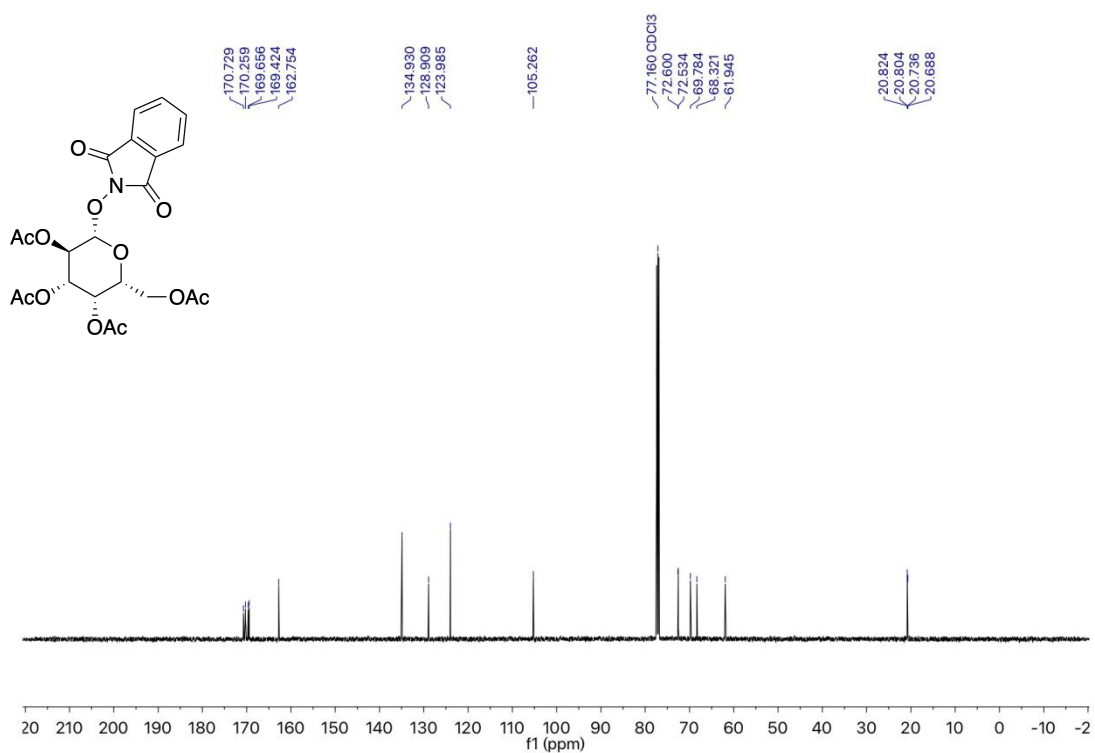


**<sup>13</sup>C NMR spectrum (101 MHz, CDCl<sub>3</sub>) of 6**

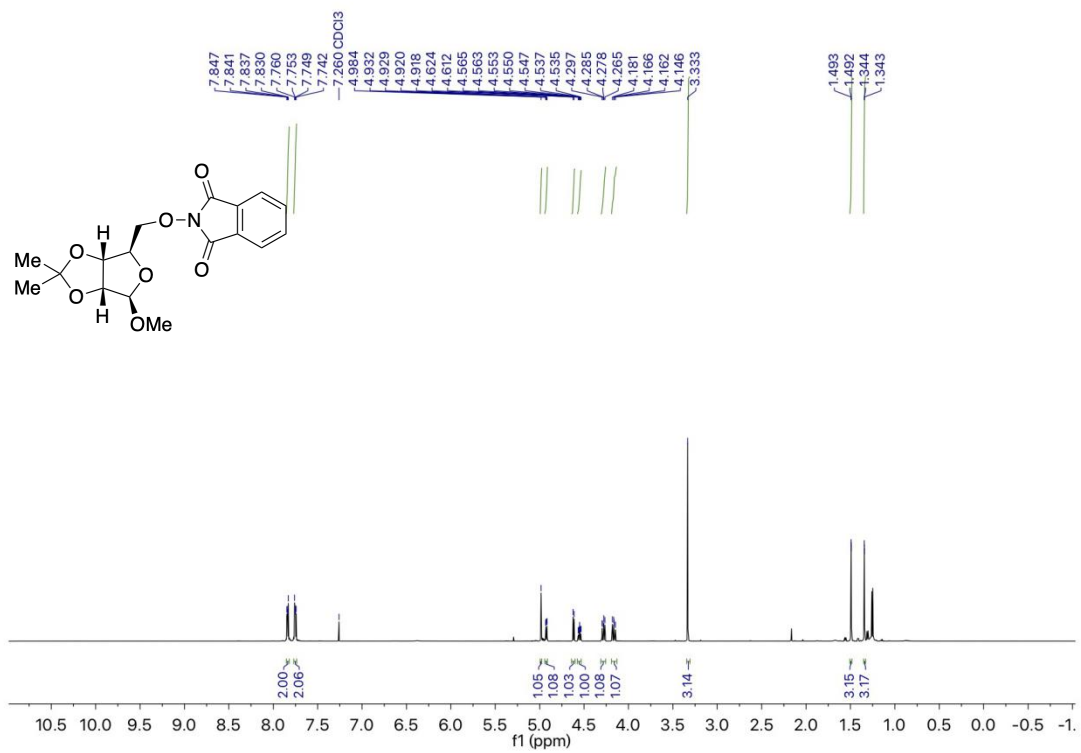




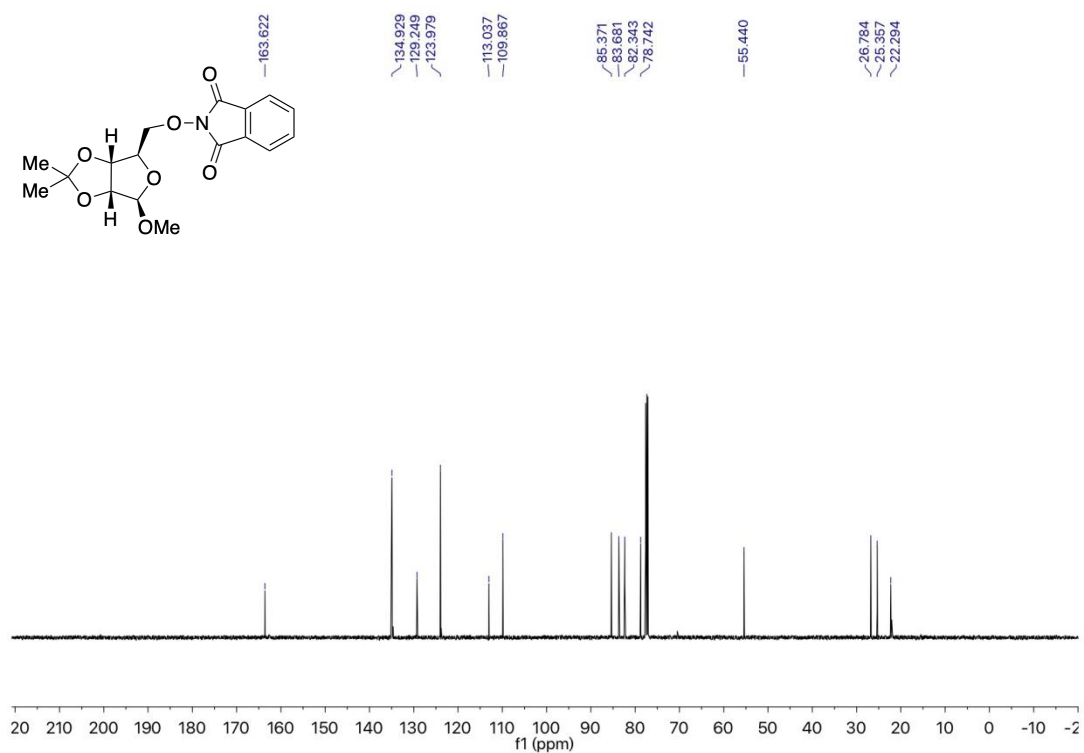
<sup>1</sup>H NMR spectrum (400 MHz, CDCl<sub>3</sub>) of **8**



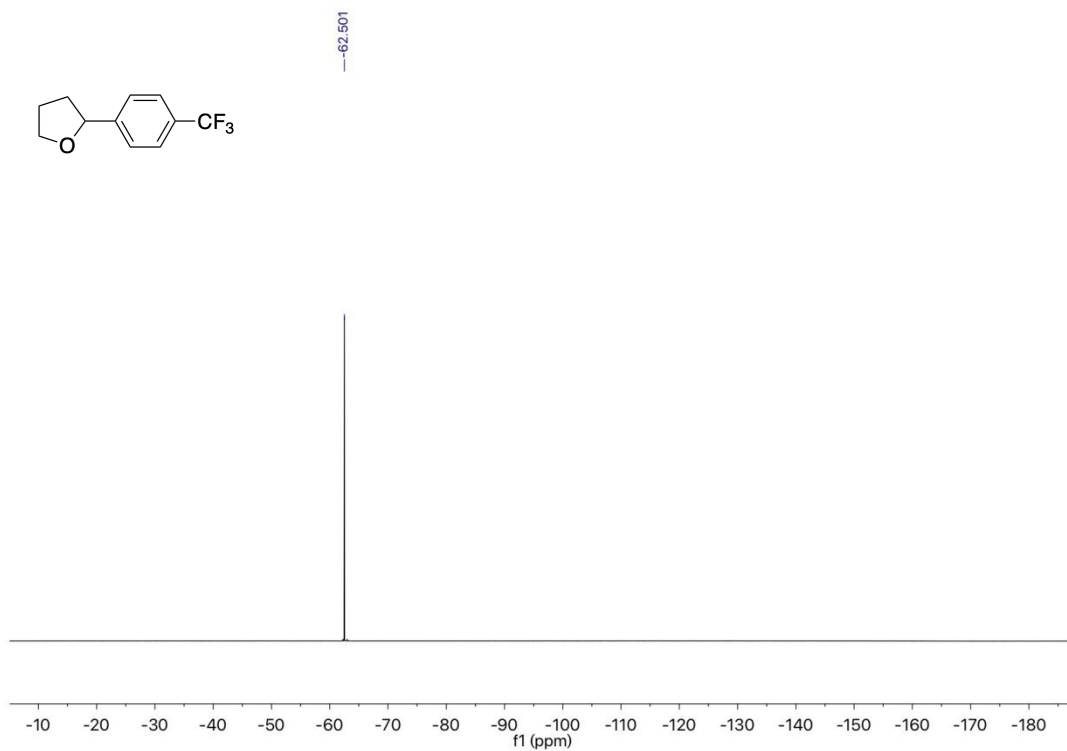
<sup>13</sup>C NMR spectrum (101 MHz, CDCl<sub>3</sub>) of **8**



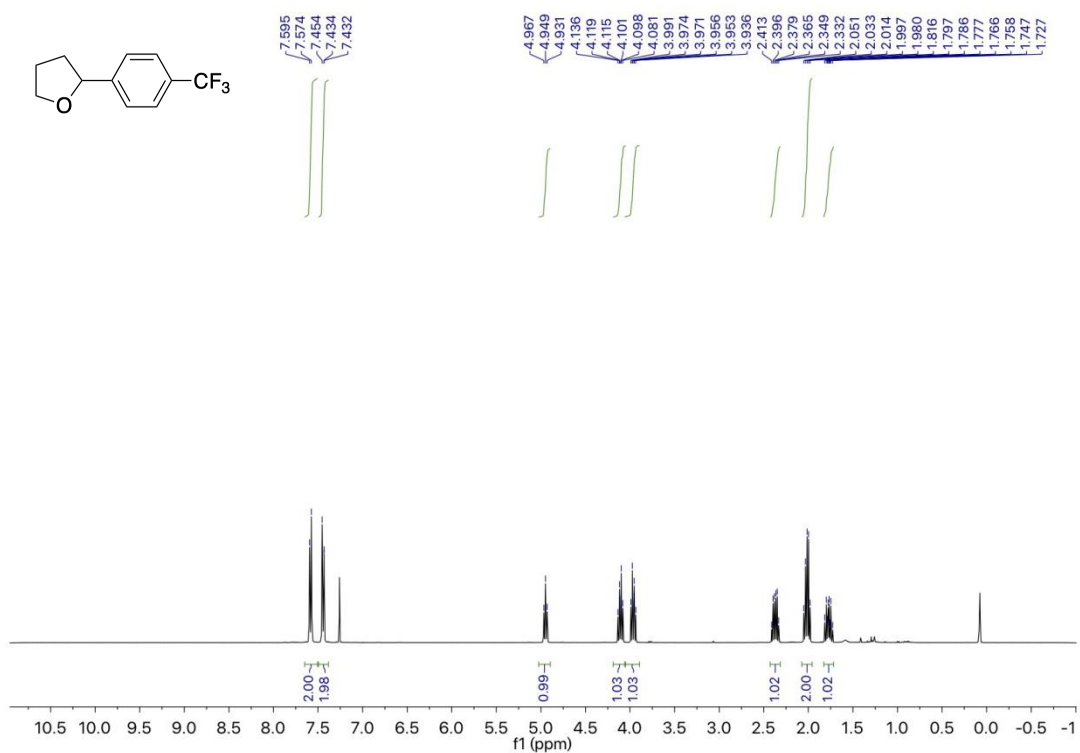
**<sup>1</sup>H NMR spectrum (400 MHz, CDCl<sub>3</sub>) of **10****



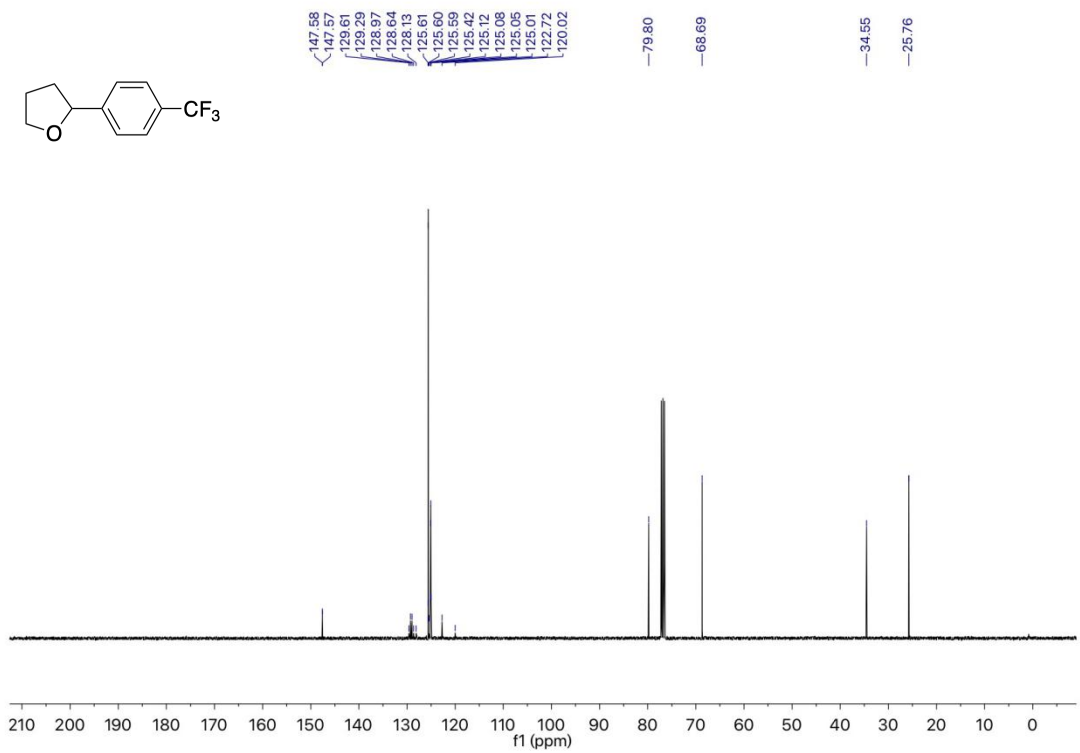
**<sup>13</sup>C NMR spectrum (101 MHz, CDCl<sub>3</sub>) of **10****



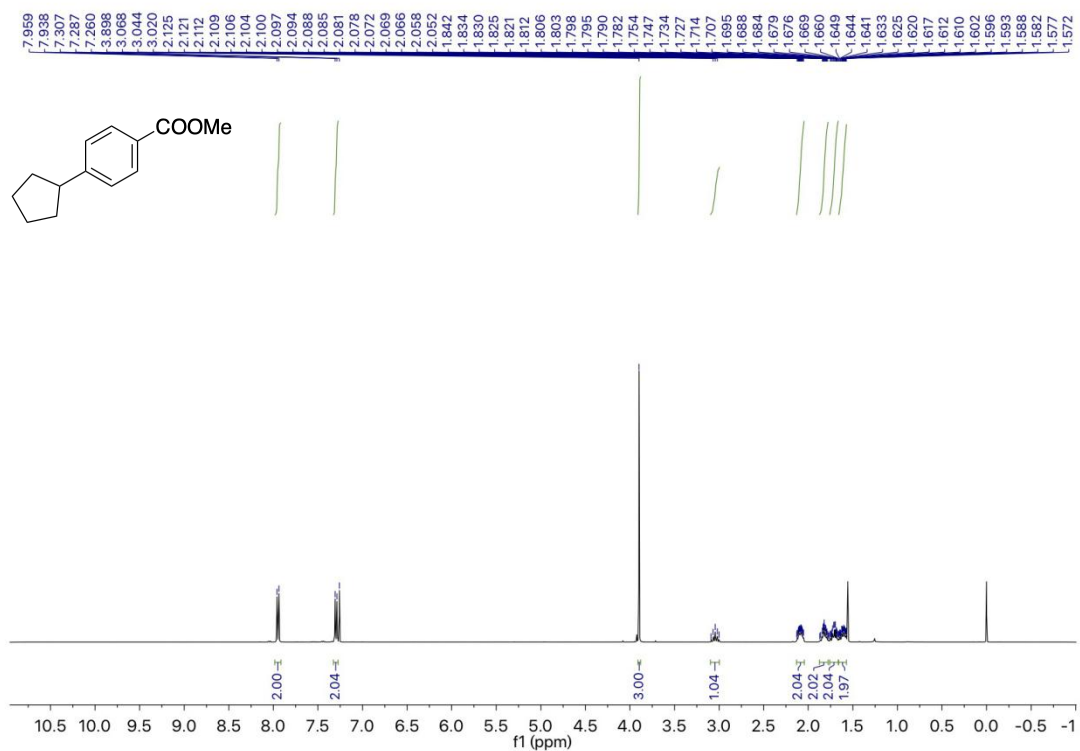
$^{19}\text{F}$  NMR spectrum (375 MHz,  $\text{CDCl}_3$ ) of **3a**



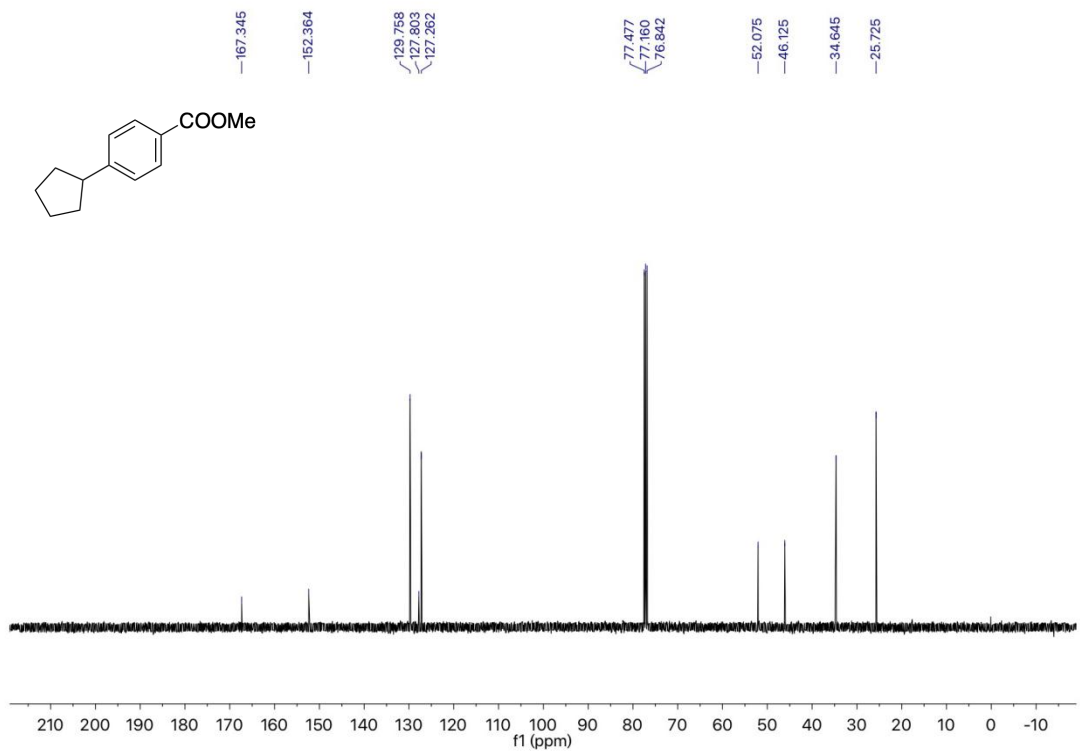
$^1\text{H}$  NMR spectrum (500 MHz,  $\text{CDCl}_3$ ) of **3a**



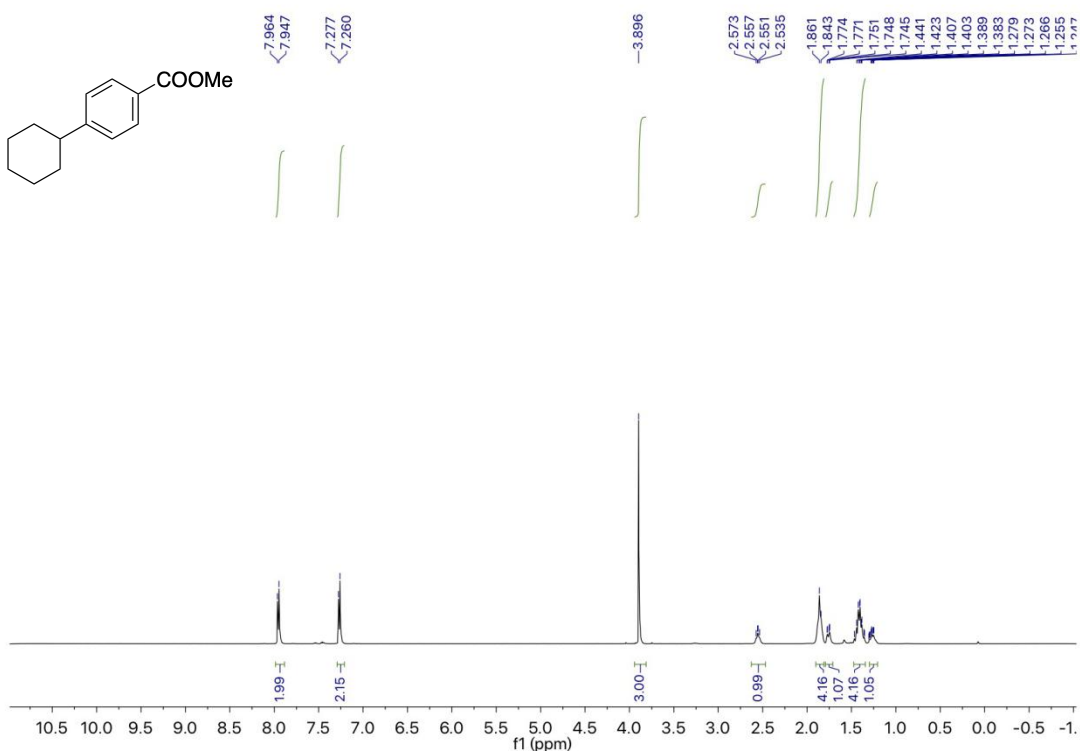
$^{13}\text{C}$  NMR spectrum (126 MHz,  $\text{CDCl}_3$ ) of 3a



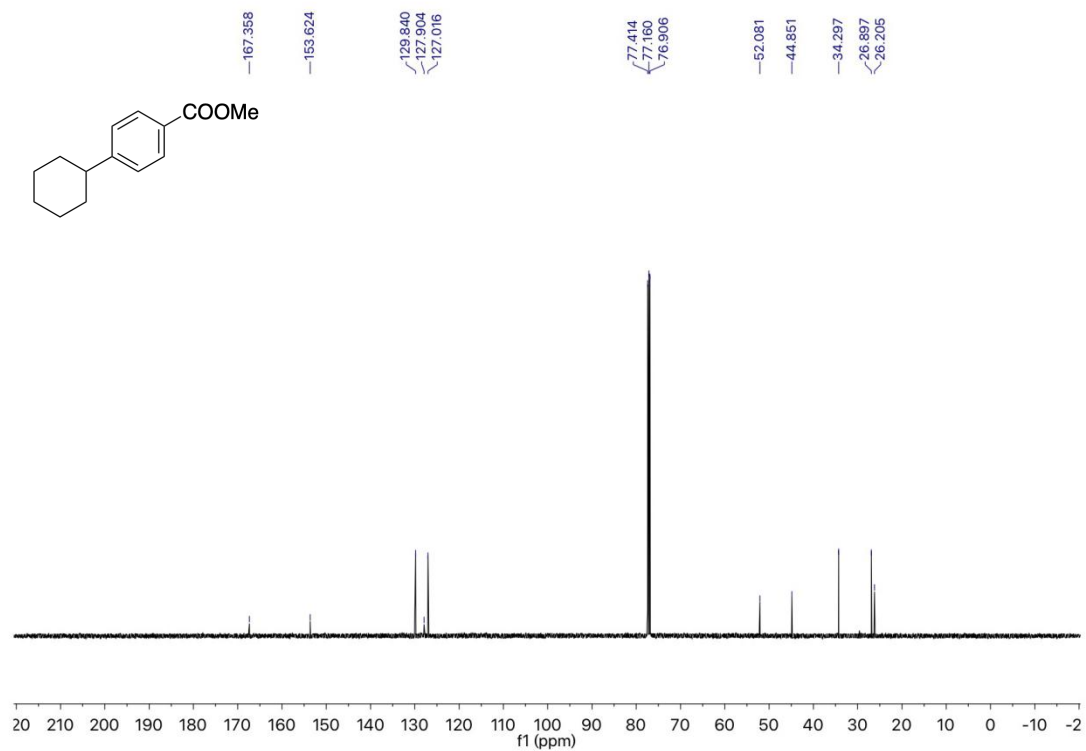
$^1\text{H}$  NMR spectrum (400 MHz,  $\text{CDCl}_3$ ) of 3b



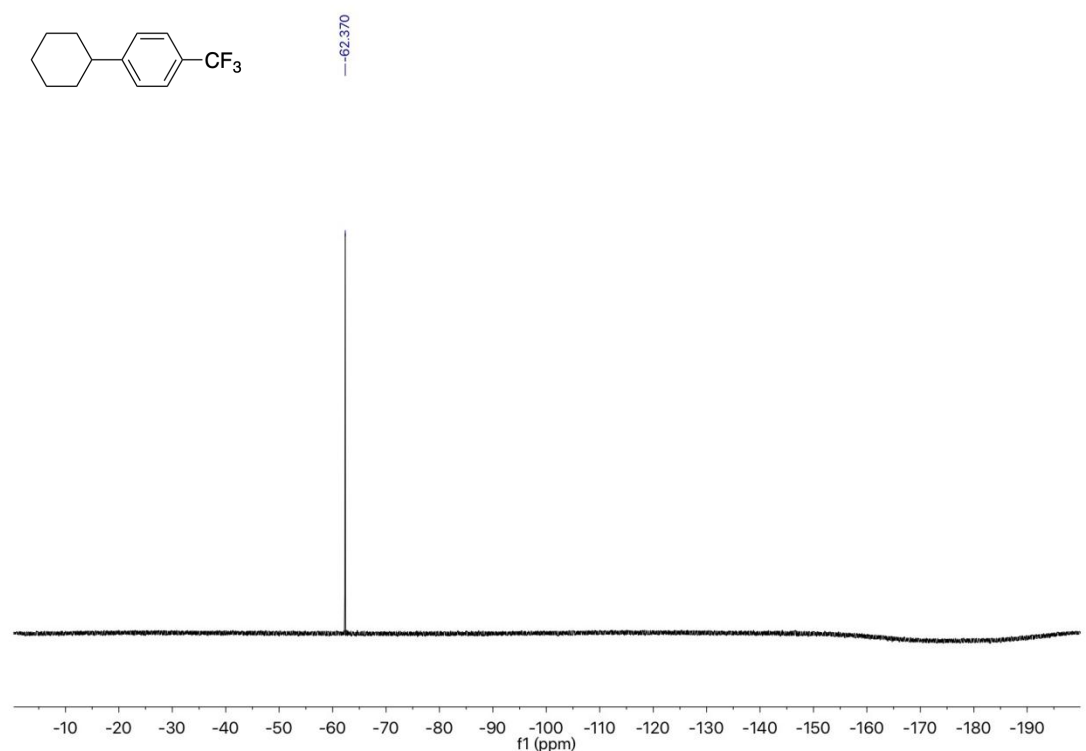
$^{13}\text{C}$  NMR spectrum (101 MHz,  $\text{CDCl}_3$ ) of **3b**



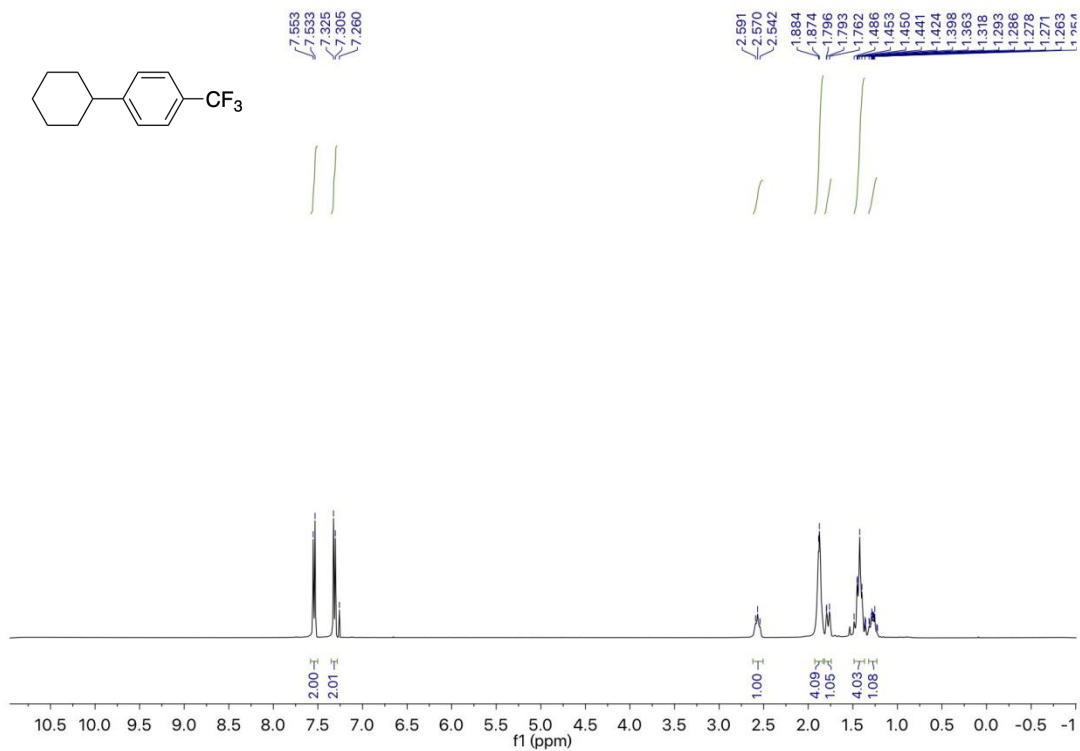
$^1\text{H}$  NMR spectrum (400 MHz,  $\text{CDCl}_3$ ) of **3c**



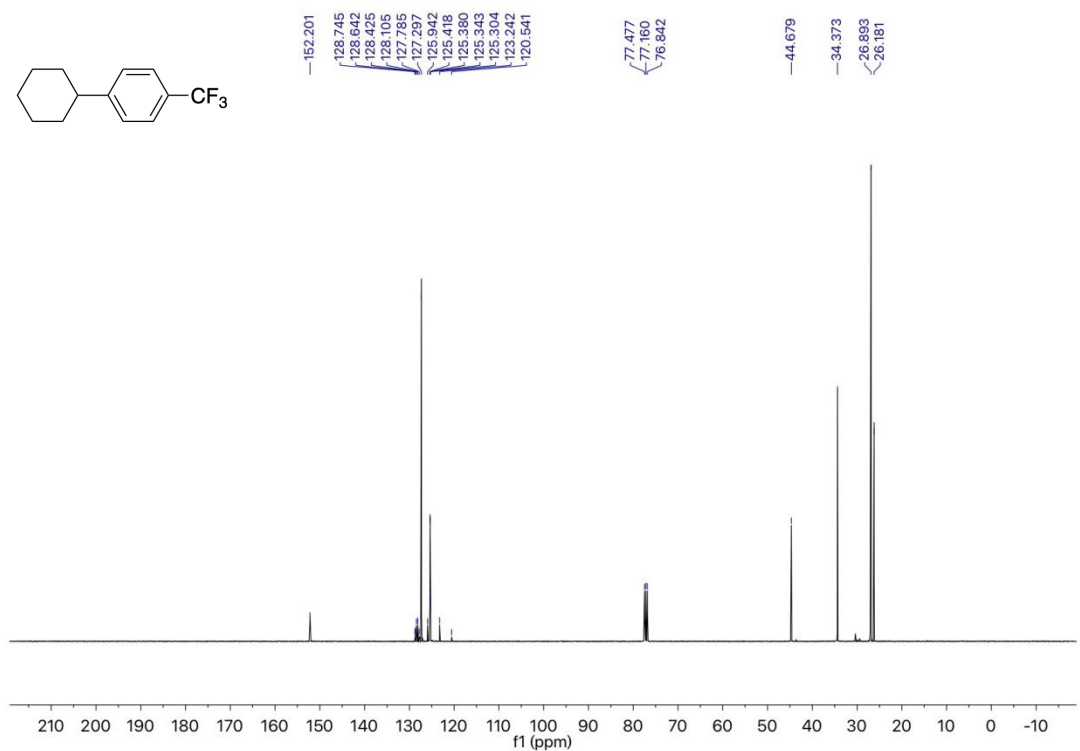
$^{13}\text{C}$  NMR spectrum (101 MHz,  $\text{CDCl}_3$ ) of **3c**



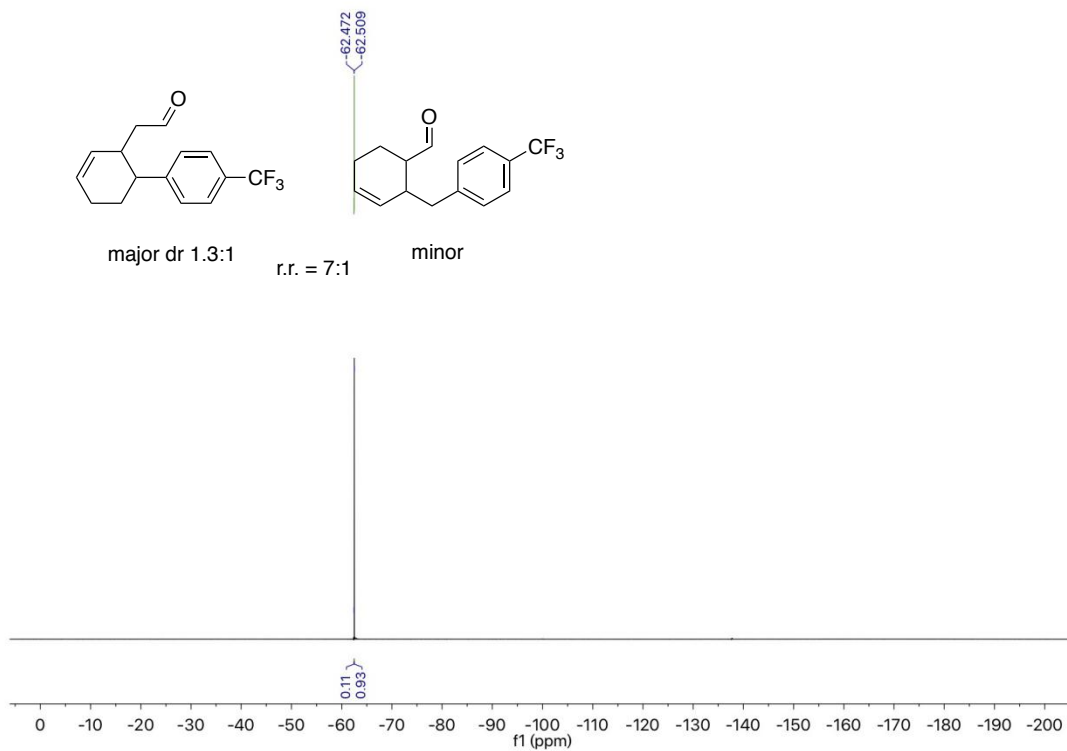
$^{19}\text{F}$  NMR spectrum (375 MHz,  $\text{CDCl}_3$ ) of **3d**



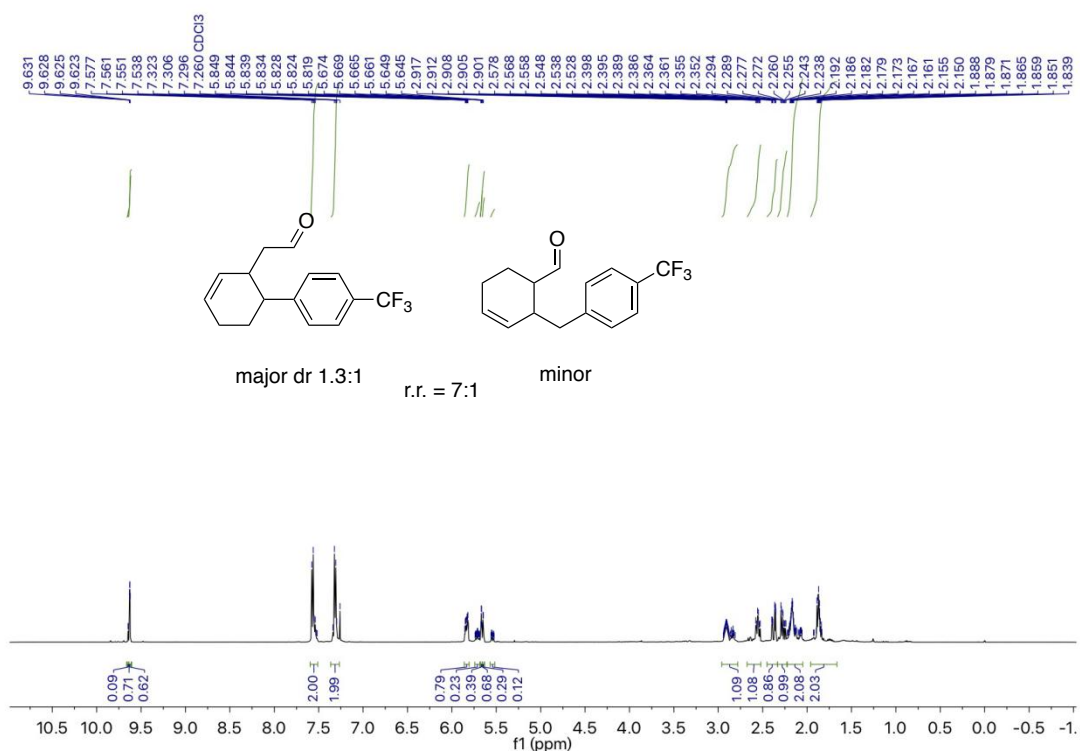
$^1\text{H}$  NMR spectrum (400 MHz,  $\text{CDCl}_3$ ) of **3d**



$^{13}\text{C}$  NMR spectrum (126 MHz,  $\text{CDCl}_3$ ) of **3d**

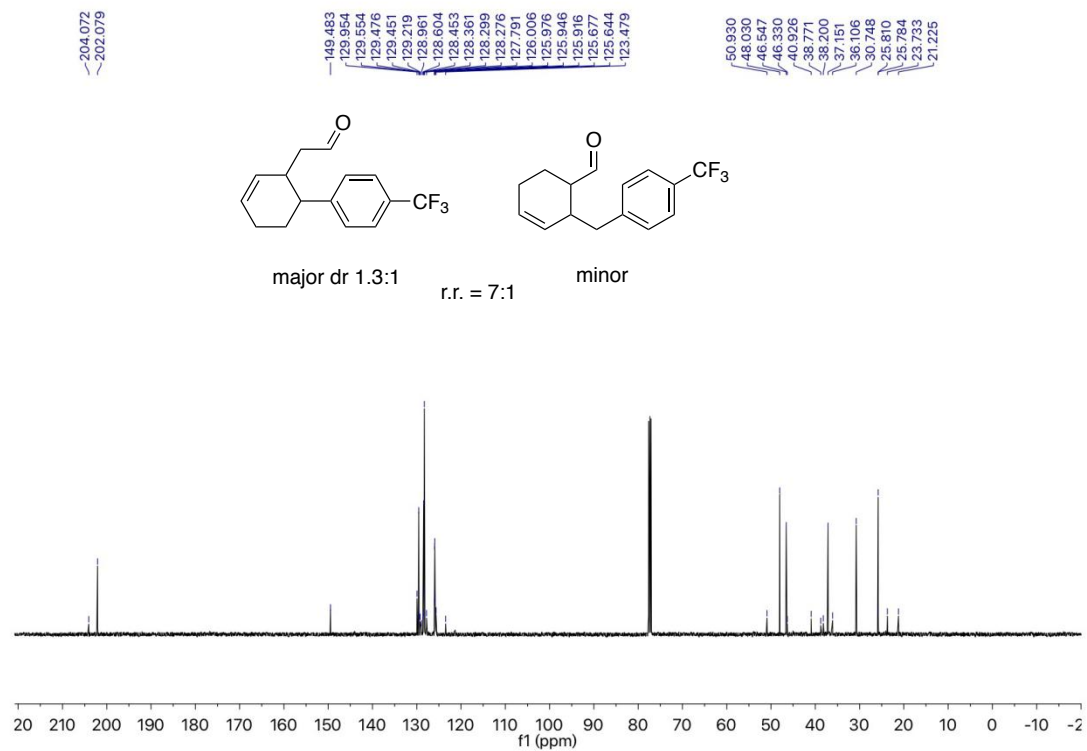


$^{19}\text{F}$  NMR spectrum (376 MHz,  $\text{CDCl}_3$ ) of **3e**

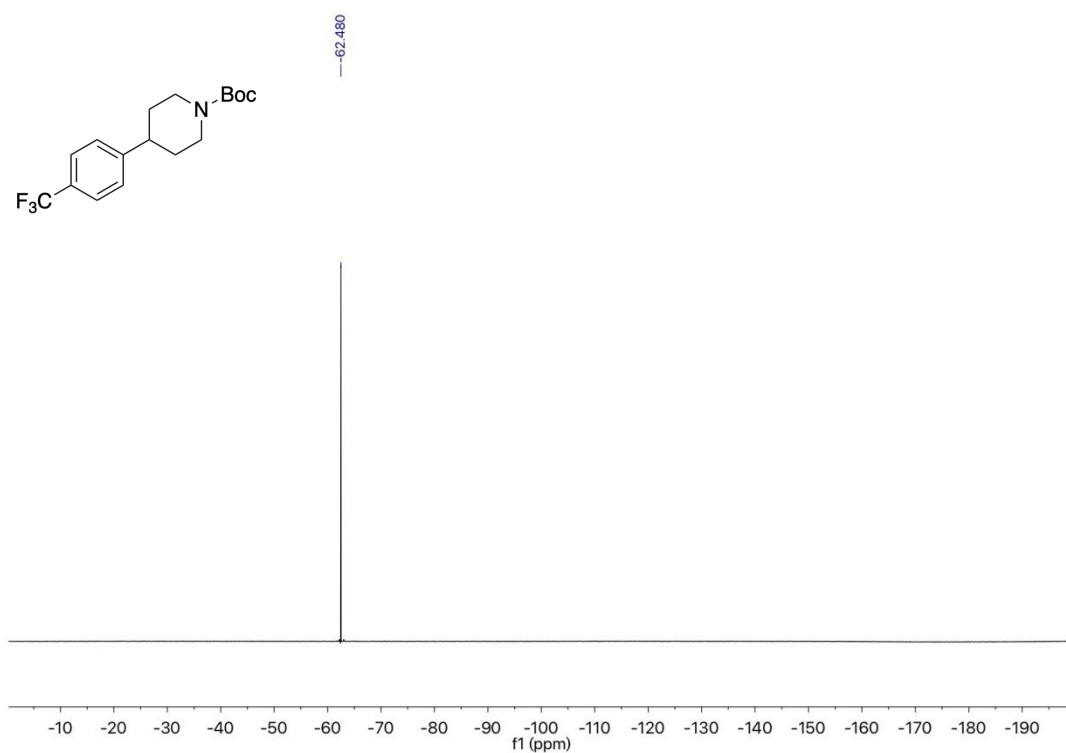


$^1\text{H}$  NMR spectrum (400 MHz,  $\text{CDCl}_3$ ) of **3e**

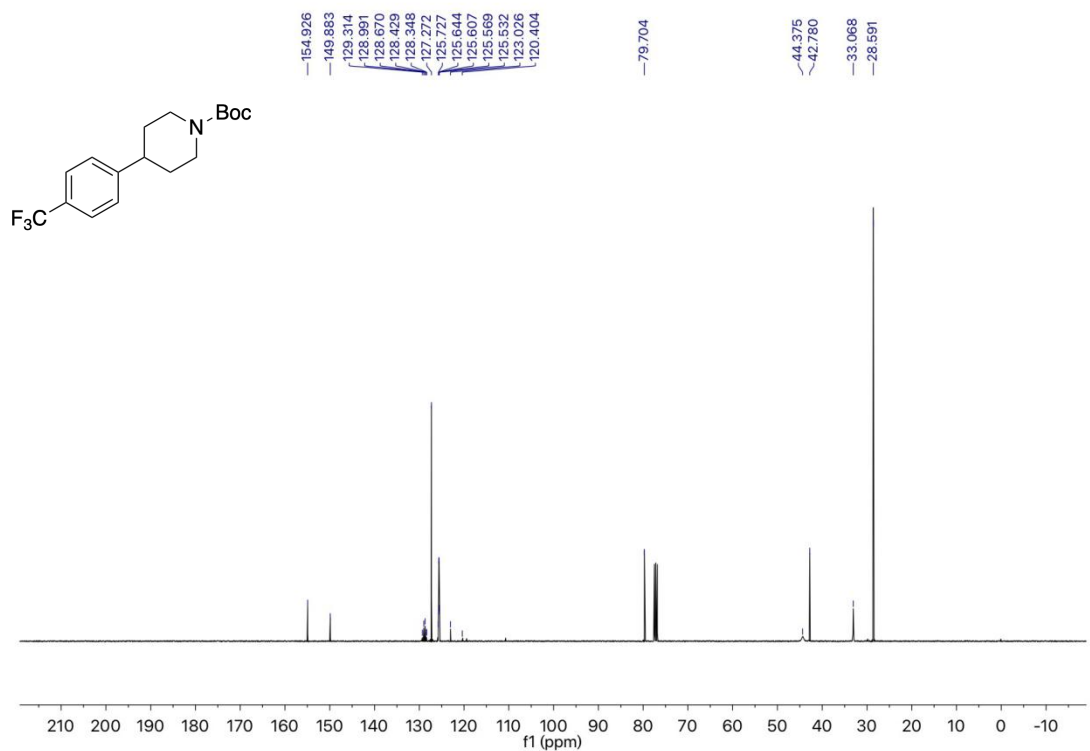
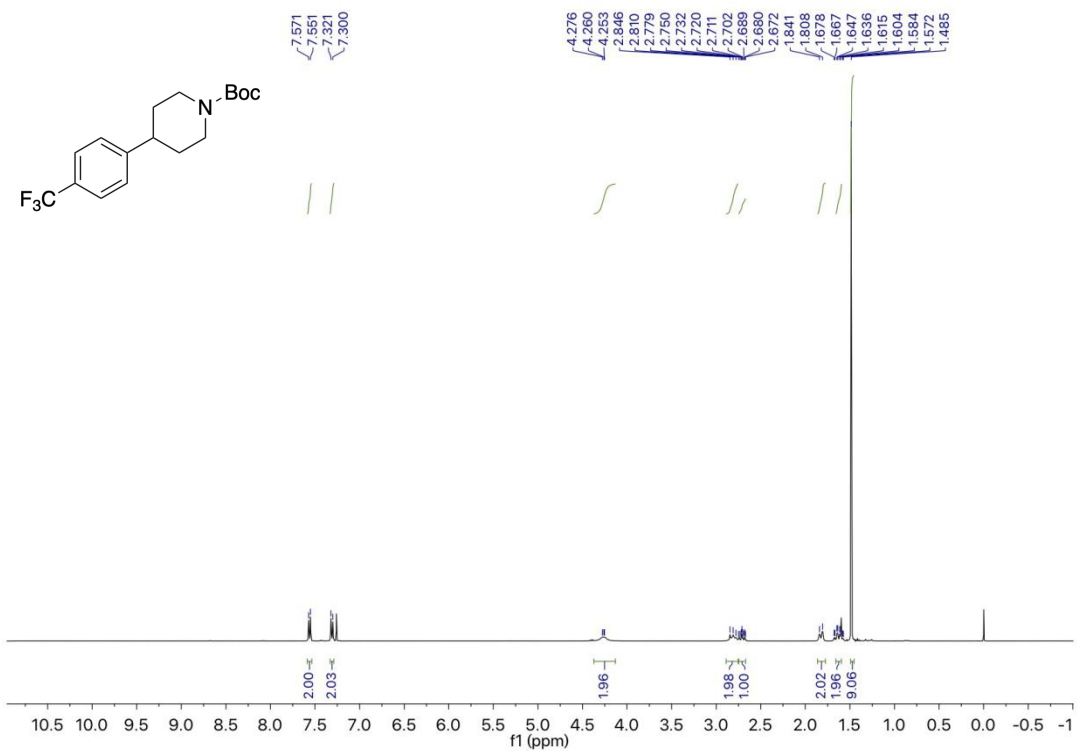


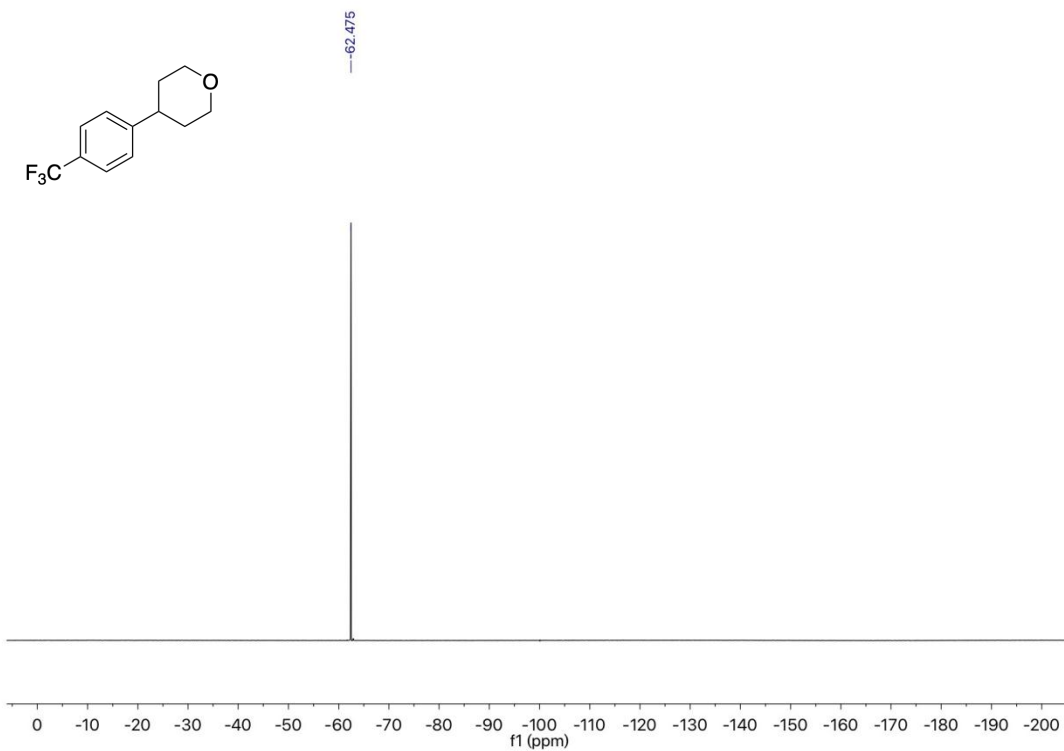


<sup>13</sup>C NMR spectrum (101 MHz, CDCl<sub>3</sub>) of **3e**

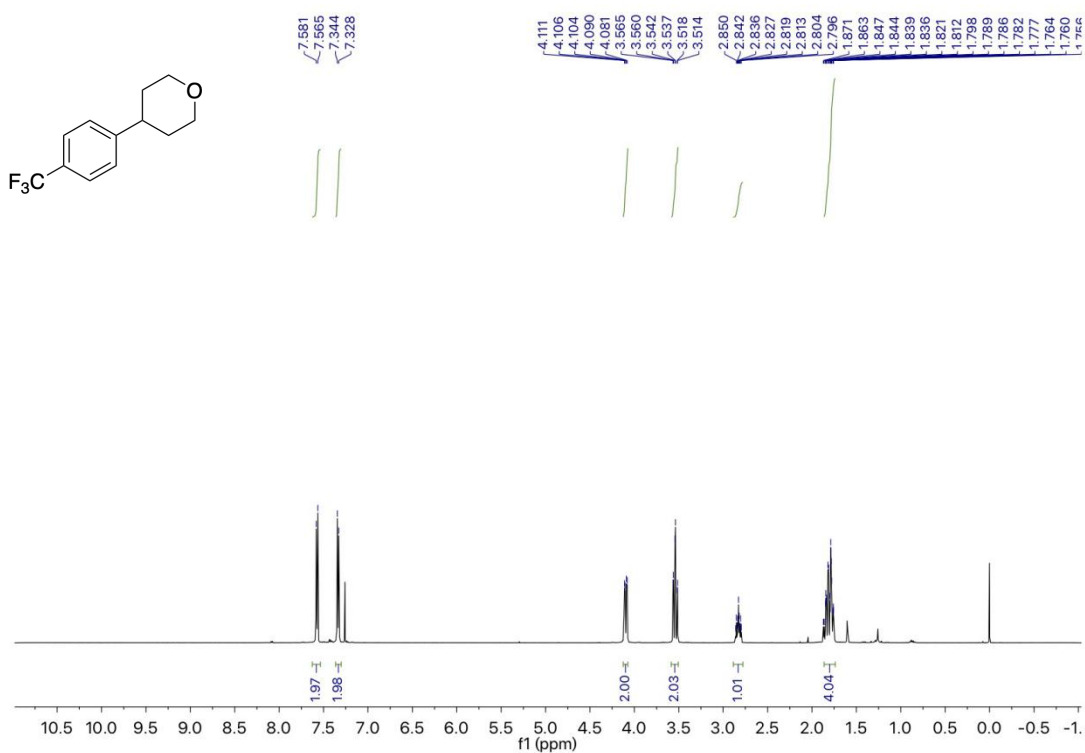


<sup>19</sup>F NMR spectrum (375 MHz, CDCl<sub>3</sub>) of **3f**

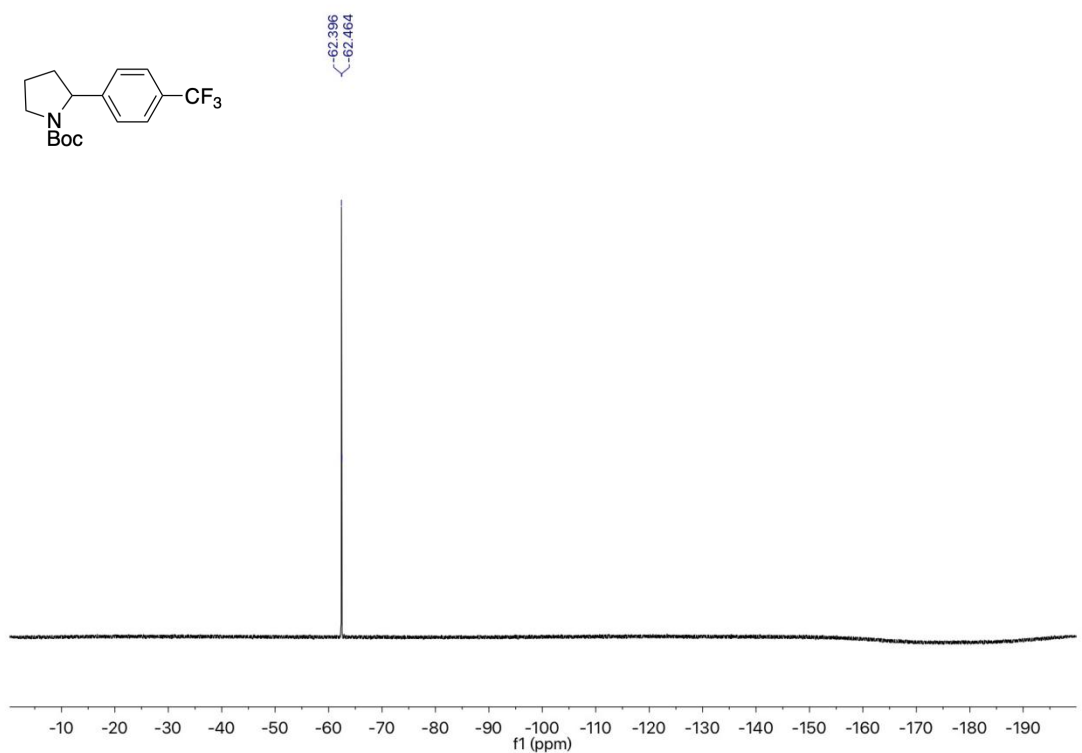
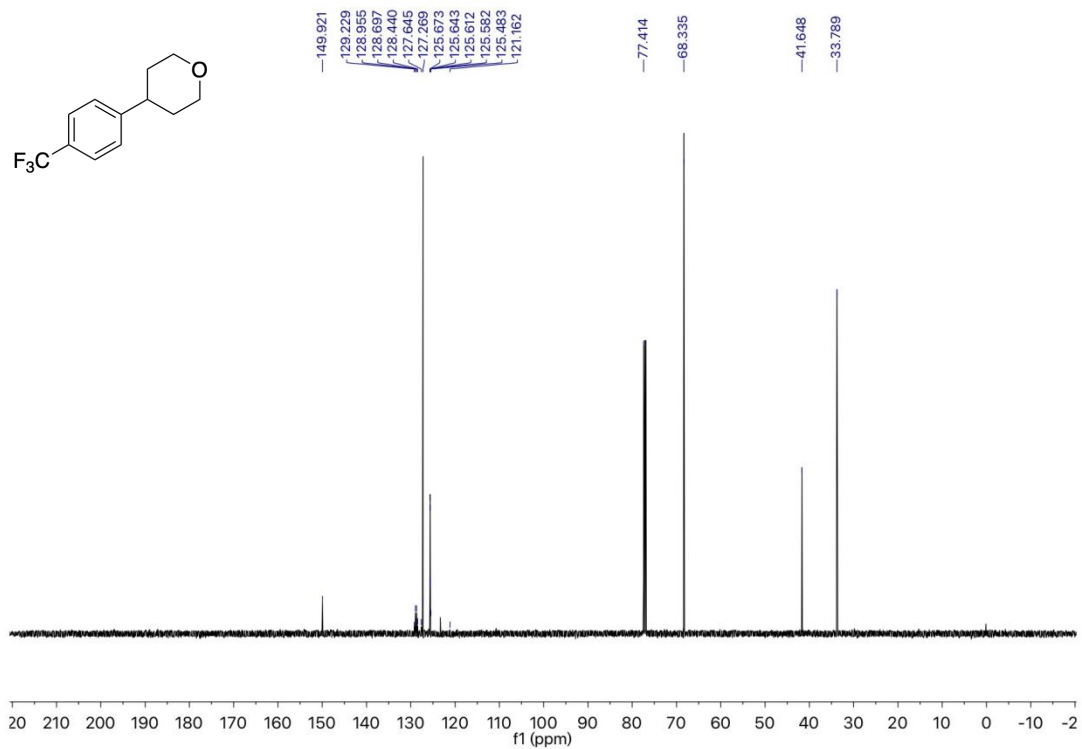


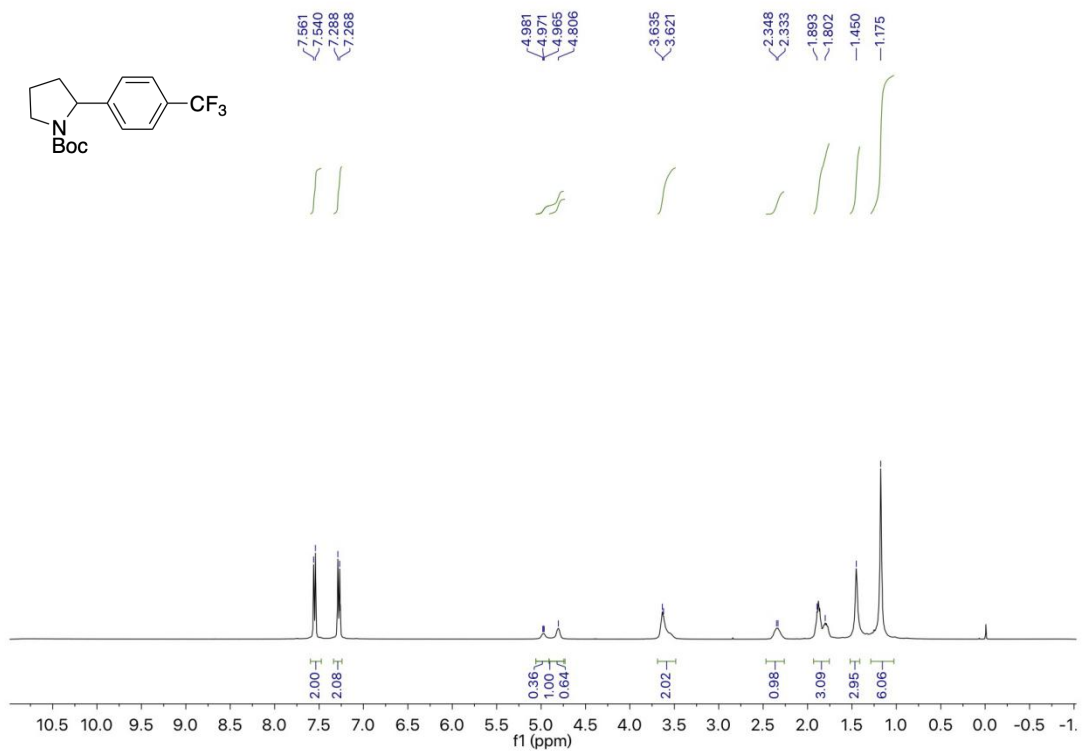


$^{19}\text{F}$  NMR spectrum (375 MHz,  $\text{CDCl}_3$ ) of **3g**

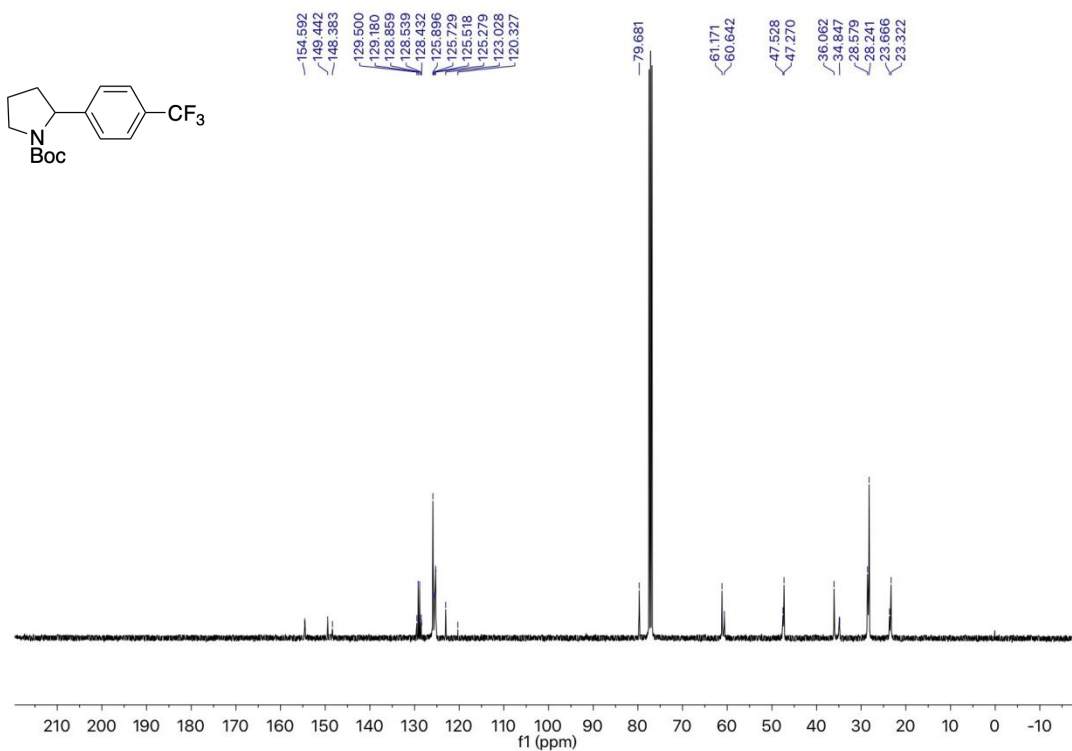


$^1\text{H}$  NMR spectrum (400 MHz,  $\text{CDCl}_3$ ) of **3g**

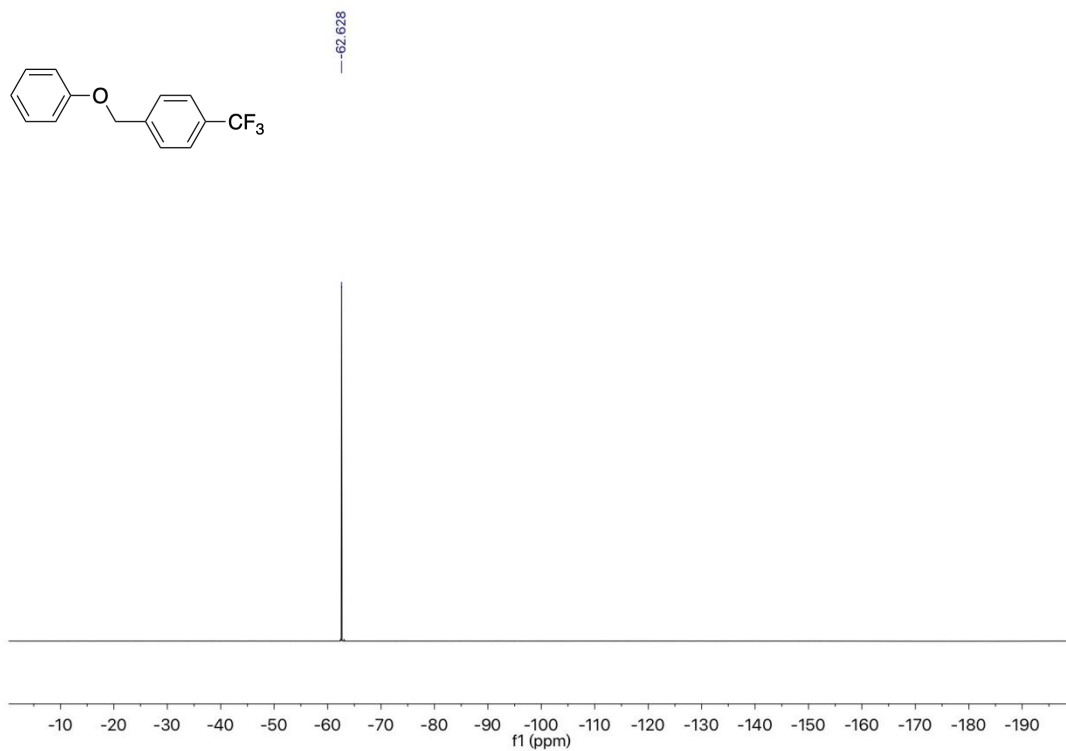




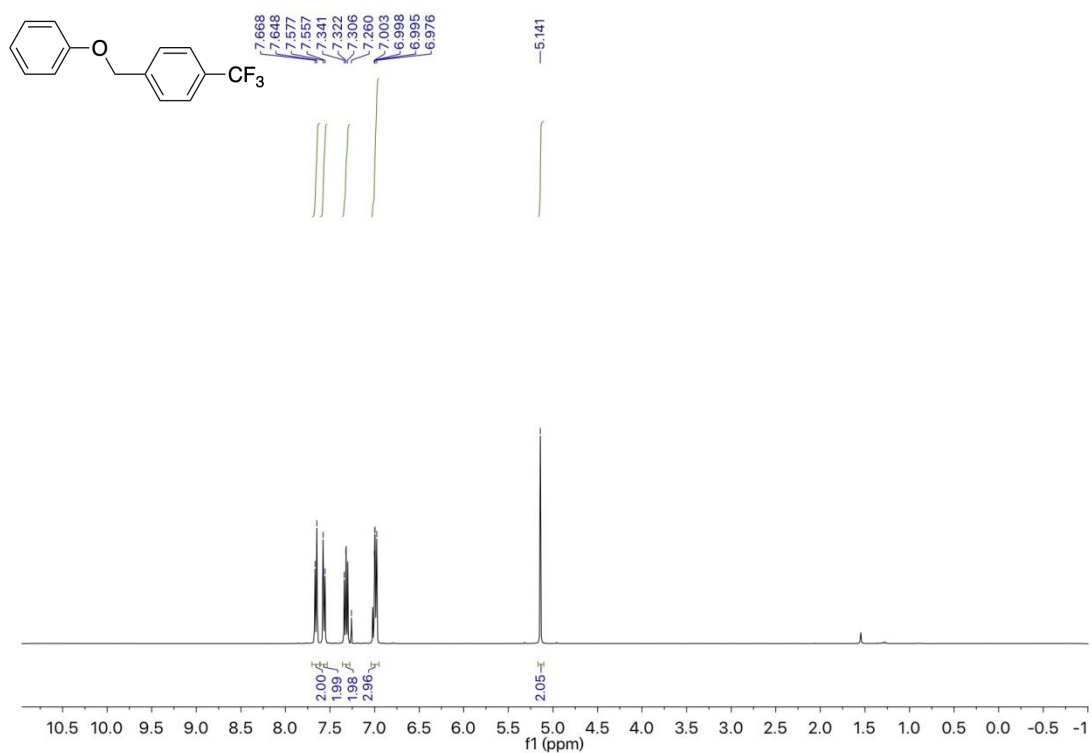
<sup>1</sup>H NMR spectrum (400 MHz, CDCl<sub>3</sub>) of **3h**



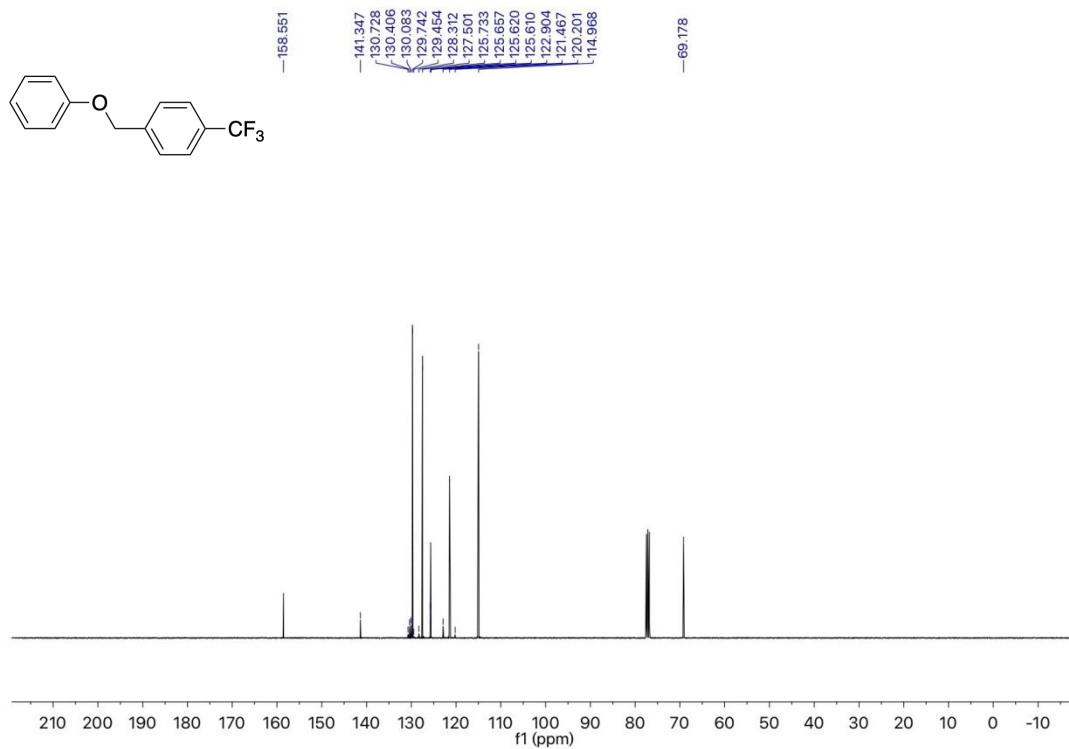
<sup>13</sup>C NMR spectrum (101 MHz, CDCl<sub>3</sub>) of **3h**



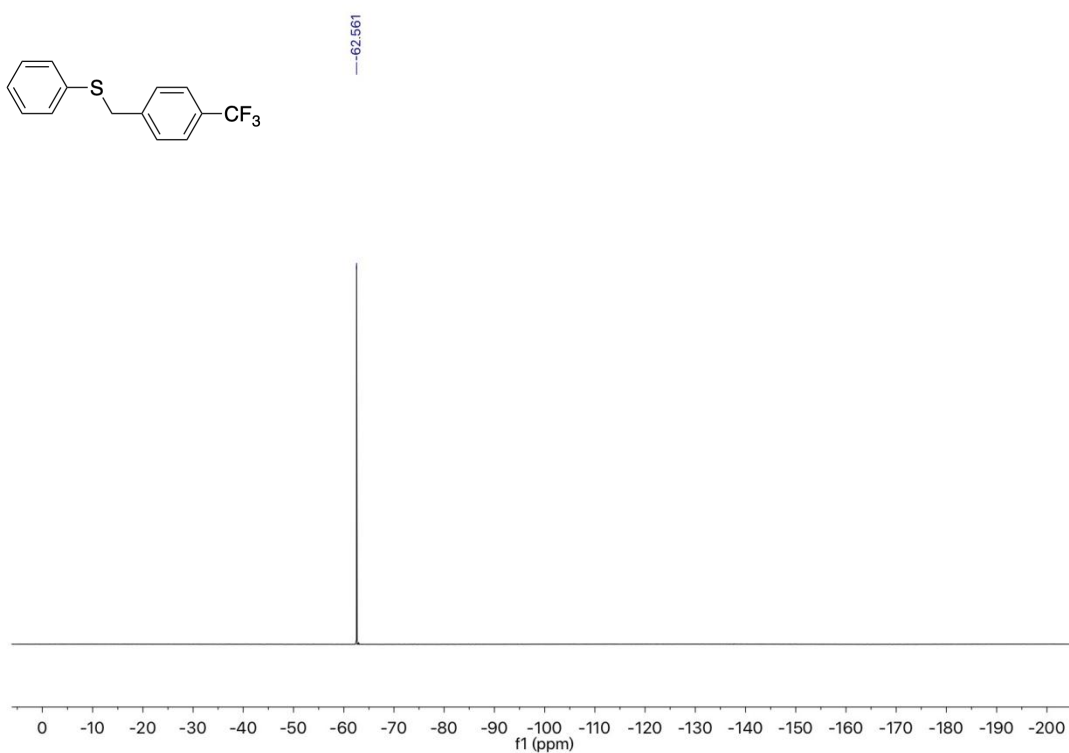
$^{19}\text{F}$  NMR spectrum (375 MHz,  $\text{CDCl}_3$ ) of **3i**



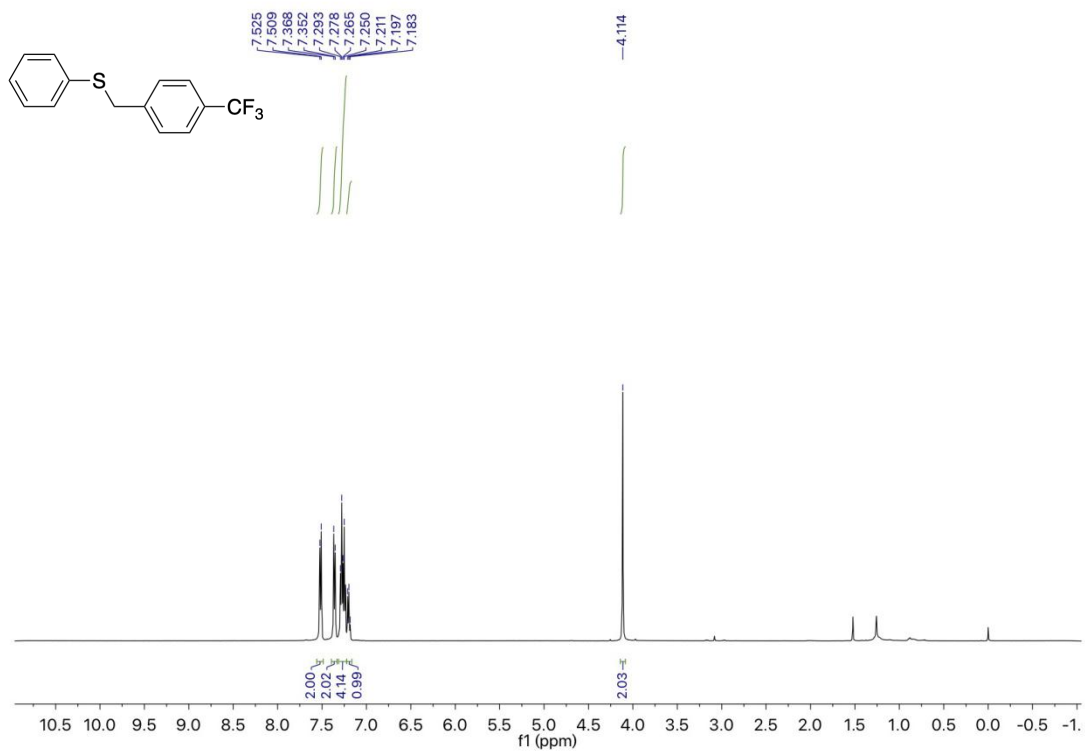
$^1\text{H}$  NMR spectrum (500 MHz,  $\text{CDCl}_3$ ) of **3i**



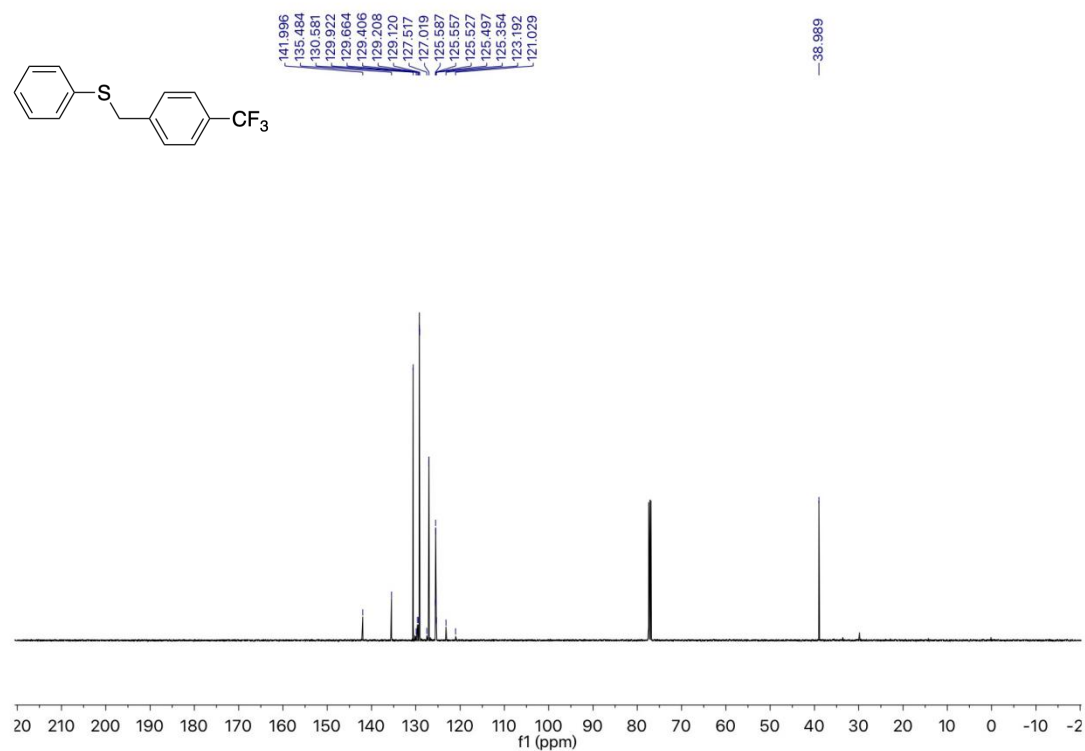
$^{13}\text{C}$  NMR spectrum (126 MHz,  $\text{CDCl}_3$ ) of **3i**



$^{19}\text{F}$  NMR spectrum (375 MHz,  $\text{CDCl}_3$ ) of **3j**

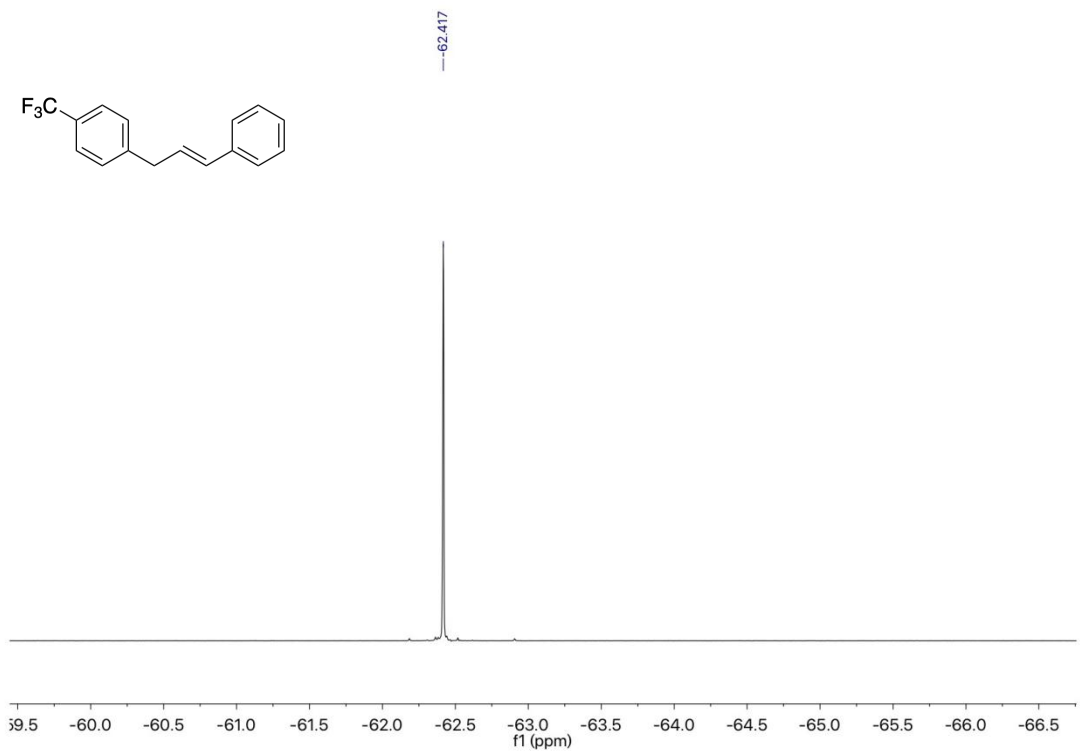


<sup>1</sup>H NMR spectrum (500 MHz, CDCl<sub>3</sub>) of **3i**

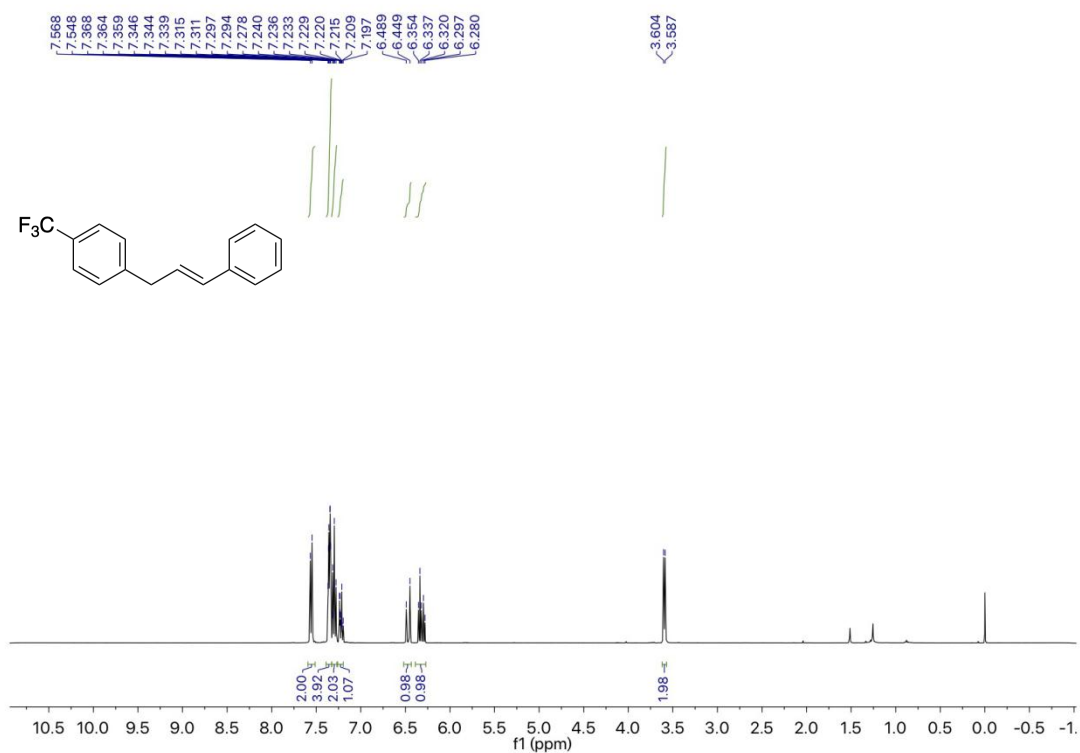


<sup>13</sup>C NMR spectrum (126 MHz, CDCl<sub>3</sub>) of **3j**

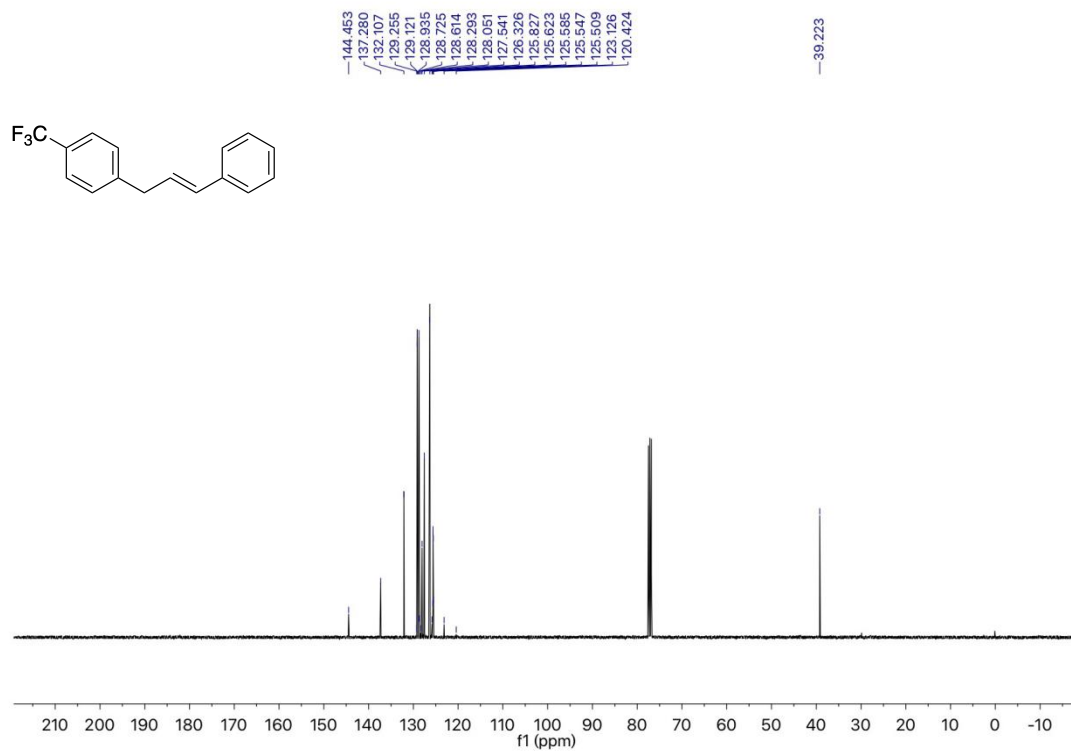




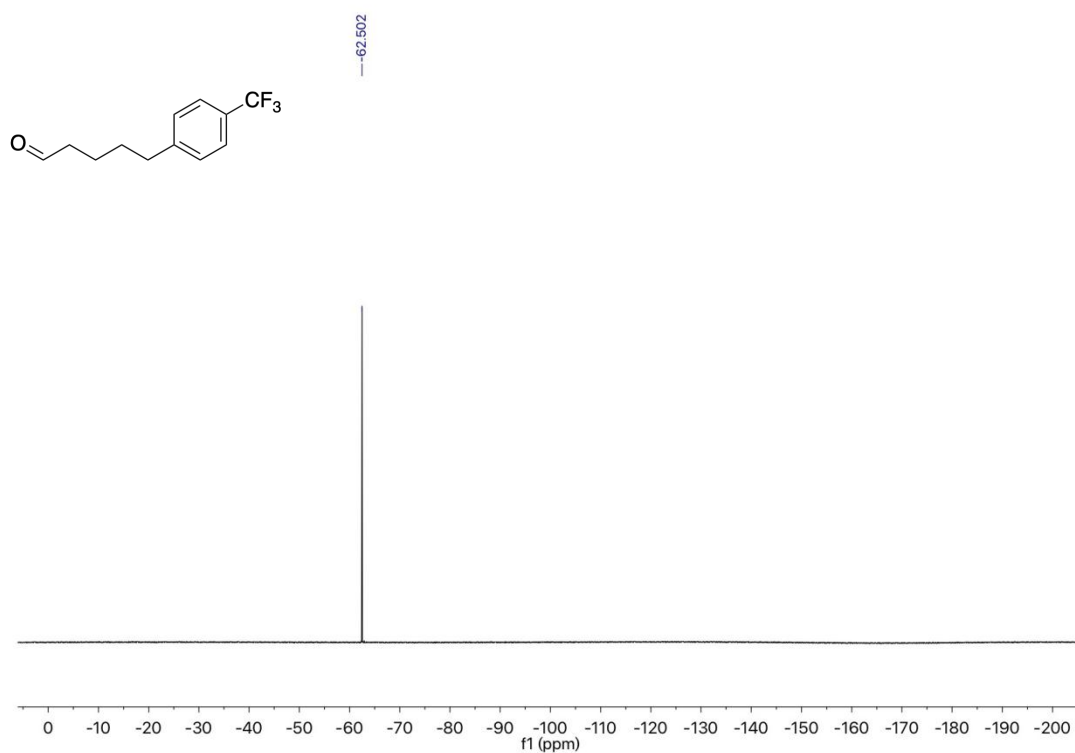
$^{19}\text{F}$  NMR spectrum (375 MHz,  $\text{CDCl}_3$ ) of **3k**



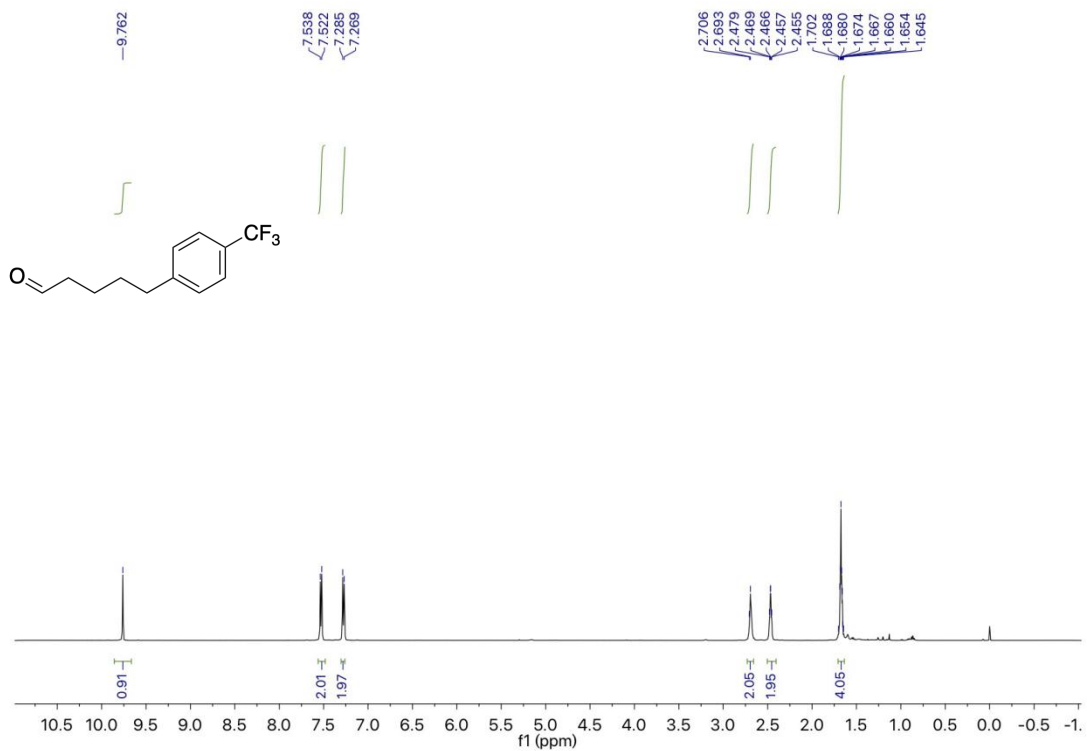
$^1\text{H}$  NMR spectrum (500 MHz,  $\text{CDCl}_3$ ) of **3k**



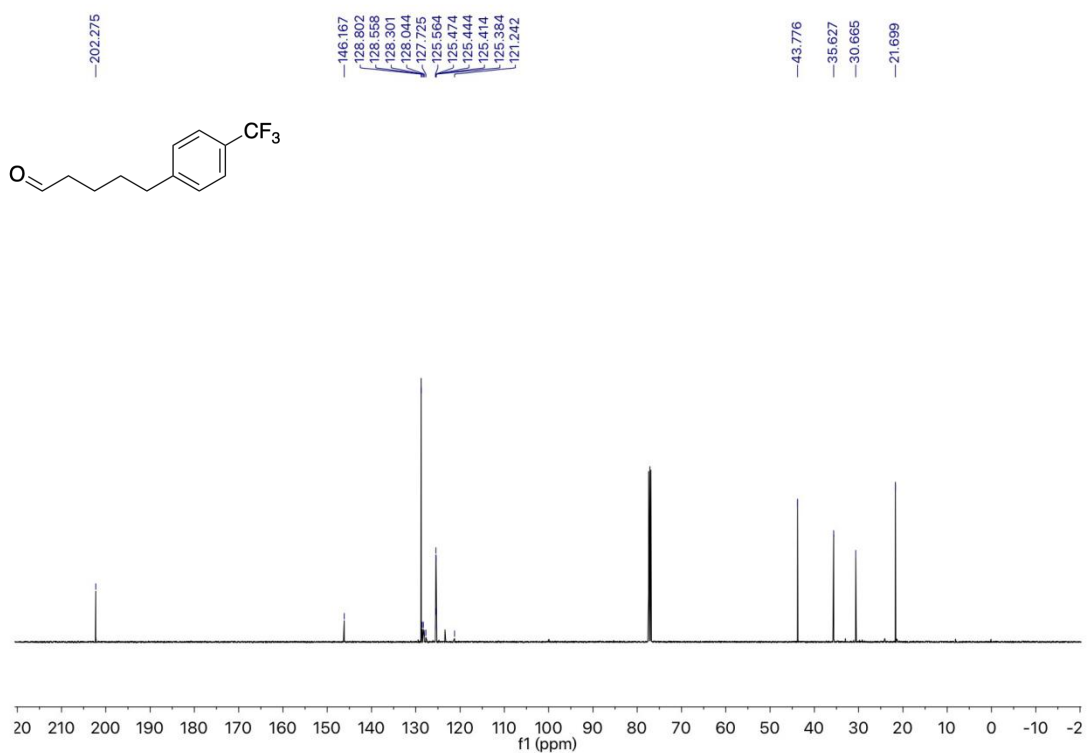
<sup>13</sup>C NMR spectrum (126 MHz, CDCl<sub>3</sub>) of **3k**



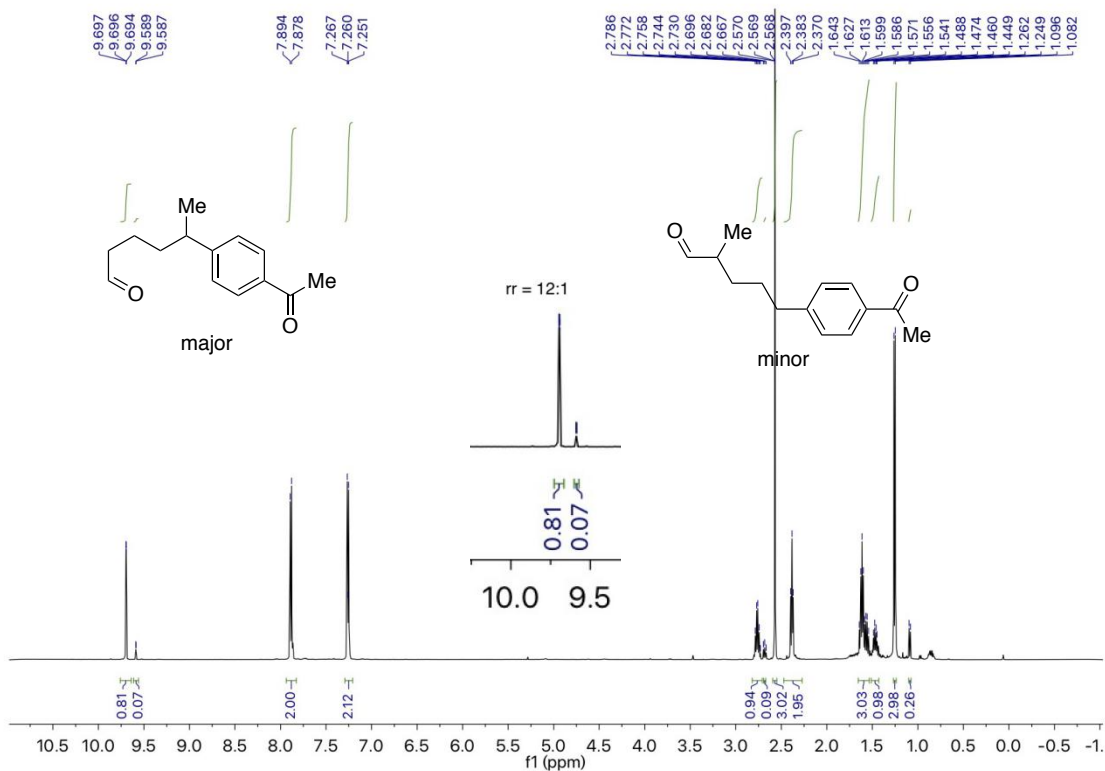
<sup>19</sup>F NMR spectrum (375 MHz, CDCl<sub>3</sub>) of **3l**



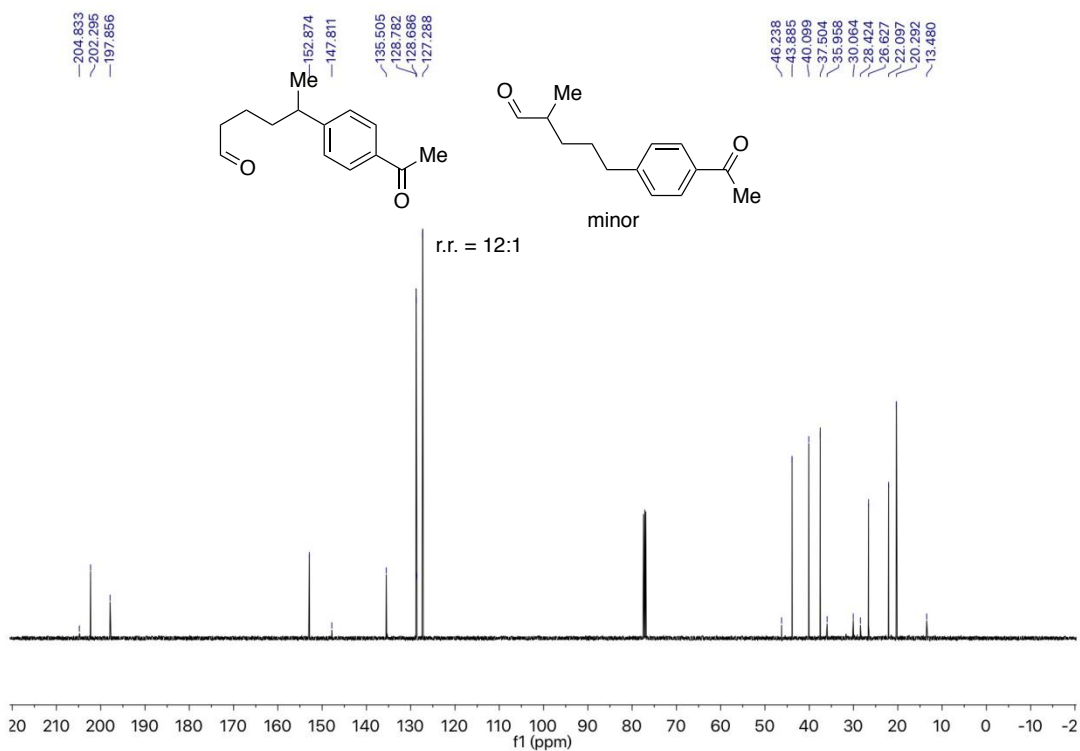
<sup>1</sup>H NMR spectrum (400 MHz, CDCl<sub>3</sub>) of **3I**



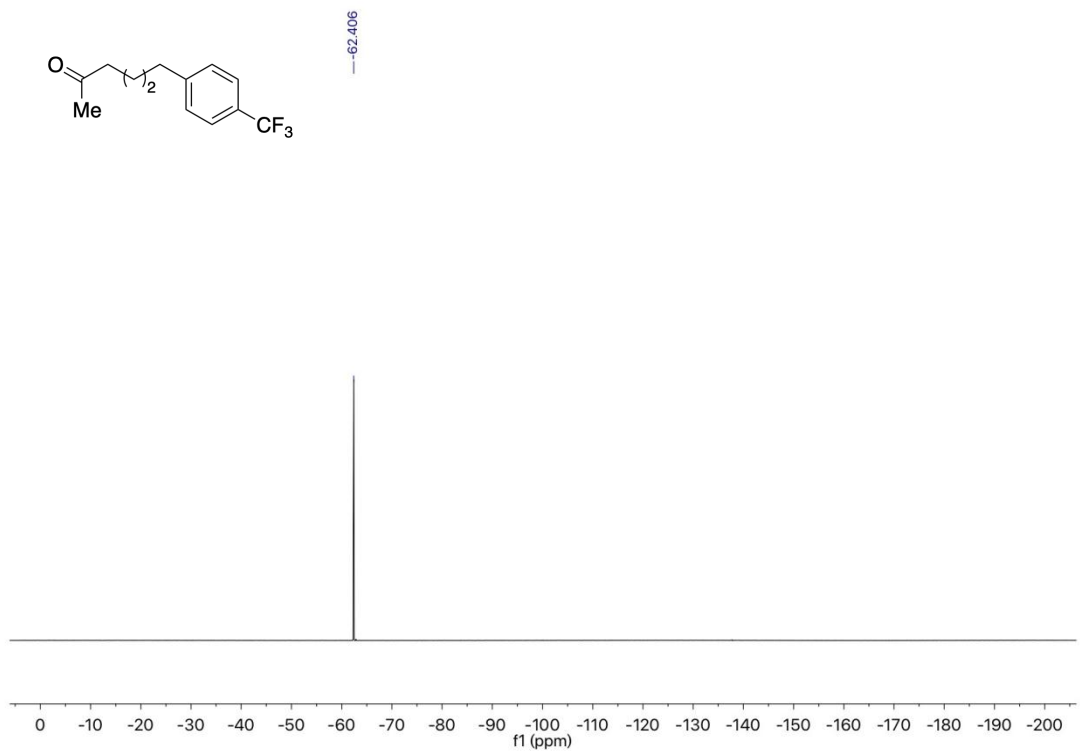
<sup>13</sup>C NMR spectrum (101 MHz, CDCl<sub>3</sub>) of **3I**



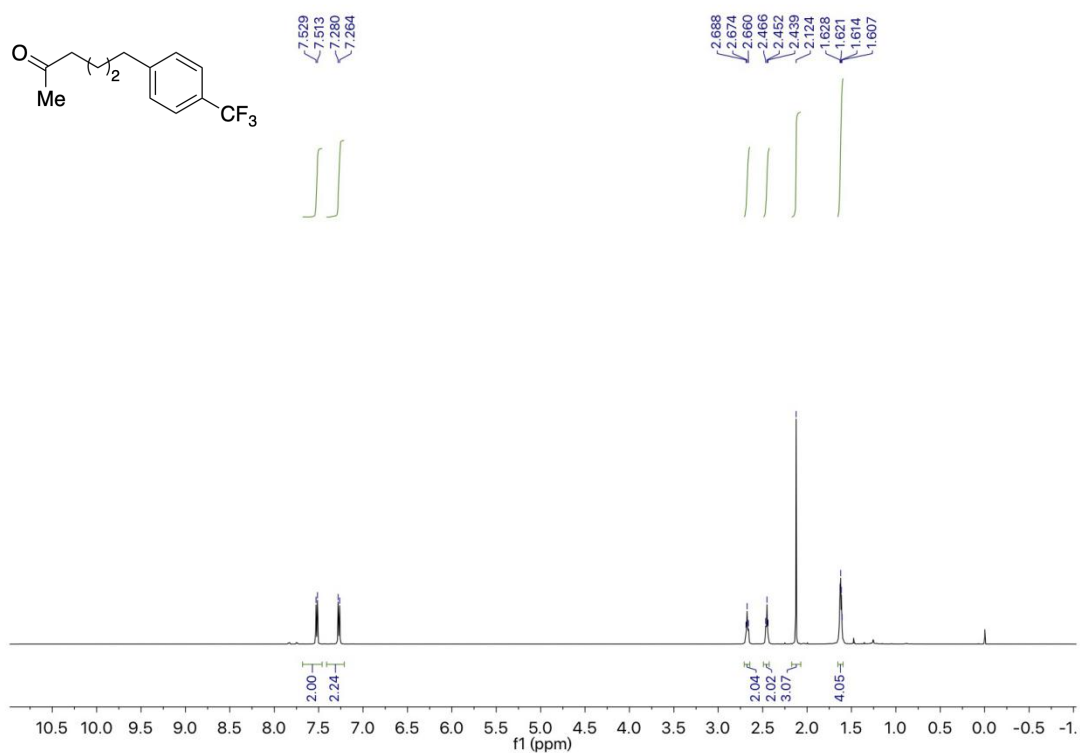
**<sup>1</sup>H NMR spectrum (400 MHz, CDCl<sub>3</sub>) of **3m****



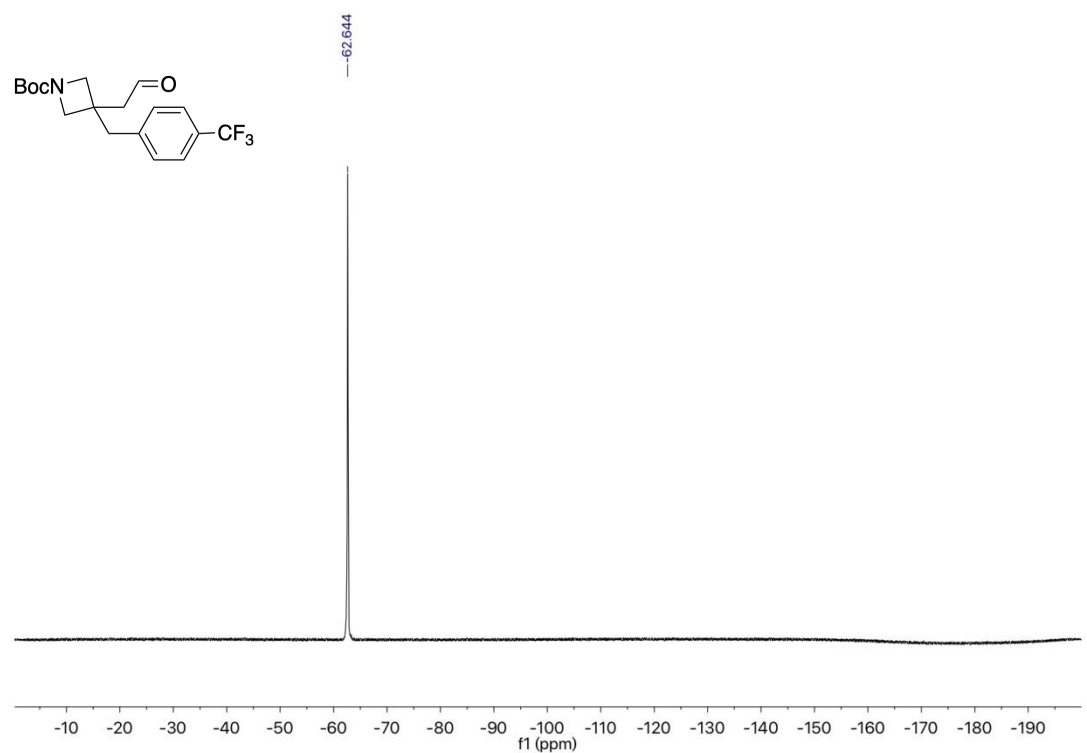
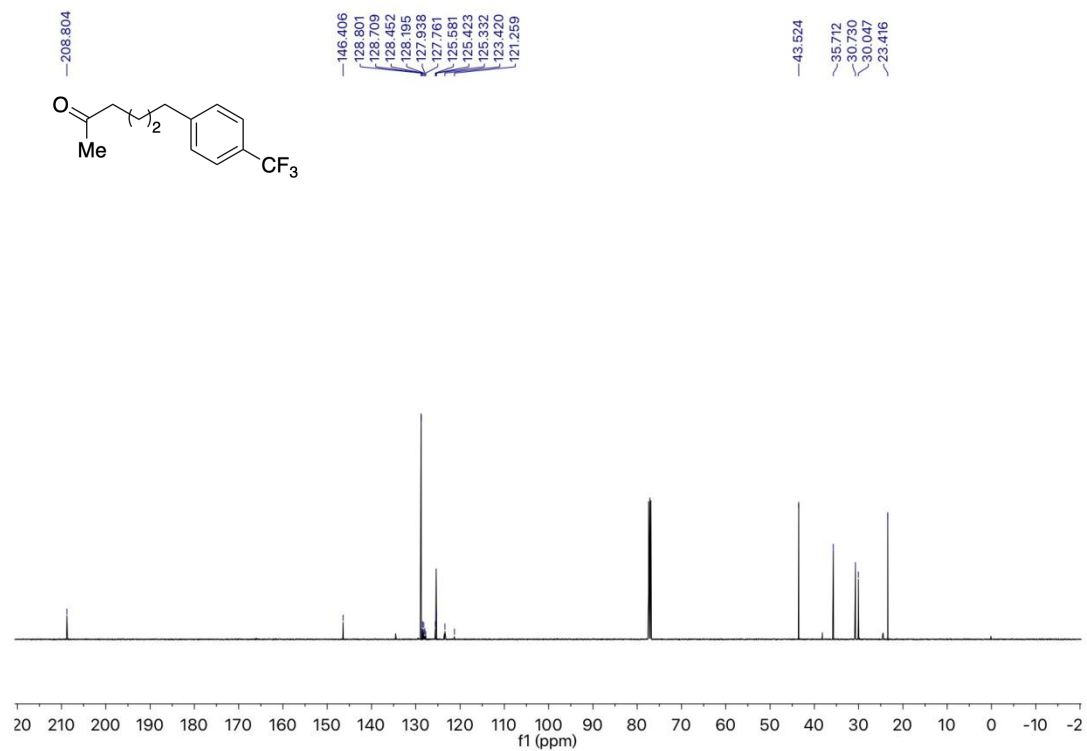
**<sup>13</sup>C NMR spectrum (101 MHz, CDCl<sub>3</sub>) of **3m****

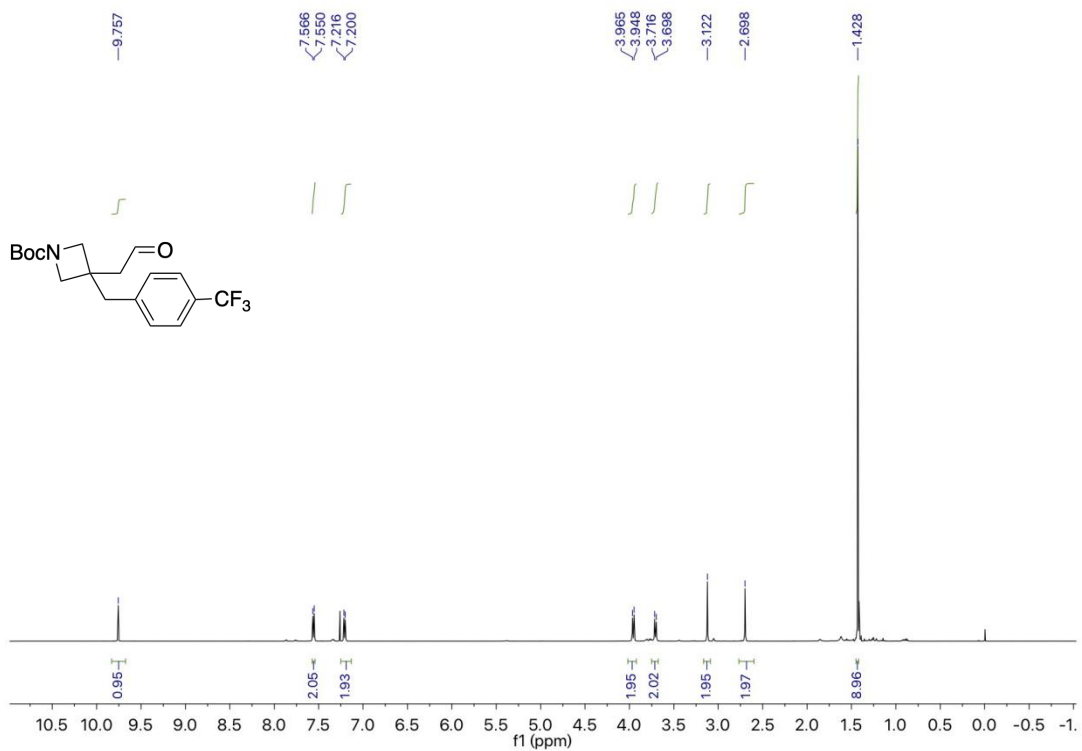


$^{19}\text{F}$  NMR spectrum (375 MHz,  $\text{CDCl}_3$ ) of **3n**

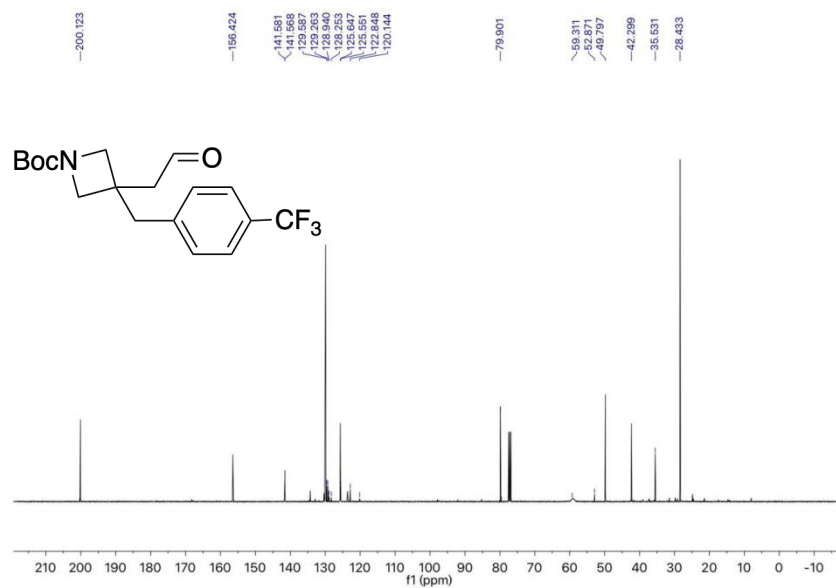


$^1\text{H}$  NMR spectrum (500 MHz,  $\text{CDCl}_3$ ) of **3n**

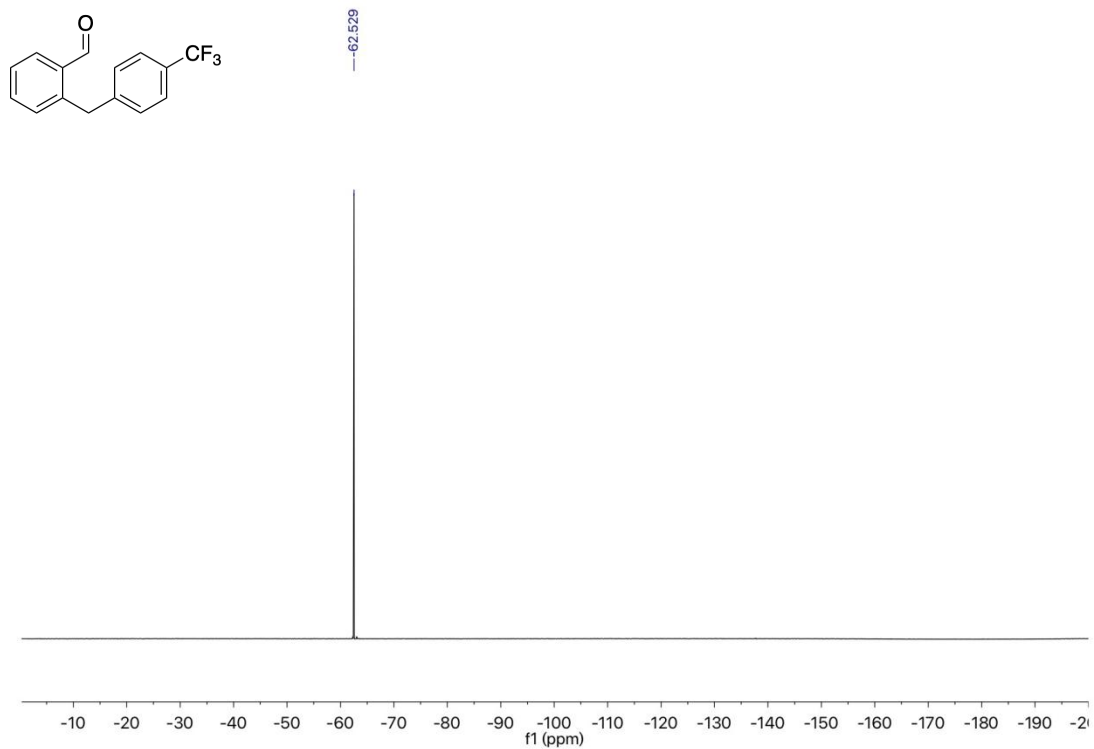




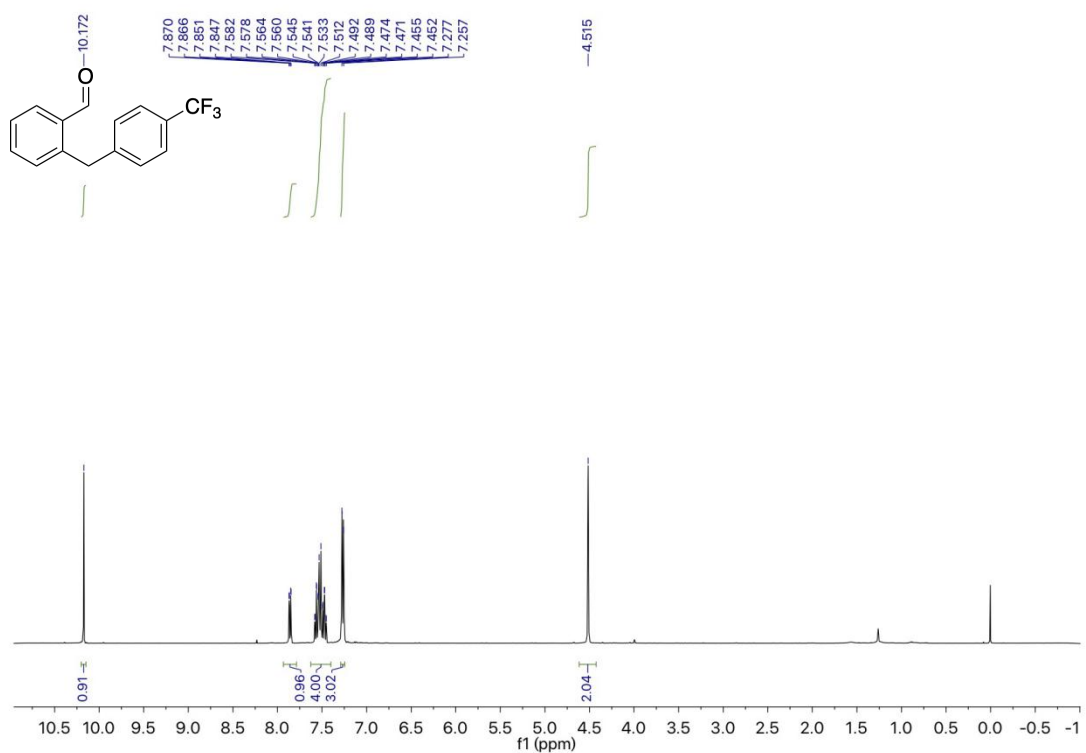
<sup>1</sup>H NMR spectrum (400 MHz, CDCl<sub>3</sub>) of **3o**



<sup>13</sup>C NMR spectrum (101 MHz, CDCl<sub>3</sub>) of **3o**

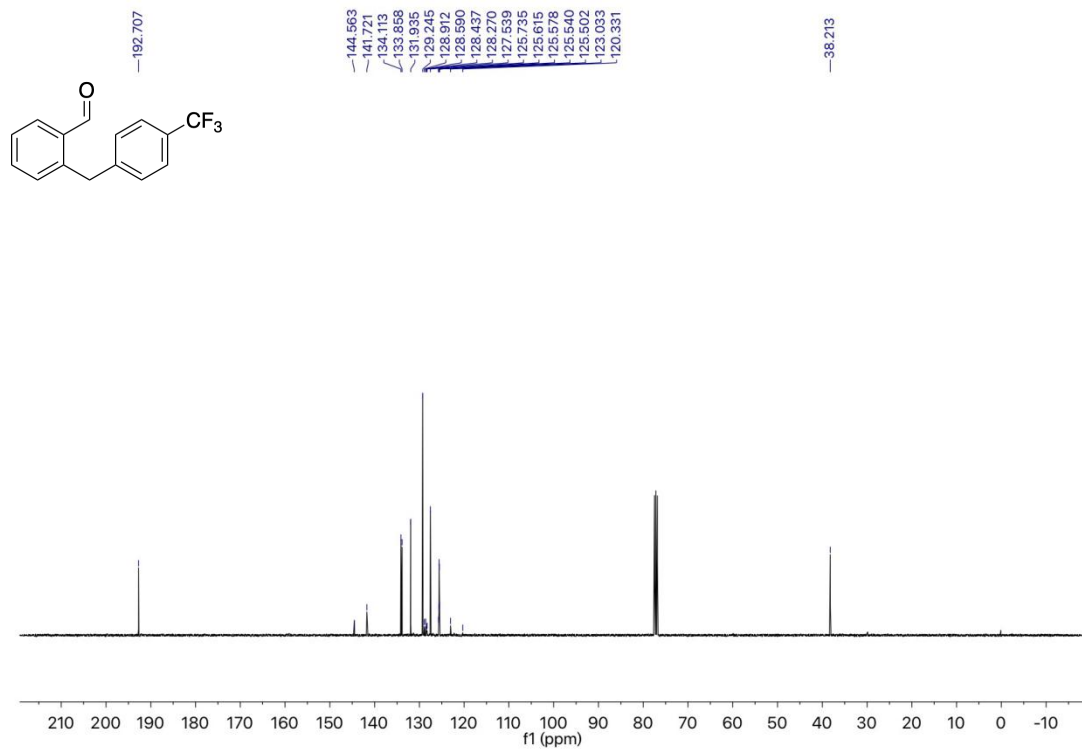


$^{19}\text{F}$  NMR spectrum (375 MHz,  $\text{CDCl}_3$ ) of **3p**

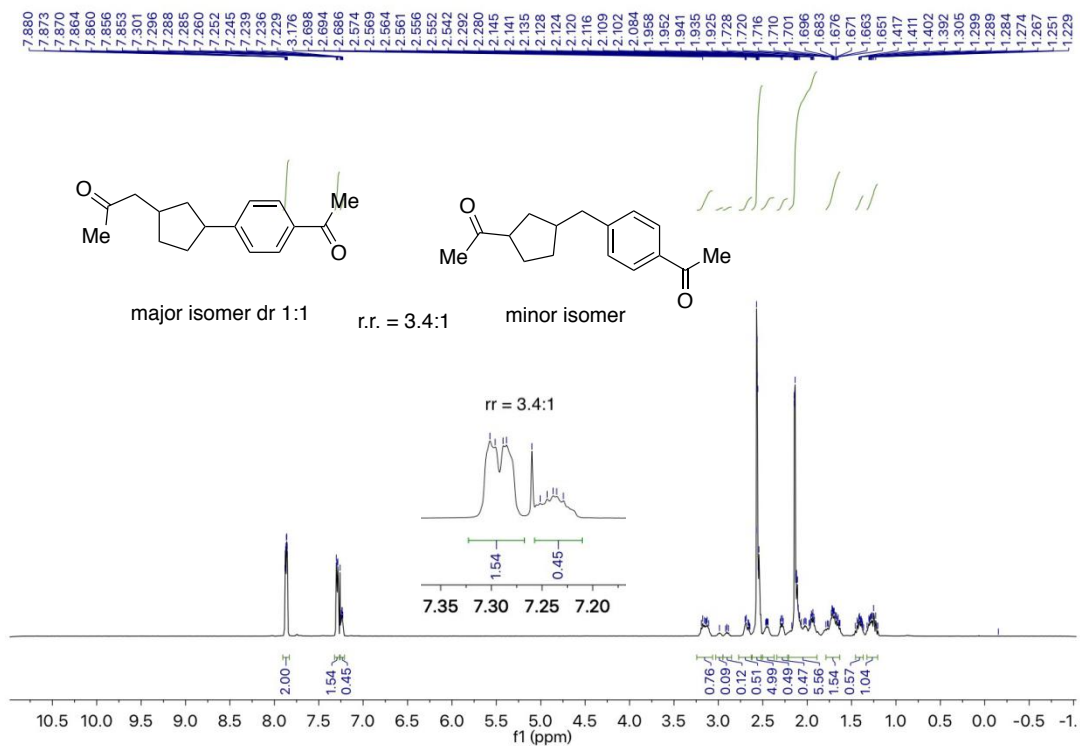


$^1\text{H}$  NMR spectrum (400 MHz,  $\text{CDCl}_3$ ) of **3p**

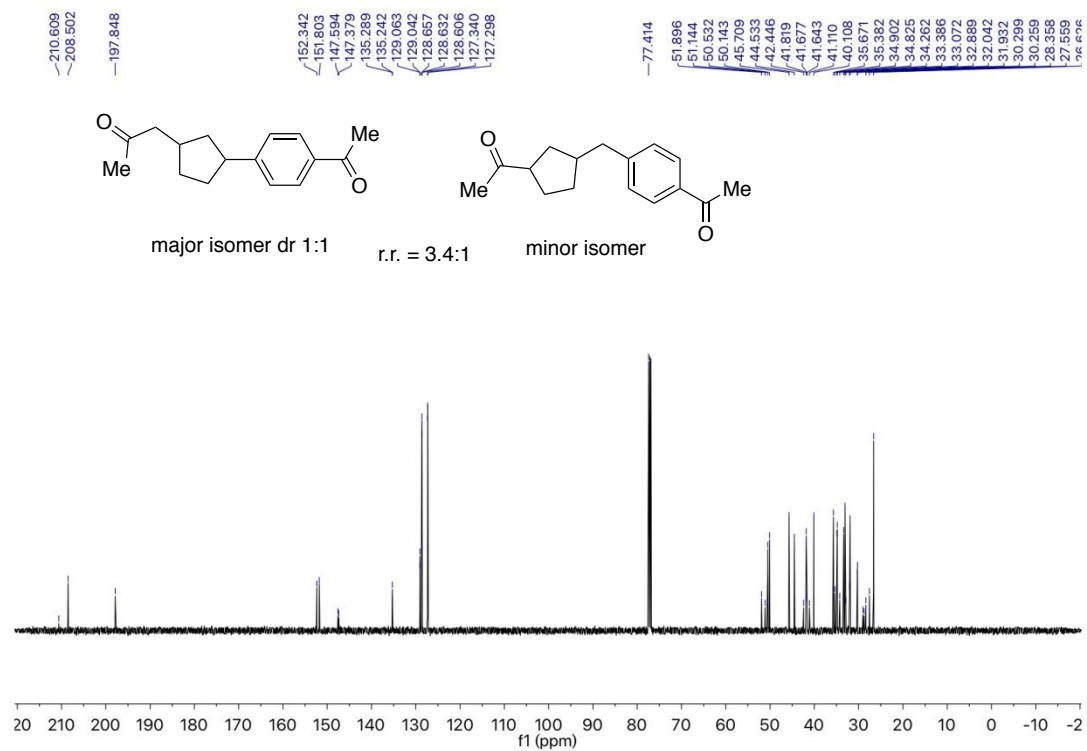




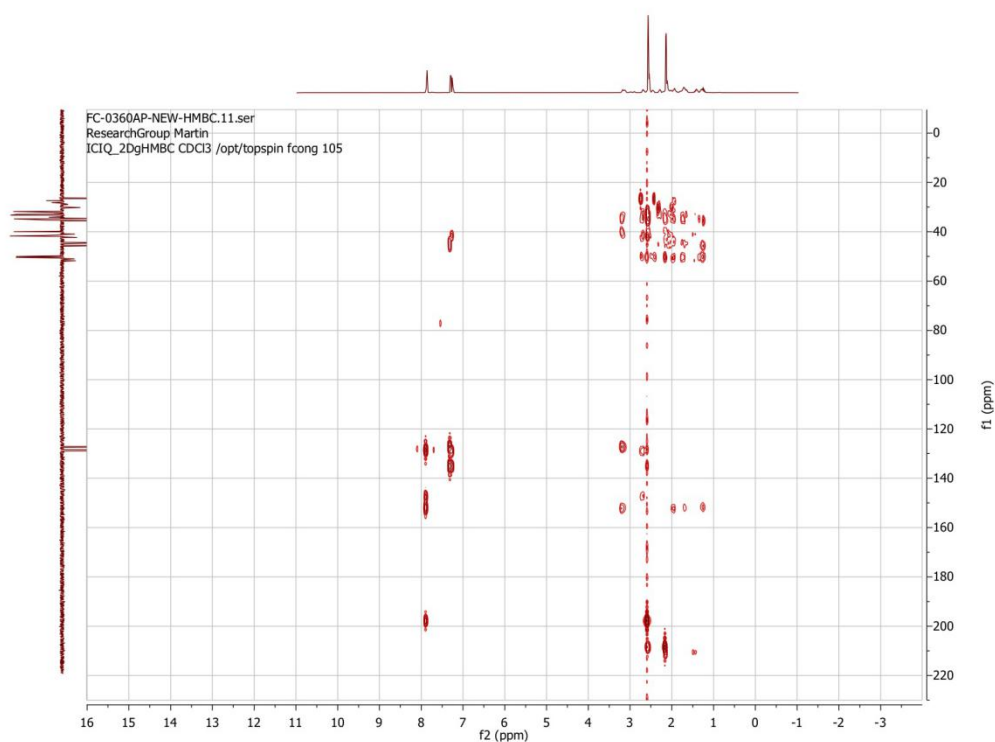
<sup>13</sup>C NMR spectrum (101 MHz, CDCl<sub>3</sub>) of **3p**



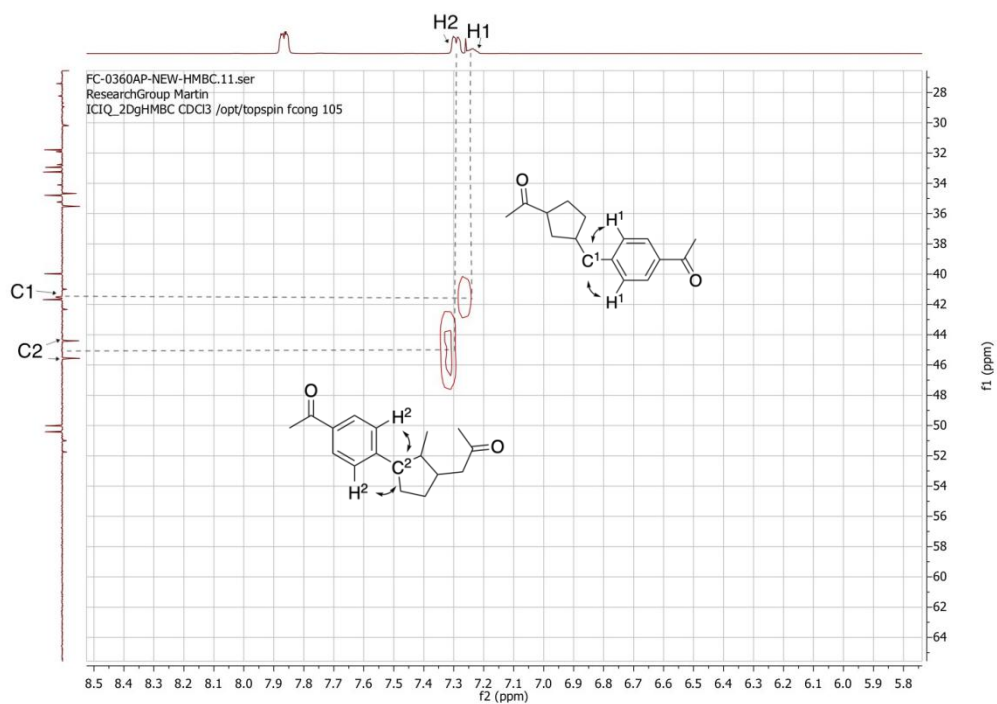
<sup>1</sup>H NMR spectrum (400 MHz, CDCl<sub>3</sub>) of **3q**



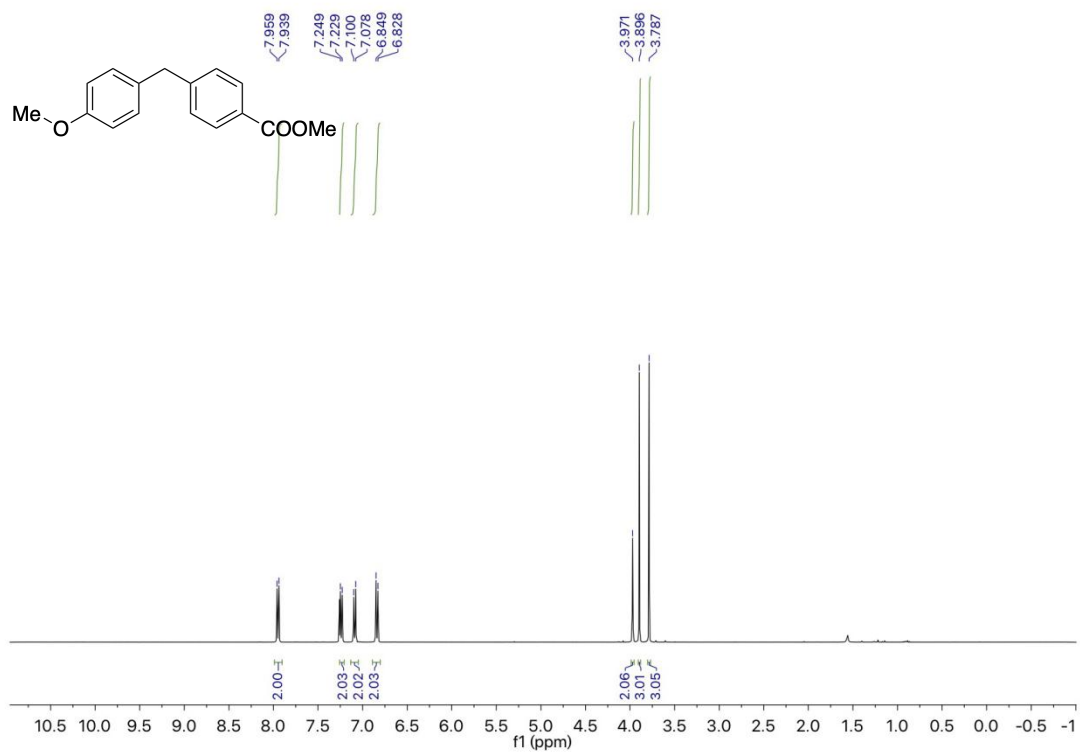
$^{13}\text{C}$  NMR spectrum (101 MHz,  $\text{CDCl}_3$ ) of **3q**



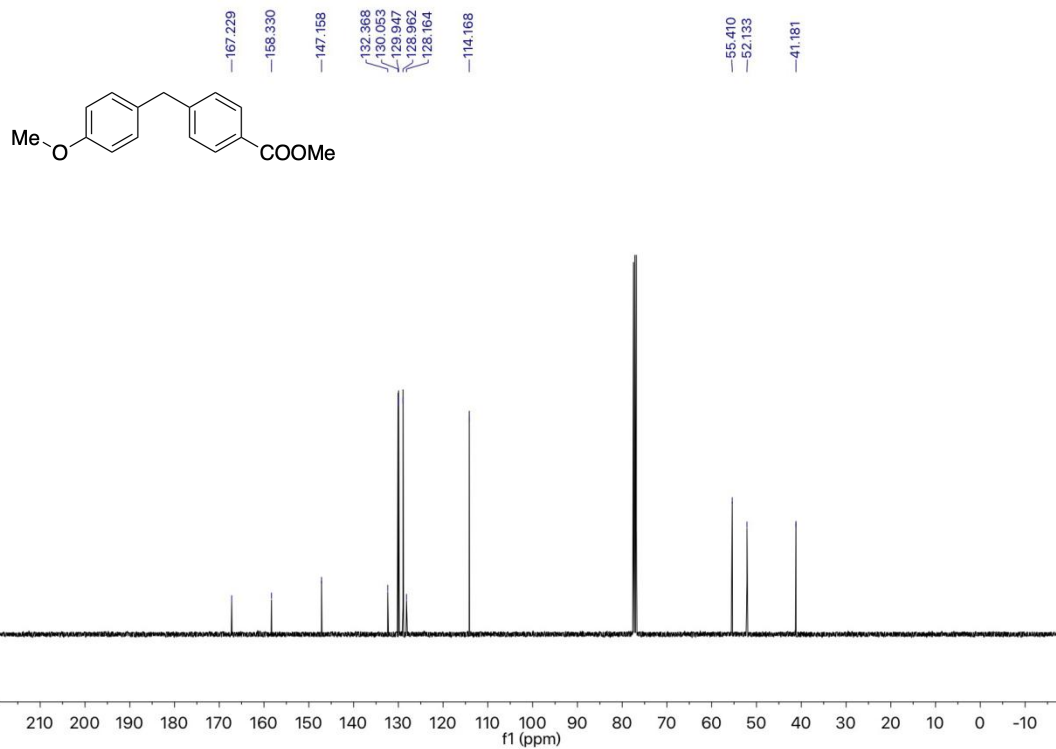
HMBC spectrum ( $\text{CDCl}_3$ ) of **3q**



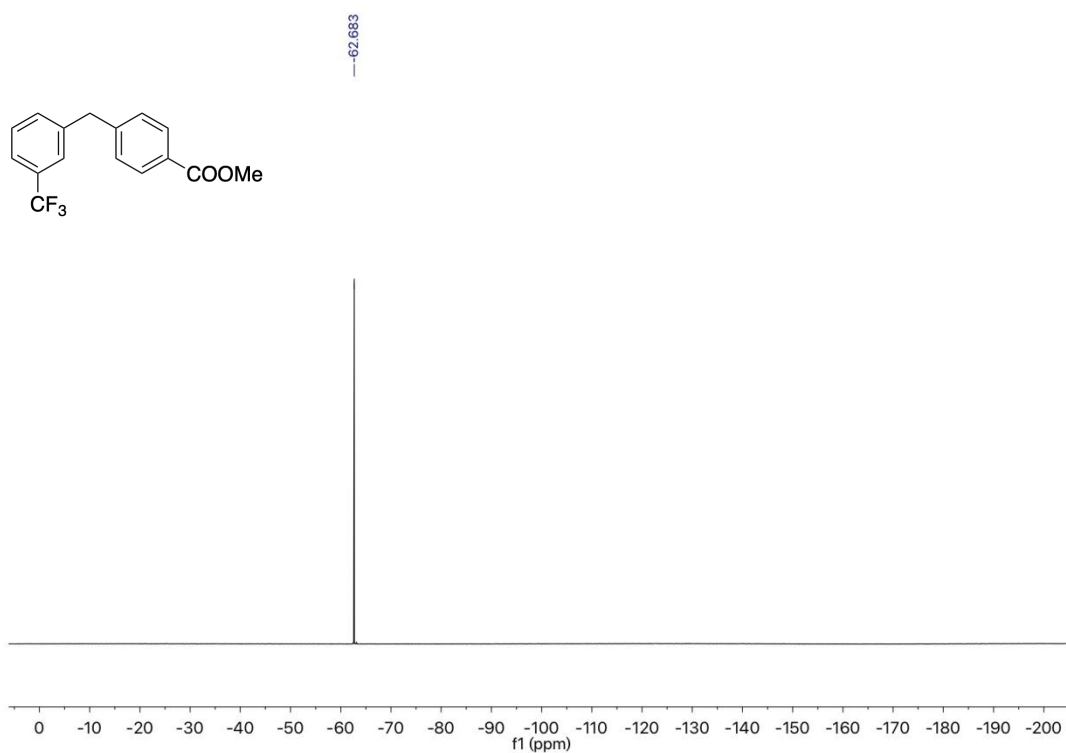
HMBC spectrum ( CDCl<sub>3</sub>) of **3q**



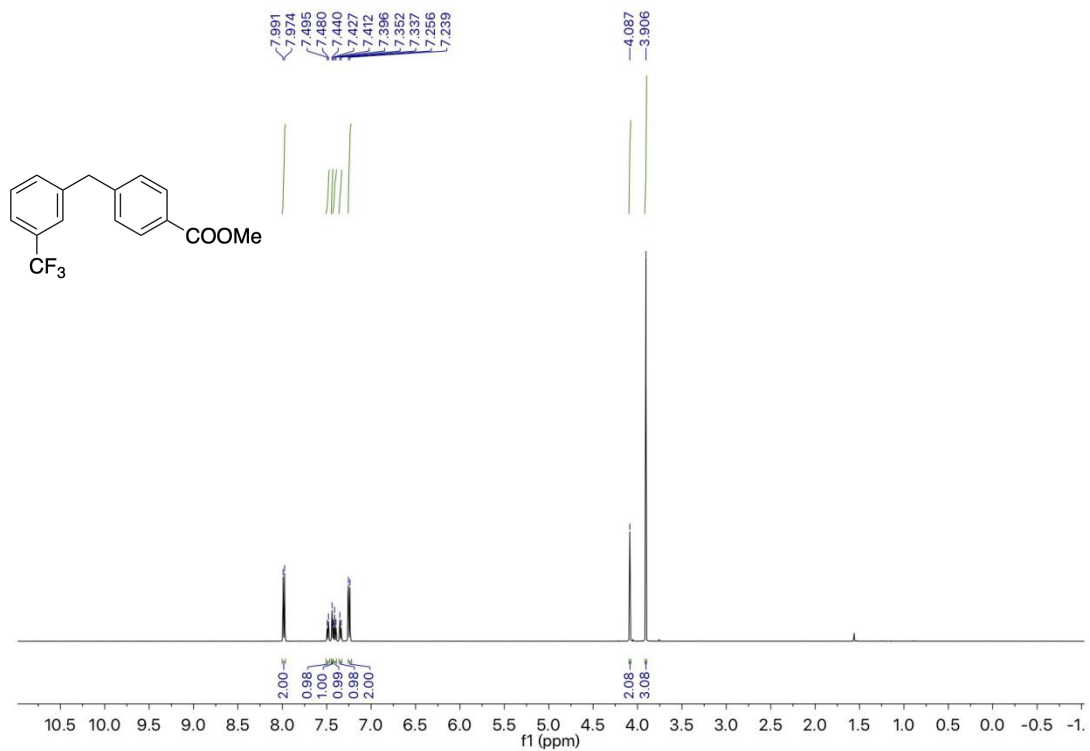
<sup>1</sup>H NMR spectrum (400 MHz, CDCl<sub>3</sub>) of **3r**



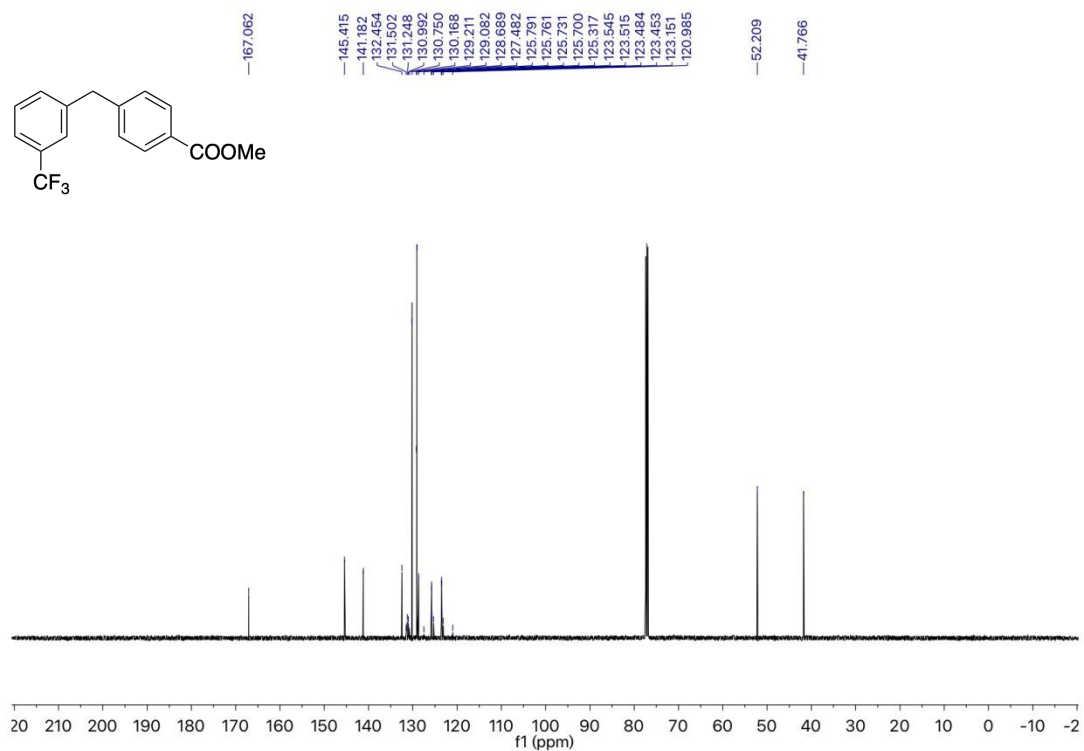
<sup>13</sup>C NMR spectrum (101 MHz, CDCl<sub>3</sub>) of **3r**



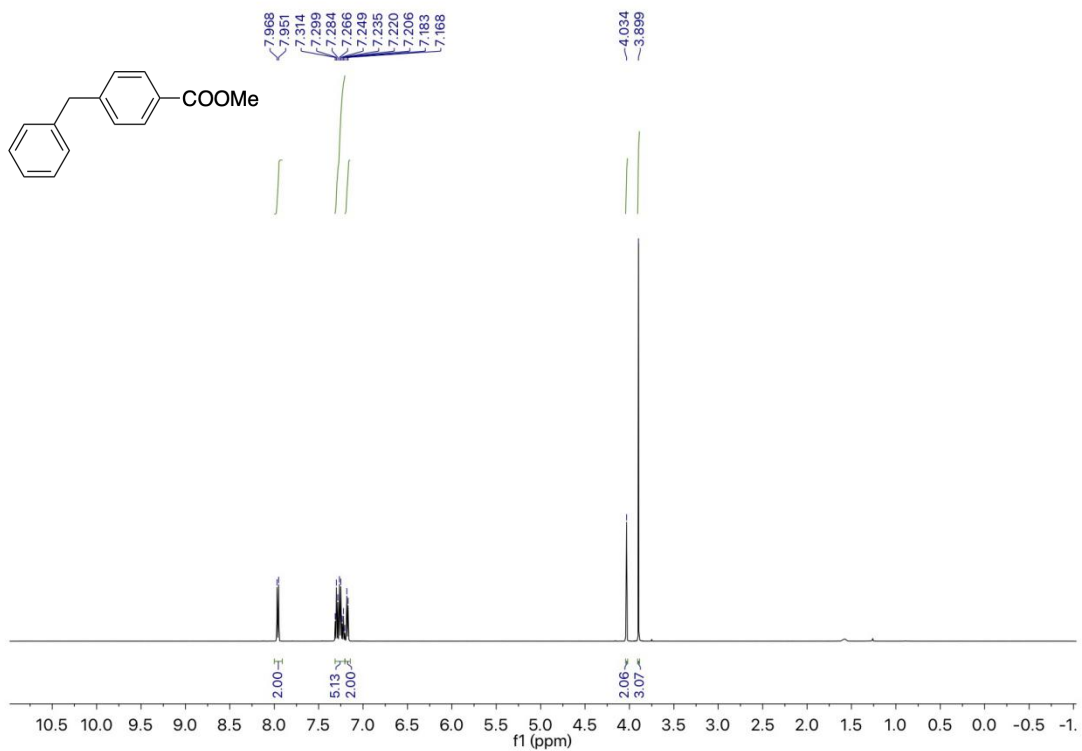
<sup>19</sup>F NMR spectrum (375 MHz, CDCl<sub>3</sub>) of **3s**



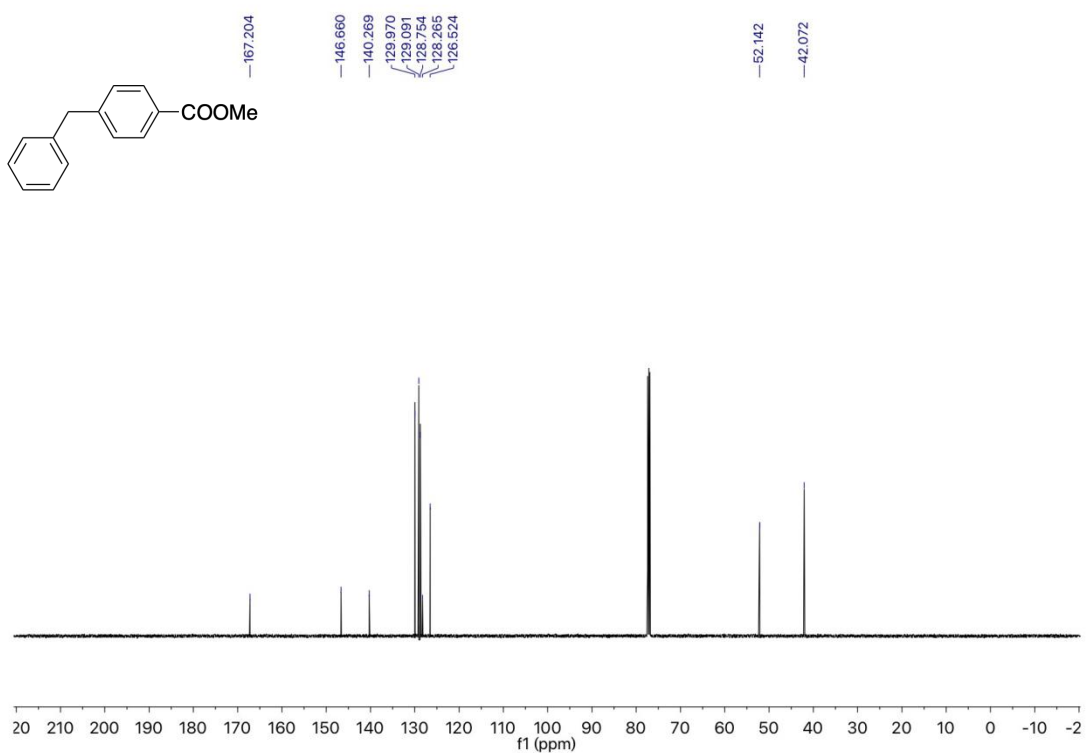
<sup>1</sup>H NMR spectrum (400 MHz, CDCl<sub>3</sub>) of **3s**



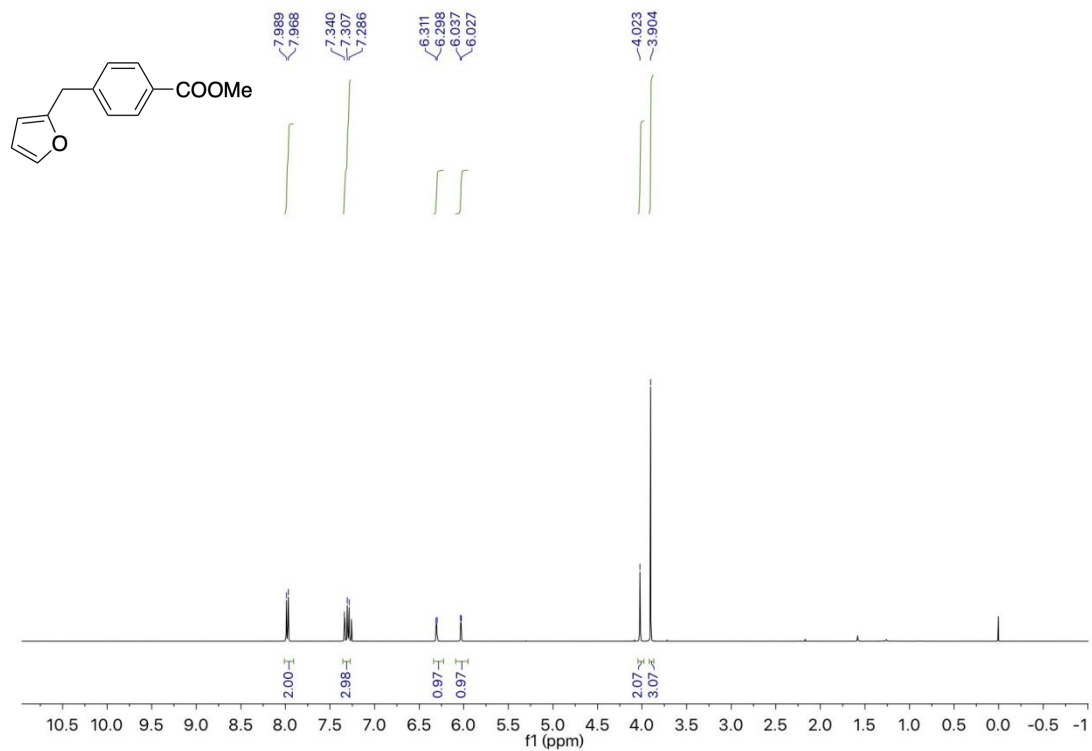
<sup>13</sup>C NMR spectrum (101 MHz, CDCl<sub>3</sub>) of **3s**



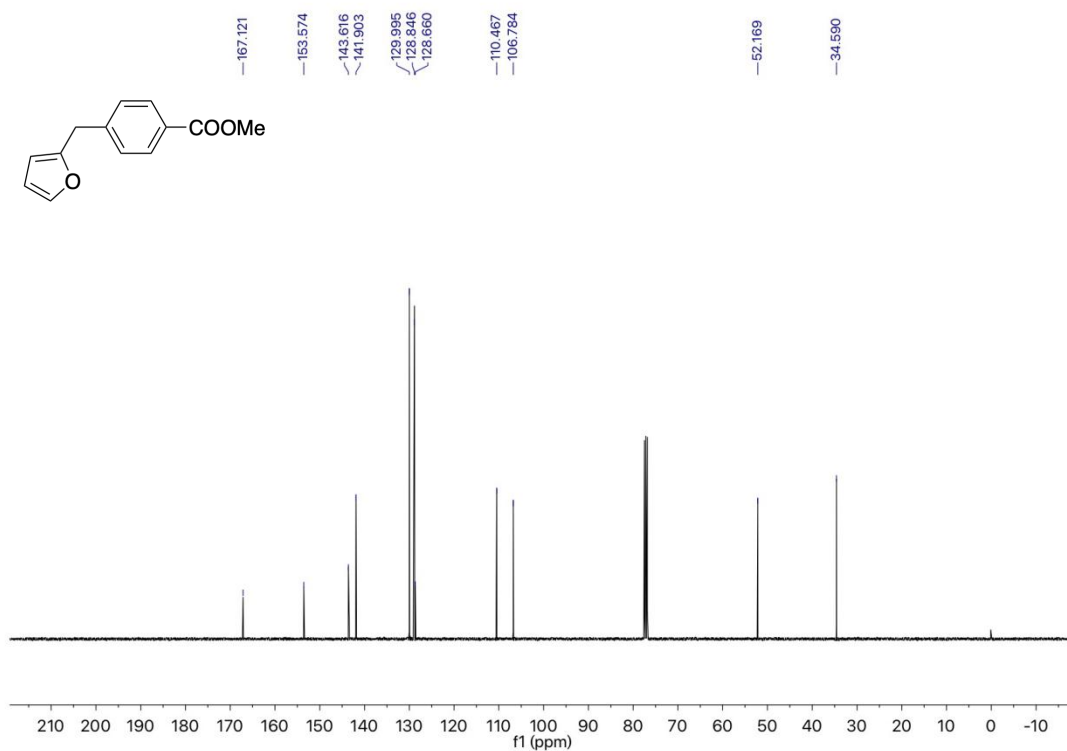
<sup>1</sup>H NMR spectrum (400 MHz, CDCl<sub>3</sub>) of **3t**



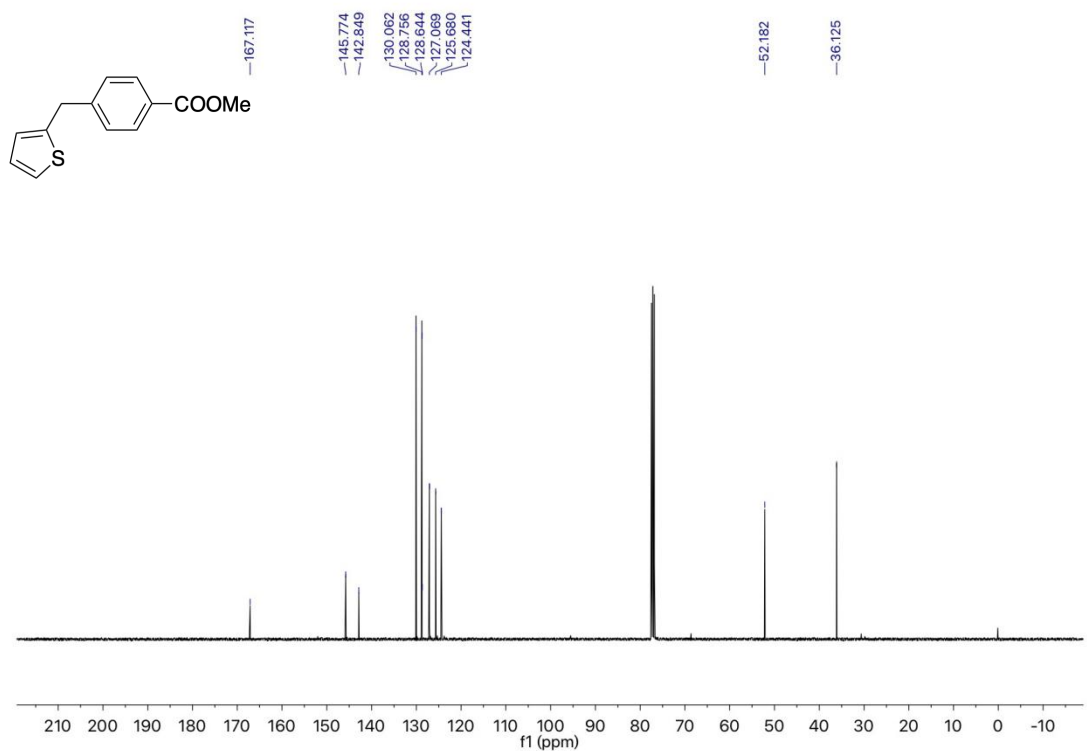
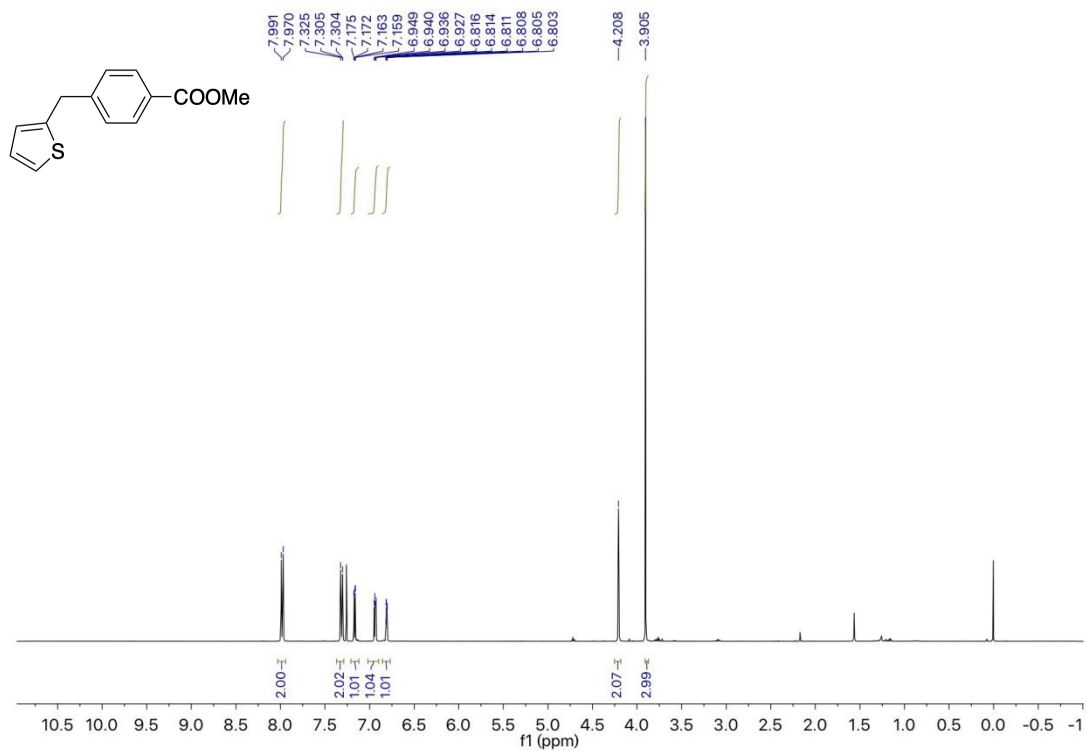
<sup>13</sup>C NMR spectrum (101 MHz, CDCl<sub>3</sub>) of **3t**



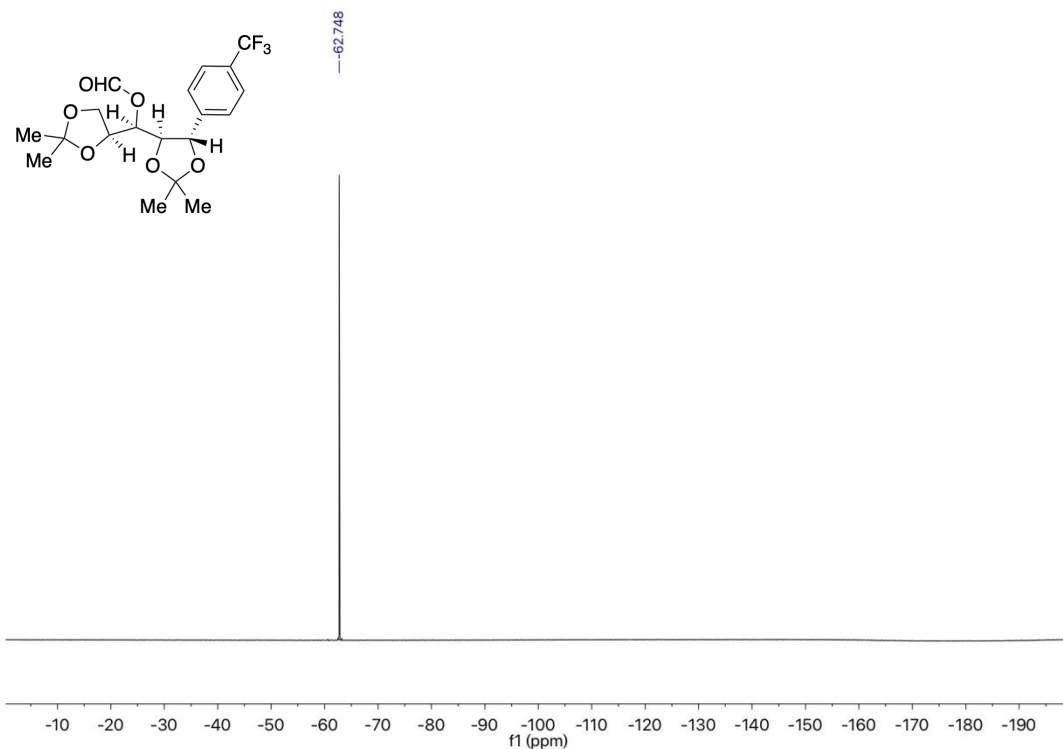
<sup>1</sup>H NMR spectrum (400 MHz, CDCl<sub>3</sub>) of **3v**



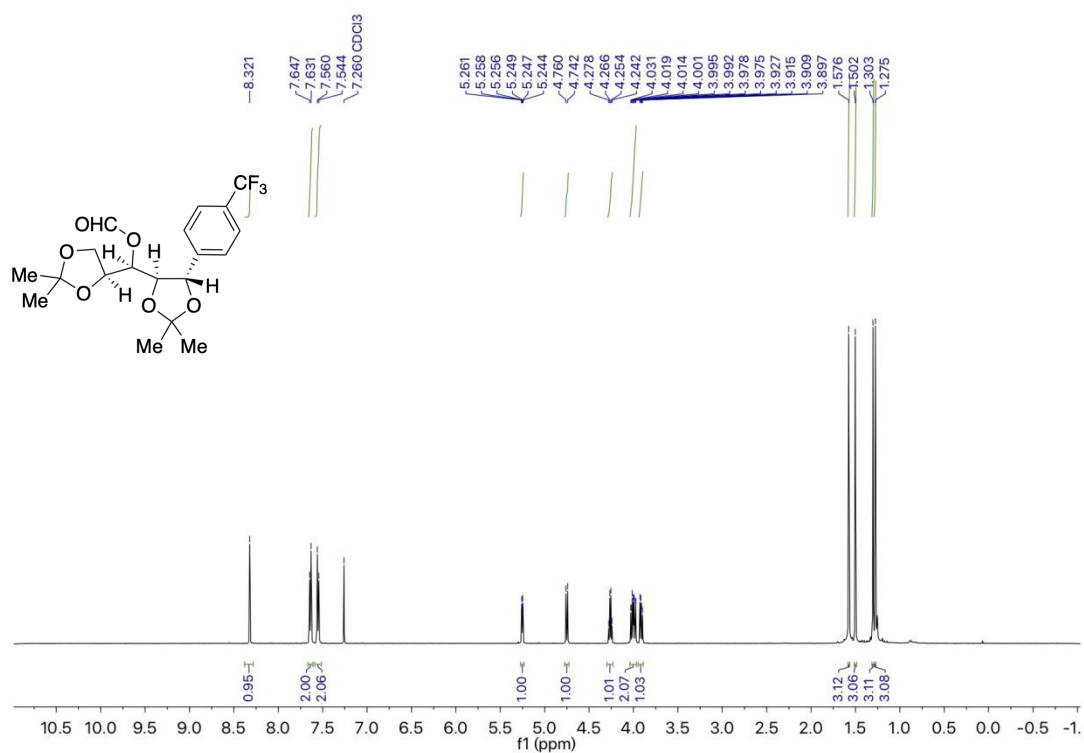
<sup>13</sup>C NMR spectrum (101 MHz, CDCl<sub>3</sub>) of **3v**



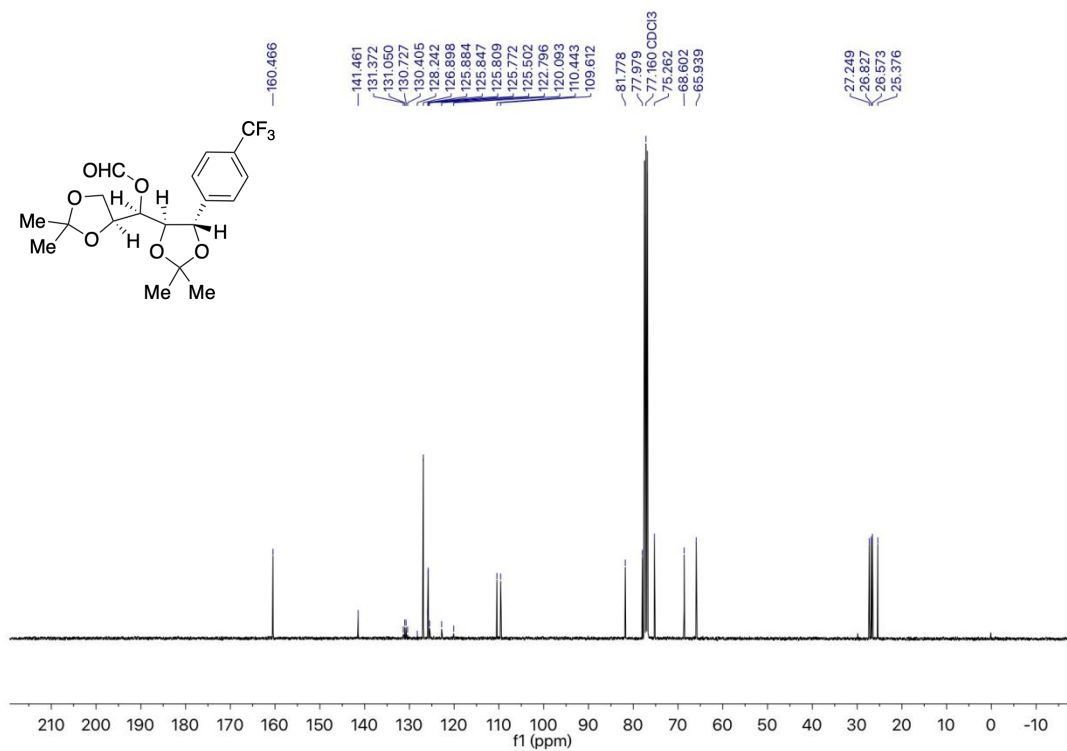




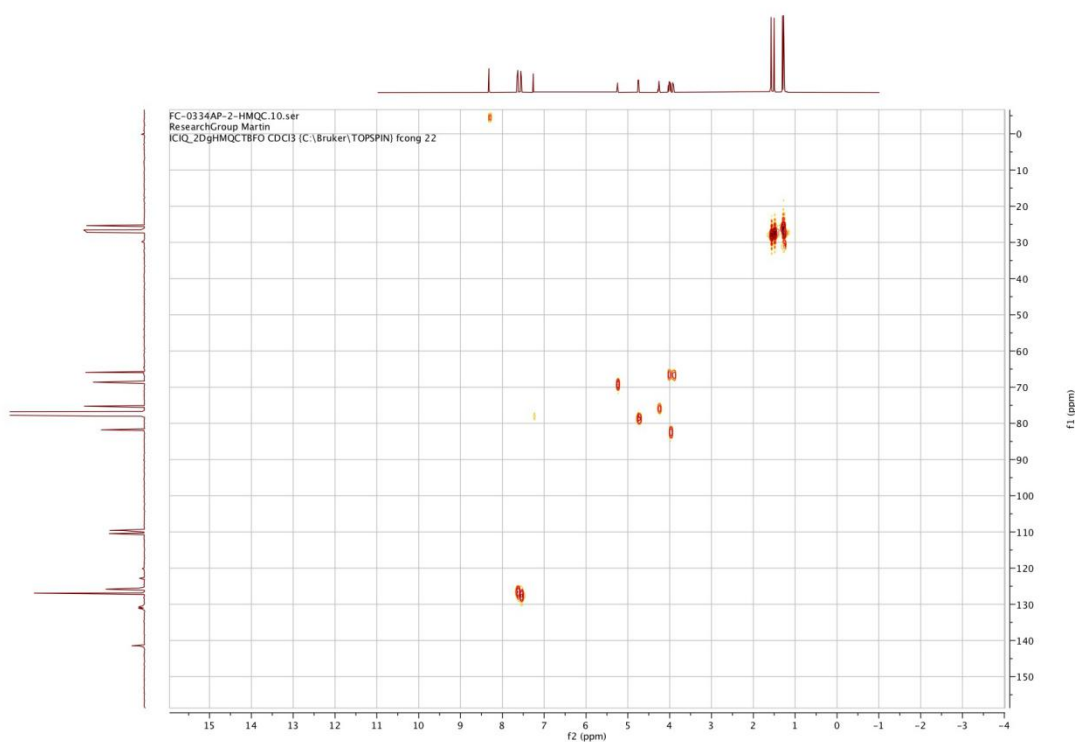
$^{19}\text{F}$  NMR spectrum (375 MHz,  $\text{CDCl}_3$ ) of **7**



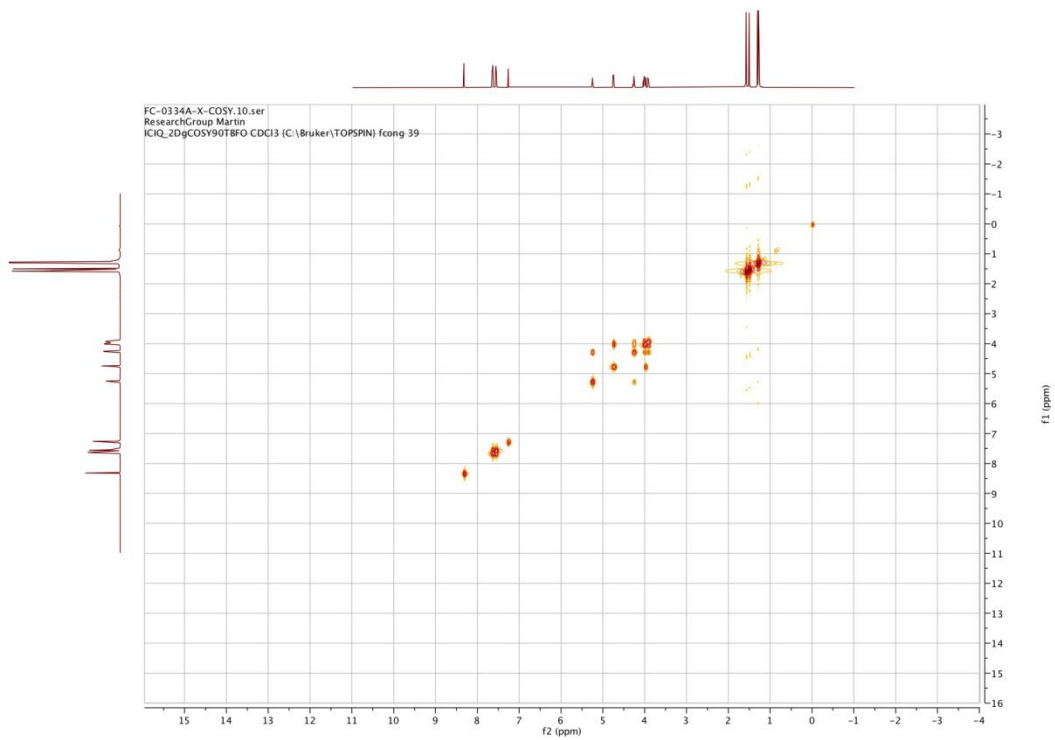
$^1\text{H}$  NMR spectrum (400 MHz,  $\text{CDCl}_3$ ) of **7**



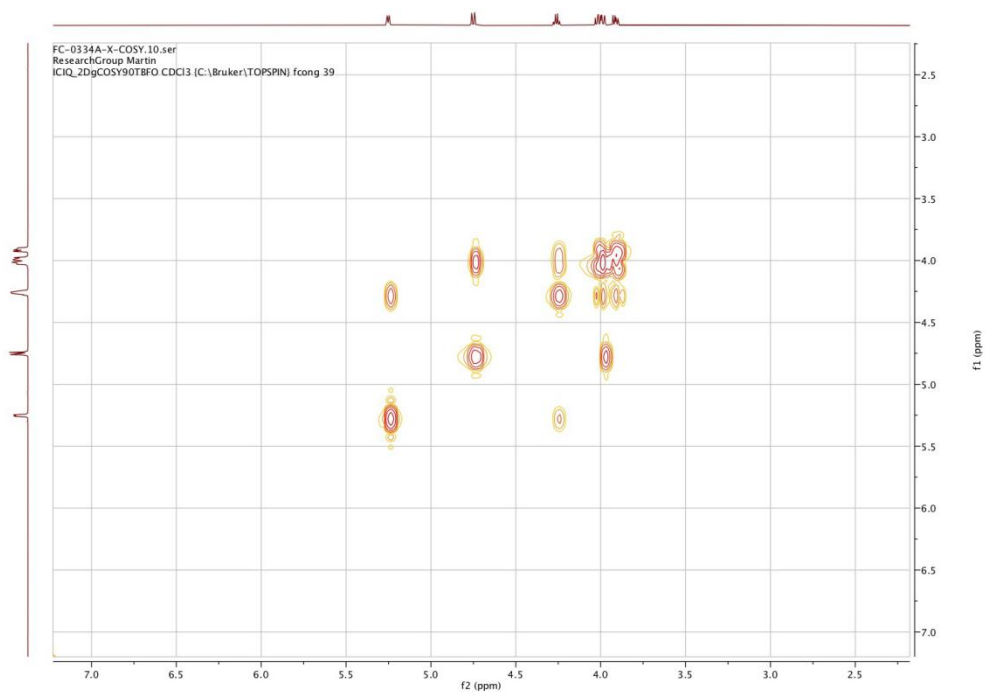
<sup>13</sup>C NMR spectrum (101 MHz, CDCl<sub>3</sub>) of 7



HMQC spectrum(CDCl<sub>3</sub>) of 7



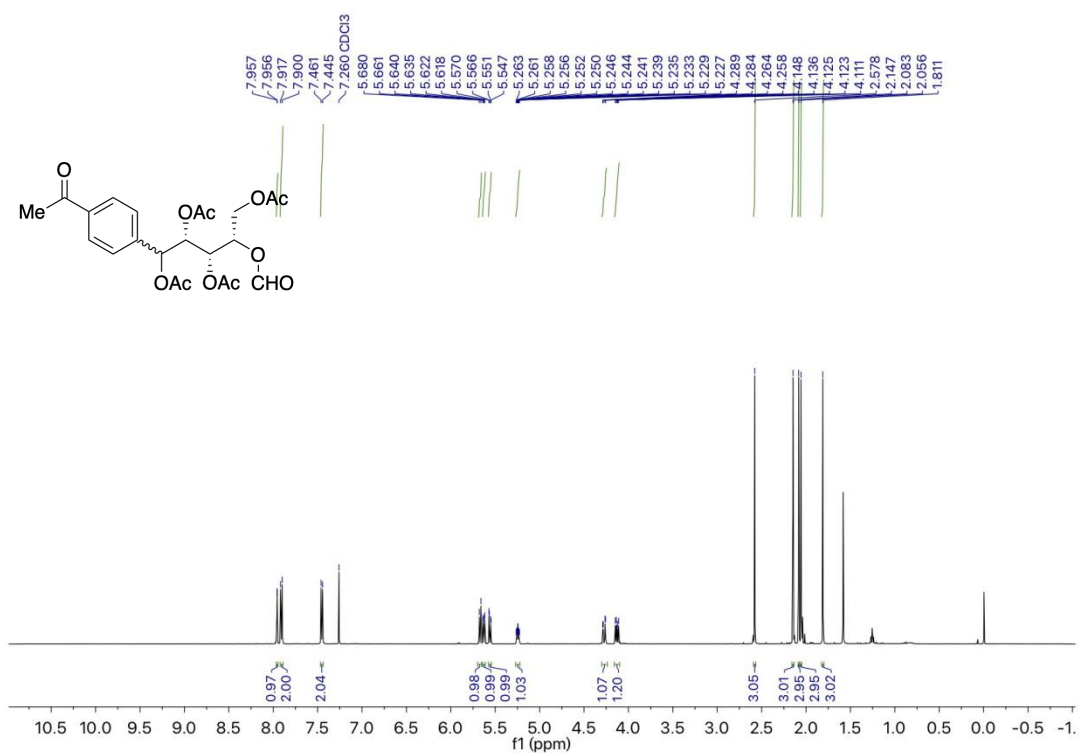
COSY spectrum (CDCl<sub>3</sub>) of **7**



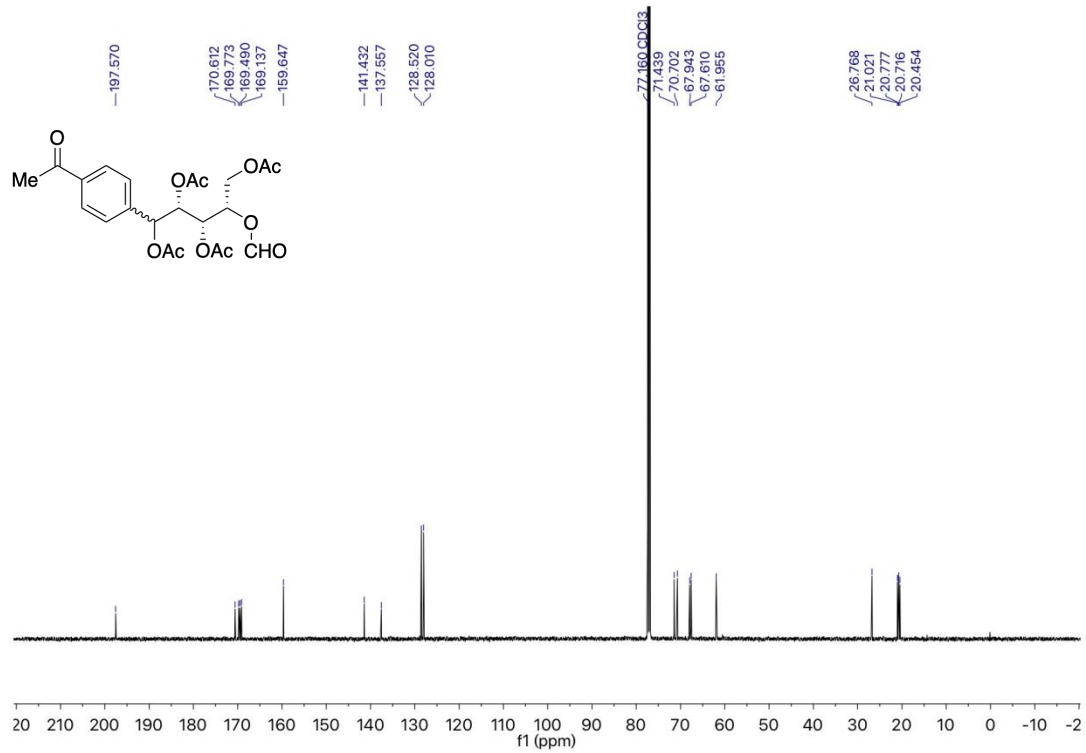
COSY spectrum (CDCl<sub>3</sub>) of **7**



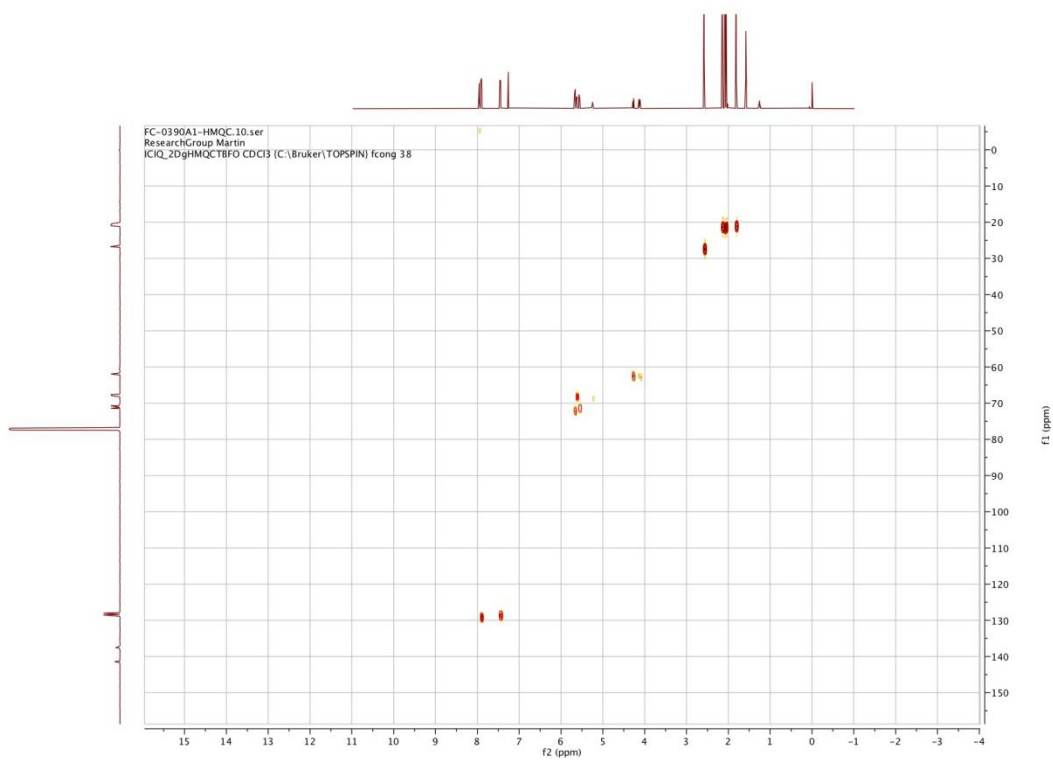
NOE spectrum (CDCl<sub>3</sub>) of **7**



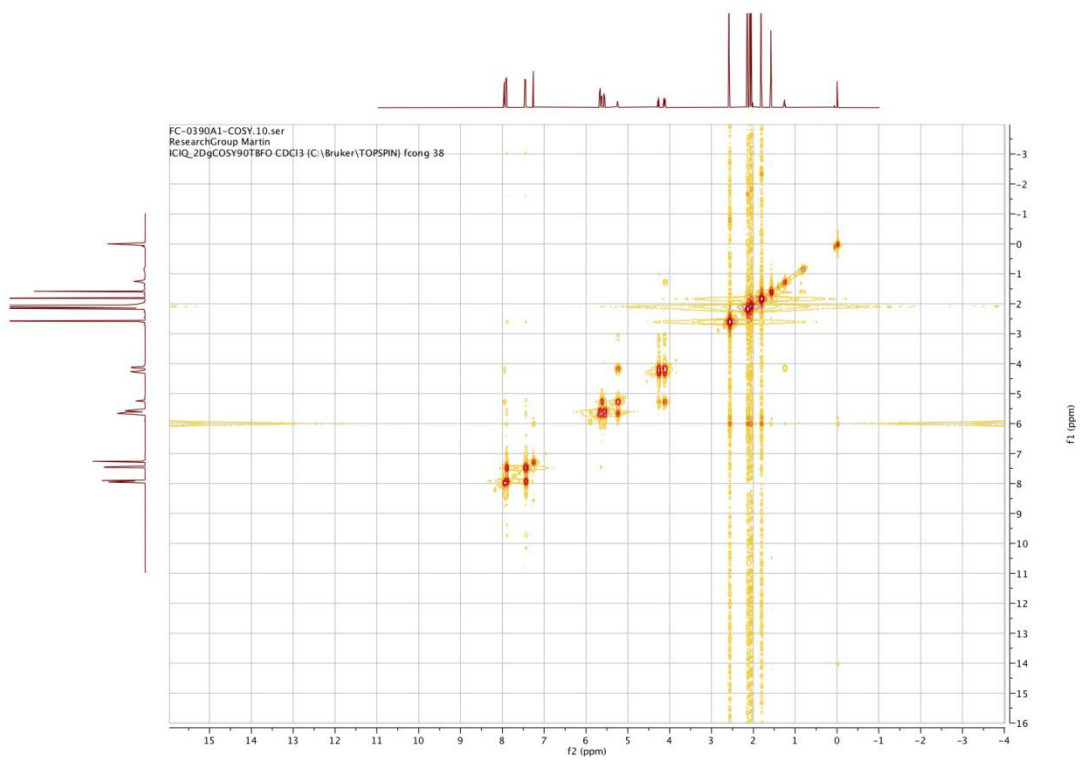
<sup>1</sup>H NMR spectrum (400 MHz, CDCl<sub>3</sub>) of **9-1**



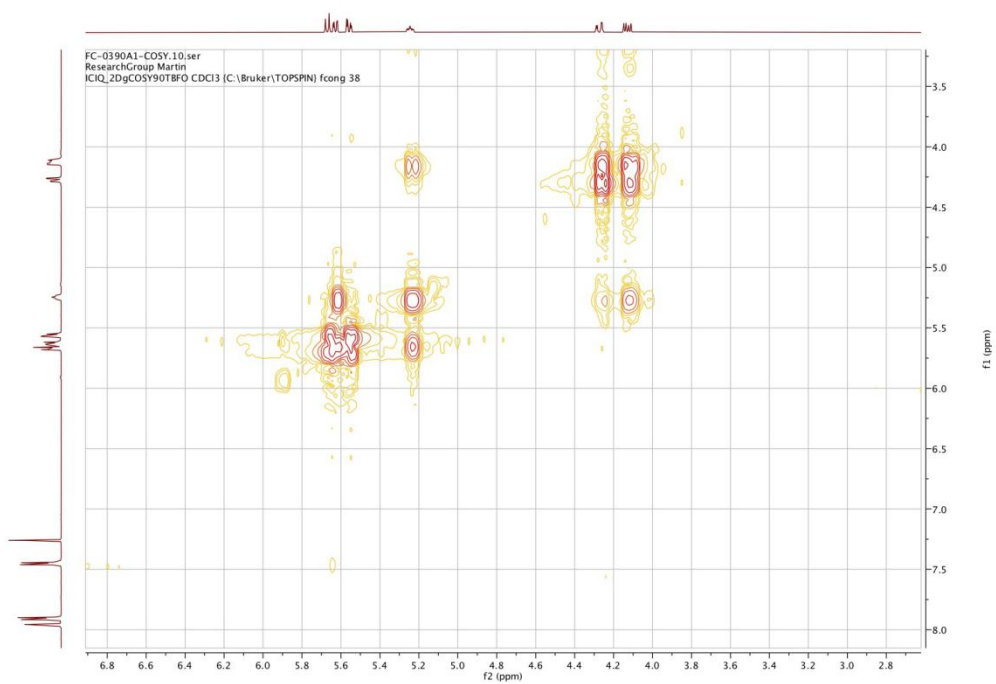
$^{13}\text{C}$  NMR spectrum (101 MHz, CDCl<sub>3</sub>) of **9-1**



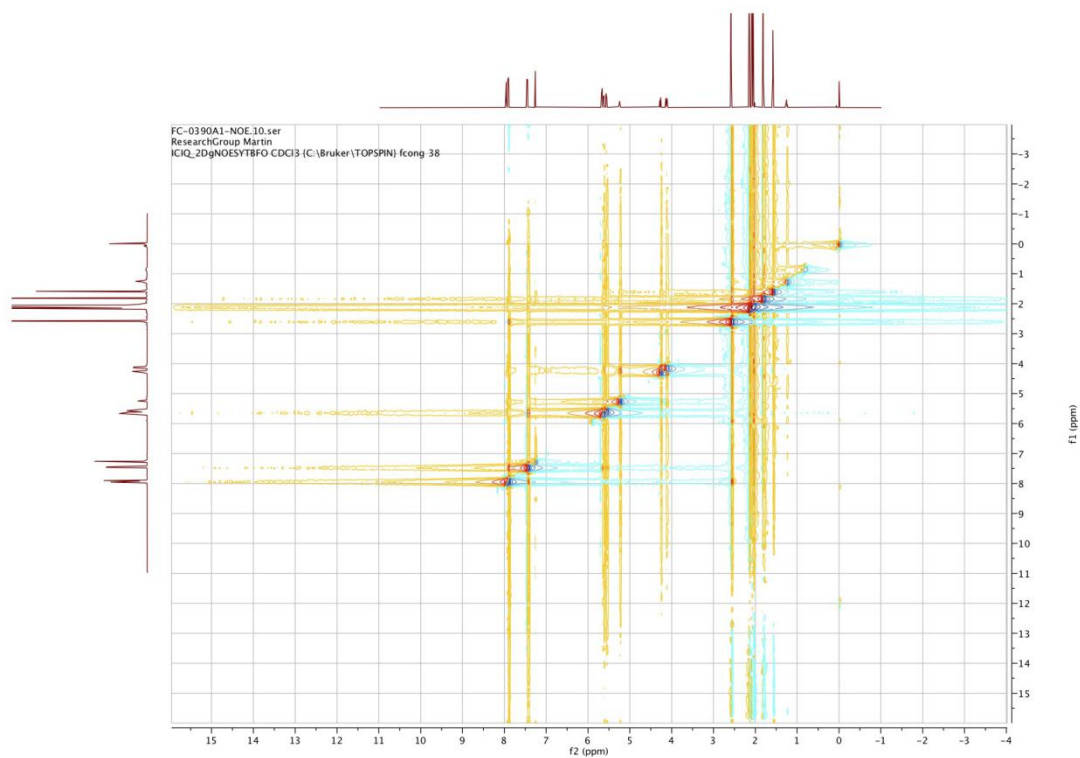
HMBC spectrum (CDCl<sub>3</sub>) of **9-1**



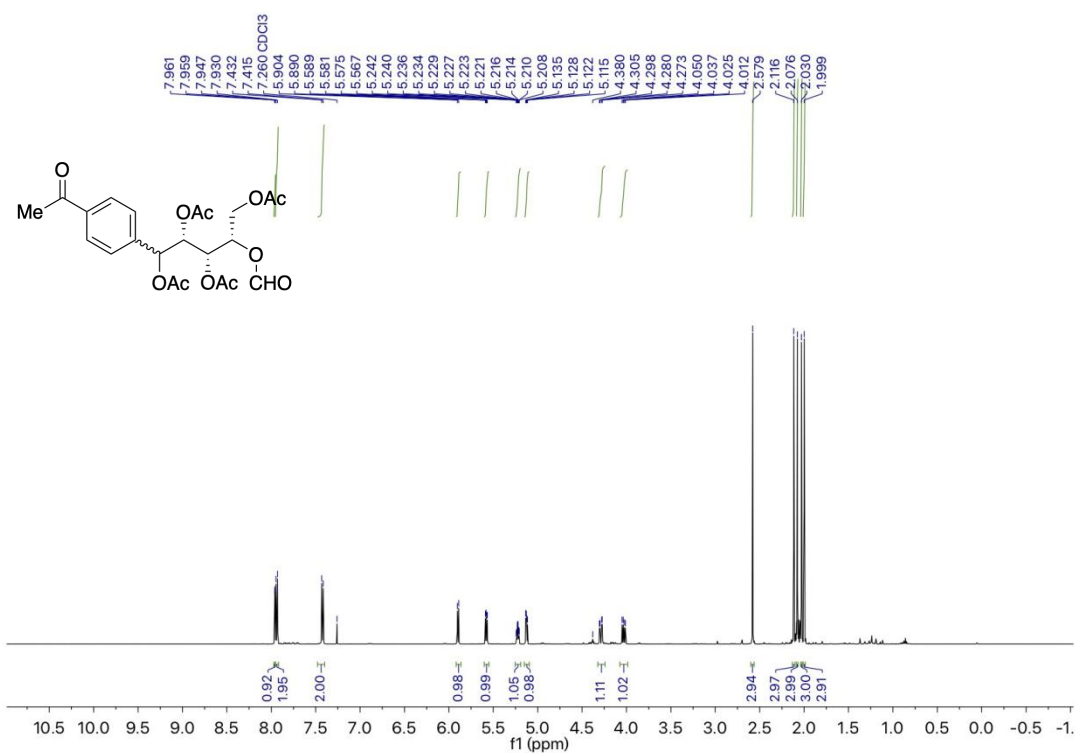
COSY spectrum (CDCl<sub>3</sub>) of 9-1



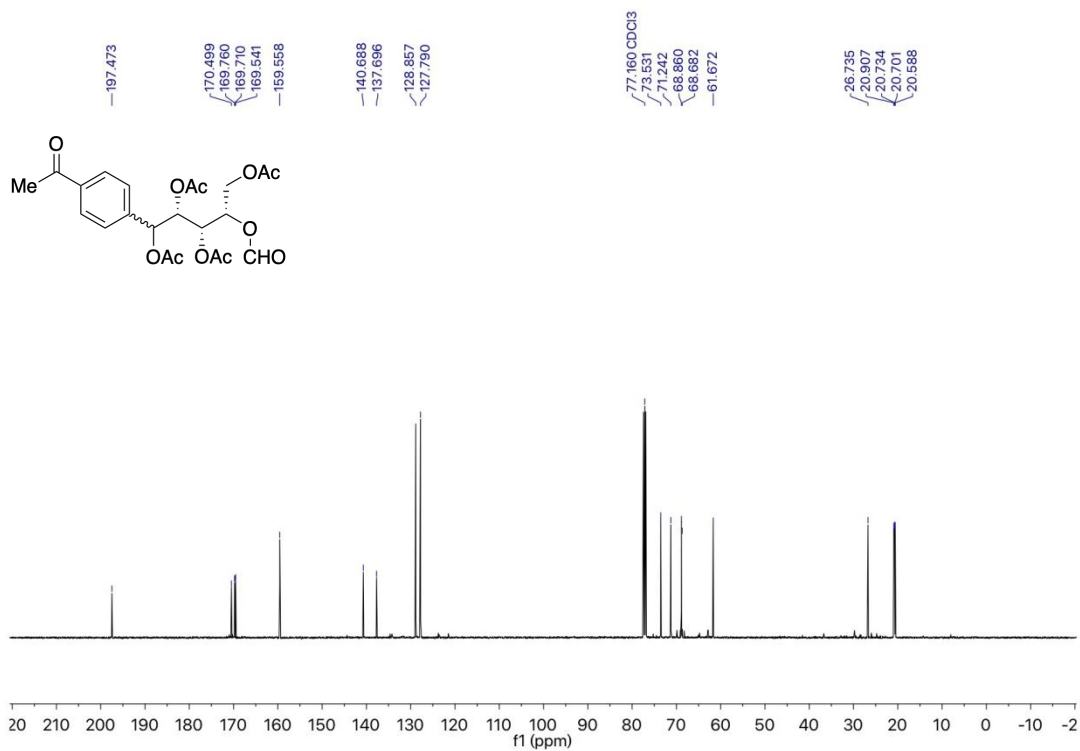
COSY spectrum (CDCl<sub>3</sub>) of 9-1



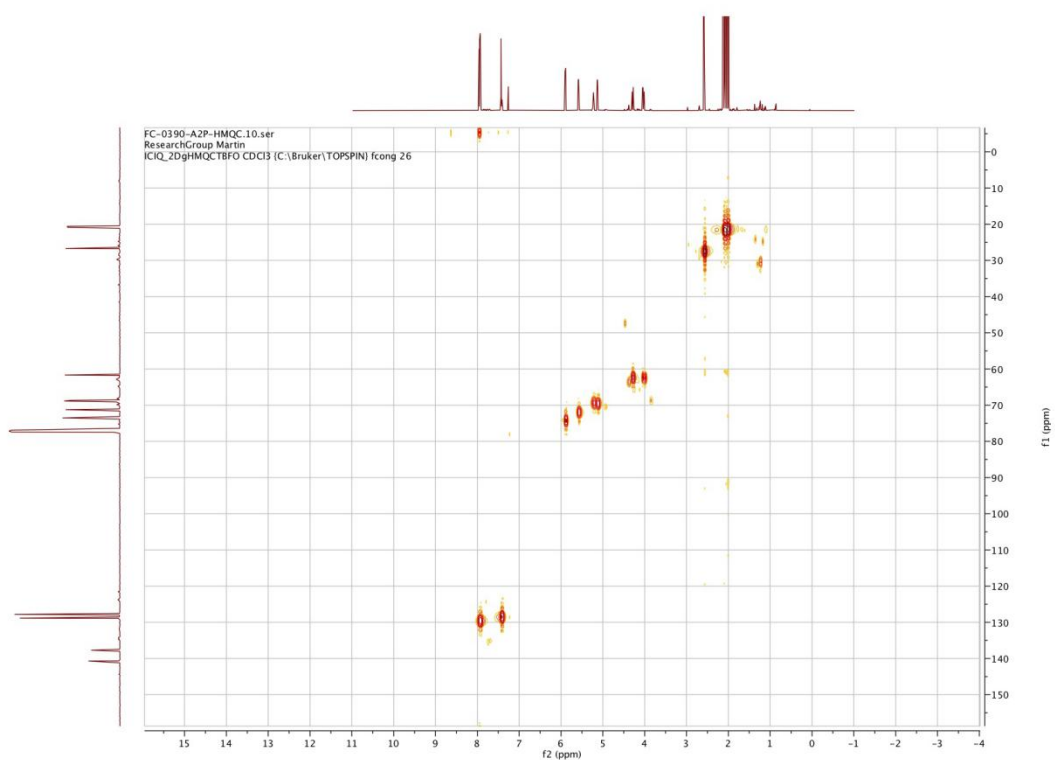
NOE spectrum ( $\text{CDCl}_3$ ) of **9-1**



$^1\text{H}$  NMR spectrum (400 MHz,  $\text{CDCl}_3$ ) of **9-2**

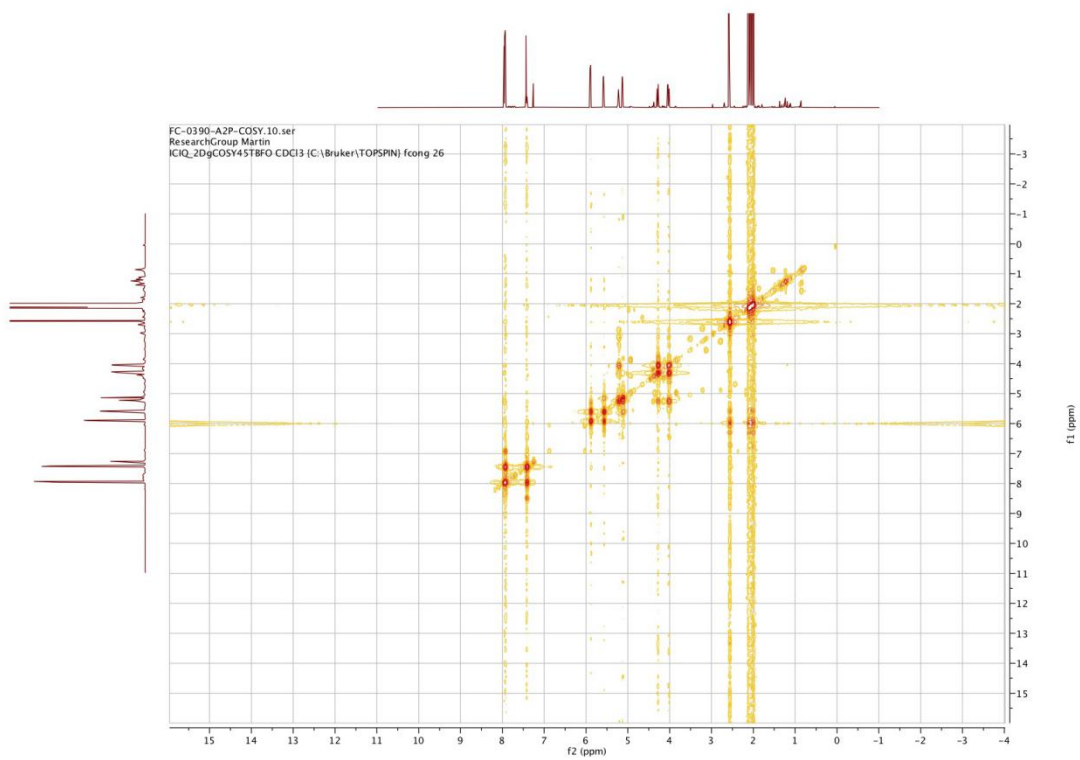


<sup>13</sup>C NMR spectrum (101 MHz, CDCl<sub>3</sub>) of **9-2**

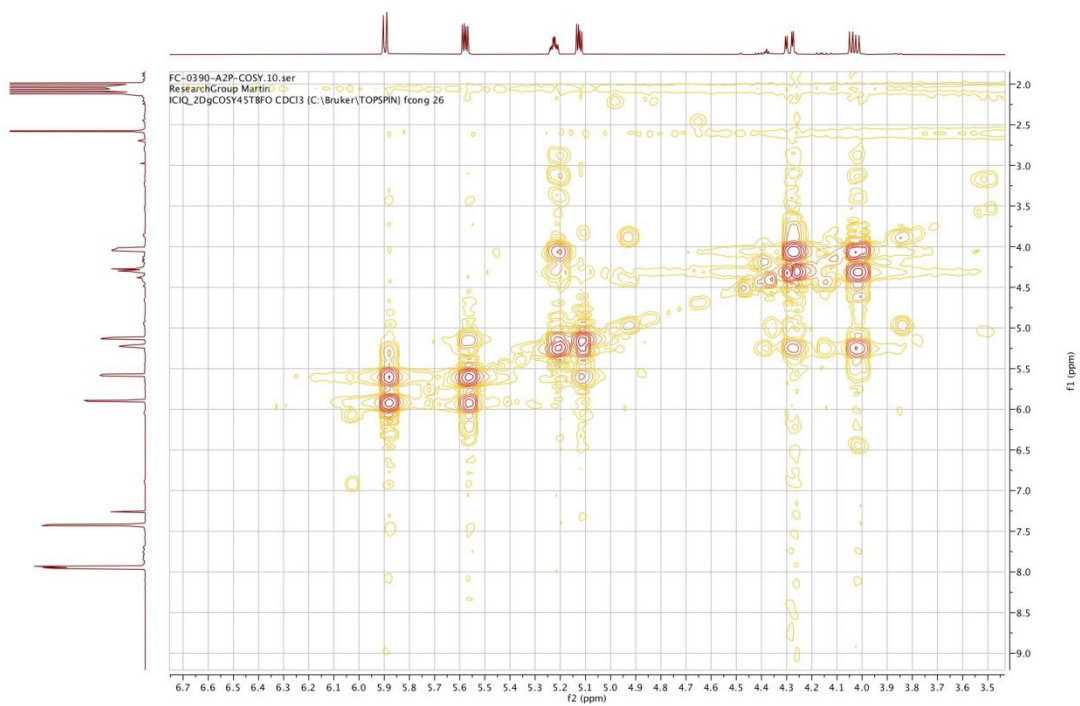


HMQC spectrum (CDCl<sub>3</sub>) of **9-2**

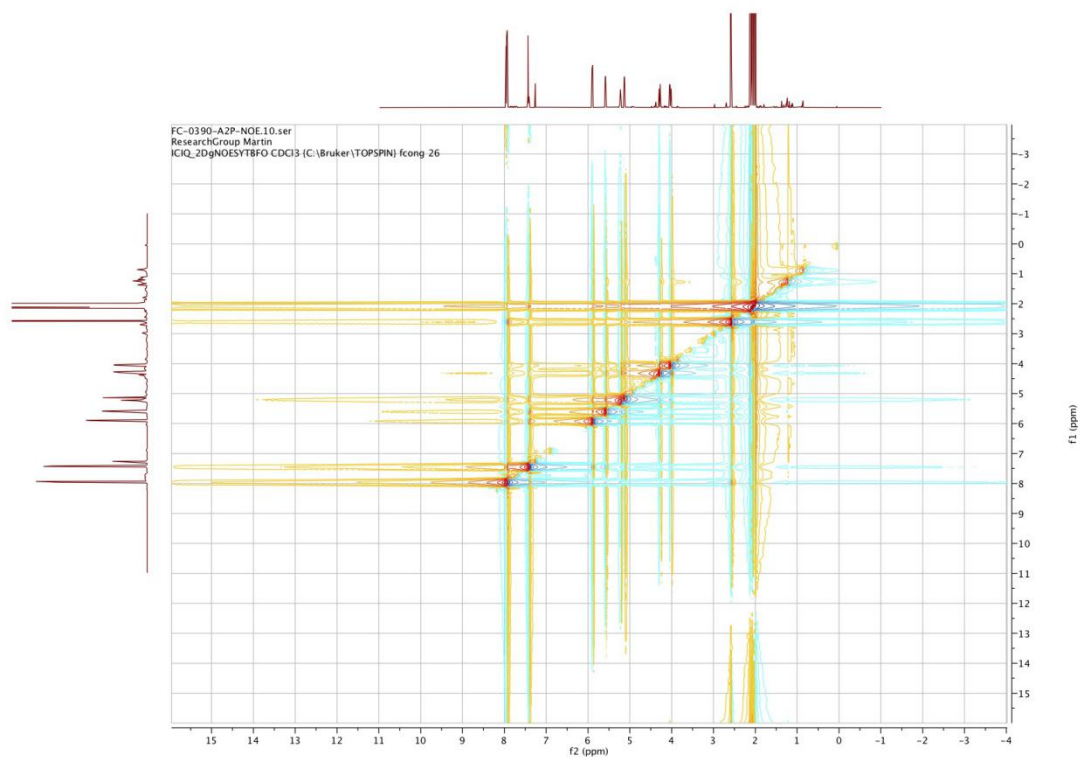




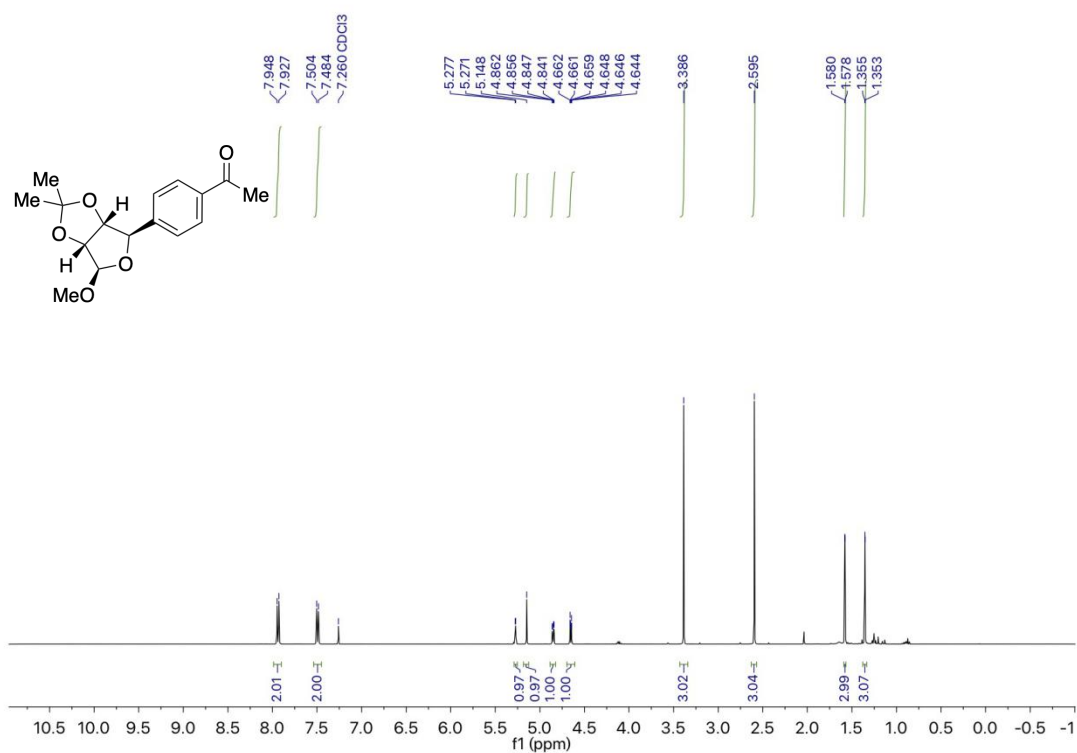
COSY spectrum (CDCl<sub>3</sub>) of 9-2



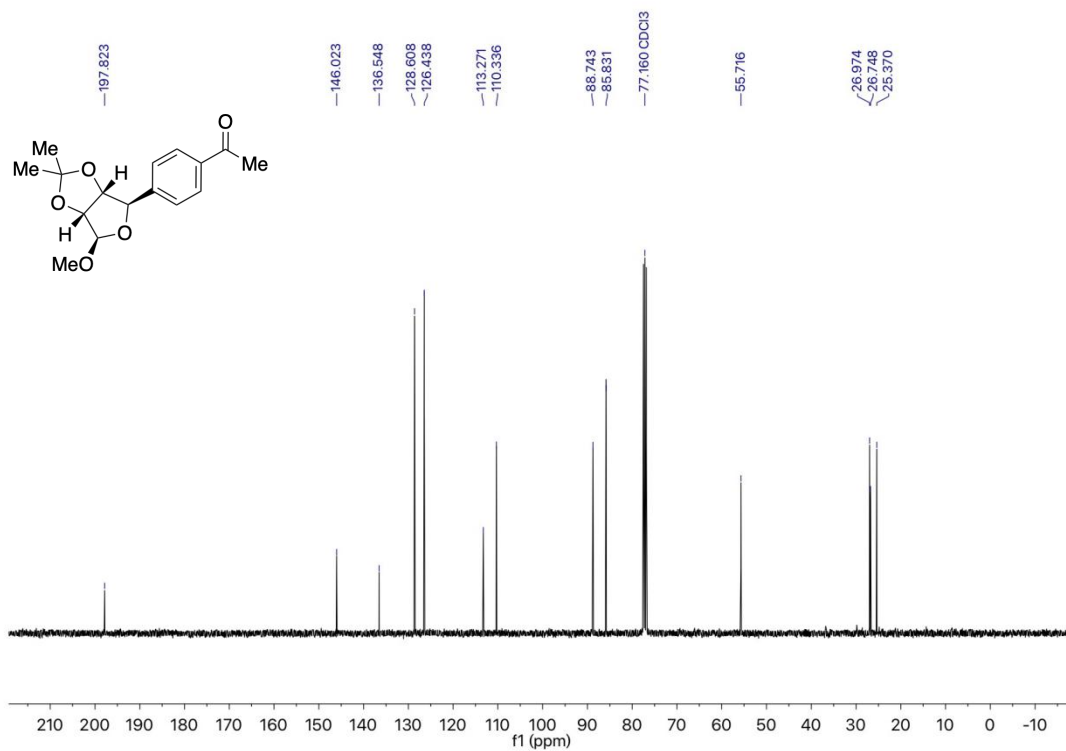
COSY spectrum (CDCl<sub>3</sub>) of 9-2



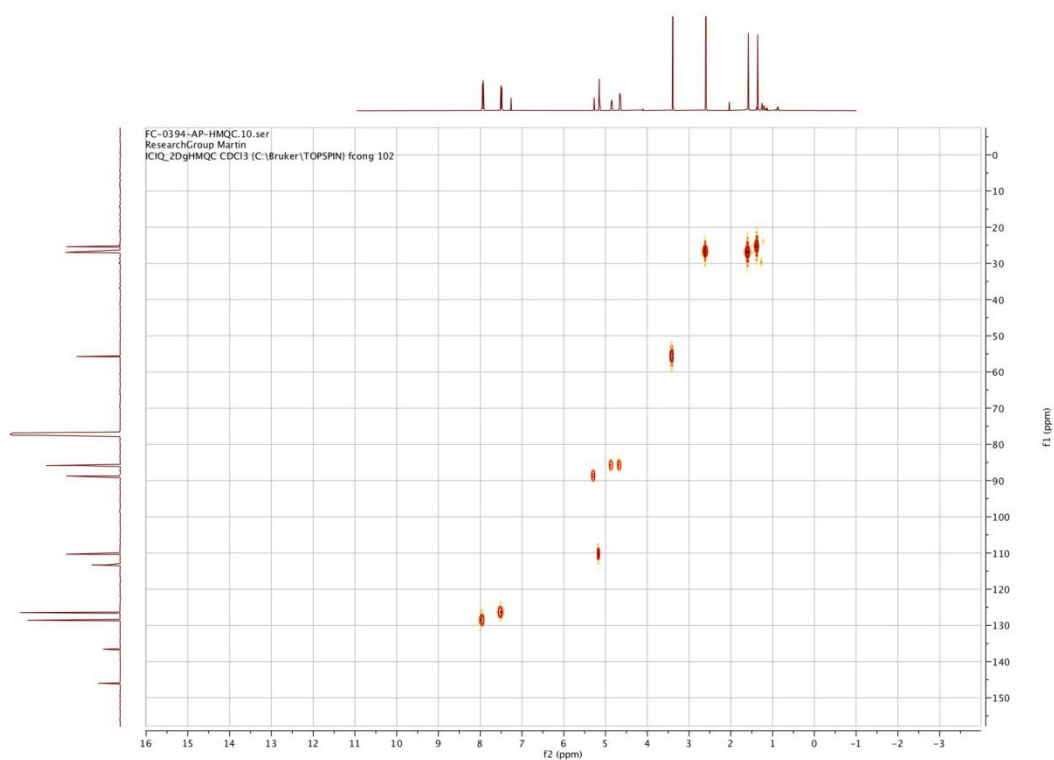
NOE spectrum ( $\text{CDCl}_3$ ) of **9-2**



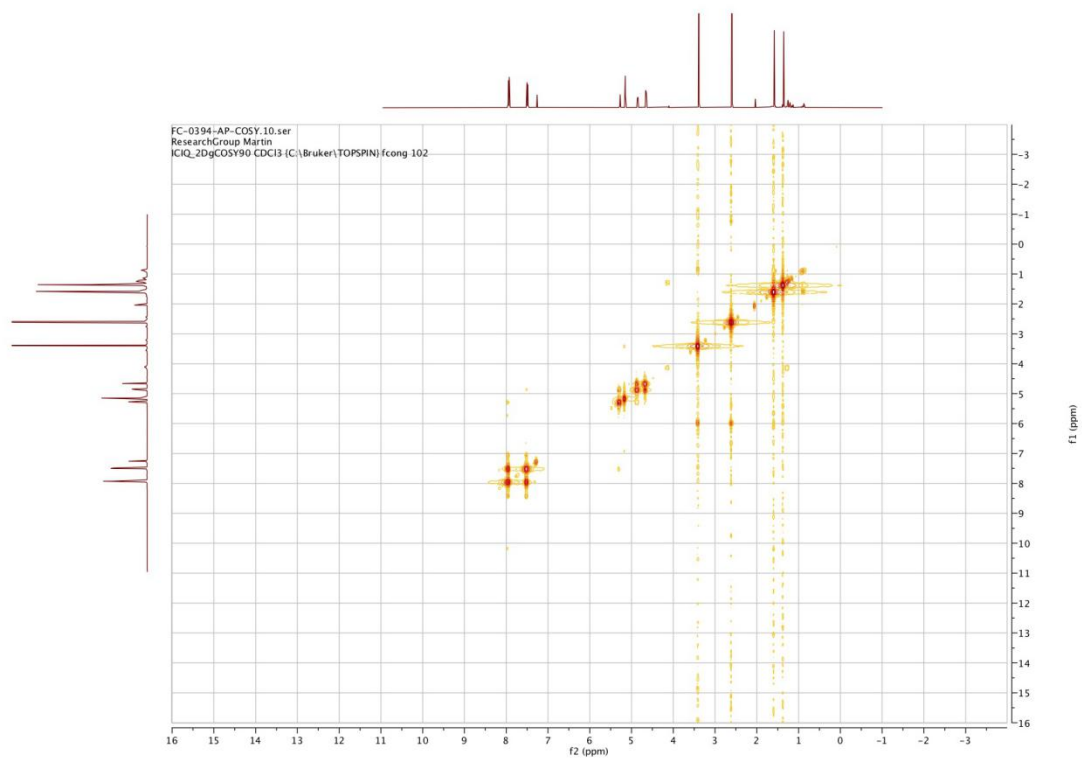
$^1\text{H}$  NMR spectrum (400 MHz,  $\text{CDCl}_3$ ) of **11**



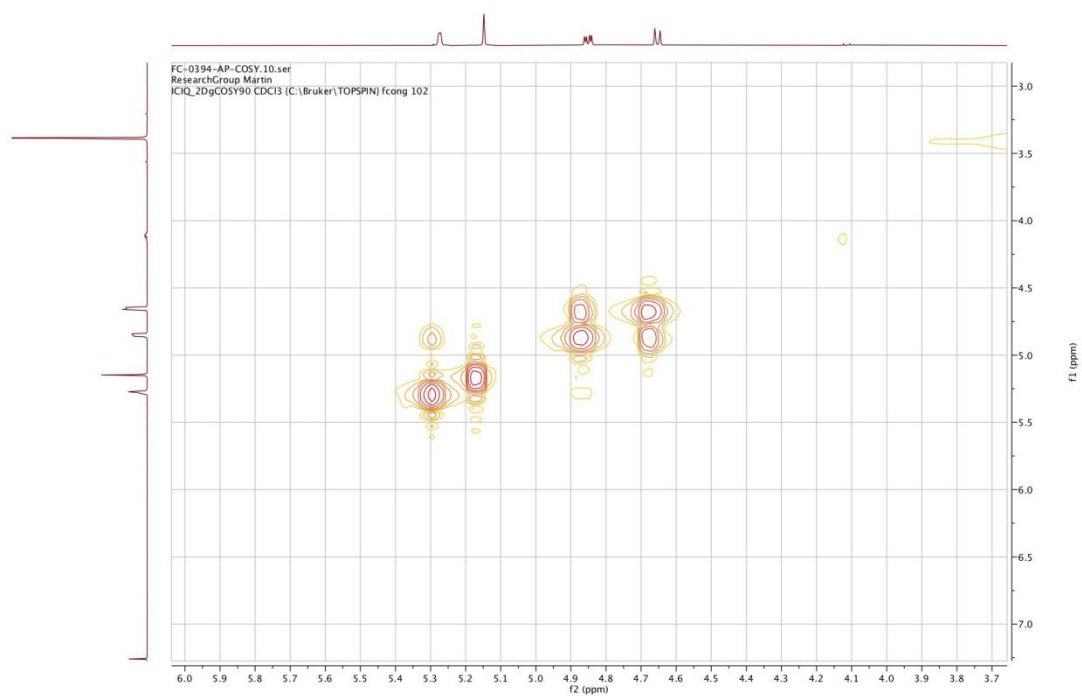
$^{13}\text{C}$  NMR spectrum (101 MHz,  $\text{CDCl}_3$ ) of **11**



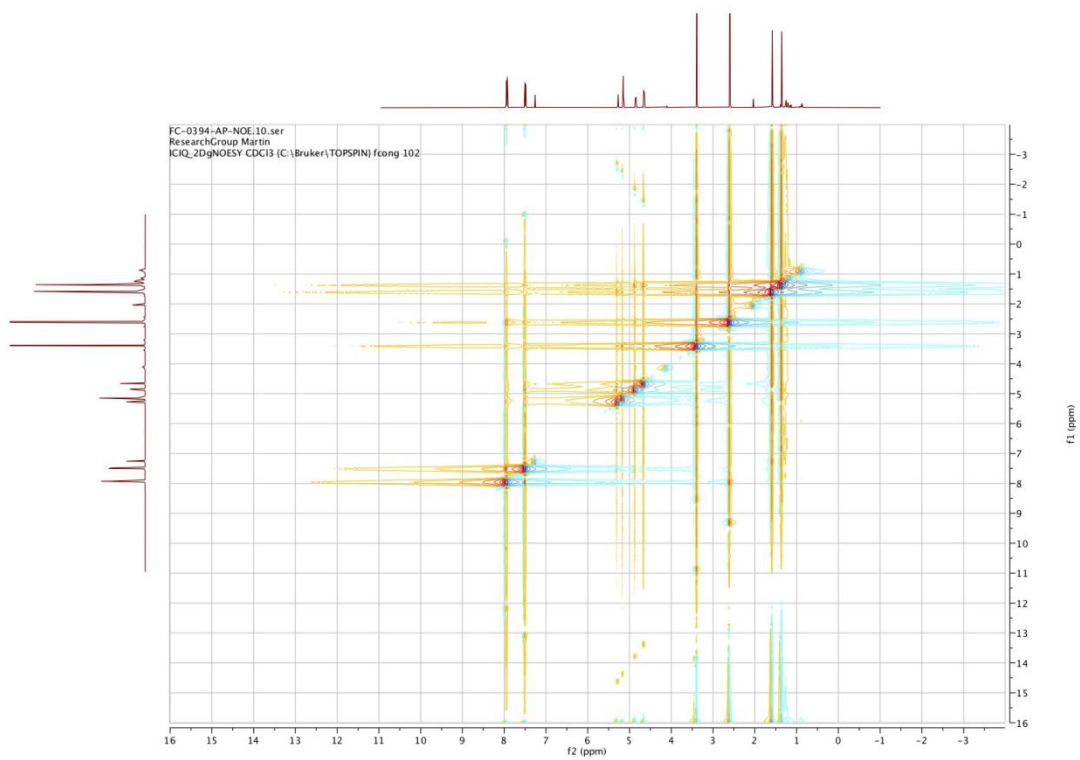
HMBC spectrum ( $\text{CDCl}_3$ ) of **11**



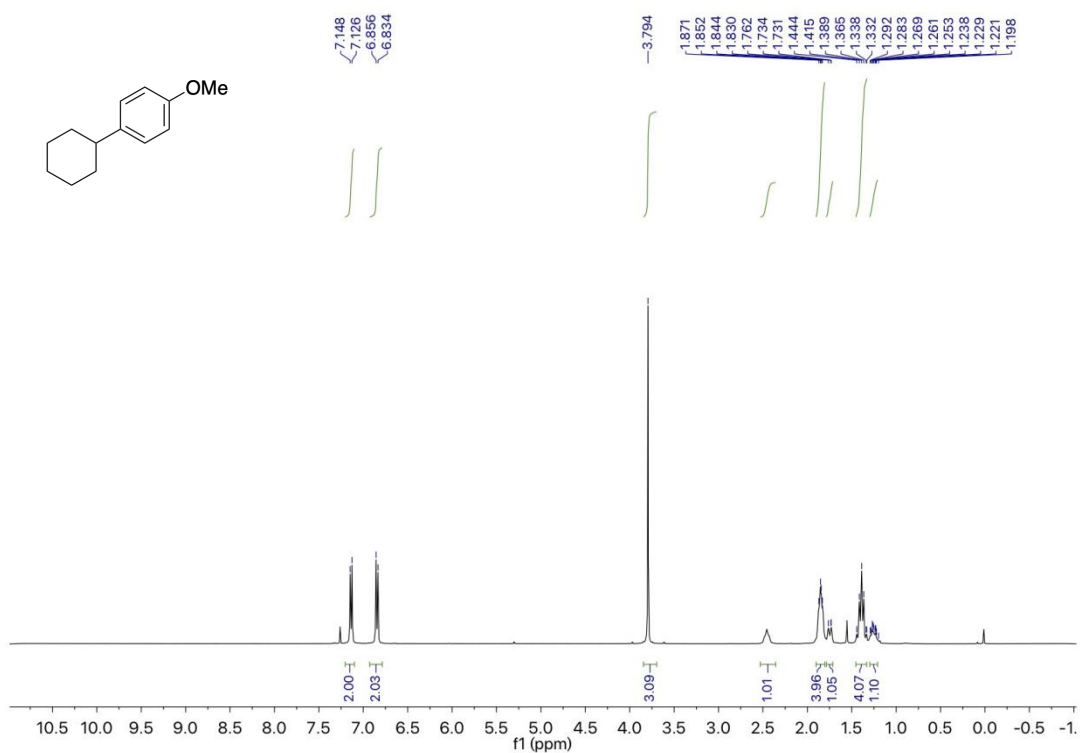
COSY spectrum (CDCl<sub>3</sub>) of **11**



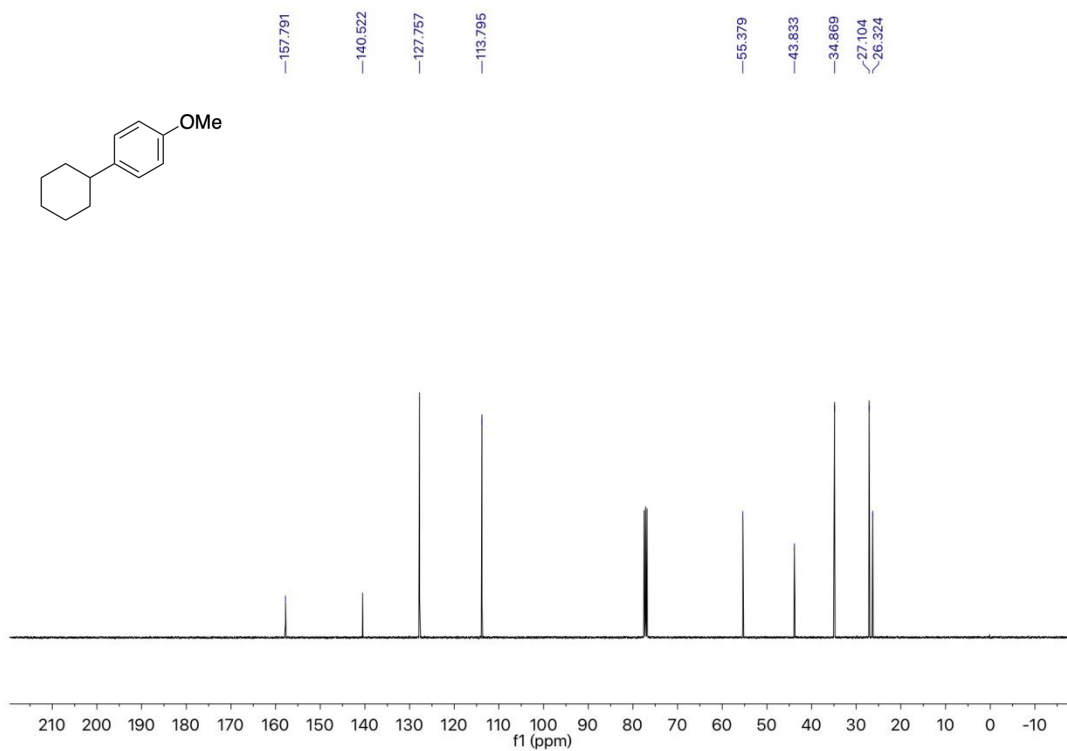
COSY spectrum (CDCl<sub>3</sub>) of **11**



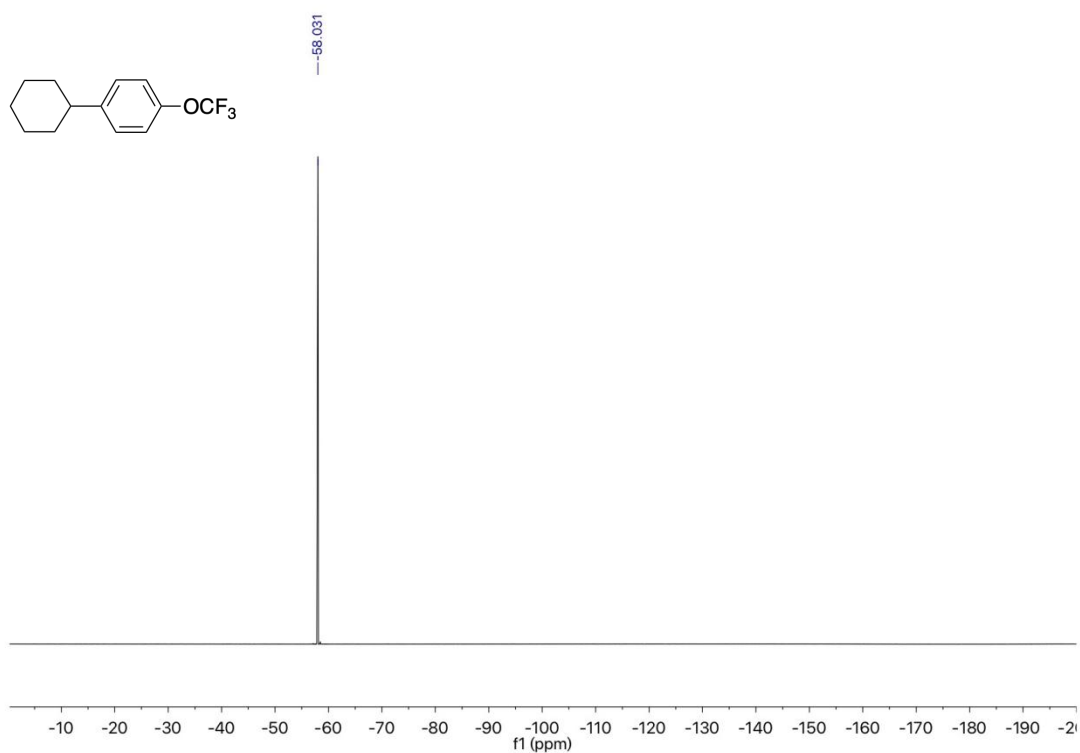
NOE spectrum (CDCl<sub>3</sub>) of **11**



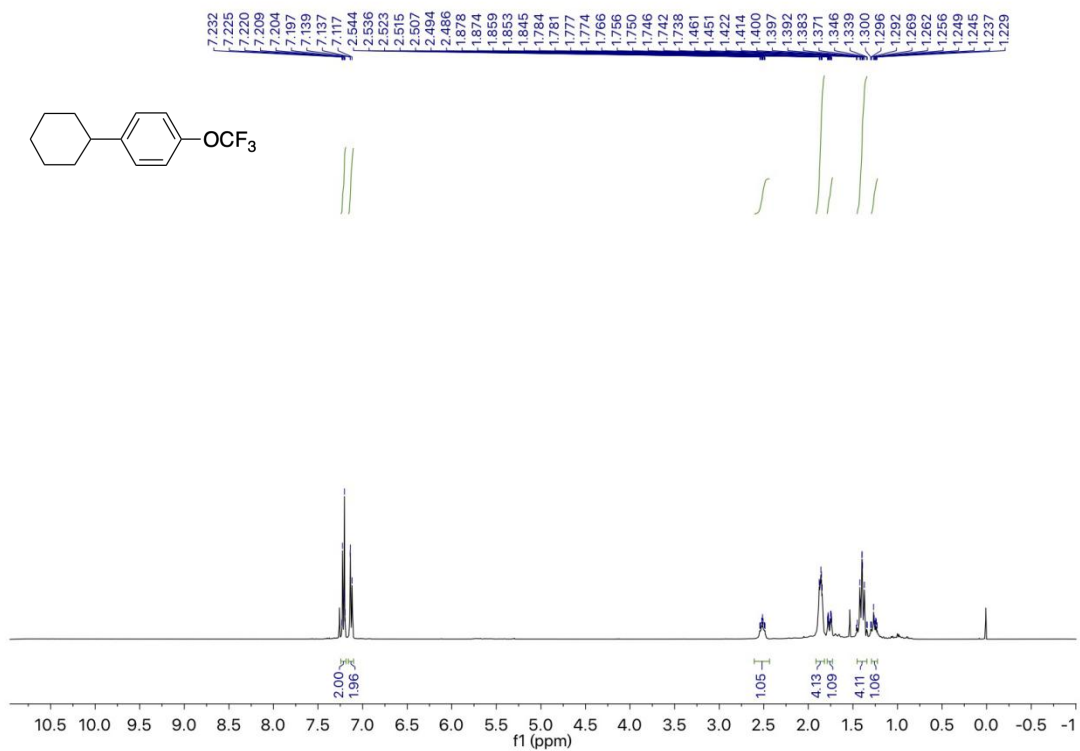
<sup>1</sup>H NMR spectrum (400 MHz, CDCl<sub>3</sub>) of **4a**



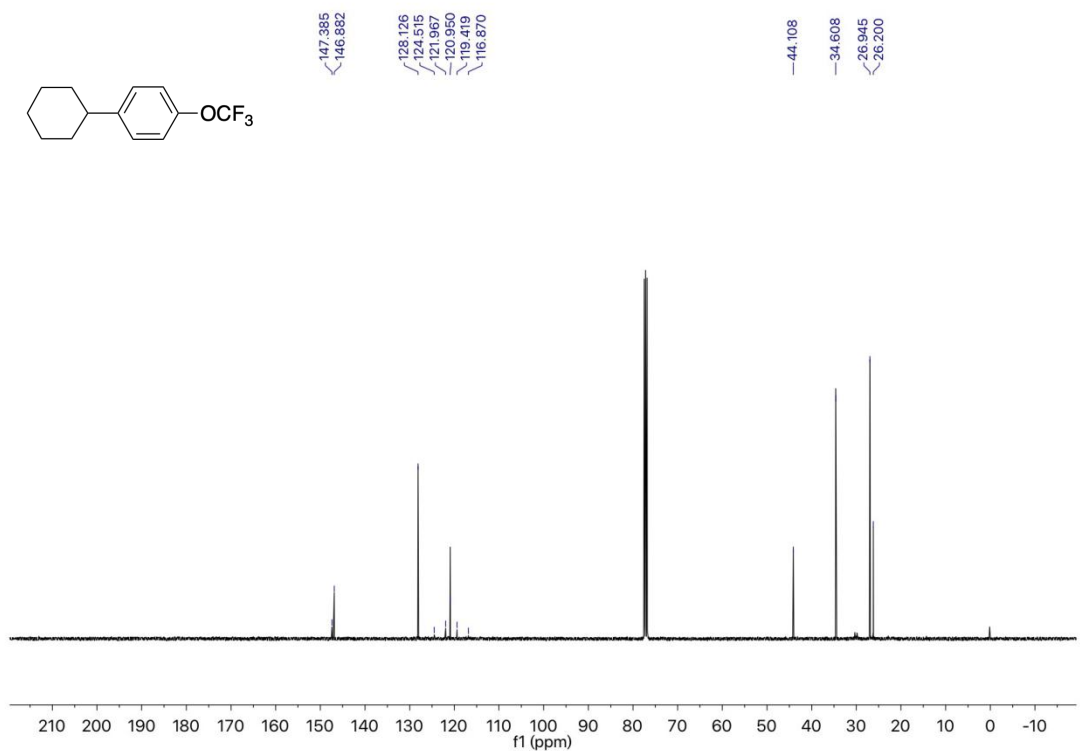
<sup>13</sup>C NMR spectrum (101 MHz, CDCl<sub>3</sub>) of **4a**



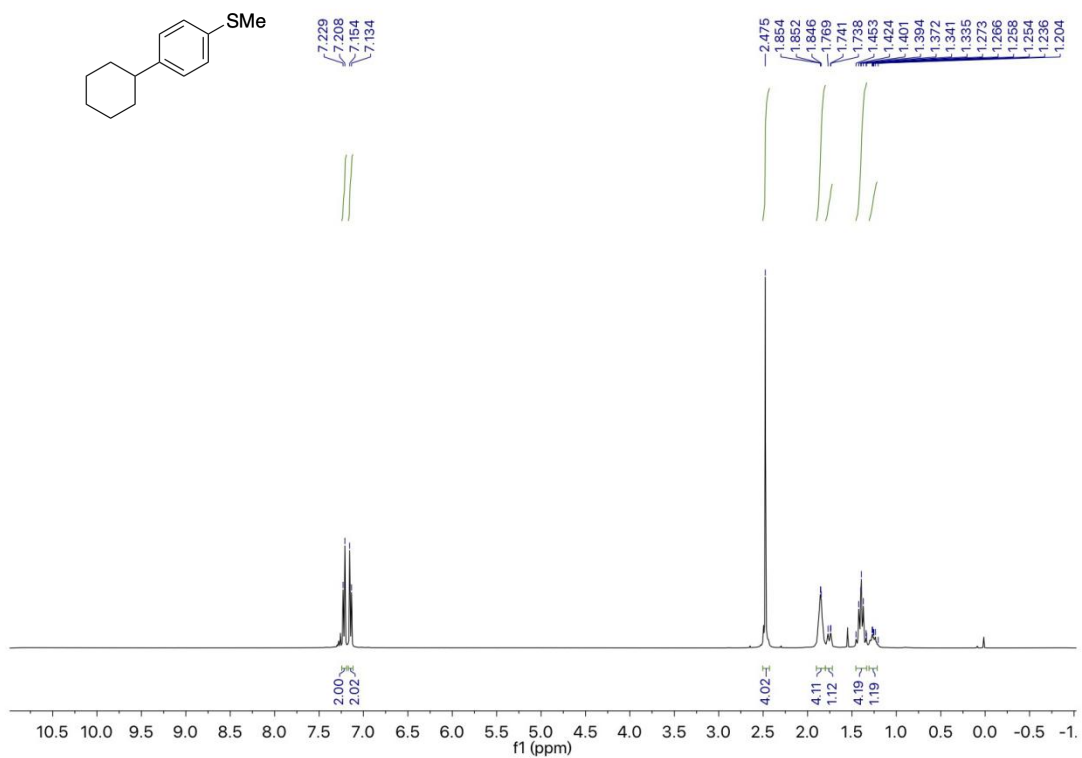
<sup>19</sup>F NMR spectrum (375 MHz, CDCl<sub>3</sub>) of **4b**



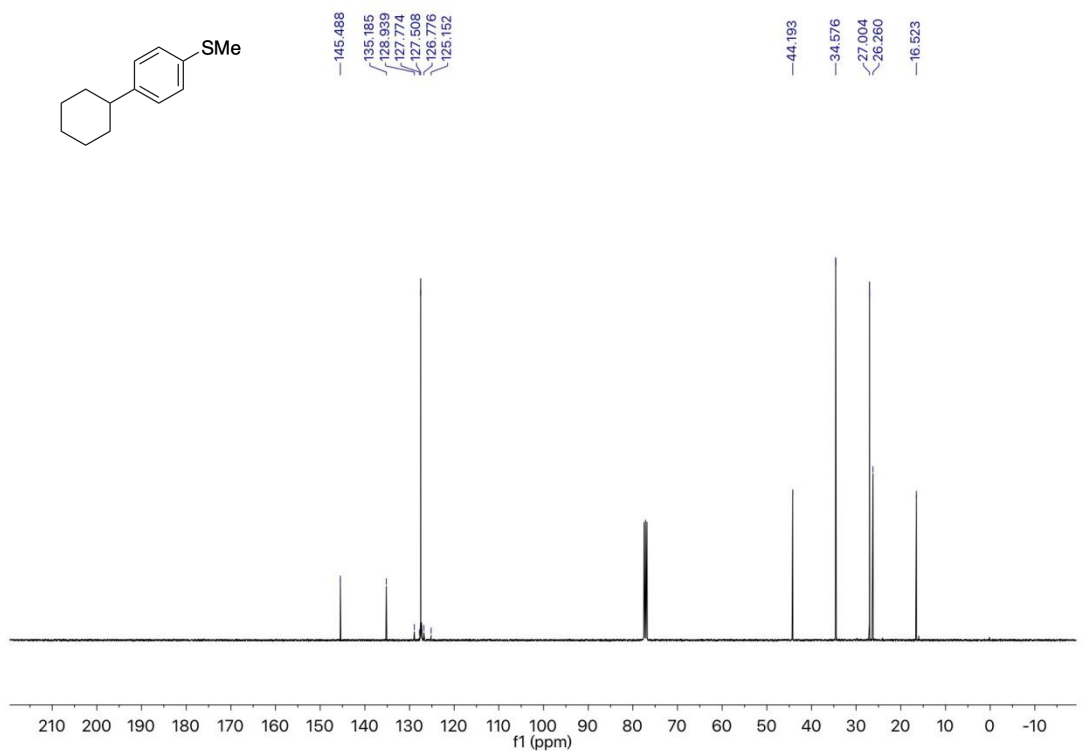
<sup>1</sup>H NMR spectrum (400 MHz, CDCl<sub>3</sub>) of **4b**



<sup>13</sup>C NMR spectrum (101 MHz, CDCl<sub>3</sub>) of **4b**

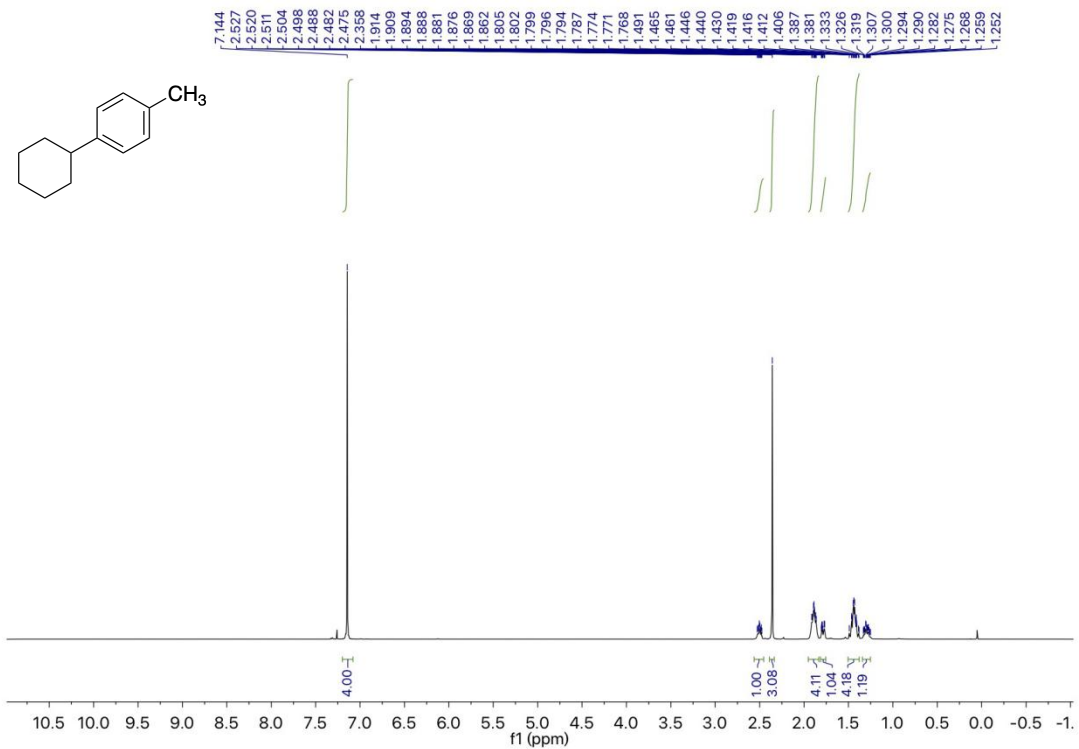


$^1\text{H}$  NMR spectrum (400 MHz,  $\text{CDCl}_3$ ) of **4c**

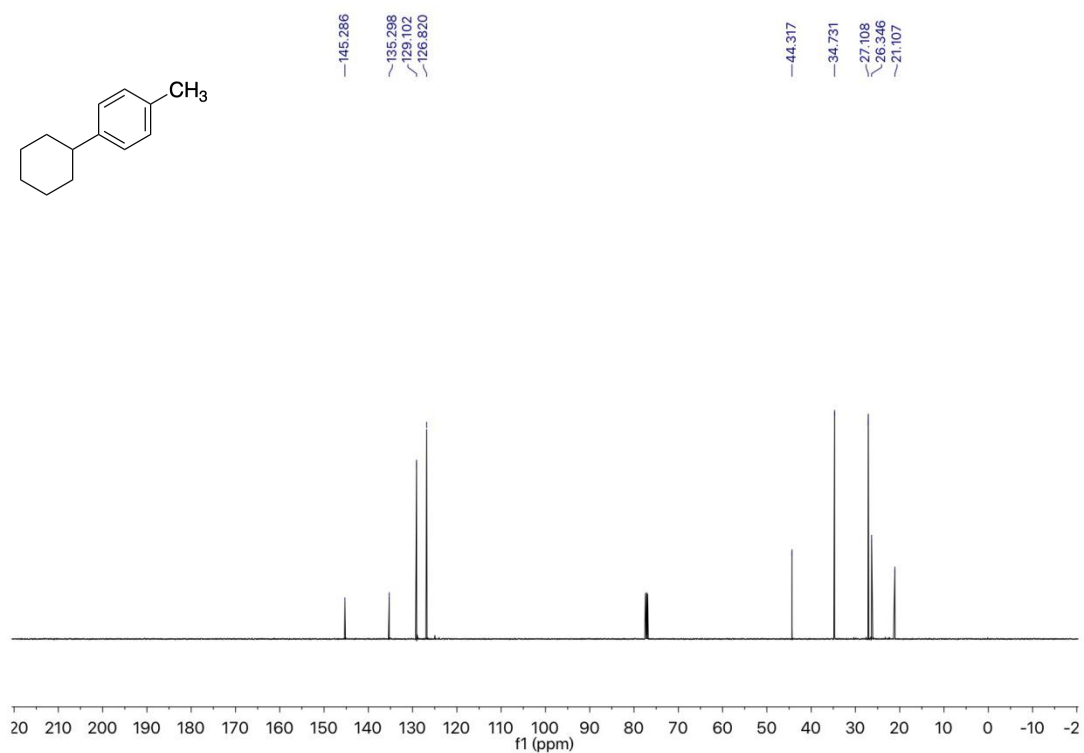


$^{13}\text{C}$  NMR spectrum (101 MHz,  $\text{CDCl}_3$ ) of **4c**

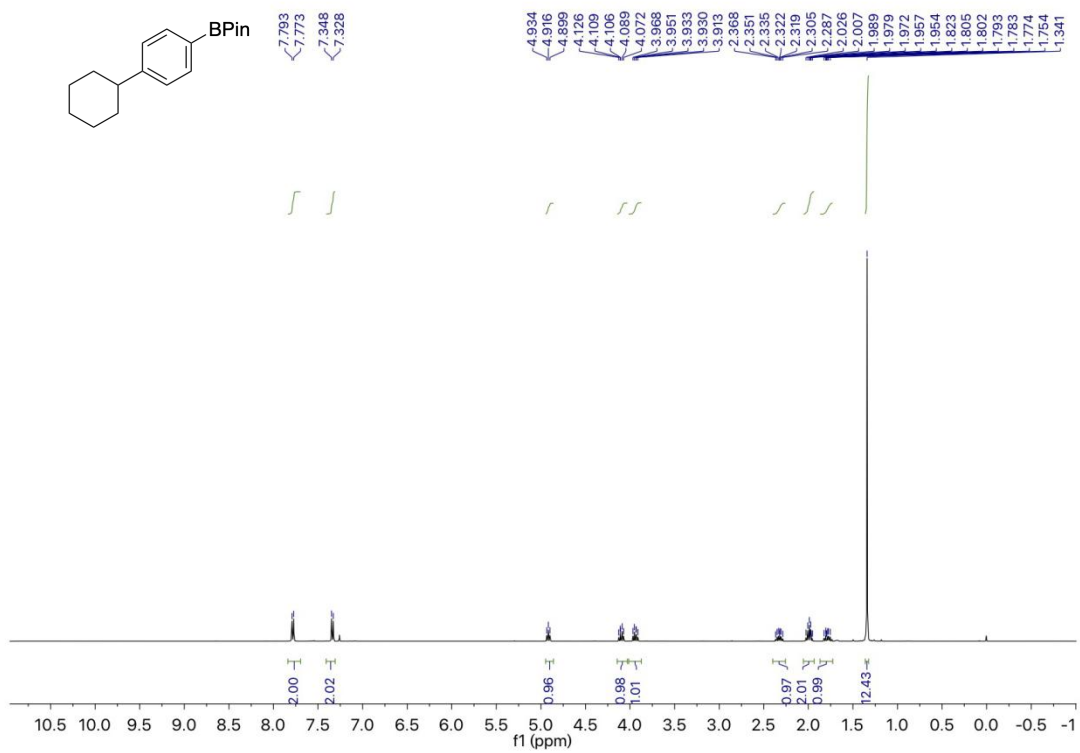




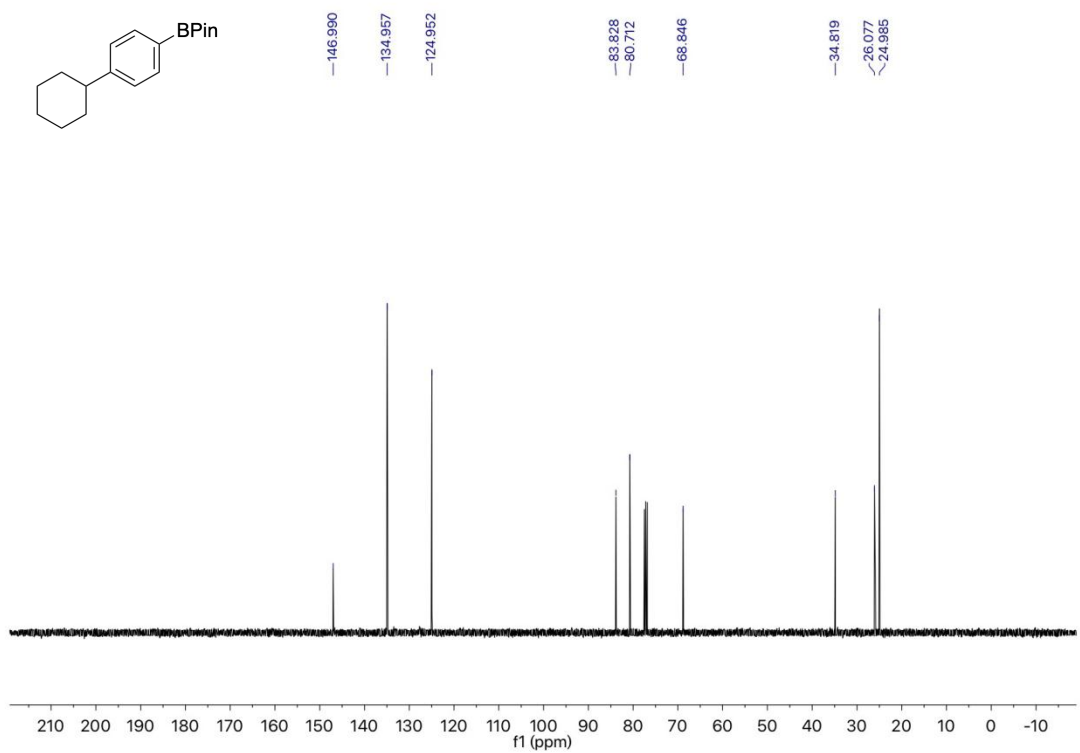
$^1\text{H}$  NMR spectrum (400 MHz,  $\text{CDCl}_3$ ) of **4d**



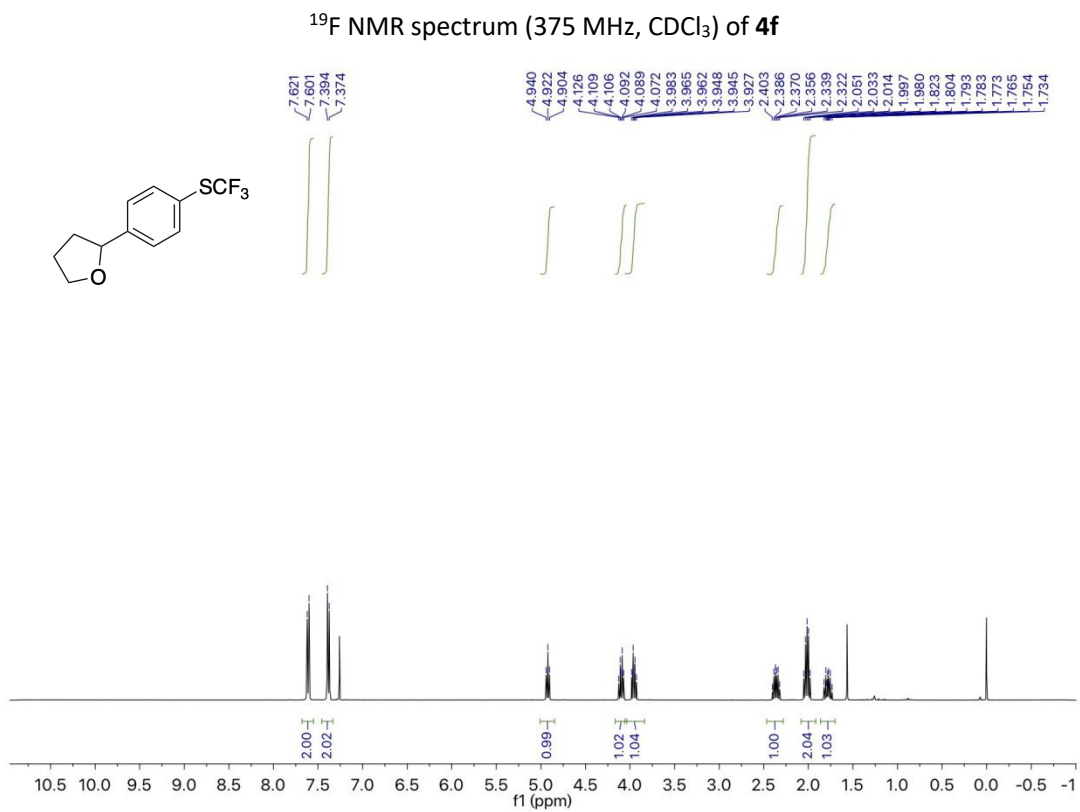
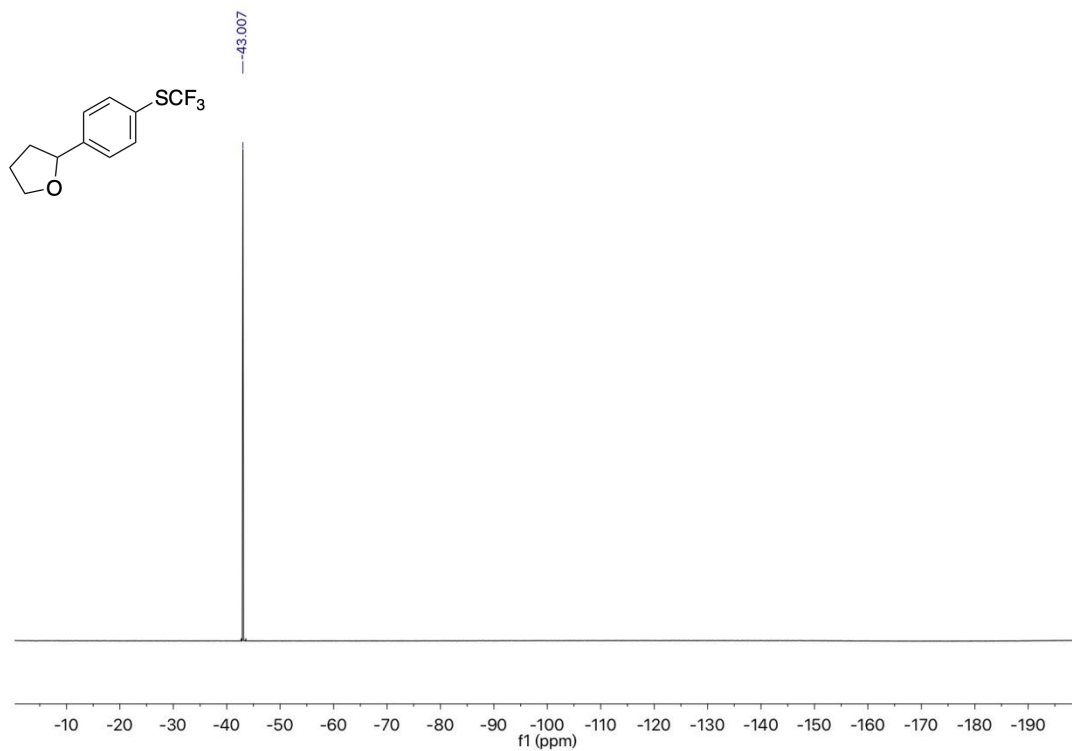
$^{13}\text{C}$  NMR spectrum (101 MHz,  $\text{CDCl}_3$ ) of **4d**



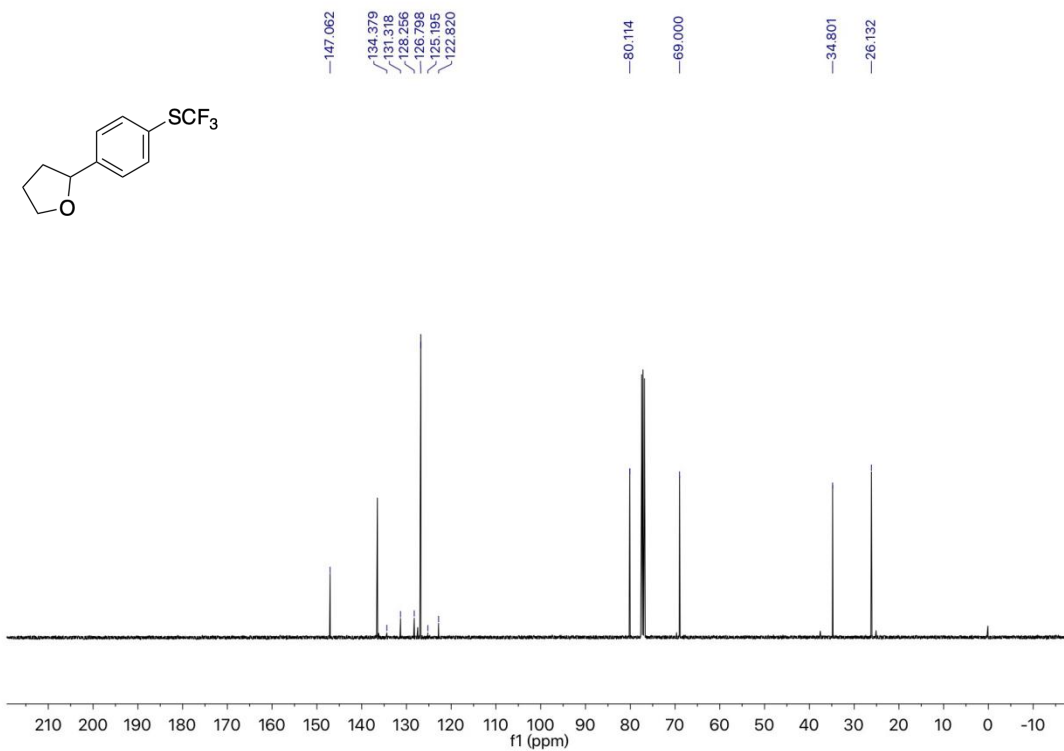
$^1\text{H}$  NMR spectrum (400 MHz,  $\text{CDCl}_3$ ) of **4e**



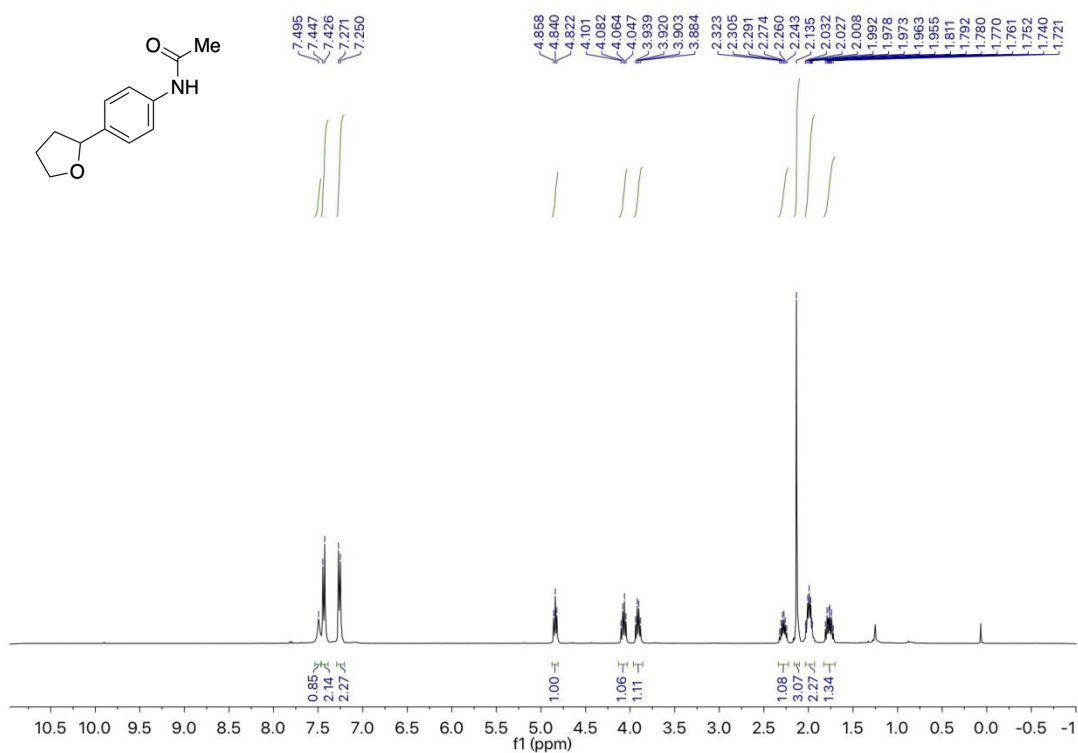
$^{13}\text{C}$  NMR spectrum (101 MHz,  $\text{CDCl}_3$ ) of **4e**



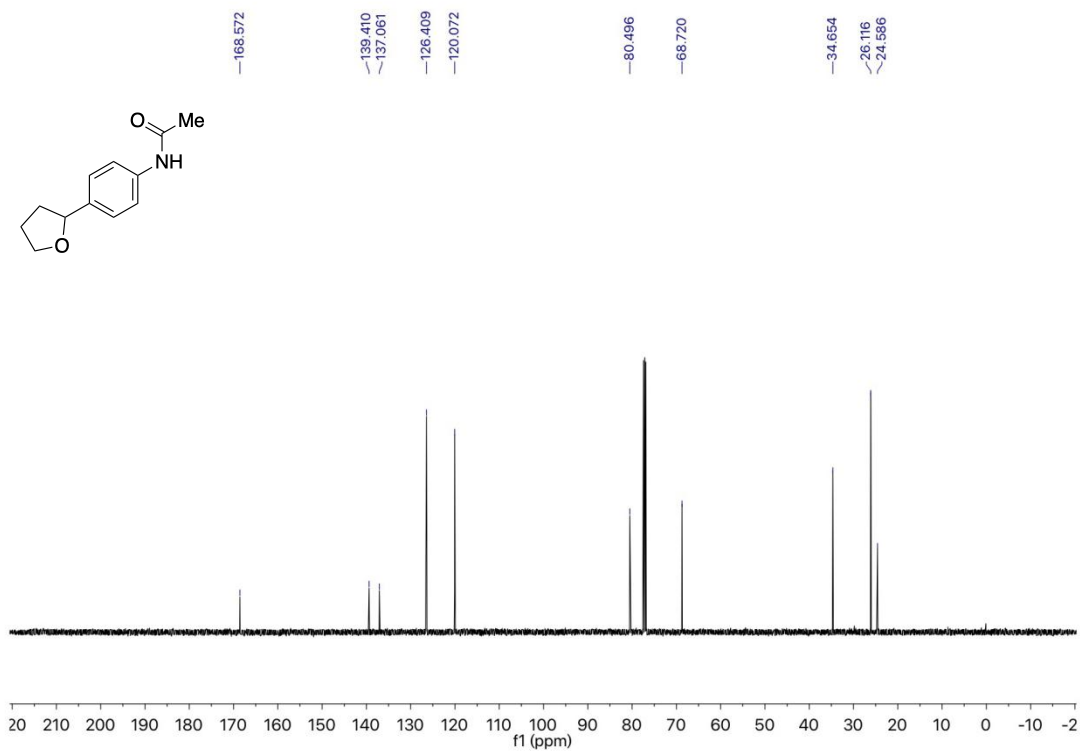
$^1\text{H}$  NMR spectrum (400 MHz,  $\text{CDCl}_3$ ) of **4f**



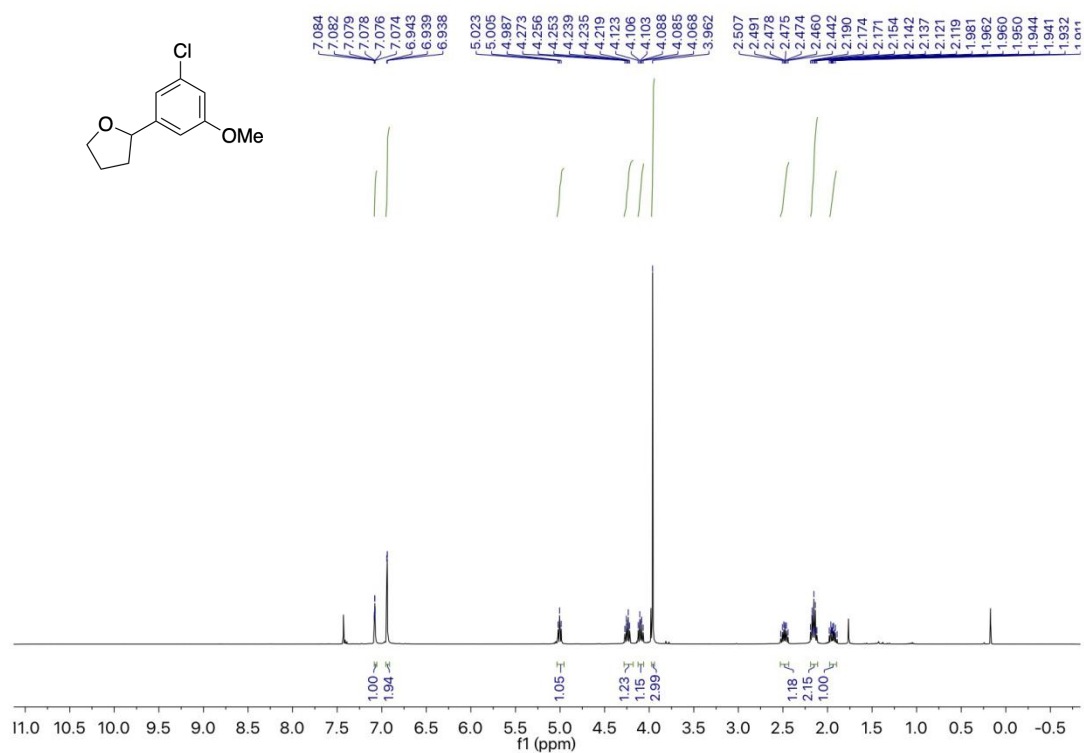
$^{13}\text{C}$  NMR spectrum (101 MHz,  $\text{CDCl}_3$ ) of **4f**



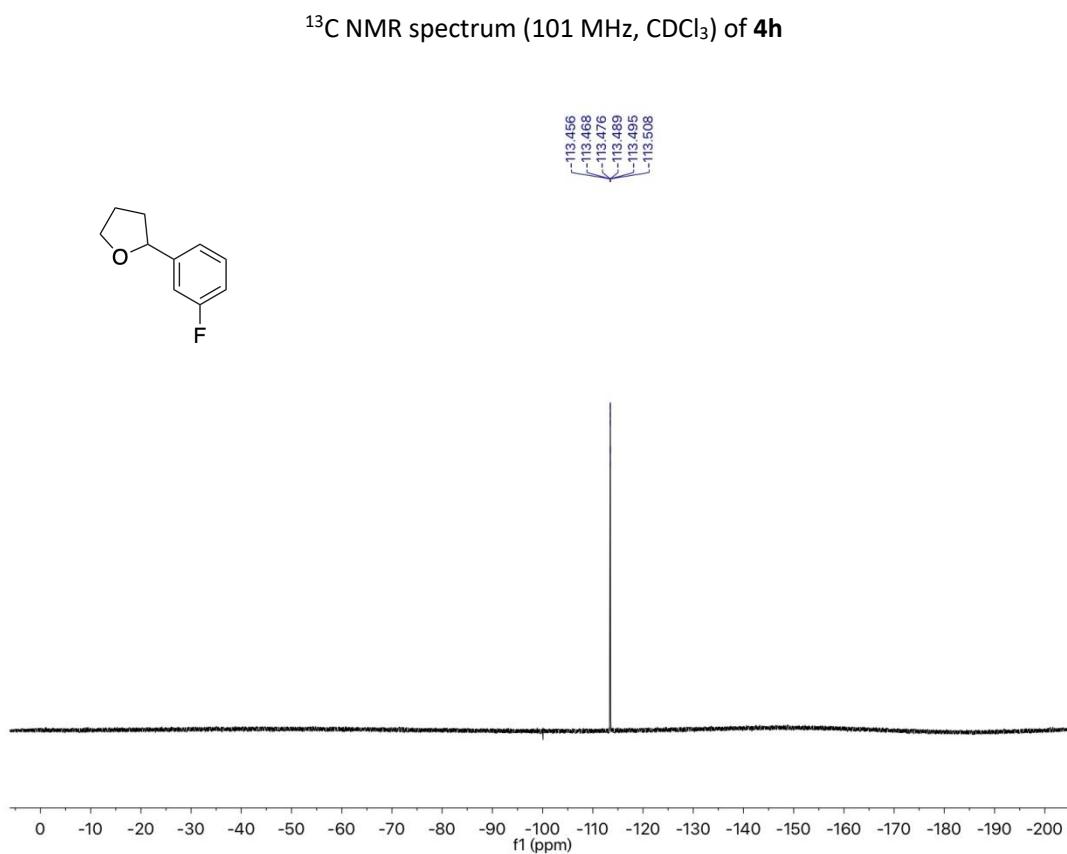
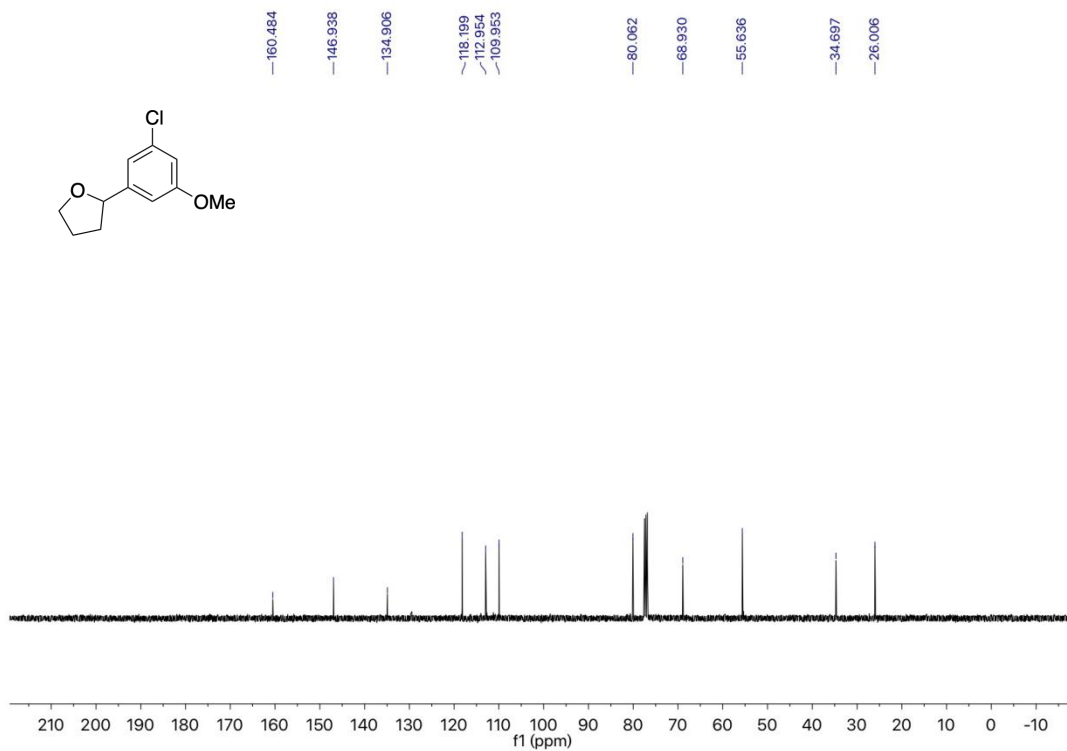
$^1\text{H}$  NMR spectrum (400 MHz,  $\text{CDCl}_3$ ) of **4g**



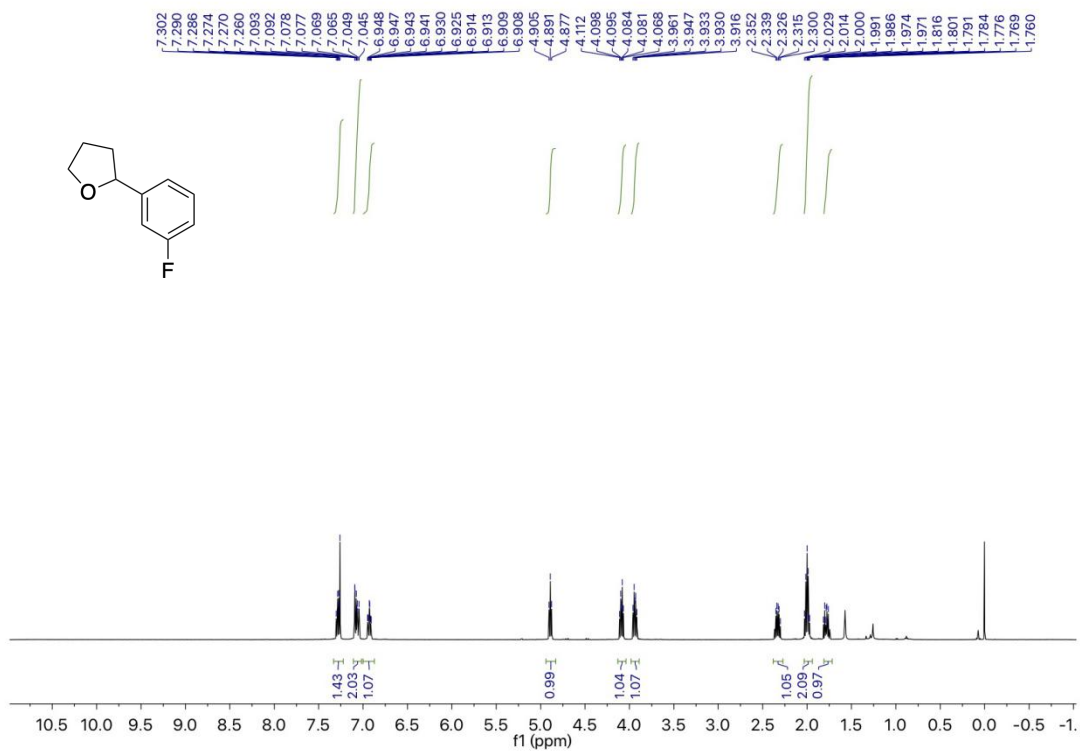
$^{13}\text{C}$  NMR spectrum (101 MHz,  $\text{CDCl}_3$ ) of **4g**



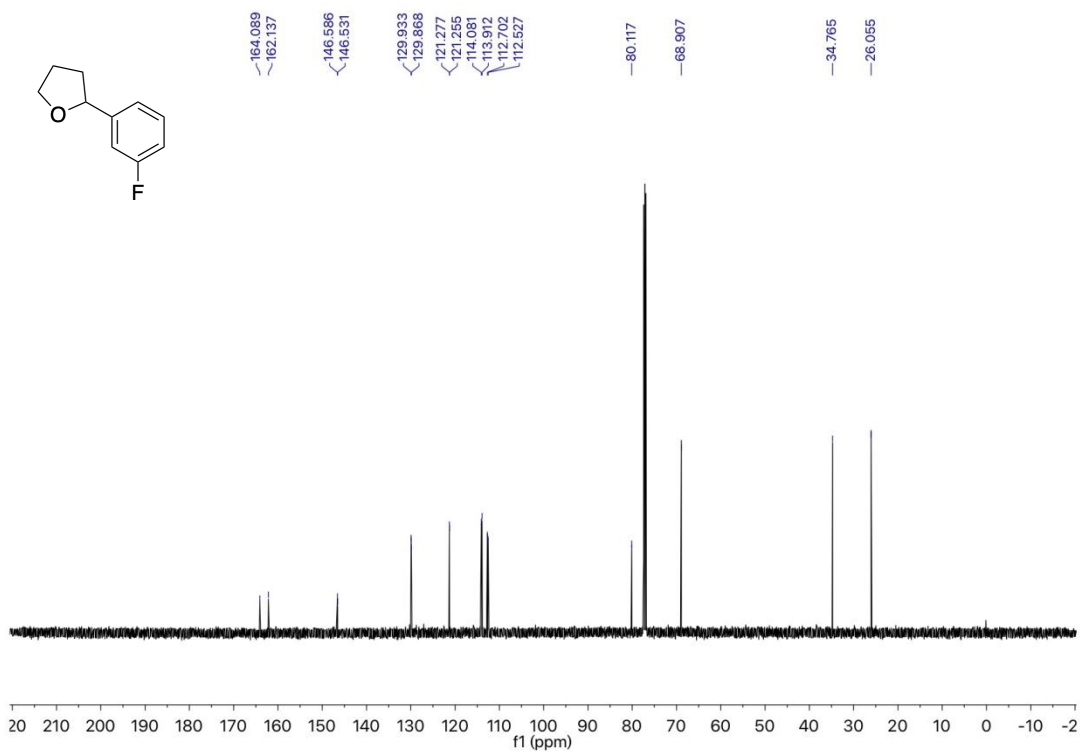
$^1\text{H}$  NMR spectrum (400 MHz,  $\text{CDCl}_3$ ) of **4h**



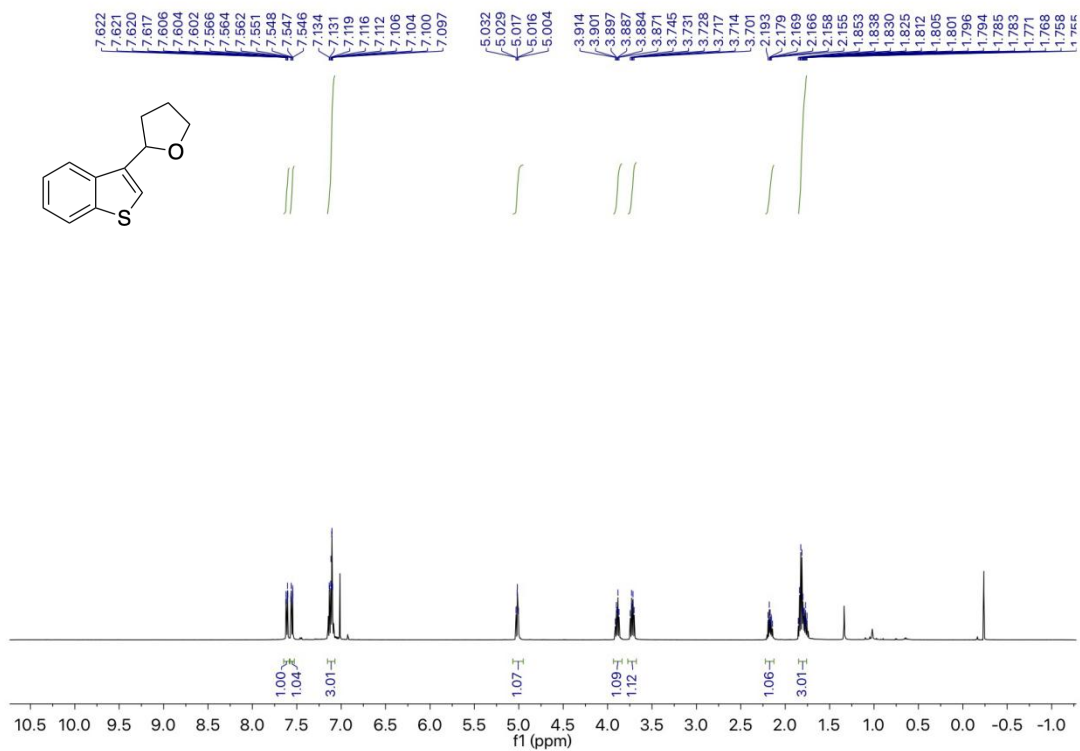
$^{19}\text{F}$  NMR spectrum (375 MHz,  $\text{CDCl}_3$ ) of **4i**



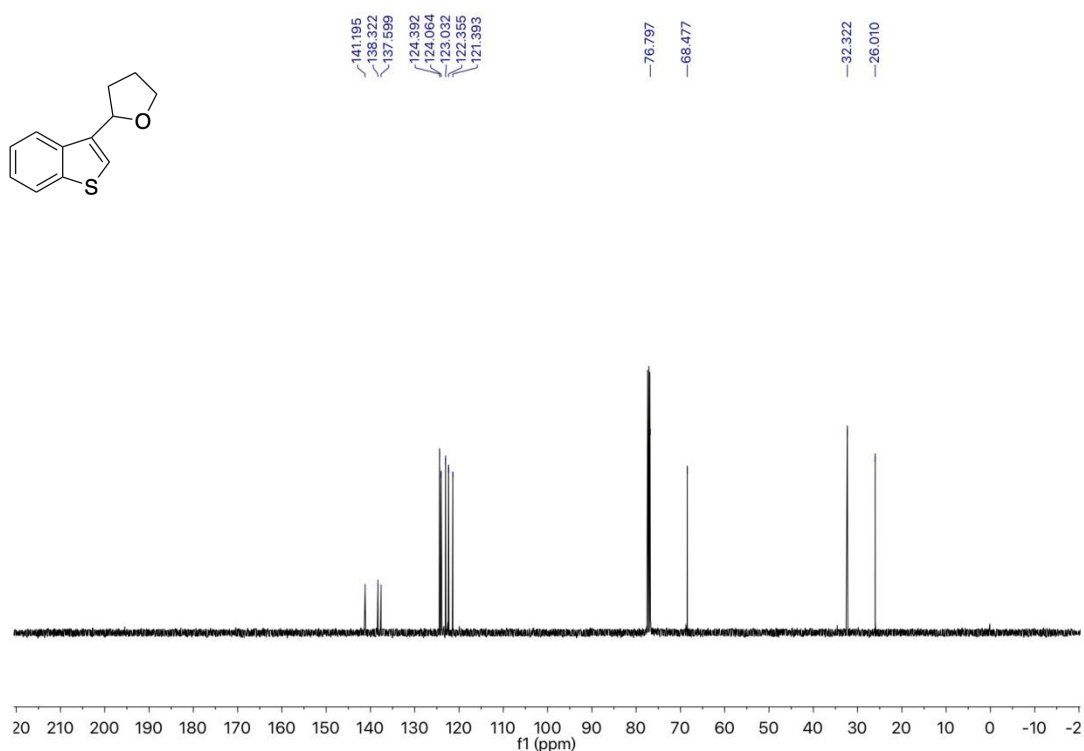
**<sup>1</sup>H NMR spectrum (400 MHz, CDCl<sub>3</sub>) of 4i**



**<sup>13</sup>C NMR spectrum (101 MHz, CDCl<sub>3</sub>) of 4i**

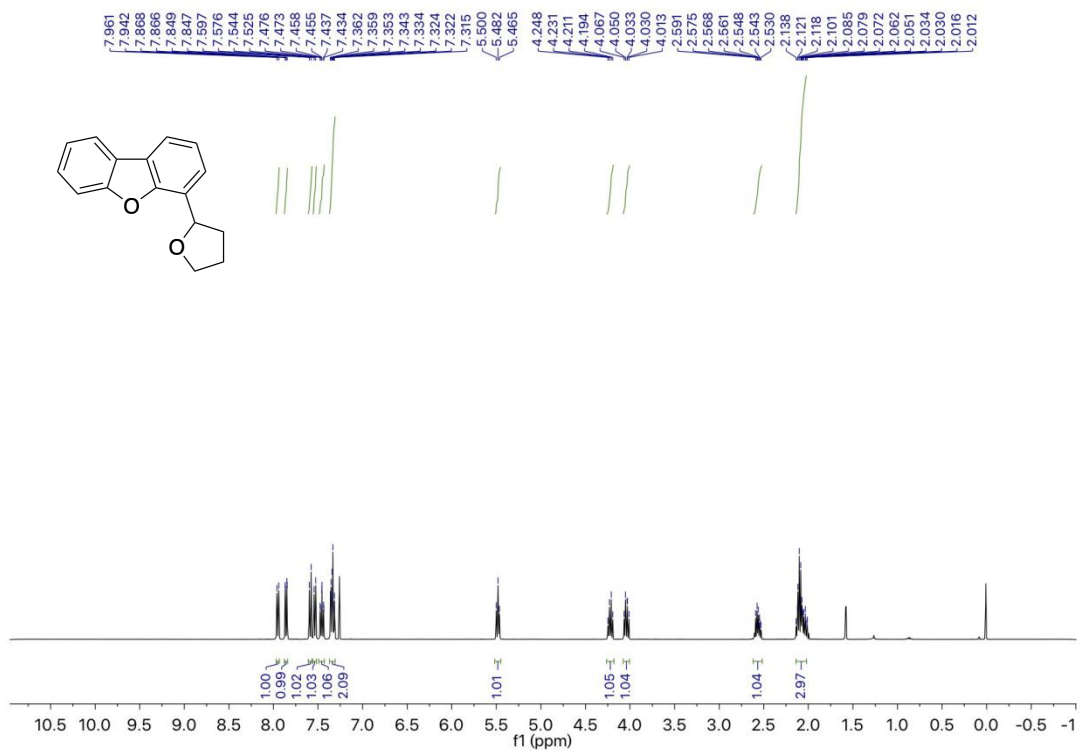


**<sup>1</sup>H NMR spectrum (400 MHz, CDCl<sub>3</sub>) of 4j**

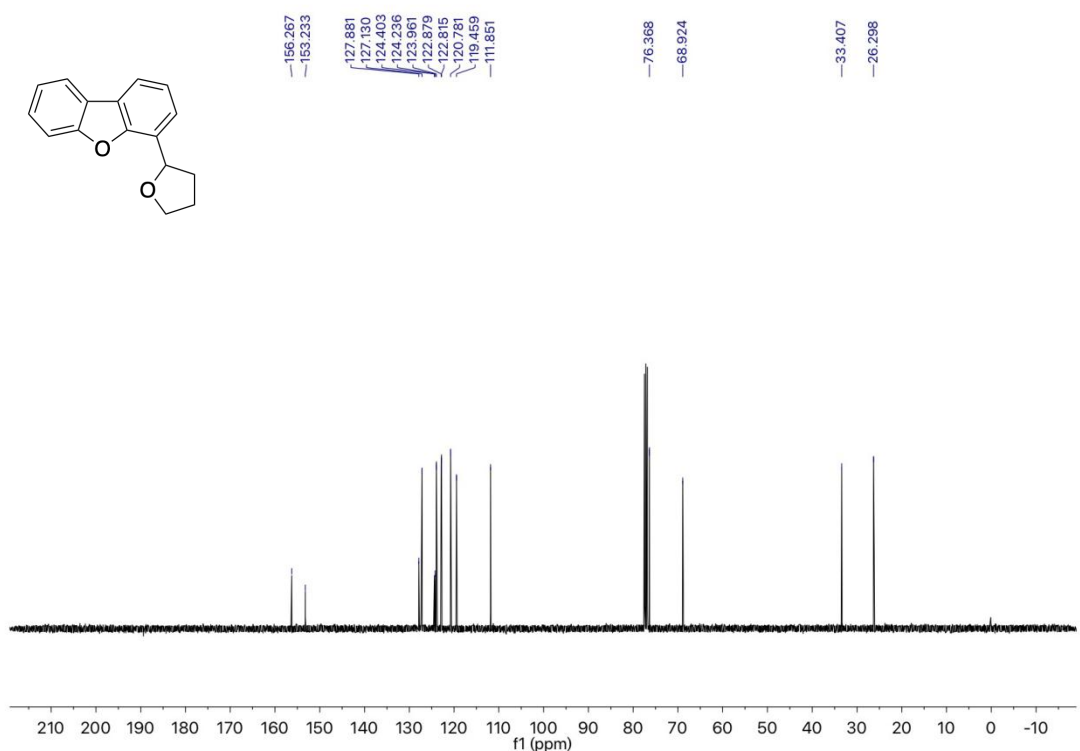


**<sup>13</sup>C NMR spectrum (101 MHz, CDCl<sub>3</sub>) of 4j**

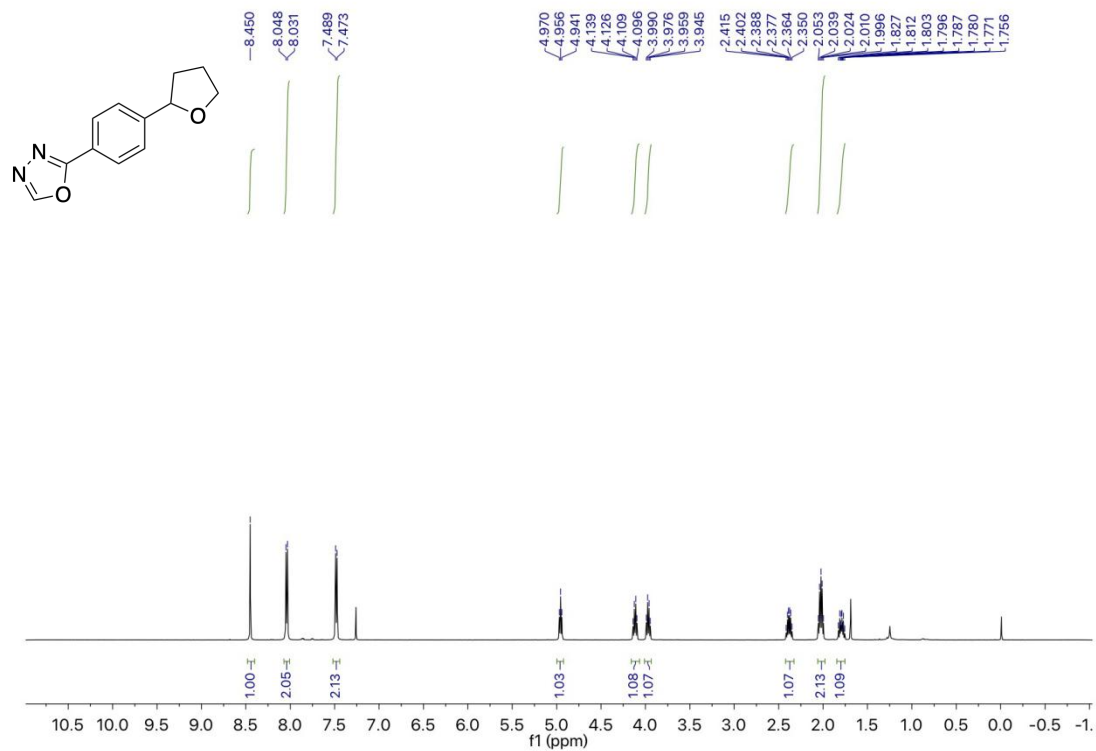




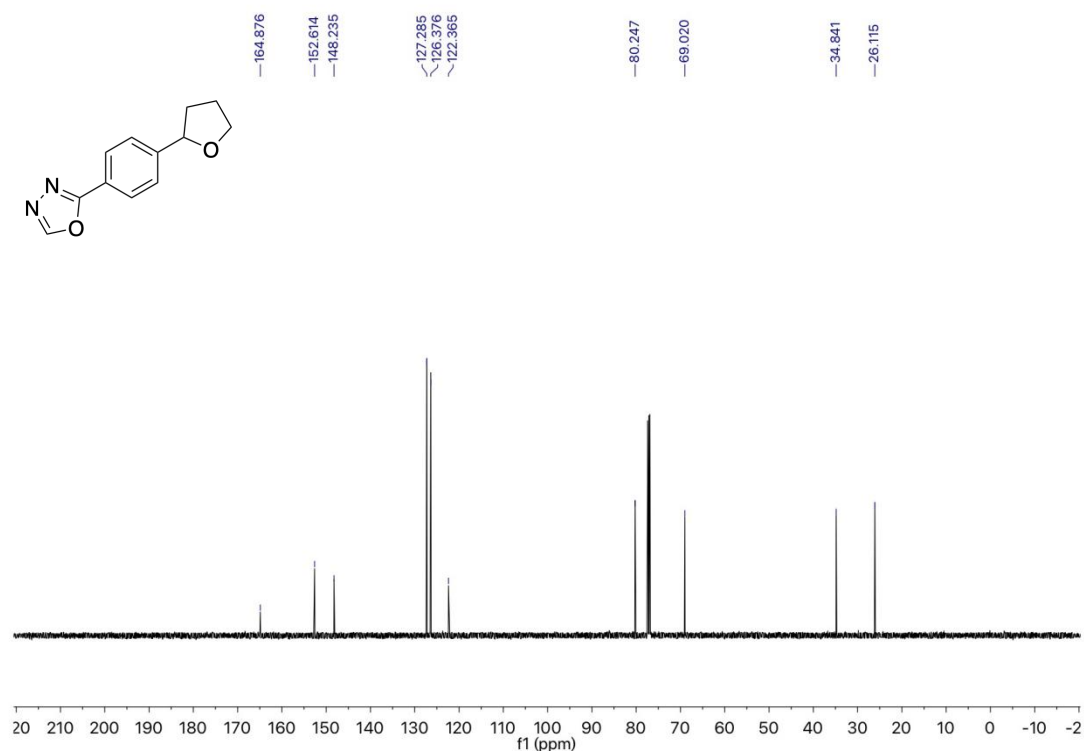
<sup>1</sup>H NMR spectrum (400 MHz, CDCl<sub>3</sub>) of 4k



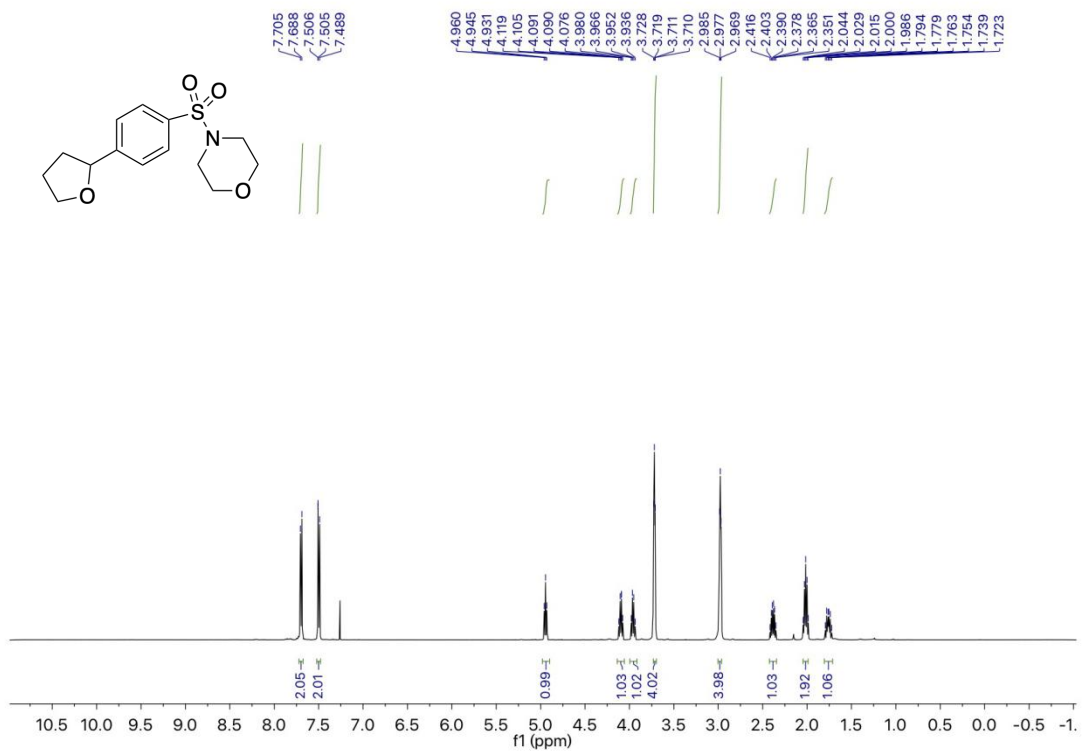
<sup>13</sup>C NMR spectrum (101 MHz, CDCl<sub>3</sub>) of 4k



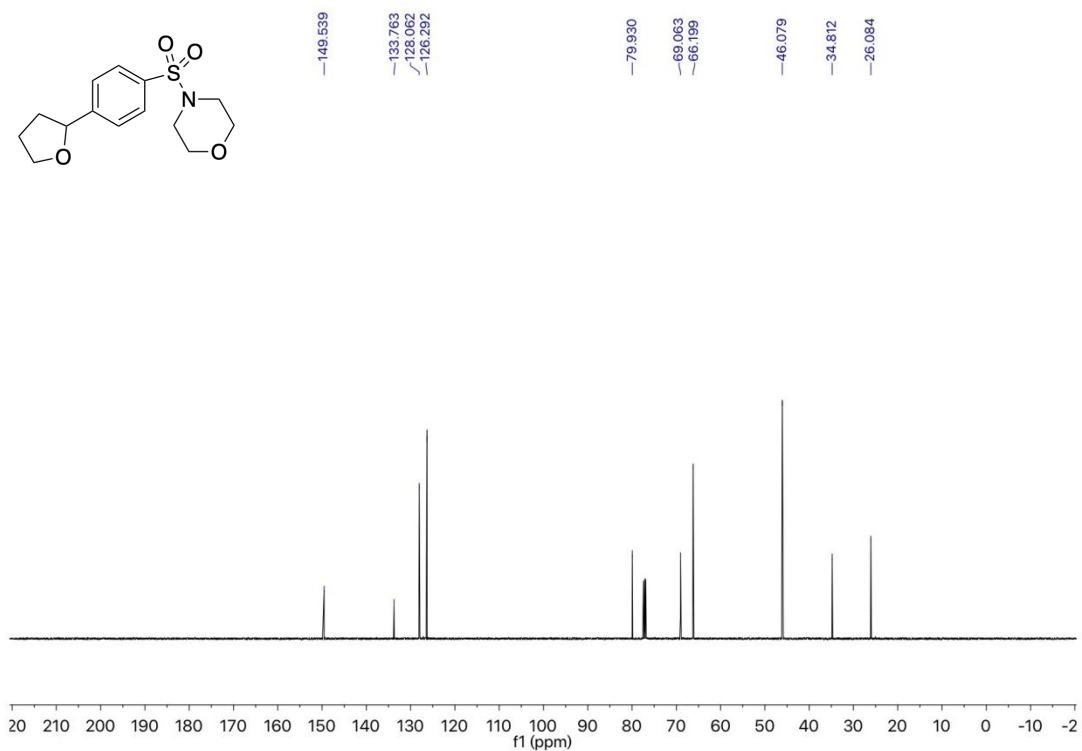
$^1\text{H}$  NMR spectrum (500 MHz,  $\text{CDCl}_3$ ) of **4I**



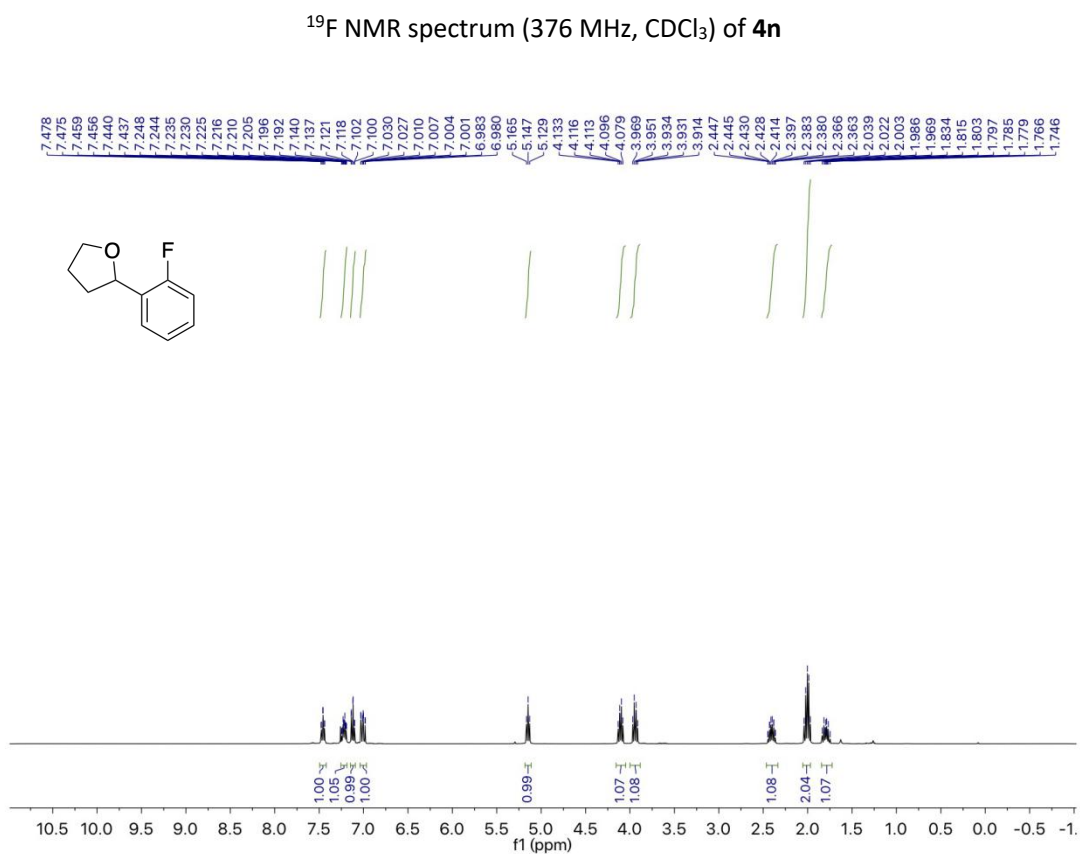
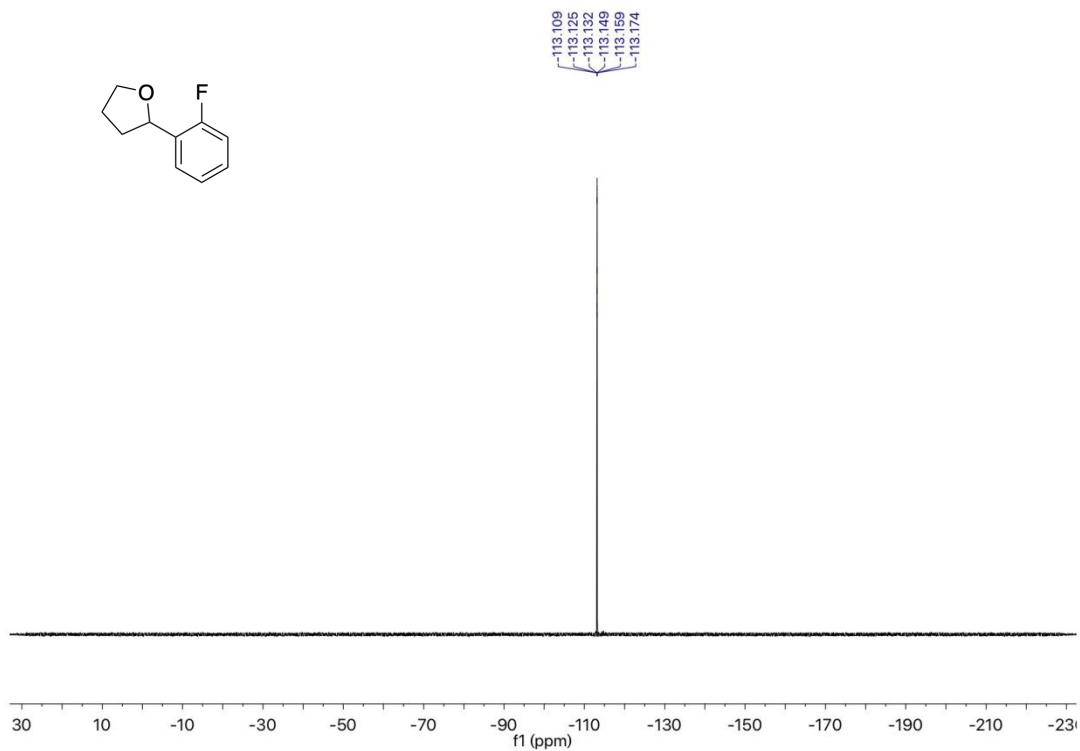
$^{13}\text{C}$  NMR spectrum (126 MHz,  $\text{CDCl}_3$ ) of **4I**

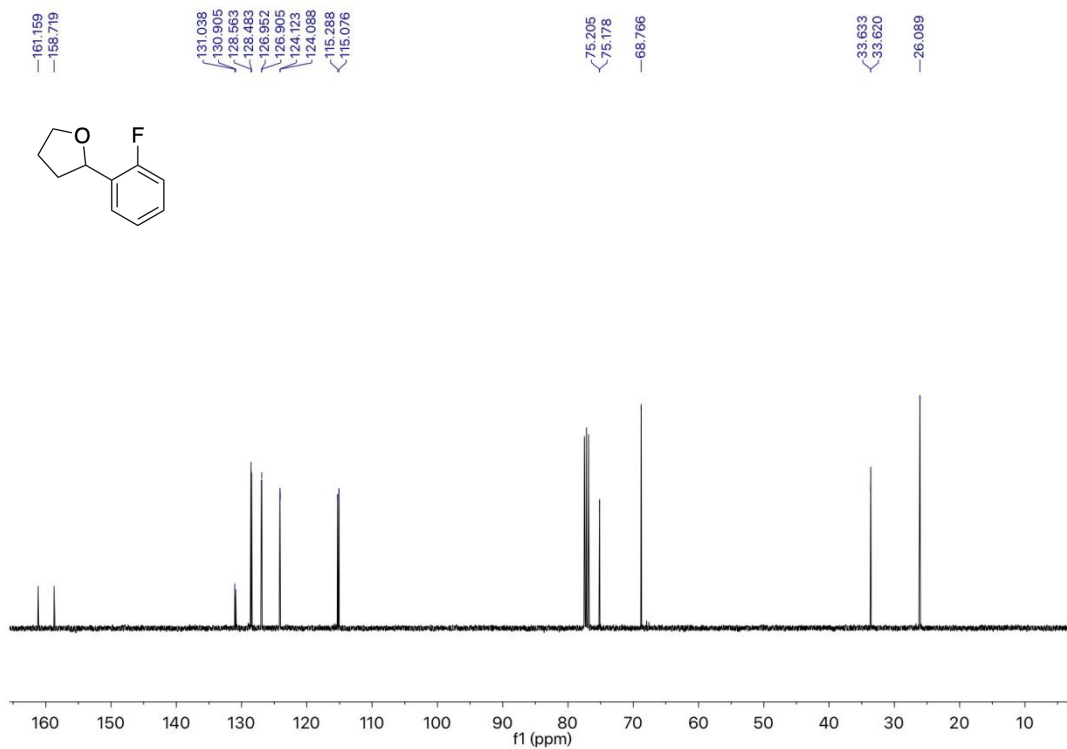


**<sup>1</sup>H NMR spectrum (400 MHz, CDCl<sub>3</sub>) of **4m****

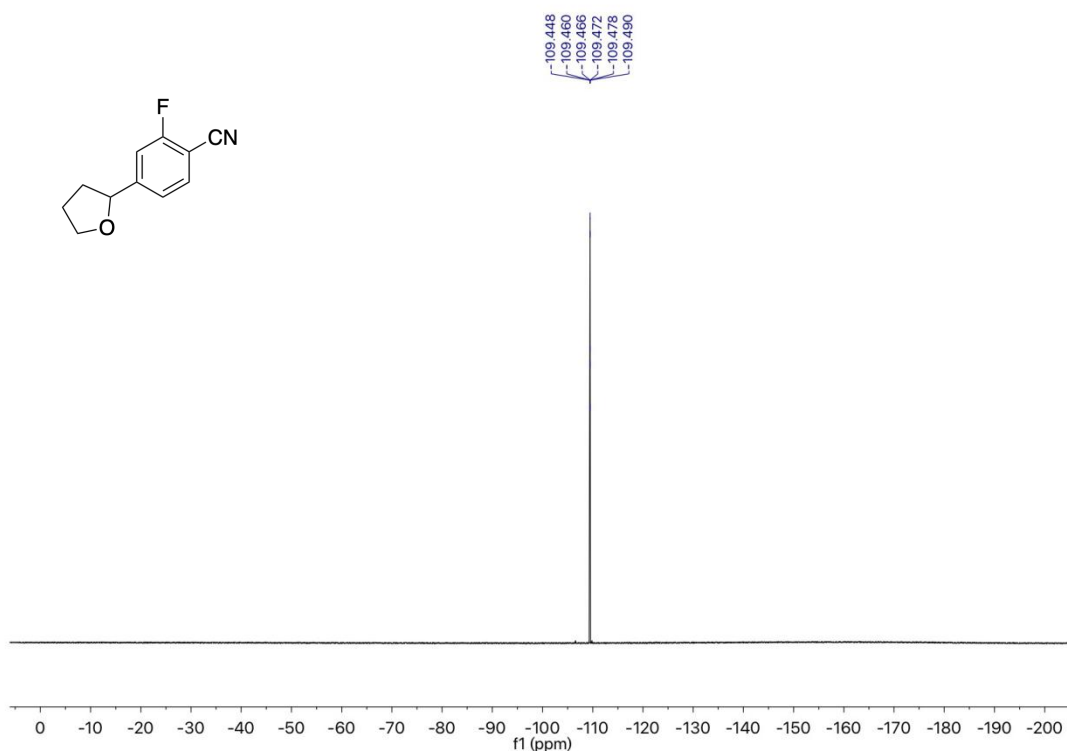


**<sup>13</sup>C NMR spectrum (101 MHz, CDCl<sub>3</sub>) of **4m****

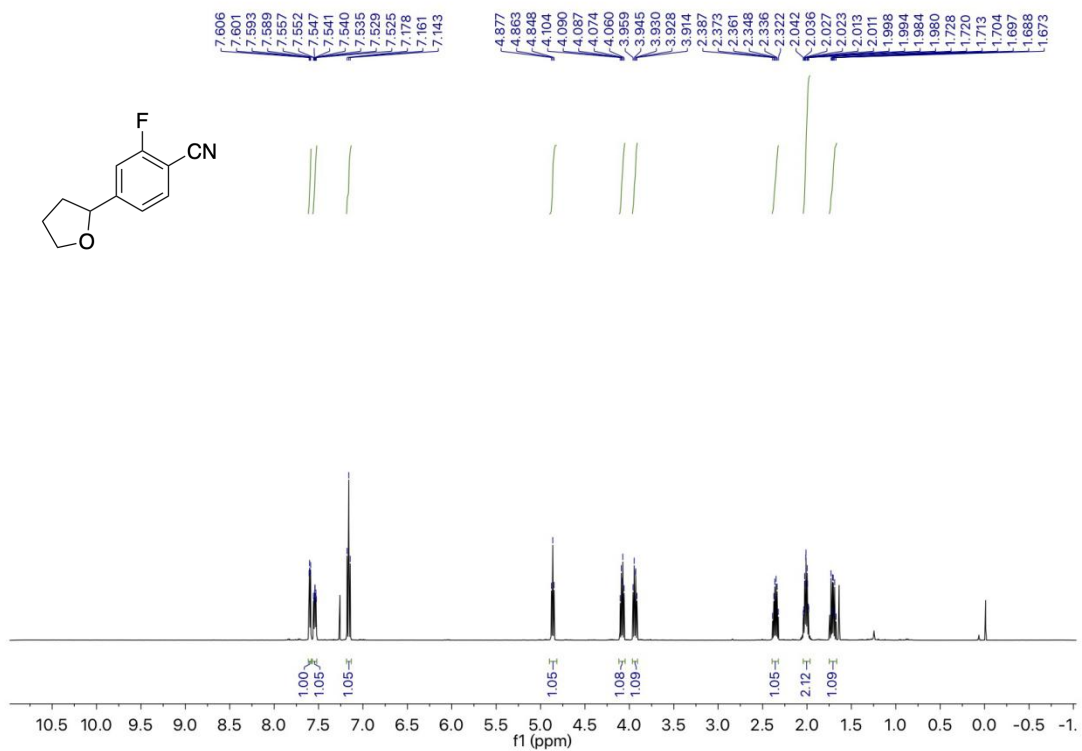




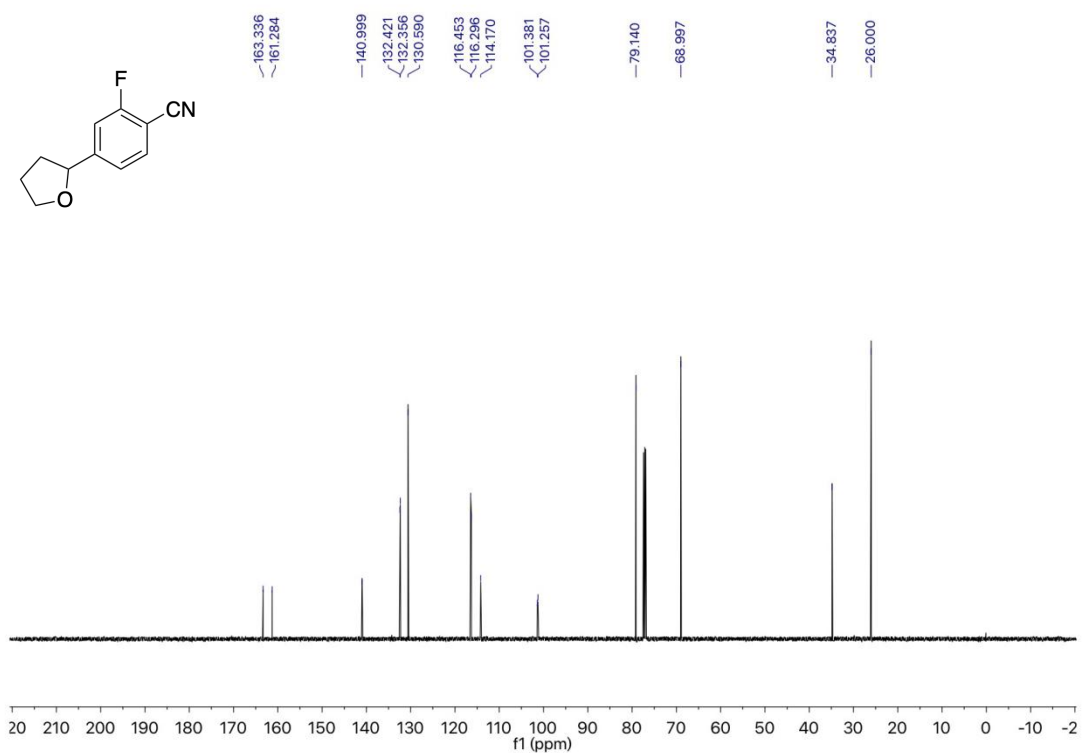
<sup>13</sup>C NMR spectrum (101 MHz, CDCl<sub>3</sub>) of **4n**



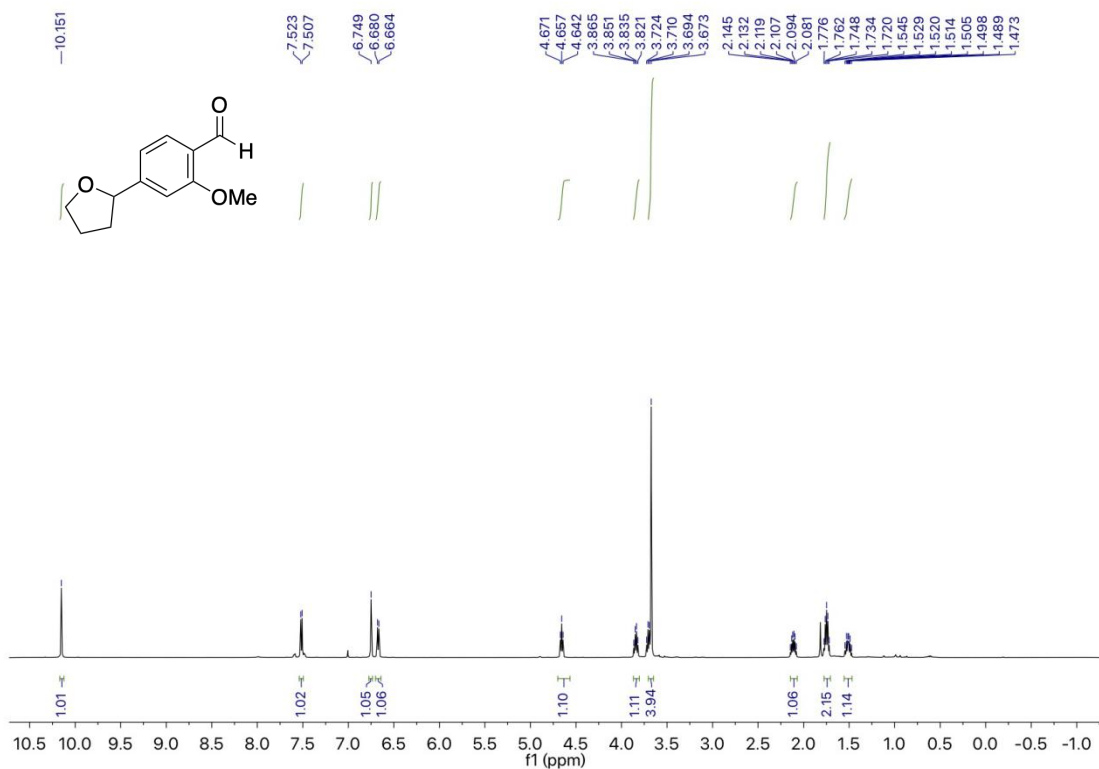
<sup>19</sup>F NMR spectrum (471 MHz, CDCl<sub>3</sub>) of **4o**



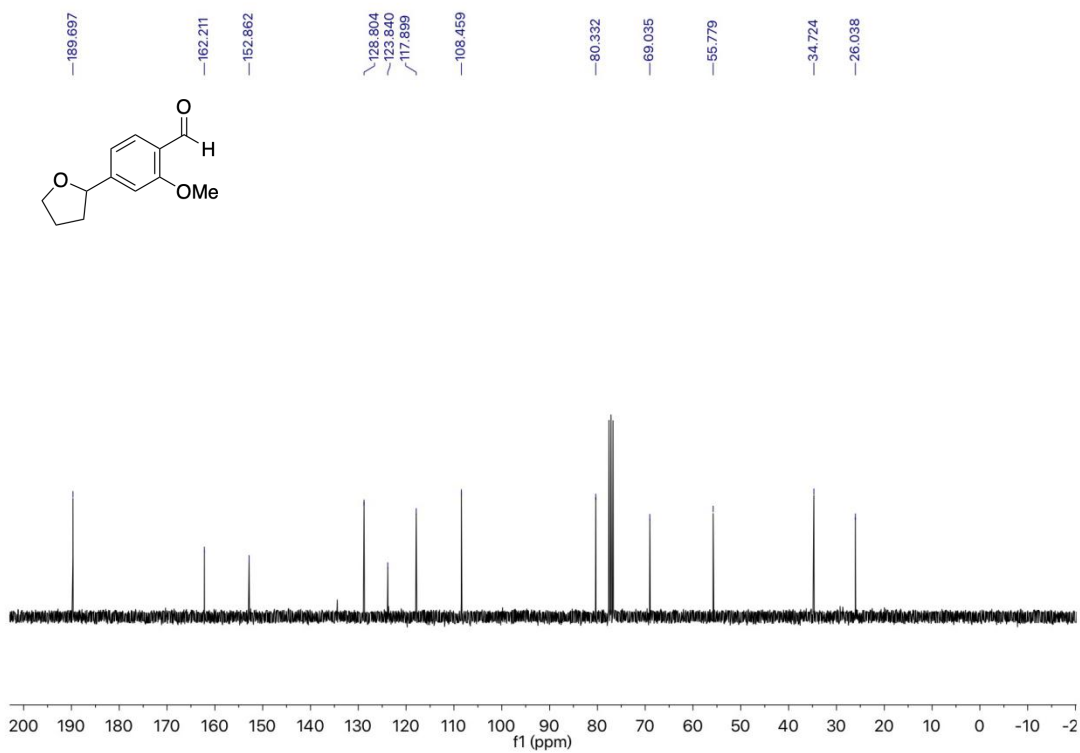
**<sup>1</sup>H NMR spectrum (500 MHz, CDCl<sub>3</sub>) of **4o****



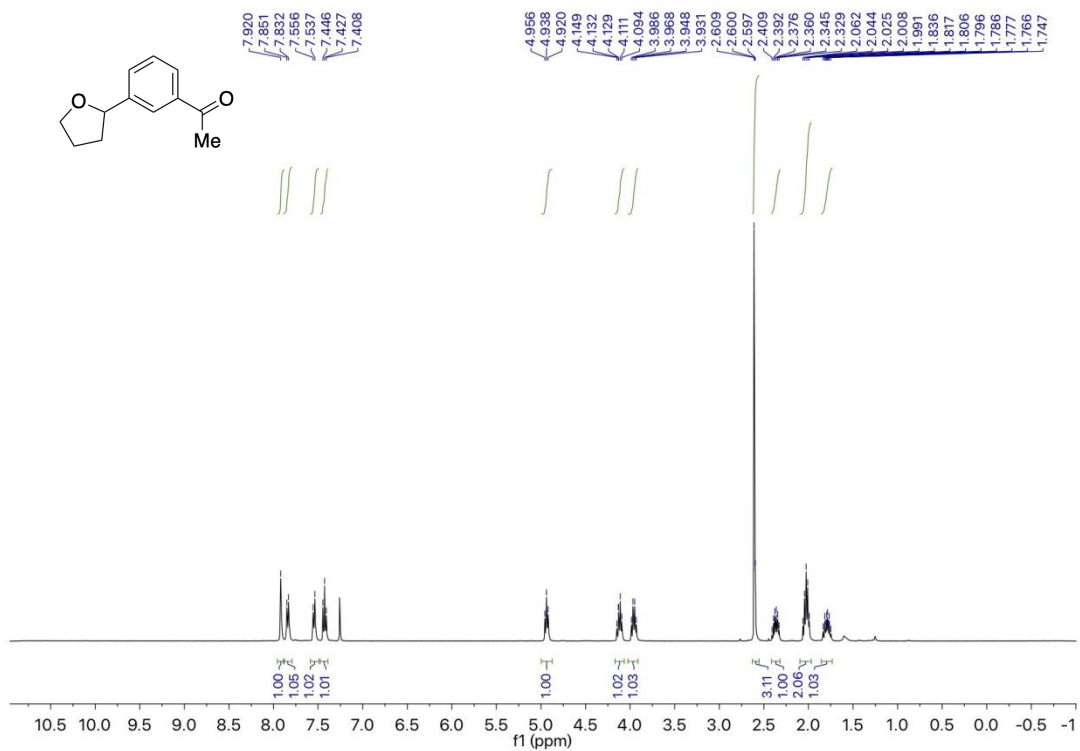
**<sup>13</sup>C NMR spectrum (126 MHz, CDCl<sub>3</sub>) of **4o****



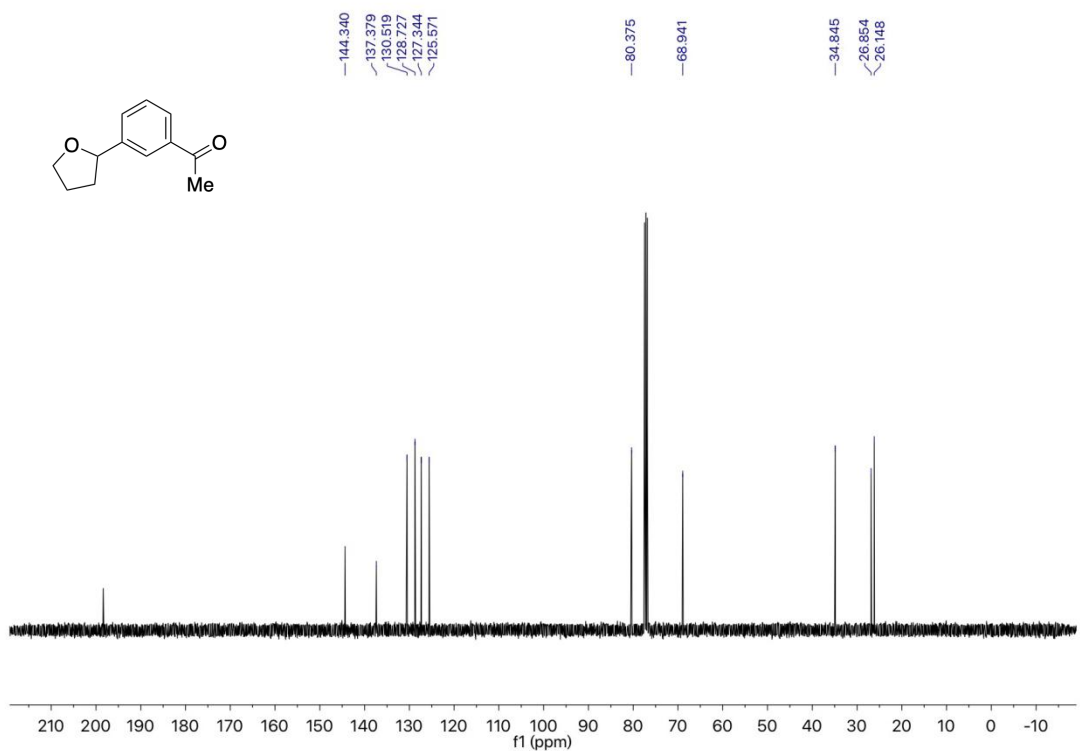
<sup>1</sup>H NMR spectrum (400 MHz, CDCl<sub>3</sub>) of **4p**



<sup>13</sup>C NMR spectrum (75 MHz, CDCl<sub>3</sub>) of **4p**

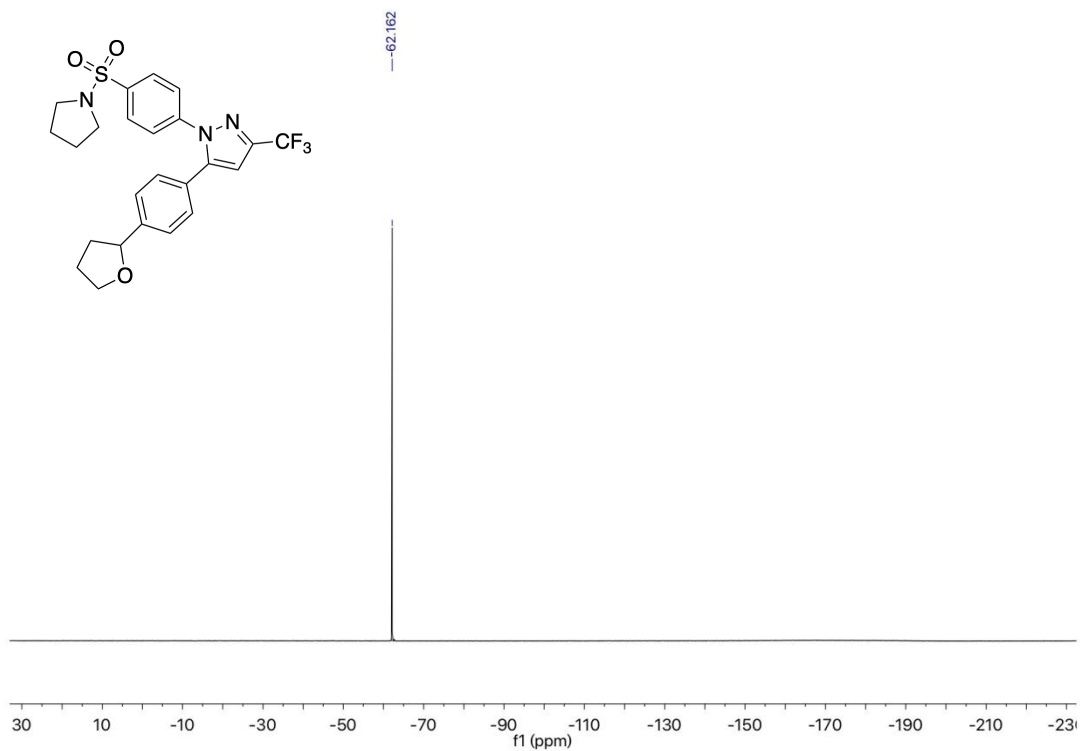


<sup>1</sup>H NMR spectrum (400 MHz, CDCl<sub>3</sub>) of **4q**

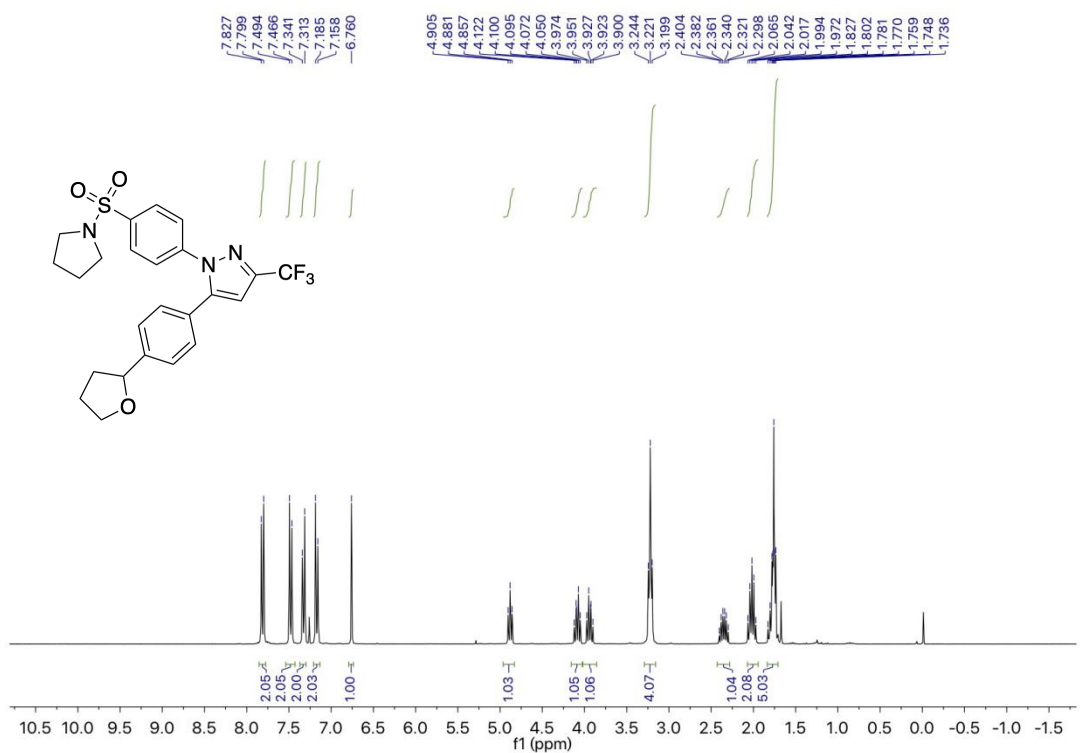


<sup>13</sup>C NMR spectrum (101 MHz, CDCl<sub>3</sub>) of **4q**

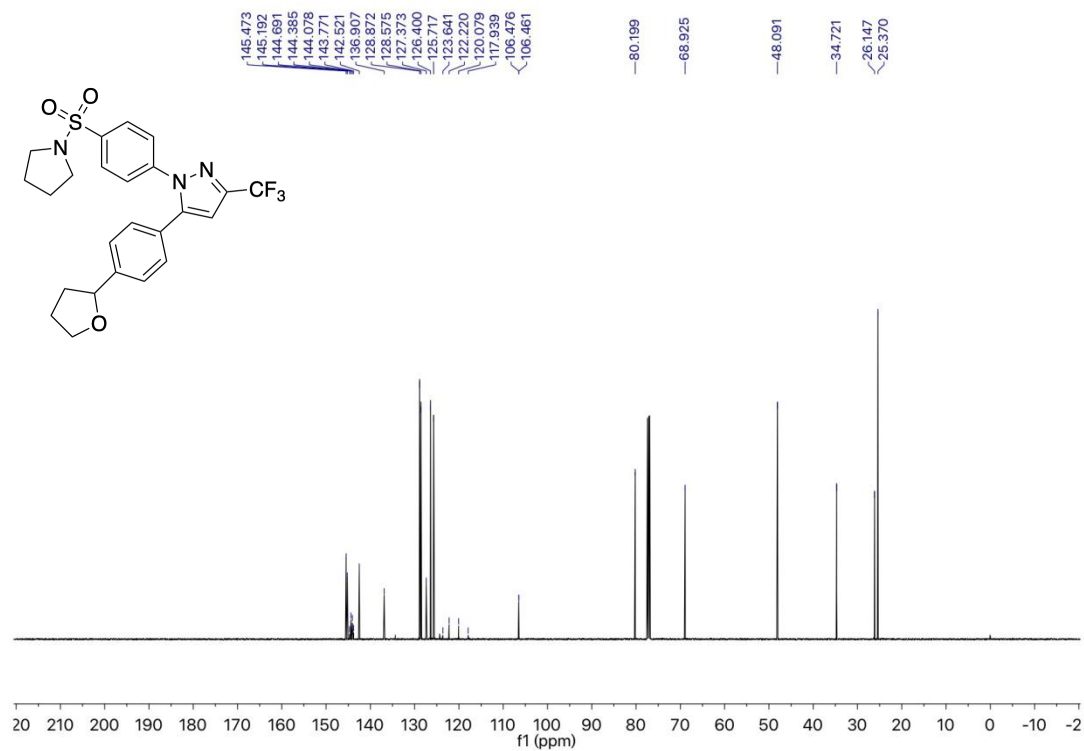




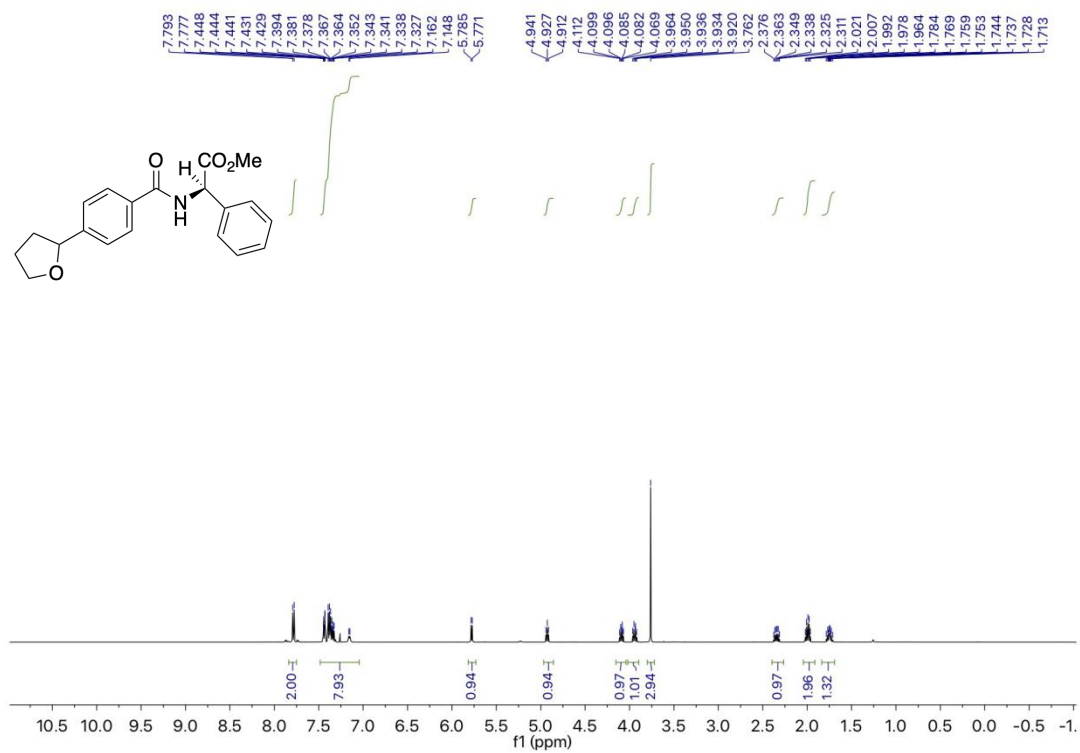
$^{19}\text{F}$  NMR spectrum (376 MHz,  $\text{CDCl}_3$ ) of **4r**



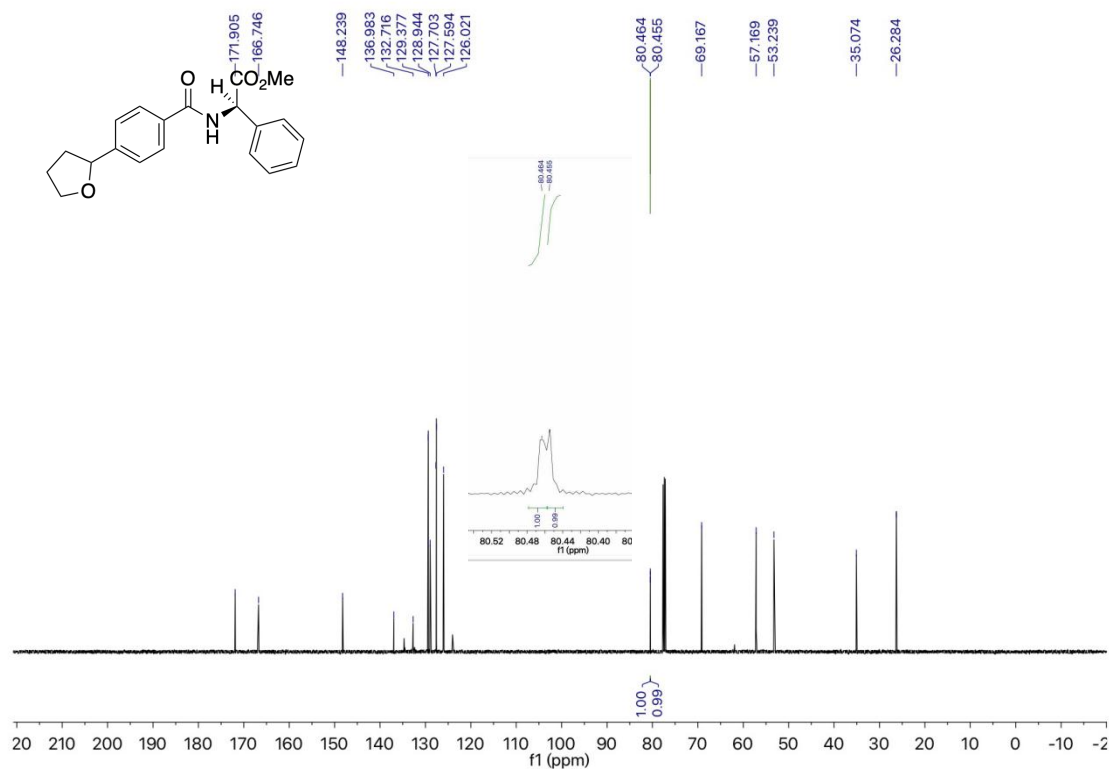
$^1\text{H}$  NMR spectrum (400 MHz,  $\text{CDCl}_3$ ) of **3r**



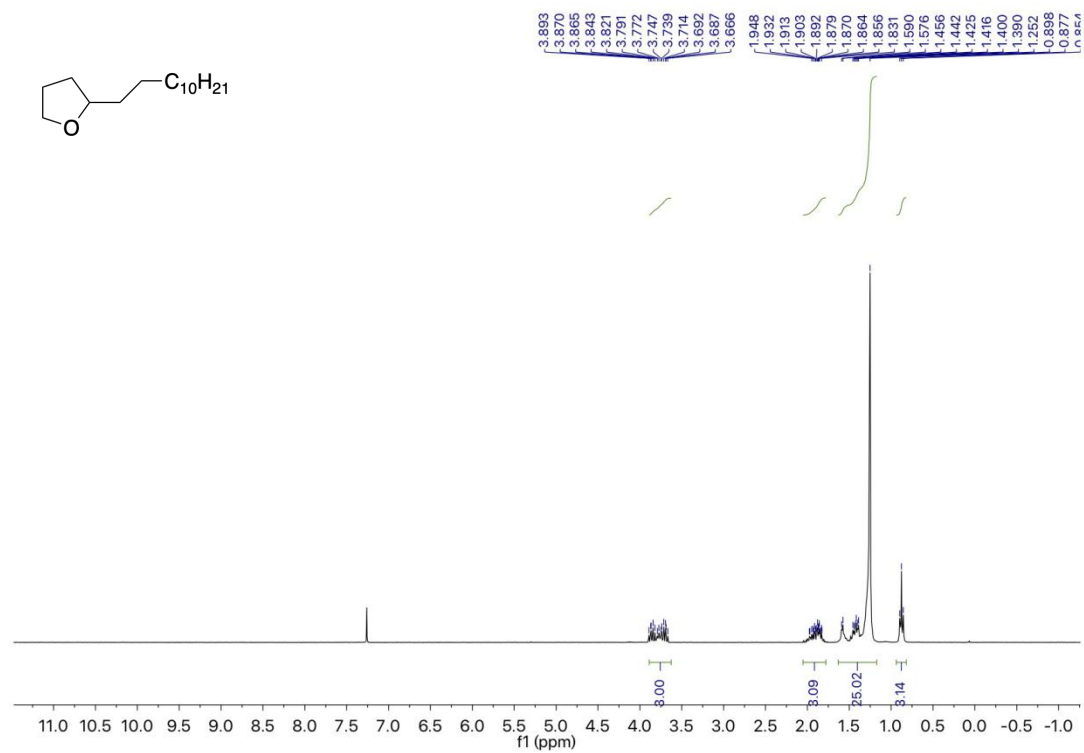
<sup>13</sup>C NMR spectrum (101 MHz, CDCl<sub>3</sub>) of **4r**



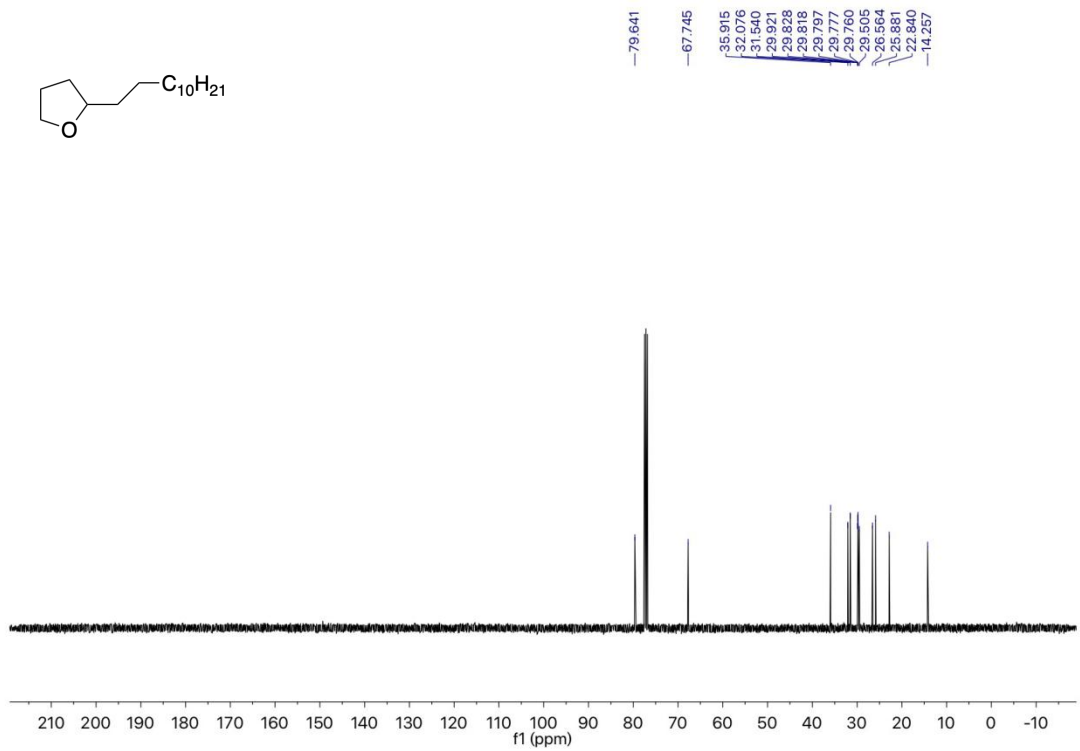
<sup>1</sup>H NMR spectrum (400 MHz, CDCl<sub>3</sub>) of **4s**



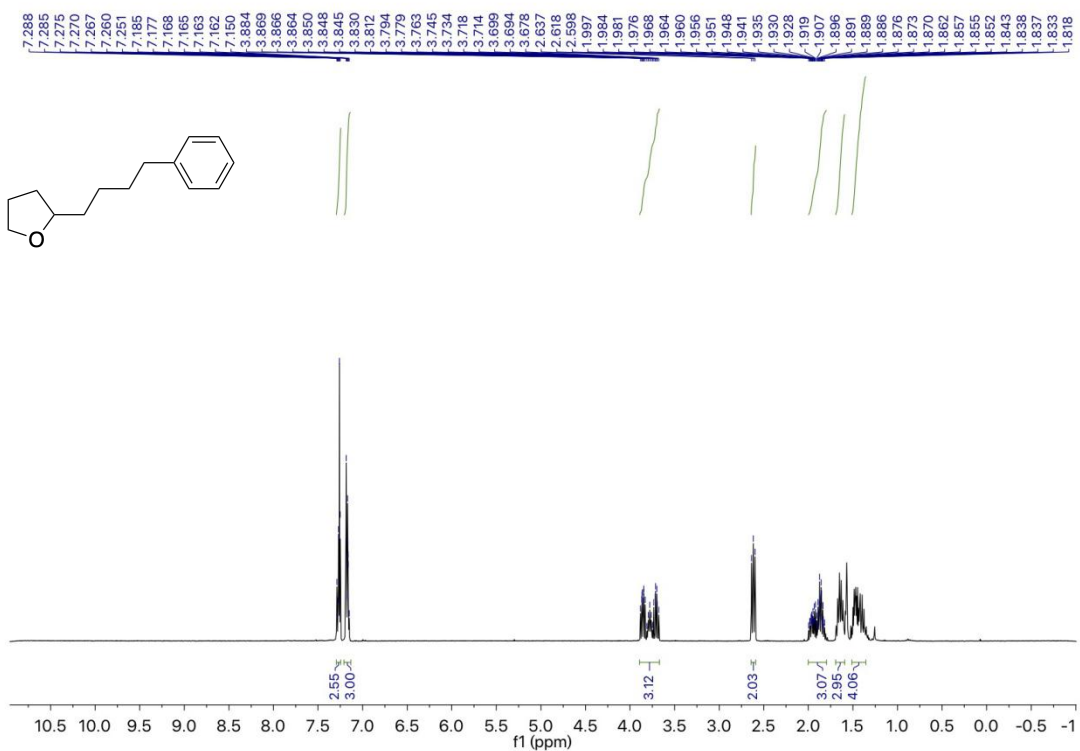
**<sup>13</sup>C NMR spectrum (101 MHz, CDCl<sub>3</sub>) of **4s****



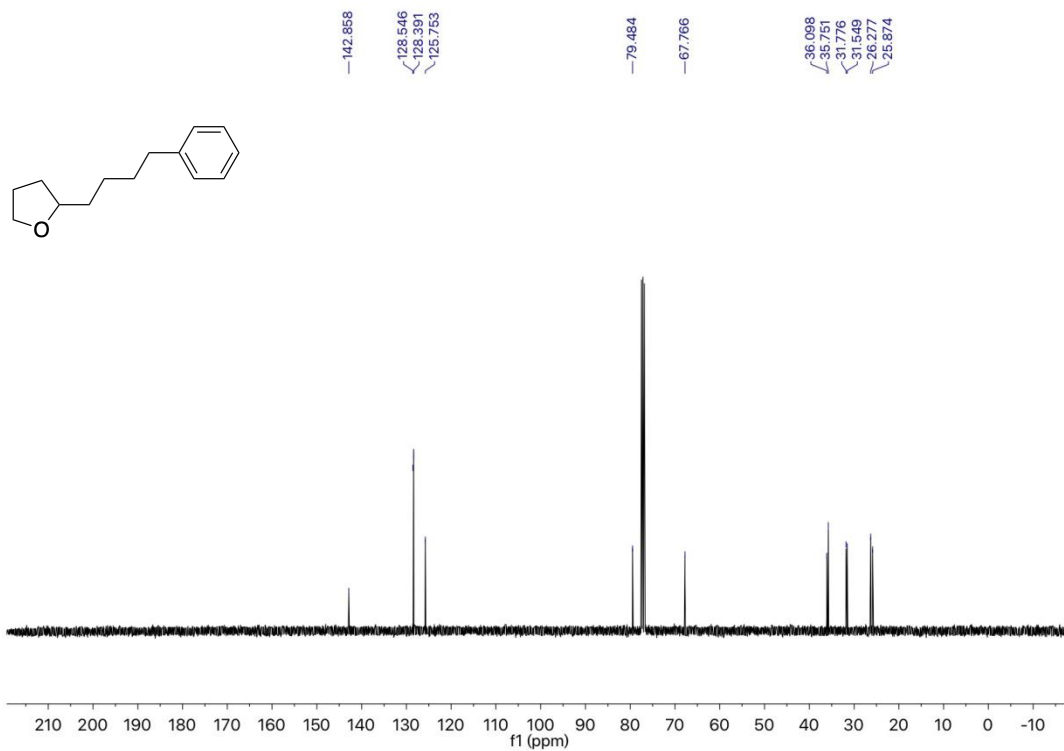
**<sup>1</sup>H NMR spectrum (300 MHz, CDCl<sub>3</sub>) of **5a****



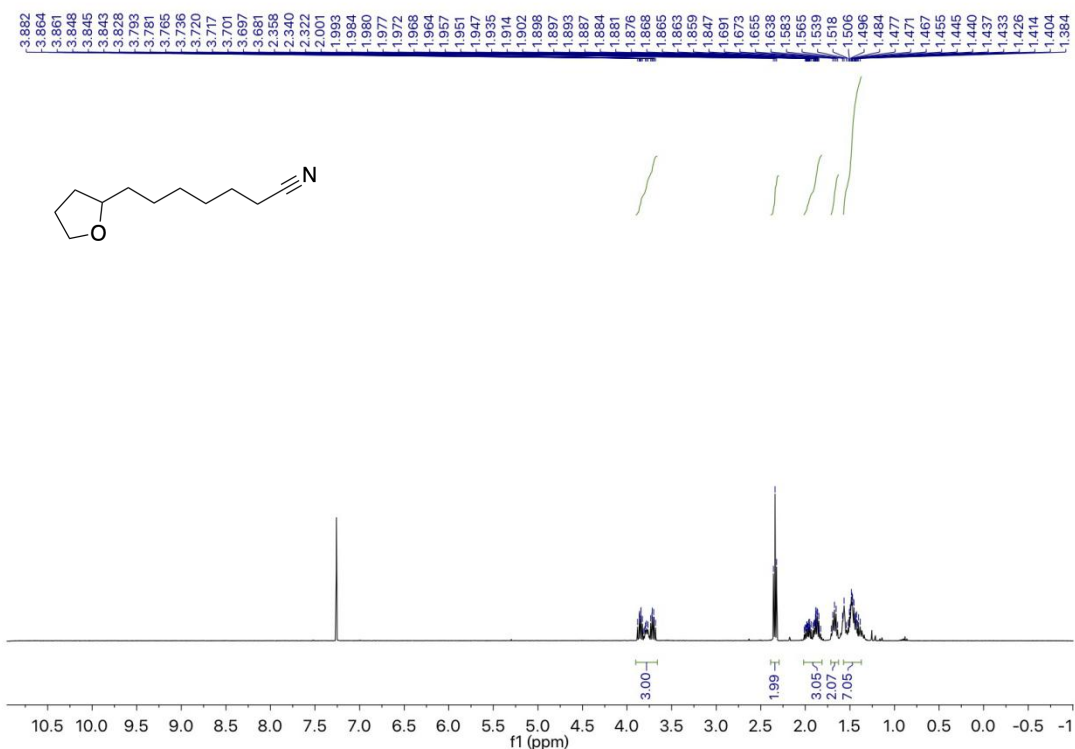
$^{13}\text{C}$  NMR spectrum (75 MHz,  $\text{CDCl}_3$ ) of **5a**



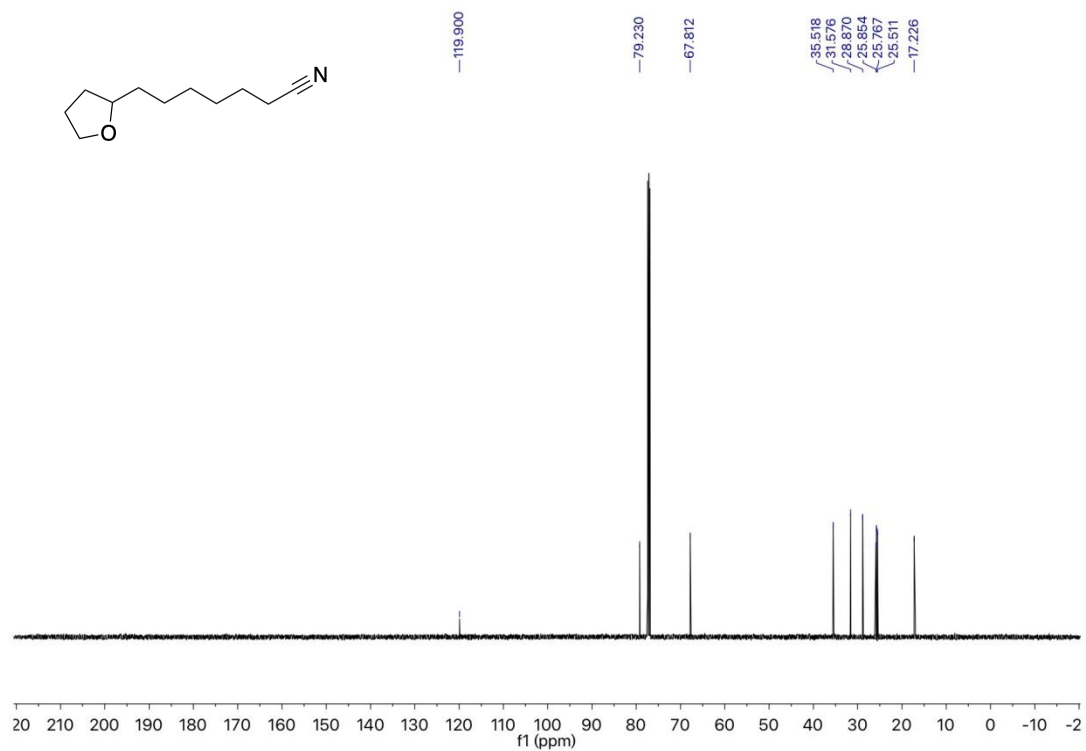
$^1\text{H}$  NMR spectrum (400 MHz,  $\text{CDCl}_3$ ) of **5b**



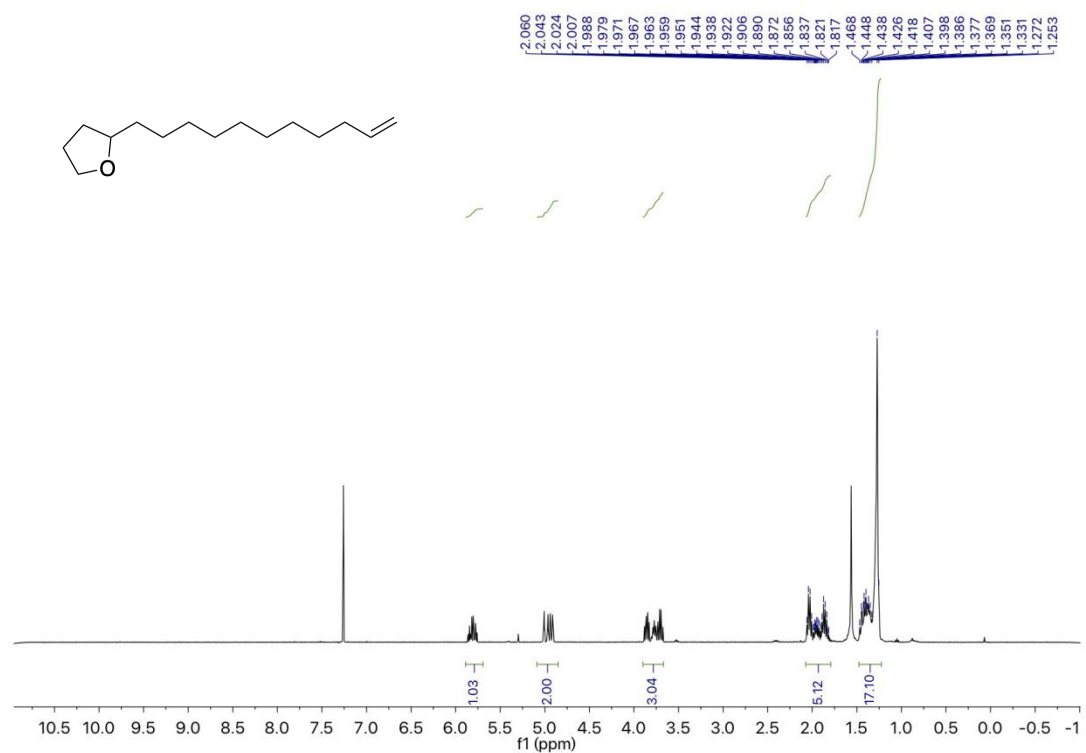
$^{13}\text{C}$  NMR spectrum (101 MHz,  $\text{CDCl}_3$ ) of 5b



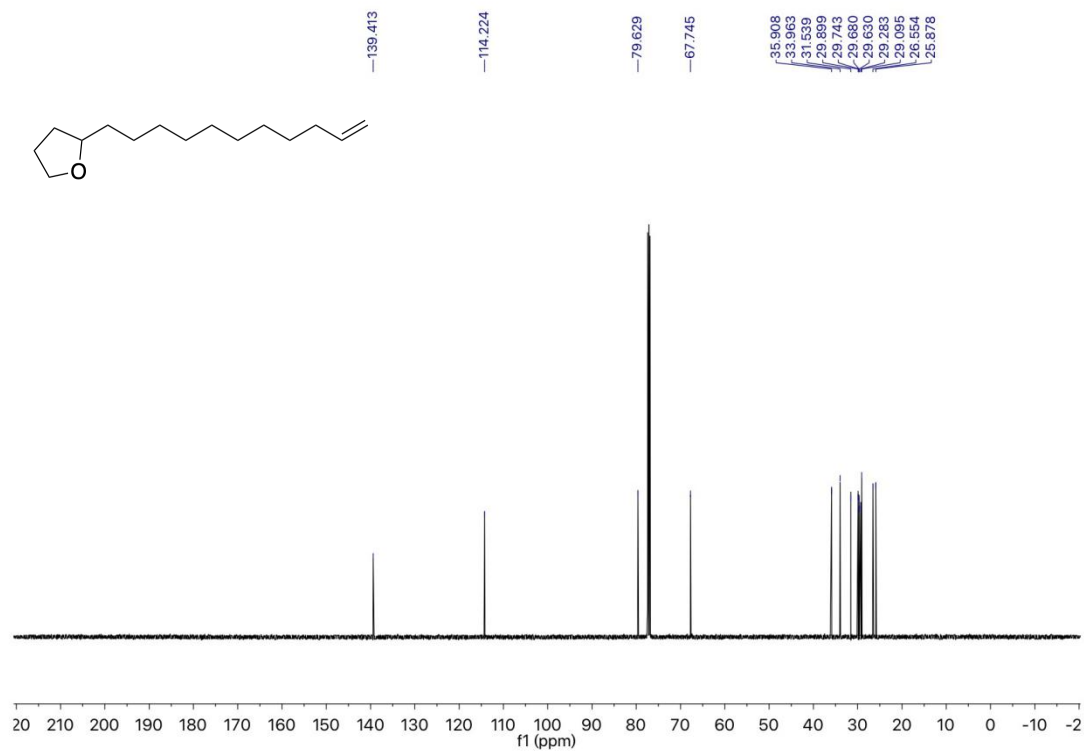
$^1\text{H}$  NMR spectrum (400 MHz,  $\text{CDCl}_3$ ) of 5c



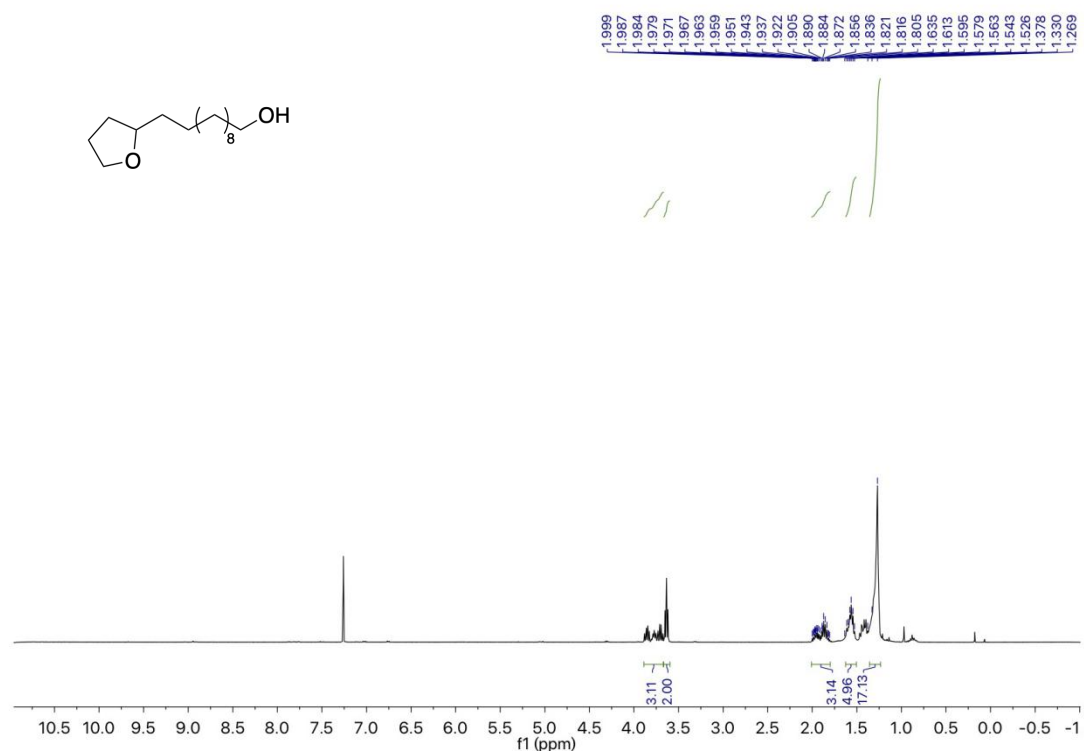
$^{13}\text{C}$  NMR spectrum (101 MHz,  $\text{CDCl}_3$ ) of 5c



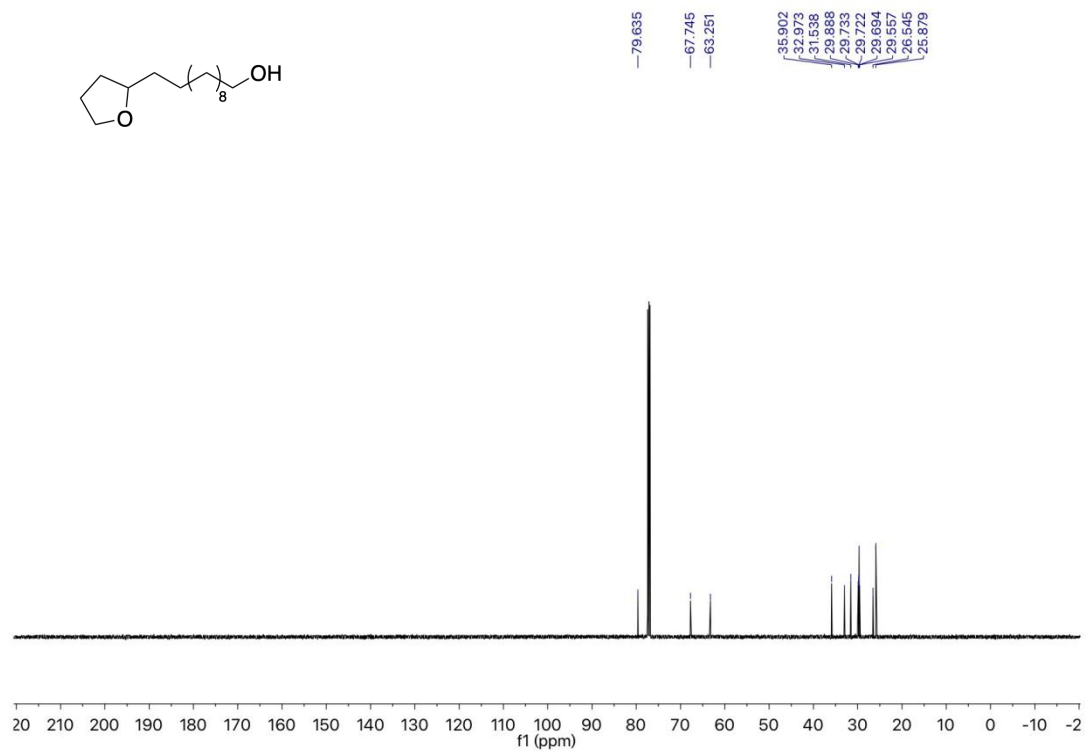
$^1\text{H}$  NMR spectrum (400 MHz,  $\text{CDCl}_3$ ) of 5d



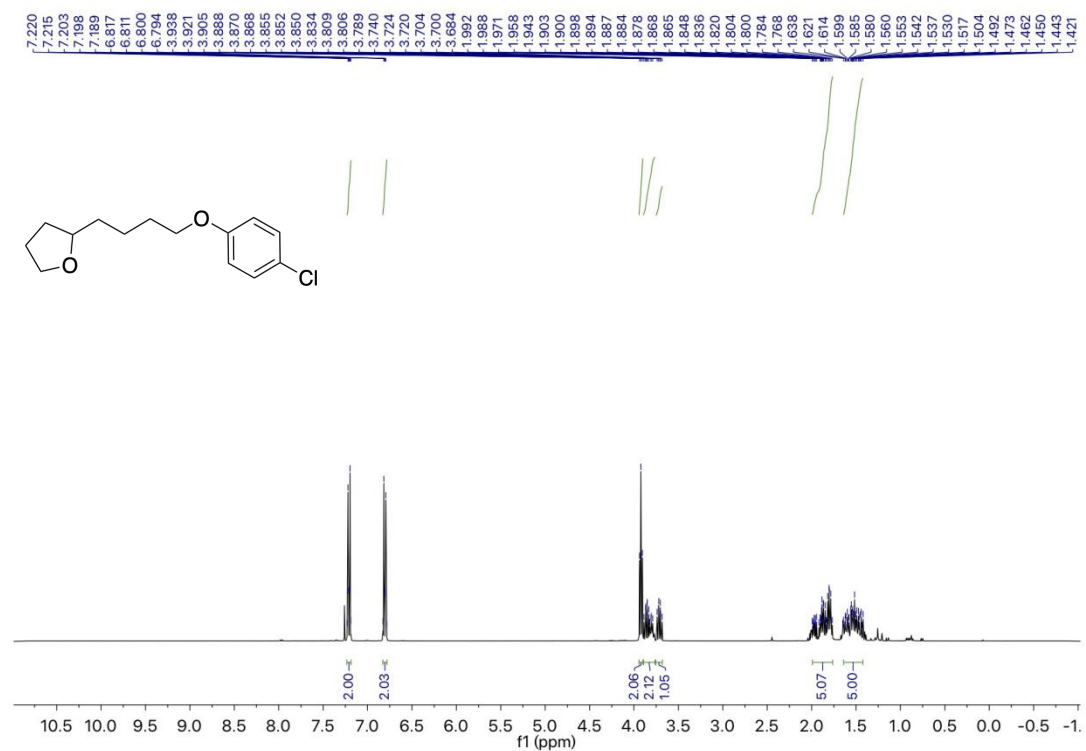
$^{13}\text{C}$  NMR spectrum (101 MHz,  $\text{CDCl}_3$ ) of **5d**



$^1\text{H}$  NMR spectrum (400 MHz,  $\text{CDCl}_3$ ) of **5e**

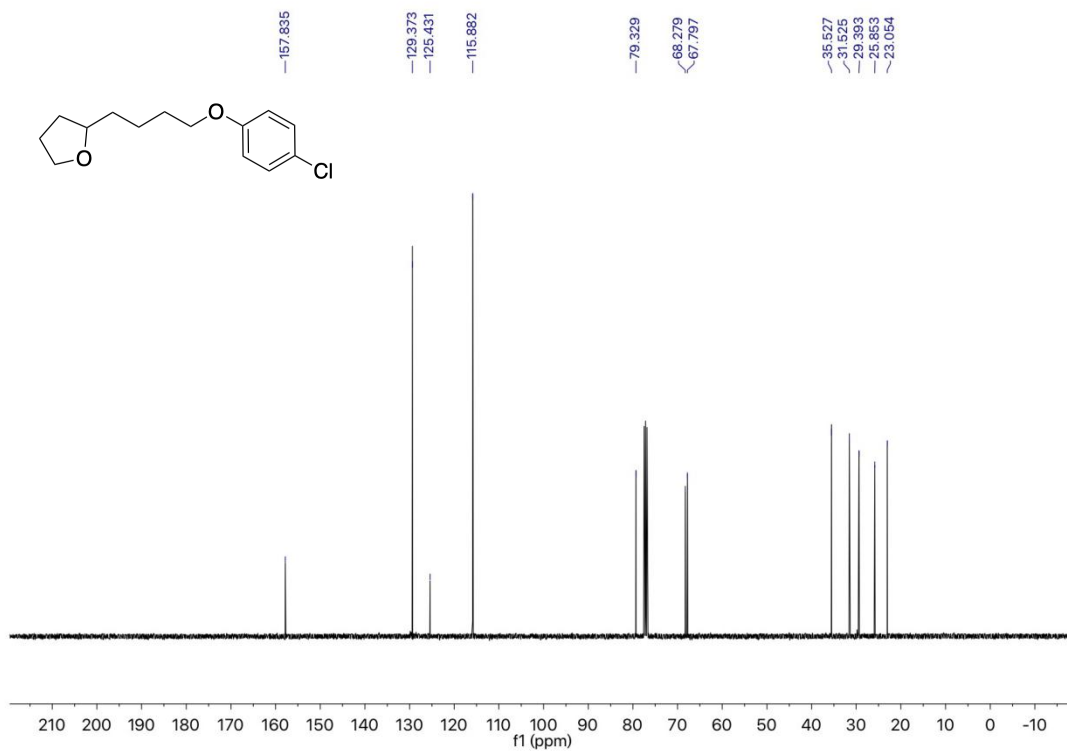


$^{13}\text{C}$  NMR spectrum (101 MHz,  $\text{CDCl}_3$ ) of **5e**

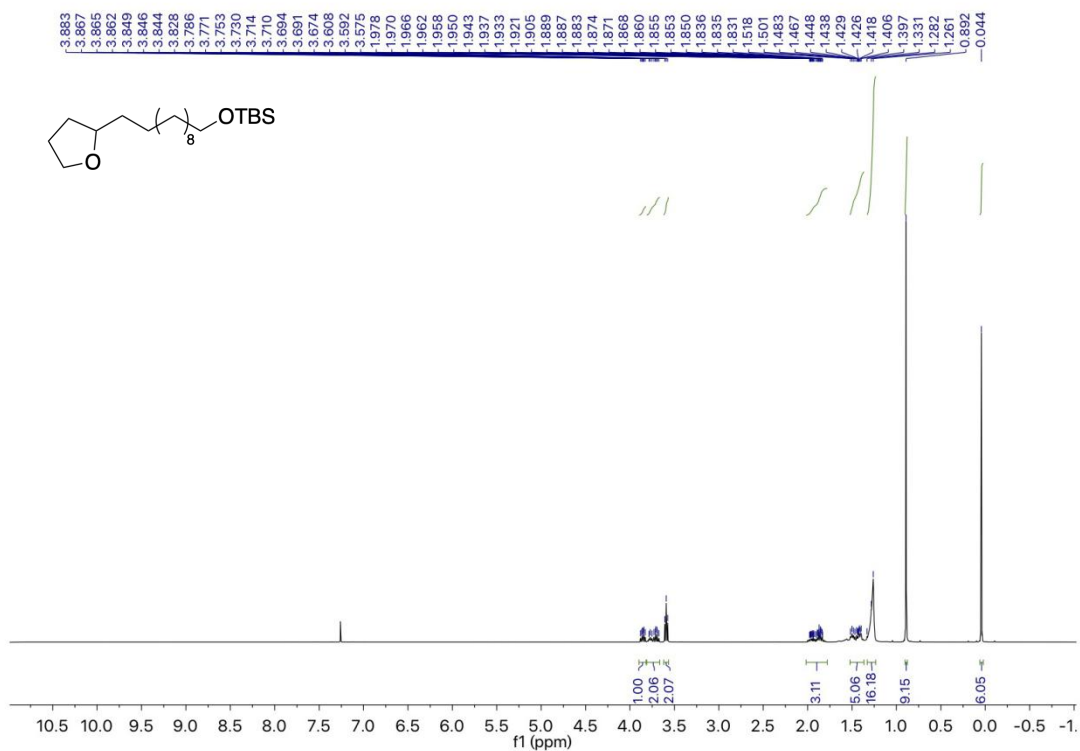


$^1\text{H}$  NMR spectrum (400 MHz,  $\text{CDCl}_3$ ) of **5f**

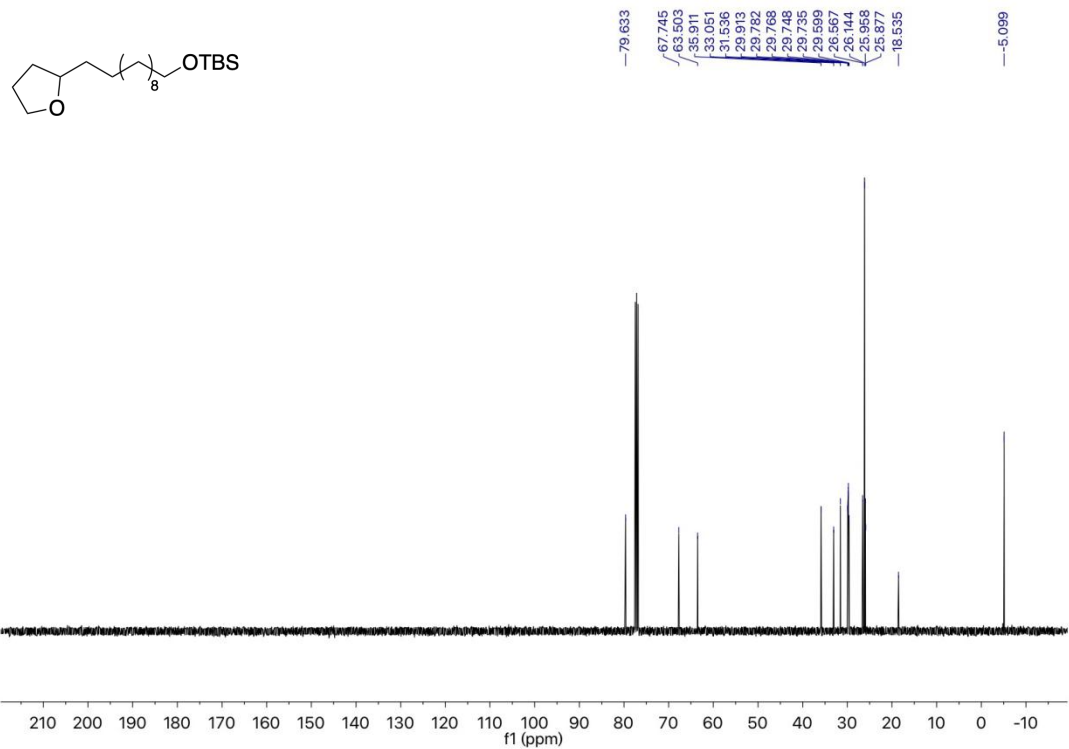




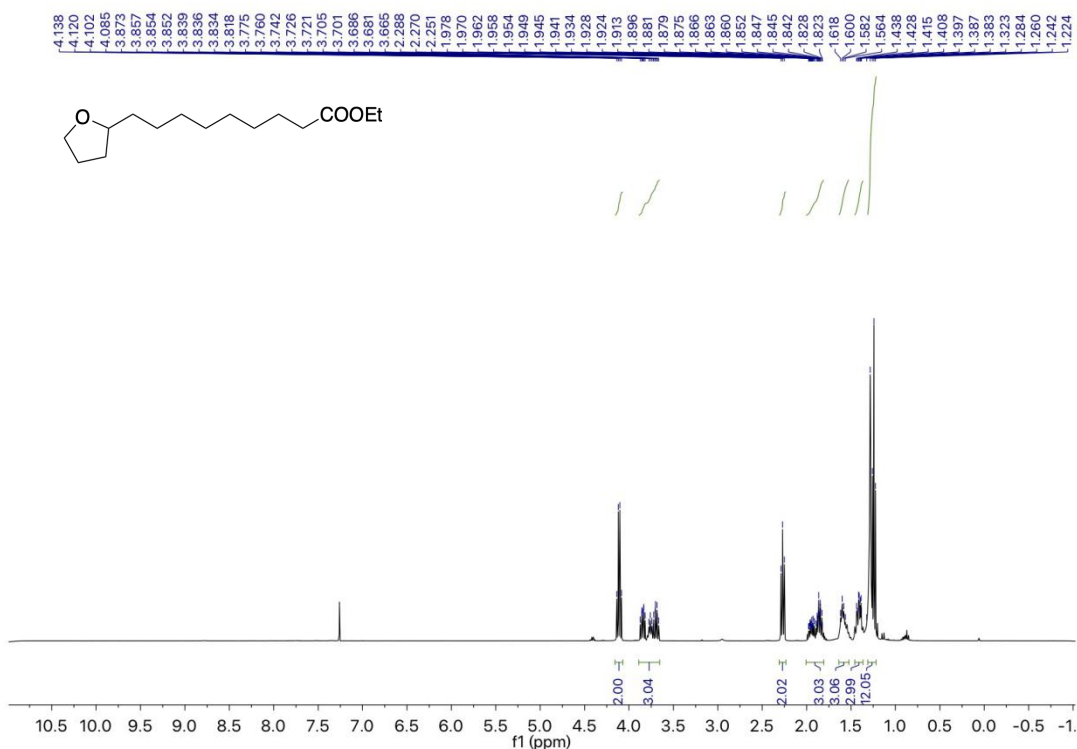
<sup>13</sup>C NMR spectrum (101 MHz, CDCl<sub>3</sub>) of 5f



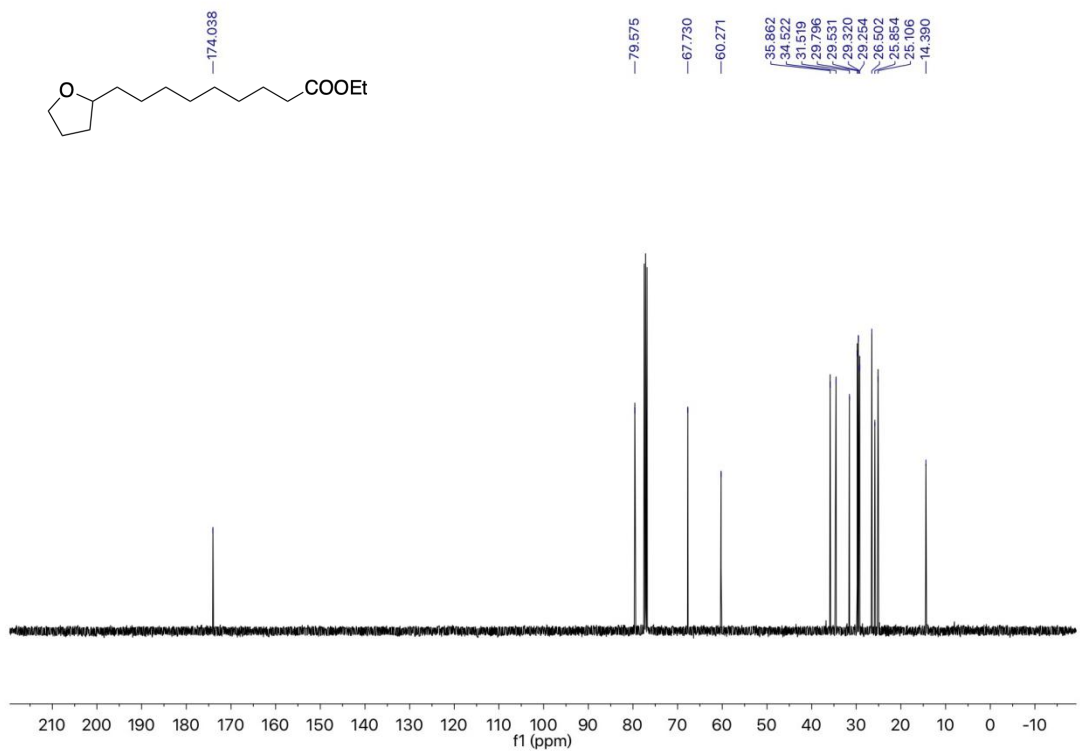
<sup>1</sup>H NMR spectrum (400 MHz, CDCl<sub>3</sub>) of 5g



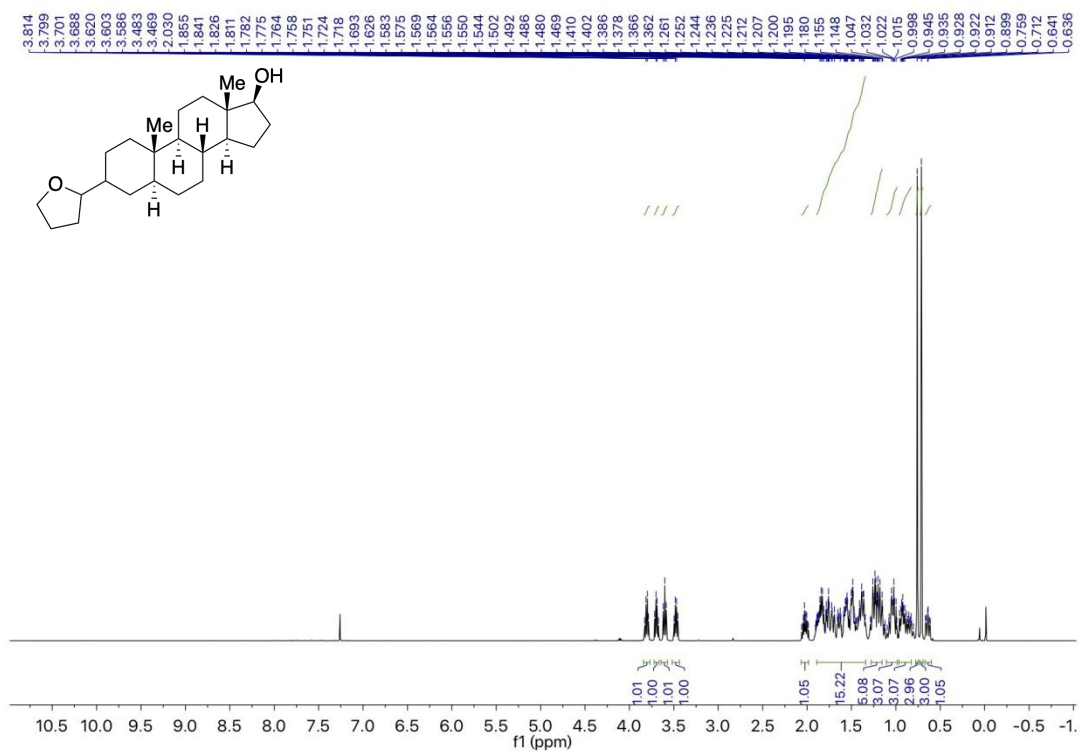
$^{13}\text{C}$  NMR spectrum (101 MHz,  $\text{CDCl}_3$ ) of **5g**



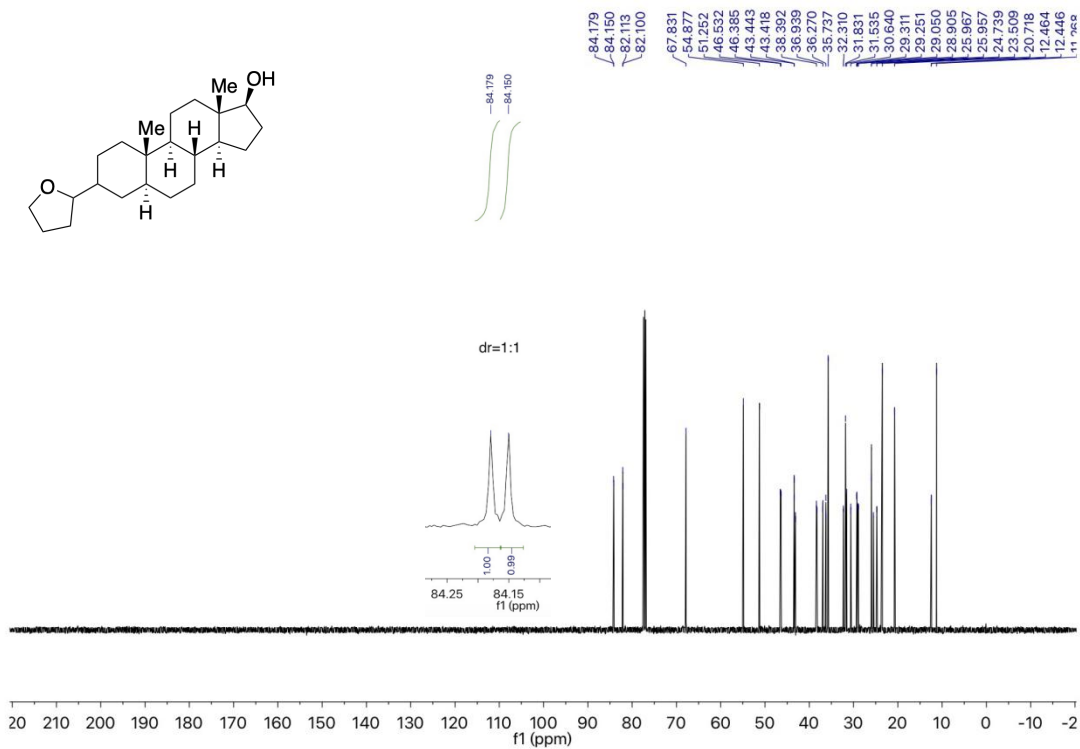
$^1\text{H}$  NMR spectrum (400 MHz,  $\text{CDCl}_3$ ) of **5h**



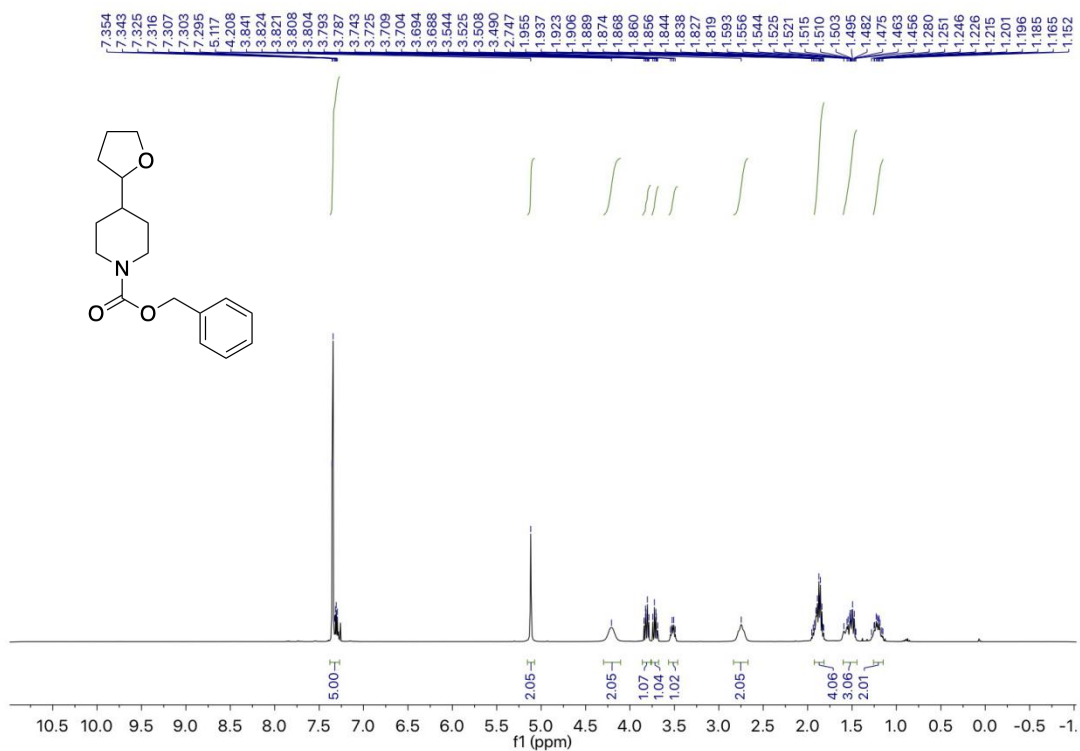
$^{13}\text{C}$  NMR spectrum (101 MHz,  $\text{CDCl}_3$ ) of **5h**



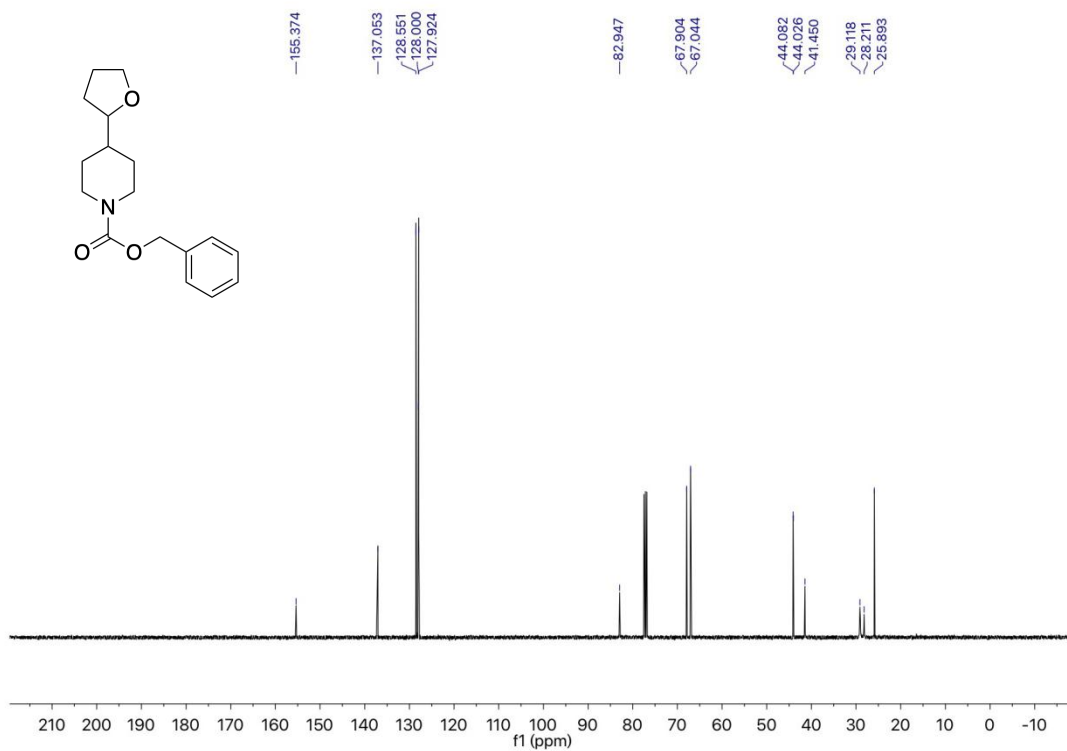
$^1\text{H}$  NMR spectrum (400 MHz,  $\text{CDCl}_3$ ) of **5i**



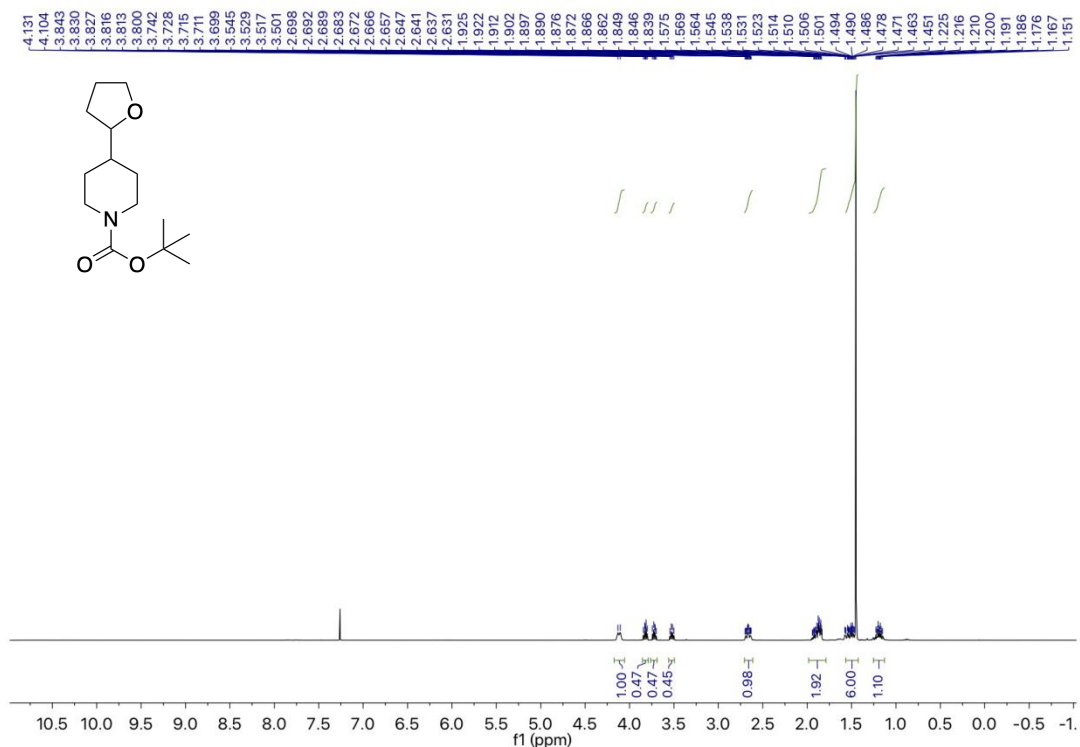
**<sup>13</sup>C NMR spectrum (101 MHz, CDCl<sub>3</sub>) of 5i**



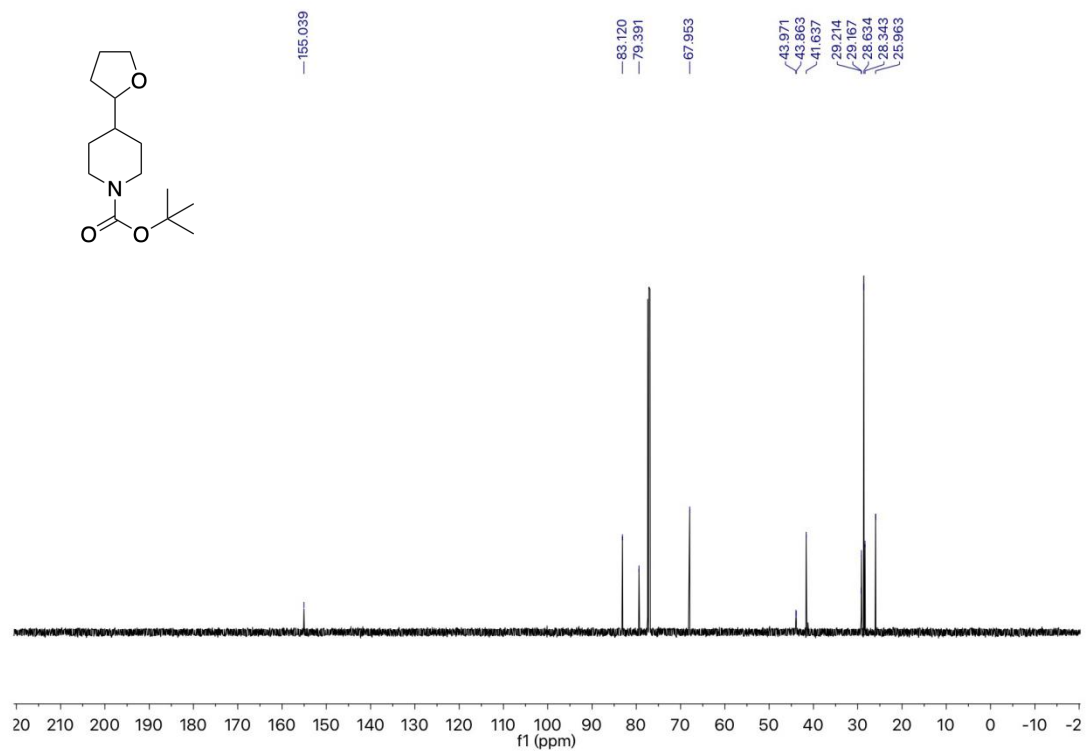
**<sup>1</sup>H NMR spectrum (400 MHz, CDCl<sub>3</sub>) of 5j**



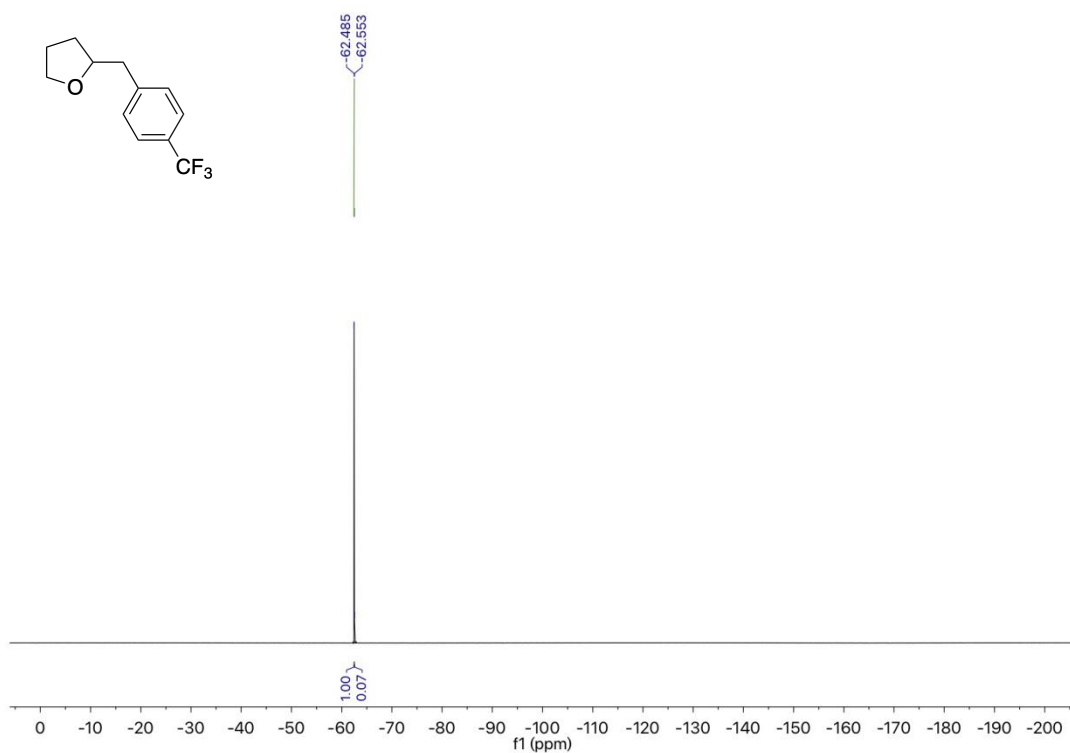
$^{13}\text{C}$  NMR spectrum (101 MHz,  $\text{CDCl}_3$ ) of **5j**



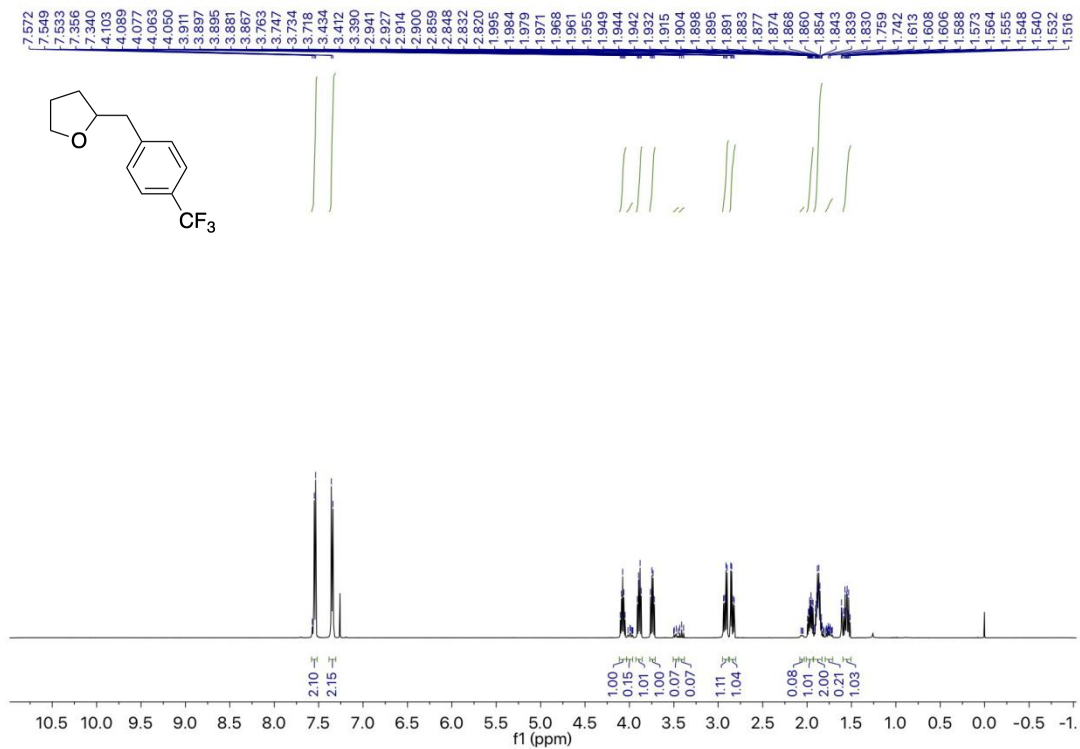
$^1\text{H}$  NMR spectrum (400 MHz,  $\text{CDCl}_3$ ) of **5k**



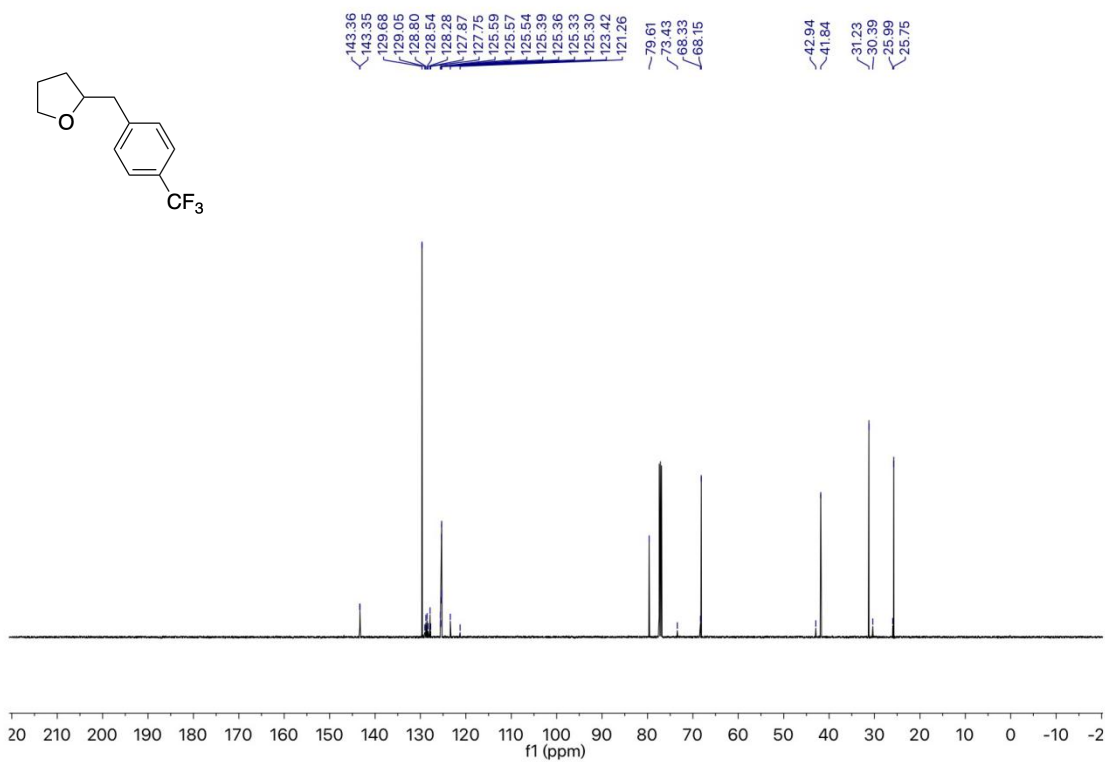
$^{13}\text{C}$  NMR spectrum (101 MHz,  $\text{CDCl}_3$ ) of **5k**



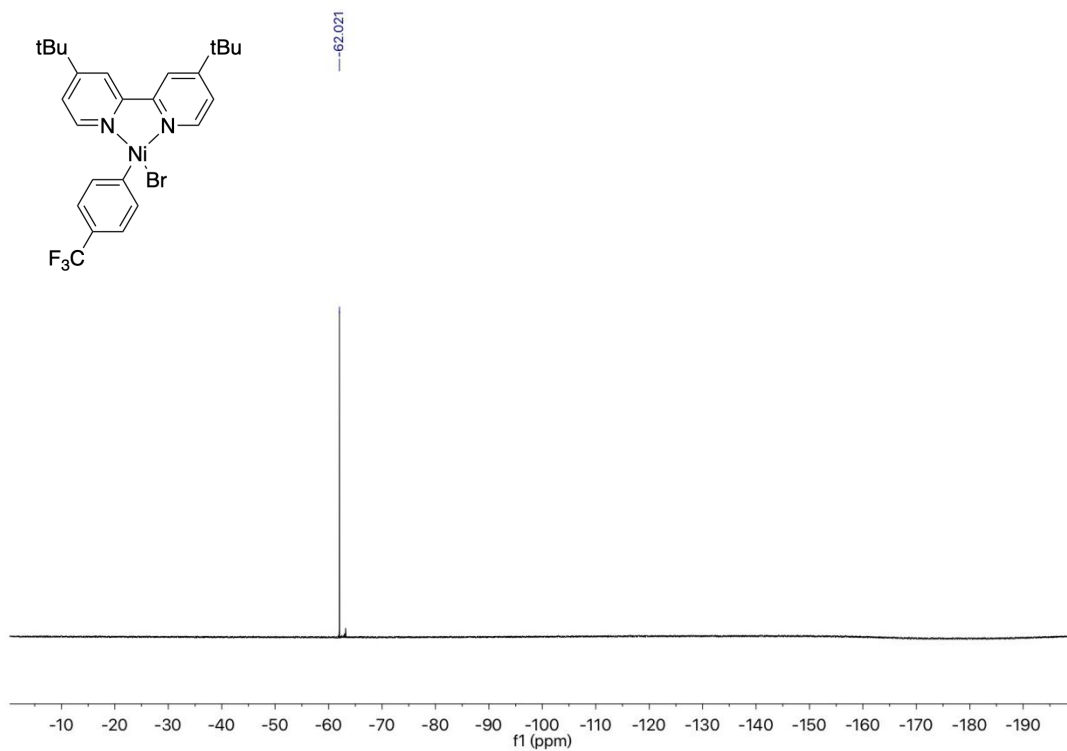
$^{19}\text{F}$  NMR spectrum (376 MHz,  $\text{CDCl}_3$ ) of **13** and **14**



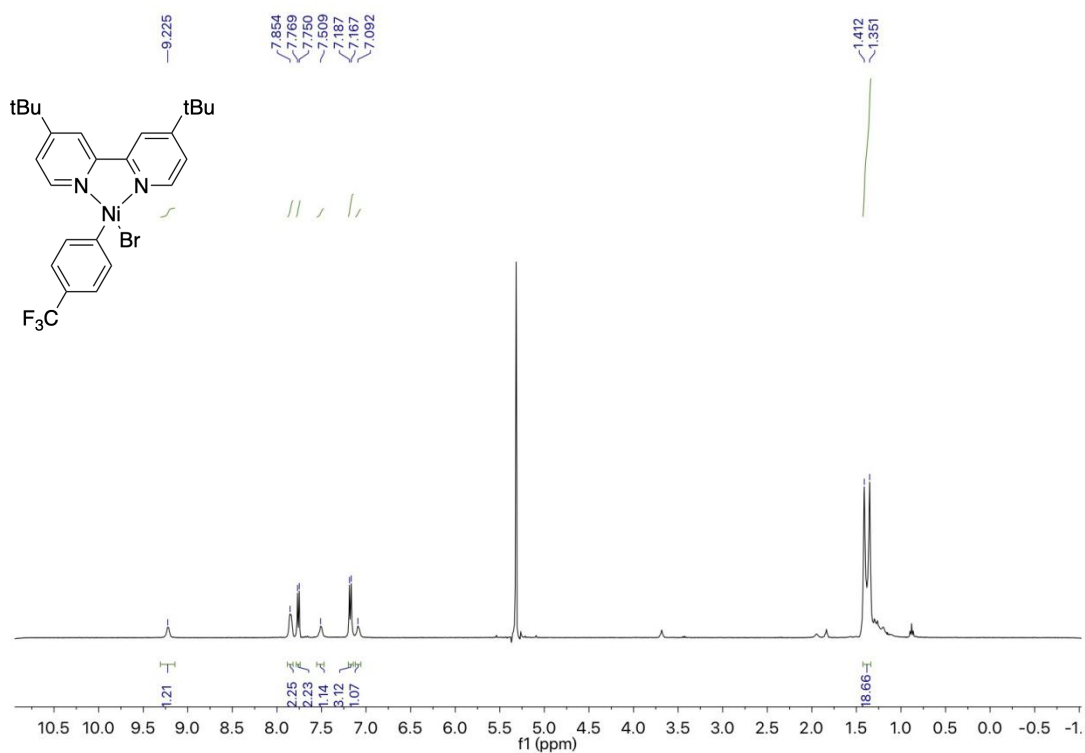
<sup>1</sup>H NMR spectrum (500 MHz, CDCl<sub>3</sub>) of **13** and **14**



<sup>13</sup>C NMR spectrum (126 MHz, CDCl<sub>3</sub>) of **13** and **14**



$^{19}\text{F}$  NMR spectrum (376 MHz,  $\text{CD}_2\text{Cl}_2$ ) of Ni-I



$^1\text{H}$  NMR spectrum (400 MHz,  $\text{CD}_2\text{Cl}_2$ ) of Ni-I



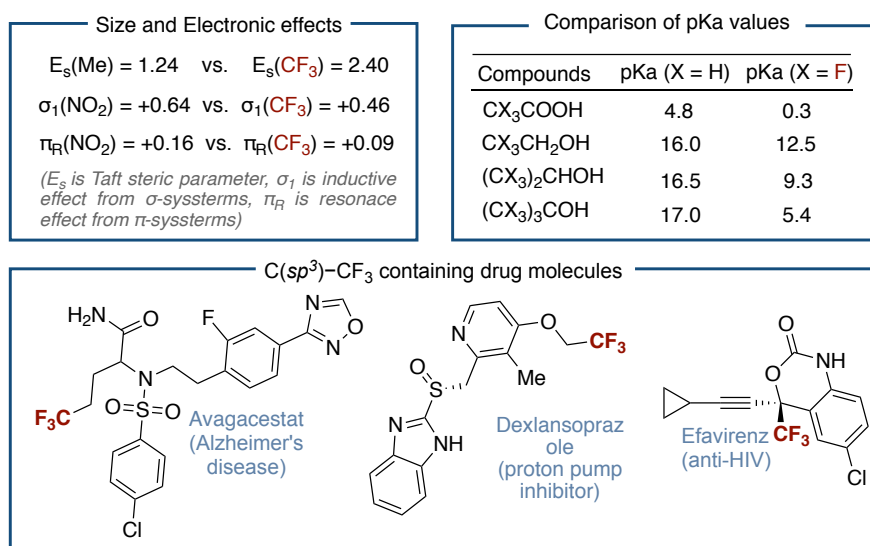
---

## Chapter 3

### *Trifluoromethylation of Carbonyl and Olefin Derivatives by C(sp<sup>3</sup>)-C Bond Cleavage*

### 3.1 General Introduction

Due to the recent development of numerous synthetic methods in organic fluorine chemistry, organic compounds containing fluorine functional group were widely studied and incorporated into pharmaceuticals, agrochemicals, and functional materials.<sup>1</sup> In particular, the trifluoromethyl group (CF<sub>3</sub>) possesses unique properties as a strong electron-withdrawing effect (Scheme 3.1, *top left*) and could increase the lipophilicity of a drug candidate upon incorporation.<sup>2</sup> The stable C–F bond can also significantly change the acidity and the dipole moment (Scheme 3.1, *top right*),<sup>3</sup> therefore increasing the polarity of the molecule.<sup>2, 3</sup> Furthermore, fluorine-containing groups were applied to tune permeability, lipophilicity and metabolic stability of drug molecules (Scheme 3.1),<sup>1</sup> therefore attracting attention from the medicinal chemists. Currently, related CF<sub>3</sub>-drug molecules such as Avagacestat (Alzheimer's disease), Dexlansoprazole (proton pump inhibitor), and Efavirenz (anti-HIV), have shown good bioactivity (Scheme 3.1, *bottom*).<sup>4</sup>

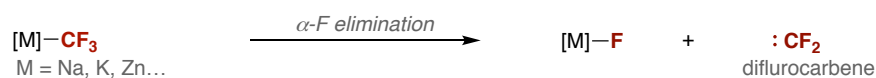


**Scheme 3.1** Properties of the trifluoromethyl group.

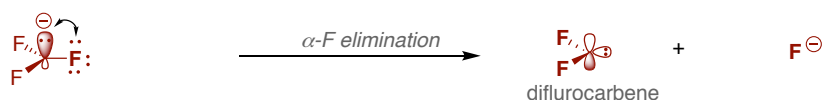
In recent years, efficient and elegant transition metal-catalyzed trifluoromethylation reactions to forge C(sp<sup>3</sup>)-CF<sub>3</sub> bonds have been developed.<sup>5</sup> Due to the large lattice energy between metal and fluorine atoms and the special nature of trifluoromethyl group, the related trifluoromethyl metal-active species is unstable and is prone to  $\alpha$ -F elimination (Scheme 3.2).<sup>6</sup> In addition, due to the acidity of fluoroform (pKa = 28),<sup>7</sup> the installation of aliphatic trifluoromethyl groups via the S<sub>N</sub>2 route is also problematic because of the instability of the CF<sub>3</sub> anion which rapidly decomposes to fluoride anion and difluorocarbenes due to negative charge-lone pair repulsion.<sup>8</sup> Therefore, the efficient

synthesis of these compounds including alkyl-trifluoromethyl motifs  $[C(sp^3)-CF_3]$  remains an important challenge.

- Unstable Metal–CF<sub>3</sub> species



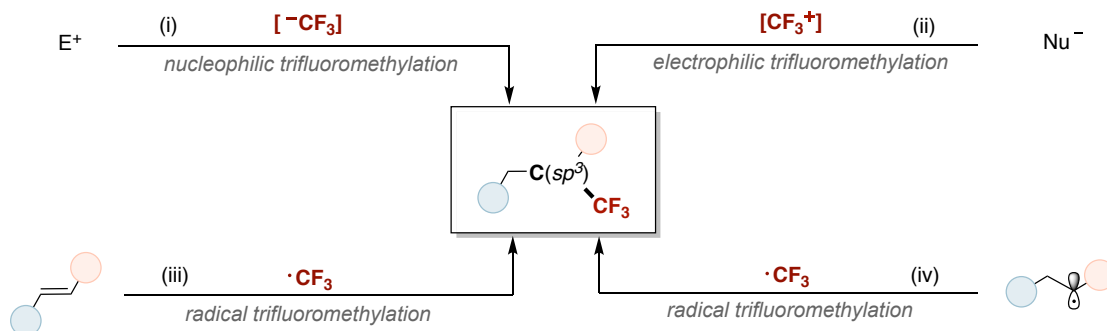
- Rapidly decomposed CF<sub>3</sub> anion



**Scheme 3.2**  $\alpha$ -F elimination of CF<sub>3</sub> anions or metal-bound CF<sub>3</sub>.

### 3.1.1 Radical Trifluoromethylation to Forge $C(sp^3)-CF_3$ Bonds

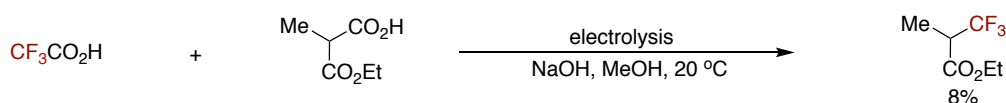
In contrast to the numerous strategies to assemble trifluoromethylated arenes via  $C(sp^2)-CF_3$  bond formation,<sup>5a, 5b, 9</sup> synthetic methods to build up aliphatic  $C(sp^3)-CF_3$  bonds are still limited due to  $sp^3$  hybridized carbon centers are prone to chemoselectivity problems of protonation and  $\beta$ -H elimination.<sup>5</sup> Current synthetic methods can be grouped into four different classes (Scheme 3.3): (i) Trifluoromethylation of carbon-centered electrophiles with  $[CF_3^-]$  reagents (nucleophilic trifluoromethylation),<sup>5a, 10</sup> (ii) Trifluoromethylation of carbon-centered nucleophiles with  $[CF_3^+]$  reagents (electrophilic trifluoromethylation),<sup>11</sup> (iii) Difunctionalization of unsaturated bonds such as alkenes via  $CF_3$  radical addition,<sup>12</sup> (iv) Trifluoromethylation of carbon-centered radicals.<sup>12a, 13</sup> The mild generation of radical intermediates applying (metalla)photoredox chemistry has driven the development of new methods to form  $C(sp^3)-CF_3$  bonds via radical trifluoromethylation reactions.<sup>5c</sup> This enables traditionally unreactive substrates to undergo trifluoromethylation accompanied by unique chemoselectivity and excellent functional group compatibility. In recent years, radical trifluoromethylation has been the latest research trend in the formation of  $C(sp^3)-CF_3$  bonds.<sup>5,12,13</sup>



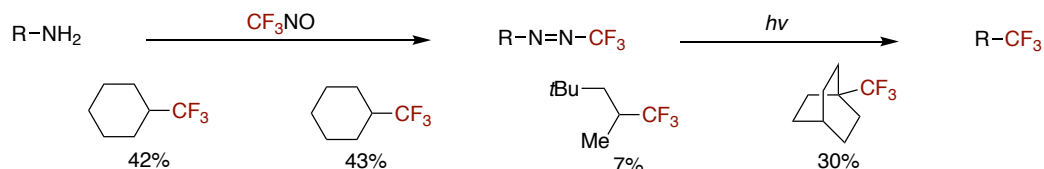
**Scheme 3.3** Classical approaches of trifluoromethylation.

Back in the 1970s, Metal-free radical cross-coupling reactions between trifluoromethyl radicals and alkyl radicals were initially investigated and discovered by Renaud,<sup>14</sup> de Meijere et al.<sup>15</sup> (Scheme 3.4). They found that given the mismatch between the two transient radicals, this type of reaction usually provided the desired product in very low yields. It was not until more than 30 years later that more efficient and versatile methods of radical trifluoromethylation were discovered,<sup>5,12,13</sup> driven by the development of new trifluoromethylation reagents,<sup>11a, 16</sup> particularly preparable isolated metal-CF<sub>3</sub> reagents.<sup>9e,9g, 17</sup>

In 1975, Renaud:



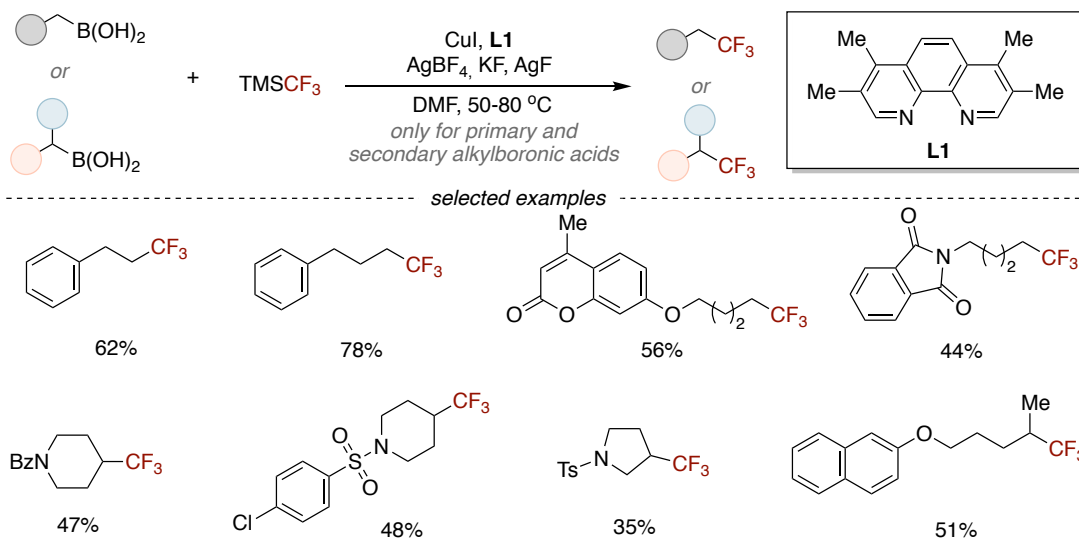
In 1977, de Meijere:



**Scheme 3.4** Cross-coupling between alkyl radical and CF<sub>3</sub> radical.

In 2012, the Fu group reported the successful trifluoromethylation of primary and secondary alkylboronic acids.<sup>18</sup> Herein, Ruppert's reagent (TMS-CF<sub>3</sub>)<sup>19</sup> was used as the trifluoromethylation source in the presence of Ag<sup>+</sup> as stoichiometric oxidant and CuI as the catalyst.

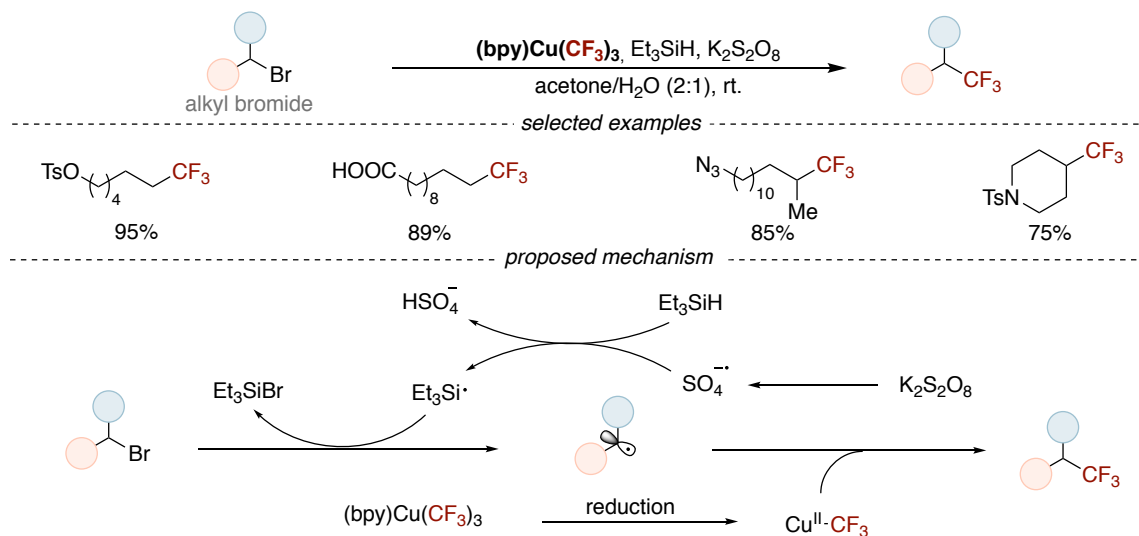
In 2012, Fu:



**Scheme 3.5** Cu-catalyzed trifluoromethylation of primary and secondary alkylboronic acids.

The related breakthrough study was reported by Li's group in 2017,<sup>20</sup> they discovered the copper-mediated trifluoromethylation of alkyl bromides using stoichiometric reagent  $(\text{bpy})\text{Cu}(\text{CF}_3)_3$  as trifluoromethylation source in the presence of  $\text{K}_2\text{S}_2\text{O}_8$ ,  $\text{Et}_3\text{SiH}$  and aqueous acetone (Scheme 3.6). A plausible mechanism proposes the initial reduction of  $\text{K}_2\text{S}_2\text{O}_8$  via SET producing a sulphate radical anion ( $^-\text{SO}_4$ ), which could abstract a hydrogen atom from  $\text{Et}_3\text{SiH}$  to produce an  $\alpha$ -silicon-centered radical ( $\text{Me}_3\text{Si}^\cdot$ ). These radical intermediates are known to undergo halogen atom transfer (XAT) processes to generate the related alkyl radical from the corresponding bromide. Simultaneously, the  $\text{Cu}^{\text{II}}\text{-CF}_3$  intermediate is formed upon reduction of  $(\text{bpy})\text{Cu}(\text{CF}_3)_3$ , which finally will form the trifluoromethylated product via cross-coupling. The regenerated  $\text{Cu}^{\text{I}}$  species will be reoxidized by  $\text{S}_2\text{O}_8^{2-}$  initiating again the HAT/XAT-process. Although copper-catalyzed nucleophilic trifluoromethylation has been previously reported for alkyl halides, these strategies were limited to highly reactive substrates as benzylic or allylic positions. However, Li's copper-mediated trifluoromethylation of alkyl halides showcased a broad substrate scope and wide functional group compatibility with high yields under mild conditions. This lays the foundation for the development of new methods to form  $\text{C}(\text{sp}^3)\text{-CF}_3$  bonds via radical trifluoromethylation process.

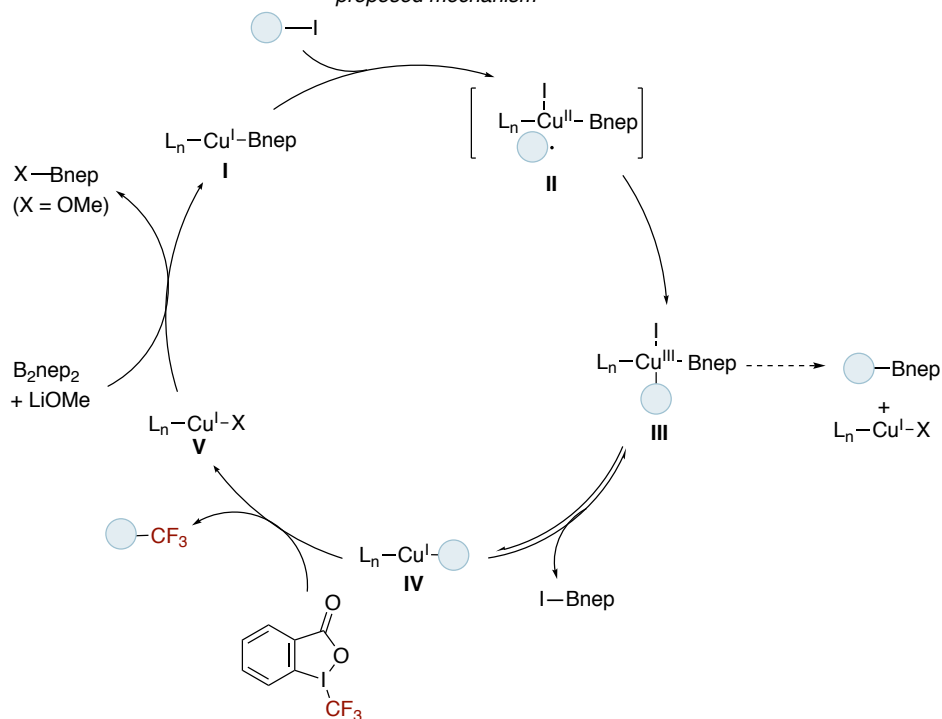
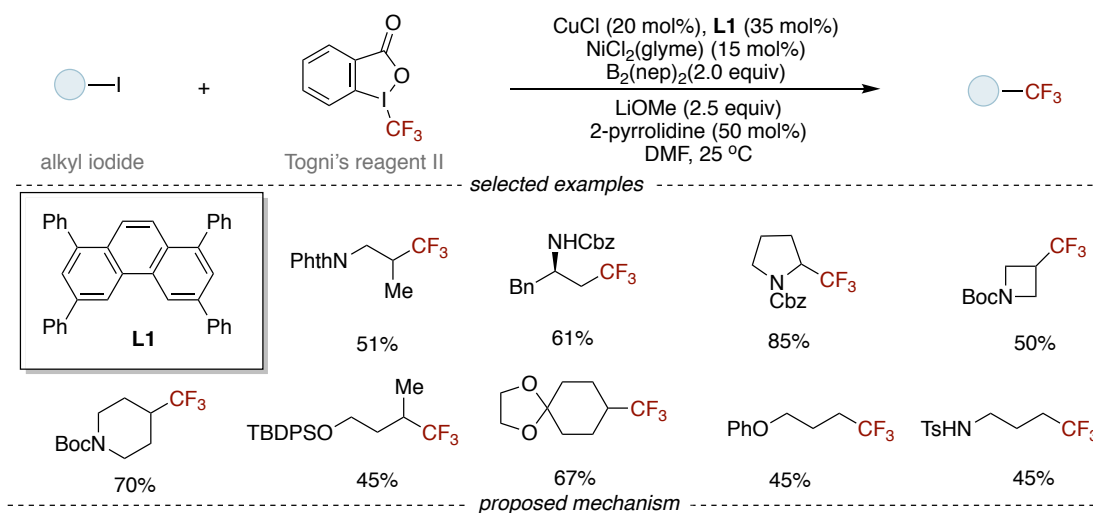
In 2017, Li:



**Scheme 3.6** Cu-mediated trifluoromethylation of alkyl bromides with  $(bpy)Cu(CF_3)_3$ .

In 2018, Gong and his colleagues reported a Cu/Ni-cocatalyzed reductive coupling of alkyl iodides with Togni's reagent II (Scheme 3.7).<sup>21</sup> Copper(I) chloride ( $CuCl$ ) and  $NiCl_2 \cdot glyme$  were employed as catalysts and  $B_2(nep)_2$  (bis(nepentylglycolato)diboron) as the terminating reductant. The authors proposed that the interaction of  $Cu^I$ -Bnep intermediates (**A**) with alkyl iodides to produce alkyl radicals and  $I-Cu^{II}$ -Bnep species (**B**). Following this, the alkyl  $I-Cu^{III}$ -B(nep) intermediate (**C**) is rapidly formed and to produce  $R-Cu^I$  intermediate (**D**) upon reductive elimination. Finally, reaction of  $R-Cu^I$  with Togni reagent II produced the trifluoromethylated product and regenerates  $Cu^I$  (**V**).

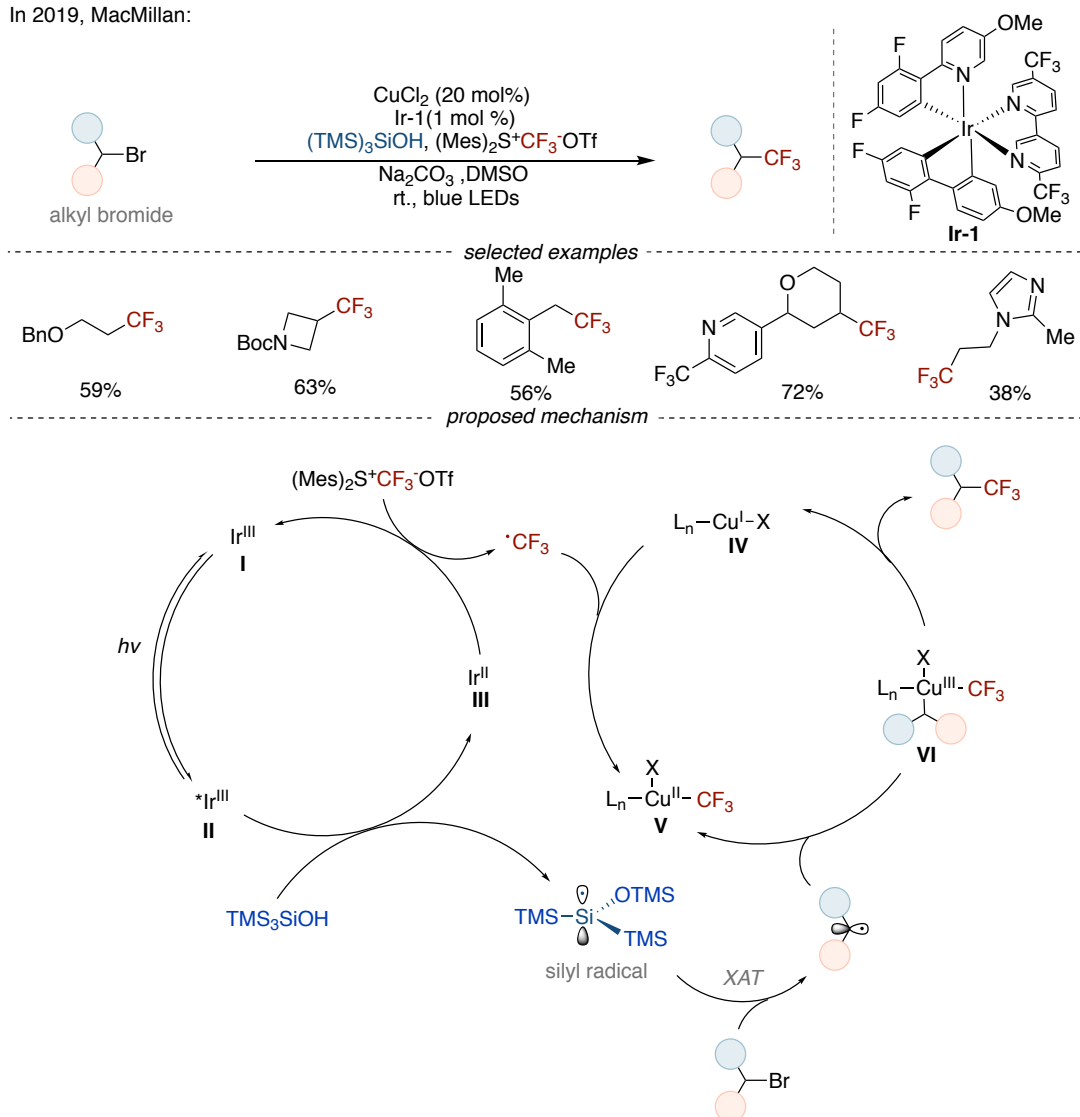
In 2018, Gong:



**Scheme 3.7** Dual Ni/Cu-catalyzed reductive coupling of alkyl iodides with Togni's reagent II.

In 2019, the MacMillan group developed the dual copper/photo-redox catalyzed trifluoromethylation of alkyl bromides employing the electrophilic trifluoromethylation reagent  $[(\text{Mes})_2\text{S}^+\text{CF}_3\text{-OTf}]$ .<sup>22</sup> Herein, tris(trimethylsilyl)silanol  $(\text{TM}_3\text{SiOH})$  served as XAT catalyst via oxidative SET of the excited Iridium<sup>III</sup> complex (. The so generated alkyl radicals recombine with  $\text{LnX-Cu}^{\text{II}}\text{-CF}_3$  to give alkyl- $\text{Cu}^{\text{III}}\text{-CF}_3$  intermediates similar to those reported previously (Scheme 3.8).

In 2019, MacMillan:

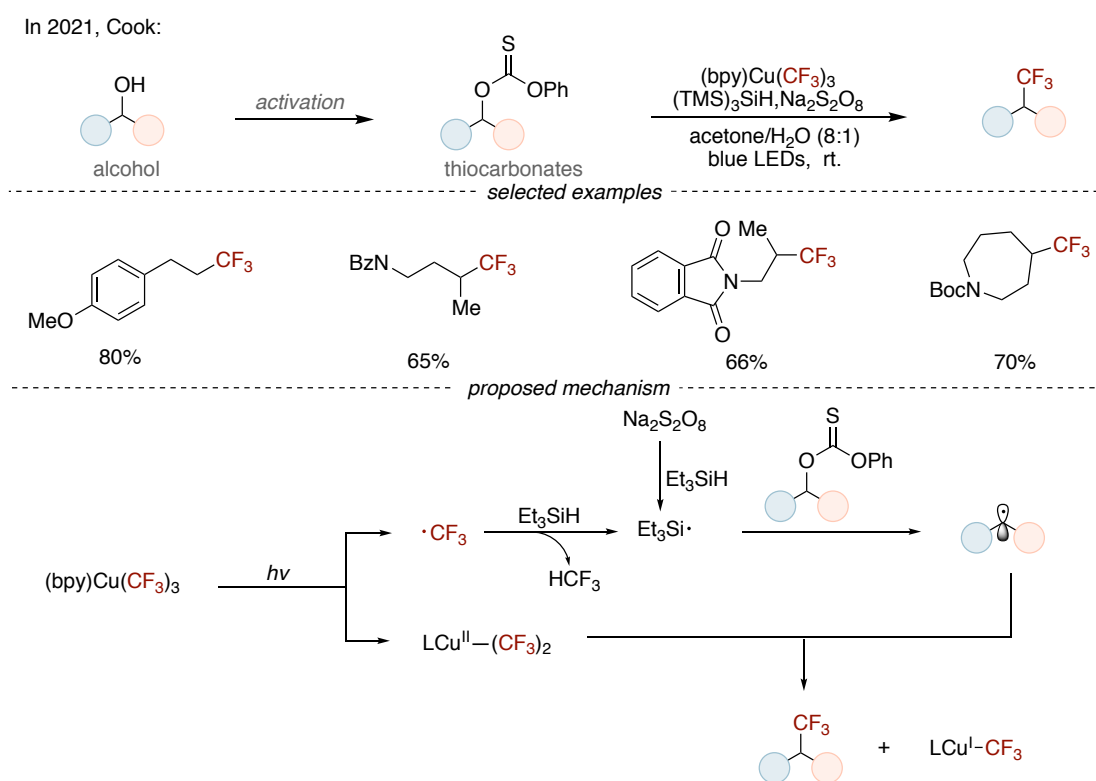


**Scheme 3.8** The dual copper/photoredox-catalyzed trifluoromethylation of alkyl bromides employing a sulfonium reagent.

Aliphatic alcohols are highly abundant and were recently developed as alkyl radical precursors upon activation and allowing to participate in trifluoromethylation strategies. In 2021, the Cook group presented the deoxytrifluoromethylation of aliphatic alcohols using O-alkyl thiocarbonates as mode of activation. Under blue LED irradiation and in the presence of  $(\text{bpy})\text{-Cu}(\text{CF}_3)_3$ ,  $(\text{TMS})_3\text{SiH}$  and  $\text{Na}_2\text{S}_2\text{O}_8$  (Scheme 3.9),<sup>23</sup> photolysis of  $(\text{bpy})\text{Cu}(\text{CF}_3)_3$  results in the generation of  $\text{CF}_3$  radicals and  $(\text{bpy})\text{Cu}(\text{CF}_3)_2$ . The reaction of the silyl radical formed by  $(\text{TMS})_3\text{SiH}$  and O-alkyl thiocarbonate initiates the generation of the corresponding alkyl radicals, which can be trapped by  $(\text{bpy})\text{Cu}^{\text{II}}(\text{CF}_3)_2$  to produce alkyl- $\text{CF}_3$  products. Recently, The MacMillan group has applied the concept of in situ

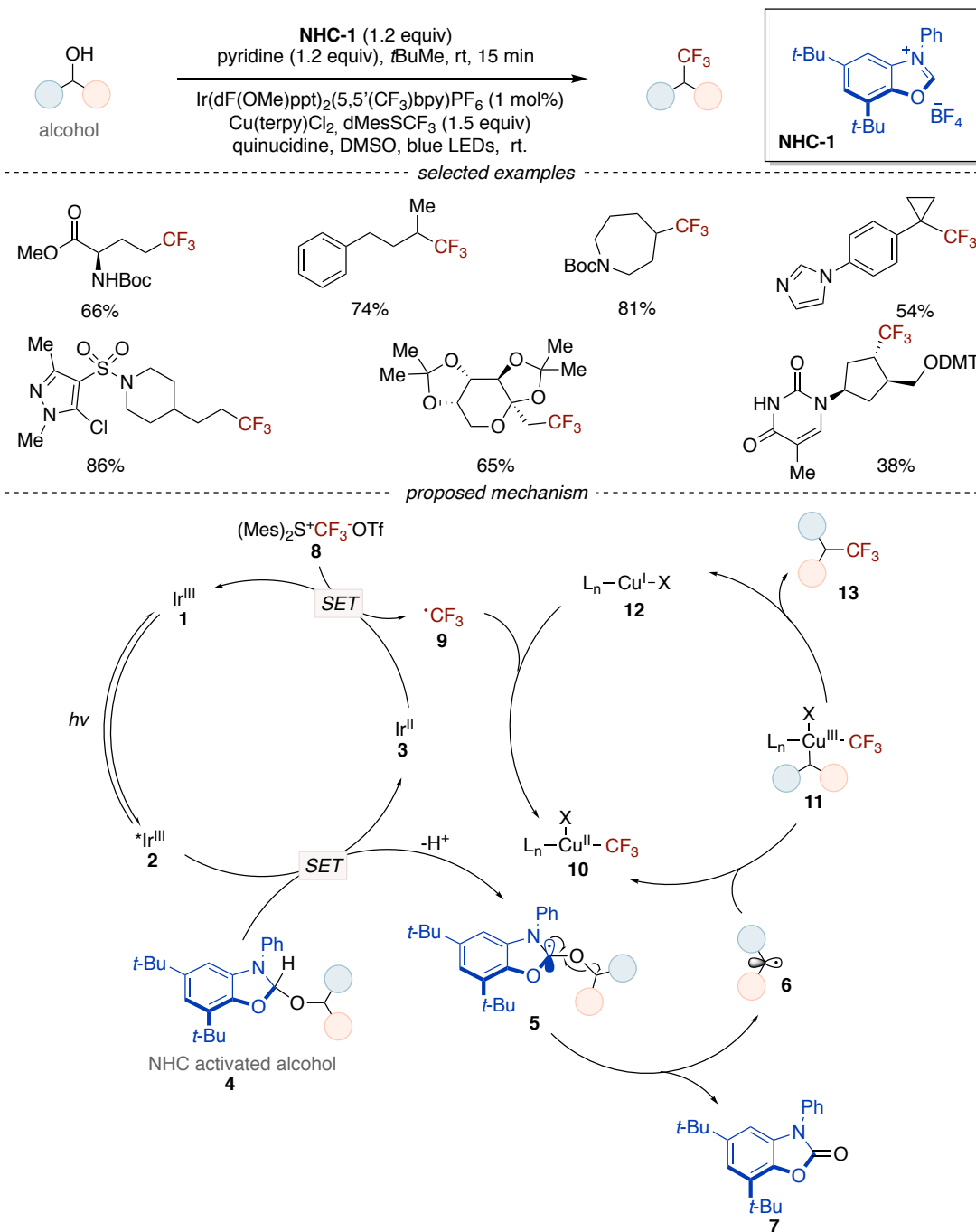


activation of free alcohols via benzoxazolium salts (N-heterocyclic carbene precursors) to the platform about copper metallaphotoredox catalyzed deoxytrifluoromethylation (Scheme 3.10).<sup>24</sup> The mild conditions and excellent chemoselectivity of this method make it suitable for a wide range of primary, secondary and tertiary alcohol substrates and even complex drug molecules such as monosaccharides and nucleosides. Regarding the mechanism, they proposed that the aliphatic alcohol firstly condenses with **NHC-1** to produce NHC-alcohol adduct (**4**) in situ. The photocatalyst  $[\text{Ir}(\text{dF}(\text{OMe})\text{ppy})_2(5,5'(\text{CF}_3)\text{bpy})\text{PF}_6]$  (**1**) produces a highly oxidative excited state **2** under light excitation. NHC-alcohol adduct **4** undergoes deprotonation and quenches **2** via single electron transfer (SET) to provide radical intermediate **5**, which can undergo C–O bond cleavage to provide alkyl radical **6** and by-product **7**. At the same time,  $\text{Cu}^{\text{I}}$  captures the  $\text{CF}_3$  radicals generated from the reduction of the electrophilic  $\text{CF}_3$  source **8** by **3**. the formed  $\text{Cu}^{\text{II}}\text{-CF}_3$  species **19** is able to trap the alkyl radicals **6** and give the alkyl- $\text{Cu}^{\text{III}}\text{-CF}_3$  intermediate **11**, which next produces the desired aliphatic trifluoromethylated product **13** via reductive elimination.



**Scheme 3.9** Cu-mediated trifluoromethylation of alcohols via thiocarbonates.

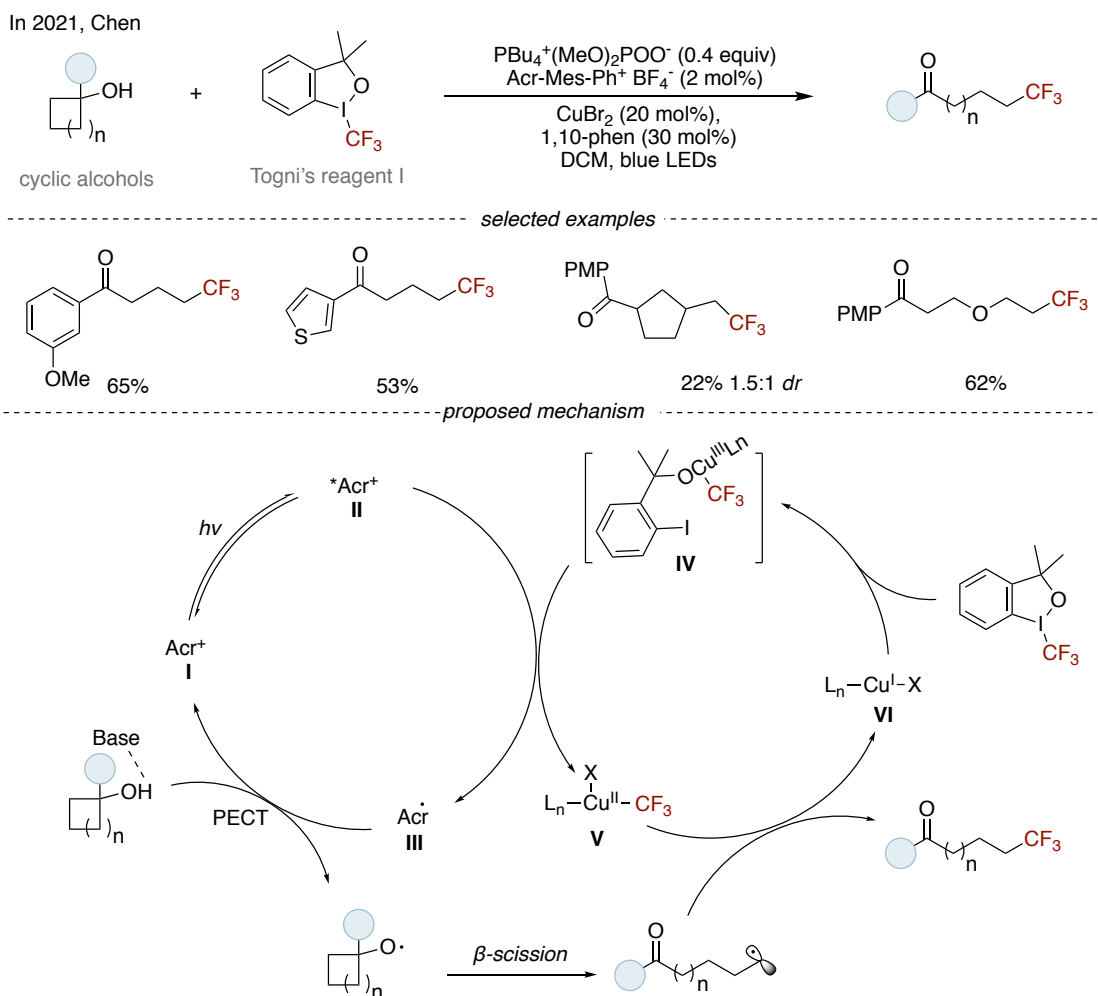
In 2022, MacMillan:



**Scheme 3.10** Cu-catalyzed trifluoromethylation of alcohols via in situ activation of NHC.

Chen's group reported that alkoxy radicals generated from cycloalkanols can achieve selectively  $\beta$  C–C bond cleavage/trifluoromethylation (Scheme 3.11).<sup>25</sup> They used cycloalkanols as substrates to generate the corresponding alkoxy radicals via the PECT pathway. the alkyl radicals generated from  $\beta$ -scission of alkoxy radicals can be trapped by

$\text{LnCu}^{\text{II}}\text{-CF}_3$  intermediate to give the final product.

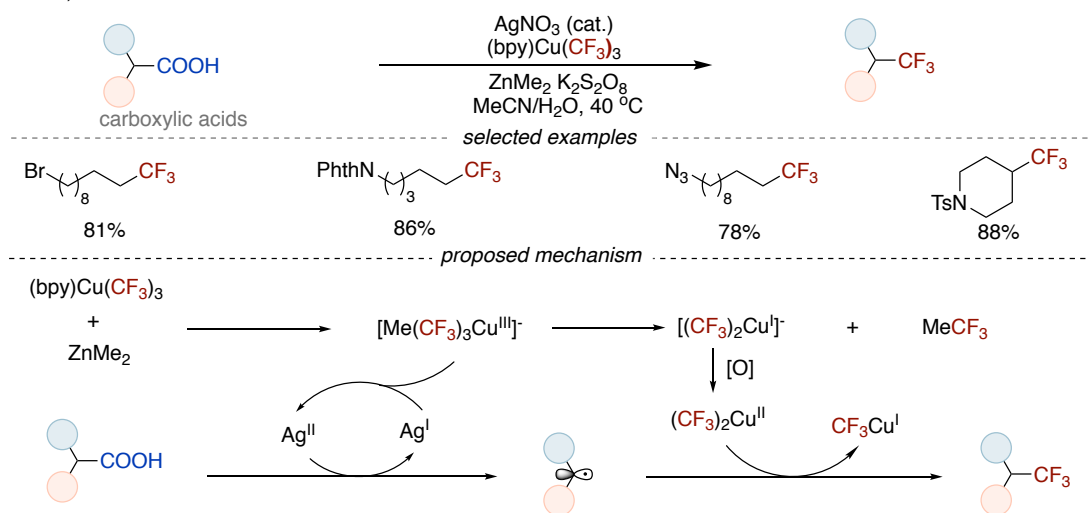


**Scheme 3.11** Cu-catalyzed  $\beta$  C–C bond cleavage/trifluoromethylation of cycloalkanols.

Carboxylic acids as a highly stable, of low cost and naturally abundant feedstock chemicals, which can be applied in the dual catalytic platform to effectively achieve the decarboxylative  $\text{C}(\text{sp}^3)\text{-CF}_3$  bond formation. The groups of Li and MacMillan have reported two different approaches for the decarboxylative trifluoromethylation of aliphatic carboxylic acids.<sup>26</sup> Firstly, Li and coworkers described the conversion of aliphatic acids to the corresponding alkyl- $\text{CF}_3$  in aqueous acetonitrile solution using  $\text{AgNO}_3$  as catalyst,  $\text{K}_2\text{S}_2\text{O}_8$  as oxidant,  $(\text{bpy})\text{Cu}(\text{CF}_3)_3$  as  $\text{CF}_3$  source, and  $\text{ZnMe}_2$  as activator (Scheme 3.12, *top*).<sup>26a</sup> They proposed that the single electron oxidation of alkyl carboxylic acids by  $\text{Ag}^{2+}$  can result in alkyl radicals, which could be trapped by  $\text{LnCu}^{\text{II}}(\text{CF}_3)_2$  to form alkyl- $\text{Cu}^{\text{III}}(\text{CF}_3)_2$  intermediates, and then alkyl- $\text{Cu}^{\text{III}}(\text{CF}_3)_2$  intermediates would undergo reductive elimination to produce the product (Scheme 3.12, *bottom*). Subsequently, the

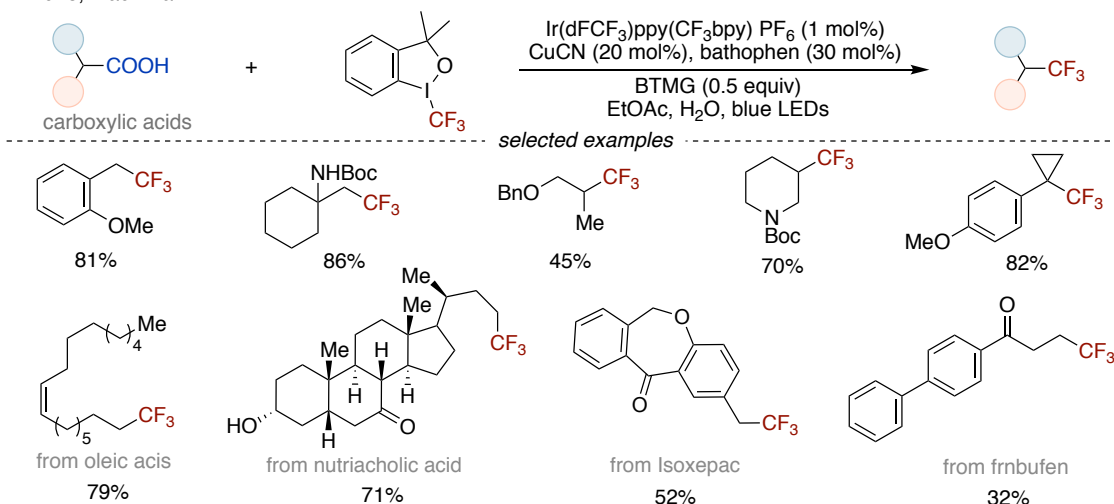
MacMillan group developed an elegant method for metal photoredox-catalyzed decarboxylative trifluoromethylation (Scheme 3.13).<sup>26b</sup> In contrast to previous work on trifluoromethylation using stoichiometric metal reagents ( $[\text{CuCF}_3]$  as a  $\text{CF}_3$  source), they used Togni's reagent I as  $\text{CF}_3$  source to successfully demonstrate the broad functional group tolerance of the reaction and its potential for late-stage diversification of complex molecules employing catalytic amounts of copper catalysis under visible light conditions.

In 2017, Li:



**Scheme 3.12** Ag catalyzed decarboxylated trifluoromethylation.

In 2018, MacMillan:

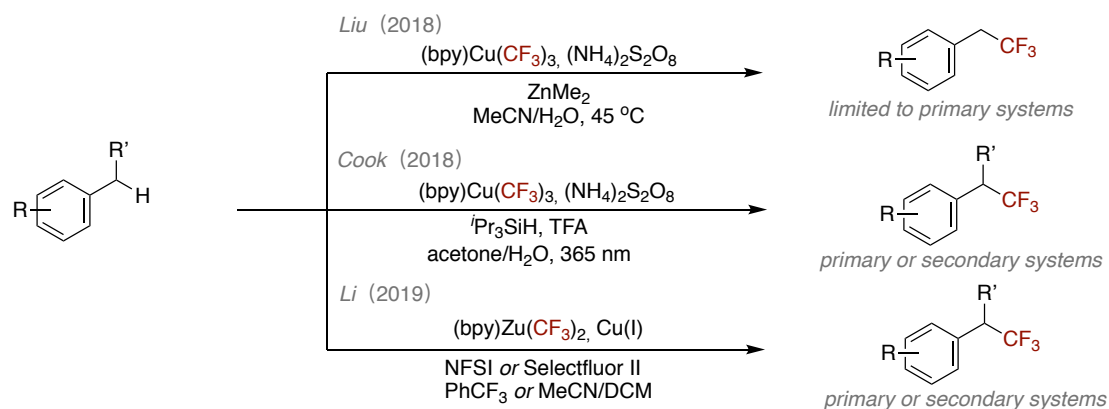


**Scheme 3.13** Photoredox-catalyzed decarboxylative trifluoromethylation cross-coupling.

Trifluoromethylation methods via  $\text{C}(\text{sp}^3)\text{-H}$  activation display one of the most atom-economical and step-efficient strategy, therefore has attracted much attention from chemists. In preliminary studies, the copper-mediated benzyl  $\text{C}(\text{sp}^3)\text{-H}$

trifluoromethylation have been independently reported by the groups of Cook, Liu and Li (Scheme 3.14).<sup>27</sup> Liu's group used  $\text{ZnMe}_2$  as a reductant to reduce  $(\text{bpy})\text{Cu}^{\text{III}}(\text{CF}_3)_3$  to trigger the generation of  $(\text{bpy})\text{Cu}^{\text{II}}(\text{CF}_3)_2$  and trifluoromethyl radicals,<sup>27b</sup> while Cook's group discovered the homolysis nature of  $(\text{bpy})\text{Cu}^{\text{III}}(\text{CF}_3)_3$  under photoexcitation to generate  $(\text{bpy})\text{Cu}^{\text{II}}(\text{CF}_3)_2$  intermediates.<sup>27a</sup> In contrast to the two previously methods, the Li group designed a catalytic amount of copper to promote the benzyl trifluoromethylation and employ NFSI or Selectfluor to oxidize  $\text{Cu}^{\text{I}}$  while acting as a HAT reagent to activate benzylic C–H bonds.<sup>27c</sup> However, the cores of the three different reaction conditions all undergo the combination of alkyl radicals with  $\text{LnCu}^{\text{II}}\text{CF}_3\text{X}$  to generate the  $\text{R-Cu}^{\text{III}}\text{-CF}_3$  intermediate, which subsequently give the benzylic  $\text{C}(\text{sp}^3)\text{-CF}_3$  product by reductive elimination.

■ Trifluoromethylation of benzylic  $\text{C}(\text{sp}^3)\text{-H}$

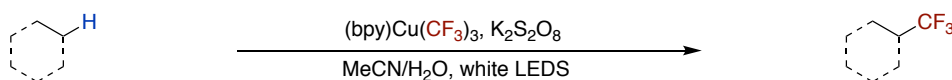


**Scheme 3.14** Benzylic C–H bond trifluoromethylation.

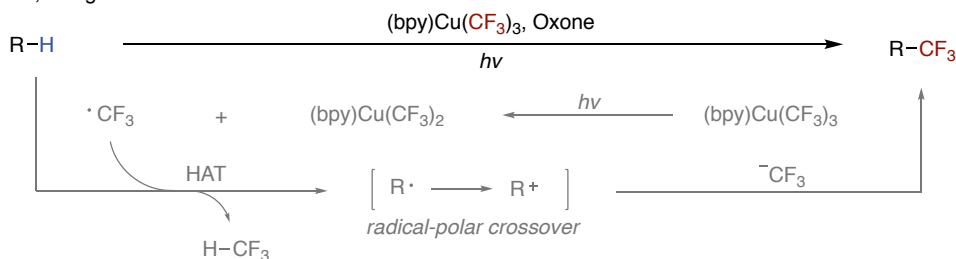
In 2021, both the Cook group and Hong's group have discovered valuable methods for the trifluoromethylation of highly unactivated  $\text{C}(\text{sp}^3)\text{-H}$  bonds of alkanes (Scheme 3.15).<sup>28</sup> However, these reactions require a large excesses of the substrate (alkane) employing a copper- $\text{CF}_3$  reagent as the limiting reagent. Herein, Hong's group utilized highly reactive  $\text{CF}_3$  radicals as HAT reagents to functionalize the inert  $\text{C}(\text{sp}^3)\text{-H}$  bond (Scheme 3.15, bottom).<sup>28b</sup> According to DFT studies, the reaction undergoes a radical-polar crossover pathway instead of reductive elimination pathway due to the strong oxidation potential of Oxone ( $E_p = +1.81\text{V}$ ).

■ Trifluoromethylation of unactivated C(sp<sup>3</sup>)-H

In 2021, Cook:



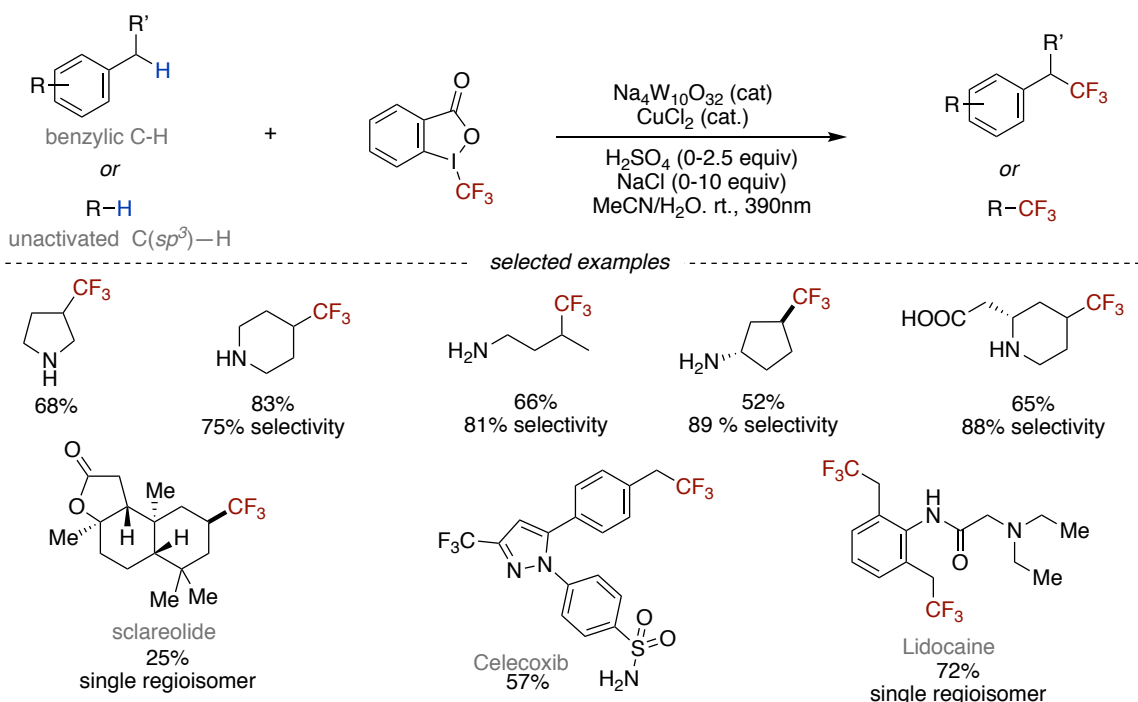
In 2021, Hong:



**Scheme 3.15** Aliphatic C(sp<sup>3</sup>)-H bond trifluoromethylation.

In 2020, MacMillan and his colleagues reported an elegant method for the direct trifluoromethylation of aliphatic and benzylic C(sp<sup>3</sup>)-H bonds employing decatungstate (Na<sub>4</sub>W<sub>10</sub>O<sub>32</sub>) and copper(II) chloride Cu<sup>II</sup>Cl<sub>2</sub> (Scheme 3.16).<sup>29</sup> Herein, β-trifluoromethylated amines could be obtained applying primary or secondary amines under slightly acidic conditions in the presence of Togni's reagent II and ultraviolet irradiation (390 nm). This method demonstrated high efficiency and a broad substrate scope including the late-stage diversification of several natural products and drug molecules. Mechanistic studies showed that the excited state of Na<sub>4</sub>W<sub>10</sub>O<sub>32</sub> acts as an HAT-catalyst and the in situ generated Cu<sup>II</sup>-CF<sub>3</sub> species is involved in the formation of the crucial C(sp<sup>3</sup>)-CF<sub>3</sub> bond.

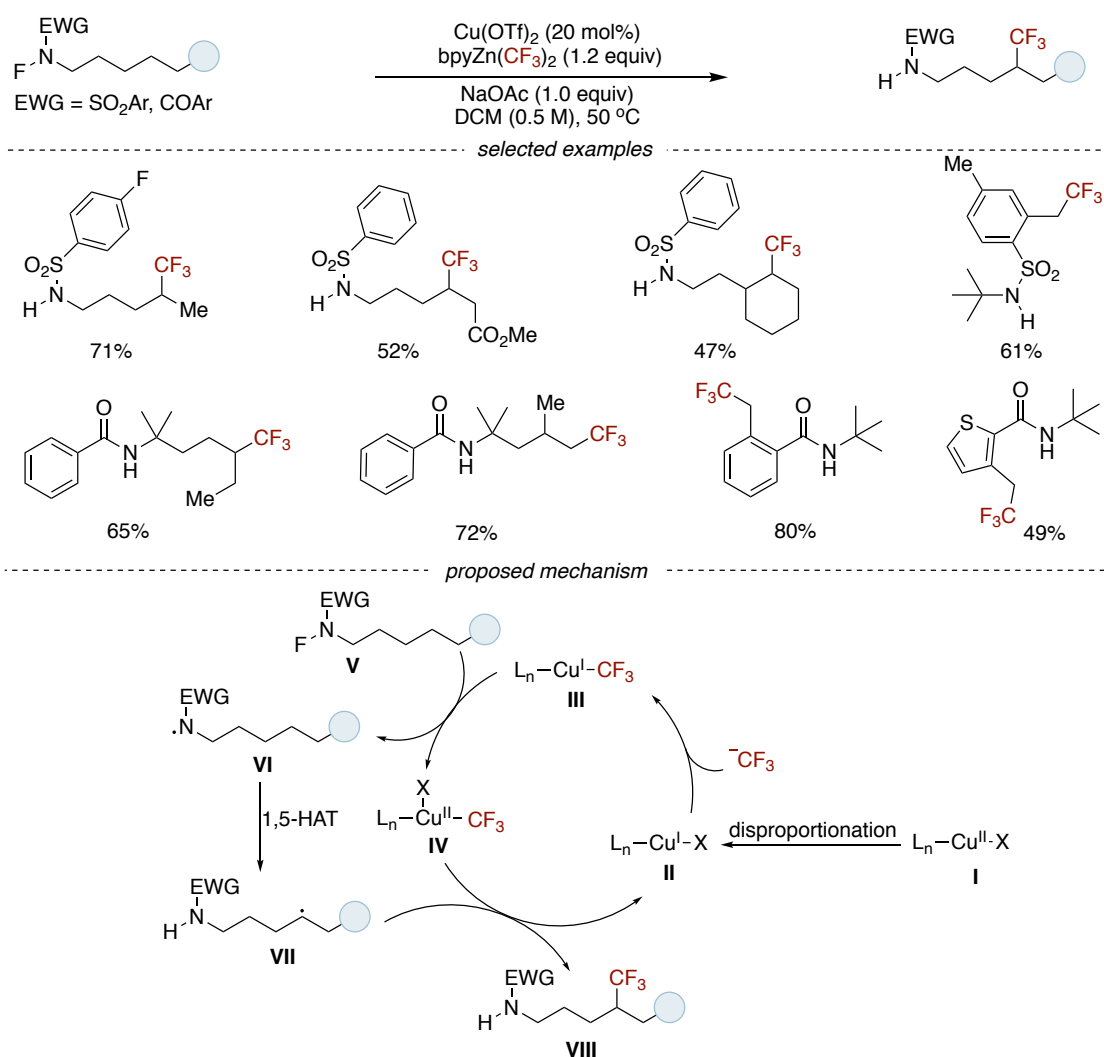
In 2020, MacMillan:



**Scheme 3.16** W/Cu-cocatalysed C(sp<sup>3</sup>)-H bond trifluoromethylation.

In 2018, Li's group reported the first remote C(sp<sup>3</sup>)-H bond activation of trifluoromethylation through the use of Cu(OTf)<sub>2</sub> as a catalyst and Zn(CF<sub>3</sub>)<sub>2</sub> as a source of trifluoromethyl, involving 1,5-hydrogen atom transfer from the N-fluoro-substituted carboxamides (or sulfonamides) (Scheme 3.17).<sup>30</sup> They hypothesised that the key intermediate Cu<sup>I</sup>-CF<sub>3</sub> (**III**) could be transferred to the N-fluoroamine substrate (**V**) via a single electron transfer to produce the Cu<sup>II</sup>-CF<sub>3</sub> intermediate (**IV**) and the corresponding N-radical (**VI**). **VI** followed by 1,5-HAT to give the alkyl radical **VII**. The subsequent transfer of the CF<sub>3</sub> group from the Cu<sup>II</sup>-CF<sub>3</sub> intermediate (**IV**) to provided remote C(sp<sup>3</sup>)-H trifluoromethylation product (**VIII**) and the generation of Cu<sup>I</sup>X (**II**) salts to complete the catalytic cycle.

In 2019, Li:

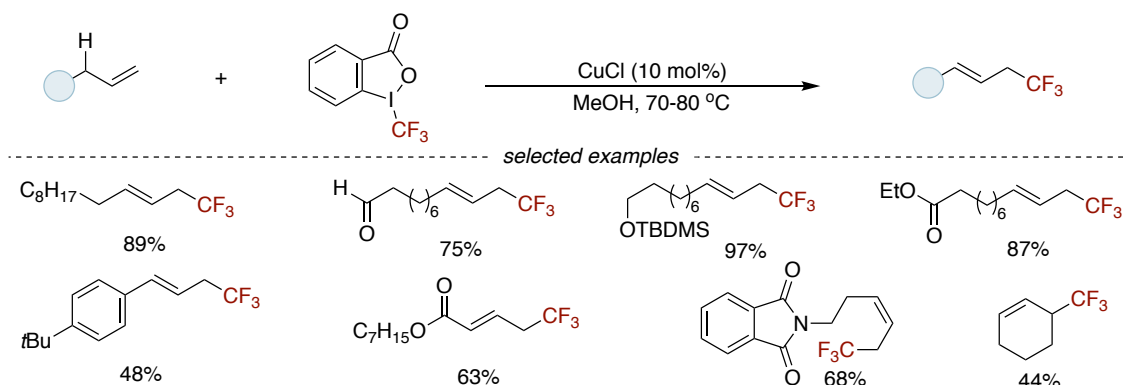


**Scheme 3.17** Remote  $\text{C}(\text{sp}^3)\text{-H}$  bond activation of trifluoromethylation.

A site-specific allylic  $\text{C-H}$  bond activation via an efficient copper-catalyzed trifluoromethylation reaction has been achieved by Wang's group (Scheme 3.18).<sup>31</sup> They built a diverse range of allyl trifluoromethylation compounds using  $\text{CuCl}$  as the catalyst, a hypervalent iodine(III) reagent as the oxidant and  $\text{CF}_3$  source, and simple olefins as substrates. They suggested allyl radical or allyl cation intermediates generated from alkenes can be attacked by the nucleophilic  $\text{Cu}^{\text{I}}\text{-CF}_3$  species to give the desired product, but the details of the  $\text{C-CF}_3$  bond-forming step are not clear.



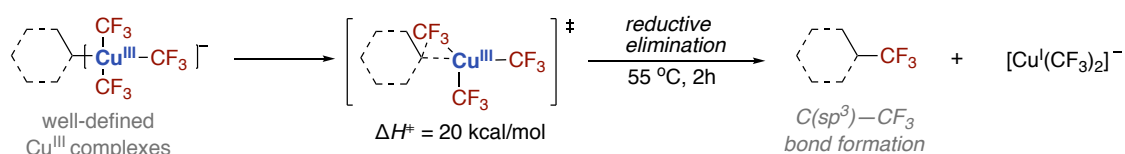
In 2011, Wang:



**Scheme 3.18** Direct allylic C–H bond activation of trifluoromethylation.

A large amount of Cu-promoted  $C(sp^3)$ -trifluoromethylation reactions have been reported in recent years suggesting the reductive elimination of  $R-Cu^{III}-CF_3$  intermediates to form  $C(sp^3)-CF_3$  bond as the key step. Although the reductive elimination for the  $C(sp^2)-CF_3$  bond formation has been explored for  $Pd^{II}$ ,  $Pd^{IV}$ ,  $Ni^{III}$  and  $Au^{III}$  complexes,<sup>9e, 9g, 32</sup> the formation of  $C(sp^3)-CF_3$  bonds via reductive elimination from any transition metal complex with a well-defined structure is still unknown. Finally, Liu's group reported the synthesis of  $[alkyl-Cu^{III}(CF_3)_3]$  complexes and it has been demonstrated that these high-valent organocopper (III) species can undergo reductive elimination following first-order kinetics to form the corresponding alkyl- $CF_3$  compounds (Scheme 3.19).<sup>33</sup> Mechanistically, this transformation is following a concerted transition state  $[Cu^I(CF_3)_3]^{2-}$  with an activation barrier of  $\Delta H^\ddagger = 20$  kcal/mol calculated by DFT.

In 2019, Liu:

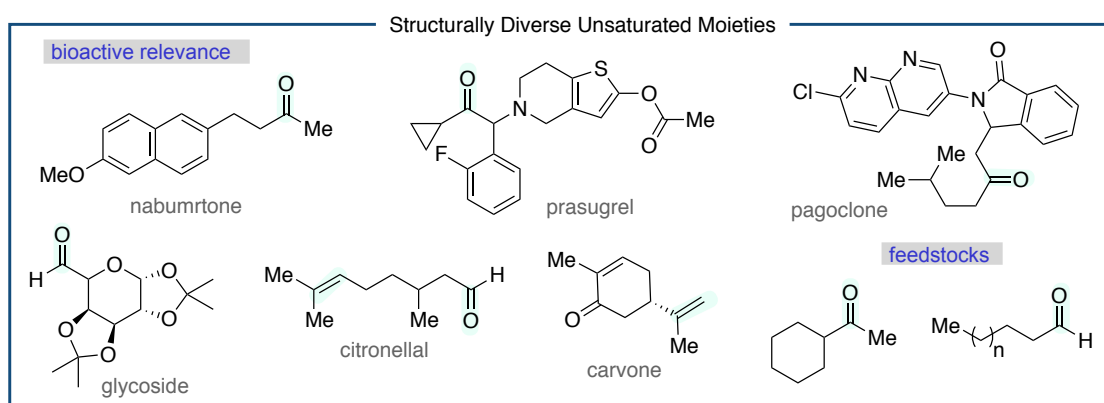


**Scheme 3.19** Forming  $C(sp^3)-CF_3$  bonds via reductive elimination of  $[Cu^{III}]$  complexes.

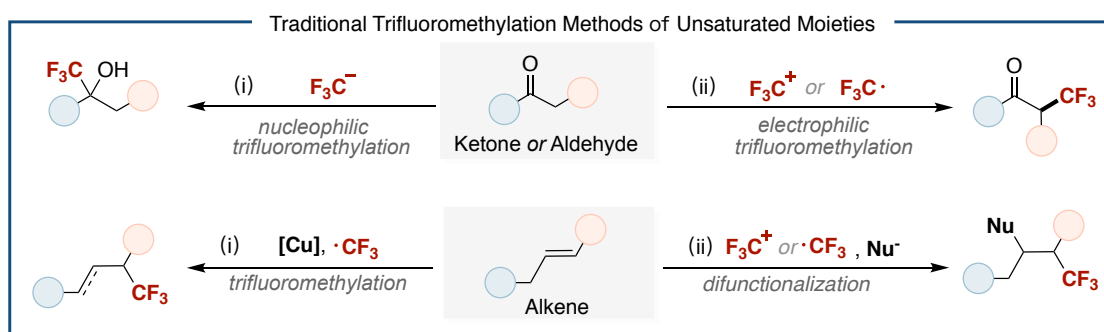
### 3.1.2 Addition of Trifluoromethyl Group to Unsaturated Moieties for Forging $C(sp^3)-CF_3$ Bonds

Unsaturated compounds, such as ketones, aldehydes and alkenes, are widely used as chemical feedstocks and represent frequently found functional groups in pharmaceutical molecules (Scheme 3.20).<sup>34</sup> The incorporation of  $CF_3$  groups across unsaturated moieties

is a common and powerful functionalization tool to access  $C(sp^3)-CF_3$  bonds.<sup>35</sup> Conventional approaches for the trifluoromethylation of carbonyl compounds fall into two main categories (Scheme 3.21): (i) Nucleophilic trifluoromethylation of carbonyl compounds via 1,2-addition allow for the preparation of  $CF_3$ -substituted alcohols.<sup>10, 35a</sup> (ii) Enolates derived from ketones react with either an electrophilic  $CF_3$  or a radical  $CF_3$  source to form the  $\alpha$ - $CF_3$ -substituted carbonyl compounds (Scheme 3.21, *top*).<sup>11,35</sup> In the case of alkenes, (i) hydrotrifluoromethylation reactions of alkenes.<sup>12</sup> (ii) difunctionalization,  $CF_3$  radicals are added to the terminal position of the alkene allowing for subsequent functionalization of the internal carbon employing copper-catalyzed cross-coupling or radical cross-coupling (Scheme 3.21, *bottom*).<sup>12</sup>



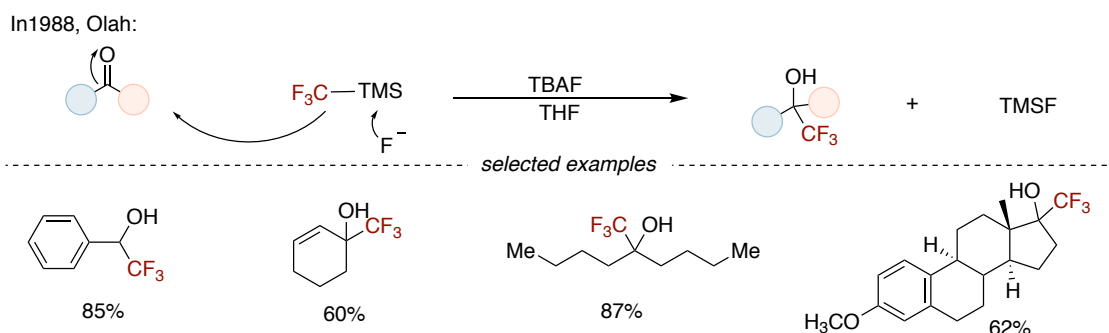
**Scheme 3.20** Structurally diverse unsaturated compounds.



**Scheme 3.21** Traditional methods of introducing  $CF_3$  groups onto unsaturated moieties.

For many years, nucleophilic trifluoromethylation has been the most convenient strategy for the incorporation of trifluoromethyl groups into unsaturated organic molecules containing carbonyl groups. As already in 1988, Olah's group reported a very efficient nucleophilic trifluoromethylation of carbonyl compounds using the Ruppert-Prakash reagent ( $TMSCF_3$ ) initiated by TBAF (Scheme 3.22).<sup>36</sup>  $TMSCF_3$  is more stable than

[metal]-CF<sub>3</sub> reagents, since its usually require an initiator for activation thus ensuring the activity and effectiveness of CF<sub>3</sub> anions and avoiding CF<sub>3</sub> anions fastly undergo  $\alpha$ -elimination of the fluoride.

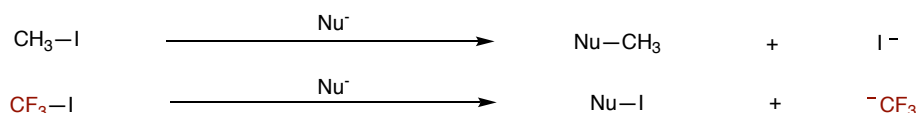


**Scheme 3.22** Nucleophilic trifluoromethylation of carbonyl compounds by TMSCF<sub>3</sub>.

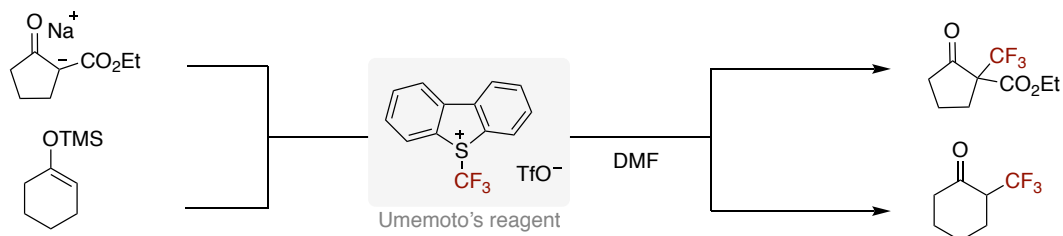
Since then, a series of studies on the nucleophilic trifluoromethylation of aldehydes and activated ketones employing TMSCF<sub>3</sub> have been reported. Notably, the different types of initiators such as alkoxides, N-oxides, phosphines and acetates have shown efficient reactivity to activate TMSCF<sub>3</sub> in situ.<sup>37</sup> In recent years, Shreeve and Kim et al. have also developed a new class of ionic liquids as reaction media for nucleophilic trifluoromethylation reactions.<sup>38</sup> In addition, the field of asymmetric nucleophilic trifluoromethylation of carbonyl groups has also been extensively studied.<sup>39</sup>

The introduction of CF<sub>3</sub> groups by activating the C(sp<sup>3</sup>)-H bond at the  $\alpha$ -position of carbonyl compounds including ketones, aldehydes, esters and amides was intensively studied to build C(sp<sup>3</sup>)-trifluoromethylated motifs.<sup>40</sup> However, due to the negative polarization of the CF<sub>3</sub> group, the typical S<sub>N</sub>2 approach via deprotonation/formation of the enolates from carbonyl compounds and then trapping to electrophilic reagents is usually not applicable to trifluoromethylation.<sup>41</sup> Take trifluoroiodomethane reagent as an example, the strong electron withdrawing effect of CF<sub>3</sub> results in the electron density around iodine being more dense toward the more electronegative (Scheme 3.23, *top*).<sup>42</sup> To circumvent the use of these reagents, some novel electrophilic trifluoromethylation agents were designed to convert enolates (or enolate equivalents) into  $\alpha$ -trifluoromethylated carbonyl groups. In 1998, Shreve and coworkers reported the electrophilic trifluoromethylation of enolates using dibenzothiophene trifluoromethylsulfonium triflate (Umemoto's reagent) as CF<sub>3</sub><sup>+</sup> reagent avoiding the reversal of polarization (Scheme 3.23, *bottom*).<sup>43</sup>

■ Reversal of polarisation in CF<sub>3</sub>I



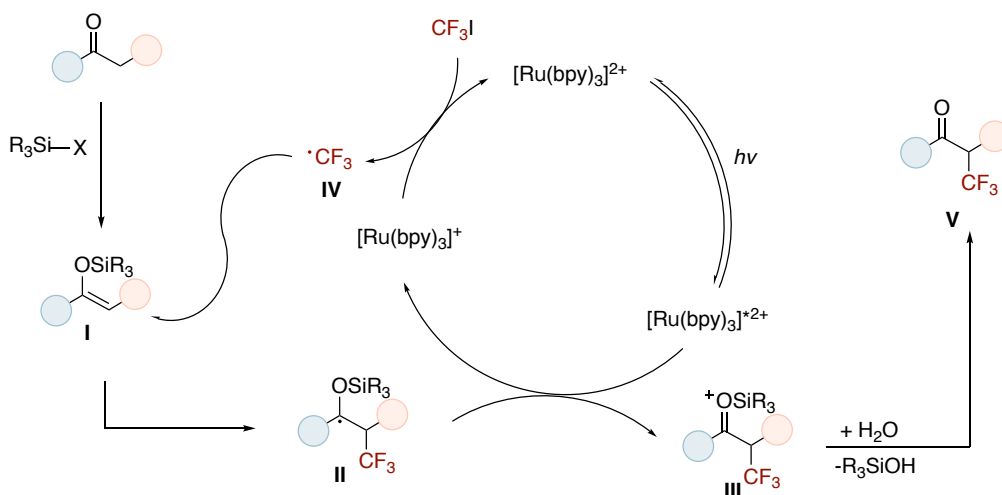
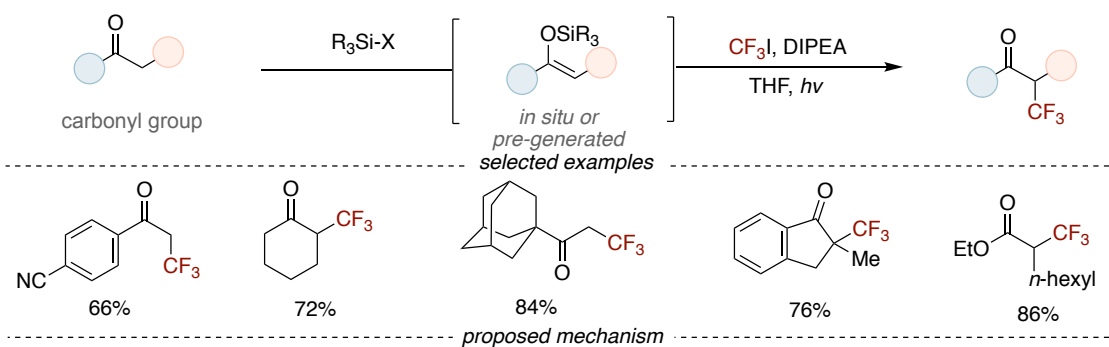
■ Electrophilic trifluoromethylation of enolates via Umemoto's reagent



**Scheme 3.23**  $\alpha$ -Trifluoromethylation of carbonyl compounds by electrophilic trifluoromethylation reagents.

Although these new electrophilic trifluoromethyl reagents<sup>11a,16d</sup> have made progress allowing for  $\alpha$ -trifluoromethylation of carbonyl compounds,<sup>40</sup> the applicability of the reactions remain limited to activated substrates. In 2011, MacMillan and colleagues described a simple method for preparing  $\alpha$ -trifluoromethyl carbonyl compounds from methylsilyl enol derivatives and CF<sub>3</sub>I employing photoredox-catalysis (Scheme 3.24).<sup>44</sup> Proposing, the electrophilic trifluoromethyl radical is generated via SET from the reductive photocatalyst [Ru(bpy)<sub>3</sub>]<sup>+</sup>. Following this, the CF<sub>3</sub> adds into the silyl enol ether **I** to provide a highly stabilized  $\alpha$ -methanosiloxy radical **II**. Final oxidation mediated by [Ru(bpy)<sub>3</sub>]<sup>\*2+</sup> ( $E_{1/2\text{red}} = 0.79$  V vs. SCE in MeCN)<sup>45</sup> forms silyloxocarbenium **III** which rapidly hydrolyzes to deliver the desired  $\alpha$ -CF<sub>3</sub> carbonyl product.

In 2011, MacMillan:



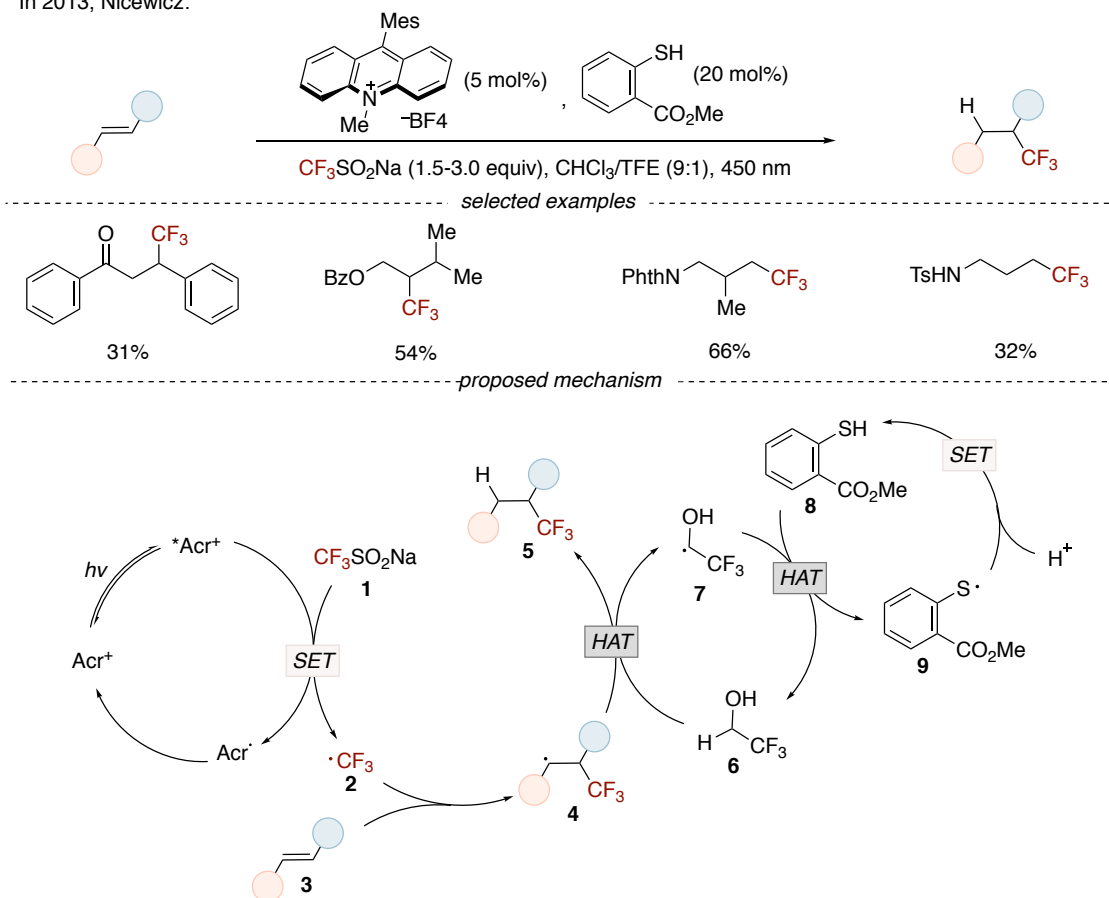
**Scheme 3.24** Photoredox-catalyzed  $\alpha$ -trifluoromethylation of carbonyl group by  $CF_3I$ .

Alkenes display another prominent class of abundant organic compounds, available from petrochemical feedstocks being widely present in natural products and pharmaceutical molecules.<sup>34c, 34d</sup> The application of radical  $CF_3$  sources have attracted chemists to add into unsaturated double bonds forming  $C(sp^3)-CF_3$  bonds.<sup>12</sup> Thereby,  $CF_3$  radical has electrophilic nature with a low-lying singly occupied molecular orbital (SOMO) and therefore can react faster with electron-rich alkenes with high-lying highest occupied molecular orbitals (HOMOs).<sup>46</sup>

In the late 1980s, the electrochemical hydrotrifluoromethylation of olefins have been started to study.<sup>47</sup> However, hydrotrifluoromethylation of unactivated olefins by electrochemical oxidation has remained underexplored due to the disadvantages of low chemoselectivity and harsh reaction conditions.<sup>48</sup> Based on the development of photocatalytic reactions, a series of hydrotrifluoromethylation reactions of olefins via photocatalytic oxidation have been successively reported.<sup>49</sup> For example, in 2013, the Nicewicz group developed a metal-free photoredox process that successfully achieved hydrotrifluoromethylation of unactivated mono-, di- and tri-substituted olefins (Scheme

3.25).<sup>50</sup> They hypothesised that TFE acts as a co-solvent while the  $\alpha$  C–H bond of TFE also acts as a hydrogen atom source, methyl thiosalicylate can provide a hydrogen atom and facilitate the regeneration of TFE.

In 2013, Nicewicz:

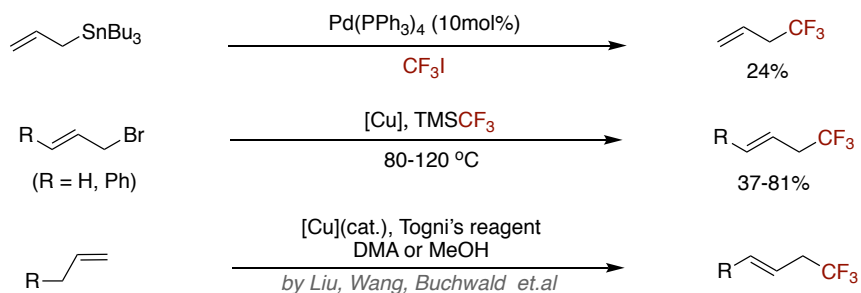


### Scheme 3.25 Hydrotrifluoromethylation of alkenes via an organic photoredox system

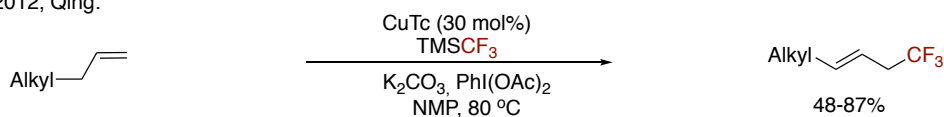
For the establishment of allylic trifluoromethylations, both the use of "prefunctionalized" starting materials containing double bonds (such as allylstannanes or allyl halides) and non-activated terminal double bonds were successfully applied to forge allylic  $C(sp^3)$ – $CF_3$  bonds.<sup>51</sup> A related series of studies was reported independently by the group of Buchwald,<sup>52</sup> Liu<sup>53</sup> and Qing<sup>54</sup> et.al (Scheme 3.26, *top*), relying on the copper-catalyzed trifluoromethylation of olefins by using Togni's and Umemoto's reagent as electrophilic trifluoromethylation reagents. They suggested that radicals or cationic species generated after the addition of  $CF_3$  to the terminal double bond serve as intermediates, but the precise mechanism of these transformations has not yet been clarified. Particularly, Qing's group reported preliminary studies on catalytic trifluoromethylation to form allylic  $C(sp^3)$ – $CF_3$  bonds by Cu-catalyzed oxidative  $C(sp^3)$ –H activation (Scheme 3.26,

bottom).<sup>54</sup>

■ Formation of Allyl C(sp<sup>3</sup>)-CF<sub>3</sub>



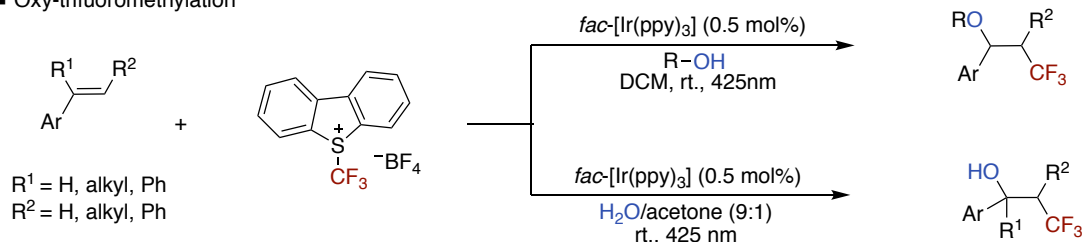
In 2012, Qing:



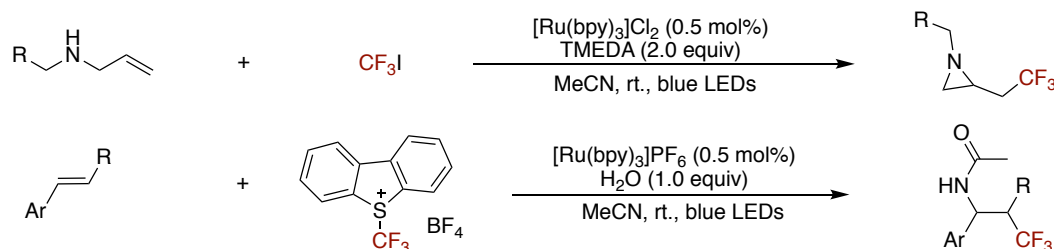
**Scheme 3.26** Forging allyl C(sp<sup>3</sup>)-CF<sub>3</sub> bonds via trifluoromethylation of double bonds.

At the same time, the trifluoromethylative difunctionalization of alkenes has attracted increasing interest. Typically, CF<sub>3</sub> radicals were added to electron rich olefins to generate alkyl radicals, which can be oxidized to the corresponding carbocations and finally trapped by intramolecular or intermolecular nucleophiles such as aliphatic alcohols or amines (Scheme 3.27).<sup>12f</sup> For example, Akita and Koike et.al. used *fac*-[Ir(ppy)<sub>3</sub>] as the photocatalyst to achieve a three-component oxygen-trifluoromethylation of alkenes.<sup>55</sup> Based on their previous work, they subsequently reported the acylamino-trifluoromethylation of styrene derivatives relying on a Ritter-type reaction.<sup>56</sup>

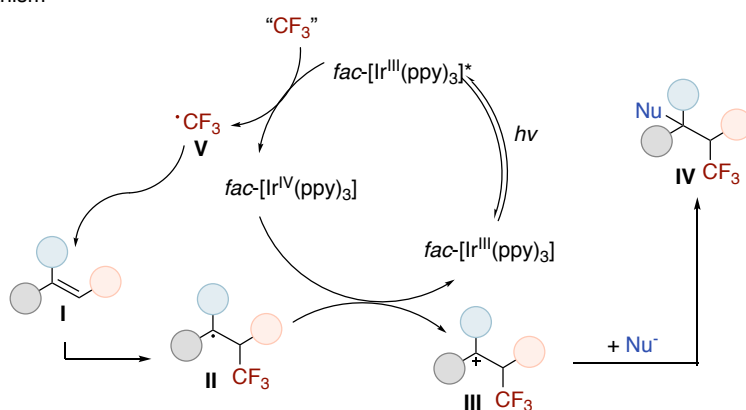
■ Oxy-trifluoromethylation



■ Alkylamino-trifluoromethylation



■ Proposed mechanism

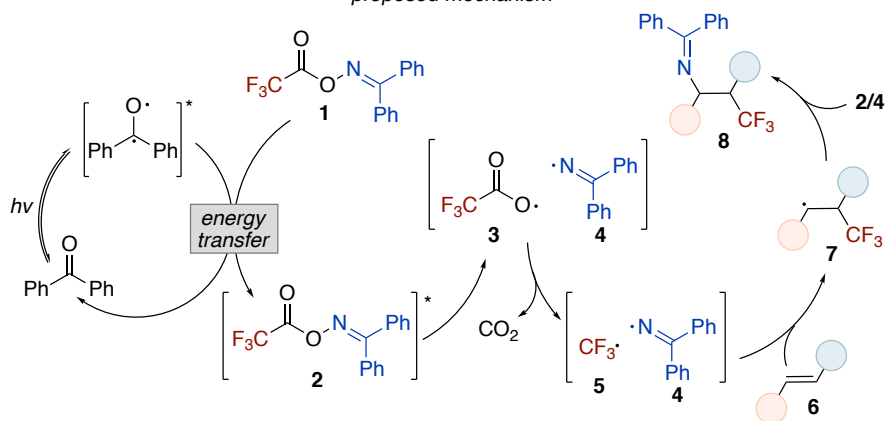
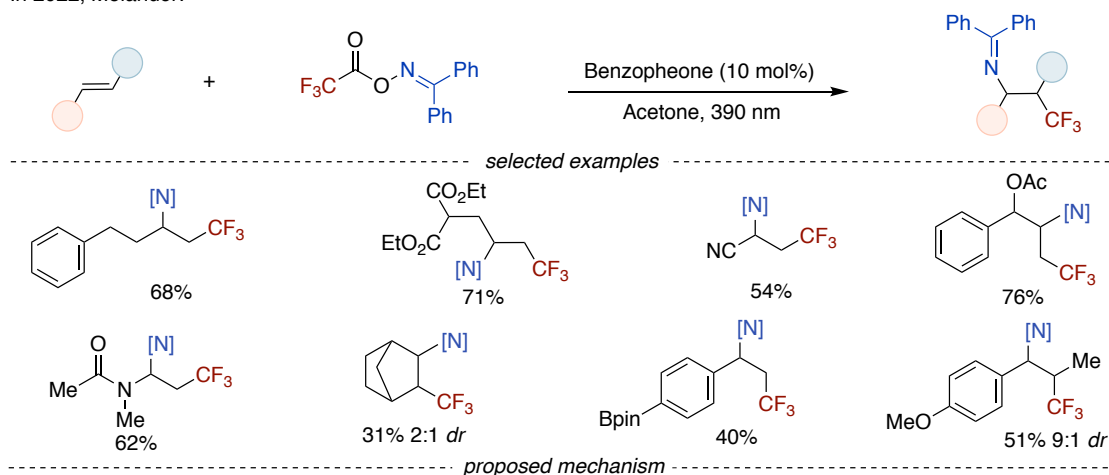


**Scheme 3.27** Difunctionalized trifluoromethylation of alkenes.

Recently, the Molander group reported an outstanding strategy to achieve direct and metal-free alkene difunctionalization to install  $C(sp^3)\text{-CF}_3$  and nitrogen-based functional groups (Scheme 3.28).<sup>57</sup> This approach provides an efficient alternative to the conventional approach of simultaneously accessing  $C(sp^3)\text{-CF}_3$  and  $C(sp^3)\text{-[N]}$  motifs based on a wide range of easily accessible alkene feedstocks under mild as well as scalable conditions. They suggested that selective radical cross-coupling between oxime (**1**) and alkene (**6**) is kinetically feasible based on persistent radical effects. Mechanistically, energy transfer between the photocatalyst (Benzophenone) and the oxime (**1**) could allow **1** to undergo rapid fragmentation/decarboxylation due to the low energy barrier when the N–O bond in the excited triplet state **1** is broken. The subsequent  $\text{CF}_3$  radical reacts with the alkene to generate an alkyl radical intermediate (**7**), and **7** undergoes radical cross-coupling with **1** or **4** to produce the final product (**8**).



In 2022, Molander:



**Scheme 3.28** Metal-free catalytic imino-trifluoromethylation of alkenes.

Until now, approaches to introduce  $\text{CF}_3$  into unsaturated moieties have mainly focused on addition reactions, the strategy of directly using unsaturated compounds as a source of  $sp^3$ -hybridized carbon intermediates to form  $\text{C}-\text{CF}_3$  bonds remains incomplete. Therefore, we hope to achieve fast and efficient trifluoromethylation reactions by using a wide range of unsaturated compounds as  $sp^3$  alkyl synthons.

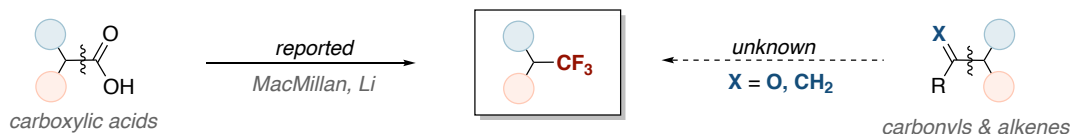
### 3.2 General Aim of the Project

Based on the current state of research, unsaturated compounds such as ketones aldehydes and alkenes display a challenging substrate class for  $\text{C}(sp^3)-\text{CF}_3$  bond formation, thereby an appealing opportunity to develop novel synthetic disconnections to incorporate trifluoromethyl groups into organic molecules. Simultaneously, the creation of new trifluoromethylation blueprints via  $\text{C}(sp^3)-\text{C}$  cleavage from unsaturated compounds may hold promise for accelerating access to important  $\text{C}(sp^3)-\text{CF}_3$  architectures from the path

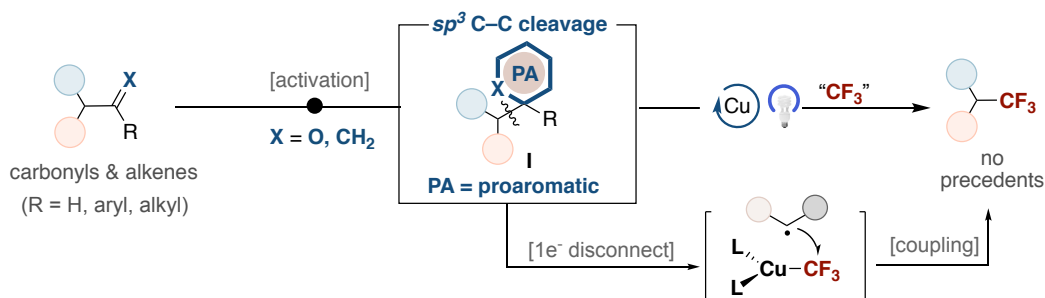
to drug discovery. Prompted by our interest in activating strong  $C(sp^3)$ -C bonds and by the prevalence of carbonyl compounds and unactivated olefins in biologically-relevant molecules, we wondered whether we could reverse the innate reactivity of these building blocks with  $CF_3$  sections by promoting a  $C(sp^3)$ - $CF_3$  bond-formation via  $C(sp^3)$ -C cleavage instead. If successful, the merger of these disciplines would offer a new technique to rapidly build  $C(sp^3)$ - $CF_3$  architectures from a simple unsaturated motif with the advantage of producing useful chemicals for downstream applications.

Our trifluoromethylation study will merge two different strategies, decarbonylative and dealkenylative, for the generation of radicals and their application in Cu-mediated trifluoromethylation reactions. The generation of alkyl radicals from carbonyl compounds via the formation of dihydroquinazoline radical precursors, was demonstrated by the Zhu group and our group (see Chapter 1, Scheme 1.24). On the other hand, the Luo group demonstrated the generation of radicals from alkenes enabled by reaction with tetrazine and photoexcitation to conduct a nickel-catalyzed arylation (Chapter 1, Scheme 1.25). We designed that the conversion of a carbonyl compound or an olefin into a proaromatic precursor (I) might set the basis for enabling a homolytic cleavage of the adjacent  $\alpha$ -C-C bond via photoinduced single-electron transfer (Scheme 3.29). The subsequent open-shell alkyl radical might then be interfaced with  $[Cu]$ - $CF_3$  species, thus leading to the targeted products via reductive elimination from alkyl- $Cu^{III}$ - $CF_3$  intermediate.

- Previous work: decarboxylated trifluoromethylation via  $C(sp^3)$ -C cleavage



- This chapter: trifluoromethylation of unsaturated moieties via  $C(sp^3)$ -C cleavage

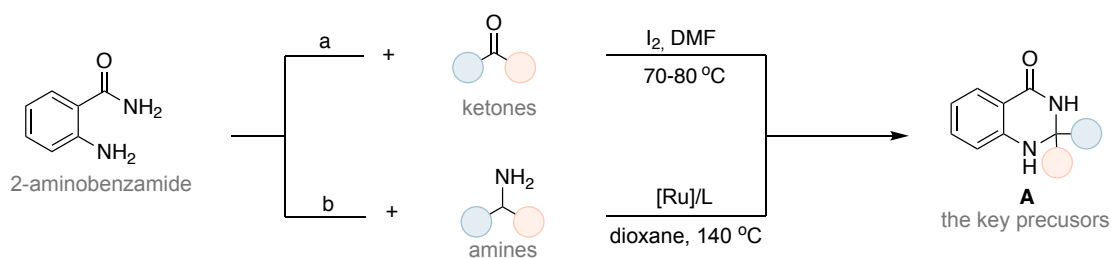


**Scheme 3.29** Alkyl trifluoromethylation from unsaturated moieties.

## 3.3 Trifluoromethylation of Carbonyl and Unactivated Olefin Derivatives via $sp^3$ C–C Bond Cleavage

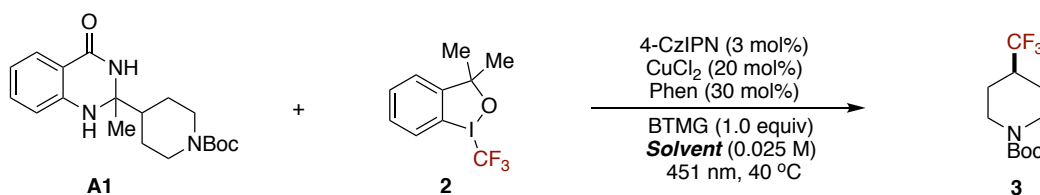
### 3.3.1 Optimization of the Reaction Conditions

We began our investigation by exploring the generation of alkyl radicals from ketones via the formation of dihydroquinazoline radical precursors **A**, which could undergo radical or nickel-catalyzed cross-coupling reactions (see Chapter 1, Scheme 1.24). Proaromatic precursor **A** was easily obtained in a single step operation from the condensation between ketone and 2-aminobenzamide (Scheme 3.30, a). In addition, the other reason to use this kind of activate precursors **A** is as reported work that **A** can even be accessed from the corresponding cyclohexanamine and 2-aminobenzamide under Ruthenium-catalyzed conditions, which would open a new platform to give an alternative deaminative trifluoromethylation (Scheme 3.30, b).<sup>58</sup>



**Scheme 3.30** Methods to prepare dihydroquinazoline radical precursors **A**

Initially, we started to screen the different solvents, as depicted in Table 3.1. When utilizing polar aprotic solvents, including DMA, DMF, NMP, DMSO, DCE, EA or acetone, moderate yields could be obtained (entry 1-7, 43-78% yield). Acetonitrile furnished the product in 29% yield but other nitrile-containing solvents only provided traces of **3**. Also etheral solvents and non-polar solvents (entry 11-12) are less efficient for the copper-catalyzed trifluoromethylation reaction. When screening different solvents, the  $^{19}F$ -NMR spectra of the crude reaction conducted in DMF or acetonitrile showed evidence for the trifluoromethylation of the solvent due to the HAT effect of  $CF_3$  radicals. The highest yields of 78% were obtained when employing acetone as the solvent. In addition, we found that the reaction proceeded better under dilute concentrations (0.025M), which is consistent with the previously reported copper-catalyzed trifluoromethylation: Herein, a significant concentration effect on the stability of  $[Cu-CF_3]$  intermediates was proposed.<sup>59</sup>

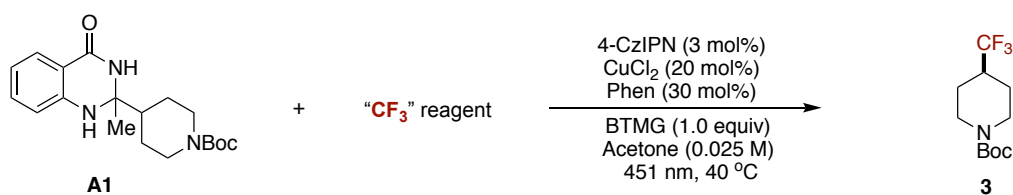


Entry	Solvent	<b>3</b> Yield (%) <sup>b</sup>
1	DMA	54
2	DMF	64
3	NMP	43
4	DMSO	48
5	DCE	62
6	EA	44
7	<b>Acetone</b>	<b>78</b>
8	CH <sub>3</sub> CN	29
9	<i>t</i> Bu-CN	trace
10	Ph-CN	trace
11	<i>i</i> Pr <sub>2</sub> O	0
12	PhMe	0
13	Acetone (0.05M)	56
14	Acetone (0.02M)	68

Conditions: <sup>a</sup> **A1** (0.05 mmol), **2** (0.1 mmol), CuCl<sub>2</sub> (20 mol%), Phen (30 mol%), 4-CzIPN (3 mol%), BTMG (0.05 mmol), in solvent (0.025 M) at 40 °C under irradiation of blue LEDs for 16 hours. <sup>b</sup> <sup>19</sup>F NMR yields using (trifluoromethyl)benzene as internal standard. BTMG = 2-tert-Butyl-1,1,3,3-tetramethylguanidine.

**Table 3.1** Screening of solvents.<sup>a</sup>

Afterwards, we examined the impact of various electrophilic trifluoromethylation reagents: Togni's reagent I (**2**) ( $E_p[2^{*+}] = -1.91$  V vs SCE in MeCN) is the most suitable for this reaction (Table 3.2, entry 1). More oxidizing CF<sub>3</sub>-sources such as Umemoto reagent ( $E_p = -0.32$  V vs SCE in MeCN, entry 2)<sup>26b</sup> and Togni's reagent II ( $E_p = -0.79$  V vs SCE in MeCN, entry 3)<sup>26b</sup> were not effective, probably as a result of the undesired reduction by the reduced 4-CzIPN photocatalyst ( $E_{1/2}[PC^{-1}/PC] = -1.24$  V vs. SCE in MeCN).<sup>60</sup>



Entry	"CF <sub>3</sub> " reagent	3 Yield (%) <sup>b</sup>
1	2	78
2	2-1	0
3	2-2	0
4	2-3	0

**2**  
E<sub>p</sub> = -1.91 V

**2-1**  
E<sub>p</sub> = -0.79 V

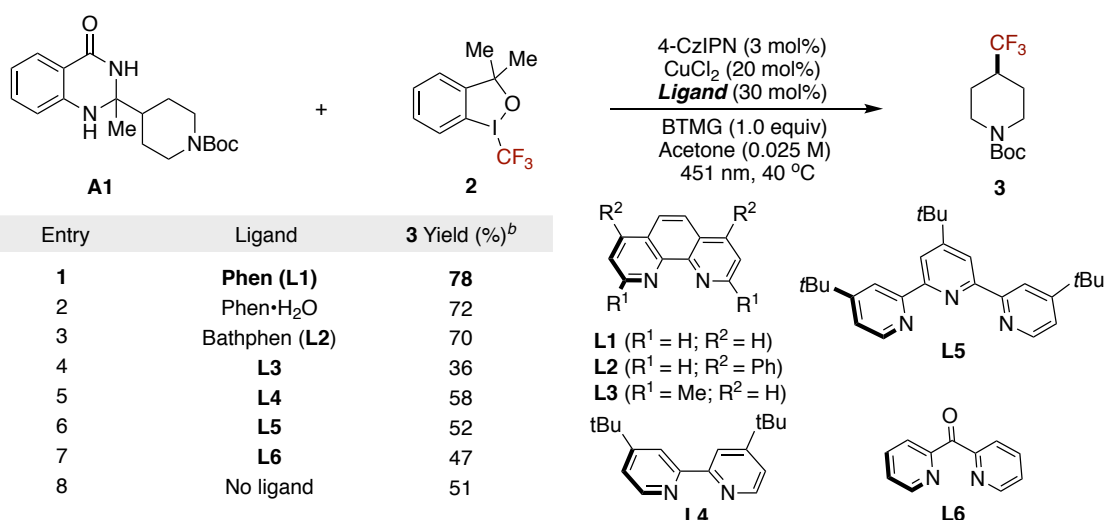
**2-2**  
E<sub>p</sub> = -0.32 V

**2-3**  
E<sub>p</sub> = -0.52 V

Conditions: <sup>a</sup> **A1** (0.05 mmol), "**CF<sub>3</sub>**" (0.1 mmol), CuCl<sub>2</sub> (20 mol%), Phen (30 mol%), 4-CzIPN (3 mol%), BTMG (0.05 mmol), in Acetone (0.025 M) at 40 °C under irradiation of blue LEDs for 16 hours. <sup>b</sup> <sup>19</sup>F NMR yields using (trifluoromethyl)benzene as internal standard. BTMG = 2-tert-Butyl-1,1,3,3-tetramethylguanidine.

**Table 3.2** Screening of "**CF<sub>3</sub>**" reagents.<sup>a</sup>

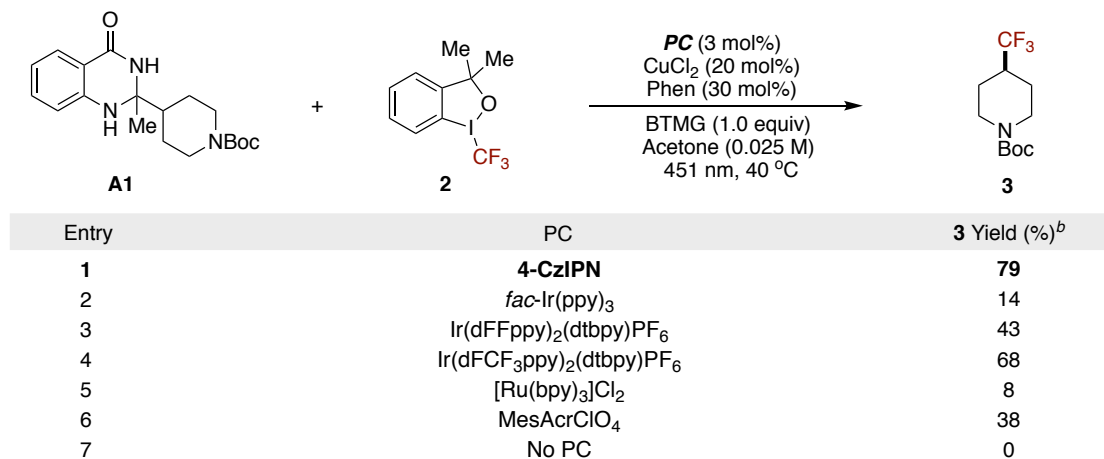
Considering the influence of the ligand on the reactivity, we began to screen different ligands (Table 3.3). Bipyridines, phenanthrolines, and other *N,N*-bidentate ligands were used to study the reactivity of various [LnCu-CF<sub>3</sub>] intermediates. 1,10-Phenanthroline (**L1**) turned out to be the best phen-type ligand, but employment of **L1** monohydrate or bathocuproine (**L2**) led to slightly lower yields (entry 2-3, 70-72% yield). neocuproine possessing 6,6'-methyl groups inhibit the reaction (**L3**). Compared with the planar phen-type ligand, the bipyridine (**L4**), tridentate nitrogen ligand (**L5**) or di(pyridin-2-yl)methanone (**L6**) showed lower yields. Specially, without Ligand can also give medium yields of product.



Conditions: <sup>a</sup> **A1** (0.05 mmol), **2** (0.1 mmol), CuCl<sub>2</sub> (20 mol%), **Ligand** (30 mol%), 4-CzIPN (3 mol%), BTMG (0.05 mmol), in Acetone (0.025 M) at 40 °C under irradiation of blue LEDs for 16 hours. <sup>b</sup> <sup>19</sup>F NMR yields using (trifluoromethyl)benzene as internal standard. BTMG = 2-tert-Butyl-1,1,3,3-tetramethylguanidine.

**Table 3.3** Screening of ligands.<sup>a</sup>

Further evaluation then revealed that using 4CzIPN as a photocatalyst led to higher yields (table 3.4, entry 1) and lower yields were obtained when the reaction was conducted using other photocatalysts such as Ir(dFFppy)<sub>2</sub>(dtbpy)PF<sub>6</sub> and [Ru(bpy)<sub>3</sub>]Cl<sub>2</sub> (entry 2-6, up to 68% yield). Concludingly, the reaction could not be initiated in the absence of a photocatalyst (entry 7).

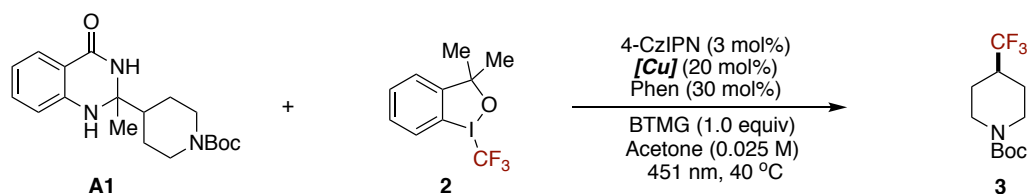


Conditions: <sup>a</sup> **A1** (0.05 mmol), **2** (0.1 mmol), CuCl<sub>2</sub> (20 mol%), Phen (30 mol%), **PC** (3 mol%), BTMG (0.05 mmol), in Acetone (0.025 M) at 40 °C under irradiation of blue LEDs for 16 hours. <sup>b</sup> <sup>19</sup>F NMR yields using (trifluoromethyl)benzene as internal standard. BTMG = 2-tert-Butyl-1,1,3,3-tetramethylguanidine.

**Table 3.4** Screening of different photocatalysts.<sup>a</sup>

To further improve the yield, we turned our attention to test the influence of other reaction parameters as the copper precatalysts (Table 2.4). Herein, copper(II) chloride

provided the best result (entry 1, 78%), while other inorganic copper salts as catalysts such as CuCl or CuBr<sub>2</sub> only gave moderate yields (entry 2-3, 53-58%). To increase the solubility of the copper catalyst, Cu(CH<sub>3</sub>CN)<sub>2</sub>PF<sub>4</sub> and Cu(OTf)<sub>2</sub> were investigated, which gave similar yields as CuCl<sub>2</sub> (entry 4-5, 67-71%). Variation of the catalyst loading had a drastic influence in decreasing the yield by 14-16% (entry 9-10). No product is formed in the absence of the copper precatalyst, which is consistent with previous reports - Direct radical coupling between alkyl radicals and trifluoromethyl radicals is very difficult due to the high transition state energy barrier to be crossed when the two transient radicals are combining.



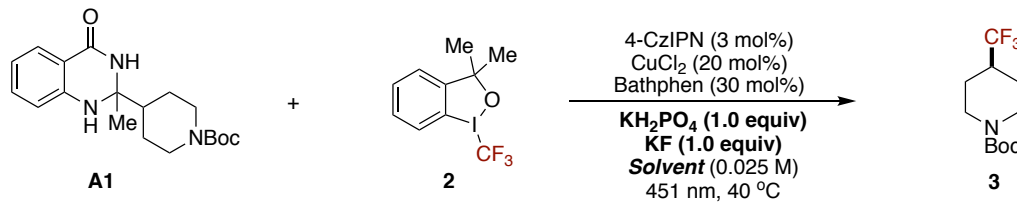
Entry	[Cu] cat.	<b>3</b> Yield (%) <sup>b</sup>
1	<b>CuCl<sub>2</sub></b>	<b>79</b>
2	CuCl	53
3	CuBr <sub>2</sub>	58
4	CuCN	35
5	Cu(CH <sub>3</sub> CN) <sub>2</sub> PF <sub>4</sub>	71
6	Cu(OTf) <sub>2</sub>	67
7	Cu(TMHD) <sub>2</sub>	62
8	Cu(acac) <sub>2</sub>	38
9	CuCl <sub>2</sub> (10 mol%)	62
10	CuCl <sub>2</sub> (30 mol%)	64
11	No Cu cat.	0

Conditions: <sup>a</sup> **A1** (0.05 mmol), **2** (0.1 mmol), Copper precatalyst (20 mol%), Phen (30 mol%), 4-CzIPN (3 mol%), BTMG (0.05 mmol), in Acetone (0.025 M) at 40 °C under irradiation of blue LEDs for 16 hours. <sup>b</sup> <sup>19</sup>F NMR yields using (trifluoromethyl)benzene as internal standard. BTMG = 2-tert-Butyl-1,1,3,3-tetramethylguanidine.

**Table 3.5** Screening of copper precatalysts.<sup>a</sup>

Next, we examined the role of bases for the decarbonylative trifluoromethylation reaction. A screen of different bases including inorganic and organic bases is presented. On the one hand, we found using KH<sub>2</sub>PO<sub>4</sub> and KF as an additive in DMF led to product **3** formation in 62% yield (Table 3.7, entry 1), and product **12** formation in 83% yield (Scheme 3.31). However, by scaling up the reaction (0.05 mol to 0.20 mmol, Scheme 3.29), the yield of **3** significantly dropped by 14%. Presumably, this was caused by the low solubility of the reagents resulting in diminished light transmission of the reaction mixture. On the one hand, we started to re-examine the organic bases (Table 3.7). Fortunately, we obtained the expected yields when using BTMG and needing to be under acetone conditions. Noteworthy, Hünig's base (DIPEA) only led to traces of the product (Table 3.7,

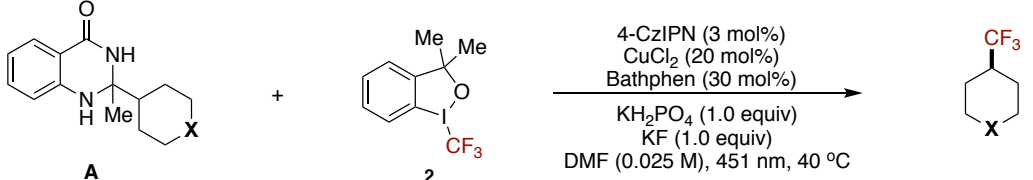
Entry 3). Proposingly, this is a result of undesired quenching of the photoexcited state of the photocatalyst (4CzIPN\*  $E_{\text{red}} = +1.35$  V vs SCE), whereas DIPEA ( $E_{\text{ox}} = +0.86$  V vs SCE)<sup>61</sup> is a better quencher than the substrate **A1** ( $E_{\text{ox}} = +1.21$  V vs SCE). Without adding a base, the yield of the product decreased to 28% (Table 3.7, entry 9).



Entry	Solvent	<b>3</b> Yield (%) <sup>b</sup>
1	DMF	62
2	DEF	20
3	NMP	33
4	DMSO	39
5	DCE	30
6	DMA	54
7	Acetone	45
8	CH <sub>3</sub> CN	29
9	<i>t</i> Bu-CN	12
10	<i>i</i> Pr <sub>2</sub> O	0
11	PhCF <sub>3</sub>	0
12	DMF, No KF	46

Conditions: <sup>a</sup> **A1** (0.05 mmol), **2** (0.1 mmol), CuCl<sub>2</sub> (20 mol%), Phen (30 mol%), 4-CzIPN (3 mol%), KH<sub>2</sub>PO<sub>4</sub> (0.05 mmol), KF (0.05 mmol) in solvent (0.025 M) at 40 °C under irradiation of blue LEDs for 16 hours. <sup>b</sup> <sup>19</sup>F NMR yields using (trifluoromethyl)benzene as internal standard.

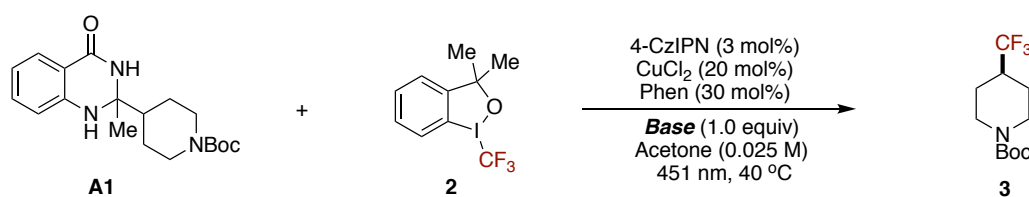
**Table 3.6** Screening of solvents based on KH<sub>2</sub>PO<sub>4</sub> as base and KF as additive.<sup>a</sup>



<b>X=CH<sub>2</sub></b> , 0.05 mmol 0.20 mmol	<b>12</b> , 83% <sup>19</sup> F NMR yield <b>12</b> , 71% <sup>19</sup> F NMR yield
<b>X=NBoc</b> , 0.05 mmol 0.20 mmol	<b>3</b> , 62% <sup>19</sup> F NMR yield <b>3</b> , 48% <sup>19</sup> F NMR yield

**Scheme 3.31** Decrease yield scaling up the amount of substrate.





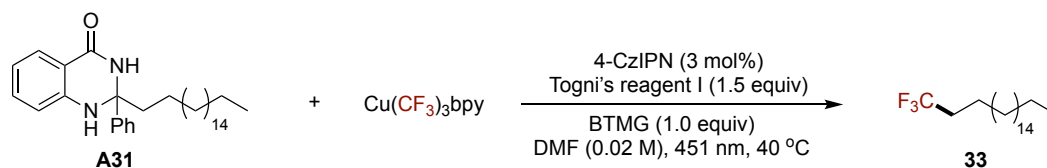
Entry	Base	<b>3</b> Yield (%) <sup>b</sup>
1	<b>BTMG</b>	<b>78</b>
2	TMG	44
3	DIPEA	trace
4	Et <sub>3</sub> N	7
5	Pyridine	28
6	K <sub>2</sub> HPO <sub>4</sub>	20
7	K <sub>2</sub> CO <sub>3</sub>	29
8	K <sub>3</sub> PO <sub>4</sub>	19
9	No base	28

Conditions: <sup>a</sup> **A1** (0.05 mmol), **2** (0.1 mmol), CuCl<sub>2</sub> (20 mol%), Phen (30 mol%), 4-CzIPN (3 mol%), base (0.05 mmol), in Acetone (0.025 M) at 40 °C under irradiation of blue LEDs for 16 hours. <sup>b</sup> <sup>19</sup>F NMR yields using (trifluoromethyl)benzene as internal standard. BTMG = 2-tert-Butyl-1,1,3,3-tetramethylguanidine.

**Table 3.7** Screening of bases.<sup>a</sup>

With these optimized conditions in hand, the scope was extended to aliphatic ketones via in situ generated, unstable primary radicals that are notoriously challenging in C(sp<sup>3</sup>)-CF<sub>3</sub> bond functionalization reactions. However, only lower yields of **33** were obtained (table 3.8, entry 1, 42%). Further optimization studies finally revealed (table 3.8 entry 2-15), that stoichiometric amounts of (bpy)Cu(CF<sub>3</sub>)<sub>3</sub> as trifluoromethylating source significantly improved the reaction outcome. Furthermore, a combination of (bpy)Cu(CF<sub>3</sub>)<sub>3</sub>, Togni's reagent I (**2**), BTMG, substrate (**A31**), and 4-CzIPN under blue light irradiation in DMF at 40 °C provided trifluoromethylated target **33** in 67% isolated yield (entry 2). Other solvents as are tolerated (entries 5-8), albeit providing **33** in lower yield (up to 56%). Togni's reagent I (**2**) plays an important role in this reaction, potentially facilitating the regeneration of Cu(CF<sub>3</sub>)<sub>3</sub>(bpy) or LnCu<sup>II</sup>CF<sub>3</sub>X intermediates. On the other hand, Togni's reagent I could act as a role of oxidant, which was further studied by the addition of other oxidants (entries 9-11). However, the reaction proceeded but delivered the desired product in lower yields (22-28 %). Next, we examined the role of BTMG by replacing it with inorganic base NaHCO<sub>3</sub> or by omitting it (entry 12-13) which again led to diminished yields (15-18%). This indicated the crucial role of BTMG for the success of the reaction, in which the base presumably promotes the release of the corresponding CF<sub>3</sub> radicals by interaction with Togni's reagent I (**2**) (See Mechanism experiments for details). In addition, the reaction proceeded well in the absence of the photocatalyst but not without light (entry 14-15), which is also consistent with the previous work in the literature that

Cu(CF<sub>3</sub>)<sub>3</sub>(bpy) could undergo homolysis under light excitation to provide the reactive bpyCu<sup>II</sup>-(CF<sub>3</sub>)<sub>2</sub> intermediate.

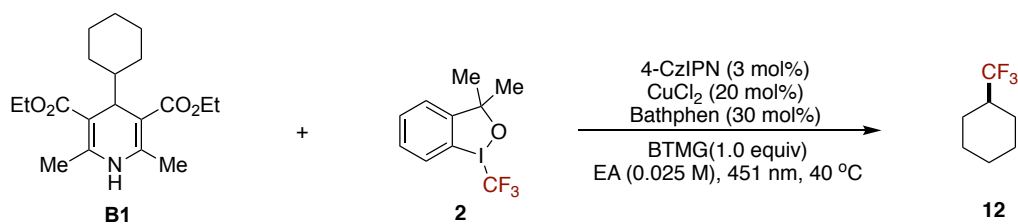


Entry	Deviation from standard conditions	<b>3</b> Yield (%) <sup>b</sup>
1	20 mol% CuCl <sub>2</sub> and 30 mol% Phen instead of Cu(CF <sub>3</sub> ) <sub>3</sub> bpy	42
<b>2</b>	<b>none</b>	<b>71 (67)<sup>c</sup></b>
3	No Togni's reagent	48
4	No Cu(CF <sub>3</sub> ) <sub>3</sub> bpy	0
5	DMA instead of DMF	56
6	Acetone instead of DMF	34
7	DCE instead of DMF	37
8	CH <sub>3</sub> CN instead of DMF	46
9	Togni's reagent II instead of Togni's reagent I	22
10	PhI(OAc) <sub>2</sub> instead of Togni's reagent I	25
11	K <sub>2</sub> S <sub>2</sub> O <sub>8</sub> instead of Togni's reagent I	28
12	NaHCO <sub>3</sub> instead of BTMG	15
13	No BTMG	18
14	No 4-CzIPN	66
15	No light (40 °C)	0

Conditions: <sup>a</sup> **A31** (0.05 mmol), Cu(CF<sub>3</sub>)<sub>3</sub>bpy (0.05 mmol), Togni's reagent I (**2**) (0.075 mmol), 4-CzIPN (3 mol%), BTMG (0.05 mmol), in DMF (0.02 M) at 40 °C under irradiation of blue LEDs for 16 hours. <sup>b</sup> <sup>19</sup>F NMR yields using (trifluoromethyl)benzene as internal standard. <sup>c</sup> Isolated yield. BTMG = 2-tert-Butyl-1,1,3,3-tetramethylguanidine.

**Table 3.8** Optimization of the reaction conditions with Cu(CF<sub>3</sub>)<sub>3</sub>(bpy) by using primary radical precursor **A31**.<sup>a</sup>

Encouraged by the successful results of trifluoromethylation performed by aliphatic ketones via *sp*<sup>3</sup> C–C bond cleavage, we wondered whether copper mediated transfer of CF<sub>3</sub> groups to alkyl radicals from ketones could be extended to other activated precursor which could generate the active open-shell carbon via aromatization-promoted processes. Firstly, Hantzsch esters were investigated which would allow for the decarbonylative coupling of aldehydes. Based on the beforementioned optimization studies on ketone-derived precursors, we rapidly observed productive reactivity (Table 3.9). Careful screening of different solvents (entry 2-5), bases (entry 6-8), copper salts (entry 9-10) and ligands (entry 11-13) indicated the ideal reaction conditions for the coupling of **B1** with **2**: CuCl<sub>2</sub> (20 mol%), BTMG (1.0 equiv), Togni's reagent I (**2**, 2.0 equiv), and 4-CzIPN (3 mol%) under blue light irradiation in ethyl acetate at 40 °C to provide trifluoromethyl-cyclohexane **12** in 65% yield.

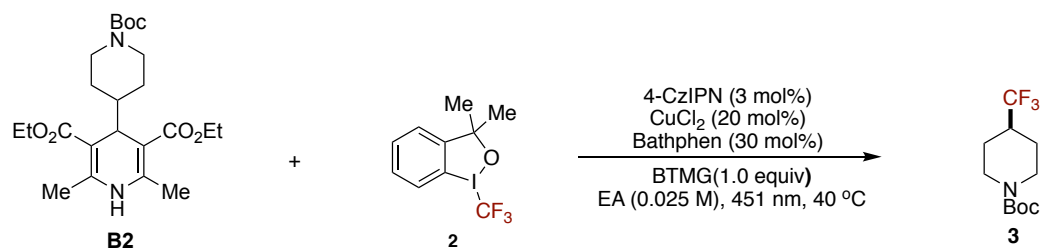


Entry	Deviation from standard conditions	12 Yield (%) <sup>b</sup>
1	none	65
2	CH <sub>3</sub> CN instead of EA	34
3	Acetone instead of DMF	58
4	DMF instead of DMF	57
5	DCE instead of DMF	64
6	NaHCO <sub>3</sub> instead of BTMG	58
7	KH <sub>2</sub> PO <sub>4</sub> instead of BTMG	60
8	No BTMG	61
9	CuBr <sub>2</sub> instead of CuCl <sub>2</sub>	11
10	Cu(CH <sub>3</sub> CN) <sub>2</sub> PF <sub>4</sub> instead of CuCl <sub>2</sub>	50
11	dtbpy instead of BathPhen	56
12	terbpy instead of BathPhen	14
13	No ligand	16
14	No light (40 °C)	0

Conditions: <sup>a</sup> **B1** (0.05 mmol), **2** (0.1 mmol), CuCl<sub>2</sub> (20 mol%), BathPhen (30 mol%), 4-CzIPN (3 mol%), BTMG (0.05 mmol), in EA (0.025 M) at 40 °C under irradiation of blue LEDs for 16 hours. <sup>b</sup> <sup>19</sup>F NMR yields using (trifluoromethyl)benzene as internal standard. BTMG = 2-tert-Butyl-1,1,3,3-tetramethylguanidine.

**Table 3.9** Optimization studies using Hantzsch ester **B1** as radical precursor.<sup>a</sup>

However, when changing to substrate **B2**, lower yields of 26% of **3** were obtained as illustrated in Table 3.10. Assuming that solubility of the substrates plays a crucial role, different solvents were examined (entry 2-6), which improved the yield to 48% employing acetonitrile as the solvent.



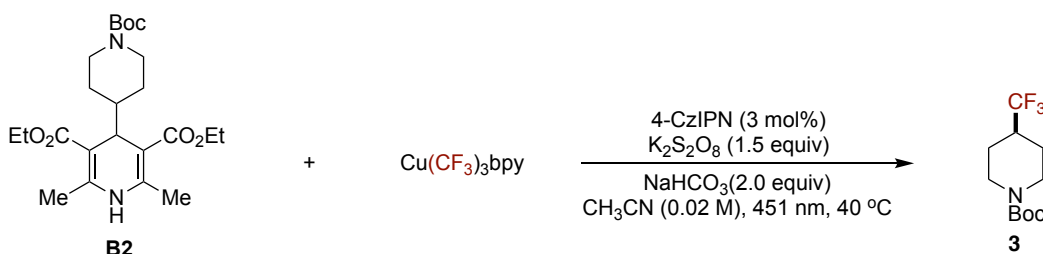
Entry	Deviation from standard conditions	3 Yield (%) <sup>b</sup>
1	none	26
2	CH <sub>3</sub> CN instead of EA	48
3	Acetone instead of EA	47
4	DMF instead of DMF	29
5	DCE instead of EA	41
6	DMA instead of EA	12

Conditions: <sup>a</sup> **B2** (0.05 mmol), **2** (0.1 mmol), CuCl<sub>2</sub> (20 mol%), BathPhen (30 mol%), 4-CzIPN (3 mol%), BTMG (0.05 mmol), in solvent (0.025 M) at 40 °C under irradiation of blue LEDs for 16 hours. <sup>b</sup> <sup>19</sup>F NMR

yields using (trifluoromethyl)benzene as internal standard. BTMG = 2-tert-Butyl-1,1,3,3-tetramethylguanidine.

**Table 3.10** Screening of solvents by using **B2** as the substrate.<sup>a</sup>

Further improvements were achieved by using stoichiometric amounts of Grushin's reagent ( $\text{Cu}(\text{CF}_3)_3(\text{bpy})$ ) as the trifluoromethylating reagent (Table 3.11). After screening of different solvents (entry 2-9), oxidants (entry 10-15), bases (entry 16-19) and photocatalysts (entry 20-21), we found the optimal featuring  $\text{Cu}(\text{CF}_3)_3(\text{bpy})$  (1.0 equiv),  $\text{K}_2\text{S}_2\text{O}_8$  (1.5 equiv),  $\text{NaHCO}_3$  (2.0 equiv) and 4-CzIPN (3 mol%) under blue LED irradiation in MeCN at 40 °C can provide 80% yield of the target product **3**. Notably,  $\text{K}_2\text{S}_2\text{O}_8$  was added as an oxidant, which potentially facilitates the oxidation of either Hantzsch ester **B2** or Cu(I) to Cu(II) species.<sup>27b, 62</sup> In the absence of oxidant (entry 15), base (entry 19) or photocatalyst (entry 21), the yield of **3** decreased significantly.



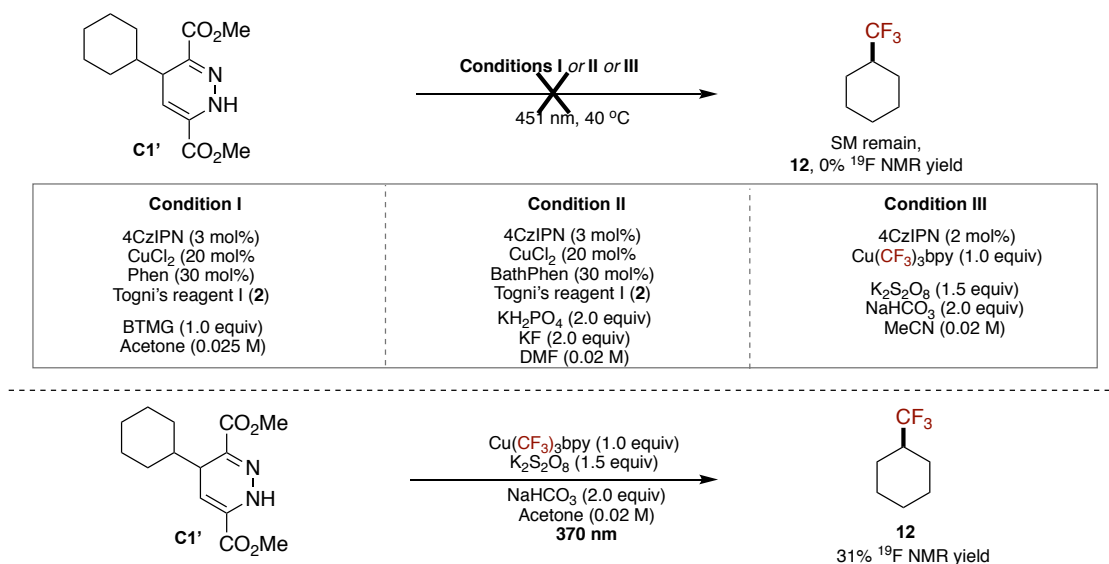
Entry	Deviation from standard conditions	<b>3</b> Yield (%) <sup>b</sup>
<b>1</b>	<b>none</b>	<b>80(71)<sup>c</sup></b>
2	EA instead of $\text{CH}_3\text{CN}$	55
3	DMF instead of $\text{CH}_3\text{CN}$	18
4	DMA instead of $\text{CH}_3\text{CN}$	43
5	DCE instead of $\text{CH}_3\text{CN}$	68
6	Acetone instead of $\text{CH}_3\text{CN}$	70
7	DMSO instead of $\text{CH}_3\text{CN}$	68
8	1,4-Dioxane instead of $\text{CH}_3\text{CN}$	24
9	$\text{CH}_3\text{CN}$ (0.05M)	66
10	$\text{Na}_2\text{S}_2\text{O}_8$ instead of $\text{K}_2\text{S}_2\text{O}_8$	75
11	OXONE instead of $\text{K}_2\text{S}_2\text{O}_8$	78
12	Togni's reagent I ( <b>2</b> ) instead of $\text{K}_2\text{S}_2\text{O}_8$	4
13	Togni's reagent II ( <b>2-1</b> ) instead of $\text{K}_2\text{S}_2\text{O}_8$	40
14	TBPB instead of $\text{K}_2\text{S}_2\text{O}_8$	26
15	No $\text{K}_2\text{S}_2\text{O}_8$	35
16	BTMG instead of $\text{NaHCO}_3$	66
17	$\text{KH}_2\text{PO}_4$ instead of $\text{NaHCO}_3$	69
18	$\text{NaOAc}$ instead of $\text{NaHCO}_3$	54
19	No $\text{NaHCO}_3$	64
20	$\text{Ru}(\text{bpy})\text{PF}_6$ instead of 4-CzIPN	78
21	No 4-CzIPN	37
22	No light (40 °C)	0

Conditions: <sup>a</sup> **B2** (0.05 mmol),  $\text{Cu}(\text{CF}_3)_3\text{bpy}$  (0.05 mmol),  $\text{K}_2\text{S}_2\text{O}_8$  (0.075 mmol), 4-CzIPN (3 mol%),  $\text{NaHCO}_3$  (0.1 mmol), in  $\text{CH}_3\text{CN}$  (0.02 M) at 40 °C under irradiation of blue LEDs for 16 hours. <sup>b</sup>  $^{19}\text{F}$  NMR yields using (trifluoromethyl)benzene as internal standard. <sup>c</sup> Isolated yield.

**Table 3.11** Optimization of the trifluoromethylation of using **B2** using stoichiometric

amounts of  $\text{Cu}(\text{CF}_3)_3(\text{bpy})$ .<sup>a</sup>

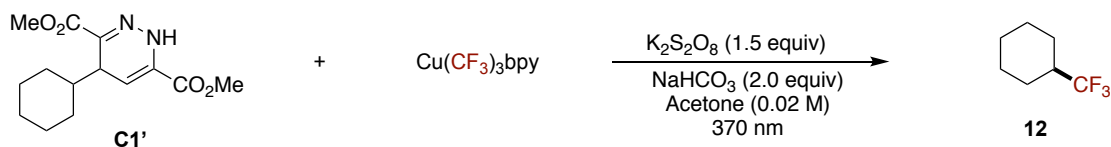
Finally, we turned our attention to apply trifluoromethylation techniques to convert aliphatic alkenes following a dealkenylative trifluoromethylation pathway. This approach was based on Luo work demonstrating the generation of alkyl radicals from alkenes enabled by the activation with tetrazine and photoexcitation to conduct a nickel-catalyzed arylation. Considering the structural similarity of alkyl-1,4-dihydropyridazine precursors **C** and Hantzsch esters (**B**), and their C–C bond cleavage mechanism following SET or photoexcitation pathways, 1,4-dihydropyridazine (**C**) could be emphasized as radical precursors for Cu-mediated trifluoromethylation reactions. For this purpose, previous reactions conditions were applied to convert proaromatic precursor **C1'** into its trifluoromethylated product **12** (Scheme 3.32, *top*). Unfortunately, no desired reactivity was observed when employing conditions I, II or III. Referring to the results reported by Luo's group, the maximum absorption of the alkyl-1,4-dihydropyridazine precursors is around at 365 nm, and they more likely undergo homolysis from excitation state **C1'** ( $\Delta G = -32.7$  kcal/mol) instead of the mesolytic cleavage from radical cation  $[\text{C1}']^+$ . To address this, the wavelength of irradiation was changed to 370 nm. In addition, these conditions would also allow for the release of trifluoromethyl radicals from  $\text{Cu}(\text{CF}_3)_3(\text{bpy})$  to obtain  $\text{Cu}^{\text{II}}(\text{CF}_3)_2(\text{bpy})$  intermediate upon light irradiation. To our delight, the desired  $\text{C}(\text{sp}^3)\text{--CF}_3$  backbone **12** was obtained in 31% yield employing  $\text{Cu}(\text{CF}_3)_3(\text{bpy})$  (1.0 equiv),  $\text{K}_2\text{S}_2\text{O}_8$  (1.5 equiv) and  $\text{NaHCO}_3$  (2.0 equiv) in acetone (Scheme 3.32, *bottom*).



**Scheme 3.32** Reactivity tests using 1,4-dihydropyridazine (**C**) as radical precursors.

Next, further optimization studies were conducted investigating different solvents (Table

3.12, entry 1-7), whereby acetone was identified as the best solvent gave relatively high yield. However, in the process of screening different bases and different oxidants, we found that base and oxidant are not necessarily needed for product formation (Table 3.12, entry 8 and entry 14), but the reaction could not proceed without light excitation. (Note: These optimization studies were conducted in assistance of Dr. Riccardo S. Mega)

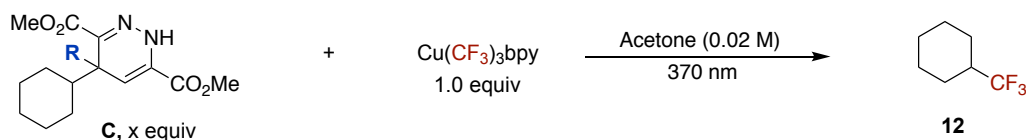


Entry	Deviation from standard conditions	12 Yield (%) <sup>b</sup>
1	<b>none</b>	<b>34</b>
2	EA instead of Acetone	32
3	DMF instead of Acetone	12
4	DMA instead of Acetone	14
5	DCE instead of Acetone	23
6	NMP instead of Acetone	13
7	DMSO instead of Acetone	0
8	<b>No NaHCO<sub>3</sub></b>	<b>33</b>
9	K <sub>3</sub> PO <sub>4</sub> instead of NaHCO <sub>3</sub>	20
10	DIPEA instead of NaHCO <sub>3</sub>	27
11	Na <sub>2</sub> S <sub>2</sub> O <sub>8</sub> instead of K <sub>2</sub> S <sub>2</sub> O <sub>8</sub>	35
12	OXONE instead of K <sub>2</sub> S <sub>2</sub> O <sub>8</sub>	34
13	(NH <sub>4</sub> ) <sub>2</sub> S <sub>2</sub> O <sub>8</sub> instead of K <sub>2</sub> S <sub>2</sub> O <sub>8</sub>	12
14	<b>No K<sub>2</sub>S<sub>2</sub>O<sub>8</sub></b>	<b>34</b>
15	No light (40 °C)	0

Conditions: <sup>a</sup> **C1'** (0.05 mmol), Cu(CF<sub>3</sub>)<sub>3</sub>bpy (0.05 mmol), K<sub>2</sub>S<sub>2</sub>O<sub>8</sub> (0.075 mmol), NaHCO<sub>3</sub> (0.1 mmol), in Acetone (0.02 M) at 35 °C under irradiation of 370 nm for 16 hours. <sup>b</sup> <sup>19</sup>F NMR yields using (trifluoromethyl)benzene as internal standard.

**Table 3.12** Optimized conditions by using **C1'** and Cu(CF<sub>3</sub>)<sub>3</sub>(bpy).<sup>a</sup>

When increasing the amount of radical precursor to 1.5 equivalents, the yield of **12** was improved to 45% (Table 3.13, entry 2). Further tuning of the reactivity (activation energy of carbon-carbon bond cleavage in the excited substrate) of the proaromatic precursor revealed better results when the R group was changed from hydrogen atom to a methyl group (Table 3.13, entry 3). In contrast, the phenyl substituted derivative provided the desired product **12** in only 29% yield.



Entry	Deviation from standard conditions	12 Yield (%) <sup>b</sup>
1	R = H, x = 1.0 equiv	34
2	R = H, x = 1.5 equiv	45
3	<b>R = Me, x = 1.5 equiv</b>	<b>57</b>
4	R = Ph, x = 1.0 equiv	29

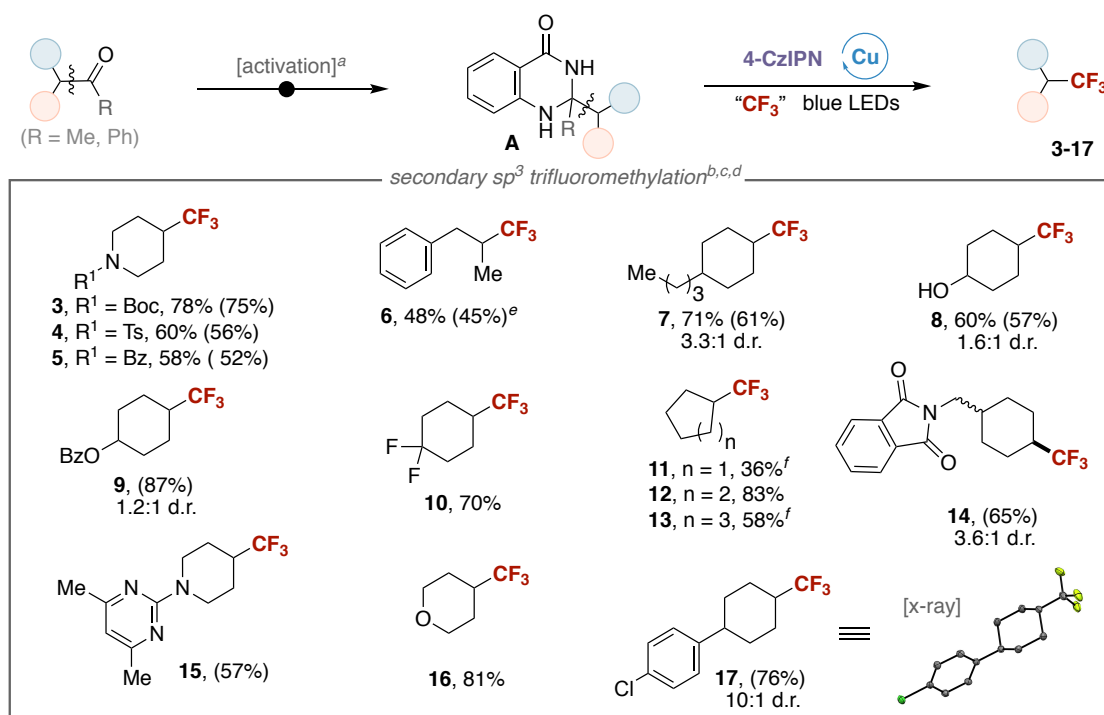
Conditions: <sup>a</sup> C (0.05-0.10 mmol) and Cu(CF<sub>3</sub>)<sub>3</sub>bpy (0.05 mmol) in Acetone (0.02 M) at 35 °C under irradiation of 370 nm for 16 hours. <sup>b</sup> <sup>19</sup>F NMR yields using (trifluoromethyl)benzene as internal standard.

**Table 3.13** Optimized conditions by changing C and stoichiometry.<sup>a</sup>

### 3.3.2 Substrate Scope

#### 3.3.2.1 Scope of Trifluoromethylation of Alkyl ketones

With optimized conditions in hand, we evaluated the scope of the C(sp<sup>3</sup>)-CF<sub>3</sub> bond-forming reaction. As shown in Scheme 3.33, a wide range of differentially substituted secondary alkyl ketone derivatives were readily converted to their corresponding trifluoromethylated products (**3-17**) in good to excellent yields. Sensitive functional groups such as alcohol (**8**), protected amines (**3-5**), phthalimide (**14**) and nitrogen-containing heterocycles (**15**) were well tolerated, highlighting the chemoselectivity of this protocol.

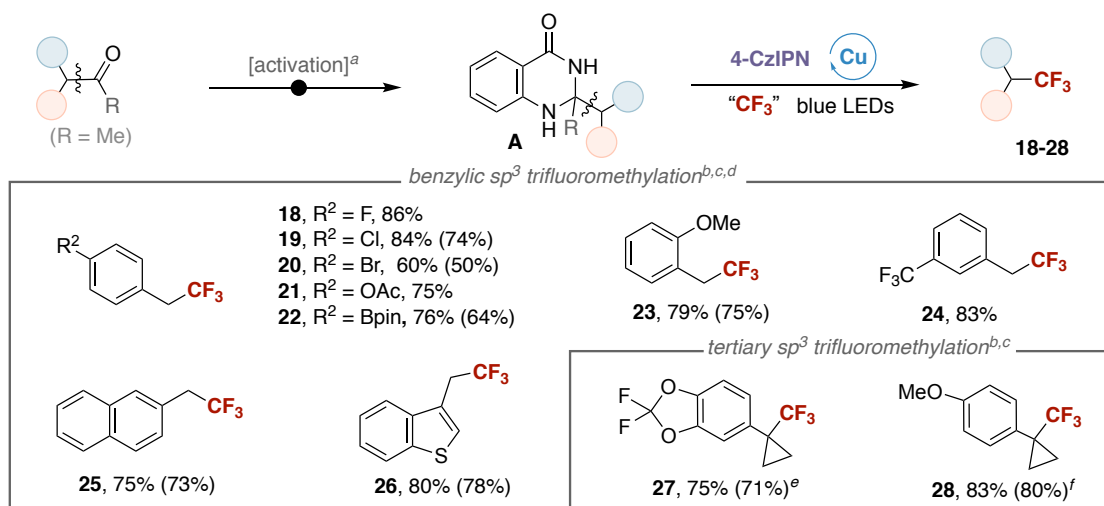


Conditions: <sup>a</sup> A: Ketone (1.05 equiv), aminobenzamide (1.0 equiv), I<sub>2</sub> (5 mol%) in DMF (0.67 M) at 80 °C, see supporting information for characterization data of A. <sup>b</sup> A (0.20 mmol), 2 (0.40 mmol), CuCl<sub>2</sub> (20 mol %), 4-CzIPN (3 mol %), under blue LED irradiation, R = Me. <sup>c</sup> Using: L1 (30 mol %), BTMG (1.0 equiv), in acetone (0.025 M). <sup>d</sup> Yields are reported on the basis of <sup>19</sup>F NMR analysis using PhCF<sub>3</sub> as internal standard; Isolated yields are in parentheses, thus showing how the volatility of some products affects the yield loss. <sup>e</sup> R = Ph. <sup>f</sup> Using L2 (30 mol%), KH<sub>2</sub>PO<sub>4</sub> (2.0 equiv), KF (2.0 equiv) in DMF (0.02 M).

**Scheme 3.33** Scope of trifluoromethylation of secondary alkyl ketones.

Next, we investigated benzylic CF<sub>3</sub>-bond formation and the desired trifluoromethylated products were successfully prepared (**18-26**) (Scheme 3.34). An array of aryl halides (**18-**

20), electron-rich arenes (**21**, **23**, **25**) electron-deficient arenes (**24**), boronic esters (**22**) and sulfur-containing heterocycles (**26**) were all tolerated under the reaction conditions delivering the products in 50-86% yield. In addition, the tertiary alkyl ketones (**27**, **28**) were also successfully converted to trifluoromethylated products in excellent yields. Noteworthy, minor modifications of the reaction conditions were made to improve the yields in certain cases. For example, for some specific substrates (**11**, **13**, **28**), KF was added to inhibit F-elimination from Cu–CF<sub>3</sub>.<sup>33</sup>



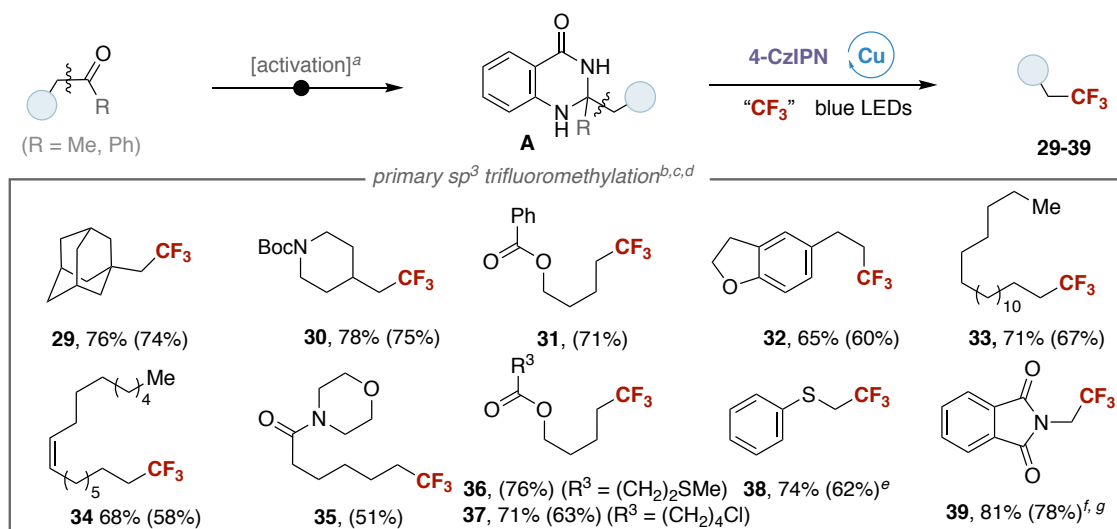
Conditions: <sup>a</sup> A: Ketone (1.05 equiv), aminobenzamide (1.0 equiv), I<sub>2</sub> (5 mol%) in DMF (0.67 M) at 80 °C, see supporting information for characterization data of A. <sup>b</sup> A (0.20 mmol), **2** (0.40 mmol), CuCl<sub>2</sub> (20 mol%), 4-CzIPN (3 mol %), under blue LED irradiation, R = Me. <sup>c</sup> Yields are reported on the basis of <sup>19</sup>F NMR analysis using PhCF<sub>3</sub> as internal standard; Isolated yields are in parentheses, thus showing how the volatility of some products affects the yield loss. <sup>d</sup> Using di(pyridin-2-yl)methanone (30 mol%), KH<sub>2</sub>PO<sub>4</sub> (2.0 equiv) in DMF (0.02 M), <sup>e</sup> Using **L2** (30 mol%), BTMG (1.0 equiv) in DMF (0.02 M). <sup>f</sup> Using **L2** (30 mol%), KH<sub>2</sub>PO<sub>4</sub> (2.0 equiv), KF (2.0 equiv) in DMF (0.02 M).

**Scheme 3.34** Scope of benzylic CF<sub>3</sub>-bond formation.

However, when we turned our attention to primary alkyl ketones, we found that the current reaction conditions only giving lower yields for this fragmentation mode representing a significant barrier in C–C bond cleavage reactions. To address this challenge, we conducted further optimization studies (Table 3.8), in which we found that using stoichiometric (bpy)Cu(CF<sub>3</sub>)<sub>3</sub> as a trifluoromethylating source significantly improved the reaction outcome. We attributed the lower yields of primary substrates to the increased promiscuity of high energy primary radicals which must rapidly react with a trifluoromethylating reagent before undergoing undesired side reactions as HAT or radical disproportionation. A combination of substrate, (bpy)Cu(CF<sub>3</sub>)<sub>3</sub>, Togni's reagent I (**2**), BTMG, and 4-CzIPN in DMF at 40 °C under blue light irradiation finally provided the trifluoromethylated product. Critical for success was the use of both, **2** and BTMG, probably by facilitating the regeneration of Cu(CF<sub>3</sub>)<sub>3</sub>(bpy) and Cu(CF<sub>3</sub>)<sub>2</sub>(bpy). Next, we



explored the scope of primary alkyl substrates (Scheme 3.35, **29-37**). Good yields (51-78%) were obtained across the scope, with broad functional group compatibility. Particularly, the efficacy of the reaction is not affected by steric hindrance (**29**) or some functional groups such as alkene (**34**), amide (**30, 35, 39**), thioether (**36, 38**) and chloride (**37**). Although it might be predicted from the outset that the presence of tertiary  $sp^3$  alkyl or allylic C–H sites would be unfavorable for the reaction because of competitive HAT at such activated positions, no significant loss in product formation was observed (**29, 32, 38, 39**).

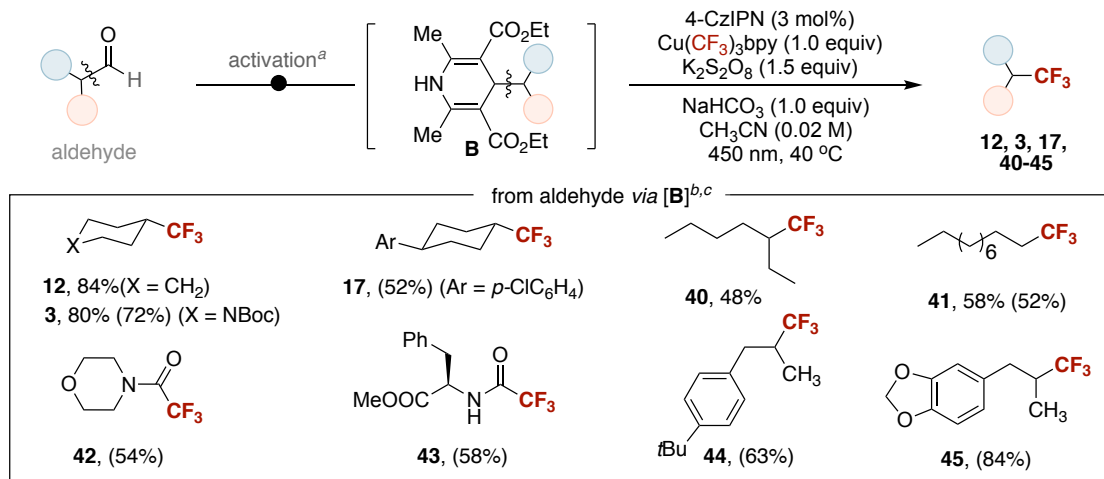


Conditions: <sup>a</sup> **A**: Ketone (1.05 equiv), aminobenzamide (1.0 equiv),  $I_2$  (5 mol%) in DMF (0.67 M) at 80 °C, see supporting information for characterization data of **A**. <sup>b</sup> **A** (0.20 mmol),  $Cu(CF_3)_3bpy$  (0.20 mmol), 4-CzIPN (3 mol %) under blue LED irradiation, R = Ph. <sup>c</sup> Yields are reported on the basis of  $^{19}F$  NMR analysis using  $PhCF_3$  as internal standard; Isolated yields are in parentheses, thus showing how the volatility of some products affects the yield loss. <sup>d</sup> Using **2** (0.30 mmol), BTMG (1.0 equiv) in DMF (0.02 M). <sup>e</sup> **A** (0.20 mmol),  $Cu(CF_3)_3bpy$  (0.20 mmol), 4-CzIPN (3 mol %) under blue LED irradiation, R = Ph. <sup>f</sup> Using  $K_2S_2O_8$  (1.5 equiv),  $KH_2PO_4$  (2.0 equiv) in  $CH_3CN$  (0.025 M). <sup>g</sup> R = Me.

**Scheme 3.35** Scope of trifluoromethylation of primary alkyl ketones.

### 3.3.2.2 Scope of Trifluoromethylation of Alkyl aldehydes

By attempting to expand the substrate scope to aldehydes, we began evaluating the trifluoromethylation using  $(bpy)Cu(CF_3)_3$ , a base and an oxidant under photocatalytic conditions employing Hantzsch ester (**B**), which could be easily accessed by condensation from the corresponding aldehyde. As shown in Scheme 3.36, a range of aldehydes leading to intermediary cyclic secondary radicals (**12, 3, 17**), unactivated primary radicals (**41**) and even unstrained secondary radicals (**40, 44, 45**) successfully participated in the desired reaction. Remarkable, this strategy also provides a mild pathway to construct trifluoroacetamide substrates (**42, 43**).

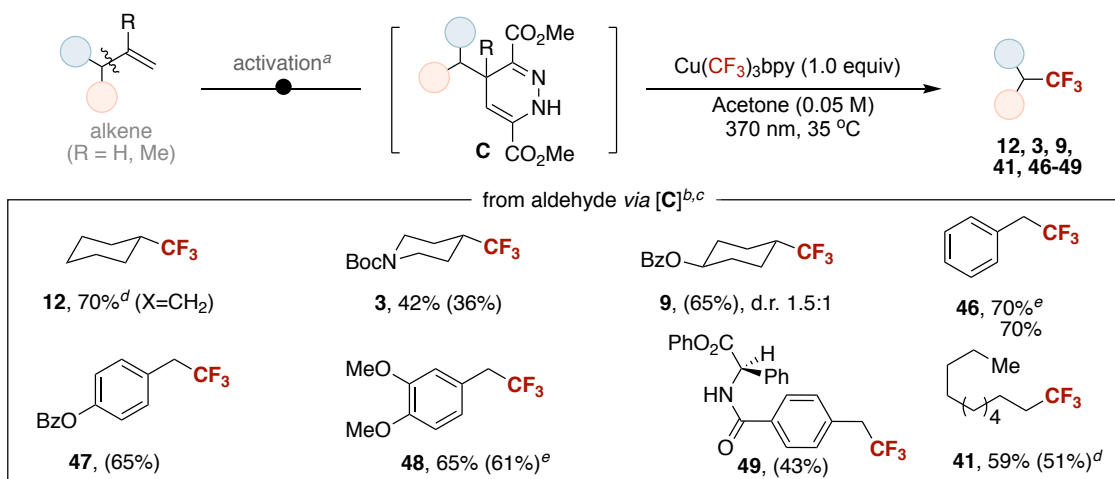


Conditions: <sup>a</sup> **B**: Aldehyde (1.0 equiv), Bu<sub>4</sub>NHSO<sub>4</sub> (12 mol%), ethyl 3-aminocrotonate (1.0 equiv), ethyl acetoacetate (1.0 equiv) in ethylene glycol (2.5 M) at 80 °C; see supporting information for characterization of data of **B**. <sup>b</sup> **B** (0.20 -0.30 mmol), Cu(CF<sub>3</sub>)<sub>3</sub>bpy (0.20 mmol), K<sub>2</sub>S<sub>2</sub>O<sub>8</sub> (0.30 mmol), 4-CzIPN (3 mol %), NaHCO<sub>3</sub> (0.40 mmol) in CH<sub>3</sub>CN (0.02 M) at 40 °C under blue LED irradiation. <sup>c</sup> Yields are reported on the basis of <sup>19</sup>F NMR analysis using PhCF<sub>3</sub> as internal standard; Isolated yields are in parentheses, thus showing how the volatility of some products affects the yield loss.

**Scheme 3.36** Scope of decarbonylative trifluoromethylation of aldehydes.

### 3.3.2.3 Scope of Trifluoromethylation of Alkyl alkenes

Furthermore, we applied our strategy to the trifluoromethylation event at a *sp*<sup>3</sup>-sites in the allylic position via formal release of isopropene (R = Me, Scheme 3.37), which stands in sharp contrast to previous methodologies that incorporate the trifluoromethyl moiety across the *sp*<sup>2</sup>-moiety. By applying this technology, the CF<sub>3</sub> fragment could be included at either benzylic moieties (**46-49**) with 43-70% yields, unactivated secondary (**22, 3, 19**) with 36-70% yields or primary alkyl sites with 51% yield (**41**).



Conditions: <sup>a</sup> **C**: Alkene (1.0 equiv), dimethyl 1,2,4,5-tetrazine-3,6-dicarboxylate (1.05 equiv) in DCM (0.2 M); see supporting information for characterization of data of **C**. <sup>b</sup> **C** (0.20 - 0.30 mmol), Cu(CF<sub>3</sub>)<sub>3</sub>bpy (0.2

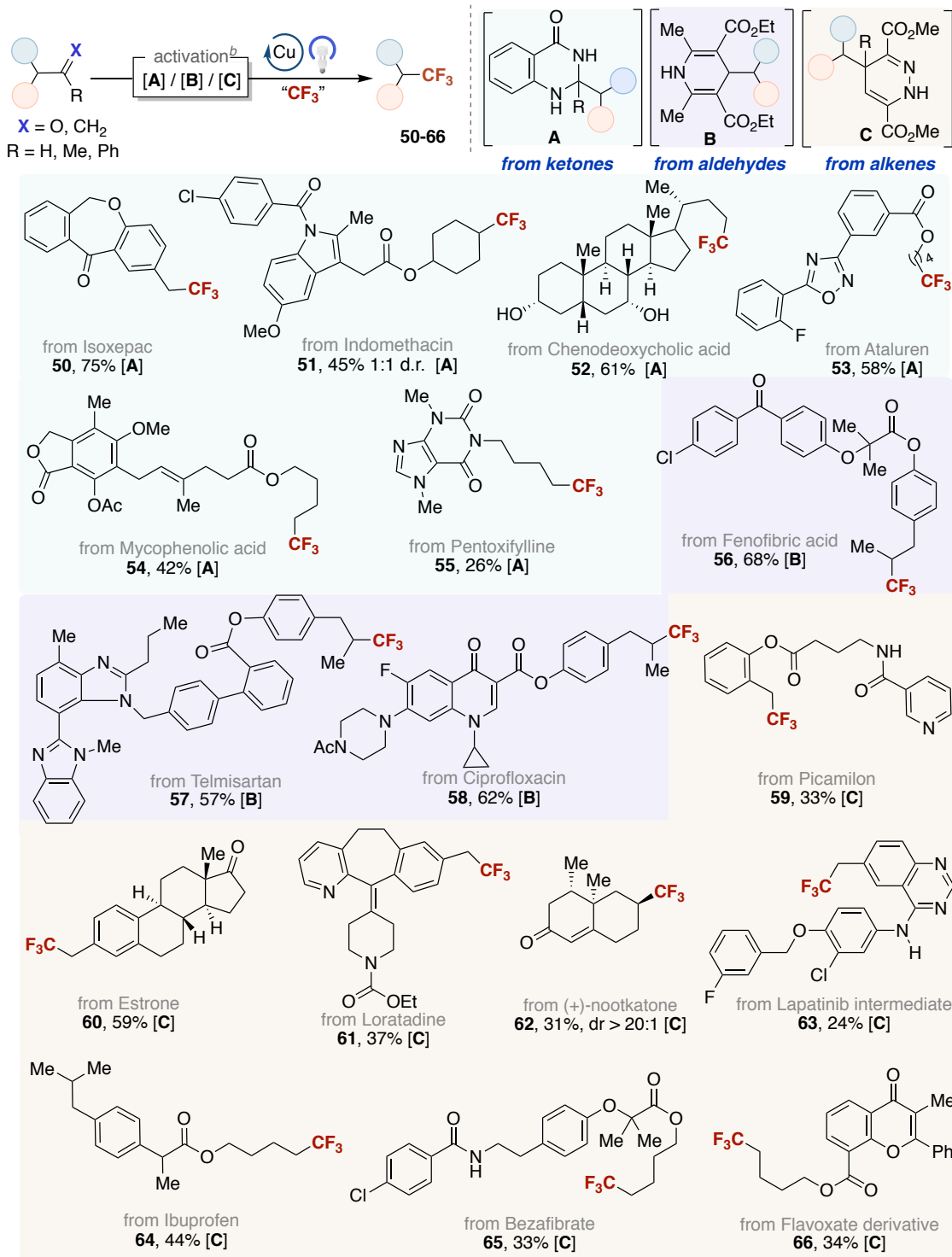
---

mmol) at 35 °C under irradiation of 370 nm, R = Me. <sup>e</sup> Yields are reported on the basis of <sup>19</sup>F NMR analysis using PhCF<sub>3</sub> as internal standard; Isolated yields are in parentheses since volatility of some products diminished the isolated yield. <sup>d</sup> C (0.30 mmol), Cu(CF<sub>3</sub>)<sub>3</sub>bpy (0.2 mmol), **2** (0.5 equiv) and BTMG (0.5 equiv). <sup>e</sup> R = H.

### Scheme 3.37 Scope of trifluoromethylation of alkenes.

#### 3.3.2.4 Late-stage trifluoromethylation of natural products and medicinal agents

Finally, we focused on ketones, aldehydes and alkenes stemming from a variety of highly functionalized natural products and medicinal agents to further demonstrate the efficiency of our strategy (Scheme 3.38). Generally, we found that the developed reaction conditions could tolerate a wide range of functional groups and heterocyclic motifs, enabling the installation of the CF<sub>3</sub> group on densely functionalized molecules with ease and in good yields. Advanced synthetic intermediates possessing ketones (**50**, **56**, **60**), free alcohols (**52**), amides (**51**, **55**, **58**, **59**, **61**, **65**), halides (**53**, **56**, **58**, **63**, **65**) or amines (**58**, **63**), which are vulnerable to single-electron oxidation, and free hydroxyl groups underwent chemoselective trifluoromethylation. Moreover, a range of nitrogen- and oxygen-containing heterocycles (**51**, **53**, **55**, **57-59**, **61**, **63**, **66**), could be employed as substrates, thus holding promise for the implementation of this technology in medicinal chemistry programs. Particularly noteworthy are examples bearing benzylic and allylic sites (**50**, **51**, **54**, **56-58**, **61**, **63-65**), which are highly susceptible to C–H trifluoromethylation but also these targets showed high chemoselectivity for the desired trifluoromethylation. Moreover, internal alkenes (**54**) and  $\alpha,\beta$ -unsaturated ketones (**58**, **62**, **66**), that might a priori intercept the in situ generated open-shell intermediate generated from the *sp*<sup>3</sup> C–C bond-cleavage of the proaromatic precursors or CF<sub>3</sub> radicals, remained intact, again highlighting the chemoselectivity profile of this reaction. All these examples showcased the versatility and applicability that this technique has unmasking valuable C(*sp*<sup>3</sup>)–CF<sub>3</sub> architectures from unsaturated moieties.

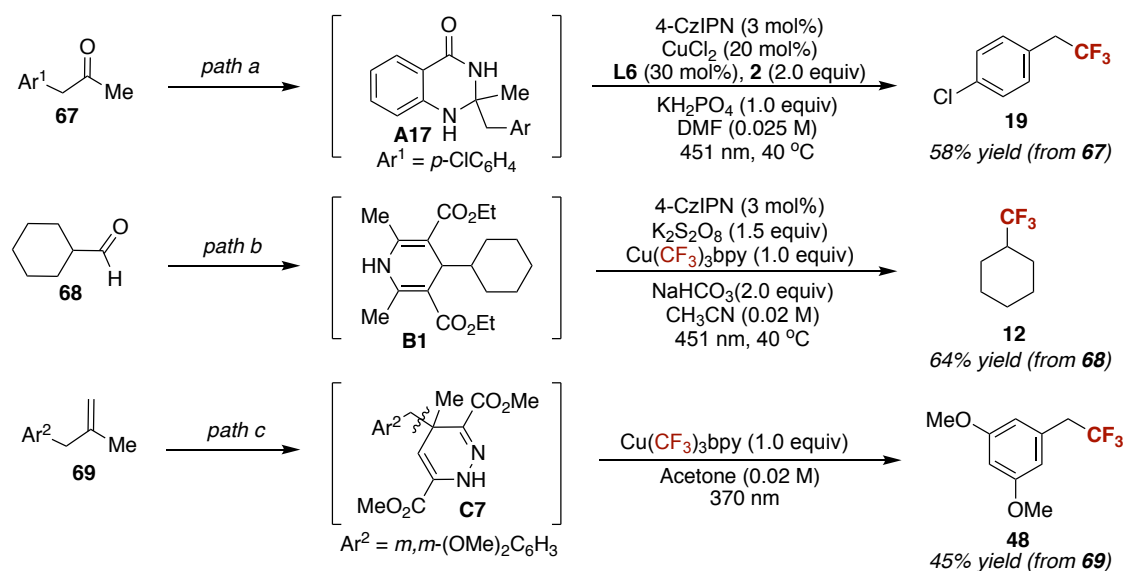


<sup>a</sup> Isolated yields. <sup>b</sup> **A** (0.20 mmol), Cu(CF<sub>3</sub>)<sub>3</sub>bpy (0.20 mmol), **2** (0.30 mmol), 4-CzIPN (3 mol %), BTMG (0.20 mmol) in DMF (0.02 M); **B** (0.30 mmol), Cu(CF<sub>3</sub>)<sub>3</sub>bpy (0.20 mmol), K<sub>2</sub>S<sub>2</sub>O<sub>8</sub> (0.45 mmol), 4-CzIPN (3 mol %), NaHCO<sub>3</sub> (0.60 mmol) in CH<sub>3</sub>CN (0.02 M); **C** (0.30 mmol), Cu(CF<sub>3</sub>)<sub>3</sub>bpy (0.20 mmol) at 35 °C under 370 nm irradiation. See supporting information for characterization of **A-C**.

**Scheme 3.38** Late-stage trifluoromethylation of advanced synthetic intermediates.

### 3.3.2.5 Synthetic Applicability

To further illustrate the combined value of our protocol, **19**, **12**, and **48** can all be used to forge C(sp<sup>3</sup>)-CF<sub>3</sub> structures from the corresponding ketones (**67**), aldehydes (**68**), and olefins (**69**) in a one-pot fashion without the need to isolate the pre-aromatic precursors **A17**, **B1**, and **C7** (Scheme 3.39).

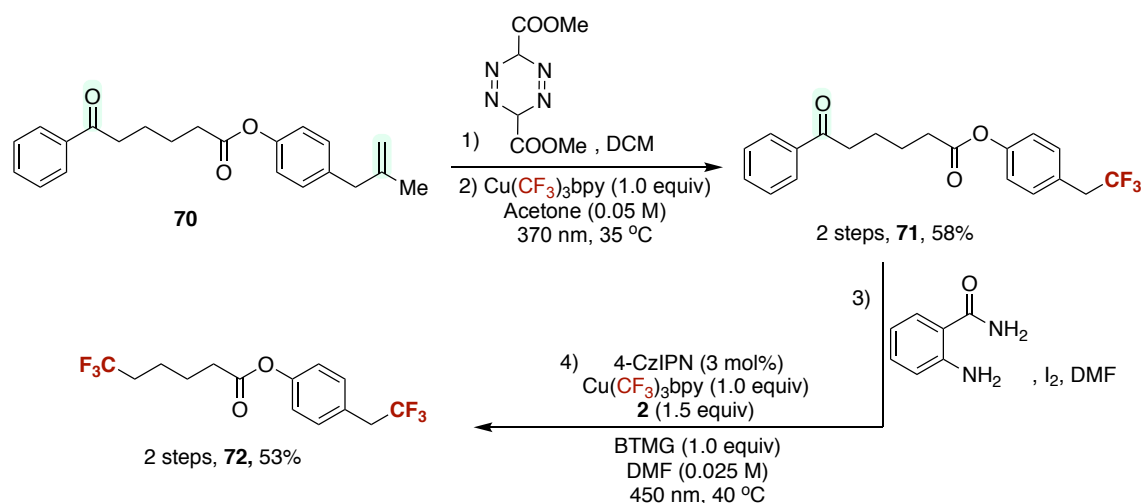


Conditions: <sup>a</sup> *path a*: using **67** (1.05 equiv), aminobenzamide (1.0 equiv), I<sub>2</sub> (5 mol%) in DMF (0.67 M) at 80 °C; *path b*: using **68** (1.0 equiv), Bu<sub>4</sub>NHSO<sub>4</sub> (12 mol%), ethyl 3-aminocrotonate (1.0 equiv), ethyl acetoacetate (1.0 equiv) in ethylene glycol (2.5 M) at 80 °C; *path c*: using **69** (1.0 equiv), dimethyl 1,2,4,5-tetrazine-3,6-dicarboxylate (1.05 equiv) in DCM (0.2 M).

**Scheme 3.39** One-pot trifluoromethylation without isolation of proaromatic precursors.

Next, we targeted a consecutive trifluoromethylation approach to selectively activate two different positions (ketone vs. terminal alkene) and install two trifluoromethyl groups (Scheme 3.40). First, the alkene was converted into its corresponding proaromatic precursor and underwent the desired trifluoromethylation in 58 % total yield keeping the ketone intact. Subsequent ketone activation and second

trifluoromethylation delivered the doubly polyfluorinated product **72** in 53 % yield by two steps.

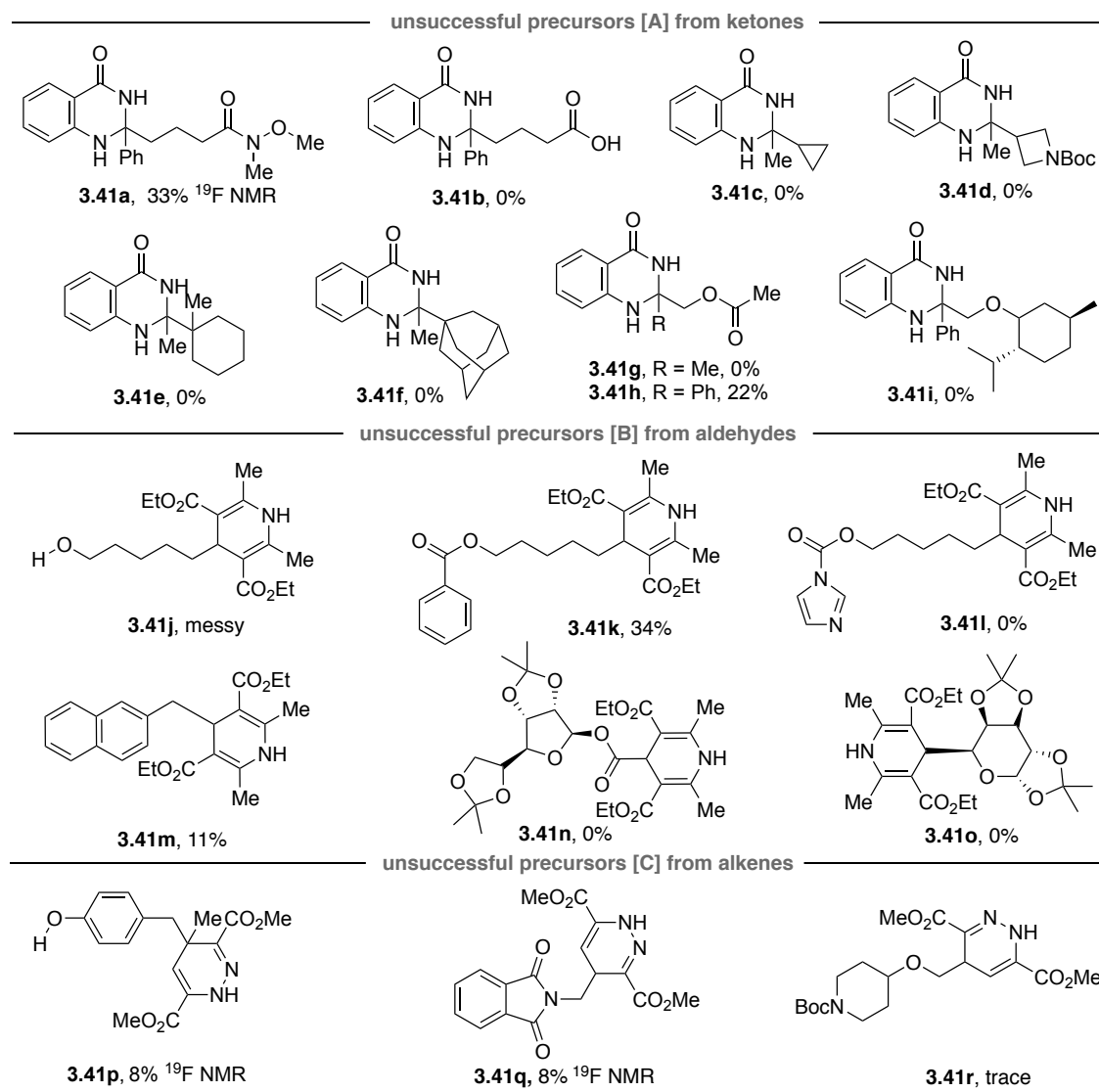


**Scheme 3.40** sequential trifluoromethylation events via  $sp^3$  C–C cleavage.

### 3.3.2.6 Unsuccessful Substrates

Unfortunately, some substrates did not participate in the desired trifluoromethylation reaction or only showed low reactivity (Scheme 3.41). Ketone-derived radical precursors bearing a Weinreb amide (**3.41a**) or carboxylic acid (**3.41b**) were not well tolerated. Cyclic secondary precursors including strained 3- and 4- membered rings (**3.41c**, **3.41d**) were identified as not reactive under the reaction conditions. Tertiary radical precursors of cyclohexane (**3.41e**) or adamantane (**3.41f**) also failed to productively undergo the reaction. Primary radical precursors required phenyl ketones as precursors but only delivered the desired product in low yields 22% (**3.41g**), whereas no reactivity was observed employing the corresponding Me-ketone (**3.41h**). In addition, some limitations were observed for the activation of aliphatic aldehydes via their corresponding Hantzsch esters. Whereas the proaromatic precursors for primary radicals delivered the product in low yield 34% (**3.41k**), other precursors did not participate in the desired decarbonylative trifluoromethylation reaction. In addition, sugar derivatives did not deliver the expected product but a partially protonated side product (**3.41n**, **3.41o**), probably due to steric repulsion and polarity-mismatched. Finally, 1,4-dihydropyridazines (**C**) as radical precursors were not suitable for dealkenylative trifluoromethylations even if the resulting radical intermediates are

stabilized due to the  $\alpha$ -position of oxygen or nitrogen (**3.41q**, **3.41r**).



**Scheme 3.41** Unsuccessful substrates.

### 3.3.3 Mechanistic Proposal

In seminal work, the generation of alkyl radicals from proaromatic precursors as dihydroquinazoline (decarbonylation of ketones), Hantzsch esters (decarbonylation of aldehydes) and 1,4-dihydropyridazines (dealkenylation of alkenes) has been extensively studied through Giese-type addition or nickel-catalyzed arylation and alkylation reactions. Thus, alkyl radical trapped experiments have been demonstrated before and in this study, we focused on relevant mechanistic experiments to further understand the copper-mediated trifluoromethylation. To support our mechanistic

proposal, dihydroquinazoline radical precursor were studied to examine the reaction pathway for C(*sp*<sup>3</sup>)-CF<sub>3</sub> bond-formation.

### 3.3.3.1 Deprotonation of A1 with BTMG by <sup>1</sup>H NMR

To find out whether **A1** is deprotonated or undergoes hydrogen bonding with 2-*tert*-butyl-1,1,3,3-tetramethylguanidine (BTMG), we monitored the chemical shift of **A1** upon reaction with BTMG by using trimethoxybenzene (TMB) as internal standard. **A1** (4.2 mg, 0.01 mmol) and TMB (2.5 mg) were added to a 3 mL vial and dissolved in 1 mL MeCN-*d*<sub>3</sub>. This solution was then transferred to an NMR tube, and the chemical shifts were measured. To this solution, BTMG (2.9 μL, 2 equiv) was added and measured by <sup>1</sup>H NMR. Subsequently, BTMG (14.3 μL, 10 equiv) was added and the mixture was analyzed again by <sup>1</sup>H NMR. *Conclusion*; Chemical shift of **A1** moves slightly downfield, with additional line broadening supporting a weak interaction between BTMG and substrate (Figure 1).

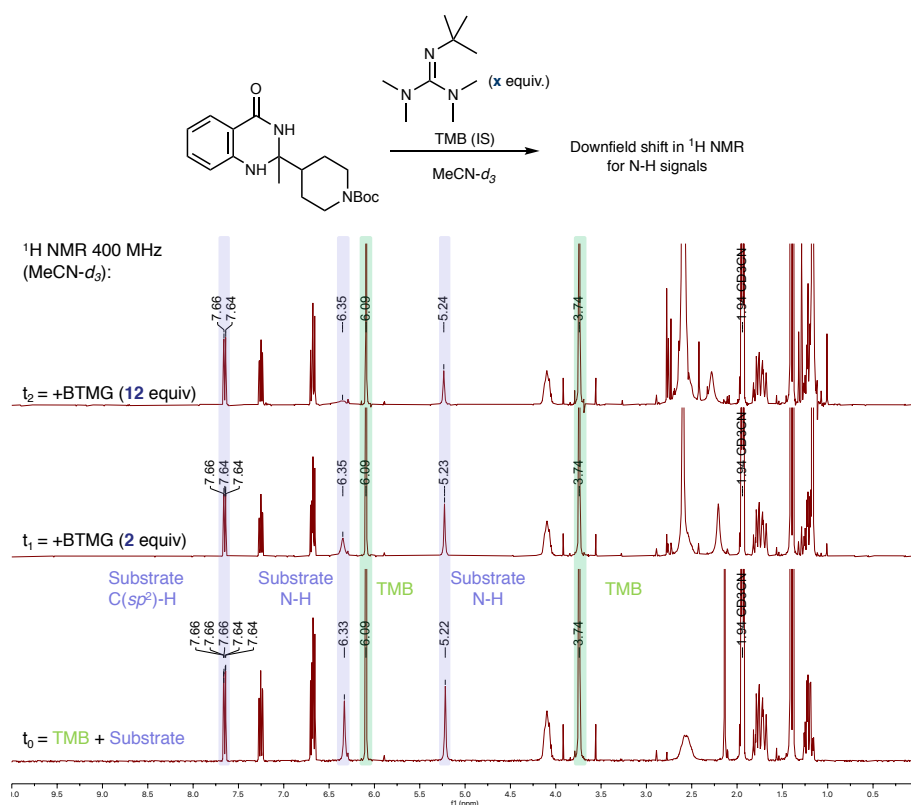


**Figure 1.** <sup>1</sup>H spectra (MeCN-*d*<sub>3</sub>, 400 MHz) of the **A1** (blue) and BTMG (internal standard = TMB (green)).



---

### 3.3.3.2 Photocatalyst Quenching with substrate and BTMG

A series of experiments were conducted to test whether there exists quenching of the photocatalyst with the reaction components. **(a-b)** To a quartz cuvette containing 4-CzIPN (10  $\mu\text{M}$ ) in MeCN was added increasing concentrations of **A1** solution and the emission spectra was recorded. (Figure 2) **(c-d)** To a quartz cuvette containing 4-CzIPN (10  $\mu\text{M}$ ) in MeCN was added increasing concentrations of BTMG solution and the emission spectra was recorded. (Figure 2) **(e-f)** To a quartz cuvette containing 4-CzIPN (10  $\mu\text{M}$ ) in MeCN was added increasing concentrations of 1:1 ratio of BTMG and **A1** solution and the emission spectra was recorded. (Figure 2) **(g-h)** To a quartz cuvette containing 4-CzIPN (10  $\mu\text{M}$ ) in MeCN was added increasing concentrations of Togni's reagent and the emission spectra was recorded. (Figure 2). *Conclusion*; **A1** and BTMG have similar quenching ability.

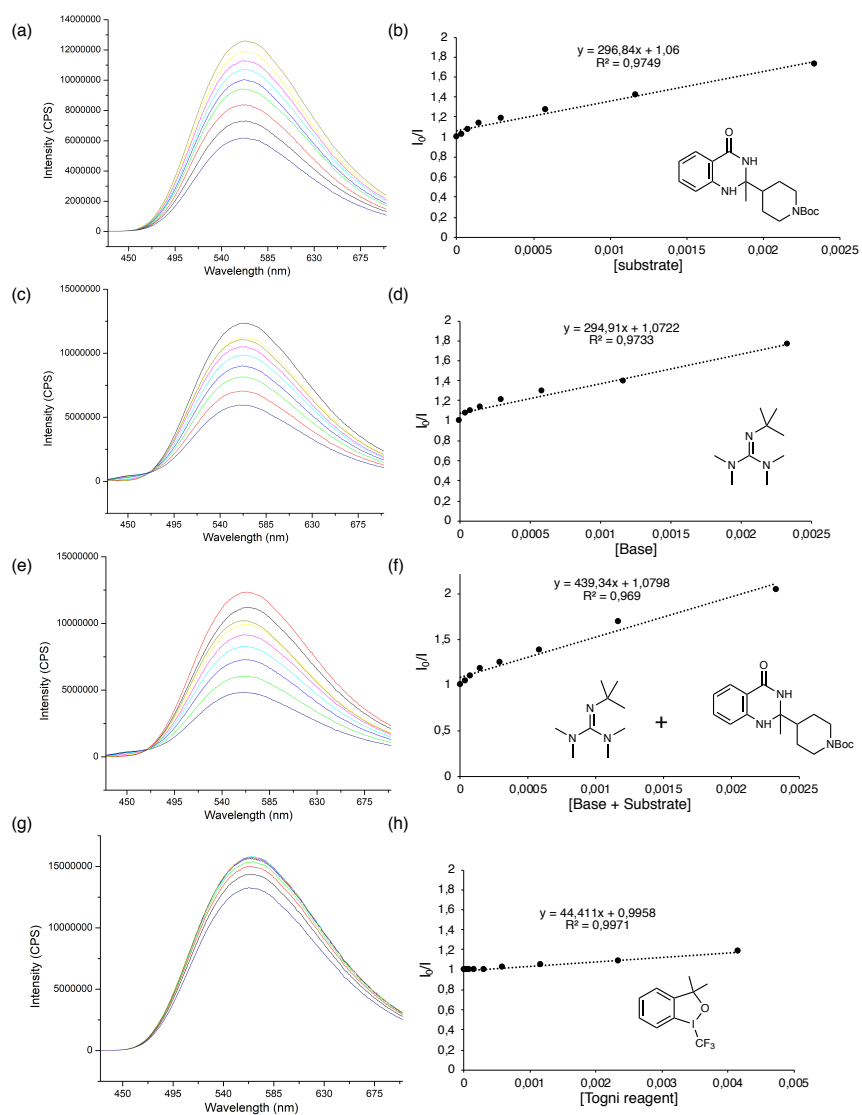


**Figure 2.** Quenching experiments of individual reaction components of substrate **A1**, BTMG, and Togni's reagent along with the combined quenching of BTMG and substrate.

Experimental results from chemical shift of  $^1\text{H}$  NMR experiments between the substrate **A1** and BTMG, as well as from photocatalyst quenching experiments, suggest an electron transfer-deprotonated process between substrate and photocatalyst rather than a PECT process.

### 3.3.3.3 Cyclic Voltammetry Experiments

Cyclic voltammetry (CV) analysis of the substrate **A1** (Figure 3), BTMG (Figure 3), Togni's reagent **I** (**2**) (Figure 4-5) and  $(\text{bpy})\text{Cu}^{\text{II}}\text{Cl}_2$  (Figure 5) showed that the excited-

state 4-CzIPN\* ( $E_{1/2}([4CzIPN]^*/[4CzIPN]) = +1.35$  V vs SCE in MeCN) could oxidize the activated precursor **A1** ( $E_{ox} = +1.21$  V vs SCE) to generate the tentative alkyl radical via SET. Furthermore, the Cu(I) species ( $E_p = -2.12$  V vs SCE in MeCN) could get reduced by Togni's reagent I (**2**) ( $E_p = -2.17$  V vs SCE in MeCN) but not by the photocatalyst 4-CzIPN ( $E_{1/2}(4CzIPN)/[4CzIPN]^{\cdot-} = -1.24$  V vs SCE in MeCN).

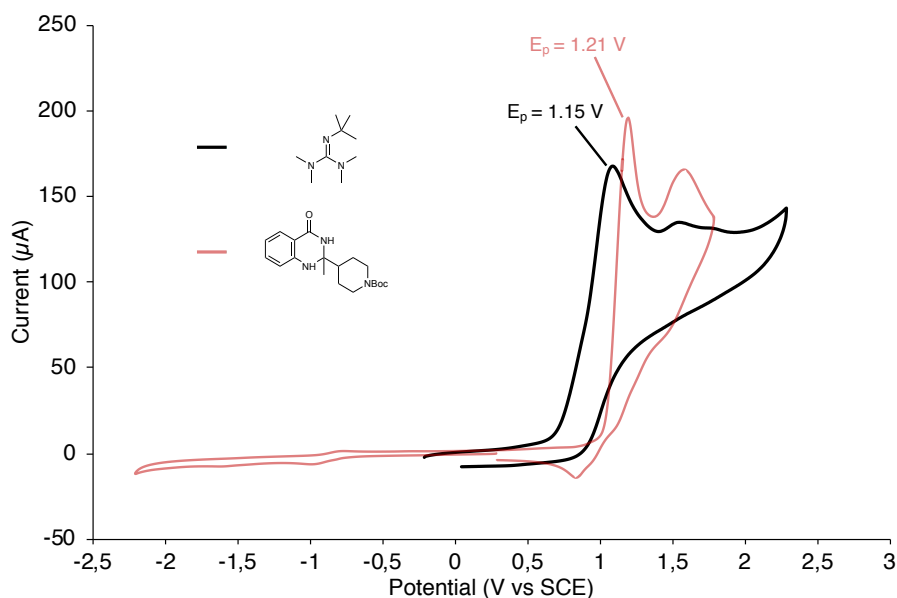


**Figure 3.** Cyclic voltammogram of **A1** (red trace) and BTMG (black trace). Voltammograms were taken using a glassy carbon working electrode in a 0.1 M [ $n$ Bu $_4$ N][PF $_6$ ] supporting electrolyte MeCN solution with a 100 mV/s scan rate and 0.01 M of sample referenced to Fc (+0.38 V vs SCE, external). Scans were started at the open-circuit potential; the first cycle is shown here.  $E_p$  values for BTMG oxidation are + 1.15 V vs SCE and **A1** are + 1.21 V vs SCE.

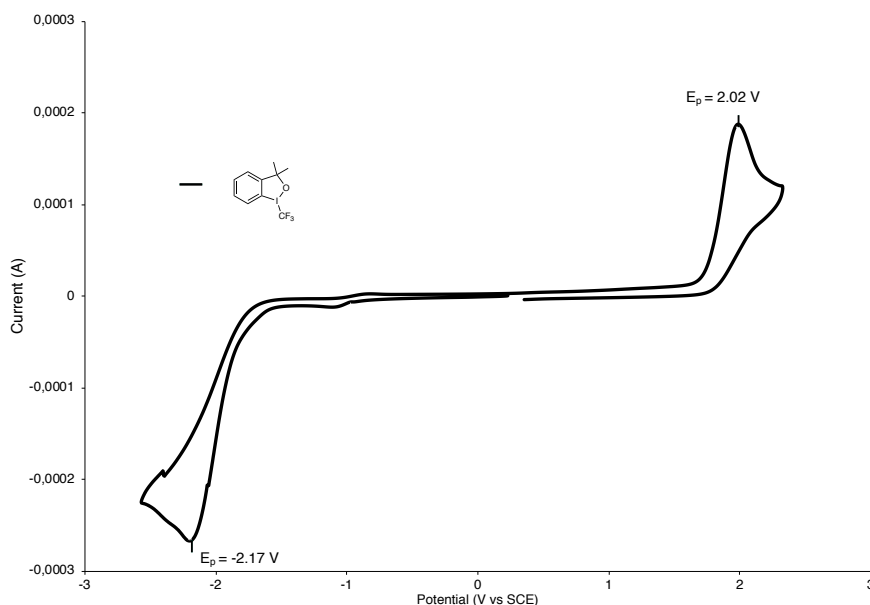


**Figure 4.** Cyclic voltammogram of Togni's reagent I. Voltammograms were taken using a glassy carbon working electrode in a 0.1 M  $[\text{nBu}_4\text{N}][\text{PF}_6]$  supporting electrolyte MeCN solution with a 100 mV/s scan rate and 0.01 M of sample referenced to Fc (+0.38 V vs SCE, external). Scans were started at the open-circuit potential and scanned in the cathode direction first; the first cycle is shown here.  $E_p$  values for Togni's reagent I are -2.17 V vs SCE for reduction and + 2.02 V vs SCE for oxidation.

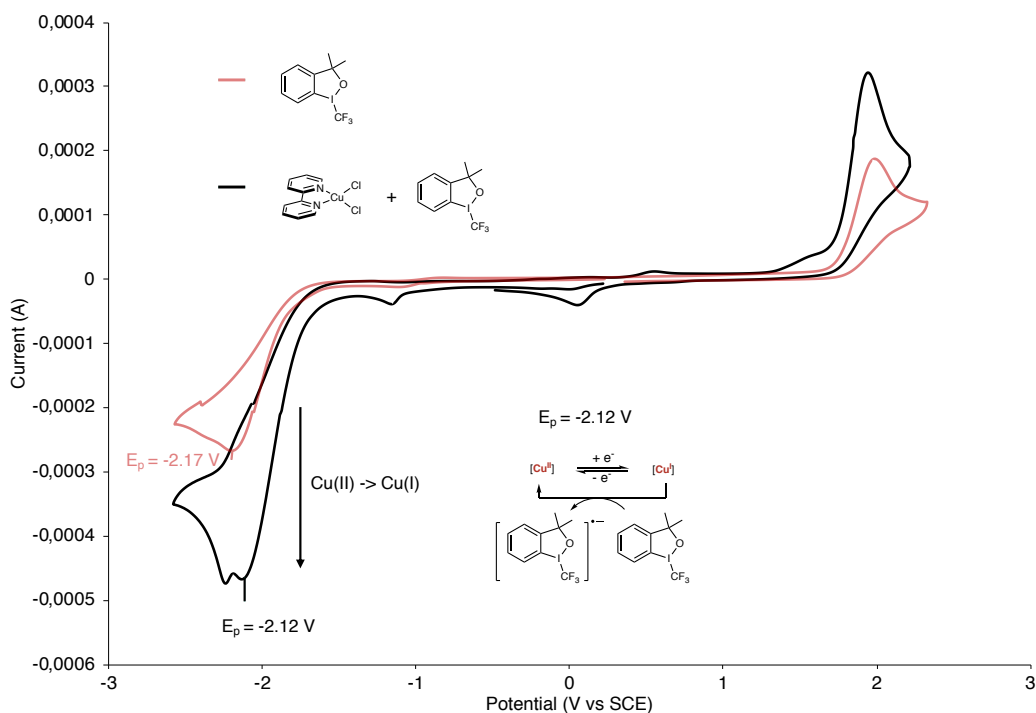


**Figure 5.** Cyclic voltammogram of  $(\text{bpy})\text{CuCl}_2$  with Togni's reagent I overlaid.

Voltammograms were taken using a glassy carbon working electrode in a 0.1 M [<sup>n</sup>Bu<sub>4</sub>N][PF<sub>6</sub>] supporting electrolyte MeCN solution with a 100 mV/s scan rate and 0.01 M of sample referenced to Fc (+ 0.38 V vs SCE, external). Scans were started at the open-circuit potential and scanned in the anode direction first; the first cycle is shown here. The new reduction peak at -2.12 V vs SCE is consistent with Cu(I) oxidizing Togni's reagent I where the catalytic electrochemical reduction of Cu(II) to Cu(I) occurs along with chemical oxidation of Cu(I) to Cu(II) by Togni's reagent I.

### 3.3.3.4 Interactions of BTMG with Togni's reagent I by UV-Vis

The UV-Vis absorption spectra of DCM solutions of BTMG (0.05 M), DCM solutions of Togni's reagent (0.05 M), DCM solutions of a mixture of BTMG (0.023 M) and Togni's reagent (0.023 M) three were recorded in 1 cm path quartz cuvettes using an Agilent Technologies Cary 300 UV-Vis spectrophotometer. As Figure 6 shown, the spectra for both BTMG and Togni's reagent have absorption tails that extend to 450 nm.

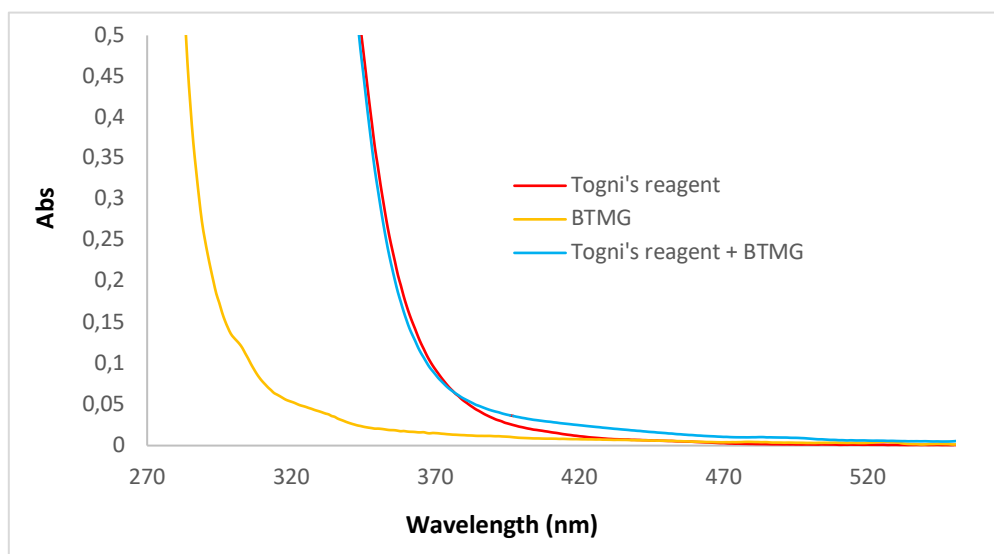


**Figure 6.** The interaction between BTMG and Togni's reagent I in DCM.

To find out whether an interaction between the BTMG and Togni's reagent I occurs, the change in UV-Vis absorption of Togni's reagent I was monitored during the addition of BTMG (**a**). To a quartz cuvette containing Togni's reagent I (0.777 mM) in MeCN was added Togni's reagent I (from 0.2 to 10 equiv) (Figure 7). *Conclusion*; the shift in UV-Vis spectra of Togni's reagent I upon adding BTMG reagent supports an interaction

between BTMG and Togni's reagent I.

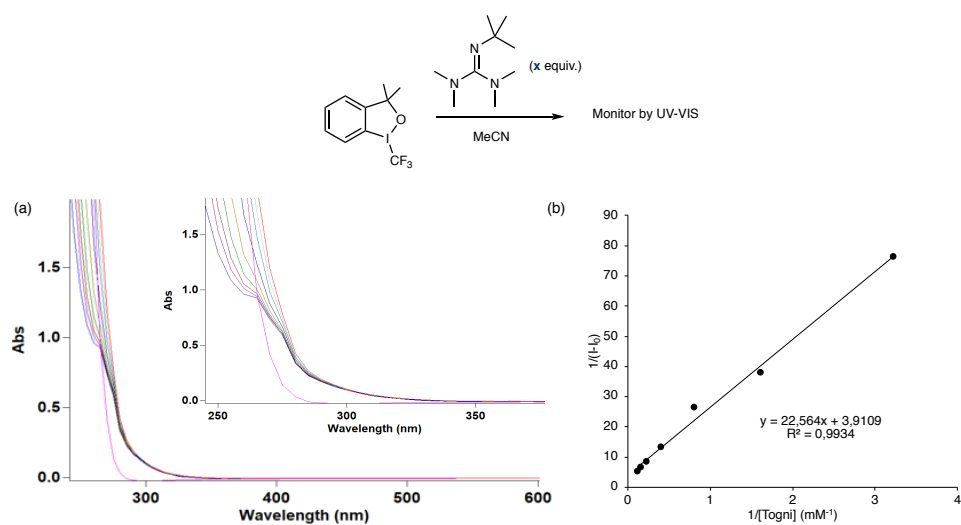


**Figure 7.** Monitoring UV-Vis of Togni's reagent with addition of BTMG. (a) The UV-Vis spectra of substrate (0.78 mM), and the titration of BTMG to Togni's reagent. Pink trace is only BTMG (7.8 mM) (b) Plotted change in absorption intensity at 275 nm vs concentration.

### 3.3.3.5 Interactions of BTMG with Togni's reagent I by <sup>1</sup>H NMR

To further test whether an interaction between the BTMG and Togni's reagent I occurs, we monitor a reaction between these species by <sup>1</sup>H NMR. Solutions containing equal molar concentrations of the BTMG (0.1 M in CDCl<sub>3</sub>) and Togni's reagent I (0.1 M in CDCl<sub>3</sub>) were prepared and mixed to cover Togni's reagent I / BTMG ratio from 0%, 10%, 20% to 100% BTMG (in Figure 8). *Conclusion*; Chemical shift of Togni's reagent moves slightly upfield, supporting an interaction between these species.

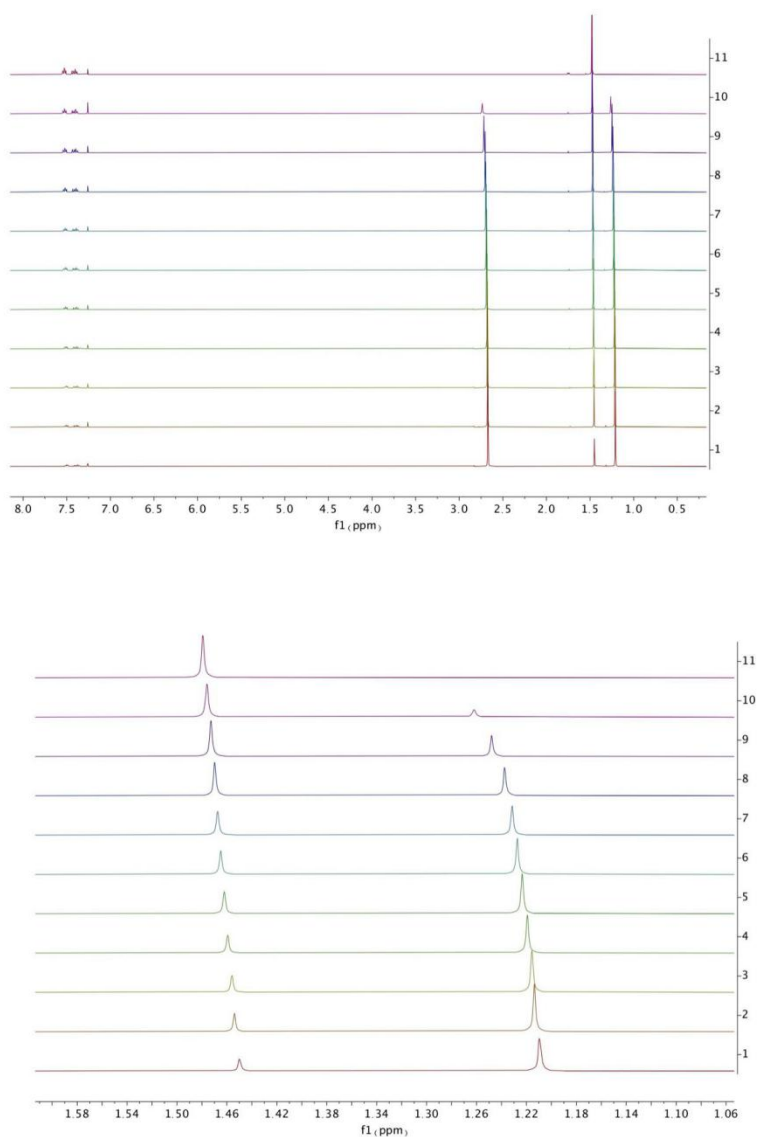


**Figure 8.**  $^1\text{H}$  spectra ( $\text{CDCl}_3$ , 400 MHz) of BTMG and Togni's reagent I. Top: full spectra, increasing equivalents of BTMG. Bottom: zoomed in region depicting shift in signals of Togni's reagent I (2x Me) and BTMG (*t*-Bu).

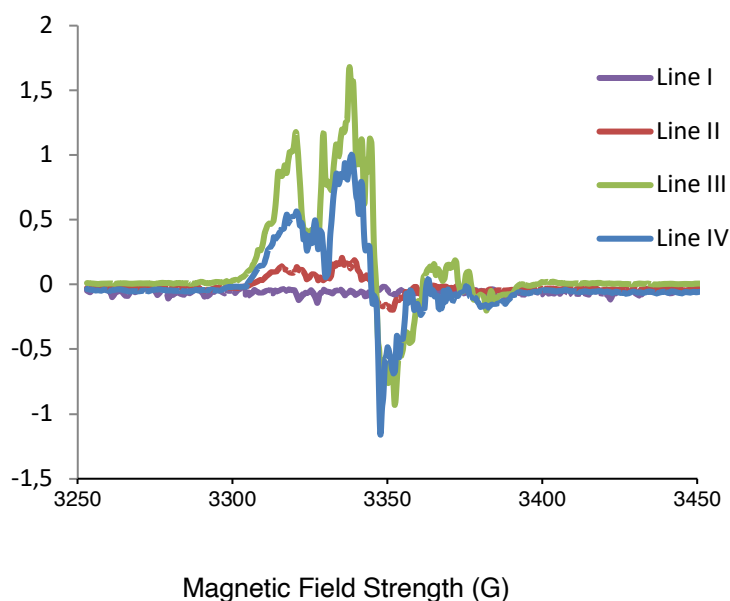
### 3.3.3.6 Interactions of BTMG with Togni's reagent I by EPR Spectrum

**Line I (blank):** An oven-dried 20 mL Schlenk tube containing a stir bar was charged with PBN (PBN = *N*-tert-Butyl- $\alpha$ -phenylnitron) (17.7 mg, 0.1 mmol) and DMF (1.0 mL), then the tube was stirred at 40 °C for 16 h. The Schlenk tube was introduced in an argon-filled glovebox, the reaction mixture was transferred to EPR tube. The sample was brought out from glovebox and was recorded by EMX Micro EPR spectrometer immediately.

**Line II:** An oven-dried 20 mL Schlenk tube containing a stir bar was charged with PBN (17.7 mg, 0.1 mmol), Togni's reagent (16.5 mg, 0.05 mmol) and DMF (1.0 mL), then the tube was stirred at 40 °C under irradiation of blue LEDs 450 nm for 16 h. The Schlenk tube was introduced in an argon-filled glovebox, the reaction mixture was transferred to EPR tube. The sample was brought out from glovebox and was recorded by EMX Micro EPR spectrometer immediately. *Conclusion:* Togni's reagent undergoes spontaneous homolysis to form radicals that react with PBN.

**Line III:** An oven-dried 20 mL Schlenk tube containing a stir bar was charged with PBN (17.7mg, 0.1 mmol), Togni's reagent (16.5 mg, 0.05 mmol) BTMG (0.05 mmol) and DMF (1.0 mL), then the tube was stirred at 40 °C under irradiation of blue LEDs 450 nm for 16 h. The Schlenk tube was introduced in an argon-filled glovebox, the reaction mixture was transferred to EPR tube. The sample was brought out from glovebox and was recorded by EMX Micro EPR spectrometer immediately. *Conclusion:* the increase in signal intensity compared to Line II supports BTMG assists in the homolysis of Togni's reagent.

**Line IV:** An oven-dried 20 mL Schlenk tube containing a stir bar was charged with PBN (17.7mg, 0.1 mmol), Togni's reagent (16.5 mg, 0.05 mmol) BTMG (0.05 mmol) and DMF (1.0 mL), then the tube was stirred at 40 °C for 16 h. The Schlenk tube was introduced in an argon-filled glovebox, the reaction mixture was transferred to EPR tube. The sample was brought out from glovebox and was recorded by EMX Micro EPR spectrometer immediately. *Conclusion:* the EPR signal observed without irradiation supports that Togni's reagent can undergo thermal homolysis at 40 °C.





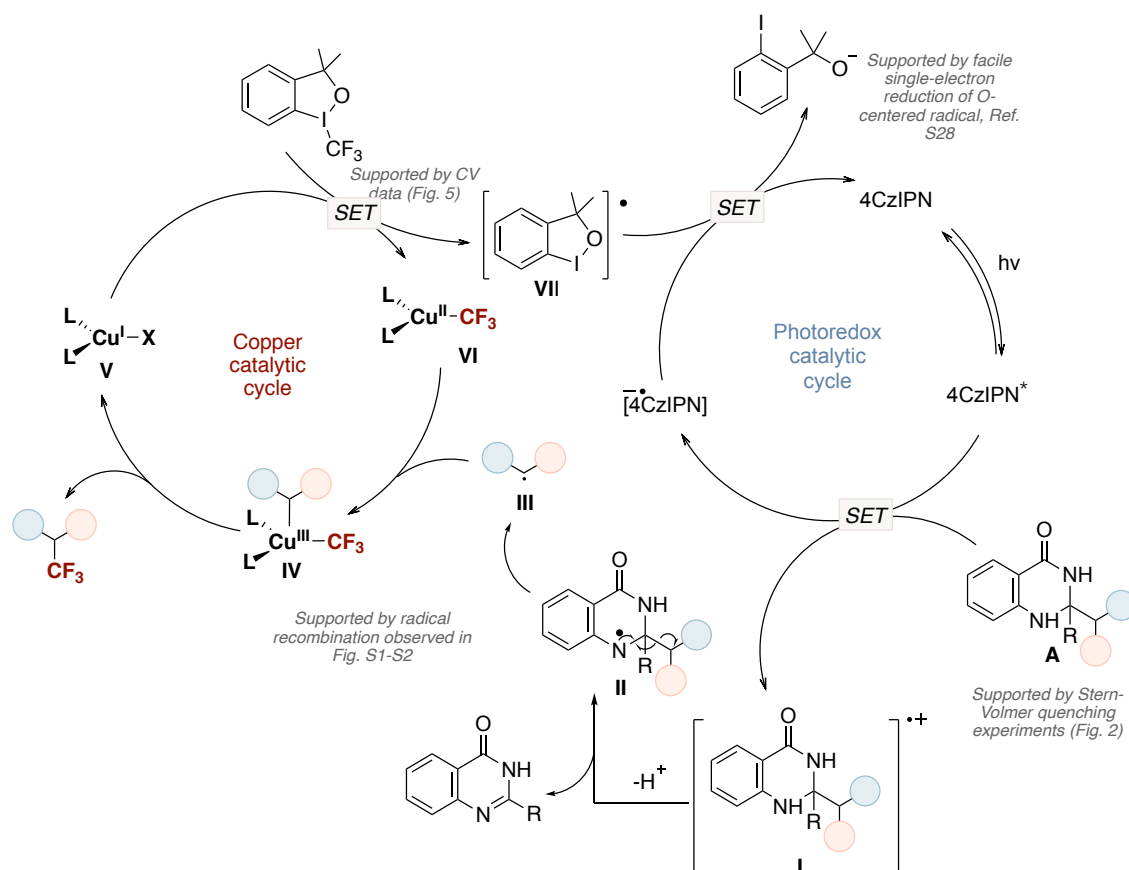
---

**Figure 9.** EPR spectrum.

UV-Vis, NMR and EPR data revealed an interaction between BTMG and Togni's reagent, thus likely promoting the release of the corresponding CF<sub>3</sub> radicals.

### 3.3.3.7 Proposed Catalytic Cycle

Based on these mechanistic studies, a plausible reaction pathway is proposed in Scheme 3.42. Herein, photoexcitation of 4-CzIPN would generate a highly oxidizing excited state 4-CzIPN\*, which could oxidize the activated precursor (**A**) to intermediate (**I**) following a SET process. Aromatization as a thermodynamic driving force triggers a site-selective fragmentation to expel the alkyl radical (**III**) from the radical cation (**II**) after a deprotonation step. At this point, we hypothesize that a single-electron transfer would occur between L<sub>n</sub>Cu<sup>I</sup>X and Togni's reagent **I** (**2**) to form L<sub>n</sub>Cu<sup>II</sup>CF<sub>3</sub> (**VI**) and related O-centered radical (**VII**). L<sub>n</sub>Cu<sup>II</sup>CF<sub>3</sub> (**VI**) would trap the alkyl radical (**III**) to deliver a high-valent alkyl-Cu<sup>III</sup>CF<sub>3</sub> complex, which affords the alkyl-CF<sub>3</sub> product via C(*sp*<sup>3</sup>)-CF<sub>3</sub> bond-forming reductive elimination and regenerates the Cu(I) catalyst. Simultaneously, SET between 4-CzIPN\* and O-radical species (**VII**) would regenerate photocatalyst 4-CzIPN to close the catalytic cycle.

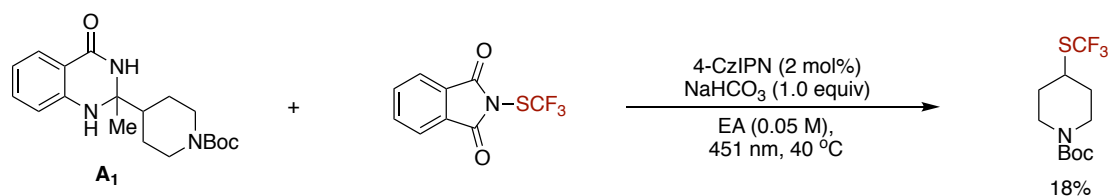


**Scheme 3.42** Mechanistic proposal.

### 3.4 Extended Research and Future outlook

Trifluoromethylthioether groups (SCF<sub>3</sub>) display an important structural motif with high electronegativity and lipophilicity (Hansch parameter  $\pi_R=1.43$ ),<sup>63</sup> which in turn could improve the metabolic stability and transmembrane permeability of drug candidates.<sup>64</sup> To extend our methodology from trifluoromethylarion to C(sp<sup>3</sup>)-SCF<sub>3</sub> bond formation, dihydroquinazolinone precursors (A) were employed as radical precursors. This would present a complementary strategy to literature-know procedures relying on the decarbonylative coupling of ketones to construct C(sp<sup>3</sup>)-SCF<sub>3</sub> bonds. Initial studies demonstrated that dihydroquinazolinone precursors (A) were able to undergo oxidative fragmentation under photo-redox conditions, and the resulting alkyl radicals were shown to successfully react with N-(trifluoromethylthio)-phthalimide to form the desired product under transition metal-free conditions (Scheme 3.43) Optimization studies and exploration of the substrate scope are currently under investigation and will be reported in due course.

In addition, Various C–C bond cleavages by de-aromatization – an important thermodynamic driving force from the formation of N-heterocycles – will remain a powerful tool for achieving a range of different transformations. In particular, the two kind of radical precursors involving dihydroquinazolinone precursors (**A**) and 1,4-dihydropyridazines precursors (**C**), which still have the potential to develop.



**Scheme 3.43** Extended research.

### 3.5 Conclusion

In summary, we have developed an efficient protocol for the conversion of structurally diverse feedstocks containing ketones, aldehydes, and alkenes to the corresponding trifluoromethylated analogues by inert C(*sp*<sup>3</sup>)–C bond cleavage. This technology offers an unconventional manifold enabling trifluoromethylation events with excellent and diverse chemoselectivity under mild reaction conditions. The applicability and functional group tolerance was further demonstrated by the late-stage functionalization of natural products and drug molecules. We believe that this process will complement current trifluoromethylation methods and would be of considerable value to chemical industry and academia.

### 3.6 References

- (a) Purser, S.; Moore, P. R.; Swallow, S.; Gouverneur, V. Fluorine in medicinal chemistry. *Chem. Soc. Rev.* **2008**, *37*, 320. (b) Muller, K.; Faeh, C.; Diederich, F. Fluorine in pharmaceuticals: Looking beyond Intuition. *Science* **2007**, *317*, 1881. (c) Wang, J.; Sanchez-Rosello, M.; Acena, J. L.; del Pozo, C.; Sorochinsky, A. E.; Fustero, S.; Soloshonok, V. A.; Liu, H. Fluorine in pharmaceutical industry: Fluorine-containing drugs introduced to the market in the last decade (2001–2011). *Chem. Rev.* **2014**, *114*, 2432. (d) Meanwell, N. A. Fluorine and fluorinated motifs in the design and application of bioisosteres for drug design. *J. Med. Chem.* **2018**,

- 
- 61, 5822. (e) Gouverneur, V. Radiochemistry: Flipping fluoride's reactivity. *Nat. Chem.* **2012**, *4*, 152.
2. (a) Hansch, C.; Leo, A.; Taft, R. W. A survey of hammett substituent constants and resonance and field parameters. *Chem. Rev.* **1991**, *91*, 165. (b) Liang, T.; Neumann, C. N.; Ritter, T. Introduction of fluorine and fluorine-containing functional groups. *Angew. Chem., Int. Ed.* **2013**, *52*, 8214.
3. Ballinger, P.; Long, F. A. Acid ionization constants of alcohols. II. Acidities of some substituted methanols and related compounds. *J. Am. Chem. Soc.* **1960**, *82*, 795.
4. Zhou, Y.; Wang, J.; Gu, Z.; Wang, S.; Zhu, W.; Aceña, J. L.; Soloshonok, V. A.; Izawa, K.; Liu, H. Next generation of fluorine-containing pharmaceuticals, compounds currently in phase II-III clinical trials of major pharmaceutical companies: New structural trends and therapeutic areas. *Chem. Rev.* **2016**, *116*, 422.
5. (a) Alonso, C.; de Marigorta, E. M.; Rubiales, G.; Palacios, F. Carbon trifluoromethylation reactions of hydrocarbon derivatives and heteroarenes. *Chem. Rev.* **2015**, *115*, 1847. (b) Schlosser, M. CF<sub>3</sub>-bearing aromatic and heterocyclic building blocks. *Angew. Chem., Int. Ed.* **2006**, *45*, 5432. (c) Ma, J.-A.; Cahard, D. Strategies for nucleophilic, electrophilic, and radical trifluoromethylation. *J. Fluorine Chem.* **2007**, *128*, 975. (d) Egami, H.; Sodeoka, M. Trifluoromethylation of alkenes with concomitant introduction of additional functional groups. *Angew. Chem., Int. Ed.* **2014**, *53*, 8294. (e) Xu, J.; Liu, X.; Fu, Y. Recent advances in transition-metal-mediated trifluoromethylation for the construction of C (*sp*<sup>3</sup>)-CF<sub>3</sub> bonds. *Tetrahedron Letters.* **2014**, *55*, 585. (f) Furuya, T.; Kamlet, A.S.; Ritter, Tobias. Catalysis for fluorination and trifluoromethylation. *Nature* **2011**, *473*, 470.
6. McClinton, M.A.M.; McClinton, D.A.M. Trifluoromethylations and related reactions in organic chemistry. *Tetrahedron* **1992**, *48*, 6555.
7. Geri, J. B.; Szymczak, N. K. Recyclable trifluoromethylation reagents from fluoroform. *J. Am. Chem. Soc.* **2017**, *139*, 9811.
8. (a) Prakash, G. K. S.; Jog, P. V.; Batamack, P. T. D.; Olah, G. A. Taming of fluoroform: direct nucleophilic trifluoromethylation of Si, B, S, and C centers. *Science*, **2012**, *338*, 1324. (b) Prakash, G. K. S.; Wang, F.; Zhang, Z.; Haiges, R.; Rahm, M.; Christe, K. O.; Mathew, T. Olah, G. A. Long-lived trifluoromethanide anion: a key intermediate in nucleophilic trifluoromethylations. *Angew. Chem. Int. Ed.* **2014**, *53*, 11575. (c) Lishchynskyi, A.; Miloserdov, F. M.; Martin, E.; Benet-

- 
- Buchholz, J.; Escudero- Adán, E. C.; Konovalov, A. I.; Grushin, V. V. The trifluoromethyl anion. *Angew. Chem. Int. Ed.* **2015**, *54*, 15289.
9. (a) Wu, X-F.; Neumann, H.; Beller, M. Recent developments on the trifluoromethylation of (hetero) arenes. *Chem. Asian J.* **2012**, *7*, 1744. (b) Liu, T.; Shen, Q. Progress in copper-mediated formation of trifluoromethylated arenes. *Eur. J. Org. Chem.* **2012**, *2012*, 6679. (c) Besset, T.; Schneider, C.; Cahard, D. Tamed arene and heteroarene trifluoromethylation. *Angew. Chem. Int. Ed.* **2012**, *51*, 5048. (d) Liu, H.; Gu, Zh.; Jiang, X. Direct trifluoromethylation of the C–H bond. *Adv. Synth. Catal.* **2013**, *355*, 617. (e) Lu, Z. H.; Liu, H.; Liu, S. H.; Leng, X. B.; Lan, Y.; Shen, Q. L. A key intermediate in copper mediated arene trifluoromethylation, [nBu<sub>4</sub>N][Cu(Ar)(CF<sub>3</sub>)<sub>3</sub>]: synthesis, characterization, and C(sp<sup>2</sup>)–CF<sub>3</sub> reductive elimination. *Angew. Chem., Int. Ed.* **2019**, *58*, 8510. (f) Yingda Ye, Stefan A. Künzi, and Melanie S. Sanford. Practical method for the Cu-mediated trifluoromethylation of arylboronic acids with CF<sub>3</sub> radicals derived from NaSO<sub>2</sub>CF<sub>3</sub> and tert-Butyl Hydroperoxide (TBHP). *Org. Lett.* **2012**, *14*, 4979. (g) Grushin, V. V.; Marshall, W. J. Facile Ar–CF<sub>3</sub> bond formation at Pd. strikingly different outcomes of reductive elimination from [(Ph<sub>3</sub>P)<sub>2</sub>Pd(CF<sub>3</sub>)Ph] and [(Xantphos)Pd(CF<sub>3</sub>)Ph]. *J. Am. Chem. Soc.* **2006**, *128*, 39, 12644. (h) Tomashenko, O. A.; Grushin, V. V. Aromatic trifluoromethylation with metal complexes. *Chem. Rev.* **2011**, *111*, 4475
10. Liu, X.; Xu, C.; Wang, M.; Liu, Q. Trifluoromethyltrimethylsilane: nucleophilic trifluoromethylation and beyond. *Chem. Rev.* **2015**, *115*, 683.
11. (a) Shibata, N.; Matsnev, A.; Cahard, D. Shelf-stable electrophilic trifluoromethylating reagents: A brief historical perspective. *Beilstein J. Org. Chem.* **2010**, *6*, 1860. (b) Barata-Vallejo, S; Lantaño, B.; Postigo, A. Recent advances in trifluoromethylation reactions with electrophilic trifluoromethylating reagents. *Chem. Eur. J.* **2014**, *20*, 16806.
12. (a) Studer, A. A “renaissance” in radical trifluoromethylation. *Angew. Chem., Int. Ed.* **2012**, *51*, 8950. (b) Koike, T.; Akita, M. Fine design of photoredox systems for catalytic fluoromethylation of carbon–carbon multiple bonds. *Acc. Chem. Res.* **2016**, *49*, 1937. (c) Nguyen, J. D.; Tucker, J. W.; Konieczynska, M. D.; Stephenson, C. R. Intermolecular atom transfer radical addition to olefins mediated by oxidative quenching of photoredox catalysts. *J. Am. Chem. Soc.* **2011**, *133*, 4160. (d) Chu, L.; Qing, F. L. Copper-catalyzed oxidative trifluoromethylation of terminal alkenes using nucleophilic CF<sub>3</sub>SiMe<sub>3</sub>: efficient C(sp<sup>3</sup>)–CF<sub>3</sub> bond formation. *Org.*

- 
- Lett.* **2012**, *14*, 2106. (e) Tang, X. J.; Dolbier Jr, W. R. Efficient Cu-catalyzed atom transfer radical addition reactions of fluoroalkylsulfonyl chlorides with electron-deficient alkenes induced by visible light. *Angew. Chem., Int. Ed.* **2015**, *54*, 4246. (f) Merino, E.; Nevado, C.; Addition of CF<sub>3</sub> across unsaturated moieties: a powerful functionalization tool. *Chem. Soc. Rev.*, **2014**, *43*, 6598.
13. (a) Zeng, H.; Luo, Z. Han, X.; Li, C. J. Metal-free construction of the C(sp<sup>3</sup>)-CF<sub>3</sub> bond: trifluoromethylation of hydrazones with tognì's reagent under mild conditions. *Org. Lett.* **2019**, *21*, 594. (b) Zhu, L.; Fang, Y.; Li, C. Trifluoromethylation of alkyl radicals: breakthrough and challenges. *Chin. J. Chem.* **2020**, *38*, 787. (c) Xiao, H.; Zhang, Z.; Fang, Y.; Zhu, L.; Li, C. Radical trifluoromethylation. *Chem. Soc. Rev.* **2021**, *50*, 6308.
14. Renaud, R. N.; Champagne, P. J. Electrochemical oxidation of trifluoroacetic acid in an organic substrate. III. In the presence of substituted malonic acid half esters and unsaturated carboxylic acid. *Can. J. Chem.*, 1975, *53*, 529.
15. Go'ltz, P.; de Meijere, A. A new method for the introduction of trifluoromethyl groups. *Angew. Chem., Int. Ed.* **1977**, *16*, 854.
16. (a) Bhowmick, A. C.; Recent development of trifluoromethyl reagents: A review. *Journal of Scientific Research*, **2021**, *13*, 317. (b) Umemoto, T. Organic polyvalent iodine compounds. *Chem. Rev.* **1996**, *96*, 1757. (c) Merritt, E. A.; Olofsson, B.  $\alpha$ -Functionalization of carbonyl compounds using hypervalent iodine reagents. *Synthesis*. **2011**, *2011*, 517. (d) Charpentier, J.; Frueh, N.; Togni, A. Electrophilic trifluoromethylation by use of hypervalent iodine reagents. *Chem. Rev.* **2015**, *115*, 650.
17. Romine, A. M.; Nebra, N.; Konovalov, A. I.; Martin, E.; Benet- Buchholz, J.; Grushin, V. V. Easy access to the copper(III) anion [Cu(CF<sub>3</sub>)<sub>4</sub>]<sup>-</sup>. *Angew. Chem., Int. Ed.* **2015**, *54*, 2745. (c) Tomashenko, O. A.; Escudero-Adan, E. C.; Belmonte, M. M.; Grushin, V. V. Simple, stable, and easily accessible well-defined CuCF<sub>3</sub> aromatic trifluoromethylating agents. *Angew. Chem., Int. Ed.* **2011**, *50*, 7655.
18. Xu, J.; Xiao, B.; Xie, C-Q.; Luo, D-F.; Liu, L.; Fu Y. Copper-promoted trifluoromethylation of primary and secondary alkylboronic acids. *Angew. Chem. Int. Ed.* **2012**, *51*, 12551.
19. Ruppert, I.; Schlich, K.; Volbach, W. Die ersten CF<sub>3</sub>-substituierten organyl(chlor)silane. *Tetrahedron. lett.* **1984**, *25*, 2195.

- 
20. Shen, H.; Liu, Z.; Zhang, P.; Tan, X.; Zhang, Z.; Li, C. Trifluoromethylation of alkyl radicals in aqueous solution. *J. Am. Chem. Soc.*, **2017**, *139*, 9843.
21. Chen, Y.; Ma, G.; Gong, H. Copper-catalyzed reductive trifluoromethylation of alkyl iodides with Togni's reagent. *Org. Lett.*, **2018**, *20*, 4677.
22. Kornfilt, D. J. P.; MacMillan, D. W. C. Copper-catalyzed trifluoromethylation of alkyl bromides. *J. Am. Chem. Soc.*, **2019**, *141*, 6853.
23. Liu, Z.-Y.; Cook, S. P. Interrupting the Barton-McCombie reaction: Aqueous deoxygenative trifluoromethylation of O-alkyl thiocarbonates. *Org. Lett.* **2021**, *23*, 808.
24. Intermaggio, N. E.; Millet, A.; Davis, D. L.; MacMillan, D. W. C. Deoxytrifluoromethylation of alcohols. *J. Am. Chem. Soc.* **2022**, *144*, 11961.
25. Wu, S.; Li, J.; He, R.; Jia, K.; Chen, Y. Terminal trifluoromethylation of ketones via selective C–C cleavage of cycloalkanols enabled by hypervalent iodine reagents. *Org. Lett.* **2021**, *23*, 9204.
26. (a) Tan, X.; Liu, Z.; Shen, H.; Zhang, P.; Zhang, Z.; Li, C. Silver-catalyzed decarboxylative trifluoromethylation of aliphatic carboxylic acids. *J. Am. Chem. Soc.* **2017**, *139*, 12430. (b) Kautzky, J. A.; Wang, T.; Evans, R. W.; MacMillan, D. W. C. Decarboxylative trifluoromethylation of aliphatic carboxylic acids. *J. Am. Chem. Soc.* **2018**, *140*, 6522.
27. (a) Guo, S.; AbuSalim, D. I.; Cook, S. P. Aqueous benzylic C–H trifluoromethylation for late-stage functionalization. *J. Am. Chem. Soc.* **2018**, *140*, 12378. (b) Paeth, M.; Carson, W.; Luo, J.; Tierney, D.; Cao, Z.; Cheng, M.; Liu, W. Copper-mediated trifluoromethylation of benzylic Csp<sup>3</sup>–H bonds. *Chem. – Eur. J.* **2018**, *24*, 11559. (c) Xiao, H.; Liu, Z.; Shen, H.; Zhang, B.; Zhu, L.; Li, C. Copper-catalyzed late-stage benzylic C (sp<sup>3</sup>)–H trifluoromethylation. *Chem* **2019**, *5*, 940.
28. (a) He, J.; Nguyen, T. N.; Guo, S.; Cook, S. P. Csp<sup>3</sup>–H trifluoromethylation of unactivated aliphatic systems. *Org. Lett.* **2021**, *23*, 702. (b) Choi, G.; Lee, G. S.; Park, B.; Kim, D.; Hong, S. H. Direct C(sp<sup>3</sup>)–H trifluoromethylation of unactivated alkanes enabled by multifunctional trifluoromethyl copper complexes. *Angew. Chem., Int. Ed.* **2021**, *60*, 5467.
29. Sarver, P. J.; Bacauanu, V.; Schultz, D. M.; DiRocco, D. A.; Lam, Y.; Sherer, E. C.; MacMillan, D. W. C. The merger of decatungstate and copper catalysis to enable aliphatic C(sp<sup>3</sup>)–H trifluoromethylation. *Nat. Chem.* **2020**, *12*, 459.

- 
30. Liu, Z.; Xiao, H.; Zhang, B.; Shen, H.; Zhu, L.; Li, C. Copper-catalyzed remote C(sp<sup>3</sup>)-H trifluoromethylation of carboxamides and sulfonamides. *Angew. Chem., Int. Ed.* **2019**, *58*, 2510.
31. Wang, X.; Ye, Y.; Zhang, S.; Feng, J.; Xu, Y.; Zhang, Y.; Wang, J. Copper-catalyzed C(sp<sup>3</sup>)-C(sp<sup>3</sup>) bond formation using a hypervalent iodine reagent: an efficient allylic trifluoromethylation. *J. Am. Chem. Soc.* **2011**, *133*, 16410.
32. (a) Ball, N. D.; Kampf, J. W.; Sanford, M. S. Aryl-CF<sub>3</sub> Bond-forming reductive elimination from palladium(IV). *J. Am. Chem. Soc.* **2010**, *132*, 2878. (b) Bour, J. R.; Camasso, N. M.; Meucci, E. A.; Kampf, J. W.; Canty, A. J.; Sanford, M. S. Carbon-carbon bond-forming reductive elimination from isolated nickel(III) complexes. *J. Am. Chem. Soc.* **2016**, *138*, 16105. (c) Winston, M. S.; Wolf, W. J.; Toste, F. D. Photoinitiated oxidative addition of CF<sub>3</sub>I to gold(I) and facile aryl-CF<sub>3</sub> reductive elimination. *J. Am. Chem. Soc.* **2014**, *136*, 7777.
33. Paeth, M.; Tyndall, S. B.; Chen, L. Y.; Hong, J. C.; Carson, W. P.; Liu, X.; Sun, X.; Liu, J.; Yang, K.; Hale, E. M.; Tierney, D. L.; Liu, B.; Cao, Z.; Cheng, M. J.; Goddard, W. A.; Liu, W. Csp<sup>3</sup>-Csp<sup>3</sup> bond-forming reductive elimination from well-defined copper(III) complexes. *J. Am. Chem. Soc.* **2019**, *141*, 3153.
34. (a) Foley, D. J.; Waldmann, H. Ketones as strategic building blocks for the synthesis of natural product-inspired compounds. *Chem. Soc. Rev.*, **2022**, *51*, 4094. (b) Garattini, E.; Terao, M. Increasing recognition of the importance of aldehyde oxidase in drug development and discovery, *Drug Metabolism Reviews*, **2011**, *43*, 374.
35. For selected references:(a) Prakash, G. K. S.; Krishnamurti, R.; Olah, G. A. Synthetic methods and reactions. 141. Fluoride-induced trifluoromethylation of carbonyl compounds with trifluoromethyltrimethylsilane (TMS-CF<sub>3</sub>). A trifluoromethide equivalent. *J. Am. Chem. Soc.* **1989**, *111*, 393. (b) Wu, L.; Wang, F.; Wan, X.; Wang, D.; Chen, P.; Liu, G. Asymmetric Cu-catalyzed intermolecular trifluoromethylarylation of styrenes: enantioselective arylation of benzylic radicals. *J. Am. Chem. Soc.* **2017**, *139*, 2904. (c) Ye, K. Y.; Pombar, G.; Fu, N.; Sauer, G. S.; Kereszte, I.; Lin, S. Anodically coupled electrolysis for the heterodifunctionalization of alkenes. *J. Am. Chem. Soc.* **2018**, *140*, 2438. (d) Novak, P.; Lishchynskyi, A.; Grushin, V. V. Trifluoromethylation of α-Haloketones. *J. Am. Chem. Soc.* **2012**, *134*, 16167.



- 
36. (a) Prakash, G. K. S.; Mandal, M. Nucleophilic trifluoromethylation tamed. *J. Fluorine Chem.* **2001**, *112*, 123. (b) Nelson, D. W.; Easley, R. A.; Pinteá, B. N. V. Nucleophilic perfluoroalkylation of nitrones. *Tetrahedron Lett.* **1999**, *40*, 25.
37. (a) Nelson, D. W.; Owens, J.; Hiraldo, D.  $\alpha$ -(Trifluoromethyl)amine derivatives via nucleophilic trifluoromethylation of nitrones. *J. Org. Chem.* **2001**, *66*, 2572. (b) Hagiwara, T.; Kobayashi, T.; Fuchikami, T. Lewis base catalyzed trifluoromethylation of carbonyl compounds with trialkyl(trifluoromethyl)silanes. *Main Group Chem.* 1997, *2*, 13. (c) Surya Prakash, G. K.; Mandal, M.; Panja, C.; Mathew, T.; Olah, G. A. Preparation of TMS protected trifluoromethylated alcohols using trimethylamine N-oxide and trifluoromethyltrimethylsilane (TMSCF<sub>3</sub>). *J. Fluorine Chem.* **2003**, *123*, 61. (d) Prakash, G. K. S.; Panja, C.; Vaghoo, H.; Surampudi, V.; Kultyshev, R.; Mandal, M.; Rasul, G.; Mathew, T.; Olah, G. A. *J. Org. Chem.* **2006**, *71*, 6806. (e) Mukaiyama, T.; Kawano, Y.; Fujisawa, H. Lithium acetate-catalyzed trifluoromethylation of carbonyl compounds with (trifluoromethyl) trimethylsilane. *Chem. Lett.* 2005, *34*, 88. (f) Song, J. J.; Tan, Z.; Reeves, J. T.; Gallou, F.; Yee, N. K.; Senanayake, C. H. N-heterocyclic carbene catalyzed trifluoromethylation of carbonyl compounds. *Org. Lett.* **2005**, *7*, 2193.
38. Kim, J.; Shreeve, J. M. The first Cu (I)-mediated nucleophilic trifluoromethylation reactions using (trifluoromethyl) trimethylsilane in ionic liquids. *Org. Biomol. Chem.* **2004**, *2*, 2728.
39. (a) Ma, J.-A.; Cahard, D. Asymmetric fluorination, trifluoromethylation, and perfluoroalkylation reactions. *Chem. Rev.* **2004**, *104*, 6119. (b) Kawano, Y.; Mukaiyama, T. Diastereoselective trifluoromethylation of chiral N-(Tolylsulfinyl)imines in the presence of lewis bases. *Chem. Lett.* **2005**, *34*, 894.
40. (a) Xu, J.; Liu, X.; Fu, Y. Recent advance in transition-metal-mediated trifluoromethylation for the construction of C (*sp*<sup>3</sup>)-CF<sub>3</sub> bonds. *Tetrahedron Lett.* **2014**, *55*, 585. (b) Sato, K.; Yuki, T.; Yamaguchi, R.; Hamano, T.; Tarui, A.; Omote, M.; Kumadaki, I.; Ando, A. Mechanistic studies on  $\alpha$ -trifluoromethylation of Ketones via silyl enol ethers and its application to other carbonyl compounds. *J. Org. Chem.* **2009**, *74*, 3815. (c) Itoh, Y.; Mikami, K. Radical trifluoromethylation of titanium ate enolate. *Org. Lett.* **2005**, *7*, 649. (d) Itoh, Y.; Mikami, K. Facile radical trifluoromethylation of lithium enolates. *Org. Lett.* **2005**, *7*, 4883. (e) Mikami, K.; Tomita, Y.; Ichikawa, Y.; Amikura, K.; Itoh, Y. Radical trifluoromethylation of ketone silyl enol ethers by activation with dialkylzinc. *Org.*

- 
- Lett.* **2006**, *8*, 4671. (f) Itoh, Y.; Mikami, K. Radical trifluoromethylation of Ti ate enolate: possible intervention of transformation of Ti (IV) to Ti (III) for radical termination. *J. Fluor. Chem.* **2006**, *127*, 539. (g) Sato, K.; Yuki, T.; Tarui, A.; Omote, M.; Kumadaki, I.; Ando, A. Zn-mediated rhodium-catalyzed  $\alpha$ -trifluoromethylation of ketones via silyl enol ethers. *Tetrahedron Lett.* **2008**, *49*, 3558.
41. Ono, T.; Umemoto, T. Kinetic study of trifluoromethylation with S-(trifluoromethyl) dibenzothiophenium salts. *J. Fluorine Chem.* **1996**, *80*, 163. (b) Blazejewski, J. C.; Wilmshurst, M. P.; Popkin, M. D.; Wakselman, C.; Laurent, G.; Nonclercq, D.; Cleeren, A.; Seo, M. Y. H-S.; Leclercq, G. Synthesis, characterization and biological evaluation of  $7\alpha$ -perfluoroalkylestradiol derivatives. *Bioorg. Med. Chem.* **2003**, *11*, 335.
42. (a) Umemoto, T. Electrophilic perfluoroalkylating agents. *Chem. Rev.* **1996**, *96*, 1757. (b) Martinez, H.; Rebeyrol, A.; Nelms, T. B.; Dolbier Jr, W. R. Impact of fluorine substituents on the rates of nucleophilic aliphatic substitution and  $\beta$ -elimination. *J. Fluorine Chem.* **2012**, *135*, 167. (c) Howell, J. L.; Muzzi, B. J.; Rider, N. L.; Aly, E. M.; Abouelmagd, M. K. On the preparation of 1H-perfluoroalkanes and a mechanism for the reduction of perfluoroalkyl iodides. *J. Fluorine Chem.* **1995**, *72*, 61.
43. Muralidharan, K.; Chakraborty, R. J.; Shreeve, M. Electrophilic trifluoromethylation of simple inorganic salts: a one step route to trifluoromethylnitromethane,  $\text{CF}_3\text{NO}_2$ . *J. Fluorine Chem.* **2004**, *125*, 1967.
44. Pham, P. V.; Nagib, D. A.; MacMillan, D. W. C. Photoredox catalysis: A mild, operationally simple approach to the synthesis of  $\alpha$ -trifluoromethyl carbonyl compounds. *Angew. Chem., Int. Ed.* **2011**, *50*, 6119.
45. (a) Juris, A.; Balzani, V.; Barigelletti, F.; Campagna, S.; Belser, P.; Zelewsky, A. Ru (II) polypyridine complexes: photophysics, photochemistry, electrochemistry, and chemiluminescence. *Chem. Rev.* **1988**, *84*, 85. (b) K. Kalyanasundaram, Coord. Photophysics, photochemistry and solar energy conversion with tris (bipyridyl) ruthenium (II) and its analogues. *Chem. Rev.* **1982**, *46*, 159.
46. Krusic, P. J.; Bingham, R. C. An electron spin resonance study of the substituent effects causing nonplanarity in alkyl radicals. Electronegativity vs.. pi.-conjugative destabilization. *J. Am. Chem. Soc.* **1976**, *98*, 230.

- 
47. Muller, N. Anodic trifluoromethylation of acrylic acid. Synthesis of diethyl (2, 2, 2-trifluoroethyl) malonate and trifluorinated analogs of barbital and amobarbital. *J. Org. Chem.*, **1986**, *51*, 263.
48. (a) Tommasino, J-B.; Brondex, A.; M'edebielle, M.; Thomalla, M.; Langlois B. R.; Billard, T. Trifluoromethylation reactions with potassium trifluoromethanesulfinate under electrochemical oxidation. *Synlett*, **2002**, 1697. (b) Sato, K.; Omote, M.; Ando, A.; Kumadaki, I. Rhodium-catalyzed novel trifluoromethylation at the  $\alpha$ -position of  $\alpha$ ,  $\beta$ -unsaturated ketones. *Org. Lett.*, **2004**, *6*, 4359. (c) Erdbrink, H.; Peuser, I.; Gerling, U. I.; Lentz, M. D.; Koksich, B.; Czekelius, C. Conjugate hydrotrifluoromethylation of  $\alpha$ ,  $\beta$ -unsaturated acyl-oxazolidinones: synthesis of chiral fluorinated amino acids. *Org. Biomol. Chem.*, **2012**, *10*, 8583. (d) Wu, X.; Chu, L.; Qing, F-L. Silver-catalyzed hydrotrifluoromethylation of unactivated alkenes with  $\text{CF}_3\text{SiMe}_3$ . *Angew. Chem., Int. Ed.*, **2013**, *52*, 2198.
49. Mizuta, S.; Verhoog, S.; Engle, K. M.; Khotavivattana, T.; O'Duill, M.; Wheelhouse, K.; Rassias, G.; M'edebielle, M.; Gouverneur, V. Catalytic hydrotrifluoromethylation of unactivated alkenes. *J. Am. Chem. Soc.*, **2013**, *135*, 2505.
50. Wilger, D. J.; Gesmundo, N. J.; Nicewicz, D. A. A practical method for metal-free radical trifluoromethylation of styrenes with  $\text{NaSO}_2\text{CF}_3$ . *Chem. Sci.*, **2013**, *4*, 3160.
51. (a) Kitazume, T.; Ishikawa, N. Ultrasound-promoted selective perfluoroalkylation on the desired position of organic molecules. *J. Am. Chem. Soc.* **1985**, *107*, 518. (b) Matsubara, S.; Mitani, M.; Utimoto, K. A facile preparation of 1-perfluoroalkylalkenes and alkynes. Palladium catalyzed reaction of perfluoroalkyl iodides with organotin compounds. *Tetrahedron Lett.* **1987**, *28*, 5857. (c) Urata, H.; Fuchikami, T. A novel and convenient method for trifluoromethylation of organic halides using  $\text{CF}_3\text{SiR}'_3/\text{KF}/\text{Cu}$  (I) system. *Tetrahedron Lett.* **1991**, *32*, 91. (d) Su, D-B.; Duan, J-X.; Chen, Q-Y. Methyl chlorodifluoroacetate a convenient trifluoromethylating agent. *Tetrahedron Lett.* **1991**, *32*, 7689. (e) Bouillon, J-P.; Maliverney, C.; MerØnyi, R.; Viehe, H. G. Trifluoromethylation of aliphatic halogen compounds. *J. Chem. Soc. Perkin Trans.* 1991, *1*, 2147.
52. Parsons, A. T.; Buchwald, S. L. Copper-catalyzed trifluoromethylation of unactivated olefins. *Angew. Chem., Int. Ed.*, **2011**, *50*, 9120.

- 
53. Xu, J.; Fu, Y.; Luo, D-F.; Jiang, Y-Y.; Xiao, B.; Liu, Z-J. Gong, T-J.; Liu, L. Copper-catalyzed trifluoromethylation of terminal alkenes through allylic C–H bond activation. *J. Am. Chem. Soc.*, **2011**, *133*, 15300.
54. Chu, L.; Qing, F-L. Copper-catalyzed oxidative trifluoromethylation of terminal alkenes using nucleophilic  $\text{CF}_3\text{SiMe}_3$ : Efficient  $\text{C}(\text{sp}^3)\text{--CF}_3$  bond formation. *Org. Lett.* **2012**, *14*, 2106.
55. Yasu, Y.; Koike, T.; Akita, M. Three-component oxytrifluoromethylation of alkenes: Highly efficient and regioselective difunctionalization of C–C bonds mediated by photoredox catalysts. *Angew. Chem. Int. Ed.* **2012**, *124*, 9705.
56. (a) Yasu, Y.; Koike, T.; Akita, M. Intermolecular aminotrifluoromethylation of alkenes by visible-light-driven photoredox catalysis. *Org. Lett.* **2013**, *15*, 2136. (b) Kim, E.; Choi, S.; Kim, H.; Cho, E. J.; Generation of  $\text{CF}_3$ -containing epoxides and aziridines by visible-light-driven trifluoromethylation of allylic alcohols and amines. *Chem. Eur. J.* **2013**, *19*, 6209.
57. Majhi, J.; Dhungana, R. K.; Rentería-Gómez, A.; Sharique, M.; Li, L.; Dong, W.; Gutierrez, O.; Molander, G. A. Metal-free photochemical imino-alkylation of alkenes with bifunctional oxime esters. *J. Am. Chem. Soc.* **2022**, *144*, 15871.
58. Gnyawali, K.; Arachchige, P. T. K.; Yi, C. S. Synthesis of flavanone and quinazolinone derivatives from the ruthenium-catalyzed deaminative coupling reaction of 2'-hydroxyaryl ketones and 2-aminobenzamides with simple amines. *Org. Lett.* **2022**, *24*, 218
59. Zanardi, A.; Novikov, M. A.; Martin, E.; Benet-Buchholz, J.; Grushin, V. V. Direct cupration of fluoroform. *J. Am. Chem. Soc.* **2011**, *133*, 20901.
60. Luo, J.; Zhang, J. Donor–acceptor fluorophores for visible-light-promoted organic synthesis: photoredox/Ni dual catalytic  $\text{C}(\text{sp}^3)\text{--C}(\text{sp}^2)$  cross-coupling. *ACS Catal.* **2016**, *6*, 873
61. Yue, W-J.; Day, C. S.; Brenes Rucinski, A. J.; Martin, R. Catalytic hydrodifluoroalkylation of unactivated olefins. *Org. Lett.* **2022**, *24*, 5109.
62. Liu, X.; Liu, R.; Dai, J.; Cheng, X.; Li, G. Application of Hantzsch ester and Meyer nitrile in radical alkynylation reactions. *Org. Lett.* **2018**, *20*, 6906.
63. (a) Hansch, C.; Leo, A.; Taft, R. W. Survey of Hammett substituent constants and resonance and field parameters. *Chem. Rev.* **1991**, *91*, 16. (b) Toulgoat, F.; Alazet, S.; Billard, T. Direct trifluoromethylthiolation reactions: the “renaissance” of an old concept. *Eur. J. Org. Chem.* **2014**, *2014*, 2415. (c) Barata-Vallejo, S.; Bonesi, S.;

---

Postigo, A. Late stage trifluoromethylthiolation strategies for organic compounds. *Org. Biomol. Chem.* **2016**, *14*, 7150. (d) Xu, X-H.; Matsuzaki, K.; Shibata, N. Synthetic methods for compounds having CF<sub>3</sub>-S units on carbon by trifluoromethylation, trifluoromethylthiolation, triflylation, and related reactions. *Chem. Rev.* **2015**, *115*, 731.

64. (a) Zheng, H.; Huang, Y.; Weng, Z. Recent advances in trifluoromethylthiolation using nucleophilic trifluoromethylthiolating reagents. *Tetrahedron Lett.* **2016**, *57*, 1397. (b) Zhang, C. J. Advances in trifluoromethylation or trifluoromethylthiolation with copper CF<sub>3</sub> or SCF<sub>3</sub> complexes. *Chem. Sci.* **2017**, *129*, 1795

## 3.7 Experimental Section

### 3.7.1 General Considerations

**Analytical methods:** <sup>1</sup>H and <sup>13</sup>C NMR spectra were recorded on Bruker 300 MHz, Bruker 400 MHz and Bruker 500 MHz at 20 °C. Chemical shifts (δ) are given in parts per million (ppm) and referenced to CDCl<sub>3</sub> (<sup>1</sup>H: 7.26 ppm, <sup>13</sup>C: 77.17 ppm), unless otherwise stated. <sup>19</sup>F NMR was obtained with <sup>1</sup>H decoupling unless otherwise stated. Coupling constants (*J*) are given in Hertz (Hz). Melting points were measured in degrees Celsius (°C) using open glass capillaries in a Büchi B540 apparatus. Infra-red spectra (FT-IR) measurements were carried out on a Bruker Optics FT-IR Alpha spectrometer equipped with a DTGS detector, KBr beamsplitter at 4 cm<sup>-1</sup> resolution using a one bounce ATR accessory with diamond windows. Selected absorption maxima (ν<sub>max</sub>) are reported in wavenumbers (cm<sup>-1</sup>). High-resolution mass spectra (HRMS) were recorded on a Waters LCT Premier spectrometer or in a MicroTOF Focus, Bruker Daltonics spectrometer. UV-Vis absorption spectra were recorded using a Agilent Technologies Cary 300 UV-Vis spectrophotometer in quartz cuvettes with a path length of 1.0 cm. Bulk electrolysis was conducted on a PARSTAT 2273 potentiometer using a 3-electrode cell configuration at room temperature, the same electrodes were used for cyclic voltammetry (CV) experiments, namely a glassy carbon working electrode, platinum flag counter electrode and Ag/AgCl (KCl sat.) reference electrode. Flash column chromatography was performed with EM Science silica gel 60 (230-400 mesh). Analytical thin-layer chromatography (TLC) was performed using aluminium-backed silica plates (Merck, silica gel 60 F<sub>254</sub>). Compounds were visualized

---

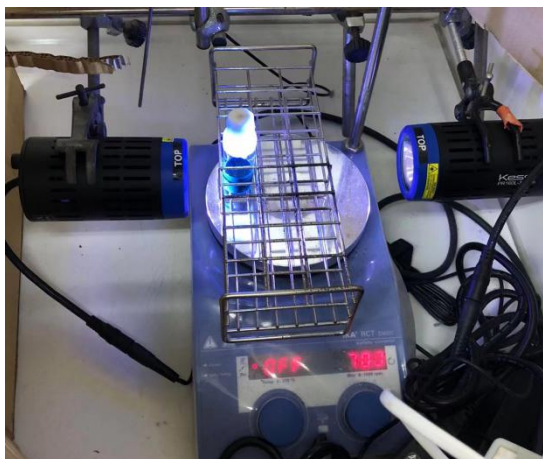
under UV light and/or staining with aqueous basic potassium permanganate (KMnO<sub>4</sub>) or cerium molybdate solution. The yields reported refer to isolated yields and represent an average of at least two independent runs. The procedures described in this section are representative. Thus, the yields may differ slightly from those given in the tables of the manuscript.

**Reagents:** Commercially available materials were used as received without further purification. Anhydrous copper(II) chloride (97% purity) was purchased from Alfa Aesar. Phenanthroline (99% purity) was purchased from Aldrich. Togni's reagent I (98% purity) was purchased from CF Plus Chemicals. 2-tert-Butyl-1,1,3,3-tetramethylguanidine (BTMG) was purchased from Aldrich (98% purity). Anhydrous N,N-dimethylformamide (DMF, 99.5% purity) was purchased from Acros. Anhydrous acetone (99.5% purity) was purchased from Acros. Anhydrous acetonitrile (99.5% purity) was purchased from Acros.

Trifluoromethylation reactions from ketones and aldehydes were performed with 451 nm blue LEDs (OSRAM Oslon® SSL 80 royal-blue LEDs) installed at the bottom of a custom-made photoreactor, which was designed to hold 8 flat-bottom Schlenk tubes (the distance between the flat-bottom Schlenk tube and the light source was measured to be ~7 mm). The photoreactor was equipped with a liquid cooling system (the thermostat was set at 40 °C) and a magnetic stirrer (~700 rpm).

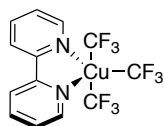


Trifluoromethylations from alkenes were performed with 2×370nm Kessil lamps (PR160L-370 nm, 40 W) without cooling (35 °C), and a magnetic stirrer (~700 rpm).



### 3.7.2 Synthesis of Starting Materials

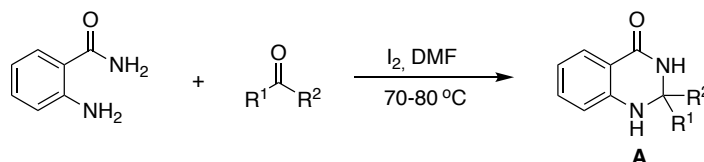
#### Synthesis of $\text{Cu}(\text{CF}_3)_3(\text{bpy})$



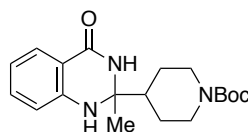
$\text{Cu}(\text{CF}_3)_3(\text{bpy})$  was prepared following a modified literature procedure.<sup>[1]</sup> To a dry 250 mL round-bottom flask were added copper (I) iodide (10 mmol), 2,2'-bipyridine (10 mmol), silver (I) fluoride (40 mmol) in an argon-filled glove box. DMF (13 mL) was added outside of glove box, and stirred for 30 min.  $\text{TMSCF}_3$  (65 mmol) was slowly added (10 mL/h) under argon flow. The resulting mixture was stirred for 18 h at room temperature. The resulting mixture was filtered through a pad of Celite®, eluted with acetone, and concentrated under reduced pressure. Methanol was added (200 mL) to the resulting residue, and recrystallized at  $-20\text{ }^\circ\text{C}$  overnight, filtered, washed with cold methanol and dried under vacuum to afford pure  $\text{Cu}(\text{CF}_3)_3(\text{bpy})$  as a yellow solid. Spectroscopic data for  $\text{Cu}(\text{CF}_3)_3(\text{bpy})$  match those previously reported in the literature.<sup>1</sup>  $^{19}\text{F}$  NMR (376 MHz, Acetone- $\text{d}_6$ )  $\delta$  -24.83 (t,  $J = 9.3$  Hz), -37.82 (q,  $J = 9.1$  Hz) ppm.  $^1\text{H}$  NMR (400 MHz, Acetone- $\text{d}_6$ )  $\delta$  9.28 (d,  $J = 5.2$  Hz, 2H), 8.85 (d,  $J = 8.1$  Hz, 2H), 8.43 (td,  $J = 7.9, 1.6$  Hz, 2H), 7.96 (ddd,  $J = 7.7, 5.2, 1.1$  Hz, 2H) ppm.

#### Synthesis of Radical Precursors (A) from Ketones

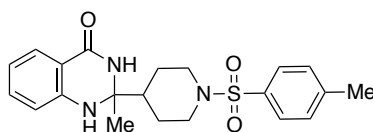
##### Method A



Following a literature procedure,<sup>[2]</sup> a dry flask was charged with 2-aminobenzamide (1.00 equiv), ketone (1.05 equiv), I<sub>2</sub> (5 mol%) and DMF (0.67 M). The reaction mixture was stirred at 70-80 °C for 12-16 h. After completion of the reaction, the reaction mixture was cooled to room temperature. Water was added to the mixture, and the solid was collected by filtration. The crude products were washed with water and purified by recrystallization from Et<sub>2</sub>O and hexane.



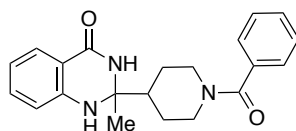
**tert-butyl 4-(2-methyl-4-oxo-1,2,3,4-tetrahydroquinazolin-2-yl)piperidine-1-carboxylate (A1)** Following Method A, the utilization of *tert*-butyl 4-acetylpiperidine-1-carboxylate (1.14 g, 5.0 mmol) afforded the title compound as a white solid (1.43 g, 83% yield). <sup>1</sup>H NMR (400 MHz, CDCl<sub>3</sub>) δ 7.84 (dd, *J* = 7.8, 1.6 Hz, 1H), 7.37 – 7.21 (m, 1H), 6.86 (s, 1H), 6.82 – 6.74 (m, 1H), 6.58 (dd, *J* = 8.1, 1.0 Hz, 1H), 4.22 – 4.18 (m, 3H), 2.62 – 2.56 (m, 2H), 2.01 – 1.68 (m, 3H), 1.46 (s, 3H), 1.43 (s, 9H), 1.32-1.25 (m, 2H) ppm. <sup>13</sup>C NMR (101 MHz, CDCl<sub>3</sub>) δ 164.3, 154.7, 145.7, 134.2, 128.3, 118.5, 114.4, 114.3, 79.7, 71.6, 46.7, 28.5, 26.5, 26.2. IR (neat): 3300, 3173, 2951, 2863, 1687, 1632, 1610, 1581, 1483, 1317, 1239, 1162, 1067, 1029, 941, 865, 805, 756, 580, 527 cm<sup>-1</sup>. Mp: 191 °C. HRMS *calcd.* for (C<sub>19</sub>H<sub>27</sub>N<sub>3</sub>NaO<sub>3</sub>) [M+Na]<sup>+</sup>: 368.1950, *found* 368.1943.



**2-methyl-2-(1-tosylpiperidin-4-yl)-2,3-dihydroquinazolin-4(1H)-one (A2)** Following Method A, the utilization of 1-(1-tosylpiperidin-4-yl)ethan-1-one (0.92 g, 3.3 mmol) afforded the title compound as a white solid (0.96 g, 69% yield). <sup>1</sup>H NMR (400 MHz, CDCl<sub>3</sub>) δ 7.80 (dd, *J* = 7.8, 1.7 Hz, 1H), 7.63 – 7.57 (m, 2H), 7.33 – 7.28 (m, 2H), 7.26 (m, 2H), 6.78 (d, *J* = 6.8 Hz, 1H), 6.63 – 6.50 (m, 1H), 6.31 (s, 1H), 4.22 – 4.15 (m, 1H), 3.85 (d, *J* = 13.4 Hz, 2H), 2.41 (s, 3H), 2.23 – 2.06 (m, 2H), 1.95 – 1.85 (m, 1H), 1.78 (dd, *J* = 12.5, 2.9 Hz, 1H), 1.53-1.47 (m, 2H), 1.43 (s, 3H) ppm. <sup>13</sup>C NMR (126 MHz, DMF-d<sub>7</sub>) δ 164.1, 148.2, 144.7, 134.3, 134.0, 130.8, 128.8, 128.3,

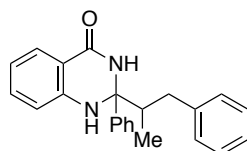


117.3, 115.2, 115.1, 72.1, 47.7, 47.6, 46.8, 26.9, 26.6, 25.5, 21.6 ppm. **IR (neat):** 3362, 3278, 2963, 2929, 2847, 2166, 1654, 1630, 1609, 1588, 1484, 1333, 1150, 937, 816, 761, 727, 711, 651, 591, 548  $\text{cm}^{-1}$ . **Mp:** 234 °C. **HRMS** *calcd.* for  $(\text{C}_{21}\text{H}_{25}\text{N}_3\text{NaO}_3\text{S})$   $[\text{M}+\text{Na}]^+$ : 422.1514, *found* 422.1510.



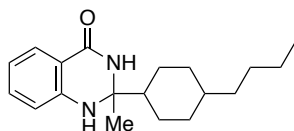
**2-(1-benzoylpiperidin-4-yl)-2-methyl-2,3-dihydroquinazolin-4(1H)-one (A3)**

Following Method A, the utilization of 1-(1-benzoylpiperidin-4-yl)ethan-1-one (331 mg, 1.43 mmol) afforded the title compound as a pale yellow solid after column chromatography (5% MeOH/EtOAc) (112 mg, 24% yield).  **$^1\text{H}$  NMR (300 MHz, DMF- $d_7$ )**  $\delta$  7.91 – 7.77 (m, 1H), 7.68 (dd,  $J = 7.7, 1.7$  Hz, 1H), 7.60 – 7.36 (m, 5H), 7.24 (m, 1H), 6.84 – 6.76 (m, 1H), 6.70 (s, 1H), 6.64 (ddd,  $J = 8.0, 7.2, 1.1$  Hz, 1H), 4.70 (br, 1H), 3.74 (br, 1H), 2.96 (br, 1H), 2.74 (br, 1H), 2.10 – 1.96 (m, 2H), 1.87 (s, 2H), 1.49 – 1.45 (m, 4H) ppm.  **$^{13}\text{C}$  NMR (75 MHz, DMF- $d_7$ )**  $\delta$  170.2, 164.2, 148.4, 138.0, 134.4, 130.4, 129.4, 128.3, 127.9, 117.3, 115.2, 115.1, 72.3, 47.8, 25.9 ppm. **IR (neat):** 3280, 2927, 1609, 1485, 1435, 1371, 1313, 1277, 1151, 1121, 1006, 752, 705  $\text{cm}^{-1}$ . **Mp:** 140 °C. **HRMS** *calcd.* for  $(\text{C}_{21}\text{H}_{23}\text{N}_3\text{NaO}_2)$   $[\text{M}+\text{Na}]^+$ : 372.1688, *found* 372.1684.

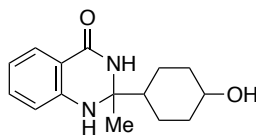


**2-phenyl-2-(1-phenylpropan-2-yl)-2,3-dihydroquinazolin-4(1H)-one (A4)**

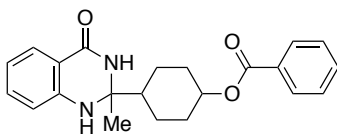
Following Method A, the utilization of 2-methyl-1,3-diphenylpropan-1-one (1.44 g, 6.4 mmol) afforded the title compound as a white solid (1.20 g, 55% yield).  **$^1\text{H}$  NMR (400 MHz,  $\text{CD}_2\text{Cl}_2$ )**  $\delta$  7.85 – 7.80 (m, 1H), 7.45-7.48 (m, 2H), 7.38 – 7.10 (m, 9H), 6.88 – 6.71 (m, 2H), 5.33 – 5.29 (s, 1H), 5.03 (s, 1H), 3.20 (dd,  $J = 34.5, 11.6$  Hz, 1H), 2.55 – 2.25 (m, 2H), 0.83 (dd,  $J = 9.5, 6.3$  Hz, 3H) ppm.  **$^{13}\text{C}$  NMR (101 MHz,  $\text{CD}_2\text{Cl}_2$ )**  $\delta$  146.8, 145.5/145.2, 141.2, 141.0, 134.4, 134.3, 129.6, 129.5, 128.89/128.84, 128.7, 128.6, 128.53/128.50, 128.1, 127.9, 126.4, 126.3, 126.1, 126.0, 119.06/119.00, 115.18/115.16, 46.3, 37.96/37.93, 13.59/13.50 ppm. **IR (neat):** 3302, 3023, 2180, 1721, 1649, 1610, 1483, 1447, 1373, 1251, 1149, 1030, 751, 697, 557  $\text{cm}^{-1}$ . **Mp:** 135 °C. **HRMS** *calcd.* for  $(\text{C}_{23}\text{H}_{22}\text{N}_2\text{NaO})$   $[\text{M}+\text{Na}]^+$ : 365.1630, *found* 365.1621.



**2-(4-butylcyclohexyl)-2-methyl-2,3-dihydroquinazolin-4(1H)-one (A5)** Following Method A, the utilization of 1-(4-butylcyclohexyl)ethan-1-one (0.38 g, 2.1 mmol) afforded the title compound as a white solid (0.38 g, 60% yield), as a mixture of two isomers (3:7 ratio). **<sup>1</sup>H NMR (400 MHz, CDCl<sub>3</sub>)** δ 7.85 (dd, *J* = 7.8, 1.9 Hz, 1H), 7.41 – 7.06 (m, 1H), 6.77 (td, *J* = 7.6, 1.2 Hz, 1H), 6.69 – 6.52 (m, 1H), 6.02 (s, 1H), 4.43 – 3.83 (m, 1H), 1.85 – 1.78 (m, 1H), 1.71 – 1.51 (m, 5H), 1.44 – 1.41 (m, 4H), 1.35 – 1.05 (m, 9H), 0.89 (t, *J* = 7.3 Hz, 3H) ppm. **<sup>13</sup>C NMR (101 MHz, CDCl<sub>3</sub>)** δ 164.1, 146.0, 134.0, 128.4, 118.4, 118.3, 114.3, 114.3, 72.3, 72.2, 48.2, 48.1, 37.5, 36.8, 32.9, 32.1, 30.5, 30.2, 29.9, 29.8, 29.2, 27.0, 26.8, 25.6, 25.5, 23.1, 23.0, 21.5, 21.3, 14.3, 14.2 ppm. **IR (neat):** 3312, 3183, 2919, 2867, 1631, 1609, 1570, 1506, 1484, 1449, 1399, 1328, 1275, 1150, 803, 754 cm<sup>-1</sup>. **Mp:** 175 °C. **HRMS** *calcd.* for (C<sub>19</sub>H<sub>28</sub>N<sub>2</sub>NaO) [M+Na]<sup>+</sup>: 323.2099, *found* 323.2098.

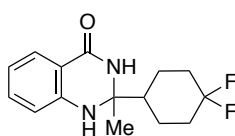


**2-(4-hydroxycyclohexyl)-2-methyl-2,3-dihydroquinazolin-4(1H)-one (A6)** Following Method A, the utilization of 1-(4-hydroxycyclohexyl)ethan-1-one (0.43g, 3.0 mmol) afforded the title compound as a white solid (0.26 g, 33% yield), as a mixture of two isomers (*cis* : *trans* = 1:1). **<sup>1</sup>H NMR (500 MHz, DMF-d<sub>7</sub>)** δ 7.72 (s, 1H), 7.66 (dd, *J* = 7.7, 1.7 Hz, 1H), 7.22 (m, 1H), 6.79 (dd, *J* = 8.3, 1.3 Hz, 1H), 6.70 – 6.49 (m, 2H), 4.25 (d, *J* = 3.1 Hz, 1H), 3.88 (q, *J* = 2.9 Hz, 1H), 1.91 – 1.55 (m, 7H), 1.44 (s, 3H), 1.42 – 1.22 (m, 2H) ppm. **<sup>13</sup>C NMR (126 MHz, DMF-d<sub>7</sub>)** δ 164.2, 148.6, 134.2, 128.3, 117.0, 115.4, 115.0, 72.8, 65.0, 49.1, 34.0, 33.9, 25.5, 21.8, 21.4 ppm. **IR (neat):** 3440, 3289, 2933, 2204, 1606, 1517, 1484, 1392, 1279, 1188, 1147, 898, 817, 749, 582 cm<sup>-1</sup>. **Mp:** 226 °C. **HRMS** *calcd.* for (C<sub>15</sub>H<sub>20</sub>N<sub>2</sub>NaO<sub>2</sub>) [M+Na]<sup>+</sup>: 283.1422, *found* 283.1418.



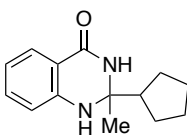
**4-(2-methyl-4-oxo-1,2,3,4-tetrahydroquinazolin-2-yl)cyclohexyl benzoate (A7)** Following Method A, the utilization of 4-acetylcyclohexyl benzoate (1.46 g, 5.9 mmol)

afforded the title compound as a white solid (1.20 g, 56% yield), as a mixture of two isomers (*cis* : *trans* = 1:1). **<sup>1</sup>H NMR (400 MHz, CDCl<sub>3</sub>)** δ 8.14 – 7.97 (m, 2H), 7.89 (dd, *J* = 7.8, 1.7 Hz, 1H), 7.68 – 7.55 (m, 1H), 7.52 – 7.42 (m, 2H), 7.38 – 7.13 (m, 1H), 6.86 – 6.76 (m, 1H), 6.63 (dd, *J* = 8.1, 1.1 Hz, 1H), 6.43 (s, 1H), 5.29 (s, 1H), 4.46 – 4.07 (m, 1H), 2.28 – 2.08 (m, 2H), 1.97 – 1.75 (m, 3H), 1.68 – 1.39 (m, 7H) ppm. **<sup>13</sup>C NMR (101 MHz, CDCl<sub>3</sub>)** δ 165.7, 164.0, 145.7, 134.0, 132.9, 130.7, 129.4, 128.4, 128.3, 118.4, 114.5, 114.2, 71.9, 69.1, 47.0, 29.9, 21.6, 21.3 ppm. **IR (neat):** 3292, 3173, 2941, 1714, 1640, 1614, 1525, 1488, 1449, 1398, 1229, 1312, 1272, 1173, 1106, 1069, 923, 752, 707 cm<sup>-1</sup>. **Mp:** 182 °C. **HRMS *calcd.*** for (C<sub>22</sub>H<sub>24</sub>N<sub>2</sub>NaO<sub>3</sub>) [M+Na]<sup>+</sup>: 387.1685, *found* 387.1679.



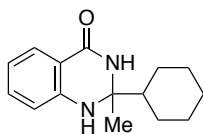
**2-(4,4-difluorocyclohexyl)-2-methyl-2,3-dihydroquinazolin-4(1H)-one (A8)**

Following Method A, the utilization of 1-(4,4-difluorocyclohexyl)ethan-1-one (1.00 g, 9.8 mmol) afforded the title compound as a white solid (1.79 g, 74% yield). **<sup>19</sup>F NMR (376 MHz, DMF-*d*<sub>7</sub>)** δ -91.60 (d, *J* = 232.3 Hz), -102.62 (m) ppm. **<sup>1</sup>H NMR (500 MHz, DMF-*d*<sub>7</sub>)** δ 7.32 – 6.95 (m, 2H), 6.67 (m, 1H), 6.21 (dd, *J* = 8.2, 1.4 Hz, 1H), 6.19 – 6.15 (m, 1H), 6.07 (m, 1H), 1.52 – 1.26 (m, 7H), 0.91 (s, 5H) ppm. **<sup>13</sup>C NMR (126 MHz, DMF-*d*<sub>7</sub>)** δ 164.1, 148.3, 134.3, 128.3, 117.3, 115.1, 115.0, 72.2 (d, *J* = 2.8 Hz), 47.4, 34.5 (d, *J* = 9.2 Hz), 34.2 (d, *J* = 9.2 Hz), 34.07 (d, *J* = 8.7 Hz), 25.9, 24.5 (d, *J* = 10.1 Hz), 24.1 (d, *J* = 10.1 Hz) ppm. **IR (neat):** 3313, 3170, 2967, 1532, 1608, 1579, 1505, 1483, 1449, 1379, 1360, 1324, 1268, 1197, 1152, 1126, 1106, 1028, 966, 931, 803, 754, 582, 491 cm<sup>-1</sup>. **Mp:** 215 °C. **HRMS *calcd.*** for (C<sub>15</sub>H<sub>18</sub>F<sub>2</sub>N<sub>2</sub>NaO) [M+Na]<sup>+</sup>: 303.1285, *found* 303.1288.

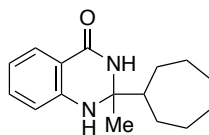


**2-cyclopentyl-2-methyl-2,3-dihydroquinazolin-4(1H)-one (A9)** Following Method A, the utilization of 1-cyclopentylethan-1-one (0.50 g, 4.5 mmol) afforded the title compound as a white solid (0.80 g, 78% yield). **<sup>1</sup>H NMR (400 MHz, CDCl<sub>3</sub>)** δ 7.85 (dd, *J* = 7.8, 1.8 Hz, 1H), 7.42 – 7.21 (m, 1H), 6.78 (t, *J* = 7.5, 1.1 Hz, 1H), 6.58 (dd, *J* = 8.1, 1.1 Hz, 1H), 6.03 (s, 1H), 4.11 (s, 1H), 2.50 – 2.20 (m, 1H), 1.90 – 1.30 (m, 11H) ppm. **<sup>13</sup>C NMR (101 MHz, CDCl<sub>3</sub>)** δ 164.2, 146.1, 134.0, 128.4, 118.4, 114.5, 114.3,

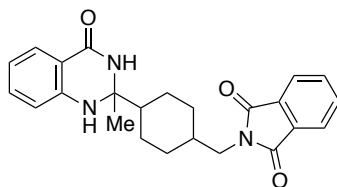
71.9, 50.8, 27.3, 27.2, 26.7, 26.0, 25.8 ppm. **IR (neat):** 3308, 3108, 2952, 2867, 1632, 1608, 1579, 1502, 1483, 1453, 1420, 1326, 1272, 1150, 801, 755  $\text{cm}^{-1}$ . **Mp:** 185 °C. **HRMS calcd.** for  $(\text{C}_{14}\text{H}_{18}\text{N}_2\text{NaO})$   $[\text{M}+\text{Na}]^+$ : 253.1317, *found* 253.1310.



**2-cyclohexyl-2-methyl-2,3-dihydroquinazolin-4(1H)-one (A10)** Following Method A, the utilization of 1-cyclohexylethan-1-one (0.63 g, 5.0 mmol) afforded the title compound as a white solid (0.83 g, 68% yield).  **$^1\text{H}$  NMR (400 MHz,  $\text{CDCl}_3$ )**  $\delta$  7.85 (d,  $J = 6.1$  Hz, 1H), 7.36 – 7.16 (m, 1H), 6.78 (t,  $J = 7.0$  Hz, 1H), 6.57 (d,  $J = 7.5$  Hz, 1H), 5.85 (s, 1H), 4.15 (s, 1H), 2.02 – 1.64 (m, 6H), 1.44 (s, 3H), 1.28 – 0.99 (m, 5H) ppm.  **$^{13}\text{C}$  NMR (126 MHz,  $\text{CDCl}_3$ )**  $\delta$  164.0, 145.9, 134.1, 128.4, 118.4, 114.4, 114.3, 72.2, 48.0, 31.0, 27.2, 27.0, 26.3, 26.2, 25.4 ppm. **IR (neat):** 3329, 3175, 2929, 2851, 1631, 1606, 1577, 1504, 1482, 1447, 1397, 1328, 1273, 1149, 1132, 1026, 802, 750, 572  $\text{cm}^{-1}$ . **Mp:** 210 °C. **HRMS calcd.** for  $(\text{C}_{15}\text{H}_{20}\text{N}_2\text{NaO})$   $[\text{M}+\text{Na}]^+$ : 267.1473, *found* 267.1469.

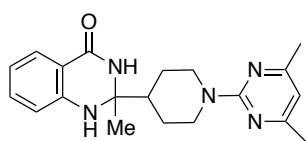


**2-cycloheptyl-2-methyl-2,3-dihydroquinazolin-4(1H)-one (A11)** Following Method A, the utilization of 1-cycloheptylethan-1-one (1.50 g, 10.7 mmol) afforded the title compound as a white solid (1.60 g, 54% yield).  **$^1\text{H}$  NMR (400 MHz,  $\text{CDCl}_3$ )**  $\delta$  7.85 (dd,  $J = 7.8, 1.7$  Hz, 1H), 7.42 – 7.17 (m, 1H), 6.80–6.78 (m, 1H), 6.58 (dd,  $J = 8.1, 1.1$  Hz, 1H), 6.23 (s, 1H), 4.25 (s, 1H), 2.15 – 1.64 (m, 5H), 1.64 – 1.07 (m, 11H) ppm.  **$^{13}\text{C}$  NMR (101 MHz,  $\text{CDCl}_3$ )**  $\delta$  164.1, 145.9, 134.0, 128.4, 118.4, 114.7, 114.4, 73.0, 48.7, 28.8, 28.3, 28.1, 28.0, 27.4, 27.2, 24.8 ppm. **IR (neat):** 3310, 3180, 2917, 2851, 1631, 1609, 1518, 1484, 1455, 1397, 1279, 1150, 800, 750  $\text{cm}^{-1}$ . **Mp:** 192 °C. **HRMS calcd.** for  $(\text{C}_{16}\text{H}_{22}\text{N}_2\text{NaO})$   $[\text{M}+\text{Na}]^+$ : 281.1630, *found* 281.1625.

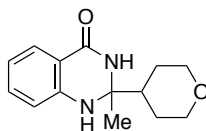


**2-((4-(2-methyl-4-oxo-1,2,3,4-tetrahydroquinazolin-2-yl)cyclohexyl)methyl)isoindoline-1,3-dione (A12)** Following Method A, the utilization of 2-((4-acetylcyclohexyl)methyl)isoindoline-1,3-dione (0.90 g, 3.1 mmol)

afforded the title compound as a white solid (0.80 g, 65% yield) as a mixture of two isomers (*cis* : *trans* = 1:1.8). <sup>1</sup>H NMR (400 MHz, CD<sub>2</sub>Cl<sub>2</sub>) δ 7.88 – 7.65 (m, 5H), 7.36 – 7.16 (m, 1H), 7.00 – 6.86 (m, 1H), 6.81 – 6.49 (m, 2H), 4.50 (br, 1H), 3.80 – 3.39 (m, 2H), 2.26 – 1.27 (m, 11H), 1.21 – 0.86 (m, 2H) ppm. <sup>13</sup>C NMR (101 MHz, CD<sub>2</sub>Cl<sub>2</sub>) δ 168.4, 163.9, 163.8, 146.2, 146.1, 133.9, 133.8, 133.7, 133.7, 132.1, 132.0, 127.9, 127.8, 122.9, 122.9, 117.8, 117.7, 114.4, 114.3, 114.2, 114.1, 71.9, 71.8, 47.7, 47.6, 43.6, 39.2, 36.9, 31.3, 30.3, 30.2, 27.5, 27.4, 26.1, 25.9, 25.0, 24.8, 21.4, 21.0 ppm. IR (neat): 3369, 2931, 1770, 1702, 1658, 1610, 1511, 1485, 1395, 1243, 1151, 1068, 945, 755, 721, 530 cm<sup>-1</sup>. Mp: 150 °C. HRMS *calcd.* for (C<sub>24</sub>H<sub>25</sub>N<sub>3</sub>NaO<sub>3</sub>) [M+Na]<sup>+</sup>: 426.1794, *found* 426.1785.

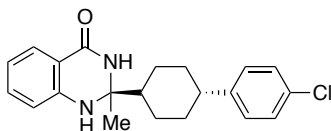


**2-(1-(4,6-dimethylpyrimidin-2-yl)piperidin-4-yl)-2-methyl-2,3-dihydroquinazolin-4(1H)-one (A13)** Following Method A, the utilization of 1-(1-(4,6-dimethylpyrimidin-2-yl)piperidin-4-yl)ethan-1-one (576 mg, 2.47 mmol) afforded the title compound as a white solid (320 mg, 39% yield). <sup>1</sup>H NMR (300 MHz, DMF-d<sub>7</sub>) δ 7.83 – 7.78 (m, 1H), 7.67 (dd, *J* = 7.7, 1.7 Hz, 1H), 7.27 – 7.16 (m, 1H), 6.77 (dd, *J* = 8.2, 1.1 Hz, 1H), 6.73 – 6.57 (m, 2H), 6.36 (s, 1H), 5.11 – 4.87 (m, 2H), 2.77 – 2.50 (m, 2H), 2.23 (s, 6H), 2.09 – 1.82 (m, 3H), 1.51 – 1.32 (m, 5H) ppm. <sup>13</sup>C NMR (126 MHz, DMF-d<sub>7</sub>) δ 168.0, 164.2, 162.4, 148.5, 134.3, 128.3, 117.2, 115.2, 114.9, 109.1, 72.4, 48.7, 44.6, 44.6, 27.4, 27.1, 26.1, 24.4 ppm. IR (neat): 3319, 2990, 2925, 2848, 1642, 1659, 1519, 1476, 1371, 1336, 1309, 1259, 1145, 1109, 754, 697, 574 cm<sup>-1</sup>. Mp: 250 °C. HRMS *calcd.* for (C<sub>20</sub>H<sub>26</sub>N<sub>5</sub>O) [M+H]<sup>+</sup>: 352.2137, *found* 352.2133.

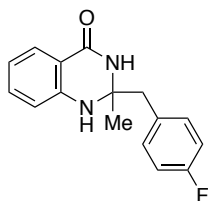


**2-methyl-2-(tetrahydro-2H-pyran-4-yl)-2,3-dihydroquinazolin-4(1H)-one (A14)** Following Method A, the utilization of 1-(tetrahydro-2H-pyran-4-yl)ethan-1-one (1.28 g, 10.0 mmol) afforded the title compound as a white solid (1.24 g, 50% yield). <sup>1</sup>H NMR (400 MHz, CDCl<sub>3</sub>) δ 7.85 (dd, *J* = 7.7, 1.7 Hz, 1H), 7.44 – 7.21 (m, 1H), 6.79 (m, 1H), 6.70 – 6.43 (m, 2H), 4.20 (s, 1H), 4.05-3.99 (m, 2H), 3.35-3.26 (m, 2H), 2.01 – 1.83 (m, 1H), 1.76 – 1.67 (m, 1H), 1.67 – 1.60 (m, 1H), 1.58 – 1.45 (m, 5H) ppm. <sup>13</sup>C NMR (101 MHz, CDCl<sub>3</sub>) δ 164.2, 145.7, 134.2, 128.4, 118.6, 114.5, 114.3, 71.6, 67.8,

67.8, 45.6, 27.1, 27.0, 25.2 ppm. **IR (neat):** 3333, 3173, 2968, 2839, 2204, 1632, 1606, 1578, 1504, 1482, 1390, 1326, 1271, 1174, 1149, 1113, 1095, 1070, 852, 803, 753, 580  $\text{cm}^{-1}$ . **Mp:** 202 °C. **HRMS calcd.** for  $(\text{C}_{14}\text{H}_{18}\text{N}_2\text{NaO}_2)$   $[\text{M}+\text{Na}]^+$ : 269.1266, *found* 269.1259.

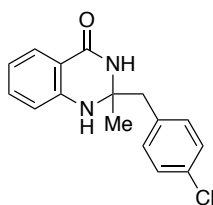


**(S)-2-((1S,4R)-4-(4-chlorophenyl)cyclohexyl)-2-methyl-2,3-dihydroquinazolin-4(1H)-one (A15)** Following Method A, the utilization of 1-((1S,4S)-4-(4-chlorophenyl)cyclohexyl)ethan-1-one (1.40 g, 5.9 mmol) afforded the title compound as a white solid (1.29 g, 62% yield).  **$^1\text{H}$  NMR (400 MHz,  $\text{CDCl}_3$ )**  $\delta$  7.87 (dd,  $J = 7.8, 1.7$  Hz, 1H), 7.41 – 7.19 (m, 3H), 7.17 – 7.02 (m, 2H), 6.80 (t,  $J = 7.5$ , 1H), 6.60 (dd,  $J = 8.1, 1.1$  Hz, 1H), 6.14 (s, 1H), 4.35 – 3.99 (m, 1H), 2.55 – 2.36 (m, 1H), 2.06 (d,  $J = 12.7$  Hz, 1H), 1.97 (d,  $J = 4.2$  Hz, 3H), 1.88 – 1.69 (m, 1H), 1.50 (s, 3H), 1.46 – 1.21 (m, 4H) ppm.  **$^{13}\text{C}$  NMR (101 MHz,  $\text{CDCl}_3$ )**  $\delta$  164.1, 145.9, 145.2, 134.2, 131.8, 128.6, 128.4, 128.2, 118.5, 114.5, 114.3, 72.1, 47.6, 43.6, 33.8, 33.8, 27.2, 27.0, 25.6 ppm. **IR (neat):** 3332, 3194, 2919, 1652, 1633, 1606, 1520, 1488, 1453, 1399, 1339, 1279, 1146, 1090, 1009, 820, 753, 530  $\text{cm}^{-1}$ . **Mp:** 205 °C. **HRMS calcd.** for  $(\text{C}_{21}\text{H}_{23}\text{ClN}_2\text{NaO})$   $[\text{M}+\text{Na}]^+$ : 377.1397, *found* 377.1395.

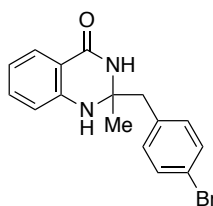


**2-(4-fluorobenzyl)-2-methyl-2,3-dihydroquinazolin-4(1H)-one (A16)** Following Method A, the utilization of 1-(4-fluorophenyl)propan-2-one (0.76 g, 5.0 mmol) afforded the title compound as a white solid (1.00 g, 74% yield).  **$^{19}\text{F}$  NMR (376 MHz,  $\text{CDCl}_3$ )**  $\delta$  -115.34 (m).  **$^1\text{H}$  NMR (400 MHz,  $\text{CDCl}_3$ )**  $\delta$  7.91 (d,  $J = 7.7$  Hz, 1H), 7.39 – 7.32 (m, 1H), 7.16 – 7.06 (m, 2H), 7.01 (t,  $J = 8.7$  Hz, 2H), 6.86 (t,  $J = 7.5$  Hz, 1H), 6.63 (d,  $J = 8.6$  Hz, 1H), 6.29 (s, 1H), 4.20 (s, 1H), 3.14 (d,  $J = 13.3$  Hz, 1H), 2.95 (d,  $J = 13.3$  Hz, 1H), 1.45 (s, 3H) ppm.  **$^{13}\text{C}$  NMR (126 MHz,  $\text{DMF-d}_7$ )**  $\delta$  164.4, 162.72 (d,  $J = 241.8$  Hz), 148.3, 134.3, 134.1 (d,  $J = 3.2$  Hz), 133.7 (d,  $J = 7.8$  Hz), 128.3, 117.5, 115.5, 115.4, 115.3 (d,  $J = 12.4$  Hz), 70.8, 47.1, 28.3 ppm. **IR (neat):** 3319, 3189, 2974, 1626, 1509, 1485, 1418, 1387, 1335, 1276, 1221, 1175, 1156, 1100, 827, 801, 760, 582, 464  $\text{cm}^{-1}$ . **Mp:** 178 °C. **HRMS calcd.** for  $(\text{C}_{16}\text{H}_{15}\text{FN}_2\text{NaO})$   $[\text{M}+\text{Na}]^+$ : 293.1066, *found*

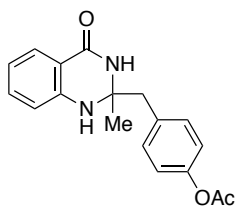
293.1061.



**2-(4-chlorobenzyl)-2-methyl-2,3-dihydroquinazolin-4(1H)-one (A17)** Following Method A, the utilization of 1-(4-chlorophenyl)propan-2-one (0.84 g, 5.0 mmol) afforded the title compound as a white solid (0.93 g, 65% yield). **<sup>1</sup>H NMR (400 MHz, CDCl<sub>3</sub>)** δ 7.90 (dd, *J* = 7.8, 1.6 Hz, 1H), 7.37-7.32 (m, 1H), 7.31 – 7.25 (m, 3H), 7.12 – 6.99 (m, 2H), 6.85 (m, 1H), 6.69 – 6.58 (m, 1H), 4.31 (s, 1H), 3.17 (d, *J* = 13.3 Hz, 1H), 2.94 (d, *J* = 13.3 Hz, 1H), 1.47 (s, 3H) ppm. **<sup>13</sup>C NMR (101 MHz, CDCl<sub>3</sub>)** δ 164.6, 145.6, 134.3, 134.2, 133.2, 131.8, 128.7, 128.5, 119.0, 115.1, 114.7, 69.5, 46.6, 26.9 ppm. **IR (neat):** 3302, 3177, 2971, 1600, 1484, 1428, 1384, 1333, 1273, 1155, 1085, 1017, 840, 801, 759, 681, 463 cm<sup>-1</sup>. **Mp:** 157 °C. **HRMS calcd.** for (C<sub>16</sub>H<sub>15</sub>ClN<sub>2</sub>NaO) [M+Na]<sup>+</sup>: 309.0771, *found* 309.0768.

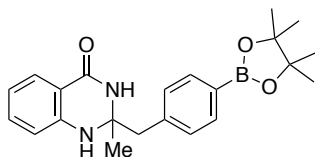


**2-(4-bromobenzyl)-2-methyl-2,3-dihydroquinazolin-4(1H)-one (A18)** Following Method A, the utilization of 1-(4-bromophenyl)propan-2-one (1.06 g, 5.0 mmol) afforded the title compound as a white solid (1.25 g, 76% yield). **<sup>1</sup>H NMR (400 MHz, CD<sub>2</sub>Cl<sub>2</sub>)** δ 7.82 (dd, *J* = 7.8, 1.6 Hz, 1H), 7.52 – 7.41 (m, 2H), 7.35-7.33 (m, 1H), 7.15 – 7.00 (m, 2H), 6.91 – 6.81 (m, 1H), 6.65 (d, *J* = 8.3 Hz, 1H), 6.17 (s, 1H), 4.32 (s, 1H), 3.10 (d, *J* = 13.2 Hz, 1H), 2.94 (d, *J* = 13.2 Hz, 1H), 1.43 (s, 3H) ppm. **<sup>13</sup>C NMR (101 MHz, CD<sub>2</sub>Cl<sub>2</sub>)** δ 164.0, 146.0, 135.2, 134.5, 132.6, 131.9, 128.5, 121.4, 119.1, 115.3, 115.1, 69.8, 47.0, 27.1 ppm. **IR (neat):** 3260, 3171, 3043, 2919, 1651, 1613, 1520, 1484, 1434, 1407, 1383, 1298, 1153, 1094, 1069, 1031, 1009, 859, 761, 724, 662, 607, 522, 478 cm<sup>-1</sup>. **Mp:** 85 °C. **HRMS calcd.** for (C<sub>16</sub>H<sub>16</sub>BrN<sub>2</sub>O) [M+H]<sup>+</sup>: 331.0446, *found* 331.0441.



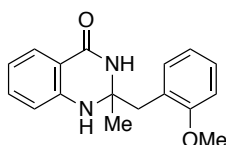
**4-((2-methyl-4-oxo-1,2,3,4-tetrahydroquinazolin-2-yl)methyl)phenyl acetate (A19)**

Following Method A, the utilization of 4-(2-oxopropyl)phenyl acetate (0.96 g, 5.0 mmol) afforded the title compound as a white solid (0.90 g, 58% yield). **<sup>1</sup>H NMR (400 MHz, CDCl<sub>3</sub>)** δ 7.92 (dd, *J* = 7.8, 1.8 Hz, 1H), 7.34 (m, 1H), 7.14 (s, 2H), 7.04 (d, *J* = 8.6 Hz, 2H), 6.85 (t, *J* = 7.0 Hz, 1H), 6.67 – 6.54 (m, 2H), 4.28 (s, 1H), 3.19 (d, *J* = 13.3 Hz, 1H), 2.94 (d, *J* = 13.2 Hz, 1H), 2.30 (s, 3H), 1.46 (s, 3H) ppm. **<sup>13</sup>C NMR (101 MHz, CDCl<sub>3</sub>)** δ 169.6, 164.4, 149.9, 145.7, 134.4, 133.2, 131.5, 128.6, 121.8, 119.0, 115.0, 114.8, 69.6, 46.7, 26.9, 21.2 ppm. **IR (neat):** 3281, 3178, 3052, 2923, 1751, 1649, 1611, 1505, 1484, 1420, 1368, 1274, 1192, 1151, 1017, 914, 859, 749, 663, 575 cm<sup>-1</sup>. **Mp:** 45 °C. **HRMS calcd.** for (C<sub>18</sub>H<sub>18</sub>N<sub>2</sub>NaO<sub>3</sub>) [M+Na]<sup>+</sup>: 333.1215, *found* 333.1210.



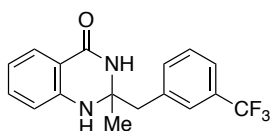
**2-methyl-2-(4-(4,4,5,5-tetramethyl-1,3,2-dioxaborolan-2-yl)benzyl)-2,3-**

**dihydroquinazolin-4(1H)-one (A20)** Following Method A, the utilization of 1-(4-(4,4,5,5-tetramethyl-1,3,2-dioxaborolan-2-yl)phenyl)propan-2-one (1.40 g, 5.4 mmol) afforded the title compound as a white solid (0.92 g, 45% yield). **<sup>1</sup>H NMR (500 MHz, DMF-d<sub>7</sub>)** δ 7.86 (s, 1H), 7.69 (dd, *J* = 7.7, 1.6 Hz, 1H), 7.65 – 7.59 (m, 2H), 7.35 – 7.22 (m, 3H), 6.84 – 6.77 (m, 2H), 6.67 (ddd, *J* = 8.0, 7.2, 1.1 Hz, 1H), 3.12 (d, *J* = 13.0 Hz, 1H), 3.04 (d, *J* = 13.0 Hz, 1H), 1.49 (s, 3H), 1.33 (s, 12H) ppm. **<sup>13</sup>C NMR (126 MHz, DMF-d<sub>7</sub>)** δ 163.3, 147.2, 140.4, 134.1, 133.3, 130.4, 127.4, 116.6, 114.5, 114.4, 83.7, 69.7, 46.9, 26.9, 24.6, 24.4, 24.2 ppm. **IR (neat):** 3345, 3184, 2978, 1637, 1611, 1516, 1487, 1388, 1354, 1323, 1272, 1141, 1086, 1023, 961, 858, 826, 799, 759, 666, 582 cm<sup>-1</sup>. **Mp:** 170 °C. **HRMS calcd.** for (C<sub>22</sub>H<sub>27</sub>BN<sub>2</sub>NaO<sub>3</sub>) [M+Na]<sup>+</sup>: 401.2012, *found* 401.2011.

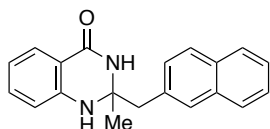




**2-(2-methoxybenzyl)-2-methyl-2,3-dihydroquinazolin-4(1H)-one (A21)** Following Method A, the utilization of 1-(2-methoxyphenyl)propan-2-one (0.86 g, 5.2 mmol) afforded the title compound as a white solid (1.12 g, 80% yield).  $^1\text{H NMR}$  (500 MHz,  $\text{DMF-d}_7$ )  $\delta$  7.86 (d,  $J = 7.8$  Hz, 1H), 7.24 (s, 1H), 7.11 (dd,  $J = 7.4, 1.7$  Hz, 2H), 6.96 (dd,  $J = 8.2, 1.1$  Hz, 1H), 6.85 (m, 1H), 6.79 (dd,  $J = 8.1, 1.1$  Hz, 2H), 6.70 – 6.56 (m, 2H), 3.79 (s, 3H), 3.20 – 3.02 (m, 2H), 1.47 (s, 3H) ppm.  $^{13}\text{C NMR}$  (126 MHz,  $\text{DMF-d}_7$ )  $\delta$  164.4, 159.3, 148.5, 134.1, 133.4, 128.9, 128.2, 125.9, 120.9, 117.4, 115.8, 115.6, 111.6, 71.3, 56.0, 41.4, 27.9 ppm. **IR** (neat): 3394, 3172, 3043, 2972, 1660, 1613, 1484, 1460, 1417, 1388, 1325, 1289, 1270, 1248, 1155, 1129, 1079, 1026, 816, 769, 752, 578, 518  $\text{cm}^{-1}$ . **Mp**: 158 °C. **HRMS** *calcd.* for  $(\text{C}_{17}\text{H}_{18}\text{N}_2\text{NaO}_2)$   $[\text{M}+\text{Na}]^+$ : 305.1266, *found* 305.1263.

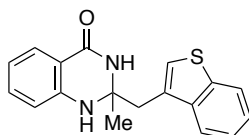


**2-methyl-2-(3-(trifluoromethyl)benzyl)-2,3-dihydroquinazolin-4(1H)-one (A22)** Following Method A, the utilization of 1-(3-(trifluoromethyl)phenyl)propan-2-one (0.81 g, 4.8 mmol) afforded the title compound as a white solid (1.10 g, 72% yield).  $^{19}\text{F NMR}$  (376 MHz,  $\text{CDCl}_3$ )  $\delta$  -62.73 ppm.  $^1\text{H NMR}$  (400 MHz,  $\text{CDCl}_3$ )  $\delta$  7.89 (dd,  $J = 7.8, 1.7$  Hz, 1H), 7.57 – 7.30 (m, 6H), 6.90 – 6.78 (m, 1H), 6.62 (dd,  $J = 8.1, 1.5$  Hz, 1H), 4.37 – 4.09 (m, 1H), 3.29 (d,  $J = 13.2$  Hz, 1H), 2.99 (d,  $J = 13.2$  Hz, 1H), 1.50 (s, 3H) ppm.  $^{13}\text{C NMR}$  (101 MHz,  $\text{CDCl}_3$ )  $\delta$  164.7, 145.5, 136.8, 134.5, 133.9, 130.9 (q,  $J = 31.8$  Hz), 129.0, 128.5, 127.2 (q,  $J = 4.0$  Hz), 124.1 (q,  $J = 272.2$  Hz), 124.0 (q,  $J = 4.0$  Hz), 119.1, 115.1, 114.7, 69.4, 47.1, 27.0 ppm. **IR** (neat): 3255, 3177, 3039, 1613, 1524, 1488, 1452, 1437, 1387, 1330, 1278, 1205, 1116, 1073, 926, 854, 797, 749, 705, 531, 475  $\text{cm}^{-1}$ . **Mp**: 123 °C. **HRMS** *calcd.* for  $(\text{C}_{17}\text{H}_{15}\text{F}_3\text{N}_2\text{NaO})$   $[\text{M}+\text{Na}]^+$ : 343.1034, *found* 343.1029.



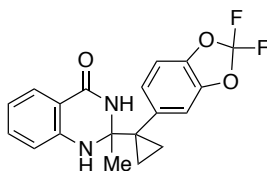
**2-methyl-2-(naphthalen-2-ylmethyl)-2,3-dihydroquinazolin-4(1H)-one (A23)** Following Method A, the utilization of 1-(naphthalen-2-yl)propan-2-one (0.55 g, 3.0 mmol) afforded the title compound as a white solid (0.76 g, 84% yield).  $^1\text{H NMR}$  (400 MHz,  $\text{CDCl}_3$ )  $\delta$  7.95 (dd,  $J = 7.7, 1.7$  Hz, 1H), 7.86 – 7.76 (m, 3H), 7.61 – 7.57 (m, 1H), 7.52 – 7.45 (m, 2H), 7.38 (m, 1H), 7.28 (d,  $J = 1.8$  Hz, 1H), 6.88 (m, 1.1 Hz, 1H),

6.80 (s, 1H), 6.65 (dd,  $J = 8.1, 1.2$  Hz, 1H), 4.43 – 4.15 (s, 1H), 3.38 (d,  $J = 13.1$  Hz, 1H), 3.11 (d,  $J = 13.2$  Hz, 1H), 1.50 (s, 3H) ppm.  $^{13}\text{C}$  NMR (101 MHz,  $\text{CDCl}_3$ )  $\delta$  164.4, 145.8, 134.3, 133.4, 133.2, 132.5, 129.3, 128.6, 128.2, 127.7, 126.4, 126.1, 119.0, 115.2, 114.8, 69.8, 47.42, 27.0 ppm. IR (neat): 3291, 3173, 3052, 1629, 1508, 1484, 1392, 1327, 1261, 1159, 1086, 815, 760, 670, 579, 473  $\text{cm}^{-1}$ . Mp: 132 °C. HRMS calcd. for  $(\text{C}_{20}\text{H}_{18}\text{N}_2\text{NaO})$   $[\text{M}+\text{Na}]^+$ : 325.1317, found 325.1311.



**2-(benzo[*b*]thiophen-3-ylmethyl)-2-methyl-2,3-dihydroquinazolin-4(1*H*)-one (A24)**

Following Method A, the utilization of 1-(benzo[*b*]thiophen-3-yl)propan-2-one (0.88 g, 4.6 mmol) afforded the title compound as a white solid (1.00 g, 77% yield).  $^1\text{H}$  NMR (500 MHz,  $\text{DMF-d}_7$ )  $\delta$  7.99 – 7.96 (m, 1H), 7.91 (s, 1H), 7.90 – 7.84 (m, 1H), 7.68 (dd,  $J = 7.7, 1.6$  Hz, 1H), 7.46 (s, 1H), 7.43 – 7.34 (m, 2H), 7.23 (m, 1H), 6.83 (d,  $J = 1.7$  Hz, 1H), 6.72 (dd,  $J = 8.1, 1.0$  Hz, 1H), 6.65 (m, 1H), 3.43 – 3.31 (m, 2H), 1.56 (s, 3H) ppm.  $^{13}\text{C}$  NMR (126 MHz,  $\text{DMF-d}_7$ )  $\delta$  163.3, 147.1, 140.0, 139.9, 133.2, 131.6, 127.2, 125.7, 124.0, 123.9, 122.6, 122.4, 116.5, 114.4, 70.1, 39.3, 27.5 ppm. IR (neat): 3287, 3171, 2991, 1609, 1523, 1481, 1422, 1383, 1335, 1275, 1148, 748, 732  $\text{cm}^{-1}$ . Mp: 177 °C. HRMS calcd. for  $(\text{C}_{18}\text{H}_{17}\text{N}_2\text{OS})$   $[\text{M}+\text{H}]^+$ : 309.1062, found 309.1056.

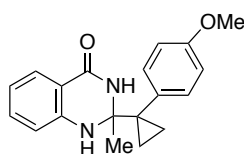


**2-(1-(2,2-difluorobenzo[*d*][1,3]dioxol-5-yl)cyclopropyl)-2-methyl-2,3-**

**dihydroquinazolin-4(1*H*)-one (A25)**

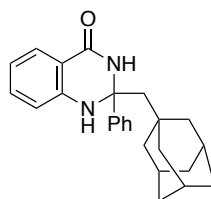
Following Method A, the utilization of 1-(1-(2,2-difluorobenzo[*d*][1,3]dioxol-5-yl)cyclopropyl)ethan-1-one (1.09 g, 4.5 mmol) afforded the title compound as a white solid (0.68 g, 42% yield).  $^{19}\text{F}$  NMR (376 MHz,  $\text{CDCl}_3$ )  $\delta$  -50.06 (s) ppm.  $^1\text{H}$  NMR (400 MHz,  $\text{CDCl}_3$ )  $\delta$  7.84 (dd,  $J = 7.7, 1.7$  Hz, 1H), 7.33 (m, 1H), 7.18 – 7.04 (m, 2H), 6.98 (d,  $J = 8.1$  Hz, 1H), 6.87 – 6.69 (m, 2H), 6.54 (dd,  $J = 8.1, 1.1$  Hz, 1H), 4.15 (s, 1H), 1.55 (s, 3H), 1.17 – 1.07 (m, 1H), 1.02 – 0.91 (m, 1H), 0.72-0.71 (m, 2H) ppm.  $^{13}\text{C}$  NMR (126 MHz,  $\text{CDCl}_3$ )  $\delta$  164.5, 145.7, 143.5, 143.0, 137.9, 134.4, 131.7 (t,  $J = 255.5$  Hz), 128.3, 127.4, 118.7, 114.9, 114.0, 113.2, 109.1, 70.5, 35.9, 27.9, 11.3, 8.2 ppm. IR (neat): 3286, 3184, 1634, 1532, 1490, 1434, 1388, 1344, 1237, 1152, 1127, 1069, 1030, 914, 796, 776, 750, 704, 633  $\text{cm}^{-1}$ . Mp: 168 °C.

**HRMS** *calcd.* for (C<sub>19</sub>H<sub>17</sub>F<sub>2</sub>N<sub>2</sub>O<sub>3</sub>) [M+H]<sup>+</sup>: 359.1207, *found* 359.1204.



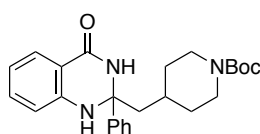
**2-(1-(4-methoxyphenyl)cyclopropyl)-2-methyl-2,3-dihydroquinazolin-4(1H)-one**

**(A26)** Following Method A, the utilization of 1-(1-(4-methoxyphenyl)cyclopropyl)ethan-1-one (0.75 g, 3.9 mmol) afforded the title compound as a white solid (0.61 g, 51% yield). **<sup>1</sup>H NMR (400 MHz, CDCl<sub>3</sub>)** δ 7.85 (dd, *J* = 7.7, 1.7 Hz, 1H), 7.38 – 7.24 (m, 3H), 6.92 – 6.75 (m, 3H), 6.63 – 6.50 (m, 1H), 6.33 (s, 1H), 4.17 (s, 1H), 3.80 (s, 3H), 1.53 (s, 3H), 1.07 – 1.04 (m, 1H), 0.89 – 0.82 (m, 1H), 0.73 – 0.67 (m, 2H) ppm. **<sup>13</sup>C NMR (101 MHz, CDCl<sub>3</sub>)** δ 164.5, 158.9, 146.1, 134.3, 133.5, 133.1, 128.3, 118.4, 114.9, 114.1, 113.8, 70.7, 55.4, 35.0, 28.2, 10.8, 7.7 ppm. **IR (neat):** 3267, 3002, 1610, 1511, 1488, 1538, 1379, 1289, 1247, 1174, 1152, 1134, 1085, 1023, 834, 789, 763, 740, 607, 552 cm<sup>-1</sup>. **Mp:** 158 °C. **HRMS** *calcd.* for (C<sub>19</sub>H<sub>20</sub>N<sub>2</sub>NaO<sub>2</sub>) [M+Na]<sup>+</sup>: 331.1422, *found* 331.1427.



**2-(((1S,3S)-adamantan-1-yl)methyl)-2-phenyl-2,3-dihydroquinazolin-4(1H)-one**

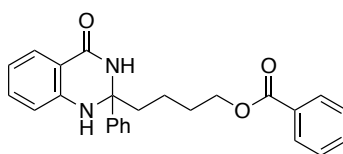
**(A27)** Following Method A, the utilization of 2-((1S,3S)-adamantan-1-yl)-1-phenylethan-1-one (1.00 g, 3.93 mmol) afforded the title compound as a white solid (0.32 g, 22% yield). **<sup>1</sup>H NMR (400 MHz, CD<sub>2</sub>Cl<sub>2</sub>)** δ 7.74 (dd, *J* = 7.8, 1.6 Hz, 1H), 7.70 – 7.65 (m, 1H), 7.50 – 7.39 (m, 2H), 7.27 (td, *J* = 7.5, 1.3 Hz, 3H), 7.23 – 7.16 (m, 1H), 6.80 – 6.69 (m, 2H), 5.21 – 5.06 (m, 1H), 1.99 – 1.77 (m, 5H), 1.77 – 1.43 (m, 12H) ppm. **<sup>13</sup>C NMR (101 MHz, CD<sub>2</sub>Cl<sub>2</sub>)** δ 164.9, 147.5, 146.3, 134.2, 128.7, 128.4, 127.8, 125.6, 118.8, 115.9, 115.1, 74.5, 56.3, 44.0, 37.1, 34.8, 29.2 ppm. **IR (neat):** 3307, 3052, 2902, 2848, 1728, 1652, 1612, 1484, 1447, 1373, 1264, 1191, 1154, 1045, 733, 699 cm<sup>-1</sup>. **Mp:** 40 °C. **HRMS** *calcd.* for (C<sub>25</sub>H<sub>28</sub>N<sub>2</sub>NaO) [M+Na]<sup>+</sup>: 395.2099, *found* 395.2090.



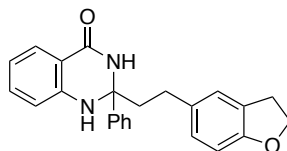
**tert-butyl**

**4-((4-oxo-2-phenyl-1,2,3,4-tetrahydroquinazolin-2-**

**yl)methyl)piperidine-1-carboxylate (A28)** Following Method A, the utilization of *tert*-butyl 4-(2-oxo-2-phenylethyl)piperidine-1-carboxylate (1.78 g, 5.9 mmol) afforded the title compound as a white solid (1.07 g, 44% yield). <sup>1</sup>H NMR (400 MHz, CDCl<sub>3</sub>) δ 7.80 (m, 2H), 7.51 – 7.40 (m, 2H), 7.33 – 7.12 (m, 4H), 6.76 (m, 1H), 6.70 (d, *J* = 8.1 Hz, 1H), 4.87 (s, 1H), 3.96 (s, 2H), 2.81 – 2.47 (m, 2H), 2.01 – 1.74 (m, 4H), 1.64 (d, *J* = 13.2 Hz, 1H), 1.42 (s, 9H), 1.27 – 1.10 (m, 2H) ppm. <sup>13</sup>C NMR (101 MHz, CDCl<sub>3</sub>) δ 165.4, 154.8, 145.8, 134.2, 128.7, 128.5, 128.0, 125.1, 119.2, 115.6, 114.9, 79.4, 73.8, 49.4, 33.7, 33.3, 32.1, 28.5 ppm. IR (neat): 3304, 2913, 1653, 1612, 1482, 1431, 1365, 1231, 1148, 753, 731, 698 cm<sup>-1</sup>. Mp: 250 °C. HRMS *calcd.* for (C<sub>25</sub>H<sub>31</sub>N<sub>3</sub>NaO<sub>3</sub>) [M+Na]<sup>+</sup>: 444.2263, *found* 444.2258.

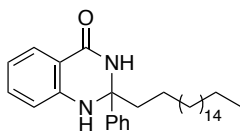


**4-(4-oxo-2-phenyl-1,2,3,4-tetrahydroquinazolin-2-yl)butyl benzoate (A29)** Following Method A, the utilization of 5-oxo-5-phenylpentyl benzoate (1.50 g, 5.3 mmol) afforded the title compound as a white solid (1.33 g, 63% yield). <sup>1</sup>H NMR (400 MHz, CDCl<sub>3</sub>) δ 8.05 – 7.94 (m, 2H), 7.81 (dd, *J* = 7.8, 1.6 Hz, 1H), 7.54 (dd, *J* = 7.1, 1.1 Hz, 1H), 7.49 – 7.35 (m, 4H), 7.34 – 7.20 (m, 5H), 6.76-6.75 (m, 1H), 6.68 (dd, *J* = 8.1, 1.0 Hz, 1H), 4.85 (s, 1H), 4.30 (dt, *J* = 8.7, 6.3 Hz, 2H), 2.26 – 2.08 (m, 2H), 1.96 – 1.75 (m, 2H), 1.69 – 1.50 (m, 2H) ppm. <sup>13</sup>C NMR (101 MHz, CDCl<sub>3</sub>) δ 166.7, 164.9, 145.7, 144.7, 133.9, 132.9, 130.1, 129.5, 128.61, 128.4, 128.3, 127.9, 125.1, 119.0, 115.5, 114.8, 73.3, 64.1, 42.0, 28.5, 20.3 ppm. IR (neat): 3374, 3168, 3058, 2920, 1698, 1660, 1612, 1482, 1281, 1124, 1072, 806, 757, 719, 552 cm<sup>-1</sup>. Mp: 185 °C. HRMS *calcd.* for (C<sub>25</sub>H<sub>24</sub>N<sub>2</sub>NaO<sub>3</sub>) [M+Na]<sup>+</sup>: 423.1685, *found* 423.1680.

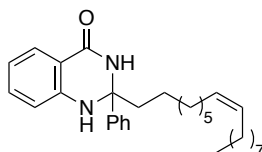


**2-(2-(2,3-dihydrobenzofuran-5-yl)ethyl)-2-phenyl-2,3-dihydroquinazolin-4(1H)-one (A30)** Following Method A, the utilization of 3-(2,3-dihydrobenzofuran-5-yl)-1-phenylpropan-1-one (1.08 g, 4.3 mmol) afforded the title compound as a white solid (1.18 g, 73% yield). <sup>1</sup>H NMR (400 MHz, DMF-*d*<sub>7</sub>) δ 8.82 (d, *J* = 8.2 Hz, 1H), 7.76 (s, 1H), 7.74 – 7.57 (m, 3H), 7.48 – 7.15 (m, 4H), 7.12 (d, *J* = 1.9 Hz, 1H), 7.06 – 6.87 (m, 2H), 6.75 – 6.43 (m, 2H), 4.50 (t, *J* = 8.7 Hz, 2H), 3.16 (t, *J* = 8.7 Hz, 2H), 2.99 – 2.84 (m, 2H), 2.21 (t, *J* = 11.4, 2H) ppm. <sup>13</sup>C NMR (101 MHz, DMF-*d*<sub>7</sub>) δ 165.7, 165.6,

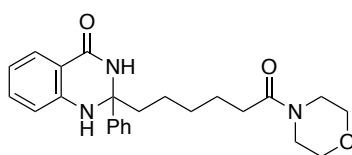
159.4, 149.3, 149.0, 134.9, 134.3, 129.1, 128.6, 128.5, 128.2, 126.6, 126.0, 117.9, 116.6, 115.7, 109.6, 74.4, 71.9, 46.5 ppm. **IR (neat):** 3366, 3159, 2885, 1737, 1657, 1609, 1483, 1446, 1372, 1239, 1190, 1154, 808, 753, 698  $\text{cm}^{-1}$ . **Mp:** 130 °C. **HRMS calcd.** for  $(\text{C}_{24}\text{H}_{22}\text{N}_2\text{NaO}_2)$   $[\text{M}+\text{Na}]^+$ : 393.1579, *found* 393.1571.



**2-octadecyl-2-phenyl-2,3-dihydroquinazolin-4(1H)-one (A31).** Following Method A, the utilization of 1-phenylnonadecan-1-one (1.79 g, 5.0 mmol) afforded the title compound as a white solid (1.30 g, 58% yield).  **$^1\text{H}$  NMR (500 MHz,  $\text{CDCl}_3$ )**  $\delta$  7.94 – 7.84 (m, 1H), 7.83 (dd,  $J = 7.7, 1.7$  Hz, 1H), 7.49 – 7.43 (m, 2H), 7.34 – 7.21 (m, 3H), 7.21 (d,  $J = 6.1$  Hz, 1H), 6.77–6.73 (m, 2H), 5.03 (d,  $J = 1.6$  Hz, 1H), 2.08 – 1.92 (m, 2H), 1.59 – 1.17 (m, 32H), 0.89 (t,  $J = 7.0$  Hz, 3H) ppm.  **$^{13}\text{C}$  NMR (101 MHz,  $\text{CDCl}_3$ )**  $\delta$  165.4, 146.2, 145.3, 133.9, 128.5, 128.4, 127.7, 125.4, 118.8, 115.8, 114.9, 73.5, 43.0, 32.0, 29.8, 29.7, 29.7, 29.6, 29.5, 29.4, 23.9, 22.8, 14.2 ppm. **IR (neat):** 3416, 3318, 2017, 2846, 1651, 1614, 1505, 1484, 1465, 1366, 1152, 759, 700, 548  $\text{cm}^{-1}$ . **Mp:** 85 °C. **HRMS calcd.** for  $(\text{C}_{32}\text{H}_{48}\text{N}_2\text{NaO})$   $[\text{M}+\text{Na}]^+$ : 499.3664, *found* 499.3659.

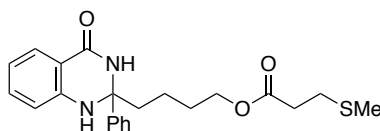


**(Z)-2-(hexadec-8-en-1-yl)-2-phenyl-2,3-dihydroquinazolin-4(1H)-one (A32).** Following Method A, the utilization of (Z)-1-phenyloctadec-9-en-1-one (2.32 g, 6.8 mmol) afforded the title compound as a liquid (1.79 g, 57% yield).  **$^1\text{H}$  NMR (500 MHz,  $\text{CDCl}_3$ )**  $\delta$  7.80 (dd,  $J = 7.8, 1.6$  Hz, 1H), 7.51 – 7.35 (m, 3H), 7.34 – 7.15 (m, 4H), 6.91 – 6.56 (m, 2H), 5.31 (d,  $J = 5.9$  Hz, 2H), 2.25 – 1.90 (m, 6H), 1.54 – 1.16 (m, 23H), 0.86 (t,  $J = 6.9$  Hz, 3H) ppm.  **$^{13}\text{C}$  NMR (126 MHz,  $\text{CDCl}_3$ )**  $\delta$  165.0, 145.9, 144.9, 133.9, 129.9, 129.7, 128.4, 128.3, 127.7, 125.2, 118.8, 115.6, 114.8, 73.4, 42.7, 31.8, 29.7, 29.6, 29.5, 29.4, 29.3, 29.3, 29.1, 27.2, 27.1, 23.7, 22.6, 14.0 ppm. **IR (neat):** 3305, 2923, 2852, 1725, 1653, 1613, 1485, 1447, 1374, 1251, 1151, 1046, 752, 698  $\text{cm}^{-1}$ . **HRMS calcd.** for  $(\text{C}_{31}\text{H}_{44}\text{N}_2\text{NaO})$   $[\text{M}+\text{Na}]^+$ : 483.3351, *found* 483.3346

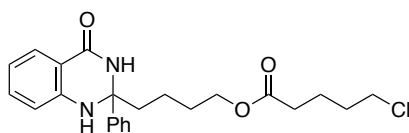


**2-(6-morpholino-6-oxohexyl)-2-phenyl-2,3-dihydroquinazolin-4(1H)-one (A33)**

Following Method A, the utilization of 1-morpholino-7-phenylheptane-1,7-dione (1.38 g, 4.7 mmol) afforded the title compound as a white solid (1.07 g, 56% yield). **<sup>1</sup>H NMR (500 MHz, DMF-d<sub>7</sub>)** δ 8.54 (s, 1H), 7.69 – 7.63 (m, 2H), 7.59 (dd, *J* = 7.8, 1.6 Hz, 1H), 7.55 (d, *J* = 1.8 Hz, 1H), 7.38 – 7.27 (m, 2H), 7.26 – 7.17 (m, 2H), 6.93 (dd, *J* = 8.3, 1.0 Hz, 1H), 6.59 (t, *J* = 6.9 Hz, 1H), 3.61 – 3.57 (m, 4H), 3.53 – 3.40 (m, 4H), 2.34 (t, *J* = 7.4 Hz, 2H), 2.08 – 1.88 (m, 2H), 1.72 – 1.50 (m, 4H), 1.35 (q, *J* = 7.5 Hz, 2H) ppm. **<sup>13</sup>C NMR (126 MHz, DMF-d<sub>7</sub>)** δ 172.1, 165.4, 149.4, 149.0, 134.2, 129.0, 128.4, 128.1, 126.7, 117.8, 116.6, 115.6, 74.5, 67.6, 55.8, 46.8, 43.8, 42.7, 33.3, 25.9, 24.9 ppm. **IR (neat):** 3318, 3247, 2949, 2850, 1645, 1611, 1515, 1485, 1445, 1361, 1270, 1118, 1028, 755, 732, 698 cm<sup>-1</sup>. **Mp:** 112 °C. **HRMS *calcd.*** for (C<sub>24</sub>H<sub>29</sub>N<sub>3</sub>NaO<sub>3</sub>) [M+Na]<sup>+</sup>: 430.2107, *found* 430.2098.

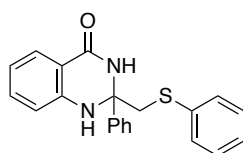


**4-(4-oxo-2-phenyl-1,2,3,4-tetrahydroquinazolin-2-yl)butyl 3-(methylthio)propanoate (A34)** Following Method A, the utilization of 5-oxo-5-phenylpentyl 3-(methylthio)propanoate (1.17 g, 4.2 mmol) afforded the title compound as a liquid (1.38 g, 81% yield). **<sup>1</sup>H NMR (500 MHz, CDCl<sub>3</sub>)** δ 8.78 (s, 1H), 7.87 (dd, *J* = 7.8, 1.6 Hz, 1H), 7.54 (d, *J* = 7.7 Hz, 2H), 7.34 – 7.19 (m, 4H), 6.87 (dd, *J* = 8.2, 1.0 Hz, 1H), 6.80 – 6.71 (m, 1H), 5.68 (s, 1H), 4.07 (m, 2H), 2.74 (t, *J* = 7.2 Hz, 2H), 2.57 (t, *J* = 7.2 Hz, 2H), 2.11 – 2.06 (m, 5H), 1.81 – 1.50 (m, 4H) ppm. **<sup>13</sup>C NMR (126 MHz, CDCl<sub>3</sub>)** δ 172.0, 165.8, 146.4, 145.5, 133.8, 128.2, 128.0, 127.4, 125.1, 118.2, 115.1, 114.7, 73.2, 64.1, 42.1, 34.1, 28.9, 28.1, 20.2, 15.2 ppm. **IR (neat):** 3293, 2917, 1717, 1646, 1611, 1484, 1447, 1380, 1248, 1149, 1030, 909, 753, 730, 699 cm<sup>-1</sup>. **HRMS *calcd.*** for (C<sub>22</sub>H<sub>26</sub>N<sub>2</sub>NaO<sub>3</sub>S) [M+Na]<sup>+</sup>: 421.1562, *found* 421.1554.



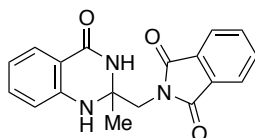
**4-(4-oxo-2-phenyl-1,2,3,4-tetrahydroquinazolin-2-yl)butyl 5-chloropentanoate (A35)** Following Method A, the utilization of 5-oxo-5-phenylpentyl 5-chloropentanoate (0.91 g, 3.1 mmol) afforded the title compound as a colorless solid (0.86 g, 67% yield). **<sup>1</sup>H NMR (500 MHz, CDCl<sub>3</sub>)** δ 8.56 (s, 1H), 7.82 (dd, *J* = 7.8, 1.6 Hz, 1H), 7.53 – 7.46 (m, 2H), 7.34 – 7.13 (m, 4H), 6.88 – 6.71 (m, 2H), 5.29 (s, 1H), 4.16 – 3.96 (m, 2H), 3.56 – 3.47 (m, 2H), 2.25 (t, *J* = 6.9 Hz, 2H), 2.17 – 1.99 (m, 2H), 1.81 – 1.67 (m, 4H),

1.69 – 1.51 (m, 4H) ppm.  $^{13}\text{C}$  NMR (75 MHz,  $\text{CDCl}_3$ )  $\delta$  173.4, 165.8, 146.3, 145.5, 134.0, 128.5, 128.3, 127.7, 125.2, 118.6, 115.4, 114.8, 73.4, 63.9, 44.5, 42.2, 33.3, 31.8, 28.4, 22.2, 20.4 ppm. IR (neat): 3355, 3177, 3043, 2952, 1710, 1658, 1610, 1510, 1483, 1445, 1375, 1305, 1265, 1150, 1065, 1032, 998, 905, 828, 772, 754, 701, 642, 552  $\text{cm}^{-1}$ . **Mp:** 94 °C. HRMS *calcd.* for ( $\text{C}_{23}\text{H}_{27}\text{ClN}_2\text{NaO}_3$ )  $[\text{M}+\text{Na}]^+$ : 437.1608, *found* 437.1602.

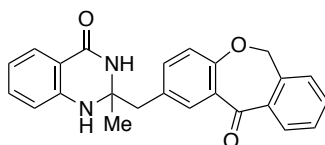


**2-phenyl-2-((phenylthio)methyl)-2,3-dihydroquinazolin-4(1H)-one (A36)**

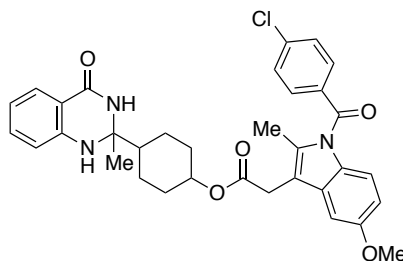
Following Method A, the utilization of 1-phenyl-2-(phenylthio)ethan-1-one (1.14 g, 5.0 mmol) afforded the title compound as a white solid (1.30 g, 75% yield).  $^1\text{H}$  NMR (400 MHz,  $\text{CDCl}_3$ )  $\delta$  7.84 (dd,  $J = 7.8, 1.6$  Hz, 1H), 7.58 – 7.48 (m, 2H), 7.39 – 7.13 (m, 9H), 7.04 (s, 1H), 6.81 (ddd,  $J = 8.1, 7.3, 1.0$  Hz, 1H), 6.54 (dd,  $J = 8.1, 1.0$  Hz, 1H), 5.14 (d,  $J = 1.7$  Hz, 1H), 3.71 (d,  $J = 3.6$  Hz, 2H) ppm.  $^{13}\text{C}$  NMR (101 MHz,  $\text{CDCl}_3$ )  $\delta$  163.8, 145.1, 141.8, 135.0, 134.0, 130.6, 129.1, 128.7, 128.6, 128.3, 127.0, 125.9, 119.4, 115.3, 115.3, 73.3, 45.7 ppm. IR (neat): 3325, 3061, 2922, 2245, 2184, 2098, 1665, 1613, 1507 1474, 1448, 1418, 1370, 1181, 1153, 750, 734, 688, 573  $\text{cm}^{-1}$ . **Mp:** 153 °C. HRMS *calcd.* for ( $\text{C}_{21}\text{H}_{18}\text{N}_2\text{NaOS}$ )  $[\text{M}+\text{Na}]^+$ : 369.1038, *found* 369.1035.



**2-((2-methyl-4-oxo-1,2,3,4-tetrahydroquinazolin-2-yl)methyl)isoindoline-1,3-dione (A37)** Following Method A, the utilization of 2-(2-oxopropyl)isoindoline-1,3-dione (2.03 g, 10.0 mmol) afforded the title compound as a yellow solid (2.86 g, 89% yield).  $^1\text{H}$  NMR (400 MHz,  $\text{CDCl}_3$ )  $\delta$  7.83 (dd,  $J = 5.5, 3.0$  Hz, 2H), 7.79 (dd,  $J = 7.8, 1.6$  Hz, 1H), 7.71 (dd,  $J = 5.5, 3.0$  Hz, 2H), 7.26 – 7.21 (m, 1H), 6.73 (t,  $J = 7.0$  Hz, 1H), 6.62 (d,  $J = 7.6$  Hz, 1H), 6.10 (s, 1H), 4.5 (s, 1H), 3.94 (d,  $J = 2.2$  Hz, 2H), 1.61 (s, 3H) ppm.  $^{13}\text{C}$  NMR (126 MHz,  $\text{DMF-d}_7$ )  $\delta$  169.2, 164.0, 148.1, 135.2, 134.2, 133.3, 128.3, 123.9, 117.9, 115.9, 115.6, 70.9, 46.5, 27.3 ppm. IR (neat): 3372, 3336, 1767, 1700, 1662, 1613, 1516, 1484, 1425, 1390, 1324, 1150, 1077, 934, 761, 727, 713, 697, 571, 531  $\text{cm}^{-1}$ . **Mp:** 228 °C. HRMS *calcd.* for ( $\text{C}_{18}\text{H}_{15}\text{N}_3\text{NaO}_3$ )  $[\text{M}+\text{Na}]^+$ : 344.1011, *found* 344.1014.



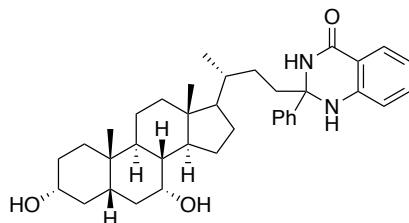
**2-methyl-2-((11-oxo-6,11-dihydrodibenzo[*b,e*]oxepin-2-yl)methyl)-2,3-dihydroquinazolin-4(1*H*)-one (A38)** Following Method A, the utilization of 2-(2-oxopropyl)dibenzo[*b,e*]oxepin-11(6*H*)-one (1.35 g, 5.0 mmol) afforded the title compound as a white solid (0.83 g, 43% yield). **<sup>1</sup>H NMR (500 MHz, DMF-*d*<sub>7</sub>)** δ 8.06 – 7.99 (m, 1H), 7.89 (d, *J* = 1.8 Hz, 1H), 7.84 (dd, *J* = 7.7, 1.4 Hz, 1H), 7.68 (dd, *J* = 7.4, 1.4 Hz, 1H), 7.63 – 7.54 (m, 3H), 7.46 (dd, *J* = 8.4, 2.4 Hz, 1H), 7.23 (m, 1H), 6.98 (d, *J* = 8.4 Hz, 1H), 6.82 (d, *J* = 1.8 Hz, 1H), 6.76 (dd, *J* = 8.2, 1.0 Hz, 1H), 6.59 (ddd, *J* = 7.9, 7.2, 1.1 Hz, 1H), 5.29 (s, 2H), 3.14 (d, *J* = 13.4 Hz, 1H), 3.05 (d, *J* = 13.4 Hz, 1H), 1.54 (s, 3H) ppm. **<sup>13</sup>C NMR (126 MHz, DMF-*d*<sub>7</sub>)** δ 191.3, 164.4, 161.1, 148.4, 141.5, 139.1, 137.4, 134.7, 134.2, 134.0, 131.7, 130.2, 130.0, 129.3, 128.2, 125.8, 121.0, 117.4, 115.5, 115.3, 74.1, 70.9, 47.2, 28.5 ppm. **IR (neat):** 3378, 3168, 2970, 2183, 1972, 1663, 1643, 1611, 1514, 1486, 1414, 1391, 1302, 1201, 1154, 1139, 1012, 827, 755, 640 cm<sup>-1</sup>. **Mp:** 196 °C. **HRMS *calcd.*** for (C<sub>24</sub>H<sub>20</sub>N<sub>2</sub>NaO<sub>3</sub>) [M+Na]<sup>+</sup>: 407.1372, *found* 407.1366.



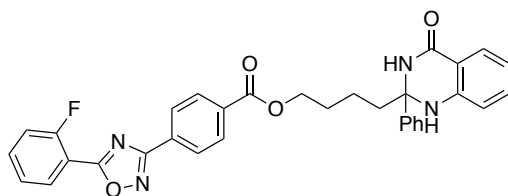
**4-(2-methyl-4-oxo-1,2,3,4-tetrahydroquinazolin-2-yl)cyclohexyl 2-(1-(4-chlorobenzoyl)-5-methoxy-2-methyl-1*H*-indol-3-yl)acetate (A39)** Following Method A, the utilization of 4-acetylcyclohexyl 2-(1-(4-chlorobenzoyl)-5-methoxy-2-methyl-1*H*-indol-3-yl)acetate (1.60 g, 3.3 mmol) afforded the title compound as a white solid (0.64 g, 32% yield), as a mixture of two isomers (*cis* : *trans* = 1:2.4). **<sup>1</sup>H NMR (400 MHz, CD<sub>2</sub>Cl<sub>2</sub>)** δ 7.75 (dd, *J* = 7.8, 1.6 Hz, 1H), 7.66 – 7.60 (m, 2H), 7.50 – 7.42 (m, 2H), 7.27 – 7.16 (m, 2H), 7.04 – 6.89 (m, 2H), 6.77 – 6.54 (m, 3H), 4.65 – 4.59 (m, 1H), 3.80 (d, *J* = 3.2 Hz, 3H), 3.64 (d, *J* = 17.6 Hz, 2H), 3.63-3.62 (m, 2H), 2.33 (s, 2H), 2.05 – 1.52 (m, 5H), 1.51 – 1.16 (m, 7H) ppm. **<sup>13</sup>C NMR (101 MHz, CD<sub>2</sub>Cl<sub>2</sub>)** δ 170.1, 169.9, 168.2, 168.1, 164.08/164.03, 156.0, 155.9, 146.1, 146.0, 138.99/138.93, 135.7, 134.0, 133.79/133.77, 131.07/131.06, 130.8, 130.7, 129.05/129.02, 127.7, 117.78/117.76, 114.9, 114.3, 114.25/114.22, 114.1, 113.1, 112.8, 111.4, 111.0, 101.6,



101.2, 73.4, 71.6, 71.5, 69.3, 55.5, 46.8/46.7, 31.2, 31.1, 30.6, 30.4, 29.69/29.62, 25.0, 24.9, 24.6, 24.4, 21.2, 20.8, 13.1 ppm. **IR (neat):** 3320, 2933, 2035, 1981, 1726, 1652, 1611, 1477, 1356, 1221, 1145, 1088, 1066, 1035, 1014, 925, 832, 752  $\text{cm}^{-1}$ . **Mp:** 126  $^{\circ}\text{C}$ . **HRMS** *calcd.* for  $(\text{C}_{34}\text{H}_{34}\text{ClN}_3\text{NaO}_5)$   $[\text{M}+\text{Na}]^+$ : 622.2085, *found* 622.2079.

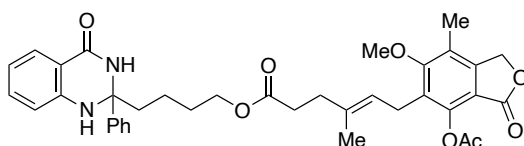


**2-((3R)-3-((3R,5S,7R,8R,9S,10S,13R,14S)-3,7-dihydroxy-10,13-dimethylhexadecahydro-1H-cyclopenta[a]phenanthren-17-yl)butyl)-2-phenyl-2,3-dihydroquinazolin-4(1H)-one (A40)** Following Method A, the utilization of (4R)-4-((3R,5S,7R,8R,9S,10S,13R,14S)-3,7-dihydroxy-10,13-dimethylhexadecahydro-1H-cyclopenta[a]phenanthren-17-yl)-1-phenylpentan-1-one (0.38 g, 0.84 mmol) afforded the title compound as a white solid (0.41 g, 86% yield).  **$^1\text{H}$  NMR (400 MHz,  $\text{CD}_2\text{Cl}_2$ )**  $\delta$  8.25 (d,  $J = 13.1$  Hz, 1H), 7.75 (ddd,  $J = 8.0, 3.3, 1.5$  Hz, 1H), 7.50 (dt,  $J = 7.5, 2.5$  Hz, 2H), 7.30 – 7.20 (m, 4H), 6.81 (d,  $J = 8.0$  Hz, 1H), 6.70 (td,  $J = 7.4, 5.3$  Hz, 1H), 5.55 (d,  $J = 7.1$  Hz, 1H), 3.77 (s, 1H), 3.41 (s, 1H), 2.91 – 2.84 (m, 1H), 2.26 – 2.04 (m, 3H), 1.95 – 0.81 (m, 30H), 0.60 – 0.56 (m, 3H) ppm.  **$^{13}\text{C}$  NMR (101 MHz,  $\text{CD}_2\text{Cl}_2$ )**  $\delta$  165.6, 165.5, 146.6, 146.6, 146.1, 146.0, 133.9, 128.3, 128.1, 127.5, 125.4, 115.4, 115.4, 114.9, 73.7, 73.7, 71.8, 55.8, 55.6, 50.3, 50.3, 42.5, 42.5, 41.7, 39.8, 39.4, 35.5, 35.5, 35.4, 345.0, 34.6, 32.8, 30.8, 29.7, 28.1, 23.6, 22.6, 20.6, 18.6, 18.5, 11.5, 11.5 ppm. **IR (neat):** 3295, 2923, 2863, 1652, 1612, 1485, 1447, 1374, 1264, 1151, 1076, 977, 753, 699  $\text{cm}^{-1}$ . **Mp:** 170  $^{\circ}\text{C}$ . **HRMS** *calcd.* for  $(\text{C}_{37}\text{H}_{50}\text{N}_2\text{NaO}_3)$   $[\text{M}+\text{Na}]^+$ : 593.3719, *found* 593.3714.



**4-(4-oxo-2-phenyl-1,2,3,4-tetrahydroquinazolin-2-yl)butyl 4-(5-(2-fluorophenyl)-1,2,4-oxadiazol-3-yl)benzoate (A41)** Following Method A, the utilization of 5-oxo-5-phenylpentyl 4-(5-(2-fluorophenyl)-1,2,4-oxadiazol-3-yl)benzoate (1.00 g, 2.2 mmol) afforded the title compound as a white solid (0.87 g, 71% yield).  **$^1\text{H}$  NMR (400 MHz,  $\text{CD}_2\text{Cl}_2$ )**  $\delta$  8.75 (td,  $J = 1.7, 0.6$  Hz, 1H), 8.36 – 8.29 (m, 2H), 8.22 (ddd,  $J = 7.9, 7.1, 1.8$  Hz, 1H), 8.11 (ddd,  $J = 7.8, 1.8, 1.2$  Hz, 1H), 7.76 (d,  $J = 1.6$  Hz, 1H), 7.67 – 7.59

(m, 1H), 7.57 – 7.46 (m, 3H), 7.40 – 7.14 (m, 7H), 6.78 (dt,  $J = 7.9, 0.8$  Hz, 1H), 6.71 (ddd,  $J = 8.2, 7.2, 1.0$  Hz, 1H), 4.43 – 4.23 (m, 2H), 2.20 – 2.02 (m, 2H), 1.87 – 1.58 (m, 4H) ppm.  $^{13}\text{C}$  NMR (101 MHz,  $\text{CD}_2\text{Cl}_2$ )  $\delta$  173.5 (d,  $J = 4.3$  Hz), 168.4, 166.1, 165.7, 162.4, 159.8, 146.7, 146.1, 135.3 (d,  $J = 8.7$  Hz), 134.2, 132.5, 131.9, 131.6, 131.3, 129.5, 128.8, 128.7, 128.4, 128.0, 127.5, 125.2 (d,  $J = 3.7$  Hz), 118.9, 117.6, 117.4, 115.9, 115.3, 112.9 (d,  $J = 11.4$  Hz), 73.8, 65.2, 54.2, 42.6, 28.8, 20.8 ppm. **IR** (neat): 3321, 3055, 2954, 2177, 2004, 1718, 1650, 1612, 1554, 1483, 1367, 1255, 1147, 1105, 824, 747, 721, 698  $\text{cm}^{-1}$ . **Mp**: 97 °C. **HRMS** *calcd.* for  $(\text{C}_{33}\text{H}_{27}\text{FN}_4\text{NaO}_4)$   $[\text{M}+\text{Na}]^+$ : 585.1914, *found* 585.1909.

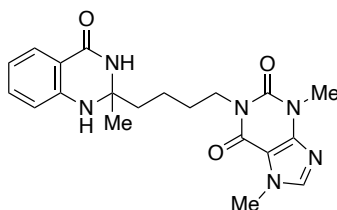


**4-(4-oxo-2-phenyl-1,2,3,4-tetrahydroquinazolin-2-yl)butyl (E)-6-(4-acetoxy-6-methoxy-7-methyl-3-oxo-1,3-dihydroisobenzofuran-5-yl)-4-methylhex-4-enoate**

**(A42)** Following Method A, the utilization of 5-oxo-5-phenylpentyl (*E*)-6-(4-acetoxy-6-methoxy-7-methyl-3-oxo-1,3-dihydroisobenzofuran-5-yl)-4-methylhex-4-enoate

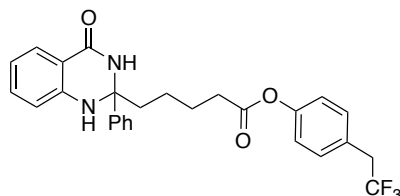
(550 mg, 1.05 mmol) afforded the title compound as a white solid (320 mg, 48% yield).

$^1\text{H}$  NMR (400 MHz,  $\text{CDCl}_3$ )  $\delta$  8.34 (s, 1H), 7.75 (d,  $J = 6.2$  Hz, 1H), 7.44 (d,  $J = 7.0$  Hz, 2H), 7.20 (t,  $J = 7.5$  Hz, 3H), 7.14 (d,  $J = 7.2$  Hz, 1H), 6.73 (d,  $J = 7.3$  Hz, 1H), 6.67 (t,  $J = 7.0$  Hz, 1H), 5.51 (s, 1H), 5.07 (s, 3H), 3.93 (d,  $J = 5.4$  Hz, 2H), 3.74 (s, 3H), 3.33 (d,  $J = 7.0$  Hz, 2H), 2.36 (s, 3H), 2.30 (d,  $J = 7.6$  Hz, 2H), 2.24 (d,  $J = 7.6$  Hz, 2H), 2.16 (s, 3H), 2.05 – 1.94 (m, 2H), 1.74 (s, 3H), 1.52 (m, 4H) ppm.  $^{13}\text{C}$  NMR (101 MHz,  $\text{CDCl}_3$ )  $\delta$  173.2, 169.0, 168.5, 165.7, 162.7, 146.5, 146.3, 145.8, 145.6, 134.5, 133.9, 129.2, 128.3, 128.1, 127.5, 125.3, 123.1, 122.2, 118.3, 115.3, 114.8, 113.3, 73.3, 68.4, 63.9, 61.2, 42.2, 34.4, 32.7, 28.3, 23.5, 20.5, 20.3, 16.2, 11.7 ppm. **IR** (neat): 3359, 3199, 3100, 2933, 1756, 1655, 1611, 1509, 1484, 1447, 1358, 1316, 1269, 1185, 1168, 1128, 1069, 1030, 1008, 976, 889, 756, 730, 700, 556, 539  $\text{cm}^{-1}$ . **Mp**: 73 °C. **HRMS** *calcd.* for  $(\text{C}_{37}\text{H}_{40}\text{N}_2\text{NaO}_8)$   $[\text{M}+\text{Na}]^+$ : 663,2682, *found* 663,2677.



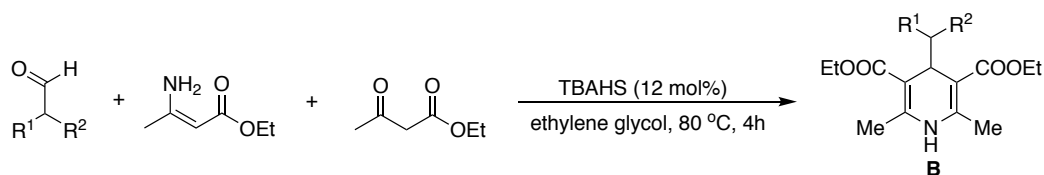
**3,7-dimethyl-1-(4-(2-methyl-4-oxo-1,2,3,4-tetrahydroquinazolin-2-yl)butyl)-3,7-**

**dihydro-1H-purine-2,6-dione (A43)** Following Method A, the utilization of Pentoxifylline (1.39 g, 5.0 mmol) afforded the title compound as a white solid (1.17 g, 59% yield).  $^1\text{H NMR}$  (400 MHz,  $\text{CDCl}_3$ )  $\delta$  7.81 (d,  $J = 6.2$  Hz, 1H), 7.49 (s, 1H), 7.23 (t,  $J = 6.9$  Hz, 1H), 6.74 (t,  $J = 7.0$  Hz, 1H), 6.57 (d,  $J = 8.1$  Hz, 1H), 6.40 (s, 1H), 4.14 – 4.04 (m, 1H), 4.02 (s, 3H), 4.02 – 3.95 (m, 1H), 3.57 (s, 3H), 1.82 – 1.75 (m, 2H), 1.67 – 1.63 (m, 2H), 1.63 (s, 3H), 1.60 – 1.49 (m, 2H) ppm.  $^{13}\text{C NMR}$  (101 MHz,  $\text{CDCl}_3$ )  $\delta$  164.4, 155.8, 151.7, 149.0, 146.2, 141.8, 133.9, 128.3, 118.4, 114.6, 114.5, 107.7, 69.9, 40.6, 40.1, 33.8, 29.9, 29.0, 27.2, 20.4 ppm. **IR (neat):** 3299, 2944, 2871, 1697, 644, 1613, 1549, 1513, 485, 1358, 1324, 1283, 1233, 1186, 115, 196, 1035, 748, 701, 611, 458  $\text{cm}^{-1}$ . **Mp:** 87 °C. **HRMS calcd.** for  $(\text{C}_{20}\text{H}_{24}\text{N}_6\text{NaO}_3)$   $[\text{M}+\text{Na}]^+$ : 419,1808, *found* 419,1802.

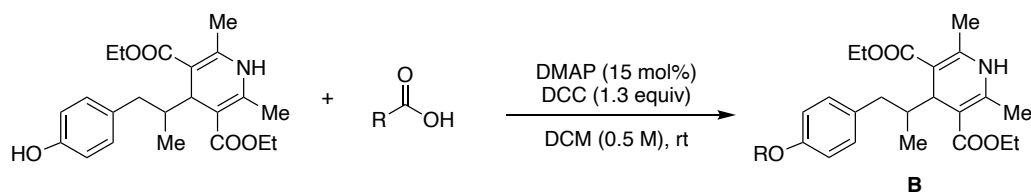


**4-(2,2,2-trifluoroethyl)phenyl 5-(4-oxo-2-phenyl-1,2,3,4-tetrahydroquinazolin-2-yl)pentanoate (A44)** Following Method A, the utilization of 4-(2,2,2-trifluoroethyl)phenyl 6-oxo-6-phenylhexanoate (182.0 mg, 0.50 mmol) afforded the title compound as a white solid (188.3 mg, 78% yield).  $^{19}\text{F NMR}$  (376 MHz,  $\text{CD}_2\text{Cl}_2$ )  $\delta$  -66.52 (t,  $J = 10.9$  Hz) ppm.  $^1\text{H NMR}$  (400 MHz,  $\text{CD}_2\text{Cl}_2$ )  $\delta$  7.84 (s, 1H), 7.79 – 7.75 (m, 1H), 7.51 – 7.42 (m, 2H), 7.35 – 7.20 (m, 6H), 7.06 – 6.95 (m, 2H), 6.75 (d,  $J = 7.8$  Hz, 2H), 5.08 (s, 1H), 3.39 (q,  $J = 10.9$  Hz, 2H), 2.54 (t,  $J = 7.3$  Hz, 2H), 2.15 – 2.05 (m, 2H), 1.79-1.71 (m, 2H), 1.68 – 1.48 (m, 2H) ppm.  $^{13}\text{C NMR}$  (101 MHz,  $\text{CD}_2\text{Cl}_2$ )  $\delta$  171.8, 165.0, 150.6, 146.1, 145.4, 133.9, 131.1, 128.5, 128.0, 127.7 (q,  $J = 3.0$  Hz), 125.8 (q,  $J = 276.6$  Hz), 127.6, 127.2, 125.3, 121.9, 118.7, 115.6, 114.9, 73.4, 42.3, 39.4 (q,  $J = 29.8$  Hz), 33.9, 24.5, 23.4 ppm. **IR (neat):** 3295, 2923, 2863, 1652, 1612, 1485, 1447, 1374, 1264, 1151, 1076, 977, 753, 699  $\text{cm}^{-1}$ . **Mp:** 121 °C. **HRMS calcd.** for  $(\text{C}_{27}\text{H}_{25}\text{F}_3\text{N}_2\text{NaO}_3)$   $[\text{M}+\text{Na}]^+$ : 505.1715, *found* 505.1720.

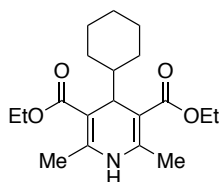
### Synthesis of Hantzsch Esters Analogues (B)



Following a literature procedure,<sup>[3]</sup> to a solution of aldehyde (1.0 equiv), ethyl 3-aminocrotonate (1.0 equiv), and ethyl acetoacetate (1.0 equiv) in ethylene glycol (2.5 M) was added Bu<sub>4</sub>NHSO<sub>4</sub> (12 mol%) in one portion. The vial was sealed and heated at 80 °C for 4 h. After consumption of the aldehyde, the reaction was cooled to r.t., diluted aq. NaCl and extracted into EtOAc. The combined organic phases were dried over anhydrous Na<sub>2</sub>SO<sub>4</sub>, filtered, and concentrated in vacuo. The crude residue was then purified by column chromatography.

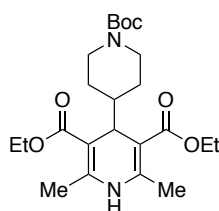


DMAP (15 mol%) was added to a stirred reaction mixture of diethyl 4-(1-(4-hydroxyphenyl)propan-2-yl)-2,6-dimethyl-1,4-dihydropyridine-3,5-dicarboxylate (1.0 equiv), carboxylic acid (1.0 equiv), and DCC (1.3 equiv) in dry DCM (0.5 M) at room temperature. The reaction mixture was filtered after 4 h (TLC control), the precipitate was rinsed with DCM. The combined filtrates were evaporated to dryness. The crude mixture was purified by flash column chromatography on silica gel to give desired product.

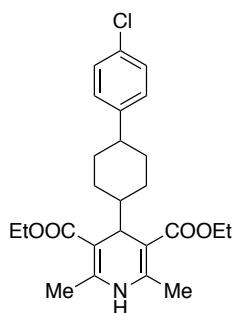


#### Diethyl 4-cyclohexyl-2,6-dimethyl-1,4-dihydropyridine-3,5-dicarboxylate (B1)

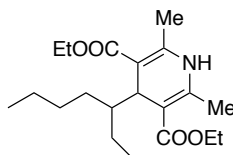
Following the procedure described, the utilization of cyclohexanecarbaldehyde (1.12 g, 10.0 mmol) afforded the title compound as a white solid (2.17 g, 65% yield). <sup>1</sup>H NMR (400 MHz, CDCl<sub>3</sub>) δ 5.57 (s, 1H), 4.38 – 4.08 (m, 4H), 3.92 (d, *J* = 5.7 Hz, 1H), 2.30 (s, 6H), 1.84 – 1.48 (m, 5H), 1.29 (t, *J* = 7.1 Hz, 6H), 1.23 – 1.16 (m, 1H), 1.13 – 1.04 (m, 3H), 0.93 (t, *J* = 11.7 Hz, 2H) ppm. <sup>13</sup>C NMR (101 MHz, CDCl<sub>3</sub>) δ 168.8, 144.5, 102.1, 59.7, 45.9, 38.5, 28.9, 26.8, 26.7, 19.5, 14.5 ppm. Spectral data was in agreement with the literature<sup>[4]</sup>.



**Diethyl 4-(1-(*tert*-butoxycarbonyl)piperidin-4-yl)-2,6-dimethyl-1,4-dihydropyridine-3,5-dicarboxylate (B2)** Following the procedure described, the utilization of *tert*-butyl 4-formylpiperidine-1-carboxylate (2.13 g, 10.0 mmol) afforded the title compound as a white solid (2.49 g, 57% yield).  $^1\text{H NMR}$  (400 MHz,  $\text{CDCl}_3$ )  $\delta$  5.89 (s, 1H), 4.17 (m, 4H), 4.06 – 3.91 (m, 2H), 2.50 (t,  $J = 12.0$  Hz, 2H), 2.30 (s, 6H), 1.48 – 1.31(m, 13H), 1.29 (t,  $J = 7.1$  Hz, 6H), 1.12 (dd,  $J = 12.4, 4.3$  Hz, 2H) ppm.  $^{13}\text{C NMR}$  (101 MHz,  $\text{CDCl}_3$ )  $\delta$  168.2, 154.8, 145.1, 101.0, 79.1, 59.6, 43.9, 37.5, 28.4, 19.4, 14.3 ppm. Spectral data was in agreement with the literature<sup>[5]</sup>.

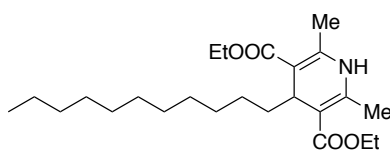


**Diethyl 4-(4-(4-chlorophenyl)cyclohexyl)-2,6-dimethyl-1,4-dihydropyridine-3,5-dicarboxylate (B3)** Following the procedure described, the utilization of 4-(4-chlorophenyl)cyclohexane-1-carbaldehyde (racemic) (1.11 g, 5.0 mmol) afforded the title compound as a white solid (1.44 g, 65% yield) by using Hexane/EtOAc (5:1) as eluent.  $^1\text{H NMR}$  (400 MHz,  $\text{CDCl}_3$ )  $\delta$  7.21 (d,  $J = 8.4$  Hz, 2H), 7.07 (d,  $J = 8.5$  Hz, 2H), 5.57 (s, 1H), 4.34 – 4.10 (m, 4H), 4.00 (d,  $J = 5.4$  Hz, 1H), 2.32 (s, 6H), 1.89 – 1.79 (m, 2H), 1.77 – 1.62 (m, 2H), 1.44 – 1.23 (m, 9H), 1.14 (td,  $J = 12.5, 3.1$  Hz, 2H) ppm.  $^{13}\text{C NMR}$  (101 MHz,  $\text{CDCl}_3$ )  $\delta$  168.7, 146.4, 144.7, 131.4, 128.4, 128.2, 101.9, 59.8, 45.3, 44.0, 38.3, 34.4, 28.9, 19.6, 14.5 ppm. Spectral data was in agreement with the literature<sup>[6]</sup>.



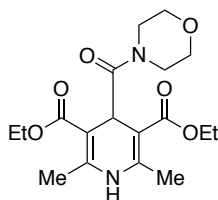
**Diethyl 4-(heptan-3-yl)-2,6-dimethyl-1,4-dihydropyridine-3,5-dicarboxylate (B4)** Following the procedure described, the utilization of 2-ethylhexanal (1.28 g, 10.0 mmol) afforded the title compound as a white solid (2.14 g, 61% yield) by using Hexane/EtOAc (5:1) as eluent.  $^1\text{H NMR}$  (400 MHz,  $\text{CDCl}_3$ )  $\delta$  5.56 (s, 1H), 4.24 – 4.00 (m, 5H), 2.27 (d,  $J = 2.2$  Hz, 6H), 1.33 – 1.05 (m, 15H), 0.85 (t,  $J = 6.9$  Hz, 6H) ppm.  $^{13}\text{C NMR}$  (101 MHz,  $\text{CDCl}_3$ )  $\delta$  168.7, 144.4, 144.3, 102.3, 102.1, 59.5, 48.0, 35.0, 29.5, 28.3, 23.1, 21.7, 19.3, 19.3, 14.2, 14.1, 11.8 ppm. Spectral data was in agreement

with the literature<sup>[3]</sup>.



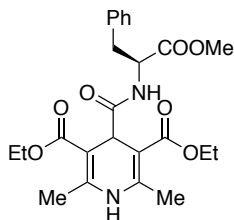
**Diethyl 2,6-dimethyl-4-undecyl-1,4-dihydropyridine-3,5-dicarboxylate (B5)**

Following a literature procedure, the utilization of dodecanal (1.84 g, 10.0 mmol) afforded the title compound as a white solid (2.48 g, 61% yield) by using Hexane/EtOAc (8:1) as eluent. <sup>1</sup>H NMR (400 MHz, CDCl<sub>3</sub>) δ 5.50 (s, 1H), 4.29 – 4.07 (m, 4H), 3.92 (t, *J* = 5.8 Hz, 1H), 2.28 (s, 6H), 1.41 – 1.18 (m, 26H), 0.98 – 0.81 (m, 3H) ppm. <sup>13</sup>C NMR (101 MHz, CDCl<sub>3</sub>) δ 168.2, 144.6, 103.6, 59.7, 37.0, 33.0, 32.0, 30.1, 29.9, 29.8, 29.8, 29.7, 29.5, 25.0, 22.8, 19.6, 14.5, 14.2 ppm. Spectral data was in agreement with the literature<sup>[7]</sup>.



**Diethyl 2,6-dimethyl-4-(morpholine-4-carbonyl)-1,4-dihydropyridine-3,5-dicarboxylate (B6)**

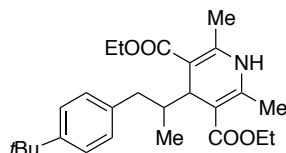
Following a literature procedure,<sup>[10]</sup> the utilization of morpholine (150 μL, 1.7 mmol, 1.2 equiv) afforded the title compound as a pale yellow solid (0.15 g, 40% yield). <sup>1</sup>H NMR (400 MHz, CDCl<sub>3</sub>) δ 7.57 (s, 1H), 5.01 (s, 1H), 4.26 – 4.09 (m, 4H), 3.99 – 3.90 (m, 2H), 3.75 (t, *J* = 4.7 Hz, 2H), 3.67 – 3.56 (m, 4H), 2.23 (s, 6H), 1.28 (t, *J* = 7.1 Hz, 6H) ppm. <sup>13</sup>C NMR (101 MHz, CDCl<sub>3</sub>) δ 174.5, 167.6, 147.6, 99.0, 67.4, 67.0, 60.0, 47.5, 42.8, 36.5, 19.6, 14.7 ppm. Spectral data was in agreement with the literature<sup>[8]</sup>.



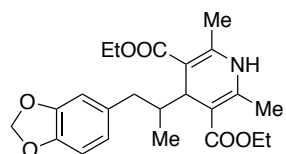
**Diethyl 4-[(2S)-1-methoxy-1-oxo-3-phenylpropan-2-yl]carbamoyl-2,6-dimethyl-1,4-dihydropyridine-3,5-dicarboxylate (B7)**

Following a literature procedure,<sup>[8]</sup> the utilization of L-Phenylalanine methyl ester hydrochloride (1.29 g, 6.0 mmol, 2 equiv) afforded the title compound as a pale yellow solid (1.23 g, 90% yield) by using Hexane/EtOAc (1:2) as eluent. <sup>1</sup>H NMR (400 MHz, CDCl<sub>3</sub>) δ 7.27 (s, 1H), 7.25 – 7.20

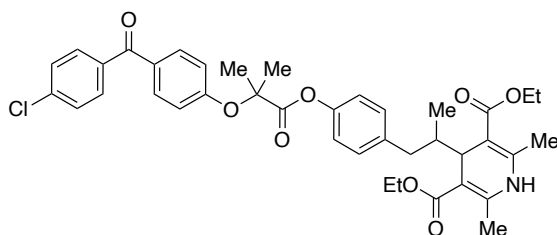
(m, 2H), 7.14 – 7.03 (m, 3H), 4.83 – 4.74 (m, 1H), 4.63 (s, 1H), 4.21 – 4.00 (m, 4H), 3.66 (s, 3H), 3.08 (m, 2H), 2.20 (dd,  $J = 4.7, 1.4$  Hz, 6H), 1.20 (t,  $J = 7.1$ , 6H) ppm.  $^{13}\text{C}$  NMR (101 MHz,  $\text{CDCl}_3$ )  $\delta$  174.0, 171.9, 167.5, 167.4, 147.4, 147.3, 136.3, 129.4, 128.5, 127.0, 98.0, 97.9, 60.2, 60.2, 53.6, 52.2, 41.3, 38.1, 19.3, 19.1, 14.4, 14.3 ppm. Spectral data was in agreement with the literature<sup>[8]</sup>.



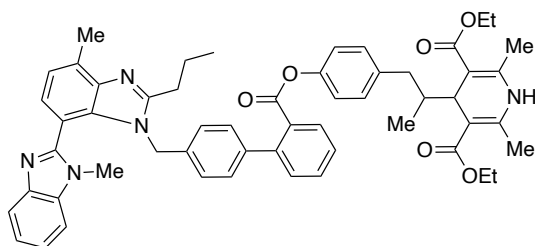
**Diethyl 4-(1-(4-(*tert*-butyl)phenyl)propan-2-yl)-2,6-dimethyl-1,4-dihydropyridine-3,5-dicarboxylate (B8)** Following the procedure described, the utilization of 3-(4-(*tert*-butyl)phenyl)-2-methylpropanal (1.02 g, 5.0 mmol) afforded the title compound as a light yellow oil (1.28 g, 60% yield) by using Hexane/EtOAc (15:1) as eluent.  $^1\text{H}$  NMR (400 MHz,  $\text{CDCl}_3$ )  $\delta$  7.24 (d,  $J = 8.2$  Hz, 2H), 7.01 (d,  $J = 8.2$  Hz, 2H), 5.60 (s, 1H), 4.21 – 4.09 (m, 5H), 2.76 (dd,  $J = 13.3, 3.6$  Hz, 1H), 2.55 (d,  $J = 6.2$  Hz, 1H), 2.31 (d,  $J = 1.6$  Hz, 6H), 1.77 – 1.67 (m, 1H), 1.33 – 1.26 (m, 15H), 0.65 (d,  $J = 6.8$  Hz, 3H) ppm.  $^{13}\text{C}$  NMR (101 MHz,  $\text{CDCl}_3$ )  $\delta$  168.8, 168.5, 148.2, 144.9, 144.8, 139.1, 128.7, 125.0, 102.1, 101.6, 59.8, 43.2, 38.8, 34.4, 31.5, 19.6, 19.5, 14.7, 14.59, 14.52 ppm. Spectral data was in agreement with the literature<sup>[9]</sup>.



**Diethyl 4-(1-(benzo[*d*][1,3]dioxol-5-yl)propan-2-yl)-2,6-dimethyl-1,4-dihydropyridine-3,5-dicarboxylate (B9)** Following the procedure described, the utilization of 3-(benzo[*d*][1,3]dioxol-5-yl)-2-methylpropanal (0.96 g, 5.0 mmol) afforded the title compound as a white solid (1.10 g, 50% yield) by using Hexane/EtOAc (4:1) as eluent.  $^1\text{H}$  NMR (400 MHz,  $\text{CDCl}_3$ )  $\delta$  6.67 (d,  $J = 7.9$  Hz, 1H), 6.57 (d,  $J = 1.6$  Hz, 1H), 6.52 (dd,  $J = 7.9, 1.7$  Hz, 1H), 5.89 (q,  $J = 1.5$  Hz, 2H), 5.59 (s, 1H), 4.37 – 4.11 (m, 4H), 4.10 (d,  $J = 4.8$  Hz, 1H), 2.71 (dd,  $J = 13.3, 3.5$  Hz, 1H), 2.32 (d,  $J = 1.3$  Hz, 6H), 2.09 – 1.97 (m, 1H), 1.67 (d,  $J = 4.2$  Hz, 1H), 1.30 (d,  $J = 9.0$ , 6H), 0.63 (d,  $J = 6.8$  Hz, 3H) ppm.  $^{13}\text{C}$  NMR (101 MHz,  $\text{CDCl}_3$ )  $\delta$  168.7, 168.5, 147.4, 145.4, 144.8, 144.8, 136.1, 121.8, 109.4, 107.9, 102.1, 101.6, 100.7, 59.8, 43.4, 39.1, 38.8, 19.6, 19.6, 14.5, 14.5 ppm. Spectral data was in agreement with the literature<sup>[9]</sup>.



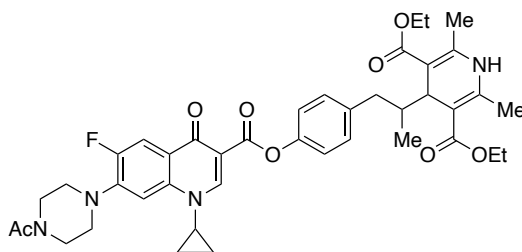
**Diethyl 4-(1-(4-((2-(4-(4-chlorobenzoyl)phenoxy)-2-methylpropanoyl)oxy)phenyl)propan-2-yl)-2,6-dimethyl-1,4-dihydropyridine-3,5-dicarboxylate (B10)** Following the procedure described, the utilization of Fenofibric acid (318 mg, 1.0 mmol, 1.0 equiv) afforded the title compound as a white solid (270 mg, 39% yield) by using Hexane/EtOAc (2:1) as eluent.  $^1\text{H NMR}$  (400 MHz,  $\text{CDCl}_3$ )  $\delta$  7.77 (d,  $J = 9.0$  Hz, 2H), 7.74 – 7.69 (m, 2H), 7.45 (d,  $J = 8.2$  Hz, 2H), 7.06 (d,  $J = 8.6$  Hz, 2H), 6.98 (d,  $J = 9.0$  Hz, 2H), 6.84 (d,  $J = 8.6$  Hz, 2H), 5.57 (s, 1H), 4.27 – 4.10 (m, 5H), 2.76 (dd,  $J = 13.6, 3.7$  Hz, 1H), 2.30 (s, 6H), 2.17 – 2.06 (m, 1H), 1.81 (s, 6H), 1.75 – 1.66 (m, 1H). 1.29 (q,  $J = 8.5$  Hz, 3H), 1.29 (q,  $J = 5.7$  Hz, 3H), 0.62 (d,  $J = 6.8$  Hz, 3H) ppm.  $^{13}\text{C NMR}$  (101 MHz,  $\text{CDCl}_3$ )  $\delta$  194.4, 172.7, 168.7, 168.5, 159.7, 148.3, 145.1, 140.4, 138.6, 136.4, 132.2, 131.3, 130.7, 130.1, 128.7, 120.6, 117.4, 101.8, 101.4, 79.6, 59.8, 43.2, 38.8, 25.6, 19.6, 19.5, 14.7, 14.6, 14.5 ppm. **IR (neat):** 2983, 2934, 1755, 1720, 1655, 1597, 1505, 1486, 1465, 1444, 1418, 1386, 1370, 1283, 1250, 1207, 1193, 1169, 1105, 1091, 1044, 1015, 971, 927, 914, 875, 853, 839, 763, 652, 477  $\text{cm}^{-1}$ . **Mp:** 40 °C. **HRMS** *calcd.* for  $(\text{C}_{39}\text{H}_{42}\text{ClNNaO}_8)$   $[\text{M}+\text{Na}]^+$ : 710,2497, *found* 710,2491. (Note: this compound is unstable and needs to be used immediately in the next step.)



**Diethyl 4-(1-(4-((1,7'-dimethyl-2'-propyl-1H,3'H-[2,4'-bibenzo[d]imidazol]-3'-yl)methyl)-[1,1'-biphenyl]-2-carbonyl)oxy)phenyl)propan-2-yl)-2,6-dimethyl-1,4-dihydropyridine-3,5-dicarboxylate (B11)** Following the procedure described, the utilization of Telmisartan (515 mg, 1.0 mmol, 1.0 equiv) afforded the title compound as a white solid (620 mg, 70% yield) by using Hexane/EtOAc (1:2) as eluent.  $^1\text{H NMR}$  (400 MHz,  $\text{CDCl}_3$ )  $\delta$  8.00 (d,  $J = 7.8$  Hz, 1H), 7.81 – 7.74 (m, 1H), 7.56 (m, 1H), 7.50 – 7.42 (m, 3H), 7.33 (dd,  $J = 8.3, 2.2$  Hz, 3H), 7.28 (m, 3H), 7.11 (d,  $J = 8.5$  Hz, 2H), 6.96 (d,  $J = 8.6$  Hz, 2H), 6.73 (d,  $J = 8.6$  Hz, 2H), 5.95 (s, 1H), 5.42 (s, 2H), 4.27 – 4.11

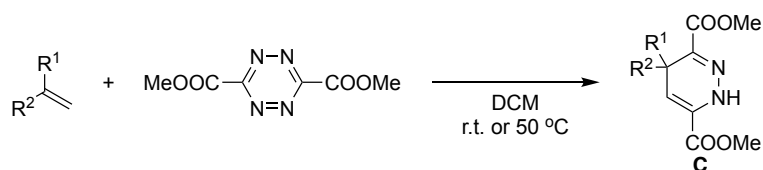


(m, 4H), 4.10 (d,  $J = 4.8$  Hz, 1H), 3.68 (s, 3H), 2.96 – 2.85 (m, 2H), 2.76 (s, 3H), 2.77 – 2.67 (m, 1H), 2.28 (d,  $J = 2.9$  Hz, 6H), 1.91 – 1.77 (m, 4H), 1.29 (dt,  $J = 8.7, 7.1$  Hz, 6H), 1.01 (t,  $J = 7.3$  Hz, 3H), 0.60 (d,  $J = 6.9$  Hz, 3H) ppm.  $^{13}\text{C}$  NMR (101 MHz,  $\text{CDCl}_3$ )  $\delta$  168.6, 168.5, 166.7, 156.4, 154.3, 148.4, 145.6, 145.6, 143.1, 142.3, 142.1, 141.0, 139.9, 136.4, 134.8, 134.8, 131.8, 130.9, 130.4, 129.9, 129.7, 129.5, 129.2, 127.5, 126.0, 123.9, 123.5, 122.6, 122.4, 120.6, 119.1, 109.6, 108.9, 101.1, 100.8, 59.5, 46.9, 43.0, 38.5, 31.7, 29.7, 29.2, 24.9, 21.7, 19.0, 18.9, 16.9, 14.6, 14.4, 14.38, 14.0 ppm. IR (neat): 2868, 2808, 2796, 2150, 2122, 1628, 1530, 1408, 1321, 1237, 1018, 928, 876, 812, 758, 704, 451  $\text{cm}^{-1}$ . Mp: 45 °C. HRMS *calcd.* for ( $\text{C}_{55}\text{H}_{58}\text{N}_5\text{O}_6$ )  $[\text{M}+\text{H}]^+$ : 884,4387, *found* 884,4382. (Note: this compound is unstable and needs to be used immediately in the next step.)

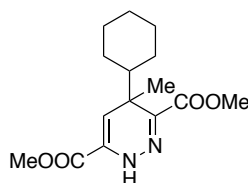


**Diethyl 4-(1-(4-((7-(4-acetylpiperazin-1-yl)-1-cyclopropyl-6-fluoro-4-oxo-1,4-dihydroquinoline-3-carbonyl)oxy)phenyl)propan-2-yl)-2,6-dimethyl-1,4-dihydropyridine-3,5-dicarboxylate (B12)** Following the procedure described, the utilization of Ciprofloxacin (373 mg, 1.0 mmol, 1.0 equiv) afforded the title compound as a white solid (330 mg, 44% yield) by using  $\text{CHCl}_3/\text{THF}$  (1:1) as eluent.  $^1\text{H}$  NMR (400 MHz,  $\text{CDCl}_3$ )  $\delta$  8.57 (s, 1H), 7.93 (d,  $J = 16.1$  Hz, 1H), 7.25 (s, 1H), 7.14 – 6.97 (m, 4H), 4.25 – 4.05 (m, 5H), 3.78 (d,  $J = 5.6$  Hz, 2H), 3.63 (d,  $J = 5.5$  Hz, 2H), 3.50 – 3.43 (m, 1H), 3.25 (t,  $J = 5.3$  Hz, 2H), 3.19 (t,  $J = 5.2$  Hz, 2H), 2.77 – 2.72 (m, 1H), 2.29 (s, 6H), 2.14 – 2.06 (m, 5H), 1.73 – 1.62 (m, 1H), 1.34 – 1.22 (m, 8H), 1.16 – 1.14 (m, 2H), 0.60 (d,  $J = 6.9$  Hz, 3H) ppm.  $^{13}\text{C}$  NMR (101 MHz,  $\text{CDCl}_3$ )  $\delta$  172.9, 169.2, 168.8, 168.7, 163.6, 153.5 (d,  $J = 249.2$  Hz), 148.8, 148.6, 145.6, 144.2 (d,  $J = 10.6$  Hz), 139.7, 138.0, 129.8, 121.4, 113.2 (d,  $J = 16.8$  Hz), 109.3, 105.5, 101.3, 101.1, 59.6, 49.6, 46.2, 43.2, 41.2, 38.7, 34.9, 21.4, 19.3, 14.9, 14.5, 14.5, 8.3 ppm. IR (neat): 3218, 2980, 2931, 2867, 1738, 1721, 1622, 1546, 1491, 1475, 1443, 1385, 130, 1348, 1330, 1315, 1283, 1248, 1228, 1209, 1167, 1105, 1071, 1043, 999, 912, 889, 872, 837, 797, 773, 728, 645, 622  $\text{cm}^{-1}$ . Mp: 146 °C. HRMS *calcd.* for ( $\text{C}_{41}\text{H}_{48}\text{FN}_4\text{O}_8$ )  $[\text{M}+\text{H}]^+$ : 743,3456, *found* 743,3451. (Note: this compound is unstable and needs to be used immediately in the next step.)

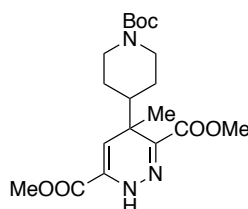
## Synthesis of Radical Precursors (C) from Alkenes



Following a literature procedure,<sup>[10]</sup> the alkene (1.0 equiv) and dimethyl 1,2,4,5-tetrazine-3,6-dicarboxylate (1.05 equiv) were combined in DCM (0.2 M). The solution was stirred at room temperature (for mono-substituted alkenes) or heated to 50 °C to maintain reflux (for 1,1-disubstituted or electron-deficient alkenes), and the reaction was monitored by TLC. The color of the solution changed from red to yellow. After complete consumption of starting materials, the solvent was removed under vacuum. The resulting crude was purified by column chromatography.

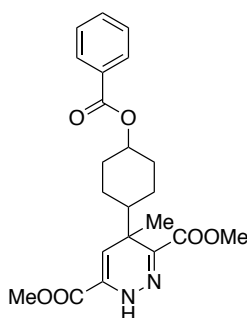


**Methyl 6-acetoxy-4-cyclohexyl-4-methyl-1,4-dihydropyridazine-3-carboxylate (C1)** Following the procedure described, the utilization of prop-1-en-2-ylcyclohexane (124.0 mg, 1.0 mmol) afforded the title compound as a liquid (276.0 mg, 94% yield) by using Hexane/EtOAc (4:1) as eluent. <sup>1</sup>H NMR (400 MHz, CDCl<sub>3</sub>) δ 7.99 (s, 1H), 5.55 (d, *J* = 2.2 Hz, 1H), 3.80 (s, 3H), 3.76 (s, 3H), 1.96 (tt, *J* = 12.3, 3.2 Hz, 1H), 1.79 – 1.64 (m, 3H), 1.62 – 1.50 (m, 2H), 1.39 (s, 3H), 1.24 – 1.12 (m, 2H), 1.09 – 0.89 (m, 3H) ppm. <sup>13</sup>C NMR (101 MHz, CDCl<sub>3</sub>) δ 164.6, 161.7, 136.6, 127.1, 114.6, 52.5, 52.1, 46.1, 39.9, 30.4, 26.6, 26.5, 26.4, 26.4, 24.5 ppm. Spectral data was in agreement with the literature.<sup>[10]</sup>

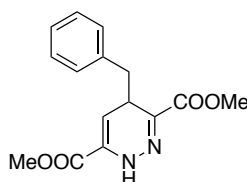


**Methyl 6-acetoxy-4-(1-(tert-butoxycarbonyl)piperidin-4-yl)-4-methyl-1,4-dihydropyridazine-3-carboxylate (C2)** Following the procedure described, the utilization of *tert*-butyl 4-(prop-1-en-2-yl)piperidine-1-carboxylate (180.0 mg, 0.8 mmol) afforded the title compound as a liquid (284.0 mg, 90% yield) by using

Hexane/EtOAc (1:1) as eluent. **<sup>1</sup>H NMR (400 MHz, CDCl<sub>3</sub>)** δ 8.01 (s, 1H), 5.51 (d, *J* = 2.3 Hz, 1H), 4.23 – 4.05 (m, 2H), 3.83 (s, 3H), 3.80 (s, 3H), 2.63 (t, *J* = 12.2 Hz, 2H), 2.32 – 2.13 (m, 1H), 1.63 (d, *J* = 15.6 Hz, 1H), 1.45 (s, 4H), 1.43 (s, 9H), 1.30 – 1.16 (m, 2H) ppm. **<sup>13</sup>C NMR (101 MHz, CDCl<sub>3</sub>)** δ 164.4, 161.4, 154.7, 135.6, 127.5, 113.4, 79.4, 52.6, 52.2, 44.6, 43.8, 39.4, 29.3, 28.4, 26.4, 23.8 ppm. **IR (neat):** 3349, 2951, 1687, 1578, 1434, 1365, 1346, 1324, 1277, 1244, 1162, 1109, 1065, 1028, 958, 865, 817, 765, 730 cm<sup>-1</sup>. **Mp:** 70 °C. **HRMS calcd.** for (C<sub>19</sub>H<sub>29</sub>N<sub>3</sub>NaO<sub>6</sub>) [M+Na]<sup>+</sup>: 418.1954, *found* 418.1947.

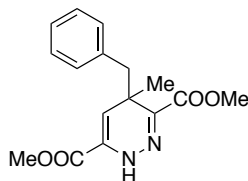


**Methyl 6-acetoxy-4-(4-(benzyloxy)cyclohexyl)-4-methyl-1,4-dihydropyridazine-3-carboxylate (C3)** Following the procedure described, the utilization of 4-(prop-1-en-2-yl)cyclohexyl benzoate (260.0 mg, 1.0 mmol) afforded the title compound as a liquid (292.0 mg, 71% yield) by using Hexane/EtOAc (1:1) as eluent. Mixture of two isomers (*cis* : *trans* = 1:3). **<sup>1</sup>H NMR (400 MHz, CDCl<sub>3</sub>)** δ 8.05 – 7.97 (m, 3H), 7.61 – 7.49 (m, 1H), 7.16 – 7.37 (m, 2H), 5.68 (d, *J* = 2.3 Hz, 0.75H), 5.58 (d, *J* = 2.2 Hz, 0.25H), 5.26 (s, 0.75H), 4.87 – 4.80 (m, 0.25H), 3.86 – 3.84 (m, 3H), 3.82 (s, 3H), 2.24 – 2.00 (m, 3H), 1.68 – 1.44 (m, 9H) ppm. **<sup>13</sup>C NMR (101 MHz, CDCl<sub>3</sub>)** δ 166.1, 165.6, 164.5, 161.5, 136.2, 136.1, 132.7, 131.0, 130.7, 129.6, 129.5, 128.3, 128.3, 127.4, 127.3, 114.1, 113.6, 73.6, 69.5, 52.6, 52.6, 52.2, 44.9, 39.8, 39.3, 31.5, 31.4, 29.9, 29.8, 28.2, 26.9, 26.5, 24.4, 22.4, 18.7 ppm. **IR (neat):** 3356, 2948, 1708, 1580, 1436, 1347, 1322, 1269, 1215, 1191, 1100, 1069, 1915, 959, 911, 816, 765, 710 cm<sup>-1</sup>. **Mp:** 56 °C. **HRMS calcd.** for (C<sub>22</sub>H<sub>26</sub>N<sub>2</sub>NaO<sub>6</sub>) [M+Na]<sup>+</sup>: 437.1689, *found* 437.1683.



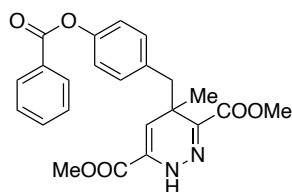
**Dimethyl 4-benzyl-1,4-dihydropyridazine-3,6-dicarboxylate (C4)** Following the procedure described, the utilization of allylbenzene (88.6 mg, 0.75 mmol) afforded the title compound as an oil (170 mg, 79% yield) by using Hexane/EtOAc (3:1) as eluent.

**<sup>1</sup>H NMR (500 MHz, CDCl<sub>3</sub>)** δ 8.31 (s, 1H), 7.31 – 7.26 (m, 2H), 7.24 – 7.19 (m, 1H), 7.14 (d, *J* = 7.2 Hz, 2H), 5.82 (dd, *J* = 6.3, 2.4 Hz, 1H), 3.92 (dt, *J* = 8.7, 5.9 Hz, 1H), 3.83 (s, 3H), 3.78 (s, 3H), 2.73 (dd, *J* = 13.0, 5.5 Hz, 1H), 2.64 (dd, *J* = 13.0, 8.7 Hz, 1H) ppm. **<sup>13</sup>C NMR (126 MHz, CDCl<sub>3</sub>)** 164.7, 161.8, 137.0, 133.5, 129.7, 129.6, 128.5, 126.7, 109.9, 52.7, 52.6, 39.7, 34.0 ppm. **IR (neat):** 3352, 3027, 2953, 2853, 1707, 1589, 1438, 1346, 1273, 1195, 1113, 958, 813, 745, 700 cm<sup>-1</sup>. **HRMS *calcd.*** for (C<sub>15</sub>H<sub>16</sub>N<sub>2</sub>NaO<sub>4</sub>) [M+Na]<sup>+</sup>: 311.1002, *found* 311.1002.



**Dimethyl 4-benzyl-4-methyl-1,4-dihydropyridazine-3,6-dicarboxylate (C5)**

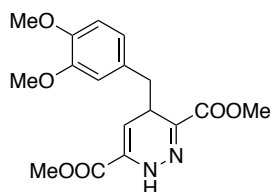
Following the procedure described, the utilization of (2-methylallyl)benzene (79.3 mg, 0.6 mmol) afforded the title compound as a gum (145 mg, 80% yield) by using Hexane/EtOAc (3:1) as eluent. **<sup>1</sup>H NMR (500 MHz, CDCl<sub>3</sub>)** δ 7.84 (s, 1H), 7.25 – 7.13 (m, 3H), 7.07 (d, *J* = 7.2 Hz, 2H), 5.52 (s, 1H), 3.81 (s, 3H), 3.80 (s, 3H), 3.35 (d, *J* = 13.4 Hz, 1H), 2.68 (d, *J* = 13.4 Hz, 1H), 1.53 (s, 3H) ppm. **<sup>13</sup>C NMR (126 MHz, CDCl<sub>3</sub>)** δ 164.7, 161.6, 137.2, 135.7, 130.5, 128.2, 127.1, 126.6, 116.5, 52.7, 52.3, 46.8, 38.0, 28.4 ppm. **IR (neat):** 3361, 3028, 2953, 2849, 1709, 1579, 1435, 1345, 1273, 1194, 1102, 958, 914, 815, 763, 740, 702 cm<sup>-1</sup>. **HRMS *calcd.*** for (C<sub>16</sub>H<sub>18</sub>N<sub>2</sub>NaO<sub>4</sub>) [M+Na]<sup>+</sup>: 325.1159, *found* 325.1150.



**Dimethyl 4-(4-(benzyloxy)benzyl)-4-methyl-1,4-dihydropyridazine-3,6-**

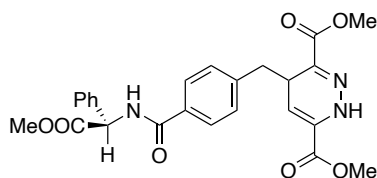
**dicarboxylate (C6)** Following the procedure described, the utilization of 4-(2-methylallyl)phenyl benzoate (151.4 mg, 0.6 mmol) afforded the title compound as a gum (183 mg, 72% yield) by using Hexane/Acetone (4:1) as eluent. **<sup>1</sup>H NMR (500 MHz, CDCl<sub>3</sub>)** δ 8.24 – 8.14 (m, 2H), 7.85 (d, *J* = 2.2 Hz, 1H), 7.67 – 7.60 (m, 1H), 7.54 – 7.47 (m, 2H), 7.14 (d, *J* = 8.6 Hz, 2H), 7.10 (d, *J* = 8.6 Hz, 2H), 5.54 (d, *J* = 2.2 Hz, 1H), 3.84 (s, 3H), 3.83 (s, 3H), 3.37 (d, *J* = 13.5 Hz, 1H), 2.73 (d, *J* = 13.5 Hz, 1H), 1.55 (s, 3H) ppm. **<sup>13</sup>C NMR (126 MHz, CDCl<sub>3</sub>)** δ 165.3, 164.7, 161.6, 149.8, 135.6, 134.9, 133.7, 131.5, 130.3, 129.8, 128.7, 127.3, 121.4, 116.2, 52.8, 52.4, 46.2, 38.0,

28.3 ppm. **IR (neat):** 3376, 2953, 2853, 1731, 1578, 1507, 1437, 1347, 1267, 1199, 1106, 1064, 1024, 765, 709  $\text{cm}^{-1}$ . **HRMS calcd.** for  $(\text{C}_{23}\text{H}_{22}\text{N}_2\text{NaO}_6)$   $[\text{M}+\text{Na}]^+$ : 445.1370, *found* 445.1375.



**Dimethyl 4-(3,4-dimethoxybenzyl)-1,4-dihydropyridazine-3,6-dicarboxylate (C7)**

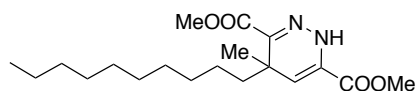
Following the procedure described, the utilization of 4-allyl-1,2-dimethoxybenzene (178.2 mg, 1.0 mmol) afforded the title compound as an off-white solid (329 mg, 94% yield) by using Hexane/Acetone (4:1) as eluent.  **$^1\text{H}$  NMR (400 MHz,  $\text{CDCl}_3$ )**  $\delta$  8.28 (d,  $J = 2.3$  Hz, 1H), 6.79 (d,  $J = 8.0$  Hz, 1H), 6.69 (d,  $J = 2.0$  Hz, 1H), 6.67 – 6.64 (m, 1H), 5.82 (dd,  $J = 6.3, 2.4$  Hz, 1H), 3.93 – 3.87 (m, 1H), 3.86 (s, 3H), 3.86 (s, 3H), 3.83 (s, 3H), 3.80 (s, 3H), 2.69 (dd,  $J = 13.1, 5.6$  Hz, 1H), 2.58 (dd,  $J = 13.1, 8.7$  Hz, 1H) ppm.  **$^{13}\text{C}$  NMR (101 MHz,  $\text{CDCl}_3$ )**  $\delta$  164.9, 161.9, 148.9, 147.9, 133.7, 129.6, 129.5, 121.7, 112.8, 111.3, 110.1, 56.0, 56.0, 52.8, 52.7, 39.2, 34.2 ppm. **IR (neat):** 3356, 2999, 2953, 2839, 1721, 1590, 1515, 1439, 1346, 1274, 1195, 1157, 1114, 1028, 761  $\text{cm}^{-1}$ . **Mp:** 105.5  $^\circ\text{C}$ . **HRMS calcd.** for  $(\text{C}_{17}\text{H}_{20}\text{N}_2\text{NaO}_6)$   $[\text{M}+\text{Na}]^+$ : 371.1214, *found* 371.1222.



**Dimethyl 4-((R)-2-methoxy-2-oxo-1-phenylethyl)carbamoylbenzyl)-1,4-dihydropyridazine-3,6-dicarboxylate (C8)**

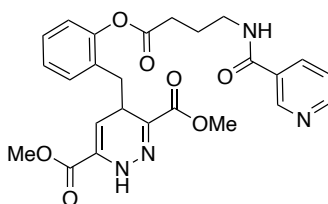
Following the procedure described, the utilization of Methyl (*R*)-2-(4-allylbenzamido)-2-phenylacetate (290 mg, 0.94 mmol) afforded the title compound as an off-white solid (400 mg, 89% yield) by using Hexane/EA (1:2) as eluent.  **$^1\text{H}$  NMR (400 MHz,  $\text{CDCl}_3$ )**  $\delta$  8.32 (s, 1H), 7.75 (d,  $J = 7.7$  Hz, 2H), 7.44 (d,  $J = 7.2$  Hz, 2H), 7.42 – 7.31 (m, 3H), 7.22 (d,  $J = 8.1$  Hz, 2H), 7.13 (d,  $J = 6.8$  Hz, 1H), 5.77 (d,  $J = 6.9$  Hz, 1H), 5.73 (m, 1H), 3.98 – 3.88 (m, 1H), 3.82 (s, 3H), 3.80 (s, 3H), 3.77 (s, 3H), 2.79 (dd,  $J = 12.8, 5.5$  Hz, 1H), 2.68 (dd,  $J = 13.0, 8.9$  Hz, 1H) ppm.  **$^{13}\text{C}$  NMR (101 MHz,  $\text{CDCl}_3$ )**  $\delta$  171.7, 166.5, 164.7, 161.7, 161.7, 141.4, 136.7, 133.0, 132.0, 129.8, 129.2, 128.7, 127.5, 127.4, 109.1, 56.9, 53.1, 52.8, 52.7, 39.5, 33.8 ppm. **IR (neat):** 3347, 3032, 3006, 2953, 1720, 1650, 1611, 1588,

1572, 1526, 1494, 1455, 1436, 1344, 1273, 1255, 1193, 1170, 1112, 1031, 1018, 991, 955, 816, 754, 728, 698, 647, 590, 542  $\text{cm}^{-1}$ . **Mp**: 56 °C. **HRMS** *calcd.* for  $(\text{C}_{25}\text{H}_{26}\text{N}_3\text{O}_7)$   $[\text{M}+\text{H}]^+$ : 480,1771, *found* 480,1765.



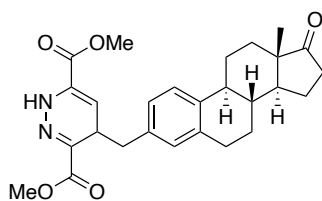
**Dimethyl 4-decyl-4-methyl-1,4-dihydropyridazine-3,6-dicarboxylate (C9)**

Following the procedure described, the utilization of 2-methyldodec-1-ene (188.0 mg, 1.0 mmol) afforded the title compound as a liquid (313.0 mg, 89% yield) by using Hexane/EtOAc (1:1) as eluent.  **$^1\text{H}$  NMR (400 MHz,  $\text{CDCl}_3$ )**  $\delta$  7.99 – 7.92 (m, 1H), 5.48 (d,  $J = 2.3$  Hz, 1H), 3.83 (s, 3H), 3.80 (s, 3H), 1.38 (s, 3H), 1.24 – 1.23 (m, 18H), 0.87 (t,  $J = 6.9$  Hz, 3H) ppm.  **$^{13}\text{C}$  NMR (101 MHz,  $\text{CDCl}_3$ )**  $\delta$  164.5, 161.8, 136.3, 127.2, 117.4, 52.6, 52.2, 41.4, 36.6, 32.0, 30.1, 29.7, 29.7, 29.6, 29.4, 28.8, 26.8, 22.8, 14.2. ppm. **IR (neat)**: 3364, 2923, 2853, 1713, 1579, 1435, 1343, 1279, 1197, 1101, 960, 816, 761, 735  $\text{cm}^{-1}$ . **HRMS** *calcd.* for  $(\text{C}_{19}\text{H}_{32}\text{N}_2\text{NaO}_4)$   $[\text{M}+\text{Na}]^+$ : 375.2260, *found* 375.2254.

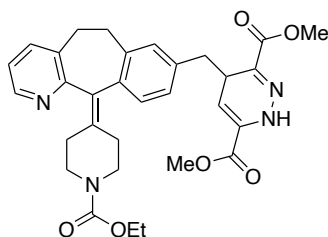


**Dimethyl 4-(2-((4-(nicotinamido)butanoyl)oxy)benzyl)-1,4-dihydropyridazine-3,6-dicarboxylate (C10)** Following the procedure described, the utilization of 2-allylphenyl 4-(nicotinamido)butanoate (324 mg, 1.0 mmol) afforded the title compound as an off-white solid (410 mg, 83% yield) by using Hexane/Acetone (1:1) as eluent.  **$^1\text{H}$  NMR (400 MHz,  $\text{CDCl}_3$ )**  $\delta$  9.04 (d,  $J = 1.5$  Hz, 1H), 8.69 (dd,  $J = 4.8, 1.7$  Hz, 1H), 8.36 (d,  $J = 2.6$  Hz, 1H), 8.16 – 8.14 (m, 1H), 7.39 – 7.33 (m, 1H), 7.29 – 7.23 (m, 1H), 7.17 – 7.09 (m, 3H), 7.04 (dd,  $J = 8.0, 1.3$  Hz, 1H), 5.70 (dd,  $J = 6.3, 2.4$  Hz, 1H), 3.90 – 3.85 (m, 1H), 3.82 (s, 3H), 3.71 (s, 3H), 3.69 – 3.58 (m, 2H), 2.87 – 2.79 (m, 2H), 2.75 (dd,  $J = 12.9, 5.3$  Hz, 1H), 2.45 (dd,  $J = 13.0, 9.4$  Hz, 1H), 2.12 (t,  $J = 6.7$  Hz, 2H) ppm.  **$^{13}\text{C}$  NMR (101 MHz,  $\text{CDCl}_3$ )**  $\delta$  172.6, 165.9, 165.0, 161.8, 152.2, 149.4, 148.2, 135.3, 133.2, 132.1, 130.4, 129.7, 128.7, 128.2, 126.1, 123.6, 122.6, 109.6, 52.8, 52.7, 39.7, 34.1, 32.4, 31.6, 24.2 ppm. **IR (neat)**: 3359, 3219, 3059, 3035, 2951, 1752, 1750, 1649, 1591, 1540, 1488, 1475, 1438, 1418, 1348, 1275, 1254, 1216, 1195, 1186, 1116, 1094, 1027, 954, 913, 813, 755, 728, 706, 646, 620, 566  $\text{cm}^{-1}$ . **Mp**: 58 °C. **HRMS**

*calcd.* for (C<sub>25</sub>H<sub>27</sub>N<sub>4</sub>O<sub>7</sub>) [M+H]<sup>+</sup> 495,1880.; *found* 495,1874.

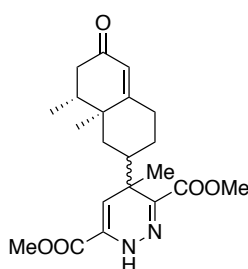


**Dimethyl 4-(((8R,9S,13S,14S)-13-methyl-17-oxo-7,8,9,11,12,13,14,15,16,17-decahydro-6H-cyclopenta[a]phenanthren-3-yl)methyl)-1,4-dihydropyridazine-3,6-dicarboxylate (C11)** Following the procedure described, the utilization of (8R,9S,13S,14S)-3-allyl-13-methyl-6,7,8,9,11,12,13,14,15,16-decahydro-17H-cyclopenta[a]phenanthren-17-one (294mg, 1.0 mmol) afforded the title compound as an off-white solid (406 mg, 88% yield) by using Hexane/EA (1:1) as eluent. <sup>1</sup>H NMR (400 MHz, CDCl<sub>3</sub>) δ 8.31 (t, *J* = 2.9 Hz, 1H), 7.20 (d, *J* = 5.6 Hz, 1H), 6.94 (d, *J* = 7.9 Hz, 1H), 6.89 (s, 1H), 5.58 – 5.56 (m, 1H), 3.92 – 3.84 (m, 1H), 3.84 (d, *J* = 1.3 Hz, 3H), 3.80 (d, *J* = 3.1 Hz, 3H), 2.92 – 2.84 (m, 2H), 2.68 (dd, *J* = 13.0, 5.2 Hz, 1H), 2.61 – 2.46 (m, 2H), 2.45 – 2.37 (m, 1H), 2.30 (d, *J* = 10.3 Hz, 1H), 2.21 – 1.91 (m, 4H), 1.66 – 1.62 (m, 1H), 1.56 – 1.44 (m, 5H), 0.91 (s, 3H) ppm. <sup>13</sup>C NMR (101 MHz, CDCl<sub>3</sub>) δ 220.9, 164.8, 161.9, 138.1, 136.6, 134.5, 133.8, 133.7, 130.2, 130.1, 129.5, 127.1, 127.0, 125.5, 110.2, 52.7, 52.6, 50.7, 48.1, 44.5, 39.2, 39.17, 38.4, 38.3, 36.0, 34.0, 31.8, 29.5, 29.4, 26.7, 26.67, 25.9, 21.7, 14.0 ppm. IR (neat): 3357, 2929, 2859, 1751, 1654, 1590, 1499, 1437, 1342, 1273, 1255, 1194, 1167, 1111, 1084, 1053, 1007, cm<sup>-1</sup>. Mp: 65 °C. HRMS *calcd.* for (C<sub>27</sub>H<sub>33</sub>N<sub>2</sub>O<sub>5</sub>) [M+H]<sup>+</sup>: 465,2389, *found* 465,2384.

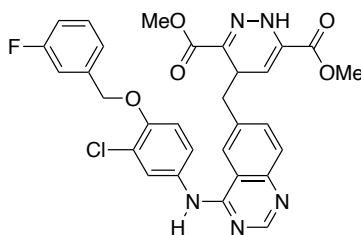


**Dimethyl 4-(((11-(1-(ethoxycarbonyl)piperidin-4-ylidene)-6,11-dihydro-5H-benzo[5,6]cyclohepta[1,2-b]pyridin-8-yl)methyl)-1,4-dihydropyridazine-3,6-dicarboxylate (C12)** Following the procedure described, the utilization of ethyl 4-(8-allyl-5,6-dihydro-11H-benzo[5,6]cyclohepta[1,2-b]pyridin-11-ylidene)piperidine-1-carboxylate (97 mg, 0.25 mmol) afforded the title compound as an off-white solid (86.5 mg, 62% yield) by using Hexane/EA (4:1) as eluent. <sup>1</sup>H NMR (400 MHz, CDCl<sub>3</sub>) δ 8.38 (d, *J* = 4.8 Hz, 1H), 8.32 (d, *J* = 5.4 Hz, 1H), 7.46 – 7.42 (m, 1H), 7.13 – 7.04 (m, 2H), 6.99 – 6.89 (m, 2H), 5.84 – 5.82 (m, 1H), 4.12 (q, *J* = 7.1 Hz, 2H), 3.91 – 3.72 (m, 6H), 3.70 – 3.59 (m, 3H), 3.35 (dtt, *J* = 13.6, 9.1, 4.6 Hz, 2H), 3.21 – 3.07 (m, 2H), 2.81

(dddd,  $J = 14.7, 12.6, 8.8, 5.5$  Hz, 2H), 2.68 – 2.53 (m, 2H), 2.50 – 2.43 (m, 1H), 2.40 – 2.24 (m, 3H), 1.24 (t,  $J = 7.1$  Hz, 3H) ppm.  $^{13}\text{C}$  NMR (101 MHz,  $\text{CDCl}_3$ )  $\delta$  164.7 (d,  $J = 2.6$  Hz), 161.8 (d,  $J = 3.3$  Hz), 157.8 (d,  $J = 11.3$  Hz), 146.6, 137.7 (d,  $J = 7.0$  Hz), 137.5, 136.8, 136.7, 136.2 (d,  $J = 2.9$  Hz), 135.1, 133.9 (d,  $J = 8.0$  Hz), 133.5 (d,  $J = 5.9$  Hz), 130.3 (d,  $J = 10.2$  Hz), 129.7, 129.4, 127.3, 127.2, 122.2 (d,  $J = 1.8$  Hz), 109.9, 61.4, 52.7, 52.4 (d,  $J = 5.5$  Hz), 44.9 (d,  $J = 6.2$  Hz), 39.3, 33.9 (d,  $J = 12.8$  Hz), 32.0, 31.9 (d,  $J = 2.9$  Hz), 31.7, 30.8, 30.6, 14.8 ppm. IR (neat): 3328, 2980, 2951, 2917, 2854, 2248, 2184, 1722, 1690, 1584, 1435, 1385, 1373, 1346, 1273, 1226, 1194, 1169, 1109, 1060, 1026, 996, 960, 817, 762, 727, 646, 541  $\text{cm}^{-1}$ . Mp: 81 °C. HRMS *calcd.* for  $(\text{C}_{31}\text{H}_{34}\text{N}_4\text{NaO}_6)$   $[\text{M}+\text{Na}]^+$ : 581,2376, *found* 581,2371.



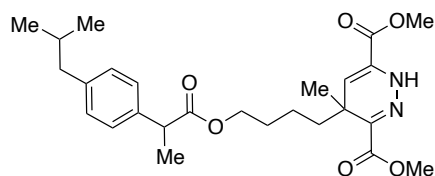
**Dimethyl 4-((8R,8aS)-8,8a-dimethyl-6-oxo-1,2,3,4,6,7,8,8a-octahydronaphthalen-2-yl)-4-methyl-1,4-dihydropyridazine-3,6-dicarboxylate (C13)** Following the procedure described, the utilization of (+)-nootkatone (174.4 mg, 0.8 mmol) afforded the title compound as a liquid (257.0 mg, 83% yield, 1:1 diastereomeric ratio) by using Hexane/EtOAc (2:1) as eluent.  $^1\text{H}$  NMR (400 MHz,  $\text{CDCl}_3$ )  $\delta$  8.01 (d,  $J = 8.5$  Hz, 1H), 5.73 (d,  $J = 5.9$  Hz, 1H), 5.51 (dd,  $J = 7.7, 2.3$  Hz, 1H), 3.84 – 3.82 (m, 6H), 2.63 – 2.36 (m, 3H), 2.31 – 2.17 (m, 2H), 1.91 (d,  $J = 13.0$  Hz, 2H), 1.79 – 1.70 (m, 1H), 1.62 (s, 1H), 1.48 (d,  $J = 6.5$  Hz, 3H), 1.27 – 1.17 (m, 1H), 1.11 – 1.02 (m, 3H), 1.01 – 0.83 (m, 5H) ppm.  $^{13}\text{C}$  NMR (101 MHz,  $\text{CDCl}_3$ )  $\delta$  199.5, 199.4, 170.06, 170.05, 164.5, 164.4, 161.4, 161.3, 136.2, 135.8, 127.6, 127.6, 124.6, 124.6, 113.0, 112.6, 52.6, 52.2, 42.8, 42.0, 41.9, 41.3, 40.9, 40.5, 40.3, 39.4, 39.3, 39.1, 36.3, 32.7, 32.7, 30.1, 26.9, 26.8, 24.5, 16.8, 16.7, 15.01, 14.95 ppm. Spectral data was in agreement with the literature.<sup>[10]</sup>



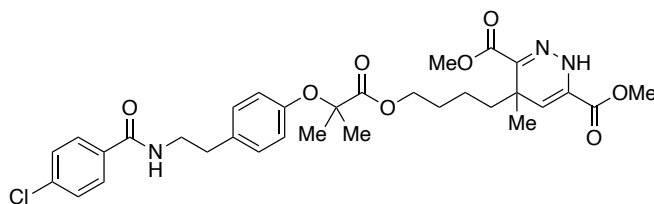
**Dimethyl 4-((4-((3-chloro-4-((3-fluorobenzyl)oxy)phenyl)amino)quinazolin-6-yl)methyl)-1,4-dihydropyridazine-3,6-dicarboxylate (C14)** Following the procedure



described, the utilization of 6-allyl-*N*-(3-chloro-4-((3-fluorobenzyl)oxy)phenyl)quinazolin-4-amine (419 mg, 1.0 mmol) afforded the title compound as an off-white solid (433 mg, 74% yield) by using Hexane/EA (1:1) as eluent. **<sup>1</sup>H NMR (400 MHz, DMF)** δ 10.59 (d, *J* = 2.5 Hz, 1H), 9.91 (s, 1H), 8.64 (s, 1H), 8.36 (d, *J* = 1.9 Hz, 1H), 8.23 (d, *J* = 2.6 Hz, 1H), 7.92 (dd, *J* = 9.0, 2.6 Hz, 1H), 7.77 (d, *J* = 8.5 Hz, 1H), 7.72 (dd, *J* = 8.5, 1.8 Hz, 1H), 7.52 (td, *J* = 8.0, 5.8 Hz, 1H), 7.46 – 7.38 (m, 2H), 7.35 (d, *J* = 9.1 Hz, 1H), 7.23 – 7.18 (m, 1H), 5.81 (dd, *J* = 6.2, 2.4 Hz, 1H), 5.34 (s, 2H), 4.17 – 3.98 (m, 1H), 3.79 (s, 3H), 3.70 (s, 3H), 2.90 – 2.79 (m, 2H) ppm. **<sup>13</sup>C NMR (101 MHz, DMF)** δ 166.1, 163.9 (d, *J* = 243.6 Hz), 162.6, 158.8, 155.2, 151.2, 150.2, 141.3 (d, *J* = 7.7 Hz), 137.0, 135.8, 135.1, 132.2, 131.6 (d, *J* = 8.4 Hz), 131.5, 129.1, 125.0, 124.5 (d, *J* = 2.9 Hz), 123.8, 123.0, 122.7, 116.3, 115.7 (d, *J* = 21.3 Hz), 115.4, 115.2 (d, *J* = 22.4 Hz), 109.3, 70.9 (d, *J* = 2.2 Hz), 53.1, 52.6, 34.4 ppm. **IR (neat):** 3347, 3330, 3020, 2952, 2900, 2846, 2805, 2702, 1725, 1716, 1628, 1593, 1496, 1455, 1438, 1418, 1391, 1272, 1221, 1201, 1111, 1061, 1013, 949, 932, 917, 853, 832, 816, 795, 776, 680, 570, 508, 441 cm<sup>-1</sup>. **Mp:** 200 °C. **HRMS** *calcd.* for (C<sub>30</sub>H<sub>26</sub>ClFN<sub>5</sub>O<sub>5</sub>) [M+H]<sup>+</sup>: 590,1606, *found* 590,1601.

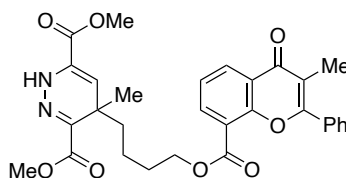


**Dimethyl 4-(4-((2-(4-isobutylphenyl)propanoyl)oxy)butyl)-4-methyl-1,4-dihydropyridazine-3,6-dicarboxylate (C15)** Following the procedure described, the utilization of 5-methylhex-5-en-1-yl 2-(4-isobutylphenyl)propanoate (302 mg, 1.0 mmol) afforded the title compound as a liquid (418 mg, 89% yield) by using Hexane/EA (10:1) as eluent. **<sup>1</sup>H NMR (400 MHz, CDCl<sub>3</sub>)** δ 7.99 (s, 1H), 7.17 (d, *J* = 8.1 Hz, 2H), 7.07 (d, *J* = 8.0 Hz, 2H), 5.45 (d, *J* = 2.3 Hz, 1H), 4.07 – 3.79 (m, 2H), 3.83 (s, 3H), 3.79 (d, *J* = 1.8 Hz, 3H), 3.66 (q, *J* = 7.2 Hz, 1H), 2.43 (d, *J* = 7.2 Hz, 2H), 2.19 (td, *J* = 11.0, 2.6 Hz, 1H), 1.83 (dt, *J* = 13.6, 6.9 Hz, 1H), 1.64 – 1.51 (m, 2H), 1.46 (d, *J* = 7.2 Hz, 3H), 1.36 (s, 3H), 1.30 – 1.13 (m, 3H), 0.90 (s, 3H), 0.88 (s, 3H) ppm. **<sup>13</sup>C NMR (101 MHz, CDCl<sub>3</sub>)** δ 174.8, 174.8, 164.5, 161.6, 140.6, 137.9, 135.8, 129.4, 127.3, 127.2, 116.8, 64.5, 64.5, 52.6, 52.2, 45.3, 45.1, 40.9, 40.8, 36.5, 30.3, 28.8, 28.7, 23.1, 23.0, 22.5, 18.6, 18.6 ppm. **IR (neat):** 3359, 2953, 2930, 2867, 1713, 1664, 1578, 1512, 1458, 1436, 1376, 1342, 1278, 1244, 1199, 1164, 1095, 959, 848, 815, 762, 736 cm<sup>-1</sup>. **HRMS** *calcd.* for (C<sub>26</sub>H<sub>36</sub>N<sub>2</sub>NaO<sub>6</sub>) [M+H]<sup>+</sup>: 495,2471, *found* 495,2466.



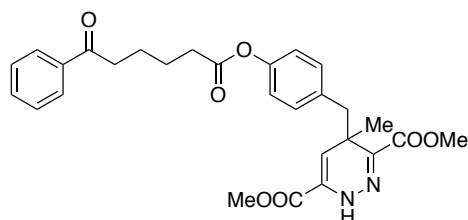
**Dimethyl 4-(4-((2-(4-(2-(4-chlorobenzamido)ethyl)phenoxy)-2-methylpropanoyl)oxy)butyl)-4-methyl-1,4-dihydropyridazine-3,6-dicarboxylate**

**(C16)** Following the procedure described, the utilization of 5-methylhex-5-en-1-yl 2-(4-(2-(4-chlorobenzamido)ethyl)phenoxy)-2-methylpropanoate (457 mg, 1.0 mmol) afforded the title compound as a white solid (584 mg, 93% yield) by using Hexane/EA (1:1) as eluent.  $^1\text{H NMR}$  (400 MHz,  $\text{CDCl}_3$ )  $\delta$  8.01 (s, 1H), 7.61 (d,  $J = 8.5$  Hz, 2H), 7.35 (d,  $J = 8.4$  Hz, 2H), 7.06 (d,  $J = 8.6$  Hz, 2H), 6.76 (d,  $J = 8.6$  Hz, 2H), 6.26 (t,  $J = 5.4$  Hz, 1H), 5.42 (d,  $J = 2.2$  Hz, 1H), 4.18 – 4.08 (m, 2H), 3.80 (s, 3H), 3.76 (s, 3H), 3.64 (q,  $J = 6.9$  Hz, 2H), 2.84 (t,  $J = 6.9$  Hz, 2H), 2.26 – 2.15 (m, 1H), 1.64 – 1.60 (m, 2H), 1.54 (d,  $J = 1.8$  Hz, 6H), 1.35 (s, 3H), 1.30 – 1.13 (m, 3H) ppm.  $^{13}\text{C NMR}$  (101 MHz,  $\text{CDCl}_3$ )  $\delta$  174.3, 166.5, 164.5, 161.6, 154.2, 137.7, 135.7, 133.2, 132.6, 129.5, 128.9, 128.4, 127.4, 119.7, 116.7, 79.3, 65.1, 52.6, 52.2, 41.4, 40.9, 36.5, 34.8, 28.8, 28.7, 25.5, 25.4, 23.0 ppm. **IR (neat):** 3340, 2992, 2951, 2862, 1715, 1641, 1611, 1596, 1541, 1508, 1486, 1436, 1380, 1365, 1343, 1278, 1234, 1197, 1176, 1137, 1014, 956, 911, 846, 815, 759, 729, 524  $\text{cm}^{-1}$ . **Mp:** 43 °C. **HRMS calcd.** for  $(\text{C}_{32}\text{H}_{39}\text{ClN}_3\text{O}_8)$   $[\text{M}+\text{H}]^+$ : 628,2426, *found* 628,2420.



**Dimethyl 4-methyl-4-(4-((3-methyl-4-oxo-2-phenyl-4H-chromene-8-carbonyl)oxy)butyl)-1,4-dihydropyridazine-3,6-dicarboxylate (C17)** Following the procedure described, the utilization of 5-methylhex-5-en-1-yl 3-methyl-4-oxo-2-phenyl-4H-chromene-8-carboxylate (376 mg, 1.0 mmol) afforded the title compound as a white solid (504 mg, 92% yield) by using Hexane/EA (2:1) as eluent.  $^1\text{H NMR}$  (400 MHz,  $\text{CDCl}_3$ )  $\delta$  8.45 (dd,  $J = 8.0, 1.8$  Hz, 1H), 8.23 (dd,  $J = 7.5, 1.8$  Hz, 1H), 7.97 (d,  $J = 2.3$  Hz, 1H), 7.82 – 7.74 (m, 2H), 7.55 – 7.49 (m, 3H), 7.43 (t,  $J = 7.7$  Hz, 1H), 5.41 (d,  $J = 2.3$  Hz, 1H), 4.31 (t,  $J = 6.8$  Hz, 2H), 3.78 (s, 3H), 3.74 (s, 3H), 2.23 (s, 3H), 1.81 – 1.68 (m, 3H), 1.38 – 1.33 (m, 4H), 1.28 – 1.18 (m, 2H) ppm.  $^{13}\text{C NMR}$  (101 MHz,  $\text{CDCl}_3$ )  $\delta$  178.4, 164.5, 164.4, 161.6, 161.2, 154.6, 136.2, 135.7, 133.2,

130.8, 130.6, 129.5, 128.5, 127.4, 124.1, 123.4, 120.9, 117.7, 116.7, 65.3 52.6, 52.2, 40.8, 36.5, 28.8, 28.7, 23.1, 11.9 ppm. **IR (neat):** 3353, 3020, 2860, 1708, 1624, 1602, 1574, 1478, 1436, 1392, 1373, 1343, 1278, 1197, 1179, 1126, 1096, 1068, 1039, 1023, 958, 916, 853, 815, 758, 730, 698, 644, 542, 471, 443  $\text{cm}^{-1}$ . **Mp:** 48 °C. **HRMS calcd.** for  $(\text{C}_{30}\text{H}_{30}\text{N}_2\text{NaO}_8)$   $[\text{M}+\text{Na}]^+$ : 569,1900, *found* 569,1894.



**Dimethyl 4-methyl-4-(4-((6-oxo-6-phenylhexanoyl)oxy)benzyl)-1,4-dihydropyridazine-3,6-dicarboxylate (C18)** Following the procedure described, the utilization of 4-(2-methylallyl)phenyl 6-oxo-6-phenylhexanoate (477.0 mg, 1.42 mmol) afforded the title compound as a liquid (608.0 mg, 85% yield) by using Hexane/EtOAc (1:1) as eluent.  **$^1\text{H}$  NMR (400 MHz,  $\text{CDCl}_3$ )**  $\delta$  7.95 (dd,  $J = 8.4, 1.3$  Hz, 2H), 7.87 (d,  $J = 2.0$  Hz, 1H), 7.58 – 7.50 (m, 1H), 7.48 – 7.40 (m, 2H), 7.10 – 7.03 (m, 2H), 6.97 – 6.91 (m, 2H), 5.50 (d,  $J = 2.3$  Hz, 1H), 3.80 (s, 6H), 3.32 (d,  $J = 13.5$  Hz, 1H), 3.03 (t,  $J = 6.8$  Hz, 2H), 2.68 (d,  $J = 13.5$  Hz, 1H), 2.59 (t,  $J = 7.0$  Hz, 2H), 1.97 – 1.75 (m, 4H), 1.51 (s, 3H) ppm.  **$^{13}\text{C}$  NMR (101 MHz,  $\text{CDCl}_3$ )**  $\delta$  199.8, 171.9, 164.6, 161.4, 149.4, 136.9, 135.5, 134.6, 133.1, 131.3, 128.7, 128.1, 127.1, 121.1, 116.1, 52.6, 52.2, 46.0, 38.1, 37.8, 34.3, 28.2, 24.6, 23.6 ppm. **IR (neat):** 3366, 2953, 1713, 1684, 1579, 1506, 1436, 1345, 1274, 1196, 1166, 1126, 1104, 909, 727, 690, 648  $\text{cm}^{-1}$ . **HRMS calcd.** for  $(\text{C}_{28}\text{H}_{30}\text{N}_2\text{NaO}_7)$   $[\text{M}+\text{Na}]^+$ : 529.1951, *found* 529.1945.

---

### 3.7.3 General Procedures for Trifluoromethylation

**General procedure A:** An oven-dried 20 mL Schlenk tube containing a stir bar was charged with 4-CzIPN (4.8 mg, 3 mol%), CuCl<sub>2</sub> (5.6 mg, 20 mol%), Phenanthroline (10.8 mg, 30 mol%), proaromatic precursor (0.2 mmol, 1.0 equiv) and Togni's reagent I (132.0 mg, 2.0 equiv). The Schlenk tube was connected to a vacuum line where it was evacuated and back-filled with Ar at least three times. Acetone (8.0 mL) was then added followed by BTMG (34.0 μL, 1.0 equiv) under argon atmosphere. The reaction mixture was sonicated, then placed in a temperature-controlled photoreactor maintained at 40 °C and stirred for 16-24 h under continuous light irradiation from blue LEDs ( $\lambda = 451$  nm). The reaction mixture was diluted with Et<sub>2</sub>O, and then quenched with aqueous NaCl. (Trifluoromethyl)benzene (internal standard, 0.2 mmol) was added to the reaction mixture for calculating the <sup>19</sup>F NMR yield. The reaction mixture was extracted into Et<sub>2</sub>O (3x). The organic phase was dried with anhydrous Na<sub>2</sub>SO<sub>4</sub>, filtered, and concentrated. The residue was purified by flash column chromatography on silica gel.

**General procedure B:** An oven-dried 20 mL Schlenk tube containing a stir bar was charged with 4-CzIPN (4.8 mg, 3 mol%), Cu(CF<sub>3</sub>)<sub>3</sub>bpy (85.2 mg, 1.0 equiv), proaromatic precursor (0.2 mmol, 1.0 equiv) and Togni's reagent I (99.2 mg, 1.5 equiv). The Schlenk tube was connected to a vacuum line where it was evacuated and back-filled with Ar at least three times. DMF (10.0 mL) was added followed by BTMG (34 μL, 1.0 equiv) under argon atmosphere. The reaction mixture was sonicated, then placed in a temperature-controlled photoreactor maintained at 40 °C and stirred for 16-24 h under continuous light irradiation from blue LEDs ( $\lambda = 451$  nm). The reaction mixture was diluted with Et<sub>2</sub>O, and then quenched with aqueous NaCl. (Trifluoromethyl)benzene (internal standard, 0.2 mmol) was added to the reaction mixture for calculating the <sup>19</sup>F NMR yield. The reaction mixture was extracted into Et<sub>2</sub>O (3x). The organic phase was dried with anhydrous Na<sub>2</sub>SO<sub>4</sub>, filtered, and concentrated. The residue was purified by flash column chromatography on silica gel.

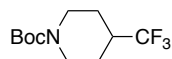
**General procedure C:** An oven-dried 20 mL Schlenk tube containing a stir bar was charged with 4-CzIPN (4.8 mg, 3 mol%), Cu(CF<sub>3</sub>)<sub>3</sub>bpy (85.2 mg, 1.0 equiv), proaromatic precursor (0.2 mmol, 1.0 – 1.5 equiv), K<sub>2</sub>S<sub>2</sub>O<sub>8</sub> (81.2 mg, 1.5 equiv) and NaHCO<sub>3</sub> (33.2 mg, 2.0 equiv). The Schlenk tube was connected to a vacuum line where

---

it was evacuated and back-filled with Ar at least three times. CH<sub>3</sub>CN (8.0 mL) was added under argon atmosphere. The reaction mixture was sonicated, then placed in a temperature-controlled photoreactor maintained at 40 °C and stirred for 16-24 h under continuous light irradiation from blue LEDs ( $\lambda = 451$  nm). The reaction mixture was diluted with Et<sub>2</sub>O, and then quenched with aqueous NaCl. (Trifluoromethyl)benzene (internal standard, 0.2 mmol) was added to the reaction mixture for calculating the <sup>19</sup>F NMR yield. The reaction mixture was extracted into Et<sub>2</sub>O (3x). The organic phase was dried with anhydrous Na<sub>2</sub>SO<sub>4</sub>, filtered, and concentrated. The residue was purified by flash column chromatography on silica gel.

**General procedure D:** An oven-dried 20 mL reaction tube containing a stir bar was charged with Cu(CF<sub>3</sub>)<sub>3</sub>bpy (85.2 mg, 1.0 equiv), Substrate (0.2 mmol, 1.0 – 1.5 equiv). The reaction tube was connected to a vacuum line where it was evacuated and back-filled with Ar at least three times. Acetone (4.0 mL) was added under argon atmosphere. The reaction mixture was stirred for 18 h under continuous light irradiation from 370 nm Kessil LED lamps. The reaction was diluted with Et<sub>2</sub>O, and then quenched with aqueous NaCl. (Trifluoromethyl)benzene (internal standard, 0.2 mmol) or 1-fluoro-3-nitrobenzene (internal standard, 0.2 mmol) was added to the reaction mixture for calculating the <sup>19</sup>F NMR yield. The reaction mixture was extracted into Et<sub>2</sub>O (3x). The organic phase was dried with anhydrous Na<sub>2</sub>SO<sub>4</sub>, filtered, and carefully concentrated. The residue was purified by flash column chromatography on silica gel.

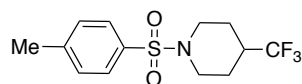
## Product Characterization



**tert-butyl 4-(trifluoromethyl)piperidine-1-carboxylate (3)** Prepared following general procedure A using 4-CzIPN (4.8 mg, 3 mol%), CuCl<sub>2</sub> (5.6 mg, 20 mol%), Phenanthroline (10.8 mg, 30 mol%), *tert*-butyl 4-(2-methyl-4-oxo-1,2,3,4-tetrahydroquinazolin-2-yl)piperidine-1-carboxylate (**A1**) (69.0 mg, 0.2 mmol, 1.0 equiv), BTMG (34 μL, 1.0 equiv), Togni's reagent I (132.0 mg, 2.0 equiv) and 8.0 mL of Acetone. Product was obtained as a colorless solid (38.1 mg, 75% yield) by using Hexane/EtOAc (10:1) as eluent. (78% <sup>19</sup>F NMR yield against internal standard). <sup>19</sup>F NMR (376 MHz, CDCl<sub>3</sub>) δ -74.04 (d, *J* = 8.5 Hz) ppm. <sup>1</sup>H NMR (400 MHz, CDCl<sub>3</sub>) δ 4.26 – 4.08 (m, 2H), 2.67 (t, *J* = 12.2 Hz, 1H), 2.20 – 2.10 (m, 1H), 1.90 – 1.74 (m, 2H), 1.44 (s, 11H) ppm. <sup>13</sup>C NMR (101 MHz, CDCl<sub>3</sub>) δ 154.5, 127.1 (q, *J* = 278.2 Hz), 79.8, 42.6 (br), 40.5 (q, *J* = 27.5 Hz), 28.3, 24.4 ppm. Spectral data was in agreement with the literature<sup>[11]</sup>.

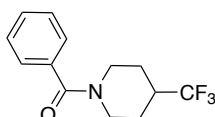
Prepared following general procedure C using 4-CzIPN (4.8 mg, 3 mol%), Cu(CF<sub>3</sub>)<sub>3</sub>bpy (85.2 mg, 0.2 mmol, 1.0 equiv), diethyl 4-(1-(*tert*-butoxycarbonyl)piperidin-4-yl)-2,6-dimethyl-1,4-dihydropyridine-3,5-dicarboxylate (**B2**) (87.3 mg, 0.2 mmol, 1.0 equiv), K<sub>2</sub>S<sub>2</sub>O<sub>8</sub> (81.2 mg, 1.5 equiv) and NaHCO<sub>3</sub> (33.2 mg, 2.0 equiv) and 8.0 mL of CH<sub>3</sub>CN. Product was obtained as a colorless solid (38.1 mg, 72% yield) by using Hexane/EtOAc (10:1) as eluent. (80% <sup>19</sup>F NMR yield against internal standard).

Prepared following general procedure D using Cu(CF<sub>3</sub>)<sub>3</sub>bpy (85.2 mg, 0.2 mmol, 1.0 equiv), dimethyl 4-(1-(*tert*-butoxycarbonyl)piperidin-4-yl)-4-methyl-1,4-dihydropyridazine-3,6-dicarboxylate (**C2**) (118.6 mg, 0.3 mmol, 1.5 equiv), and 4.0 mL of Acetone. Product was obtained as a colorless solid (18.0 mg, 36% yield) by using Hexane/EtOAc (10:1) as eluent. (42% <sup>19</sup>F NMR yield against internal standard).

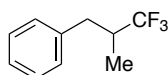


**1-tosyl-4-(trifluoromethyl)piperidine (4)** Prepared following general procedure A using 4-CzIPN (4.8 mg, 3 mol%), CuCl<sub>2</sub> (5.6 mg, 20 mol%), Phenanthroline (10.8 mg, 30 mol%), 2-methyl-2-(1-tosylpiperidin-4-yl)-2,3-dihydroquinazolin-4(1*H*)-one (**A2**) (79.8 mg, 0.2 mmol, 1.0 equiv), BTMG (34 μL, 1.0 equiv), Togni's reagent I (132.0 mg,

2.0 equiv) and 8.0 mL of Acetone. Product was obtained as a colorless solid (34.5 mg, 56% yield) by using Hexane/EtOAc (10:1) as eluent. (60%  $^{19}\text{F}$  NMR yield against internal standard).  $^{19}\text{F}$  NMR (376 MHz,  $\text{CDCl}_3$ )  $\delta$  -73.85 (d,  $J$  = 7.8 Hz) ppm.  $^1\text{H}$  NMR (400 MHz,  $\text{CDCl}_3$ )  $\delta$  7.63 (d,  $J$  = 8.3 Hz, 2H), 7.42 – 7.28 (m, 2H), 4.01 – 3.61 (m, 2H), 2.43 (s, 3H), 2.24 (t,  $J$  = 12.2, 2H), 2.00 – 1.81 (m, 3H), 1.76 – 1.57 (m, 2H) ppm.  $^{13}\text{C}$  NMR (101 MHz,  $\text{CDCl}_3$ )  $\delta$  143.9, 133.0, 129.9, 127.8, 126.9 (q,  $J$  = 278.1 Hz), 45.1, 39.8 (q,  $J$  = 27.8 Hz), 24.1 (q,  $J$  = 2.1 Hz), 21.6 ppm. Spectral data was in agreement with the literature.<sup>[12]</sup>

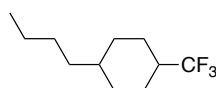


**phenyl(4-(trifluoromethyl)piperidin-1-yl)methanone (5)** Prepared following general procedure A using 4-CzIPN (4.8 mg, 3 mol%),  $\text{CuCl}_2$  (5.6 mg, 20 mol%), Phenanthroline (10.8 mg, 30 mol%), 2-(1-benzoylpiperidin-4-yl)-2-methyl-2,3-dihydroquinazolin-4(1*H*)-one (**A3**) (69.8 mg, 0.2 mmol, 1.0 equiv), BTMG (34  $\mu\text{L}$ , 1.0 equiv), Togni's reagent I (132.0 mg, 2.0 equiv) and 8.0 mL of Acetone. Product was obtained as a colorless liquid (26.7 mg, 52% yield) by using Hexane/EtOAc (50:1) as eluent. (58%  $^{19}\text{F}$  NMR yield against internal standard).  $^{19}\text{F}$  NMR (376 MHz,  $\text{CDCl}_3$ )  $\delta$  -73.93 (d,  $J$  = 8.1 Hz) ppm.  $^1\text{H}$  NMR (500 MHz,  $\text{CDCl}_3$ )  $\delta$  7.43 – 7.39 (m, 5H), 4.84 (br, 1H), 3.89 (br, 1H), 2.89 (br, 2H), 2.31 (m, 1H), 1.78 (m, 4H) ppm.  $^{13}\text{C}$  NMR (101 MHz,  $\text{CDCl}_3$ )  $\delta$  170.6, 135.8, 129.9, 128.7, 127.0 (q,  $J$  = 276.0 Hz), 125.6, 46.6, 40.8 (q,  $J$  = 27.4 Hz), 25.1 ppm. Spectral data was in agreement with the literature.<sup>[13]</sup>

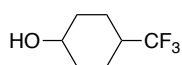


**(3,3,3-trifluoro-2-methylpropyl)benzene (6)** Prepared following general procedure A using 4-CzIPN (4.8 mg, 3 mol%),  $\text{CuCl}_2$  (5.6 mg, 20 mol%), Phenanthroline (10.8 mg, 30 mol%), 2-phenyl-2-(1-phenylpropan-2-yl)-2,3-dihydroquinazolin-4(1*H*)-one (**A4**) (68.4 mg, 0.2 mmol, 1.0 equiv), BTMG (34  $\mu\text{L}$ , 1.0 equiv), Togni's reagent I (132.0 mg, 2.0 equiv) and 8.0 mL of Acetone. Product was obtained as a colorless liquid (17.7 mg, 45% yield) by using Pentane as eluent. (48%  $^{19}\text{F}$  NMR yield against internal standard).  $^{19}\text{F}$  NMR (376 MHz,  $\text{CD}_2\text{Cl}_2$ )  $\delta$  -73.81 (d,  $J$  = 8.1 Hz) ppm.  $^1\text{H}$  NMR (400 MHz,  $\text{CD}_2\text{Cl}_2$ )  $\delta$  77.33 – 7.30 (m, 2H), 7.25 (d,  $J$  = 6.9 Hz, 1H), 7.18 (dd,  $J$  = 7.8, 1.4 Hz, 2H), 3.09 (m, 1H), 2.47– 2.44 (m, 2H), 1.00 (d,  $J$  = 6.8 Hz, 3H) ppm.  $^{13}\text{C}$  NMR (126 MHz,  $\text{CDCl}_3$ )  $\delta$  138.3, 129.2, 128.7, 128.3 (q,  $J$  = 279.5 Hz), 126.8, 40.2 (q,  $J$  = 26.1 Hz), 35.8 (q,  $J$  = 2.8 Hz), 12.2 (q,  $J$  = 2.8 Hz) ppm. Spectral data was in agreement with

the literature.<sup>[14]</sup>

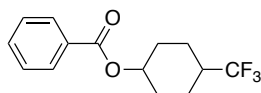


**1-butyl-4-(trifluoromethyl)cyclohexane (7)** Prepared following general procedure A using 4-CzIPN (4.8 mg, 3 mol%), CuCl<sub>2</sub> (5.6 mg, 20 mol%), Phenanthroline (10.8 mg, 30 mol%), 2-(4-butylcyclohexyl)-2-methyl-2,3-dihydroquinazolin-4(1H)-one (**A5**) (60.0 mg, 0.2 mmol, 1.0 equiv), BTMG (34  $\mu$ L, 1.0 equiv), Togni's reagent I (132.0 mg, 2.0 equiv) and 8.0 mL of Acetone. Product was obtained as a colorless liquid (25.6 mg, 61% yield) by using Hexane as eluent. (71% <sup>19</sup>F NMR yield against internal standard). Mixture of two isomers (*cis* : *trans* = 1:3.3). <sup>19</sup>F NMR (376 MHz, CDCl<sub>3</sub>)  $\delta$  -72.46 (d, *J* = 9.8 Hz), -73.97 (d, *J* = 8.5 Hz) ppm. <sup>1</sup>H NMR (400 MHz, CDCl<sub>3</sub>)  $\delta$  2.08 – 1.80 (m, 4H), 1.66 – 1.46 (m, 2H), 1.38 – 1.14 (m, 8H), 0.97 – 0.82 (m, 5H) ppm. <sup>13</sup>C NMR (101 MHz, CDCl<sub>3</sub>)  $\delta$  128.1 (q, *J* = 277.1 Hz), 127.9 (q, *J* = 277.1 Hz), 42.1 (q, *J* = 26.2 Hz), 40.9 (q, *J* = 25.6 Hz), 36.9, 36.7, 32.9, 31.6, 29.8, 29.1, 28.4, 25.1, 25.0, 25.0, 25.0, 22.92, 22.87, 20.6, 20.5, 14.08, 14.05 ppm. Spectral data was in agreement with the literature.<sup>[12]</sup>



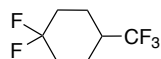
**4-(trifluoromethyl)cyclohexan-1-ol (8)** Prepared following general procedure A using 4-CzIPN (4.8 mg, 3 mol%), CuCl<sub>2</sub> (5.6 mg, 20 mol%), Phenanthroline (10.8 mg, 30 mol%), 2-(4-hydroxycyclohexyl)-2-methyl-2,3-dihydroquinazolin-4(1H)-one (**A6**) (52.0 mg, 0.2 mmol, 1.0 equiv), BTMG (34  $\mu$ L, 1.0 equiv), Togni's reagent I (132.0 mg, 2.0 equiv) and 8.0 mL of Acetone. Product was obtained as a colorless liquid (19.0 mg, 57% yield) by using Hexane/EtOAc (3:1) as eluent. (60% <sup>19</sup>F NMR yield against internal standard). Mixture of two isomers (*cis* : *trans* = 1:1.6). *cis*-diastereomer: <sup>19</sup>F NMR (376 MHz, CDCl<sub>3</sub>)  $\delta$  -73.73 (d, *J* = 8.5 Hz) ppm. <sup>1</sup>H NMR (400 MHz, CDCl<sub>3</sub>)  $\delta$  4.07 (m, 1H), 2.10 – 1.96 (m, 1H), 1.92 – 1.82 (m, 2H), 1.80 – 1.65 (m, 4H), 1.53 (m, 2H), 1.39 (br, 1H) ppm. <sup>13</sup>C NMR (126 MHz, CDCl<sub>3</sub>)  $\delta$  127.8 (q, *J* = 278.6 Hz), 65.0, 41.3 (q, *J* = 26.6 Hz), 31.3, 18.9 (d, *J* = 2.8 Hz) ppm. *trans*-diastereomer: <sup>19</sup>F NMR (376 MHz, CDCl<sub>3</sub>)  $\delta$  -73.52 (d, *J* = 7.8 Hz) ppm. <sup>1</sup>H NMR (400 MHz, CDCl<sub>3</sub>)  $\delta$  3.70 – 3.28 (m, 1H), 2.20 – 1.87 (m, 6H), 1.48 – 1.10 (m, 4H) ppm. <sup>13</sup>C NMR (101 MHz, CDCl<sub>3</sub>)  $\delta$  127.6 (q, *J* = 278.5 Hz), 69.7, 40.9 (q, *J* = 26.7 Hz), 33.8, 23.3 (q, *J* = 2.6 Hz) ppm. Spectral data was in agreement with the literature.<sup>[15]</sup>





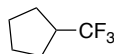
**4-(trifluoromethyl)cyclohexyl benzoate (9)** Prepared following general procedure A using 4-CzIPN (4.8 mg, 3 mol%), CuCl<sub>2</sub> (5.6 mg, 20 mol%), Phenanthroline (10.8 mg, 30 mol%), 4-(2-methyl-4-oxo-1,2,3,4-tetrahydroquinazolin-2-yl)cyclohexyl benzoate (**A7**) (72.8 mg, 0.2 mmol, 1.0 equiv), BTMG (34 μL, 1.0 equiv), Togni's reagent I (132.0 mg, 2.0 equiv) and 8.0 mL of Acetone. Product was obtained as a colorless liquid (47.8 mg, 87% yield) by using Hexane/EtOAc (10:1) as eluent. (83% <sup>19</sup>F NMR yield against internal standard). Mixture of two isomers (*cis* : *trans* = 1:1.2). **<sup>19</sup>F NMR (376 MHz, CDCl<sub>3</sub>)** δ -73.42 (d, *J* = 7.9 Hz), -73.92 (d, *J* = 8.3 Hz) ppm. **<sup>1</sup>H NMR (400 MHz, CDCl<sub>3</sub>)** δ 8.07 – 8.03 (m, 2H), 7.62 – 7.52 (m, 1H), 7.45 (ddd, *J* = 9.3, 8.2, 6.9 Hz, 2H), 5.36 – 4.87 (m, 1H), 2.31 – 1.99 (m, 4H), 1.93 – 1.46 (m, 5H) ppm. **<sup>13</sup>C NMR (101 MHz, CDCl<sub>3</sub>)** δ 166.0, 165.8, 133.1, 133.0, 130.7, 130.6, 129.69, 129.65, 128.5, 128.4, 127.7 (q, *J* = 278.4 Hz), 127.6 (q, *J* = 278.5 Hz), 72.4, 68.6, 41.3, 41.2 (q, *J* = 27.1 Hz), 41.1 (q, *J* = 27.1 Hz), 30.3, 28.7, 23.4 (q, *J* = 2.7 Hz), 19.9 (q, *J* = 2.8 Hz) ppm. **IR (neat):** 2952, 1714, 1601, 1584, 1451, 1396, 1359, 1329, 1314, 1281, 1202, 1179, 1135, 1110, 1086, 1070 1025, 998, 923, 880, 711, 649 cm<sup>-1</sup>. **HRMS *calcd.* for (C<sub>14</sub>H<sub>14</sub>F<sub>3</sub>O<sub>2</sub>) [M-H]<sup>+</sup>: 271.0946, found 271.0931.**

Prepared following general procedure D, using Cu(CF<sub>3</sub>)<sub>3</sub>bpy (85.2 mg, 0.2 mmol, 1.0 equiv), dimethyl 4-(4-(benzoyloxy)cyclohexyl)-4-methyl-1,4-dihydropyridazine-3,6-dicarboxylate (**C3**) (124.3 mg, 0.3 mmol, 1.5 equiv), and 4.0 mL of Acetone. Product was obtained as a colorless liquid (26.6 mg, 49% yield) by using Hexane/EtOAc (10:1) as eluent. (45% <sup>19</sup>F NMR yield against internal standard). Mixture of two isomers (*cis* : *trans* = 1:1.5).

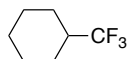


**1,1-difluoro-4-(trifluoromethyl)cyclohexane (10)** Prepared following general procedure A using 4-CzIPN (4.8 mg, 3 mol%), CuCl<sub>2</sub> (5.6 mg, 20 mol%), Phenanthroline (10.8 mg, 30 mol%), 2-(4,4-difluorocyclohexyl)-2-methyl-2,3-dihydroquinazolin-4(1*H*)-one (**A8**) (56.0 mg, 0.2 mmol, 1.0 equiv), BTMG (34 μL, 1.0 equiv), Togni's reagent I (132.0 mg, 2.0 equiv) and 8.0 mL of Acetone. Product could not be isolated due to its volatility, 1,1,1-trifluorotoluene (24.4 μL, 0.2 mmol, 1.0 equiv) was added as an internal standard for <sup>19</sup>F NMR analysis. (66% yield – average of two trials: 62% yield and 69% yield). **<sup>19</sup>F NMR (376 MHz, Acetone)** δ -73.98 (d, *J* = 8.5

Hz), -93.20 (d,  $J = 237.5$  Hz), -103.55 (d,  $J = 239.8$  Hz) ppm. Spectral data was in agreement with literature.<sup>[13]</sup>



**(Trifluoromethyl)cyclopentane (11)** Prepared following general procedure A using 4-CzIPN (4.8 mg, 3 mol%), CuCl<sub>2</sub> (5.6 mg, 20 mol%), Bathphenanthroline (20.0 mg, 30 mol%), 2-cyclopentyl-2-methyl-2,3-dihydroquinazolin-4(1*H*)-one (**A9**) (46.0 mg, 0.2 mmol, 1.0 equiv), KH<sub>2</sub>PO<sub>4</sub> (0.4 mmol, 2.0 equiv), KF (0.4 mmol, 2.0 equiv), Togni's reagent I (132.0 mg, 2.0 equiv) and 10.0 mL of DMF. Product could not be isolated due to its volatility, 1,1,1-trifluorotoluene (24.4 μL, 0.2 mmol, 1.0 equiv) was added as an internal standard for <sup>19</sup>F NMR analysis. (35% yield – average of two trials: 36% yield and 34% yield). <sup>19</sup>F NMR (376 MHz, Acetone) δ -71.99 (d,  $J = 9.8$  Hz) ppm. Data in agreement with published values.<sup>[16]</sup>

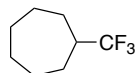


**(Trifluoromethyl)cyclohexane (12)** Prepared following general procedure A using 4-CzIPN (4.8 mg, 3 mol%), CuCl<sub>2</sub> (5.6 mg, 20 mol%), Phenanthroline (10.8 mg, 30 mol%), 2-cyclohexyl-2-methyl-2,3-dihydroquinazolin-4(1*H*)-one (**A10**) (48.8 mg, 0.2 mmol, 1.0 equiv), BTMG (34 μL, 1.0 equiv), Togni's reagent I (132.0 mg, 2.0 equiv) and 8.0 mL of Acetone. Product could not be isolated due to its volatility, 1,1,1-trifluorotoluene (24.4 μL, 0.2 mmol, 1.0 equiv) was added as an internal standard for <sup>19</sup>F NMR analysis. (83% yield – average of two trials: 82% yield and 83% yield). <sup>19</sup>F NMR (376 MHz, Acetone) δ -74.82 (d,  $J = 9.0$  Hz) ppm. Data in agreement with published values.<sup>[17]</sup>

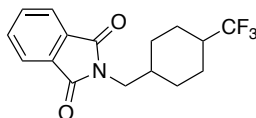
Prepared following general procedure C, using 4-CzIPN (4.8 mg, 3 mol%), Cu(CF<sub>3</sub>)<sub>3</sub>bpy (85.2 mg, 0.2 mmol, 1.0 equiv), diethyl 4-cyclohexyl-2,6-dimethyl-1,4-dihydropyridine-3,5-dicarboxylate (**B1**) (67.0 mg, 0.2 mmol, 1.0 equiv), K<sub>2</sub>S<sub>2</sub>O<sub>8</sub> (81.2 mg, 1.5 equiv) and NaHCO<sub>3</sub> (33.2 mg, 2.0 equiv) and 8.0 mL of CH<sub>3</sub>CN. Product could not be isolated due to its volatility, 1,1,1-trifluorotoluene (24.4 μL, 0.2 mmol, 1.0 equiv) was added as an internal standard for <sup>19</sup>F NMR analysis. (85% yield – average of two trials: 85% yield and 84% yield). <sup>19</sup>F NMR (376 MHz, CD<sub>3</sub>CN) δ -74.94 (d,  $J = 8.8$  Hz) ppm.

Prepared following general procedure D, using Cu(CF<sub>3</sub>)<sub>3</sub>bpy (85.2 mg, 0.2 mmol, 1.0 equiv), dimethyl 4-cyclohexyl-4-methyl-1,4-dihydropyridazine-3,6-dicarboxylate (**C1**) (88.2 mg, 0.3 mmol, 1.5 equiv), Togni's reagent I (33.0 mg, 0.5 equiv) and BTMG (16.8

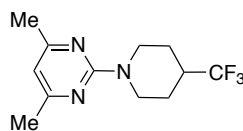
mg, 0.5 equiv) and 8.0 mL of Acetone. Product could not be isolated due to its volatility, 1,1,1-trifluorotoluene (24.4  $\mu$ L, 0.2 mmol, 1.0 equiv) was added as an internal standard for  $^{19}\text{F}$  NMR analysis. (70% yield – average of two trials: 71% yield and 70% yield).  $^{19}\text{F}$  NMR (376 MHz,  $\text{CD}_3\text{CN}$ )  $\delta$  -74.77 (d,  $J$  = 8.8 Hz) ppm.



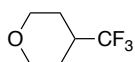
**(trifluoromethyl)cycloheptane (13)** Prepared following general procedure A using 4-CzIPN (4.8 mg, 3 mol%),  $\text{CuCl}_2$  (5.6 mg, 20 mol%), Bathphenanthroline (20.0 mg, 30 mol%), 2-cycloheptyl-2-methyl-2,3-dihydroquinazolin-4(1*H*)-one (**A11**) (51.6 mg, 0.2 mmol, 1.0 equiv),  $\text{KH}_2\text{PO}_4$  (0.4 mmol, 2.0 equiv),  $\text{KF}$  (0.4 mmol, 2.0 equiv), Togni's reagent I (132.0 mg, 2.0 equiv) and 10.0 mL of DMF. Product could not be isolated due to its volatility, 1,1,1-trifluorotoluene (24.4  $\mu$ L, 0.2 mmol, 1.0 equiv) was added as an internal standard for  $^{19}\text{F}$  NMR analysis. (58% yield – average of two trials: 58% yield and 57% yield).  $^{19}\text{F}$  NMR (376 MHz, Acetone)  $\delta$  -74.06 (d,  $J$  = 6.3 Hz) ppm. Data in agreement with published values.<sup>[16]</sup>



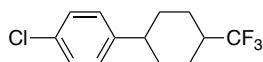
**2-((4-(trifluoromethyl)cyclohexyl)methyl)isoindoline-1,3-dione (14)** Prepared following general procedure A using 4-CzIPN (4.8 mg, 3 mol%),  $\text{CuCl}_2$  (5.6 mg, 20 mol%), Phenanthroline (10.8 mg, 30 mol%), 2-((4-(2-methyl-4-oxo-1,2,3,4-tetrahydroquinazolin-2-yl)cyclohexyl)methyl)isoindoline-1,3-dione (**A12**) (80.6 mg, 0.2 mmol, 1.0 equiv), BTMG (34  $\mu$ L, 1.0 equiv), Togni's reagent I (132.0 mg, 2.0 equiv) and 8.0 mL of Acetone. Product was obtained as a colorless liquid (40.3 mg, 65% yield) by using Hexane/DCM (1:5) as eluent. (65%  $^{19}\text{F}$  NMR yield against internal standard). Mixture of two isomers (*cis* : *trans* = 1:3.3).  $^{19}\text{F}$  NMR (376 MHz,  $\text{CDCl}_3$ )  $\delta$  -71.86 – -72.18 (br), -73.89 (d,  $J$  = 8.0 Hz) ppm.  $^1\text{H}$  NMR (400 MHz,  $\text{CDCl}_3$ )  $\delta$  8.03 – 7.75 (m, 2H), 7.78 – 7.54 (m, 2H), 3.61 (dd,  $J$  = 55.0, 7.3 Hz, 2H), 2.21 – 1.45 (m, 7H), 1.37 – 0.97 (m, 3H) ppm.  $^{13}\text{C}$  NMR (101 MHz,  $\text{CDCl}_3$ )  $\delta$  168.5, 168.4, 133.9, 132.0, 131.9, 127.9 (q,  $J$  = 277.7 Hz), 127.6 (q,  $J$  = 277.2 Hz), 123.2, 43.5, 40.2, 41.6 (q,  $J$  = 26.7 Hz), 40.4 (q,  $J$  = 26.2 Hz), 36.4, 32.3, 29.0, 26.1, 24.3 (q,  $J$  = 2.7 Hz), 20.5 (q,  $J$  = 2.7 Hz) ppm. Spectral data was in agreement with the literature.<sup>[12]</sup>



**4,6-dimethyl-2-(4-(trifluoromethyl)piperidin-1-yl)pyrimidine (15)** Prepared following general procedure A using 4-CzIPN (4.8 mg, 3 mol%), CuCl<sub>2</sub> (5.6 mg, 20 mol%), Phenanthroline (10.8 mg, 30 mol%), 2-(1-(4,6-dimethylpyrimidin-2-yl)piperidin-4-yl)-2-methyl-2,3-dihydroquinazolin-4(1*H*)-one (**A13**) (70.2 mg, 0.2 mmol, 1.0 equiv), BTMG (34 μL, 1.0 equiv), Togni's reagent I (132.0 mg, 2.0 equiv) and 8.0 mL of Acetone. Product was obtained as a colorless liquid (29.8 mg, 57% yield) by using Hexane/EtOAc (15:1) as eluent. (57% <sup>19</sup>F NMR yield against internal standard). <sup>19</sup>F NMR (376 MHz, CDCl<sub>3</sub>) δ -73.96 (d, *J* = 8.4 Hz) ppm. <sup>1</sup>H NMR (400 MHz, CDCl<sub>3</sub>) δ 6.27 (s, 1H), 4.98 (d, *J* = 15.0 Hz, 2H), 2.78 (td, *J* = 13.0, 2.7 Hz, 2H), 2.29 – 2.27 (m, 7H), 2.00 – 1.86 (m, 2H), 1.68 – 1.43 (m, 2H) ppm. <sup>13</sup>C NMR (101 MHz, CDCl<sub>3</sub>) δ 167.2, 161.7, 127.5 (q, *J* = 278.3 Hz), 109.2, 42.8, 41.1 (q, *J* = 27.2 Hz), 24.5 (q, *J* = 2.6 Hz), 24.2 ppm. IR (neat): 3009, 2948, 2866, 1570, 1492, 1436, 1377, 1335, 1279, 1250, 1166, 1145, 1093, 1008, 819, 786, 698, 687 cm<sup>-1</sup>. HRMS calcd. for (C<sub>12</sub>H<sub>17</sub>F<sub>3</sub>N<sub>3</sub>) [M+H]<sup>+</sup>: 260.1375, found 260.1369.



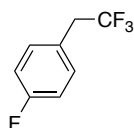
**4-(trifluoromethyl)tetrahydro-2*H*-pyran (16)** Prepared following general procedure A using 4-CzIPN (4.8 mg, 3 mol%), CuCl<sub>2</sub> (5.6 mg, 20 mol%), Phenanthroline (10.8 mg, 30 mol%), 2-methyl-2-(tetrahydro-2*H*-pyran-4-yl)-2,3-dihydroquinazolin-4(1*H*)-one (**A14**) (49.2 mg, 0.2 mmol, 1.0 equiv), BTMG (34 μL, 1.0 equiv), Togni's reagent I (132.0 mg, 2.0 equiv) and 8.0 mL of Acetone. Product could not be isolated due to its volatility, 1,1,1-trifluorotoluene (24.4 μL, 0.2 mmol, 1.0 equiv) was added as an internal standard for <sup>19</sup>F NMR analysis. (80% yield – average of two entries: 79% yield and 81% yield). <sup>19</sup>F NMR (376 MHz, Acetone) δ -75.36 (d, *J* = 8.5 Hz) ppm. Data in agreement with published values.<sup>[13]</sup>



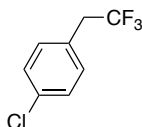
**1-chloro-4-((1*S*,4*S*)-4-(trifluoromethyl)cyclohexyl)benzene (17)** Prepared following general procedure A using 4-CzIPN (4.8 mg, 3 mol%), CuCl<sub>2</sub> (5.6 mg, 20 mol%), Phenanthroline (10.8 mg, 30 mol%), (S)-2-((1*S*,4*R*)-4-(4-chlorophenyl)cyclohexyl)-2-methyl-2,3-dihydroquinazolin-4(1*H*)-one (**A15**) (70.8 mg, 0.2 mmol, 1.0 equiv), BTMG (34 μL, 1.0 equiv), Togni's reagent I (132.0 mg, 2.0 equiv) and 8.0 mL of Acetone. Product was obtained as a colorless solid (39.8 mg, 76% yield) by using Hexane as eluent. (70% <sup>19</sup>F NMR yield against internal standard). Mixture of two isomers (*cis* : *trans* = 1:10). <sup>19</sup>F NMR (376 MHz, CDCl<sub>3</sub>) δ -68.61(br), -73.86 (d, *J* =

8.0 Hz) ppm. **<sup>1</sup>H NMR (400 MHz, CDCl<sub>3</sub>)** δ 7.34 – 7.25 (m, 2H), 7.21 – 7.08 (m, 2H), 2.74 – 2.44 (m, 1H), 2.21 – 1.88 (m, 5H), 1.60 – 1.32 (m, 4H) ppm. **<sup>13</sup>C NMR (101 MHz, CDCl<sub>3</sub>)** δ 144.9, 132.0, 128.7, 128.5 (q, *J* = 13.2 Hz), 128.2, 43.0, 41.6 (q, *J* = 26.6 Hz), 32.6, 29.0, 25.3 (q, *J* = 2.6 Hz), 23.2 ppm. **IR (neat):** 2943, 2871, 1493, 1454, 1392, 1336, 1260, 1234, 1169, 1134, 1117, 1091, 1076, 1028, 1019, 995, 971, 903, 823 cm<sup>-1</sup>. **Mp:** 40 °C. **HRMS calcd. for (C<sub>13</sub>H<sub>14</sub>ClF<sub>3</sub>) [M]<sup>+</sup>:** 262.0736, **found** 262.0734.

Prepared following general procedure C, using 4-CzIPN (4.8 mg, 3 mol%), Cu(CF<sub>3</sub>)<sub>3</sub>bpy (85.2 mg, 0.2mmol, 1.0 equiv), diethyl 2-(4-chlorophenyl)-5-(2,6-dimethyl-1,4-dihydropyridin-4-yl)cyclohexane-1,3-dicarboxylate (**B3**) (89.0 mg, 0.2 mmol, 1.0 equiv), K<sub>2</sub>S<sub>2</sub>O<sub>8</sub> (81.2 mg, 1.5 equiv) and NaHCO<sub>3</sub> (33.2 mg, 2.0 equiv) and 8.0 mL of CH<sub>3</sub>CN. Product was obtained as a colorless solid (27.2 mg, 52% yield) by using Hexane as eluent. (57% <sup>19</sup>F NMR yield against internal standard). Mixture of two isomers (*cis* : *trans* = 1:6).

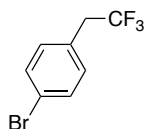


**1-fluoro-4-(2,2,2-trifluoroethyl)benzene (18)** Prepared following general procedure A using 4-CzIPN (4.8 mg, 3 mol%), CuCl<sub>2</sub> (5.6 mg, 20 mol%), di(pyridin-2-yl)methanone (11.0 mg, 30 mol%), 2-(4-fluorobenzyl)-2-methyl-2,3-dihydroquinazolin-4(1*H*)-one (**A16**) (54.0 mg, 0.2 mmol, 1.0 equiv), KH<sub>2</sub>PO<sub>4</sub> (0.4 mmol, 2.0 equiv), Togni's reagent I (132.0 mg, 2.0 equiv) and 10.0 mL of DMF. Product could not be isolated due to its volatility, 1,1,1-trifluorotoluene (24.4 μL, 0.2 mmol, 1.0 equiv) was added as an internal standard for <sup>19</sup>F NMR analysis. (86% yield – average of two trials: 85% yield and 86% yield). **<sup>19</sup>F NMR (376 MHz, CDCl<sub>3</sub>)** δ -66.40 (t, *J* = 10.7 Hz), -114.05 – -114.48 (m) ppm. Spectral data was in agreement with the literature<sup>[18]</sup>.

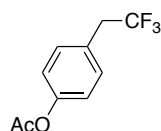


**1-chloro-4-(2,2,2-trifluoroethyl)benzene (19)** Prepared following general procedure A using 4-CzIPN (4.8 mg, 3 mol%), CuCl<sub>2</sub> (5.6 mg, 20 mol%), di(pyridin-2-yl)methanone (11.0 mg, 30 mol%), 2-(4-chlorobenzyl)-2-methyl-2,3-dihydroquinazolin-4(1*H*)-one (**A17**) (57.2 mg, 0.2 mmol, 1.0 equiv), KH<sub>2</sub>PO<sub>4</sub> (0.4 mmol, 2.0 equiv), Togni's reagent I (132.0 mg, 2.0 equiv) and 10.0 mL of DMF. Product

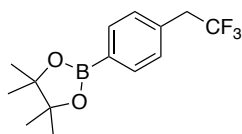
was obtained as a colorless liquid (28.9 mg, 74% yield) by using Pentane as eluent. (84%  $^{19}\text{F}$  NMR yield against internal standard).  $^{19}\text{F}$  NMR (376 MHz,  $\text{CDCl}_3$ )  $\delta$  -66.16 (t,  $J$  = 10.8 Hz) ppm.  $^1\text{H}$  NMR (400 MHz,  $\text{CDCl}_3$ )  $\delta$  7.36 – 7.32 (m, 2H), 7.25 – 7.21 (m, 2H), 3.34 (q,  $J$  = 10.7 Hz, 2H) ppm.  $^{13}\text{C}$  NMR (126 MHz,  $\text{CDCl}_3$ )  $\delta$  134.4, 131.6, 129.1, 128.73 (q,  $J$  = 2.9 Hz), 125.6 (q,  $J$  = 276.7 Hz), 39.8 (q,  $J$  = 30.0 Hz) ppm. Spectral data was in agreement with the literature.<sup>[18]</sup>



**1-bromo-4-(2,2,2-trifluoroethyl)benzene (20)** Prepared following general procedure A using 4-CzIPN (4.8 mg, 3 mol%),  $\text{CuCl}_2$  (5.6 mg, 20 mol%), di(pyridin-2-yl)methanone (11.0 mg, 30 mol%), 2-(4-bromobenzyl)-2-methyl-2,3-dihydroquinazolin-4(1H)-one (**A18**) (66.0 mg, 0.2 mmol, 1.0 equiv),  $\text{KH}_2\text{PO}_4$  (0.4 mmol, 2.0 equiv), Togni's reagent I (132.0 mg, 2.0 equiv) and 10.0 mL of DMF. Product was obtained as a colorless liquid (23.6 mg, 50% yield) by using Pentane as eluent. (60%  $^{19}\text{F}$  NMR yield against internal standard).  $^{19}\text{F}$  NMR (376 MHz,  $\text{CDCl}_3$ )  $\delta$  -62.90 (s), -66.02 (t,  $J$  = 10.6 Hz) ppm.  $^1\text{H}$  NMR (400 MHz,  $\text{CDCl}_3$ )  $\delta$  7.56 – 7.42 (m, 2H), 7.22 – 7.07 (m, 2H), 3.33 (q,  $J$  = 10.7 Hz, 2H) ppm.  $^{13}\text{C}$  NMR (126 MHz,  $\text{CDCl}_3$ )  $\delta$  132.0, 131.9, 129.2 (q,  $J$  = 3.1 Hz), 125.6 (q,  $J$  = 274.8 Hz), 39.8 (q,  $J$  = 29.6 Hz) ppm. Spectral data was in agreement with the literature.<sup>[19]</sup>

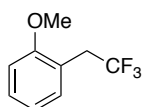


**4-(2,2,2-trifluoroethyl)phenyl acetate (21)** Prepared following general procedure A using 4-CzIPN (4.8 mg, 3 mol%),  $\text{CuCl}_2$  (5.6 mg, 20 mol%), di(pyridin-2-yl)methanone (11.0 mg, 30 mol%), 4-((2-methyl-4-oxo-1,2,3,4-tetrahydroquinazolin-2-yl)methyl)phenyl acetate (**A19**) (62.0 mg, 0.2 mmol, 1.0 equiv),  $\text{KH}_2\text{PO}_4$  (0.4 mmol, 2.0 equiv), Togni's reagent I (132.0 mg, 2.0 equiv) and 10.0 mL of DMF. Product was obtained as a colorless liquid (33.0 mg, 75% yield) by using Hexane/EtOAc (8:1) as eluent. (70%  $^{19}\text{F}$  NMR yield against internal standard).  $^{19}\text{F}$  NMR (376 MHz,  $\text{CDCl}_3$ )  $\delta$  -66.12 (t,  $J$  = 10.7 Hz) ppm.  $^1\text{H}$  NMR (400 MHz,  $\text{CDCl}_3$ )  $\delta$  7.35 – 7.27 (m, 2H), 7.09 (d,  $J$  = 8.6 Hz, 2H), 3.36 (q,  $J$  = 10.8 Hz, 2H), 2.29 (s, 3H) ppm.  $^{13}\text{C}$  NMR (101 MHz,  $\text{CDCl}_3$ )  $\delta$  169.4, 150.5, 131.3, 127.7 (q,  $J$  = 2.9 Hz), 125.6 (q,  $J$  = 276.9 Hz), 121.9, 39.6 (q,  $J$  = 29.9 Hz), 21.1 ppm. Spectral data was in agreement with the literature.<sup>[1]</sup>

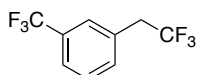


**4,4,5,5-tetramethyl-2-(4-(2,2,2-trifluoroethyl)phenyl)-1,3,2-dioxaborolane (22)**

Prepared following general procedure A using 4-CzIPN (4.8 mg, 3 mol%), CuCl<sub>2</sub> (5.6 mg, 20 mol%), di(pyridin-2-yl)methanone (11.0 mg, 30 mol%), 2-methyl-2-(4-(4,4,5,5-tetramethyl-1,3,2-dioxaborolan-2-yl)benzyl)-2,3-dihydroquinazolin-4(1*H*)-one (**A20**) (75.7 mg, 0.2 mmol, 1.0 equiv), KH<sub>2</sub>PO<sub>4</sub> (0.4 mmol, 2.0 equiv), Togni's reagent I (132.0 mg, 2.0 equiv) and 10.0 mL of DMF. Product was obtained as a colorless solid (36.6 mg, 64% yield) by using Hexane/EtOAc (20:1) as eluent. (76% <sup>19</sup>F NMR yield against internal standard). <sup>19</sup>F NMR (376 MHz, CDCl<sub>3</sub>) δ -65.80 (t, *J* = 10.9 Hz) ppm. <sup>1</sup>H NMR (400 MHz, CDCl<sub>3</sub>) δ 7.83 – 7.79 (m, 2H), 7.36 – 7.28 (m, 2H), 3.38 (q, *J* = 10.8 Hz, 2H), 1.35 (s, 12H) ppm. <sup>13</sup>C NMR (101 MHz, CDCl<sub>3</sub>) δ 135.2, 133.3 (q, *J* = 2.8 Hz), 129.7, 125.8 (q, *J* = 276.6 Hz), 125.7, 84.1, 40.5 (q, *J* = 29.8 Hz), 25.0 ppm. Spectral data was in agreement with the literature.<sup>[14]</sup>

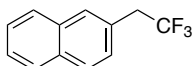


**1-methoxy-2-(2,2,2-trifluoroethyl)benzene (23)** Prepared following general procedure A using 4-CzIPN (4.8 mg, 3 mol%), CuCl<sub>2</sub> (5.6 mg, 20 mol%), di(pyridin-2-yl)methanone (11.0 mg, 30 mol%), 2-(2-methoxybenzyl)-2-methyl-2,3-dihydroquinazolin-4(1*H*)-one (**A21**) (56.4 mg, 0.2 mmol, 1.0 equiv), KH<sub>2</sub>PO<sub>4</sub> (0.4 mmol, 2.0 equiv), Togni's reagent I (132.0 mg, 2.0 equiv) and 10.0 mL of DMF. Product was obtained as a colorless liquid (28.4 mg, 75% yield) by using Hexane/EtOAc (20:1) as eluent. (79% <sup>19</sup>F NMR yield against internal standard). <sup>19</sup>F NMR (376 MHz, CDCl<sub>3</sub>) δ -65.62 (t, *J* = 10.9 Hz) ppm. <sup>1</sup>H NMR (500 MHz, CDCl<sub>3</sub>) δ 7.36 – 7.22 (m, 2H), 7.06 – 6.85 (m, 2H), 3.85 (s, 3H), 3.47 (q, *J* = 11.0 Hz, 2H) ppm. <sup>13</sup>C NMR (126 MHz, CDCl<sub>3</sub>) δ 158.1, 131.8, 129.6, 126.2 (q, *J* = 277.6 Hz), 120.6, 119.0 (q, *J* = 2.8 Hz), 111.0, 55.7, 33.5 (q, *J* = 30.3 Hz) ppm. Spectral data was in agreement with the literature.<sup>[14]</sup>

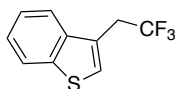


**1-(2,2,2-trifluoroethyl)-3-(trifluoromethyl)benzene (24)** Prepared following general procedure A using 4-CzIPN (4.8 mg, 3 mol%), CuCl<sub>2</sub> (5.6 mg, 20 mol%), di(pyridin-2-yl)methanone (11.0 mg, 30 mol%), 2-methyl-2-(3-(trifluoromethyl)benzyl)-2,3-

dihydroquinazolin-4(1*H*)-one (**A22**) (64.0 mg, 0.2 mmol, 1.0 equiv), KH<sub>2</sub>PO<sub>4</sub> (0.4 mmol, 2.0 equiv), Togni's reagent I (132.0 mg, 2.0 equiv) and 10.0 mL of DMF. Product could not be isolated due to its volatility, 1,1,1-trifluorotoluene (24.4  $\mu$ L, 0.2 mmol, 1.0 equiv) was added as an internal standard for <sup>19</sup>F NMR analysis. (82% yield – average of two trials: 84% yield and 80% yield). <sup>19</sup>F NMR (376 MHz, CDCl<sub>3</sub>)  $\delta$  -62.90, -66.03 (t, *J* = 10.6 Hz) ppm. <sup>1</sup>H NMR (400 MHz, CDCl<sub>3</sub>)  $\delta$  7.66 – 7.47 (m, 4H), 3.44 (q, *J* = 10.6 Hz, 2H) ppm. Spectral data was in agreement with the literature.<sup>[14]</sup>

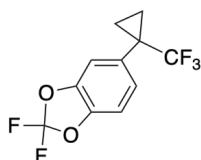


**2-(2,2,2-trifluoroethyl)naphthalene (25)** Prepared following general procedure A using 4-CzIPN (4.8 mg, 3 mol%), CuCl<sub>2</sub> (5.6 mg, 20 mol%), di(pyridin-2-yl)methanone (11.0 mg, 30 mol%), 2-methyl-2-(naphthalen-2-ylmethyl)-2,3-dihydroquinazolin-4(1*H*)-one (**A23**) (60.4 mg, 0.2 mmol, 1.0 equiv), KH<sub>2</sub>PO<sub>4</sub> (0.4 mmol, 2.0 equiv), Togni's reagent I (132.0 mg, 2.0 equiv) and 10.0 mL of DMF. Product was obtained as a white solid (30.8 mg, 73% yield) by using Hexane as eluent. (75% <sup>19</sup>F NMR yield against internal standard). <sup>19</sup>F NMR (376 MHz, CDCl<sub>3</sub>)  $\delta$  -65.70 (t, *J* = 10.9 Hz) ppm. <sup>1</sup>H NMR (400 MHz, CDCl<sub>3</sub>)  $\delta$  7.86 (d, *J* = 9.7 Hz, 3H), 7.79 (s, 1H), 7.58 – 7.52 (m, 2H), 7.48 – 7.39 (m, 1H), 3.55 (q, *J* = 10.8 Hz, 2H) ppm. <sup>13</sup>C NMR (101 MHz, CDCl<sub>3</sub>)  $\delta$  133.4, 133.0, 129.6, 128.5, 127.9, 127.7, 126.6, 126.5, 125.9 (q, *J* = 277.1 Hz), 40.5 (q, *J* = 29.7 Hz) ppm. Spectral data was in agreement with the literature.<sup>[14]</sup>

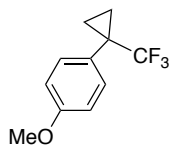


**3-(2,2,2-trifluoroethyl)benzo[*b*]thiophene (26)** Prepared following general procedure A using 4-CzIPN (4.8 mg, 3 mol%), CuCl<sub>2</sub> (5.6 mg, 20 mol%), di(pyridin-2-yl)methanone (11.0 mg, 30 mol%), 2-(benzo[*b*]thiophen-3-ylmethyl)-2-methyl-2,3-dihydroquinazolin-4(1*H*)-one (**A24**) (61.6 mg, 0.2 mmol, 1.0 equiv), KH<sub>2</sub>PO<sub>4</sub> (0.4 mmol, 2.0 equiv), Togni's reagent I (132.0 mg, 2.0 equiv) and 10.0 mL of DMF. Product was obtained as a colorless solid (33.7 mg, 78% yield) by using Hexane/EtOAc (50:1) as eluent. (80% <sup>19</sup>F NMR yield against internal standard). <sup>19</sup>F NMR (376 MHz, CDCl<sub>3</sub>)  $\delta$  -65.20 (t, *J* = 10.6 Hz) ppm. <sup>1</sup>H NMR (400 MHz, CDCl<sub>3</sub>)  $\delta$  7.96 – 7.84 (m, 1H), 7.83 – 7.70 (m, 1H), 7.54 – 7.32 (m, 3H), 3.66 (qd, *J* = 10.6, 0.8 Hz, 2H) ppm. <sup>13</sup>C NMR (101 MHz, CDCl<sub>3</sub>)  $\delta$  140.2, 138.6, 126.8, 125.7 (q, *J* = 29.7 Hz), 124.8, 124.7 (q, *J* = 3.0 Hz), 124.6, 123.0, 121.6, 33.3 (q, *J* = 31.3 Hz) ppm. Spectral data was in agreement with the literature.<sup>[14]</sup>

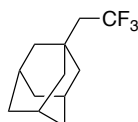




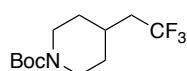
**2,2-difluoro-5-(1-(trifluoromethyl)cyclopropyl)benzo[d][1,3]dioxole (27)** Prepared following general procedure A using 4-CzIPN (4.8 mg, 3 mol%), CuCl<sub>2</sub> (5.6 mg, 20 mol%), Bathphenanthroline (20.0 mg, 30 mol%), 2-(1-(2,2-difluorobenzo[d][1,3]dioxol-5-yl)cyclopropyl)-2-methyl-2,3-dihydroquinazolin-4(1H)-one (**A25**) (71.6 mg, 0.2 mmol, 1.0 equiv), BTMG (34 μL, 1.0 equiv), Togni's reagent I (132.0 mg, 2.0 equiv) and 10.0 mL of DMF. Product was obtained as a colorless liquid (37.8 mg, 71% yield) by using Hexane as eluent. (75% <sup>19</sup>F NMR yield against internal standard). <sup>19</sup>F NMR (376 MHz, CDCl<sub>3</sub>) δ -50.00 (s, 2F), -70.51 (s, 3F) ppm. <sup>1</sup>H NMR (400 MHz, CDCl<sub>3</sub>) δ 7.19 (d, *J* = 8.1 Hz, 2H), 7.05 – 6.96 (m, 1H), 1.42 – 1.33 (m, 2H), 1.08 – 0.96 (m, 2H). <sup>13</sup>C NMR (101 MHz, CDCl<sub>3</sub>) δ 143.8, 143.6, 132.3, 131.8 (t, *J* = 255.7 Hz), 127.0, 126.2 (q, *J* = 273.5 Hz), 112.7, 109.3, 28.3 (q, *J* = 33.9 Hz), 10.2 (q, *J* = 2.3 Hz) ppm. Spectral data was in agreement with the literature.<sup>[14]</sup>



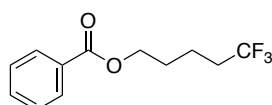
**1-methoxy-4-(1-(trifluoromethyl)cyclopropyl)benzene (28)** Prepared following general procedure A using 4-CzIPN (4.8 mg, 3 mol%), CuCl<sub>2</sub> (5.6 mg, 20 mol%), Bathphenanthroline (20.0 mg, 30 mol%), 2-(1-(4-methoxyphenyl)cyclopropyl)-2-methyl-2,3-dihydroquinazolin-4(1H)-one (**A26**) (61.6 mg, 0.2 mmol, 1.0 equiv), KH<sub>2</sub>PO<sub>4</sub> (0.4 mmol, 2.0 equiv), KF (0.4 mmol, 2.0 equiv), Togni's reagent I (132.0 mg, 2.0 equiv) and 10.0 mL of DMF. Product was obtained as a colorless liquid (34.7 mg, 80% yield) by using Hexane/EtOAc (20:1) as eluent. (83% <sup>19</sup>F NMR yield against internal standard). <sup>19</sup>F NMR (376 MHz, CDCl<sub>3</sub>) δ -70.51(s) ppm. <sup>1</sup>H NMR (400 MHz, CDCl<sub>3</sub>) δ 7.44 – 7.35 (m, 2H), 6.91 – 6.85 (m, 2H), 3.81 (s, 3H), 1.40 – 1.27 (m, 2H), 1.01 – 0.98 (m, 2H) ppm. <sup>13</sup>C NMR (101 MHz, CDCl<sub>3</sub>) δ 159.6, 132.6, 128.3, 126.6 (q, *J* = 273.3 Hz), 113.8, 55.4, 27.5 (q, *J* = 33.5 Hz), 9.9 (q, *J* = 2.3 Hz) ppm. Spectral data was in agreement with the literature.<sup>[14]</sup>



**(1*R*,3*s*)-1-(2,2,2-trifluoroethyl)adamantane (29)** Prepared following general procedure B using 4-CzIPN (4.8 mg, 3 mol%), Cu(CF<sub>3</sub>)<sub>3</sub>bpy (85.2 mg, 1.0 equiv), 2-(((1*S*,3*s*)-adamantan-1-yl)methyl)-2-phenyl-2,3-dihydroquinazolin-4(1*H*)-one (**A27**) (74.5 mg, 0.2 mmol, 1.0 equiv), Togni's reagent I (99.2 mg, 1.5 equiv), BTMG (34 μL, 1.0 equiv) and 10.0 mL of DMF. Product was obtained as a white solid (32.3 mg, 74% yield) by using Hexane as eluent. (76% <sup>19</sup>F NMR yield against internal standard). <sup>19</sup>F NMR (376 MHz, CDCl<sub>3</sub>) δ -58.87 (t, *J* = 12.3 Hz) ppm. <sup>1</sup>H NMR (500 MHz, CDCl<sub>3</sub>) δ 1.98 (br s, 3H), 1.88 (q, *J* = 12.4 Hz, 2H), 1.75 – 1.62 (m, 12H) ppm. <sup>13</sup>C NMR (126 MHz, CDCl<sub>3</sub>) δ 127.3 (q, *J* = 279.3 Hz), 46.9 (q, *J* = 25.5 Hz), 42.3, 36.7, 28.5 ppm. Spectral data was in agreement with the literature.<sup>[14]</sup>

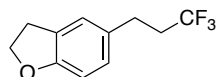


**tert-butyl 4-(2,2,2-trifluoroethyl)piperidine-1-carboxylate (30)** Prepared following general procedure B using 4-CzIPN (4.8 mg, 3 mol%), Cu(CF<sub>3</sub>)<sub>3</sub>bpy (85.2 mg, 1.0 equiv), tert-butyl 4-((4-oxo-2-phenyl-1,2,3,4-tetrahydroquinazolin-2-yl)methyl)piperidine-1-carboxylate (**A28**) (84.2 mg, 0.2 mmol, 1.0 equiv), Togni's reagent I (99.2 mg, 1.5 equiv), BTMG (34 μL, 1.0 equiv) and 10.0 mL of DMF. Product was obtained as a colorless oil (40.1 mg, 75% yield) by using Hexane/EtOAc (8:1) as eluent. (78% <sup>19</sup>F NMR yield against internal standard). <sup>19</sup>F NMR (376 MHz, CDCl<sub>3</sub>) δ -63.41 (t, *J* = 11.3 Hz) ppm. <sup>1</sup>H NMR (400 MHz, CDCl<sub>3</sub>) δ 4.14 – 3.97 (m, 2H), 2.82 – 2.62 (m, 2H), 2.02 (qd, *J* = 11.3, 6.6 Hz, 2H), 1.87 – 1.68 (m, 3H), 1.44 (s, 9H), 1.21 (m, 2H) ppm. <sup>13</sup>C NMR (101 MHz, CDCl<sub>3</sub>) δ 154.8, 126.9 (q, *J* = 277.3 Hz), 79.6, 43.6, 40.2 (q, *J* = 27.4 Hz), 32.0, 30.7 (q, *J* = 2.5 Hz), 28.5 ppm. Spectral data was in agreement with the literature.<sup>[14]</sup>

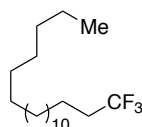


**5,5,5-trifluoropentyl benzoate (31)** Prepared following general procedure B using 4-CzIPN (4.8 mg, 3 mol%), Cu(CF<sub>3</sub>)<sub>3</sub>bpy (85.2 mg, 1.0 equiv), 4-(4-oxo-2-phenyl-1,2,3,4-tetrahydroquinazolin-2-yl)butyl benzoate (**A29**) (80.0 mg, 0.2 mmol, 1.0 equiv), Togni's reagent I (99.2 mg, 1.5 equiv), BTMG (34 μL, 1.0 equiv) and 10.0 mL of DMF. Product was obtained as a colorless liquid (34.9 mg, 71% yield) by using Hexane/EtOAc (20:1) as eluent. (71% <sup>19</sup>F NMR yield against internal standard). <sup>19</sup>F NMR (376 MHz, CDCl<sub>3</sub>) δ -66.48 (t, *J* = 10.8 Hz) ppm. <sup>1</sup>H NMR (400 MHz, CDCl<sub>3</sub>) δ 8.08 – 8.00 (m, 2H), 7.64 – 7.54 (m, 1H), 7.45 (d, *J* = 8.2, 2H), 4.35 (t, *J* = 6.3 Hz,

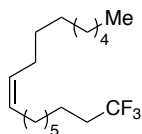
2H), 2.24 – 2.09 (m, 2H), 1.90 – 1.81 (m, 2H), 1.79 – 1.67 (m, 2H) ppm.  $^{13}\text{C}$  NMR (101 MHz,  $\text{CDCl}_3$ )  $\delta$  166.6, 133.1, 130.2, 129.6, 128.5, 127.1 (q,  $J = 276.3$  Hz), 64.2, 33.5 (q,  $J = 28.7$  Hz), 27.9, 18.9 (q,  $J = 3.0$  Hz) ppm. Spectral data was in agreement with the literature.<sup>[12]</sup>



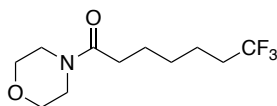
**5-(3,3,3-trifluoropropyl)-2,3-dihydrobenzofuran (32)** Prepared following general procedure B using 4-CzIPN (4.8 mg, 3 mol%),  $\text{Cu}(\text{CF}_3)_3\text{bpy}$  (85.2 mg, 1.0 equiv), 2-(2-(2,3-dihydrobenzofuran-5-yl)ethyl)-2-phenyl-2,3-dihydroquinazolin-4(1H)-one (**A30**) (74.0 mg, 0.2 mmol, 1.0 equiv), Togni's reagent I (99.2 mg, 1.5 equiv), BTMG (34  $\mu\text{L}$ , 1.0 equiv) and 10.0 mL of DMF. Product was obtained as a colorless liquid (26.0 mg, 60% yield) by using Hexane/EtOAc (20:1) as eluent. (65%  $^{19}\text{F}$  NMR yield against internal standard).  $^{19}\text{F}$  NMR (376 MHz,  $\text{CDCl}_3$ )  $\delta$  -66.73 (t,  $J = 10.7$  Hz) ppm.  $^1\text{H}$  NMR (400 MHz,  $\text{CDCl}_3$ )  $\delta$  7.04 (d,  $J = 2.0$  Hz, 1H), 6.93 (dd,  $J = 8.1, 2.0$  Hz, 1H), 6.73 (d,  $J = 8.1$  Hz, 1H), 4.57 (t,  $J = 8.7$  Hz, 2H), 3.20 (t,  $J = 8.7$  Hz, 2H), 2.93 – 2.76 (m, 2H), 2.47 – 2.24 (m, 2H) ppm.  $^{13}\text{C}$  NMR (101 MHz,  $\text{CDCl}_3$ )  $\delta$  164.8, 136.9, 133.6, 133.4, 132.7 (q,  $J = 276.7$  Hz), 130.7, 115.2, 77.1, 42.1 (q,  $J = 27.9$  Hz), 35.6, 33.5 (q,  $J = 3.3$  Hz) ppm. IR (neat): 2923, 1612, 1492, 1458, 1436, 1385, 1304, 1248, 1214, 1120, 1103, 1082, 1034, 970, 940, 896, 846, 659, 548  $\text{cm}^{-1}$ . Mp: 66 °C. HRMS *calcd.* for ( $\text{C}_{11}\text{H}_{12}\text{F}_3\text{O}$ ) [ $\text{M}+\text{H}$ ] $^+$ : 217.0840, *found* 217.0837.



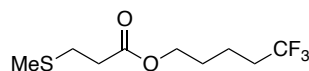
**1,1,1-trifluorononadecane (33)** Prepared following general procedure B using 4-CzIPN (4.8 mg, 3 mol%),  $\text{Cu}(\text{CF}_3)_3\text{bpy}$  (85.2 mg, 1.0 equiv), 2-octadecyl-2-phenyl-2,3-dihydroquinazolin-4(1H)-one (**A31**) (95.2 mg, 0.2 mmol, 1.0 equiv), Togni's reagent I (99.2 mg, 1.5 equiv), BTMG (34  $\mu\text{L}$ , 1.0 equiv) and 10.0 mL of DMF. Product was obtained as a colorless liquid (43.3 mg, 67% yield) by using Hexane as eluent. (71%  $^{19}\text{F}$  NMR yield against internal standard).  $^{19}\text{F}$  NMR (376 MHz,  $\text{CDCl}_3$ )  $\delta$  -66.61 (t,  $J = 11.0$  Hz) ppm.  $^1\text{H}$  NMR (400 MHz,  $\text{CDCl}_3$ )  $\delta$  2.12 – 1.98 (m, 2H), 1.55 (qd,  $J = 6.8, 4.0$  Hz, 2H), 1.38 – 1.27 (m, 30H), 0.89 (t,  $J = 6.8$  Hz, 3H) ppm.  $^{13}\text{C}$  NMR (101 MHz,  $\text{CDCl}_3$ )  $\delta$  127.5 (q,  $J = 276.2$  Hz), 33.9 (q,  $J = 28.3$  Hz), 32.1, 29.9, 29.88, 29.86, 29.81, 29.7, 29.5, 29.3, 28.9, 22.8, 22.0 (q,  $J = 2.7$  Hz), 14.2 ppm. IR (neat): 2022, 2853, 1466, 1254, 1140  $\text{cm}^{-1}$ . GCMS *calcd.* for ( $\text{C}_{19}\text{H}_{37}\text{F}_3$ ) [ $\text{M}$ ] $^+$ : 322,2847, *found* 322,2.



**(Z)-1,1,1-trifluorooctadec-9-ene (34)** Prepared following general procedure B using 4-CzIPN (4.8 mg, 3 mol%), Cu(CF<sub>3</sub>)<sub>3</sub>bpy (85.2 mg, 1.0 equiv), (Z)-2-(hexadec-8-en-1-yl)-2-phenyl-2,3-dihydroquinazolin-4(1H)-one (**A32**) (92.0 mg, 0.2 mmol, 1.0 equiv), Togni's reagent I (99.2 mg, 1.5 equiv), BTMG (34 μL, 1.0 equiv) and 10.0 mL of DMF. Product was obtained as a colorless liquid (35.8 mg, 58% yield) by using Hexane as eluent. (68% <sup>19</sup>F NMR yield against internal standard). <sup>19</sup>F NMR (376 MHz, CDCl<sub>3</sub>) δ -66.57 (t, *J* = 10.9 Hz) ppm. <sup>1</sup>H NMR (400 MHz, CDCl<sub>3</sub>) δ 5.35 (qd, *J* = 4.3, 2.6 Hz, 2H), 2.34 – 1.94 (m, 6H), 1.67 – 1.48 (m, 2H), 1.46 – 1.27 (m, 20H), 0.95 – 0.75 (m, 3H) ppm. <sup>13</sup>C NMR (101 MHz, CDCl<sub>3</sub>) δ 130.1, 129.6, 127.3 (q, *J* = 276.3 Hz), 33.7 (q, *J* = 28.3 Hz), 31.9, 29.7, 29.6, 29.5, 29.3, 29.1, 28.9, 28.6, 27.2, 27.1, 22.6, 21.8 (q, *J* = 2.9 Hz), 14.0 ppm. Spectral data was in agreement with the literature.<sup>[14]</sup>

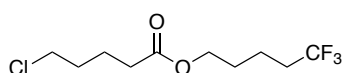


**7,7,7-trifluoro-1-morpholinoheptan-1-one (35)** Prepared following general procedure B using 4-CzIPN (4.8 mg, 3 mol%), Cu(CF<sub>3</sub>)<sub>3</sub>bpy (85.2 mg, 1.0 equiv), 2-(6-morpholino-6-oxohexyl)-2-phenyl-2,3-dihydroquinazolin-4(1H)-one (**A33**) (8.4 mg, 0.2 mmol, 1.0 equiv), Togni's reagent I (99.2 mg, 1.5 equiv), BTMG (34 μL, 1.0 equiv) and 10.0 mL of DMF. Product was obtained as a colorless liquid (25.7 mg, 51% yield) by using Hexane/EtOAc (1:2) as eluent. (48% <sup>19</sup>F NMR yield against internal standard). <sup>19</sup>F NMR (376 MHz, CDCl<sub>3</sub>) δ -66.49 (t, *J* = 11.0 Hz) ppm. <sup>1</sup>H NMR (400 MHz, CDCl<sub>3</sub>) δ 3.66 – 3.56 (m, 6H), 3.43 (t, *J* = 4.8 Hz, 2H), 2.30 (t, *J* = 7.5 Hz, 2H), 2.13 – 1.98 (m, 2H), 1.69 – 1.50 (m, 4H), 1.47 – 1.35 (m, 2H) ppm. <sup>13</sup>C NMR (101 MHz, CDCl<sub>3</sub>) δ 171.2, 127.1 (q, *J* = 276.3 Hz), 66.9, 66.6, 45.9, 41.8, 33.5 (q, *J* = 28.4 Hz), 32.5, 28.4, 24.6, 21.7 (q, *J* = 2.9 Hz) ppm. IR (neat): 2948, 2859, 1614, 1432, 1390, 1253, 1114, 1068, 1029, 921, 849, 731, 654, 571 cm<sup>-1</sup>. HRMS *calcd.* for (C<sub>11</sub>H<sub>19</sub>F<sub>3</sub>NO<sub>2</sub>) [M+H]<sup>+</sup>: 254.1368, *found* 254.1362.

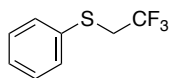


**5,5,5-trifluoropentyl 3-(methylthio)propanoate (36)** Prepared following general procedure B using 4-CzIPN (4.8 mg, 3 mol%), Cu(CF<sub>3</sub>)<sub>3</sub>bpy (85.2 mg, 1.0 equiv), 4-(4-oxo-2-phenyl-1,2,3,4-tetrahydroquinazolin-2-yl)butyl 3-(methylthio)propanoate

**(A34)** (79.6 mg, 0.2 mmol, 1.0 equiv), Togni's reagent I (99.2 mg, 1.5 equiv), BTMG (34  $\mu$ L, 1.0 equiv) and 10.0 mL of DMF. Product was obtained as a colorless liquid (37.2 mg, 76% yield) by using Hexane/EtOAc (8:1) as eluent. (74%  $^{19}\text{F}$  NMR yield against internal standard).  $^{19}\text{F}$  NMR (376 MHz,  $\text{CDCl}_3$ )  $\delta$  -66.55 (t,  $J$  = 10.8 Hz) ppm.  $^1\text{H}$  NMR (400 MHz,  $\text{CDCl}_3$ )  $\delta$  4.12 (t,  $J$  = 6.2 Hz, 2H), 2.76 (d,  $J$  = 7.8 Hz, 2H), 2.62 (t,  $J$  = 7.3 Hz, 2H), 2.14 – 2.07 (m, 5H), 1.77 – 1.56 (m, 4H) ppm.  $^{13}\text{C}$  NMR (101 MHz,  $\text{CDCl}_3$ )  $\delta$  172.0, 127.1 (q,  $J$  = 276.3 Hz), 63.9, 34.4, 33.4 (q,  $J$  = 28.6 Hz), 29.2, 27.7, 18.7 (q,  $J$  = 3.1 Hz), 15.5 ppm. IR (neat): 2921, 1733, 1439, 1392, 1337, 1249, 1135, 1073, 1038, 653  $\text{cm}^{-1}$ . HRMS *calcd.* for ( $\text{C}_9\text{H}_{15}\text{F}_3\text{NaO}_2\text{S}$ ) [ $\text{M}+\text{Na}$ ] $^+$ : 267.0643, *found* 267.0637.

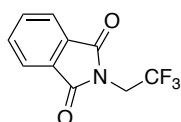


**5,5,5-trifluoropentyl 5-chloropentanoate (37)** Prepared following general procedure B using 4-CzIPN (4.8 mg, 3 mol%),  $\text{Cu}(\text{CF}_3)_3\text{bpy}$  (85.2 mg, 1.0 equiv), 4-(4-oxo-2-phenyl-1,2,3,4-tetrahydroquinazolin-2-yl)butyl 5-chloropentanoate (**A35**) (82.8 mg, 0.2 mmol, 1.0 equiv), Togni's reagent I (99.2 mg, 1.5 equiv), BTMG (34  $\mu$ L, 1.0 equiv) and 10.0 mL of DMF. Product was obtained as a colorless liquid (32.9 mg, 63% yield) by using Hexane/EtOAc (8:1) as eluent. (71%  $^{19}\text{F}$  NMR yield against internal standard).  $^{19}\text{F}$  NMR (376 MHz,  $\text{CDCl}_3$ )  $\delta$  -66.57 (t,  $J$  = 10.8 Hz) ppm.  $^1\text{H}$  NMR (400 MHz,  $\text{CDCl}_3$ )  $\delta$  4.09 (t,  $J$  = 6.2 Hz, 2H), 3.53 (t,  $J$  = 6.2 Hz, 2H), 2.42 – 2.29 (m, 2H), 2.21 – 1.99 (m, 2H), 1.92 – 1.53 (m, 8H) ppm.  $^{13}\text{C}$  NMR (101 MHz,  $\text{CDCl}_3$ )  $\delta$  173.1, 126.9 (q,  $J$  = 276.3 Hz), 63.5, 44.3, 33.31, 33.30 (q,  $J$  = 28.7 Hz), 31.8, 27.6, 22.2, 18.6 (q,  $J$  = 3.1 Hz) ppm. IR (neat): 2960, 1732, 1461, 1393, 1254, 1136, 1074, 1038, 912, 733, 652  $\text{cm}^{-1}$ . HRMS *calcd.* for ( $\text{C}_{10}\text{H}_{16}\text{ClF}_3\text{NaO}_2$ ) [ $\text{M}+\text{Na}$ ] $^+$ : 283.0689, *found* 283.0688.

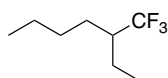


**Phenyl(2,2,2-trifluoroethyl)sulfane (38)** Prepared following general procedure C using 4-CzIPN (4.8 mg, 3 mol%),  $\text{Cu}(\text{CF}_3)_3\text{bpy}$  (85.2 mg, 1.0 equiv), 2-phenyl-2-((phenylthio)methyl)-2,3-dihydroquinazolin-4(1H)-one (**A36**) (69.2 mg, 0.2 mmol, 1.0 equiv),  $\text{K}_2\text{S}_2\text{O}_8$  (81.2 mg, 1.5 equiv) and  $\text{KH}_2\text{PO}_4$  (54.4 mg, 2.0 equiv) and 8.0 mL of  $\text{CH}_3\text{CN}$ . Product was obtained as a yellow liquid (23.9 mg, 62% yield) by using Pentane as eluent. (74%  $^{19}\text{F}$  NMR yield against internal standard).  $^{19}\text{F}$  NMR (376 MHz,  $\text{CD}_2\text{Cl}_2$ )  $\delta$  -66.88 (t,  $J$  = 9.7 Hz) ppm.  $^1\text{H}$  NMR (400 MHz,  $\text{CD}_2\text{Cl}_2$ )  $\delta$  7.53 – 7.48 (m, 2H), 7.37 – 7.30 (m, 3H), 3.45 (q,  $J$  = 9.7 Hz, 2H) ppm.  $^{13}\text{C}$  NMR (101 MHz,  $\text{CD}_2\text{Cl}_2$ )  $\delta$  133.9, 132.0, 129.4, 128.2, 125.5 (q,  $J$  = 276.5 Hz), 38.3 (q,  $J$  = 32.7 Hz) ppm. Spectral data

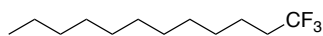
was in agreement with the literature.<sup>[20]</sup>



**2-(2,2,2-trifluoroethyl)isoindoline-1,3-dione (39)** Prepared following general procedure C using 4-CzIPN (4.8 mg, 3 mol%), Cu(CF<sub>3</sub>)<sub>3</sub>bpy (85.2 mg, 1.0 equiv), 2-((2-methyl-4-oxo-1,2,3,4-tetrahydroquinazolin-2-yl)methyl)isoindoline-1,3-dione (**A37**) (64.2 mg, 0.2 mmol, 1.0 equiv), K<sub>2</sub>S<sub>2</sub>O<sub>8</sub> (81.2 mg, 1.5 equiv) and KH<sub>2</sub>PO<sub>4</sub> (54.4 mg, 2.0 equiv) and 8.0 mL of CH<sub>3</sub>CN. Product was obtained as a yellow solid (35.6 mg, 78% yield) by using Hexane/EtOAc (5:1) as eluent. (81% <sup>19</sup>F NMR yield against internal standard). <sup>19</sup>F NMR (376 MHz, CDCl<sub>3</sub>) δ -70.63 (t, *J* = 8.6 Hz) ppm. <sup>1</sup>H NMR (400 MHz, CDCl<sub>3</sub>) δ 7.90 (dd, *J* = 5.5, 3.1 Hz, 2H), 7.77 (dd, *J* = 5.5, 3.1 Hz, 2H), 4.30 (q, *J* = 8.6 Hz, 2H) ppm. <sup>13</sup>C NMR (101 MHz, CDCl<sub>3</sub>) δ 166.8, 134.7, 131.6, 124.0, 123.3 (q, *J* = 280.0 Hz), 39.0 (q, *J* = 36.5 Hz) ppm. Spectral data was in agreement with the literature.<sup>[12]</sup>



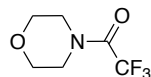
**3-(trifluoromethyl)heptane (40)** Prepared following general procedure C using 4-CzIPN (4.8 mg, 3 mol%), Cu(CF<sub>3</sub>)<sub>3</sub>bpy (85.2 mg, 0.2mmol, 1.0 equiv), Diethyl 4-(heptan-3-yl)-2,6-dimethyl-1,4-dihydropyridine-3,5-dicarboxylate (**B4**) (70.2 mg, 0.3 mmol, 1.5 equiv), K<sub>2</sub>S<sub>2</sub>O<sub>8</sub> (81.2 mg, 1.5 equiv) and NaHCO<sub>3</sub> (33.2 mg, 2.0 equiv) and 8.0 mL of CH<sub>3</sub>CN. Product could not be isolated due to its volatility, 1,1,1-trifluorotoluene (24.4 μL, 0.2 mmol, 1.0 equiv) was added as an internal standard for <sup>19</sup>F NMR analysis. (48% yield – average of two trials: 48% yield and 47% yield). <sup>19</sup>F NMR (376 MHz, Acetone) δ -70.57 (d, *J* = 9.9 Hz) ppm.



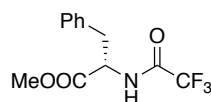
**1,1,1-trifluorododecane (41)** Prepared following general procedure C using 4-CzIPN (4.8 mg, 3 mol%), Cu(CF<sub>3</sub>)<sub>3</sub>bpy (85.2 mg, 0.2mmol, 1.0 equiv), diethyl 2,6-dimethyl-4-undecyl-1,4-dihydropyridine-3,5-dicarboxylate (**B5**) (122.1 mg, 0.3 mmol, 1.5 equiv), K<sub>2</sub>S<sub>2</sub>O<sub>8</sub> (81.2 mg, 1.5 equiv) and NaHCO<sub>3</sub> (33.2 mg, 2.0 equiv) and 8.0 mL of CH<sub>3</sub>CN. Product was obtained as a liquid (23.2 mg, 52% yield) by using Pentane as eluent. (58% <sup>19</sup>F NMR yield against internal standard). <sup>19</sup>F NMR (376 MHz, CDCl<sub>3</sub>) δ -66.55 (t, *J* = 11.0 Hz) ppm. <sup>1</sup>H NMR (400 MHz, CDCl<sub>3</sub>) δ 2.14 – 1.98 (m, 2H), 1.66 – 1.49 (m, 2H), 1.41 – 1.20 (m, 16H), 0.88 (t, *J* = 6.7 Hz, 3H) ppm. <sup>13</sup>C NMR (101 MHz, CDCl<sub>3</sub>) δ 127.4 (q, *J* = 276.2 Hz), 33.9 (q, *J* = 28.2 Hz), 32.0, 29.73, 29.71, 29.5,

29.4, 29.3, 28.8, 22.8, 22.0 (q,  $J = 2.9$  Hz), 14.2 ppm. Spectral data was in agreement with the literature.<sup>[21]</sup>

Prepared following general procedure D using  $\text{Cu}(\text{CF}_3)_3\text{bpy}$  (85.2 mg, 0.2 mmol, 1.0 equiv), methyl 6-acetoxy-4-decyl-4-methyl-1,4-dihydropyridazine-3-carboxylate (**C9**) (105.6 mg, 0.3 mmol, 1.5 equiv), Togni's reagent I (33.0 mg, 0.5 equiv) and BTMG (16.8 mg, 0.5 equiv) and 8.0 mL of Acetone. Product was obtained as a liquid (23.0 mg, 51% yield) by using pentane as eluent. (59%  $^{19}\text{F}$  NMR yield against internal standard).

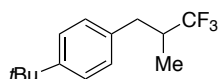


**2,2,2-trifluoro-1-morpholinoethan-1-one (42)** Prepared following general procedure C using 4-CzIPN (4.8 mg, 3 mol%),  $\text{Cu}(\text{CF}_3)_3\text{bpy}$  (85.2 mg, 0.2 mmol, 1.0 equiv), diethyl 2,6-dimethyl-4-(morpholine-4-carbonyl)-1,4-dihydropyridine-3,5-dicarboxylate (**B6**) (73.2 mg, 0.2 mmol, 1.0 equiv),  $\text{K}_2\text{S}_2\text{O}_8$  (81.2 mg, 1.5 equiv) and  $\text{NaHCO}_3$  (33.2 mg, 2.0 equiv) and 8.0 mL of  $\text{CH}_3\text{CN}$ . Product was obtained as a colorless oil (19.8 mg, 54% yield) by using Hexane/EtOAc (2:1) as eluent. (62%  $^{19}\text{F}$  NMR yield against internal standard).  $^{19}\text{F}$  NMR (376 MHz,  $\text{CDCl}_3$ )  $\delta$  -69.12 (s) ppm.  $^1\text{H}$  NMR (400 MHz,  $\text{CDCl}_3$ )  $\delta$  3.77 – 3.65 (m, 6H), 3.61 (t,  $J = 4.7$  Hz, 2H) ppm.  $^{13}\text{C}$  NMR (126 MHz,  $\text{CDCl}_3$ )  $\delta$  155.6 (q,  $J = 35.8$  Hz), 116.4 (q,  $J = 287.9$  Hz), 66.5 (d,  $J = 4.1$  Hz), 46.4 (d,  $J = 3.3$  Hz), 43.6 ppm. Spectral data was in agreement with the literature.<sup>[22]</sup>

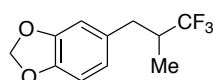


**Methyl (2,2,2-trifluoroacetyl)-L-phenylalaninate (43)** Prepared following general procedure C using 4-CzIPN (4.8 mg, 3 mol%),  $\text{Cu}(\text{CF}_3)_3\text{bpy}$  (85.2 mg, 0.2 mmol, 1.0 equiv), diethyl 4-{\{(2S)-1-methoxy-1-oxo-3-phenylpropan-2-yl\}carbamoyl}-2,6-dimethyl-1,4-dihydropyridine-3,5-dicarboxylate (**B7**) (137.4 mg, 0.3 mmol, 1.5 equiv),  $\text{K}_2\text{S}_2\text{O}_8$  (81.2 mg, 1.5 equiv) and  $\text{NaHCO}_3$  (33.2 mg, 2.0 equiv) and 8.0 mL of  $\text{CH}_3\text{CN}$ . Product was obtained as a colorless liquid (31.7 mg, 58% yield) by using Hexane/EtOAc (5:1) as eluent. (59%  $^{19}\text{F}$  NMR yield against internal standard).  $^{19}\text{F}$  NMR (376 MHz,  $\text{CDCl}_3$ )  $\delta$  -76.06 (s) ppm.  $^1\text{H}$  NMR (400 MHz,  $\text{CDCl}_3$ )  $\delta$  7.36 – 7.26 (m, 3H), 7.14 – 7.04 (m, 2H), 6.75 (s, 1H), 4.88 (dt,  $J = 7.8, 5.5$  Hz, 1H), 3.79 (s, 3H), 3.21 (qd,  $J = 14.0, 5.6$  Hz, 2H) ppm.  $^{13}\text{C}$  NMR (101 MHz,  $\text{CDCl}_3$ )  $\delta$  170.5, 156.6 (q,  $J = 37.7$  Hz), 134.6, 129.3, 128.9, 127.7, 115.6 (q,  $J = 287.6$  Hz), 53.6, 52.9, 37.4 ppm.

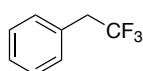
Spectral data was in agreement with the literature.<sup>[23]</sup>



**1-(tert-butyl)-4-(3,3,3-trifluoro-2-methylpropyl)benzene (44)** Prepared following general procedure C using 4-CzIPN (4.8 mg, 3 mol%), Cu(CF<sub>3</sub>)<sub>3</sub>bpy (85.2 mg, 0.2mmol, 1.0 equiv), diethyl 4-(1-(4-(tert-butyl)phenyl)propan-2-yl)-2,6-dimethyl-1,4-dihydropyridine-3,5-dicarboxylate (**B8**) (85.5 mg, 0.3 mmol, 1.5 equiv), K<sub>2</sub>S<sub>2</sub>O<sub>8</sub> (81.2 mg, 1.5 equiv) and NaHCO<sub>3</sub> (33.2 mg, 2.0 equiv) and 8.0 mL of CH<sub>3</sub>CN. Product was obtained as a liquid (30.7 mg, 63% yield) by using Hexane as eluent. (64% <sup>19</sup>F NMR yield against internal standard). <sup>19</sup>F NMR (376 MHz, CDCl<sub>3</sub>) δ -73.60 (d, *J* = 8.0 Hz) ppm. <sup>1</sup>H NMR (400 MHz, CDCl<sub>3</sub>) δ 7.44 – 7.29 (m, 2H), 7.16 – 6.94 (m, 2H), 3.12 – 3.05 (m, 1H), 2.71 – 2.34 (m, 2H), 1.32 (s, 9H), 1.03 (d, *J* = 6.4 Hz, 3H) ppm. <sup>13</sup>C NMR (101 MHz, CDCl<sub>3</sub>) δ 149.6, 135.2, 128.9, 128.4 (q, *J* = 279.5 Hz), 125.6, 40.1 (q, *J* = 26.0 Hz), 35.2 (q, *J* = 2.8 Hz), 34.5, 31.5, 12.3 (q, *J* = 2.8 Hz) ppm. IR (neat): 2964, 2870, 1514, 1465, 1376, 1265, 1167, 1121, 1093, 1012, 854, 838, 809, 642, 577, 548 cm<sup>-1</sup>. HRMS *calcd.* for (C<sub>14</sub>H<sub>18</sub>F<sub>3</sub>) [M-H]<sup>+</sup>: 243.1361, *found* 243.1354.



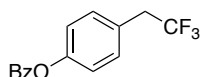
**5-(3,3,3-trifluoro-2-methylpropyl)benzo[*d*][1,3]dioxole (45)** Prepared following general procedure C using 4-CzIPN (4.8 mg, 3 mol%), Cu(CF<sub>3</sub>)<sub>3</sub>bpy (85.2 mg, 0.2mmol, 1.0 equiv), diethyl 4-(1-(benzo[*d*][1,3]dioxol-5-yl)propan-2-yl)-2,6-dimethyl-1,4-dihydropyridine-3,5-dicarboxylate (**B9**) (124.5 mg, 0.3 mmol, 1.5 equiv), K<sub>2</sub>S<sub>2</sub>O<sub>8</sub> (81.2 mg, 1.5 equiv) and NaHCO<sub>3</sub> (33.2 mg, 2.0 equiv) and 8.0 mL of CH<sub>3</sub>CN. Product was obtained as a liquid (37.1 mg, 80% yield) by using Hexane/EtOAc (50:1) as eluent. (84% <sup>19</sup>F NMR yield against internal standard). <sup>19</sup>F NMR (376 MHz, CDCl<sub>3</sub>) δ -73.51 (d, *J* = 8.2 Hz) ppm. <sup>1</sup>H NMR (400 MHz, CDCl<sub>3</sub>) δ 6.75 (d, *J* = 7.9 Hz, 1H), 6.68 – 6.54 (m, 2H), 5.94 (s, 2H), 3.04 – 3.01 (m, 1H), 2.60 – 2.30 (m, 2H), 1.05 (d, *J* = 6.8 Hz, 3H) ppm. <sup>13</sup>C NMR (101 MHz, CDCl<sub>3</sub>) δ 147.9, 146.4, 131.9, 128.2 (q, *J* = 279.6 Hz), 122.2, 109.4, 108.4, 101.1, 40.3 (q, *J* = 25.9 Hz), 35.5 (q, *J* = 2.8 Hz), 12.1 (q, *J* = 2.8 Hz) ppm. IR (neat): 2892, 1504, 1491, 1467, 1443, 1377, 1247, 1168, 1120, 1093, 1038, 1011, 930, 860, 810, 792, 673, 617, 506, 424 cm<sup>-1</sup>. HRMS *calcd.* for (C<sub>11</sub>H<sub>12</sub>F<sub>3</sub>O<sub>2</sub>) [M+H]<sup>+</sup>: 233.0789, *found* 233.0782.



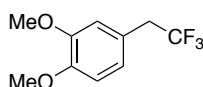


**(2,2,2-trifluoroethyl)benzene (46)** Prepared following general procedure D using  $\text{Cu}(\text{CF}_3)_3\text{bpy}$  (85.2 mg, 0.2 mmol, 1.0 equiv), dimethyl 4-benzyl-1,4-dihydropyridazine-3,6-dicarboxylate (**C4**) (86.5 mg, 0.3 mmol, 1.5 equiv), and 4.0 mL of Acetone. Product could not be isolated due to its volatility, 1-fluoro-3-nitrobenzene (20  $\mu\text{L}$ , 0.19 mmol, 0.94 equiv) was added as an internal standard for  $^{19}\text{F}$  NMR analysis. (70% yield – average of two trials: 70% yield and 69% yield).  $^{19}\text{F}$  NMR (376 MHz, Acetone)  $\delta$  -66.66 (t,  $J = 11.3$  Hz) ppm.

**(2,2,2-trifluoroethyl)benzene (46)** Prepared following general procedure D using  $\text{Cu}(\text{CF}_3)_3\text{bpy}$  (85.2 mg, 0.2 mmol, 1.0 equiv), dimethyl 4-benzyl-4-methyl-1,4-dihydropyridazine-3,6-dicarboxylate (**C5**) (60.5 mg, 0.2 mmol, 1.0 equiv), and 4.0 mL of Acetone. Product could not be isolated due to its volatility, 1-fluoro-3-nitrobenzene (20  $\mu\text{L}$ , 0.19 mmol, 0.94 equiv) was added as an internal standard for  $^{19}\text{F}$  NMR analysis. (70% yield – average of two trials: 69% yield and 71% yield).  $^{19}\text{F}$  NMR (376 MHz, Acetone)  $\delta$  -66.6 (d,  $J = 11.3$  Hz) ppm.

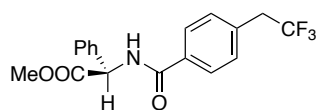


**4-(2,2,2-trifluoroethyl)phenyl benzoate (47)** Prepared following general procedure D using  $\text{Cu}(\text{CF}_3)_3\text{bpy}$  (85.2 mg, 0.2 mmol, 1.0 equiv), dimethyl 4-(4-(benzoyloxy)benzyl)-4-methyl-1,4-dihydropyridazine-3,6-dicarboxylate (**C6**) (84.5 mg, 0.2 mmol, 1.0 equiv), and 4.0 mL of Acetone. Product was obtained as a white solid (36.5 mg, 0.13 mmol, 65% yield) by using 3% acetone/hexane as eluent. (66%  $^{19}\text{F}$  NMR yield against internal standard).  $^{19}\text{F}$  NMR (471 MHz,  $\text{CDCl}_3$ )  $\delta$  -65.98 (t,  $J = 10.9$  Hz) ppm.  $^1\text{H}$  NMR (500 MHz,  $\text{CDCl}_3$ )  $\delta$  8.21 (d,  $J = 7.0$  Hz, 2H), 7.68 – 7.62 (m, 1H), 7.52 (t,  $J = 7.7$  Hz, 2H), 7.37 (d,  $J = 8.1$  Hz, 2H), 7.23 (d,  $J = 8.5$  Hz, 2H), 3.40 (q,  $J = 10.7$  Hz, 2H) ppm.  $^{13}\text{C}$  NMR (126 MHz,  $\text{CDCl}_3$ )  $\delta$  165.2, 151.0, 133.9, 131.5, 130.4, 129.5, 128.8, 127.9 (q,  $J = 2.8$  Hz), 125.8 (q,  $J = 276.8$  Hz), 122.2, 39.8 (q,  $J = 30.1$  Hz) ppm. IR (neat): 3068, 2958, 2924, 2855, 1738, 1718, 1600, 1510, 1453, 1366, 1252, 1201, 1136, 1110, 1078, 1059, 1024, 911, 711, 649, 527  $\text{cm}^{-1}$ . Mp: 89.7  $^\circ\text{C}$ . HRMS calcd. for  $(\text{C}_{15}\text{H}_{11}\text{F}_3\text{NaO}_2)$   $[\text{M}+\text{Na}]^+$ : 303.0603, found 303.0590.

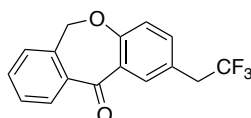


**1,2-dimethoxy-4-(2,2,2-trifluoroethyl)benzene (48)** Prepared following general procedure D using  $\text{Cu}(\text{CF}_3)_3\text{bpy}$  (85.2 mg, 0.2 mmol, 1.0 equiv), dimethyl 4-(3,4-dimethoxybenzyl)-1,4-dihydropyridazine-3,6-dicarboxylate (**C7**) (104.5 mg, 0.3 mmol,

1.5 equiv), and 4.0 mL of Acetone. Product was obtained as a colorless oil (27.0 mg, 0.12 mmol, 61% yield) by using 5% acetone/hexane as eluent. (66%  $^{19}\text{F}$  NMR yield against internal standard).  $^{19}\text{F}$  NMR (471 MHz,  $\text{CDCl}_3$ )  $\delta$  -66.20 (t,  $J$  = 11.0 Hz) ppm.  $^1\text{H}$  NMR (500 MHz,  $\text{CDCl}_3$ )  $\delta$  6.84 (s, 2H), 6.79 (s, 1H), 3.88 (s, 3H), 3.88 (s, 3H), 3.30 (q,  $J$  = 10.8 Hz, 2H) ppm.  $^{13}\text{C}$  NMR (126 MHz,  $\text{CDCl}_3$ )  $\delta$  149.1, 149.1, 126.0 (q,  $J$  = 276.7 Hz), 122.7, 122.6 (q,  $J$  = 3.1 Hz), 113.3, 111.3, 56.0, 56.0, 39.9 (q,  $J$  = 29.6 Hz) ppm. IR (neat): 2942, 2839, 1593, 1517, 1466, 1422, 1362, 1258, 1237, 1131, 1082, 1027, 908, 808, 751, 673  $\text{cm}^{-1}$ . HRMS *calcd.* for  $(\text{C}_{10}\text{H}_{11}\text{F}_3\text{NaO}_2)$   $[\text{M}+\text{Na}]^+$ : 243.0603, *found* 243.0596.

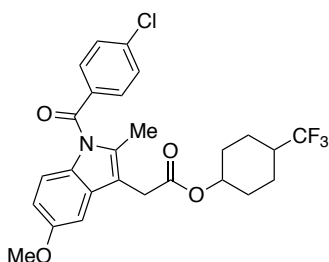


**Methyl (R)-2-phenyl-2-(4-(2,2,2-trifluoroethyl)benzamido)acetate (49)** Prepared following general procedure D using  $\text{Cu}(\text{CF}_3)_3\text{bpy}$  (85.2 mg, 0.2 mmol, 1.0 equiv), Dimethyl 4-(4-(((R)-2-methoxy-2-oxo-1-phenylethyl)carbamoyl)benzyl)-1,4-dihydropyridazine-3,6-dicarboxylate (**C8**) (143.7 mg, 0.3 mmol, 1.5 equiv), and 4.0 mL of Acetone. Product was obtained as a white solid (30.3 mg, 43% yield) by using Hexane/EtOAc (2:1) as eluent. (43%  $^{19}\text{F}$  NMR yield against internal standard).  $^{19}\text{F}$  NMR (376 MHz,  $\text{CDCl}_3$ )  $\delta$  -65.76 (t,  $J$  = 10.9 Hz) ppm.  $^1\text{H}$  NMR (400 MHz,  $\text{CDCl}_3$ )  $\delta$  7.82 (d,  $J$  = 8.5 Hz, 2H), 7.47 – 7.42 (m, 2H), 7.41 – 7.33 (m, 5H), 7.16 (d,  $J$  = 6.7 Hz, 1H), 5.77 (d,  $J$  = 6.9 Hz, 1H), 3.77 (s, 3H), 3.42 (q,  $J$  = 10.6 Hz, 2H) ppm.  $^{13}\text{C}$  NMR (101 MHz,  $\text{CDCl}_3$ )  $\delta$  171.6, 166.1, 136.6, 134.2 (q,  $J$  = 3.1 Hz), 133.6, 130.6, 129.2, 128.8, 127.7, 127.5, 125.6 (q,  $J$  = 277.0 Hz), 56.9, 53.1, 40.2 (q,  $J$  = 30.0 Hz) ppm. IR (neat): 3315, 2957, 1742, 1642, 1616, 1575, 1529, 1507, 1498, 1454, 1437, 1361, 1209, 1094, 1023, 989, 943, 829, 766, 729, 696, 667, 631, 553, 471  $\text{cm}^{-1}$ . Mp: 114  $^\circ\text{C}$ . HRMS *calcd.* for  $(\text{C}_{18}\text{H}_{17}\text{F}_3\text{NO}_3)$   $[\text{M}+\text{H}]^+$ : 352,1161, *found* 352,1158.



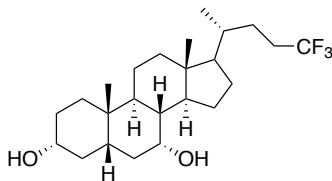
**2-(2,2,2-trifluoroethyl)dibenzo[b,e]oxepin-11(6H)-one (50)** Prepared following general procedure A using 4-CzIPN (4.8 mg, 3 mol%),  $\text{CuCl}_2$  (5.6 mg, 20 mol%), di(pyridin-2-yl)methanone (11.0 mg, 30 mol%), 2-methyl-2-((11-oxo-6,11-dihydrodibenzo[b,e]oxepin-2-yl)methyl)-2,3-dihydroquinazolin-4(1H)-one (**A38**) (76.8 mg, 0.2 mmol, 1.0 equiv),  $\text{KH}_2\text{PO}_4$  (0.4 mmol, 2.0 equiv), Togni's reagent I (132.0 mg, 2.0 equiv) and 10.0 mL of DMF. Product was obtained as a white solid (43.6 mg,

75% yield) by using Hexane/EtOAc (10:1) as eluent. (79%  $^{19}\text{F}$  NMR yield against internal standard).  $^{19}\text{F}$  NMR (376 MHz,  $\text{CDCl}_3$ )  $\delta$  -66.17 (s) ppm.  $^1\text{H}$  NMR (400 MHz,  $\text{CDCl}_3$ )  $\delta$  8.17 (d,  $J$  = 2.4 Hz, 1H), 7.89 (dd,  $J$  = 7.7, 1.4 Hz, 1H), 7.55 (td,  $J$  = 7.4, 1.4 Hz, 1H), 7.47 (td,  $J$  = 7.6, 1.3 Hz, 1H), 7.41 (dd,  $J$  = 8.6, 2.4 Hz, 1H), 7.35 (dd,  $J$  = 7.5, 1.3 Hz, 1H), 7.05 (d,  $J$  = 8.5 Hz, 1H), 5.18 (s, 2H), 3.38 (q,  $J$  = 10.7 Hz, 2H) ppm.  $^{13}\text{C}$  NMR (101 MHz,  $\text{CDCl}_3$ )  $\delta$  190.9, 161.3, 140.5, 136.7, 135.5, 133.8, 133.1, 129.7, 129.5, 128.0, 125.4, 125.8 (q,  $J$  = 277.1 Hz), 124.0 (q,  $J$  = 2.9 Hz), 121.5, 73.8, 39.5 (q,  $J$  = 30.1 Hz) ppm. Spectral data was in agreement with the literature.<sup>[12]</sup>

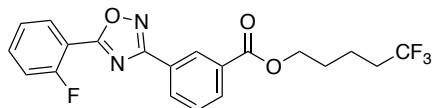


**4-(trifluoromethyl)cyclohexyl 2-(1-(4-chlorobenzoyl)-5-methoxy-2-methyl-1H-indol-3-yl)acetate (51)** Prepared following general procedure A using 4-CzIPN (4.8 mg, 3 mol%),  $\text{CuCl}_2$  (5.6 mg, 20 mol%), Phenanthroline (10.8 mg, 30 mol%), 4-(2-methyl-4-oxo-1,2,3,4-tetrahydroquinazolin-2-yl)cyclohexyl 2-(1-(4-chlorobenzoyl)-5-methoxy-2-methyl-1H-indol-3-yl)acetate (**A39**) (119.9 mg, 0.2 mmol, 1.0 equiv), BTMG (34  $\mu\text{L}$ , 1.0 equiv), Togni's reagent I (132.0 mg, 2.0 equiv) and 8.0 mL of Acetone. Product was obtained as a yellow liquid (45.7 mg, 45% yield) by using Hexane/EtOAc (6:1) as eluent. (45%  $^{19}\text{F}$  NMR yield against internal standard). Mixture of two isomers (*cis* : *trans* = 1:1). ***trans*-diastereomer:**  $^{19}\text{F}$  NMR (376 MHz,  $\text{CDCl}_3$ )  $\delta$  -73.61 (d,  $J$  = 8.0 Hz) ppm.  $^1\text{H}$  NMR (400 MHz,  $\text{CDCl}_3$ )  $\delta$  7.66 (d,  $J$  = 8.6 Hz, 2H), 7.47 (d,  $J$  = 8.5 Hz, 2H), 6.96 (d,  $J$  = 2.5 Hz, 1H), 6.87 (d,  $J$  = 9.0 Hz, 1H), 6.67 (dd,  $J$  = 9.0, 2.5 Hz, 1H), 4.70 (d,  $J$  = 4.4 Hz, 1H), 3.83 (s, 3H), 3.64 (s, 2H), 2.38 (s, 3H), 2.16 – 1.90 (m, 5H), 1.53 – 1.29 (m, 4H) ppm.  $^{13}\text{C}$  NMR (101 MHz,  $\text{CDCl}_3$ )  $\delta$  170.3, 168.4, 156.1, 139.4, 136.0, 134.0, 131.3, 130.9, 130.7, 129.2, 127.5 (q,  $J$  = 278.7 Hz), 115.0, 112.7, 111.7, 101.5, 72.6, 55.8, 40.9 (q,  $J$  = 27.0 Hz), 30.7, 30.1, 23.3 (q,  $J$  = 2.5 Hz), 13.5 ppm. ***cis*-diastereomer** (assign by X-ray):  $^{19}\text{F}$  NMR (376 MHz,  $\text{CDCl}_3$ )  $\delta$  -73.99 (d,  $J$  = 8.5 Hz) ppm.  $^1\text{H}$  NMR (500 MHz,  $\text{CDCl}_3$ )  $\delta$  7.78 – 7.57 (m, 2H), 7.46 (d,  $J$  = 8.5 Hz, 2H), 6.97 (d,  $J$  = 2.5 Hz, 1H), 6.84 (d,  $J$  = 9.0 Hz, 1H), 6.66 (dd,  $J$  = 9.0, 2.6 Hz, 1H), 5.05 (t,  $J$  = 2.9 Hz, 1H), 3.82 (s, 3H), 3.68 (s, 2H), 2.42 (s, 3H), 2.07 – 1.86 (m, 3H), 1.69 (dd,  $J$  = 12.0, 3.8 Hz, 2H), 1.57 – 1.35 (m, 4H) ppm.  $^{13}\text{C}$  NMR (126 MHz,  $\text{CDCl}_3$ )  $\delta$  170.2, 168.3, 156.2, 139.4, 135.9, 134.0, 131.2, 130.9, 130.6, 129.2,

127.5 (q,  $J = 278.6$  Hz), 115.1, 112.8, 111.8, 101.3, 68.7, 55.7, 41.0 (q,  $J = 26.8$  Hz), 30.9, 28.5, 19.5 (q,  $J = 2.7$  Hz), 13.3 ppm. **IR (neat):** 2946, 2872, 1672, 1592, 1470, 1456, 1355, 1169, 1124, 1086, 1002, 912, 856, 825, 725, 688, 635, 599, 481  $\text{cm}^{-1}$ . **Mp:** 132 °C. **HRMS** *calcd.* for  $(\text{C}_{26}\text{H}_{25}\text{ClF}_3\text{NNaO}_4)$   $[\text{M}+\text{Na}]^+$ : 530.1322, *found* 530.1314.

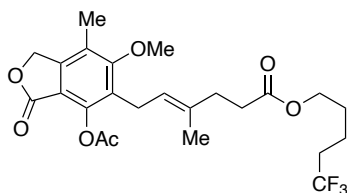


**(3R,5S,7R,8R,9S,10S,13R,14S)-10,13-dimethyl-17-((R)-5,5,5-trifluoropentan-2-yl)hexadecahydro-1H-cyclopenta[a]phenanthrene-3,7-diol (52)** Prepared following general procedure B using 4-CzIPN (4.8 mg, 3 mol%),  $\text{Cu}(\text{CF}_3)_3\text{bpy}$  (85.2 mg, 1.0 equiv), 2-(((3R)-3-((3R,5S,7R,8R,9S,10S,13R,14S)-3,7-dihydroxy-10,13-dimethylhexadecahydro-1H-cyclopenta[a]phenanthren-17-yl)butyl)-2-phenyl-2,3-dihydroquinazolin-4(1H)-one (**A40**) (114.01 mg, 0.2 mmol, 1.0 equiv), Togni's reagent I (99.2 mg, 1.5 equiv), BTMG (34  $\mu\text{L}$ , 1.0 equiv) and 10.0 mL of DMF. Product was obtained as a colorless oil (51.0 mg, 61% yield) by using Hexane/EtOAc (1:2) as eluent. (63%  $^{19}\text{F}$  NMR yield against internal standard).  $^{19}\text{F}$  NMR (376 MHz,  $\text{CDCl}_3$ ) -66.47 (t,  $J = 10.9$  Hz) ppm.  $^1\text{H}$  NMR (400 MHz,  $\text{CDCl}_3$ )  $\delta$  3.84 (q,  $J = 3.0$  Hz, 1H), 3.45 (ddd,  $J = 11.1, 6.6, 4.4$  Hz, 1H), 2.20 (td,  $J = 13.1, 11.3$  Hz, 1H), 2.13 – 2.04 (m, 1H), 2.01 – 1.77 (m, 7H), 1.75 – 1.59 (m, 5H), 1.55 – 1.09 (m, 14H), 0.96 – 0.87 (m, 6H), 0.66 (s, 3H) ppm.  $^{13}\text{C}$  NMR (101 MHz,  $\text{CDCl}_3$ )  $\delta$  127.6 (q,  $J = 276.2$  Hz), 71.9, 68.4, 55.4, 50.4, 42.6, 41.4, 39.8, 39.6, 39.4, 35.3, 35.0, 34.7, 34.6, 32.8, 30.6, 30.4 (q,  $J = 28.1$  Hz), 28.0, 27.6 (q,  $J = 2.6$  Hz), 23.6, 22.7, 20.5, 18.2, 11.7 ppm. **IR (neat):** 3379, 2927, 2865, 1447, 1378, 1254, 1141, 1077, 1001, 978, 906, 733  $\text{cm}^{-1}$ . **Mp:** 74 °C. **HRMS** *calcd.* for  $(\text{C}_{24}\text{H}_{39}\text{F}_3\text{NaO}_2)$   $[\text{M}+\text{Na}]^+$ : 439.2800, *found* 439.2794.

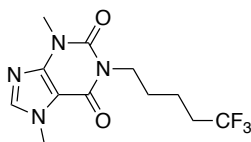


**5,5,5-trifluoropentyl 3-(5-(2-fluorophenyl)-1,2,4-oxadiazol-3-yl)benzoate (53)** Prepared following general procedure B using 4-CzIPN (4.8 mg, 3 mol%),  $\text{Cu}(\text{CF}_3)_3\text{bpy}$  (85.2 mg, 1.0 equiv), 4-(4-oxo-2-phenyl-1,2,3,4-tetrahydroquinazolin-2-yl)butyl 4-(5-(2-fluorophenyl)-1,2,4-oxadiazol-3-yl)benzoate (**A41**) (112.4 mg, 0.2 mmol, 1.0 equiv), Togni's reagent I (99.2 mg, 1.5 equiv), BTMG (34  $\mu\text{L}$ , 1.0 equiv) and 10.0 mL of DMF. Product was obtained as a white solid (47.3 mg, 58% yield) by using Hexane/EtOAc (5:1) as eluent. (61%  $^{19}\text{F}$  NMR yield against internal standard).

<sup>19</sup>F NMR (376 MHz, CDCl<sub>3</sub>) δ -66.42 (t, *J* = 10.8 Hz, 3F), -108.29 (ddd, *J* = 11.2, 6.7, 4.8 Hz, 1F) ppm. <sup>1</sup>H NMR (400 MHz, CDCl<sub>3</sub>) δ 8.83 (td, *J* = 1.8, 0.6 Hz, 1H), 8.39 (dt, *J* = 7.8, 1.5 Hz, 1H), 8.29 – 8.15 (m, 2H), 7.66 – 7.57 (m, 2H), 7.45 – 7.27 (m, 2H), 4.41 (t, *J* = 6.4 Hz, 2H), 2.27 – 2.09 (m, 2H), 1.90 (dt, *J* = 8.7, 6.5 Hz, 2H), 1.83 – 1.68 (m, 2H) ppm. <sup>13</sup>C NMR (101 MHz, CDCl<sub>3</sub>) δ 173.2 (d, *J* = 4.4 Hz), 168.2, 165.9, 160.9 (d, *J* = 260.6 Hz), 134.9 (d, *J* = 8.6 Hz), 132.3, 132.0, 131.2, 131.1, 129.2, 128.8, 127.4, 127.1 (q, *J* = 276.3 Hz), 124.9 (d, *J* = 3.7 Hz), 117.3 (d, *J* = 20.9 Hz), 112.8 (d, *J* = 11.4 Hz), 64.6, 33.5 (q, *J* = 28.7 Hz), 28.0, 18.9 (q, *J* = 3.1 Hz) ppm. IR (neat): 2964, 1714, 1620, 1598, 1556, 1470, 1418, 1390, 1296, 1253, 1218, 1136, 1106, 1037, 925, 882, 824, 783, 769, 747, 670, 651, 545 cm<sup>-1</sup>. Mp: 82 °C. HRMS *calcd.* for (C<sub>20</sub>H<sub>17</sub>F<sub>4</sub>N<sub>2</sub>O<sub>3</sub>) [M+H]<sup>+</sup>: 409.1175, *found* 409.1170.

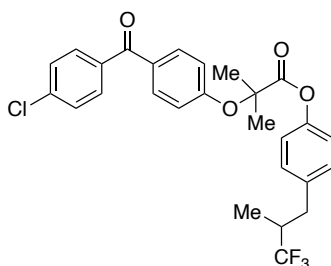


**5,5,5-trifluoropentyl** (*E*)-6-(4-acetoxy-6-methoxy-7-methyl-3-oxo-1,3-dihydroisobenzofuran-5-yl)-4-methylhex-4-enoate (**54**) Prepared following general procedure B using 4-CzIPN (4.8 mg, 3 mol%), Cu(CF<sub>3</sub>)<sub>3</sub>bpy (85.2 mg, 1.0 equiv), 4-(4-oxo-2-phenyl-1,2,3,4-tetrahydroquinazolin-2-yl)butyl (*E*)-6-(4-acetoxy-6-methoxy-7-methyl-3-oxo-1,3-dihydroisobenzofuran-5-yl)-4-methylhex-4-enoate (**A42**) (128.0 mg, 0.2 mmol, 1.0 equiv), Togni's reagent I (99.2 mg, 1.5 equiv), BTMG (34 μL, 1.0 equiv) and 10.0 mL of DMF. Product was obtained as a liquid (40.7 mg, 42% yield) by using Hexane/EtOAc (4:1) as eluent. (46% <sup>19</sup>F NMR yield against internal standard). <sup>19</sup>F NMR (376 MHz, CDCl<sub>3</sub>) δ -66.11 (t, *J* = 10.9 Hz) ppm. <sup>1</sup>H NMR (400 MHz, CDCl<sub>3</sub>) δ 5.13 (s, 2H), 5.10 (t, *J* = 6.9 Hz, 1H), 4.04 (t, *J* = 6.2 Hz, 2H), 3.78 (s, 3H), 3.34 (d, *J* = 7.0 Hz, 2H), 2.43 – 2.35 (m, 5H), 2.29 – 2.25 (m, 2H), 2.21 (s, 3H), 2.14 – 2.02 (m, 2H), 1.77 (s, 3H), 1.72 – 1.55 (m, 4H) ppm. <sup>13</sup>C NMR (101 MHz, CDCl<sub>3</sub>) δ 173.2, 169.0, 168.4, 162.8, 146.3, 146.0, 134.6, 129.2, 127.1 (q, *J* = 276.2 Hz), 123.1, 122.3, 113.6, 68.5, 63.6, 61.3, 34.5, 33.4 (q, *J* = 28.6 Hz), 32.9, 27.7, 23.6, 20.6, 18.7 (q, *J* = 3.3 Hz), 16.3, 11.9 ppm. IR (neat): 2950, 1760, 1732, 1617, 1470, 1390, 1358, 1317, 1293, 1255, 1186, 1127, 1068, 1032, 1008, 967, 950, 921, 888, 733, 651, 539 cm<sup>-1</sup>. HRMS *calcd.* for (C<sub>24</sub>H<sub>29</sub>F<sub>3</sub>NaO<sub>7</sub>) [M+Na]<sup>+</sup>: 509,1763, *found* 509,1766.



**3,7-dimethyl-1-(5,5,5-trifluoropentyl)-3,7-dihydro-1H-purine-2,6-dione (55)**

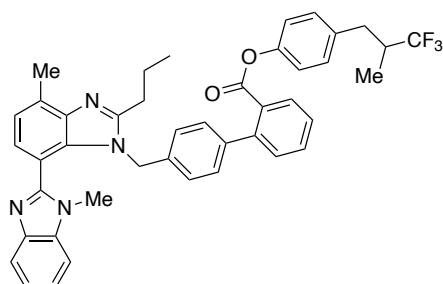
Prepared following general procedure B using 4-CzIPN (4.8 mg, 3 mol%), Cu(CF<sub>3</sub>)<sub>3</sub>bpy (85.2 mg, 1.0 equiv), 3,7-dimethyl-1-(4-(2-methyl-4-oxo-1,2,3,4-tetrahydroquinazolin-2-yl)butyl)-3,7-dihydro-1H-purine-2,6-dione (**A43**) (79.2 mg, 0.2 mmol, 1.0 equiv), Togni's reagent I (99.2 mg, 1.5 equiv), BTMG (34 μL, 1.0 equiv) and 10.0 mL of DMF. Product was obtained as a liquid (15.8 mg, 26% yield) by using Hexane/EtOAc (1:3) as eluent. (25% <sup>19</sup>F NMR yield against internal standard). <sup>19</sup>F NMR (376 MHz, CDCl<sub>3</sub>) δ -66.50 (t, *J* = 10.9 Hz) ppm. <sup>1</sup>H NMR (400 MHz, CDCl<sub>3</sub>) 7.50 (s, 1H), 4.07 – 3.98 (m, 2H), 3.98 (s, 3H), 3.57 (s, 3H), 2.26 – 2.06 (m, 2H), 1.78 – 1.70 (m, 2H), 1.68 – 1.57 (m, 3H) ppm. <sup>13</sup>C NMR (101 MHz, CDCl<sub>3</sub>) δ 155.4, 151.6, 148.9, 141.6, 127.2 (q, *J* = 276.3 Hz), 107.8, 40.7, 33.7, 33.6 (q, *J* = 86.0 Hz), 29.8, 27.2, 19.5 (q, *J* = 2.9 Hz) ppm. Spectral data was in agreement with the literature.<sup>[24]</sup>



**4-(3,3,3-trifluoro-2-methylpropyl)phenyl 2-(4-(4-chlorobenzoyl)phenoxy)-2-methylpropanoate (56)**

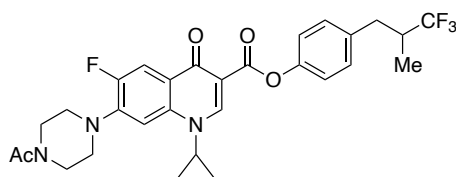
Prepared following general procedure C using 4-CzIPN (4.8 mg, 3 mol%), Cu(CF<sub>3</sub>)<sub>3</sub>bpy (85.2 mg, 0.2mmol, 1.0 equiv), Diethyl 4-(1-(4-((2-(4-(4-chlorobenzoyl)phenoxy)-2-methylpropanoyl)oxy)phenyl)propan-2-yl)-2,6-dimethyl-1,4-dihydropyridine-3,5-dicarboxylate (**B10**) (206.2 mg, 0.3 mmol, 1.5 equiv), K<sub>2</sub>S<sub>2</sub>O<sub>8</sub> (81.2 mg, 1.5 equiv) and NaHCO<sub>3</sub> (33.2 mg, 2.0 equiv) and 8.0 mL of CH<sub>3</sub>CN. Product was obtained as a liquid (68.7 mg, 68% yield) by using Hexane/EA (4:1) as eluent. (68% <sup>19</sup>F NMR yield against internal standard). <sup>19</sup>F NMR (376 MHz, CDCl<sub>3</sub>) δ -73.48 (d, *J* = 8.6 Hz) ppm. <sup>1</sup>H NMR (400 MHz, CDCl<sub>3</sub>) δ 7.79 (d, *J* = 9.0 Hz, 2H), 7.72 (d, *J* = 8.8 Hz, 2H), 7.46 (d, *J* = 8.7 Hz, 2H), 7.17 (d, *J* = 8.6 Hz, 2H), 7.00 (d, *J* = 9.0 Hz, 2H), 6.94 (d, *J* = 8.7 Hz, 2H), 3.10 – 3.06 (m, 1H), 2.53 – 2.33 (m, 2H), 1.83 (s, 6H), 1.01 (d, *J* = 6.6 Hz, 3H) ppm. <sup>13</sup>C NMR (101 MHz, CDCl<sub>3</sub>) δ 194.3, 172.6, 159.6, 149.2, 138.6, 136.4, 136.3, 132.3, 131.3, 130.8, 130.3, 128.7, 121.4, 128.2 (q, *J* = 265.6 Hz), 117.4, 79.6, 40.1 (q, *J* = 26.2 Hz), 35.2 (q, *J* = 2.9 Hz), 25.6, 12.2 (q, *J* = 2.9 Hz) ppm.

**IR (neat):** 2997, 2939, 1757, 1656, 1560, 1506, 1466, 1386, 1304, 1268, 1252, 1194, 1169, 1124, 1091, 1014, 928, 853, 763  $\text{cm}^{-1}$ . **HRMS calcd.** for  $(\text{C}_{27}\text{H}_{25}\text{ClF}_3\text{O}_4)$   $[\text{M}+\text{H}]^+$ : 505,1393, *found* 505,1388.

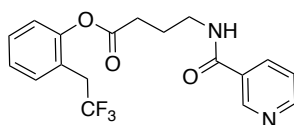


**4-(3,3,3-trifluoro-2-methylpropyl)phenyl 4'-((1,7'-dimethyl-2'-propyl-1H,3'H-[2,4'-bibenzo[d]imidazol]-3'-yl)methyl)-[1,1'-biphenyl]-2-carboxylate (57)**

Prepared following general procedure C using 4-CzIPN (4.8 mg, 3 mol%),  $\text{Cu}(\text{CF}_3)_3\text{bpy}$  (85.2 mg, 0.2 mmol, 1.0 equiv), Diethyl 4-(1-(4-((4'-((1,7'-dimethyl-2'-propyl-1H,3'H-[2,4'-bibenzo[d]imidazol]-3'-yl)methyl)-[1,1'-biphenyl]-2-carbonyl)oxy)phenyl)propan-2-yl)-2,6-dimethyl-1,4-dihydropyridine-3,5-dicarboxylate (**B11**) (264.9 mg, 0.3 mmol, 1.5 equiv),  $\text{K}_2\text{S}_2\text{O}_8$  (81.2 mg, 1.5 equiv) and  $\text{NaHCO}_3$  (33.2 mg, 2.0 equiv) and 8.0 mL of  $\text{CH}_3\text{CN}$ . Product was obtained as a white solid (81.2 mg, 58% yield) by using Hexane/EA (3:1) as eluent. (56%  $^{19}\text{F}$  NMR yield against internal standard).  $^{19}\text{F}$  NMR (376 MHz,  $\text{CDCl}_3$ )  $\delta$  -73.47 (d,  $J = 8.0$  Hz) ppm.  $^1\text{H}$  NMR (400 MHz,  $\text{CDCl}_3$ )  $\delta$  8.01 (d,  $J = 6.3$  Hz, 1H), 7.85 – 7.77 (m, 1H), 7.59 (t,  $J = 7.6$  Hz, 1H), 7.54 – 7.42 (m, 3H), 7.39 – 7.26 (m, 6H), 7.13 (d,  $J = 8.4$  Hz, 2H), 7.03 (d,  $J = 8.5$  Hz, 2H), 6.80 (d,  $J = 8.6$  Hz, 2H), 5.44 (s, 2H), 3.72 (s, 3H), 3.03 – 2.96 (m, 1H), 2.93 – 2.89 (m, 2H), 2.77 (s, 3H), 2.42 – 2.26 (m, 2H), 1.93 – 1.78 (m, 2H), 1.02 (t,  $J = 7.4$  Hz, 3H), 0.94 (d,  $J = 6.4$  Hz, 3H) ppm.  $^{13}\text{C}$  NMR (101 MHz,  $\text{CDCl}_3$ )  $\delta$  166.7, 156.6, 154.6, 149.4, 143.4, 142.5, 141.2, 136.7, 135.8, 135.2, 135.1, 132.2, 131.2, 130.6, 130.1, 129.9, 129.7, 129.4, 128.2 (q,  $J = 279.9$  Hz), 127.7, 126.2, 124.0, 122.7, 122.6, 121.5, 119.6, 109.7, 109.1, 47.2, 40.07 (q,  $J = 26.0$  Hz), 35.1, 31.9, 29.9, 21.9, 17.0, 14.2, 12.17 (q,  $J = 2.9$  Hz) ppm. **IR (neat):** 3063, 3032, 2933, 2872, 1740, 1597, 1507, 1479, 145, 1421, 1404, 1381, 1334, 1320, 1237, 1196, 1166, 1126, 1112, 1090, 1065, 1039, 1013, 875, 851, 760, 744  $\text{cm}^{-1}$ . **Mp:** 108 °C. **HRMS calcd.** for  $(\text{C}_{43}\text{H}_{40}\text{F}_3\text{N}_4\text{O}_2)$   $[\text{M}+\text{H}]^+$ : 701,3103, *found* 701,3098



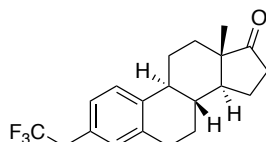
**4-(3,3,3-trifluoro-2-methylpropyl)phenyl 7-(4-acetylpiperazin-1-yl)-1-cyclopropyl-6-fluoro-4-oxo-1,4-dihydroquinoline-3-carboxylate (58)** Prepared following general procedure C using 4-CzIPN (4.8 mg, 3 mol%), Cu(CF<sub>3</sub>)<sub>3</sub>bpy (85.2 mg, 0.2 mmol, 1.0 equiv), Diethyl 4-(1-(4-((7-(4-acetylpiperazin-1-yl)-1-cyclopropyl-6-fluoro-4-oxo-1,4-dihydroquinoline-3-carbonyl)oxy)phenyl)propan-2-yl)-2,6-dimethyl-1,4-dihydropyridine-3,5-dicarboxylate (**B12**) (222.7 mg, 0.3 mmol, 1.5 equiv), K<sub>2</sub>S<sub>2</sub>O<sub>8</sub> (81.2 mg, 1.5 equiv) and NaHCO<sub>3</sub> (33.2 mg, 2.0 equiv) and 8.0 mL of CH<sub>3</sub>CN. Product was obtained as a white solid (69.4 mg, 62% yield) by using Hexane/EA (3:1) as eluent. (71% <sup>19</sup>F NMR yield against internal standard). <sup>19</sup>F NMR (282 MHz, CDCl<sub>3</sub>) δ -73.45 (d, *J* = 8.7 Hz, 3F), -123.36(m, 1F) ppm. <sup>1</sup>H NMR (400 MHz, CDCl<sub>3</sub>) δ 8.59 (s, 1H), 7.95 (d, *J* = 12.3 Hz, 1H), 7.28 (d, *J* = 7.1 Hz, 1H), 7.21 – 7.11 (m, 4H), 3.90 – 3.68 (m, 2H), 3.70 – 3.60 (m, 2H), 3.48 (dt, *J* = 7.0, 3.3 Hz, 1H), 3.27 (t, *J* = 5.0 Hz, 2H), 3.22 (d, *J* = 4.6 Hz, 2H), 3.15 – 3.03 (m, 1H), 2.58 – 2.33 (m, 2H), 2.14 (s, 3H), 1.32 (d, *J* = 7.2 Hz, 2H), 1.20 – 1.12 (m, 2H), 1.02 (d, *J* = 6.5 Hz, 3H) ppm. <sup>13</sup>C NMR (101 MHz, CDCl<sub>3</sub>) δ 172.9, 169.2, 163.7, 153.5 (d, *J* = 249.1 Hz), 149.6, 148.9, 144.3 (d, *J* = 10.6 Hz), 138.0, 135.5, 129.9, 128.2 (q, *J* = 279.5 Hz), 122.1, 113.4 (d, *J* = 23.1 Hz), 109.2, 105.5, 50.5, 49.7, 49.6, 46.3, 41.2, 40.1 (q, *J* = 26.0 Hz), 35.2 (q, *J* = 2.6 Hz), 34.9, 21.4, 12.2 (q, *J* = 2.9 Hz), 8.3 ppm. IR (neat): 2998, 2922, 2866, 2241, 1738, 1712, 1650, 1585, 1494, 1440, 1388, 1351, 1331, 1314, 1248, 1197, 1154, 1124, 1088, 1070, 1010, 998, 979, 941, 911, 890, 872, 726, 645, 589, 571, 525, 494 cm<sup>-1</sup>. Mp: 186 °C. HRMS *calcd.* for (C<sub>29</sub>H<sub>30</sub>F<sub>4</sub>N<sub>3</sub>O<sub>4</sub>) [M+H]<sup>+</sup>: 560,2172, *found* 560,2167.



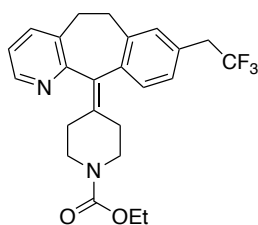
**2-(2,2,2-trifluoroethyl)phenyl 4-(nicotinamido)butanoate (59)** Prepared following general procedure D using Cu(CF<sub>3</sub>)<sub>3</sub>bpy (85.2 mg, 0.2 mmol, 1.0 equiv), Dimethyl 4-(2-((4-(nicotinamido)butanoyl)oxy)benzyl)-1,4-dihydropyridazine-3,6-dicarboxylate (**C10**) (148.2 mg, 0.3 mmol, 1.5 equiv), and 4.0 mL of Acetone. Product was obtained as a white solid (24.3 mg, 33% yield) by using acetone/hexane (1:2) as eluent. (33% <sup>19</sup>F NMR yield against internal standard). <sup>19</sup>F NMR (376 MHz, CDCl<sub>3</sub>) δ -65.43 (t, *J* = 10.9 Hz) ppm. <sup>1</sup>H NMR (400 MHz, CDCl<sub>3</sub>) δ 9.12 (s, 1H), 8.71 (s, 1H), 8.20 (d, *J* = 8.1 Hz, 1H), 7.43 (s, 1H), 7.39 – 7.30 (m, 2H), 7.23 (t, *J* = 7.3, 1H), 7.13 (d, *J* = 7.1 Hz, 1H), 7.03 (s, 1H), 3.61 (q, *J* = 6.7 Hz, 2H), 3.37 (q, *J* = 10.7 Hz, 2H), 2.74 (t, *J* = 7.0



Hz, 2H), 2.12 – 2.05 (pm, 2H) ppm.  $^{13}\text{C}$  NMR (101 MHz,  $\text{CDCl}_3$ )  $\delta$  171.8, 165.7, 151.9, 149.5, 147.8, 135.6, 132.2, 130.4, 129.6, 126.4, 125.6 (q,  $J = 277.0$  Hz), 123.8, 122.9, 122.3 (q,  $J = 2.9$  Hz), 39.6, 34.6 (q,  $J = 30.7$  Hz), 31.8, 24.5 ppm. **IR (neat):** 3316, 2931, 1747, 1665, 1635, 1592, 1493, 1473, 1450, 1416, 1369, 1326, 1312, 1305, 1265, 1243, 1220, 1177, 1142, 1113, 1091, 1065, 1028, 1016, 919, 906, 884, 860, 848, 831, 822, 773, 755, 706, 678, 656, 621, 603, 520  $\text{cm}^{-1}$ . **Mp:** 102 °C. **HRMS calcd.** for  $(\text{C}_{18}\text{H}_{18}\text{F}_3\text{N}_2\text{O}_3)$   $[\text{M}+\text{H}]^+$ : 367,1270, *found* 367,1262.

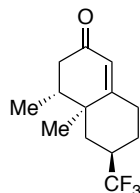


**(8R,9S,13S,14S)-13-methyl-3-(2,2,2-trifluoroethyl)-6,7,8,9,11,12,13,14,15,16-decahydro-17H-cyclopenta[*a*]phenanthren-17-one (60)** Prepared following general procedure D using  $\text{Cu}(\text{CF}_3)_3\text{bpy}$  (85.2 mg, 0.2 mmol, 1.0 equiv), Dimethyl 4-(((8R,9S,13S,14S)-13-methyl-17-oxo-7,8,9,11,12,13,14,15,16,17-decahydro-6H-cyclopenta[*a*]phenanthren-3-yl)methyl)-1,4-dihydropyridazine-3,6-dicarboxylate (**C11**) (139.2 mg, 0.3 mmol, 1.5 equiv), and 4.0 mL of Acetone. Product was obtained as a white solid (38.4 mg, 59% yield) by using hexane/EA (8:1) as eluent. (57%  $^{19}\text{F}$  NMR yield against internal standard).  $^{19}\text{F}$  NMR (376 MHz,  $\text{CDCl}_3$ )  $\delta$  -66.06 (q,  $J = 10.9$  Hz) ppm.  $^1\text{H}$  NMR (400 MHz,  $\text{CDCl}_3$ )  $\delta$  7.28 (d,  $J = 8.0$  Hz, 1H), 7.08 (d,  $J = 5.8$  Hz, 1H), 7.03 (s, 1H), 3.31 (q,  $J = 10.9$  Hz, 2H), 2.93 (dd,  $J = 8.9, 4.2$  Hz, 2H), 2.58 – 2.47 (m, 1H), 2.47 – 2.37 (m, 1H), 2.31 (td,  $J = 10.9, 5.0$  Hz, 1H), 2.22 – 1.93 (m, 4H), 1.71 – 1.41 (m, 6H), 0.92 (s, 3H) ppm.  $^{13}\text{C}$  NMR (101 MHz,  $\text{CDCl}_3$ )  $\delta$  220.9, 139.8, 137.03, 130.9, 127.7 (q,  $J = 2.9$  Hz), 127.6, 126.0 (q,  $J = 276.6$  Hz), 125.8, 50.6, 48.1, 44.4, 39.9 (q,  $J = 29.6$  Hz), 38.2, 35.9, 31.7, 29.4, 26.5, 25.8, 21.7, 13.9 ppm. Spectral data was in agreement with the literature.<sup>[25]</sup>



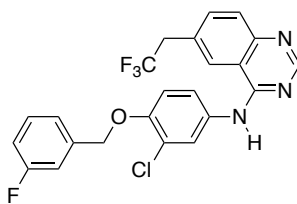
**Ethyl 4-(8-(2,2,2-trifluoroethyl)-5,6-dihydro-11H-benzo[5,6]cyclohepta[1,2-*b*]pyridin-11-ylidene)piperidine-1-carboxylate (61)** Prepared following general procedure D using  $\text{Cu}(\text{CF}_3)_3\text{bpy}$  (55.4 mg, 0.13 mmol, 1.0 equiv), Dimethyl 4-((11-(1-(ethoxycarbonyl)piperidin-4-ylidene)-6,11-dihydro-5H-benzo[5,6]cyclohepta[1,2-

*b*]pyridin-8-yl)methyl)-1,4-dihydropyridazine-3,6-dicarboxylate (**C12**) (72.4 mg, 0.13 mmol, 1.0 equiv), and 2.6 mL of Acetone. Product was obtained as a white solid (20.0 mg, 37% yield) by using hexane/DCM/EA (2:1:1) as eluent. (37%  $^{19}\text{F}$  NMR yield against internal standard).  $^{19}\text{F}$  NMR (376 MHz,  $\text{CDCl}_3$ )  $\delta$  -65.46 (t,  $J$  = 10.9 Hz) ppm.  $^1\text{H}$  NMR (400 MHz,  $\text{CDCl}_3$ )  $\delta$  8.40 (d,  $J$  = 4.8 Hz, 1H), 7.45 (d,  $J$  = 5.9 Hz, 1H), 7.18 (d,  $J$  = 8.3 Hz, 1H), 7.13 – 7.06 (m, 3H), 4.13 (q,  $J$  = 7.1 Hz, 2H), 3.81 (s, 2H), 3.50 – 3.35 (m, 2H), 3.30 (q,  $J$  = 10.9 Hz, 2H), 3.21 – 3.09 (m, 2H), 2.89 – 2.79 (m, 2H), 2.52 – 2.49 (m, 1H), 2.41 – 2.26 (m, 3H), 1.24 (t,  $J$  = 7.1 Hz, 4H) ppm.  $^{13}\text{C}$  NMR (101 MHz,  $\text{CDCl}_3$ )  $\delta$  157.3, 155.5, 146.6, 138.9, 138.0, 137.5, 137.2, 134.7, 133.6, 130.8, 129.6, 129.2 (q,  $J$  = 2.5 Hz), 127.8, 125.7 (q,  $J$  = 276.6 Hz), 122.2, 61.3, 39.9 (q,  $J$  = 29.8 Hz), 39.7, 39.4, 31.8, 31.6, 30.7, 30.5, 14.6 ppm. Spectral data was in agreement with the literature.<sup>[26]</sup>

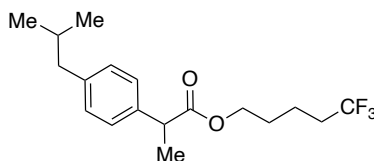


**(4R,4aS,6R)-4,4a-dimethyl-6-(trifluoromethyl)-4,4a,5,6,7,8-**

**hexahydronaphthalen-2(3H)-one (62)** Prepared following general procedure D using  $\text{Cu}(\text{CF}_3)_3\text{bpy}$  (85.2 mg, 0.2 mmol, 1.0 equiv), Dimethyl (*R*)-4-((2*S*,8*R*,8*aS*)-8,8a-dimethyl-6-oxo-1,2,3,4,6,7,8,8*a*-octahydronaphthalen-2-yl)-4-methyl-1,4-dihydropyridazine-3,6-dicarboxylate (**C13**) (77.6 mg, 0.3 mmol, 1.5 equiv), and 4.0 mL of Acetone. Product was obtained as a liquid (23.1 mg, 31% yield) by using Hexane as eluent. (30%  $^{19}\text{F}$  NMR yield against internal standard).  $^{19}\text{F}$  NMR (376 MHz,  $\text{CDCl}_3$ )  $\delta$  -72.79 (d,  $J$  = 8.8 Hz), -73.61 (d,  $J$  = 8.0 Hz) ppm.  $^1\text{H}$  NMR (400 MHz,  $\text{CDCl}_3$ )  $\delta$  5.79 (d,  $J$  = 1.4 Hz, 1H), 2.52 – 2.39 (m, 3H), 2.30 – 2.24 (m, 2H), 2.15 – 1.99 (m, 3H), 1.51 – 1.37 (m, 1H), 1.31 – 1.18 (m, 1H), 1.10 (s, 3H), 0.99 (d,  $J$  = 6.8 Hz, 3H) ppm.  $^{13}\text{C}$  NMR (101 MHz,  $\text{CDCl}_3$ )  $\delta$  198.9, 167.3, 127.5 (q,  $J$  = 278.6 Hz), 126.1, 42.1, 40.4, 38.6, 38.2 (q,  $J$  = 27.0 Hz), 36.9 (q,  $J$  = 2.3 Hz), 31.2, 25.1, 16.7, 15.0 ppm. IR (neat): 2958, 1666, 1621, 1465, 1396, 1322, 1305, 1286, 1261, 1221, 1202, 1155, 1090, 1039, 943, 906, 874, 656  $\text{cm}^{-1}$ . HRMS *calcd.* for  $(\text{C}_{13}\text{H}_{17}\text{F}_3\text{NaO})$   $[\text{M}+\text{Na}]^+$ : 269.1129, *found* 269.1124.

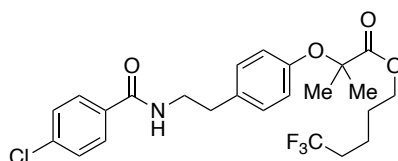


***N*-(3-chloro-4-((3-fluorobenzyl)oxy)phenyl)-6-(2,2,2-trifluoroethyl)quinazolin-4-amine (63)** Prepared following general procedure D using  $\text{Cu}(\text{CF}_3)_3\text{bpy}$  (85.2 mg, 0.2mmol, 1.0 equiv), Dimethyl 4-((4-((3-chloro-4-((3-fluorobenzyl)oxy)phenyl)amino)quinazolin-6-yl)methyl)-1,4-dihydropyridazine-3,6-dicarboxylate (**C14**) (176.7 mg, 0.3 mmol, 1.5 equiv), and 4.0 mL of Acetone. Product was obtained as a white solid (22.1 mg, 24% yield) by using Hexane/EA (2:1) and then Hexane/acetone/MeOH (2:1:5%) as eluent. (25%  $^{19}\text{F}$  NMR yield against internal standard).  $^{19}\text{F}$  NMR (376 MHz,  $\text{CDCl}_3$ )  $\delta$  -66.19 (t,  $J = 10.6$  Hz, 3F), -113.50 –113.56 (m, 1F) ppm.  $^1\text{H}$  NMR (400 MHz,  $\text{CDCl}_3$ )  $\delta$  8.70 (s, 1H), 7.93 (d,  $J = 8.4$  Hz, 1H), 7.83 (d,  $J = 2.6$  Hz, 1H), 7.72 (d,  $J = 8.4$  Hz, 1H), 7.54 (d,  $J = 8.9$  Hz, 1H), 7.35 (q,  $J = 7.2$  Hz, 1H), 7.23 – 7.19 (m, 3H), 7.08 – 6.89 (m, 2H), 5.19 – 5.09 (m, 2H), 3.56 (q,  $J = 10.6$  Hz, 2H) ppm.  $^{13}\text{C}$  NMR (101 MHz,  $\text{CD}_2\text{Cl}_2$ )  $\delta$  163.4 (d,  $J = 245.5$  Hz), 157.8, 155.5, 151.5, 150.1, 139.7 (d,  $J = 7.3$  Hz), 135.1, 132.7, 130.7 (d,  $J = 8.1$  Hz), 129.7, 129.2 (q,  $J = 3.3$  Hz), 126.1 (q,  $J = 277.0$  Hz), 125.1, 123.6, 123.1 (d,  $J = 2.9$  Hz), 122.7, 122.3, 115.4, 115.2, 114.6, 114.4 (d,  $J = 22.3$  Hz), 70.8 (d,  $J = 2.2$  Hz), 40.54 (q,  $J = 29.8$  Hz) ppm. IR (neat): 1636, 1605, 1575, 1530, 1497, 1450, 1424, 1393, 1358, 1327, 1294, 1265, 1223, 1204, 1188, 1139, 1089, 1072, 1061, 1030, 927, 903, 888, 858, 823, 808, 771, 681, 568, 516, 442  $\text{cm}^{-1}$ . Mp: 189 °C. HRMS *calcd.* for  $(\text{C}_{23}\text{H}_{17}\text{ClF}_4\text{N}_3\text{O})$   $[\text{M}+\text{H}]^+$ : 462,0996, *found* 462,0991.

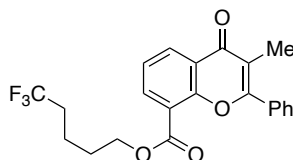


**5,5,5-trifluoropentyl 2-(4-isobutylphenyl)propanoate (64)** Prepared following general procedure D using  $\text{Cu}(\text{CF}_3)_3\text{bpy}$  (85.2 mg, 0.2mmol, 1.0 equiv), Dimethyl 4-((2-(4-isobutylphenyl)propanoyl)oxy)butyl)-4-methyl-1,4-dihydropyridazine-3,6-dicarboxylate (**C15**) (141.6 mg, 0.3 mmol, 1.5 equiv), and 4.0 mL of Acetone. Product was obtained as a liquid (28.7 mg, 44% yield) by using Hexane/EA (15:1) as eluent. (45%  $^{19}\text{F}$  NMR yield against internal standard).  $^{19}\text{F}$  NMR (376 MHz,  $\text{CDCl}_3$ )  $\delta$  -66.57 (t,  $J = 10.9$  Hz) ppm.  $^1\text{H}$  NMR (400 MHz,  $\text{CDCl}_3$ )  $\delta$  7.19 (d,  $J = 8.0$  Hz, 2H), 7.09 (d,  $J = 8.3$  Hz, 2H), 4.27 – 3.89 (m, 2H), 3.69 (q,  $J = 7.1$  Hz, 1H), 2.44 (d,  $J = 7.2$  Hz, 2H),

2.13 – 1.85 (m, 2H), 1.89 – 1.78 (m, 1H), 1.73 – 1.59 (m, 2H), 1.53 – 1.48 (m, 5H), 0.89 (d,  $J = 6.6$  Hz, 6H) ppm.  $^{13}\text{C}$  NMR (101 MHz,  $\text{CDCl}_3$ )  $\delta$  174.9, 140.8, 137.8, 129.5, 127.2, 127.1 (q,  $J = 276.2$  Hz), 63.9, 45.3, 45.2, 33.4 (q,  $J = 28.8$  Hz), 30.3, 27.7, 22.5, 18.7 (q,  $J = 3.3$  Hz), 18.4 ppm. IR (neat): 2956, 2871, 1733, 1513, 1462, 1441, 1386, 1367, 1333, 1321, 1289, 1254, 1220, 1200, 1142, 1072, 1039  $\text{cm}^{-1}$ . HRMS *calcd.* for  $(\text{C}_{18}\text{H}_{25}\text{F}_3\text{NaO}_2)$   $[\text{M}+\text{Na}]^+$ : 353,1704, *found* 353,1699.

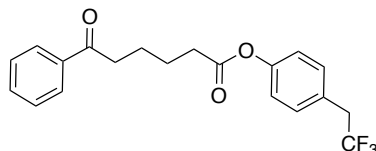


**5,5,5-trifluoropentyl 2-(4-(2-(4-chlorobenzamido)ethyl)phenoxy)-2-methylpropanoate (65)** Prepared following general procedure D using  $\text{Cu}(\text{CF}_3)_3\text{bpy}$  (85.2 mg, 0.2mmol, 1.0 equiv), Dimethyl 4-(4-((2-(4-(2-(4-chlorobenzamido)ethyl)phenoxy)-2-methylpropanoyl)oxy)butyl)-4-methyl-1,4-dihydropyridazine-3,6-dicarboxylate (**C16**) (188.2 mg, 0.3 mmol, 1.5 equiv), and 4.0 mL of Acetone. Product was obtained as a white solid (32.1 mg, 33% yield) by using Hexane/Acetone (3:1) as eluent. (35%  $^{19}\text{F}$  NMR yield against internal standard).  $^{19}\text{F}$  NMR (376 MHz,  $\text{CDCl}_3$ )  $\delta$  -66.57 (t,  $J = 10.9$  Hz) ppm.  $^1\text{H}$  NMR (400 MHz,  $\text{CDCl}_3$ )  $\delta$  7.61 (d,  $J = 8.6$  Hz, 2H), 7.37 (d,  $J = 8.6$  Hz, 2H), 7.08 (d,  $J = 8.6$  Hz, 2H), 6.78 (d,  $J = 8.6$  Hz, 2H), 6.10 (s, 1H), 4.17 (t,  $J = 6.2$  Hz, 2H), 3.65 (q,  $J = 6.8$  Hz, 2H), 2.85 (t,  $J = 6.9$  Hz, 2H), 1.71 – 1.66 (m, 2H), 1.80 – 1.65 (m, 2H), 1.59 (s, 6H), 1.56 – 1.43 (m, 2H) ppm.  $^{13}\text{C}$  NMR (101 MHz,  $\text{CDCl}_3$ )  $\delta$  174.4, 166.5, 154.3, 137.8, 133.2, 132.5, 129.6, 128.9, 128.4, 127.0 (q,  $J = 829.2$  Hz), 119.3, 79.2, 64.7, 41.3, 34.9, 33.3 (q,  $J = 28.5$  Hz), 27.6, 25.5, 18.7 (q,  $J = 3.3$  Hz) ppm. IR (neat): 3273, 2946, 2927, 1729, 1633, 1616, 1591, 1510, 1487, 1467, 1391, 1381, 1365, 11316, 1287, 1250, 1234, 1181, 1130, 1089, 1072, 1040, 1013, 980, 956, 934, 847, 836, 819, 751, 720, 680, 524  $\text{cm}^{-1}$ . **Mp**: 187 °C. HRMS *calcd.* for  $(\text{C}_{24}\text{H}_{28}\text{ClF}_3\text{NO}_4)$   $[\text{M}+\text{H}]^+$ : 486,1659, *found* 486,1653.

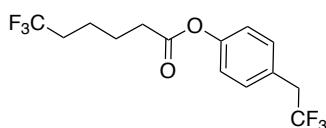


**5,5,5-trifluoropentyl 3-methyl-4-oxo-2-phenyl-4H-chromene-8-carboxylate (66)** Prepared following general procedure D using  $\text{Cu}(\text{CF}_3)_3\text{bpy}$  (85.2 mg, 0.2mmol, 1.0 equiv), Dimethyl 4-methyl-4-(4-((3-methyl-4-oxo-2-phenyl-4H-chromene-8-carbonyl)oxy)butyl)-1,4-dihydropyridazine-3,6-dicarboxylate (**C17**) (163.9 mg, 0.3 mmol, 1.5 equiv), and 4.0 mL of Acetone. Product was obtained as a white solid (27.5

mg, 34% yield) by using Hexane/EA (8:1) as eluent. (34%  $^{19}\text{F}$  NMR yield against internal standard).  $^{19}\text{F}$  NMR (376 MHz,  $\text{CDCl}_3$ )  $\delta$  -66.39 (t,  $J$  = 10.9 Hz) ppm.  $^1\text{H}$  NMR (400 MHz,  $\text{CDCl}_3$ ) 8.47 (dd,  $J$  = 7.9, 1.8 Hz, 1H), 8.26 (dd,  $J$  = 7.6, 1.8 Hz, 1H), 7.85 – 7.69 (m, 2H), 7.54 – 7.52 (m, 3H), 7.45 (t,  $J$  = 7.7 Hz, 1H), 4.36 (t,  $J$  = 6.4 Hz, 2H), 2.22 (s, 3H), 2.07 – 1.93 (m, 2H), 1.85 – 1.74 (m, 2H), 1.65 – 1.53 (m, 2H) ppm.  $^{13}\text{C}$  NMR (101 MHz,  $\text{CDCl}_3$ )  $\delta$  178.4, 164.6, 161.2, 154.6, 136.3, 133.2, 131.1, 130.6, 129.4, 128.6, 127.0 (q,  $J$  = 276.6 Hz), 124.2, 123.5, 120.7, 117.9, 64.8, 33.4 (q,  $J$  = 28.9 Hz), 27.8, 18.8 (q,  $J$  = 3.3 Hz), 11.8 ppm. IR (neat): 2964, 2925, 2896, 2856, 1709, 1637, 1623, 1599, 1582, 1496, 1479, 1469, 1436, 1395, 1366, 1331, 1288, 1270, 1251, 1236, 1216, 1184, 1135, 1091, 1067, 1039, 1024, 924, 898, 856, 837, 829, 814, 776, 756, 732, 698, 661, 487, 467  $\text{cm}^{-1}$ . Mp: 105 °C. HRMS *calcd.* for  $(\text{C}_{22}\text{H}_{20}\text{F}_3\text{O}_4)$   $[\text{M}+\text{H}]^+$ : 405,1314, *found* 405,1308.



**4-(2,2,2-trifluoroethyl)phenyl 6-oxo-6-phenylhexanoate (71)** Prepared following general procedure D using  $\text{Cu}(\text{CF}_3)_3\text{bpy}$  (85.2 mg, 0.2mmol, 1.0 equiv), dimethyl 4-methyl-4-(4-((6-oxo-6-phenylhexanoyl)oxy)benzyl)-1,4-dihydropyridazine-3,6-dicarboxylate (**C18**) (101.2 mg, 0.2 mmol, 1.0 equiv), and 4.0 mL of Acetone. Product was obtained as a liquid (49.9 mg, 68% yield) by using Hexane as eluent. (66%  $^{19}\text{F}$  NMR yield against internal standard).  $^{19}\text{F}$  NMR (376 MHz,  $\text{CDCl}_3$ )  $\delta$  -66.07 (t,  $J$  = 10.8 Hz) ppm.  $^1\text{H}$  NMR (400 MHz,  $\text{CDCl}_3$ )  $\delta$  7.97 (d,  $J$  = 7.1 Hz, 2H), 7.61 – 7.52 (m, 1H), 7.46 (t,  $J$  = 7.6 Hz, 2H), 7.29 (d,  $J$  = 8.4 Hz, 2H), 7.15 – 7.05 (m, 2H), 3.35 (q,  $J$  = 10.8 Hz, 2H), 3.05 (t,  $J$  = 6.7 Hz, 2H), 2.63 (t,  $J$  = 6.9 Hz, 2H), 2.01 – 1.80 (m, 4H) ppm.  $^{13}\text{C}$  NMR (101 MHz,  $\text{CDCl}_3$ )  $\delta$  199.7, 171.8, 150.6, 136.9, 133.1, 131.3, 128.7, 128.1, 127.7 (q,  $J$  = 2.9 Hz), 125.7 (q,  $J$  = 276.7 Hz), 121.9, 39.6 (q,  $J$  = 29.9 Hz), 38.1, 34.2, 24.6, 23.6 ppm. IR (neat): 3043, 2940, 1760, 1747, 1668, 1598, 1581, 1509, 1350, 1412, 1362, 1251, 1210, 1167, 1127, 1107, 1074, 975, 906, 831, 730, 685, 650, 573, 525  $\text{cm}^{-1}$ . HRMS *calcd.* for  $(\text{C}_{20}\text{H}_{19}\text{F}_3\text{NaO}_3)$   $[\text{M}+\text{Na}]^+$ : 387.1184, *found* 387.1187.

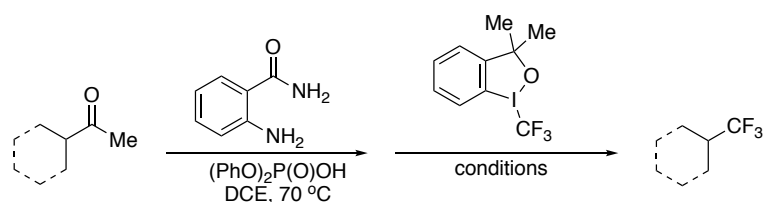


**4-(2,2,2-trifluoroethyl)phenyl 6,6,6-trifluorohexanoate (72)** Prepared following general procedure B using 4-CzIPN (4.8 mg, 3 mol%),  $\text{Cu}(\text{CF}_3)_3\text{bpy}$  (85.2 mg, 1.0

---

equiv), 4-(2,2,2-trifluoroethyl)phenyl 5-(4-oxo-2-phenyl-1,2,3,4-tetrahydroquinazolin-2-yl)pentanoate (**A44**) (96.4 mg, 0.2 mmol, 1.0 equiv), Togni's reagent I (99.2 mg, 1.5 equiv), BTMG (34  $\mu$ L, 1.0 equiv) and 10.0 mL of DMF. Product was obtained as a colorless oil (44.9 mg, 68% yield) by using Hexane/EtOAc (5:1) as eluent. (68%  $^{19}\text{F}$  NMR yield against internal standard).  $^{19}\text{F}$  NMR (376 MHz,  $\text{CDCl}_3$ )  $\delta$  -66.14 (t,  $J$  = 10.8 Hz), -66.46 (t,  $J$  = 10.8 Hz) ppm.  $^1\text{H}$  NMR (400 MHz,  $\text{CDCl}_3$ )  $\delta$  7.31 (d,  $J$  = 8.4 Hz, 2H), 7.12 – 7.02 (m, 2H), 3.36 (q,  $J$  = 10.8 Hz, 2H), 2.61 (t,  $J$  = 7.3 Hz, 2H), 2.15 (ddd,  $J$  = 10.8, 7.9, 5.4 Hz, 2H), 1.84 (dt,  $J$  = 15.0, 7.3 Hz, 2H), 1.75 – 1.65 (m, 2H) ppm.  $^{13}\text{C}$  NMR (101 MHz,  $\text{CDCl}_3$ )  $\delta$  171.5, 150.6, 131.4, 127.9 (q,  $J$  = 2.9 Hz), 126.45 (q,  $J$  = 138.9 Hz), 126.45 (q,  $J$  = 414.2 Hz), 121.9, 39.7 (q,  $J$  = 30.0 Hz), 33.9, 33.6 (q,  $J$  = 28.7 Hz), 24.0, 21.6 (q,  $J$  = 3.0 Hz) ppm. IR (neat): 2951, 1757, 1510, 1362, 1255, 1208, 1128, 1075, 1029, 909, 832, 651, 522  $\text{cm}^{-1}$ . HRMS *calcd.* for ( $\text{C}_{14}\text{H}_{14}\text{F}_6\text{NaO}_2$ )  $[\text{M}+\text{Na}]^+$ : 351.0796, *found* 351.0795.

## One-Pot Trifluoromethylation without Isolation of Proaromatic Precursors



### *tert*-butyl 4-(trifluoromethyl)piperidine-1-carboxylate (**3**)

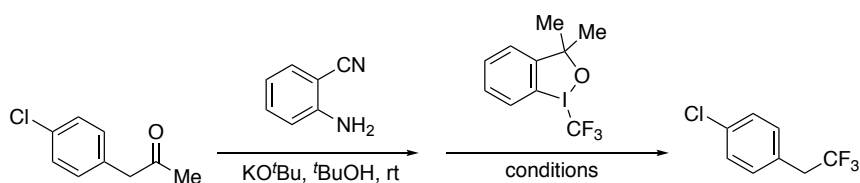
An oven-dried 8 mL screw-cap test tube was charged with a stir bar, 2-aminobenzamide (25.8 mg, 0.19 mmol), *tert*-butyl 4-acetylpiperidine-1-carboxylate (45.4 mg, 0.2 mmol), diphenyl phosphate (5.0 mg, 0.02 mmol) and DCE (0.4 mL). The reaction mixture was stirred at  $70\text{ }^\circ\text{C}$  for 24 hours. The reaction mixture was concentrated in vacuo to give the crude intermediate. An oven-dried 20 mL Schlenk tube containing a stir bar was charged with 4-CzIPN (4.8 mg, 3 mol%),  $\text{CuCl}_2$  (5.6 mg, 20 mol%), Phenanthroline (10.8 mg, 30 mol%), *tert*-butyl 4-(2-methyl-4-oxo-1,2,3,4-tetrahydroquinazolin-2-yl)piperidine-1-carboxylate (**A1**) (crude intermediate from last step) and Togni's reagent I (132.0 mg, 2.0 equiv). The Schlenk tube was connected to a vacuum line where it was evacuated and back-filled under Ar three times. Acetone (8.0 mL) was then added followed by BTMG (34.0  $\mu\text{L}$ , 1.0 equiv) under argon atmosphere. The reaction mixture was sonicated, then placed in a temperature-controlled photoreactor maintained at  $40\text{ }^\circ\text{C}$  and stirred for 18 h under continuous light irradiation from blue LEDs ( $\lambda = 451\text{ nm}$ ). The reaction mixture was diluted with  $\text{Et}_2\text{O}$ , and then quenched with aqueous NaCl. The reaction mixture was extracted into  $\text{Et}_2\text{O}$  (3x). The organic phase was dried with anhydrous  $\text{Na}_2\text{SO}_4$ , filtered, and carefully concentrated. Product was obtained as a colorless solid (38.1 mg, 43% yield) by using Hexane/EtOAc (10:1) as eluent. (50%  $^{19}\text{F}$  NMR yield against internal standard).

### 4-(trifluoromethyl)tetrahydro-2H-pyran (**16**)

An oven-dried 8 mL screw-cap test tube was charged with a stir bar, 2-aminobenzamide (25.8 mg, 0.19 mmol), 1-(tetrahydro-2H-pyran-4-yl)ethan-1-one (25.2 mg, 0.2 mmol), diphenyl phosphate (5.0 mg, 0.02 mmol) and DCE (0.4 mL). The reaction mixture was stirred at  $70\text{ }^\circ\text{C}$  for 24 hours. The reaction mixture was concentrated in vacuo to give the crude intermediate. An oven-dried 20 mL Schlenk tube containing a stirring bar was charged with 4-CzIPN (4.8 mg, 3 mol%),  $\text{CuCl}_2$  (5.6 mg, 20 mol%), Phenanthroline (10.8 mg, 30 mol%), 2-methyl-2-(tetrahydro-2H-pyran-4-yl)-2,3-dihydroquinazolin-4(1H)-one (**A14**) (crude intermediate from last step) and Togni's reagent I (132.0 mg,

2.0 equiv). The Schlenk tube was connected to a vacuum line where it was evacuated and back-filled under Ar three times. Acetone (8.0 mL) was then added followed by BTMG (34.0  $\mu$ L, 1.0 equiv) under argon atmosphere. The reaction mixture was sonicated, then placed in a temperature-controlled photoreactor maintained at 40 °C and stirred for 18 h under continuous light irradiation from blue LEDs ( $\lambda = 451$  nm). The reaction mixture was diluted with Et<sub>2</sub>O, and then quenched with aqueous NaCl. The reaction mixture was extracted into Et<sub>2</sub>O (3x). The organic phase was dried with anhydrous Na<sub>2</sub>SO<sub>4</sub>, filtered, and carefully concentrated. Product could not be isolated due to its volatility, 1,1,1-trifluorotoluene (24.4  $\mu$ L, 0.2 mmol, 1.0 equiv) was added as an internal standard for <sup>19</sup>F NMR analysis (48% yield).

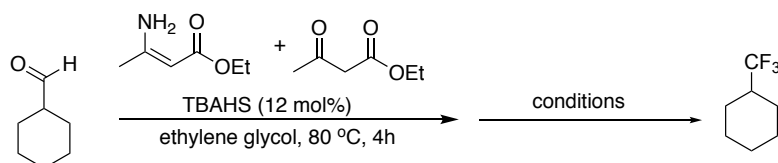
### 1-chloro-4-(2,2,2-trifluoroethyl)benzene (19)



Following a literature procedure,<sup>[27]</sup> to a mixture of 2-aminobenzonitrile (0.20 mmol, 23.6 mg) and 1-(4-chlorophenyl)propan-2-one (0.5 mmol) in dry *t*BuOH, KO<sup>t</sup>Bu (2.0 equiv) was added under Ar atmosphere. The mixture was stirred in a flame-dried sealed tube for 1 h and the progress of reaction was monitored by TLC. After completion, the mixture was diluted with aq. KHSO<sub>4</sub> solution and extracted into EtOAc (3x). The solvent was removed in vacuo to give the crude intermediate. An oven-dried 20 mL Schlenk tube containing a stir bar was charged with 4-CzIPN (4.8 mg, 3 mol%), CuCl<sub>2</sub> (5.6 mg, 20 mol%), di(pyridin-2-yl)methanone (11.0 mg, 30 mol%), 2-(4-chlorobenzyl)-2-methyl-2,3-dihydroquinazolin-4(1*H*)-one (**A17**) (crude intermediate from last step), KH<sub>2</sub>PO<sub>4</sub> (0.4 mmol, 2.0 equiv) and Togni's reagent I (132.0 mg, 2.0 equiv). The Schlenk tube was connected to a vacuum line where it was evacuated and back-filled under Ar three times. DMF (10.0 mL) was added under argon atmosphere. The Schlenk tube was closed at the atmospheric pressure of Ar and placed in temperature-controlled photoreactor maintained at 40 °C and stirred for 18 h under continuous light irradiation from blue LEDs ( $\lambda = 451$  nm). The reaction mixture was diluted with Et<sub>2</sub>O, and then quenched with aqueous NaCl. 1,1,1-trifluorotoluene (24.4  $\mu$ L, 0.2 mmol, 1.0 equiv) was added as an internal standard for <sup>19</sup>F NMR analysis (58% yield).

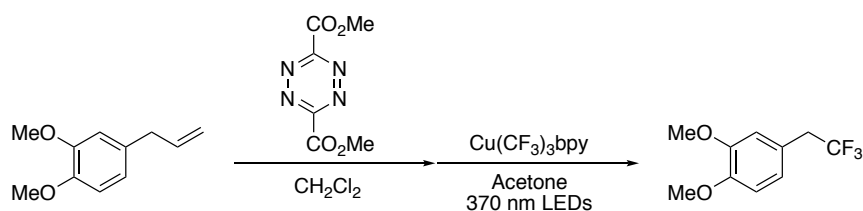
### (trifluoromethyl)cyclohexane (12)





To a solution of cyclohexanecarbaldehyde (1.2 equiv), ethyl 3-aminocrotonate (1.0 equiv) and ethyl acetoacetate (1.0 equiv) in ethylene glycol (2.5 M) was added  $\text{Bu}_4\text{NHSO}_4$  (12 mol%) in one portion. The vial was sealed and heated at 80 °C for 4 h. The mixture was then diluted with water and extracted into EtOAc (3x). The solvent was removed in vacuo to give the crude intermediate. An oven-dried 20 mL Schlenk tube containing a stir bar was charged with 4-CzIPN (4.8 mg, 3 mol%),  $\text{Cu}(\text{CF}_3)_3\text{bpy}$  (85.2 mg, 0.2 mmol, 1.0 equiv), diethyl 4-cyclohexyl-2,6-dimethyl-1,4-dihydropyridine-3,5-dicarboxylate (**B1**) (crude intermediate from last step) (1.0 equiv),  $\text{K}_2\text{S}_2\text{O}_8$  (81.2 mg, 1.5 equiv) and  $\text{NaHCO}_3$  (33.2 mg, 2.0 equiv). The Schlenk tube was connected to a vacuum line where it was evacuated and back-filled with Ar at least three times.  $\text{CH}_3\text{CN}$  (8.0 mL) was added under argon atmosphere. The Schlenk tube was closed at the atmospheric pressure of Ar and placed at a temperature-controlled photoreactor maintained at 40 °C and stirred for 16 h under continuous light irradiation from blue LEDs ( $\lambda = 451 \text{ nm}$ ). The reaction was diluted with  $\text{Et}_2\text{O}$ , and then quenched by aqueous NaCl. Product could not be isolated due to its volatility, 1,1,1-trifluorotoluene (24.4  $\mu\text{L}$ , 0.2 mmol, 1.0 equiv) was added as an internal standard for  $^{19}\text{F}$  NMR analysis. (64% yield).

#### 1,2-dimethoxy-4-(2,2,2-trifluoroethyl)benzene (**48**)



To an oven-dried vial containing a stir bar was added dimethyl 1,2,4,5-tetrazine-3,6-dicarboxylate (59 mg, 0.3 mmol, 1.5 equiv) in  $\text{CH}_2\text{Cl}_2$  (1.5 mL) under Ar. 4-Allyl-1,2-dimethoxybenzene (53.5 mg, 0.3 mmol, 1.5 equiv) was then added ( $\text{N}_2$  gas release was observed) and the reaction mixture was stirred at r.t. for 2 h (red to yellow color change observed). The solvent was removed in vacuo.  $\text{Cu}(\text{CF}_3)_3\text{bpy}$  (85.2 mg, 0.2 mmol, 1.0 equiv) and anhydrous acetone (4 mL) were then added under Ar. The reaction mixture was irradiated under 370 nm LEDs for 18 h. The reaction mixture was then diluted with  $\text{Et}_2\text{O}$  and quenched with aqueous NaCl. 1-Fluoro-3-nitrobenzene (20  $\mu\text{L}$ ) was added as

---

an internal standard for  $^{19}\text{F}$  NMR analysis (51% yield). The organics were separated and the aqueous extracted 3x into  $\text{Et}_2\text{O}$ . The organics were washed with aqueous  $\text{NaCl}$ , dried ( $\text{Na}_2\text{SO}_4$ ), and concentrated in vacuo. The crude product was purified by column chromatography (5% acetone/hexane) to give 1,2-dimethoxy-4-(2,2,2-trifluoroethyl)benzene (**48**) as a colorless oil (20 mg, 0.09 mmol, 45% yield).

### 3.7.4 Mechanistic Experiments

#### 3.7.4.1 Homolysis of (bpy)Cu(CF<sub>3</sub>)<sub>3</sub> by UV-Vis and <sup>19</sup>F NMR

To investigate the homolysis of (bpy)Cu(CF<sub>3</sub>)<sub>3</sub>, the irradiation of (bpy)Cu(CF<sub>3</sub>)<sub>3</sub> was performed in MeCN in a cuvette, and monitored by UV-Vis and <sup>19</sup>F NMR. In a 3 mL vial, (bpy)Cu(CF<sub>3</sub>)<sub>3</sub> (8.9 mg, 0.02 mmol) was dissolved in 3 mL MeCN and transferred to a sealable quartz cuvette and UV-Vis spectrum recorded. The sealed cuvette was then irradiated ( $\lambda = 450$  nm) for 30 minutes in which a new signal in the UV-Vis spectra was observed at  $\lambda_{\text{max}} = 685$  nm which is similar to Cu(II) complex (bpy)CuCl<sub>2</sub> (Figure S1. a, purple trace).

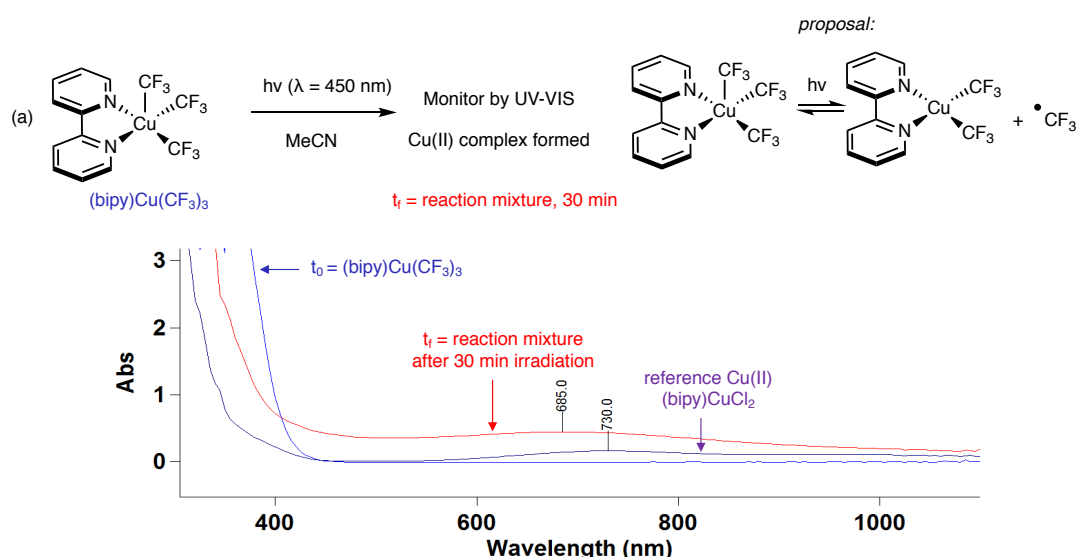


**Figure S1.** Probing products of (bpy)Cu(CF<sub>3</sub>)<sub>3</sub> homolysis by UV-Vis.

To this solution, a stock solution of trifluorotoluene (1 equiv, internal standard) in MeCN-*d*<sub>3</sub> was added and transferred to an NMR tube in which quantitative <sup>19</sup>F{<sup>1</sup>H} NMR established full conversion of (bpy)Cu(CF<sub>3</sub>)<sub>3</sub> and formation of organic products 3,3,3-trifluoropropanenitrile (63% yield) and fluoroform (41% yield). *Conclusion*; Irradiation of (bpy)Cu(CF<sub>3</sub>)<sub>3</sub> at  $\lambda = 450$  nm initiates homolysis of the Cu-CF<sub>3</sub> bond to form CF<sub>3</sub> radicals and Cu(II) complexes. These CF<sub>3</sub> radicals can then undergo HAT with a hydrogen acceptor to form HCF<sub>3</sub> and another radical intermediate.

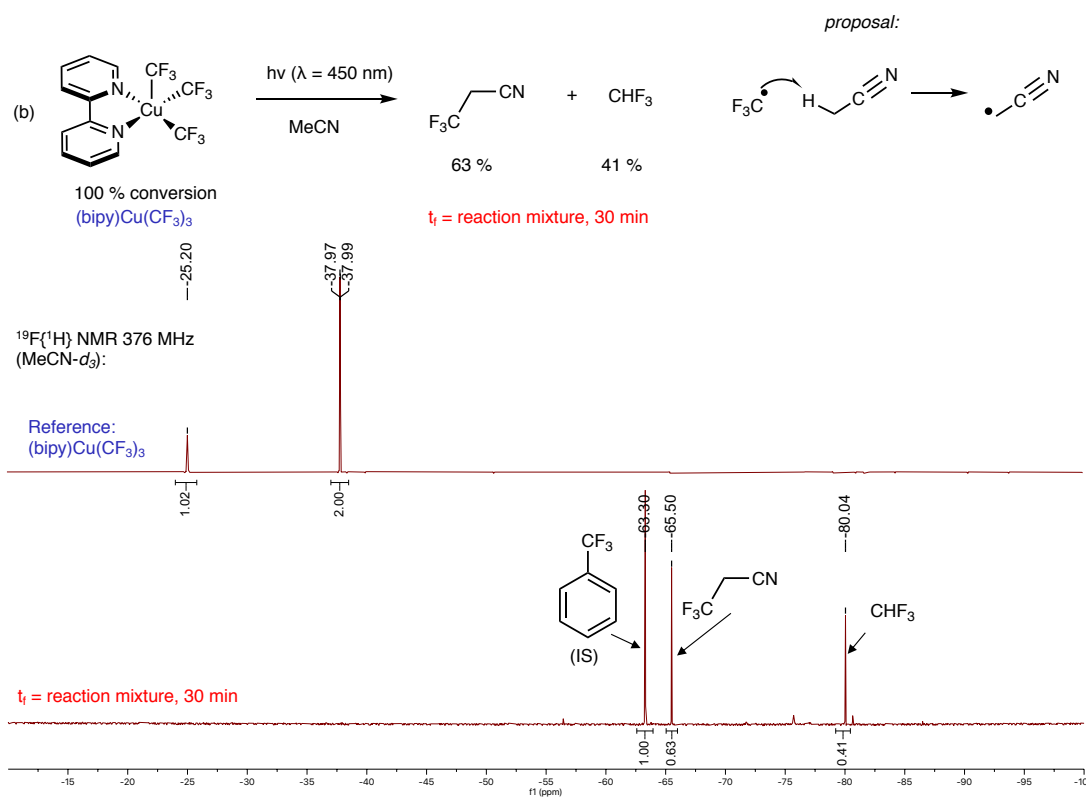


**Figure S2.** Probing products of (bpy)Cu(CF<sub>3</sub>)<sub>3</sub> homolysis by UV-Vis and <sup>19</sup>F NMR spectroscopy.

---

### 3.7.5 X-Ray Crystallography Data

#### X-Ray Data

#### X-ray diffraction of 17

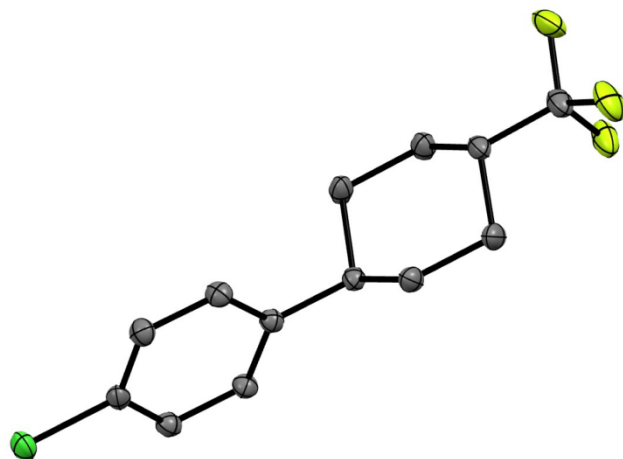


**Figure S3.** ORTEP Diagram of **CCDC-2173015**.

Table S1. Crystal data and structure refinement for **CCDC-2173015**.

---

Empirical formula	C <sub>13</sub> H <sub>14</sub> Cl F <sub>3</sub>
Formula weight	262.69
Temperature	100(2)K
Wavelength	0.71073 $\approx$
Crystal system	monoclinic
Space group	C c
Unit cell dimensions	a = 13.9995(11) $\approx$ a = 90 $\infty$ .
	b = 10.0787(8) $\approx$ b = 123.638(2) $\infty$ .
	c = 10.3743(9) $\approx$ g = 90 $\infty$ .
Volume	1218.68(17) $\approx$ 3
Z	4
Density (calculated)	1.432 Mg/m <sup>3</sup>
Absorption coefficient	0.325 mm <sup>-1</sup>
F(000)	544
Crystal size	0.300 x 0.300 x 0.200 mm <sup>3</sup>
Theta range for data collection	2.672 to 32.571 $\infty$ .
Index ranges	-21 $\leq$ h $\leq$ 17, 0 $\leq$ k $\leq$ 15, 0 $\leq$ l $\leq$ 15
Reflections collected	3896

---

Independent reflections 3896[R(int) = ?]  
Completeness to theta =32.571° 97.3%  
Absorption correction Multi-scan  
Max. and min. transmission 0.74 and 0.70  
Refinement method Full-matrix least-squares on F2  
Data / restraints / parameters 3896/ 2/ 155  
Goodness-of-fit on F2 1.099  
Final R indices [I>2sigma(I)] R1 = 0.0230, wR2 = 0.0633  
R indices (all data) R1 = 0.0239, wR2 = 0.0645  
Flack parameter x =0.11(2)  
Largest diff. peak and hole 0.323 and -0.184 e.~3

---

Table S2. Bond lengths [ $\text{\AA}$ ] and angles [ $^\circ$ ]

---

Bond lengths----

F1	C7	1.3454(19)
C11	C11	1.7335(14)
F2	C7	1.3428(18)
F3	C7	1.3373(19)
C1	C7	1.503(2)
C1	C2	1.5261(19)
C1	C6	1.5279(19)
C1	H1	1.0000
C2	C3	1.5256(19)
C2	H2A	0.9900
C2	H2B	0.9900
C3	C4	1.5280(18)
C3	H3A	0.9900
C3	H3B	0.9900
C4	C8	1.5096(17)
C4	C5	1.5277(18)
C4	H4	1.0000
C5	C6	1.5273(19)
C5	H5A	0.9900
C5	H5B	0.9900
C6	H6A	0.9900
C6	H6B	0.9900
C8	C13	1.3922(17)
C8	C9	1.4003(18)
C9	C10	1.3916(19)
C9	H9	0.9500
C10	C11	1.3871(19)
C10	H10	0.9500
C11	C12	1.3849(19)
C12	C13	1.3904(19)
C12	H12	0.9500

---

C13 H13 0.9500

Angles-----

C7	C1	C2	111.51(11)
C7	C1	C6	111.12(11)
C2	C1	C6	110.87(11)
C7	C1	H1	107.7
C2	C1	H1	107.7
C6	C1	H1	107.7
C3	C2	C1	110.46(11)
C3	C2	H2A	109.6
C1	C2	H2A	109.6
C3	C2	H2B	109.6
C1	C2	H2B	109.6
H2A	C2	H2B	108.1
C2	C3	C4	111.77(11)
C2	C3	H3A	109.3
C4	C3	H3A	109.3
C2	C3	H3B	109.3
C4	C3	H3B	109.3
H3A	C3	H3B	107.9
C8	C4	C5	110.88(10)
C8	C4	C3	112.76(10)
C5	C4	C3	110.17(11)
C8	C4	H4	107.6
C5	C4	H4	107.6
C3	C4	H4	107.6
C6	C5	C4	112.01(11)
C6	C5	H5A	109.2
C4	C5	H5A	109.2
C6	C5	H5B	109.2
C4	C5	H5B	109.2
H5A	C5	H5B	107.9
C5	C6	C1	110.45(11)



---

C5	C6	H6A	109.6
C1	C6	H6A	109.6
C5	C6	H6B	109.6
C1	C6	H6B	109.6
H6A	C6	H6B	108.1
F3	C7	F2	106.36(13)
F3	C7	F1	105.76(13)
F2	C7	F1	106.06(13)
F3	C7	C1	112.81(13)
F2	C7	C1	113.10(11)
F1	C7	C1	112.18(12)
C13	C8	C9	118.07(12)
C13	C8	C4	120.24(11)
C9	C8	C4	121.67(11)
C10	C9	C8	121.14(12)
C10	C9	H9	119.4
C8	C9	H9	119.4
C11	C10	C9	119.08(13)
C11	C10	H10	120.5
C9	C10	H10	120.5
C12	C11	C10	121.17(13)
C12	C11	C11	118.92(11)
C10	C11	C11	119.91(11)
C11	C12	C13	118.91(12)
C11	C12	H12	120.5
C13	C12	H12	120.5
C12	C13	C8	121.62(12)
C12	C13	H13	119.2
C8	C13	H13	119.2

---

Table S3. Torsion angles [ $^{\circ}$ ]

C7	C1	C2	C3	178.57(11)
C6	C1	C2	C3	-57.04(14)
C1	C2	C3	C4	56.77(14)
C2	C3	C4	C8	-179.86(10)
C2	C3	C4	C5	-55.41(13)
C8	C4	C5	C6	-179.34(11)
C3	C4	C5	C6	55.12(15)
C4	C5	C6	C1	-56.06(15)
C7	C1	C6	C5	-178.78(11)
C2	C1	C6	C5	56.62(15)
C2	C1	C7	F3	-177.05(12)
C6	C1	C7	F3	58.71(15)
C2	C1	C7	F2	62.18(16)
C6	C1	C7	F2	-62.06(16)
C2	C1	C7	F1	-57.73(15)
C6	C1	C7	F1	178.03(12)
C5	C4	C8	C13	111.54(13)
C3	C4	C8	C13	-124.39(12)
C5	C4	C8	C9	-66.51(15)
C3	C4	C8	C9	57.56(15)
C13	C8	C9	C10	0.38(19)
C4	C8	C9	C10	178.47(11)
C8	C9	C10	C11	0.0(2)
C9	C10	C11	C12	-0.70(19)
C9	C10	C11	C11	179.55(10)
C10	C11	C12	C13	0.92(19)
C11	C11	C12	C13	-179.34(9)
C11	C12	C13	C8	-0.48(19)
C9	C8	C13	C12	-0.16(18)
C4	C8	C13	C12	-178.28(11)

---

## Symmetry operations

---

- 1 'x, y, z'
- 2 'x, -y, z+1/2'
- 3 'x+1/2, y+1/2, z'
- 4 'x+1/2, -y+1/2, z+1/2'

---

### X-ray diffraction of *cis*-51

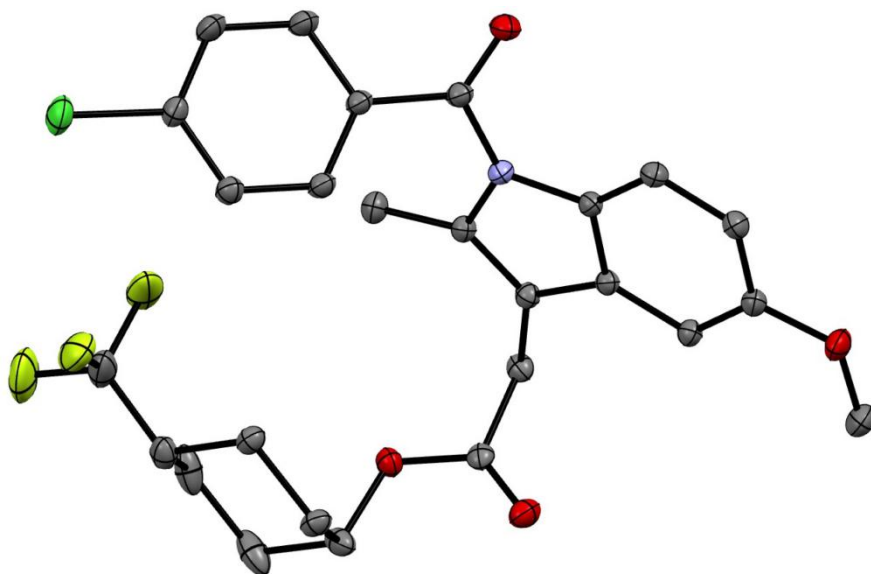


**Figure S4.** ORTEP Diagram of CCDC-2173016.

Table S4. Crystal data and structure refinement for **CCDC-2173016**.

---

Empirical formula C<sub>26</sub> H<sub>25</sub> Cl F<sub>3</sub> N O<sub>4</sub>

Formula weight 507.92

Temperature 100(2)K

Wavelength 0.71073 Å

Crystal system triclinic

Space group P -1

Unit cell dimensions a = 8.73970(10)Å a = 110.9730(10)°.

b = 11.80470(10)Å b = 96.3070(10)°.

c = 12.8546(2)Å g = 105.1810(10)°.

Volume 1164.23(3) Å<sup>3</sup>

Z 2

Density (calculated) 1.449 Mg/m<sup>3</sup>

Absorption coefficient 0.223 mm<sup>-1</sup>

F(000) 528

Crystal size 0.500 x 0.400 x 0.400 mm<sup>3</sup>

Theta range for data collection 2.479 to 34.442°.

Index ranges -13 ≤ h ≤ 13, -18 ≤ k ≤ 18, -20 ≤ l ≤ 20

Reflections collected 92449

Independent reflections 9500 [R(int) = 0.0392]

---

Completeness to theta =34.442° 96.7%  
Absorption correction Multi-scan  
Max. and min. transmission 1.00 and 0.45  
Refinement method Full-matrix least-squares on F2  
Data / restraints / parameters 9500/ 0/ 318  
Goodness-of-fit on F2 1.044  
Final R indices [ $I > 2\sigma(I)$ ] R1 = 0.0358, wR2 = 0.0975  
R indices (all data) R1 = 0.0384, wR2 = 0.0990  
Largest diff. peak and hole 0.606 and -0.662 e.Å<sup>-3</sup>

---

Table S5. Bond lengths [ $\text{\AA}$ ] and angles [ $^\circ$ ].

---

Bond lengths----

C11	C1	1.7322(8)
F1	C26	1.3468(14)
O1	C7	1.2164(9)
N1	C7	1.4054(9)
N1	C8	1.4060(9)
N1	C15	1.4160(9)
C1	C2	1.3869(11)
C1	C6	1.3893(10)
F2	C26	1.3462(11)
O2	C11	1.3743(9)
O2	C17	1.4226(11)
C2	C3	1.3870(11)
C2	H2	0.9500
F3	C26	1.3453(12)
O3	C19	1.2113(9)
C3	C4	1.3950(10)
C3	H3	0.9500
O4	C19	1.3413(9)
O4	C20	1.4605(9)
C4	C5	1.3942(10)
C4	C7	1.4895(10)
C5	C6	1.3904(10)
C5	H5	0.9500
C6	H6	0.9500
C8	C9	1.3967(10)
C8	C13	1.4017(9)
C9	C10	1.3873(10)
C9	H9	0.9500
C10	C11	1.4109(10)
C10	H10	0.9500
C11	C12	1.3885(10)

---

C12	C13	1.4013(10)
C12	H12	0.9500
C13	C14	1.4390(9)
C14	C15	1.3688(9)
C14	C18	1.5023(10)
C15	C16	1.4943(10)
C16	H16A	0.9800
C16	H16B	0.9800
C16	H16C	0.9800
C17	H17A	0.9800
C17	H17B	0.9800
C17	H17C	0.9800
C18	C19	1.5134(10)
C18	H18A	0.9900
C18	H18B	0.9900
C20	C21	1.5196(13)
C20	C25	1.5216(11)
C20	H20	1.0000
C21	C22	1.5268(17)
C21	H21A	0.9900
C21	H21B	0.9900
C22	C23	1.5315(13)
C22	H22A	0.9900
C22	H22B	0.9900
C23	C26	1.5044(13)
C23	C24	1.5333(11)
C23	H23	1.0000
C24	C25	1.5267(10)
C24	H24A	0.9900
C24	H24B	0.9900
C25	H25A	0.9900
C25	H25B	0.9900

Angles-----

---

C7	N1	C8	123.95(6)
C7	N1	C15	127.53(6)
C8	N1	C15	108.49(6)
C2	C1	C6	121.64(7)
C2	C1	C11	118.45(6)
C6	C1	C11	119.91(6)
C11	O2	C17	116.52(6)
C1	C2	C3	119.28(7)
C1	C2	H2	120.4
C3	C2	H2	120.4
C2	C3	C4	120.17(7)
C2	C3	H3	119.9
C4	C3	H3	119.9
C19	O4	C20	117.28(6)
C5	C4	C3	119.61(7)
C5	C4	C7	120.79(6)
C3	C4	C7	119.36(6)
C6	C5	C4	120.73(6)
C6	C5	H5	119.6
C4	C5	H5	119.6
C1	C6	C5	118.52(7)
C1	C6	H6	120.7
C5	C6	H6	120.7
O1	C7	N1	121.24(7)
O1	C7	C4	122.05(7)
N1	C7	C4	116.58(6)
C9	C8	C13	121.65(6)
C9	C8	N1	130.74(6)
C13	C8	N1	107.40(6)
C10	C9	C8	117.17(6)
C10	C9	H9	121.4
C8	C9	H9	121.4
C9	C10	C11	121.57(7)
C9	C10	H10	119.2



---

C11	C10	H10	119.2
O2	C11	C12	123.98(7)
O2	C11	C10	114.91(6)
C12	C11	C10	121.12(7)
C11	C12	C13	117.55(6)
C11	C12	H12	121.2
C13	C12	H12	121.2
C12	C13	C8	120.92(6)
C12	C13	C14	131.52(6)
C8	C13	C14	107.55(6)
C15	C14	C13	108.20(6)
C15	C14	C18	127.18(6)
C13	C14	C18	124.56(6)
C14	C15	N1	108.29(6)
C14	C15	C16	128.06(6)
N1	C15	C16	123.15(6)
C15	C16	H16A	109.5
C15	C16	H16B	109.5
H16A	C16	H16B	109.5
C15	C16	H16C	109.5
H16A	C16	H16C	109.5
H16B	C16	H16C	109.5
O2	C17	H17A	109.5
O2	C17	H17B	109.5
H17A	C17	H17B	109.5
O2	C17	H17C	109.5
H17A	C17	H17C	109.5
H17B	C17	H17C	109.5
C14	C18	C19	109.83(6)
C14	C18	H18A	109.7
C19	C18	H18A	109.7
C14	C18	H18B	109.7
C19	C18	H18B	109.7
H18A	C18	H18B	108.2

---

O3	C19	O4	124.49(7)
O3	C19	C18	124.66(7)
O4	C19	C18	110.81(6)
O4	C20	C21	105.45(7)
O4	C20	C25	109.63(6)
C21	C20	C25	111.48(7)
O4	C20	H20	110.1
C21	C20	H20	110.1
C25	C20	H20	110.1
C20	C21	C22	111.97(7)
C20	C21	H21A	109.2
C22	C21	H21A	109.2
C20	C21	H21B	109.2
C22	C21	H21B	109.2
H21A	C21	H21B	107.9
C21	C22	C23	110.89(8)
C21	C22	H22A	109.5
C23	C22	H22A	109.5
C21	C22	H22B	109.5
C23	C22	H22B	109.5
H22A	C22	H22B	108.0
C26	C23	C22	110.73(8)
C26	C23	C24	109.79(7)
C22	C23	C24	111.32(6)
C26	C23	H23	108.3
C22	C23	H23	108.3
C24	C23	H23	108.3
C25	C24	C23	110.80(6)
C25	C24	H24A	109.5
C23	C24	H24A	109.5
C25	C24	H24B	109.5
C23	C24	H24B	109.5
H24A	C24	H24B	108.1
C20	C25	C24	112.27(6)

---

C20	C25	H25A	109.1
C24	C25	H25A	109.1
C20	C25	H25B	109.1
C24	C25	H25B	109.1
H25A	C25	H25B	107.9
F3	C26	F2	106.43(8)
F3	C26	F1	106.35(8)
F2	C26	F1	105.12(10)
F3	C26	C23	113.19(10)
F2	C26	C23	112.31(8)
F1	C26	C23	112.84(8)

---

Table S6. Torsion angles [°].

C6	C1	C2	C3	0.08(13)
C11	C1	C2	C3	179.00(7)
C1	C2	C3	C4	1.89(13)
C2	C3	C4	C5	-2.07(12)
C2	C3	C4	C7	-176.52(7)
C3	C4	C5	C6	0.27(11)
C7	C4	C5	C6	174.64(7)
C2	C1	C6	C5	-1.84(12)
C11	C1	C6	C5	179.26(6)
C4	C5	C6	C1	1.65(11)
C8	N1	C7	O1	34.73(11)
C15	N1	C7	O1	-142.95(8)
C8	N1	C7	C4	-141.08(7)
C15	N1	C7	C4	41.23(10)
C5	C4	C7	O1	-137.35(8)
C3	C4	C7	O1	37.03(11)
C5	C4	C7	N1	38.43(10)
C3	C4	C7	N1	-147.19(7)
C7	N1	C8	C9	4.93(12)
C15	N1	C8	C9	-177.01(7)
C7	N1	C8	C13	179.63(6)
C15	N1	C8	C13	-2.30(8)
C13	C8	C9	C10	1.34(10)
N1	C8	C9	C10	175.40(7)
C8	C9	C10	C11	0.00(11)
C17	O2	C11	C12	3.46(11)
C17	O2	C11	C10	-176.86(7)
C9	C10	C11	O2	179.11(7)
C9	C10	C11	C12	-1.20(11)
O2	C11	C12	C13	-179.33(7)
C10	C11	C12	C13	1.01(11)
C11	C12	C13	C8	0.31(10)

---

C11	C12	C13	C14	-179.02(7)
C9	C8	C13	C12	-1.54(10)
N1	C8	C13	C12	-176.82(6)
C9	C8	C13	C14	177.94(6)
N1	C8	C13	C14	2.66(8)
C12	C13	C14	C15	177.35(7)
C8	C13	C14	C15	-2.06(8)
C12	C13	C14	C18	-5.39(12)
C8	C13	C14	C18	175.21(6)
C13	C14	C15	N1	0.63(8)
C18	C14	C15	N1	-176.55(7)
C13	C14	C15	C16	172.65(7)
C18	C14	C15	C16	-4.53(12)
C7	N1	C15	C14	179.01(7)
C8	N1	C15	C14	1.03(8)
C7	N1	C15	C16	6.51(11)
C8	N1	C15	C16	-171.46(6)
C15	C14	C18	C19	-93.45(9)
C13	C14	C18	C19	89.81(8)
C20	O4	C19	O3	0.96(10)
C20	O4	C19	C18	-176.91(6)
C14	C18	C19	O3	-80.17(9)
C14	C18	C19	O4	97.69(7)
C19	O4	C20	C21	-157.31(7)
C19	O4	C20	C25	82.56(8)
O4	C20	C21	C22	-64.70(8)
C25	C20	C21	C22	54.20(10)
C20	C21	C22	C23	-55.11(10)
C21	C22	C23	C26	178.02(7)
C21	C22	C23	C24	55.59(10)
C26	C23	C24	C25	-178.17(7)
C22	C23	C24	C25	-55.20(9)
O4	C20	C25	C24	62.35(8)
C21	C20	C25	C24	-54.03(9)

---

C23	C24	C25	C20	54.49(8)
C22	C23	C26	F3	57.62(10)
C24	C23	C26	F3	-179.06(8)
C22	C23	C26	F2	-62.94(11)
C24	C23	C26	F2	60.38(11)
C22	C23	C26	F1	178.46(8)
C24	C23	C26	F1	-58.22(10)

---

---

Symmetry operations

---

1 'x, y, z'

2 '-x, -y, -z'

---

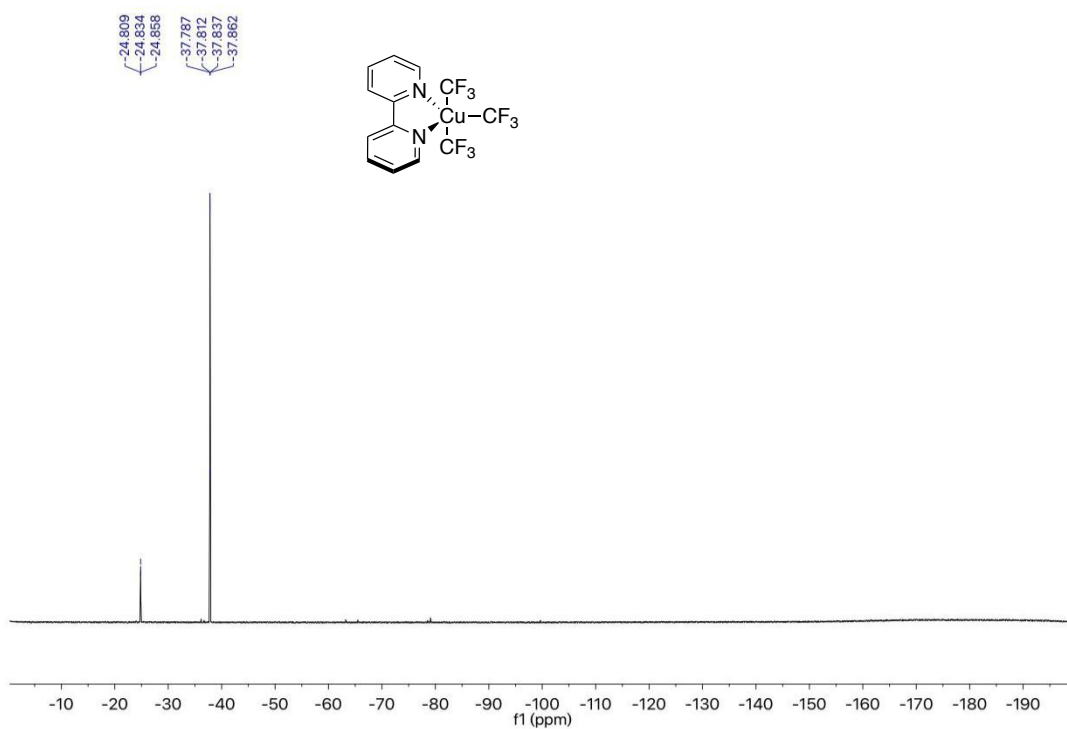
### 3.7.6 References of Experimental Procedures

1. Paeth, M.; Carson, W.; Luo, J.-H.; Tierney, D.; Cao, Z.; Cheng, M.-J.; Liu, W. *Chem. Eur. J.* **2018**, *24*, 11559–11563.
2. Li, L.; Fang, L.; Wu, W.; Zhu, J. *Org. Lett.* **2020**, *22*, 5401–5406.
3. Gutierrez-Bonet, A.; Remeur, C.; Matsui, J. K.; Molander, G. A. *J. Am. Chem. Soc.* **2017**, *139*, 12251–12258.
4. Gutierrez-Bonet, A.; Tellis, J. C.; Matsui, J. K.; Vara, Brandon A.; Molander, G. A. *ACS Catalysis*. **2016**, *6*, 8004–8008.
5. Verrier, C.; Alandini, N.; Pezzetta, C.; Moliterno, M.; Buzzetti, L.; Hepburn, H. B.; Vega-Peñaloza, A.; Silvi, M.; Melchiorre, P. *ACS Catal.* **2018**, *2*, 1062–1066.
6. Lipp, A.; Badir, S. O.; Dykstra, R.; Gutierrez, O.; Molander, G. A. *Advanced Synthesis & Catalysis*. **2021**, *363*, 3507–3520.
7. Bain, R. M.; Pulliam, C. J.; Cooks, R. G. *Chemical Science* **2015**, *6*, 397–401.
8. Alandini, N.; Buzzetti, L.; Favi, G.; Schulte, T.; Candish, L.; Collins, K. D.; Melchiorre, P. *Angew. Chem. Int. Ed.*, **2020**, *59*, 5248–5253.
9. Liang, S.; Kumon, T.; Angnes, R. A.; Sanchez, M.; Xu, B. *Organic Letters*. **2019**, *21*, 3848–3854.
10. Chen, S.; Zhu, Qi.; Cao, Y.; Li, Chen.; Guo, Y.; Kong, L.; Che, J.; Guo, Z.; Chen, H.; Zhang, N.; Fang, X.; Lu, J.; Luo, T. *J. Am. Chem. Soc.* **2021**, *35*, 14046–14052.
11. Chen, Y.; Ma, G.; Gong, H. *Org. Lett.* **2018**, *20*, 4677–4680.
12. Tan, X.; Liu, Z.; Shen, H.; Zhang, P.; Zhang, Z.; Li, C. *J. Am. Chem. Soc.* **2017**, *139*, 12430–12433.
13. Kornfilt, D. J. P.; MacMillan, D. W. C. *J. Am. Chem. Soc.* **2019**, *141*, 6853–6858.
14. Kautzky, J. A.; Wang, T.; Evans, R. W.; MacMillan, D. W. C. *J. Am. Chem. Soc.* **2018**, *21*, 6522–6526.
15. Zhang, X.; Ling, L.; Luo, M.; Zeng, X. *Angew. Chem. Int. Ed.* **2019**, *58*, 16785–16789.
16. Choi, G.; Lee, G. S.; Park, B.; Kim, D.; Hong, S. H. *Angew. Chem. Int. Ed.* **2021**, *60*, 5467–5474.
17. Ren, Y.; Zheng, X.; Zhang, X. *Synlett*. **2018**, *29*, 1028–1032
18. Guo, S.; AbuSalim, D. I.; Cook, S. P. *J. Am. Chem. Soc.* **2018**, *39*, 12378–12382.
19. Jiang, X.; Qing, F. *Beilstein J. Org. Chem.* **2013**, *9*, 2862–2865.
20. Foth, P. J.; Gu, F.; Bolduc, T. G.; Kanani, S. S.; Sammis, G. M. *Chemical Science*. **2019**, *10*, 10331–10335

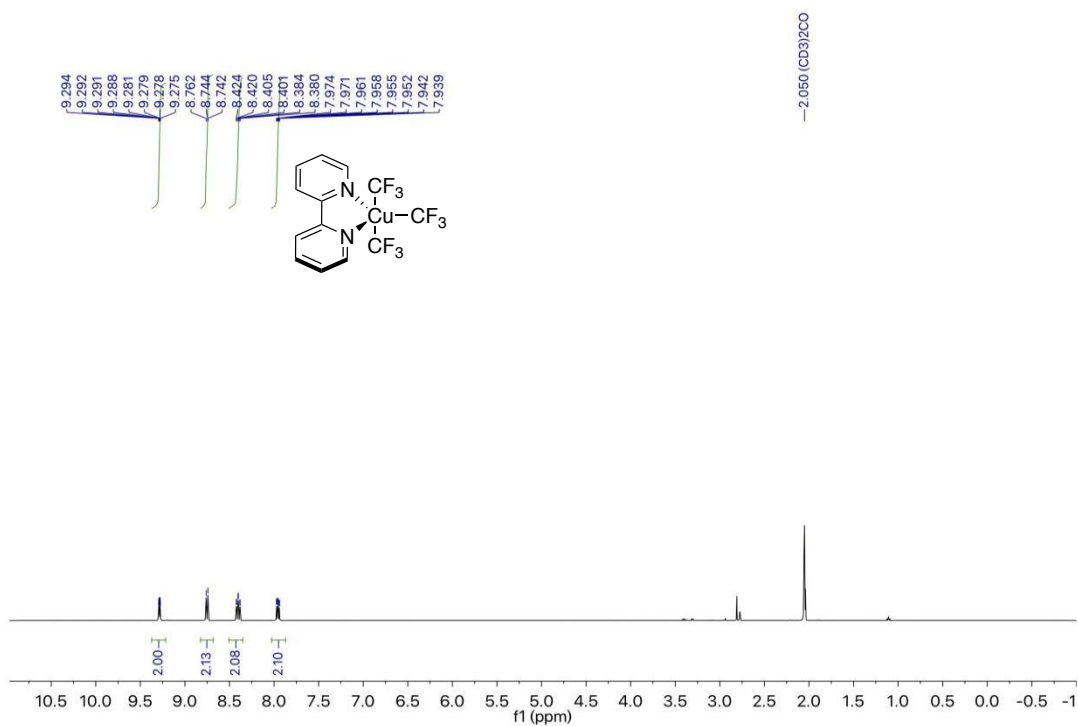


- 
21. Umemoto, T.; Singh, R. P. *Journal of Fluorine Chemistry*. **2012**, 140, 17–27.
  22. Yang, Y.; Liu, J.; Kamounah, F. S.; Ciancaleoni, G. Lee, J-W., *J. Org. Chem.* **2021**, 86, 16867–16881.
  23. Maity, S.; Kumar, R.; Maity, S. K.; Jana, P.; Bera, S. *Med. Chem. Comm.* **2013**, 4, 530–536.
  24. Xu, W.; Liu, Y.; Kato, T.; Maruoka K. *Org. Lett.* **2021**, 23, 1809.
  25. Zhao, Y.; Hu, J. *Angew. Chem. Int. Ed.* **2012**, 51, 1033.
  26. Li, H.; Sheng, J.; Liao, G-X.; Wu, B-B.; Ni, H-Q.; Li, Y.; Wang, X-S. *Adv. Synth. Catal.* **2020**, 362, 5363.
  27. Ghosh, T.; Mandal, I.; Basak, S. J.; Dash, J. *J. Org. Chem.* **2021**, 86, 14695–14704.
  28. Li, X.; Zhu, X-Q.; Zhang, F.; Wang, X-X.; Cheng, J-P, *J. Org. Chem.* **2008**, 73, 2428–2431.

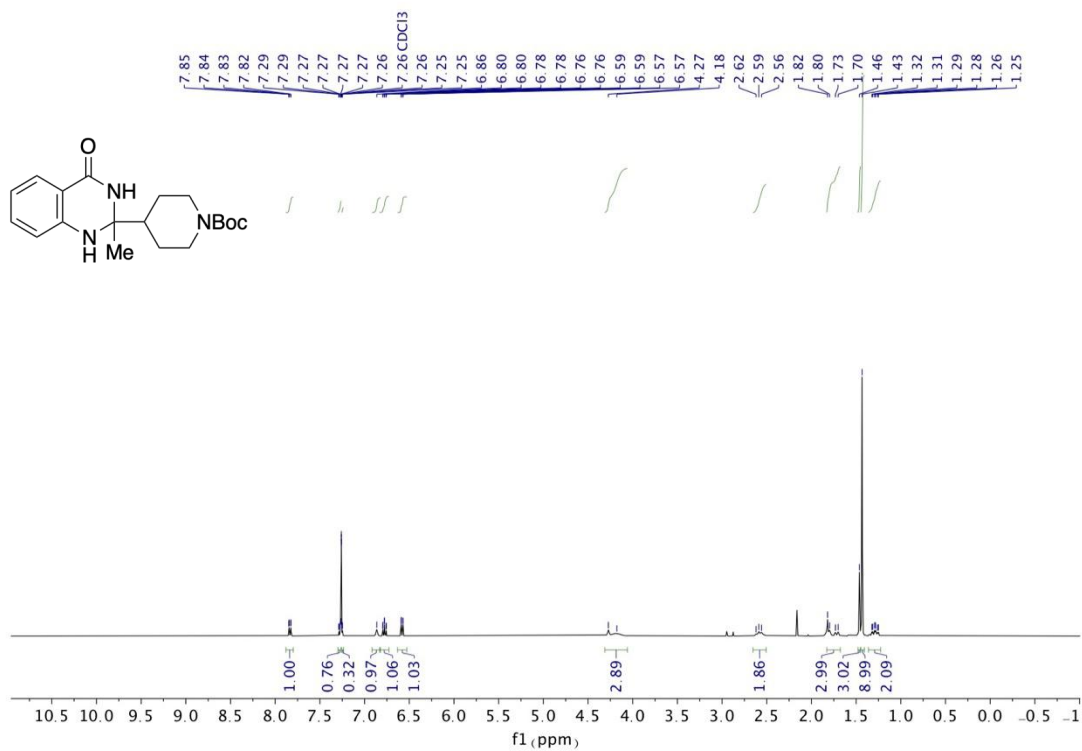
### 3.7.7 NMR Spectra



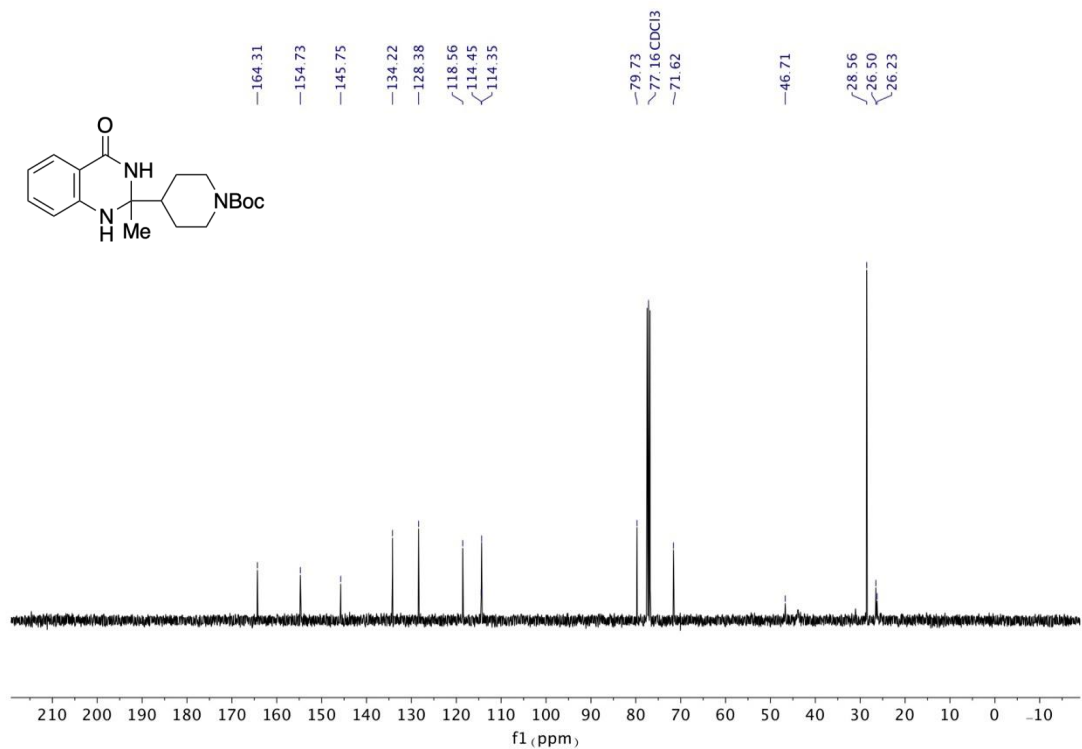
<sup>19</sup>F NMR (376 MHz, Acetone-d<sub>6</sub>) of Cu(CF<sub>3</sub>)<sub>3</sub>(bpy)



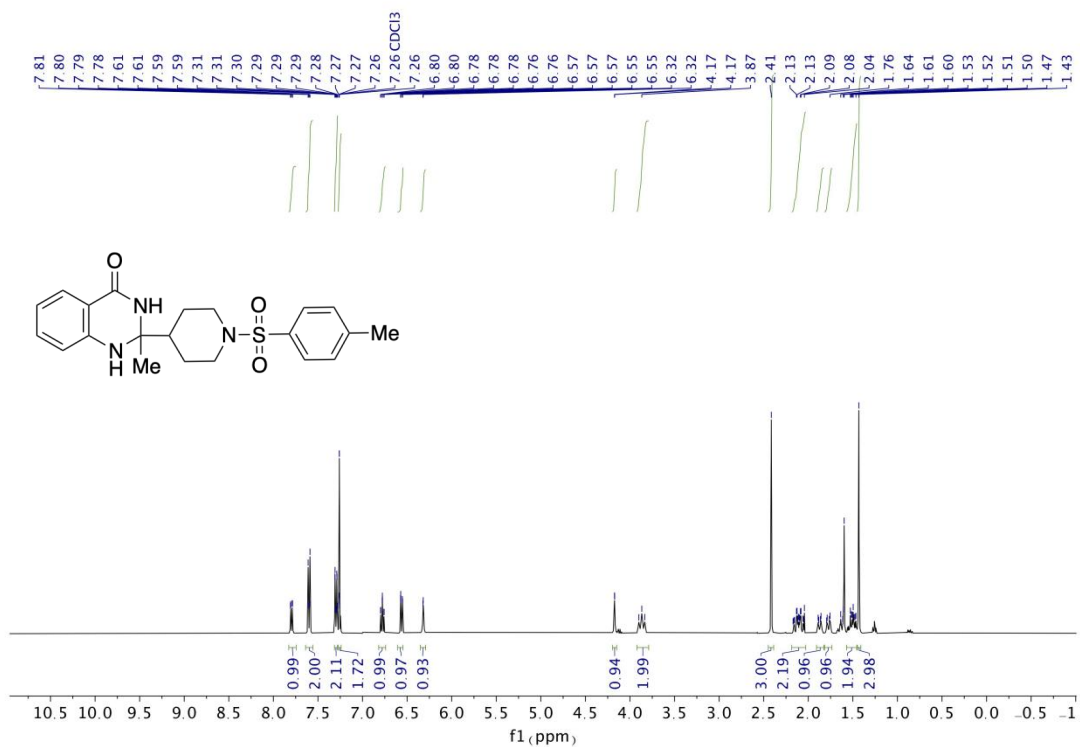
<sup>1</sup>H NMR (400 MHz, Acetone-d<sub>6</sub>) of Cu(CF<sub>3</sub>)<sub>3</sub>(bpy)



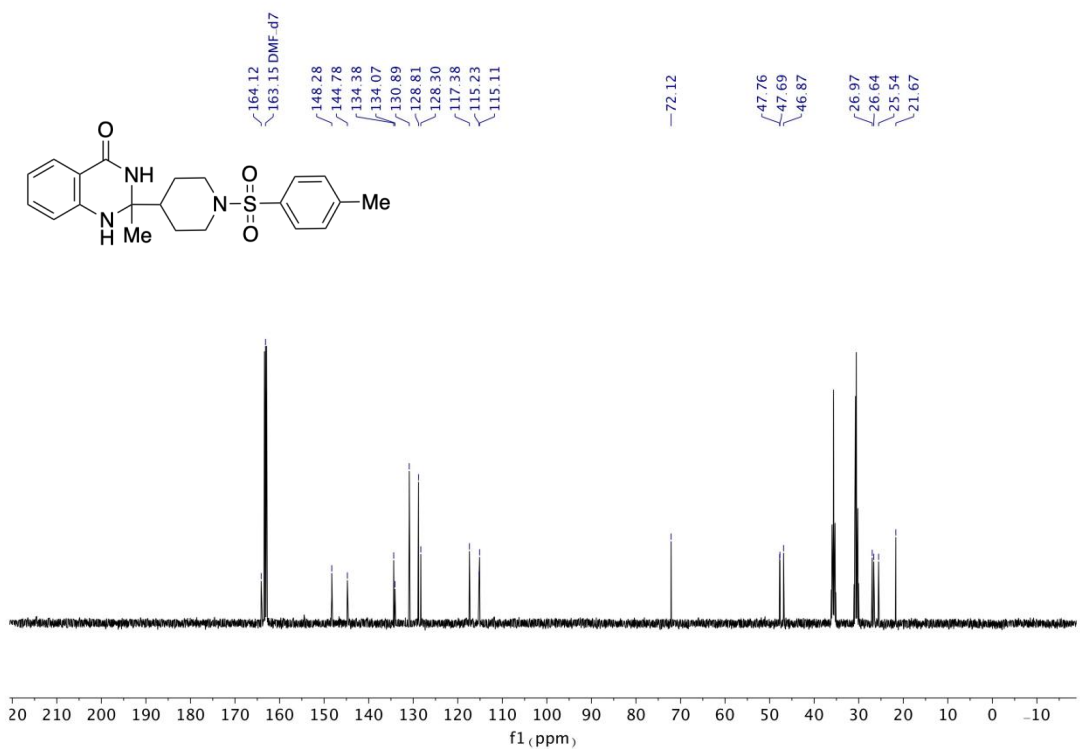
**<sup>1</sup>H NMR spectrum (400 MHz, CDCl<sub>3</sub>) of A1**



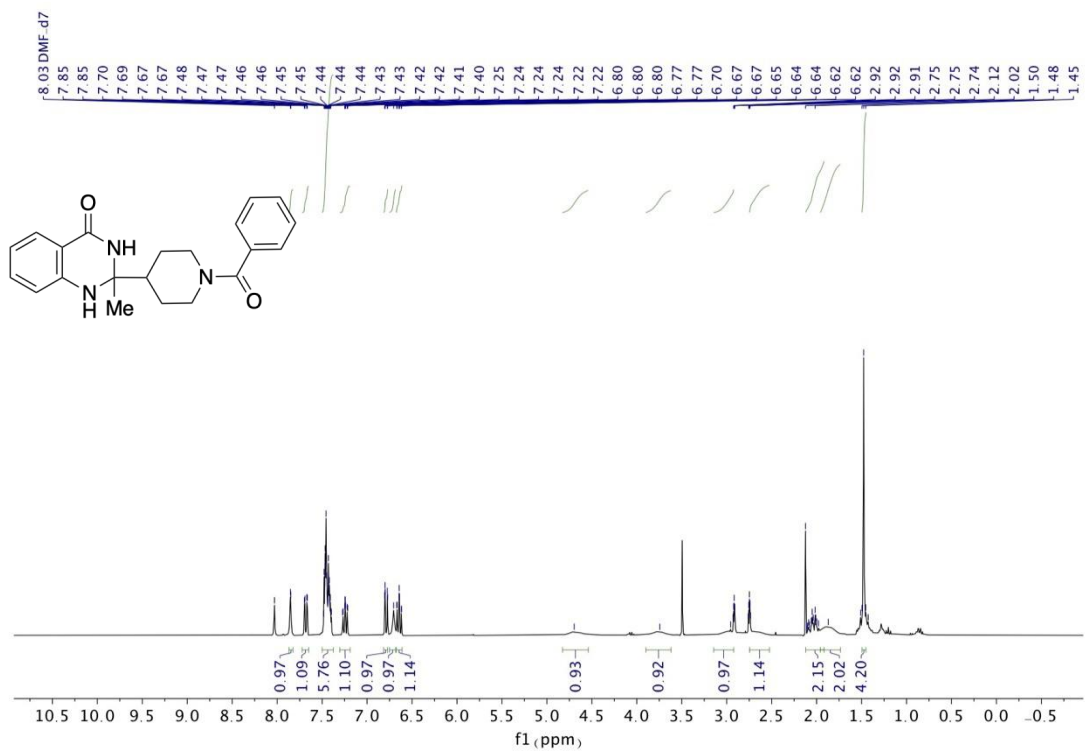
**<sup>13</sup>C NMR spectrum (101 MHz, CDCl<sub>3</sub>) of A1**



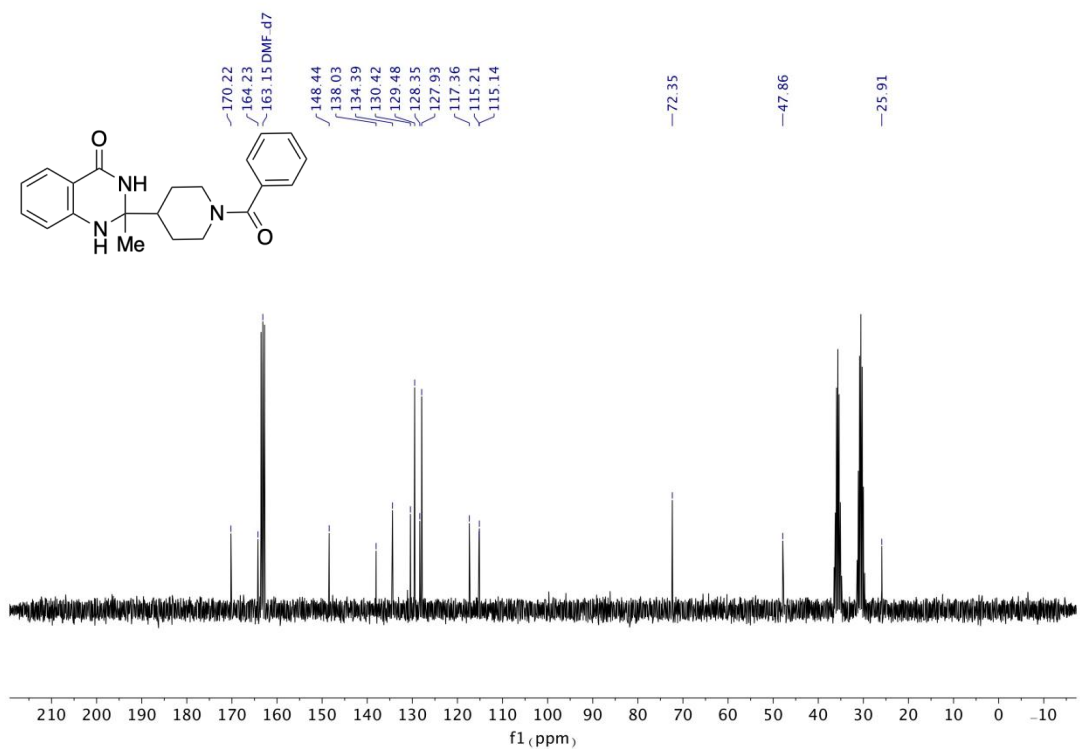
**<sup>1</sup>H NMR (400 MHz, CDCl<sub>3</sub>) of A2**



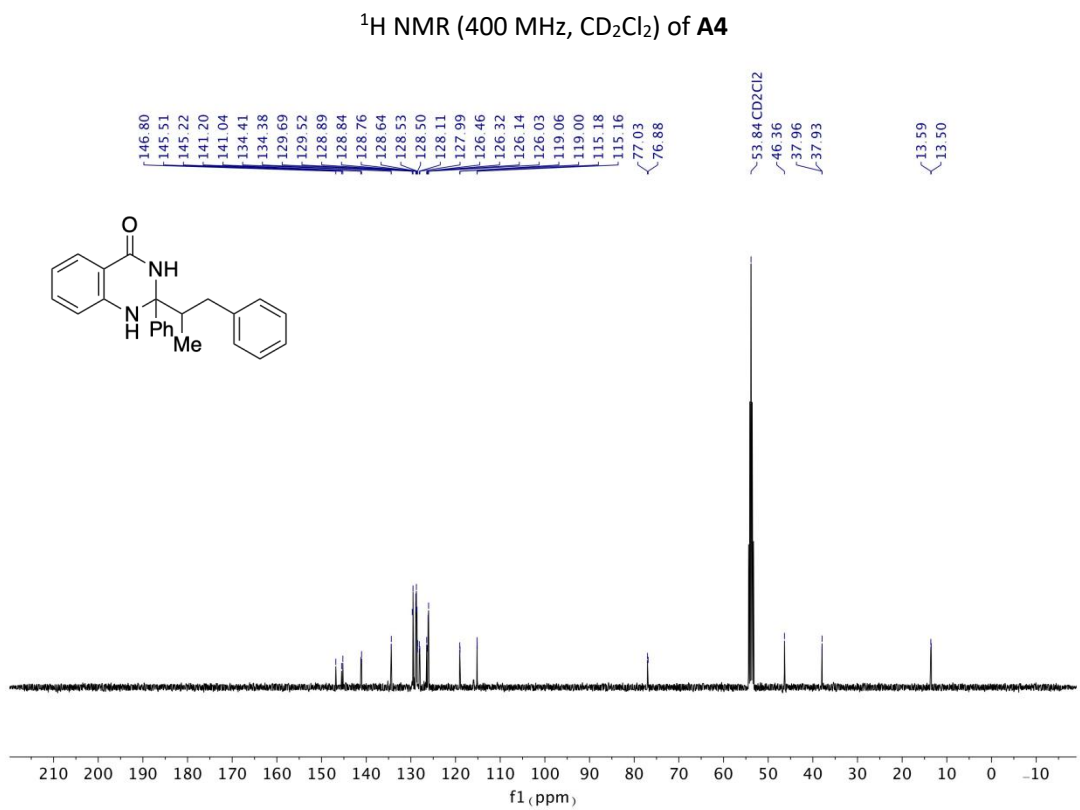
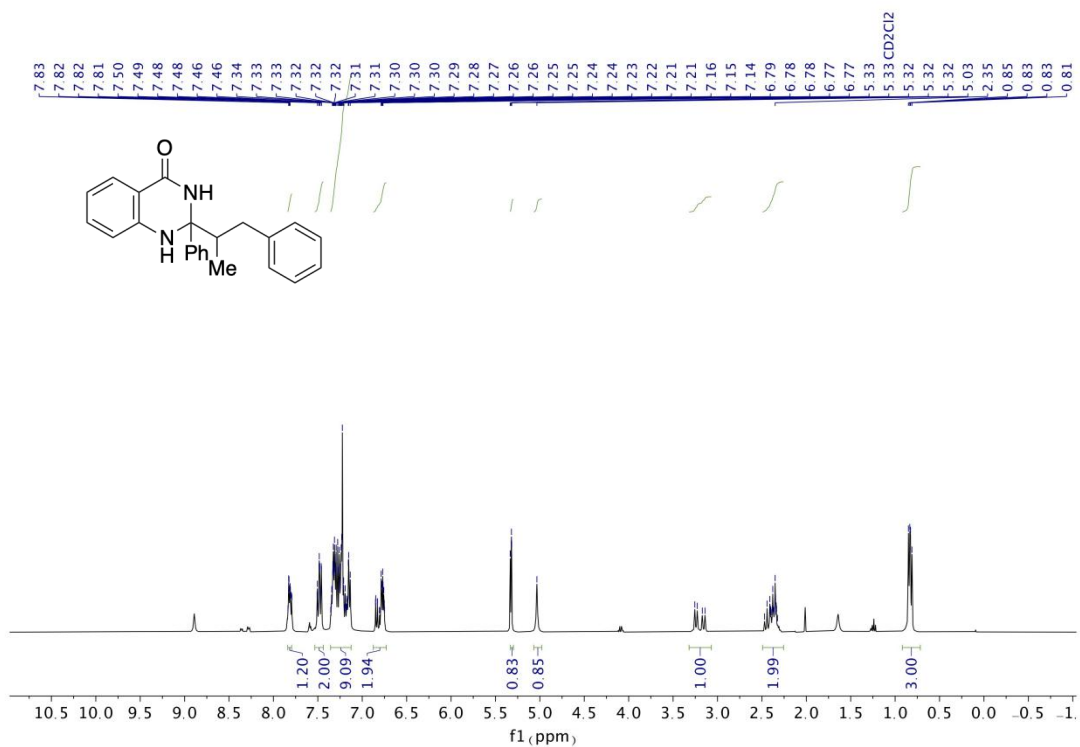
**<sup>13</sup>C NMR (126 MHz, DMF-d<sub>7</sub>) of A2**

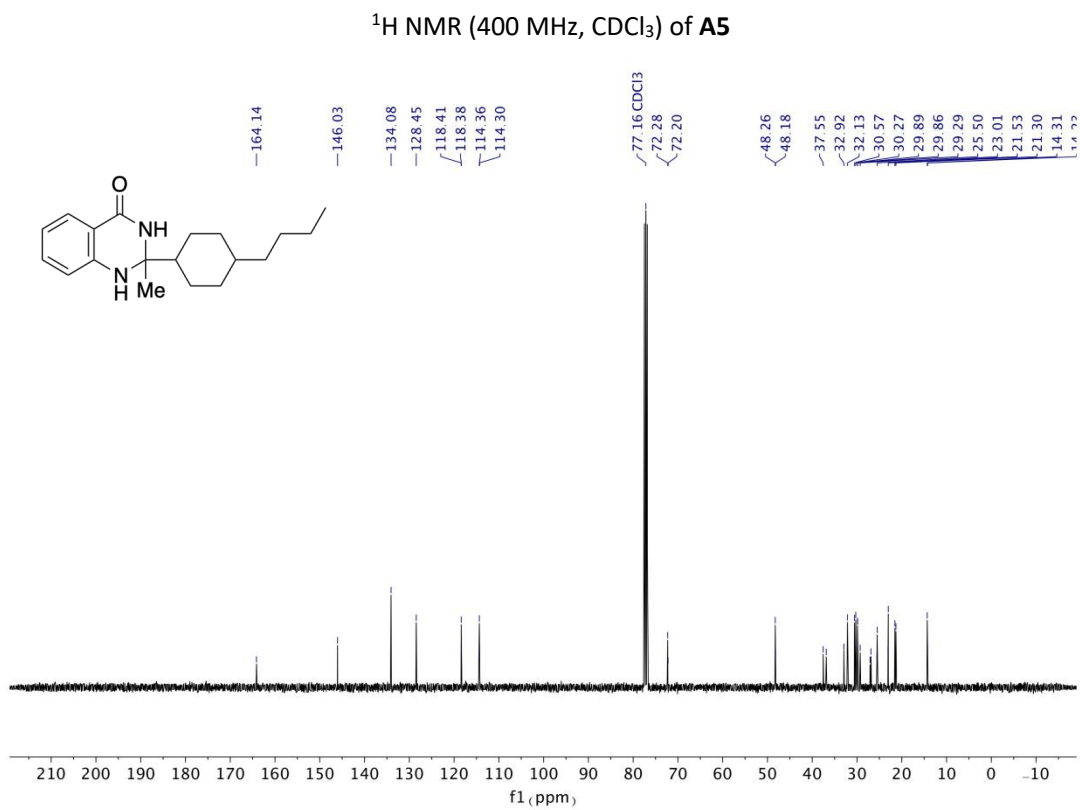
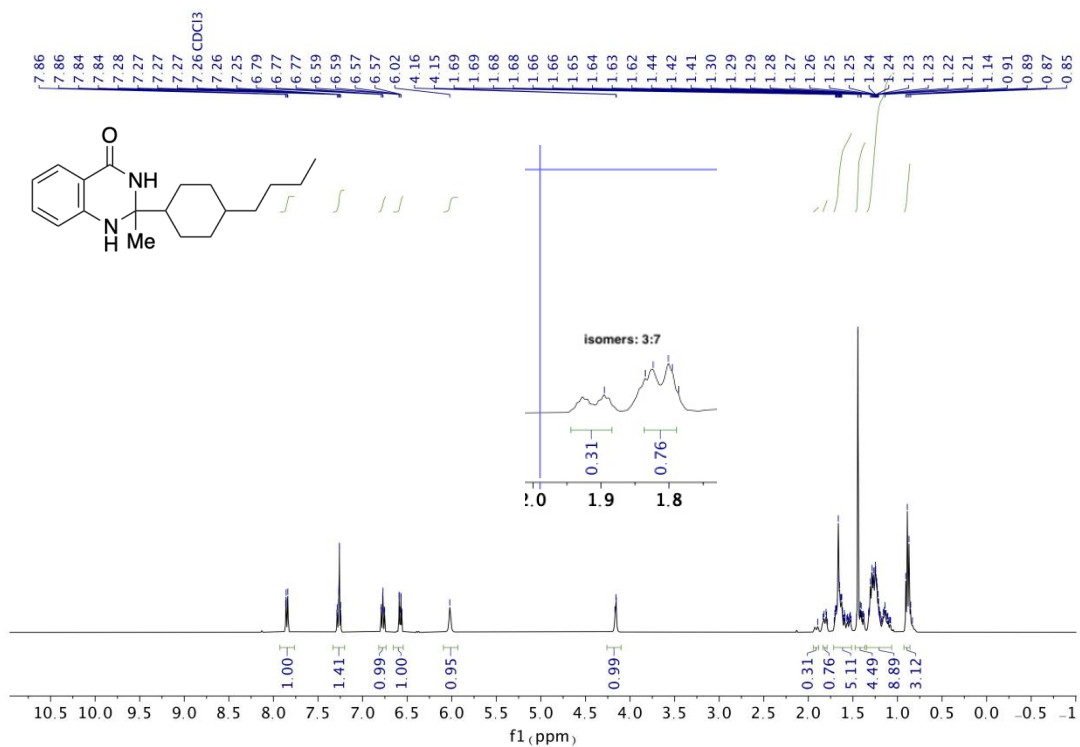


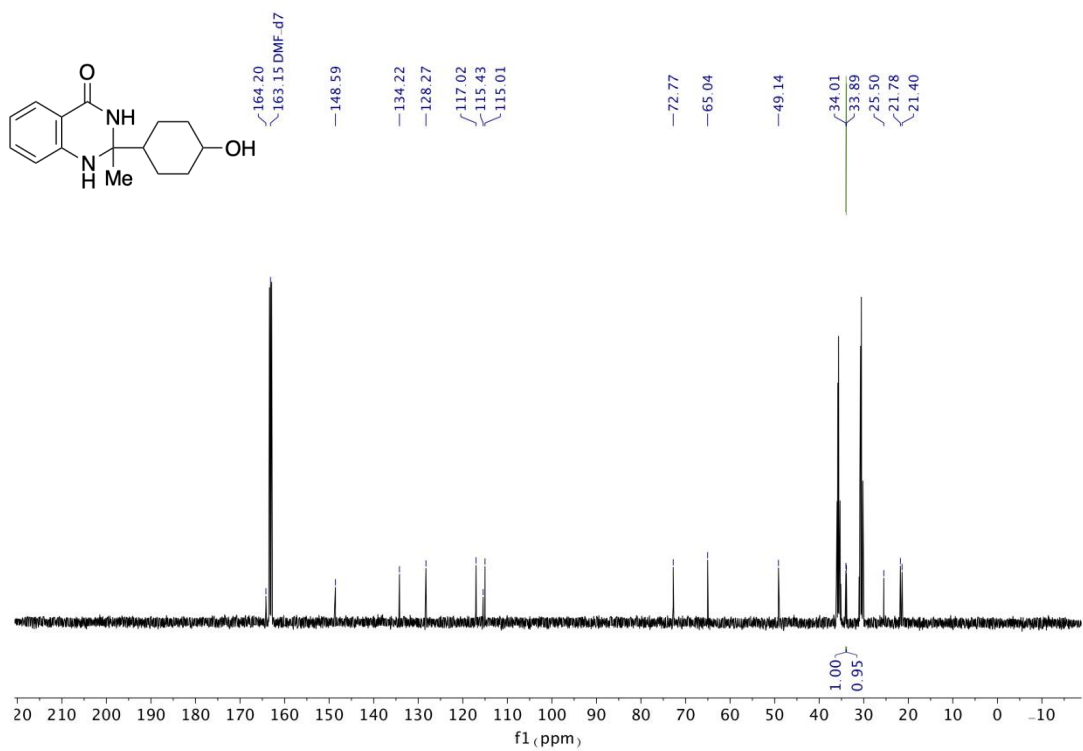
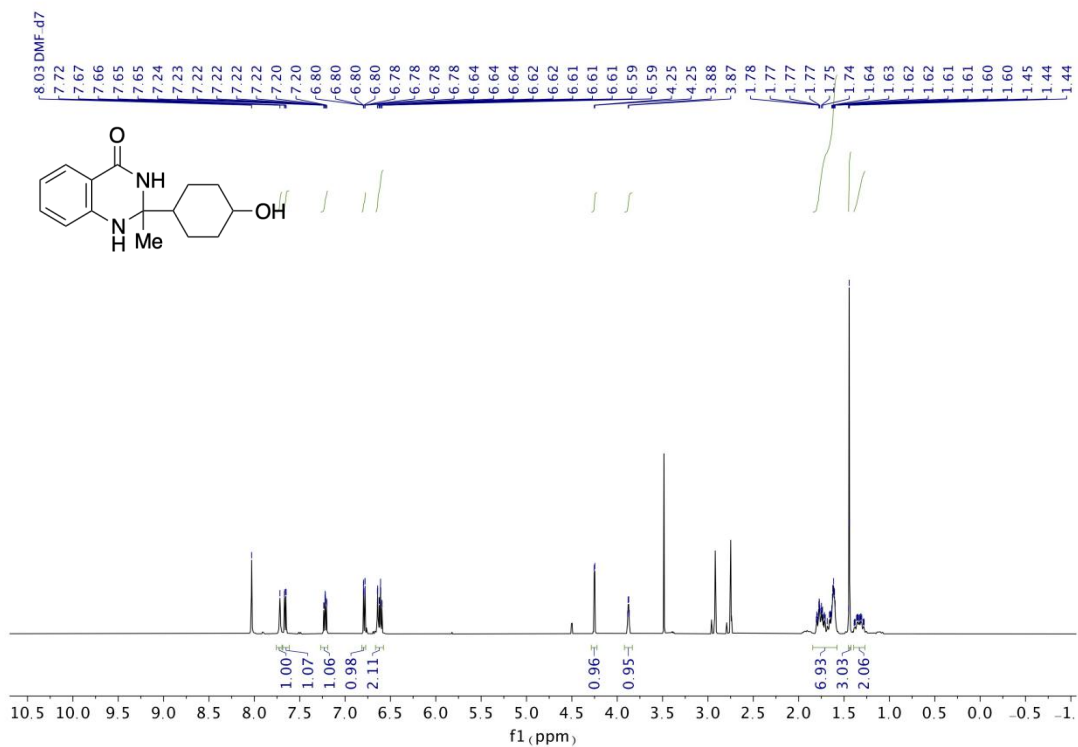
<sup>1</sup>H NMR (300 MHz, DMF-d<sub>7</sub>) of A3



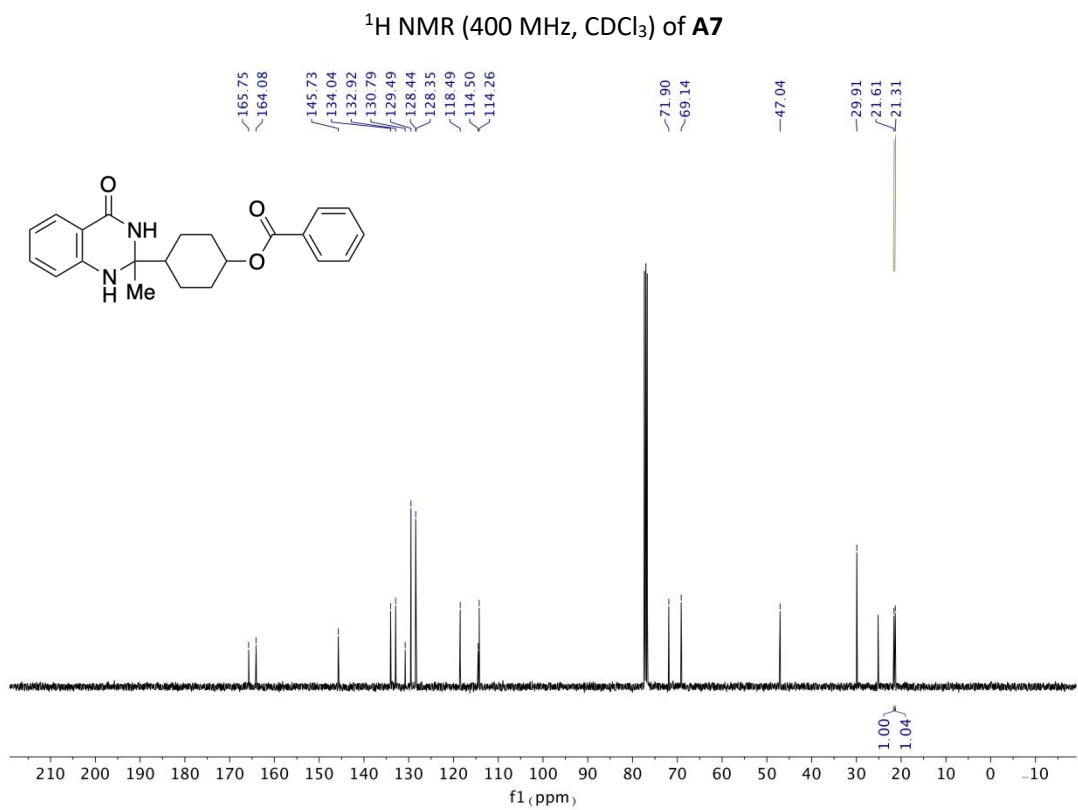
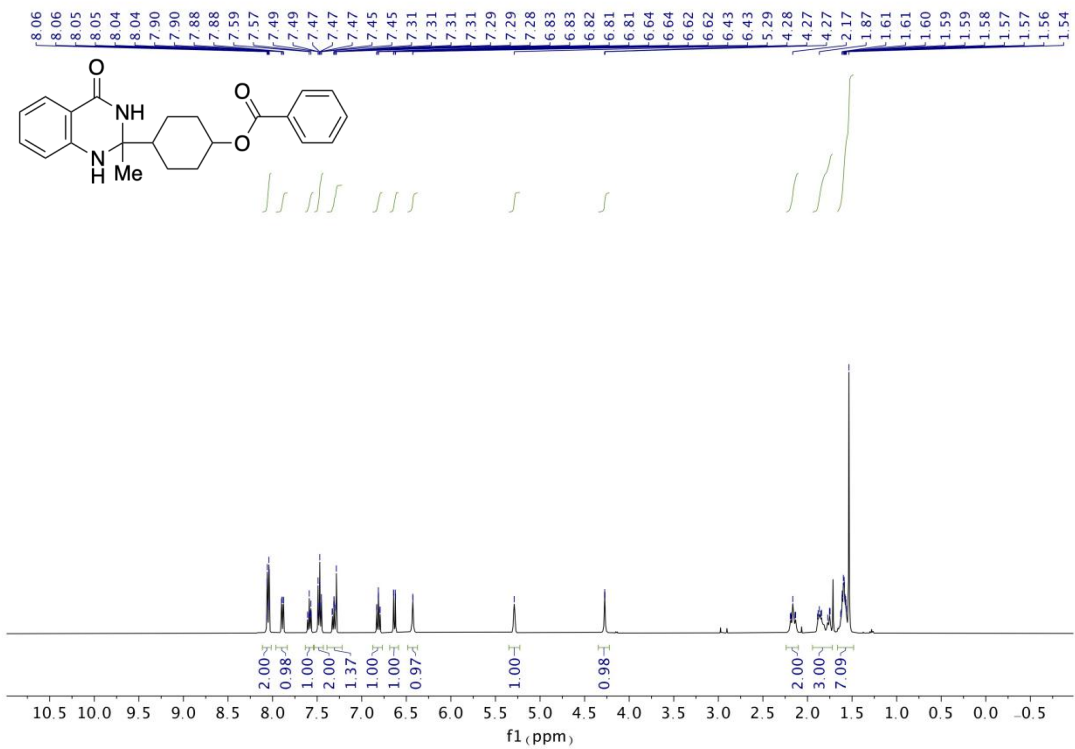
<sup>13</sup>C NMR (75 MHz, DMF-d<sub>7</sub>) of A3

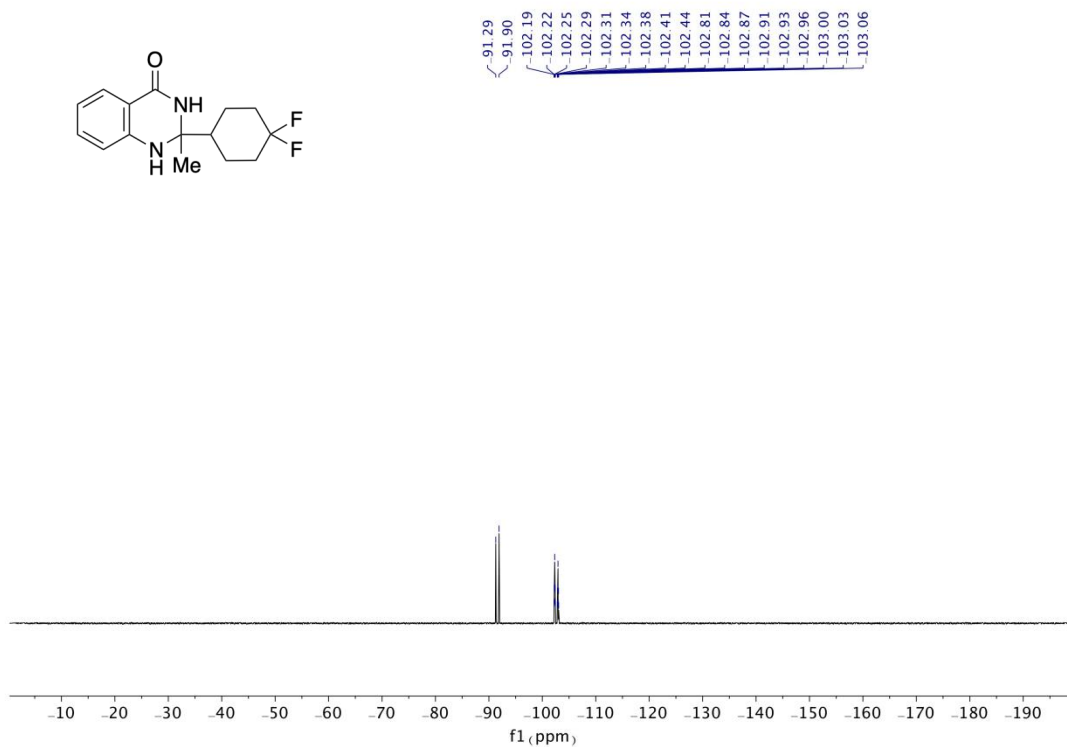




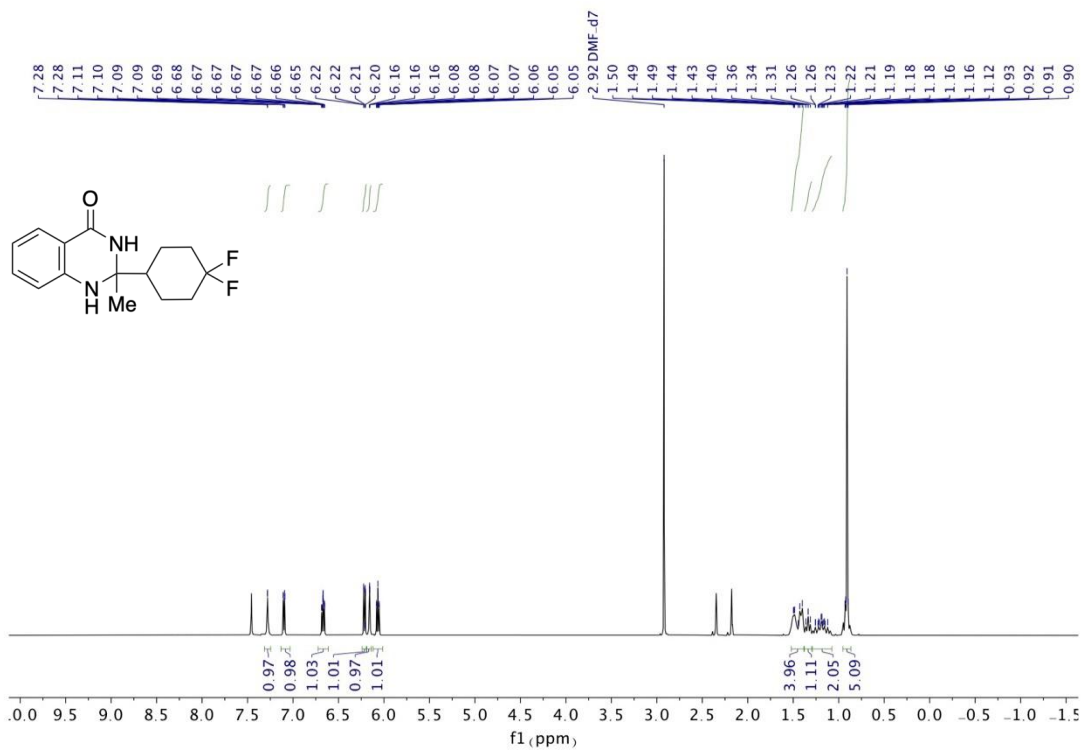




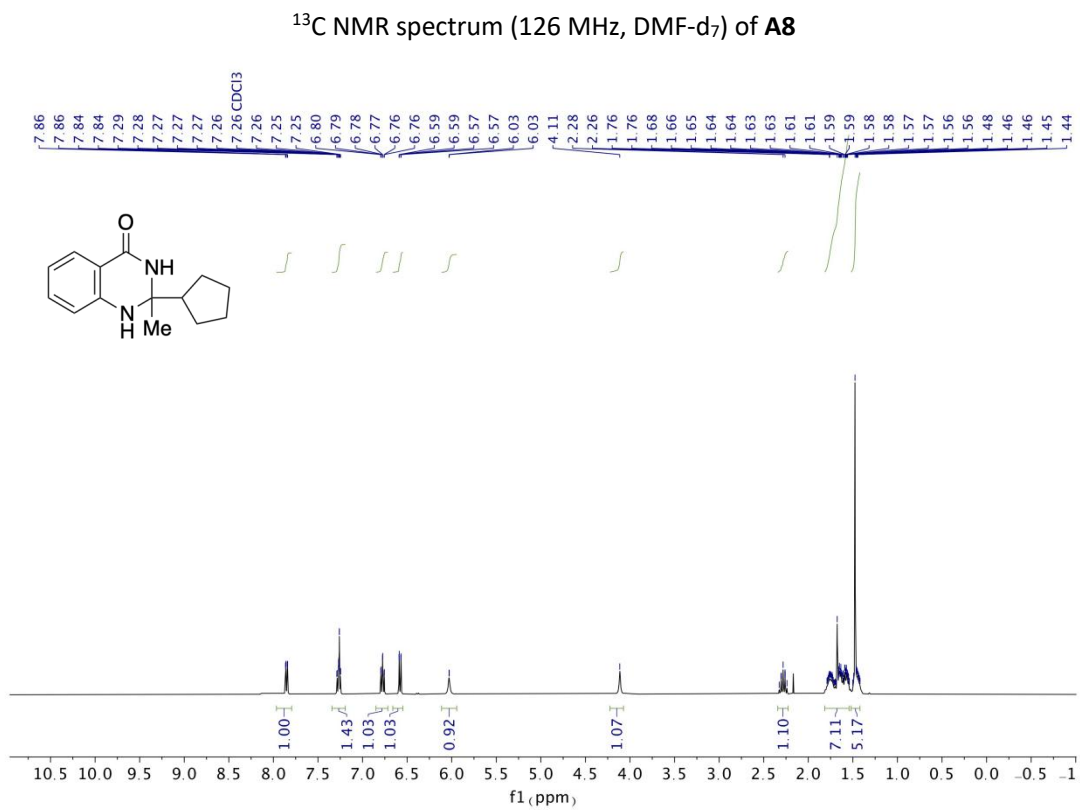
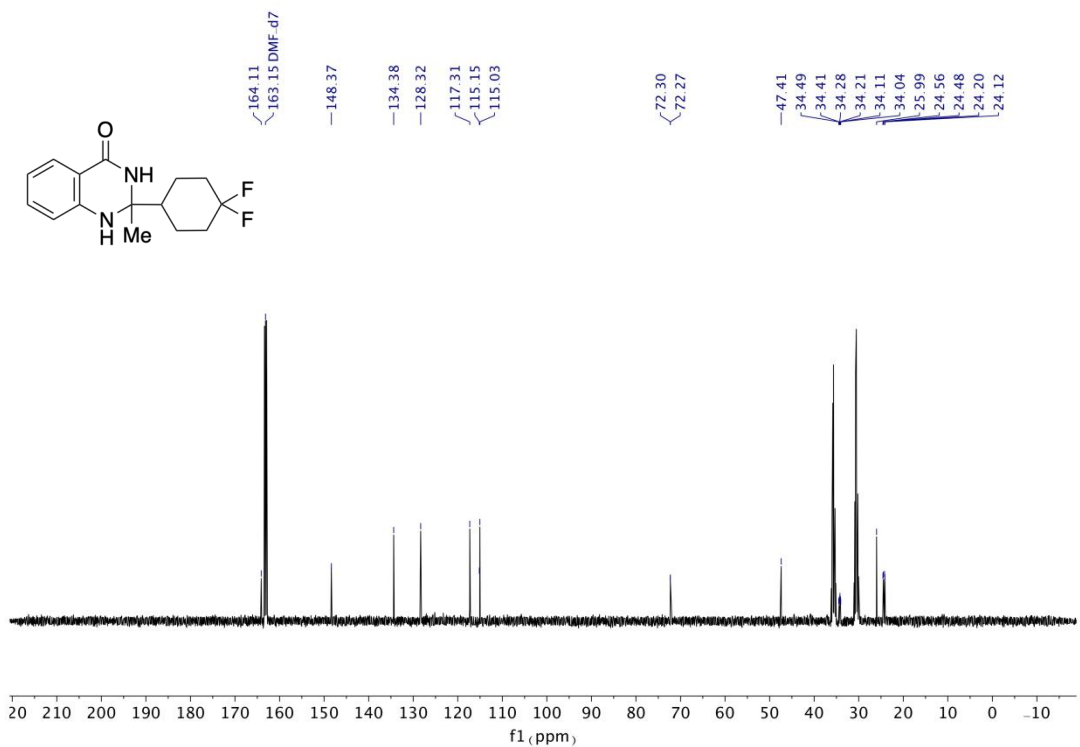


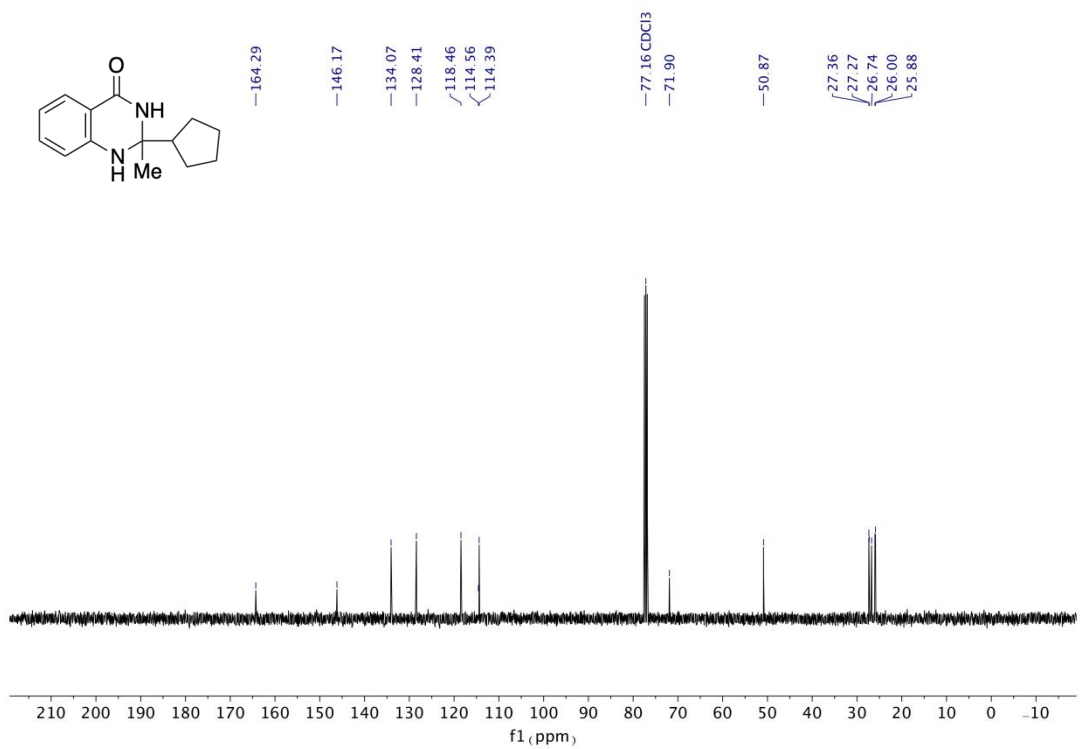


<sup>19</sup>F NMR (376 MHz, DMF-d<sub>7</sub>) of A8

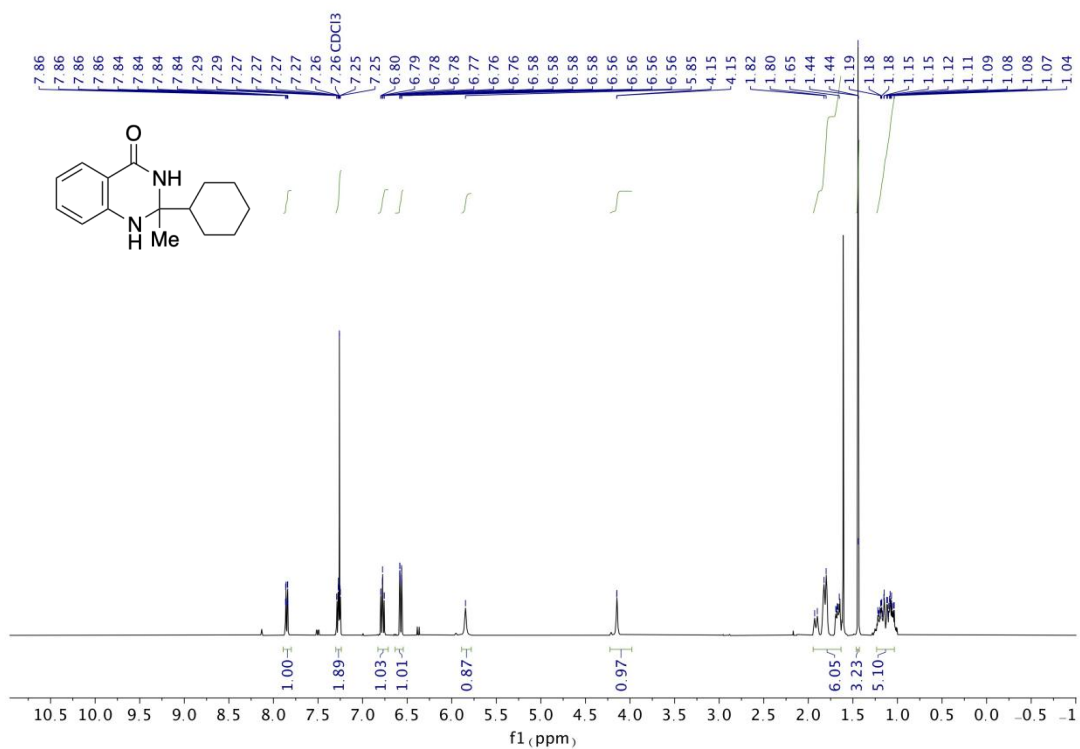


<sup>1</sup>H NMR spectrum (500 MHz, DMF-d<sub>7</sub>) of A8

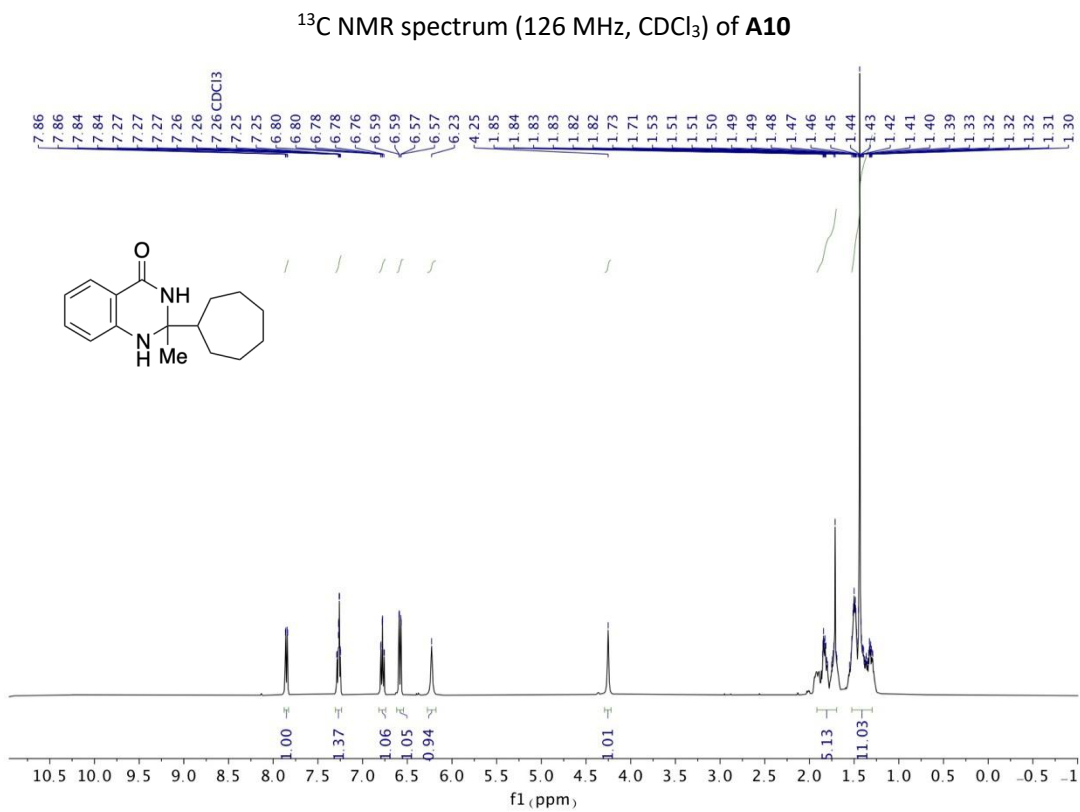
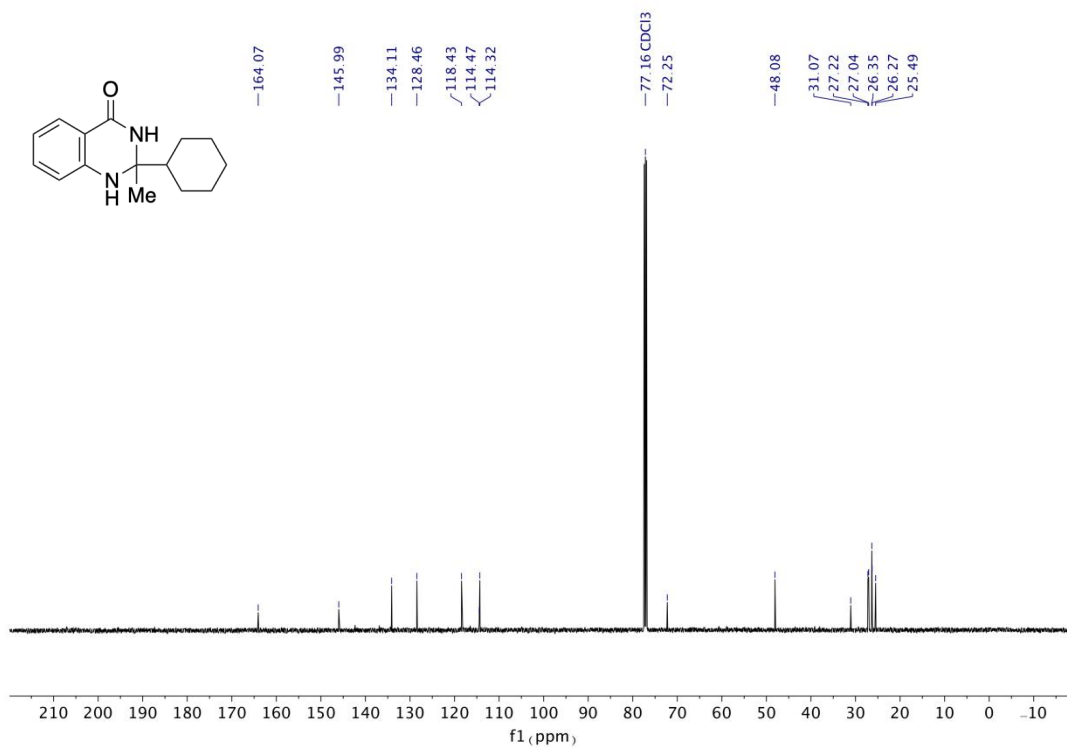


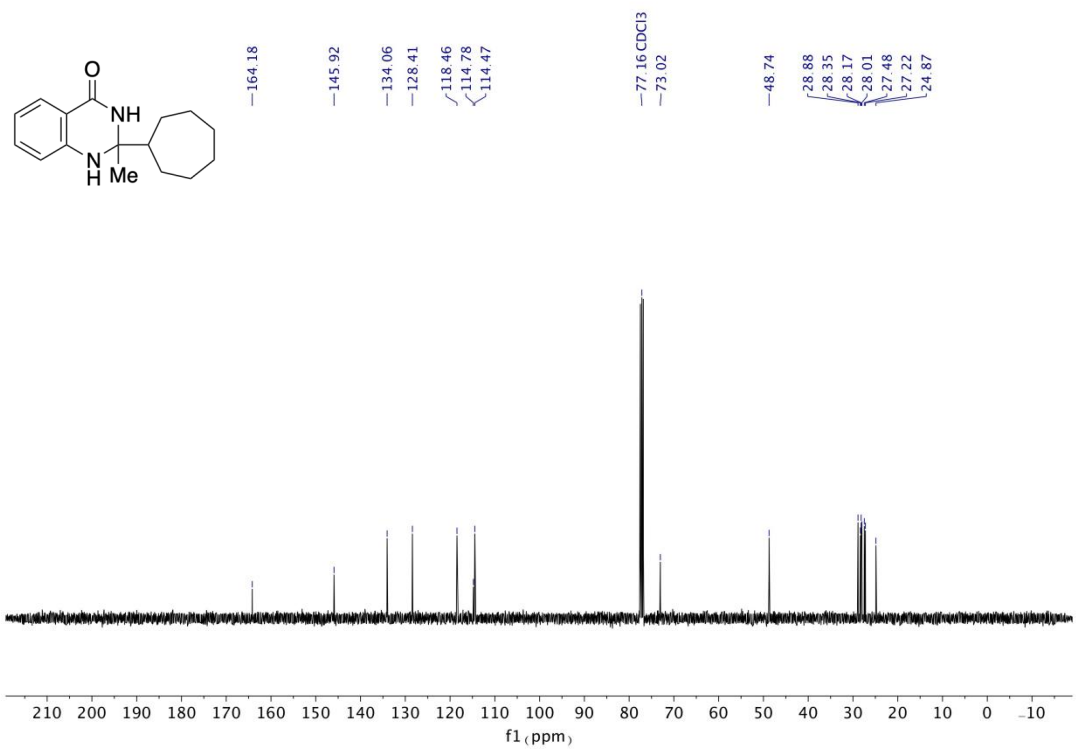


<sup>13</sup>C NMR spectrum (101 MHz, CDCl<sub>3</sub>) of A9

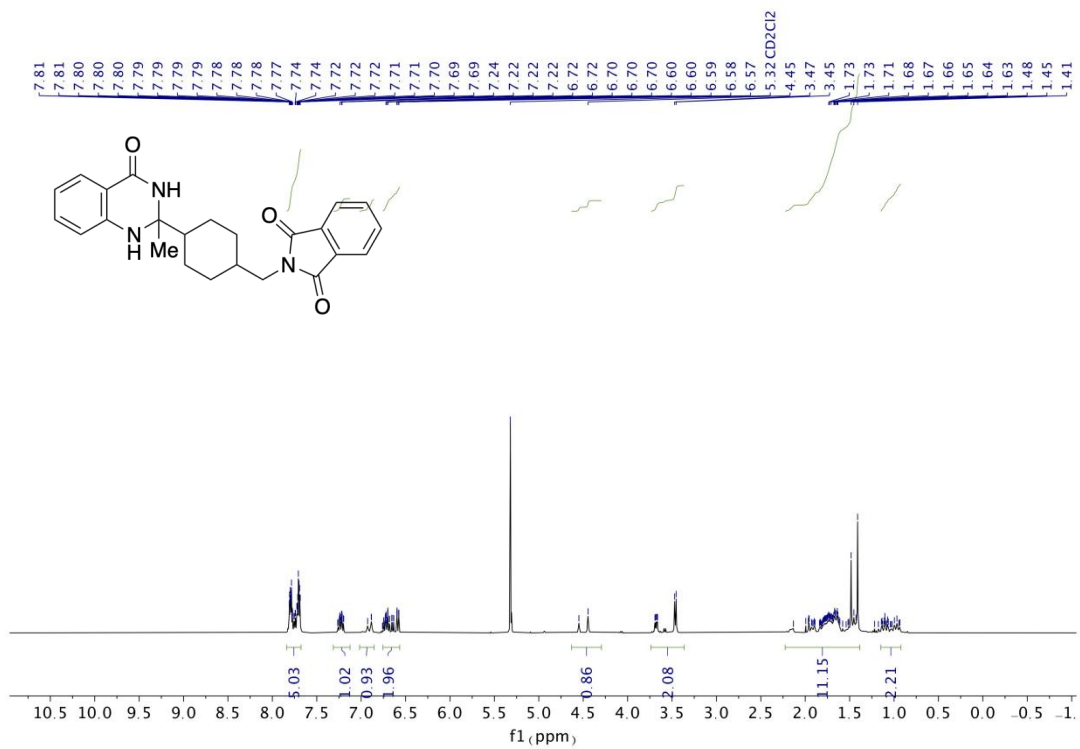


<sup>1</sup>H NMR spectrum (400 MHz, CDCl<sub>3</sub>) of A10

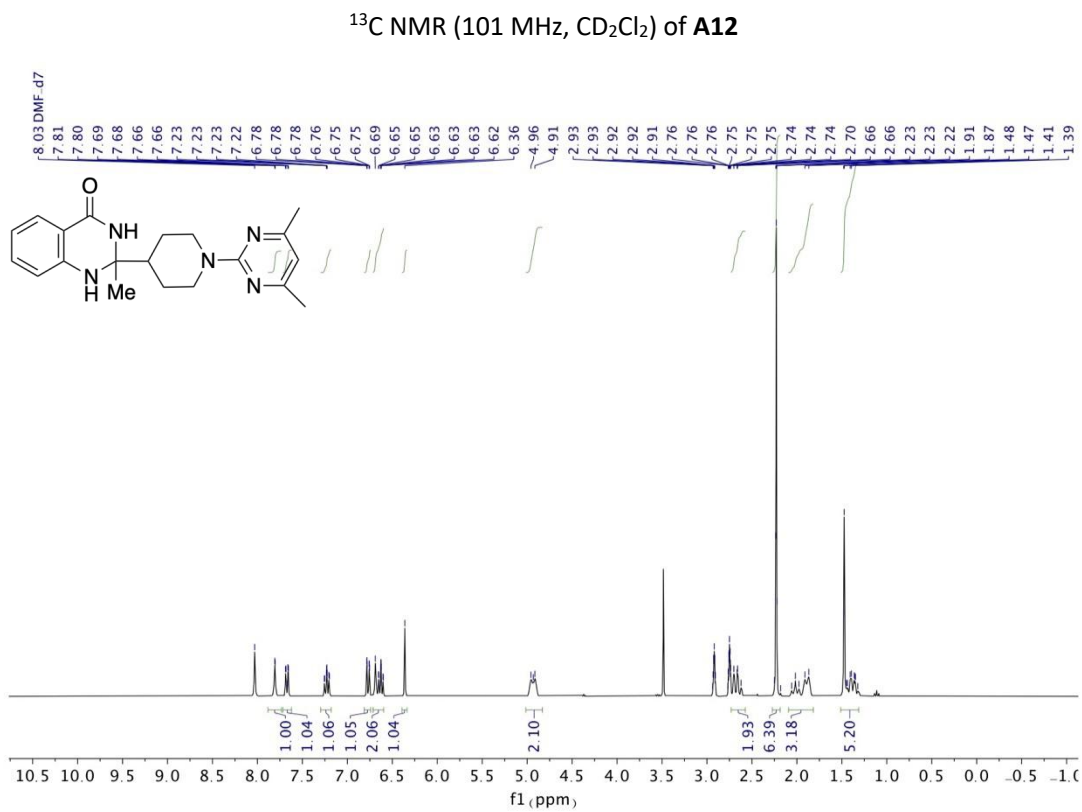
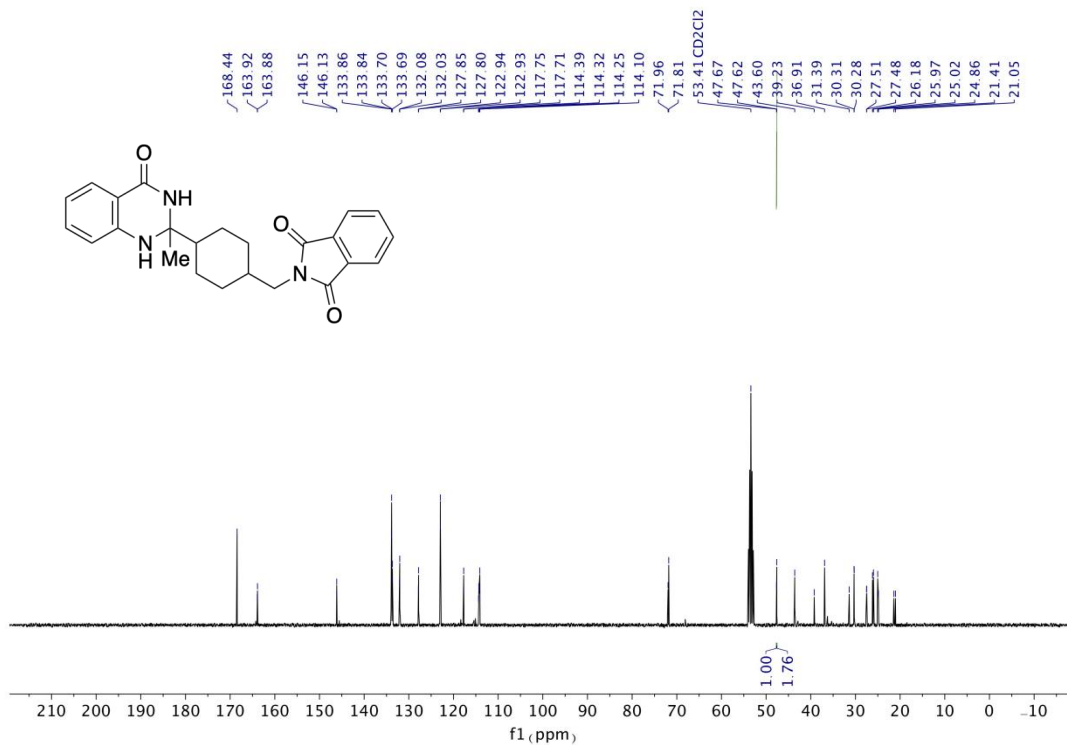


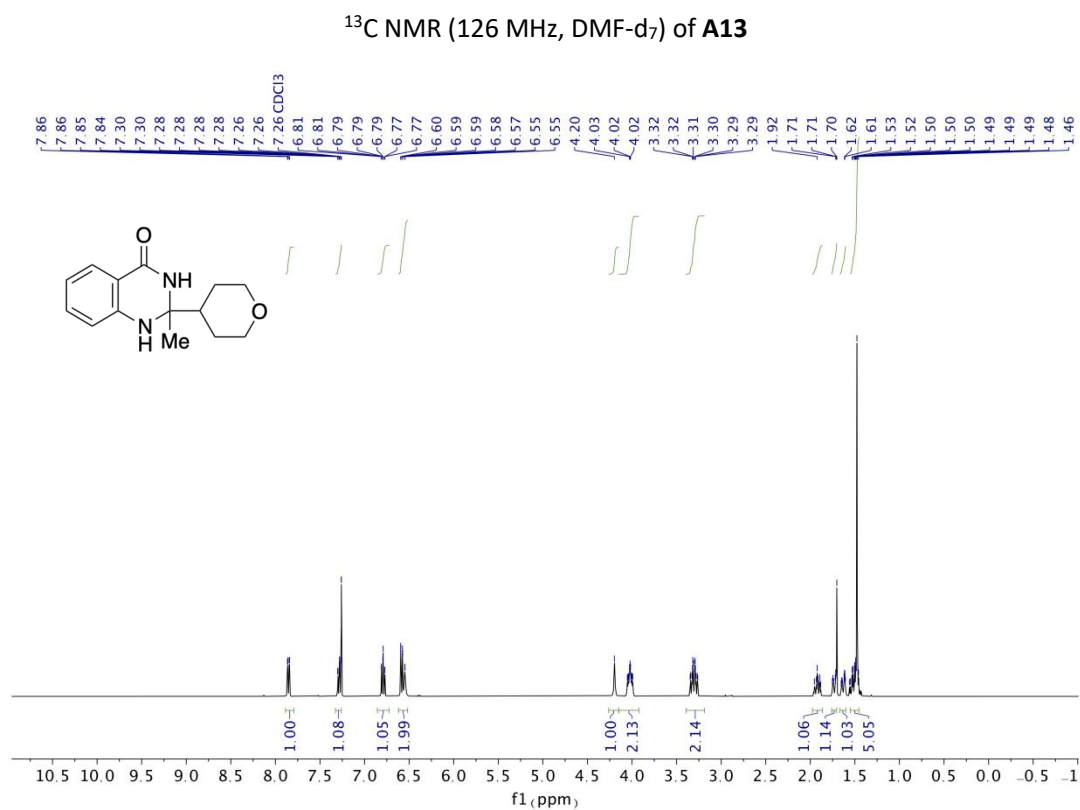
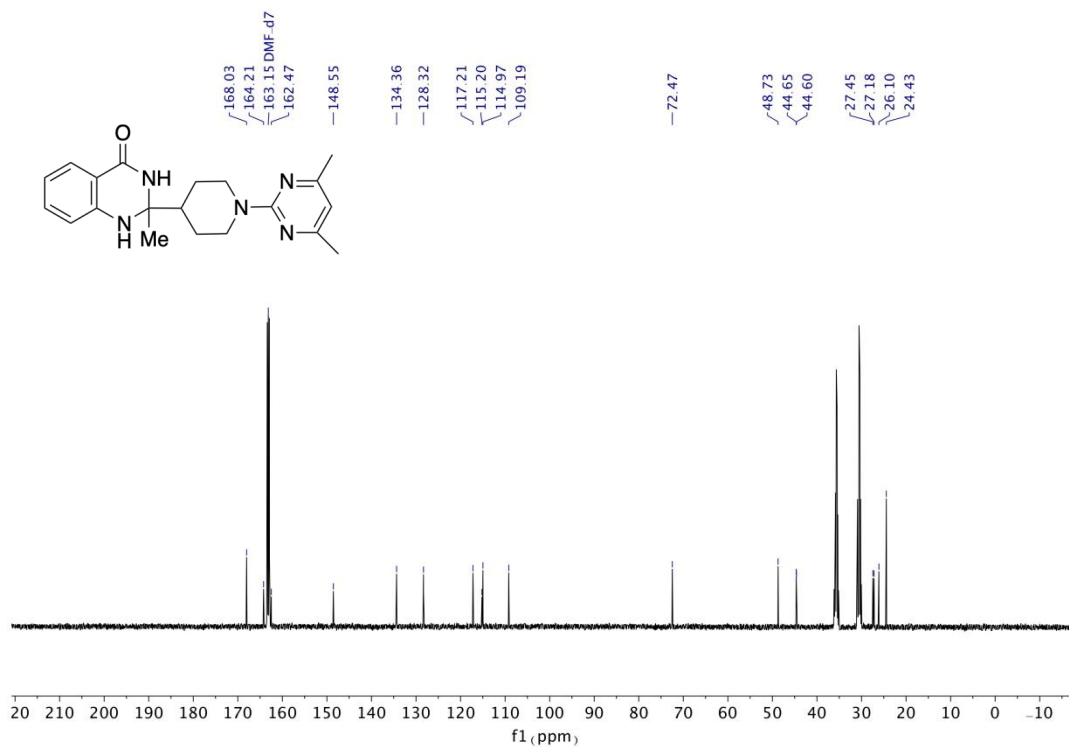


$^{13}\text{C}$  NMR spectrum (101 MHz,  $\text{CDCl}_3$ ) of **A11**

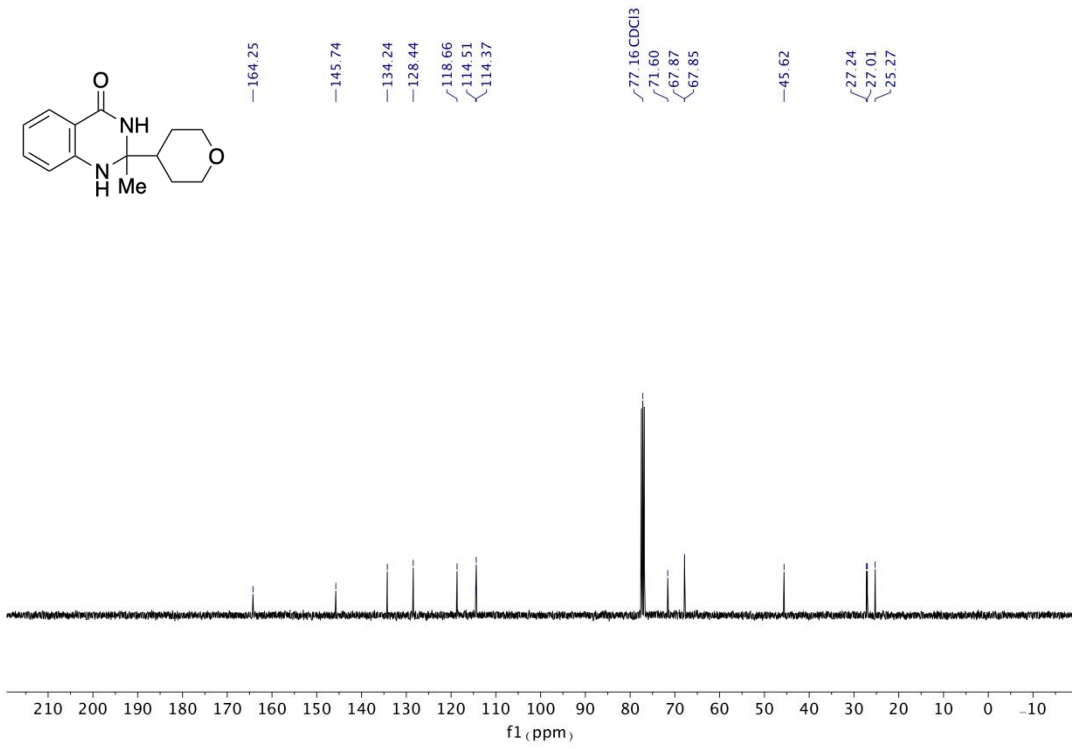


$^1\text{H}$  NMR (400 MHz,  $\text{CD}_2\text{Cl}_2$ ) of **A12**

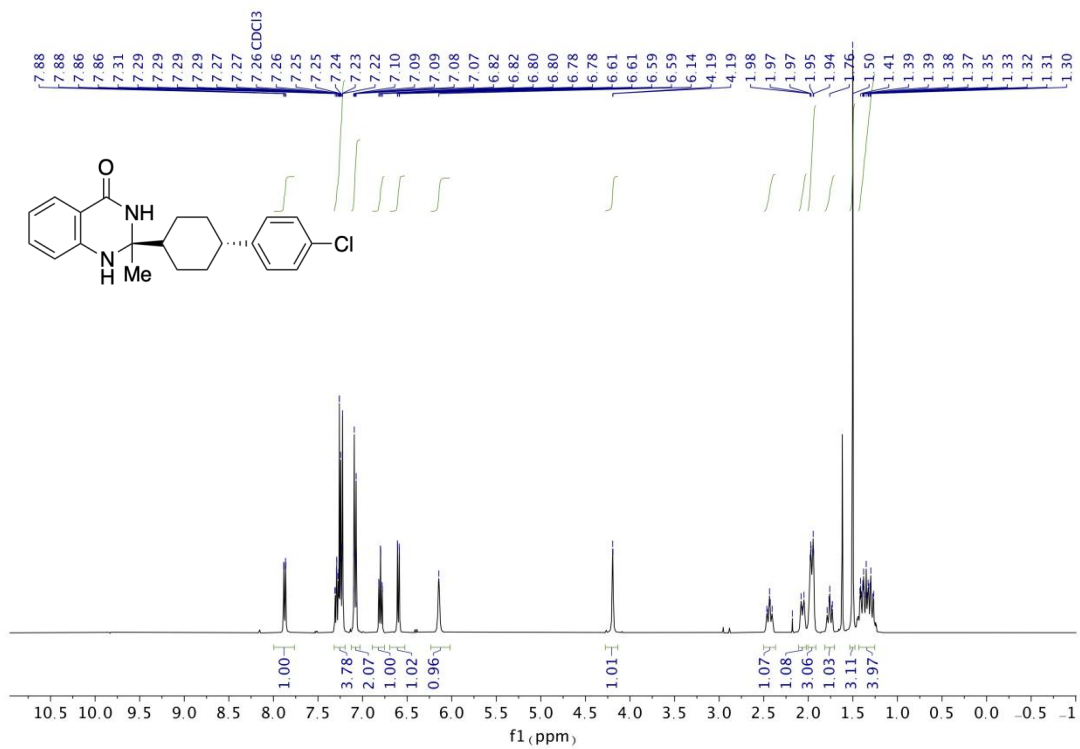




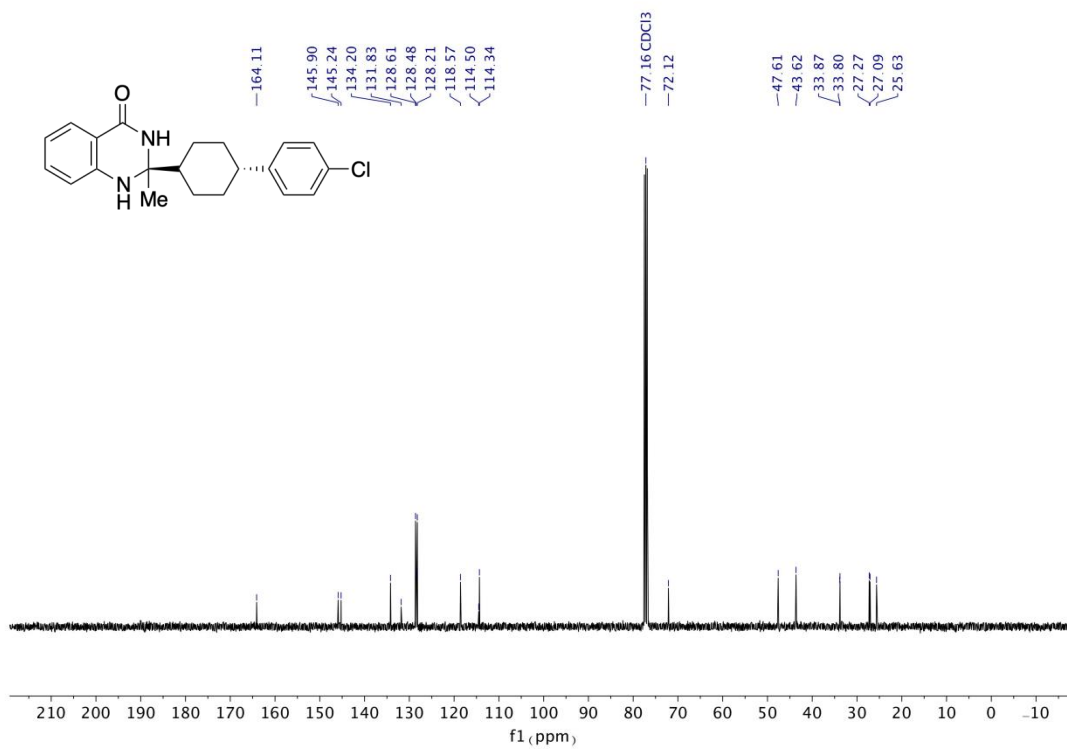




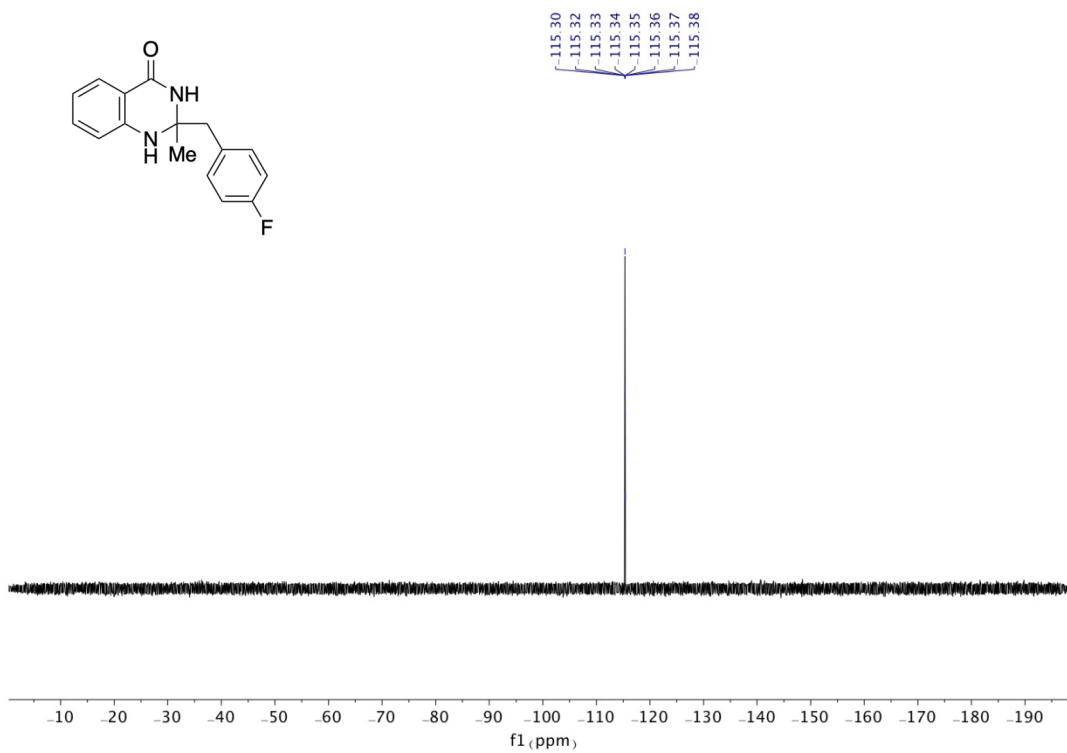
<sup>13</sup>C NMR spectrum (500 MHz, CDCl<sub>3</sub>) of **A14**



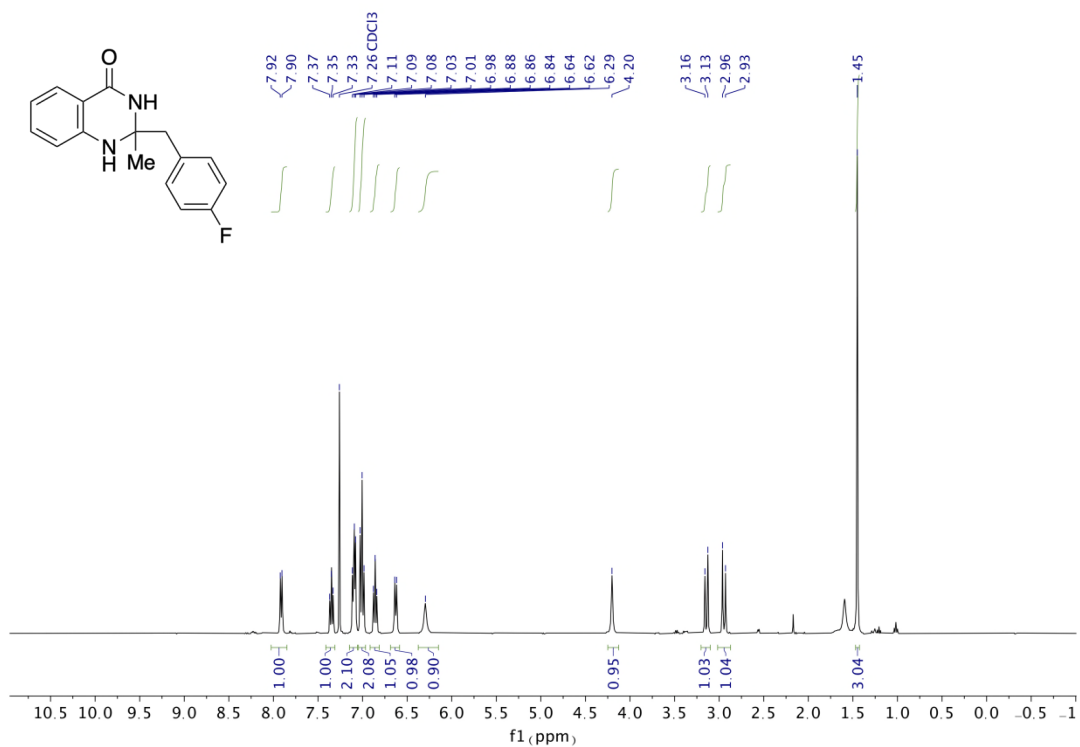
<sup>1</sup>H NMR (400 MHz, CDCl<sub>3</sub>) of **A15**



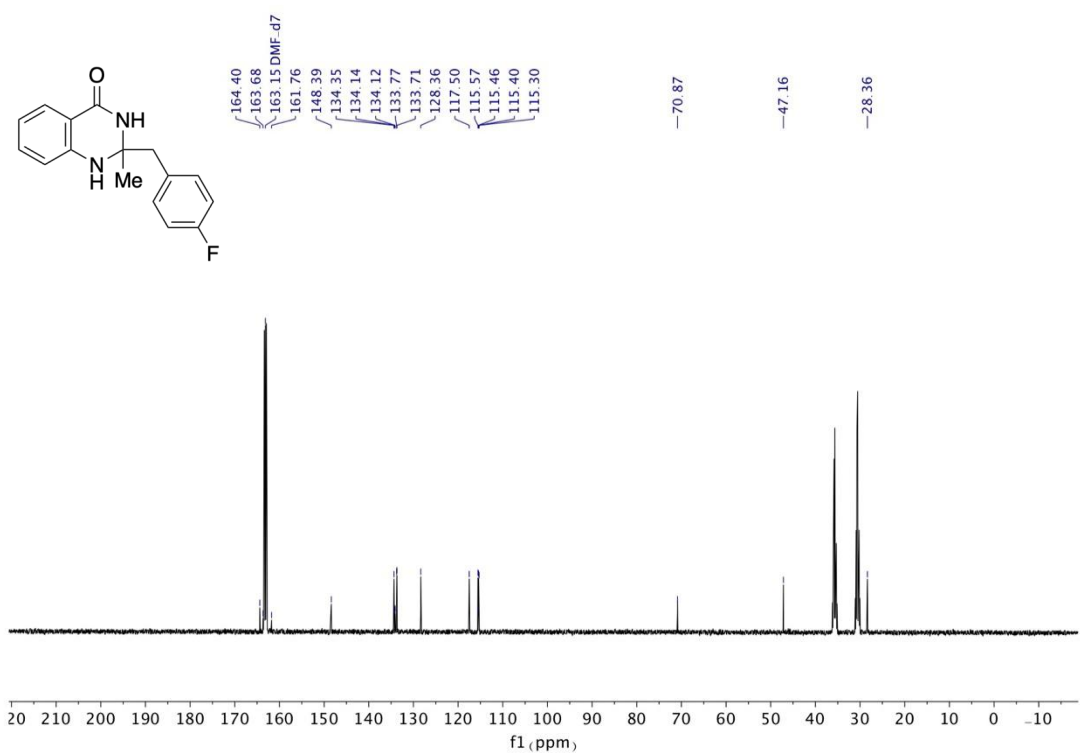
<sup>13</sup>C NMR (101 MHz, CDCl<sub>3</sub>) of **A15**



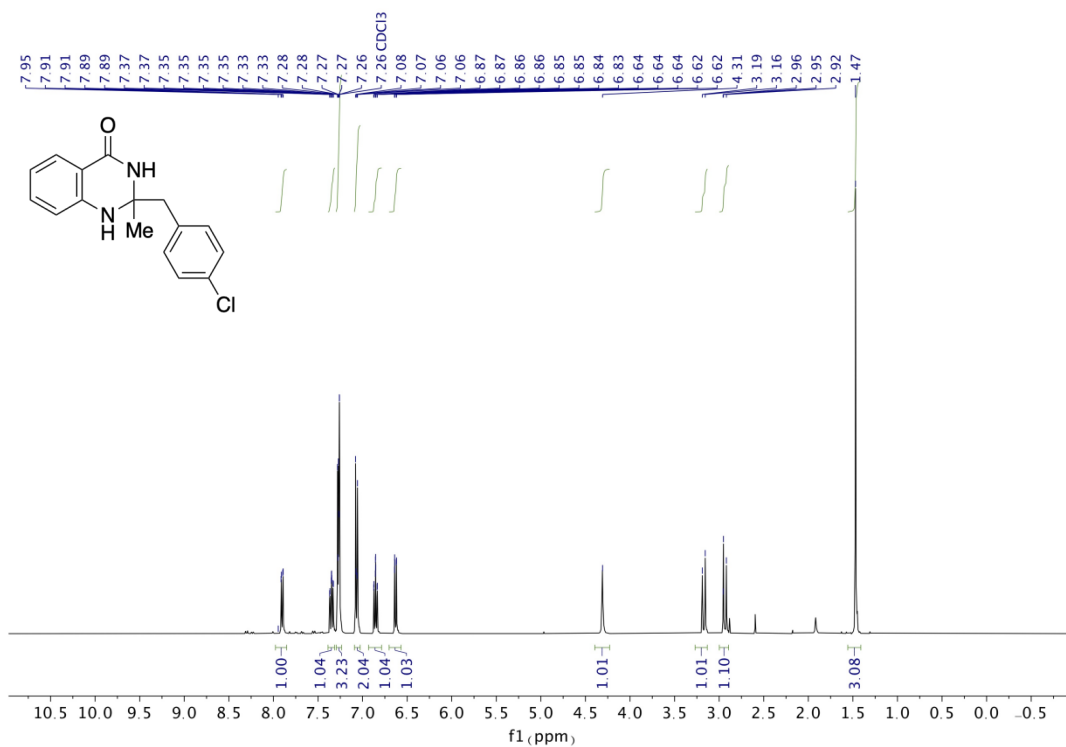
<sup>19</sup>F NMR spectrum (400 MHz, CDCl<sub>3</sub>) of **A16**



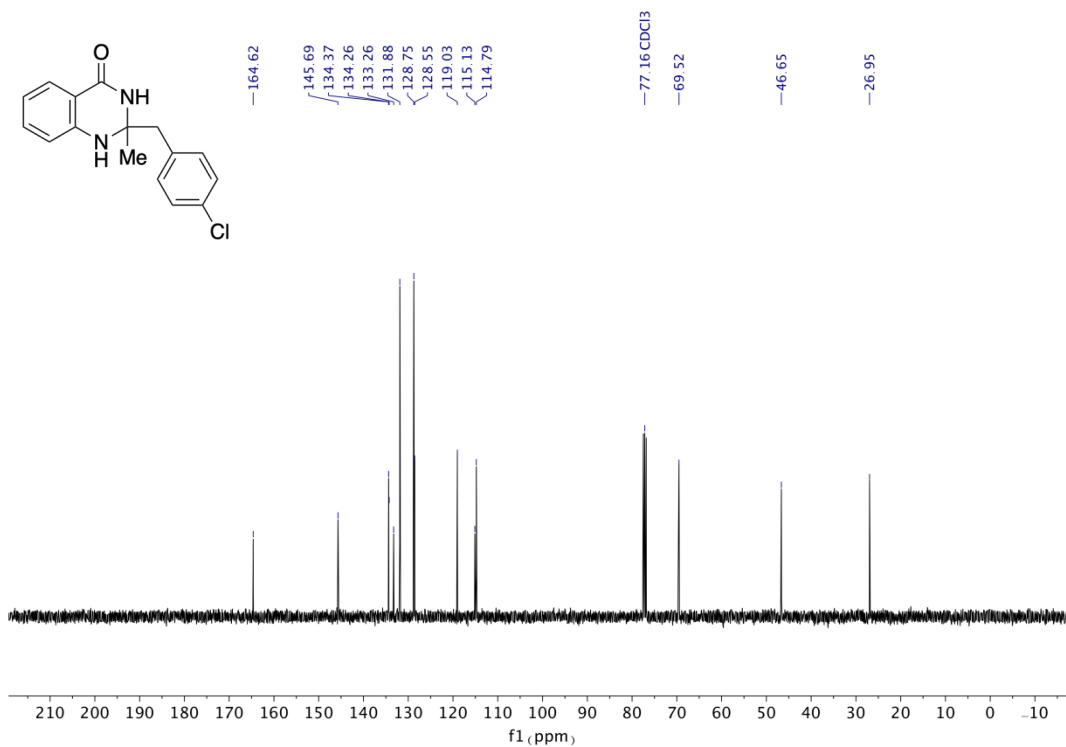
**<sup>1</sup>H NMR spectrum (400 MHz, CDCl<sub>3</sub>) of A16**



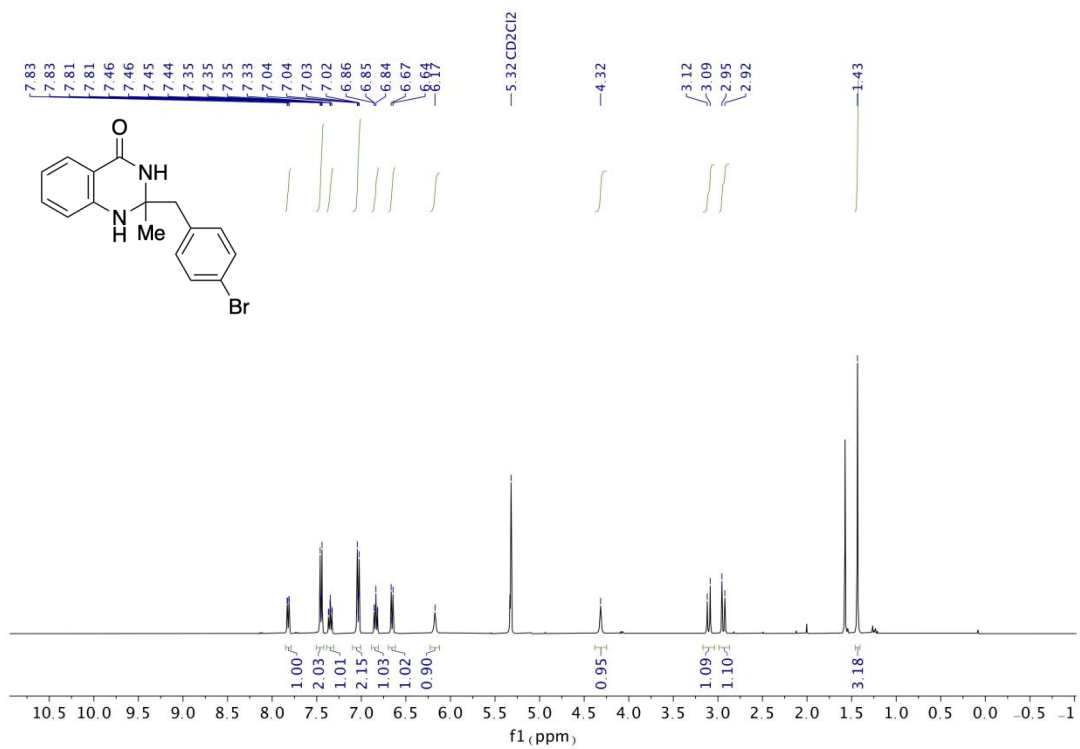
**<sup>13</sup>C NMR spectrum (126 MHz, DMF-d<sub>7</sub>) of A16**



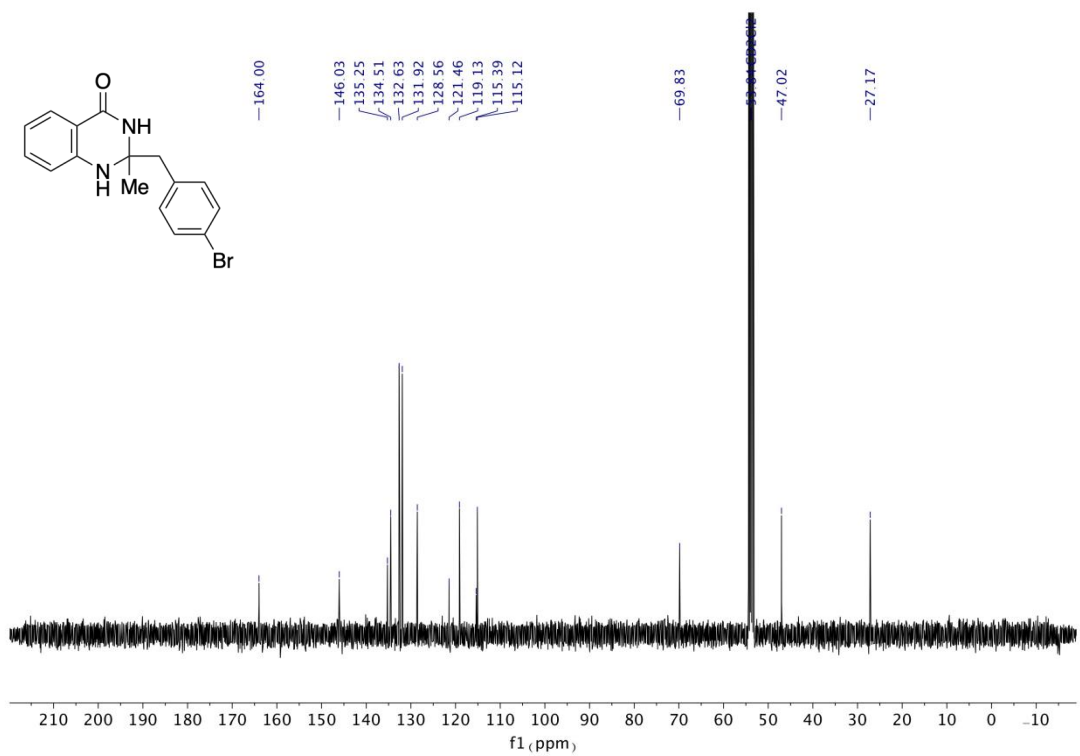
<sup>1</sup>H NMR spectrum (400 MHz, CDCl<sub>3</sub>) of A17



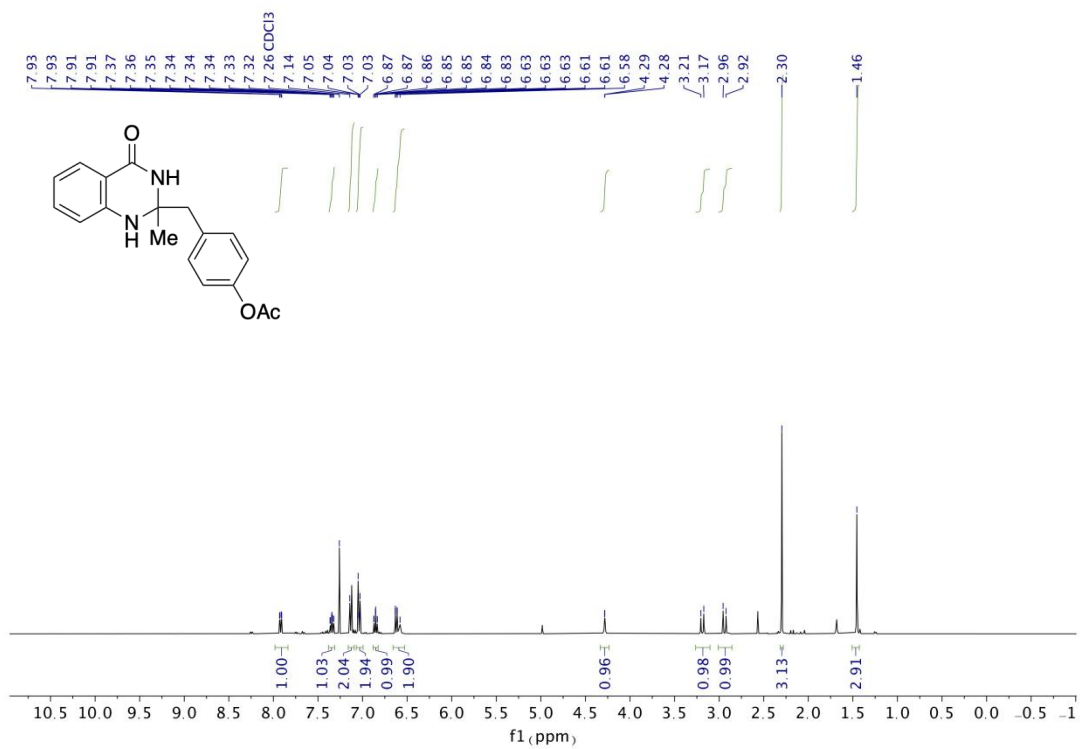
<sup>13</sup>C NMR spectrum (101 MHz, CDCl<sub>3</sub>) of A17



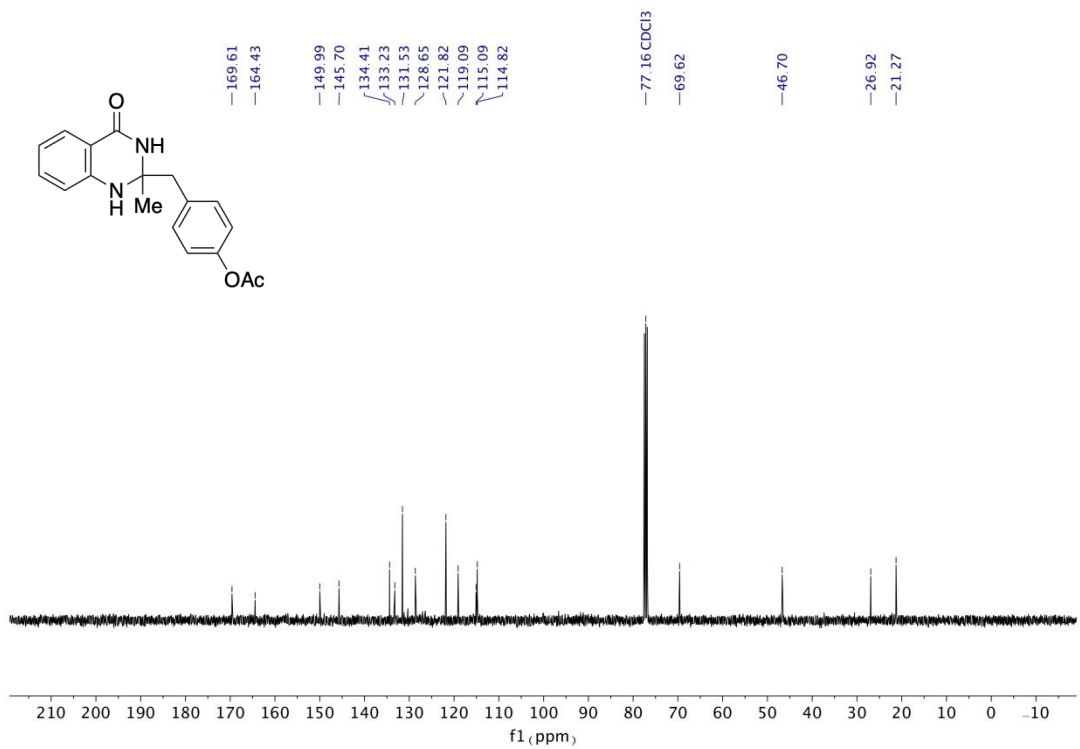
**<sup>1</sup>H NMR spectrum (400 MHz, CD<sub>2</sub>Cl<sub>2</sub>) of A18**



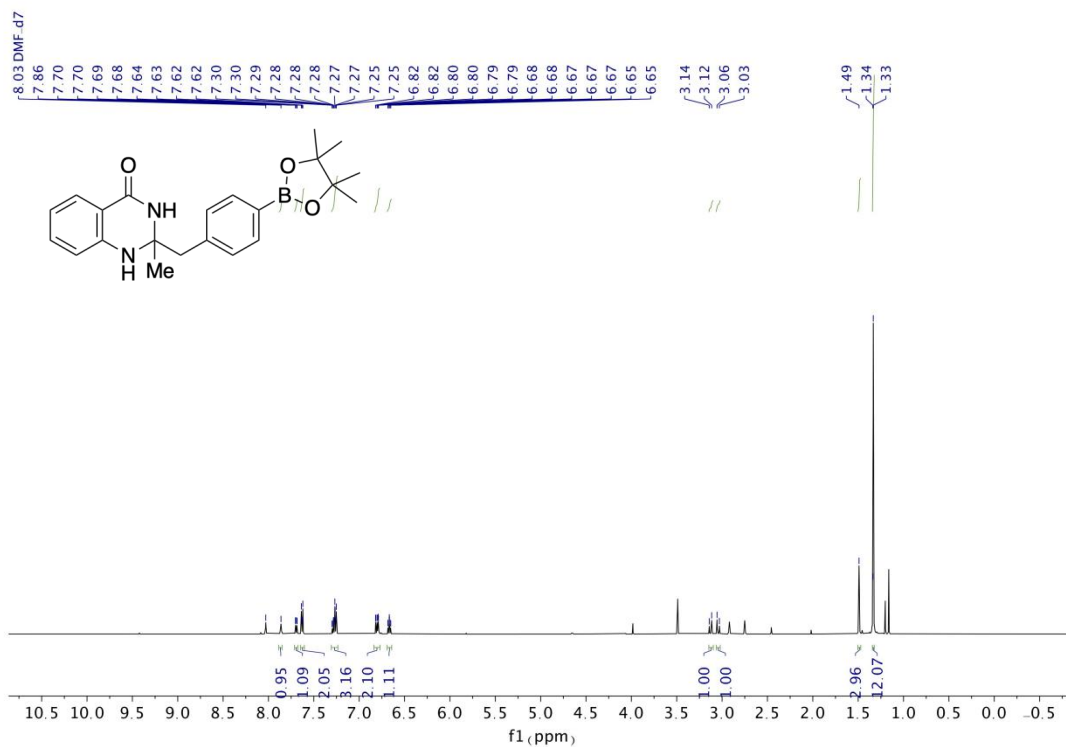
**<sup>13</sup>C NMR spectrum (101 MHz, CD<sub>2</sub>Cl<sub>2</sub>) of A18**



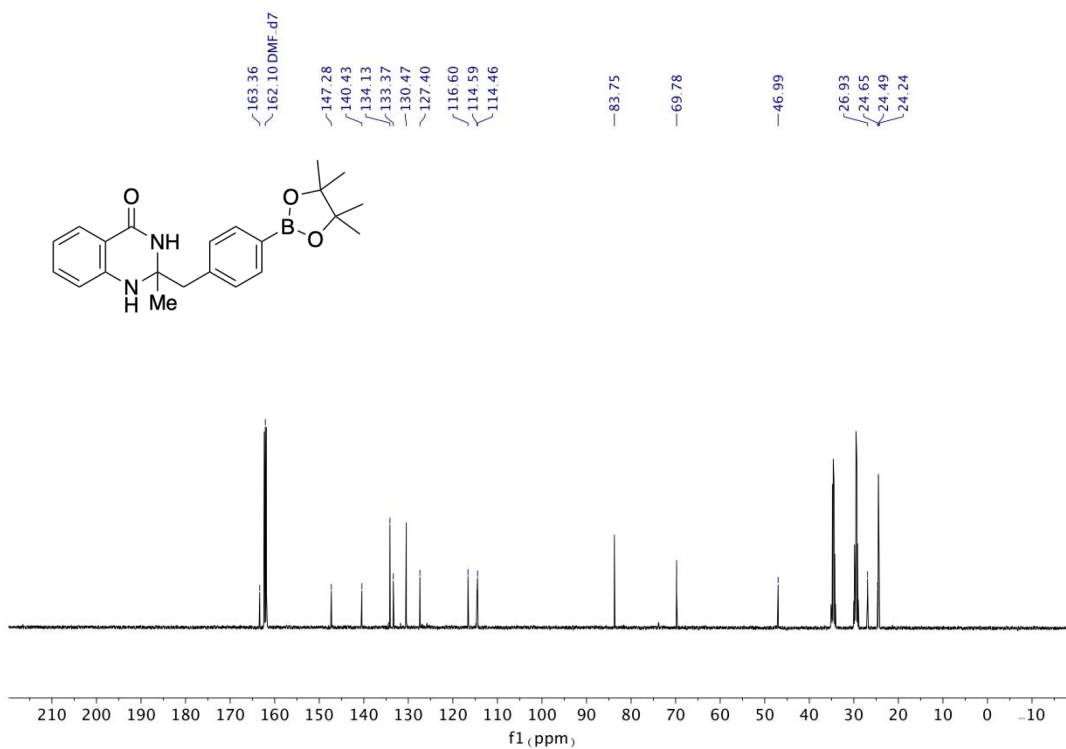
**<sup>1</sup>H NMR spectrum (400 MHz, CDCl<sub>3</sub>) of A19**



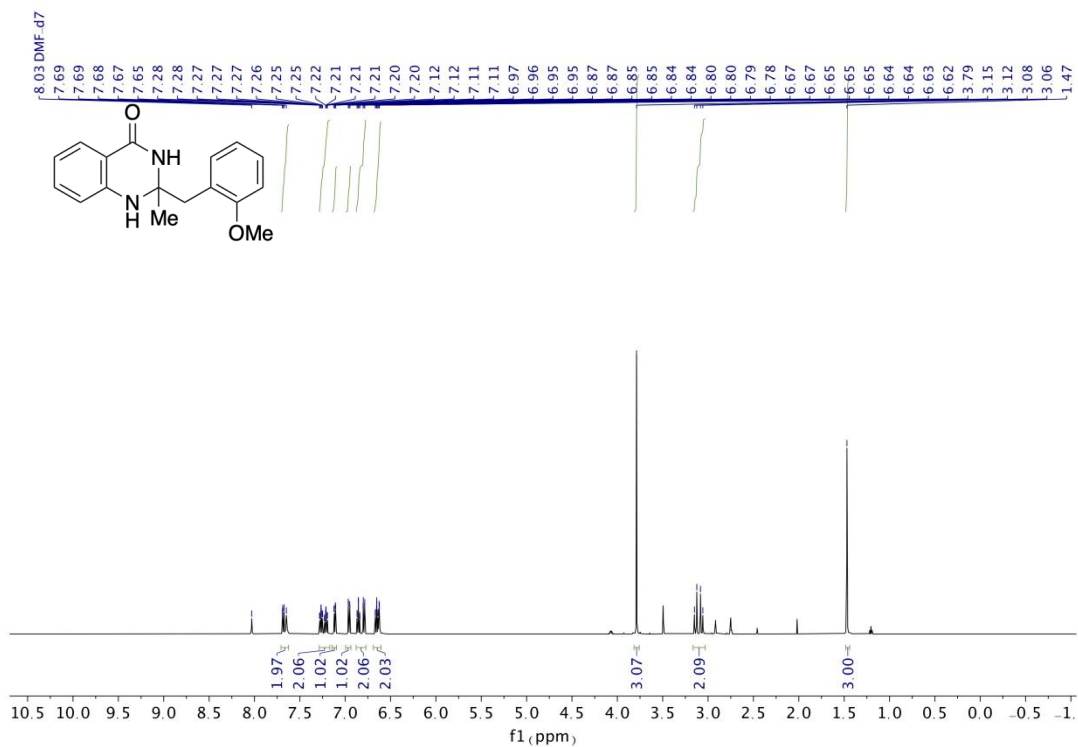
**<sup>13</sup>C NMR spectrum (101 MHz, CDCl<sub>3</sub>) of A19**



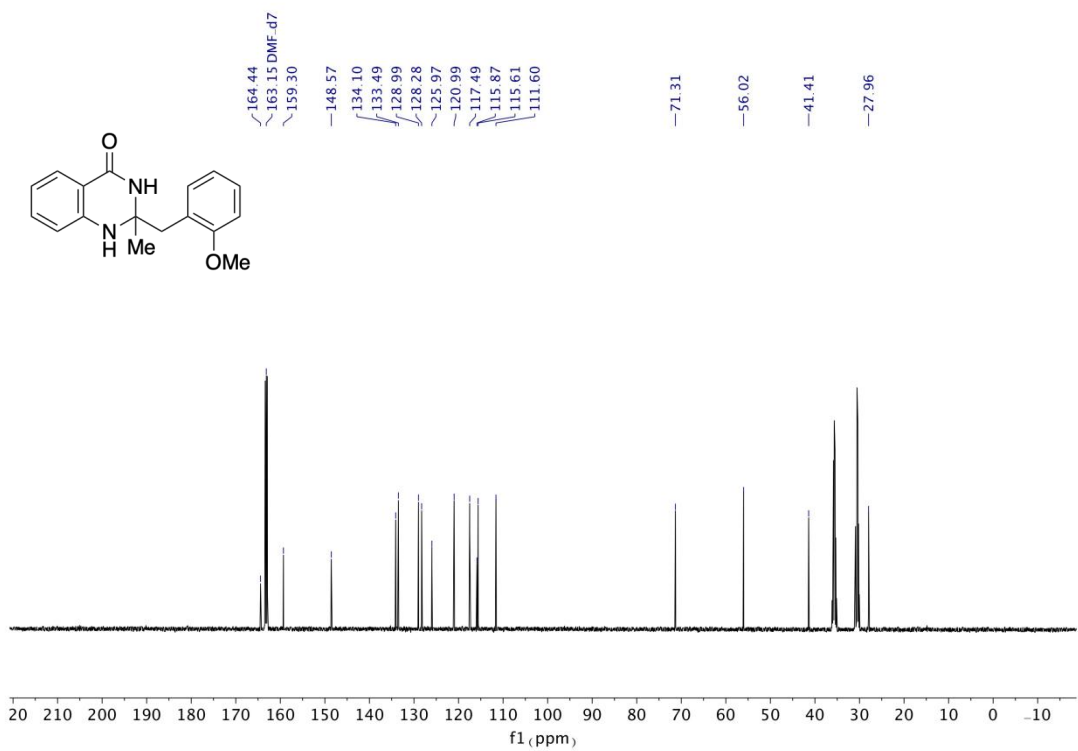
<sup>1</sup>H NMR (500 MHz, DMF-d<sub>7</sub>) of A20



<sup>13</sup>C NMR spectrum (101 MHz, DMF-d<sub>7</sub>) of A20

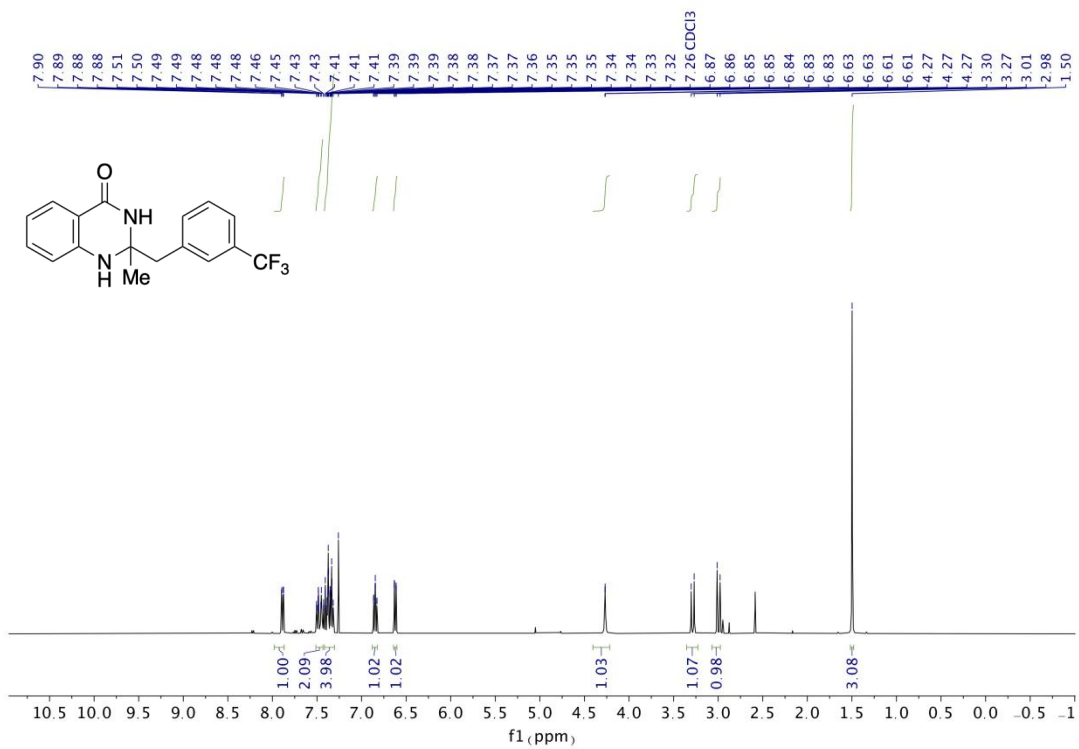
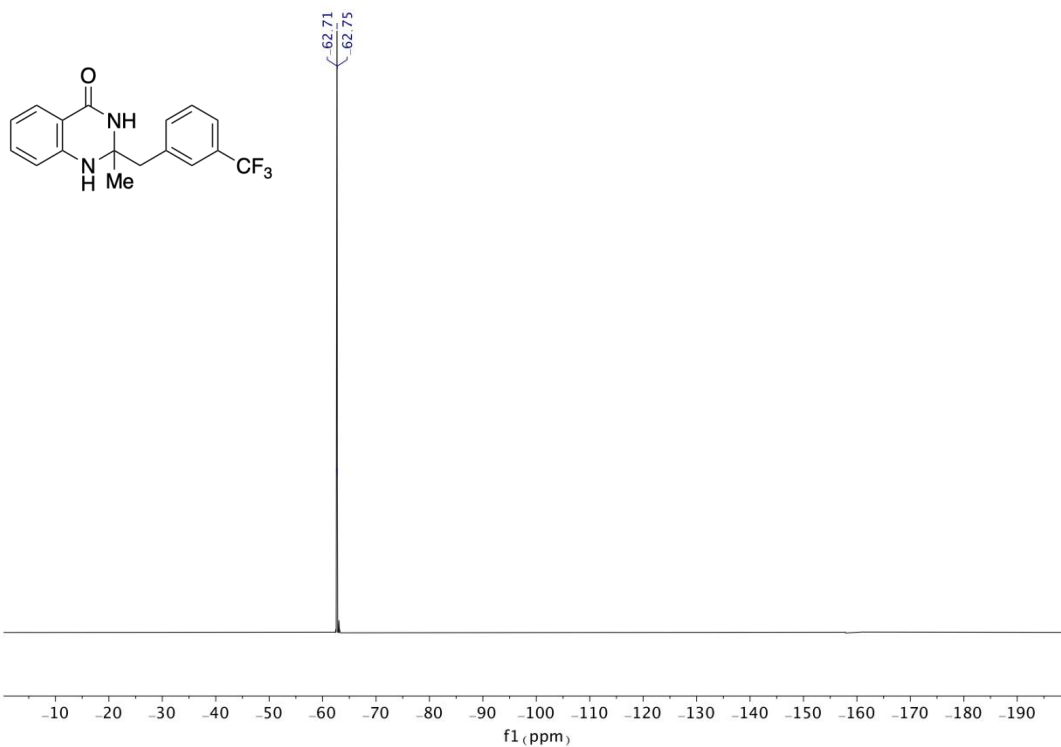


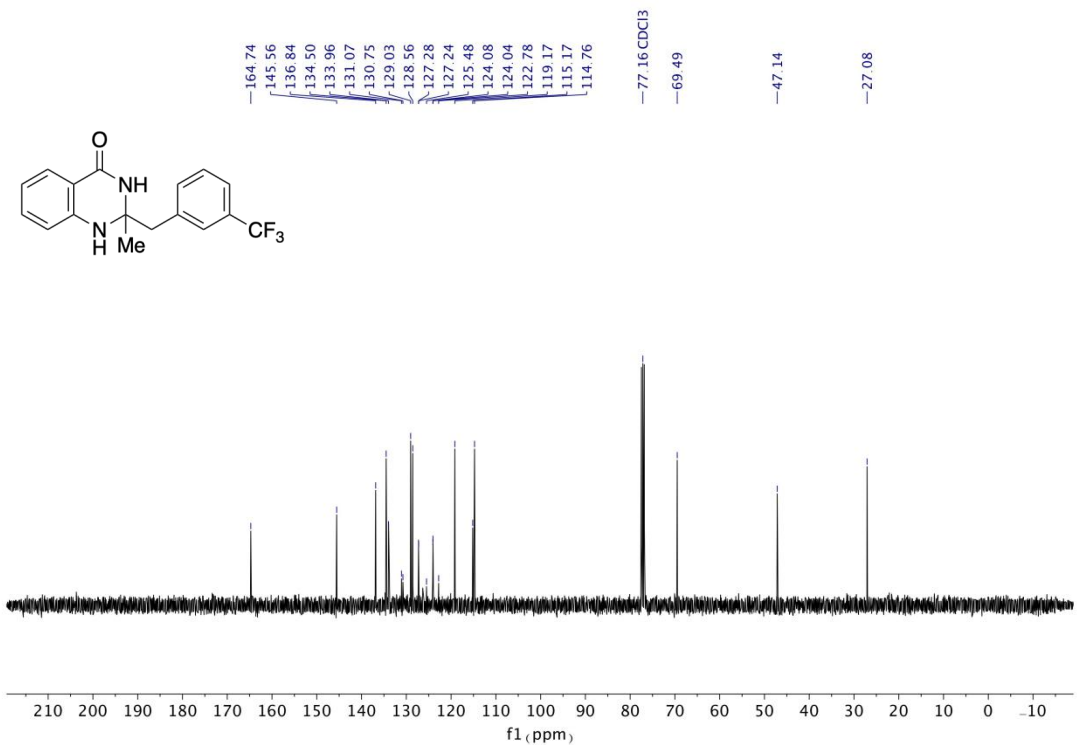
<sup>1</sup>H NMR (500 MHz, DMF-d<sub>7</sub>) of **A21**



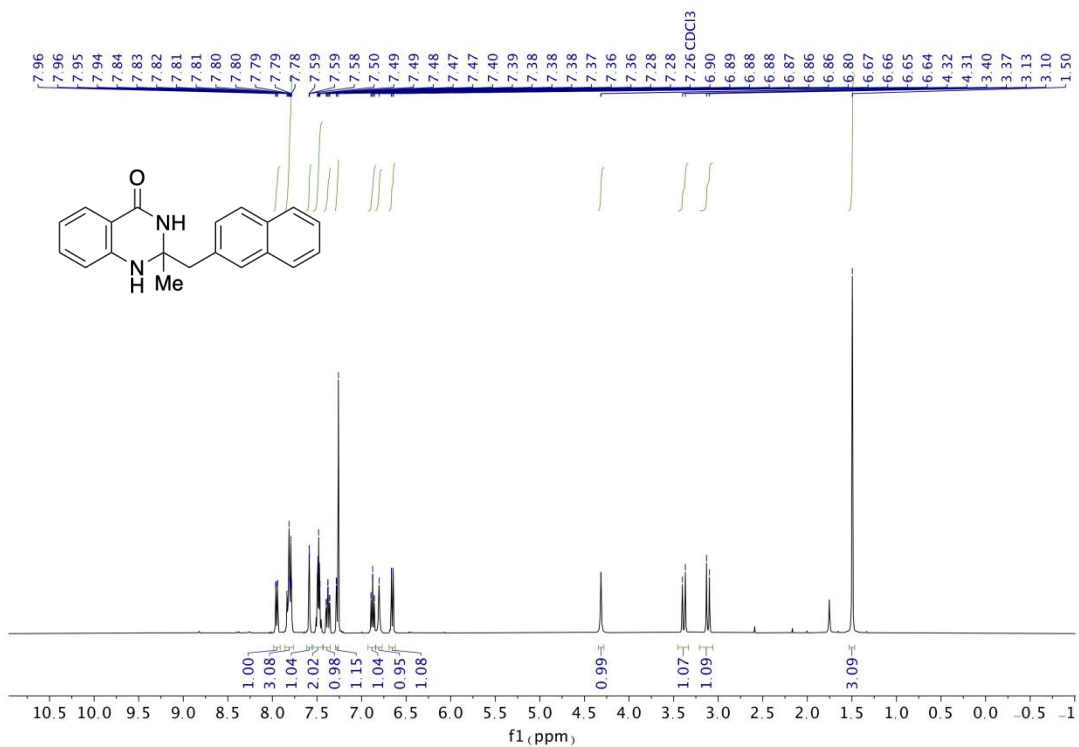
<sup>13</sup>C NMR (126 MHz, DMF-d<sub>7</sub>) of **A21**



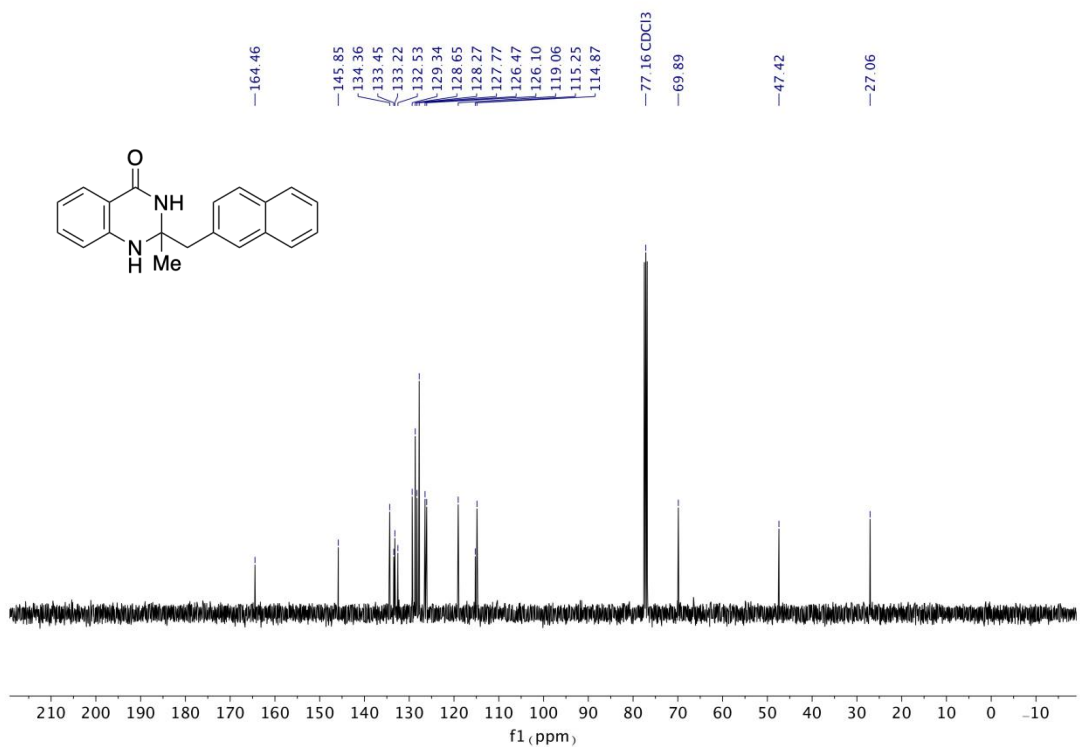




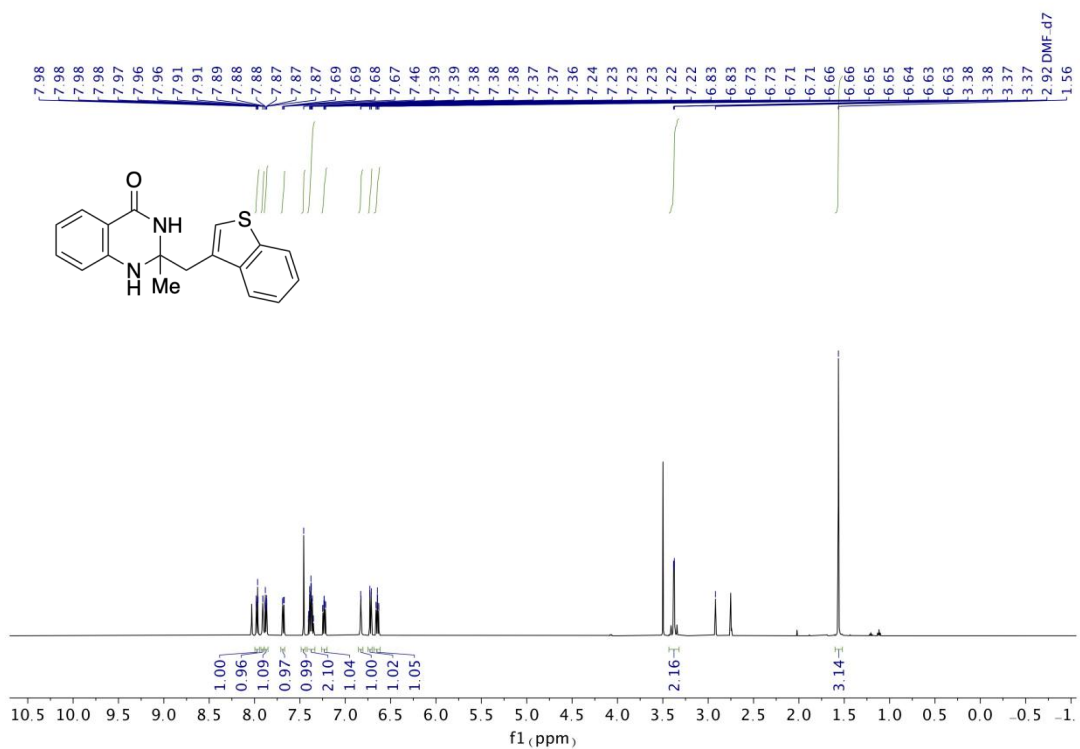
<sup>13</sup>C NMR spectrum (101 MHz, CDCl<sub>3</sub>) of A22



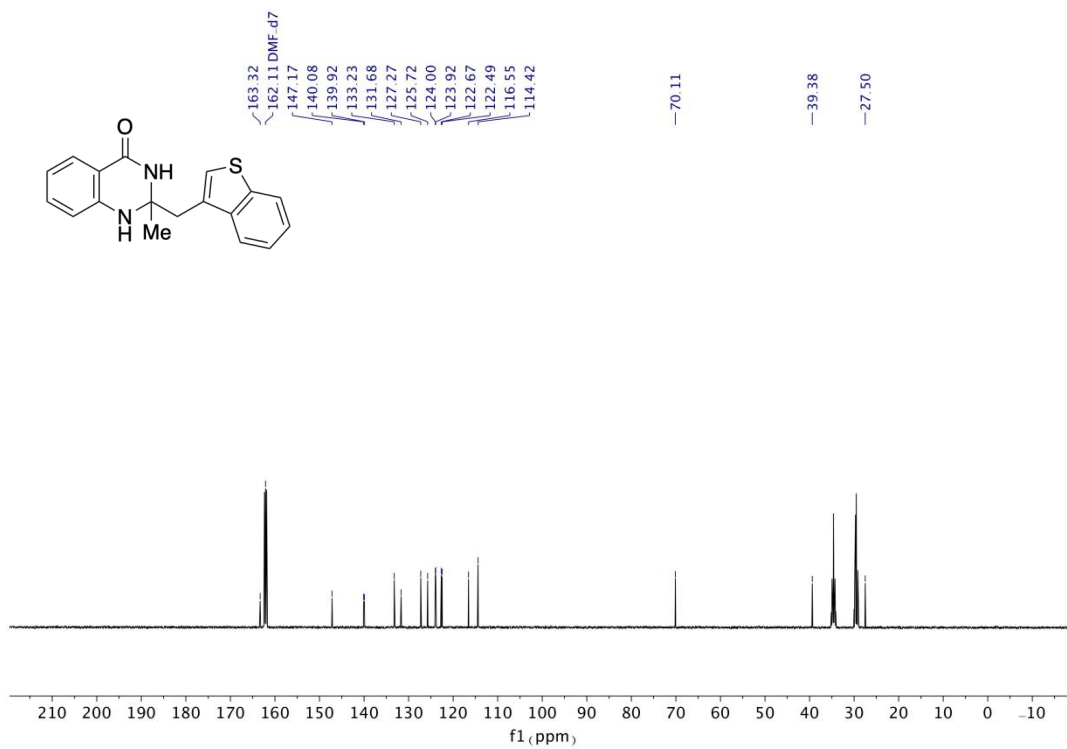
<sup>1</sup>H NMR spectrum (400 MHz, CDCl<sub>3</sub>) of A23



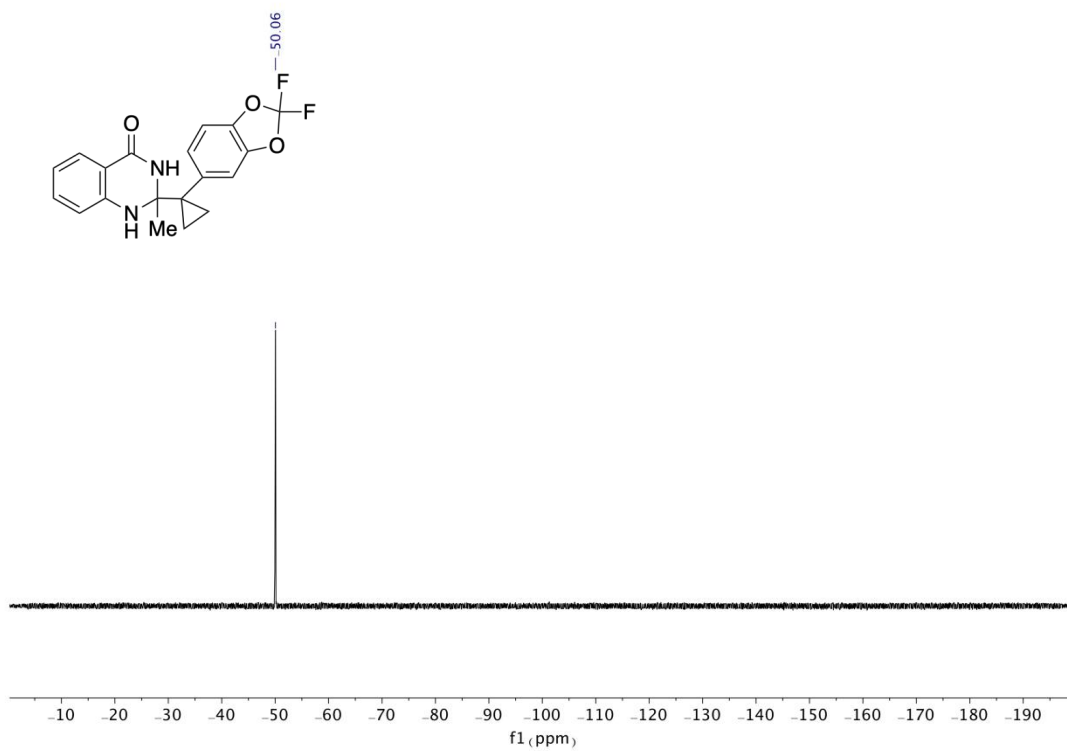
<sup>13</sup>C NMR spectrum (101 MHz, CDCl<sub>3</sub>) of **A23**



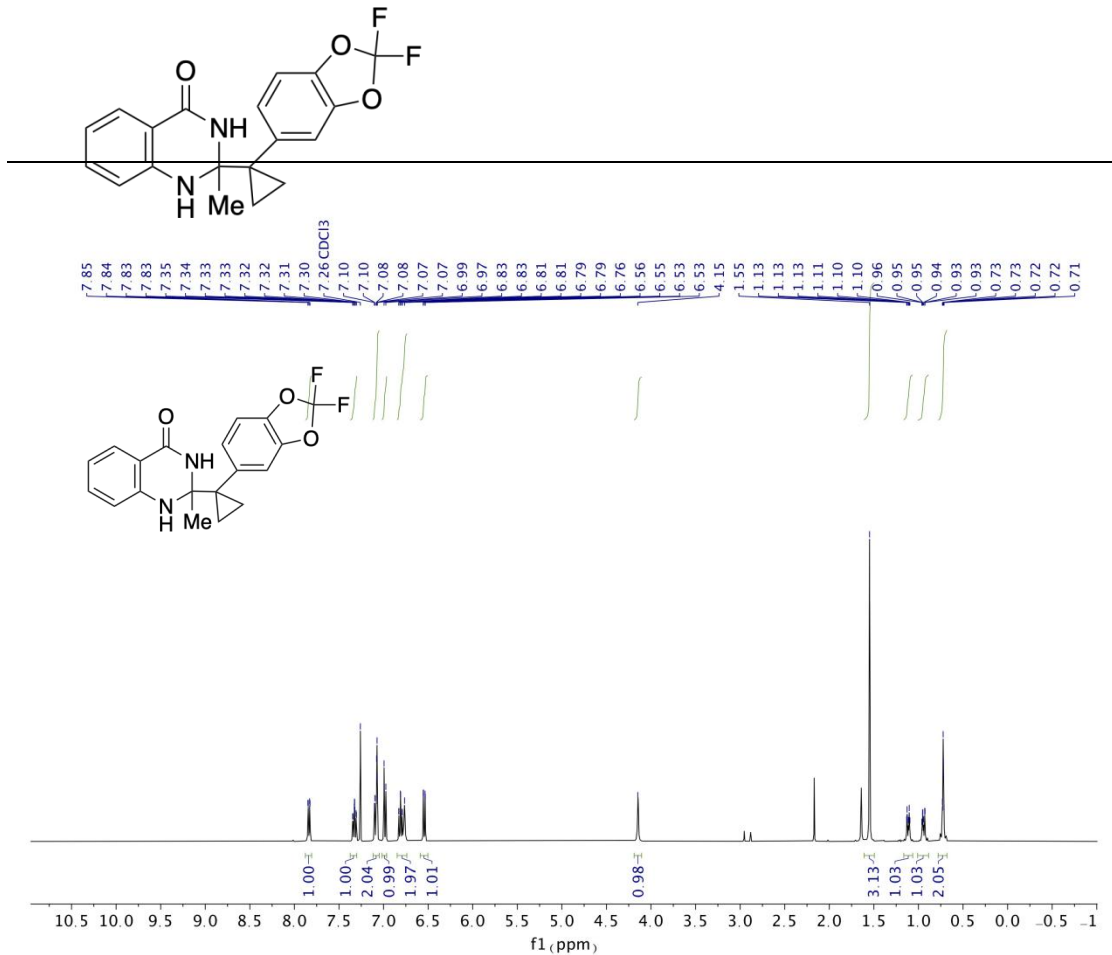
<sup>1</sup>H NMR (500 MHz, DMF-d<sub>7</sub>) of **A24**



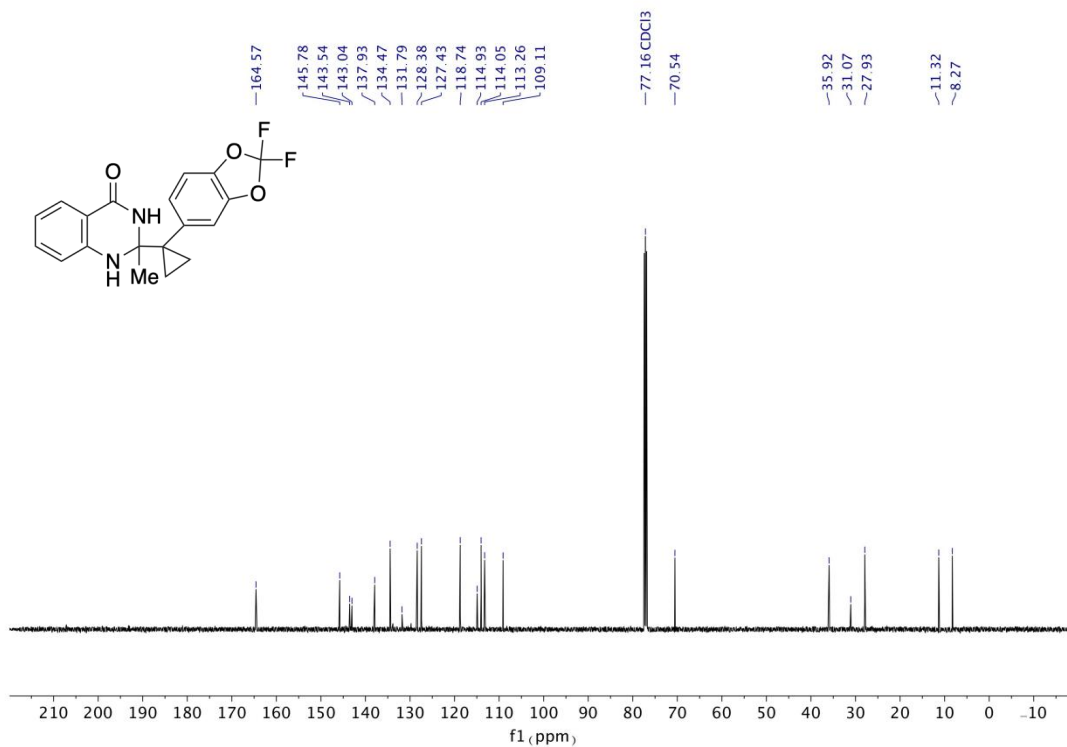
<sup>13</sup>C NMR (126 MHz, DMF-d<sub>7</sub>) of A24



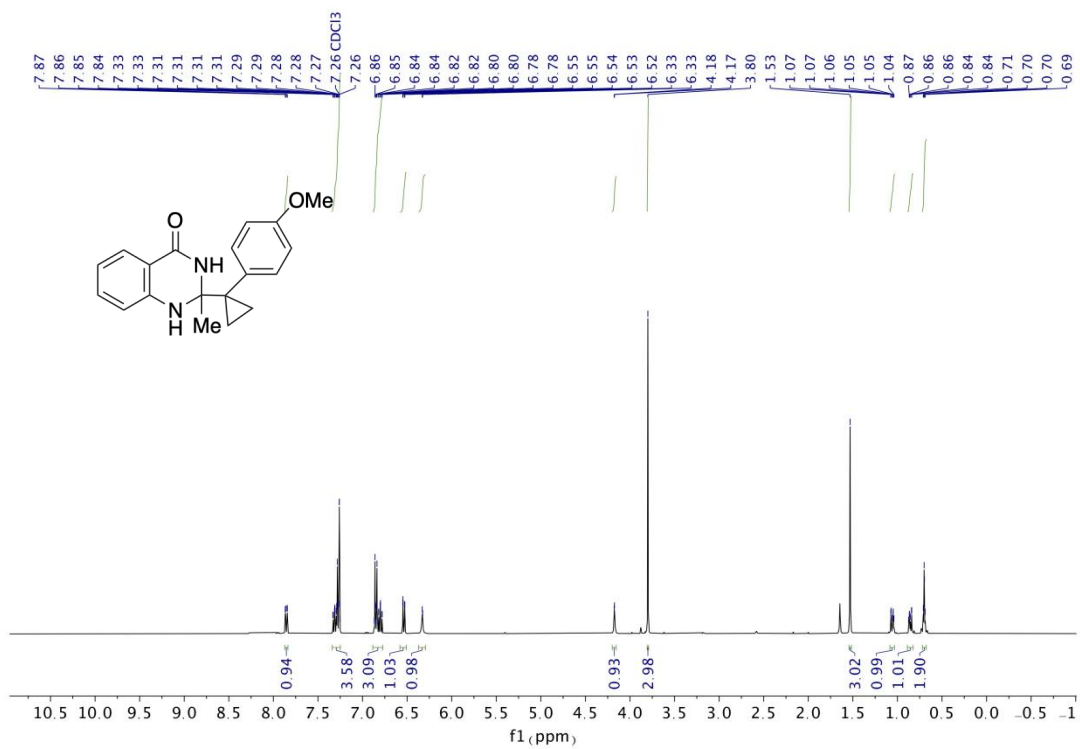
<sup>19</sup>F NMR (376 MHz, CDCl<sub>3</sub>) of A25



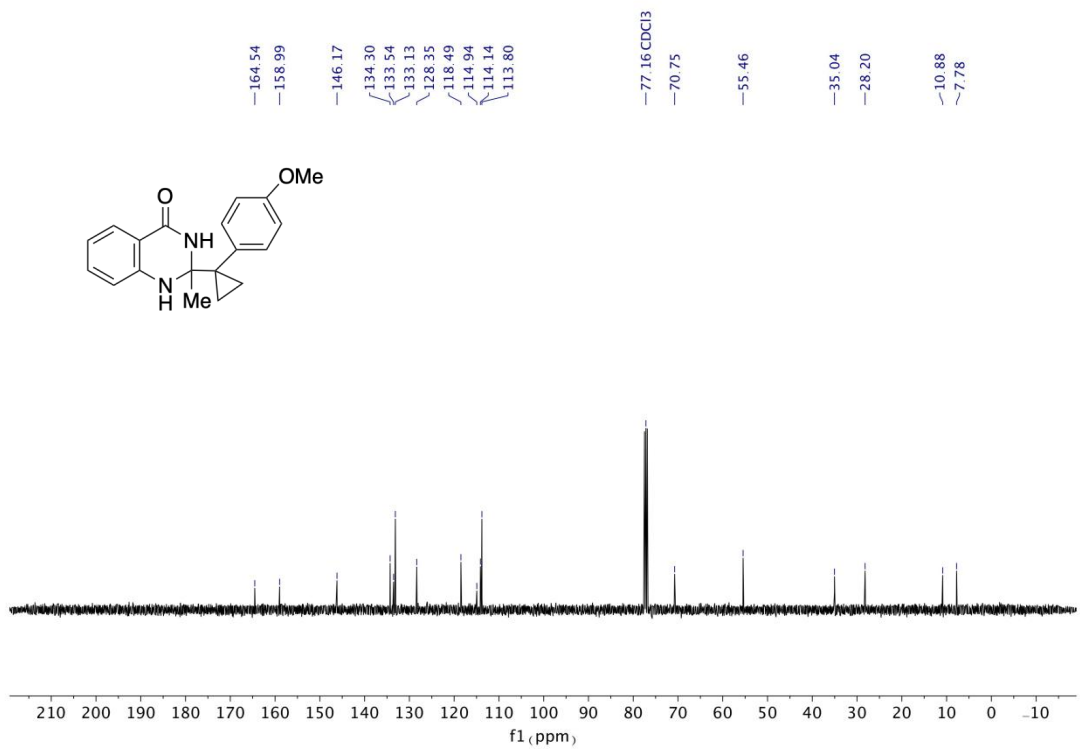
**<sup>1</sup>H NMR (400 MHz, CDCl<sub>3</sub>) of A25**



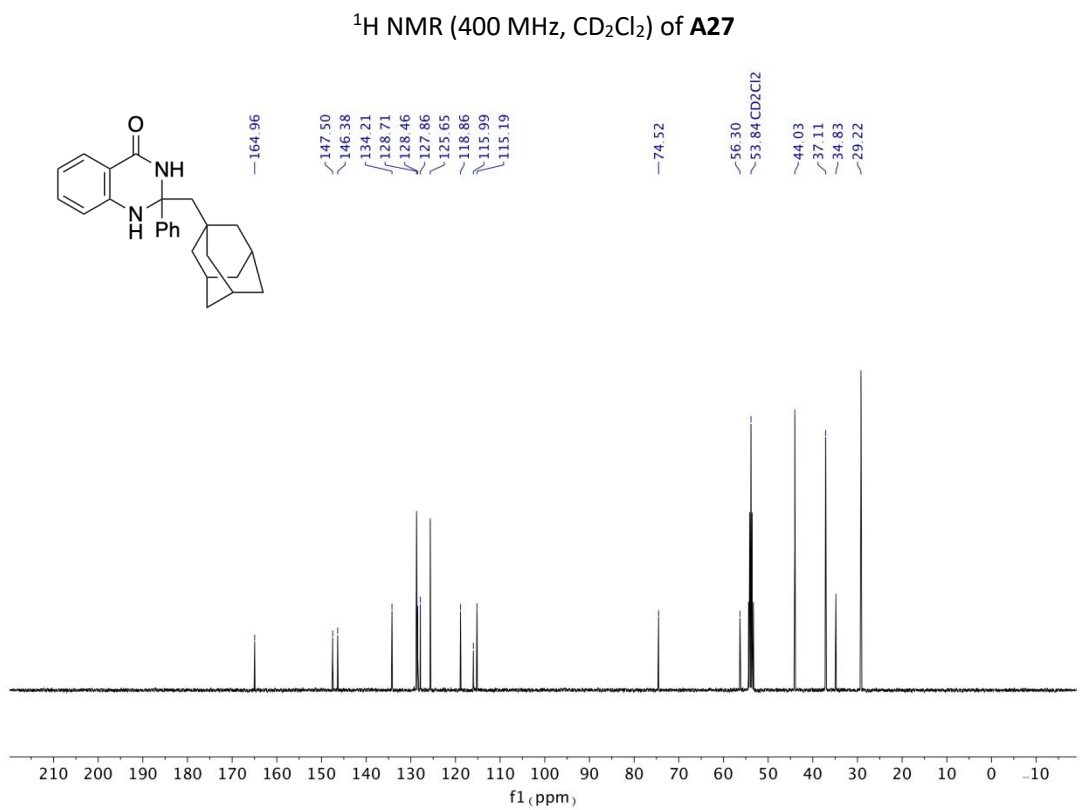
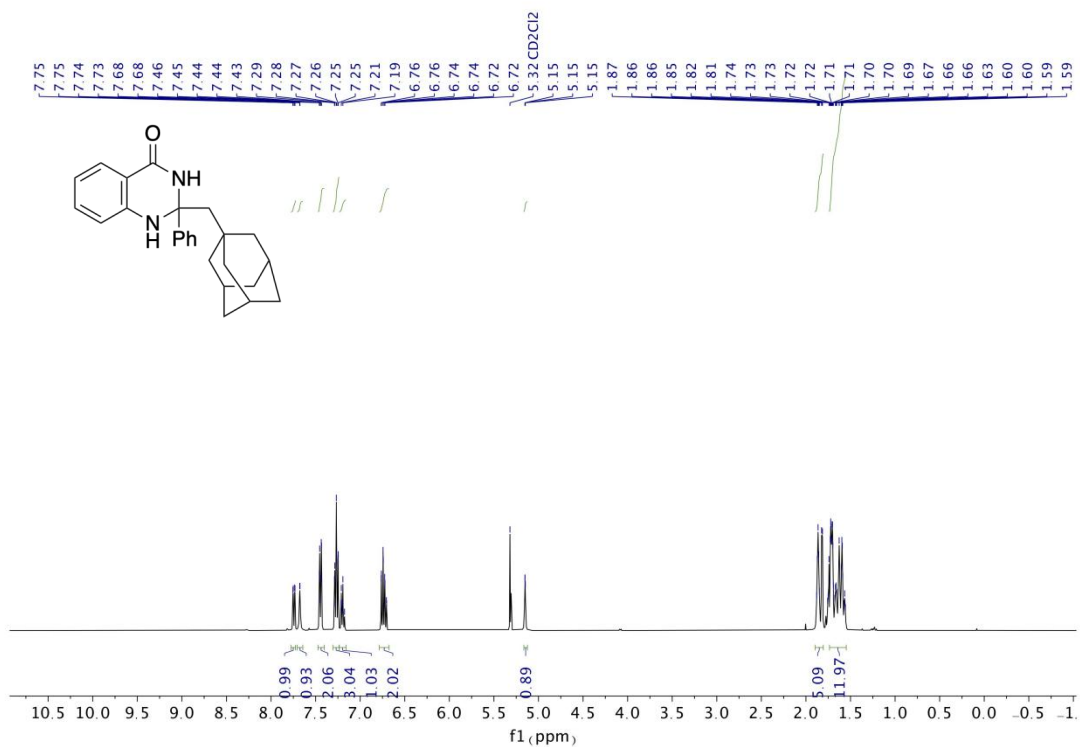
**<sup>13</sup>C NMR (126 MHz, CDCl<sub>3</sub>) of A25**

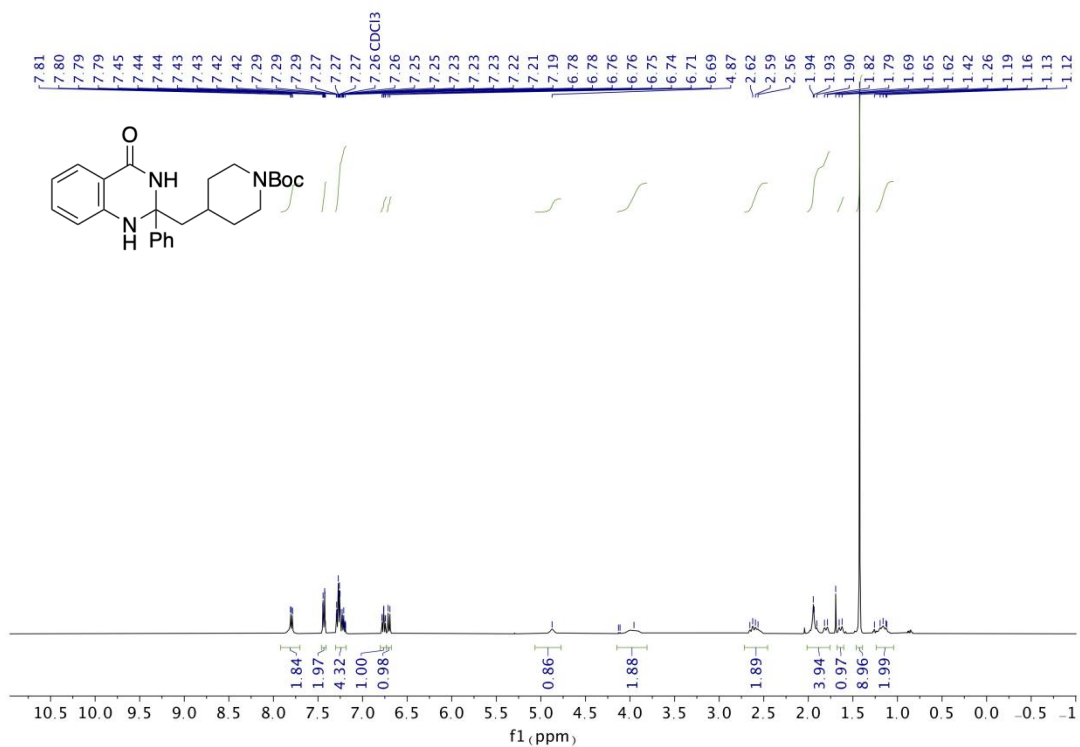


**<sup>1</sup>H NMR (400 MHz, CDCl<sub>3</sub>) of A26**

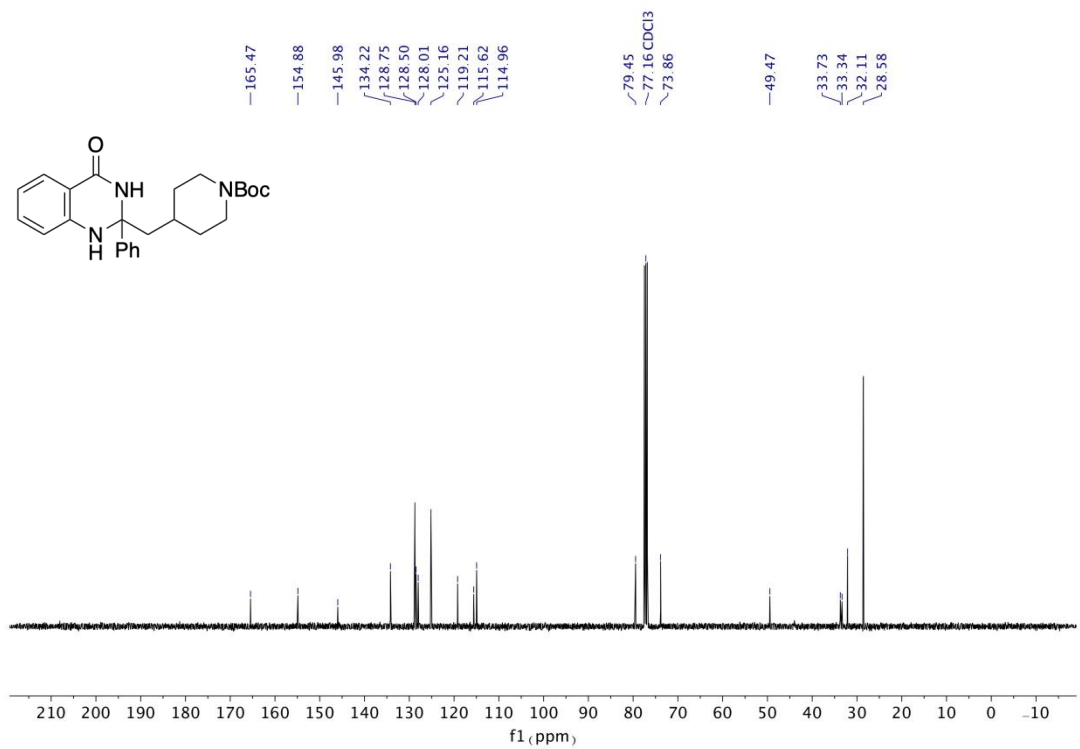


**<sup>13</sup>C NMR (101 MHz, CDCl<sub>3</sub>) of A26**



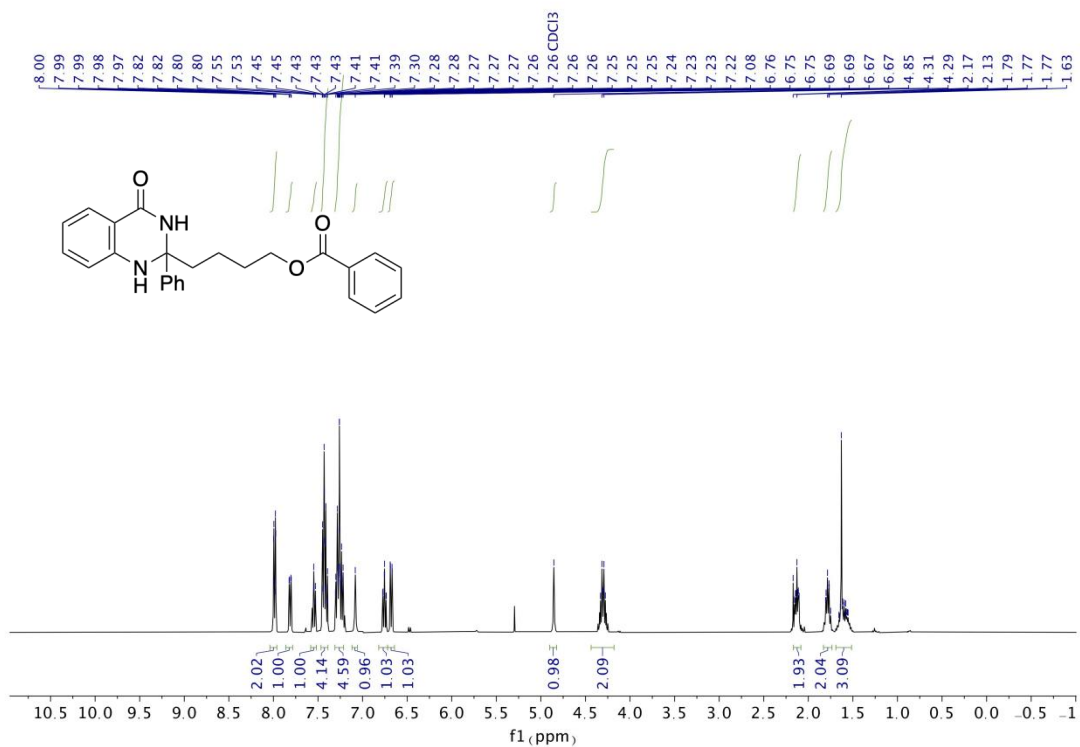


**<sup>1</sup>H NMR (400 MHz, CDCl<sub>3</sub>) of A28**

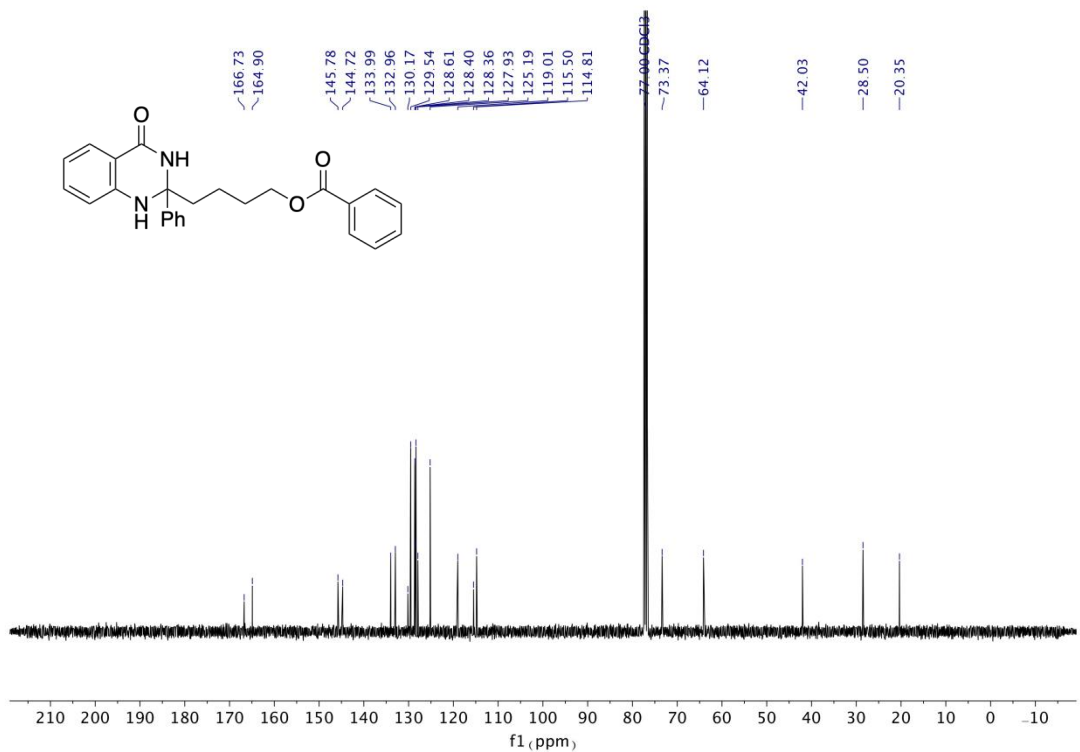


**<sup>13</sup>C NMR (101 MHz, CDCl<sub>3</sub>) of A28**

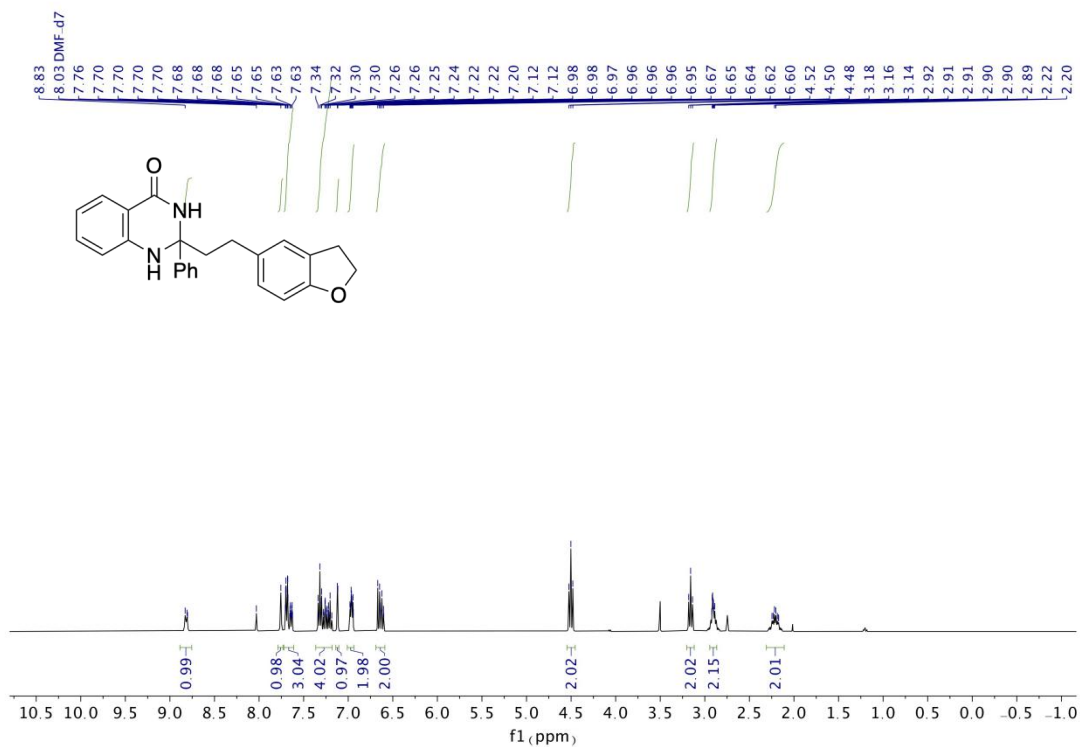




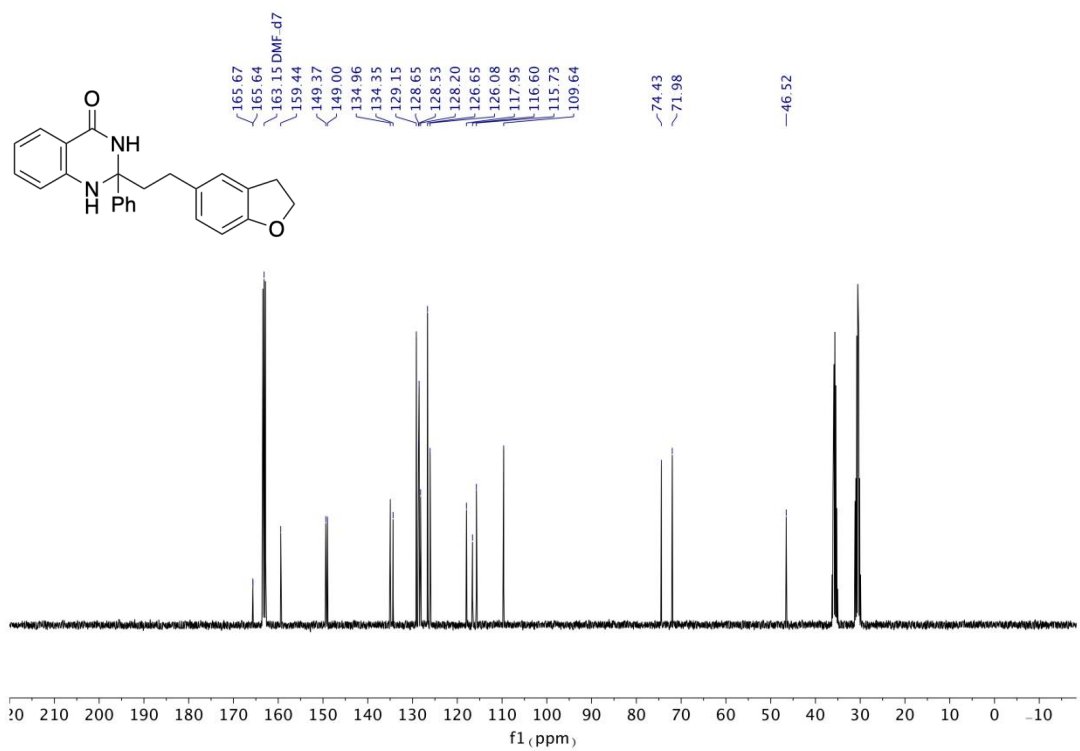
**<sup>1</sup>H NMR (400 MHz, CDCl<sub>3</sub>) of A29**



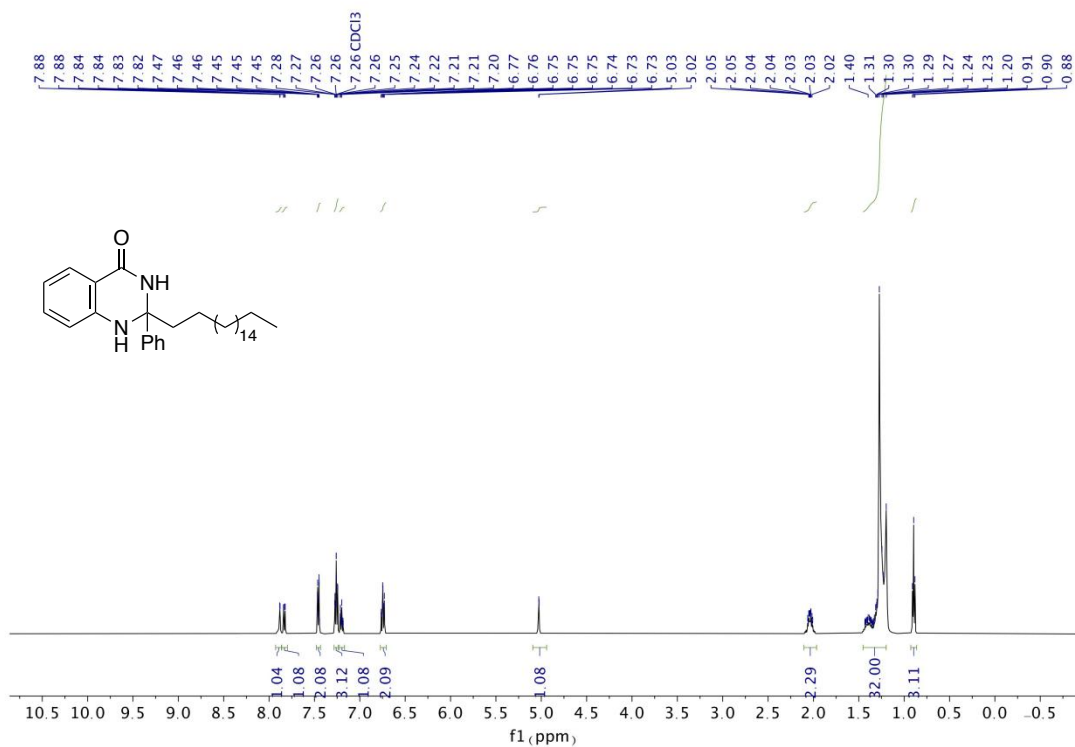
**<sup>13</sup>C NMR (101 MHz, CDCl<sub>3</sub>) of A29**



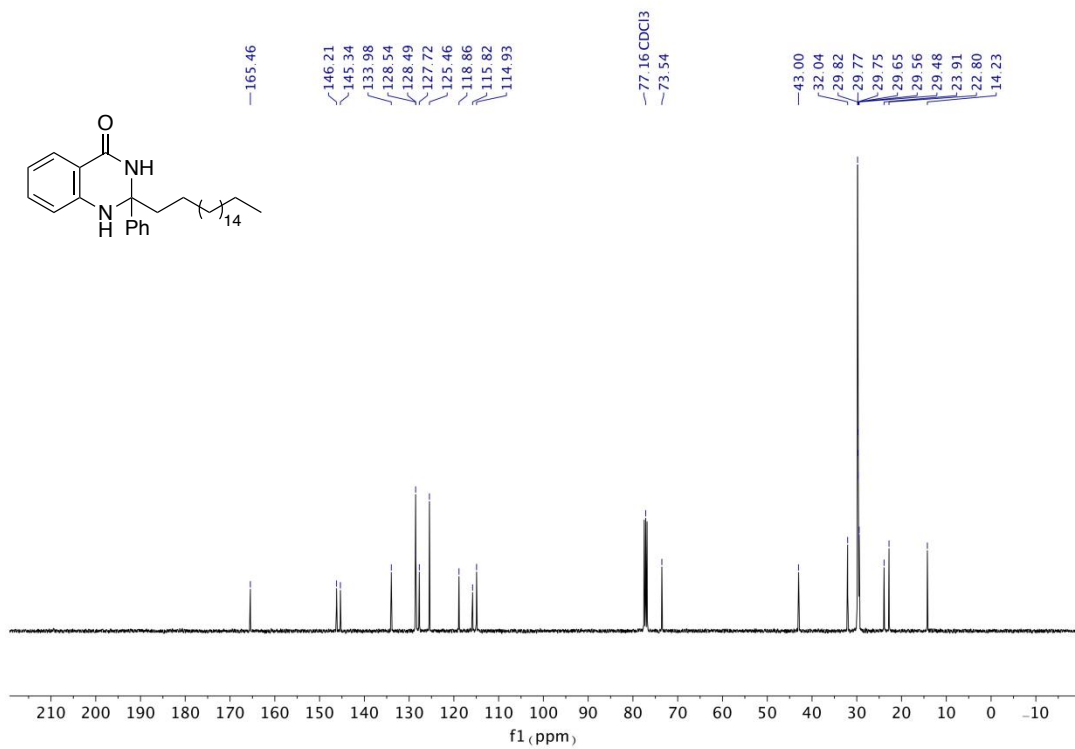
<sup>1</sup>H NMR (400 MHz, DMF-d<sub>7</sub>) of A30



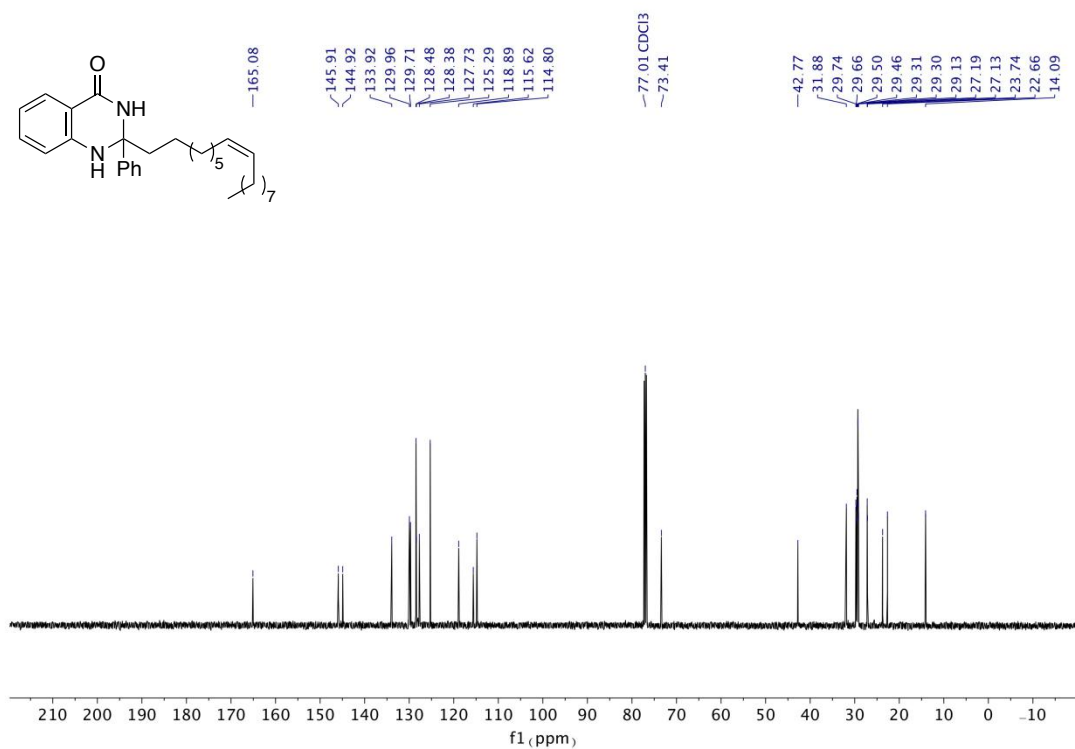
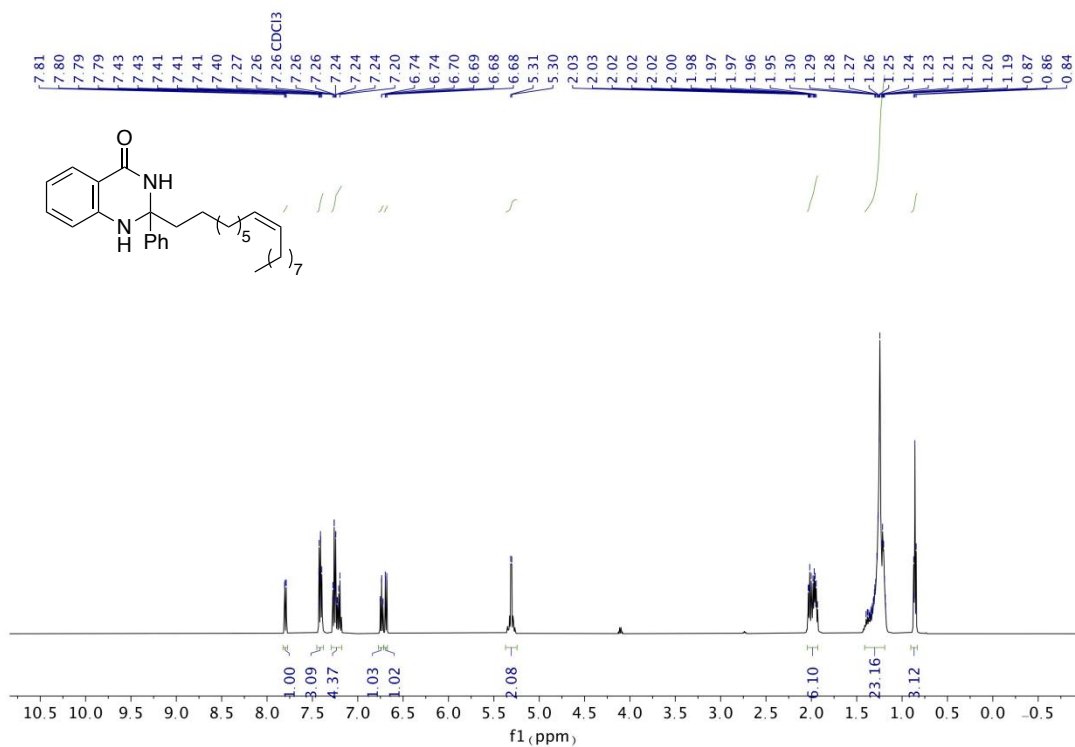
<sup>13</sup>C NMR (101 MHz, DMF-d<sub>7</sub>) of A30

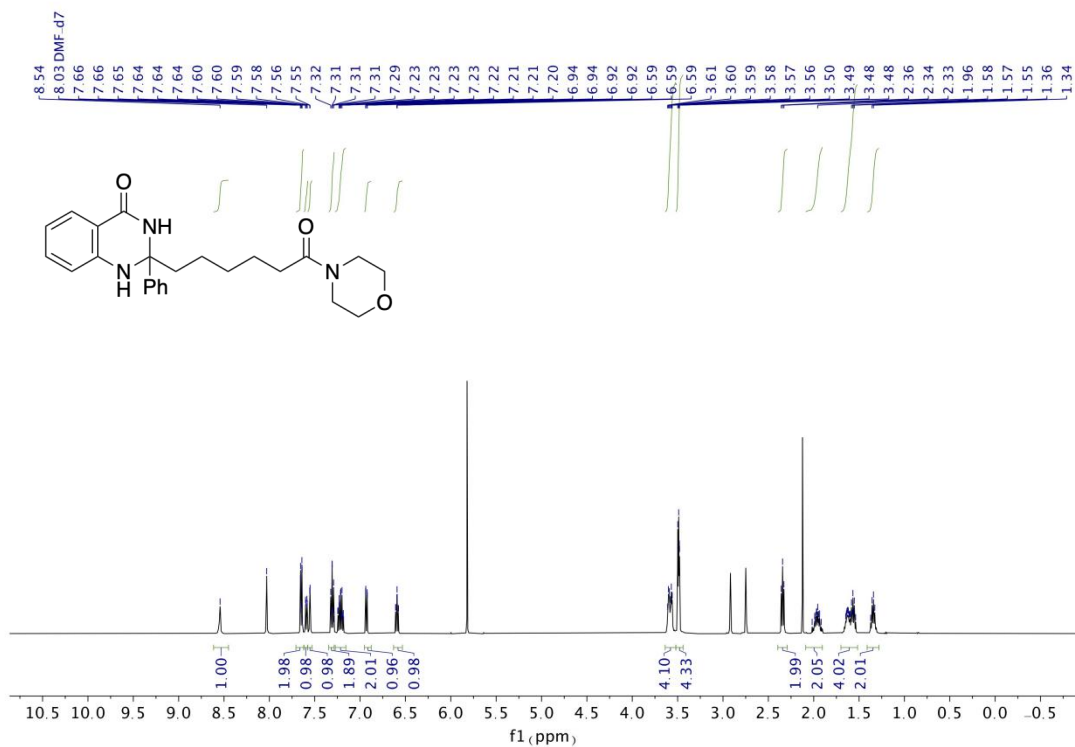


<sup>1</sup>H NMR (500 MHz, CDCl<sub>3</sub>) of A31

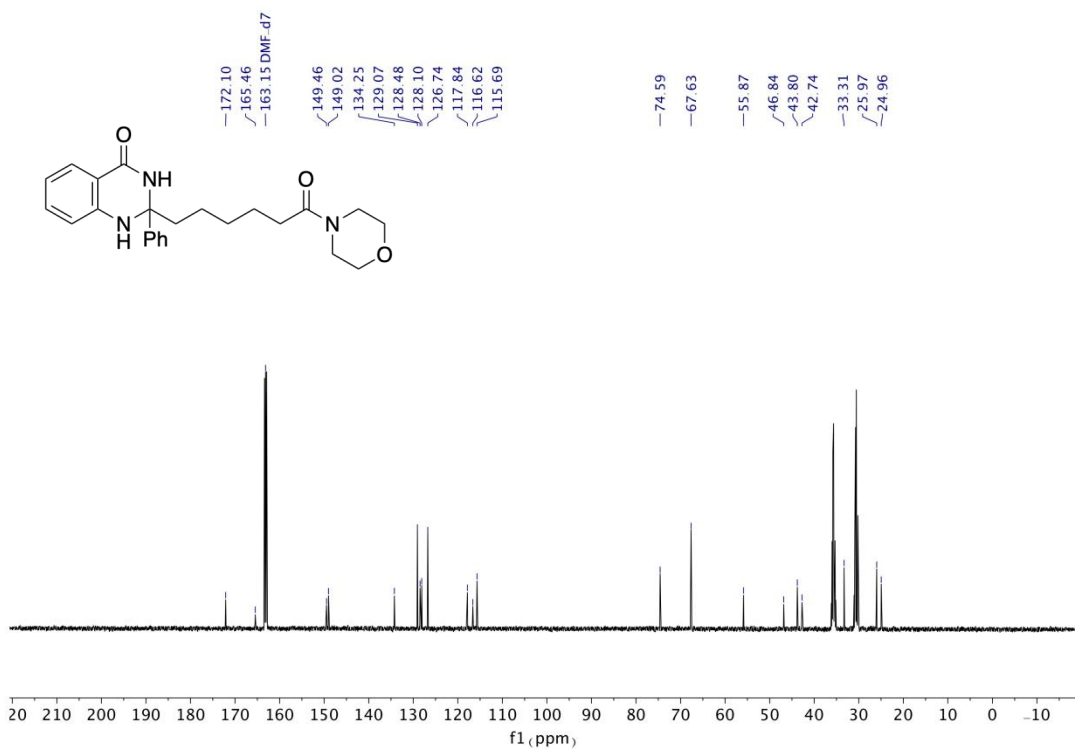


<sup>13</sup>C NMR (101 MHz, CDCl<sub>3</sub>) of A31

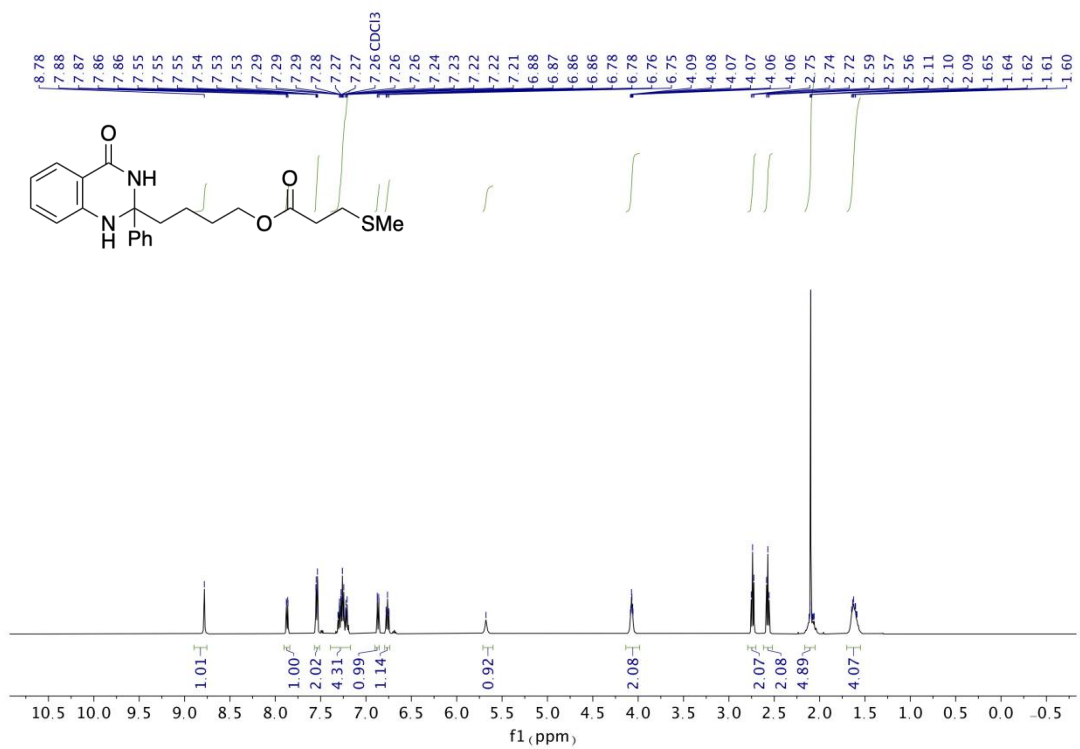




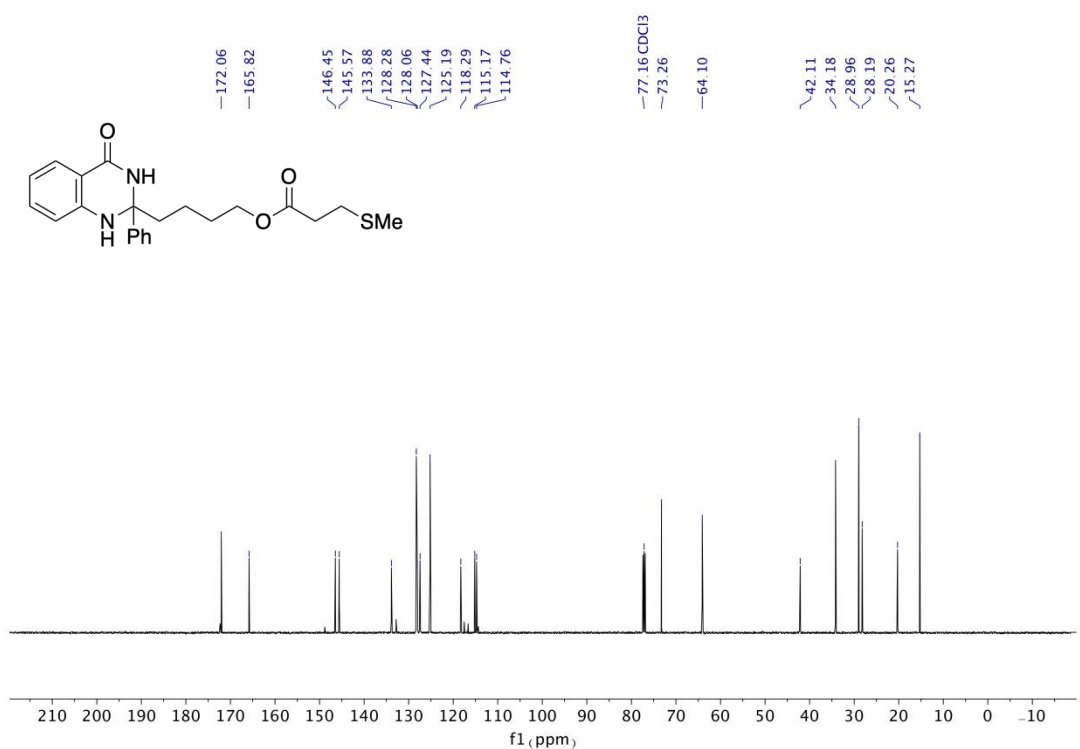
<sup>1</sup>H NMR (500 MHz, DMF-d<sub>7</sub>) of A33



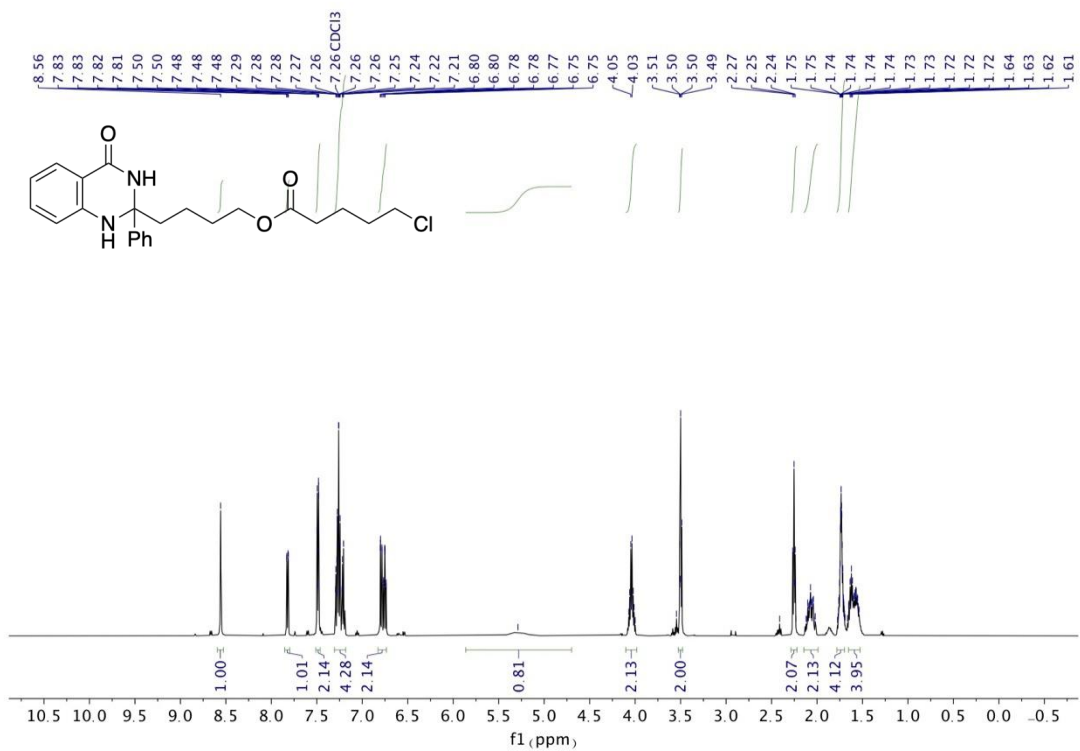
<sup>13</sup>C NMR (126 MHz, DMF-d<sub>7</sub>) of A33



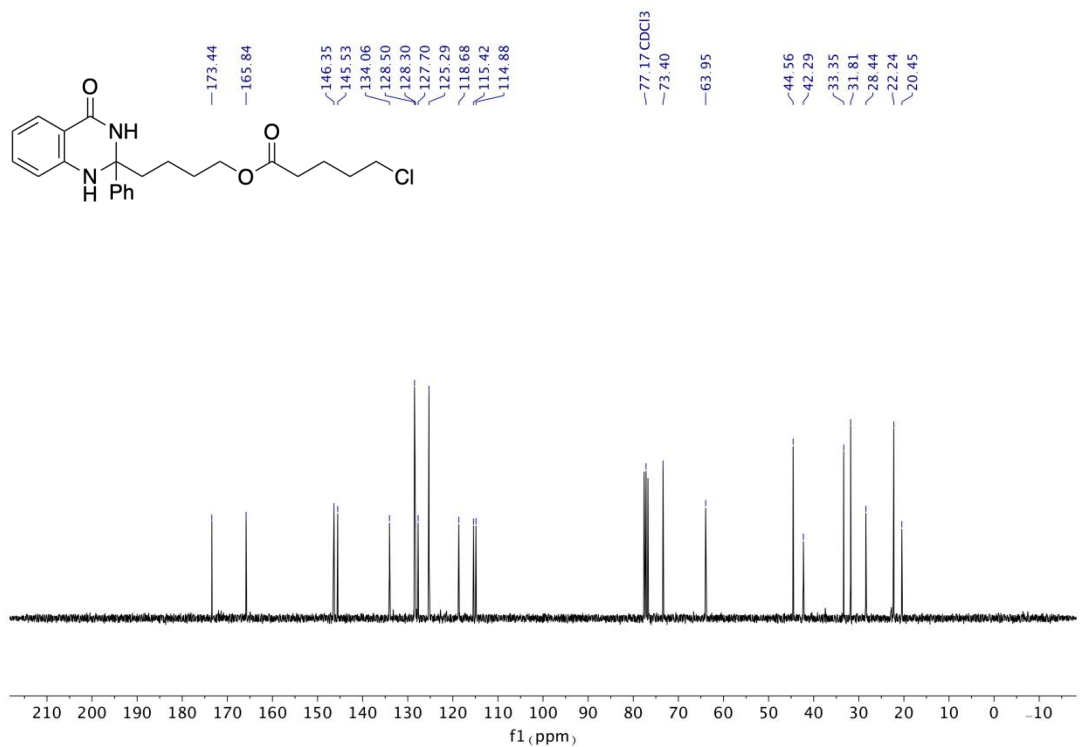
$^1\text{H NMR}$  (500 MHz,  $\text{CDCl}_3$ ) of **A34**



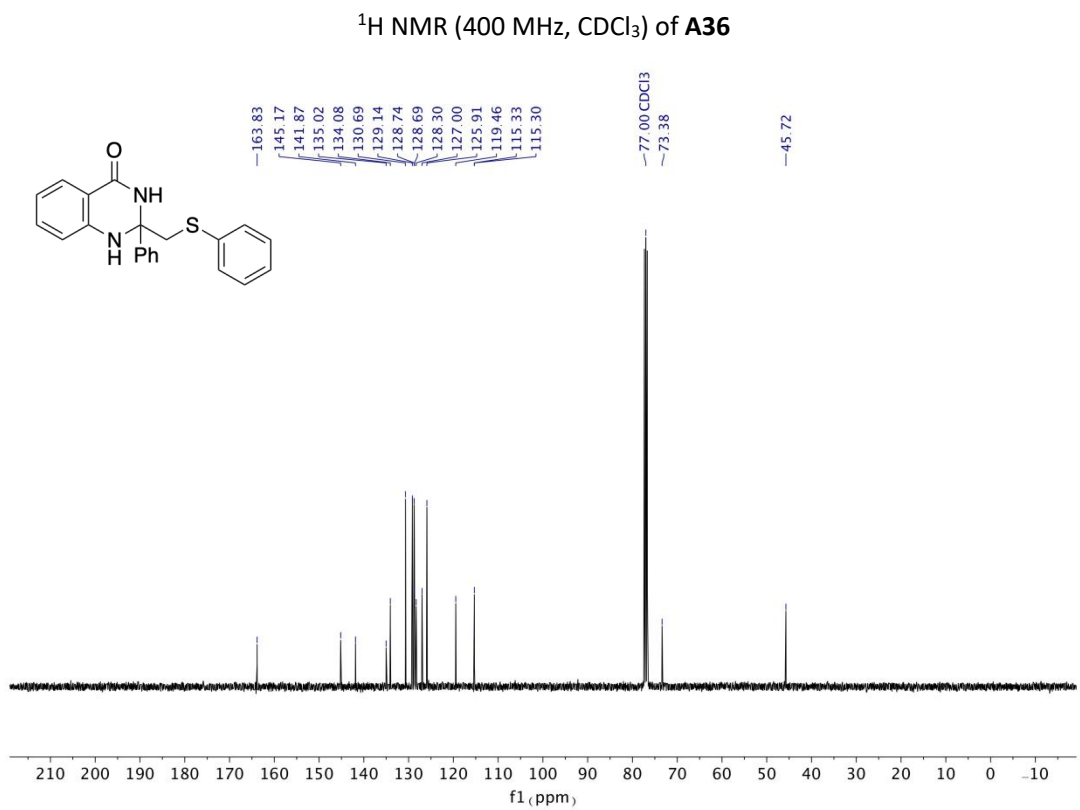
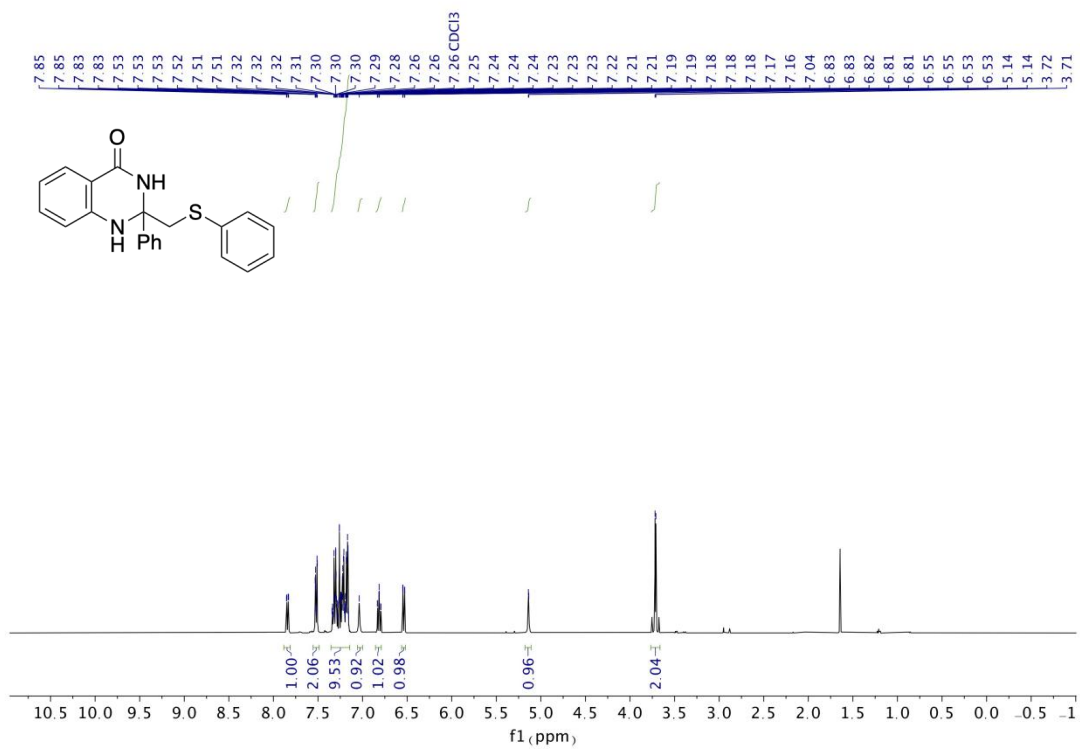
$^{13}\text{C NMR}$  (126 MHz,  $\text{CDCl}_3$ ) of **A34**



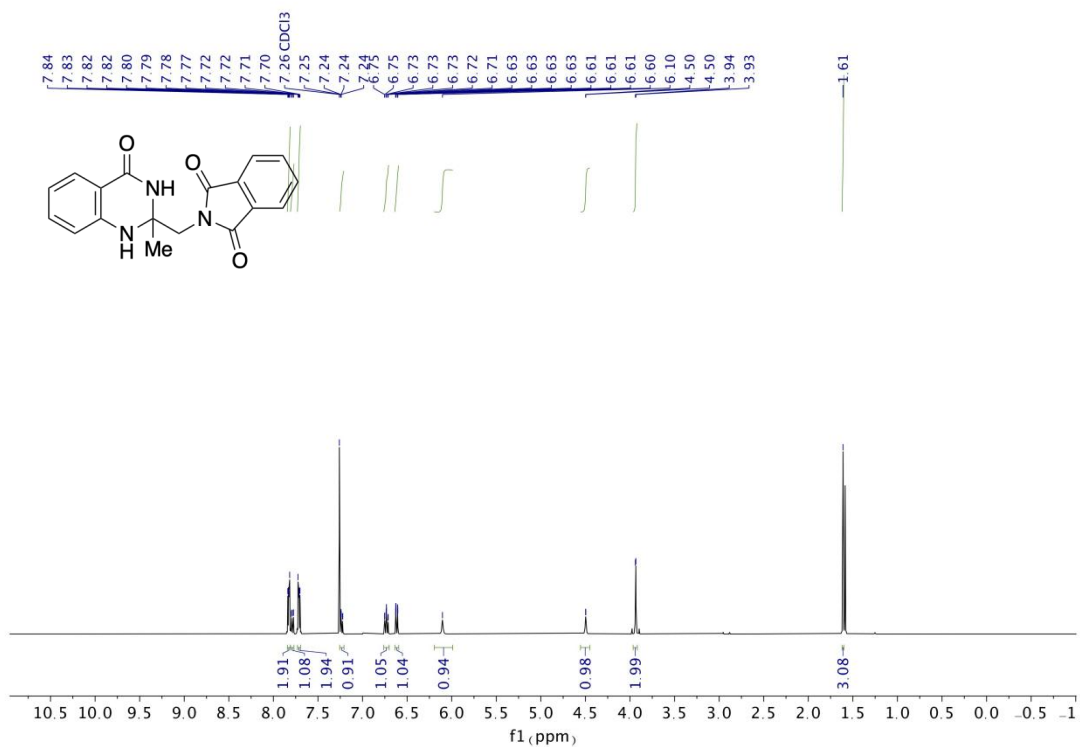
<sup>1</sup>H NMR (500 MHz, CDCl<sub>3</sub>) of A35



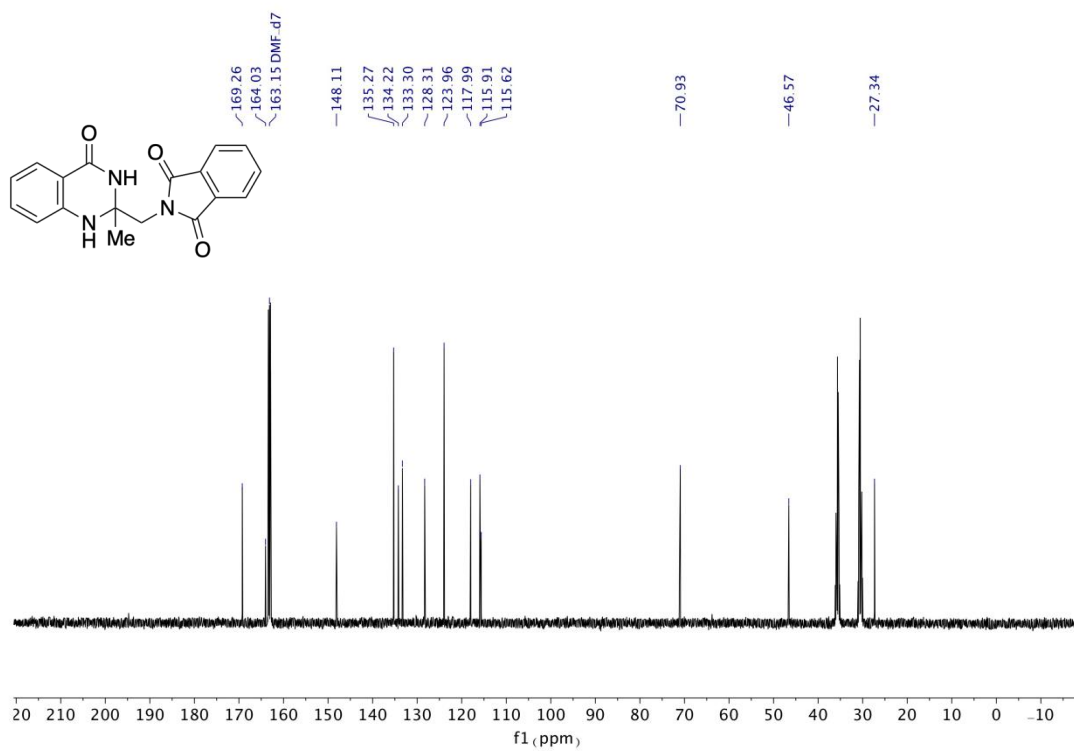
<sup>13</sup>C NMR (75 MHz, CDCl<sub>3</sub>) of A35



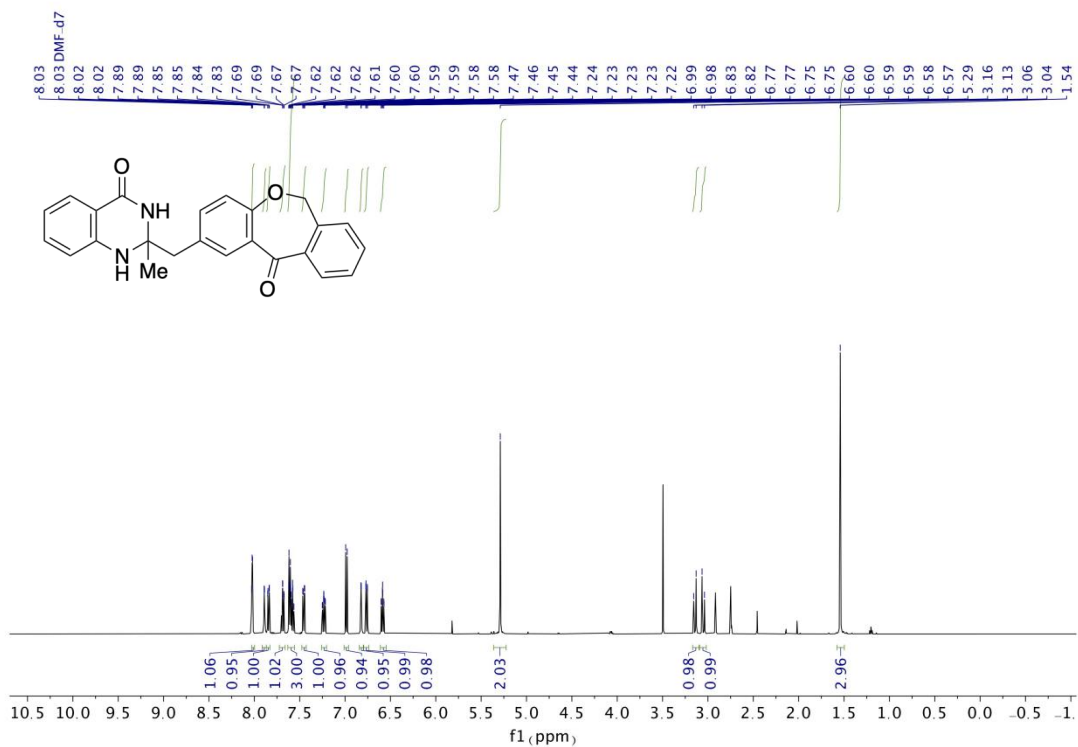




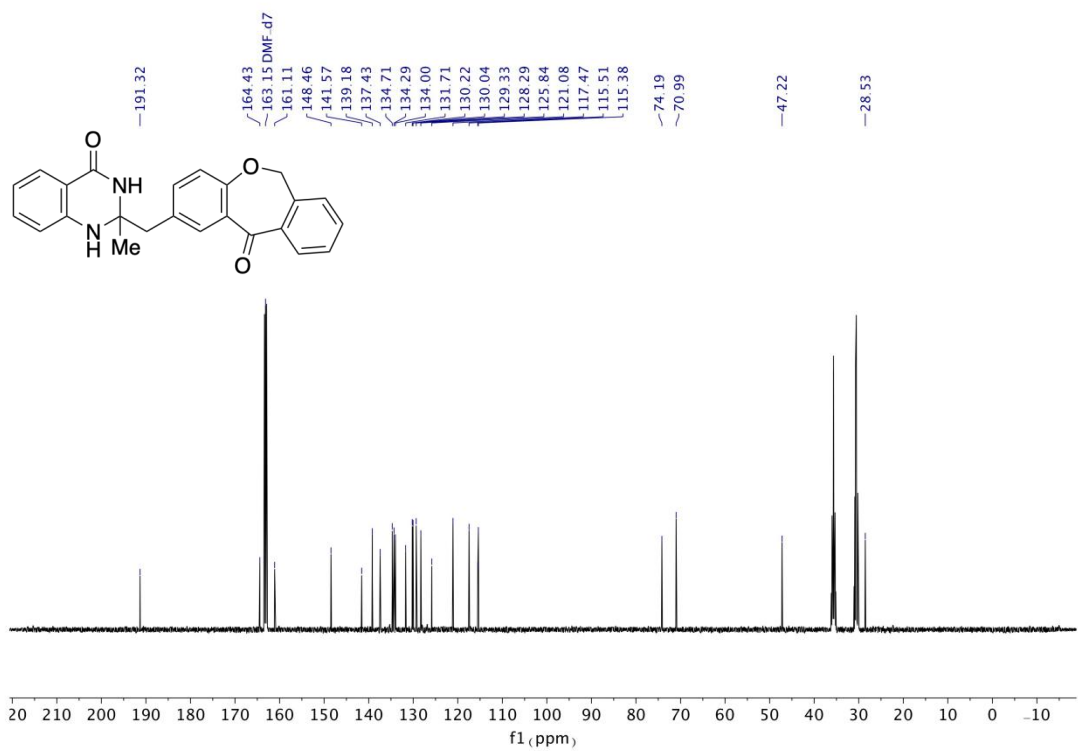
<sup>1</sup>H NMR (400 MHz, CDCl<sub>3</sub>) of A37



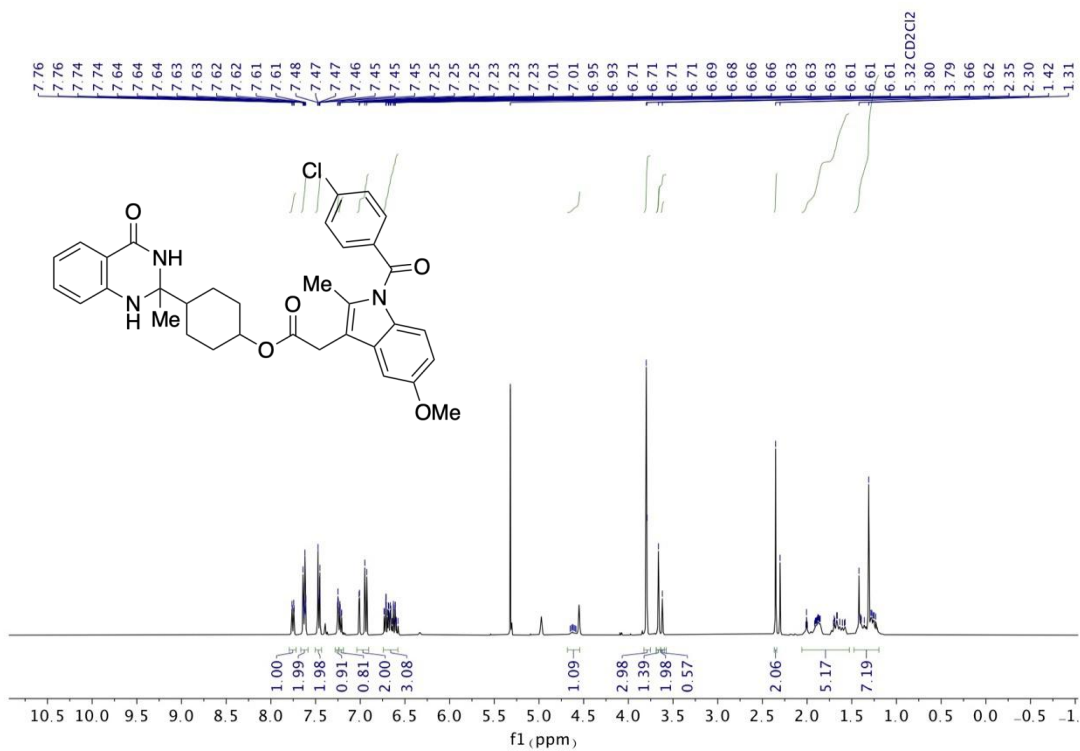
<sup>13</sup>C NMR (126 MHz, DMF-d<sub>7</sub>) of A37



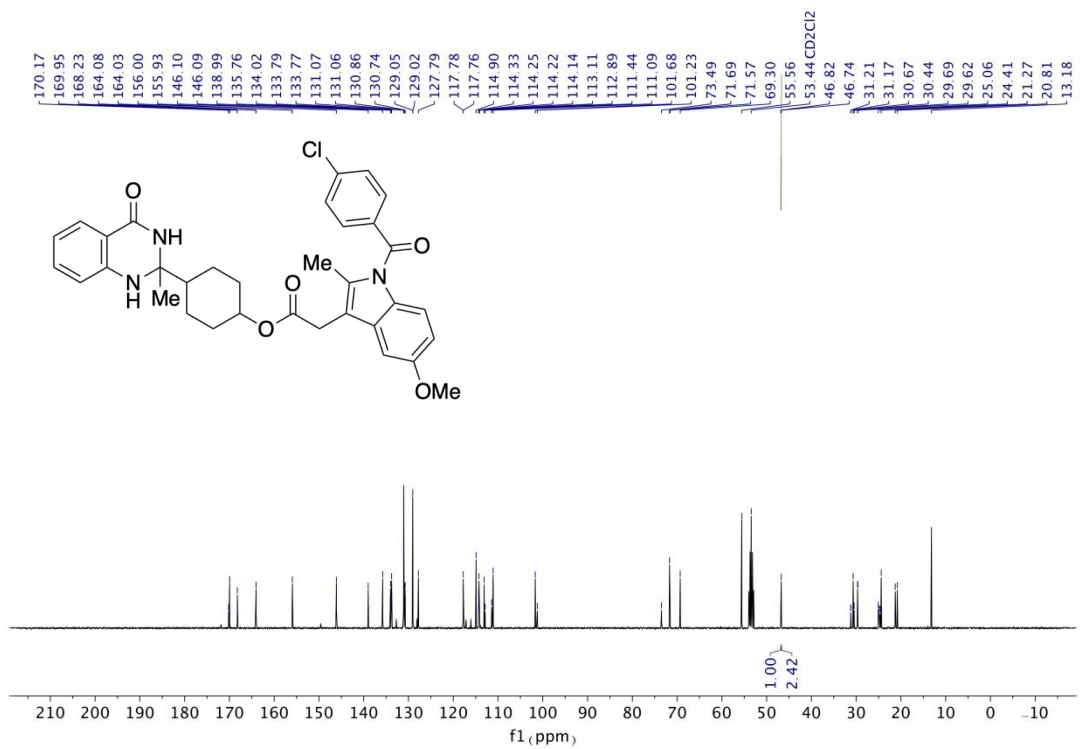
<sup>1</sup>H NMR (500 MHz, DMF-d<sub>7</sub>) of A38



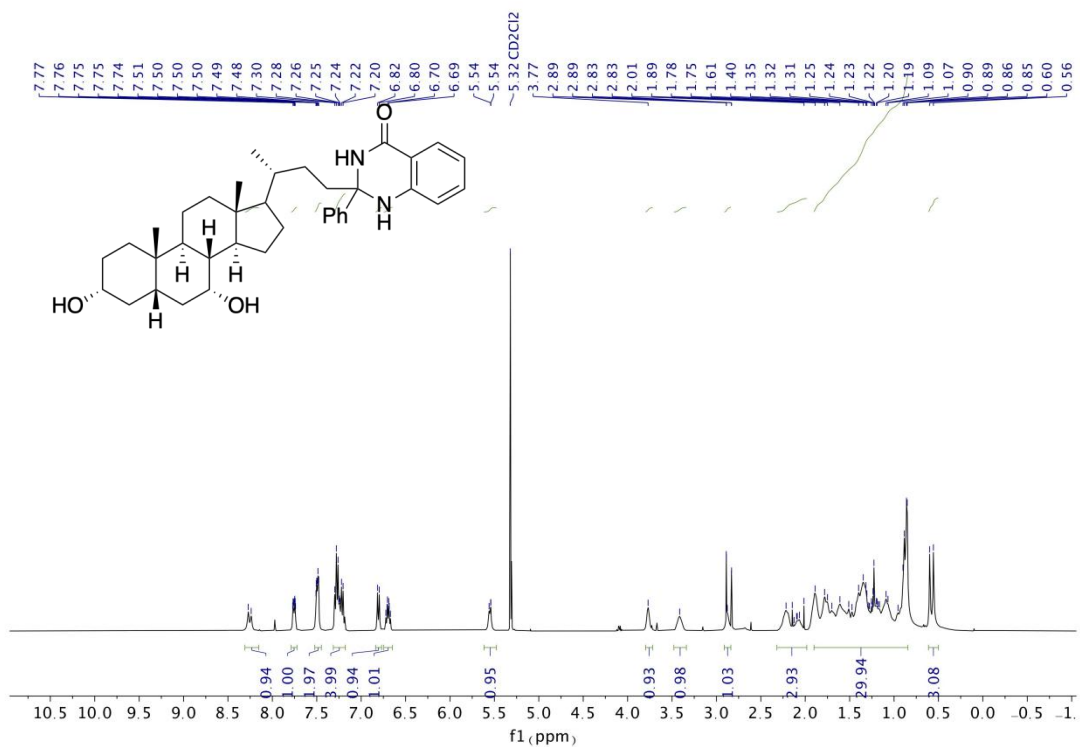
<sup>13</sup>C NMR (126 MHz, DMF-d<sub>7</sub>) of A38



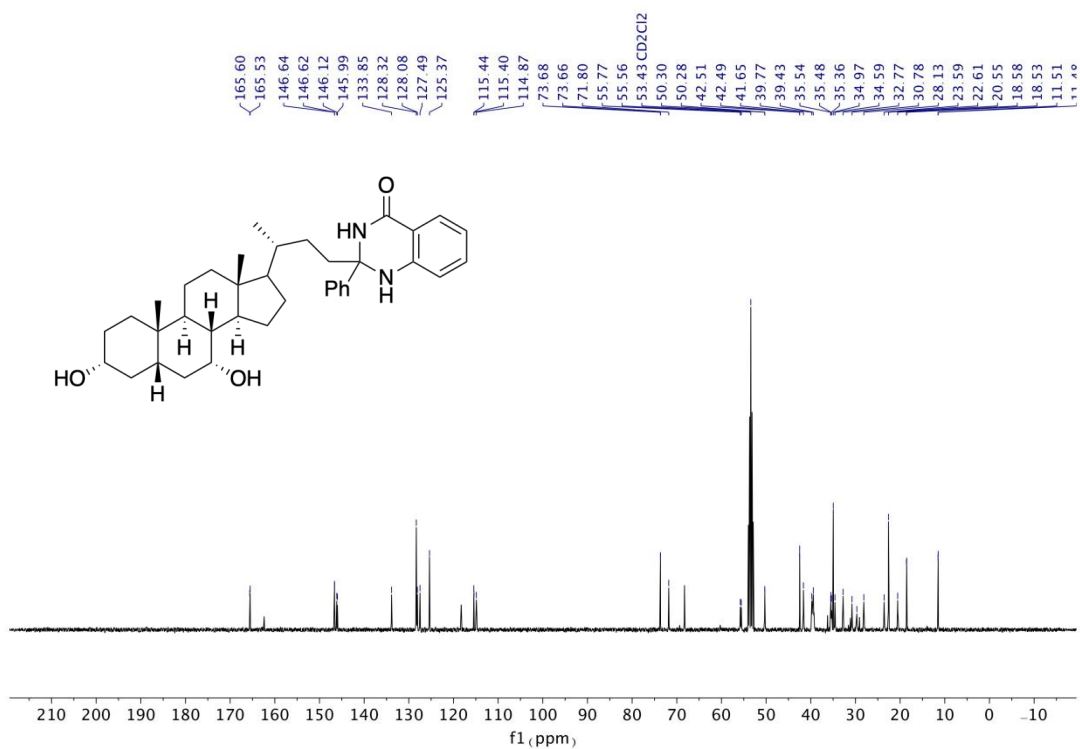
<sup>1</sup>H NMR (400 MHz, CD<sub>2</sub>Cl<sub>2</sub>) of A39



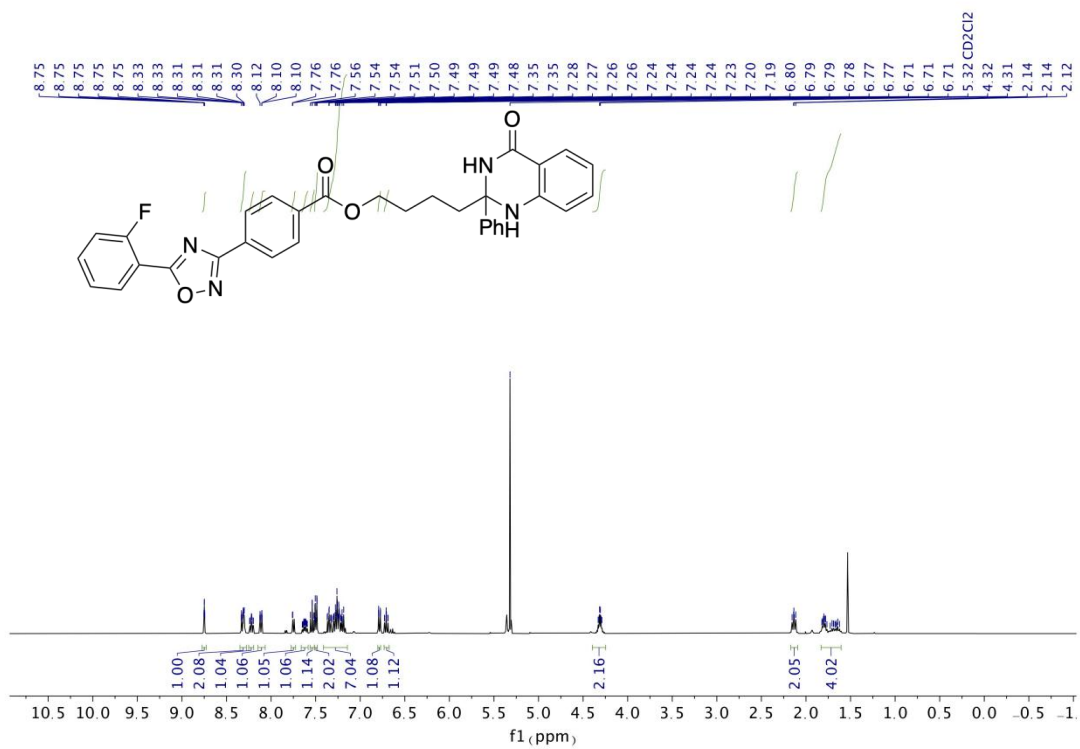
<sup>13</sup>C NMR (101 MHz, CD<sub>2</sub>Cl<sub>2</sub>) of A39



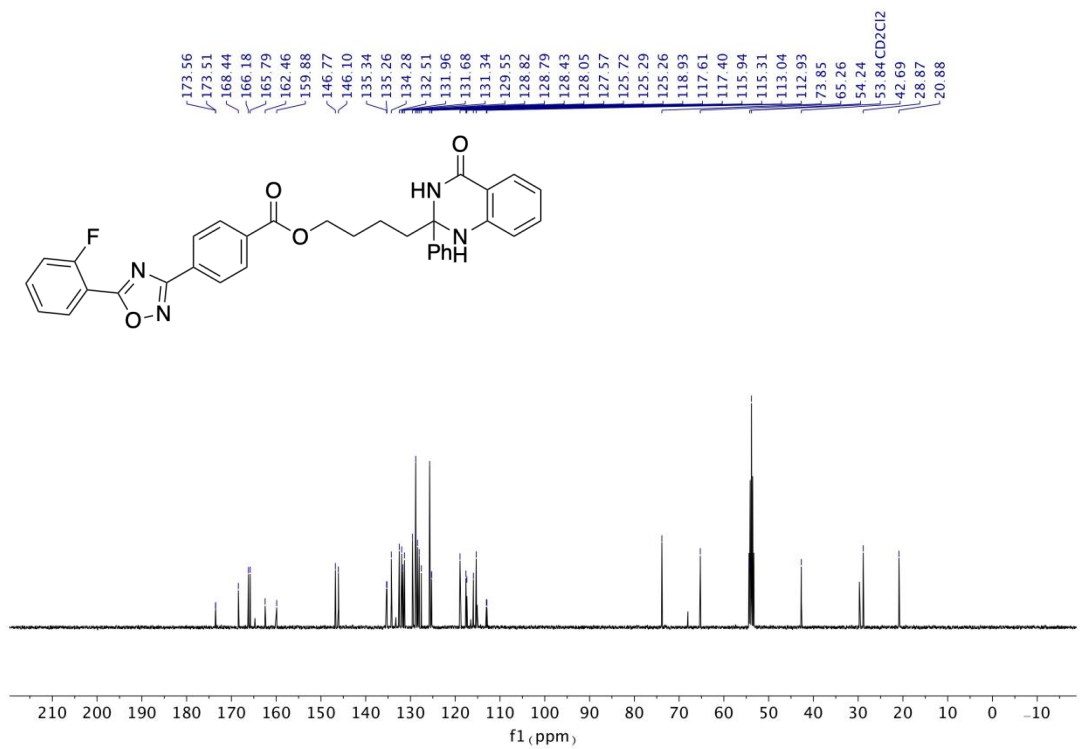
**<sup>1</sup>H NMR (400 MHz, CD<sub>2</sub>Cl<sub>2</sub>) of A40**



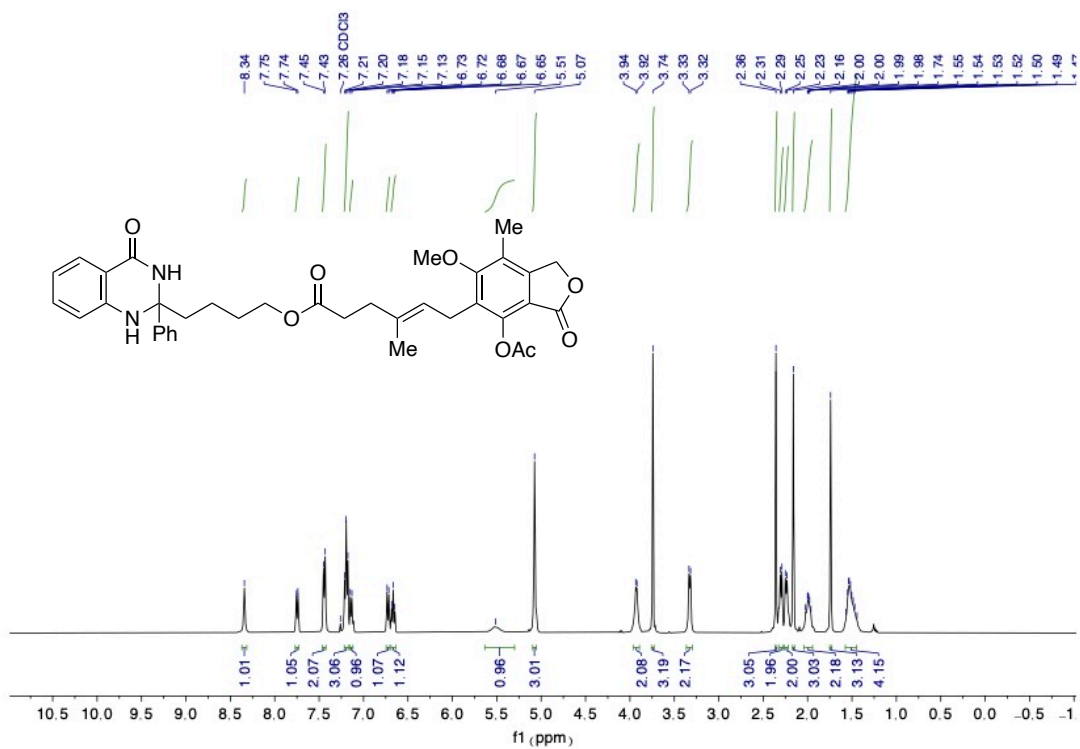
**<sup>13</sup>C NMR (101 MHz, CD<sub>2</sub>Cl<sub>2</sub>) of A40**



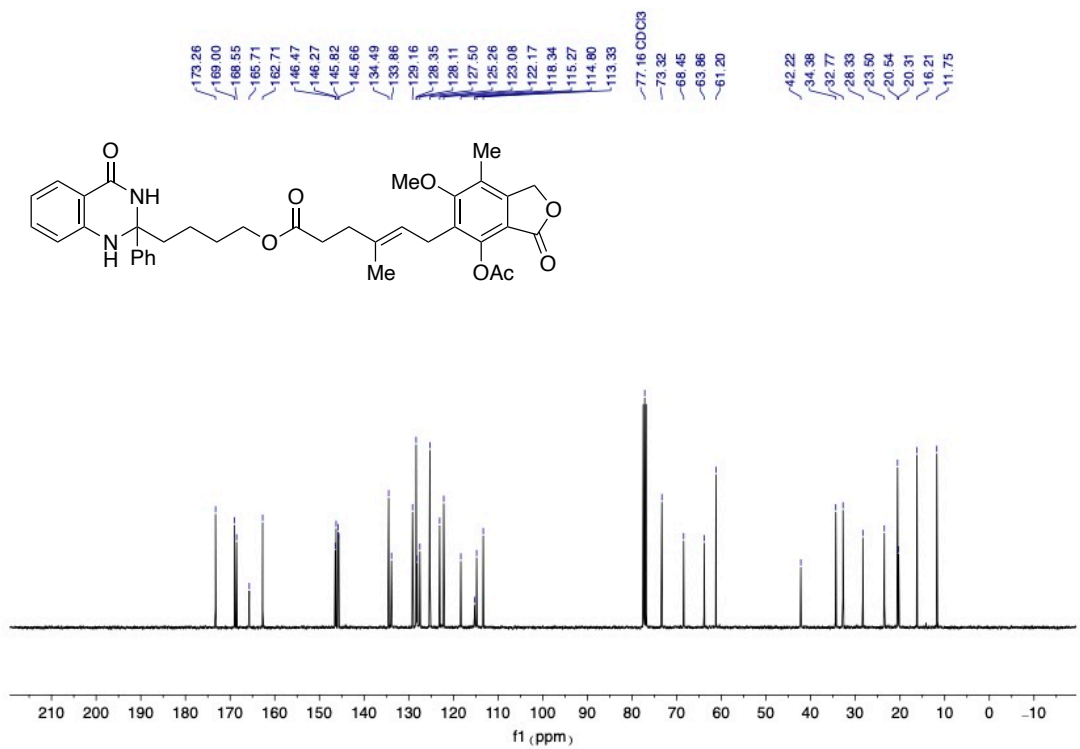
<sup>1</sup>H NMR (400 MHz, CD<sub>2</sub>Cl<sub>2</sub>) of A41



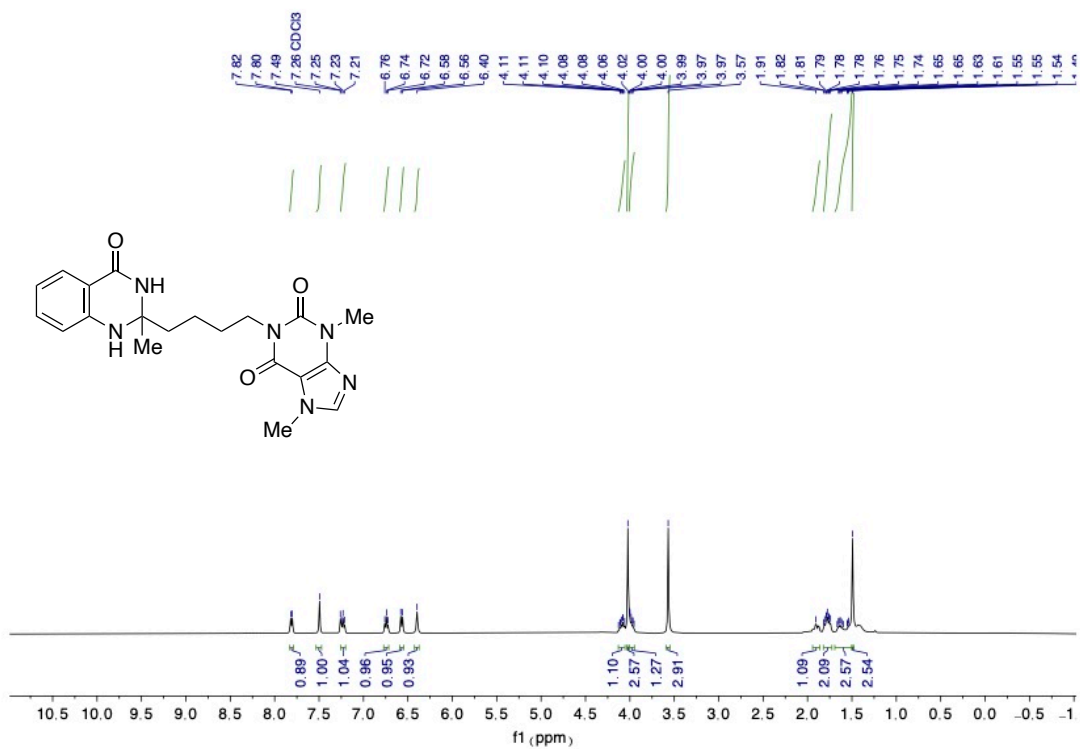
<sup>13</sup>C NMR (101 MHz, CD<sub>2</sub>Cl<sub>2</sub>) of A41



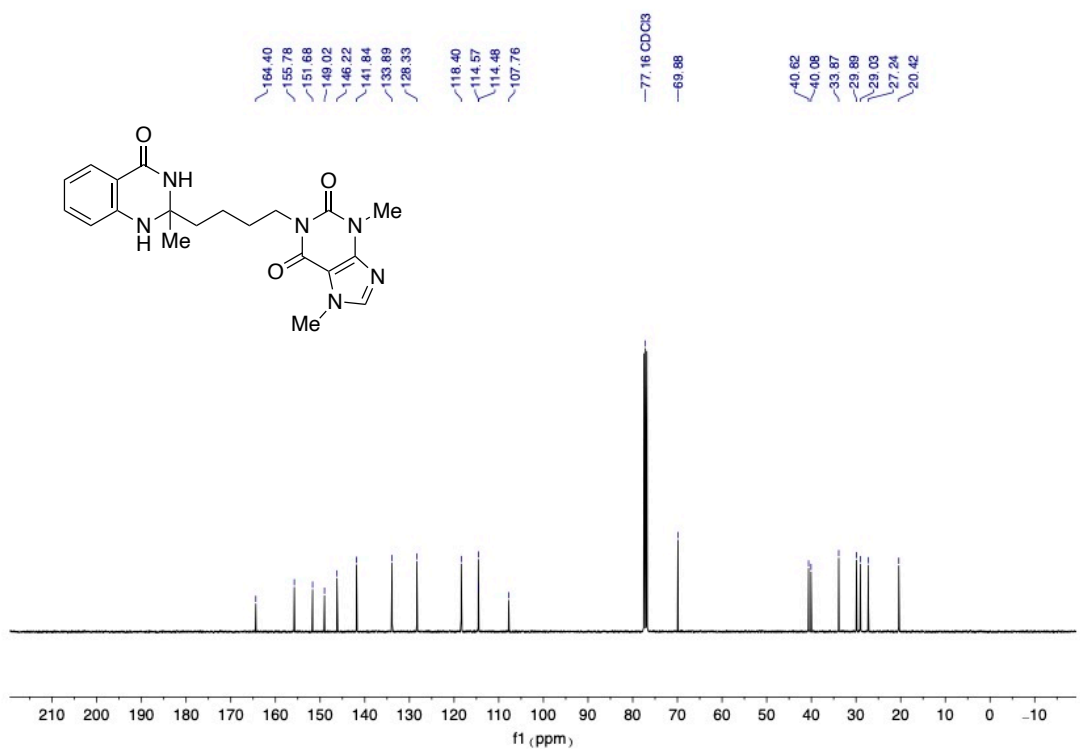
**<sup>1</sup>H NMR (400 MHz, CDCl<sub>3</sub>) of A42**



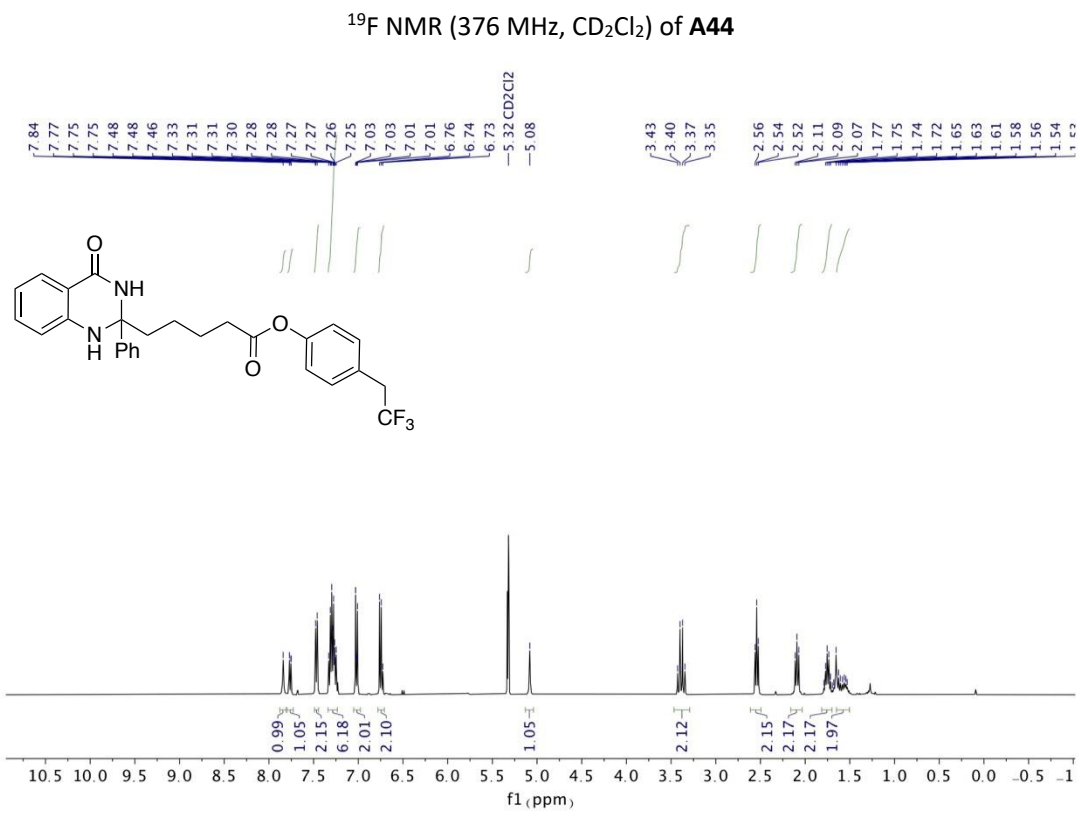
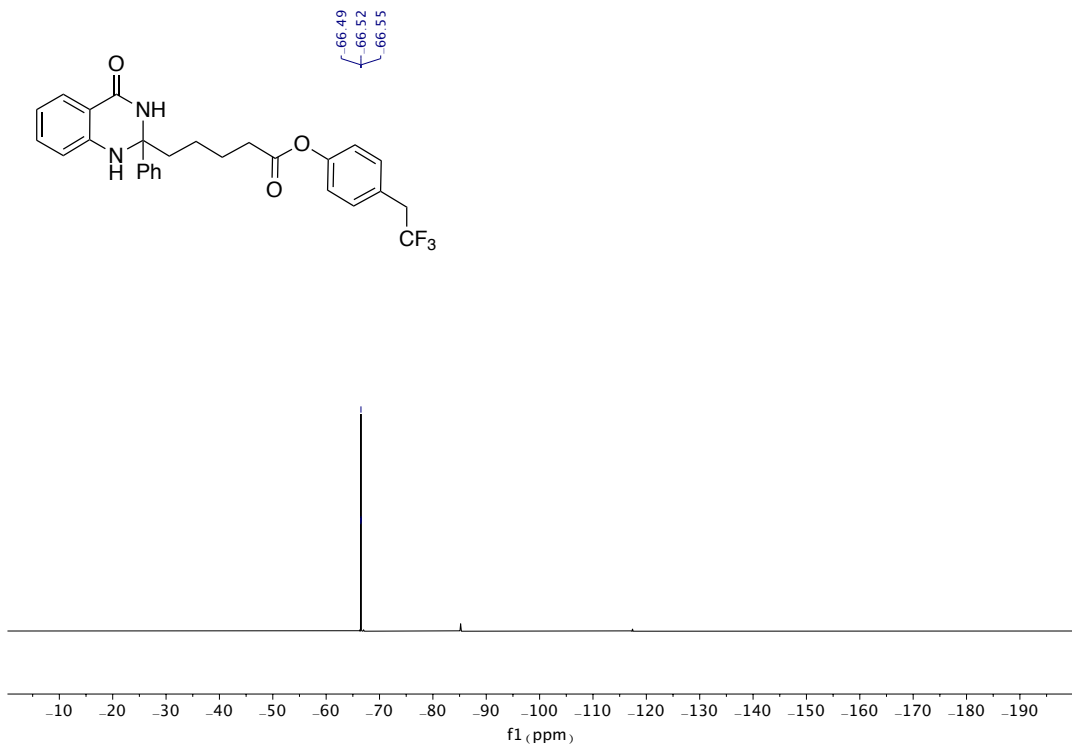
**<sup>13</sup>C NMR (101 MHz, CDCl<sub>3</sub>) of A42**



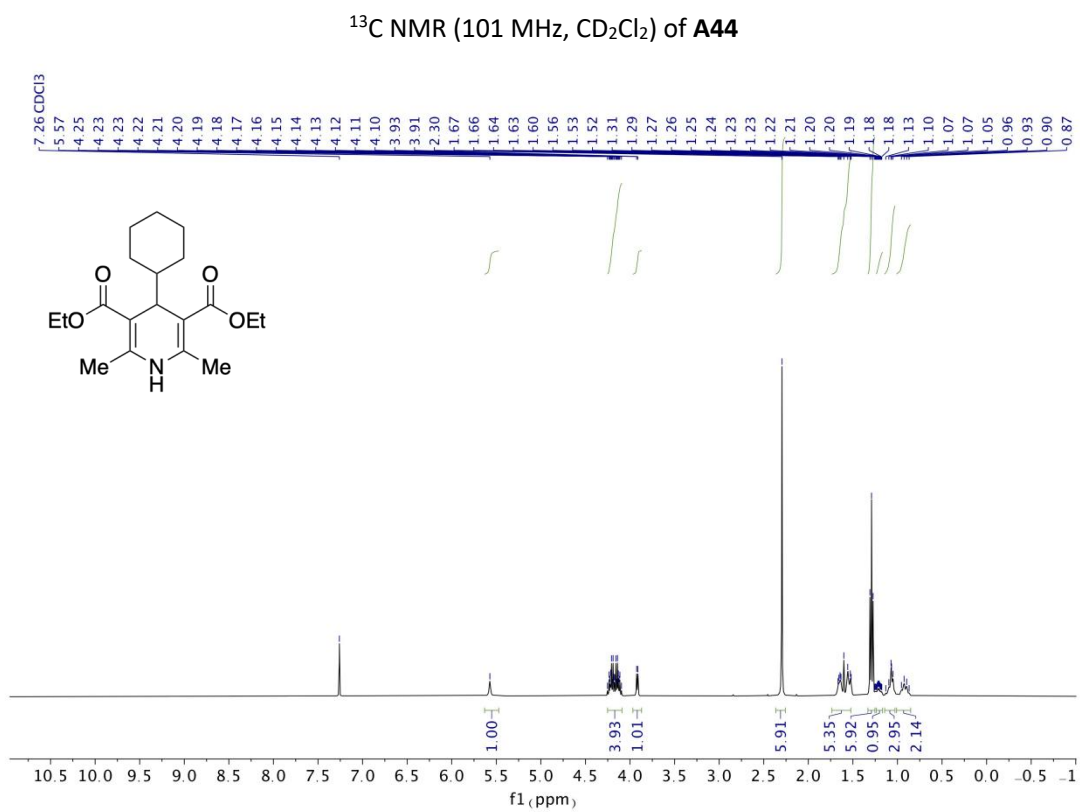
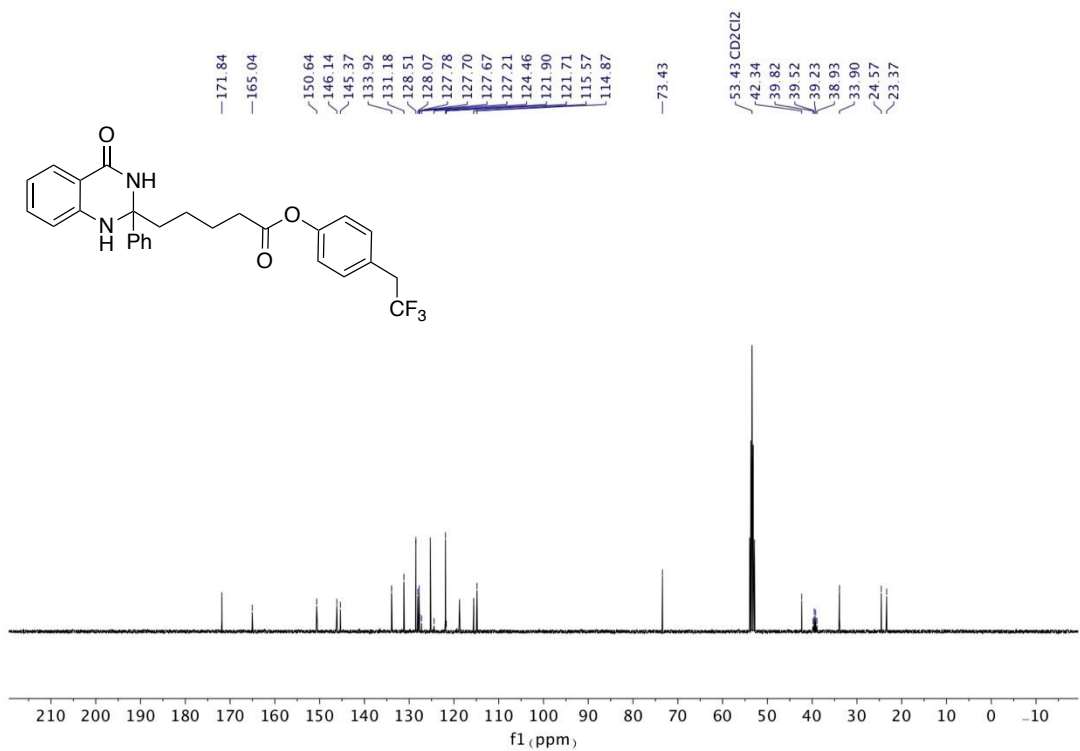
<sup>1</sup>H NMR (400 MHz, CDCl<sub>3</sub>) of A43

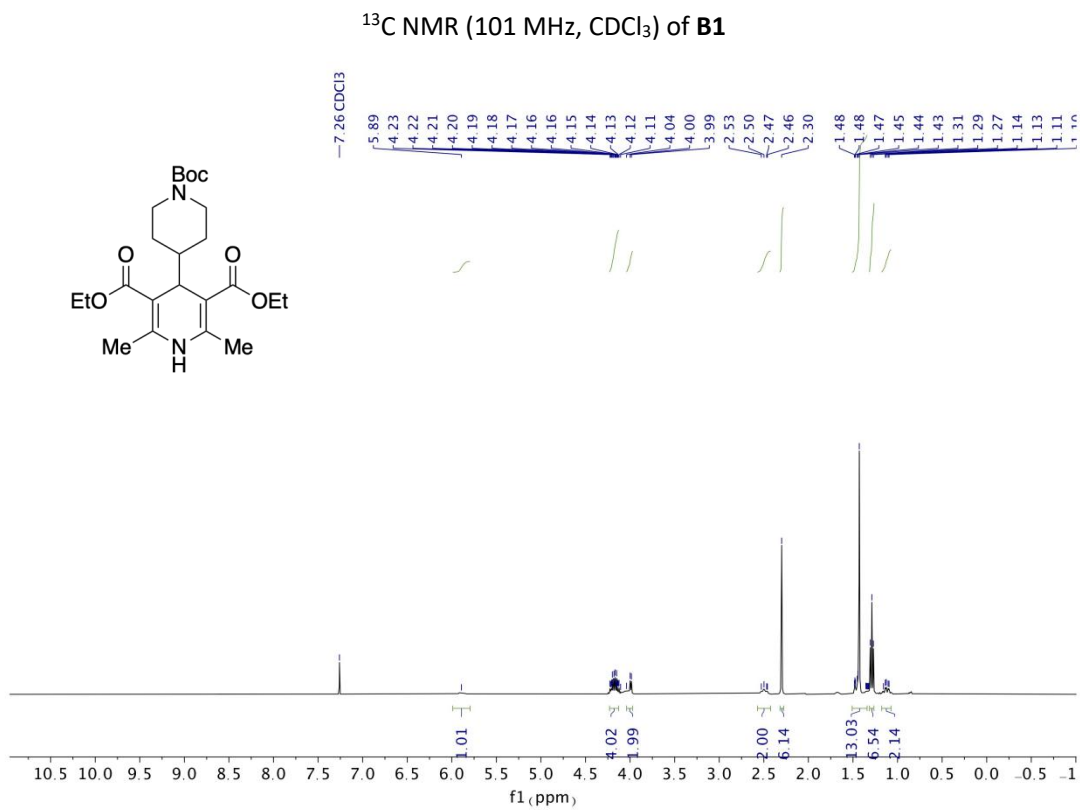
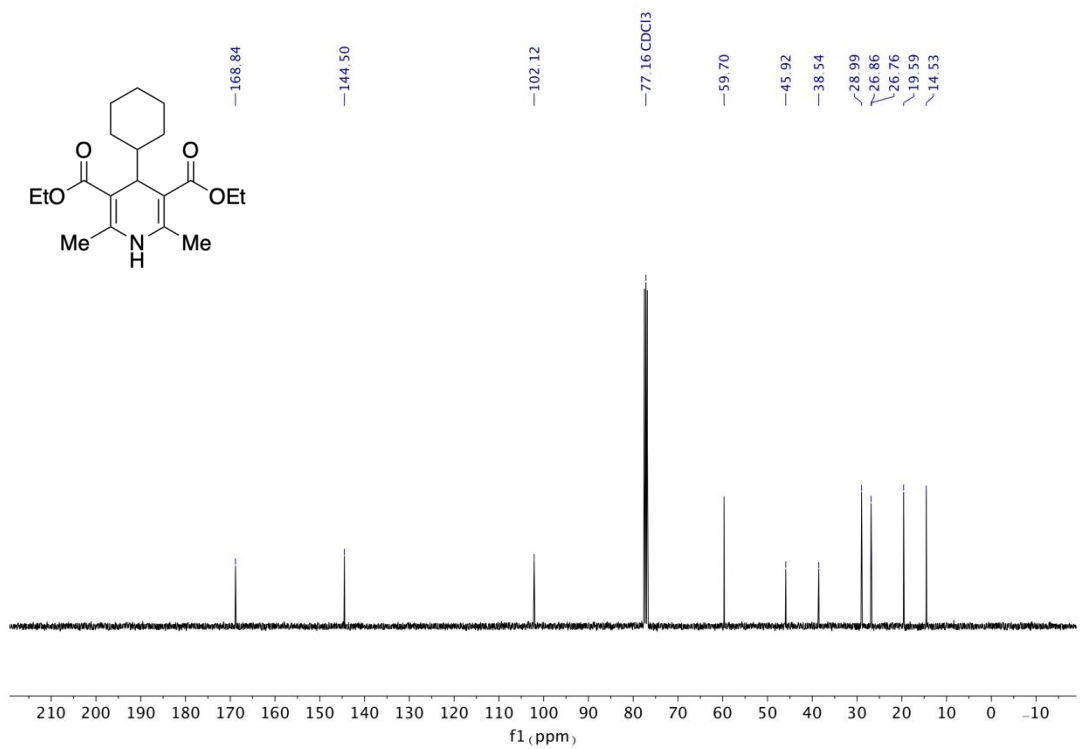


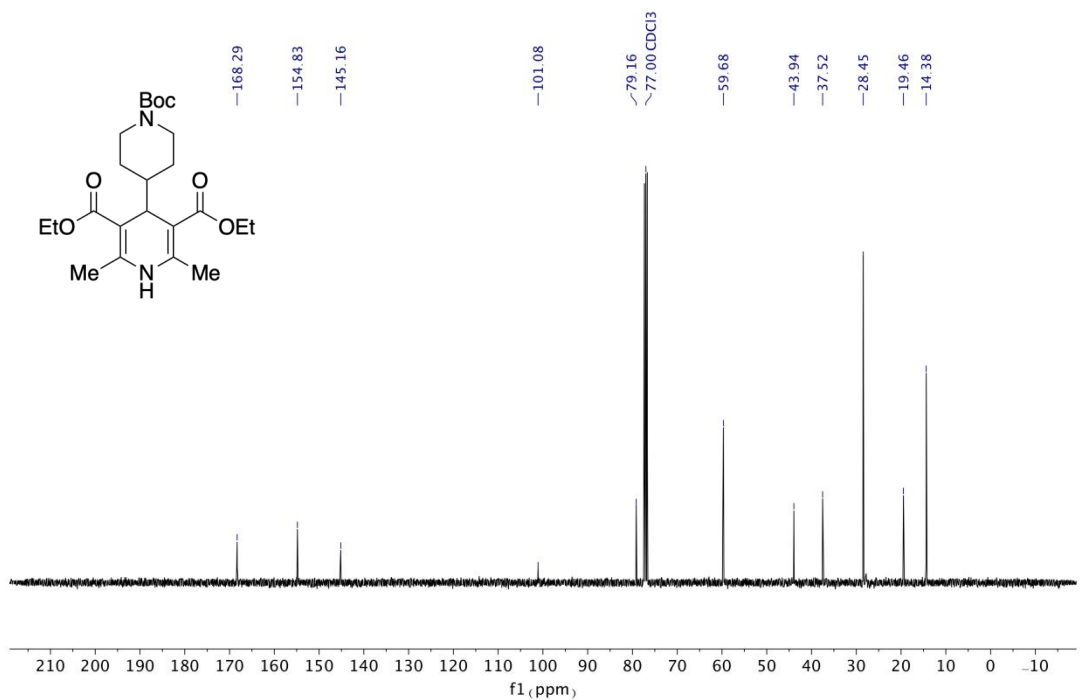
<sup>13</sup>C NMR (101 MHz, CDCl<sub>3</sub>) of A43



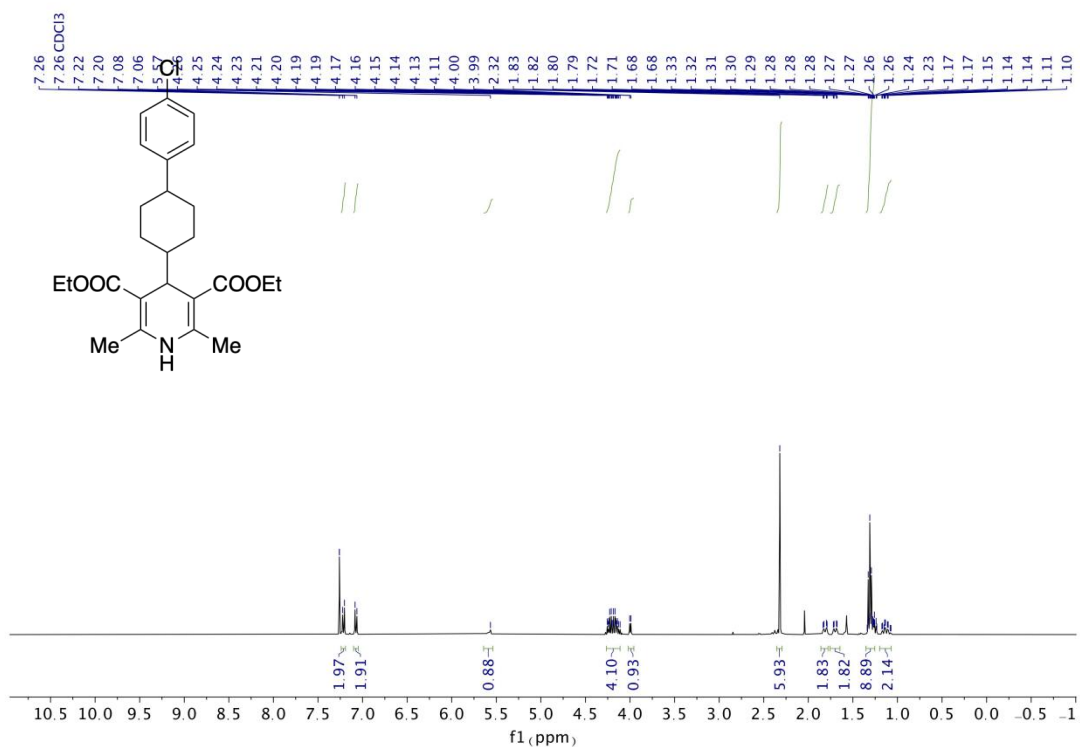




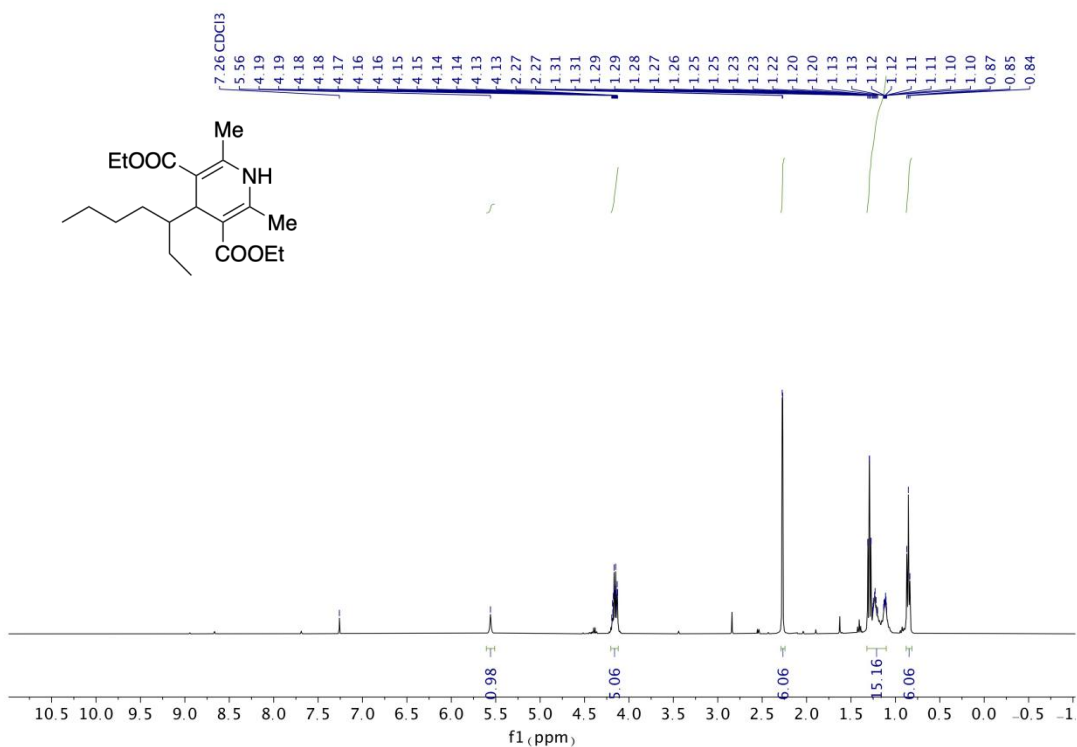
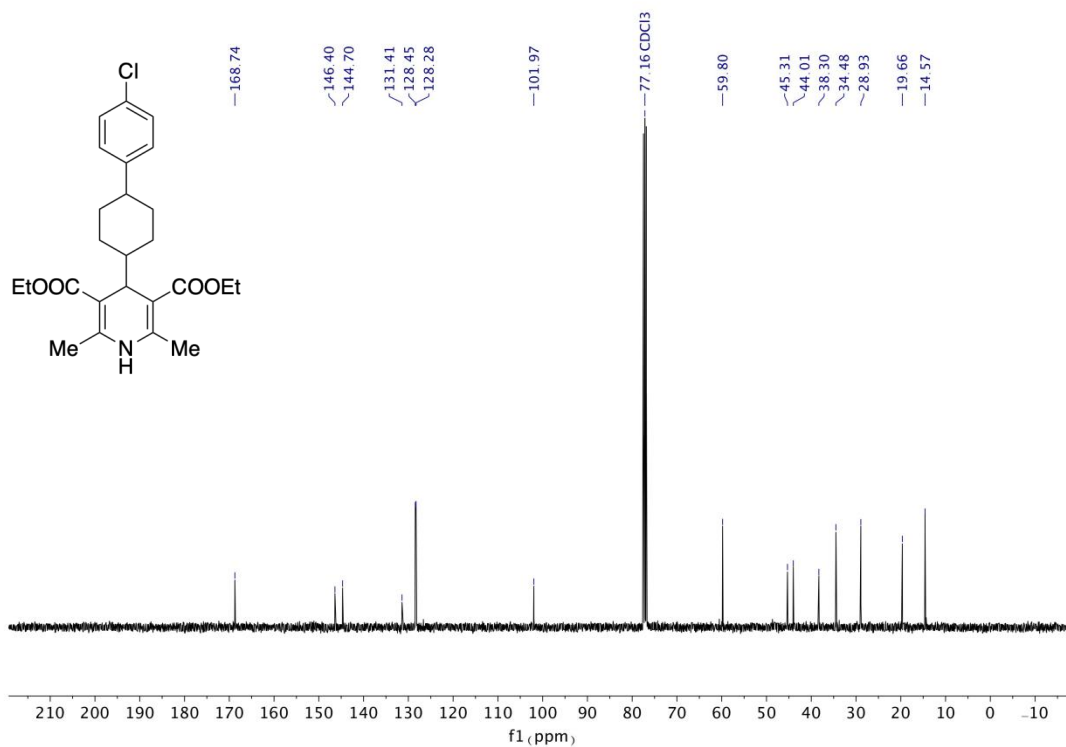


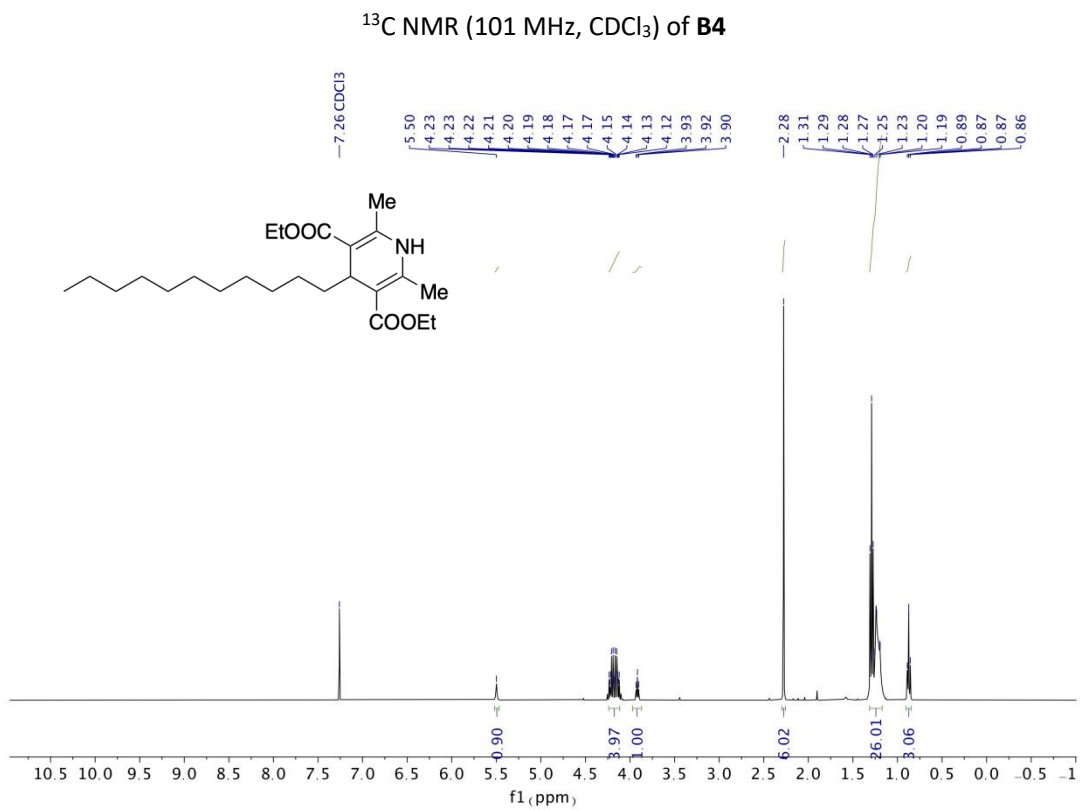
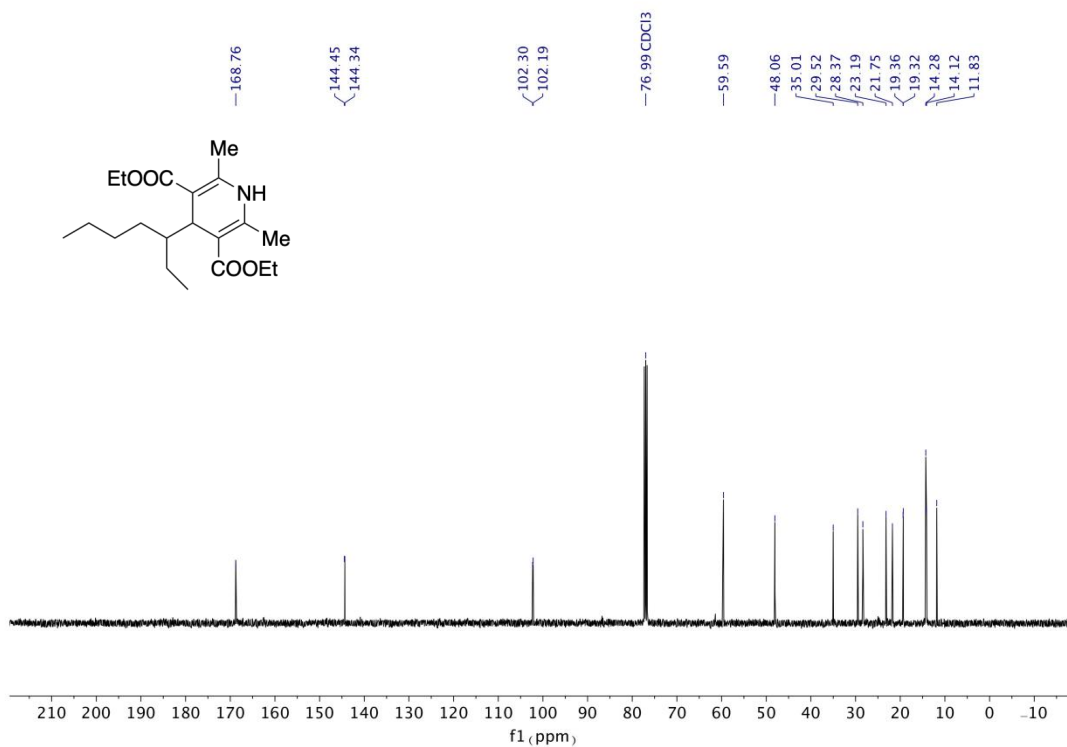


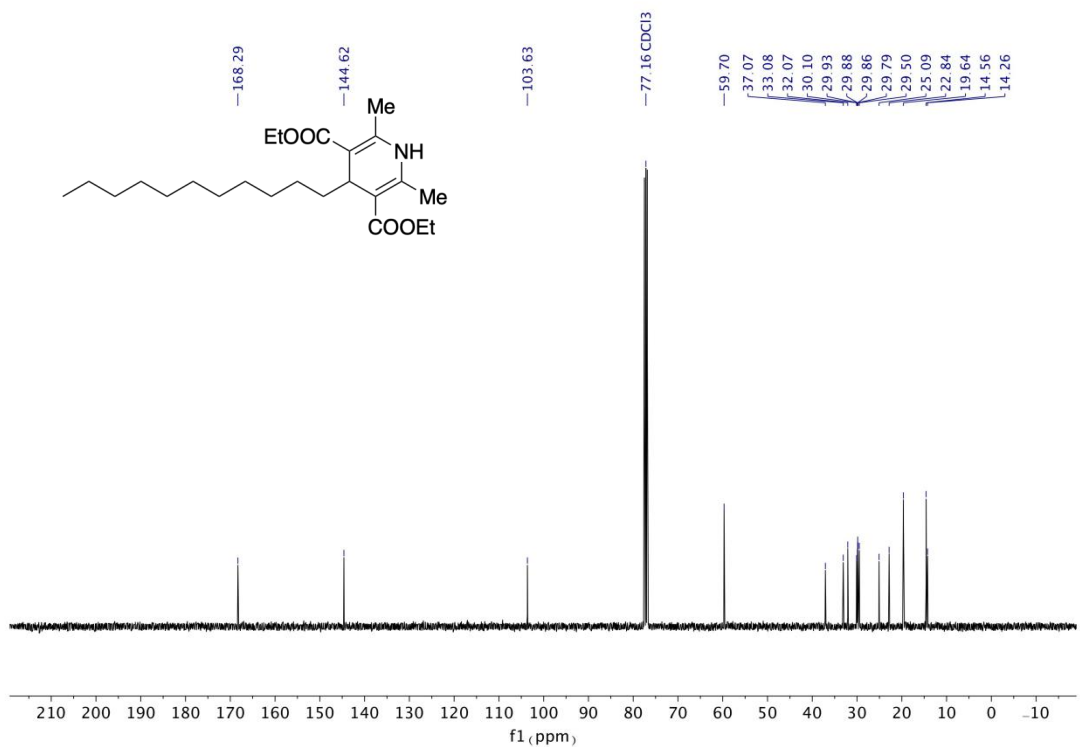
<sup>13</sup>C NMR (101 MHz, CDCl<sub>3</sub>) of B2



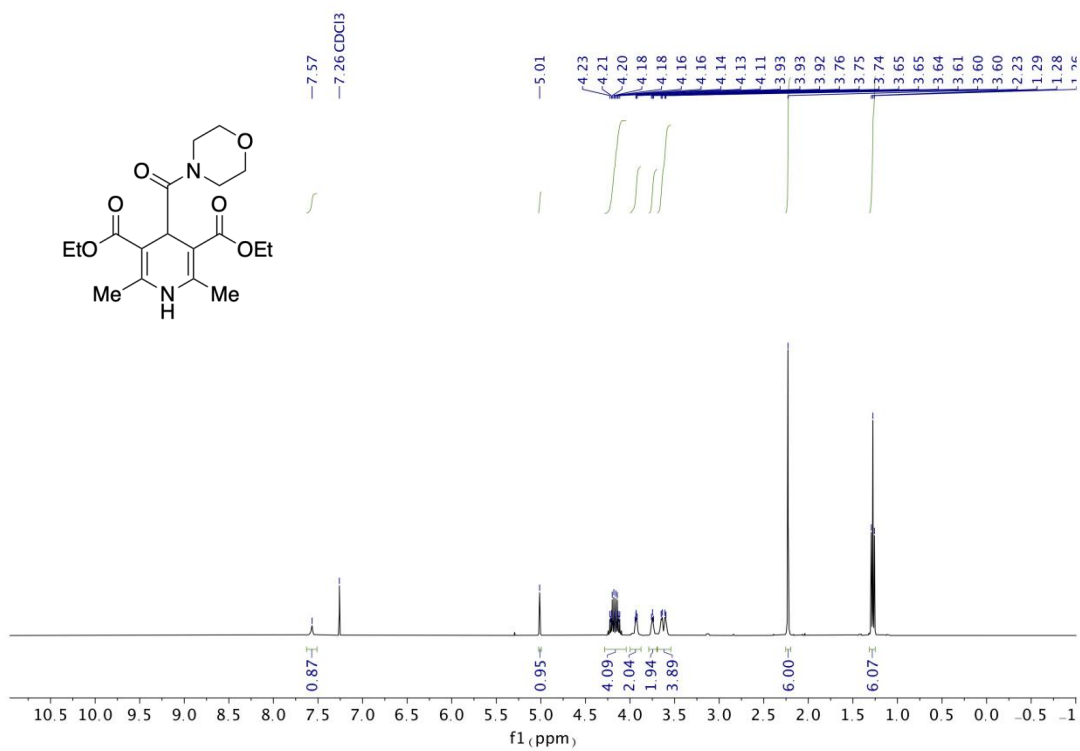
<sup>1</sup>H NMR (400 MHz, CDCl<sub>3</sub>) of B3



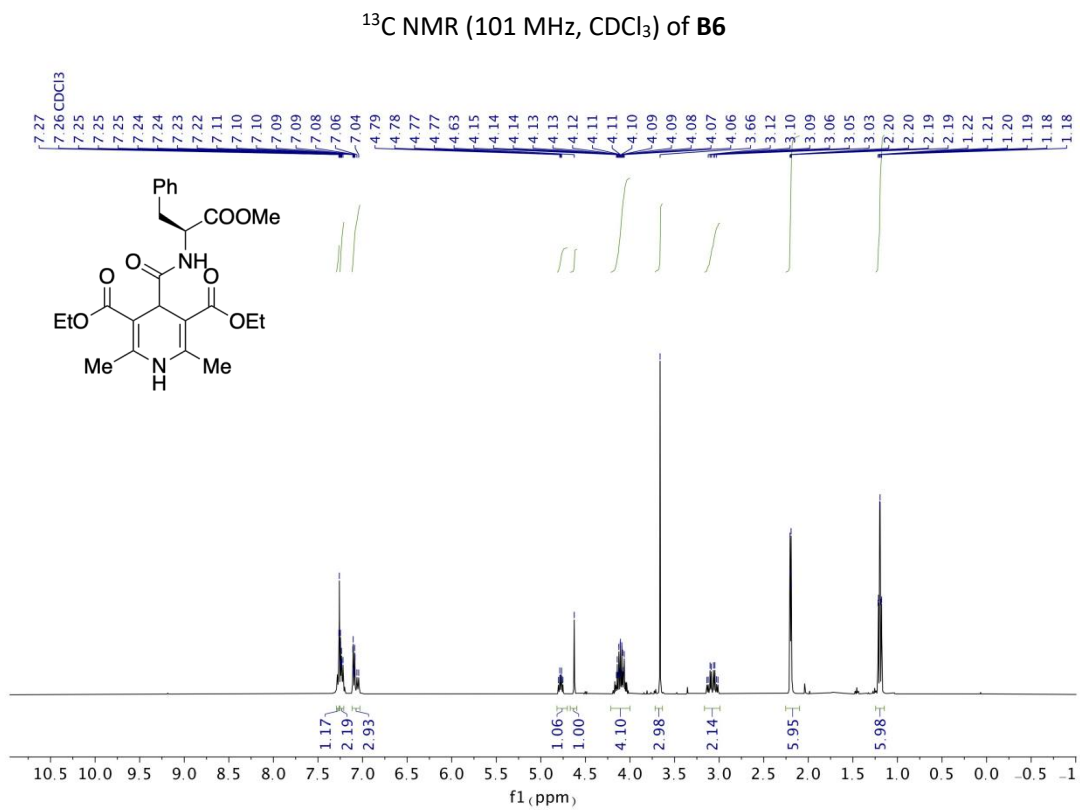
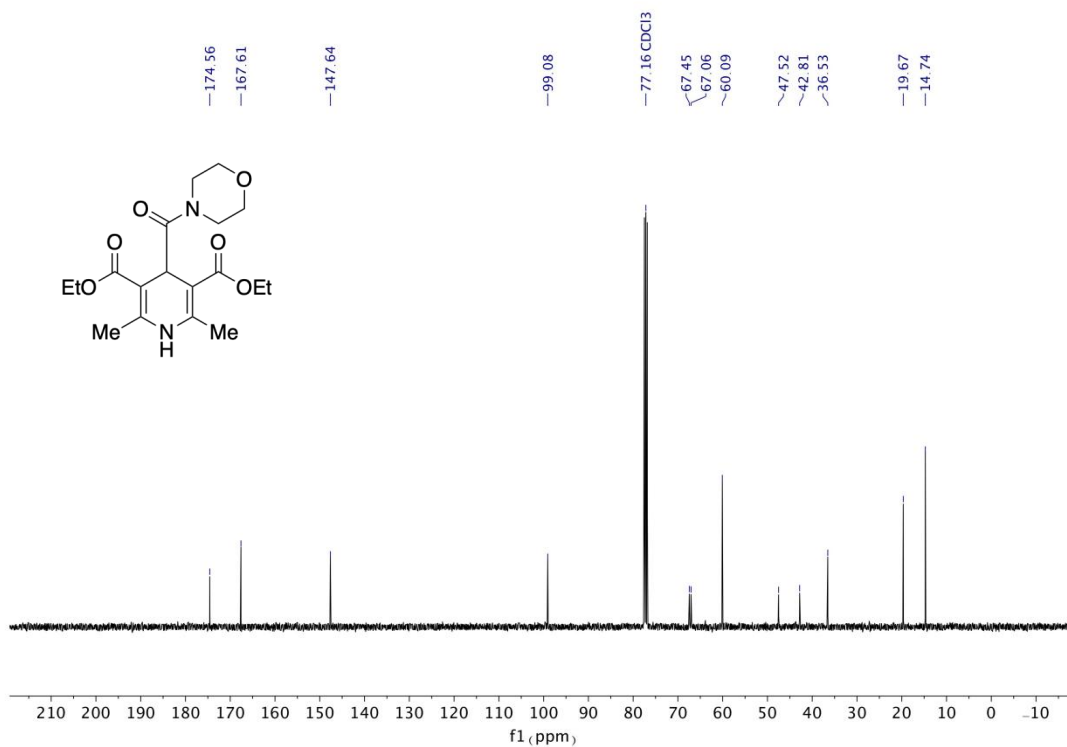


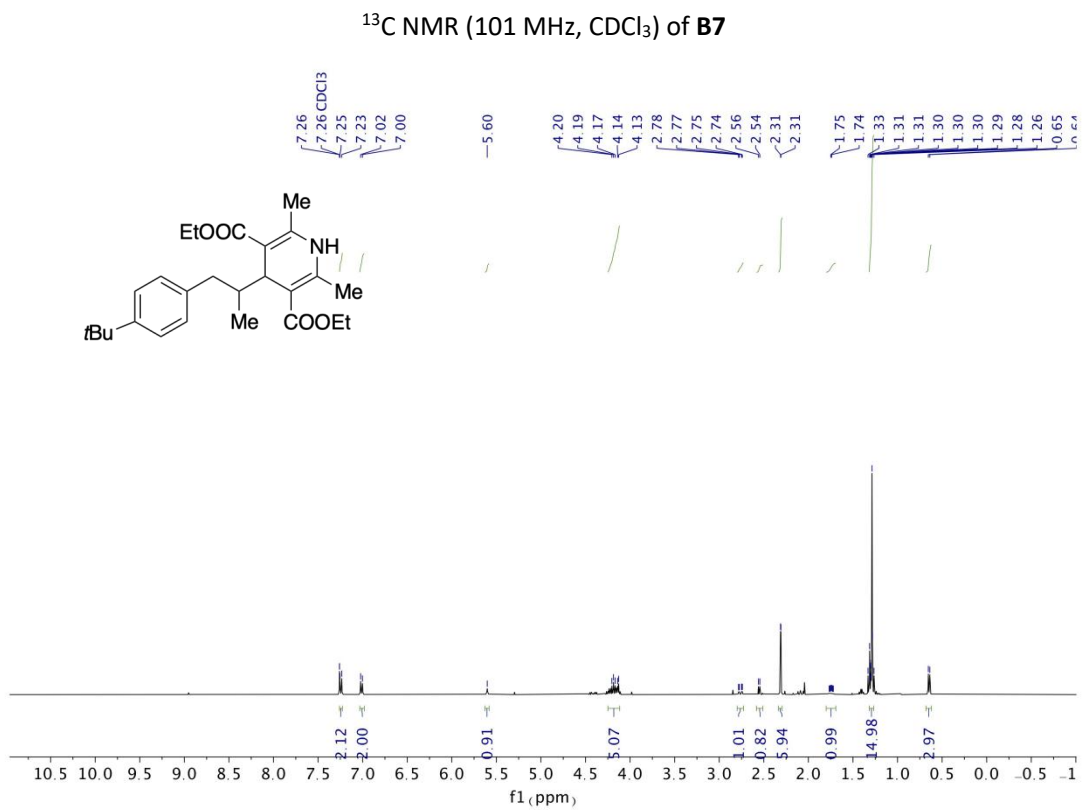
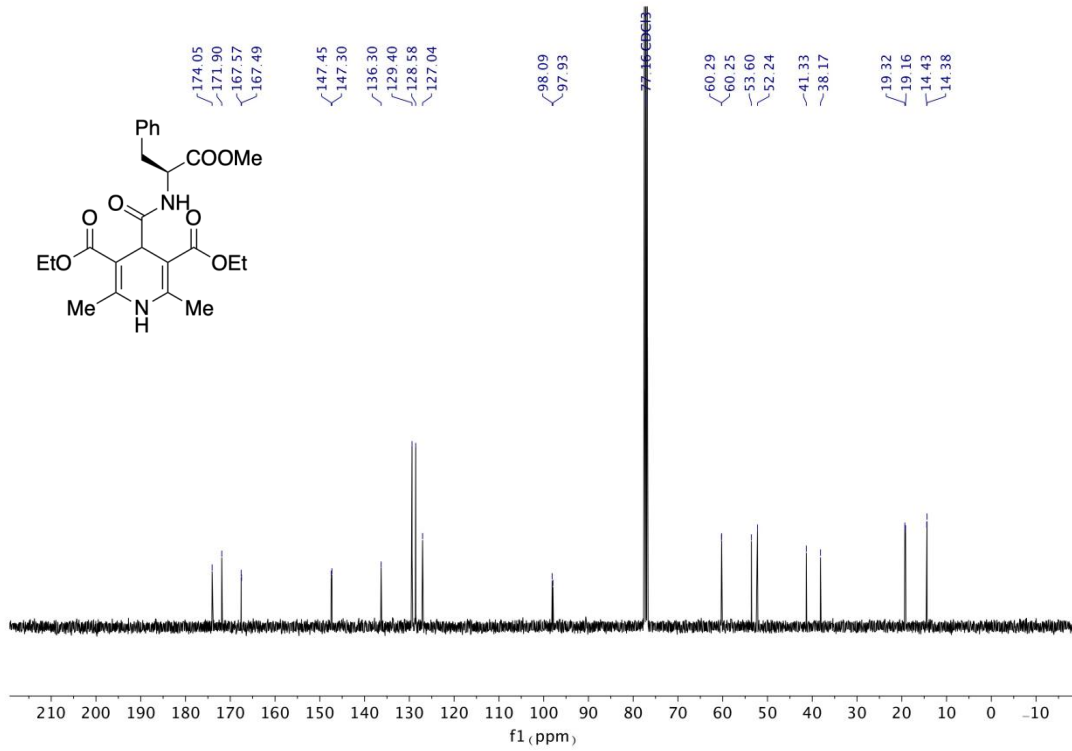


**<sup>13</sup>C NMR (101 MHz, CDCl<sub>3</sub>) of B5**

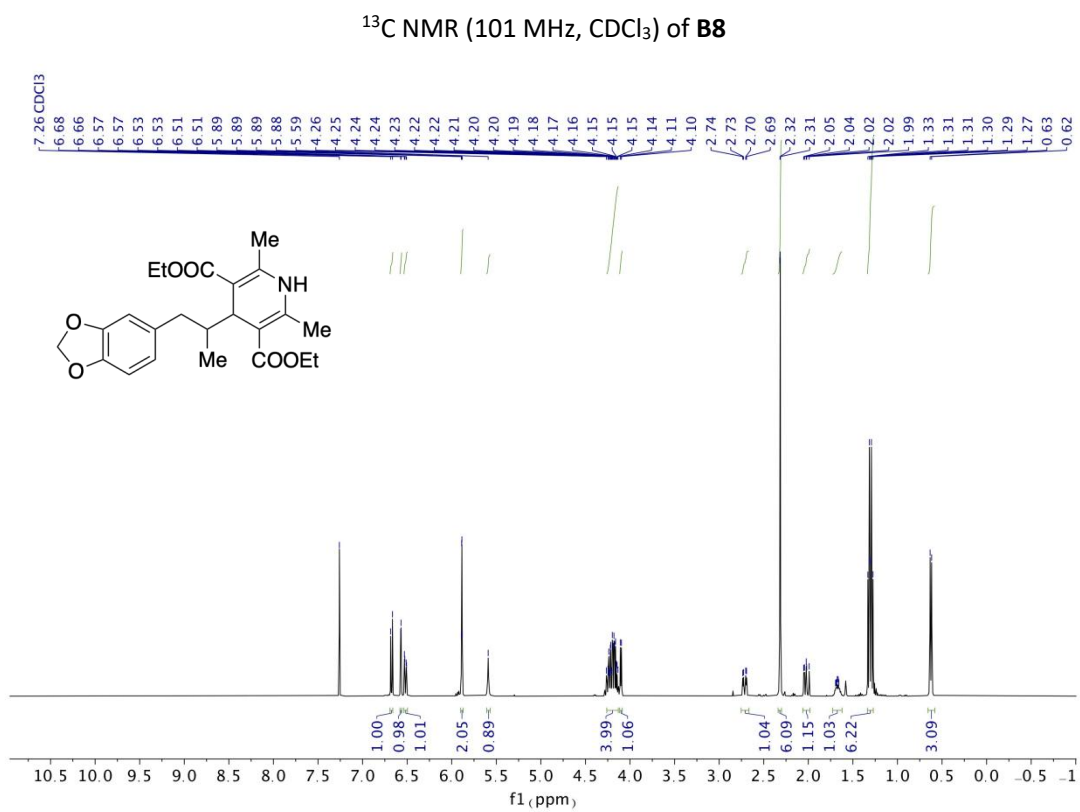
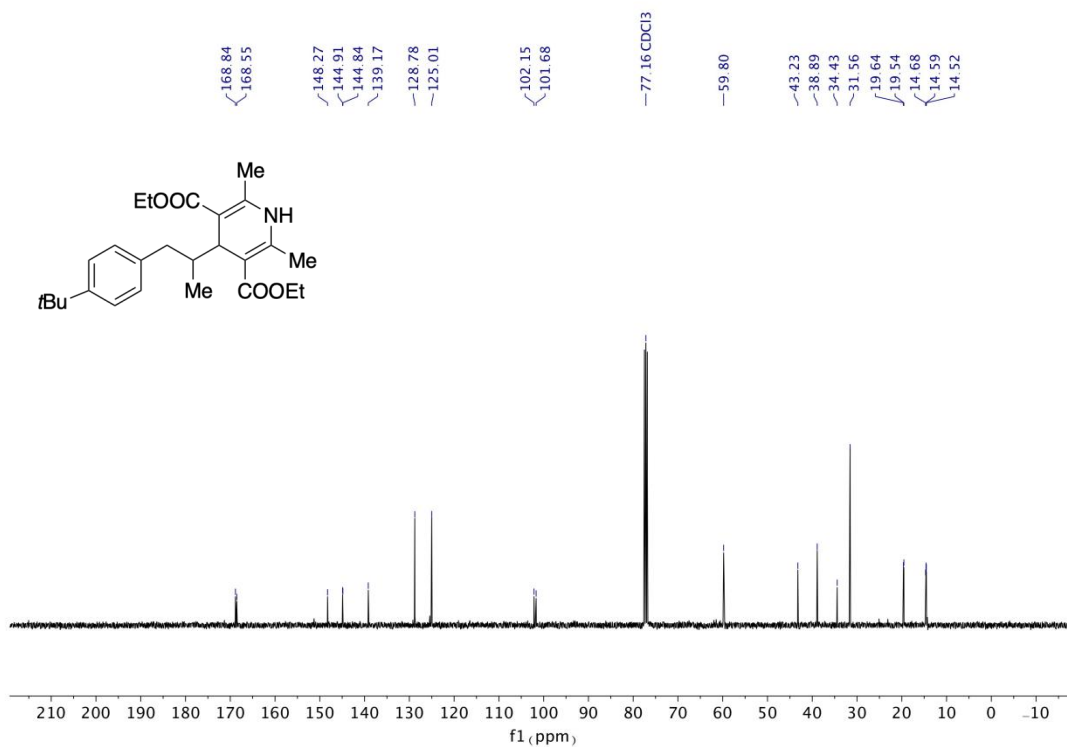


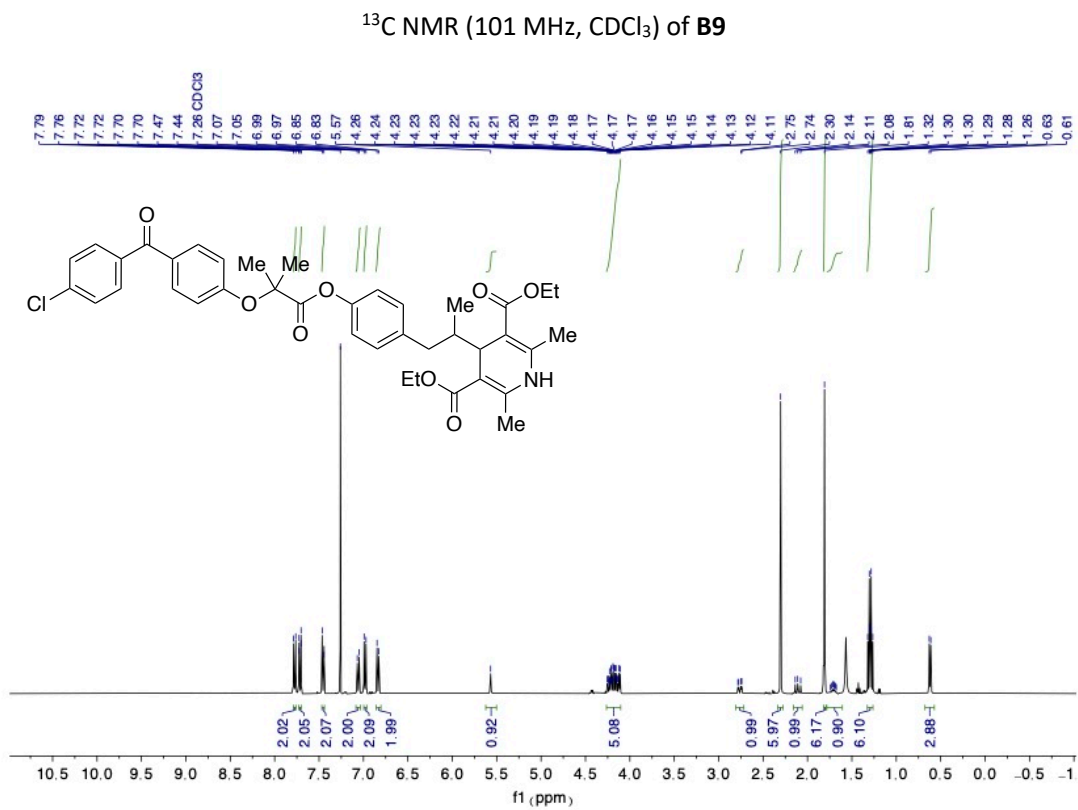
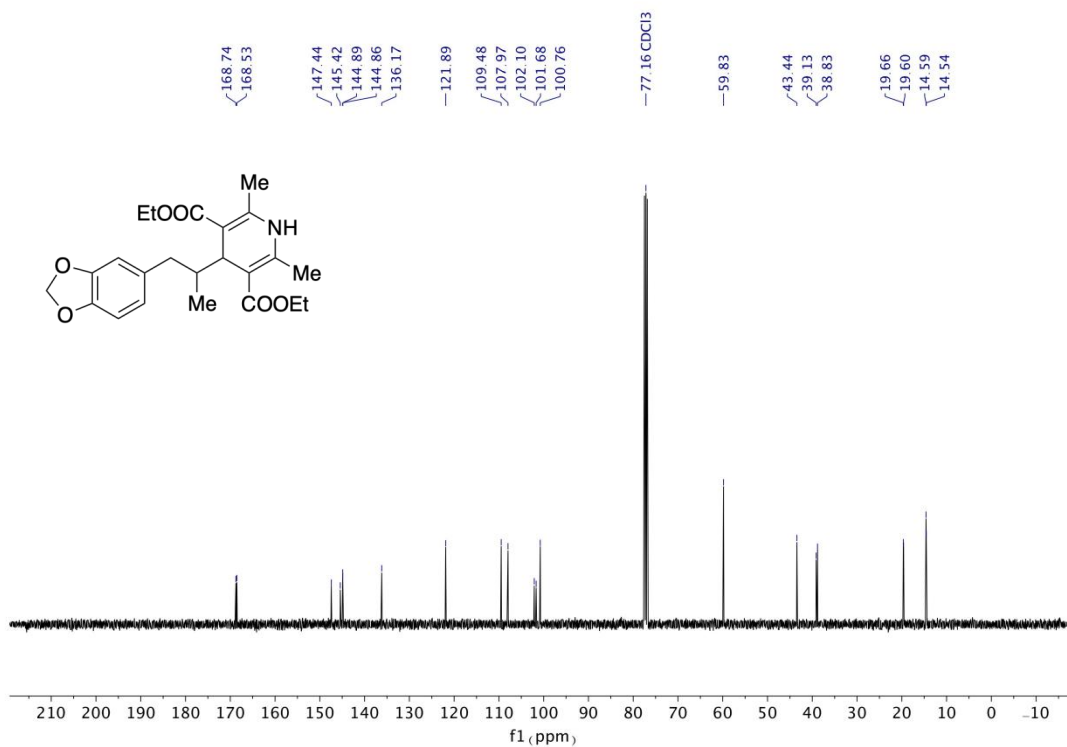
**<sup>1</sup>H NMR (400 MHz, CDCl<sub>3</sub>) of B6**



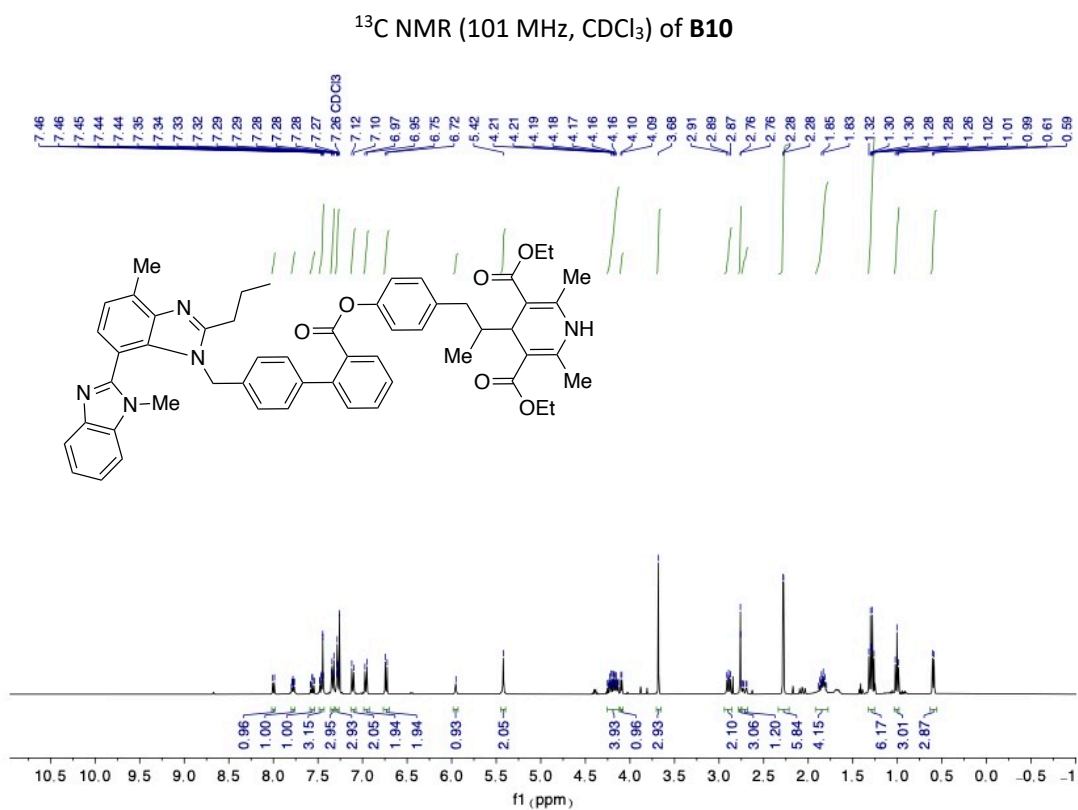
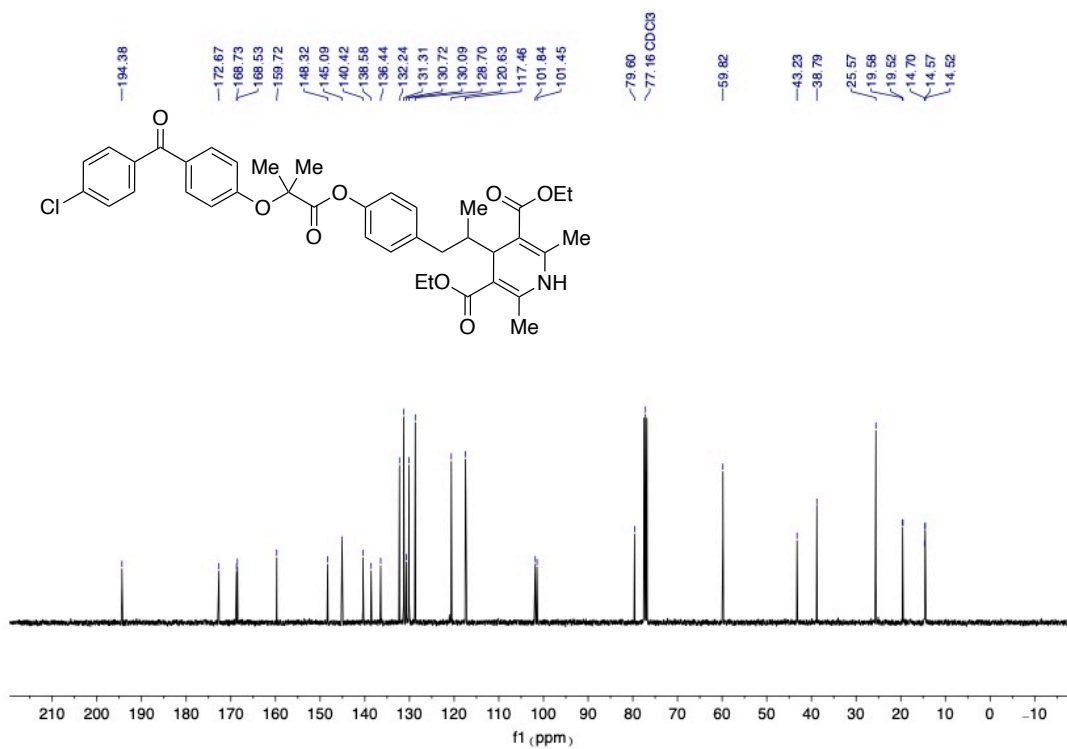


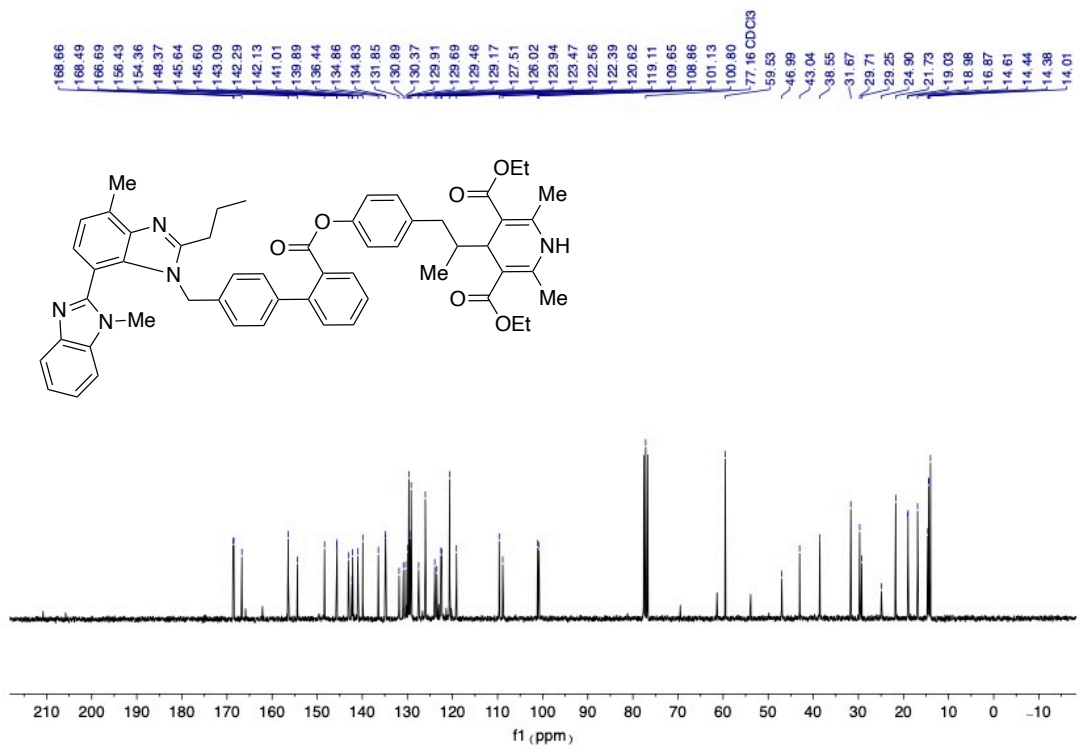




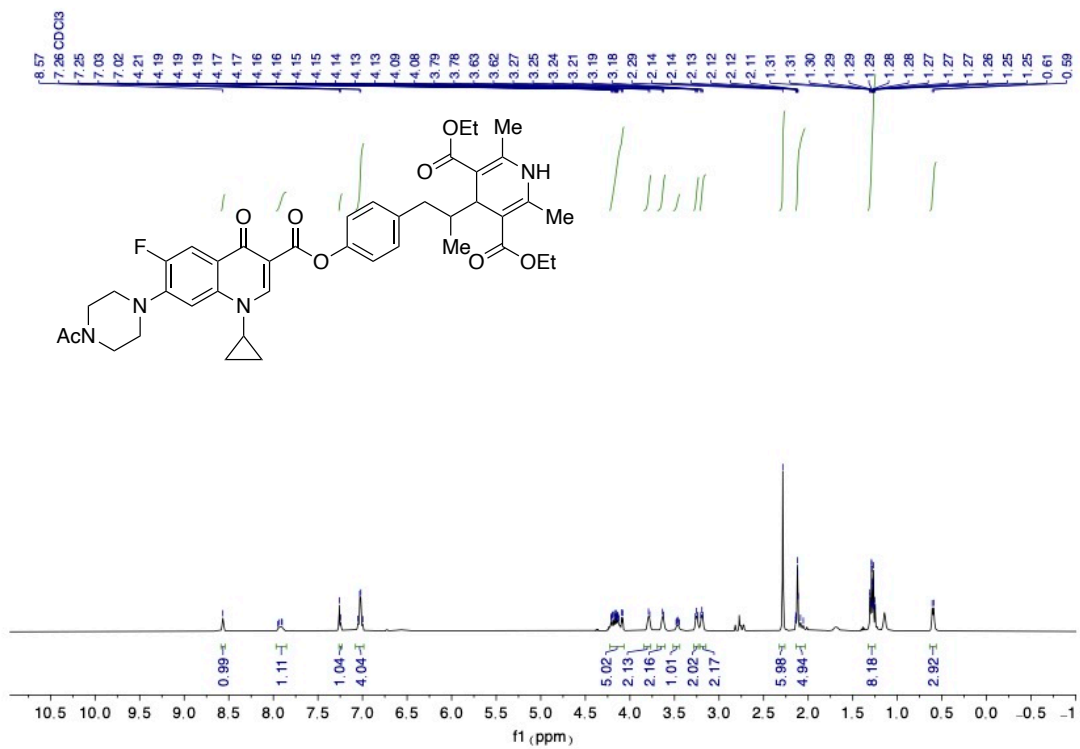


<sup>1</sup>H NMR (400 MHz, CDCl<sub>3</sub>) of B10 (note: the compound decompose)

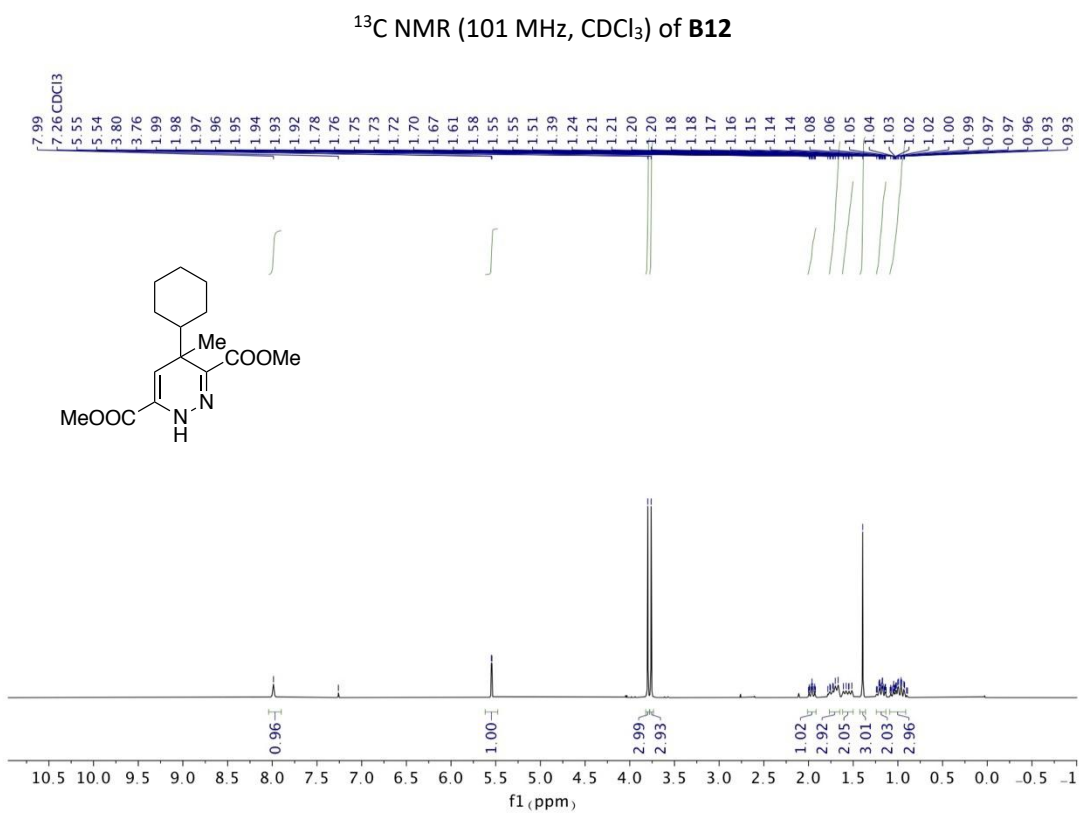
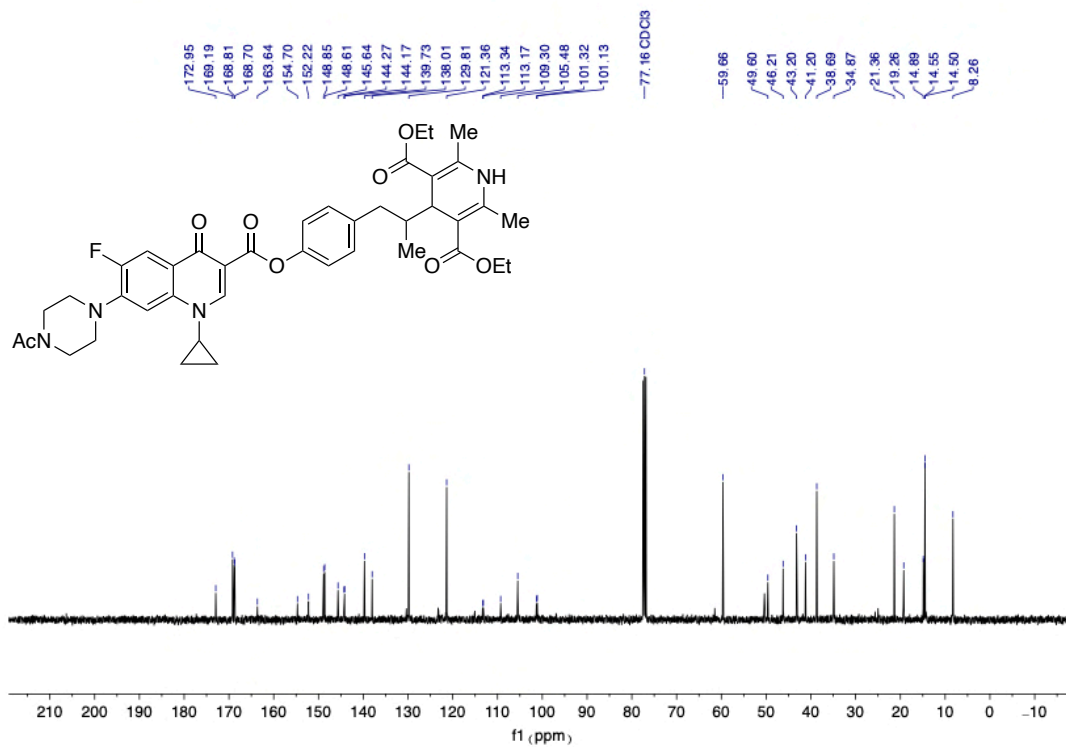


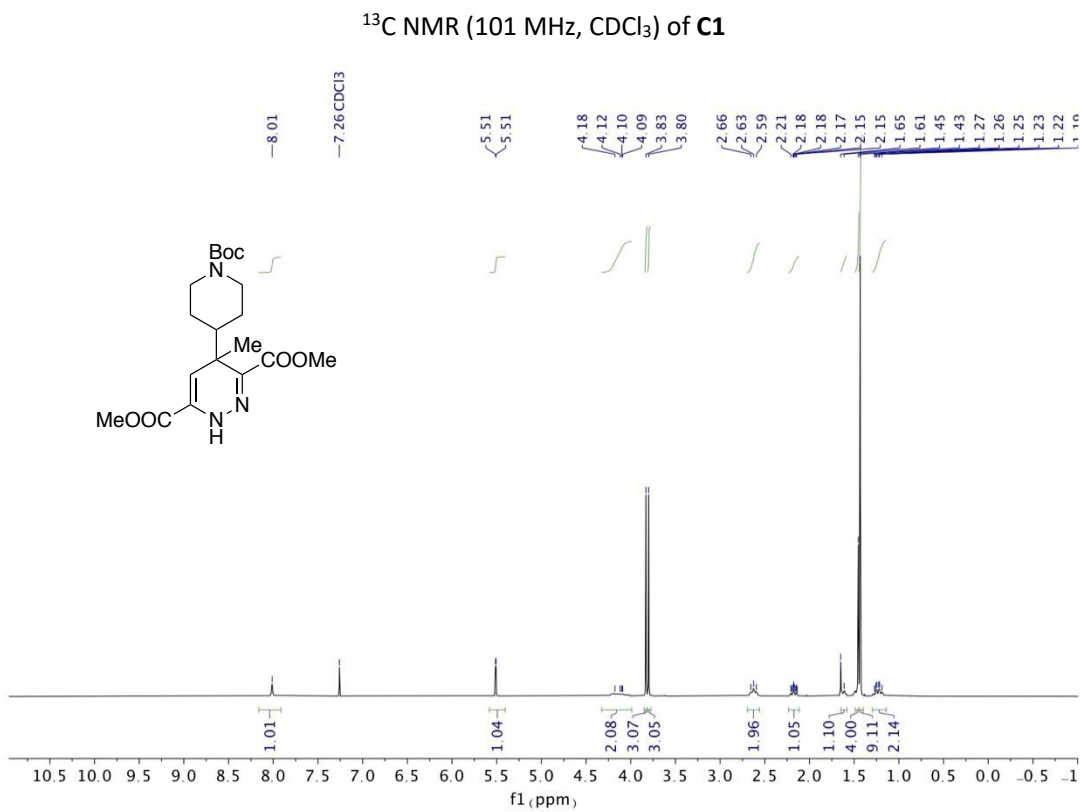
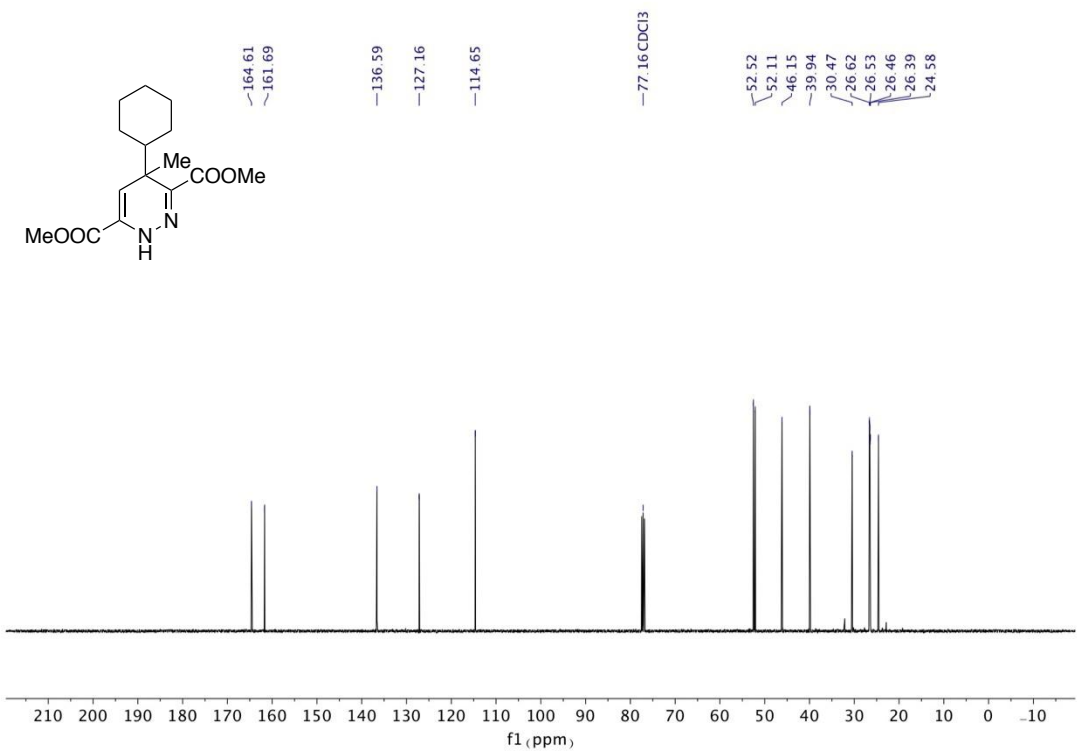


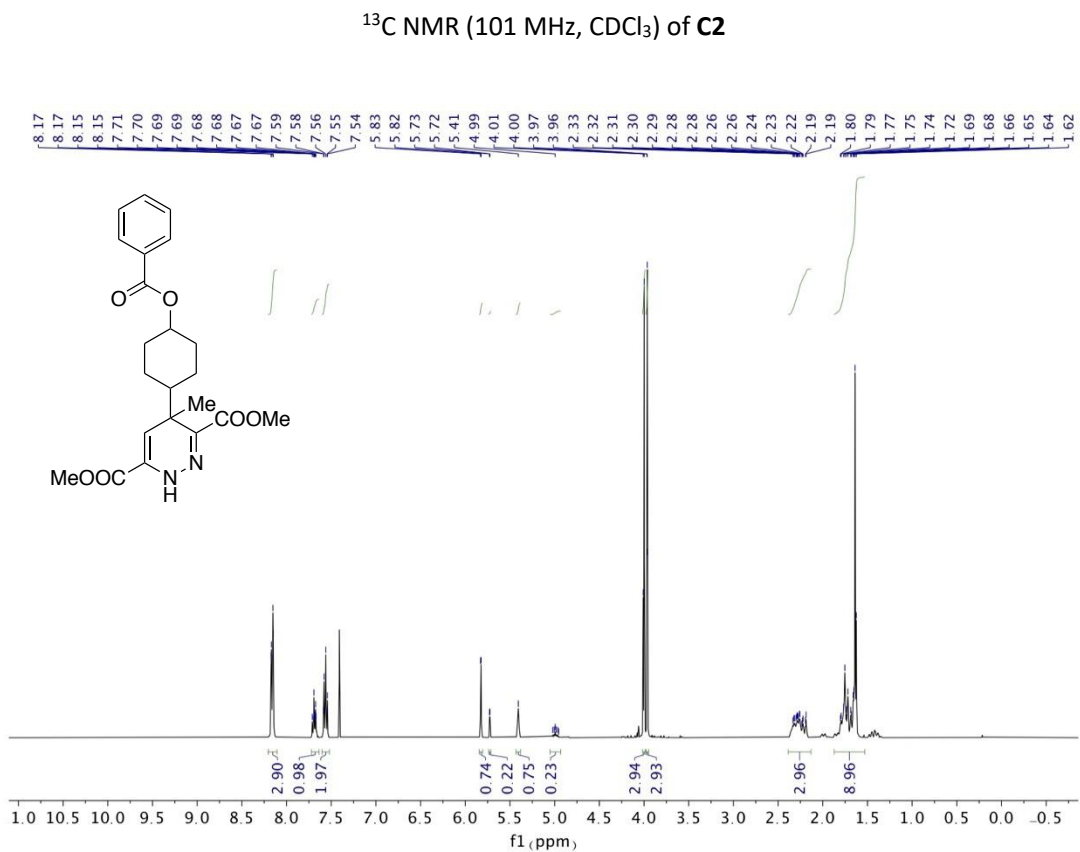
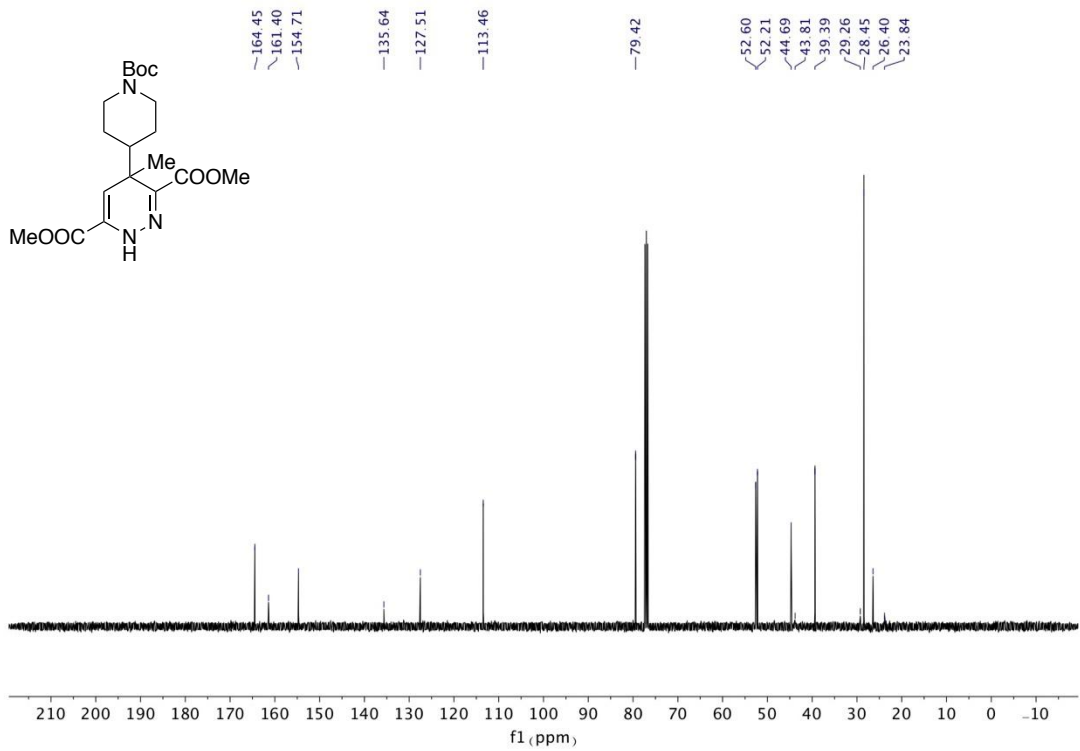
<sup>13</sup>C NMR (101 MHz, CDCl<sub>3</sub>) of **B11**



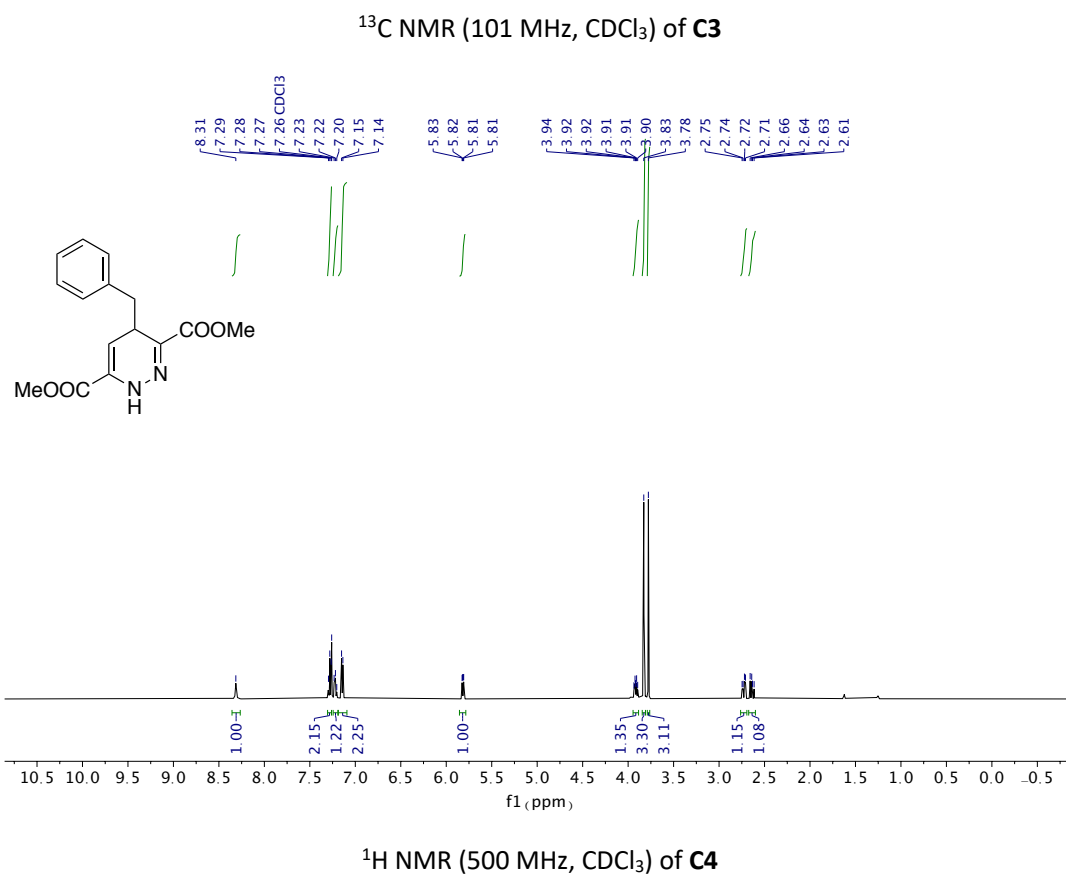
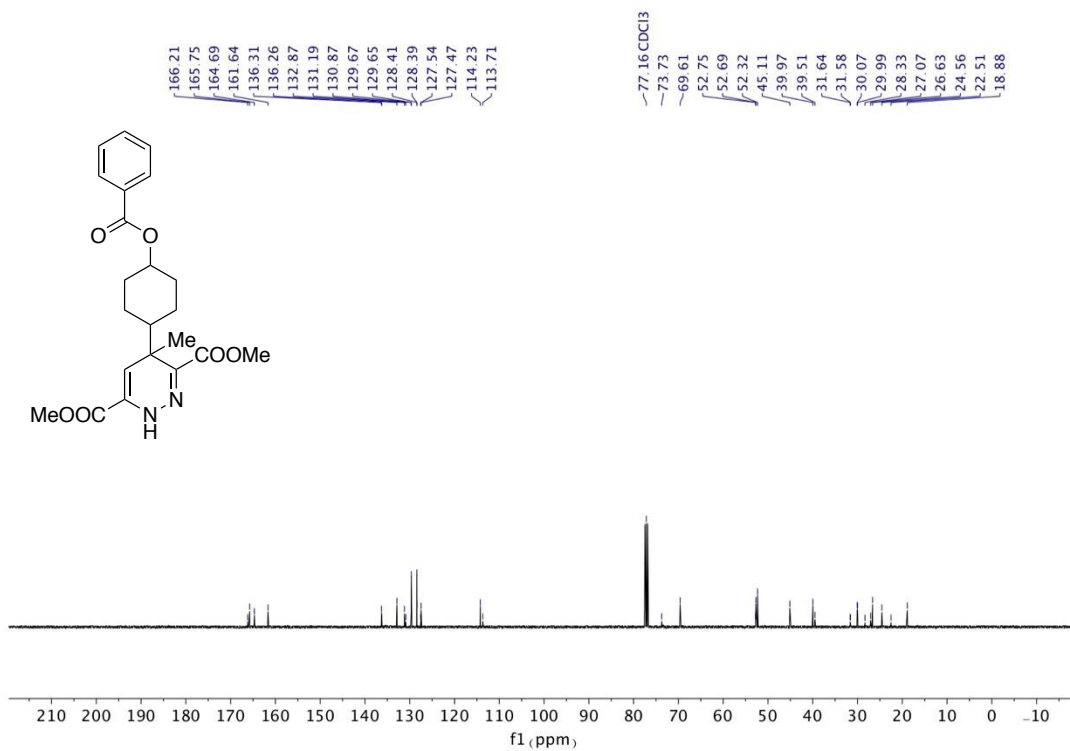
<sup>1</sup>H NMR (400 MHz, CDCl<sub>3</sub>) of **B12** (note: the compound decompose)



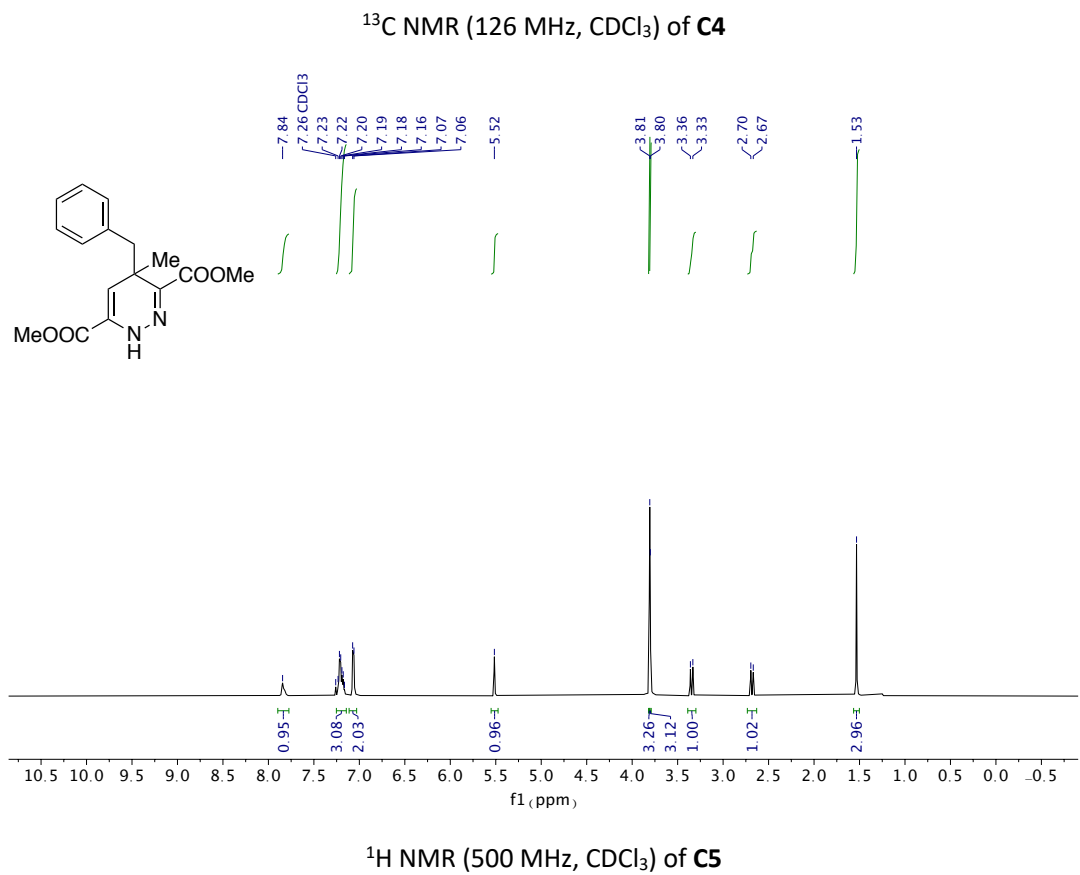
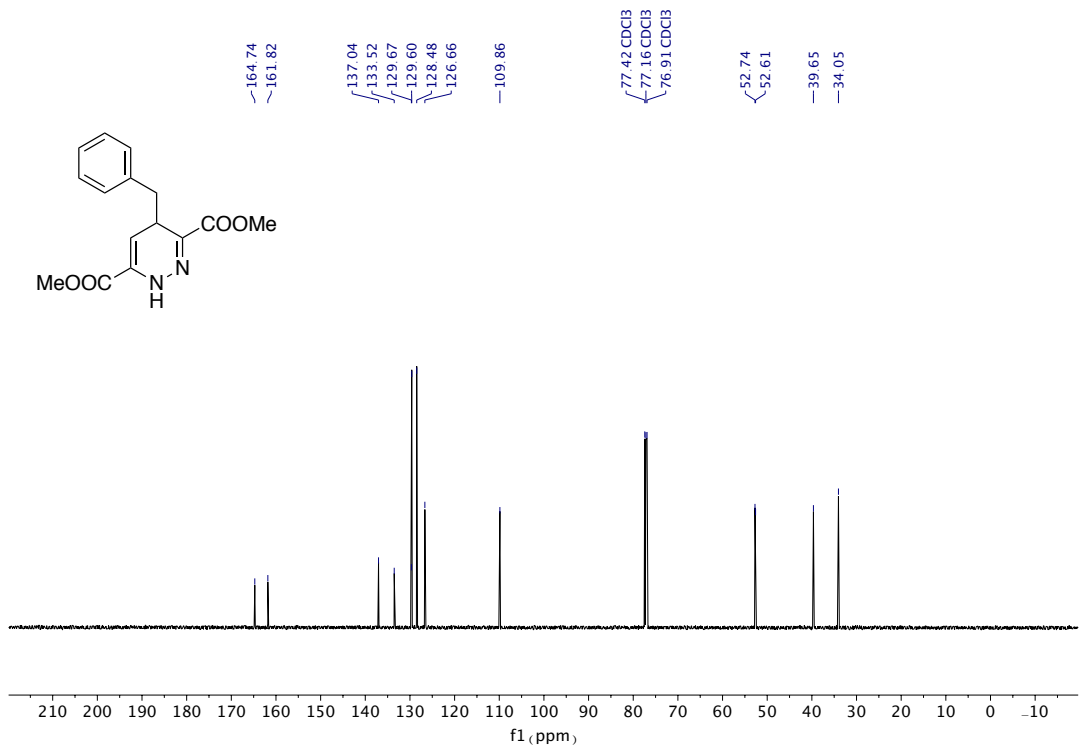


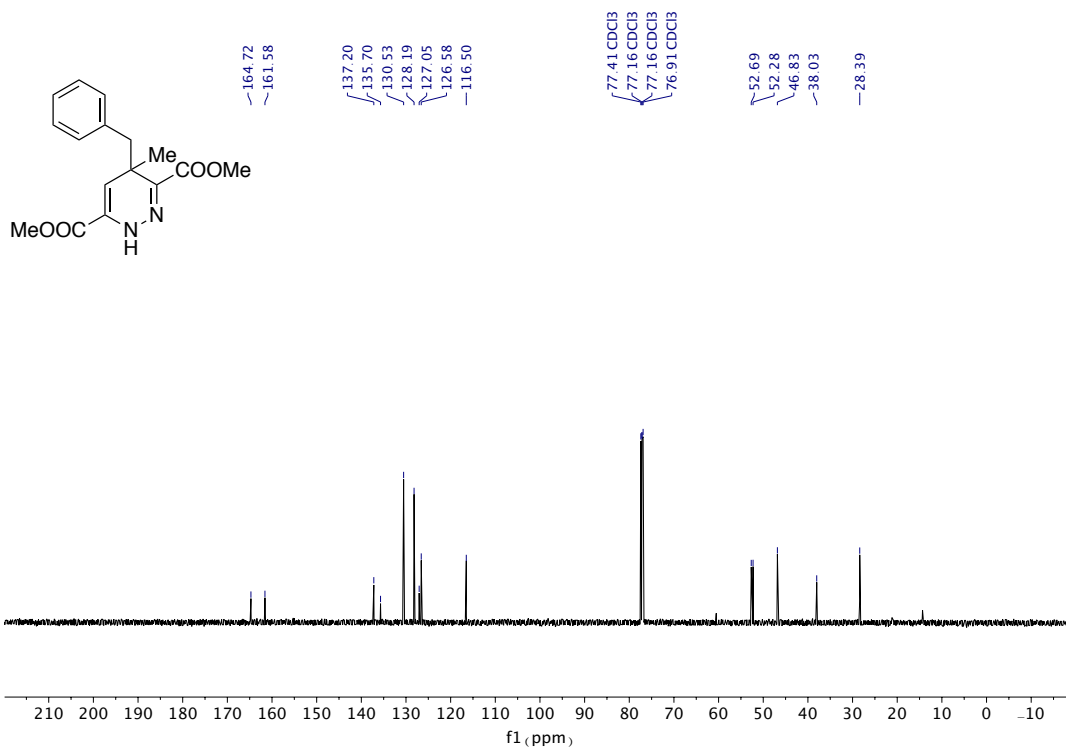


$^1\text{H}$  NMR (400 MHz,  $\text{CDCl}_3$ ) of **C3**

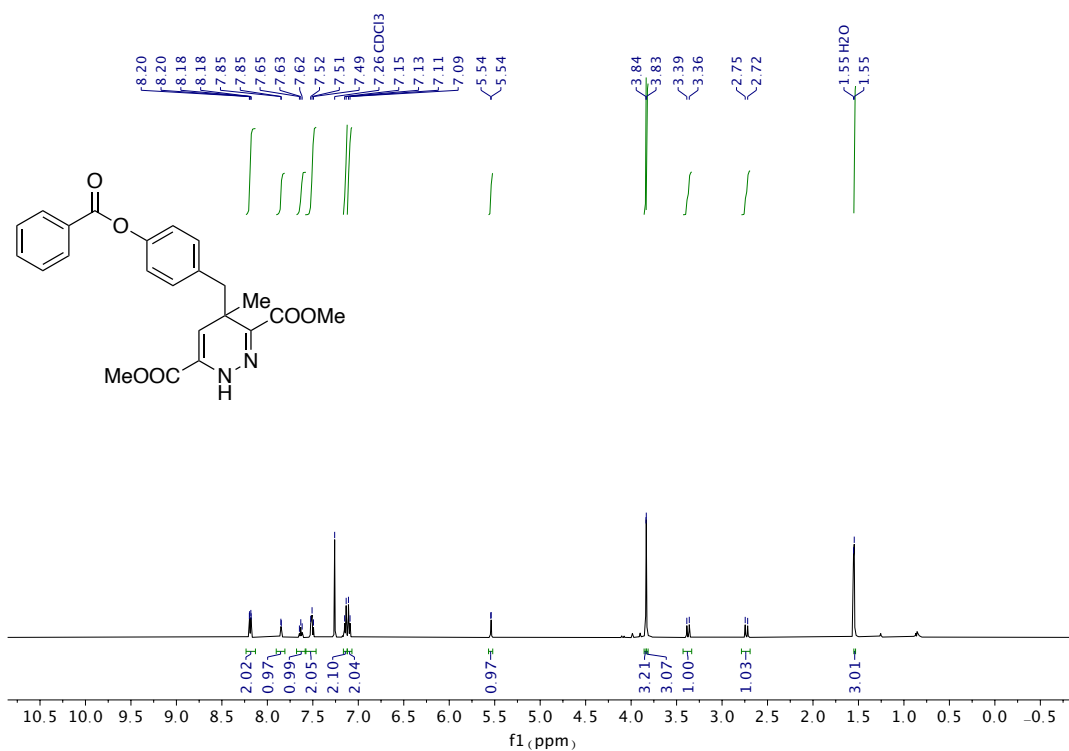




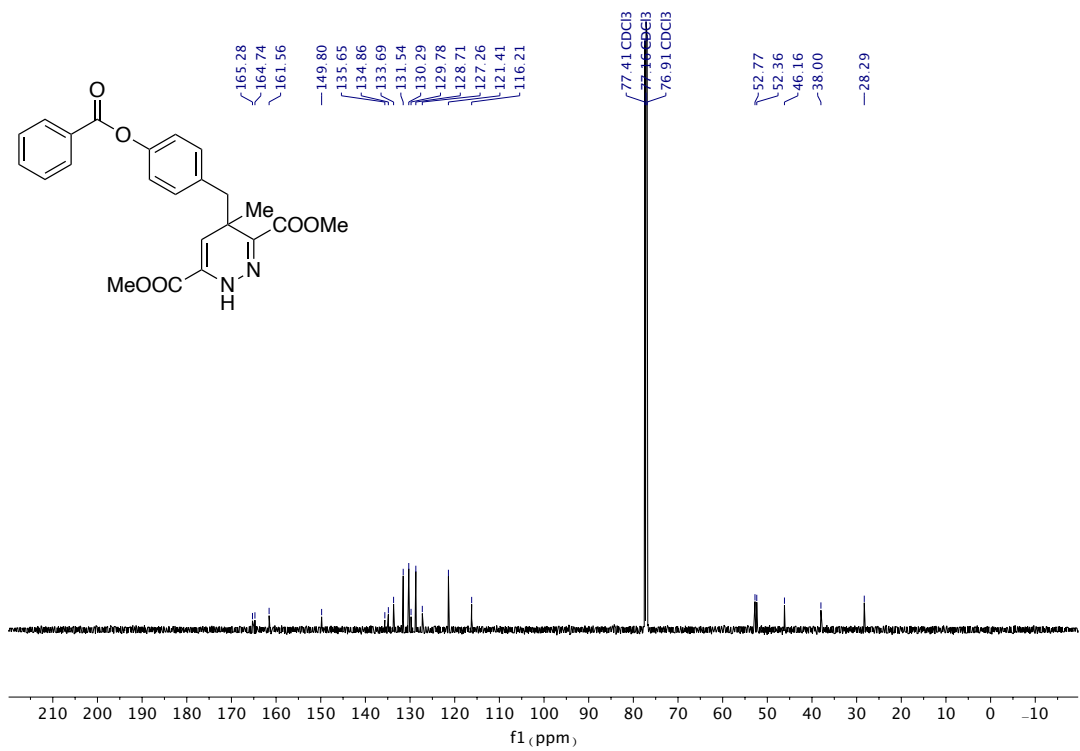




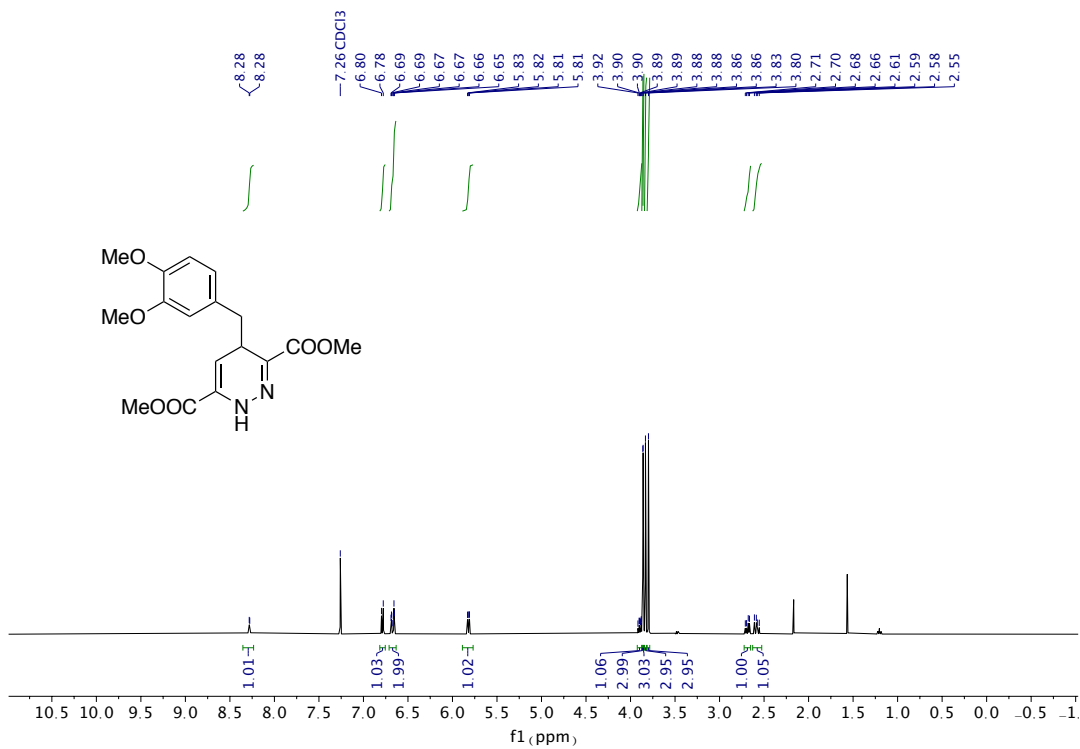
<sup>13</sup>C NMR (126 MHz, CDCl<sub>3</sub>) of **C5**



<sup>1</sup>H NMR (500 MHz, CDCl<sub>3</sub>) of **C6**

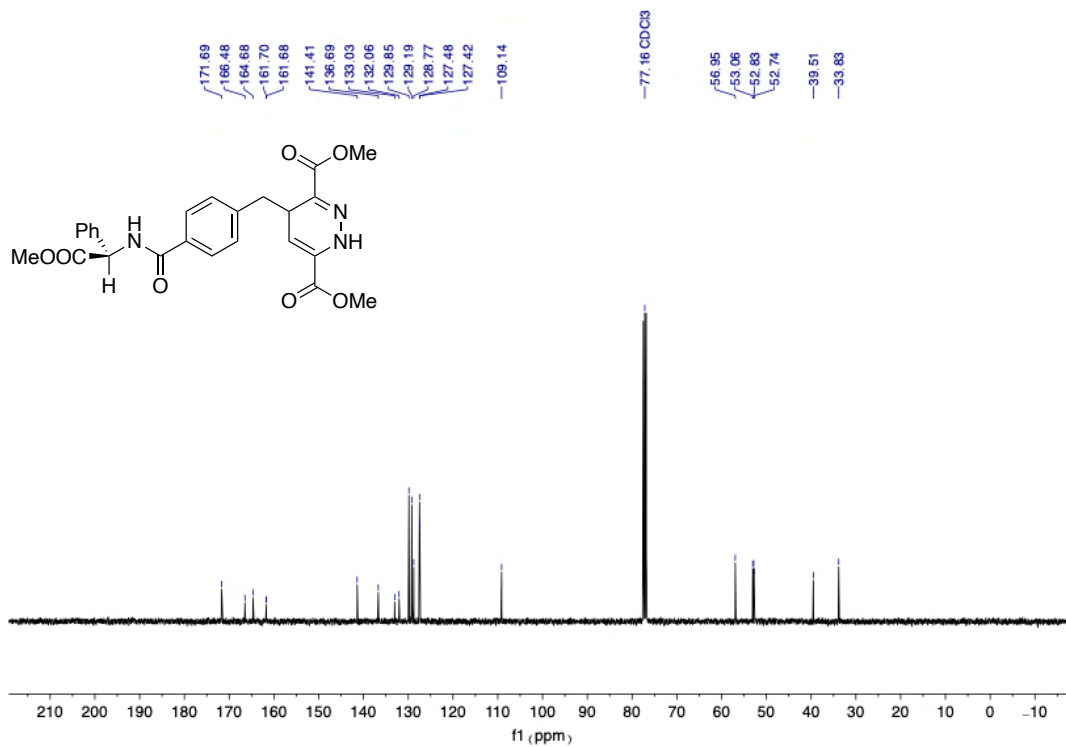


**<sup>13</sup>C NMR (126 MHz, CDCl<sub>3</sub>) of C6**

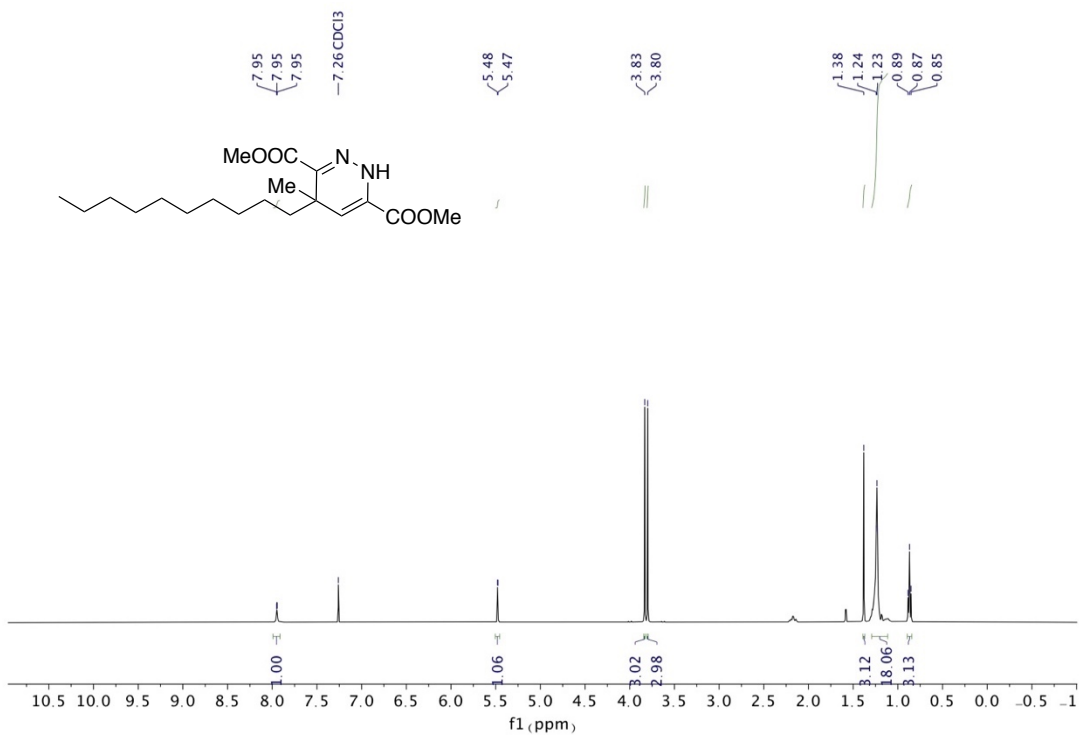


**<sup>1</sup>H NMR (400 MHz, CDCl<sub>3</sub>) of C7**

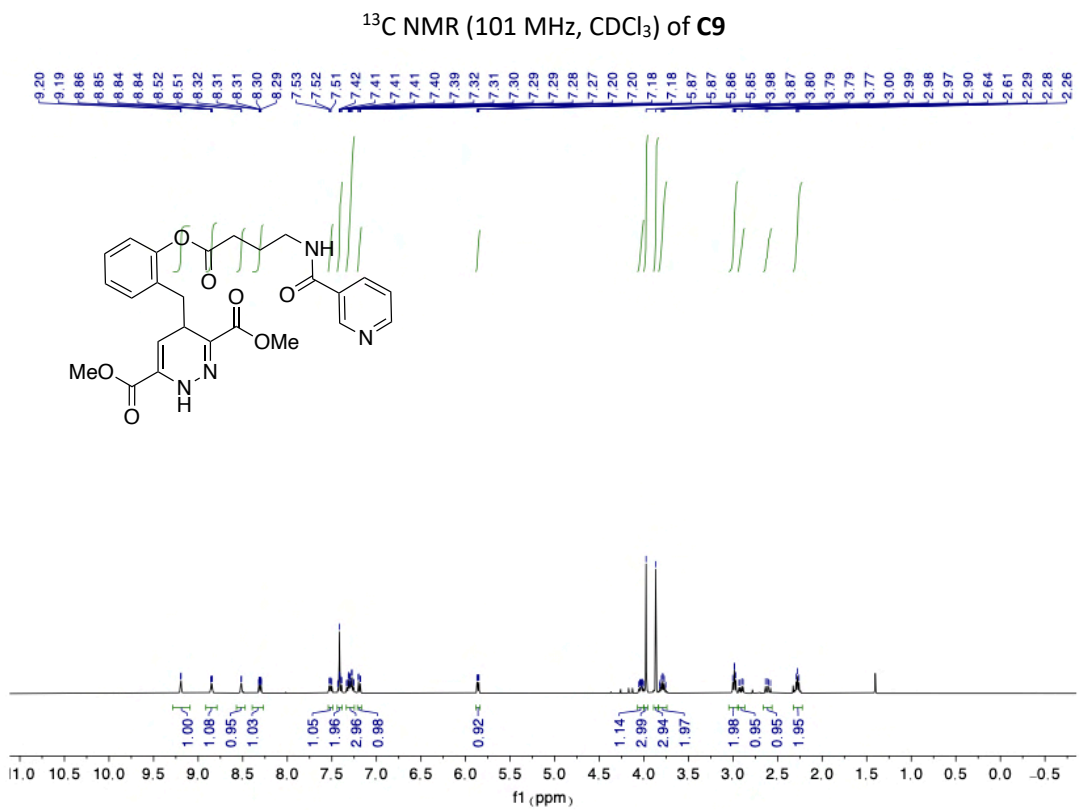
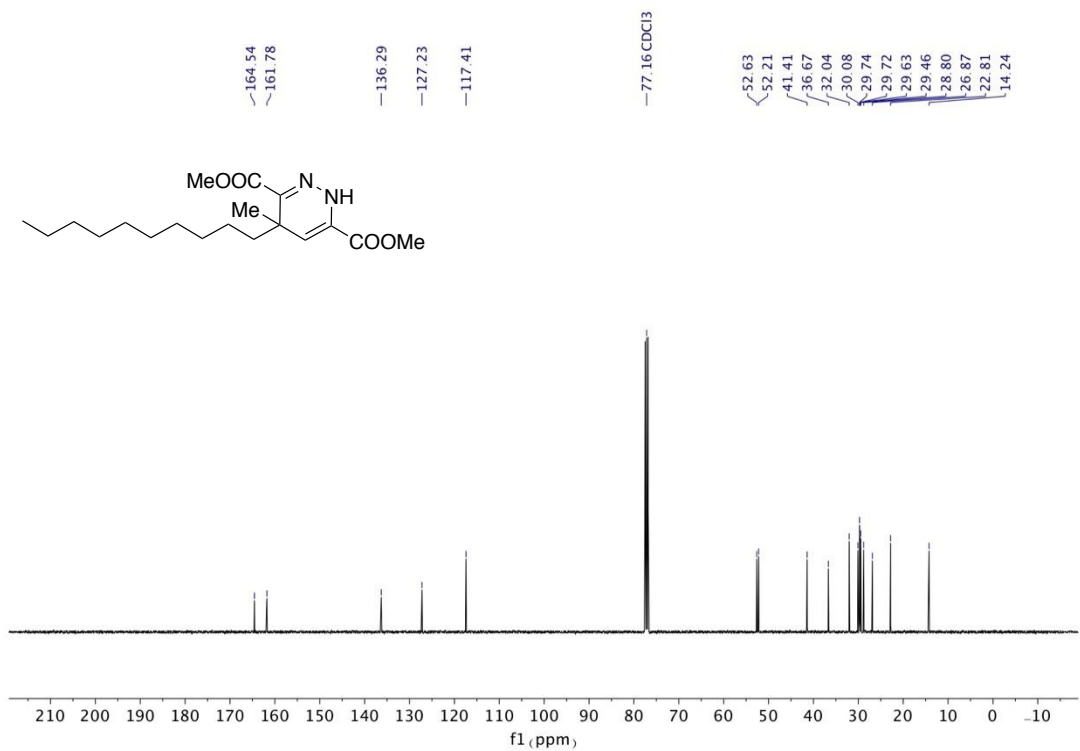


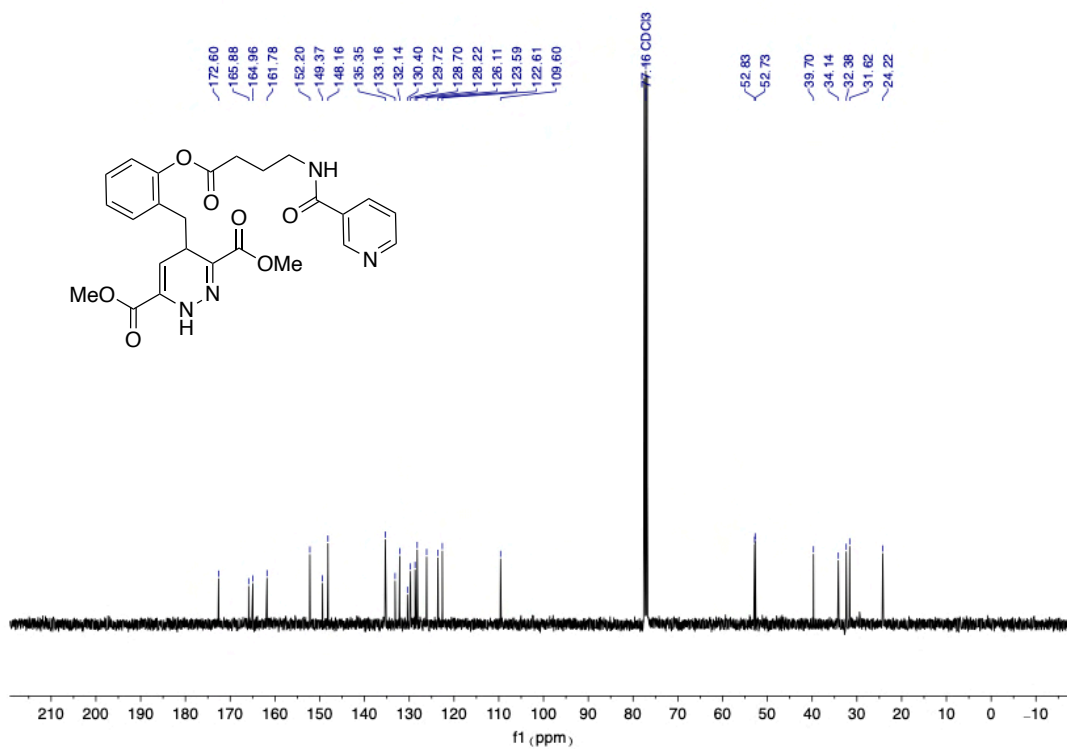


<sup>13</sup>C NMR (101 MHz, CDCl<sub>3</sub>) of **C8**

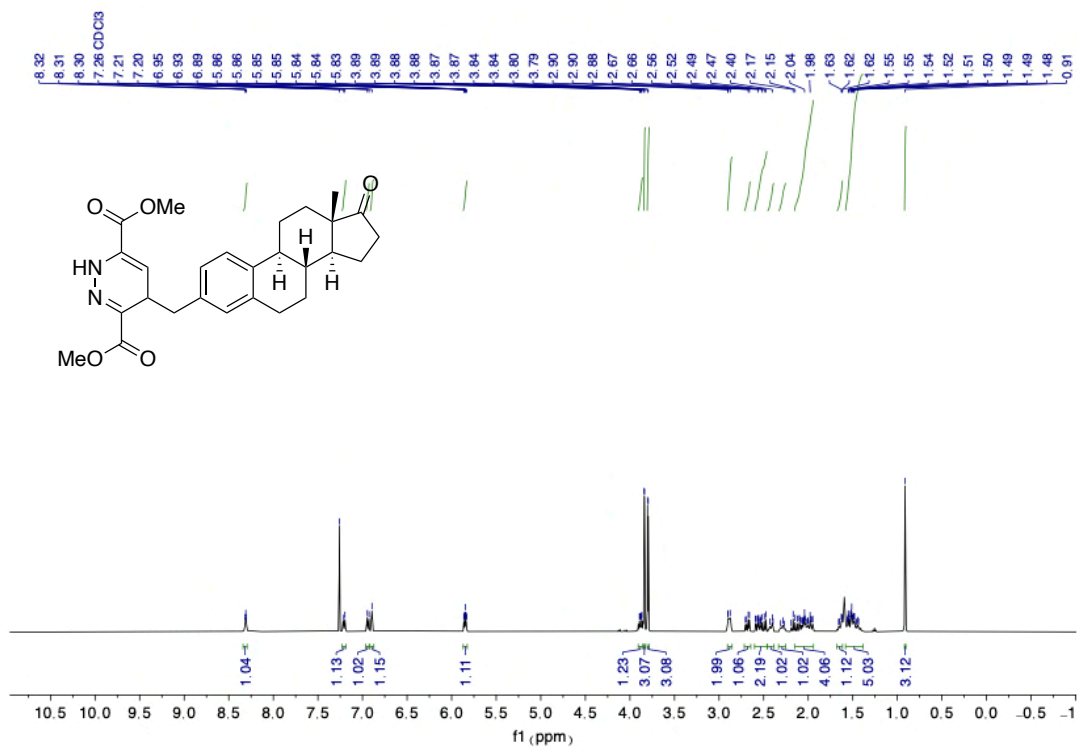


<sup>1</sup>H NMR (400 MHz, CDCl<sub>3</sub>) of **C9**

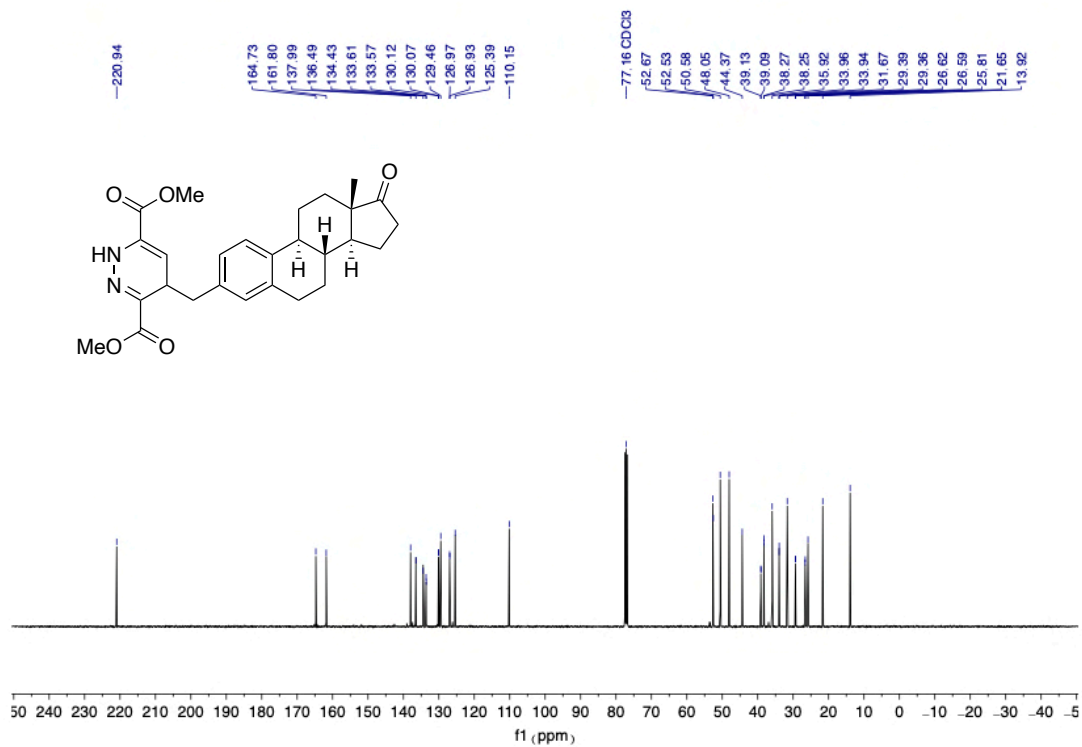




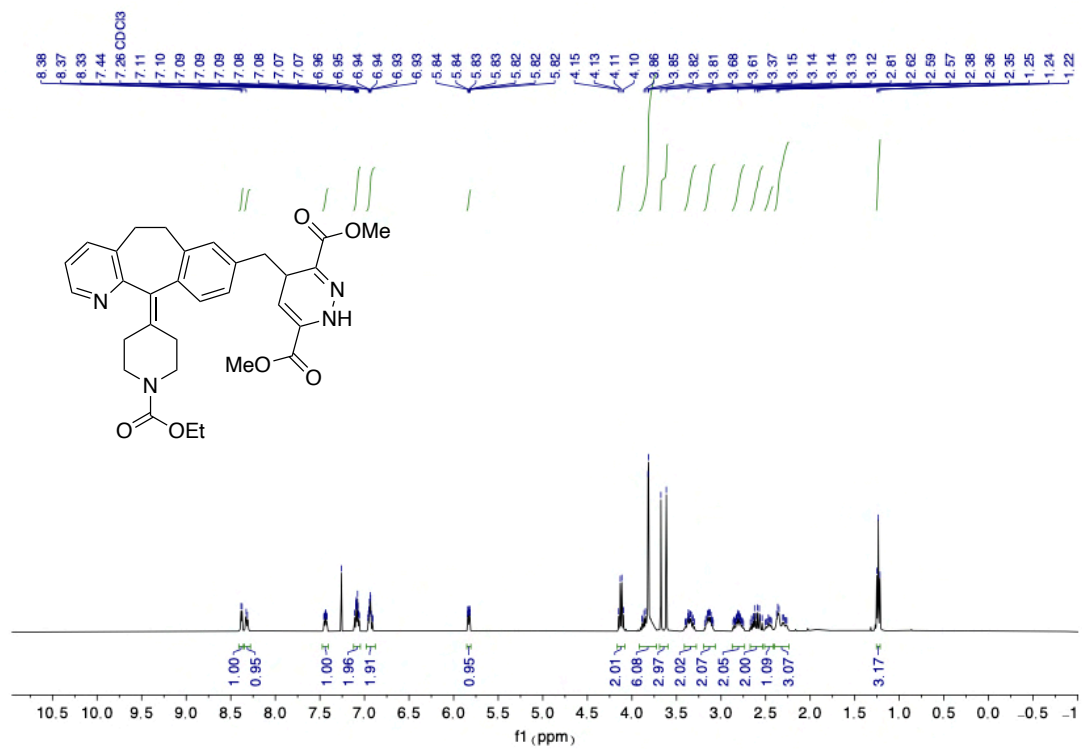
$^{13}\text{C}$  NMR (101 MHz,  $\text{CDCl}_3$ ) of **C10**



$^1\text{H}$  NMR (400 MHz,  $\text{CDCl}_3$ ) of **C11**

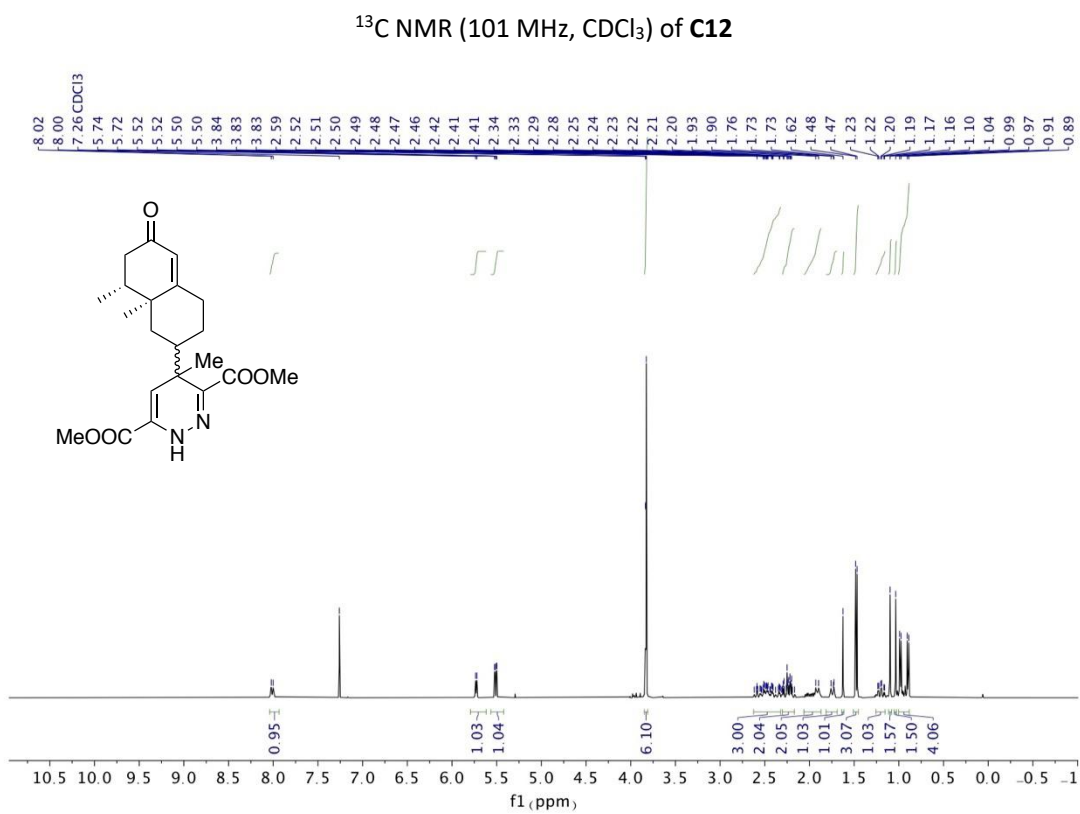
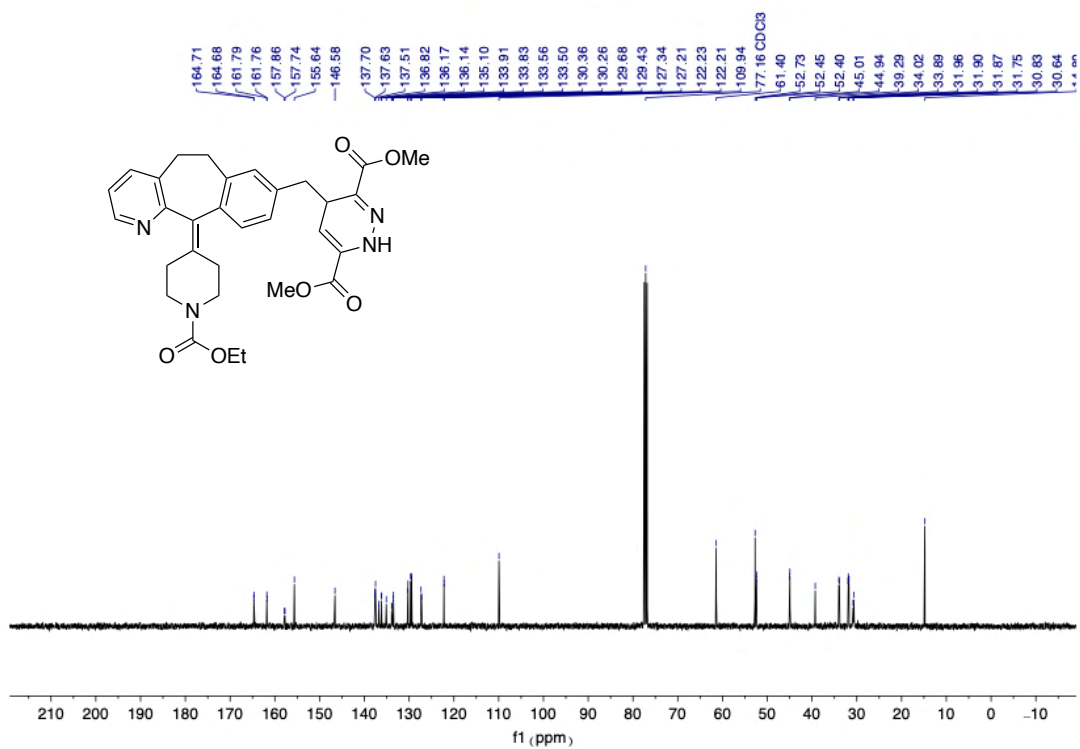


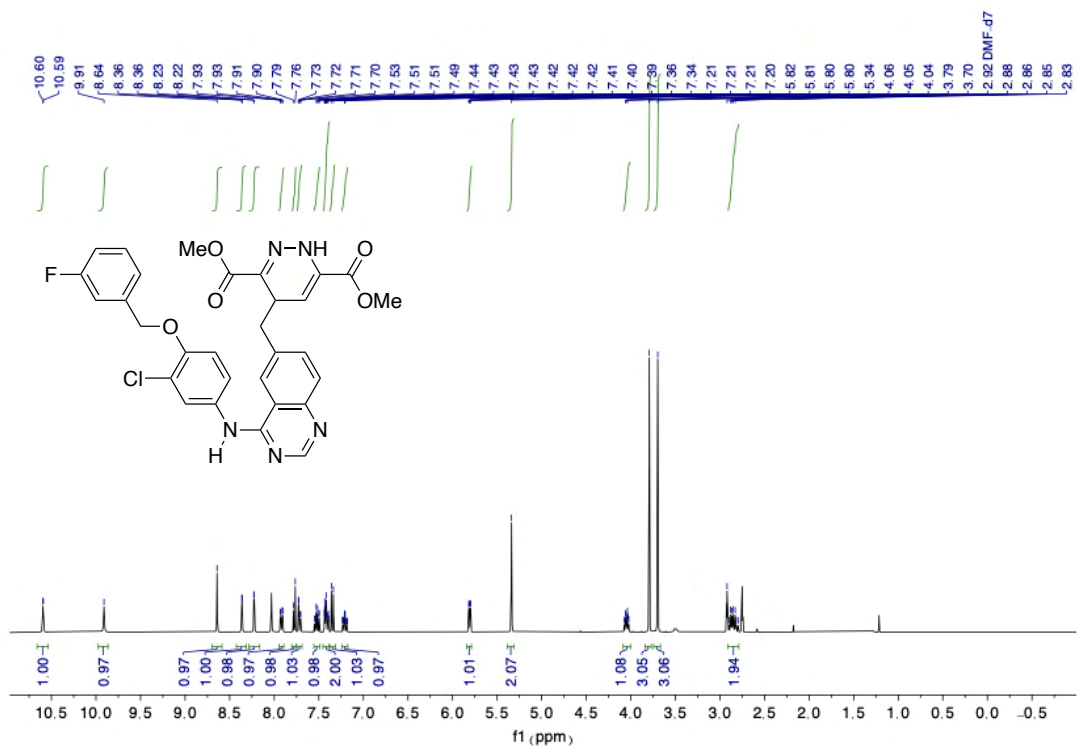
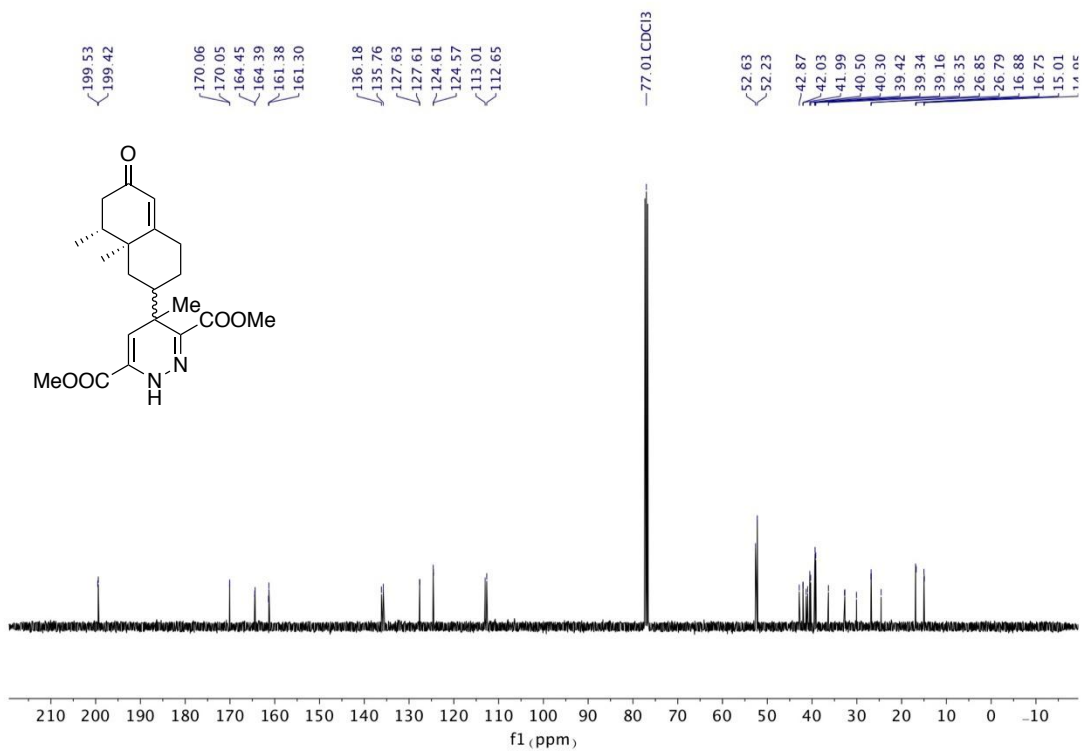
<sup>13</sup>C NMR (101 MHz, CDCl<sub>3</sub>) of **C11**

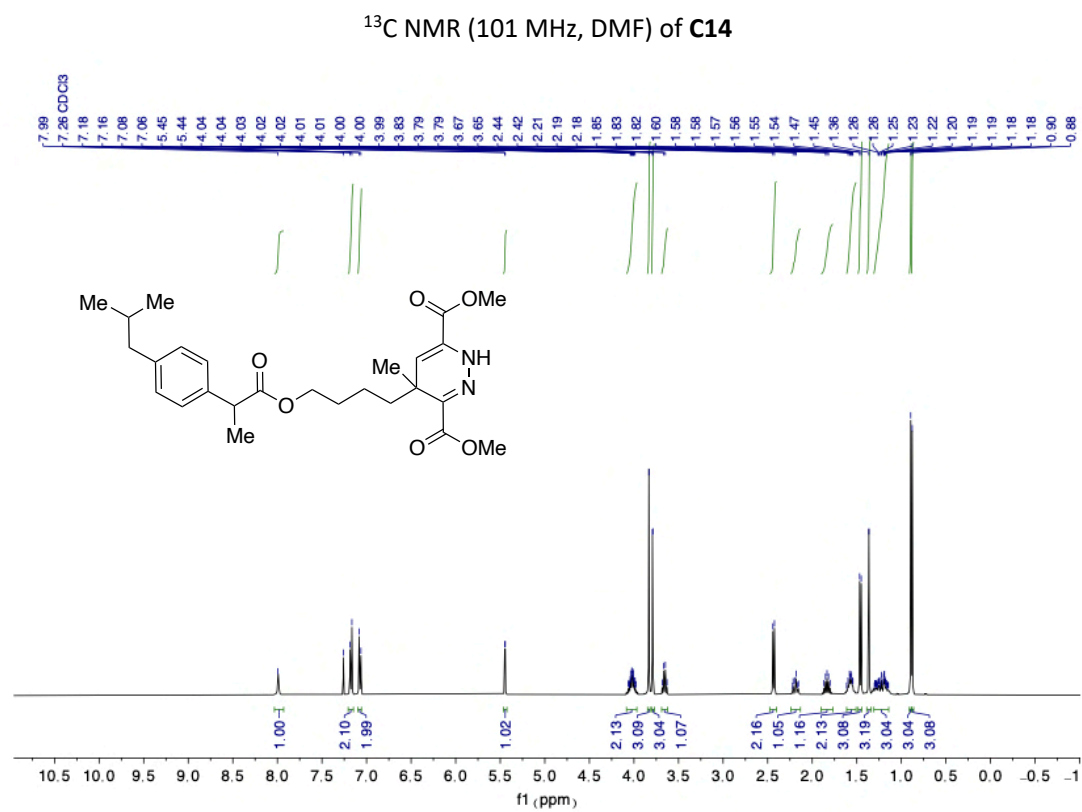
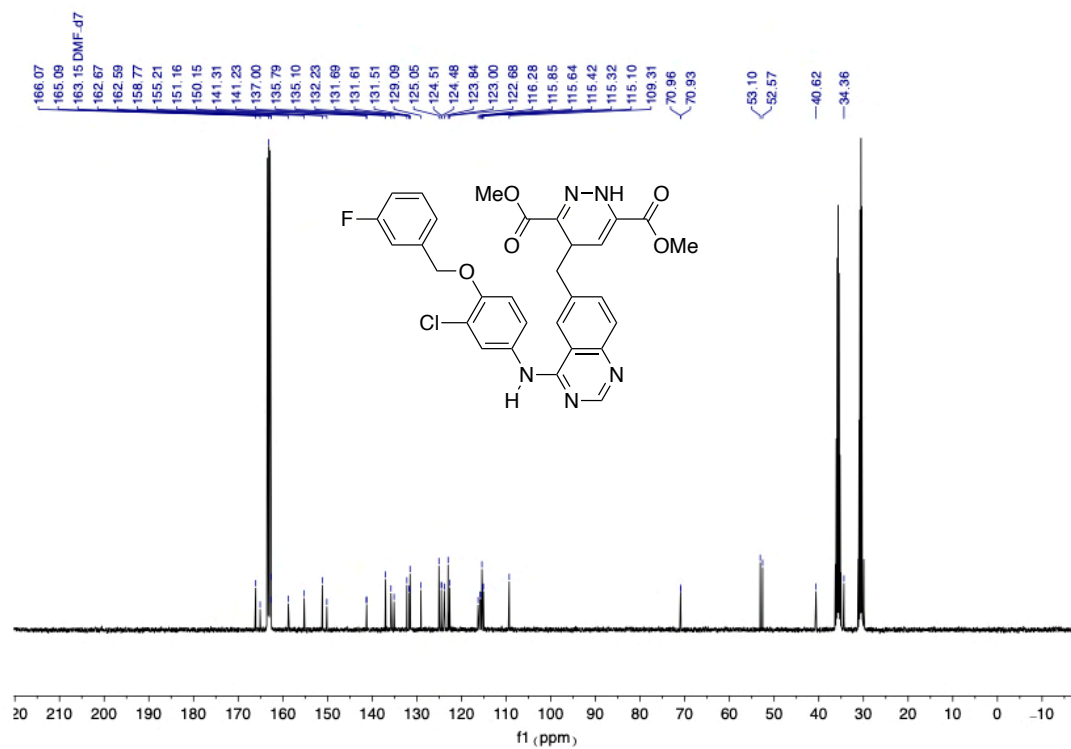


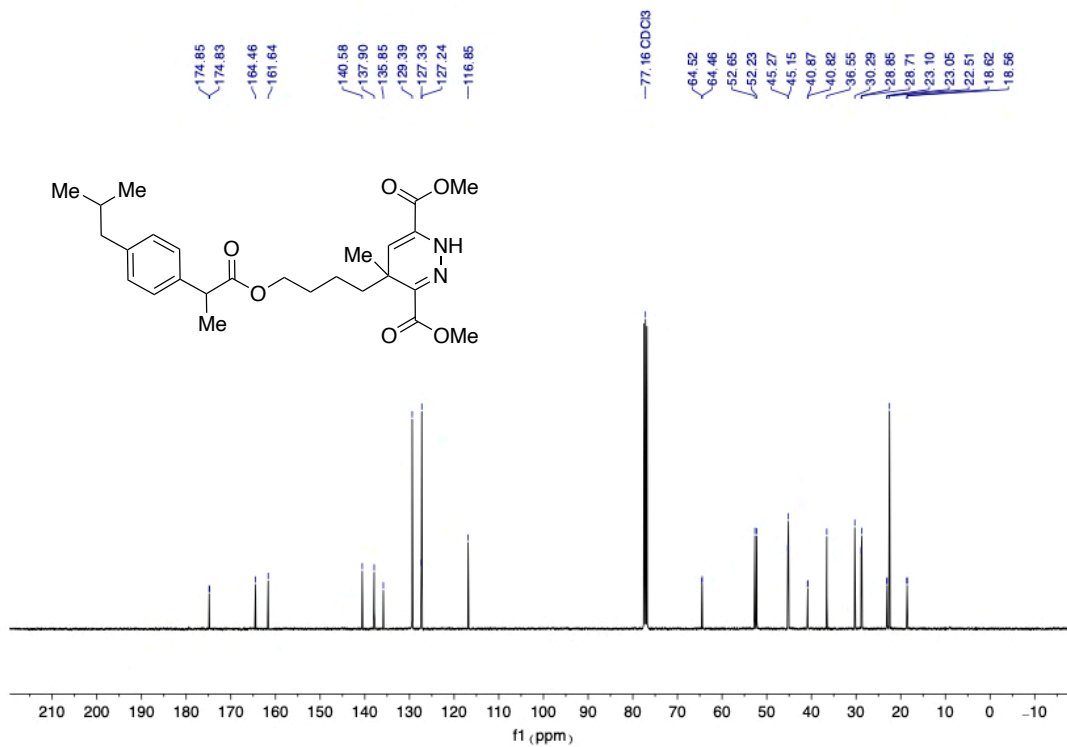
<sup>1</sup>H NMR (400 MHz, CDCl<sub>3</sub>) of **C12**



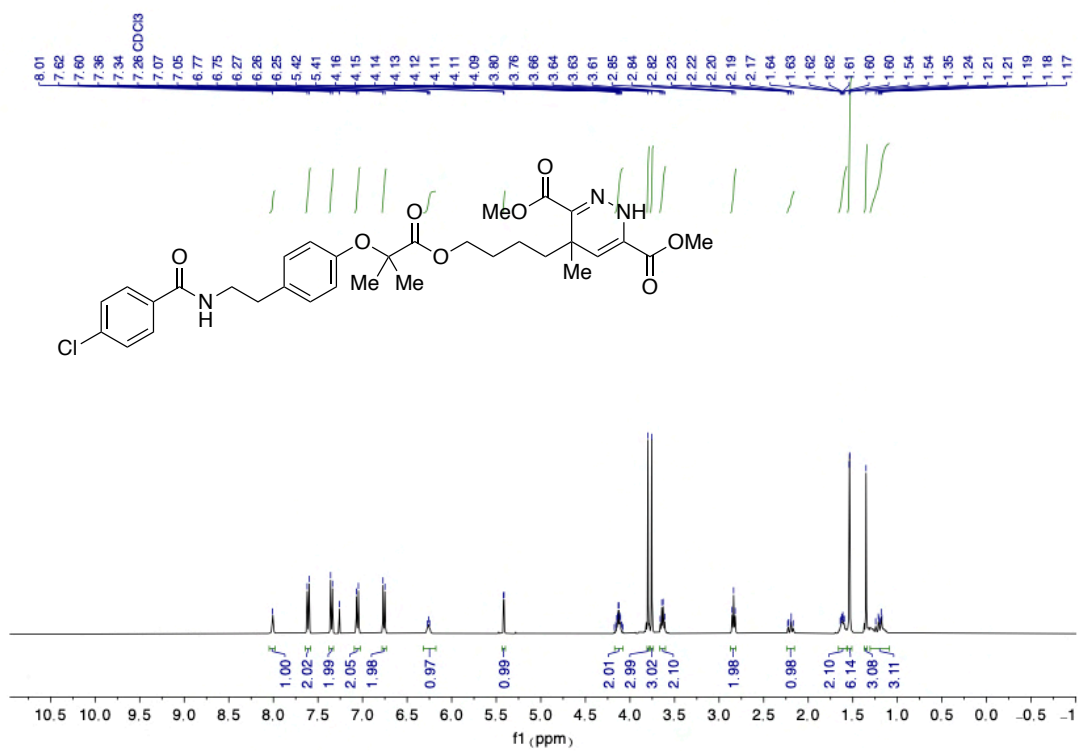




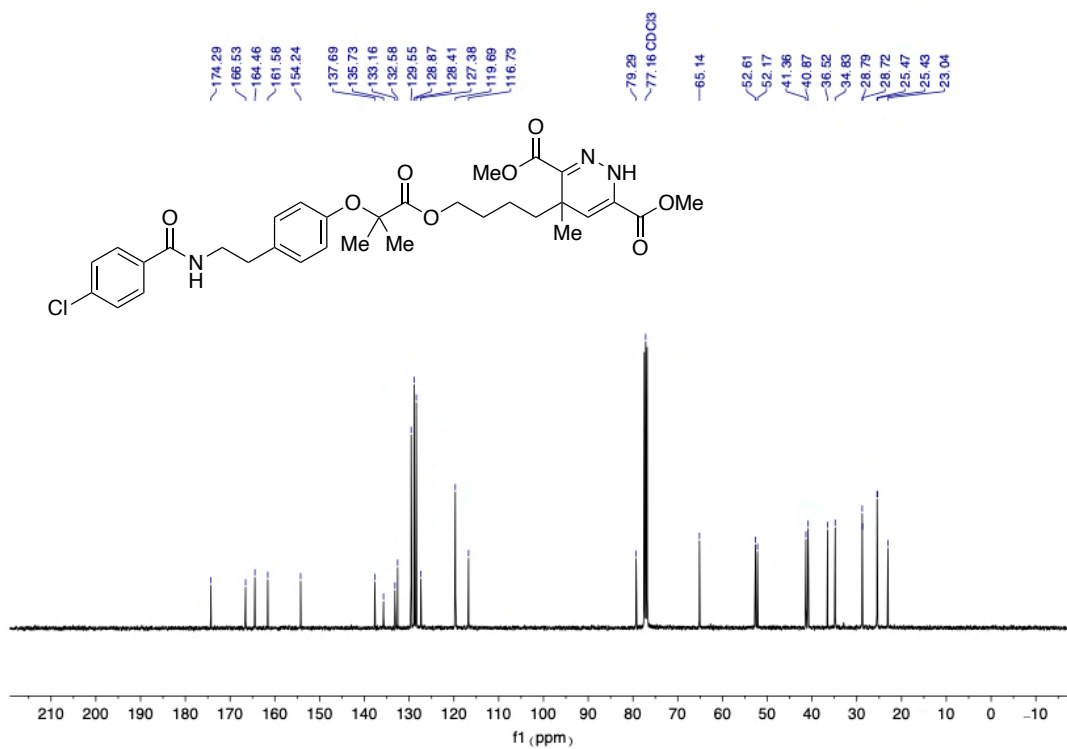




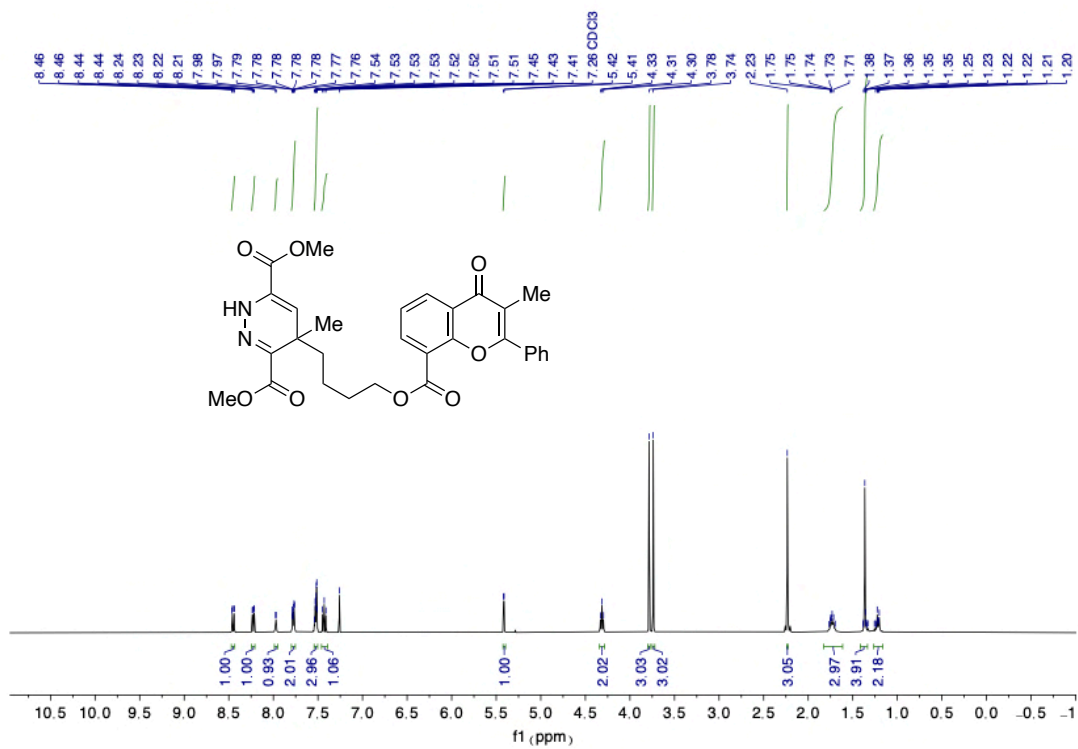
<sup>13</sup>C NMR (101 MHz, CDCl<sub>3</sub>) of **C15**



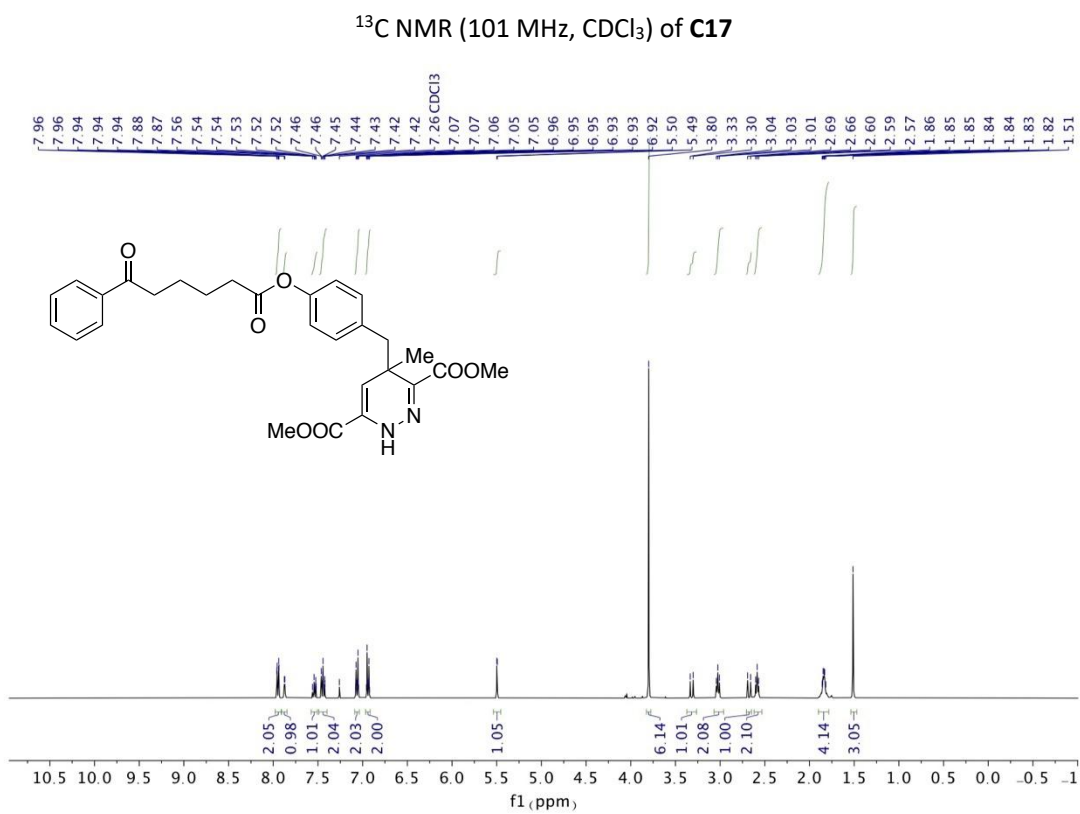
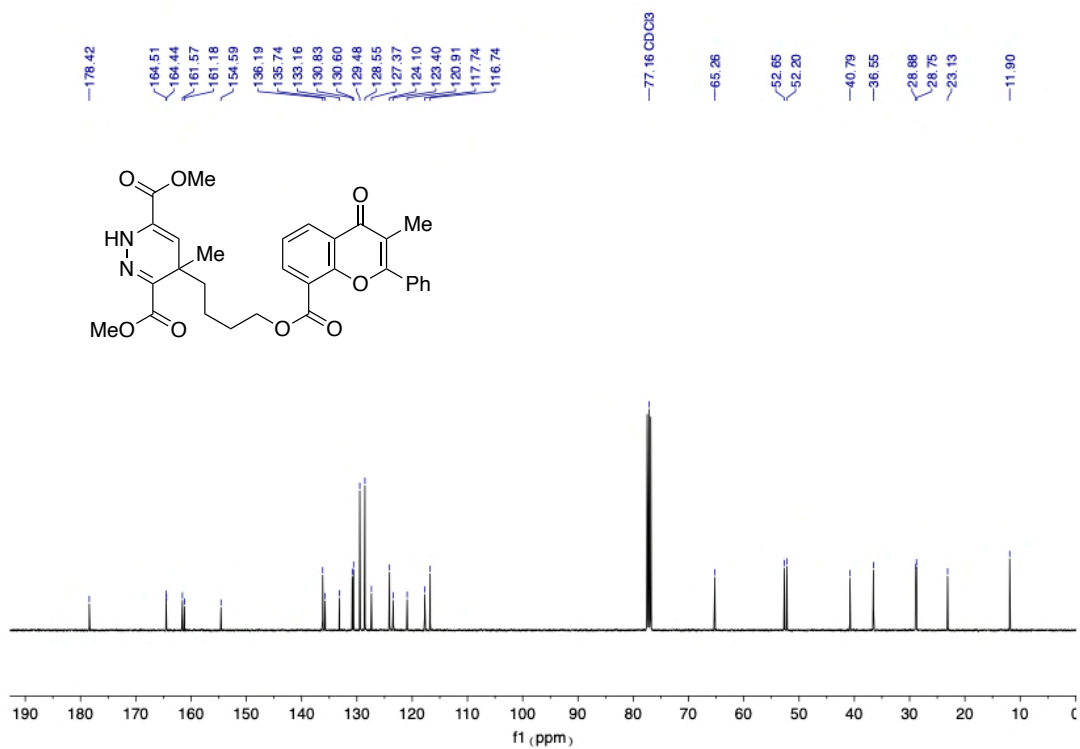
<sup>1</sup>H NMR (400 MHz, CDCl<sub>3</sub>) of **C16**



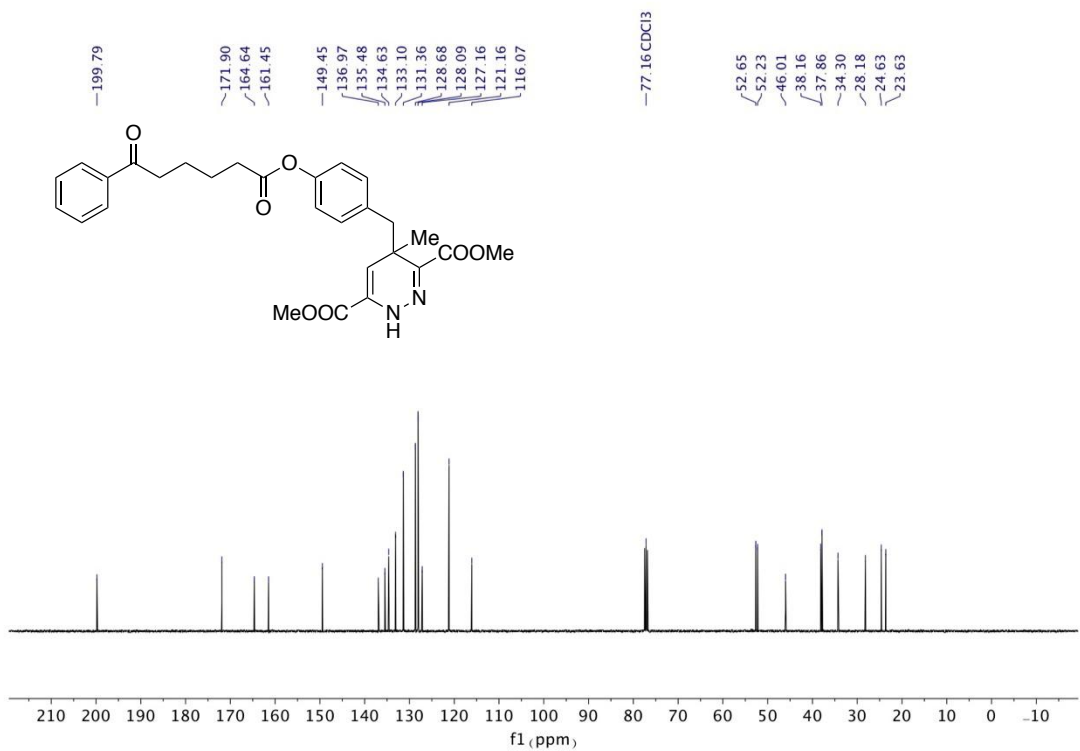
$^{13}\text{C}$  NMR (101 MHz,  $\text{CDCl}_3$ ) of **C16**



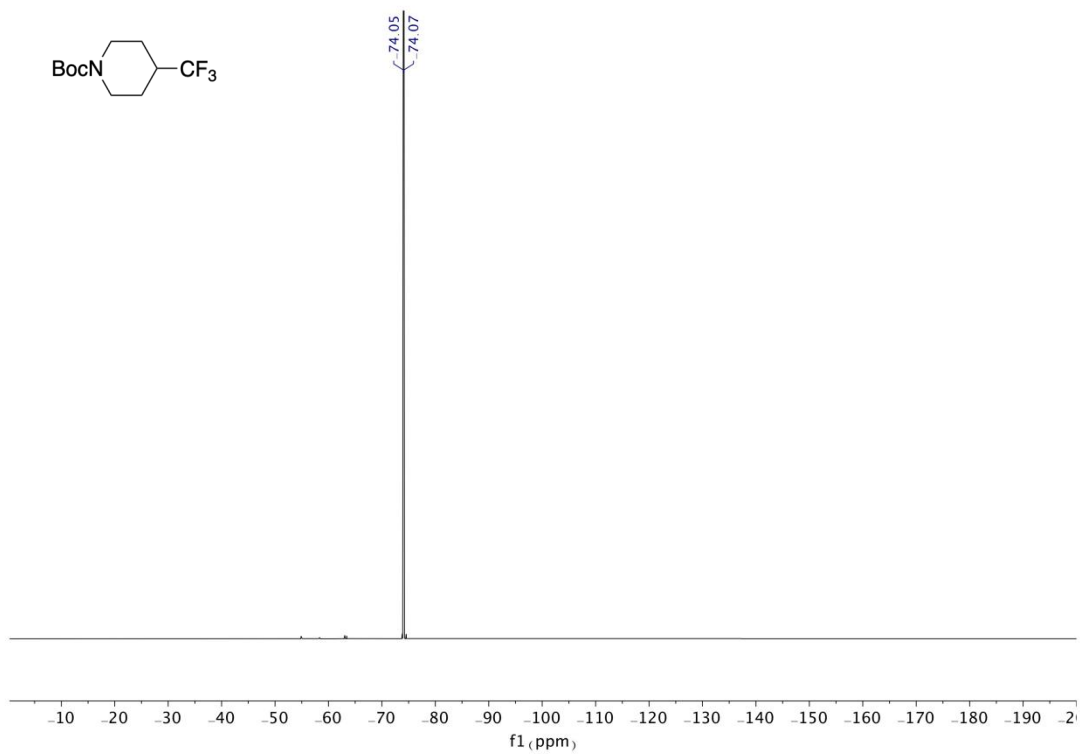
$^1\text{H}$  NMR (400 MHz,  $\text{CDCl}_3$ ) of **C17**



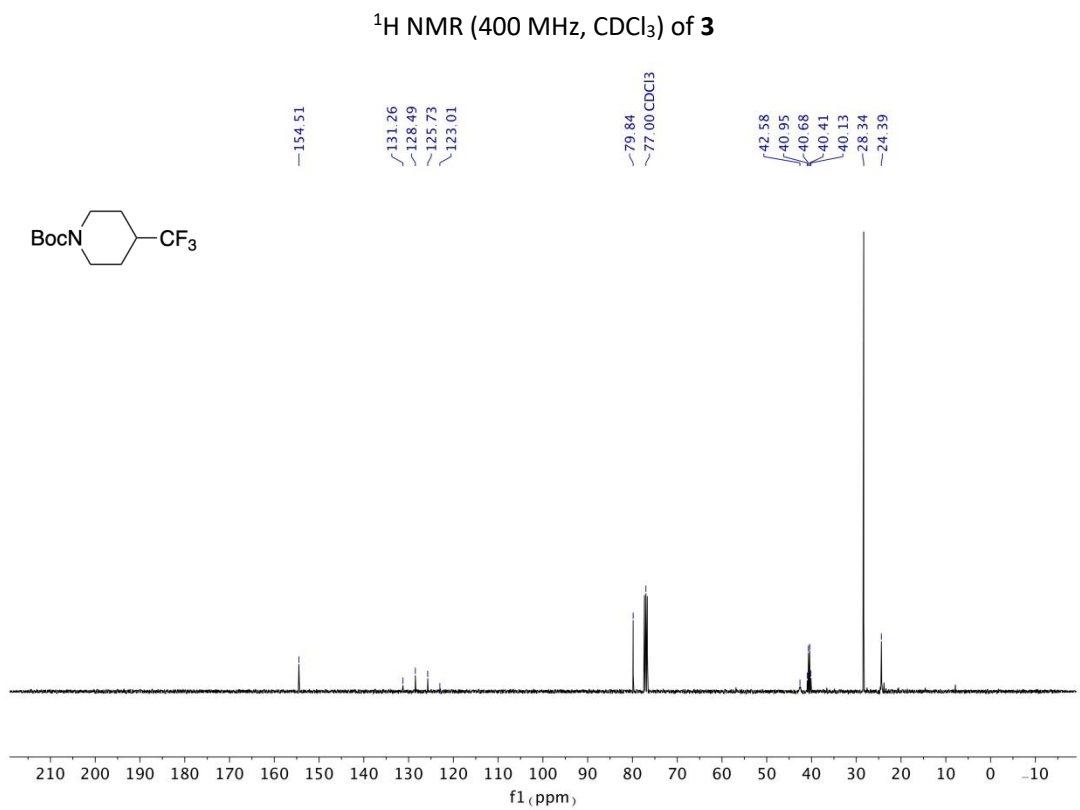
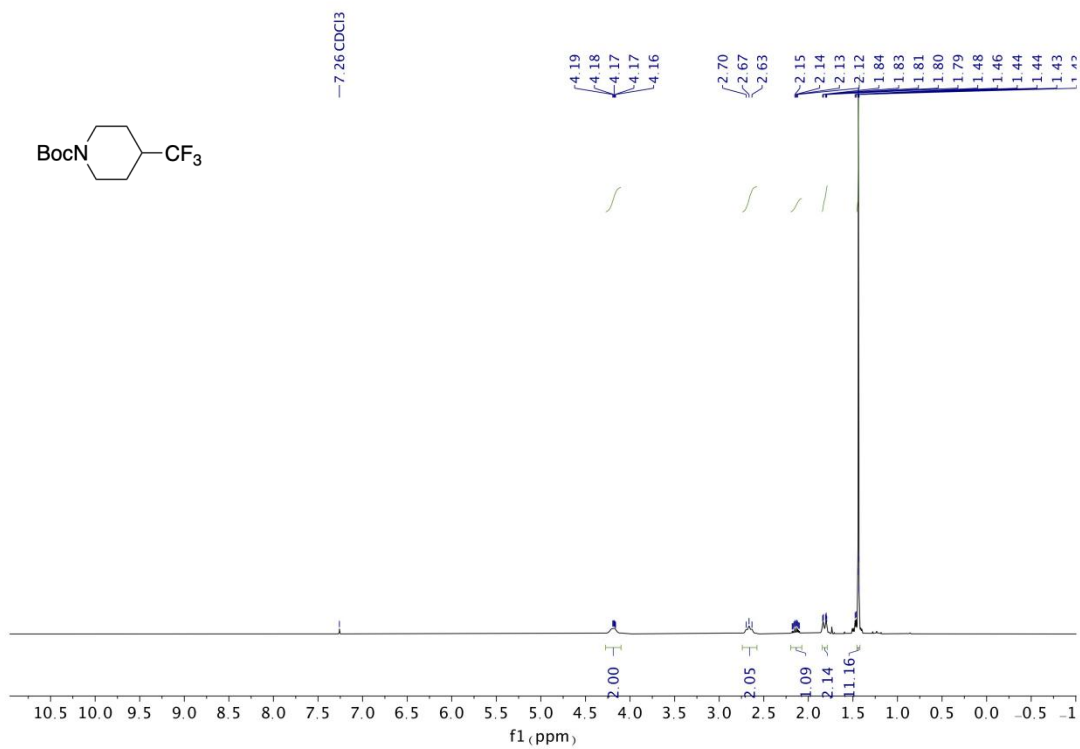
$^1\text{H}$  NMR (400 MHz,  $\text{CDCl}_3$ ) of **C18**



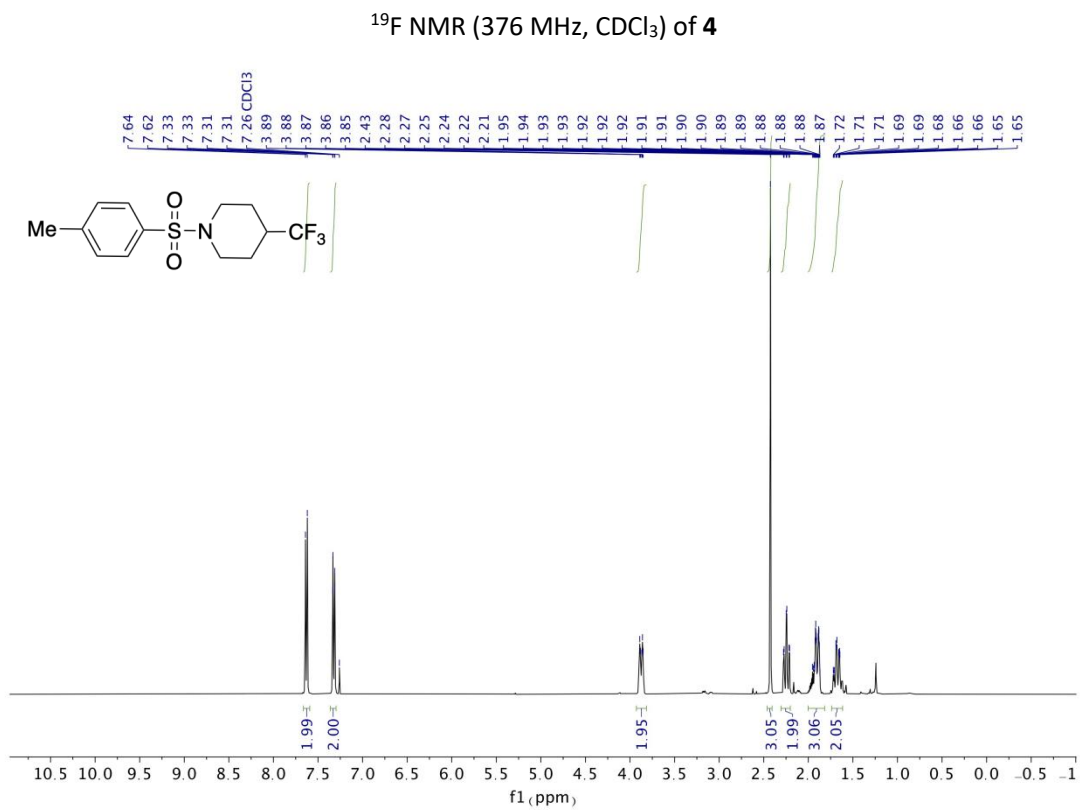
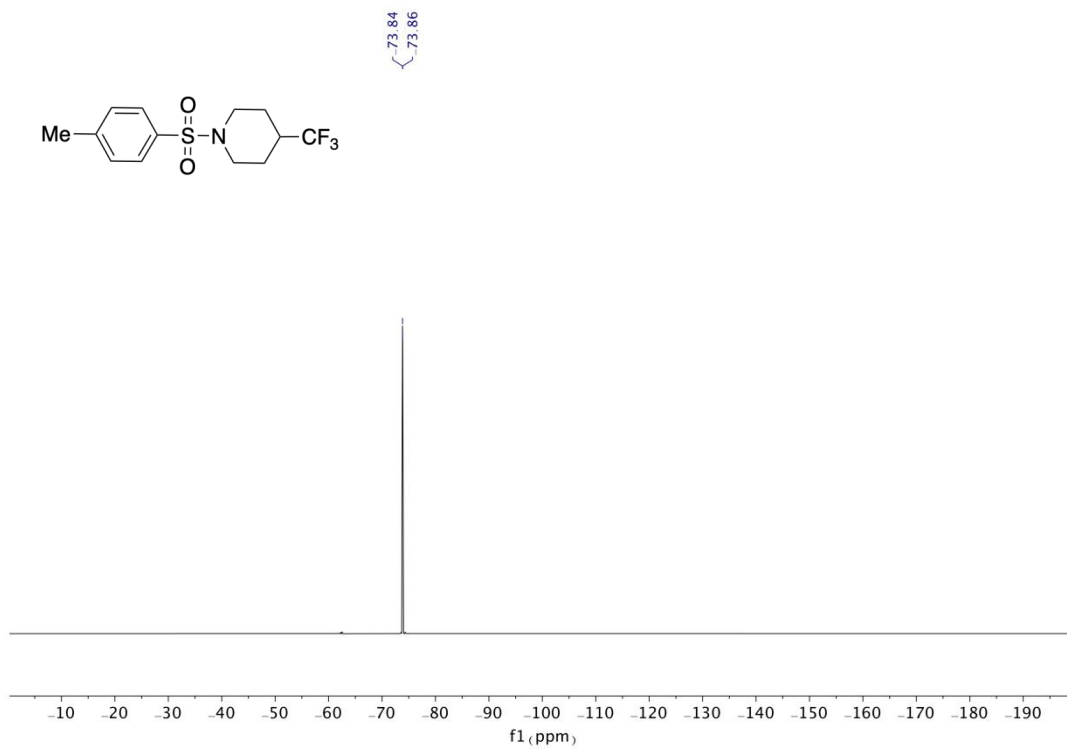
<sup>13</sup>C NMR (101 MHz, CDCl<sub>3</sub>) of **C18**

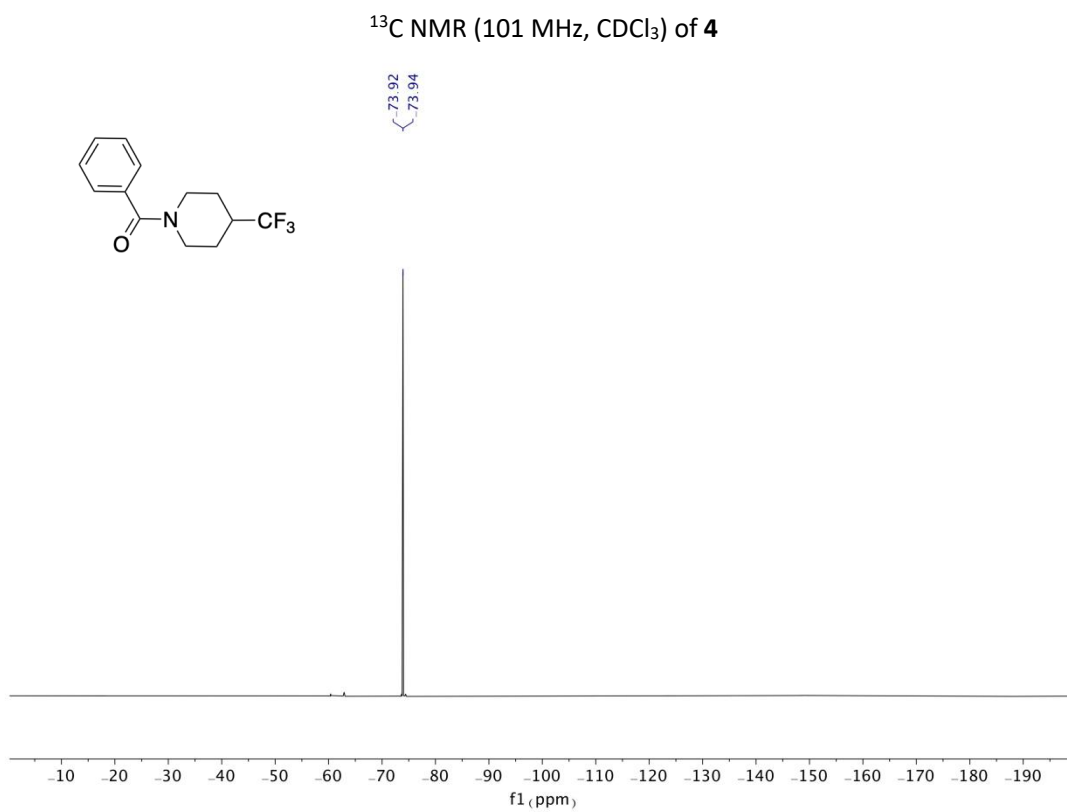
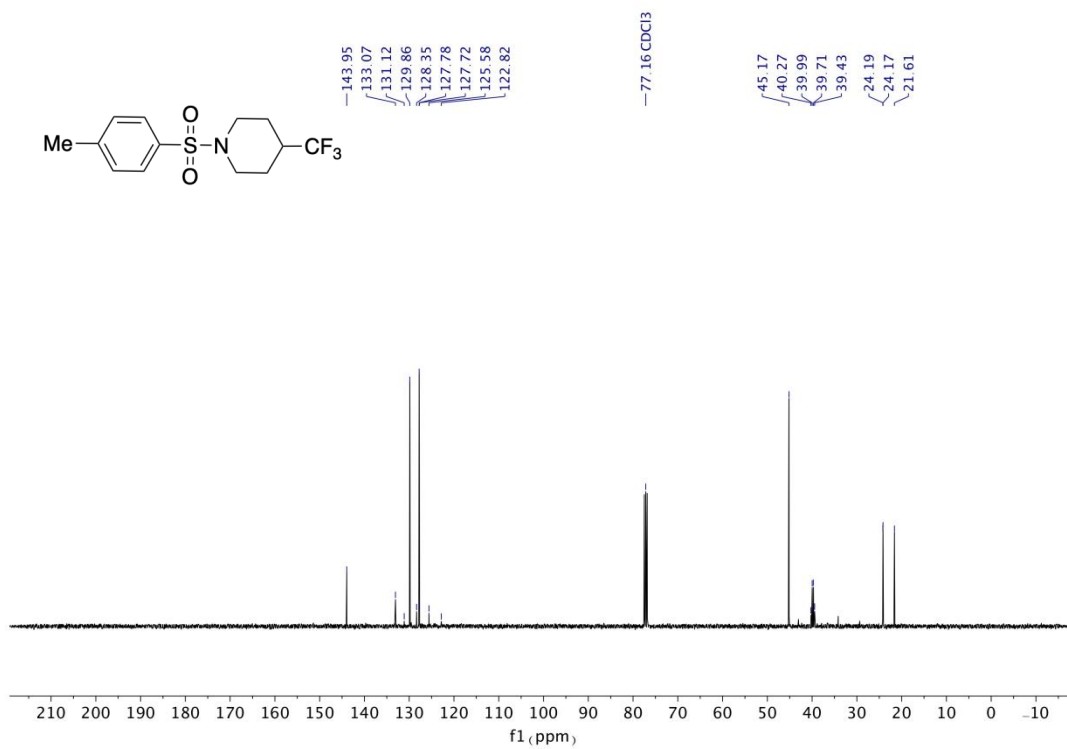


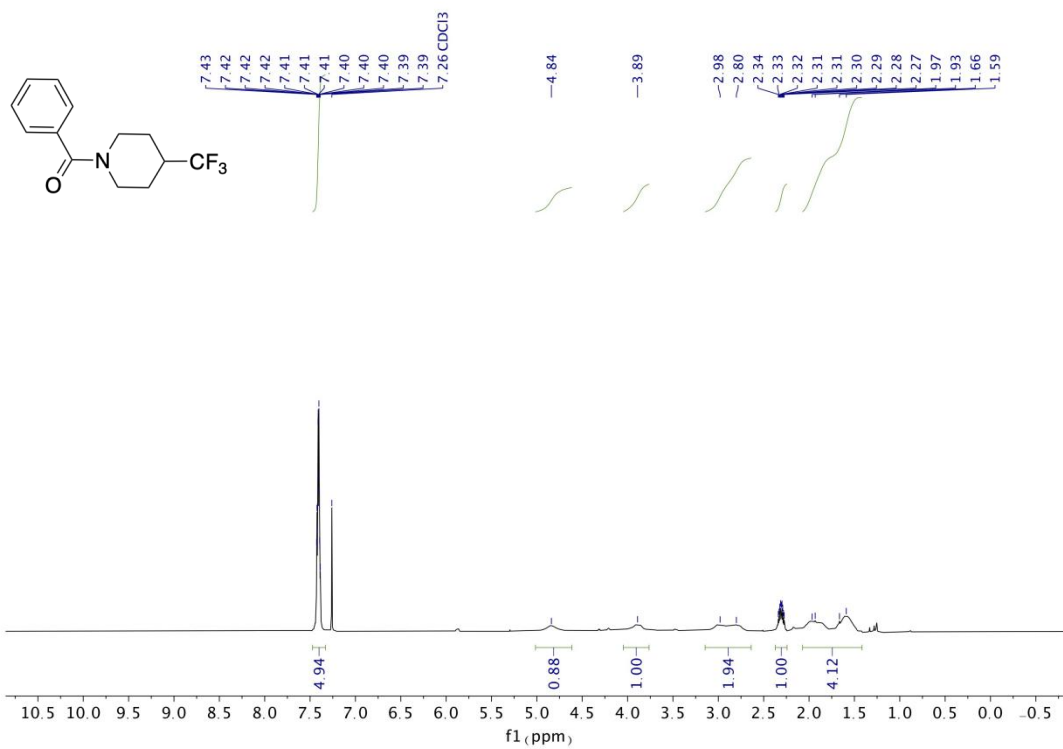
<sup>19</sup>F NMR (376 MHz, CDCl<sub>3</sub>) of **3**



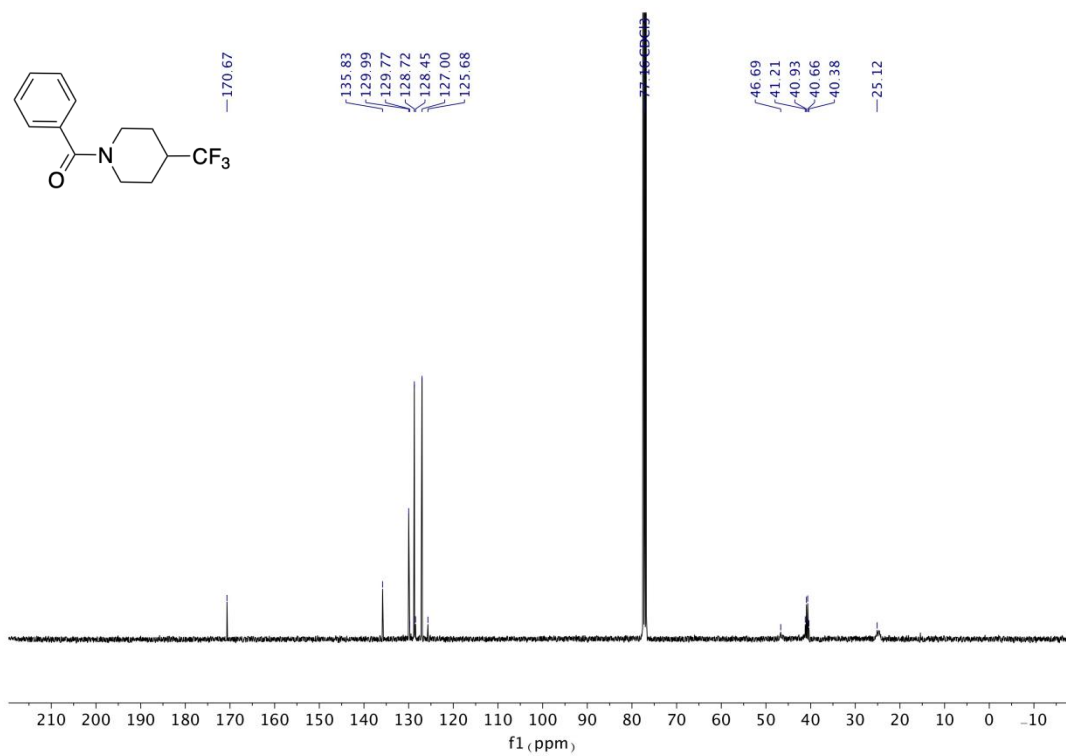




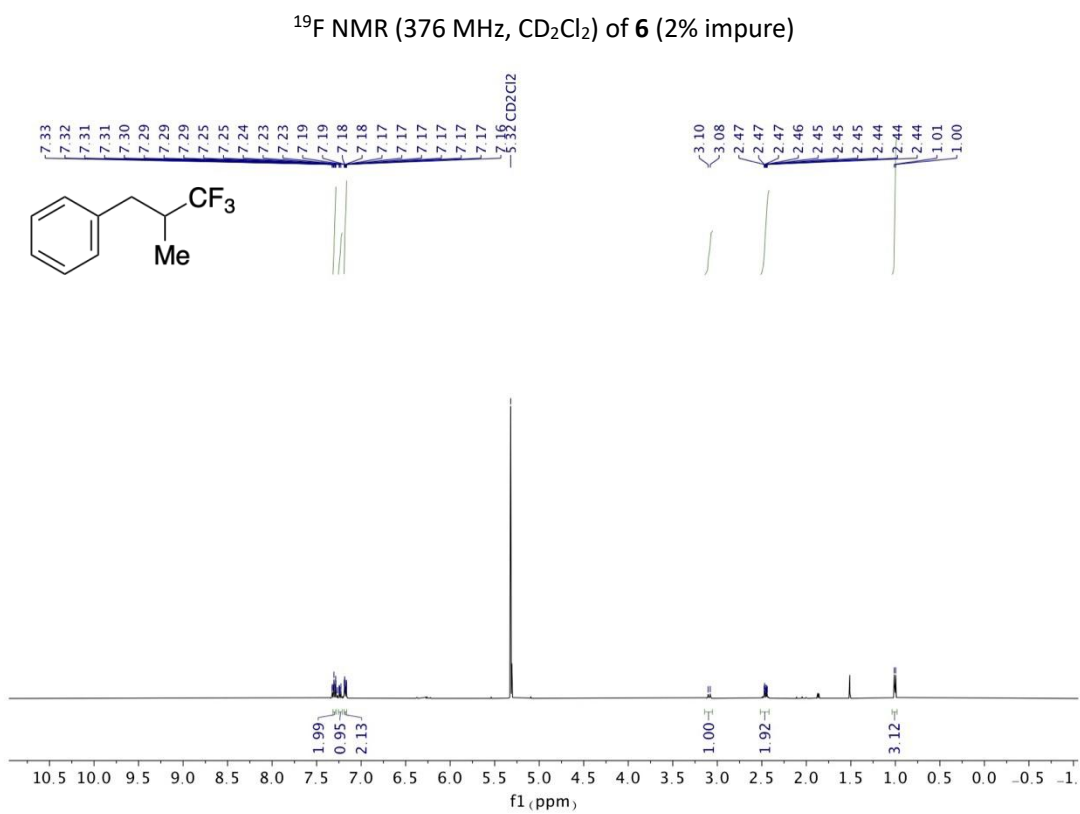
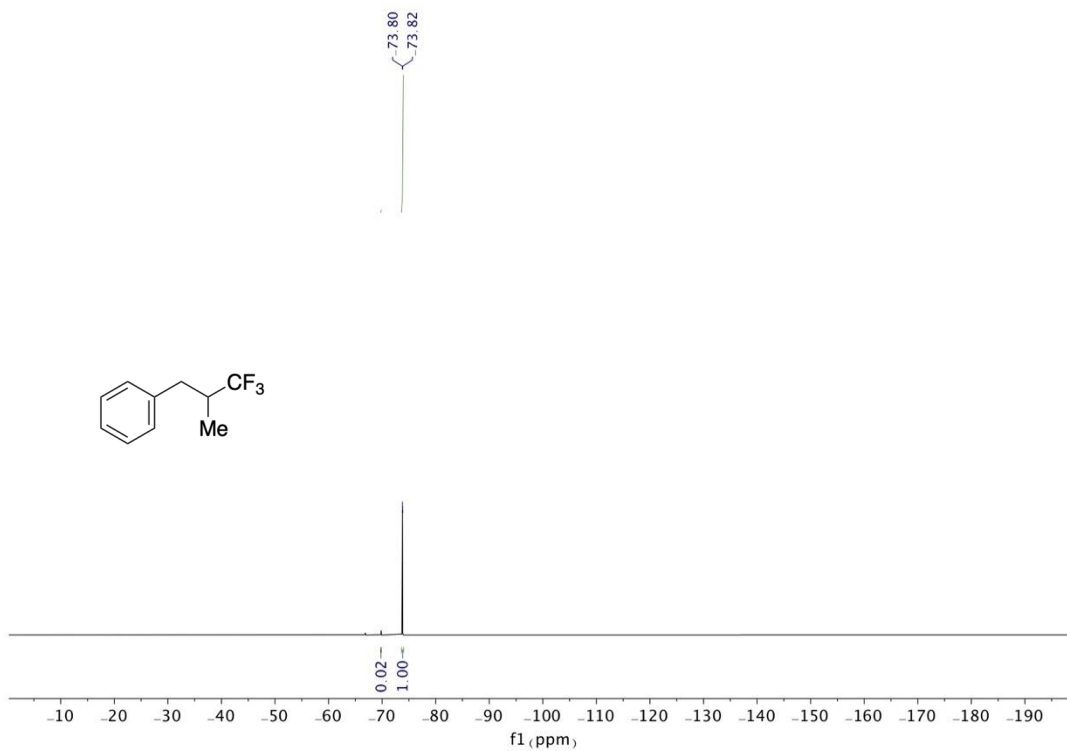


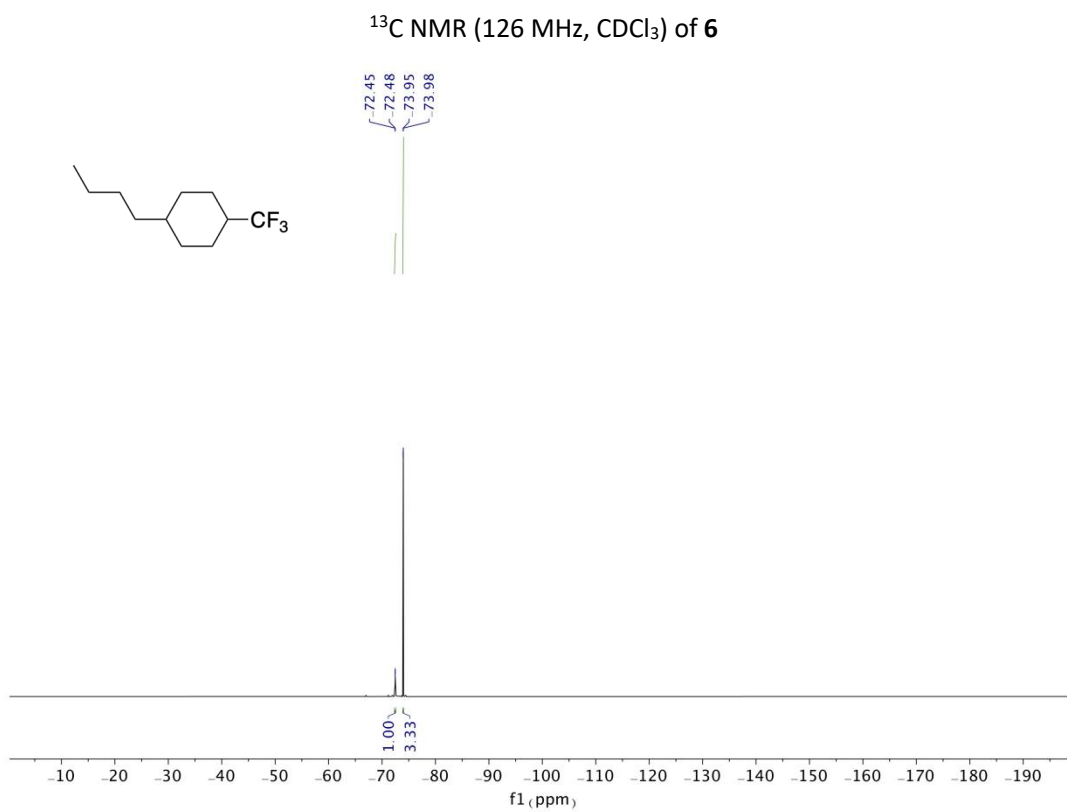
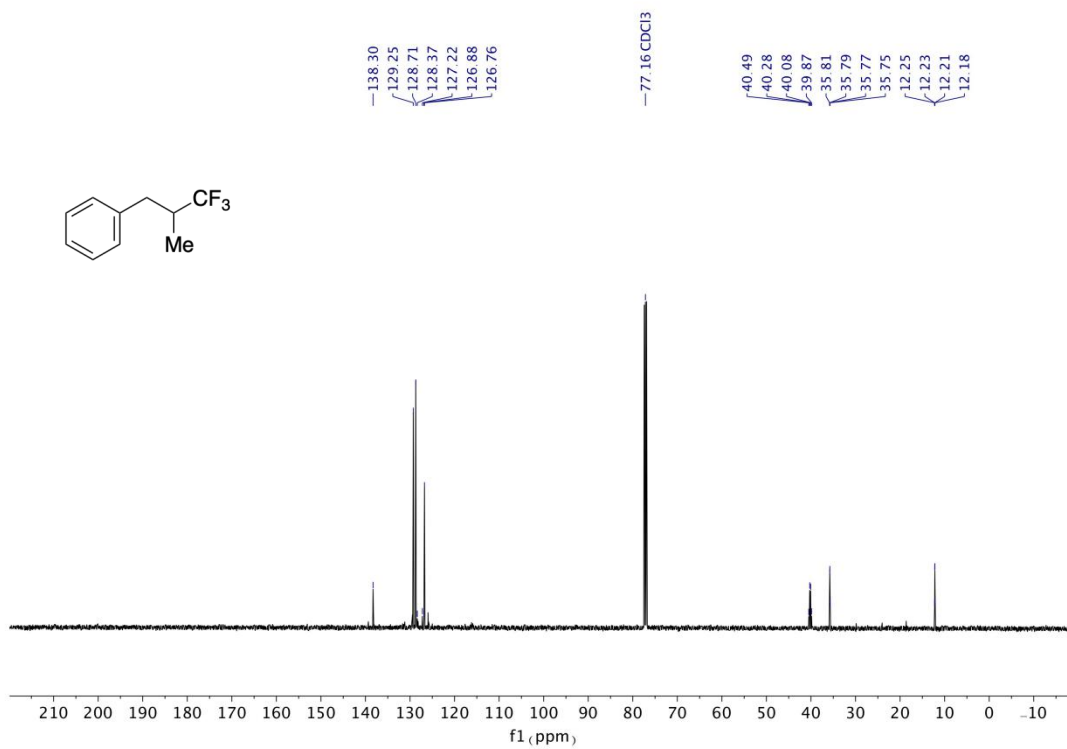


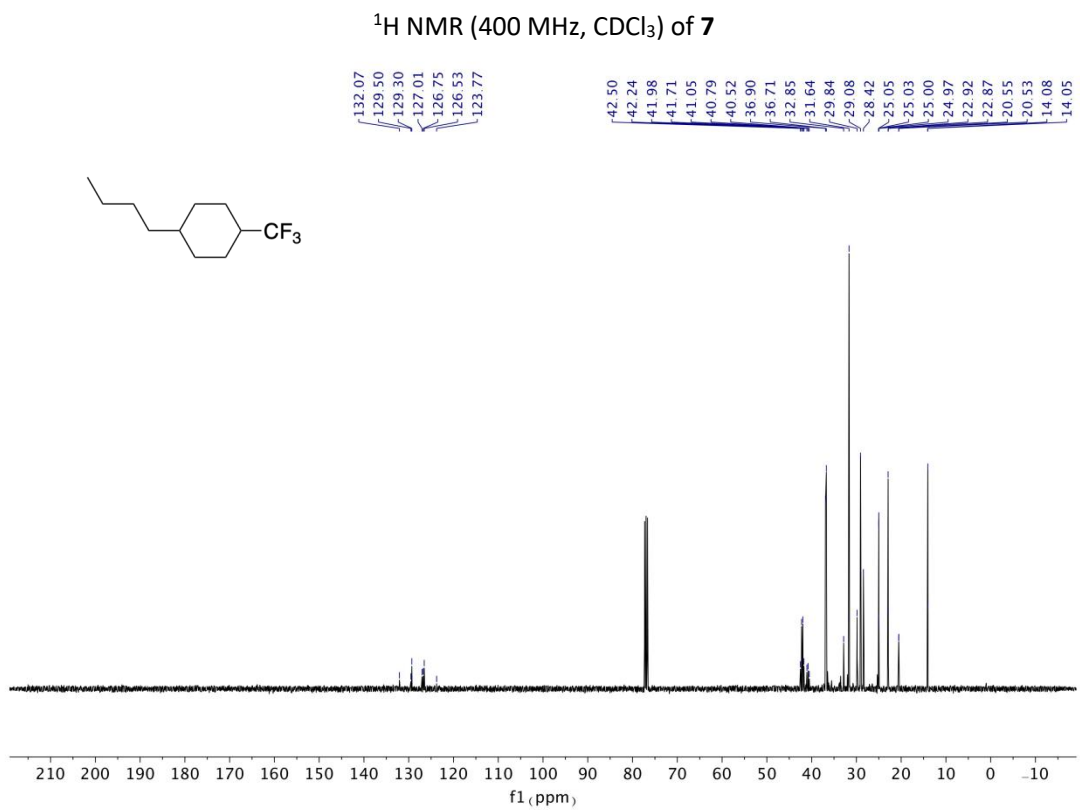
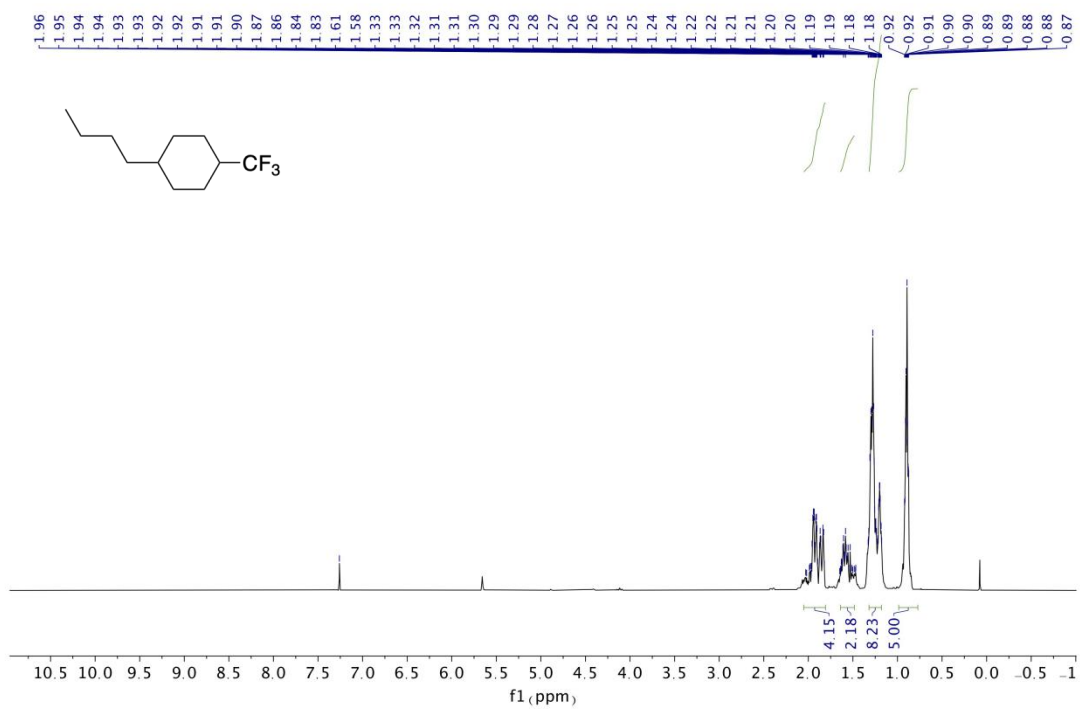
<sup>1</sup>H NMR (500 MHz, CDCl<sub>3</sub>) of 5

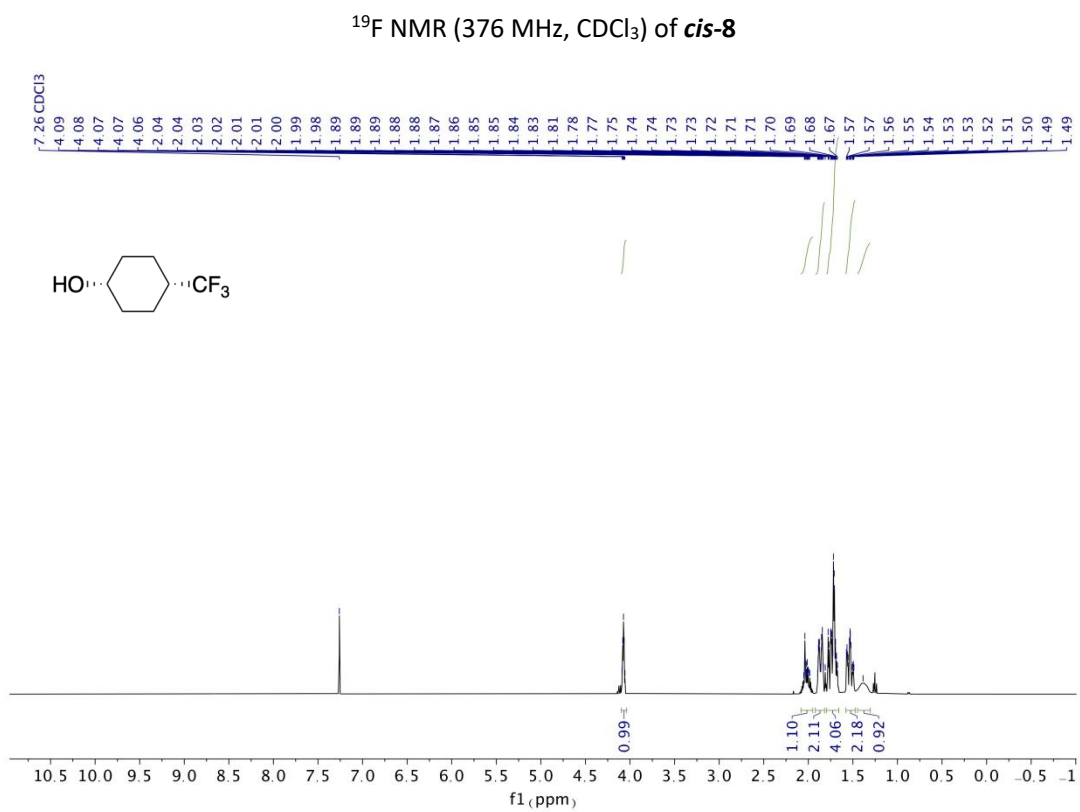
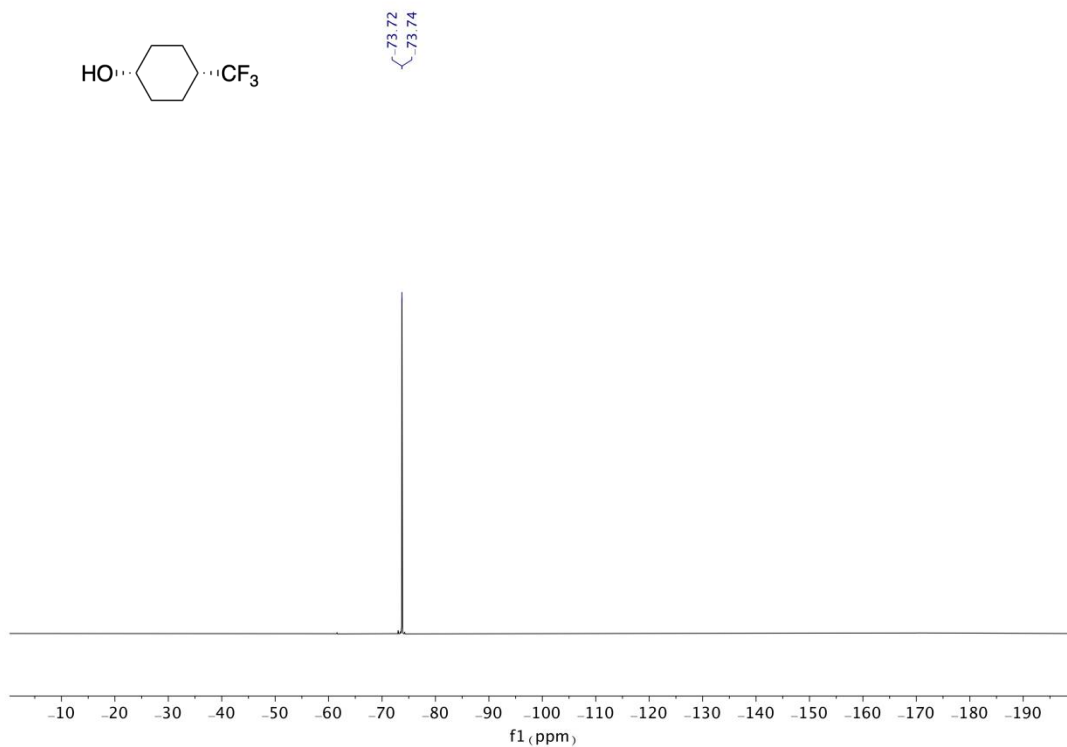


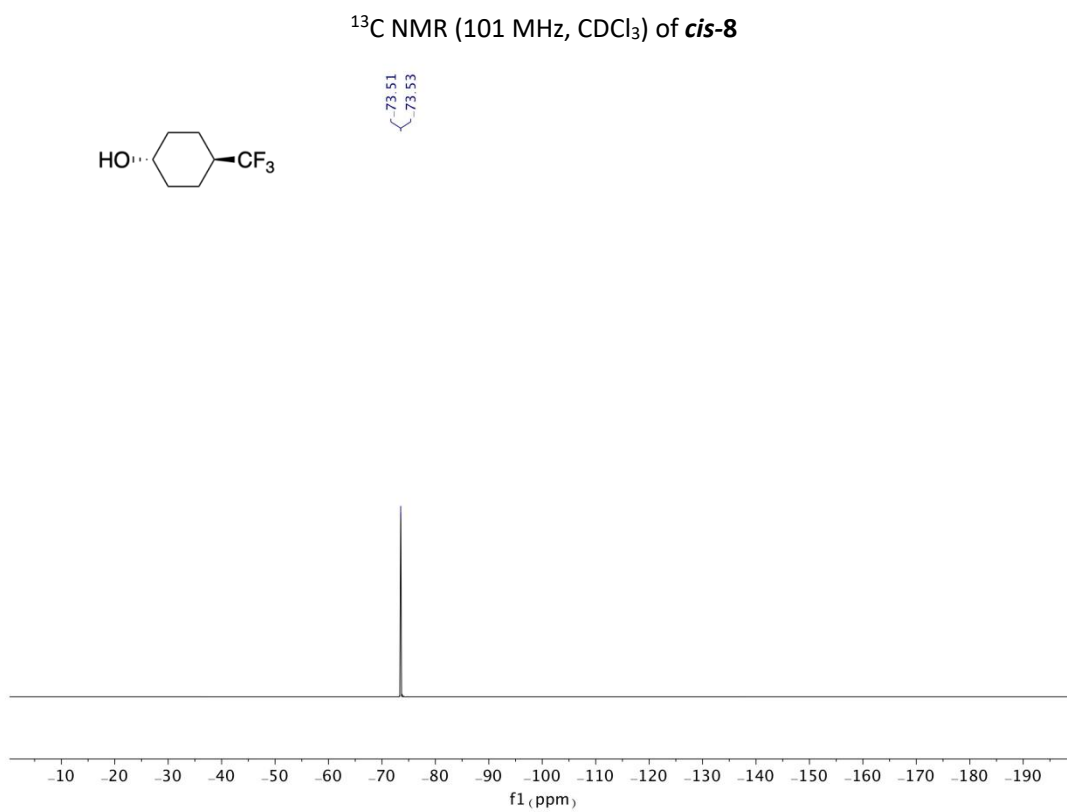
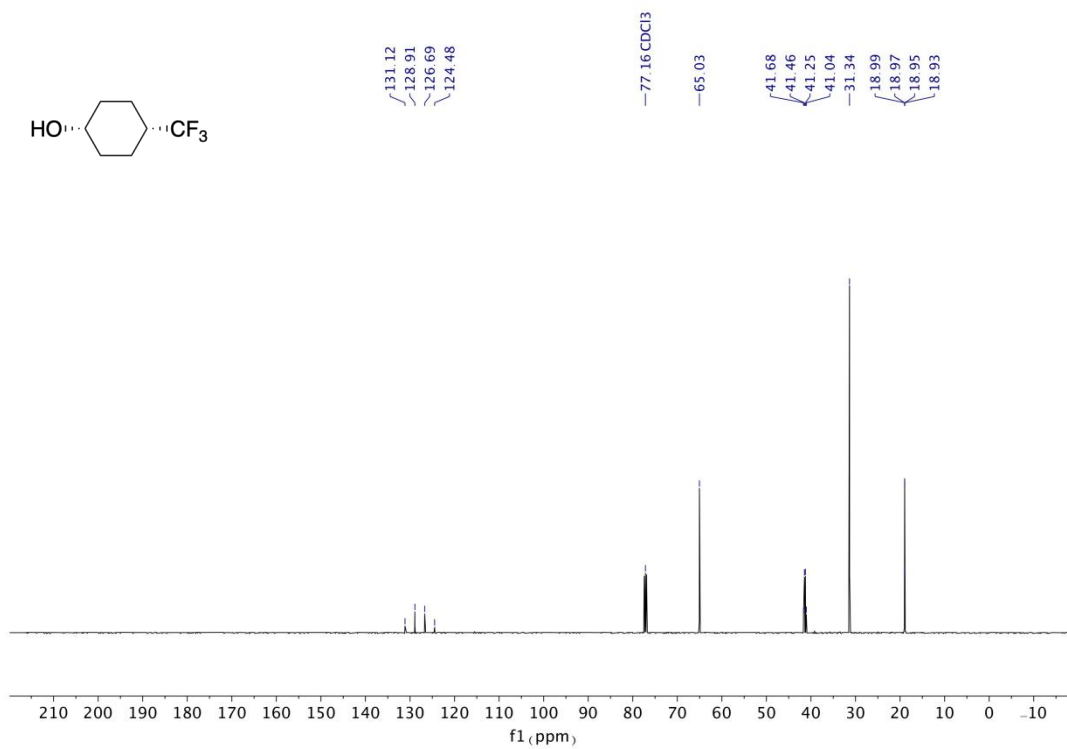
<sup>13</sup>C NMR (101 MHz, CDCl<sub>3</sub>) of 5



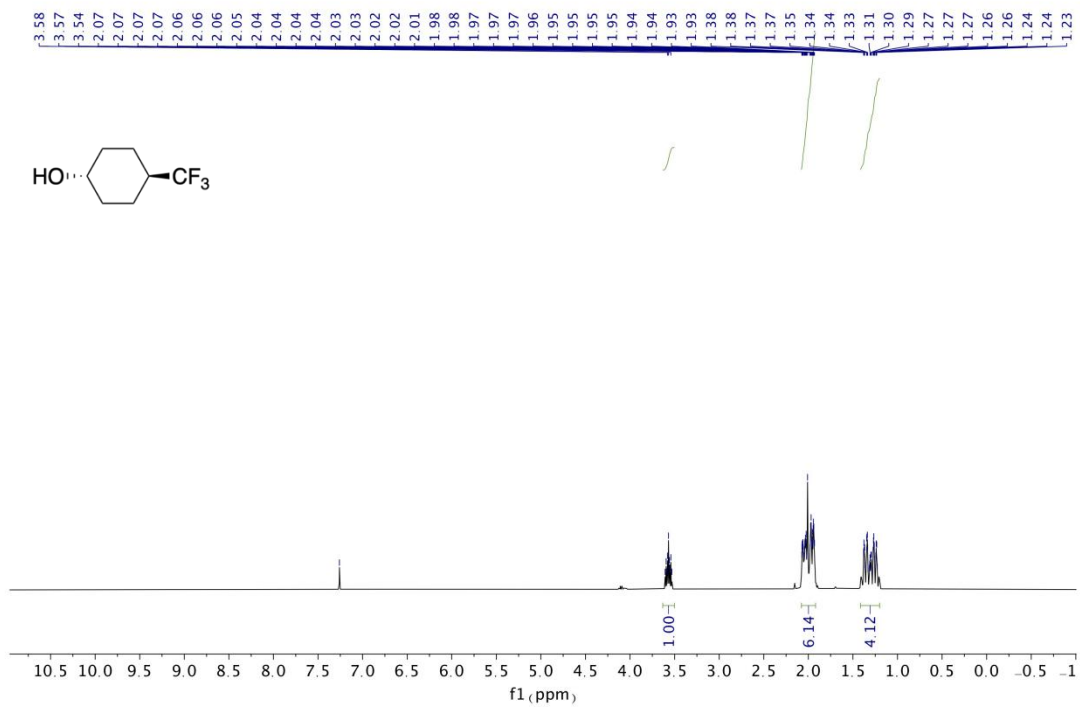




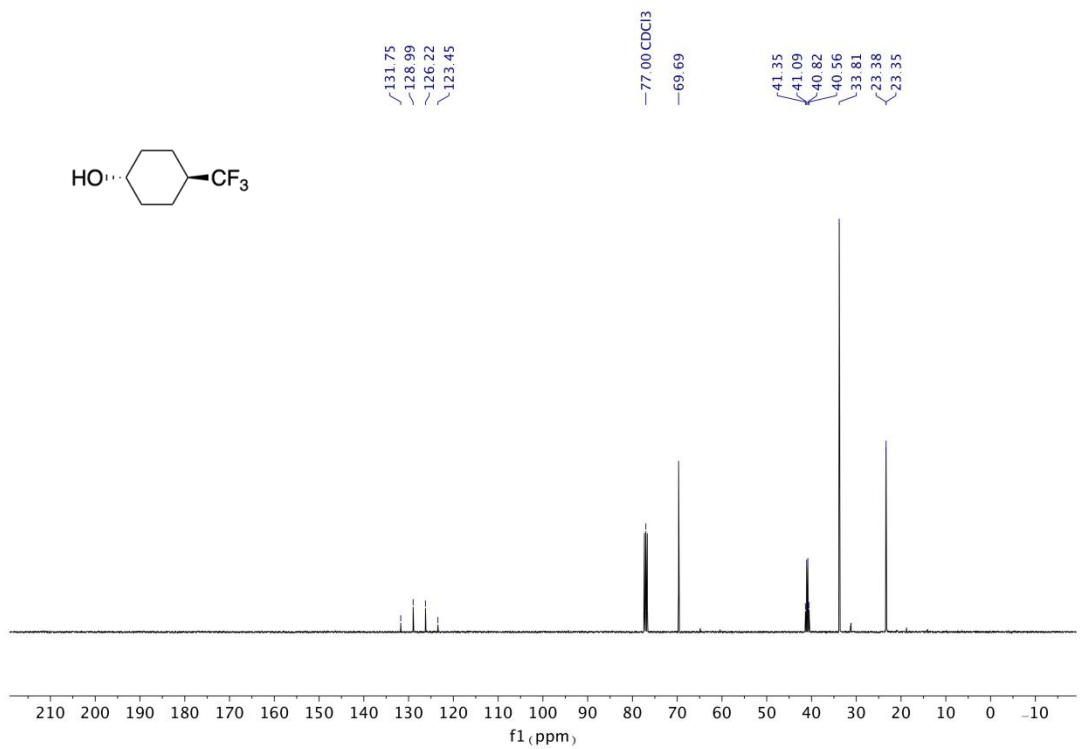




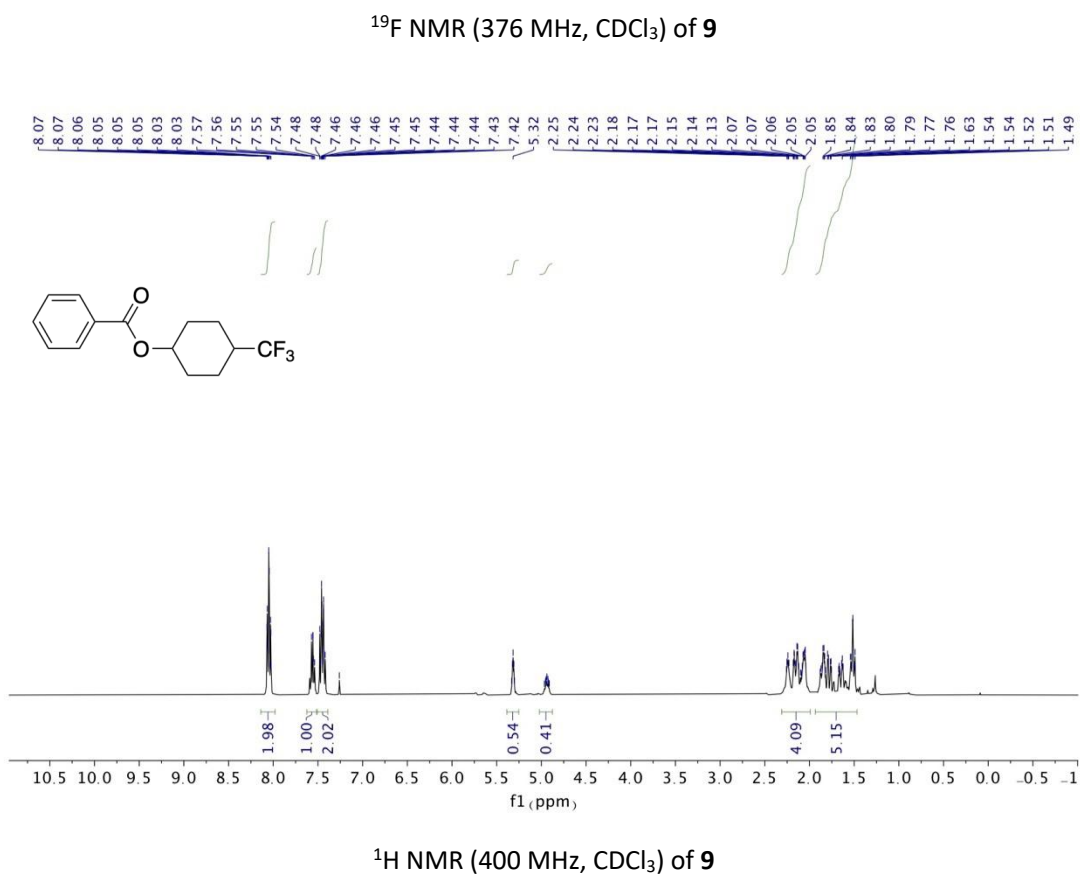
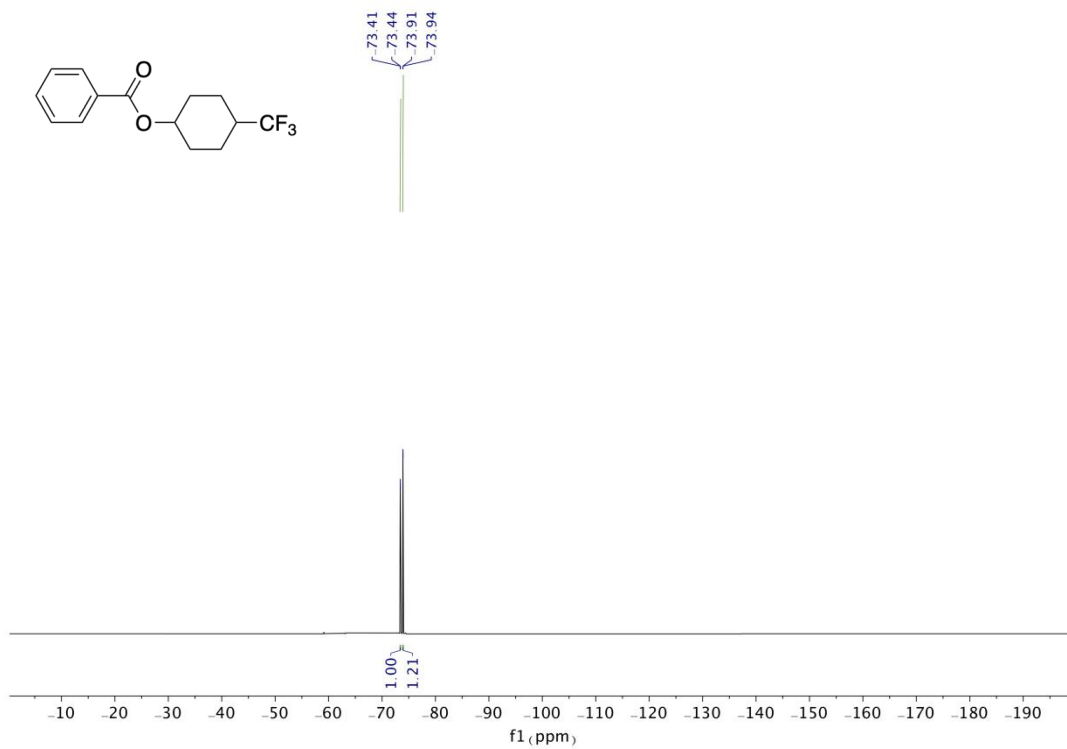


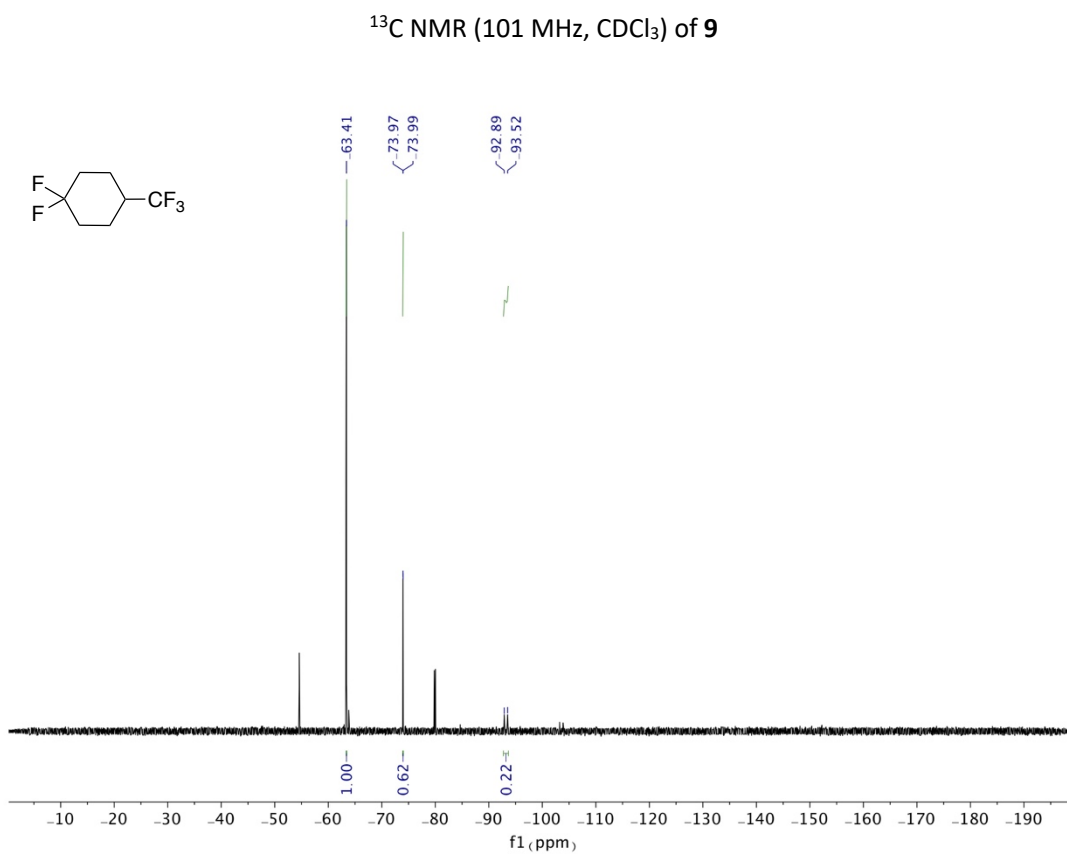
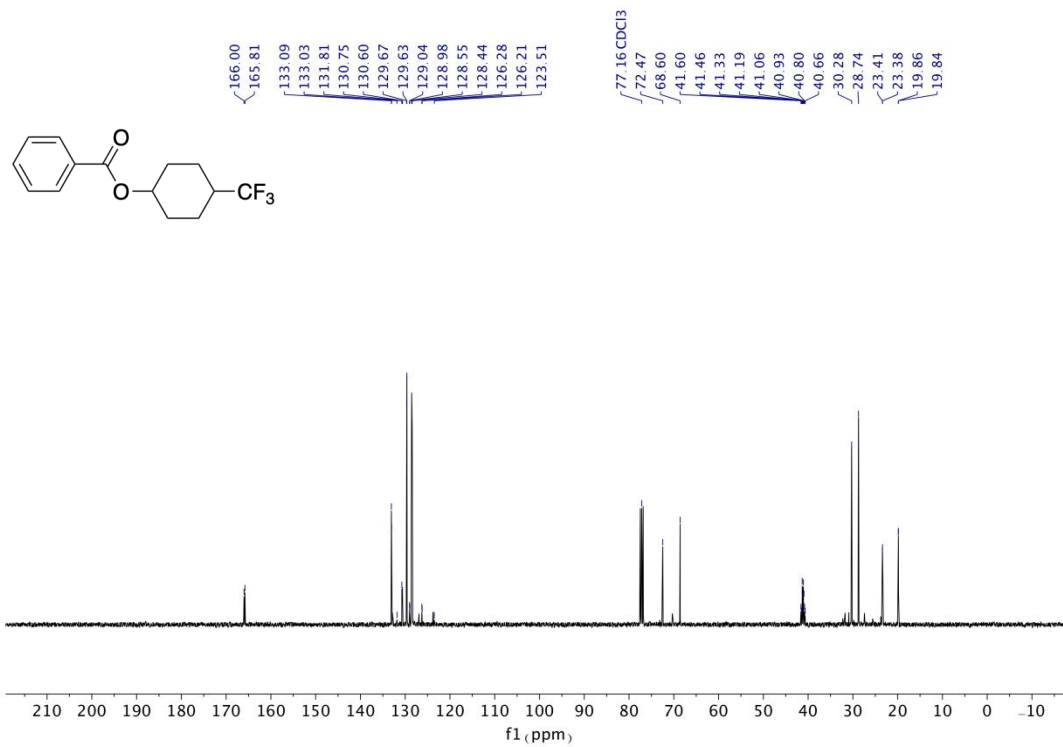


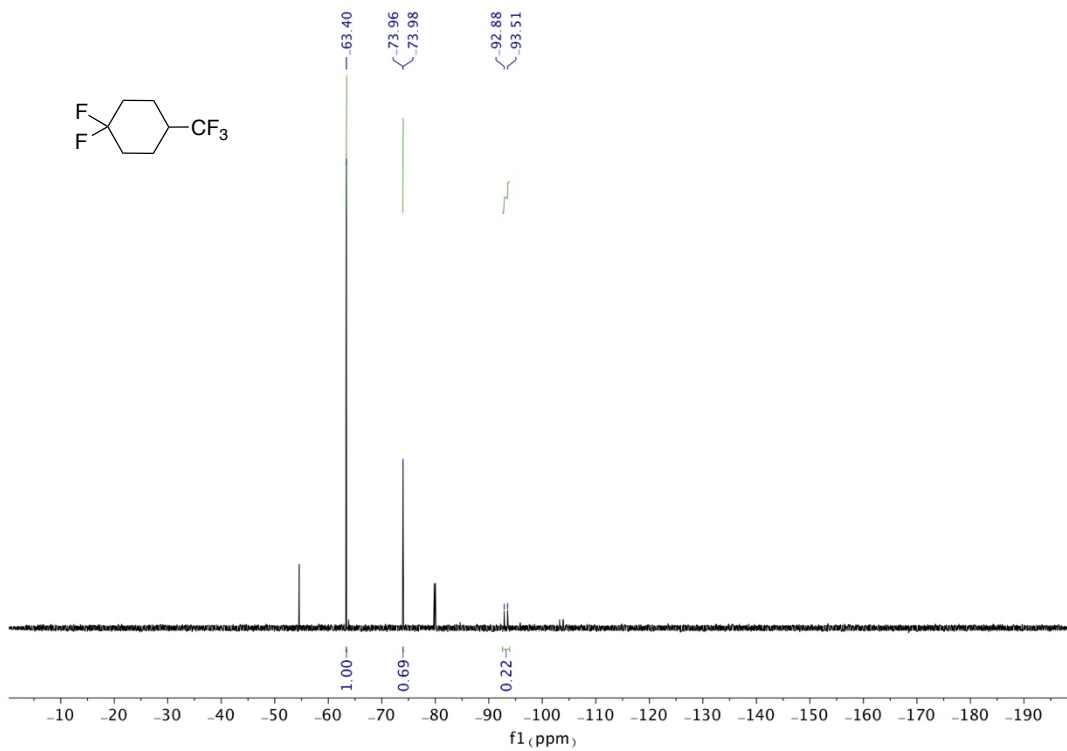
$^1\text{H}$  NMR (400 MHz,  $\text{CDCl}_3$ ) of *trans*-8



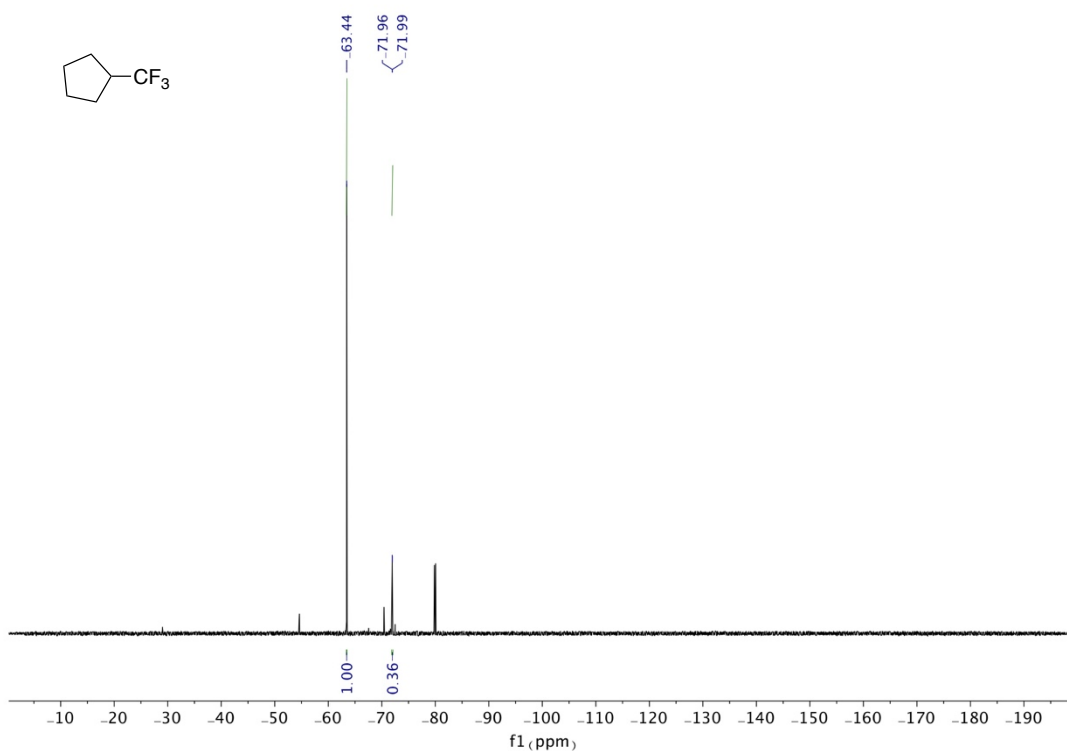
$^{13}\text{C}$  NMR (101 MHz,  $\text{CDCl}_3$ ) of *trans*-8



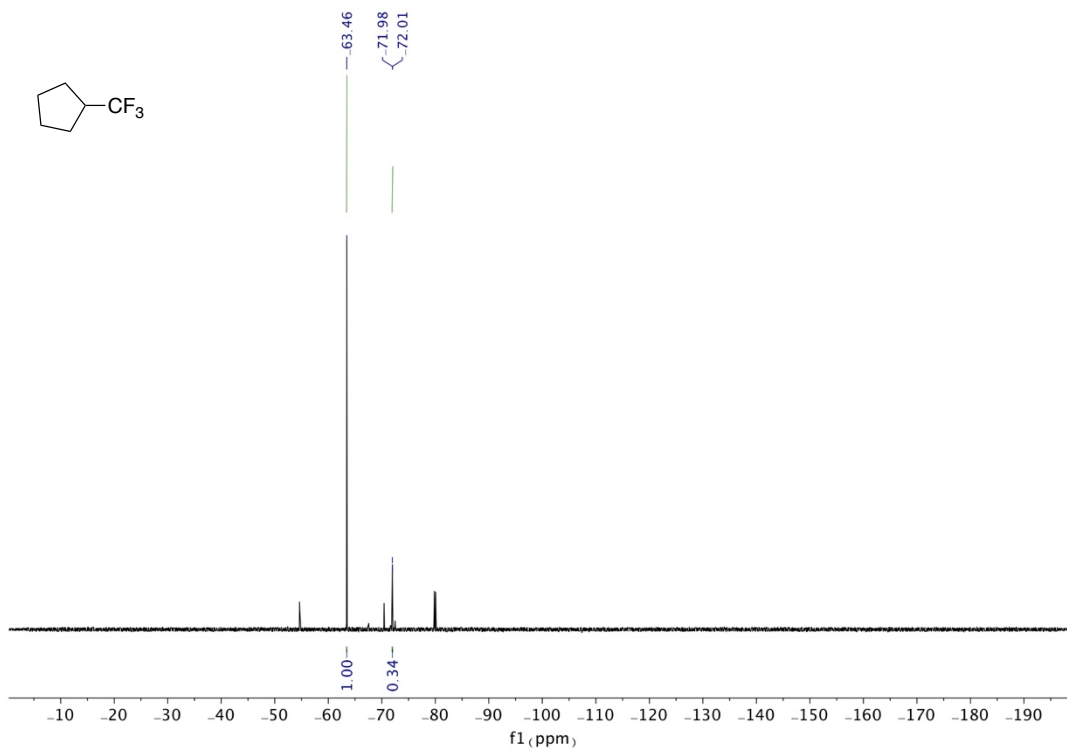




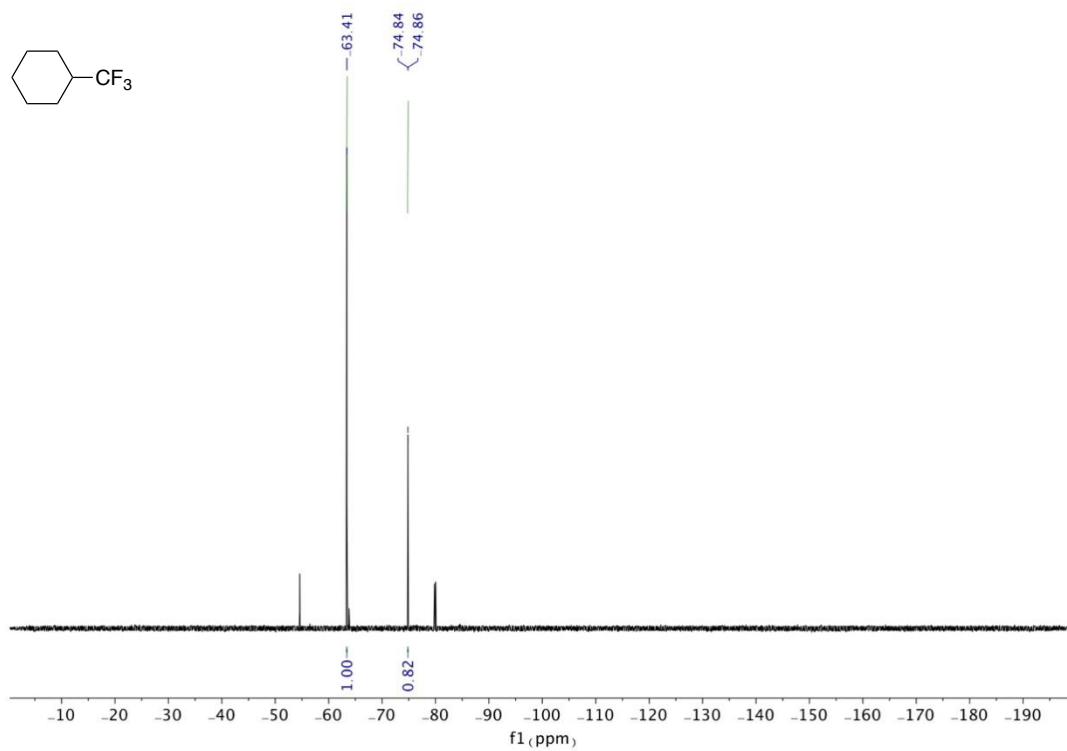
$^{19}\text{F}$  NMR assay for **10** (Experiment II)



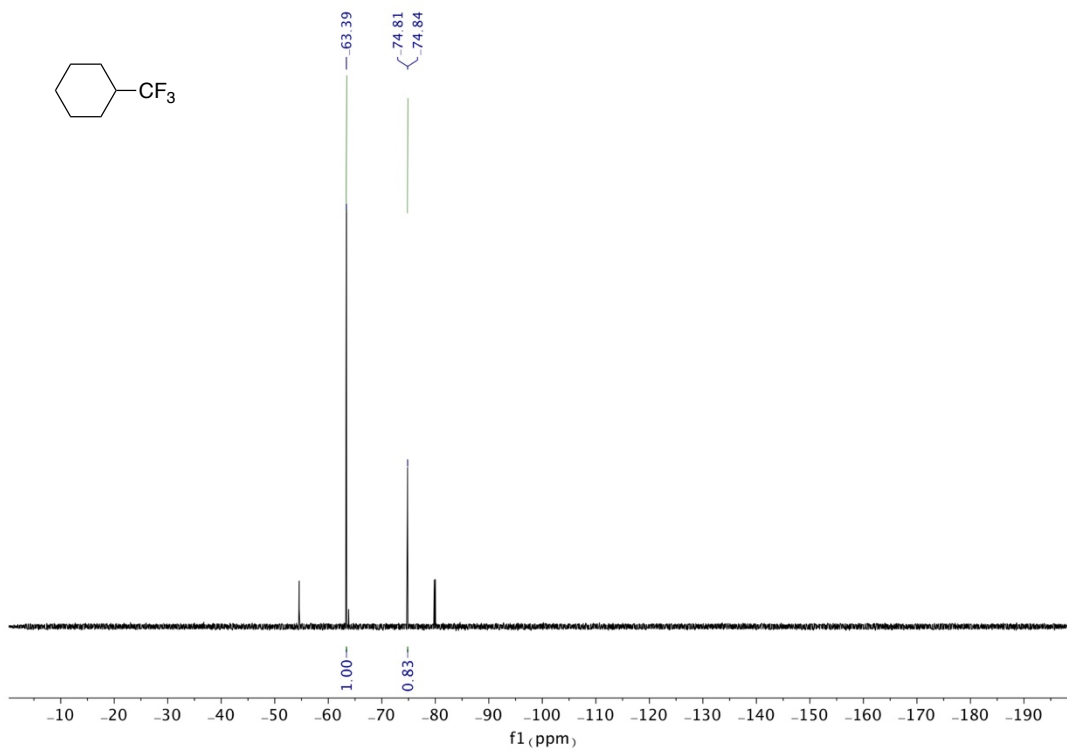
$^{19}\text{F}$  NMR assay for **11** (Experiment I)



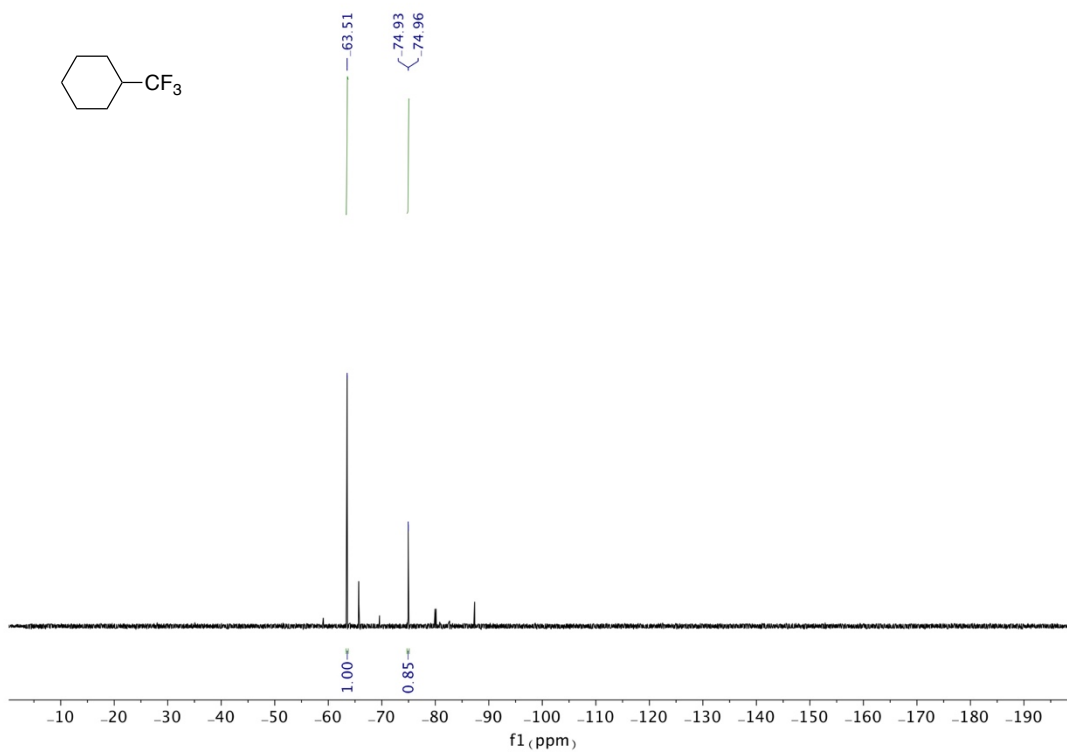
$^{19}\text{F}$  NMR assay for **11**(Experiment II)



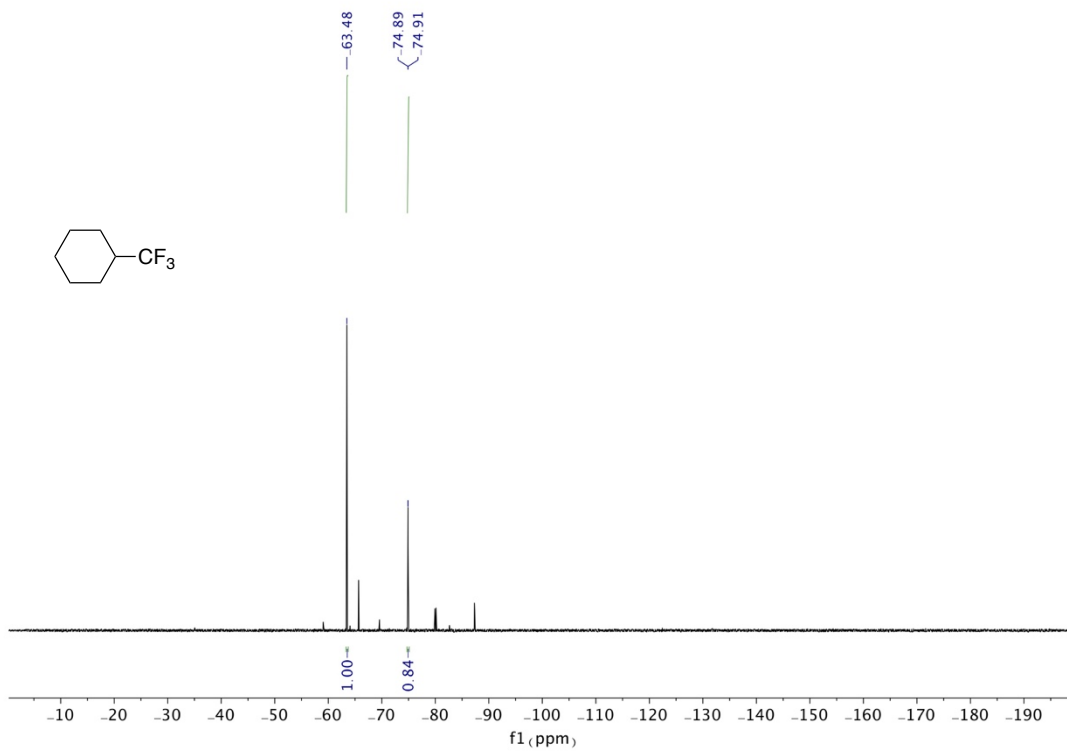
$^{19}\text{F}$  NMR assay for **12** from **A10** (Experiment I)



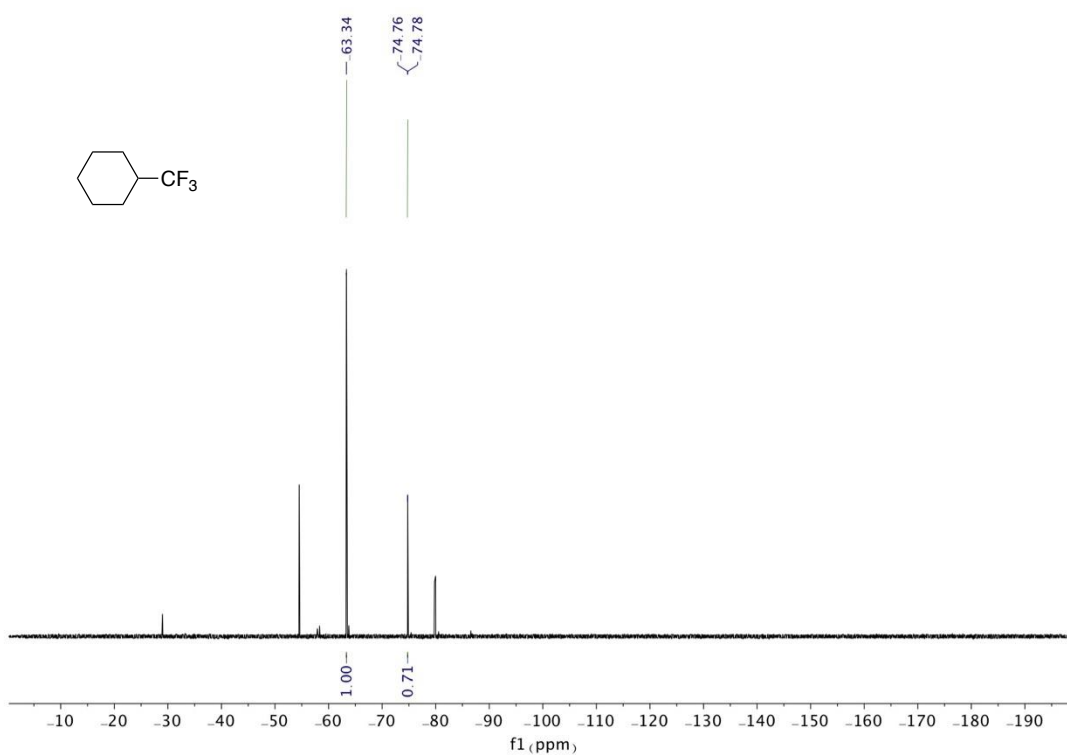
$^{19}\text{F}$  NMR assay for **12** from **A10** (Experiment II)



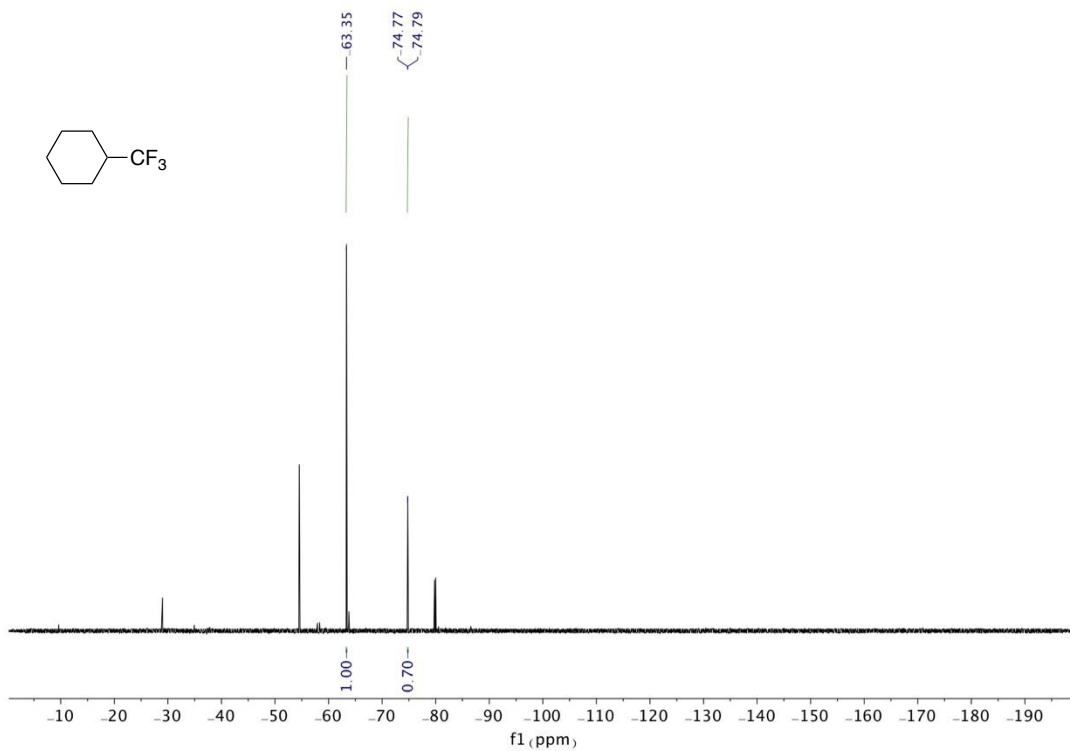
$^{19}\text{F}$  NMR assay for **12** from **B1** (Experiment I)



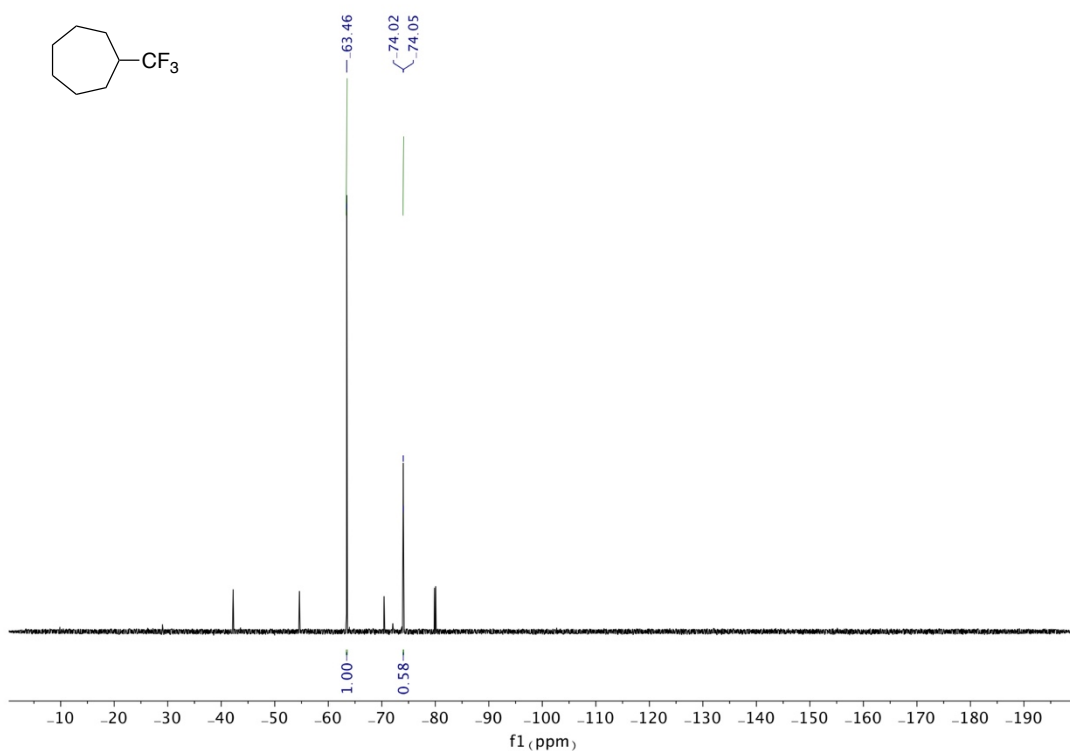
<sup>19</sup>F NMR assay for **12** from **B1** (Experiment II)



<sup>19</sup>F NMR assay for **12** from **C1** (Experiment I)

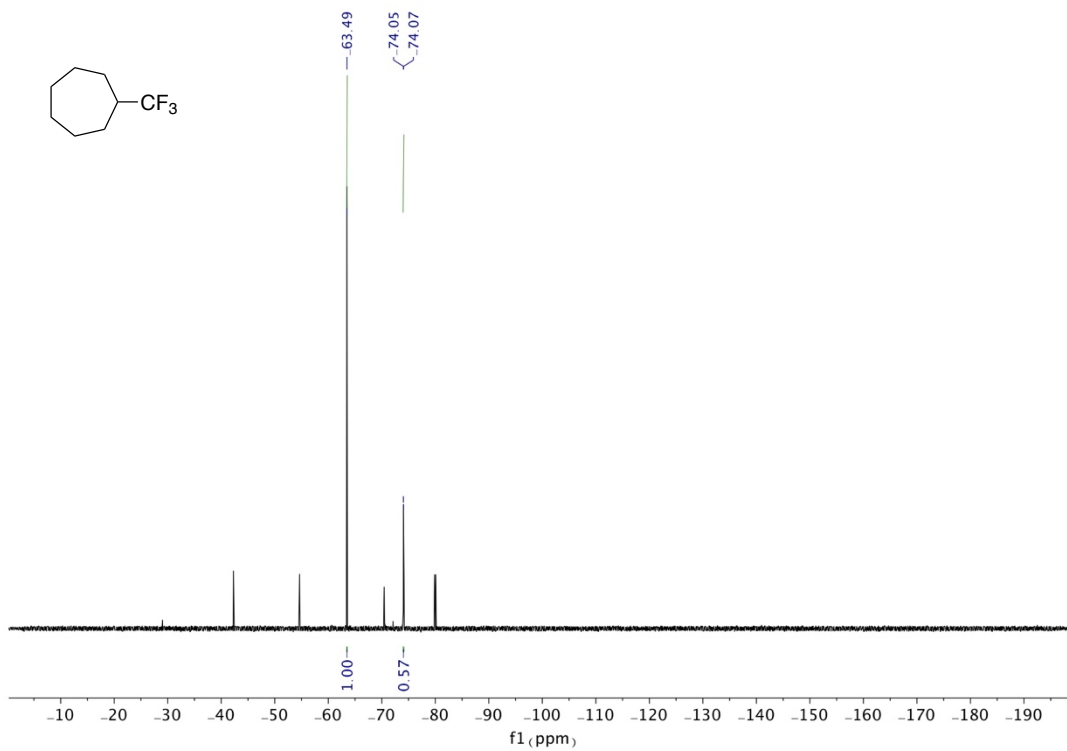


<sup>19</sup>F NMR assay for **12** from **C1** (Experiment II)

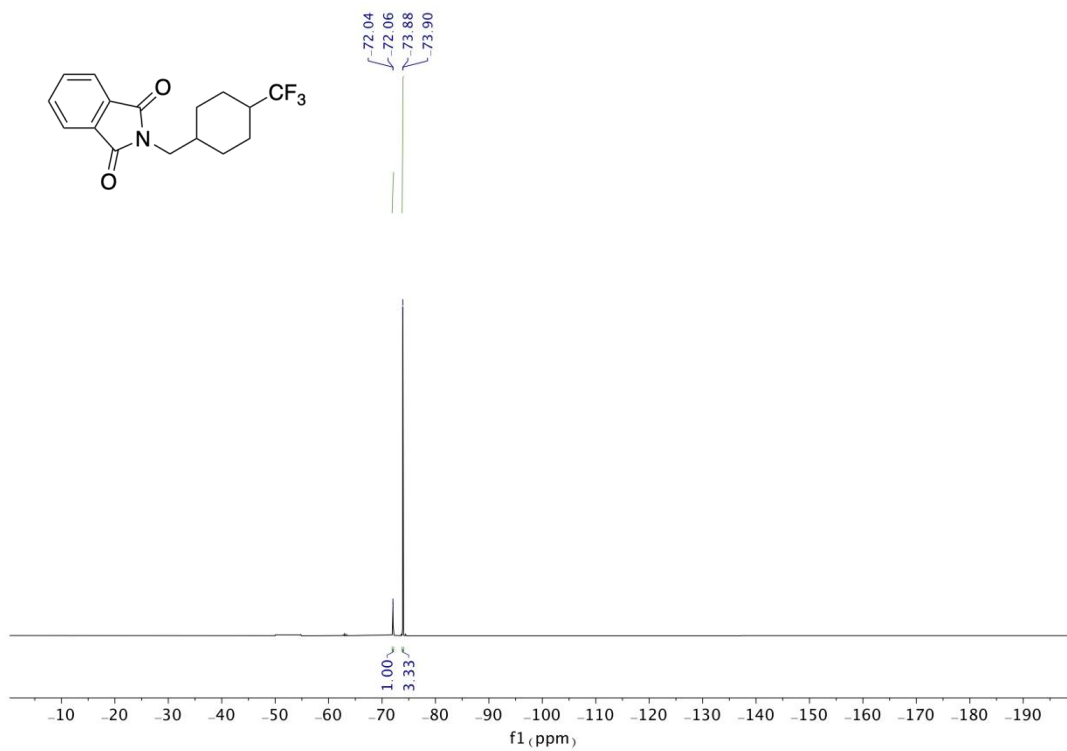


<sup>19</sup>F NMR assay for **13** (Experiment I)

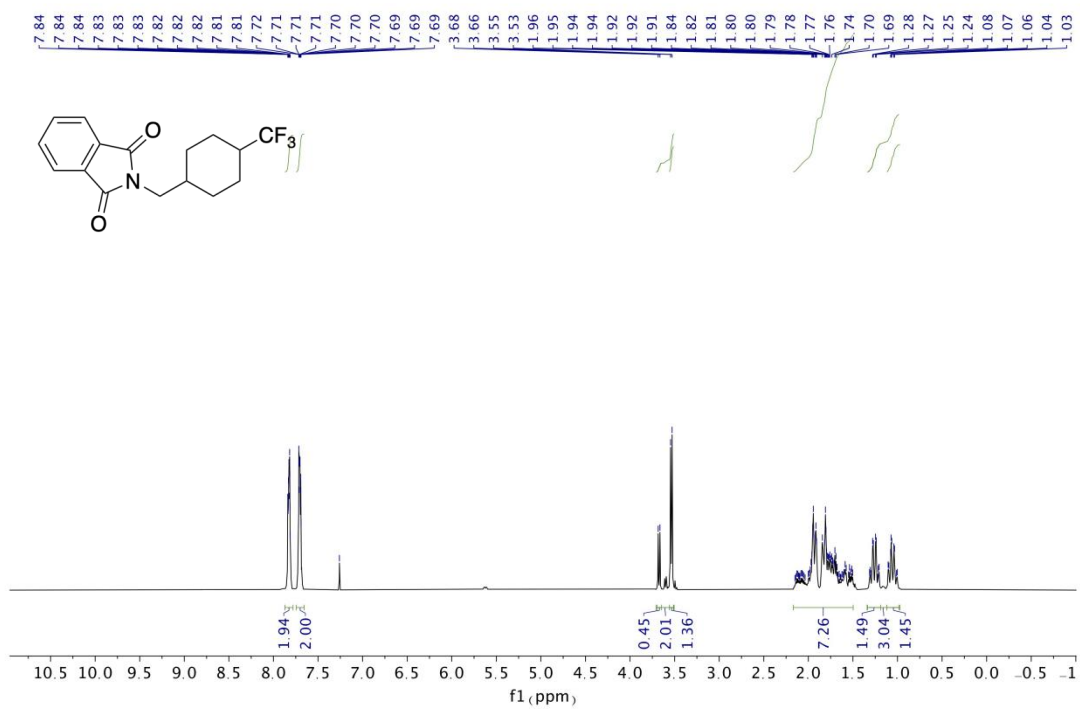




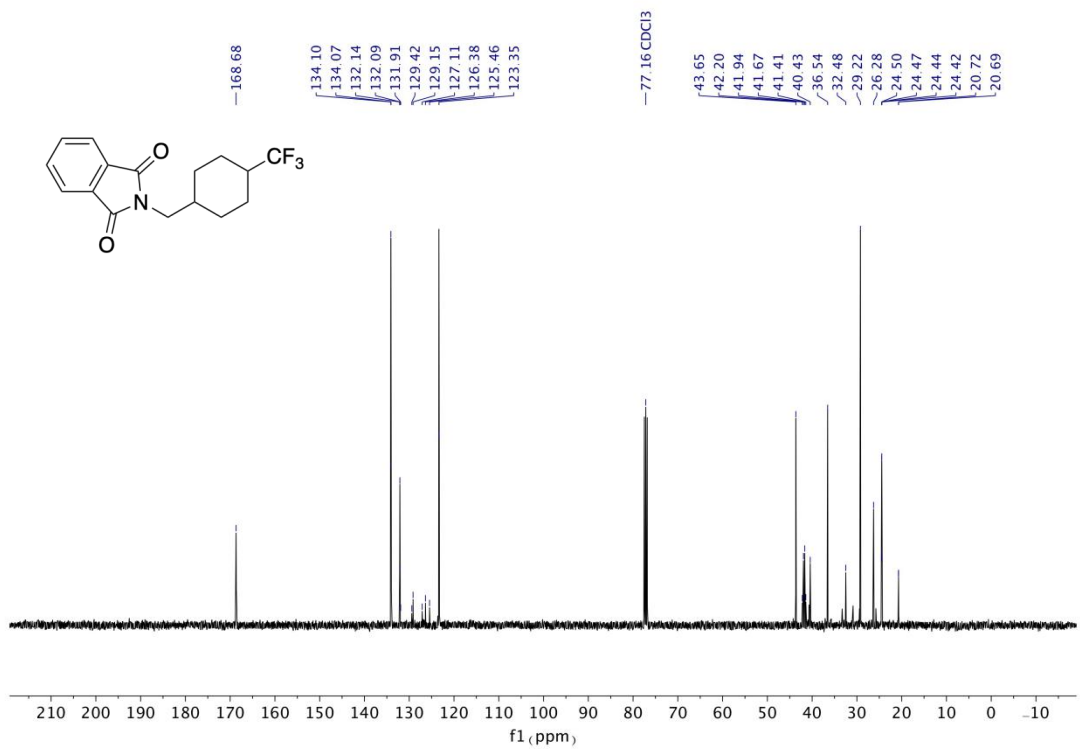
$^{19}\text{F}$  NMR assay for **13** (Experiment II)



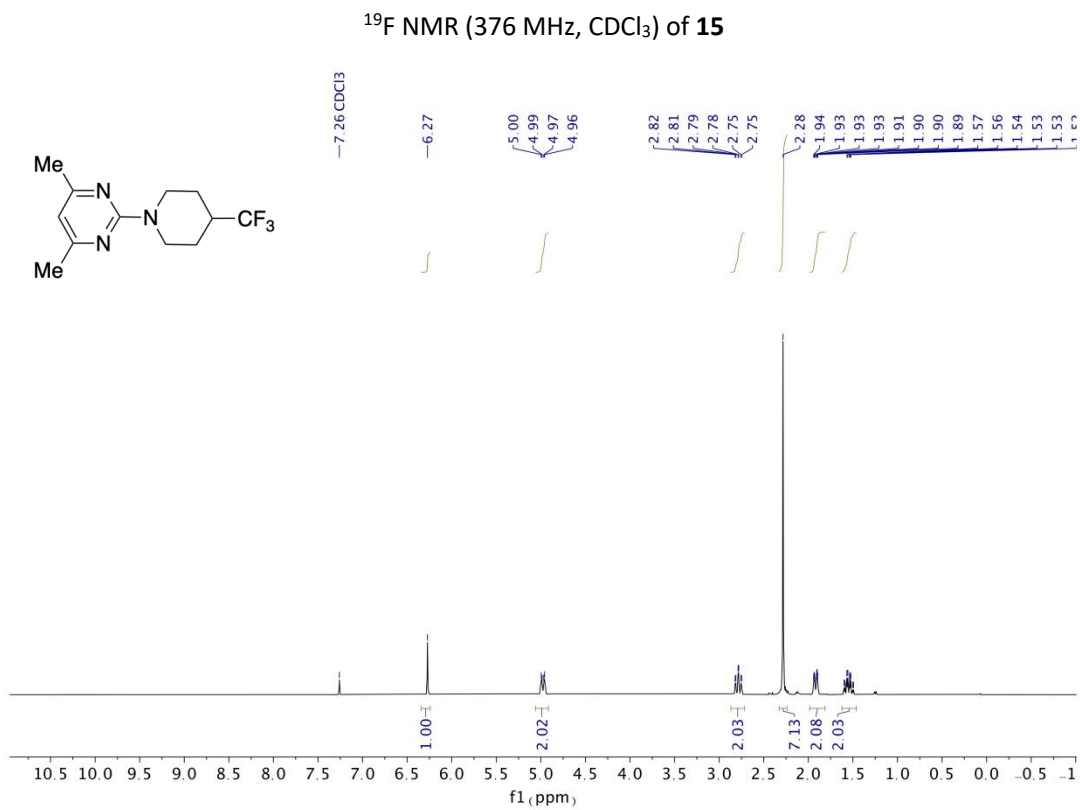
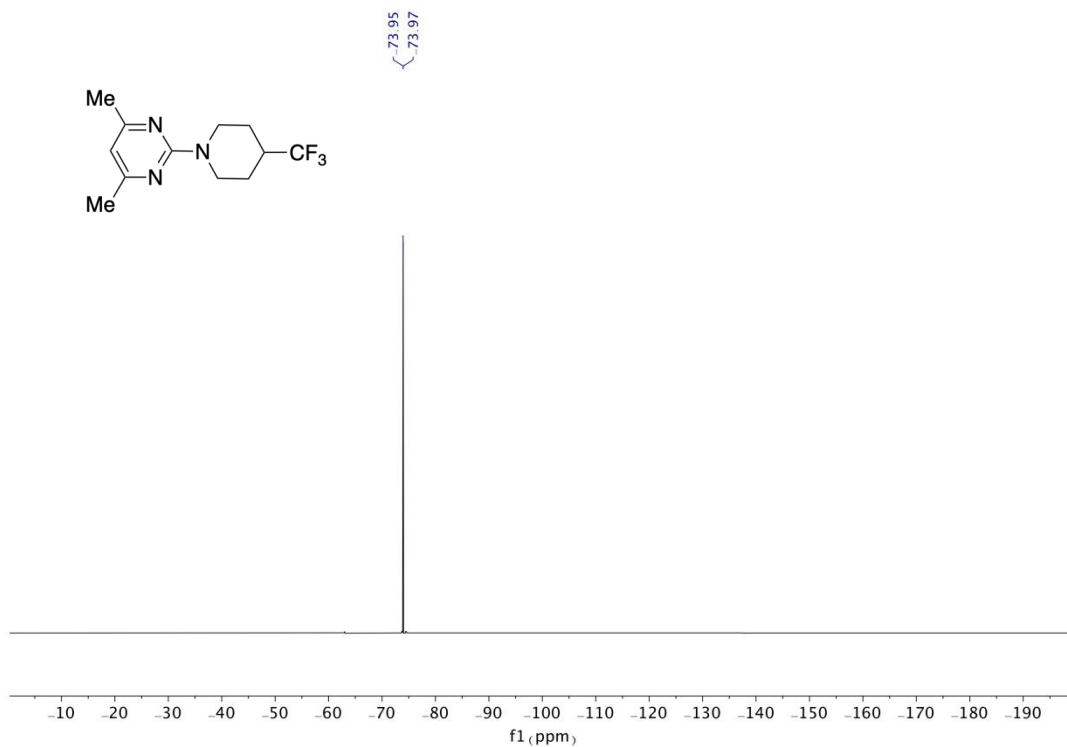
$^{19}\text{F}$  NMR (400 MHz,  $\text{CDCl}_3$ ) of **14**



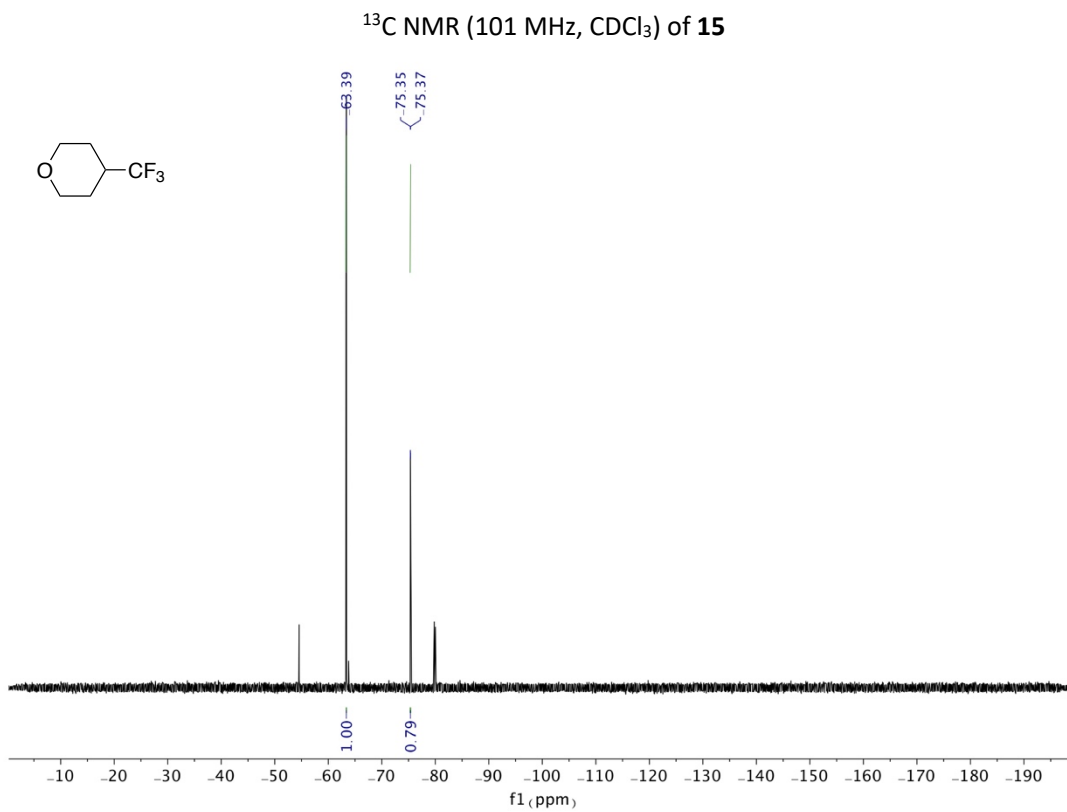
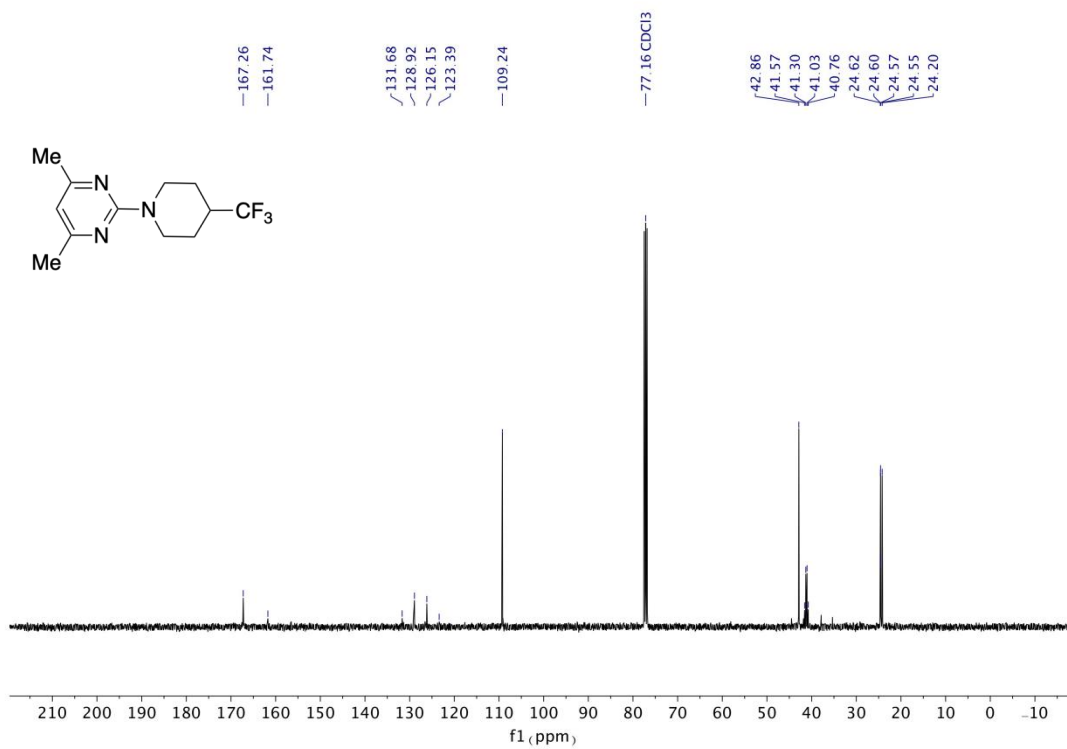
<sup>1</sup>H NMR (400 MHz, CDCl<sub>3</sub>) of **14**

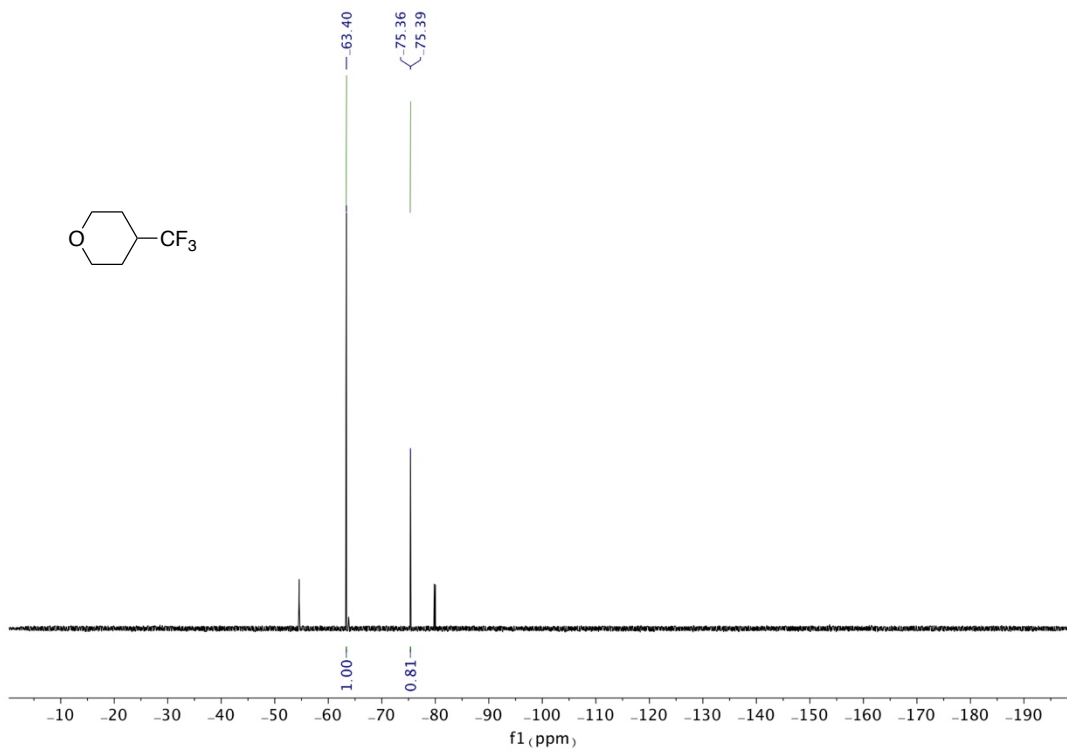


<sup>13</sup>C NMR (101 MHz, CDCl<sub>3</sub>) of **14**

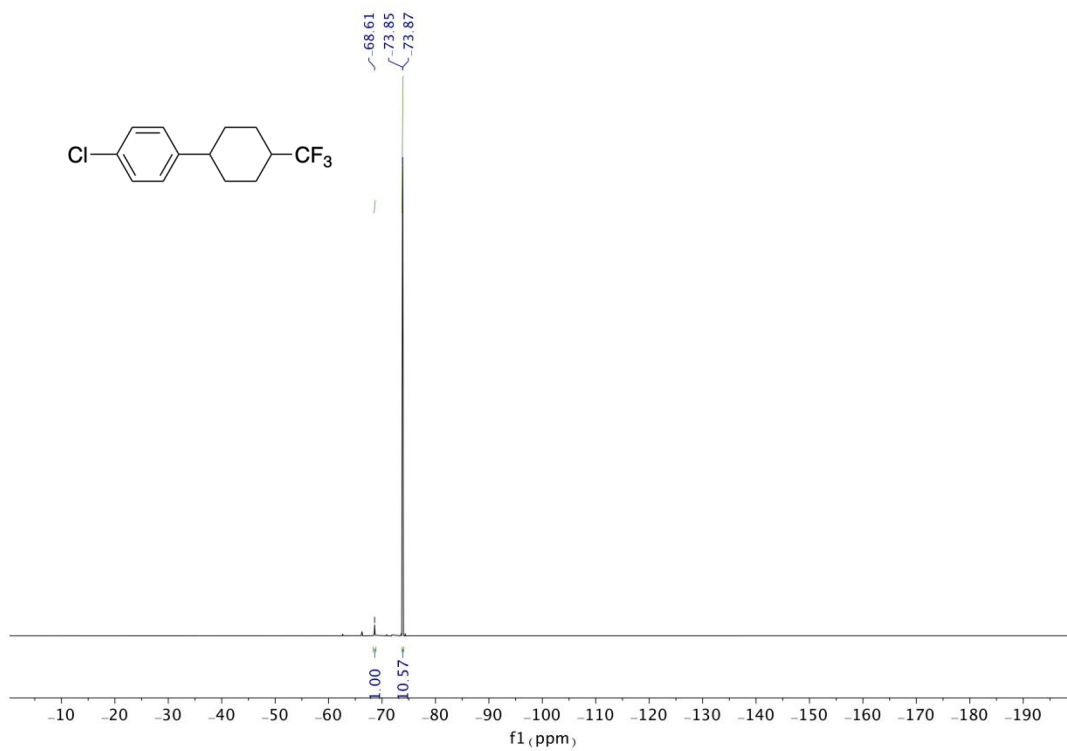


**<sup>1</sup>H NMR (400 MHz, CDCl<sub>3</sub>) of 15**

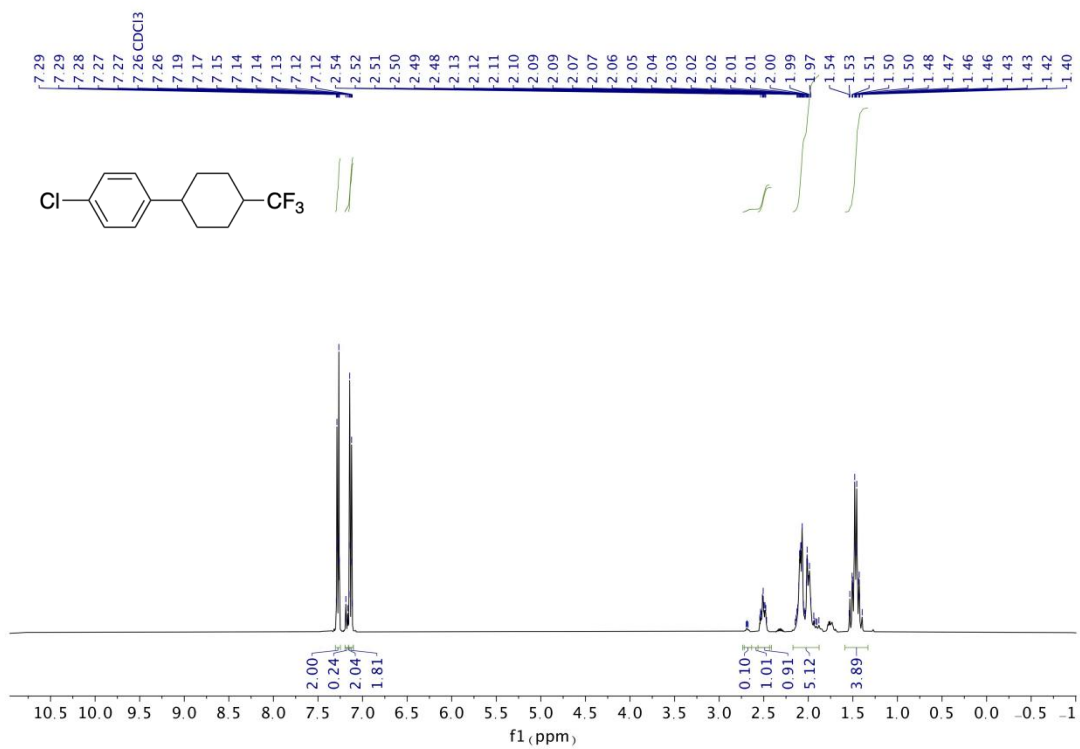




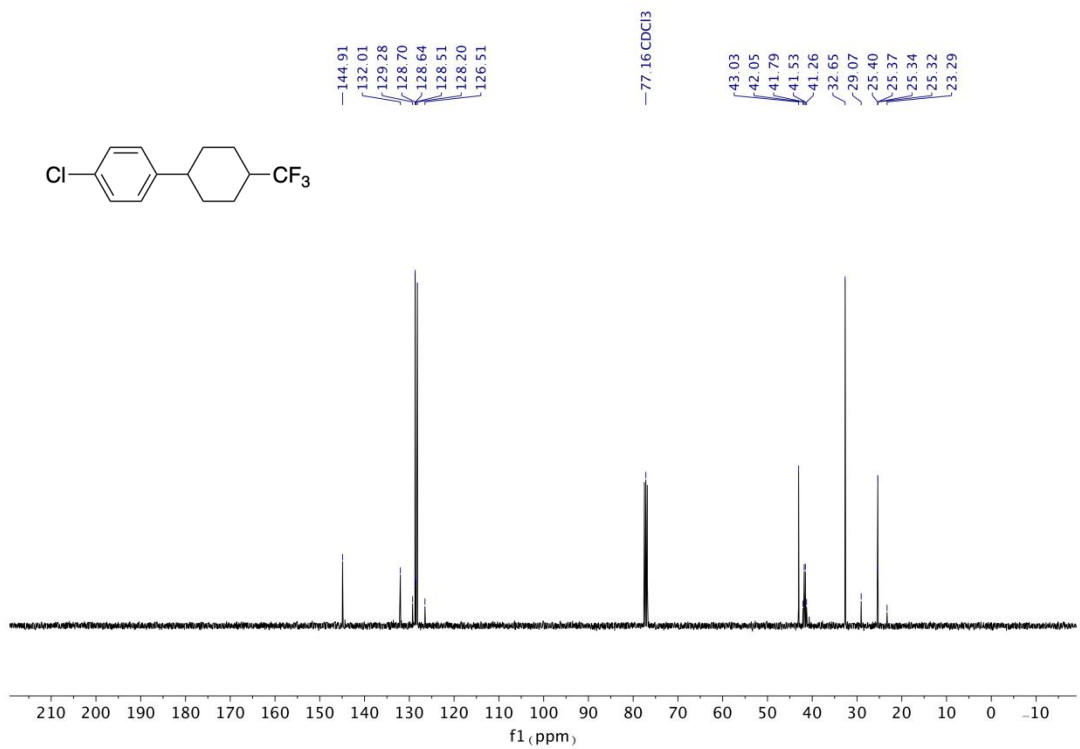
$^{19}\text{F}$  NMR assay for **16** (Experiment II)



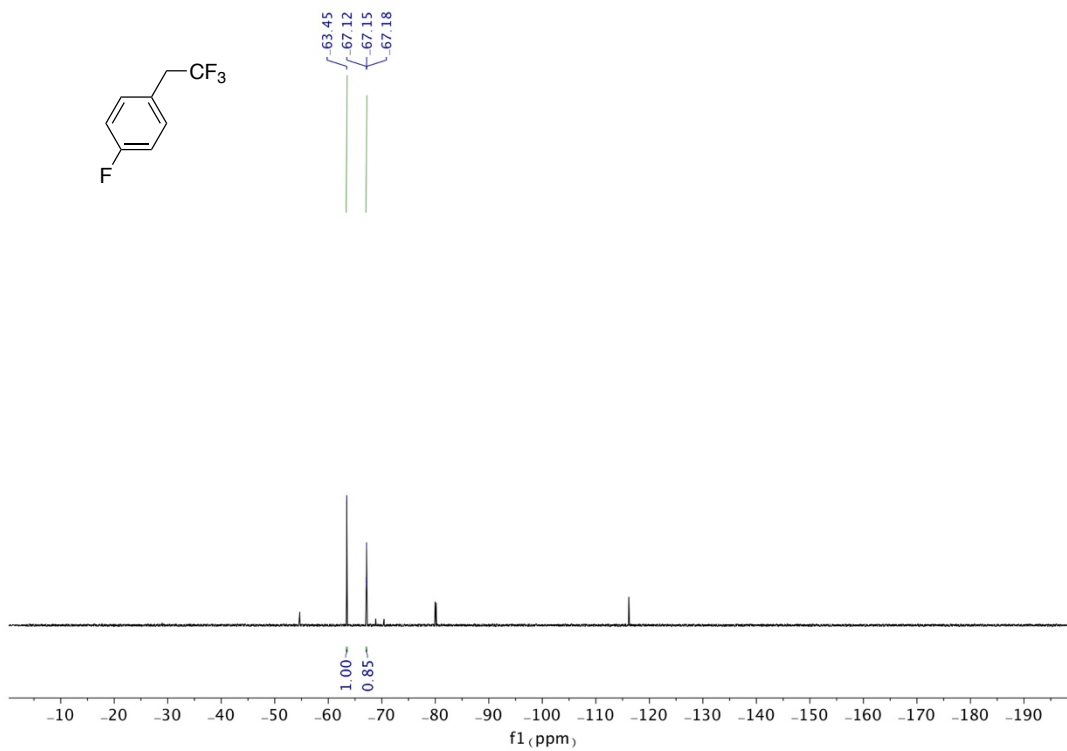
$^{19}\text{F}$  NMR (376 MHz,  $\text{CDCl}_3$ ) of **17**



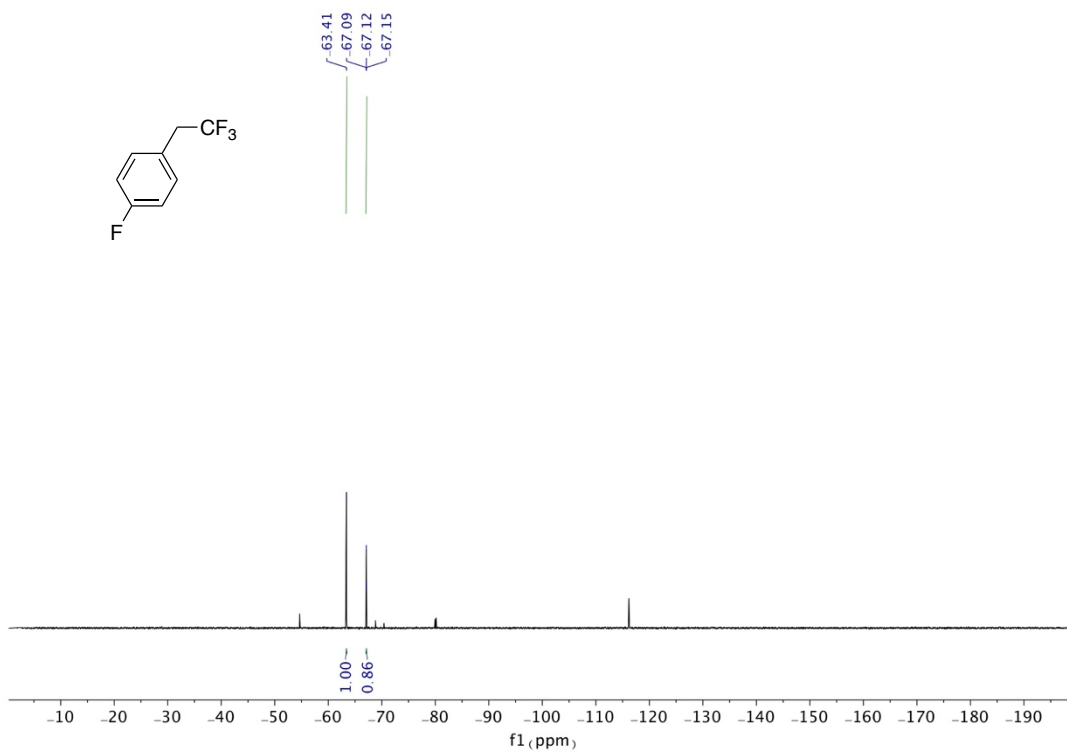
<sup>1</sup>H NMR (400 MHz, CDCl<sub>3</sub>) of **17**



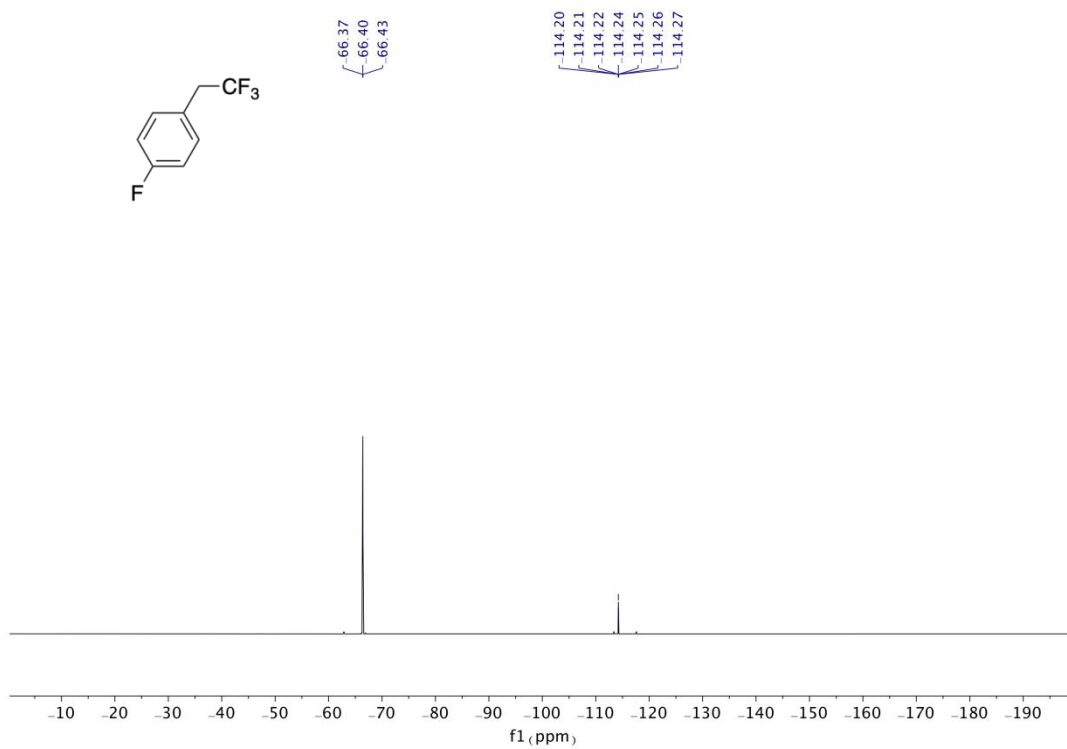
<sup>13</sup>C NMR (101 MHz, CDCl<sub>3</sub>) of **17**



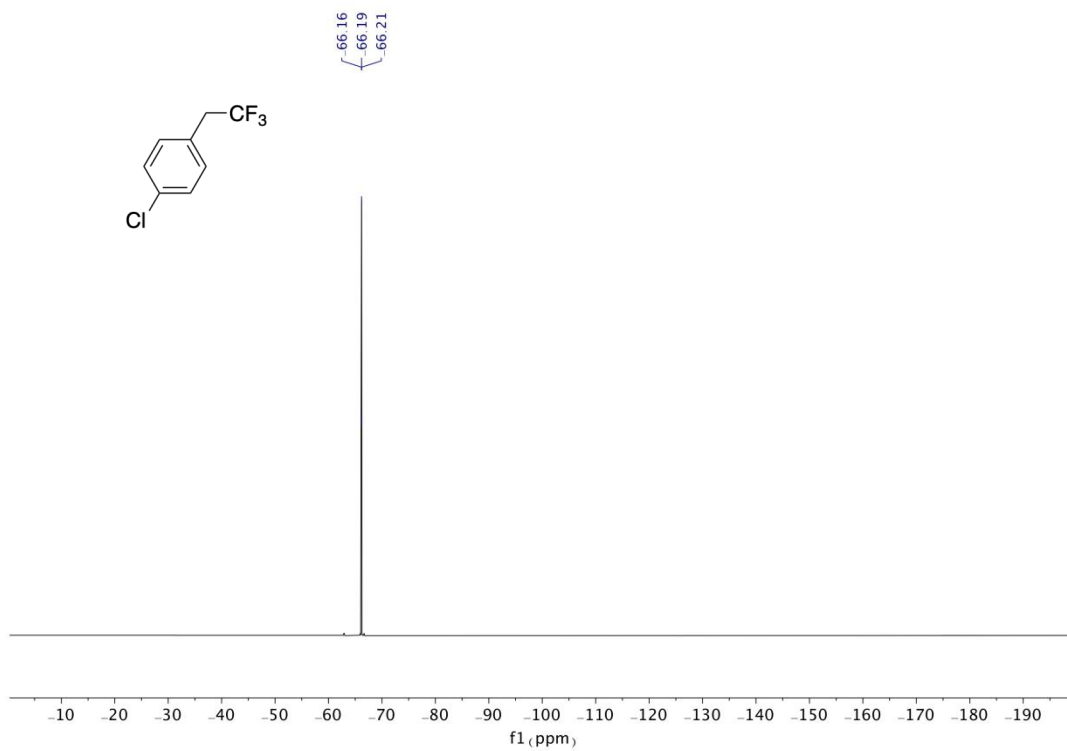
<sup>19</sup>F NMR assay for **18** (Experiment I)



<sup>19</sup>F NMR assay for **18** (Experiment II)

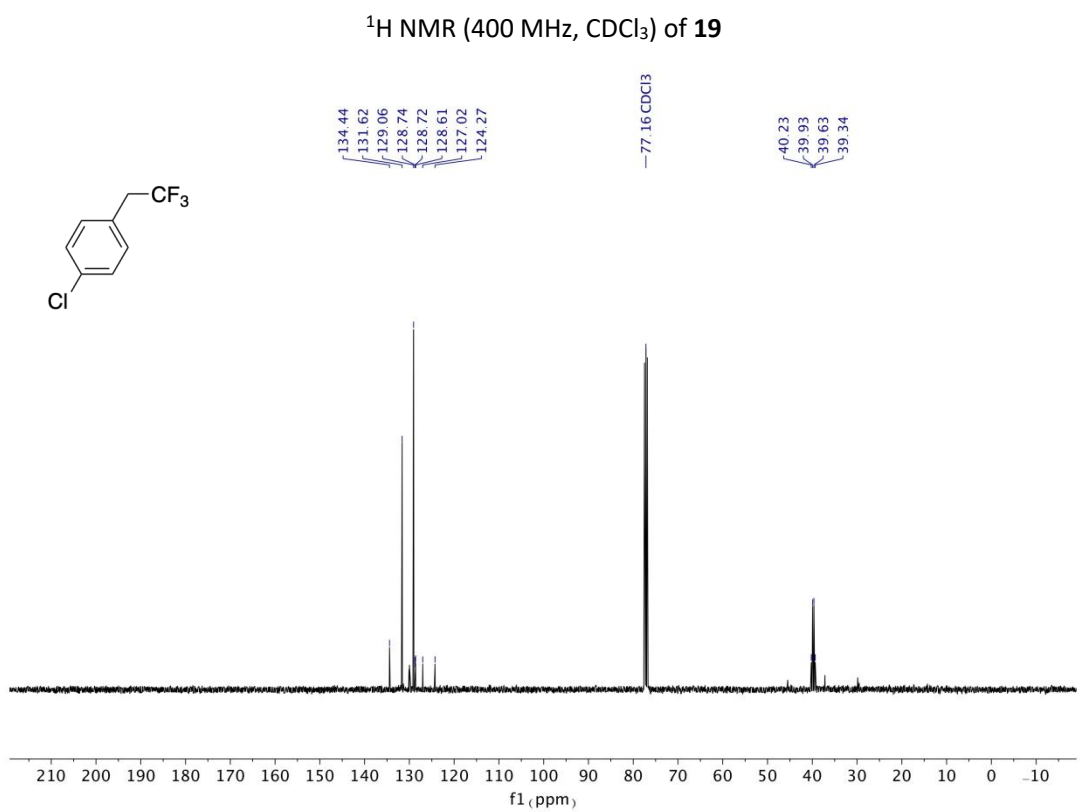
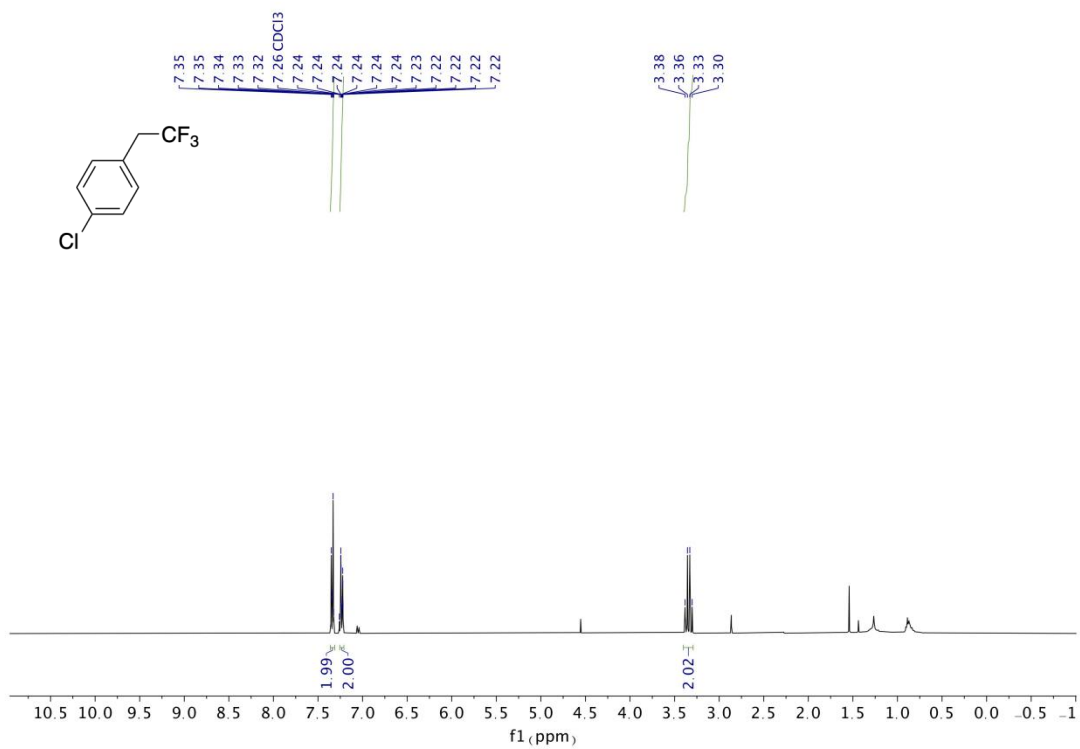


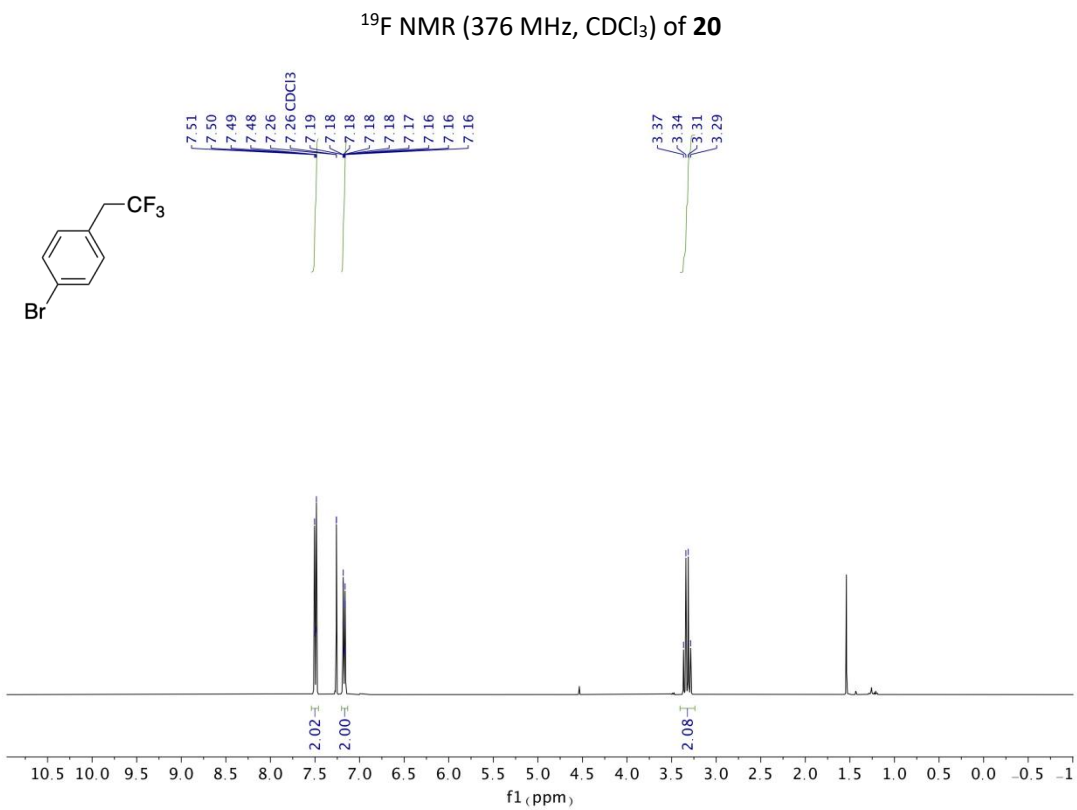
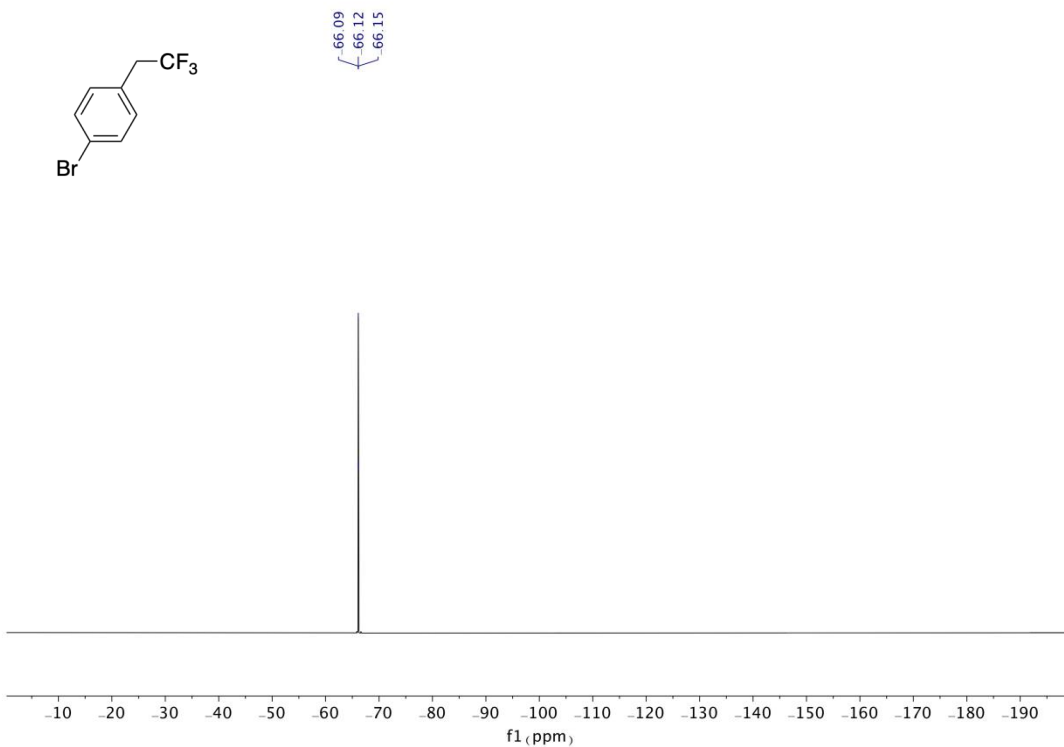
<sup>19</sup>F NMR (376 MHz, CDCl<sub>3</sub>) of **18**

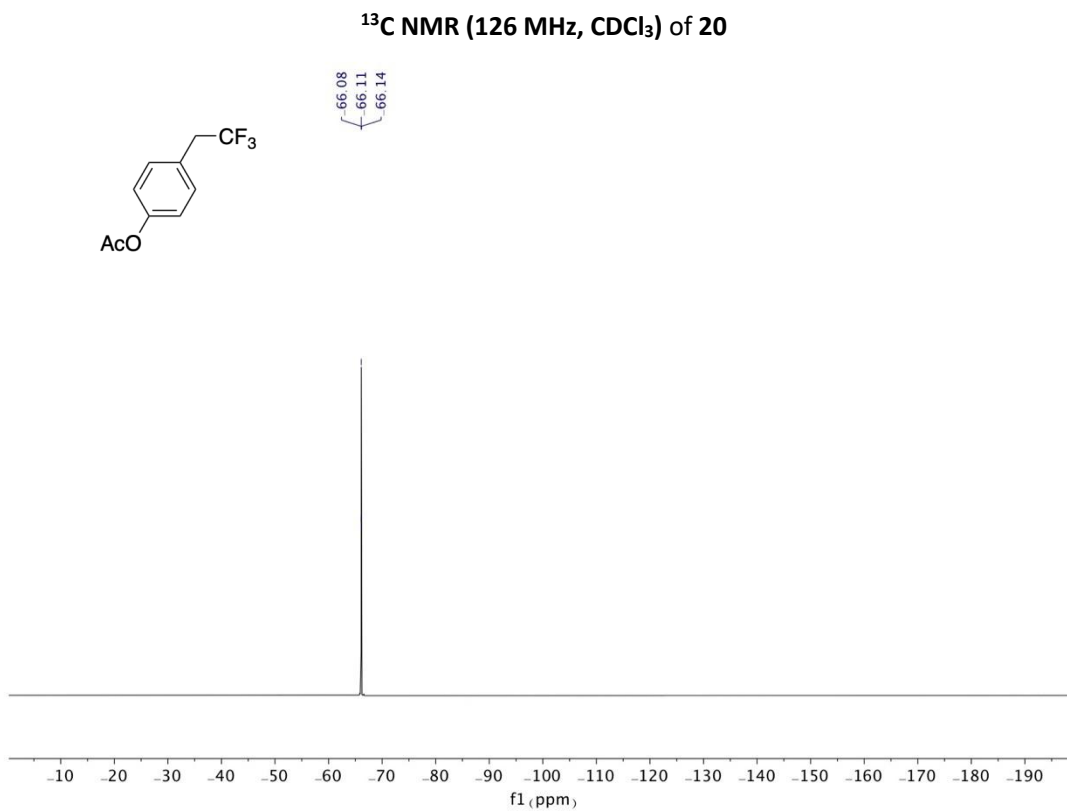
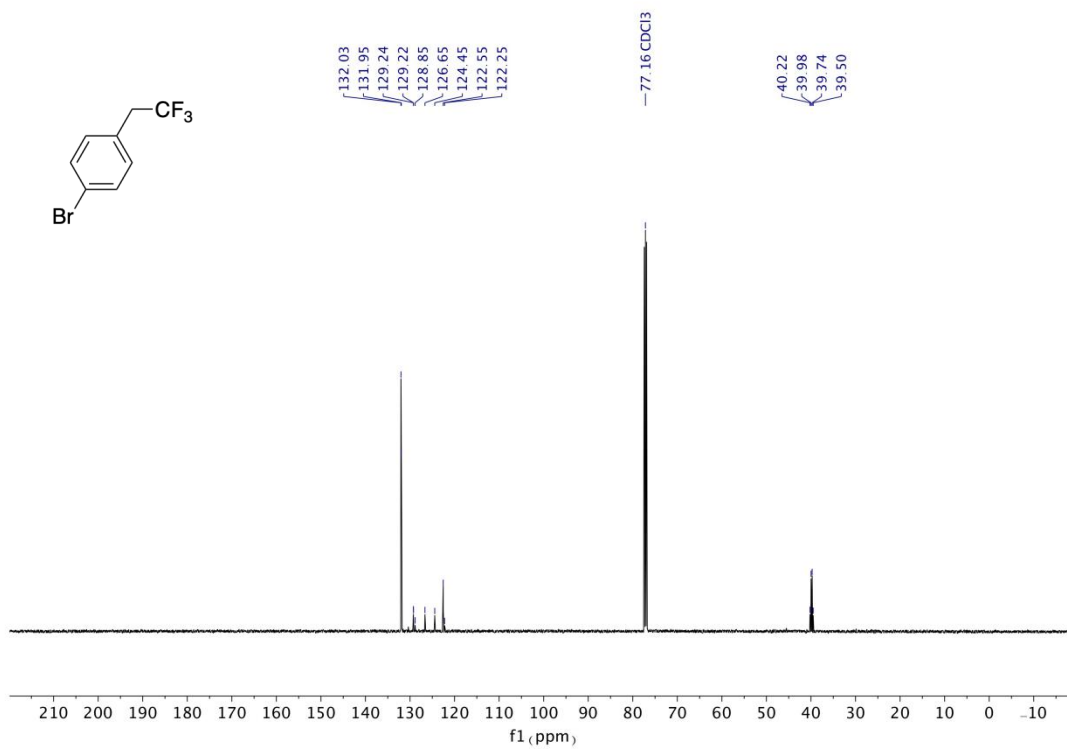


<sup>19</sup>F NMR (376 MHz, CDCl<sub>3</sub>) of **19**

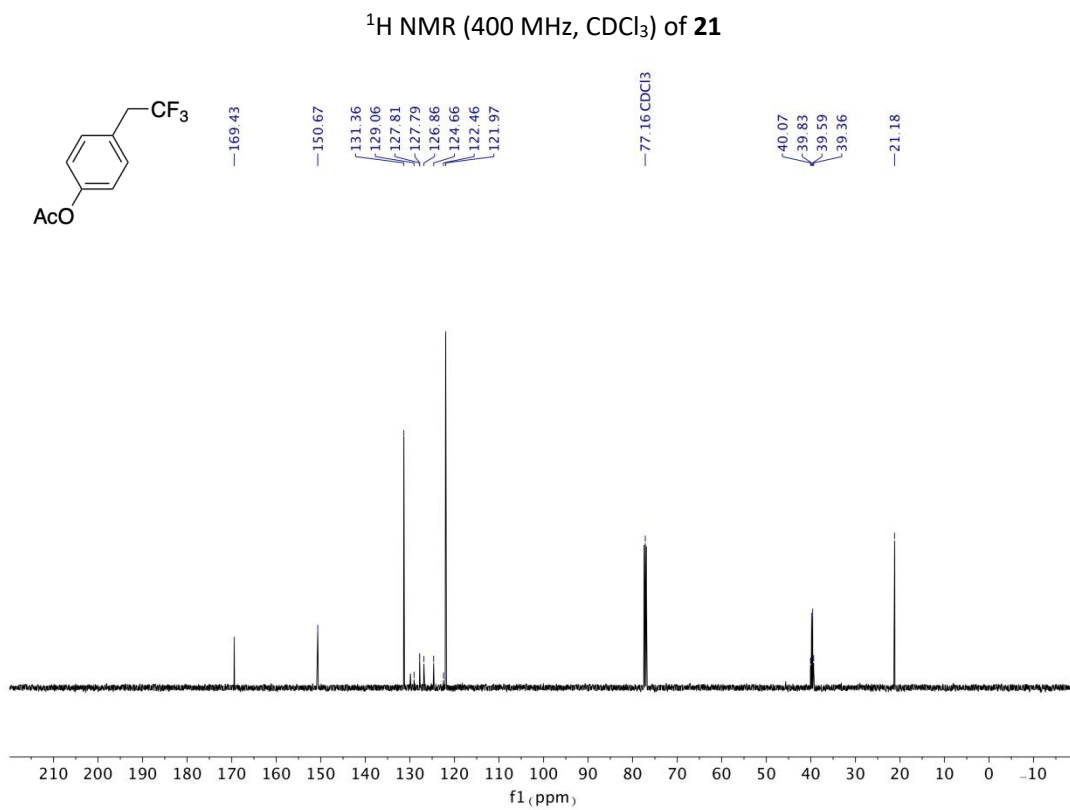
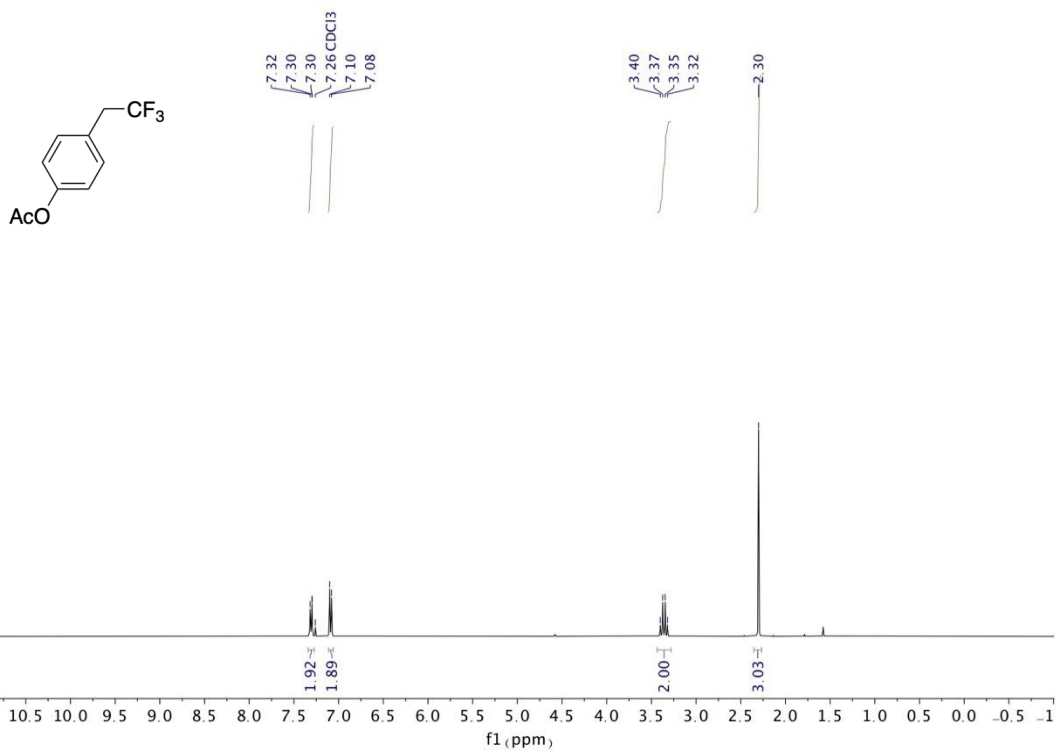


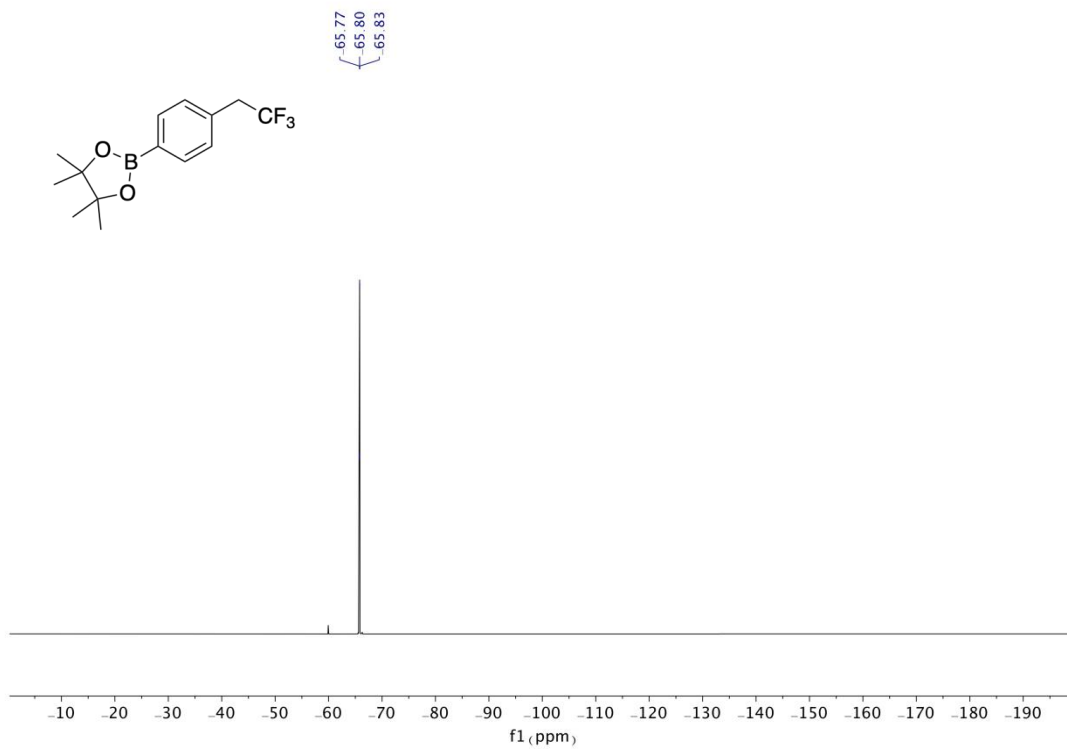




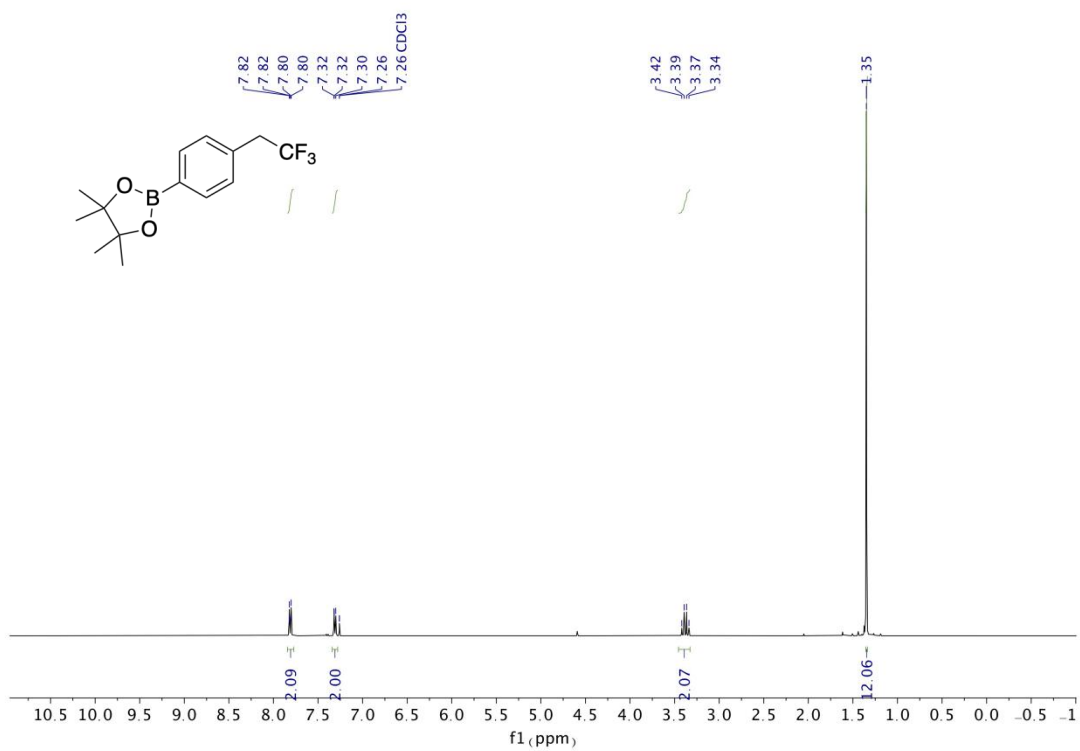


$^{19}\text{F}$  NMR (376 MHz,  $\text{CDCl}_3$ ) of 21

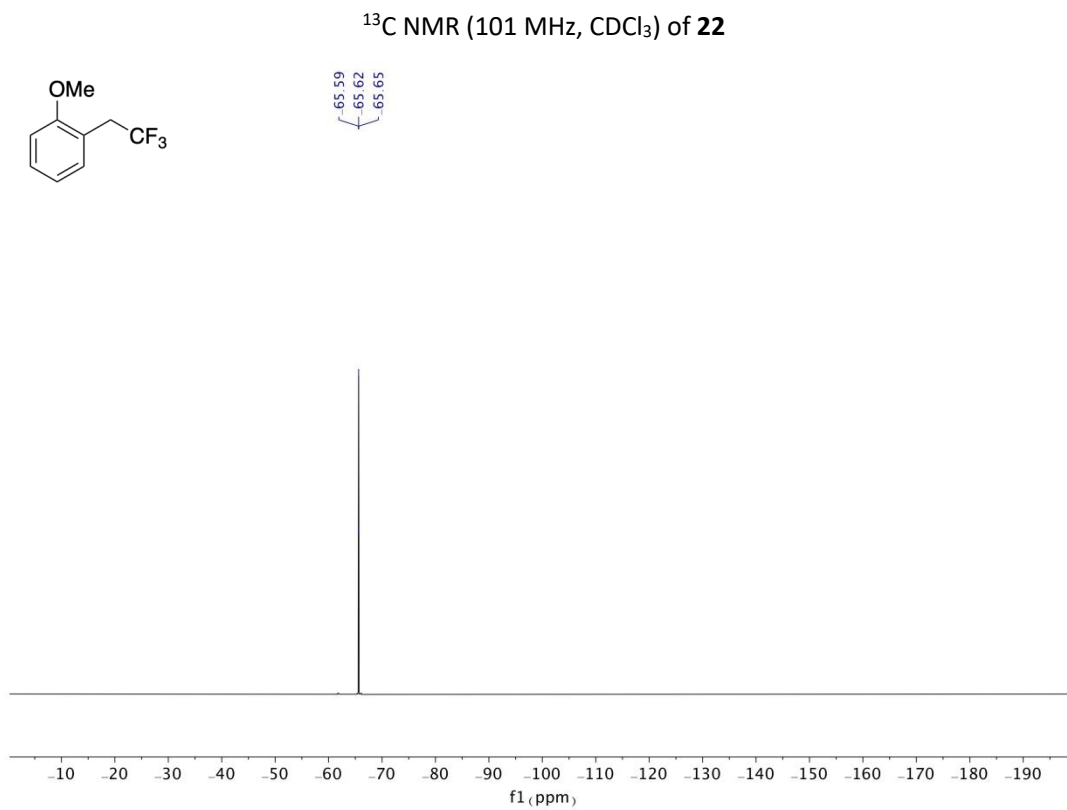
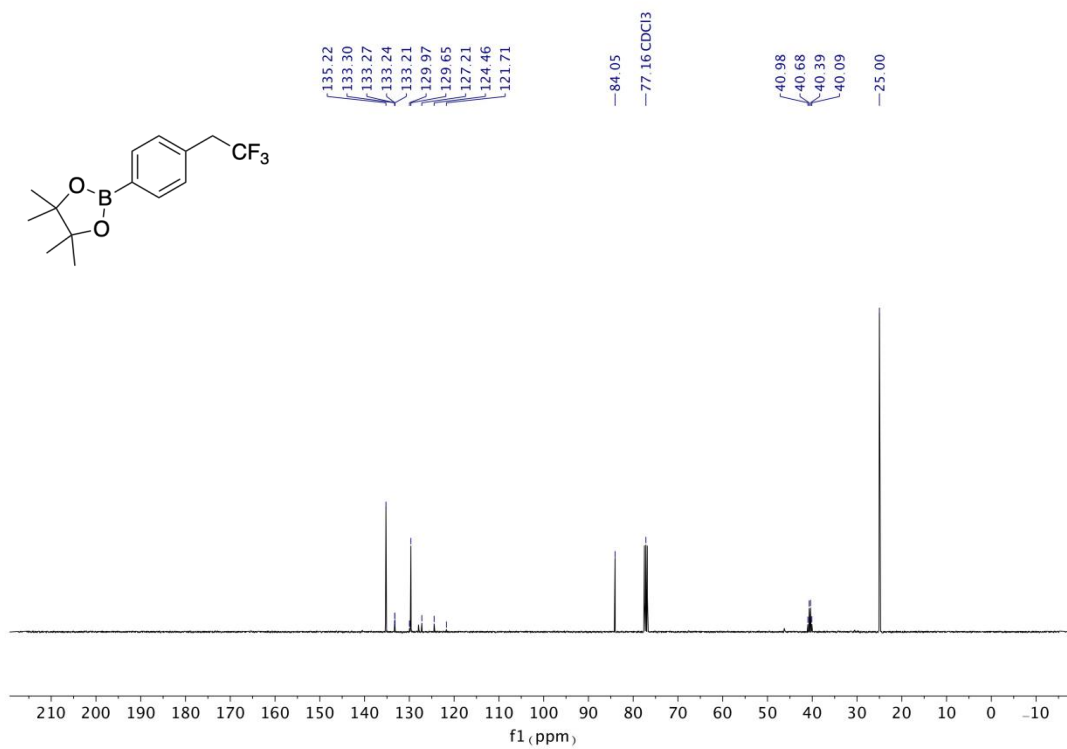


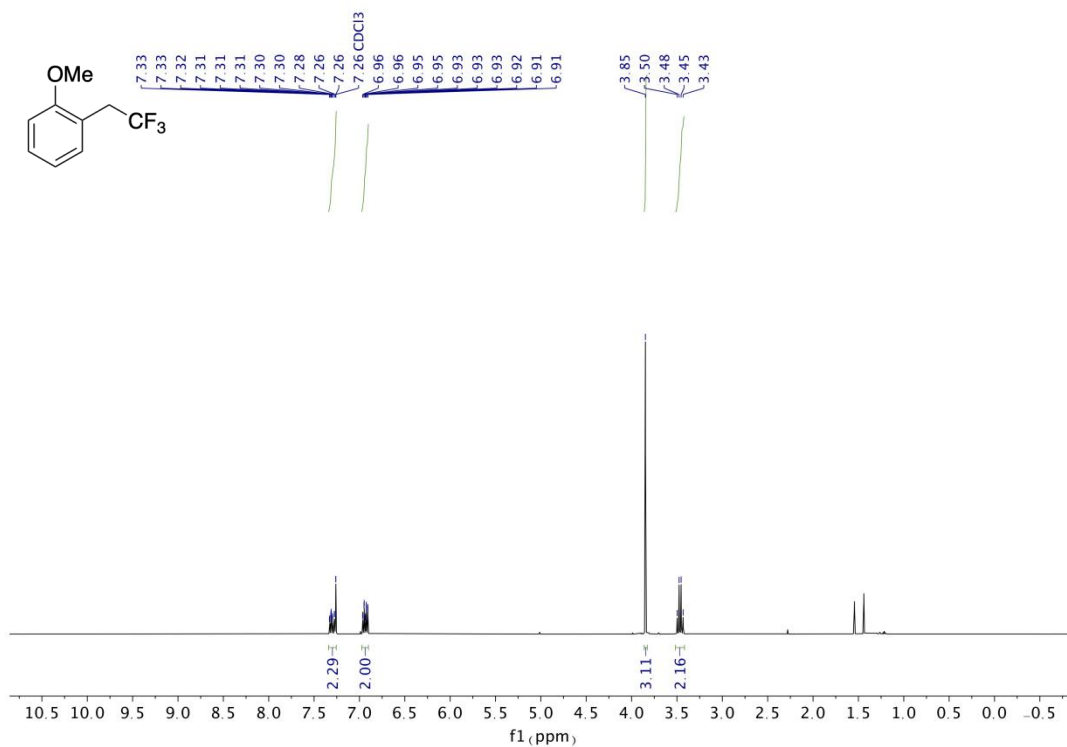


$^{19}\text{F}$  NMR (376 MHz,  $\text{CDCl}_3$ ) of **22** (1% impure)

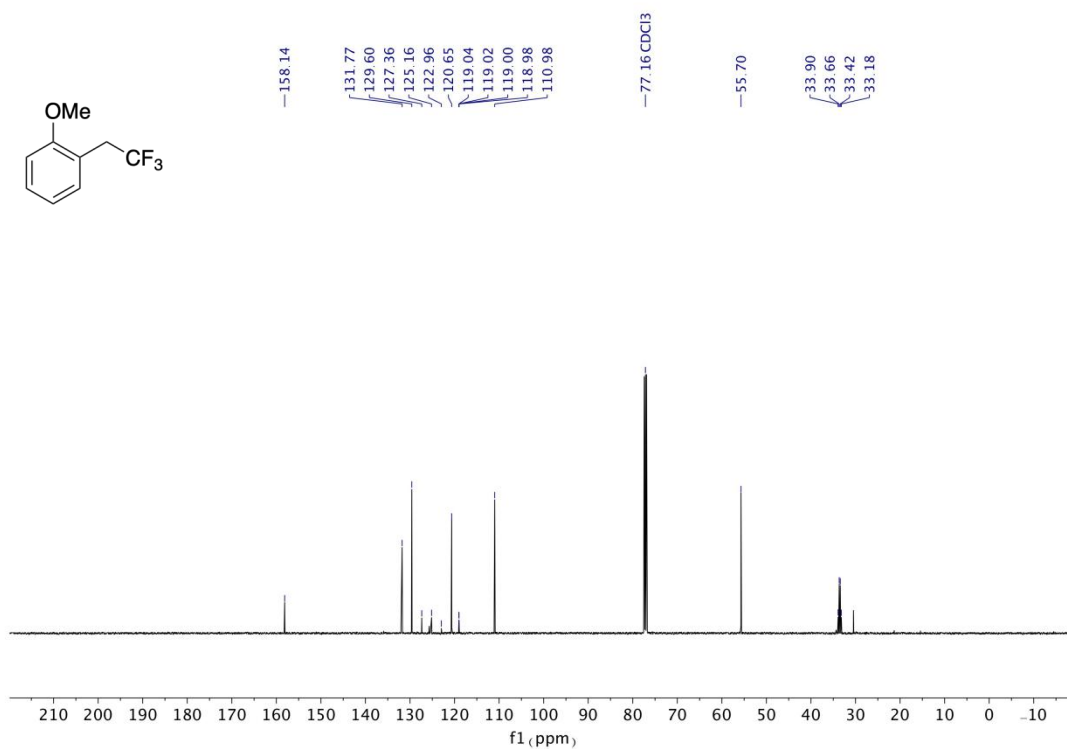


$^1\text{H}$  NMR (400 MHz,  $\text{CDCl}_3$ ) of **22**

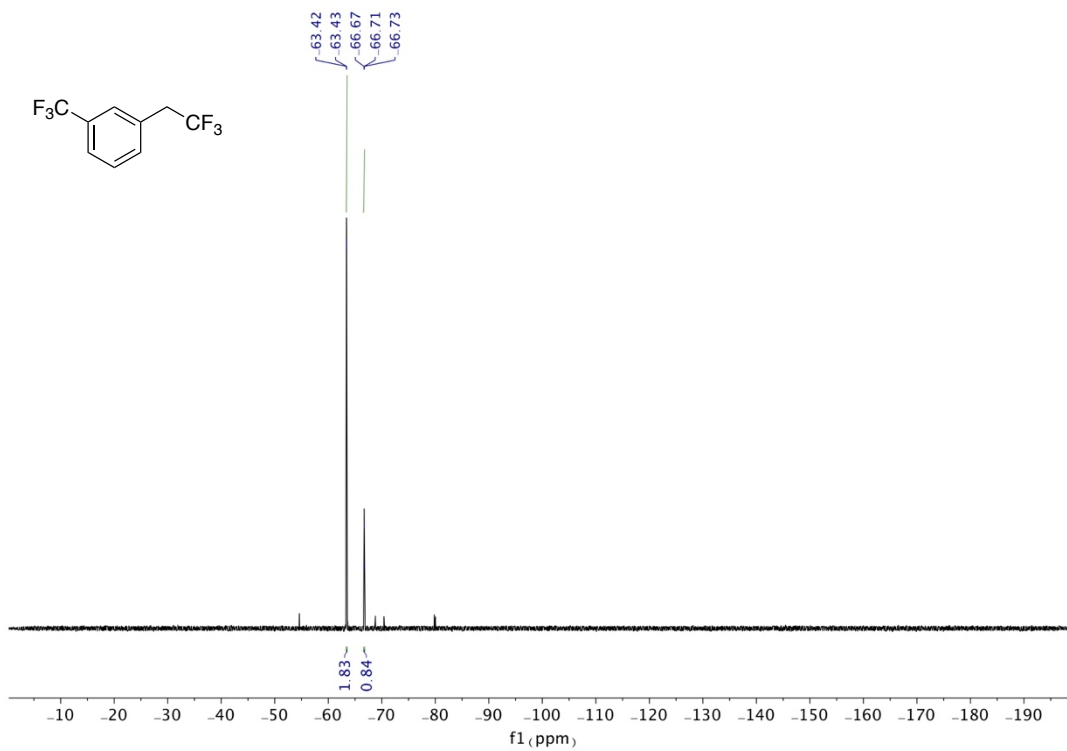




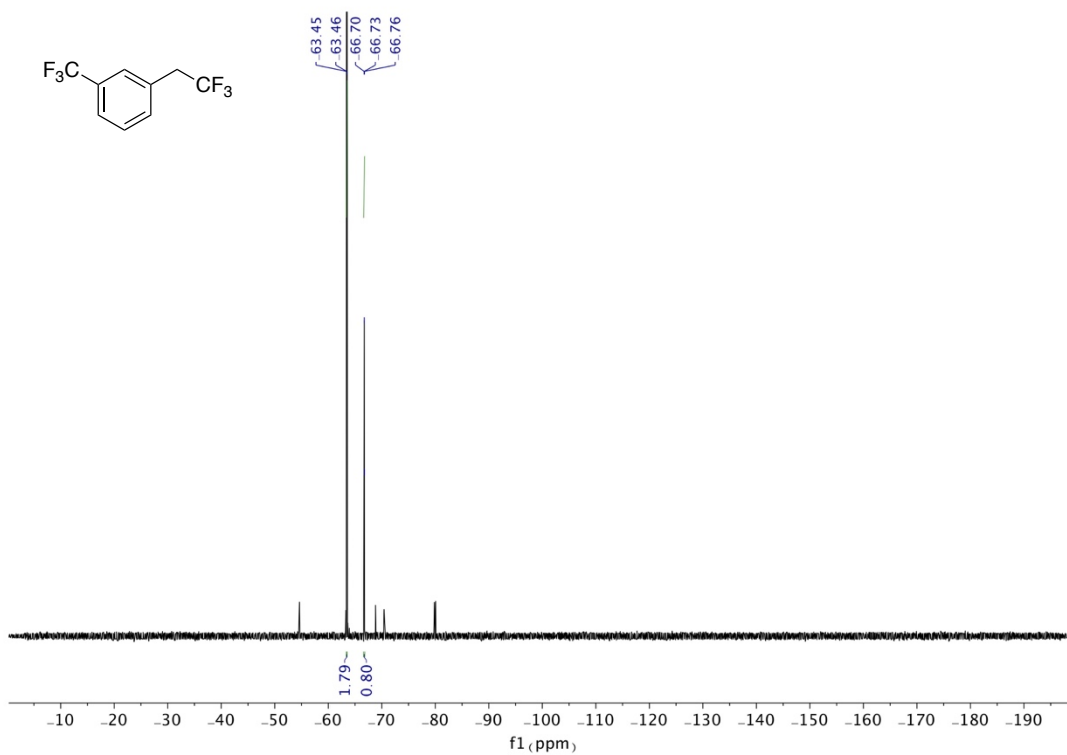
<sup>1</sup>H NMR (400 MHz, CDCl<sub>3</sub>) of 23



<sup>13</sup>C NMR (101 MHz, CDCl<sub>3</sub>) of 23

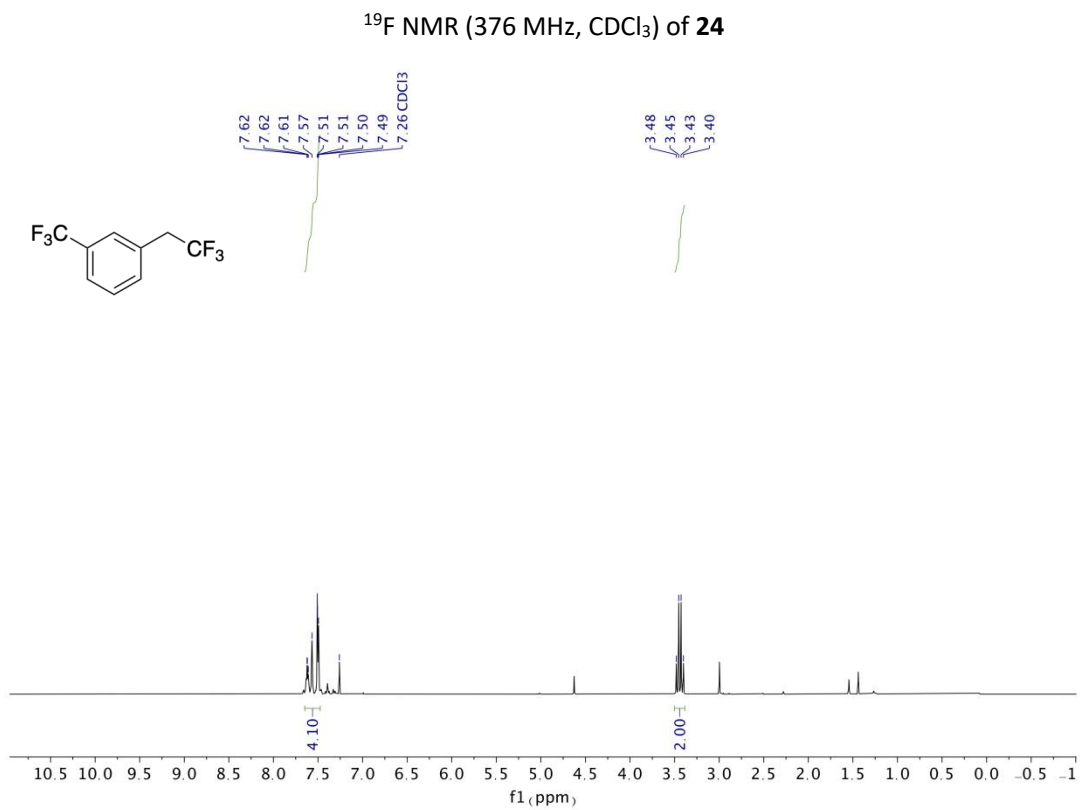
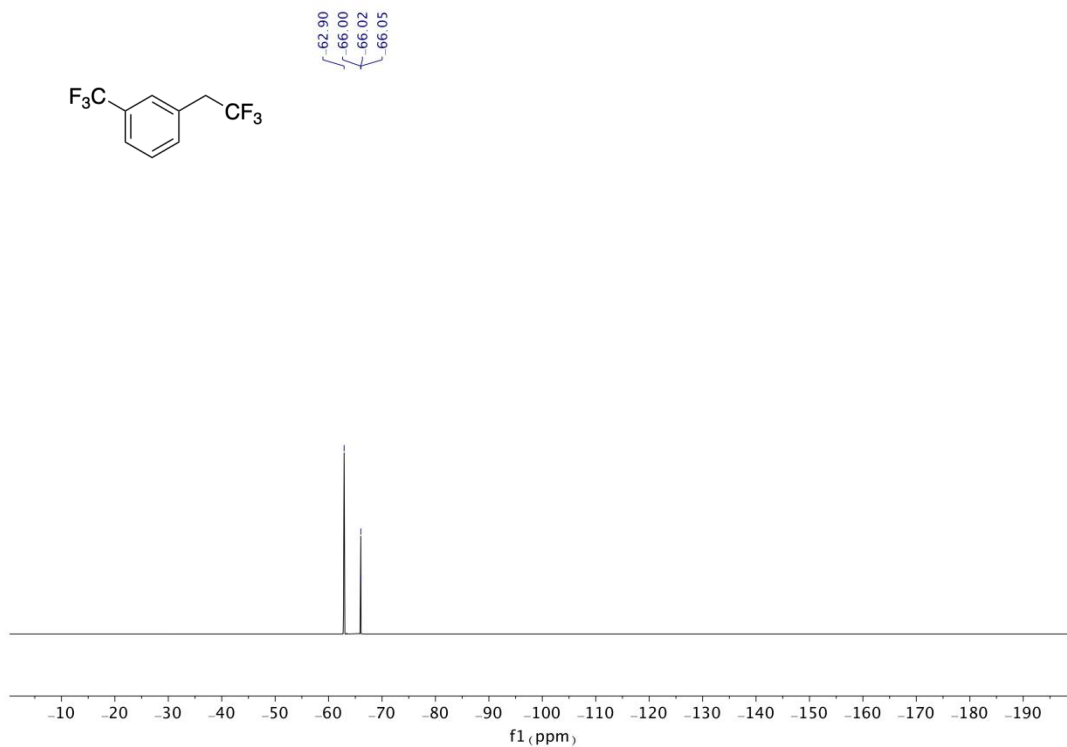


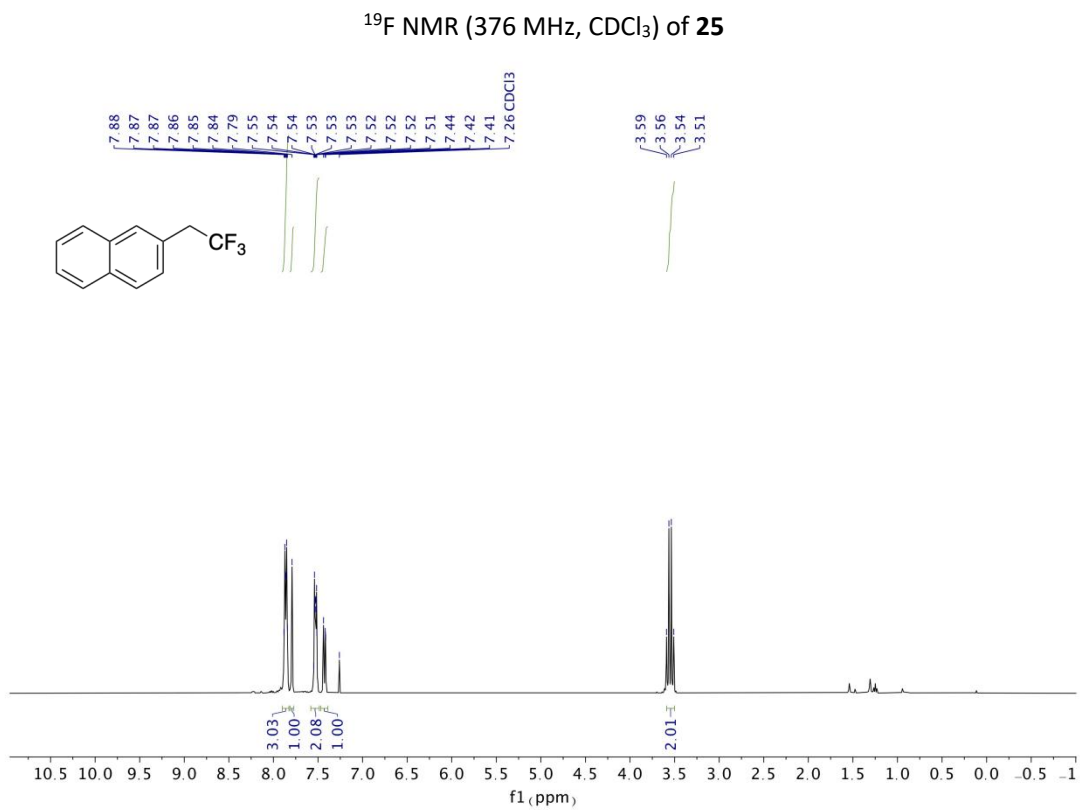
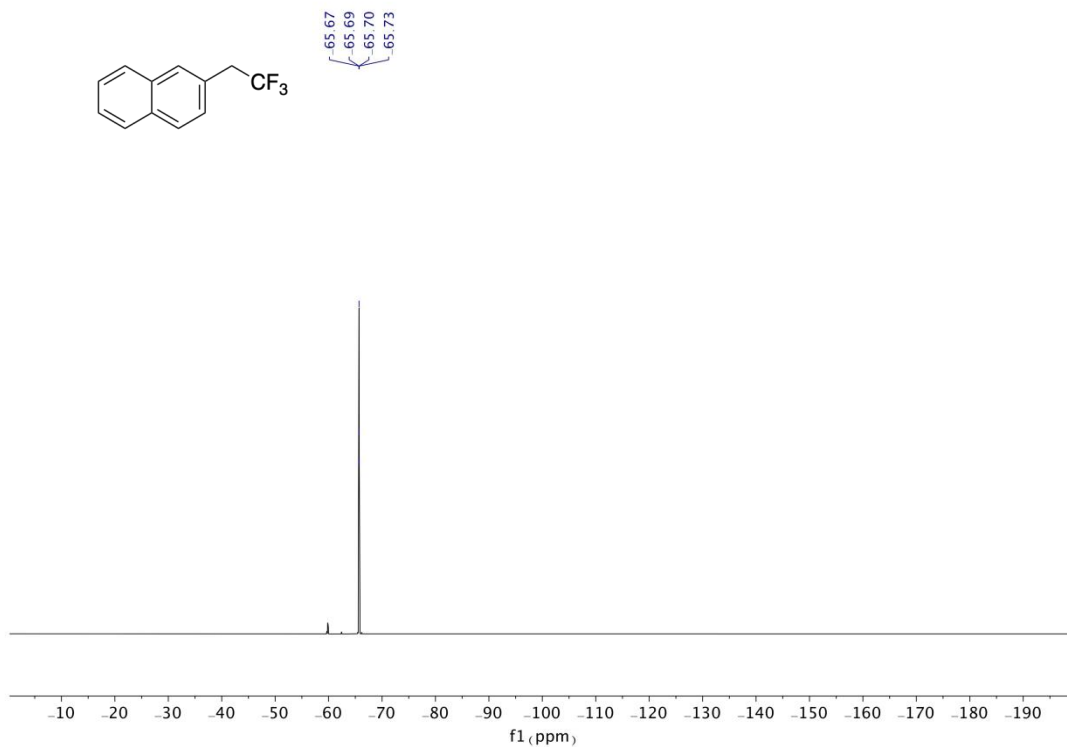
$^{19}\text{F}$  NMR assay for **24** (Experiment I)

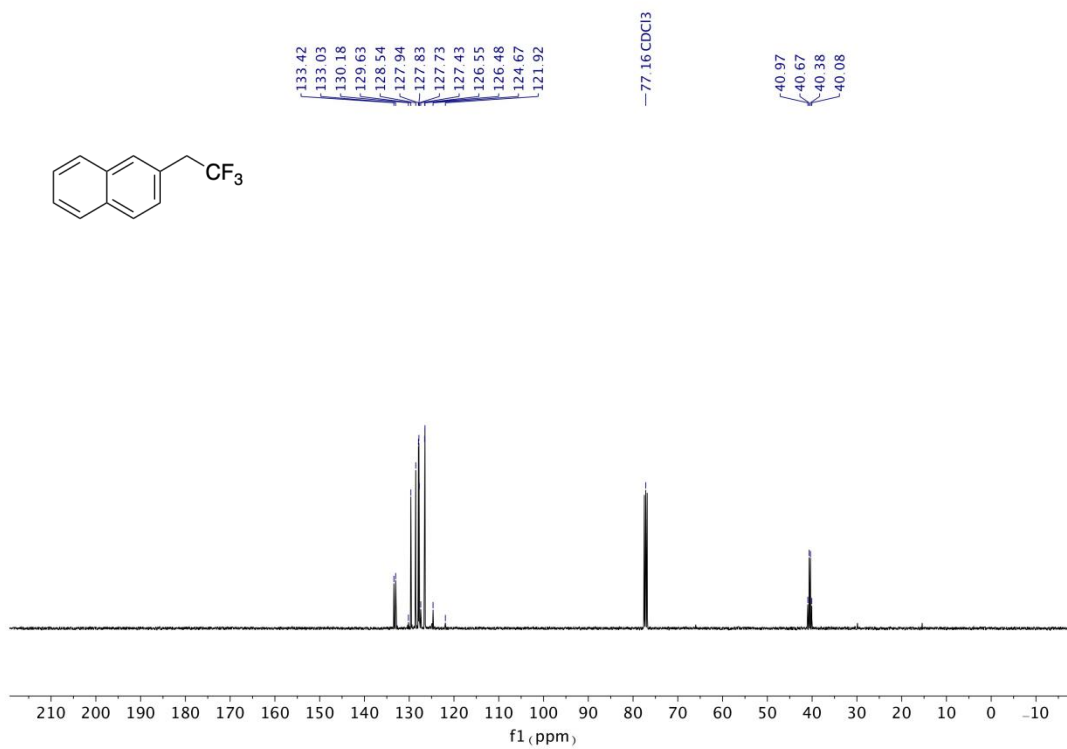


$^{19}\text{F}$  NMR assay for **24** (Experiment II)

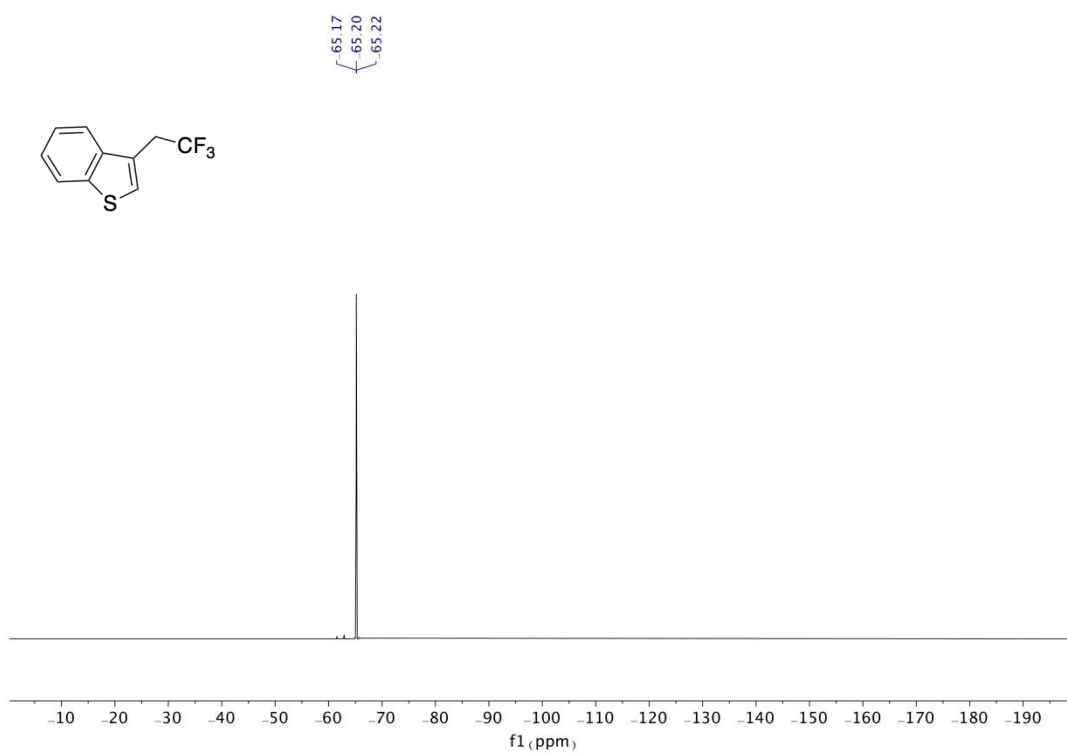




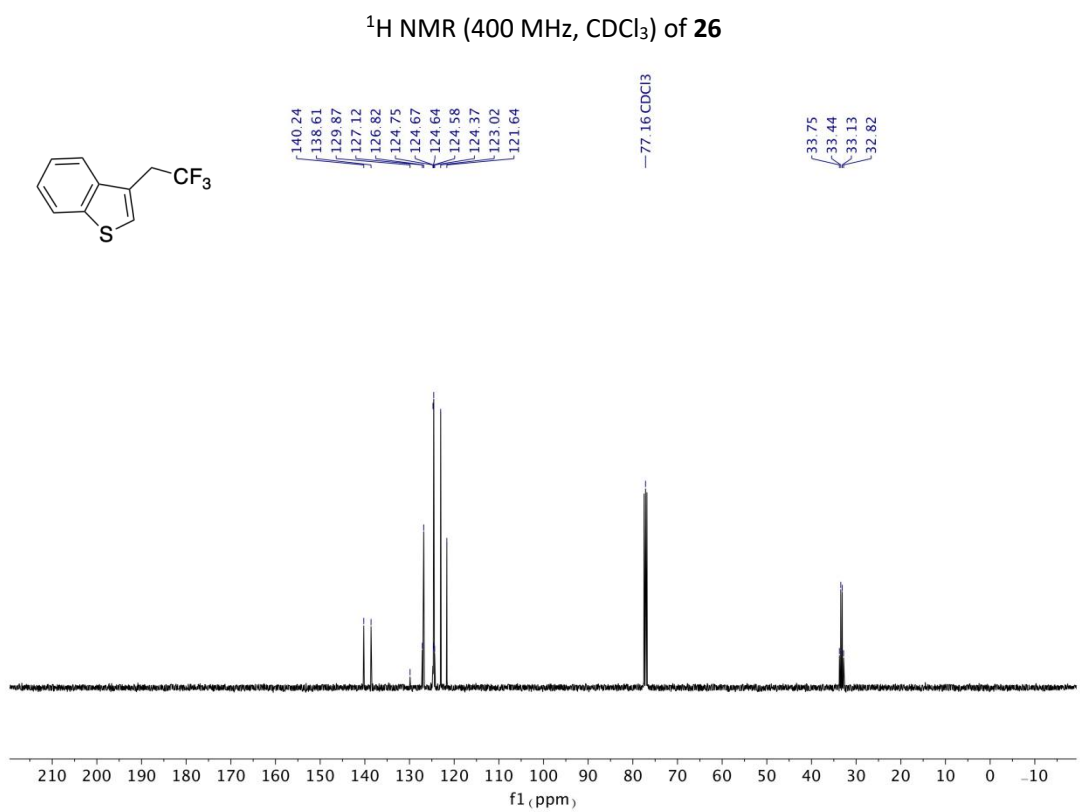
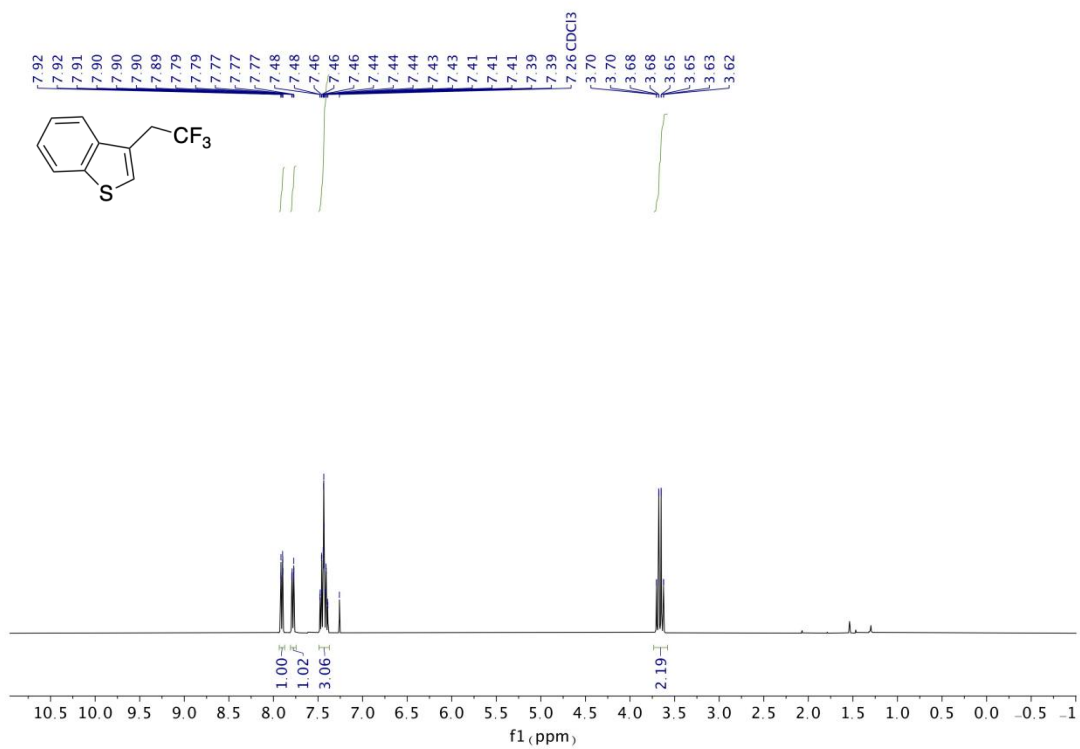


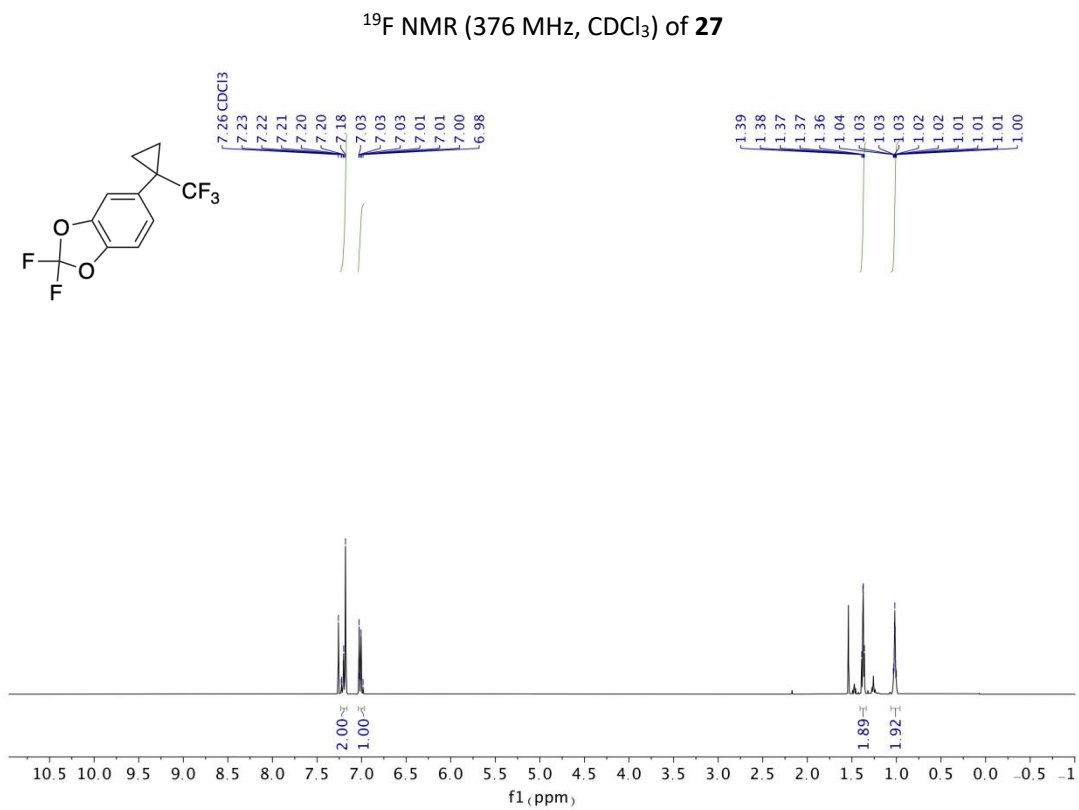
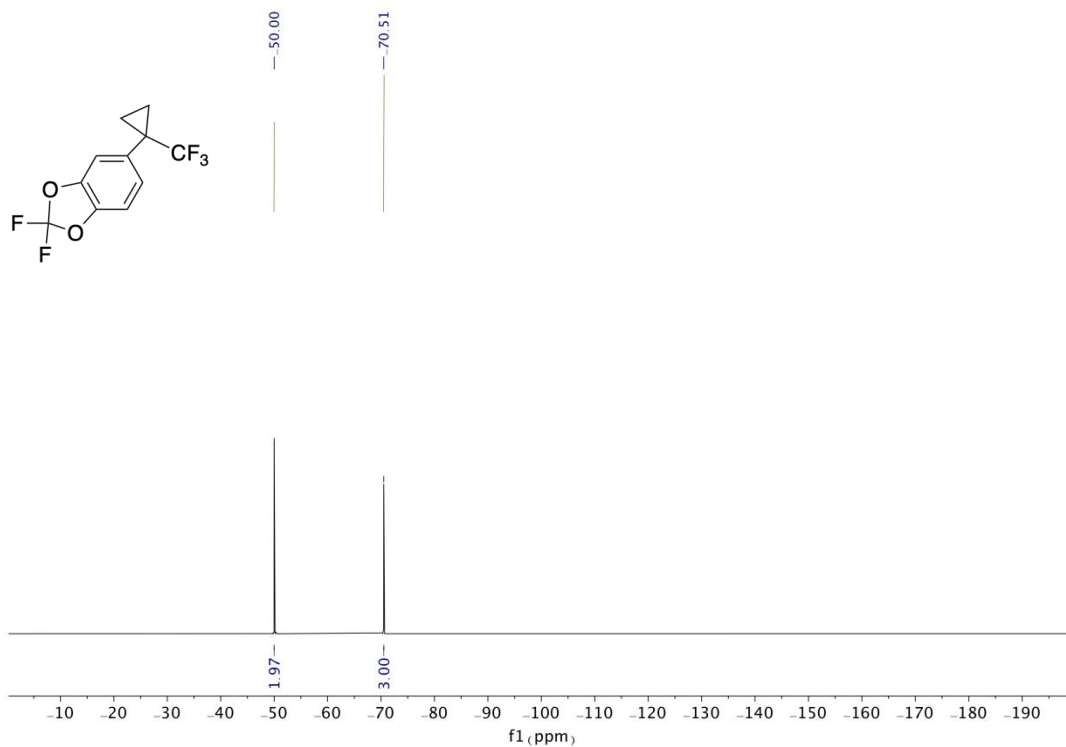


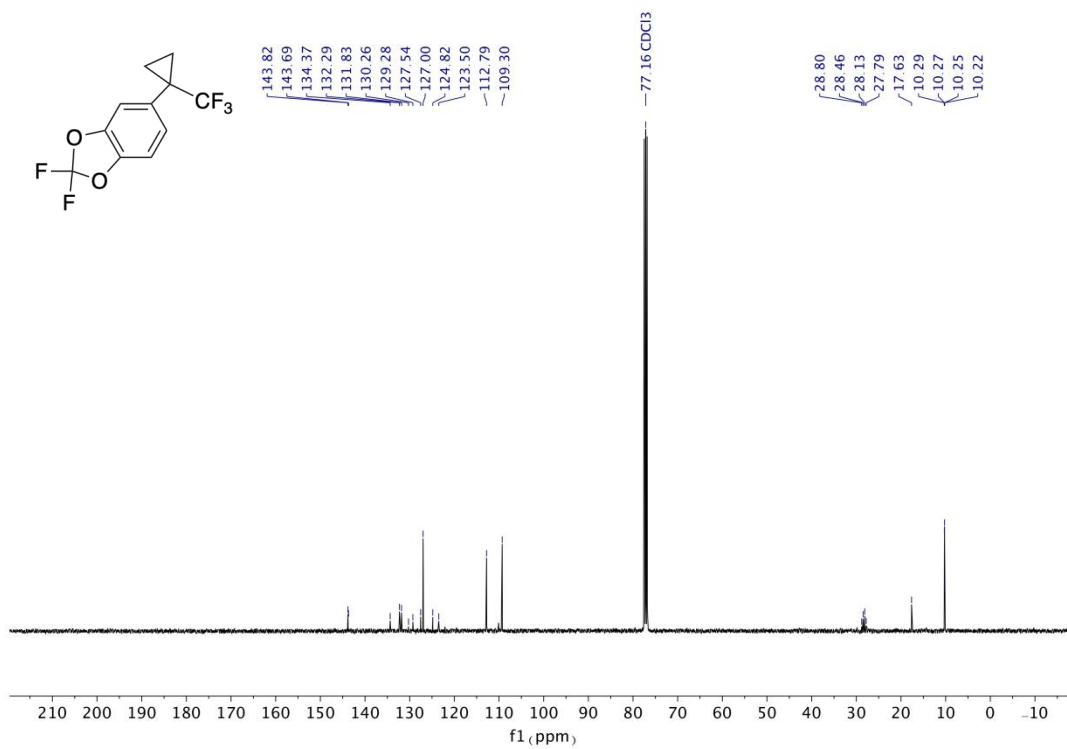
<sup>13</sup>C NMR (101 MHz, CDCl<sub>3</sub>) of **25**



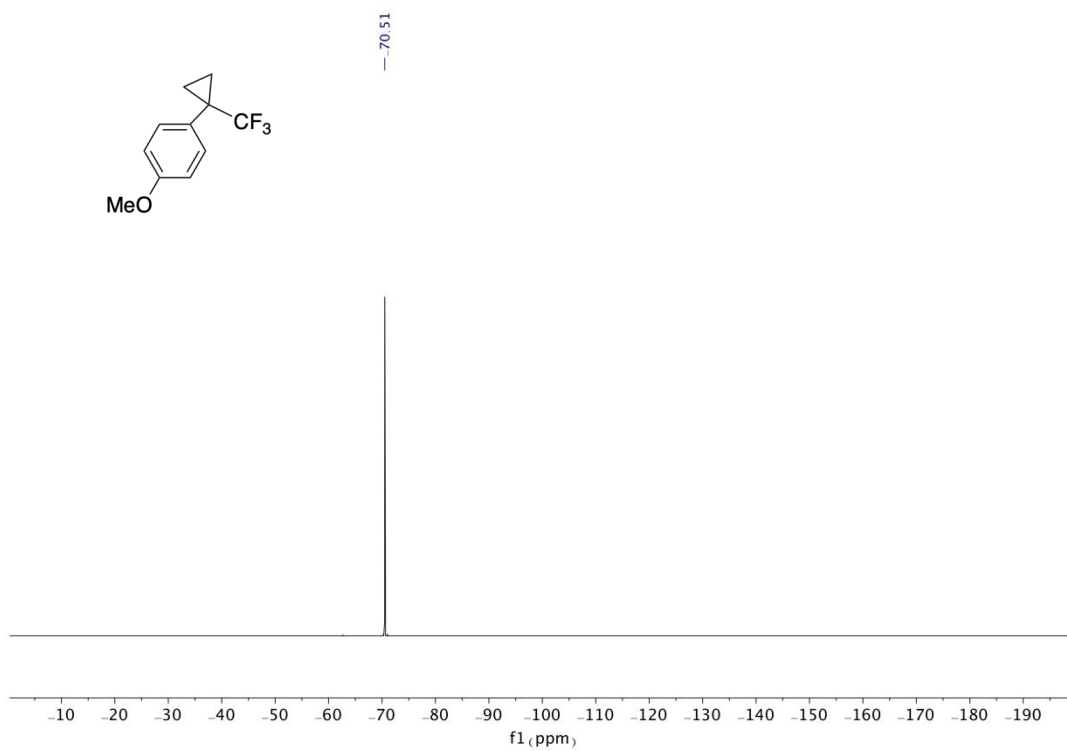
<sup>19</sup>F NMR (376 MHz, CDCl<sub>3</sub>) of **26**



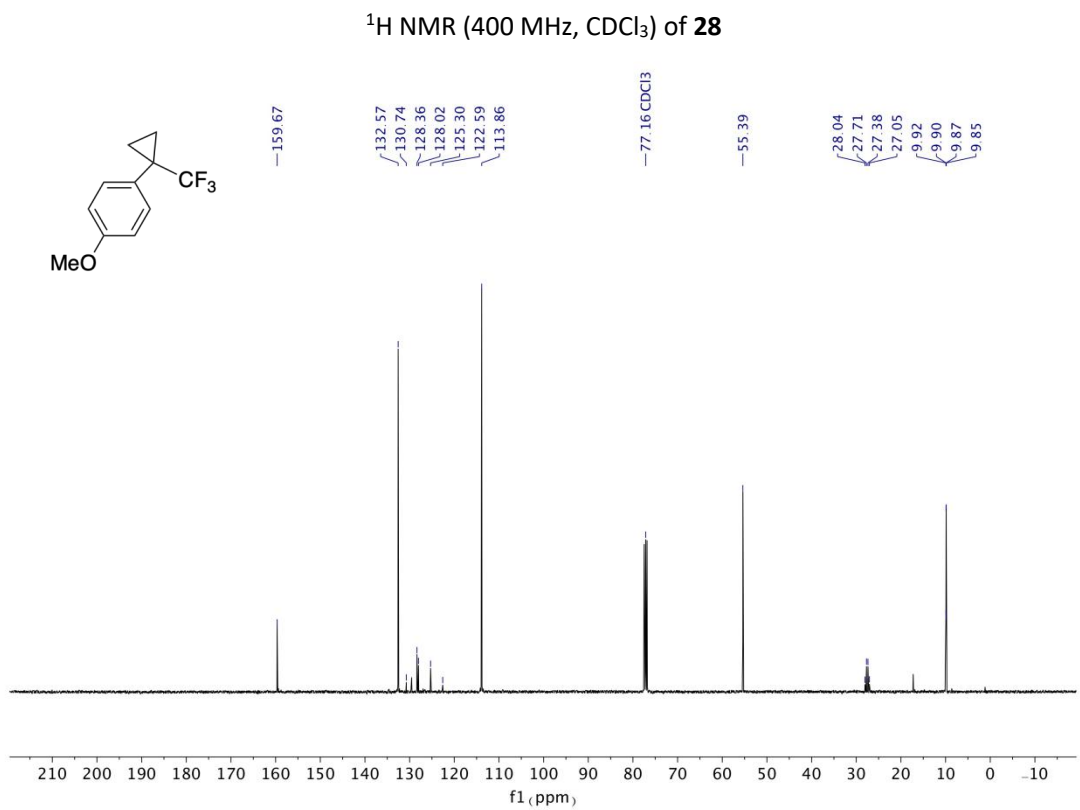
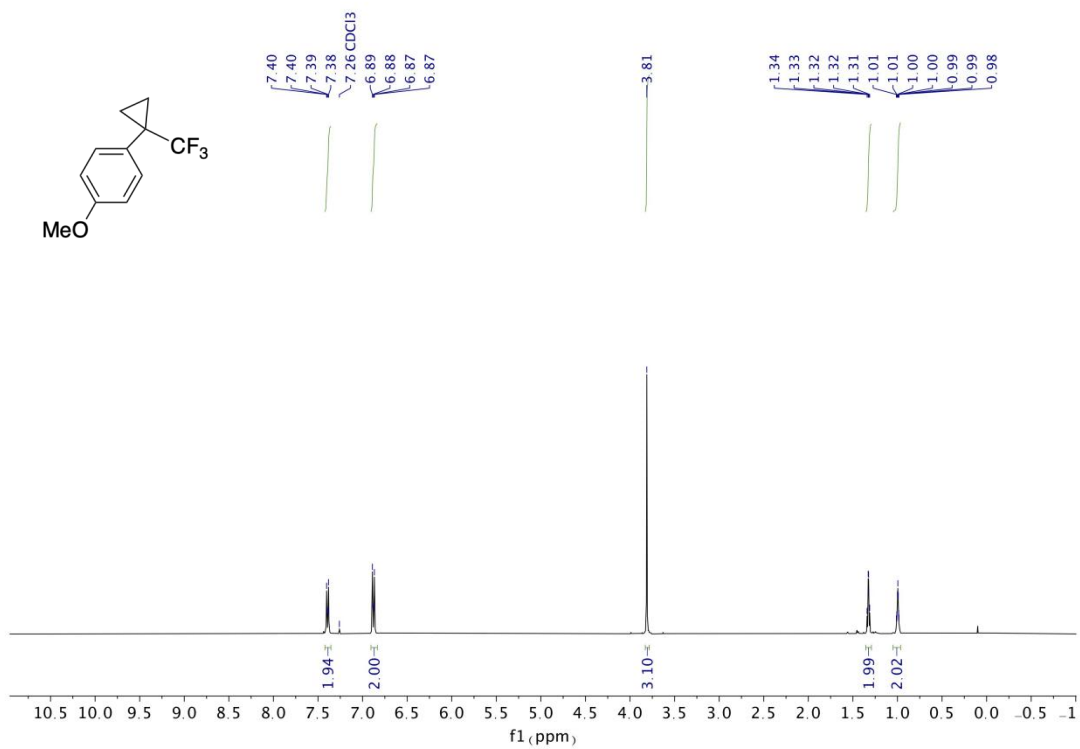


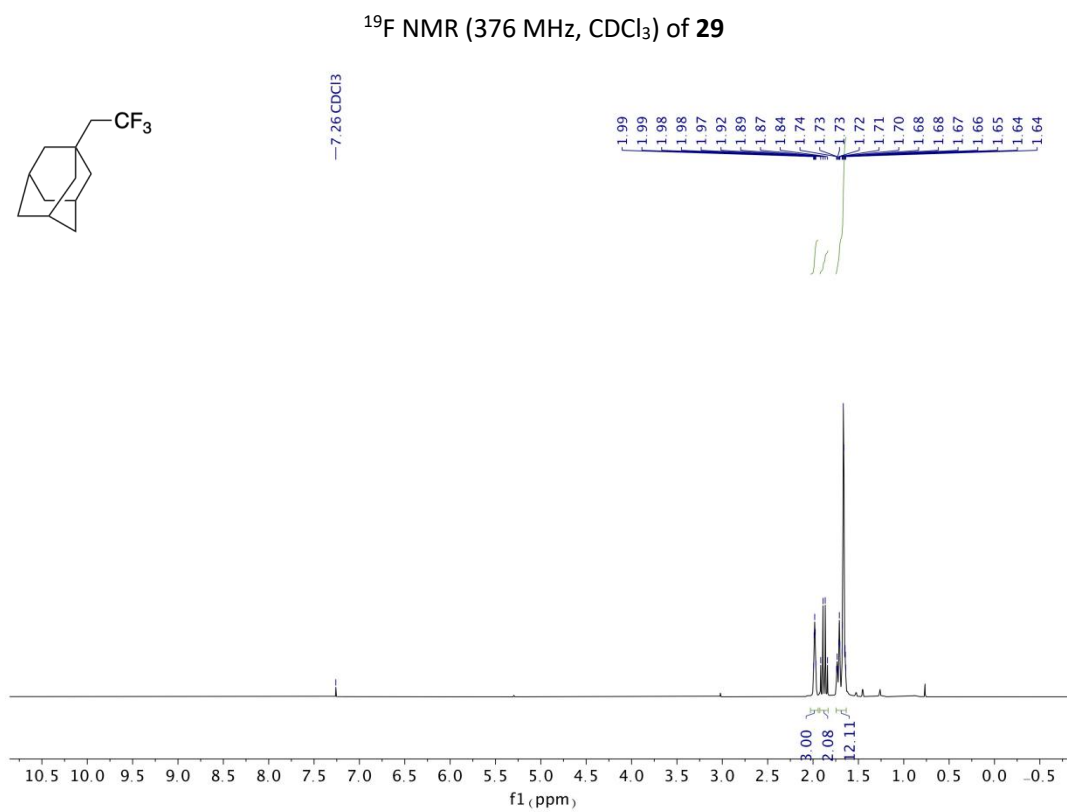
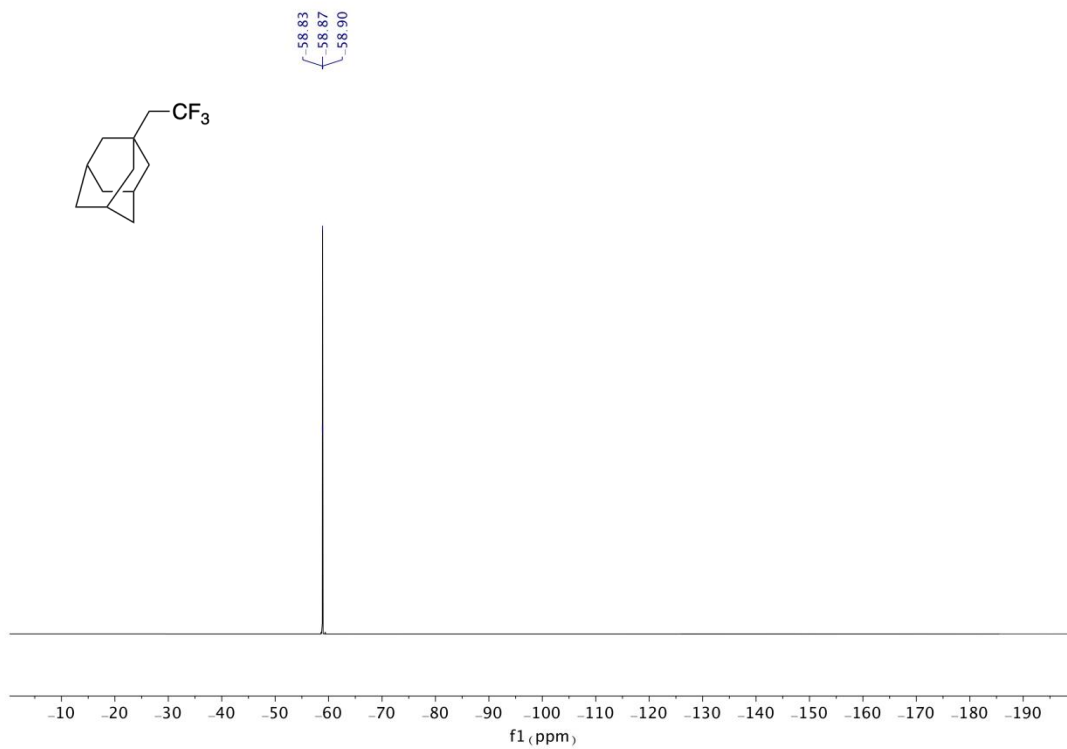


<sup>13</sup>C NMR (101 MHz, CDCl<sub>3</sub>) of **27**

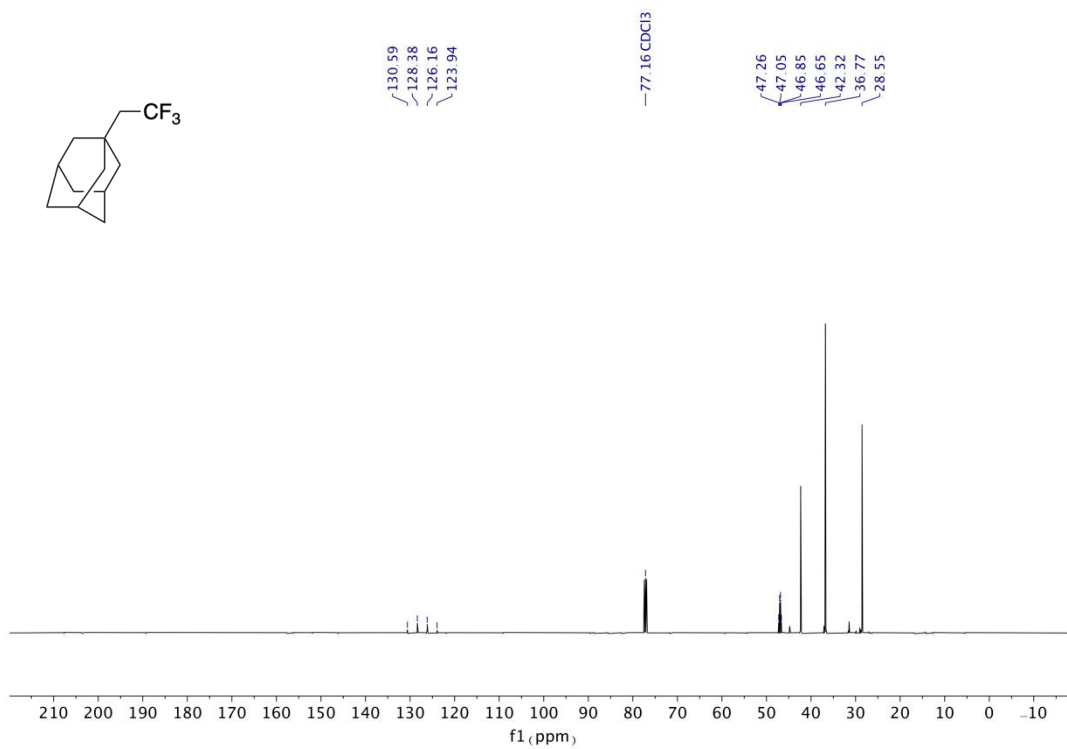


<sup>19</sup>F NMR (376 MHz, CDCl<sub>3</sub>) of **28**

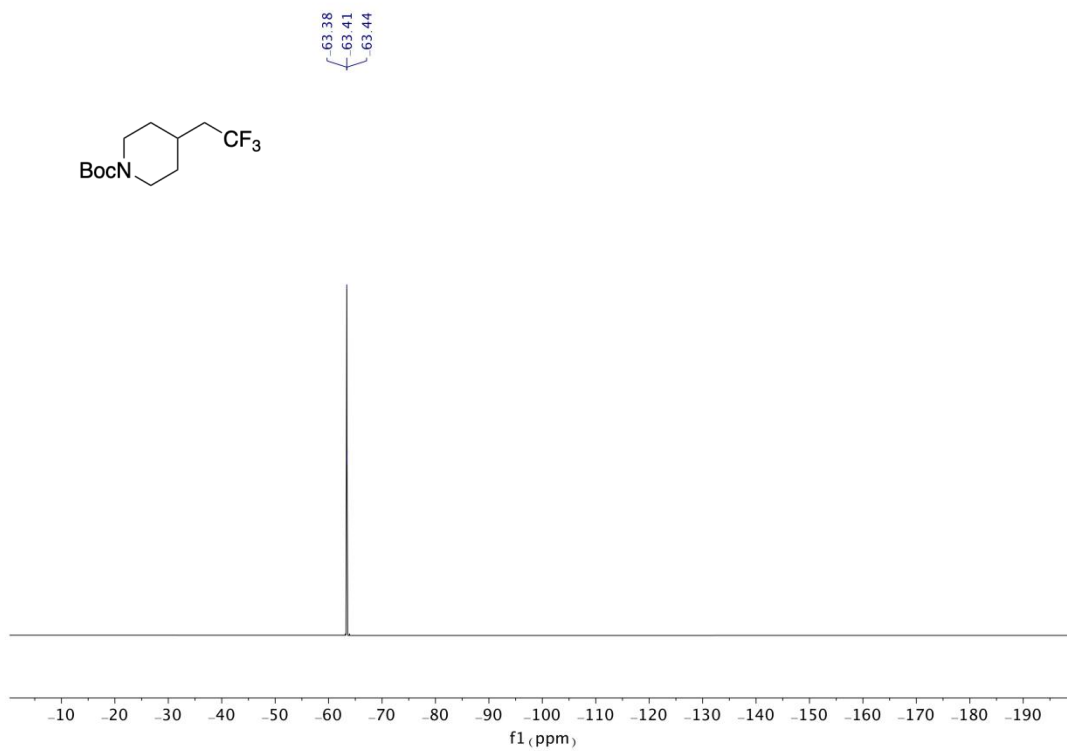




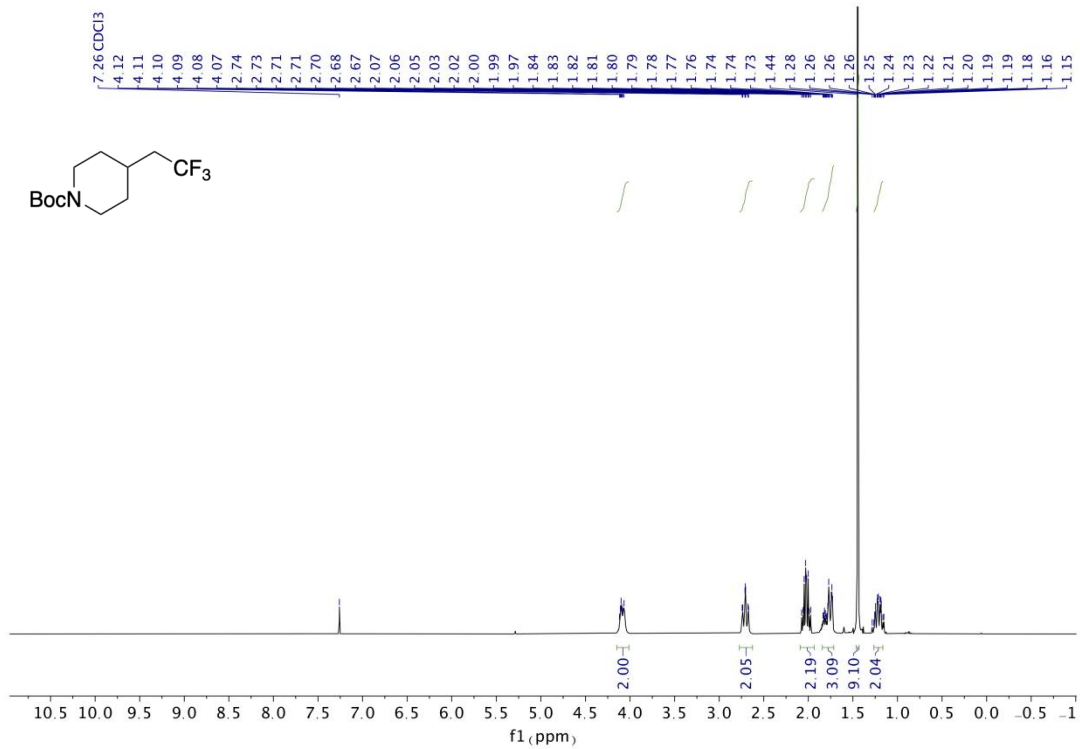




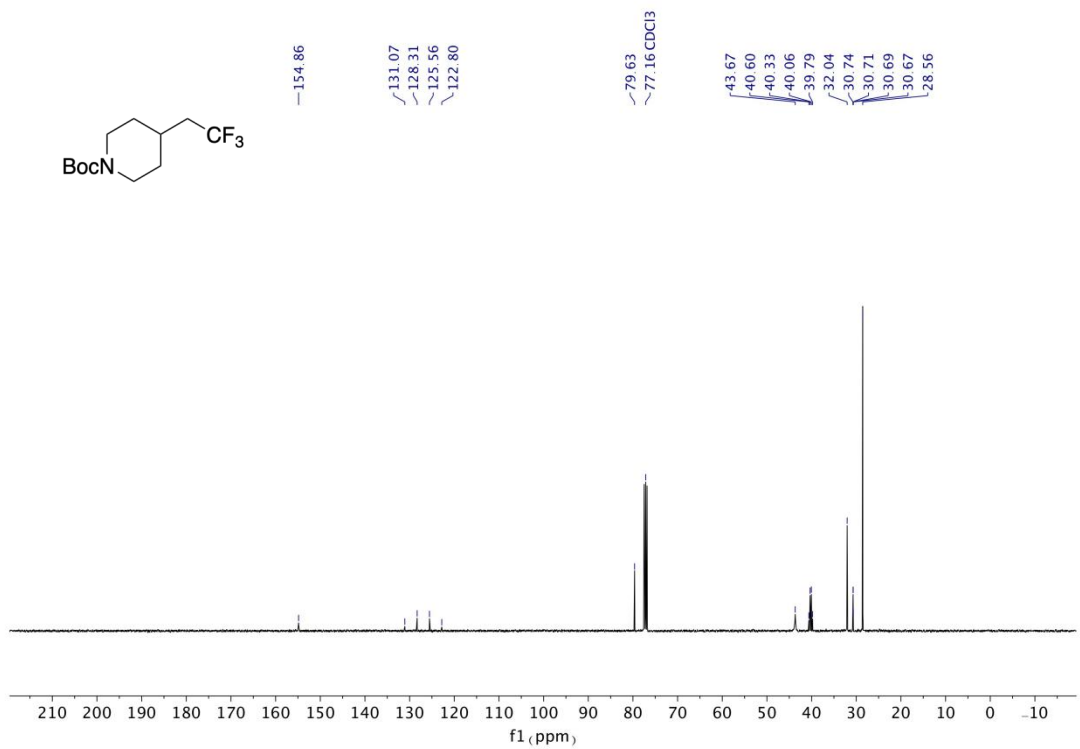
<sup>13</sup>C NMR (126 MHz, CDCl<sub>3</sub>) of **29**



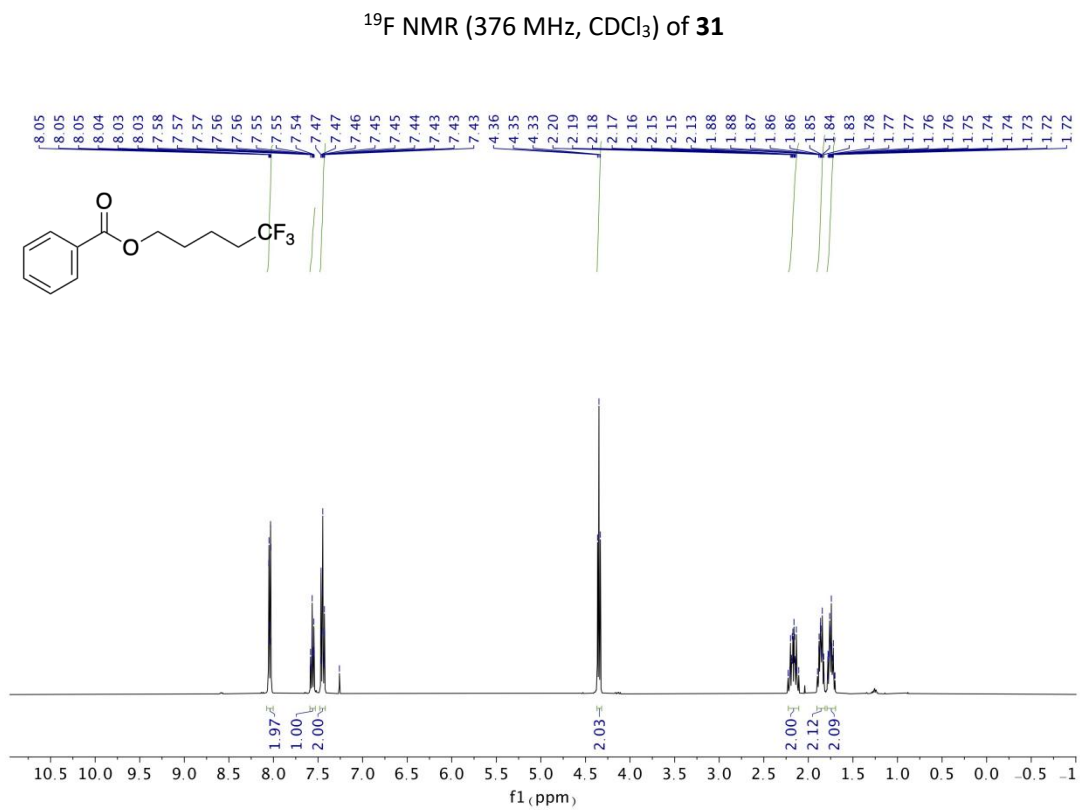
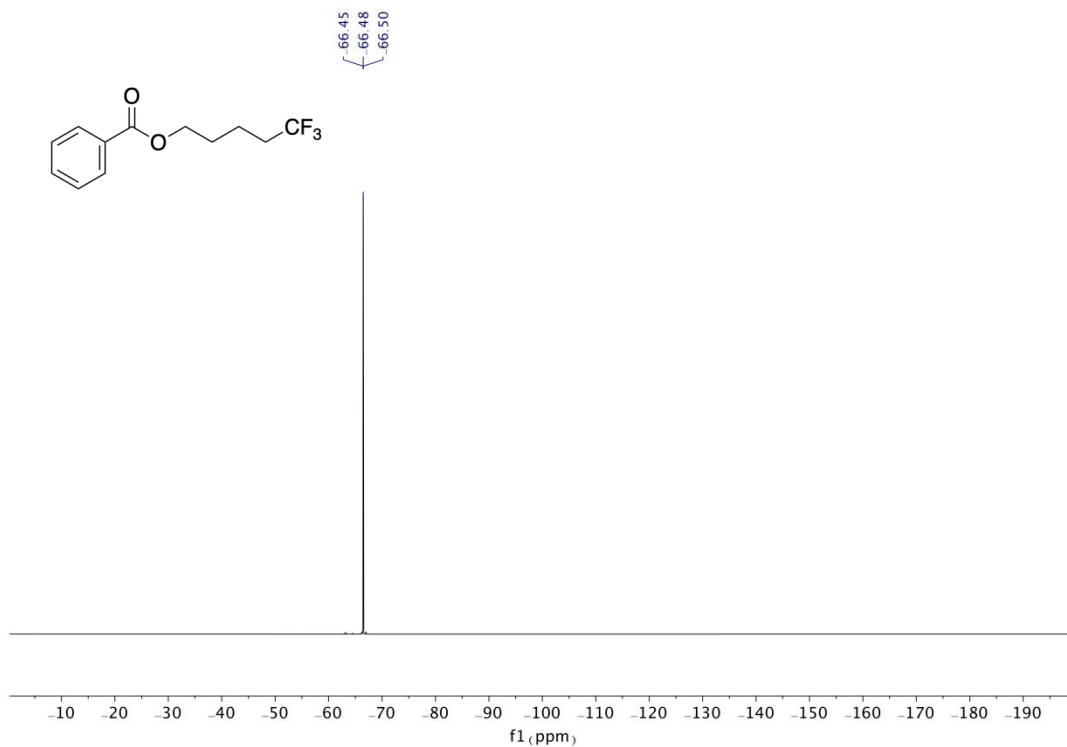
<sup>19</sup>F NMR (376 MHz, CDCl<sub>3</sub>) of **30**



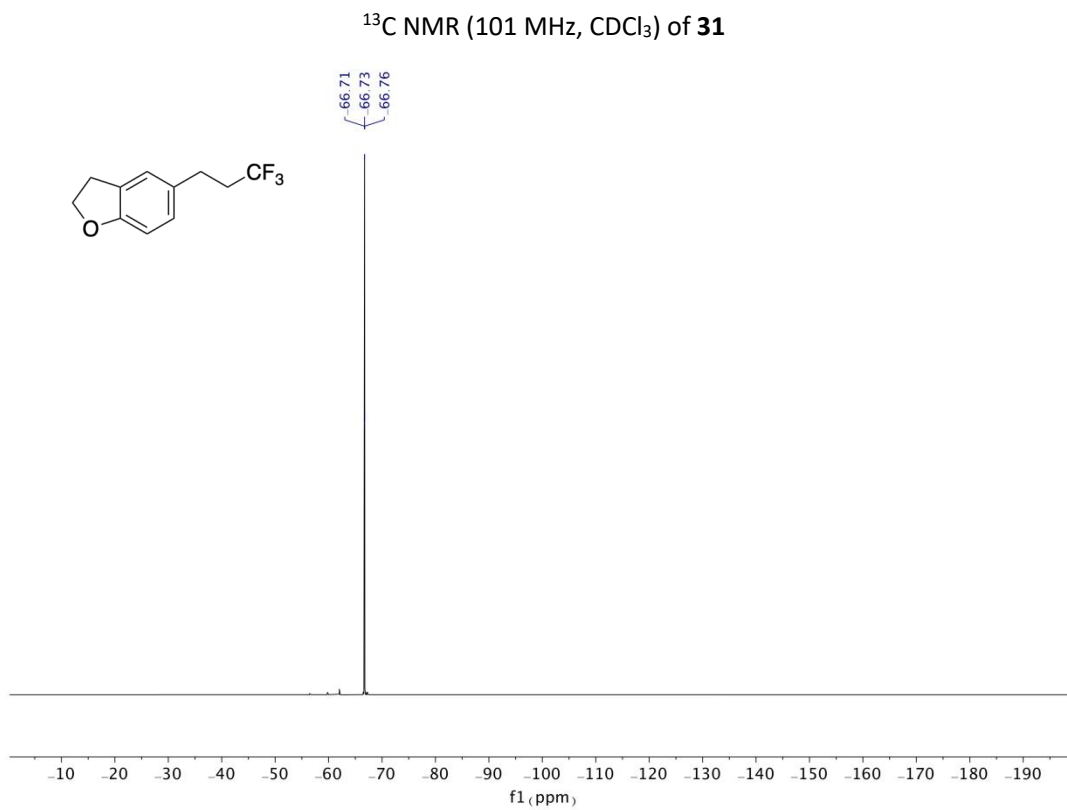
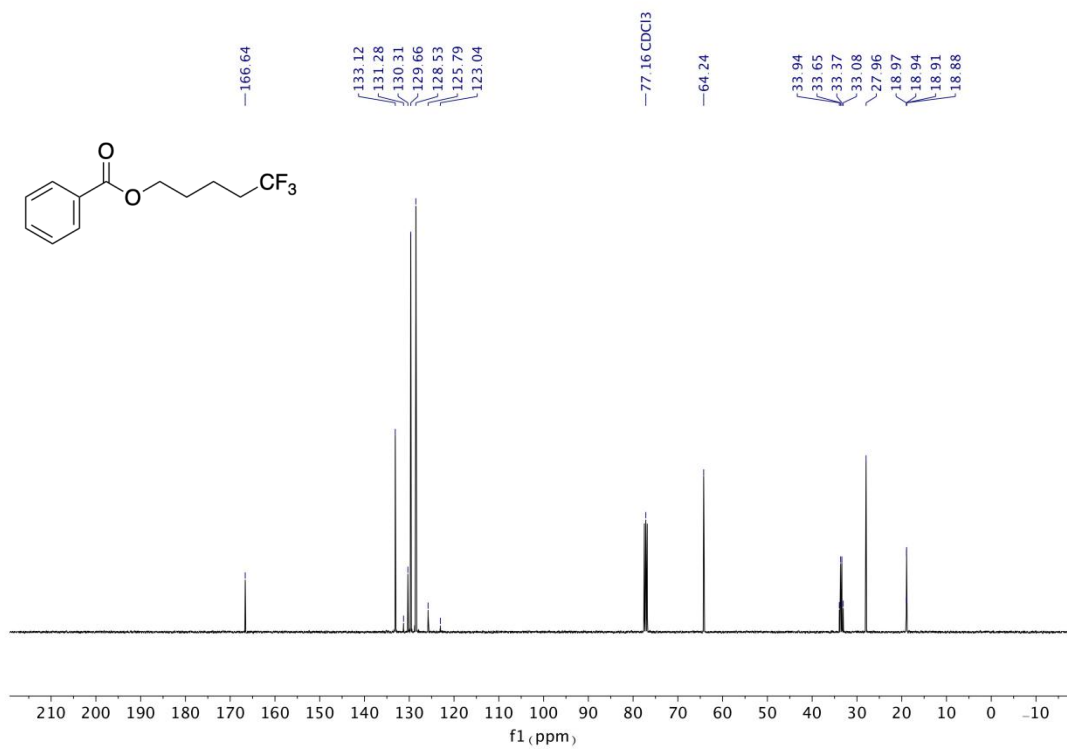
<sup>1</sup>H NMR (400 MHz, CDCl<sub>3</sub>) of **30**

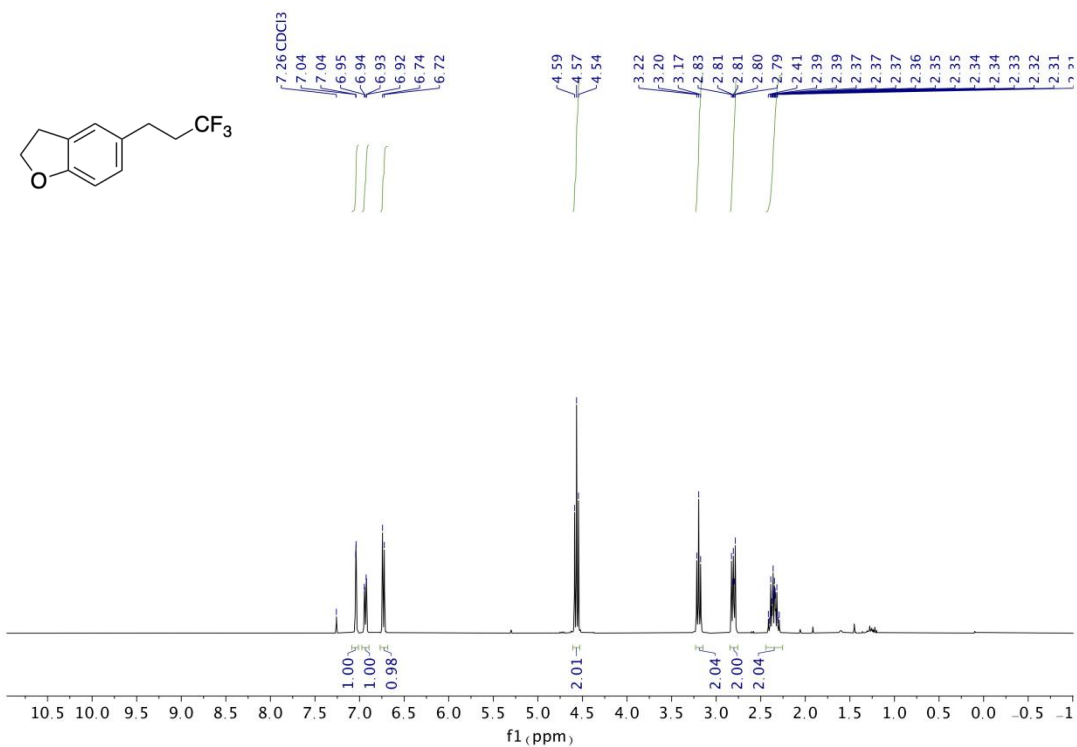


<sup>13</sup>C NMR (101 MHz, CDCl<sub>3</sub>) of **30**

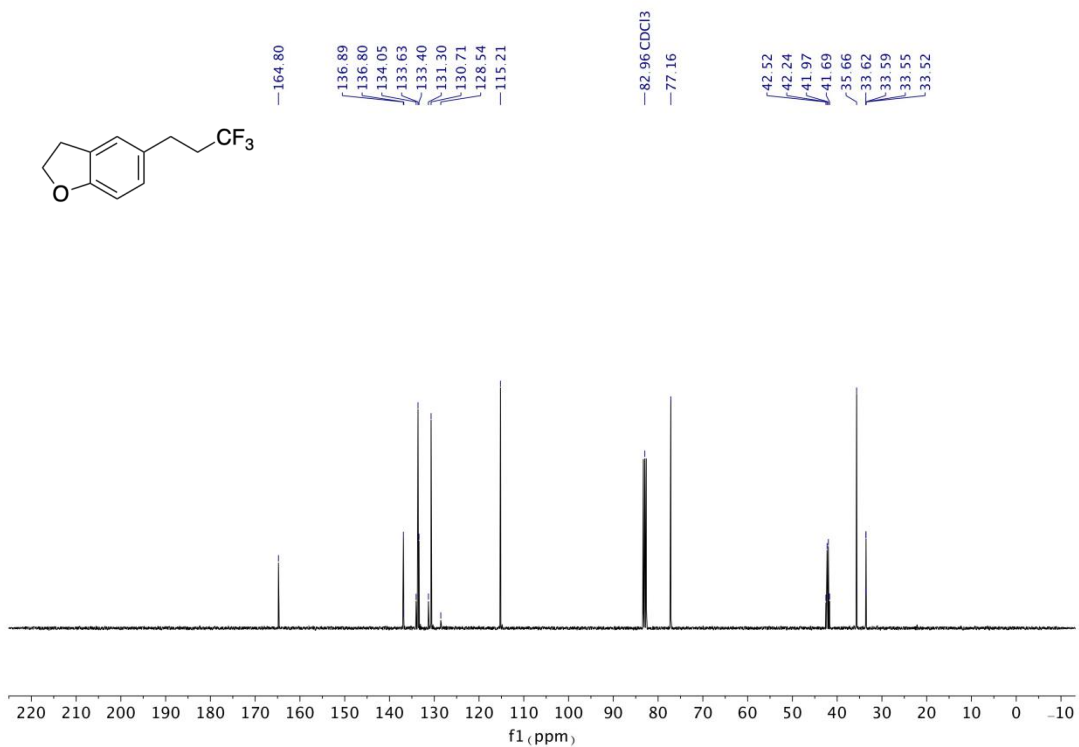


$^1\text{H}$  NMR (400 MHz,  $\text{CDCl}_3$ ) of **31**

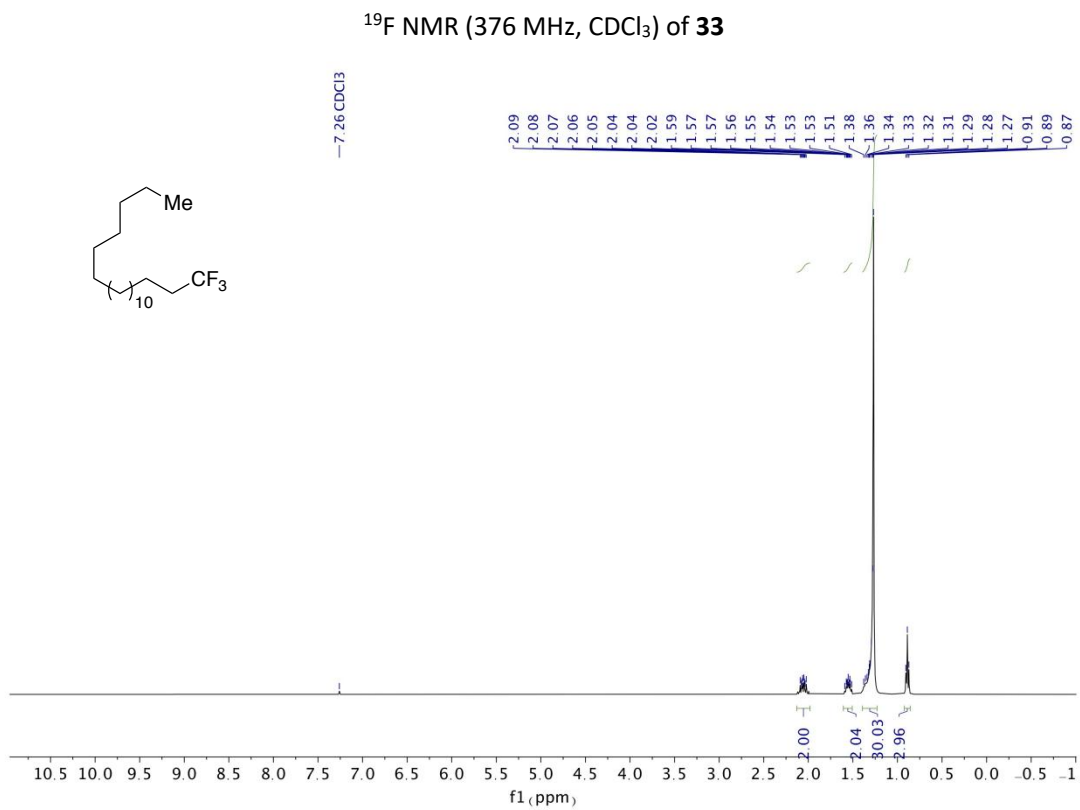
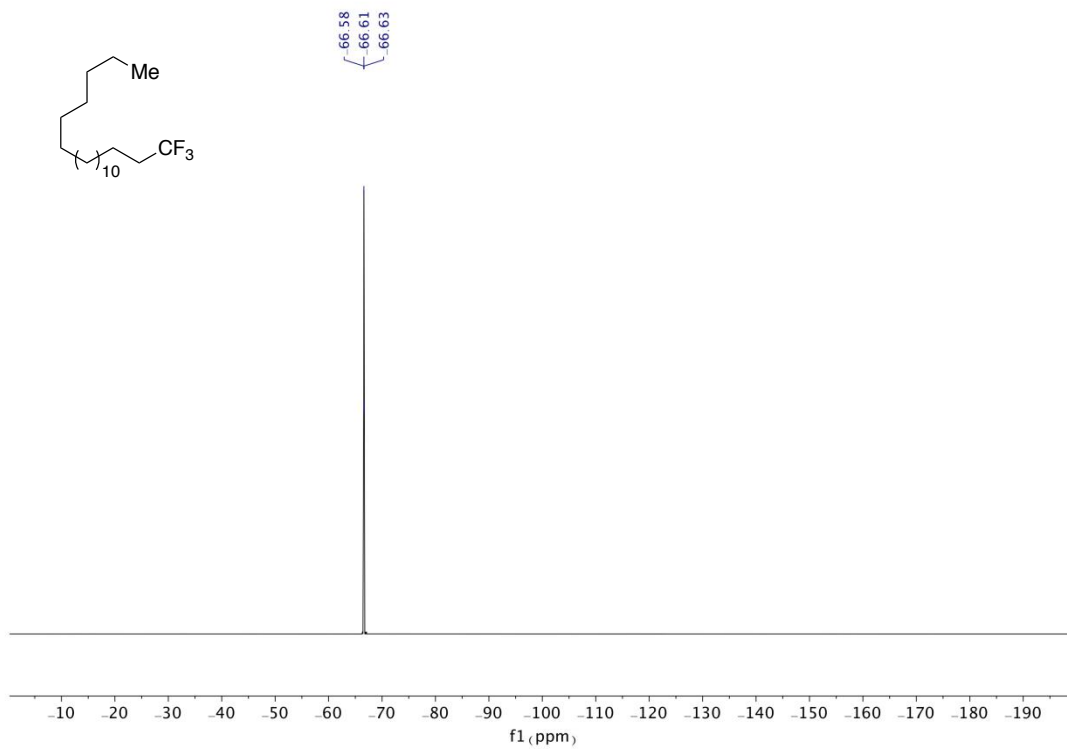


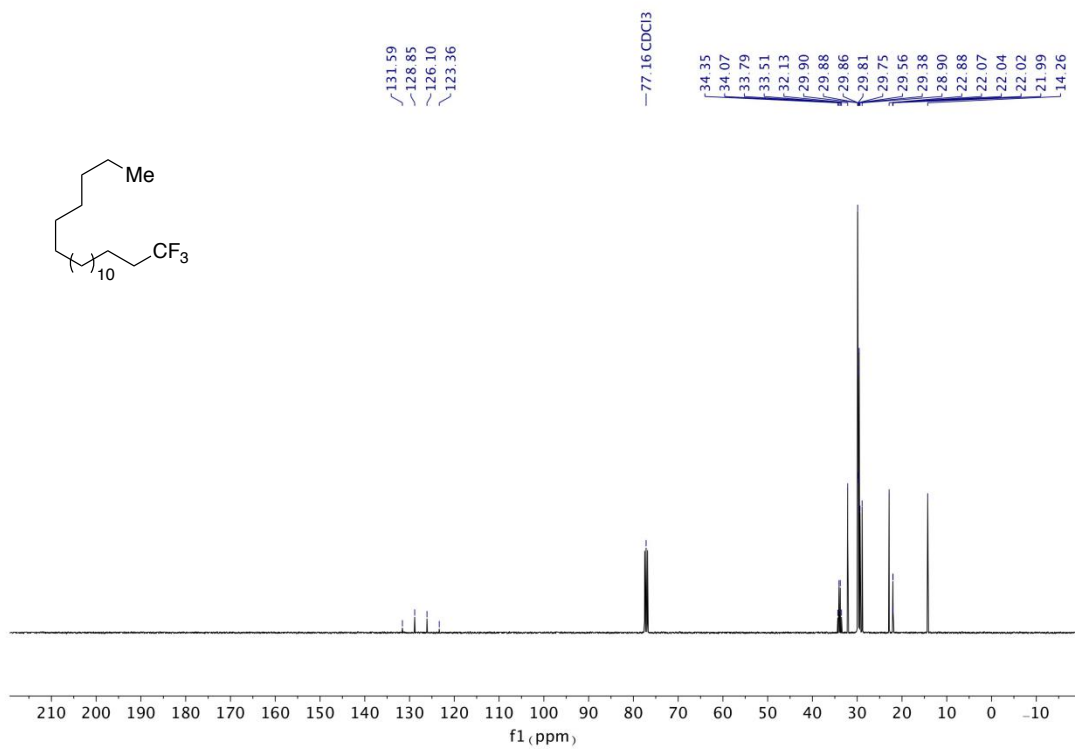


$^1\text{H}$  NMR (400 MHz,  $\text{CDCl}_3$ ) of **32**

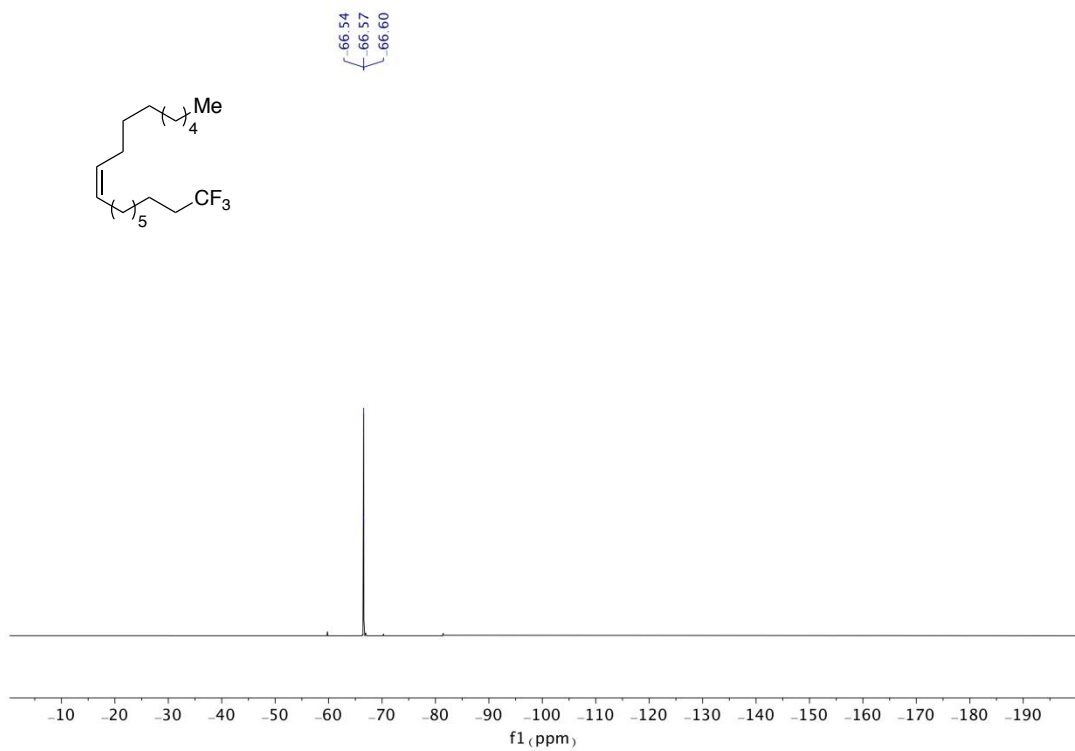


$^{13}\text{C}$  NMR (101 MHz,  $\text{CDCl}_3$ ) of **32**

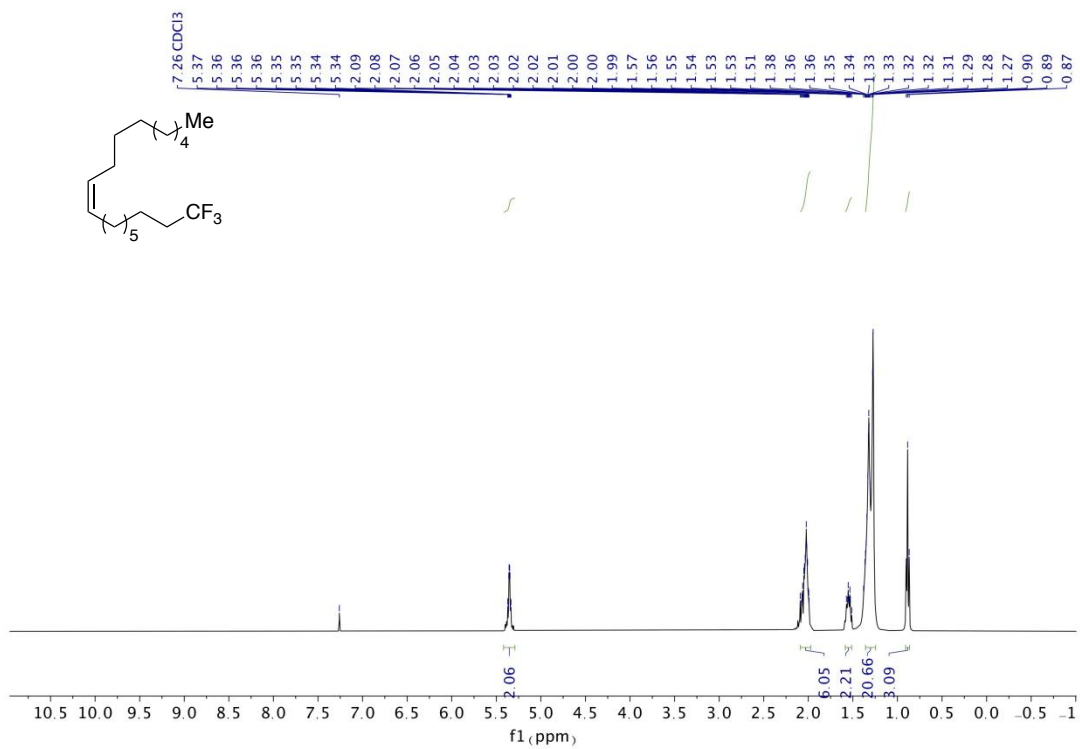




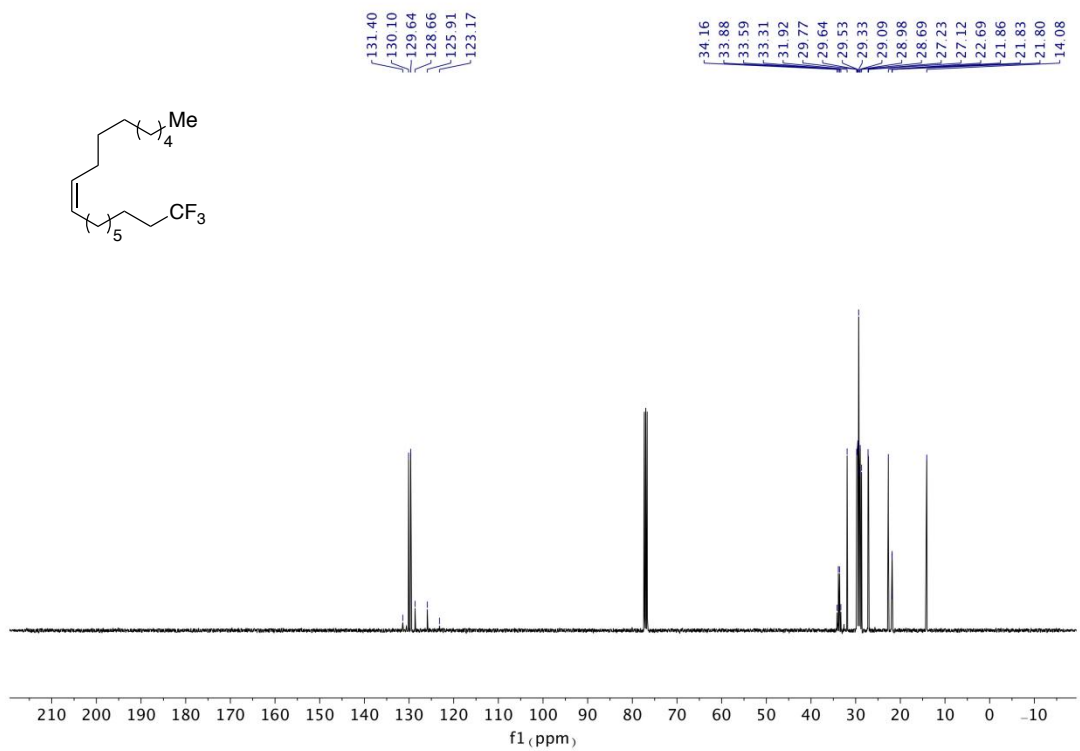
<sup>13</sup>C NMR (101 MHz, CDCl<sub>3</sub>) of **33**



<sup>19</sup>F NMR (376 MHz, CDCl<sub>3</sub>) of **34**

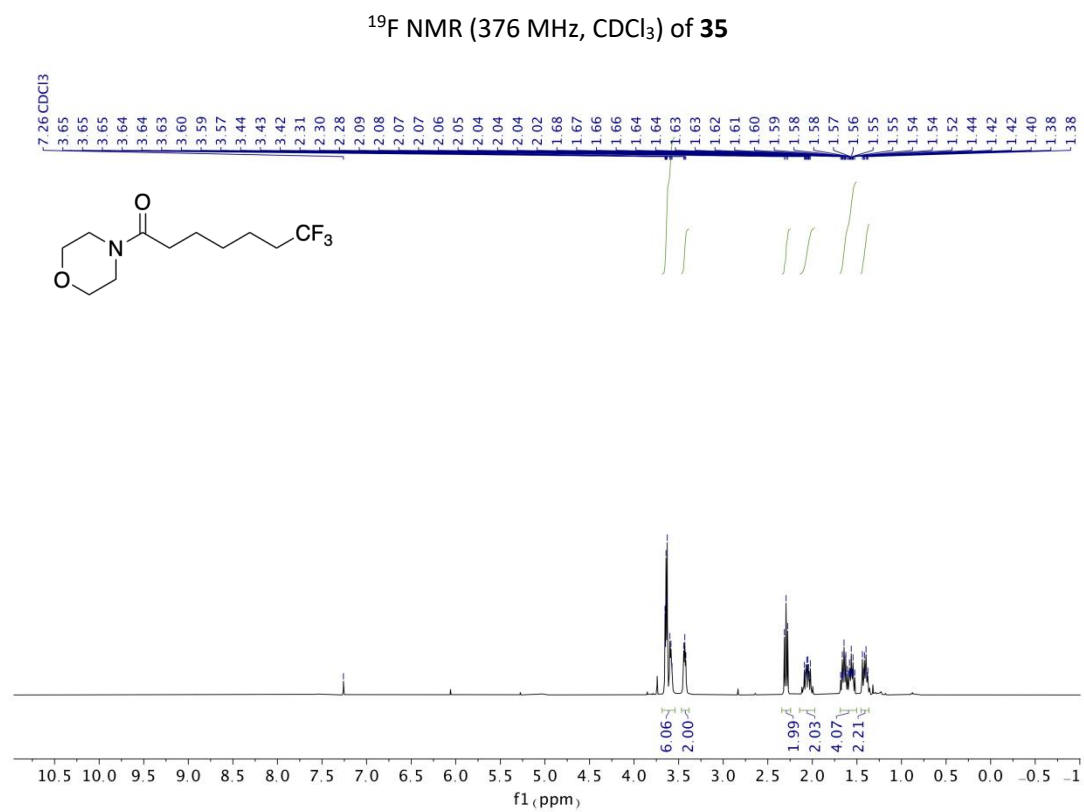
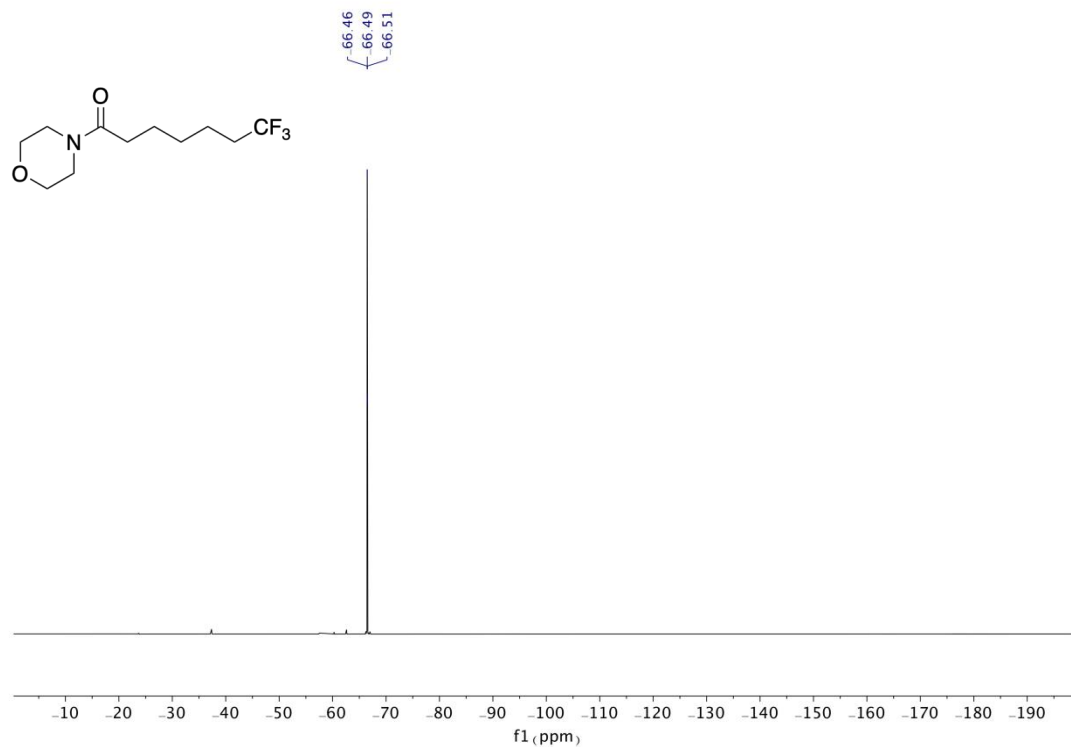


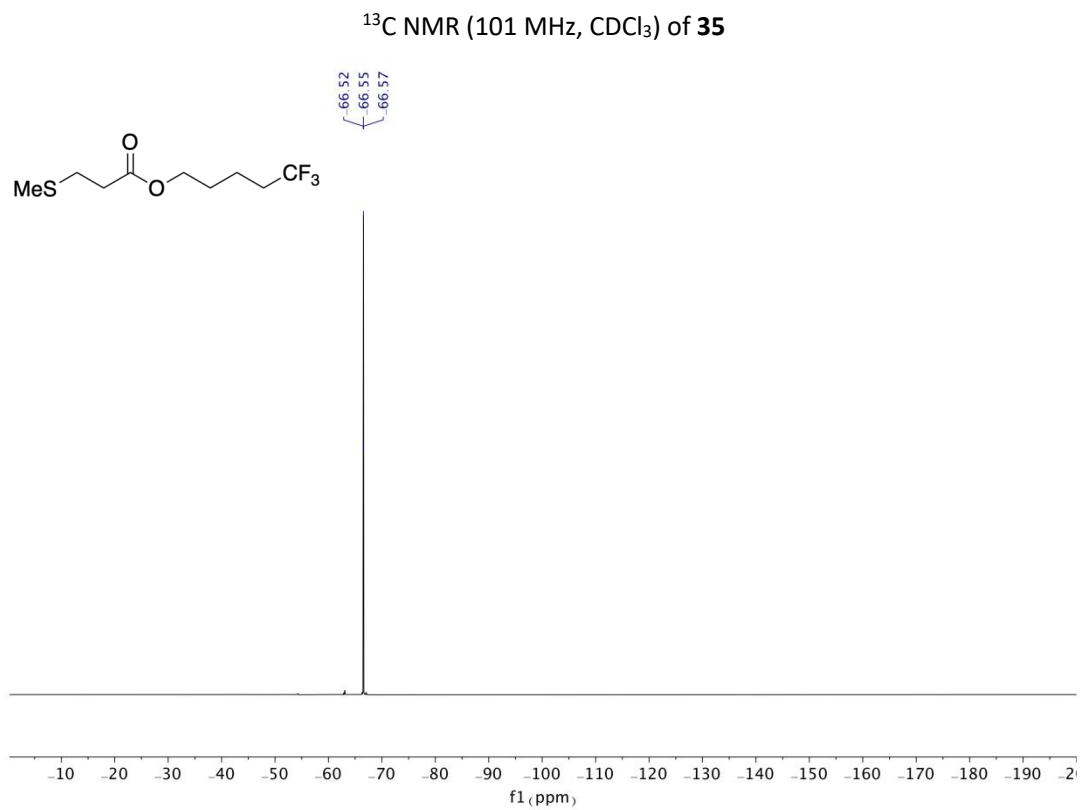
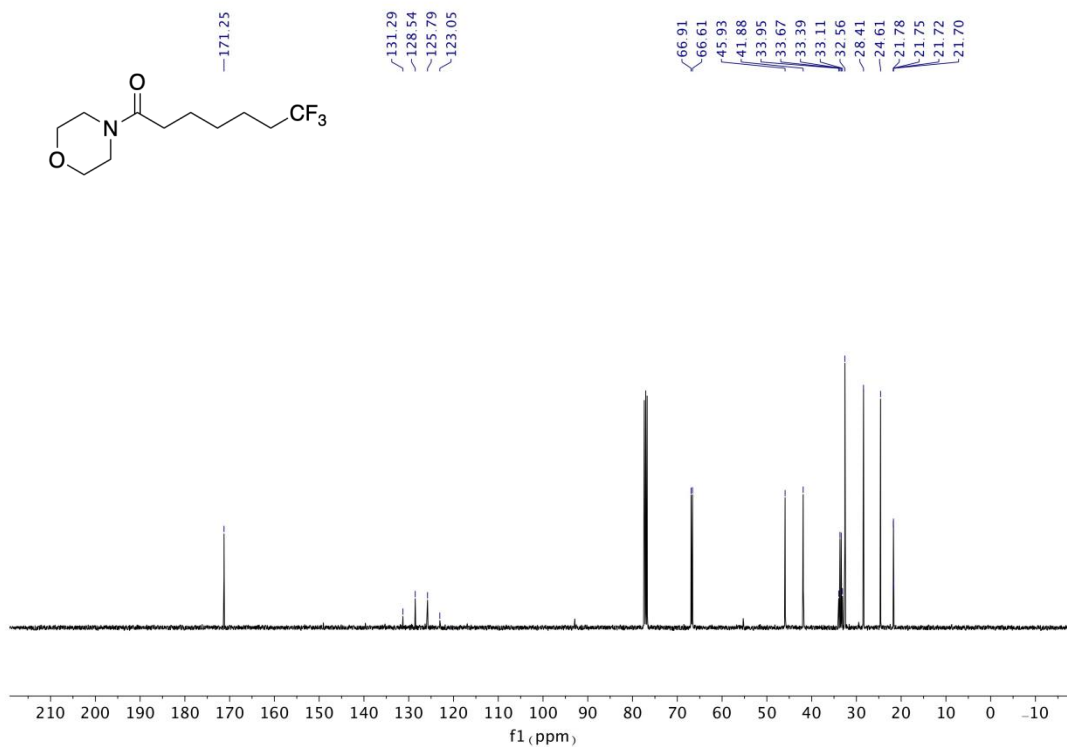
<sup>1</sup>H NMR (400 MHz, CDCl<sub>3</sub>) of **34**



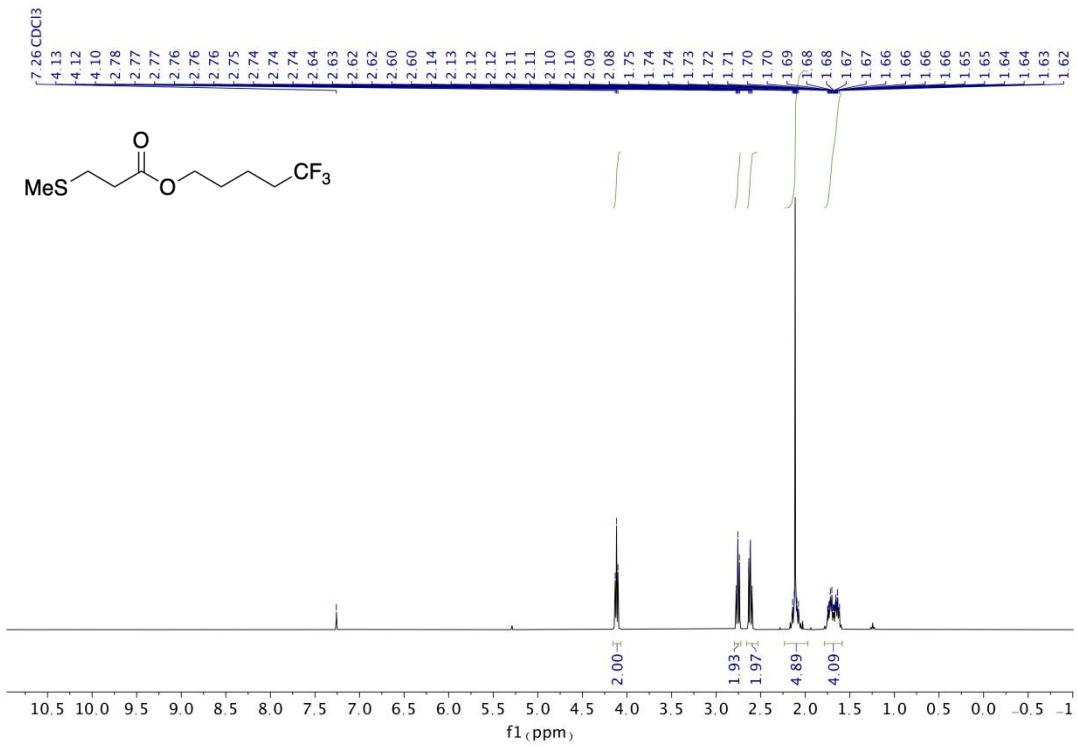
<sup>13</sup>C NMR (101 MHz, CDCl<sub>3</sub>) of **34**



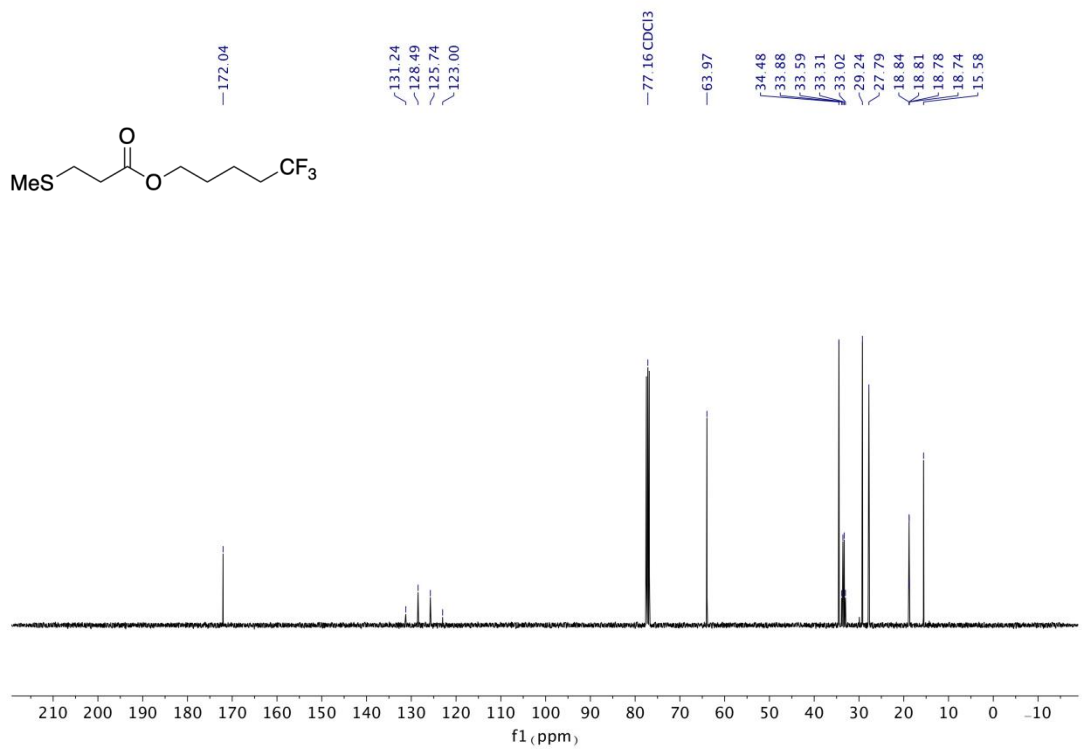




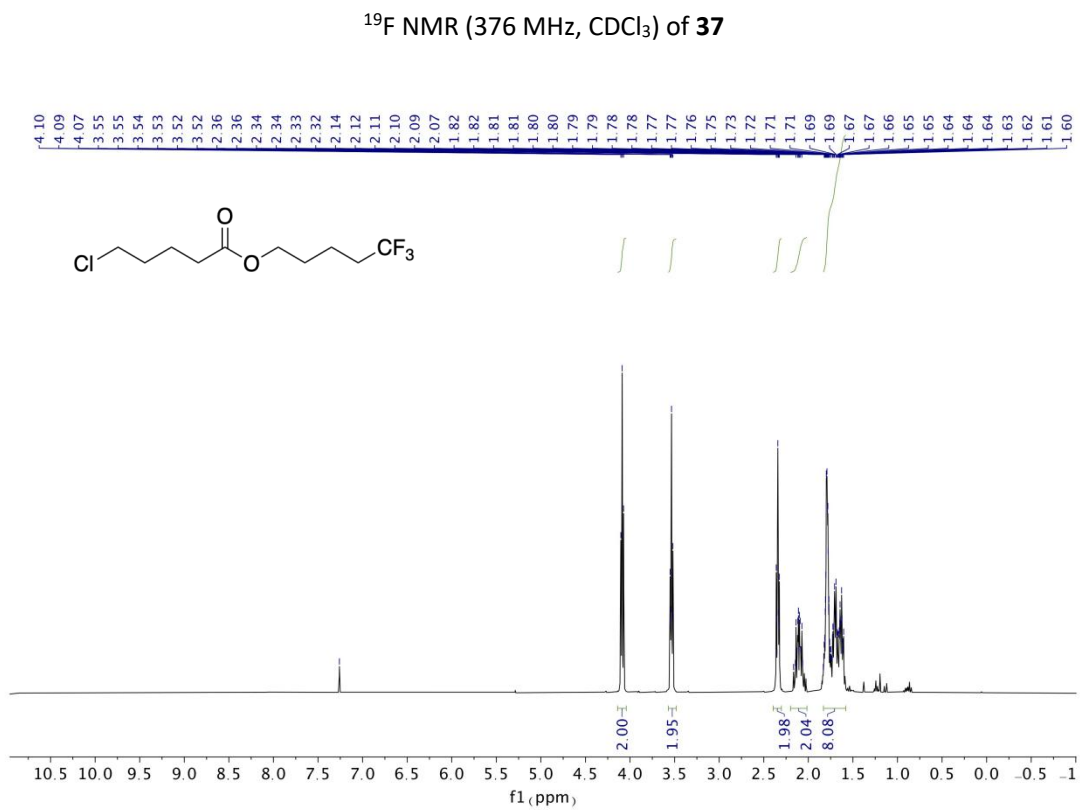
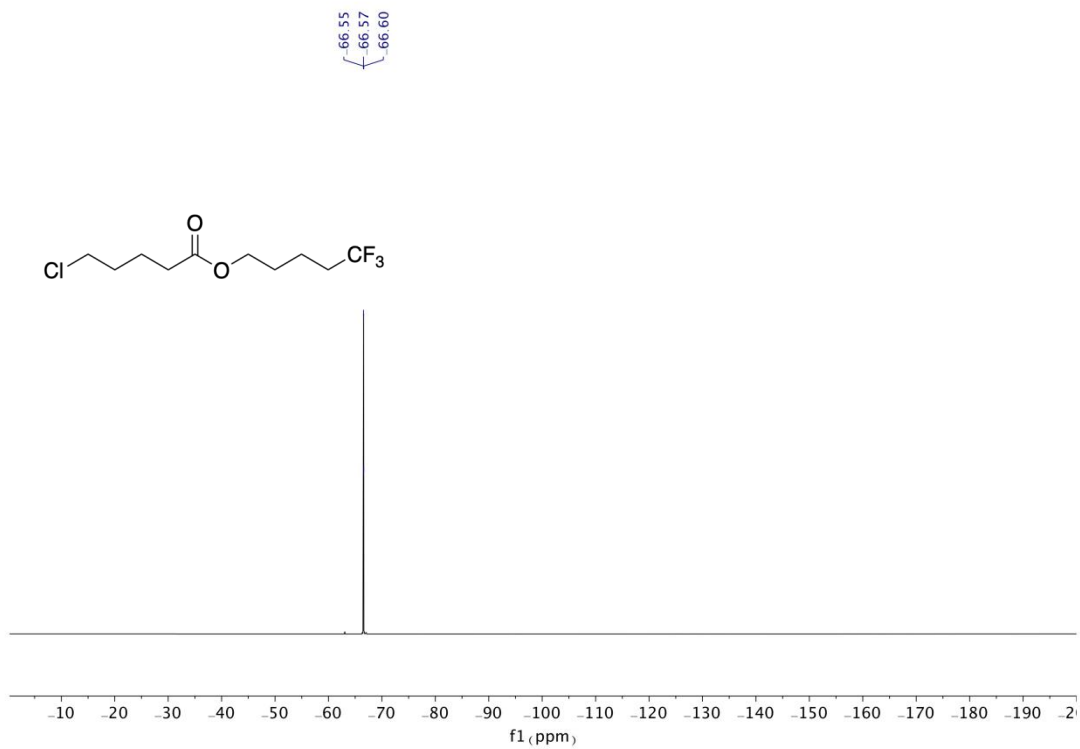
$^{19}\text{F}$  NMR (376 MHz,  $\text{CDCl}_3$ ) of **36**

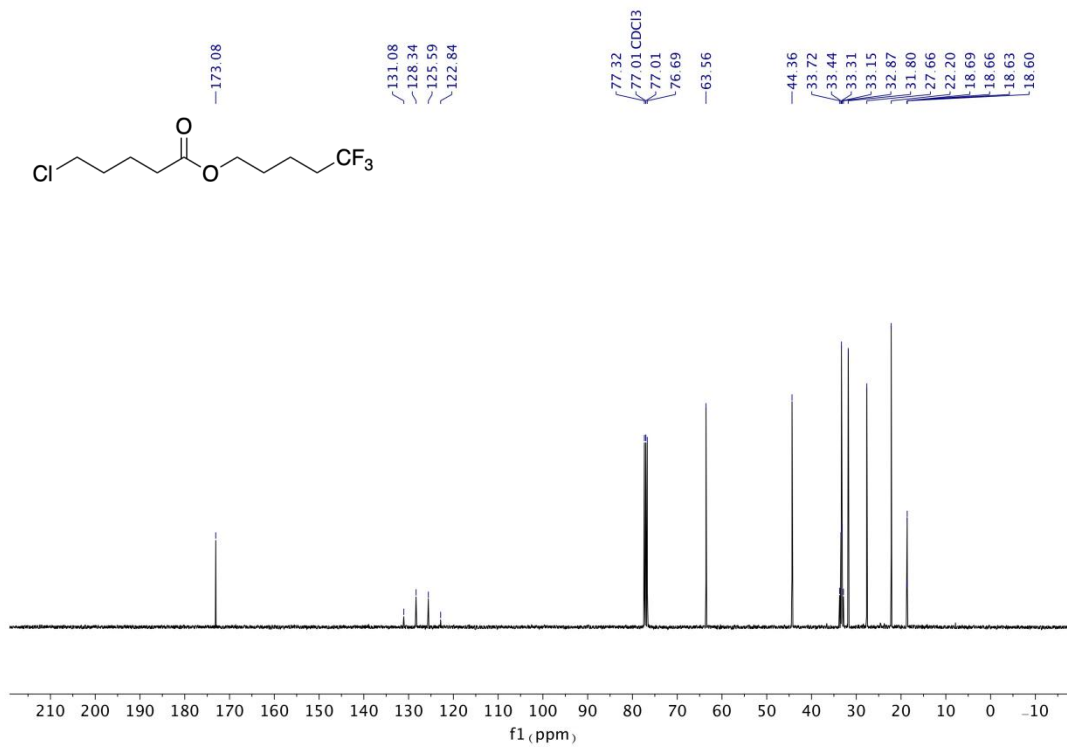


<sup>1</sup>H NMR (400 MHz, CDCl<sub>3</sub>) of **36**

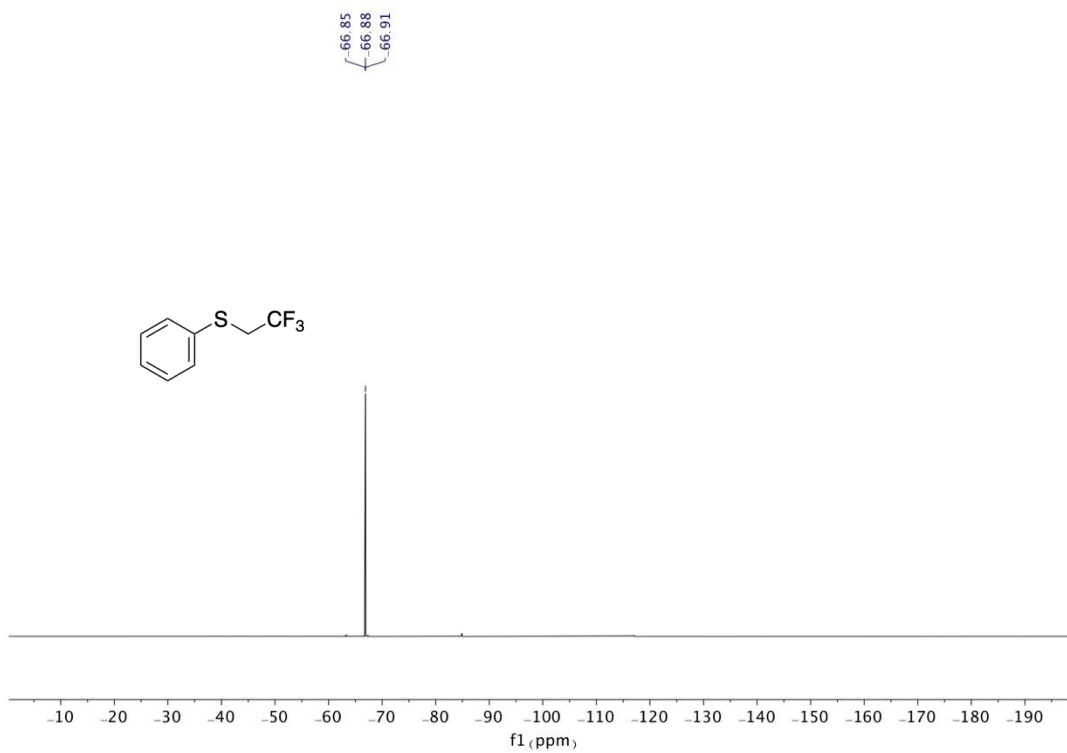


<sup>13</sup>C NMR (101 MHz, CDCl<sub>3</sub>) of **36**

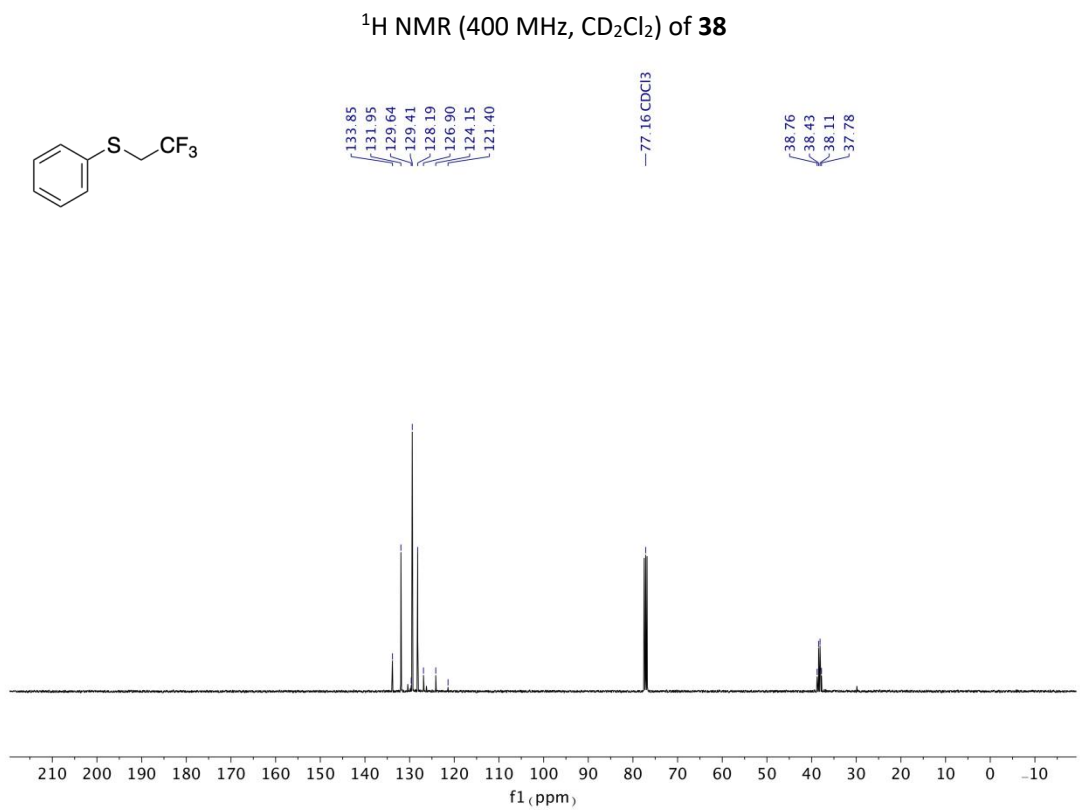
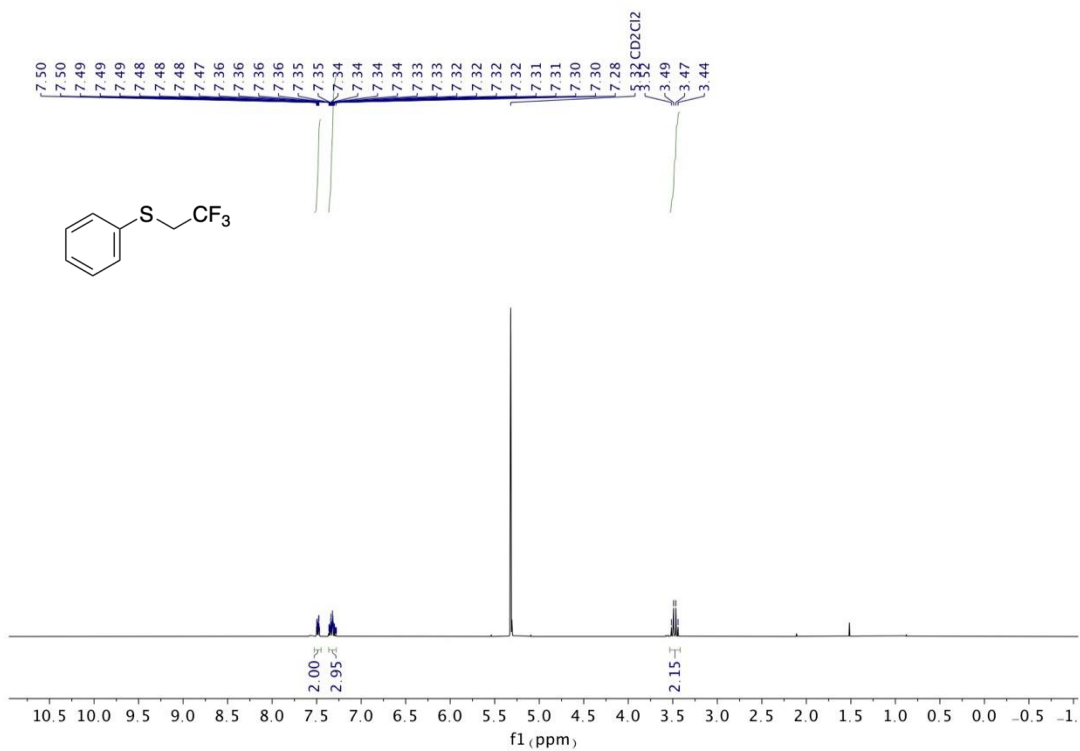


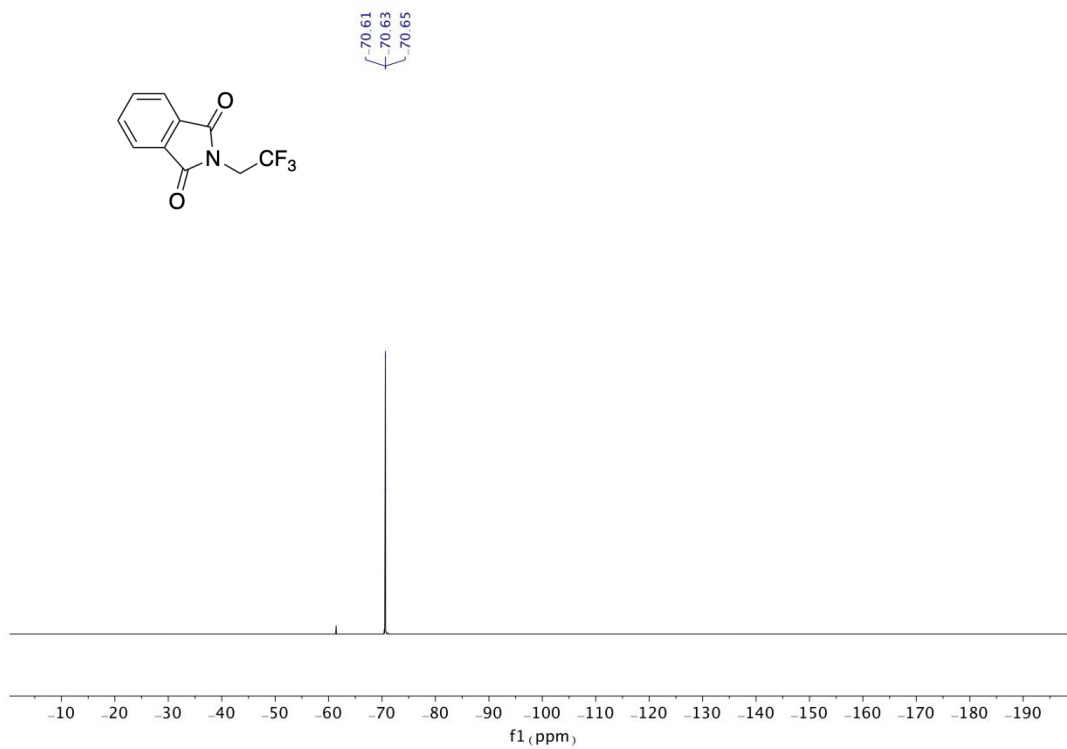


<sup>13</sup>C NMR (101 MHz, CDCl<sub>3</sub>) of **37**

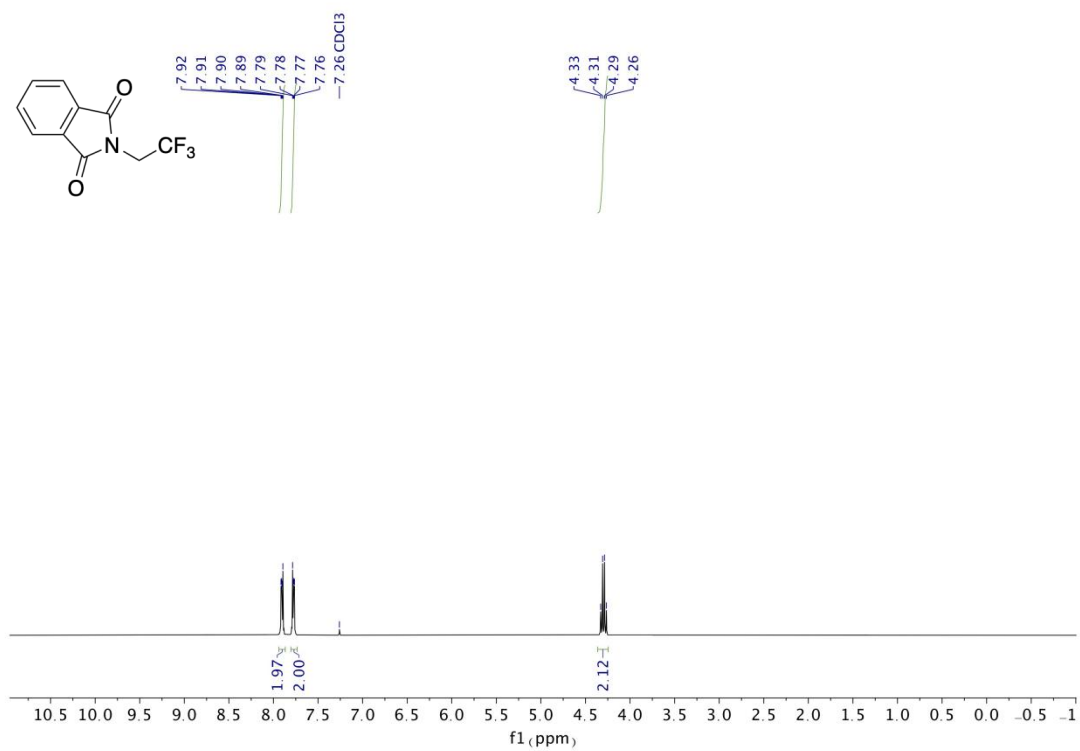


<sup>19</sup>F NMR (376 MHz, CD<sub>2</sub>Cl<sub>2</sub>) of **38**

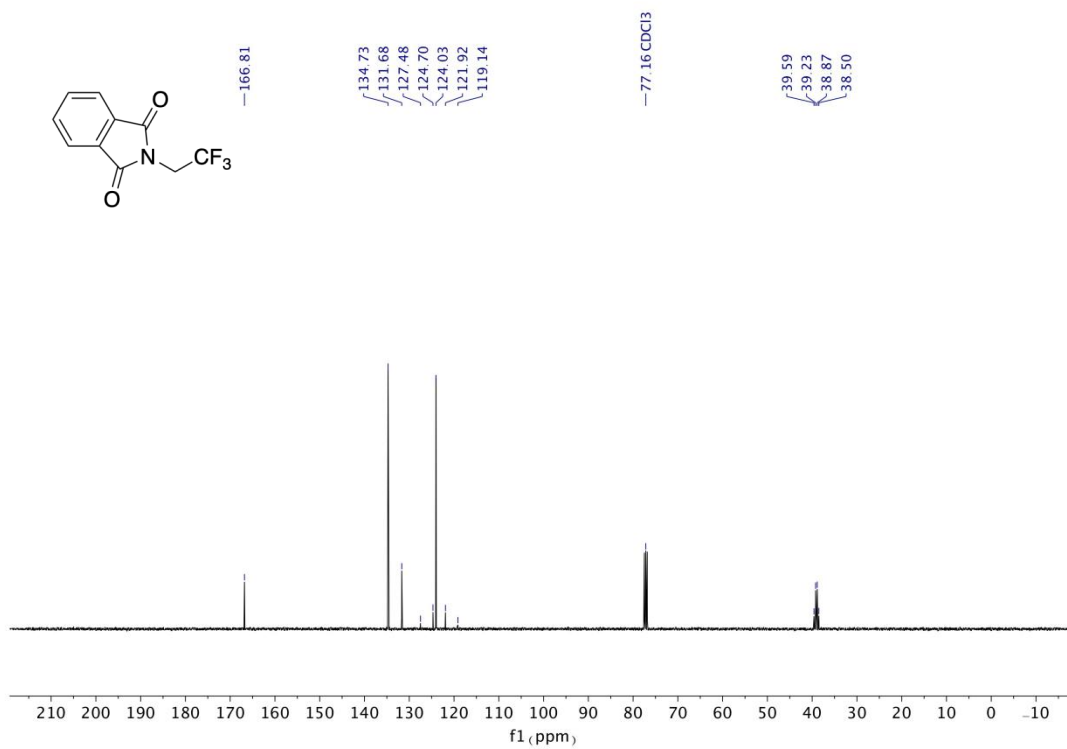




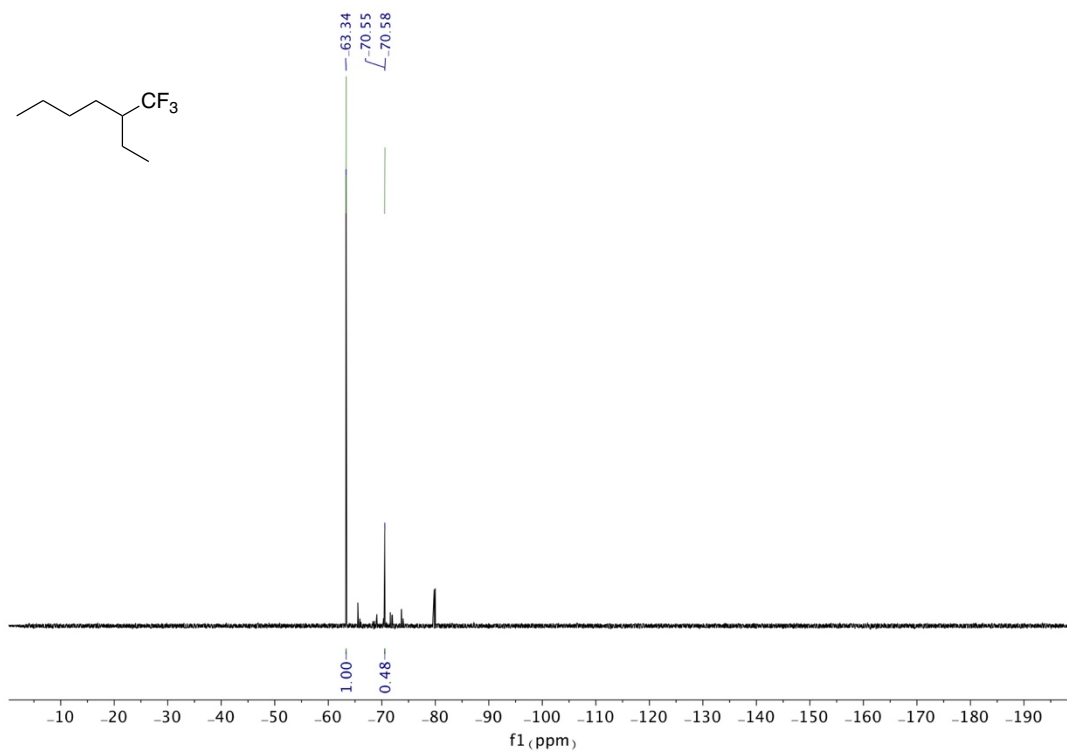
$^{19}\text{F}$  NMR (376 MHz,  $\text{CDCl}_3$ ) of **39**



$^1\text{H}$  NMR (400 MHz,  $\text{CDCl}_3$ ) of **39**

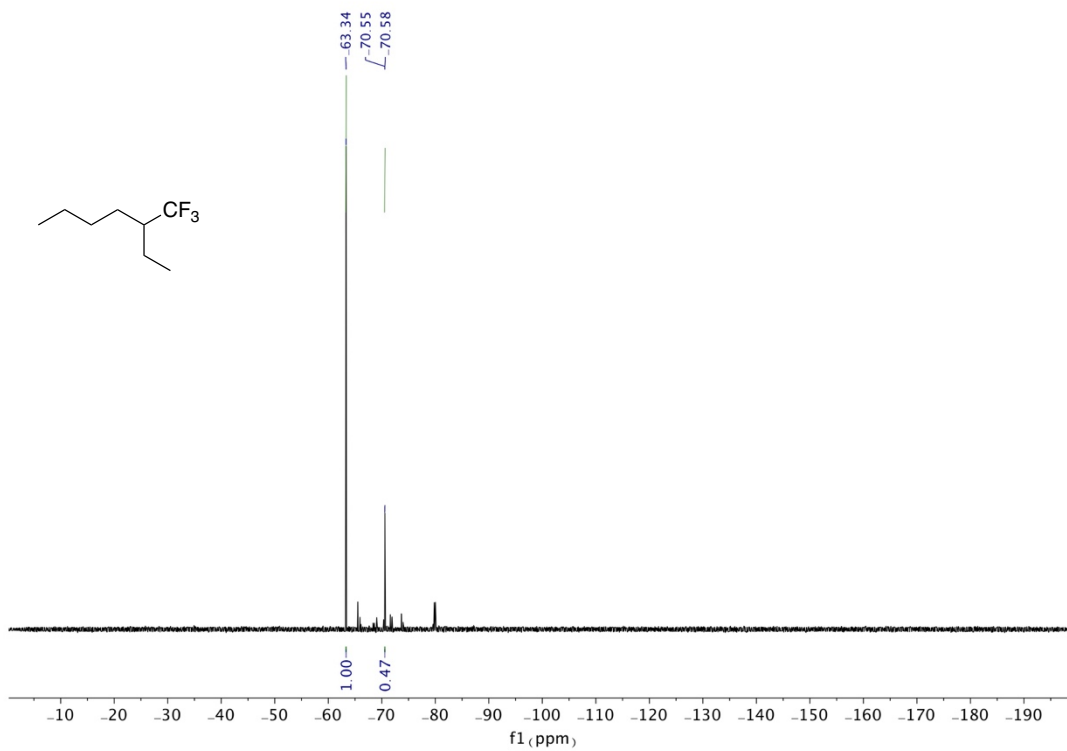


<sup>13</sup>C NMR (101 MHz, CDCl<sub>3</sub>) of **39**

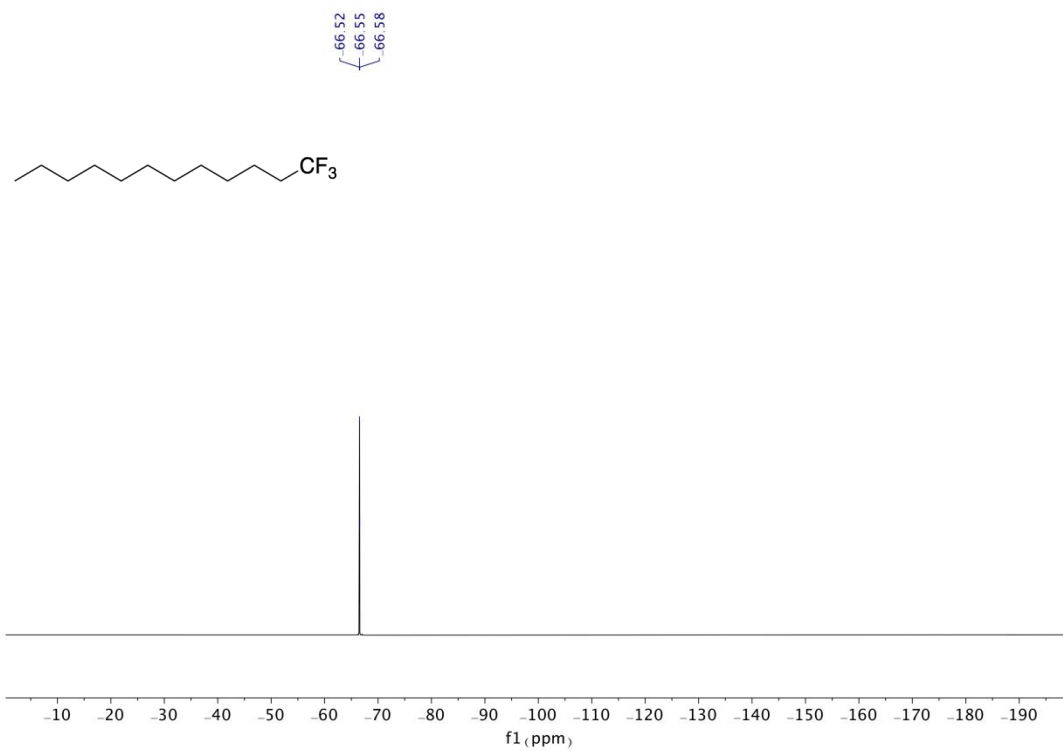


<sup>19</sup>F NMR assay for **40** (Experiment I)

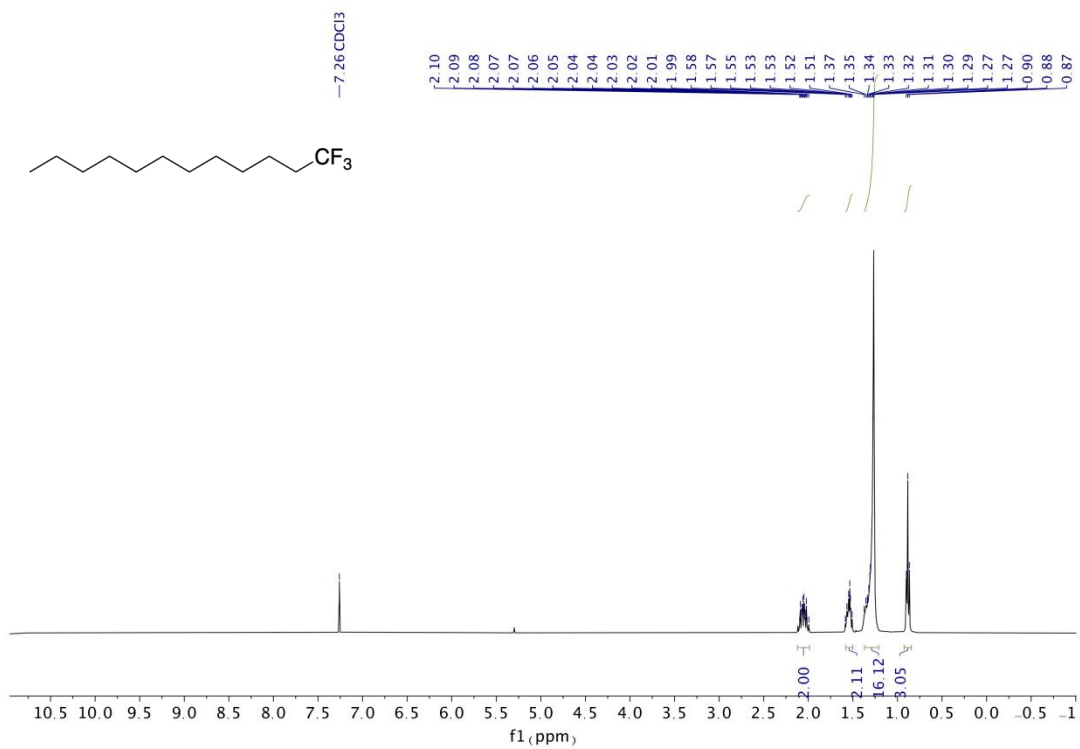




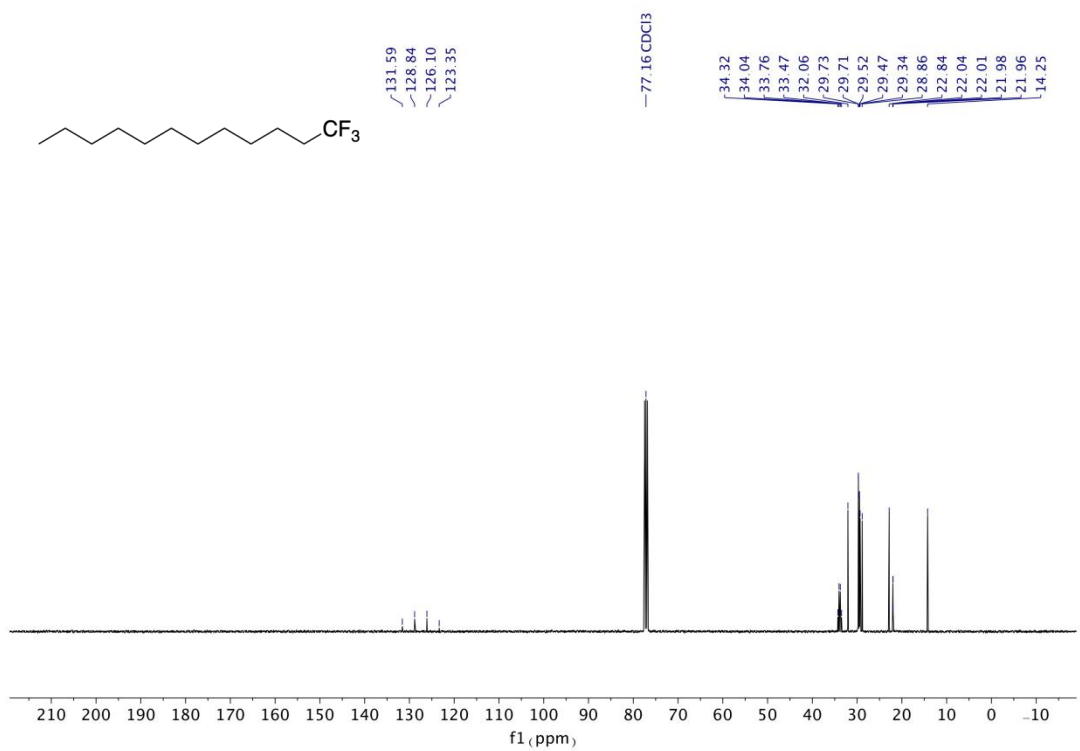
$^{19}\text{F}$  NMR assay for **40** (Experiment II)



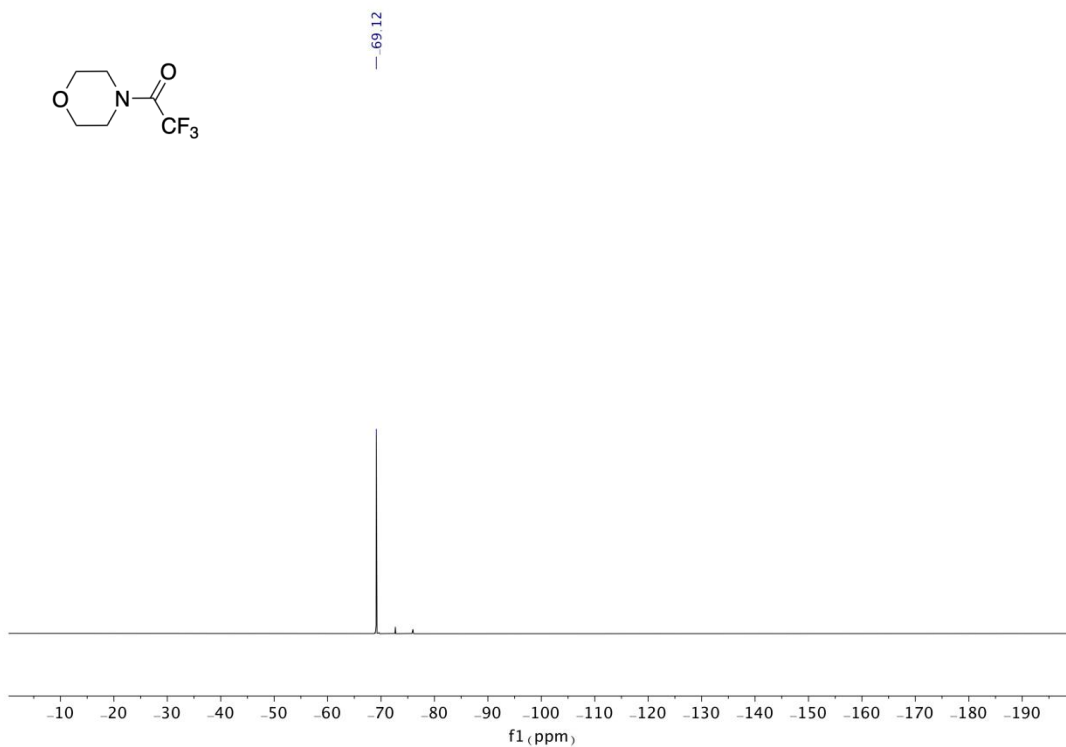
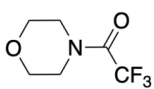
$^{19}\text{F}$  NMR (376 MHz,  $\text{CDCl}_3$ ) of **41**



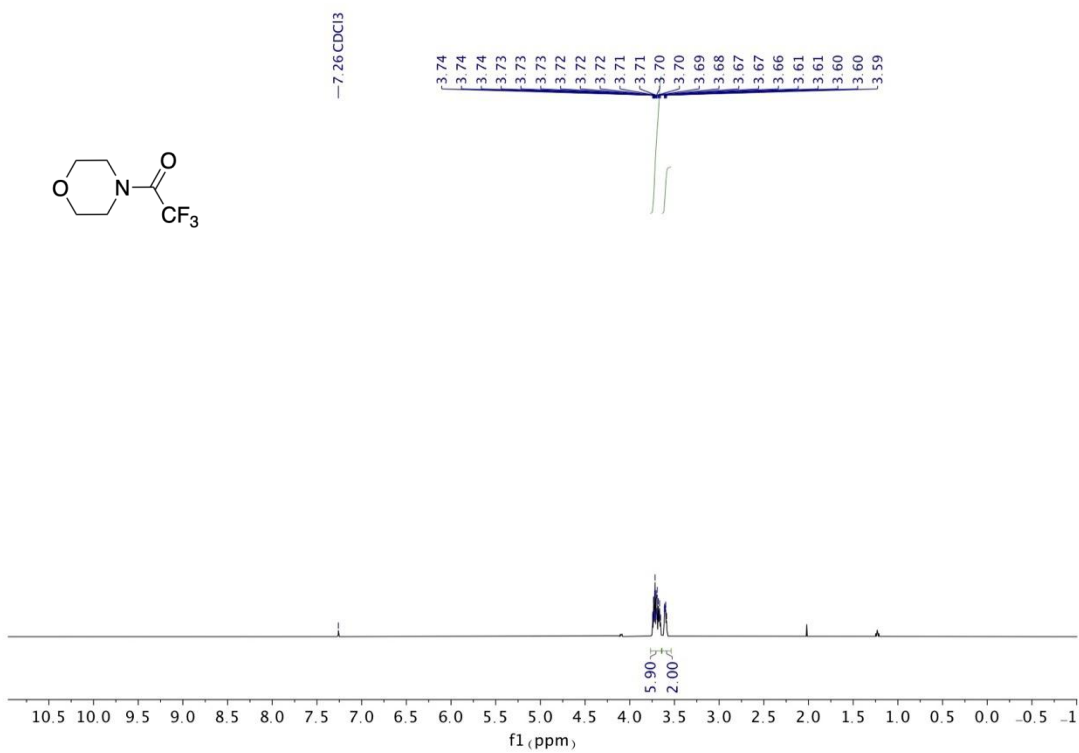
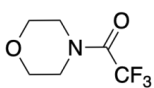
$^1\text{H}$  NMR (400 MHz,  $\text{CDCl}_3$ ) of **41**



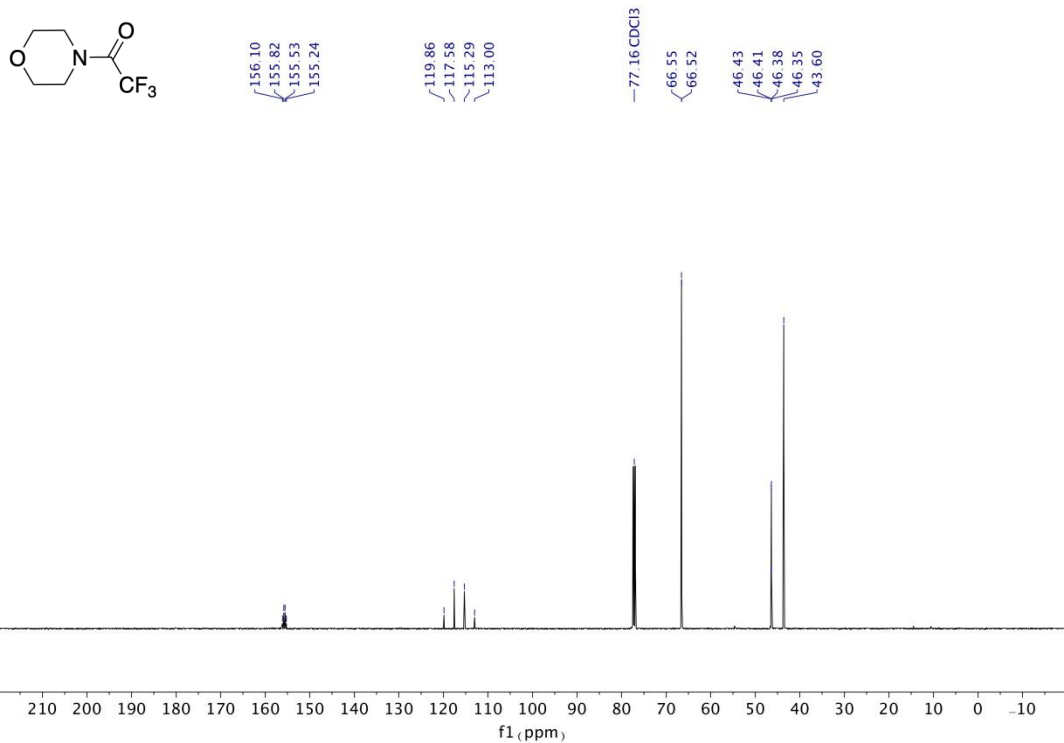
$^{13}\text{C}$  NMR (101 MHz,  $\text{CDCl}_3$ ) of **41**



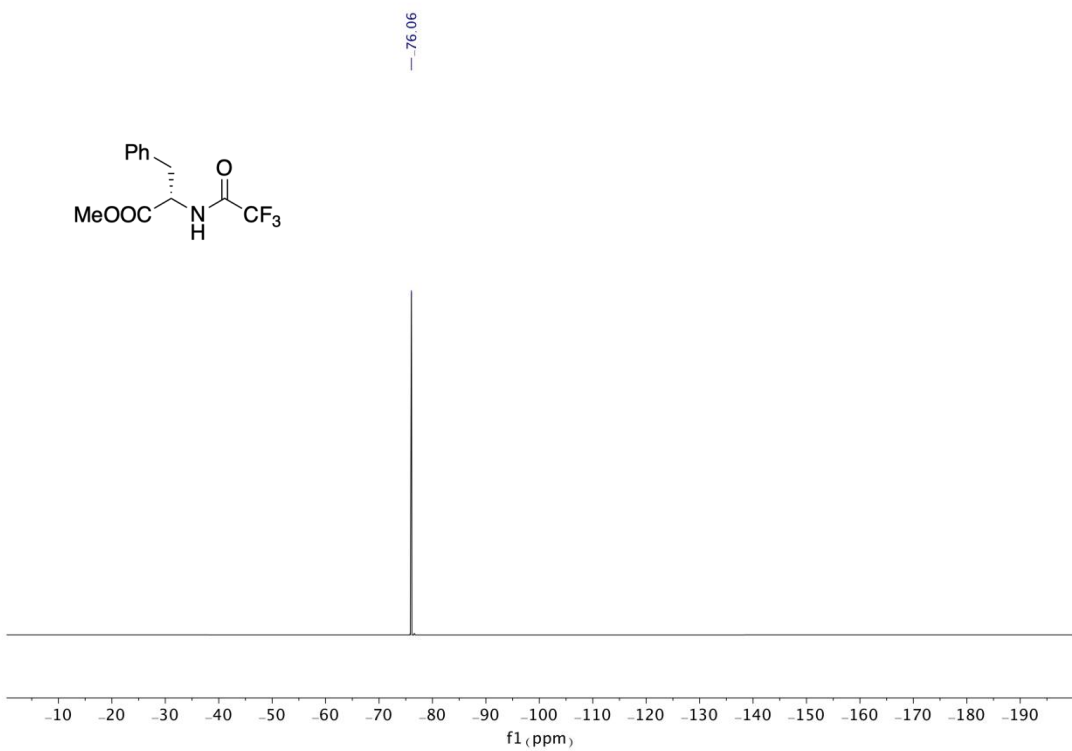
$^{19}\text{F}$  NMR (376 MHz,  $\text{CDCl}_3$ ) of **42**



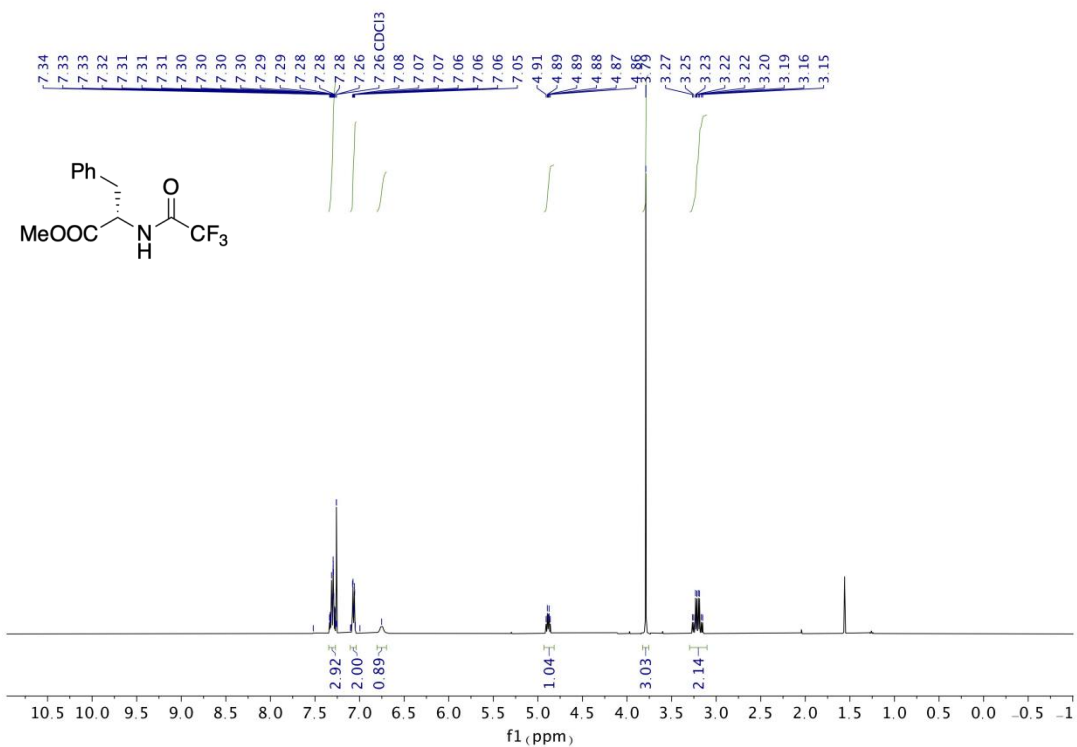
$^1\text{H}$  NMR (400 MHz,  $\text{CDCl}_3$ ) of **42**



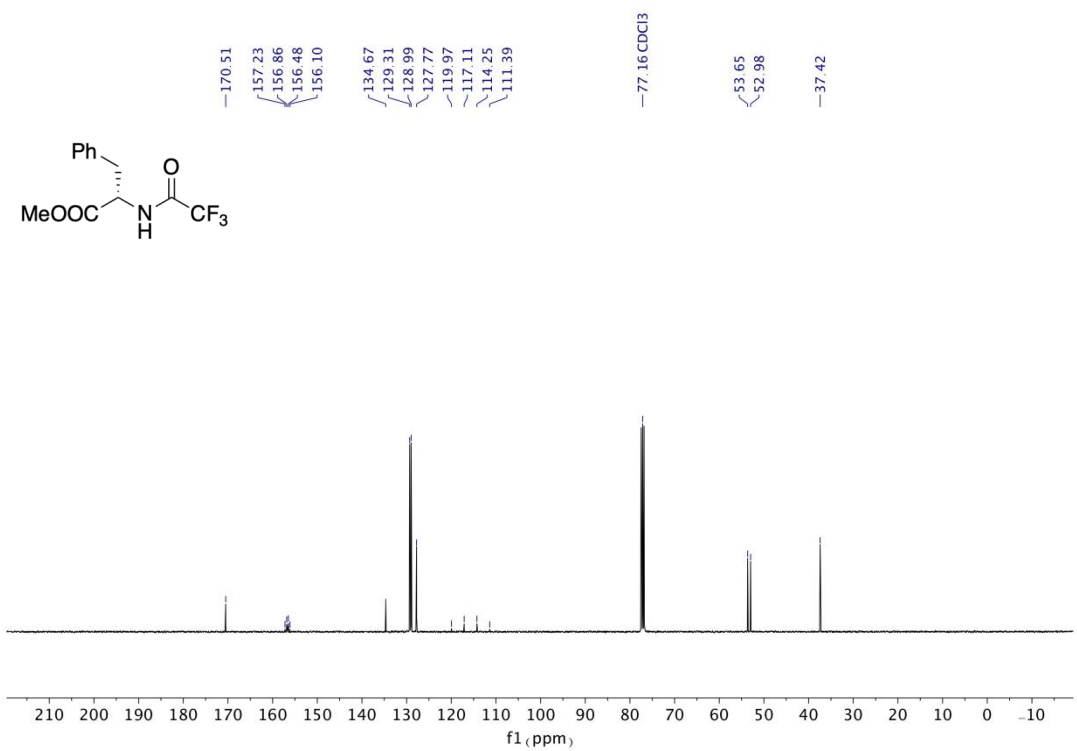
<sup>13</sup>C NMR (101 MHz, CDCl<sub>3</sub>) of 42



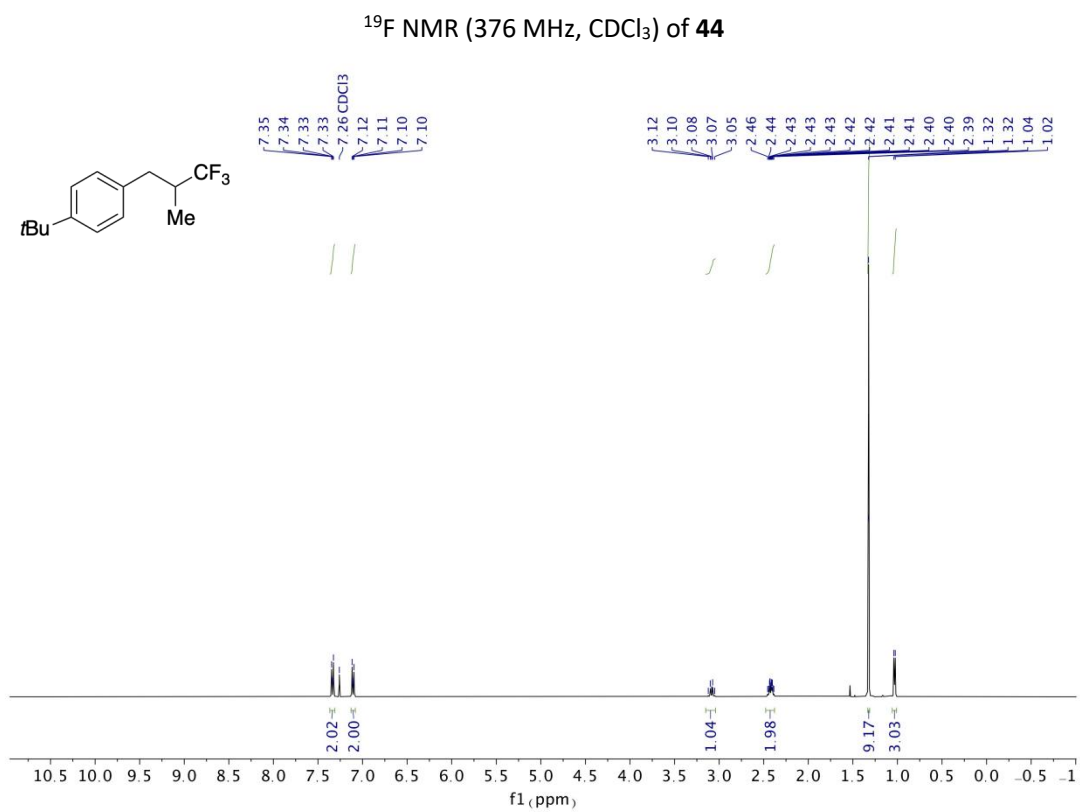
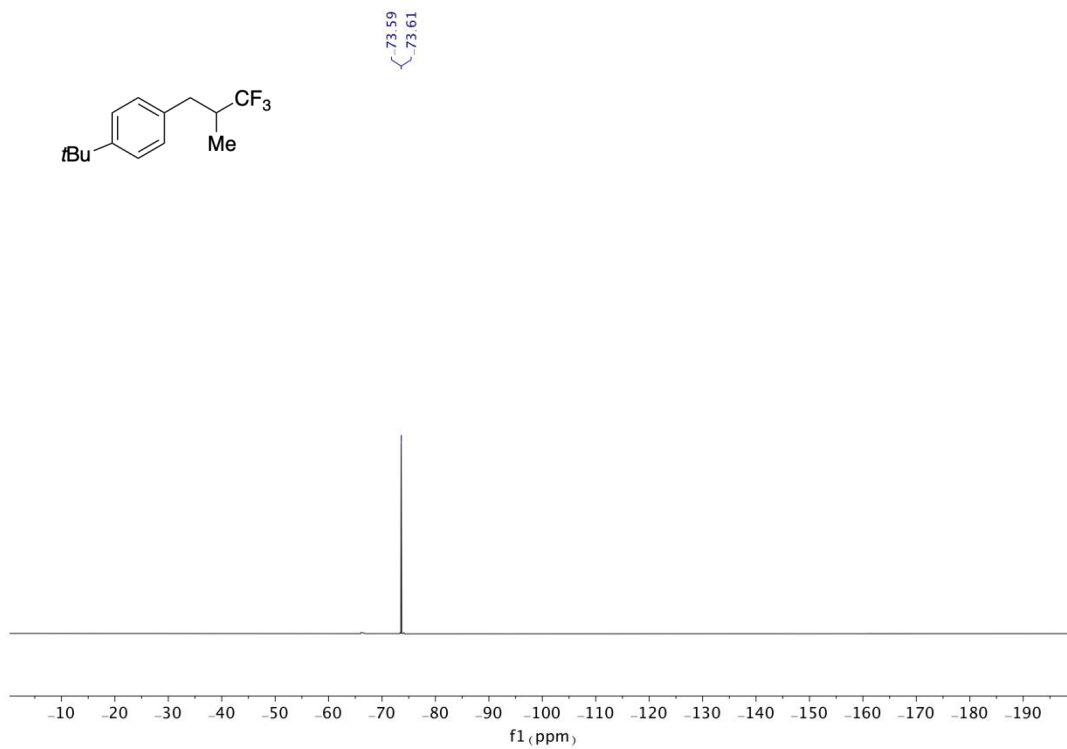
<sup>19</sup>F NMR (376 MHz, CDCl<sub>3</sub>) of 43

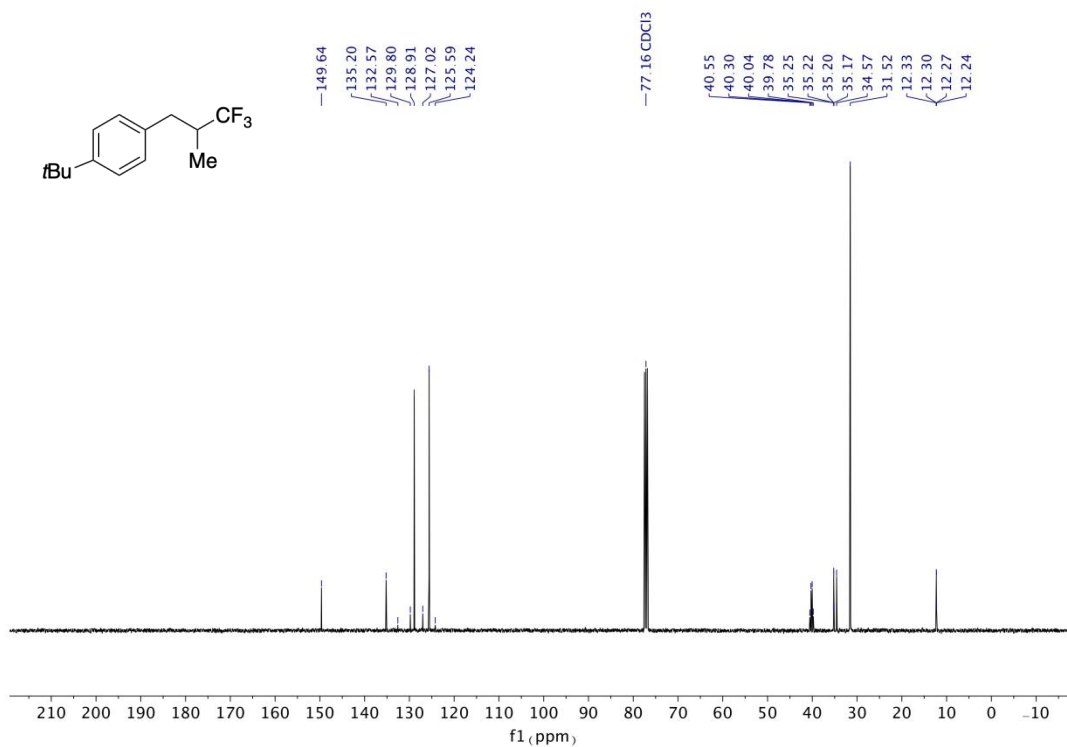


<sup>1</sup>H NMR (400 MHz, CDCl<sub>3</sub>) of 43

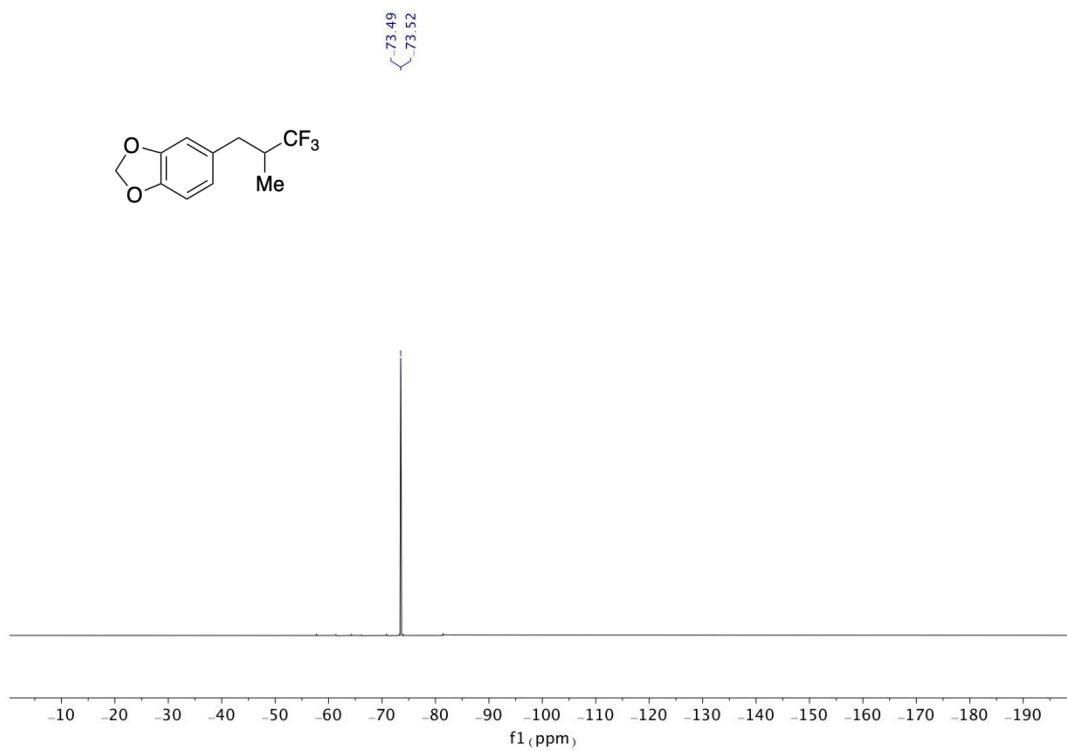


<sup>13</sup>C NMR (101 MHz, CDCl<sub>3</sub>) of 43

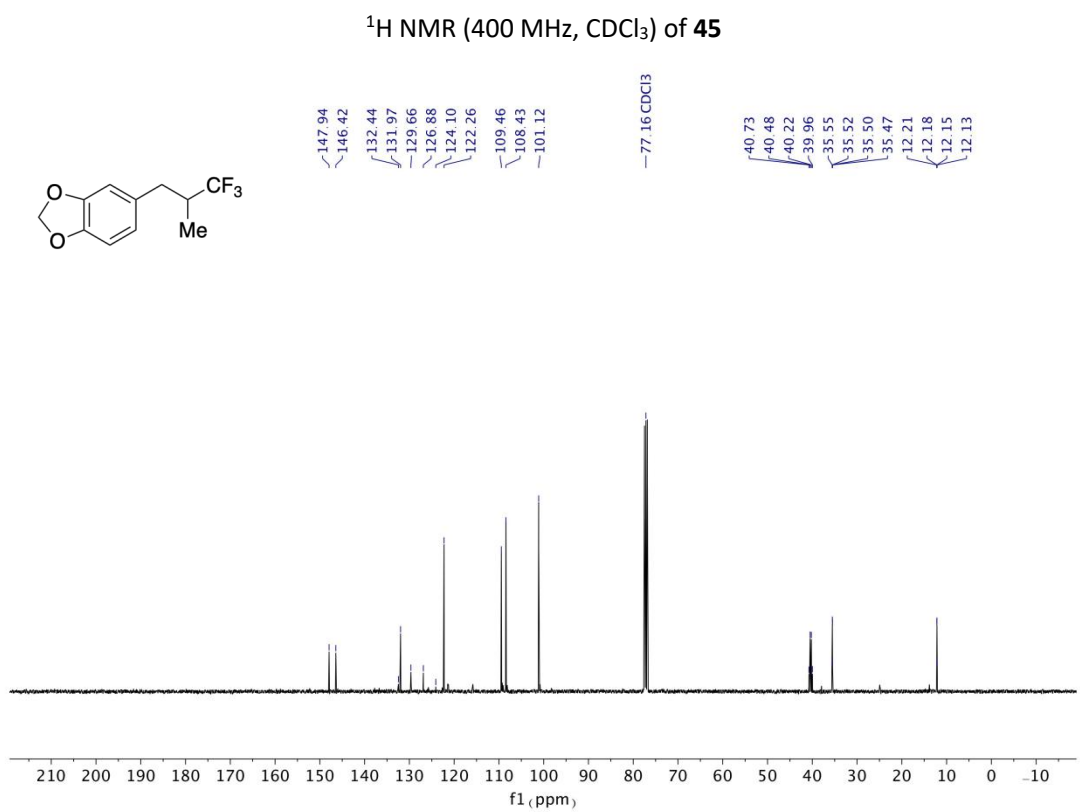
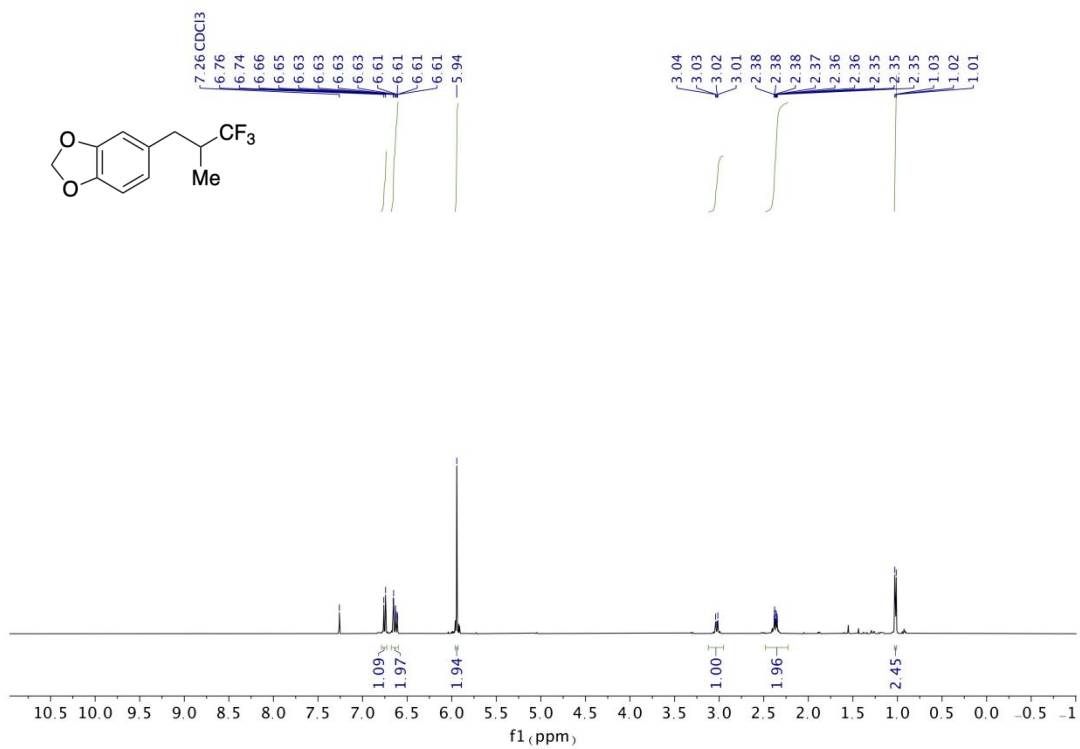




<sup>13</sup>C NMR (101 MHz, CDCl<sub>3</sub>) of **44**

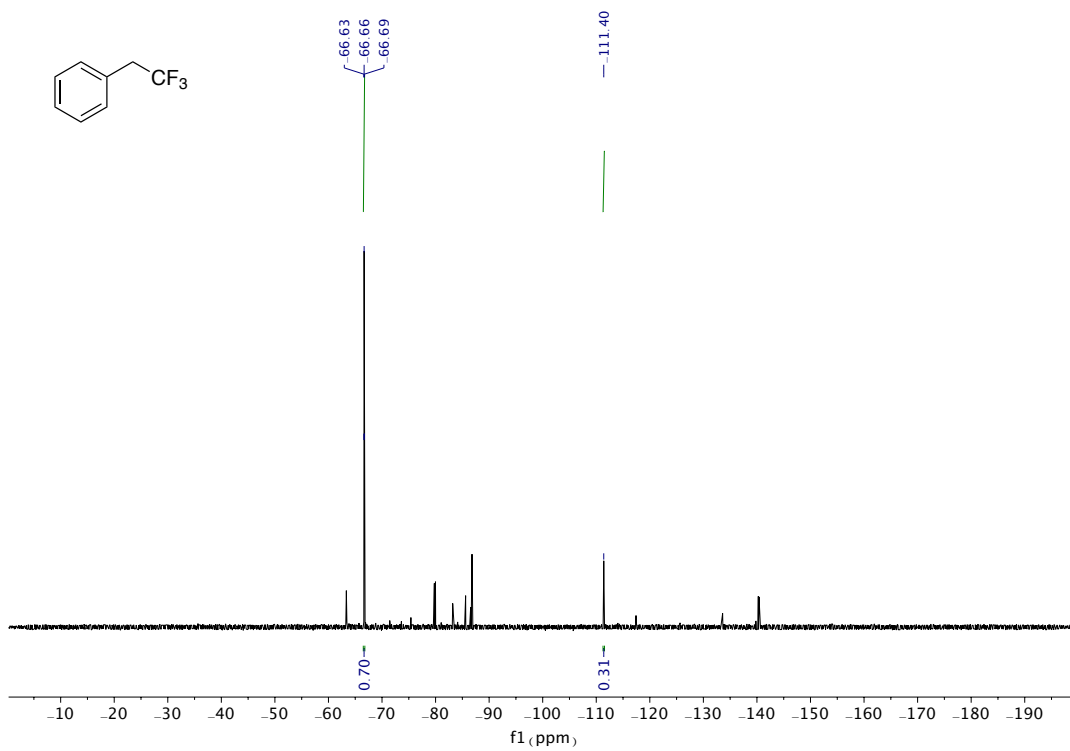


<sup>19</sup>F NMR (376 MHz, CDCl<sub>3</sub>) of **45**

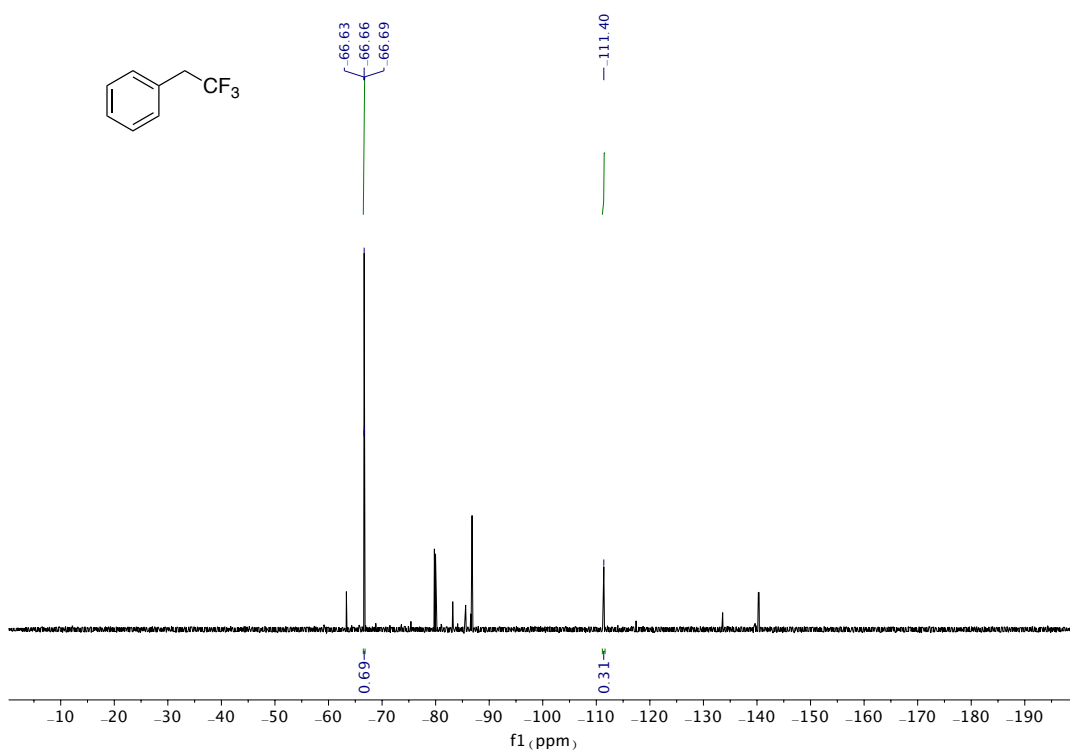


<sup>13</sup>C NMR (101 MHz, CDCl<sub>3</sub>) of 45

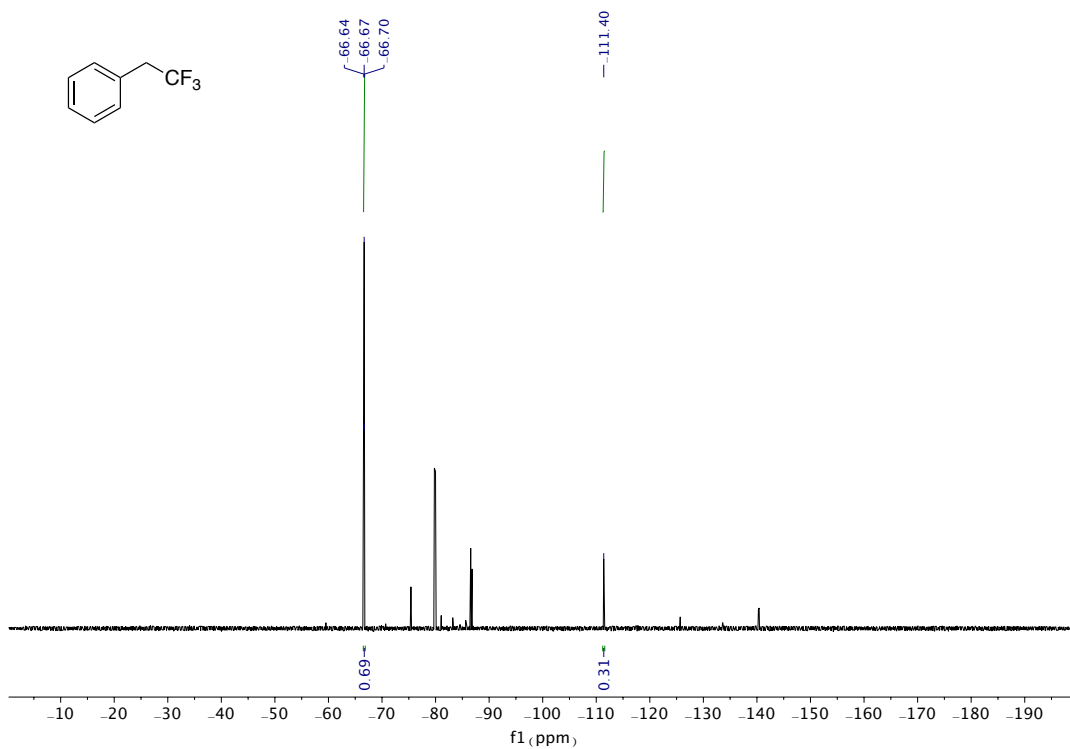




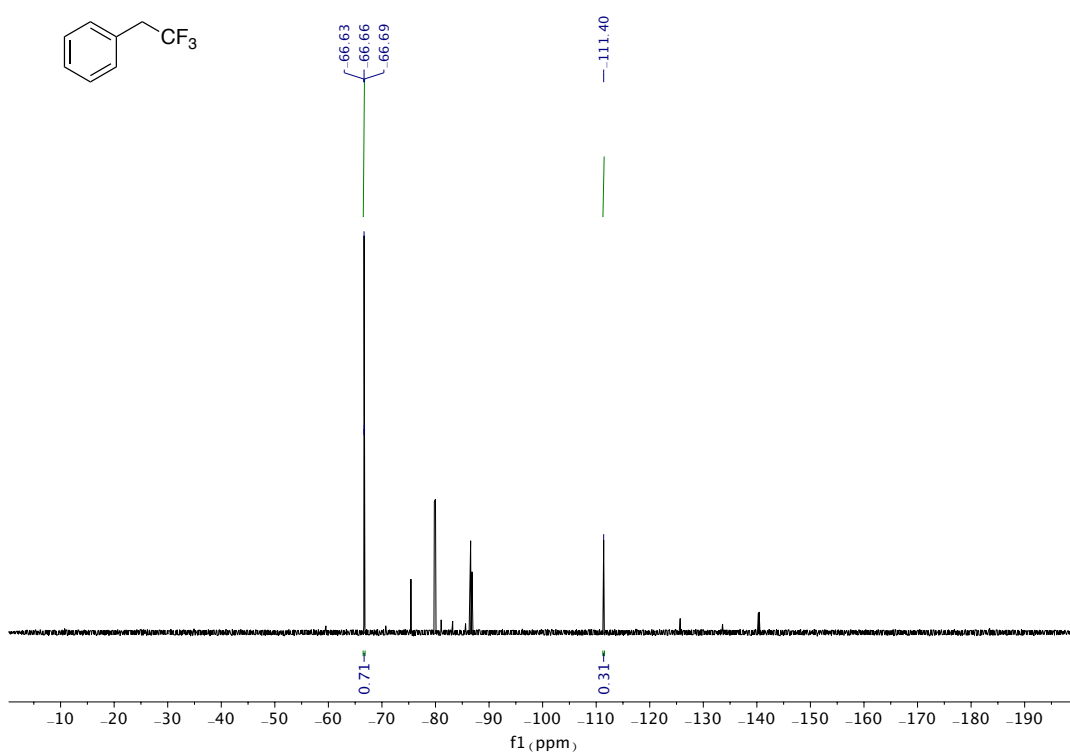
<sup>19</sup>F NMR assay for **46** from **C4** (Experiment I)



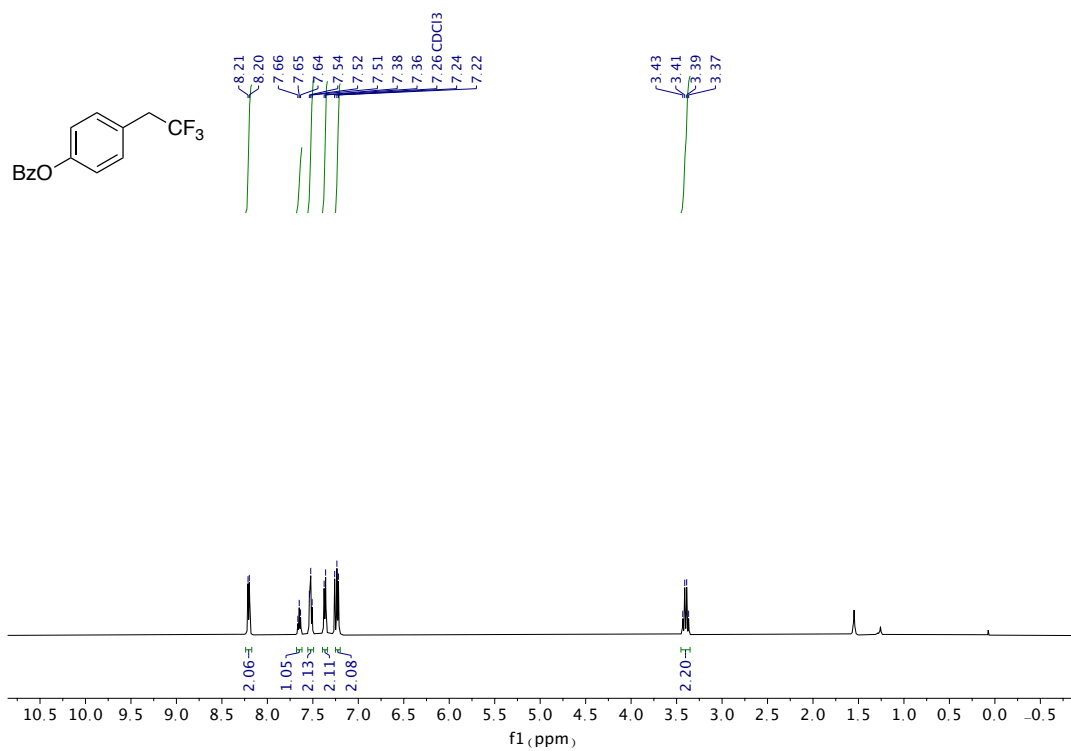
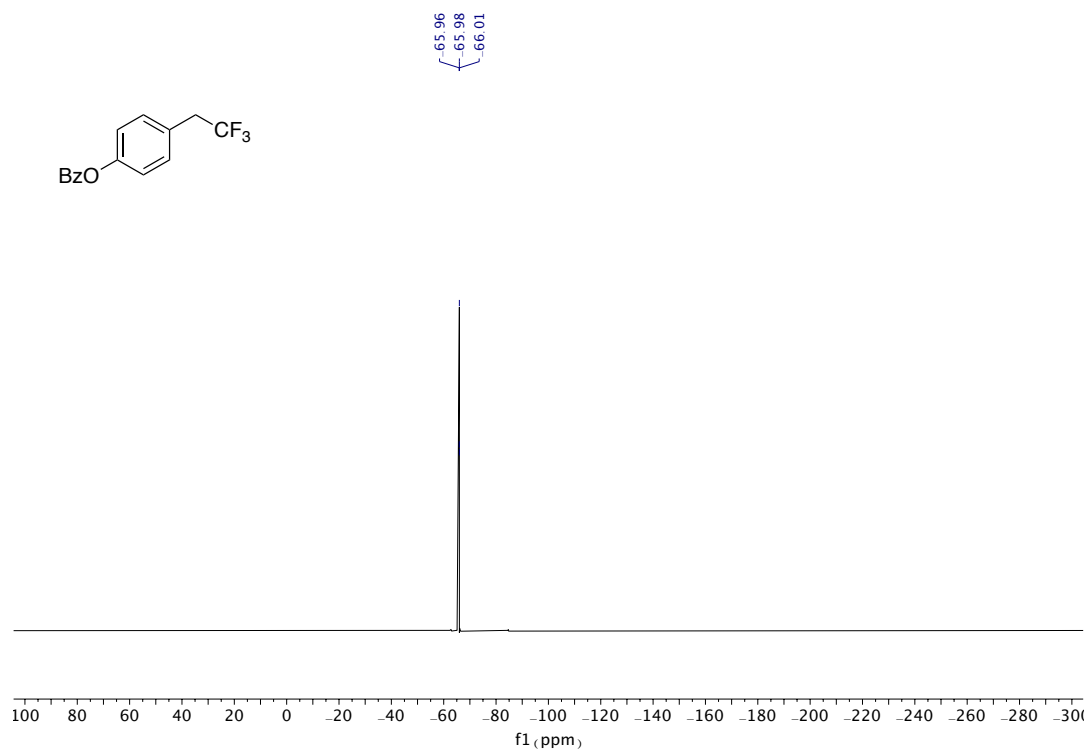
<sup>19</sup>F NMR assay for **46** from **C4** (Experiment II)

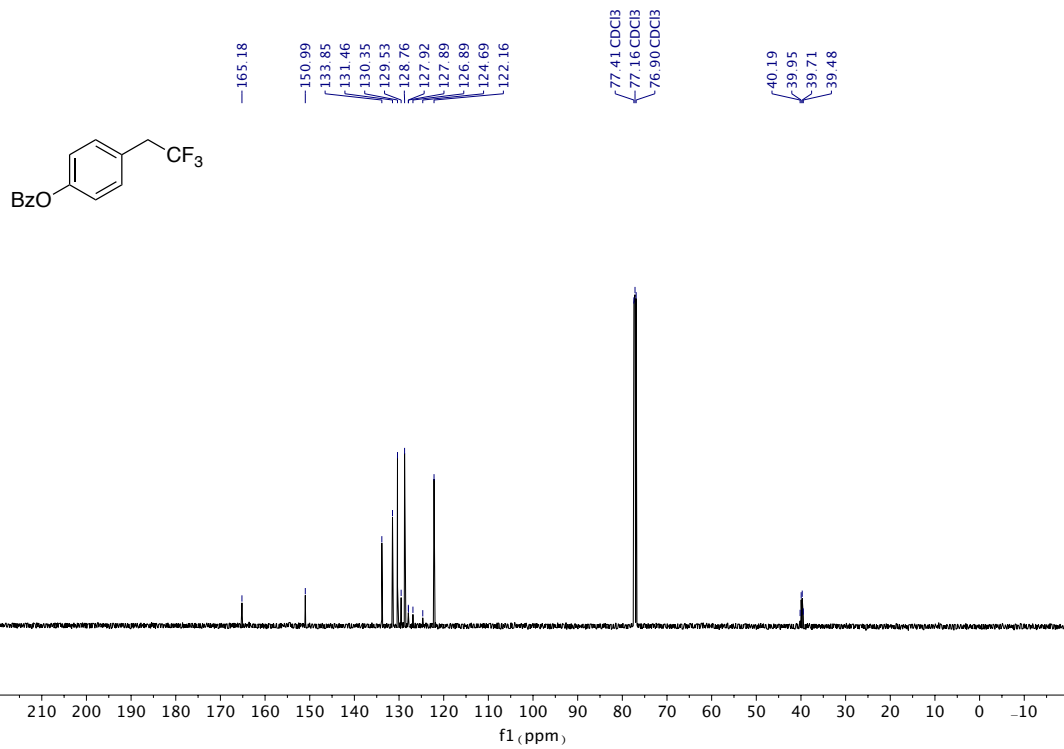


<sup>19</sup>F NMR assay for **46** from **C5** (Experiment I)

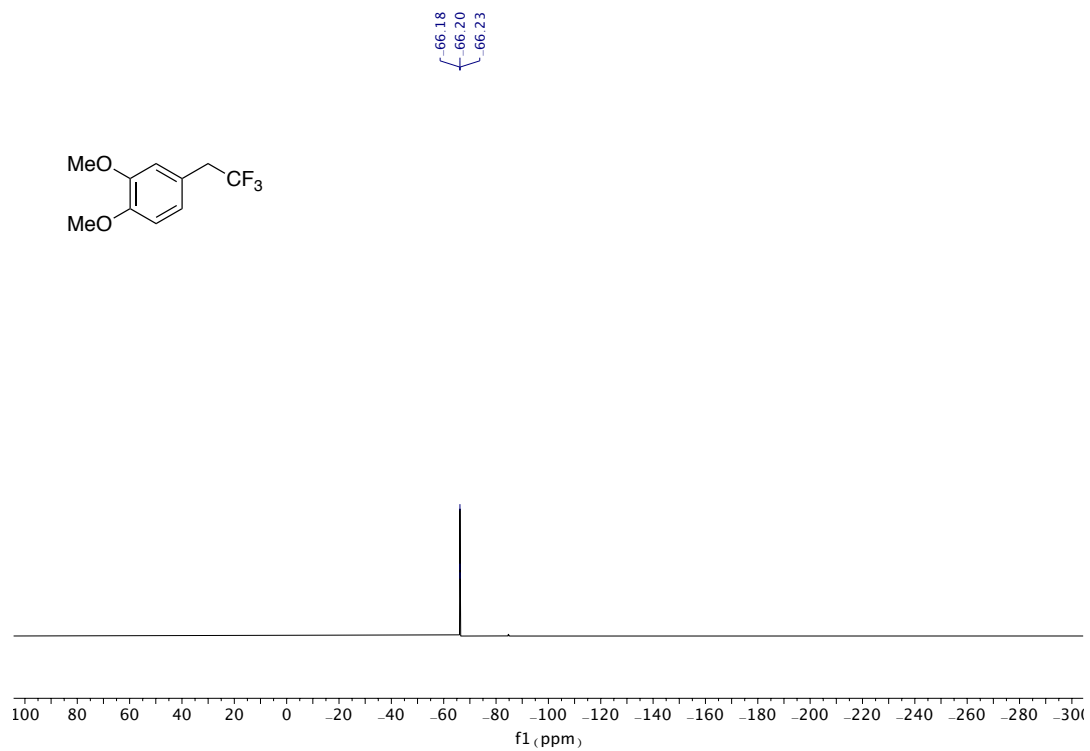


<sup>19</sup>F NMR assay for **46** from **C5** (Experiment II)

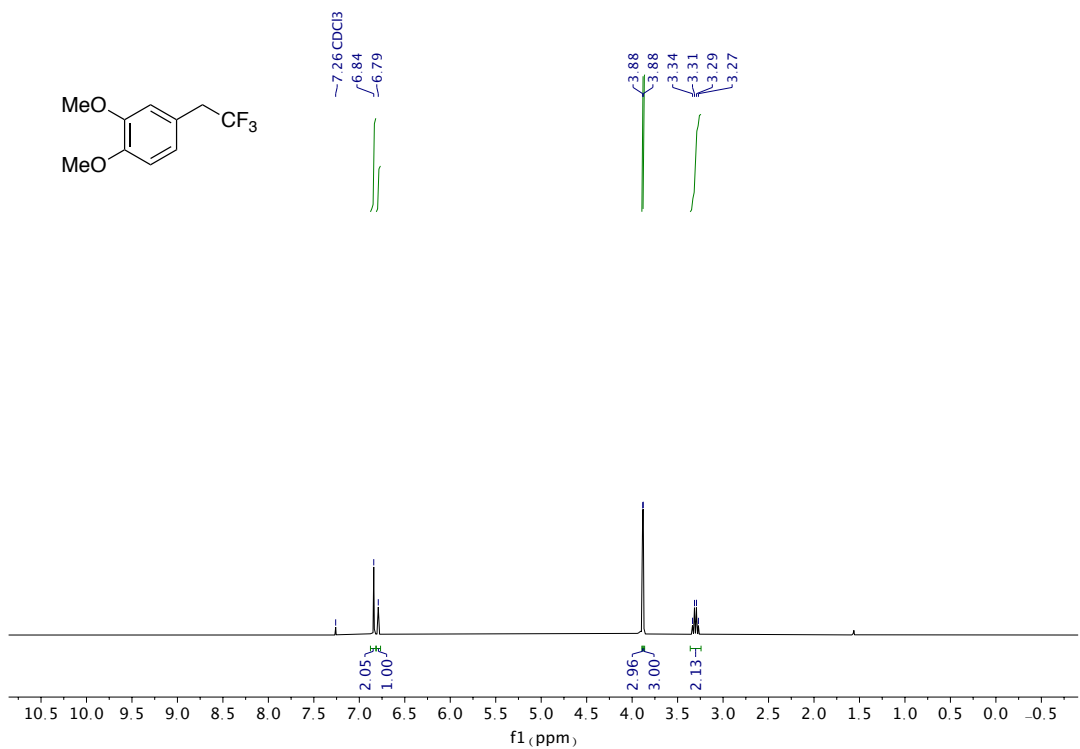




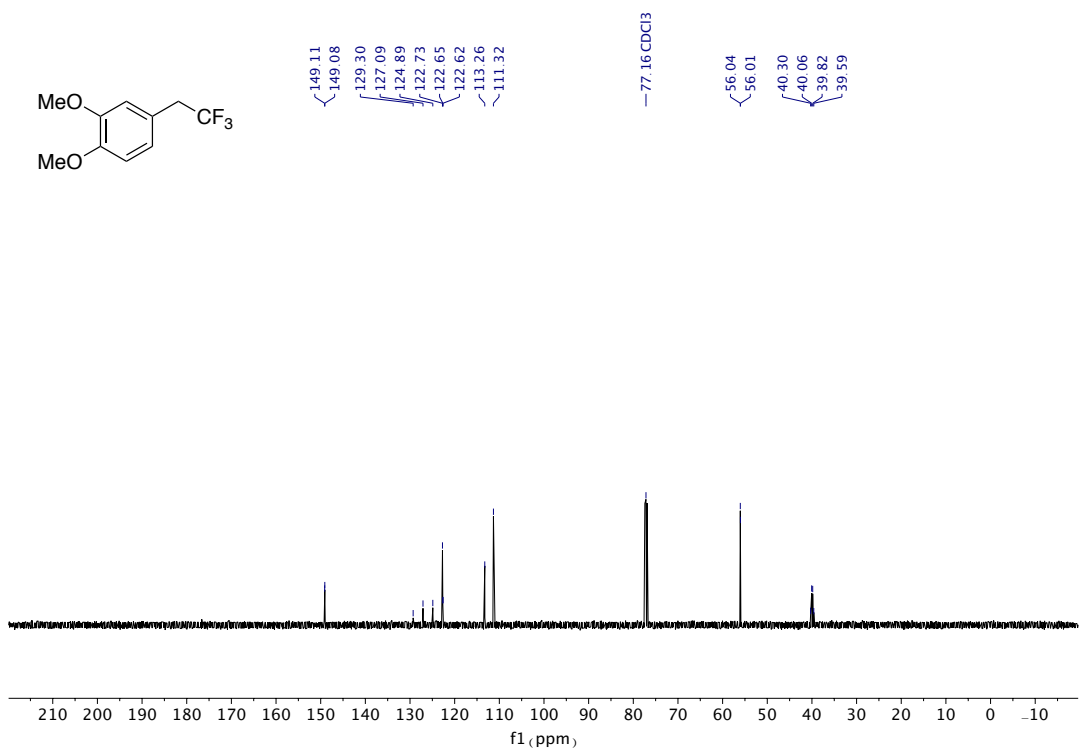
<sup>13</sup>C NMR (126 MHz, CDCl<sub>3</sub>) of **47**



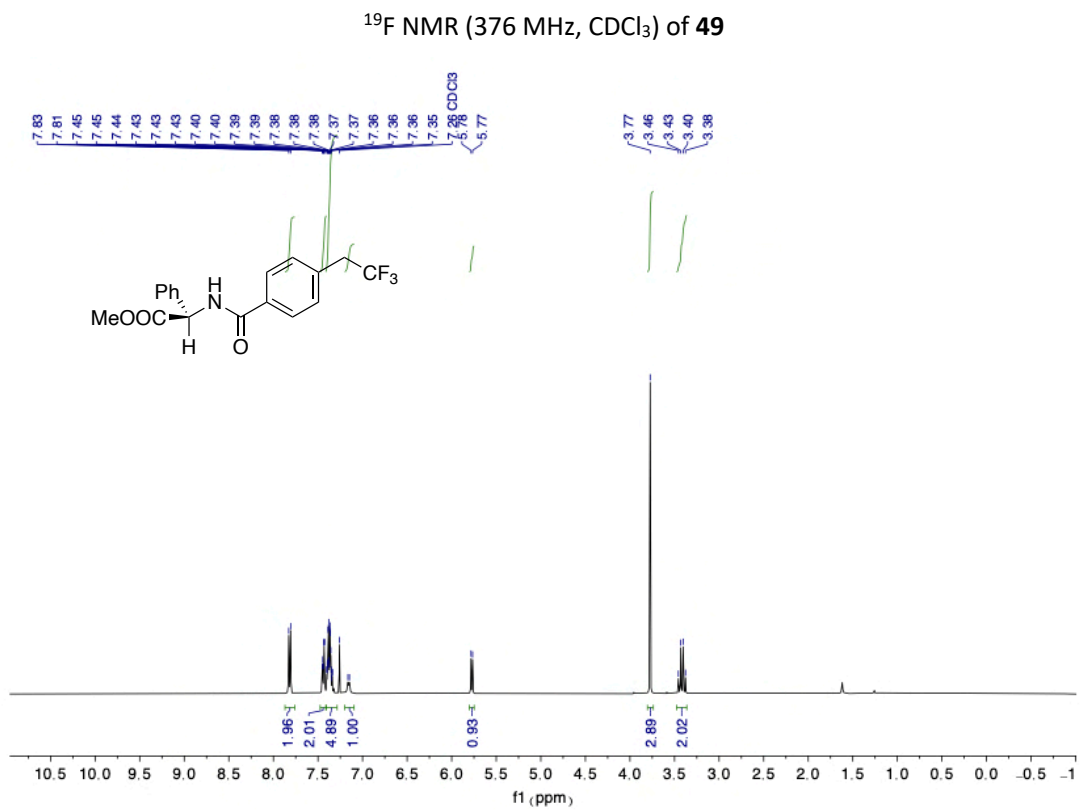
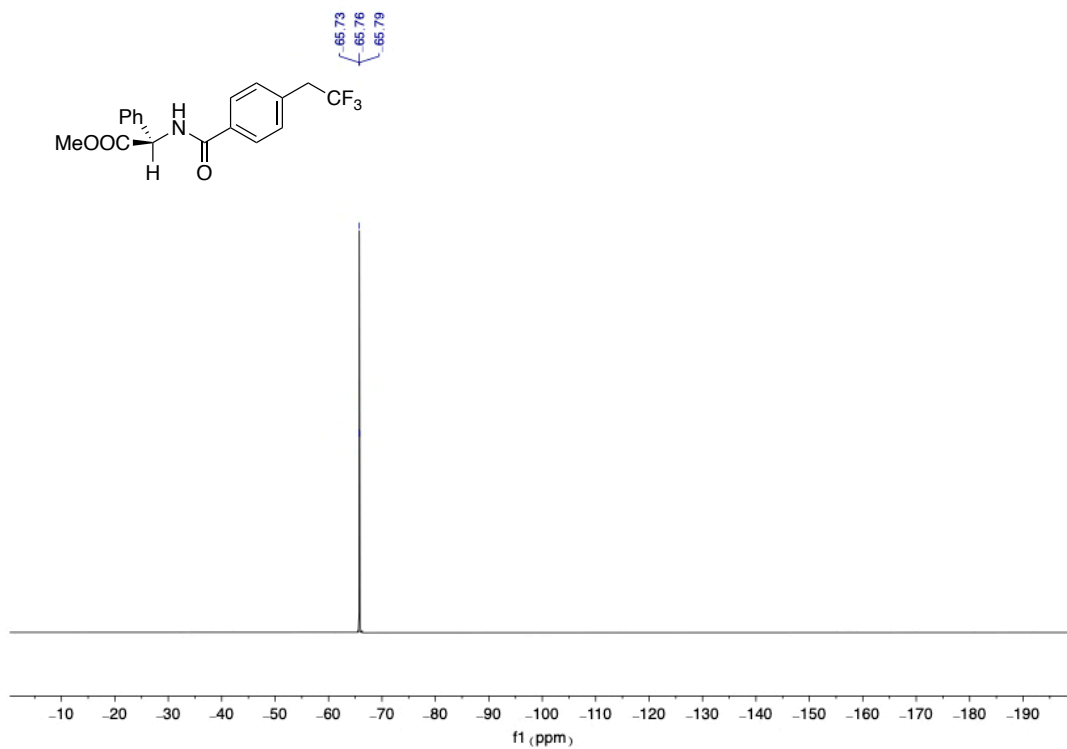
<sup>19</sup>F NMR (471 MHz, CDCl<sub>3</sub>) of **48**



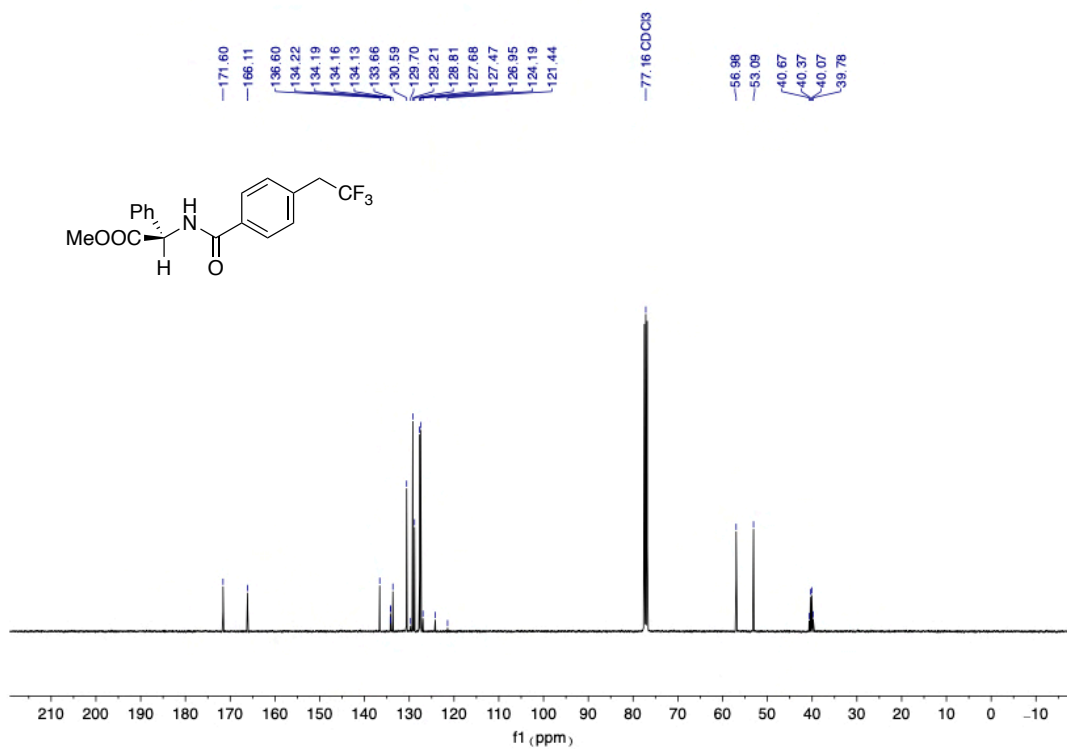
$^1\text{H}$  NMR (500 MHz,  $\text{CDCl}_3$ ) of **48**



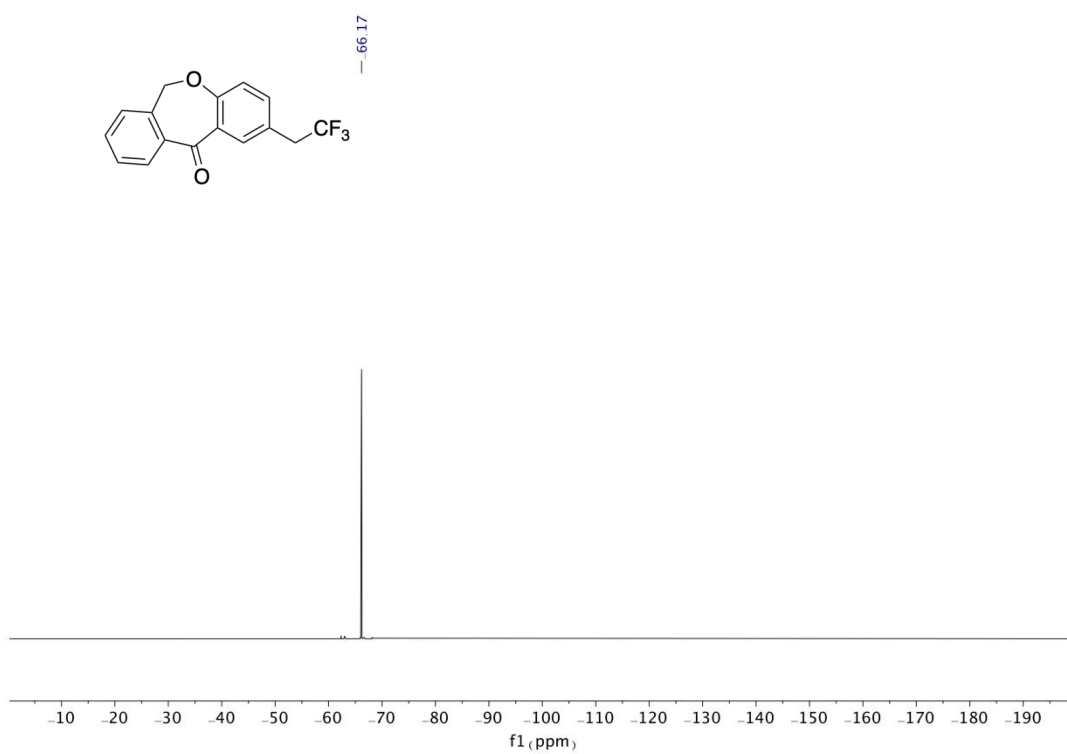
$^{13}\text{C}$  NMR (126 MHz,  $\text{CDCl}_3$ ) of **48**



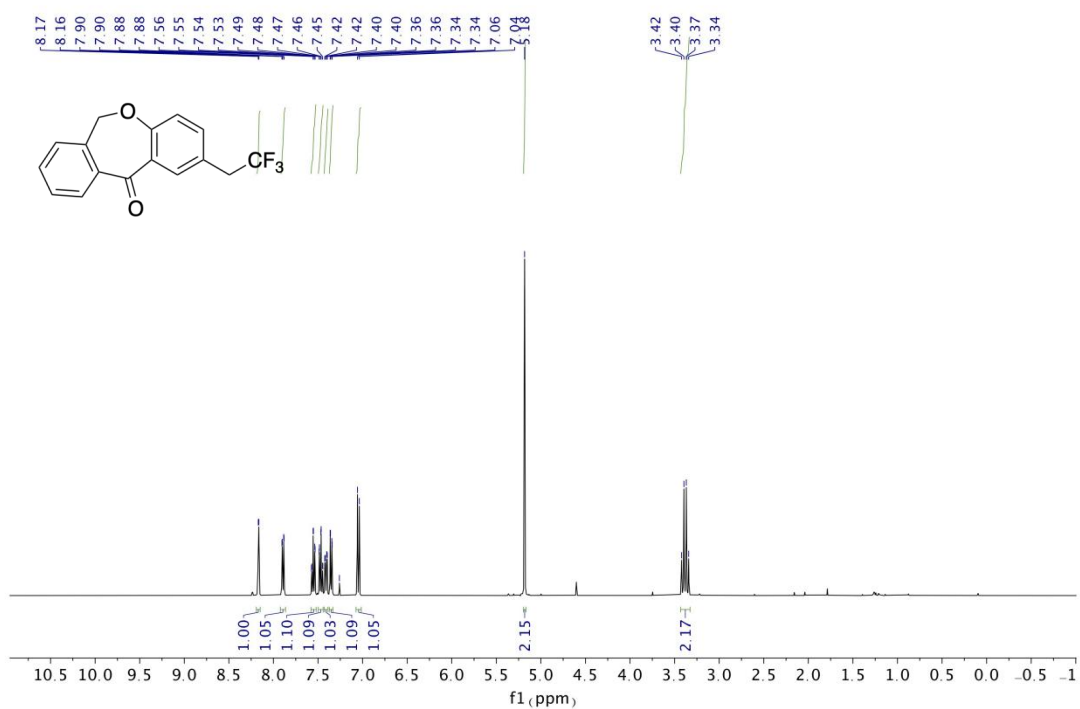
$^1\text{H}$  NMR (400 MHz,  $\text{CDCl}_3$ ) of **49**



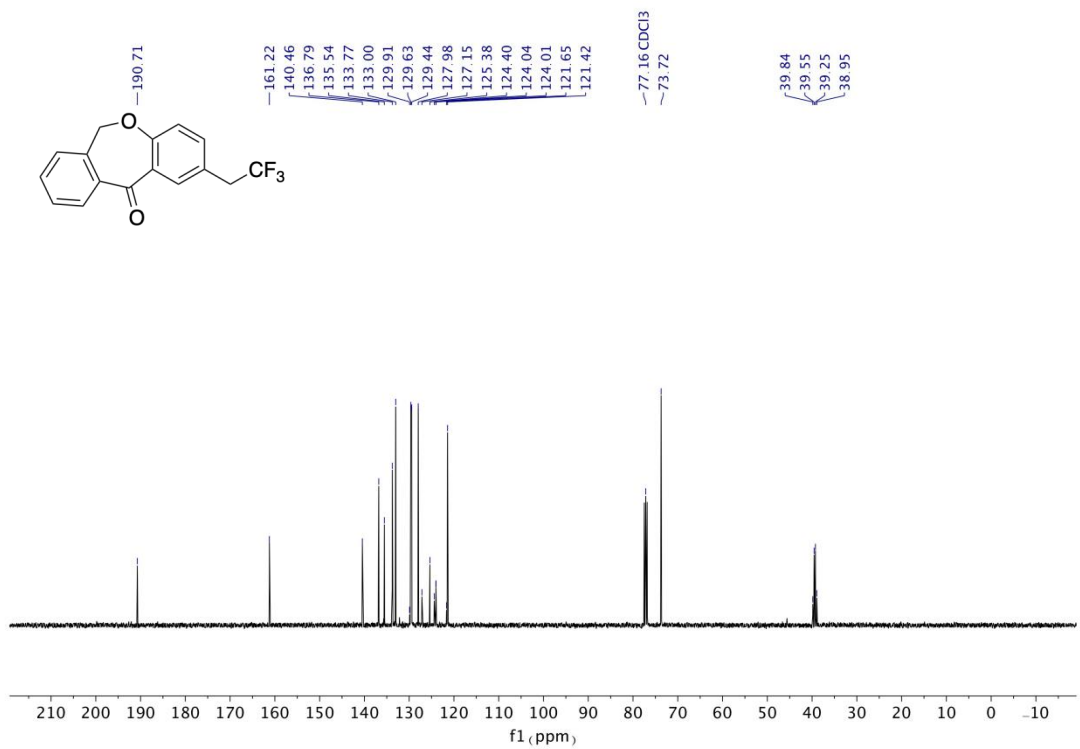
<sup>13</sup>C NMR (101 MHz, CDCl<sub>3</sub>) of **49**



<sup>19</sup>F NMR (376 MHz, CDCl<sub>3</sub>) of **50**

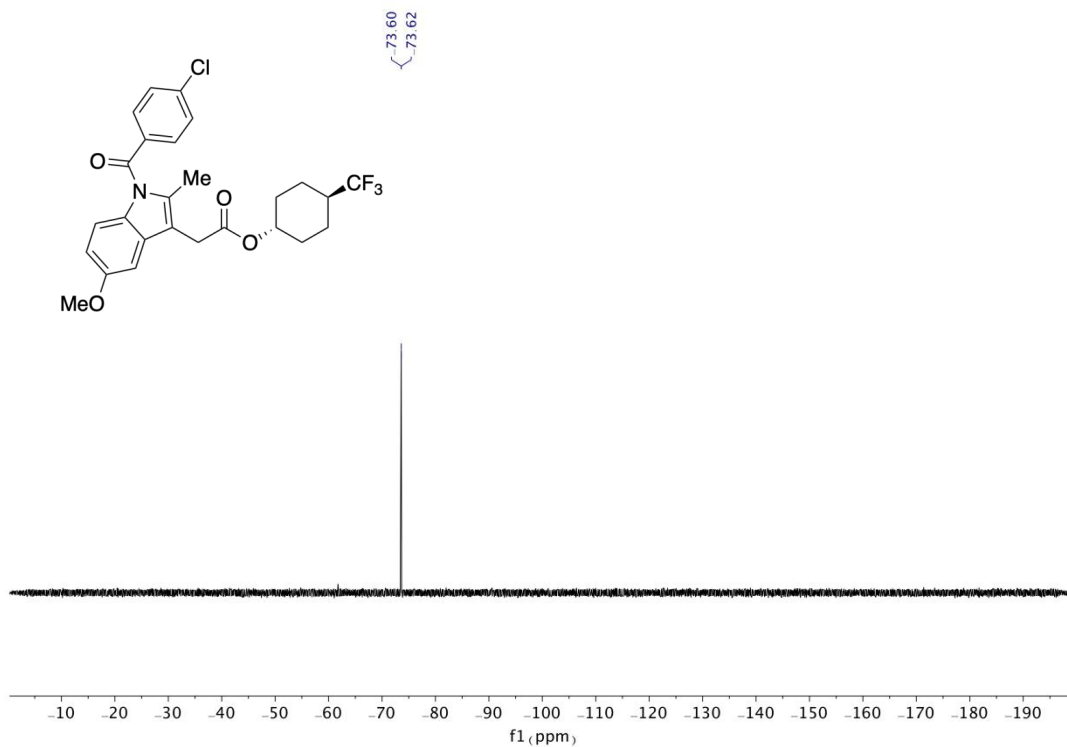


$^1\text{H}$  NMR (400 MHz,  $\text{CDCl}_3$ ) of 50

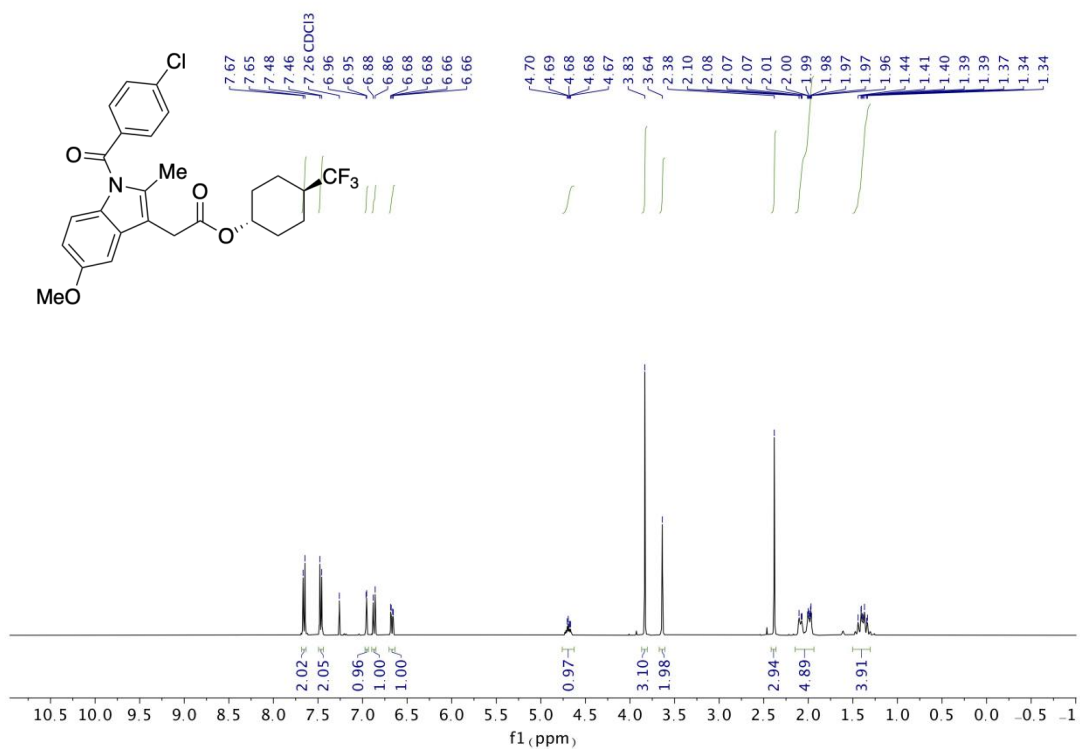


$^{13}\text{C}$  NMR (101 MHz,  $\text{CDCl}_3$ ) of 50

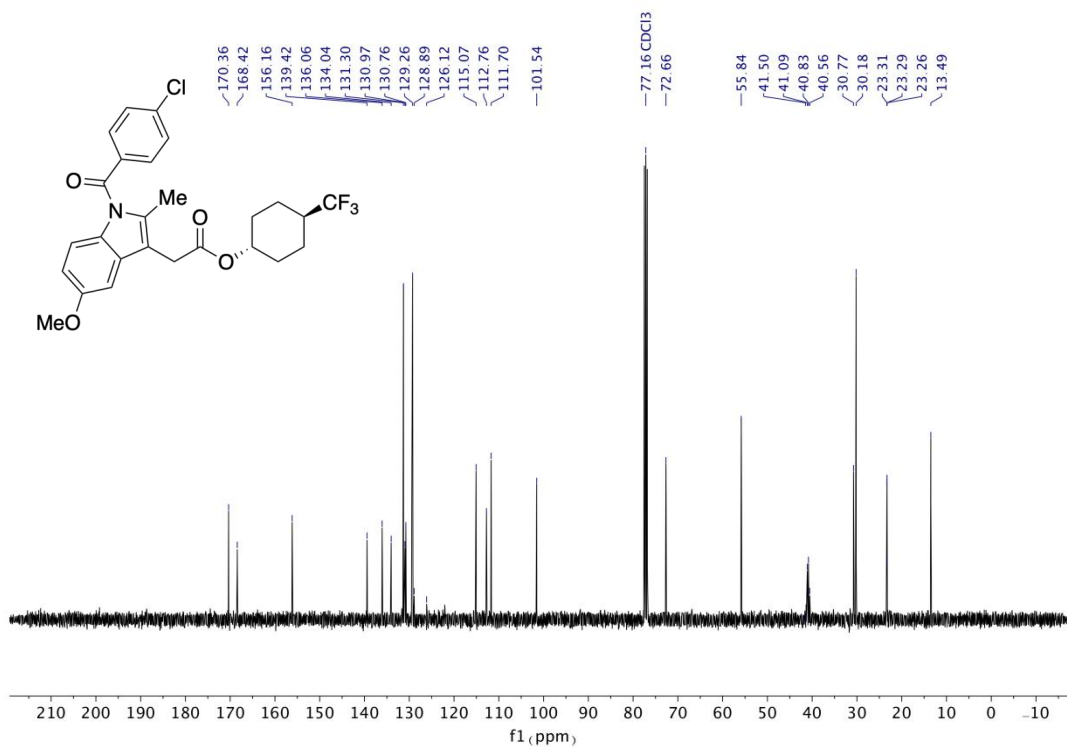




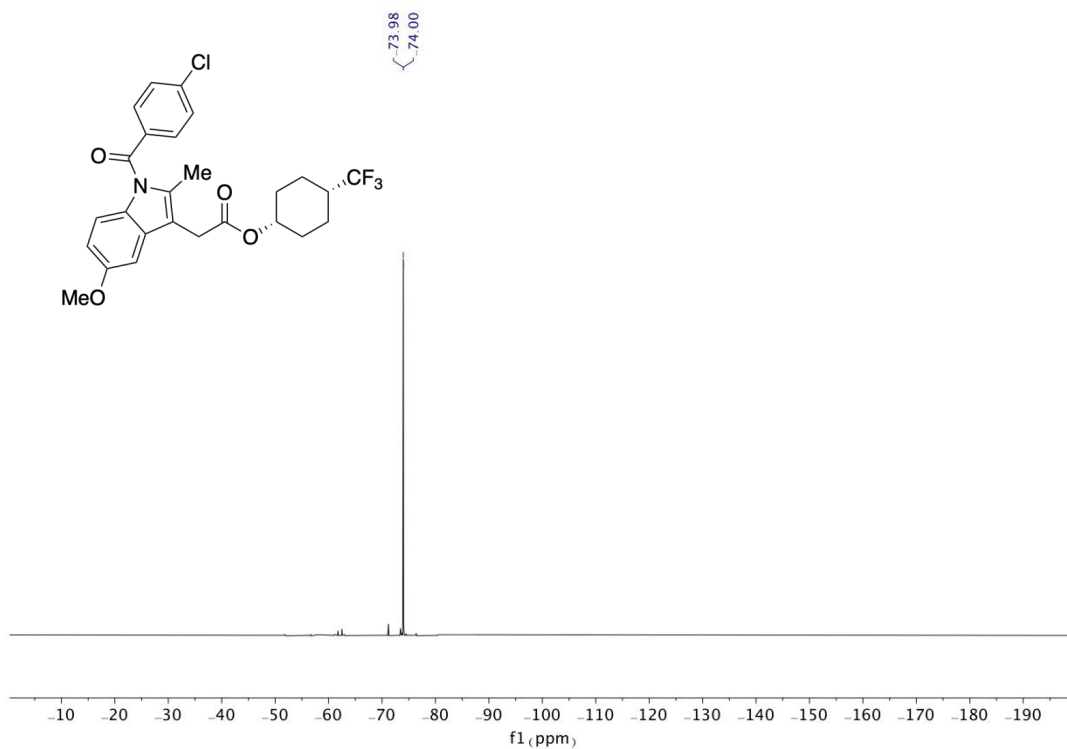
<sup>19</sup>F NMR (376 MHz, CDCl<sub>3</sub>) of *trans*-51



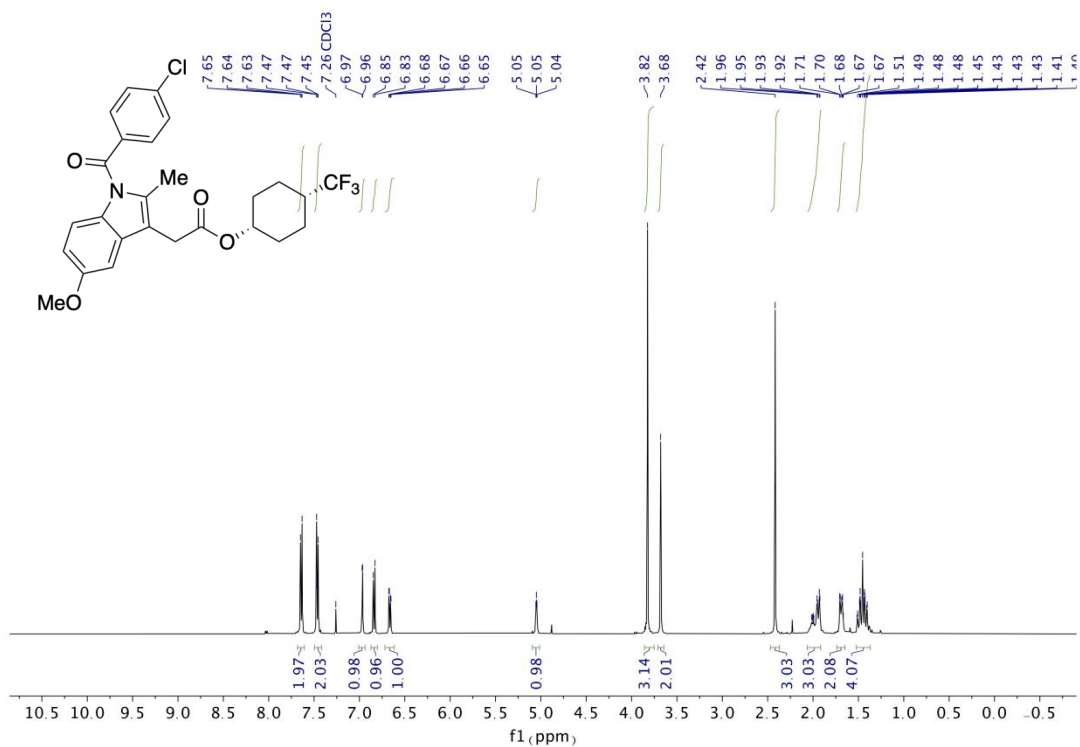
<sup>1</sup>H NMR (400 MHz, CDCl<sub>3</sub>) of *trans*-51



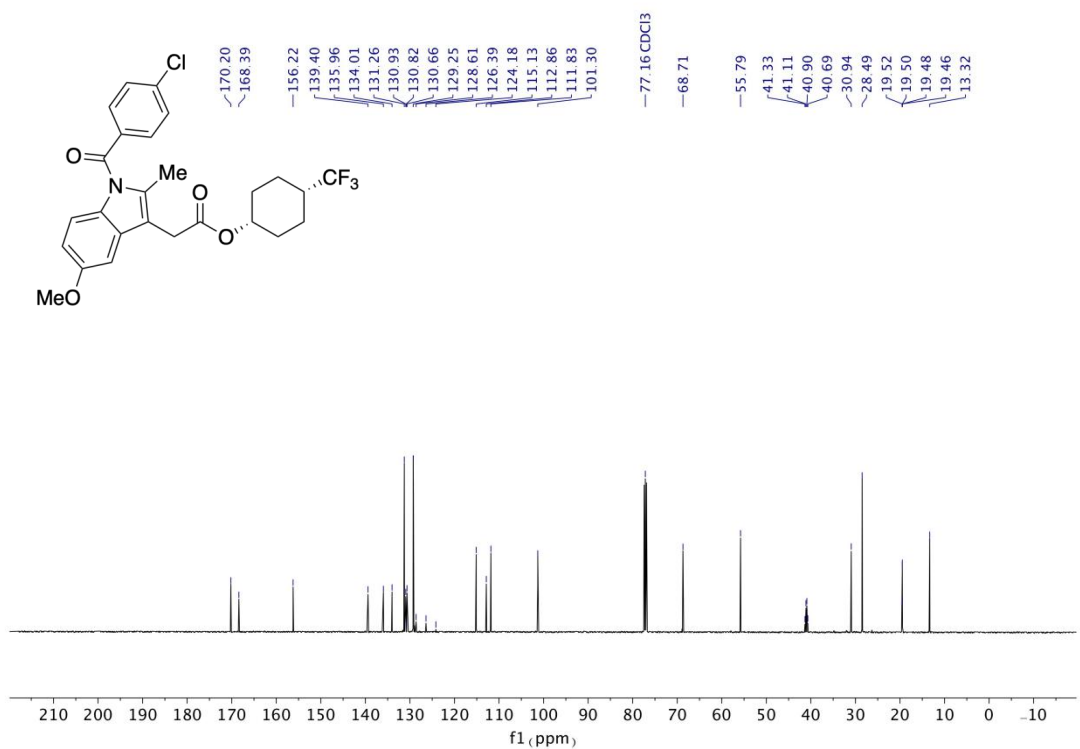
<sup>13</sup>C NMR (101 MHz, CDCl<sub>3</sub>) of *trans*-51



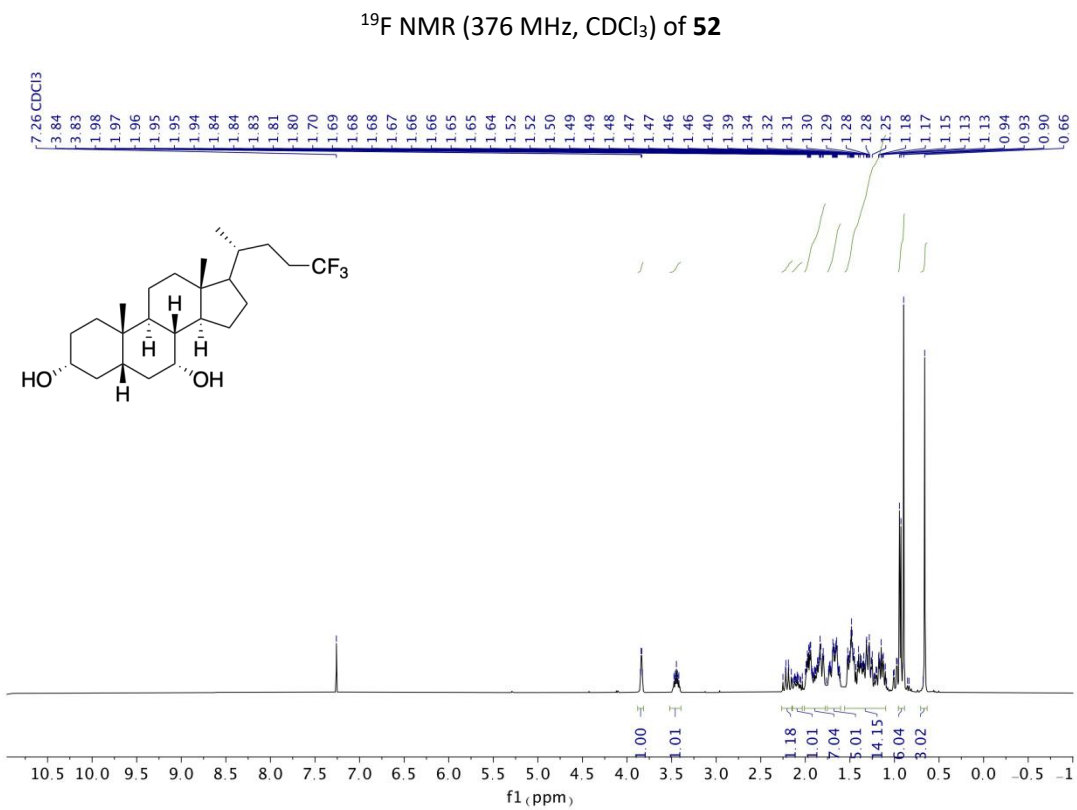
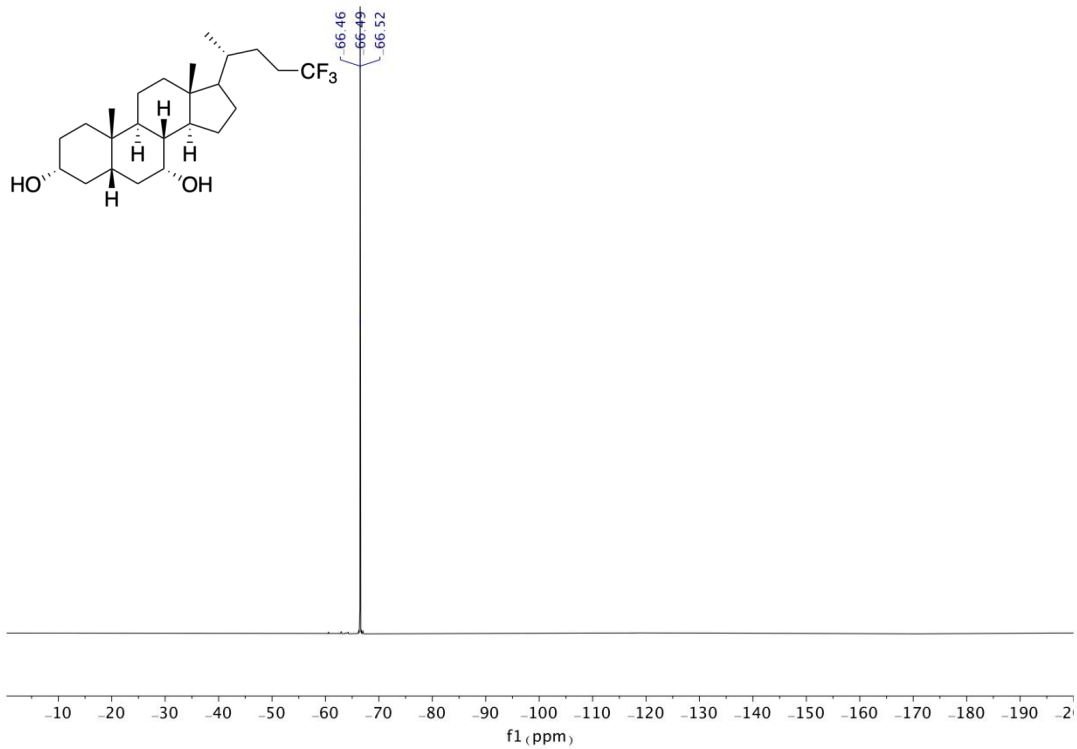
<sup>19</sup>F NMR (376 MHz, CDCl<sub>3</sub>) of *cis*-51

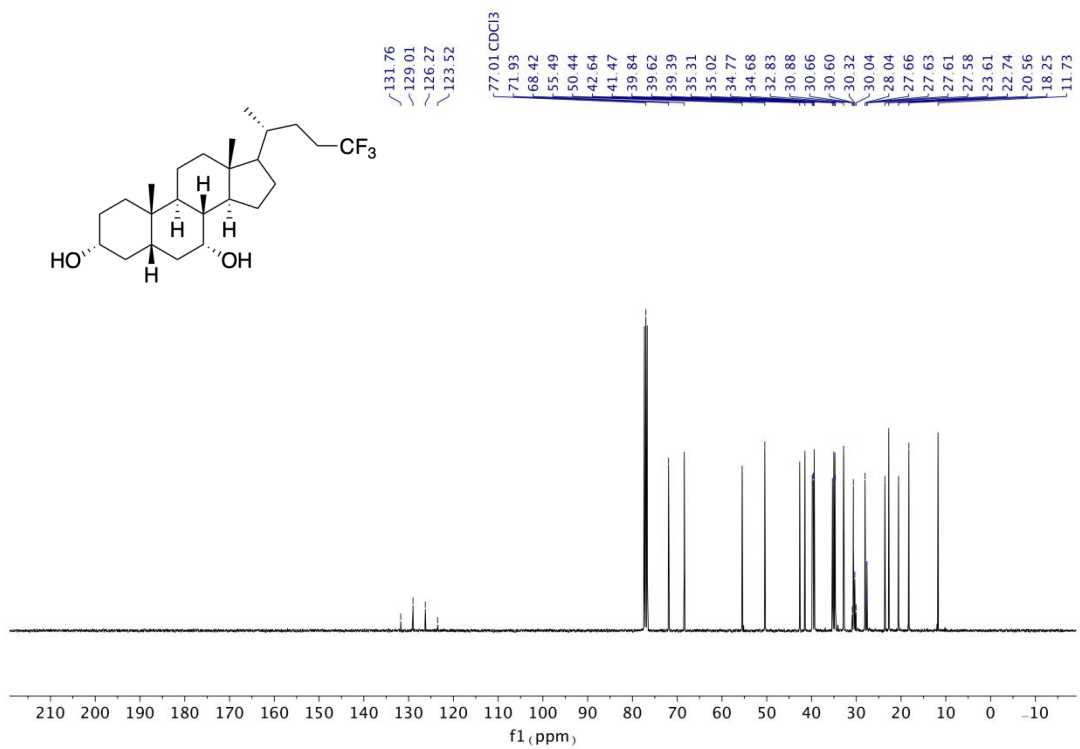


**<sup>1</sup>H NMR (400 MHz, CDCl<sub>3</sub>) of *cis*-51**



**<sup>13</sup>C NMR (101 MHz, CDCl<sub>3</sub>) of *cis*-51**

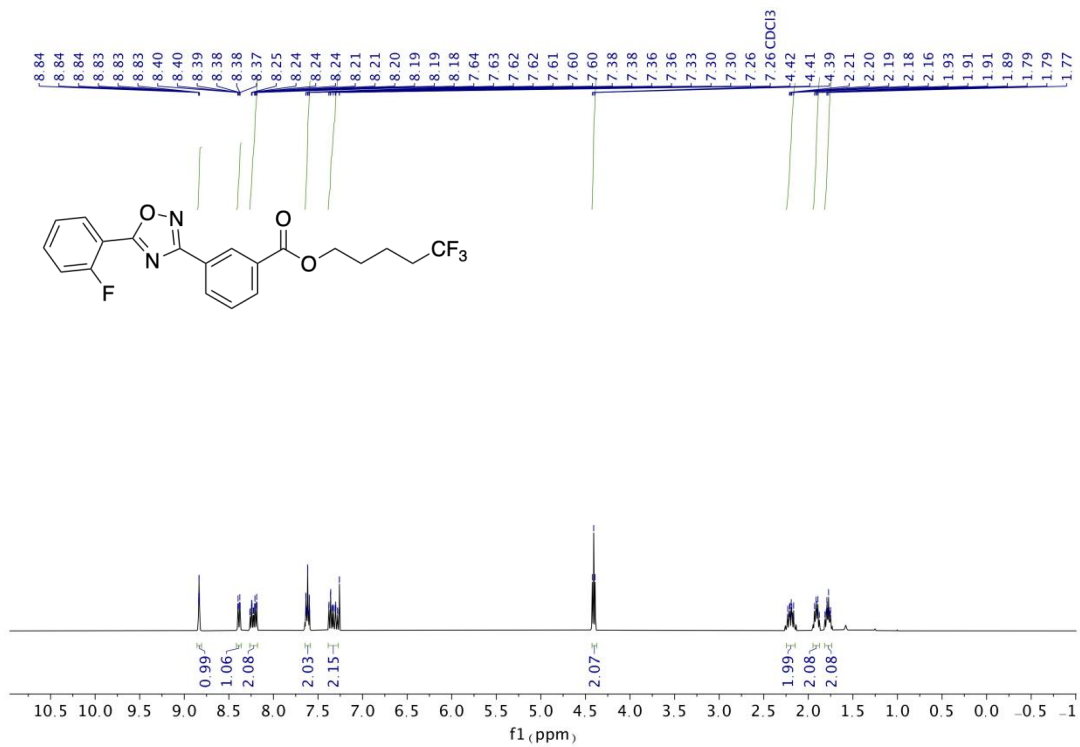




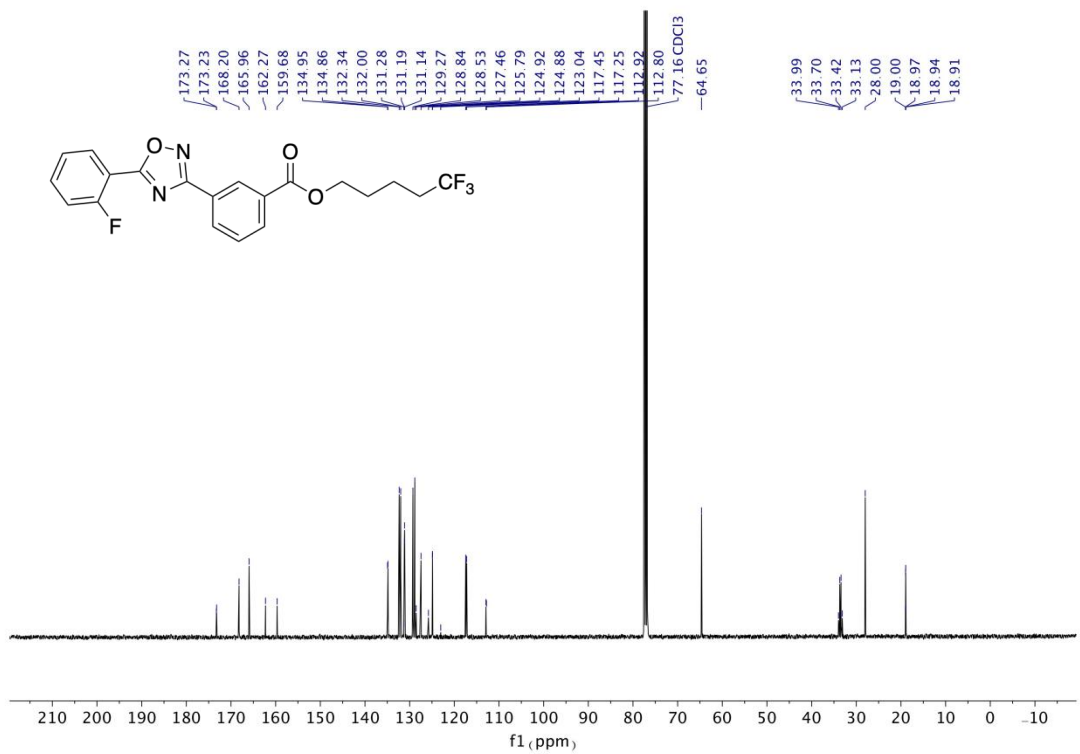
<sup>13</sup>C NMR (101 MHz, CDCl<sub>3</sub>) of **52**



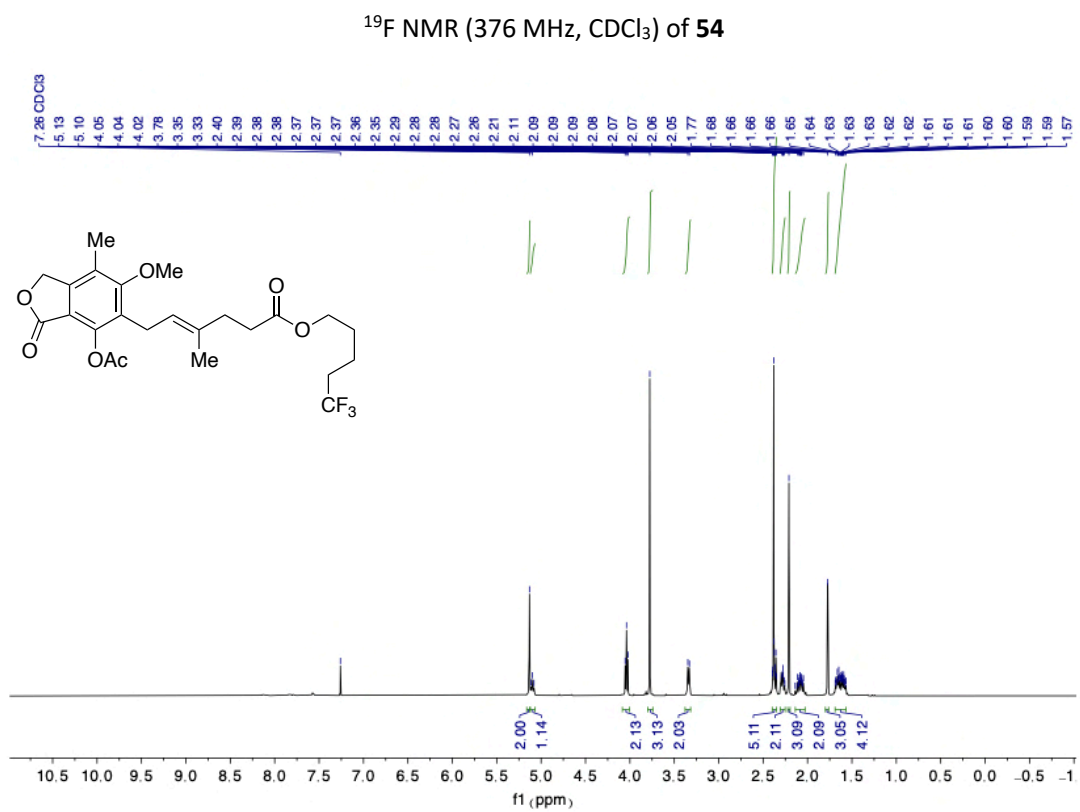
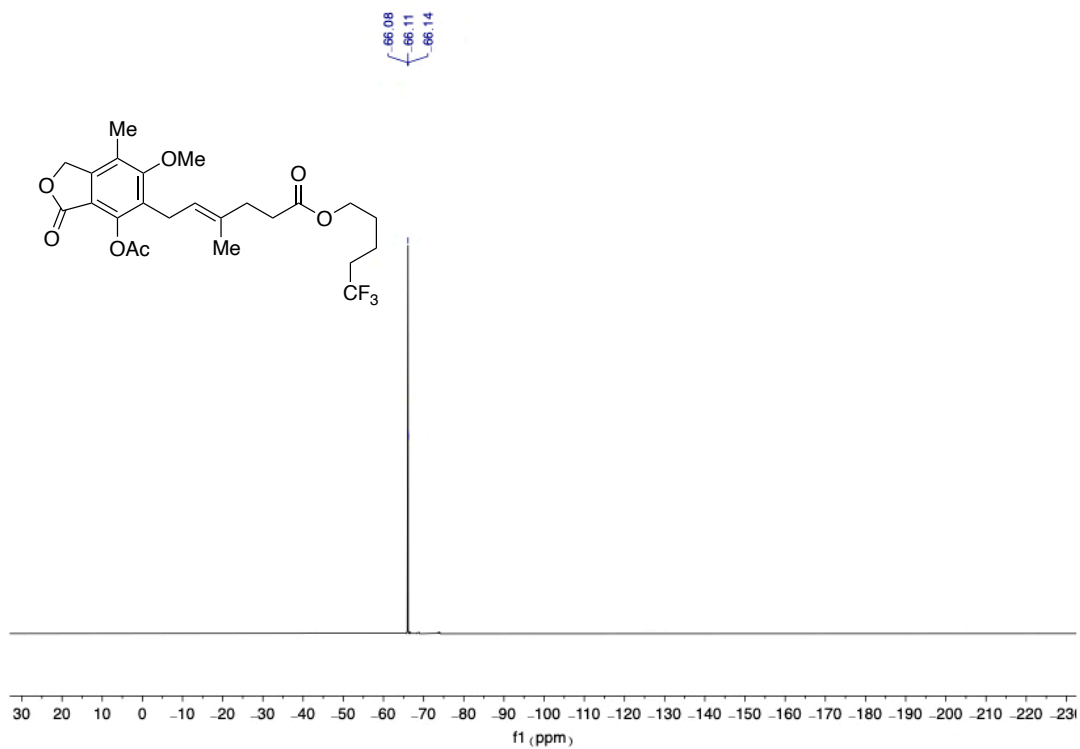
<sup>19</sup>F NMR (376 MHz, CDCl<sub>3</sub>) of **53**

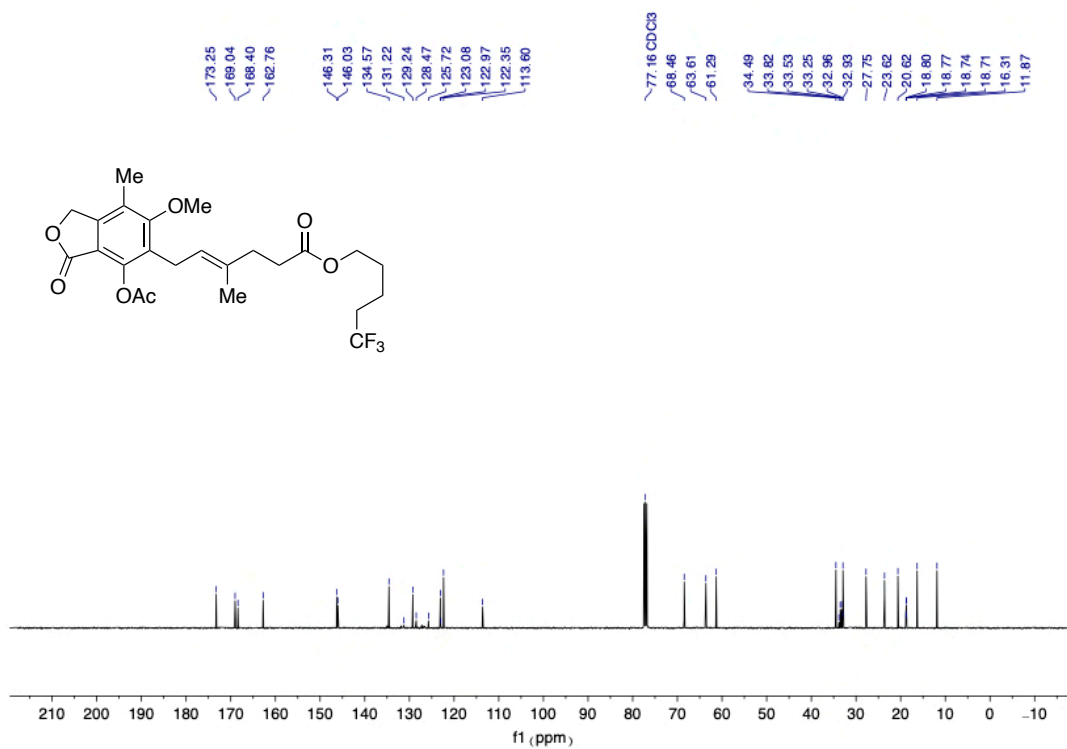


<sup>1</sup>H NMR (400 MHz, CDCl<sub>3</sub>) of **53**

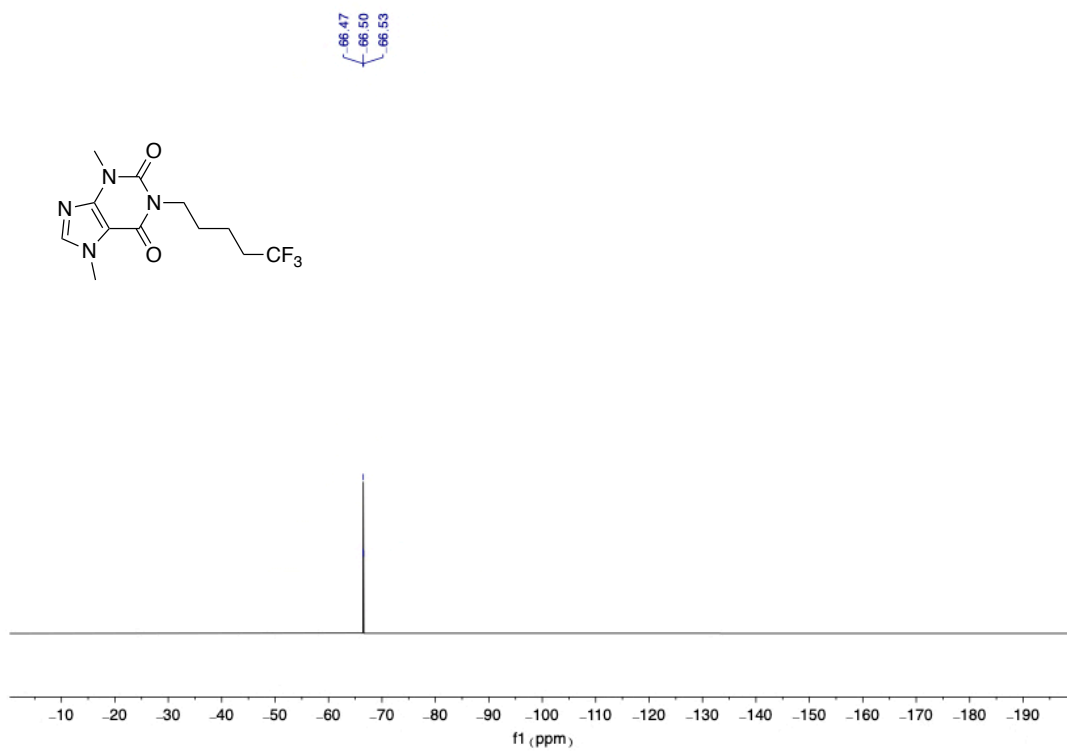


<sup>13</sup>C NMR (101 MHz, CDCl<sub>3</sub>) of **53**



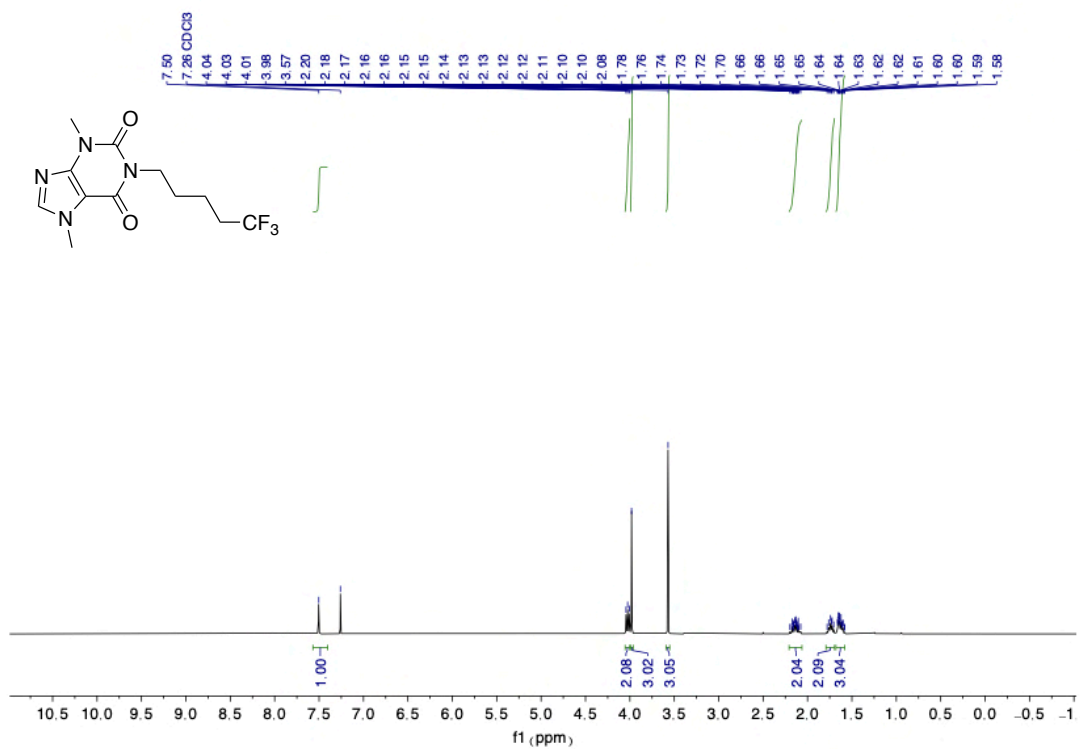


<sup>13</sup>C NMR (101 MHz, CDCl<sub>3</sub>) of **54**

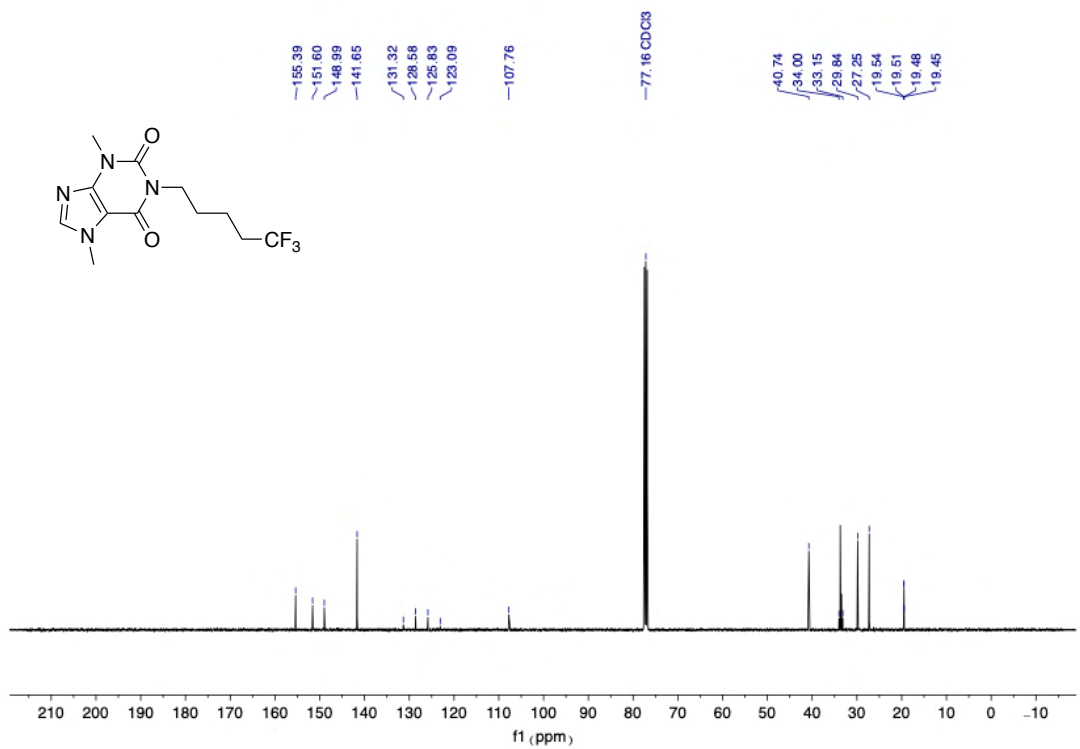


<sup>19</sup>F NMR (376 MHz, CDCl<sub>3</sub>) of **55**

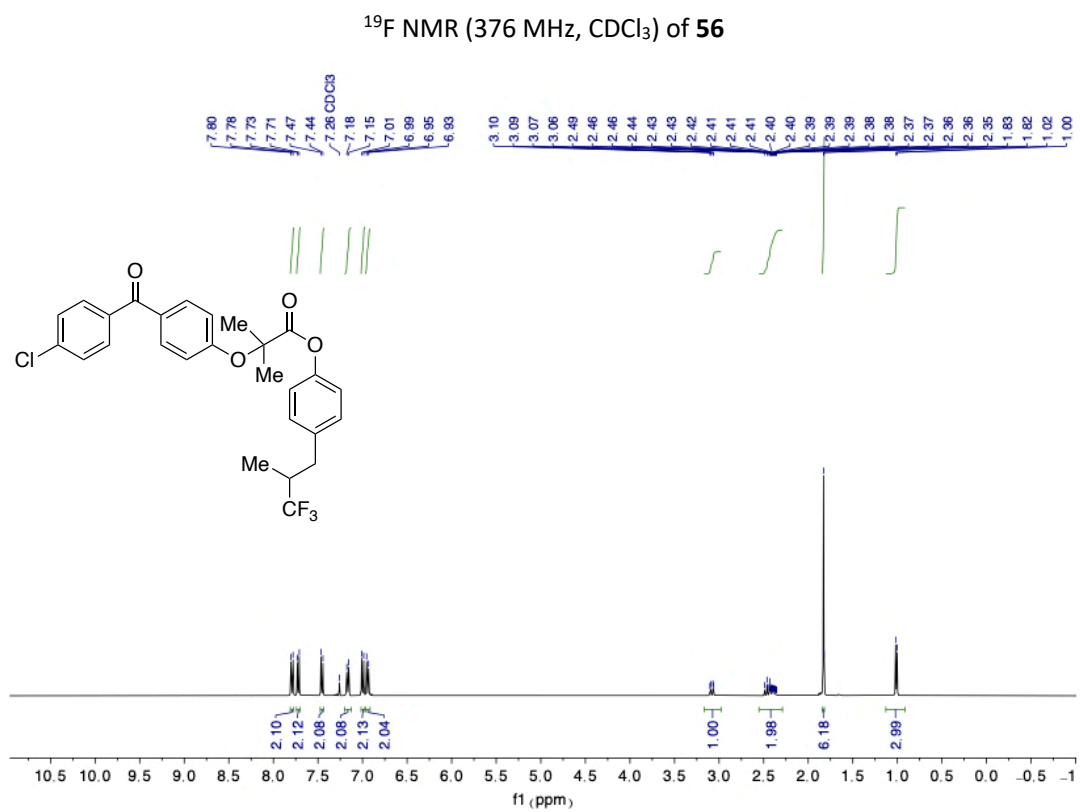
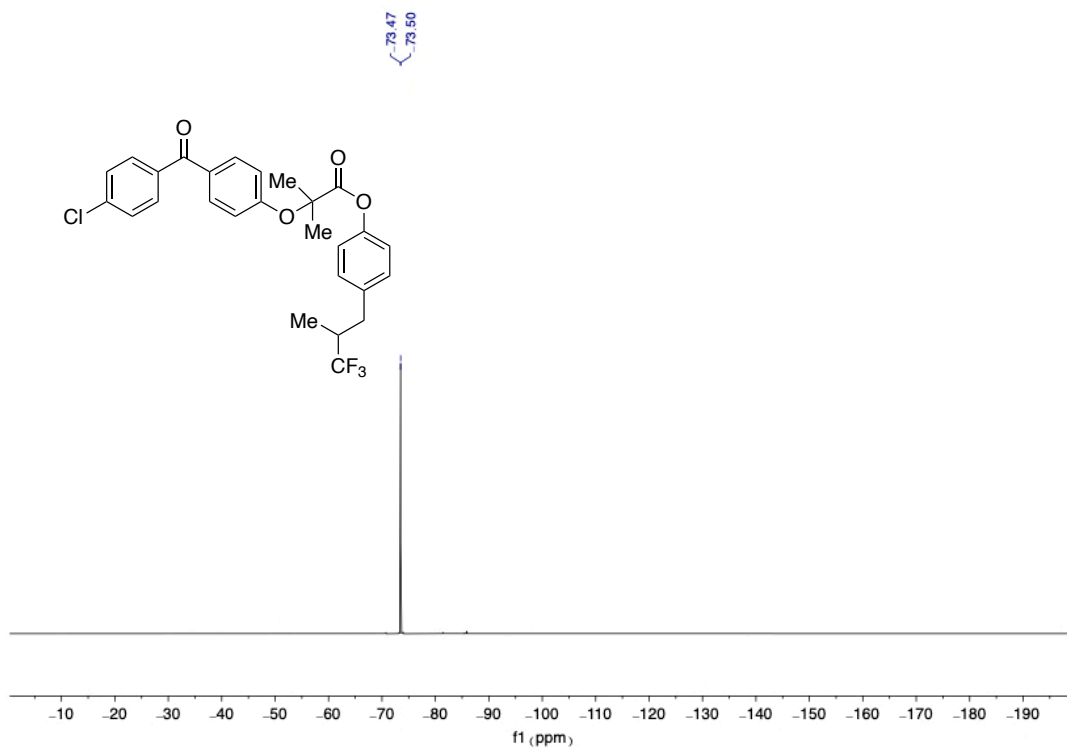


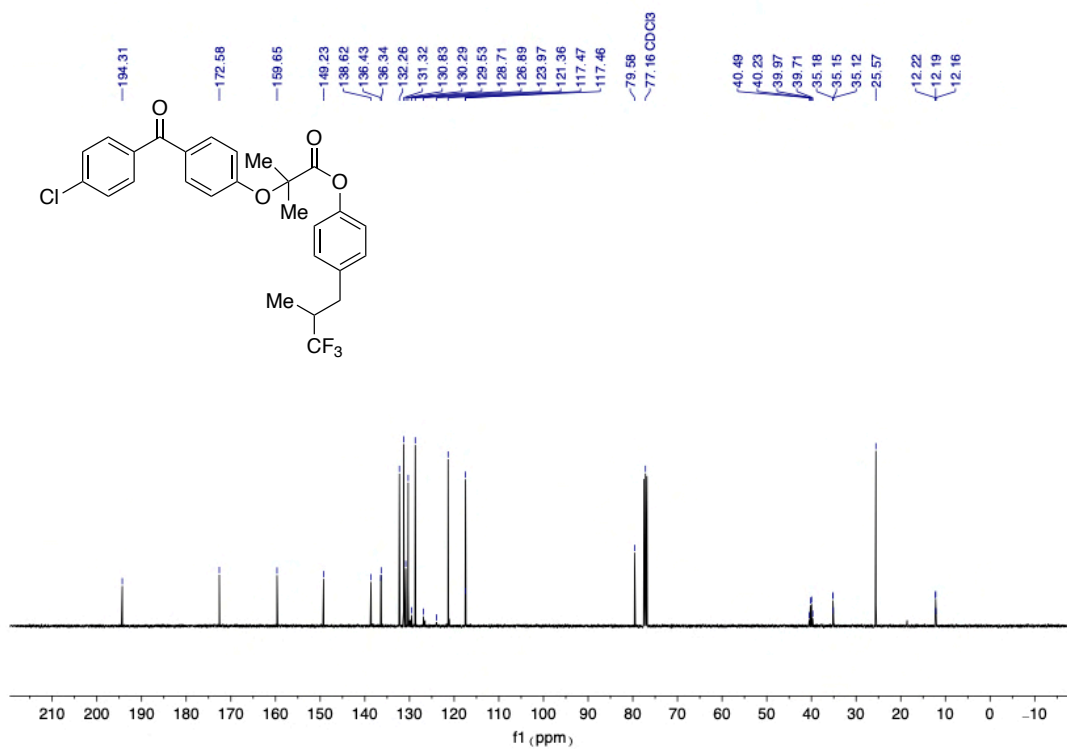


<sup>1</sup>H NMR (400 MHz, CDCl<sub>3</sub>) of 55

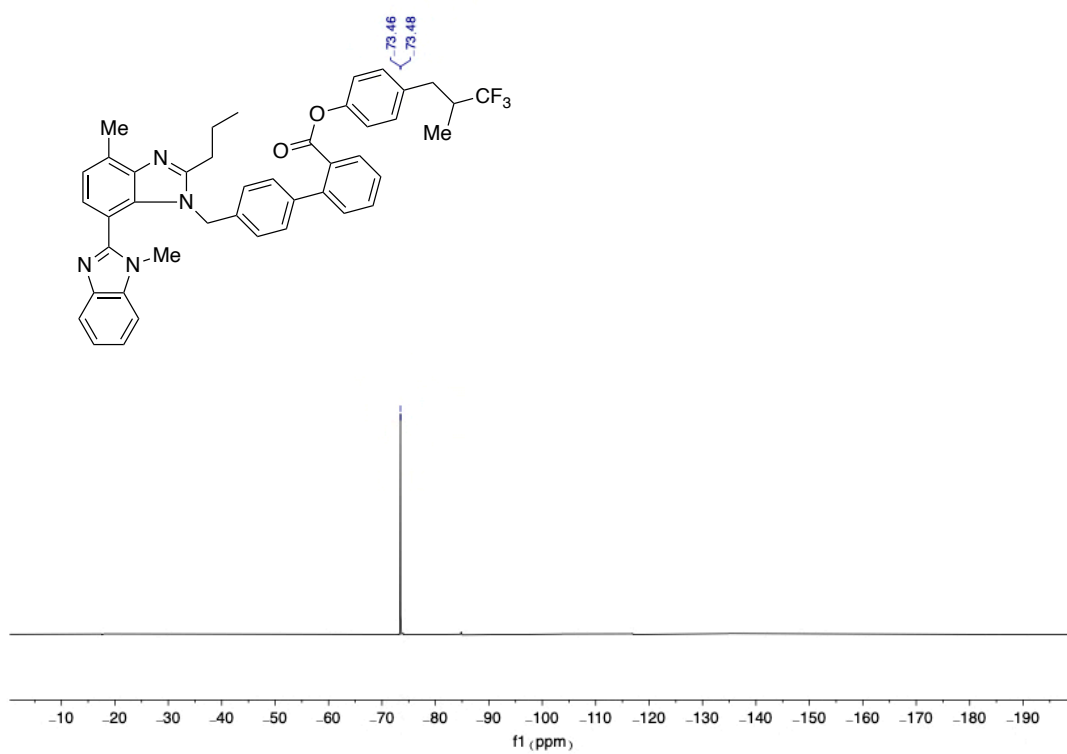


<sup>13</sup>C NMR (101 MHz, CDCl<sub>3</sub>) of 55

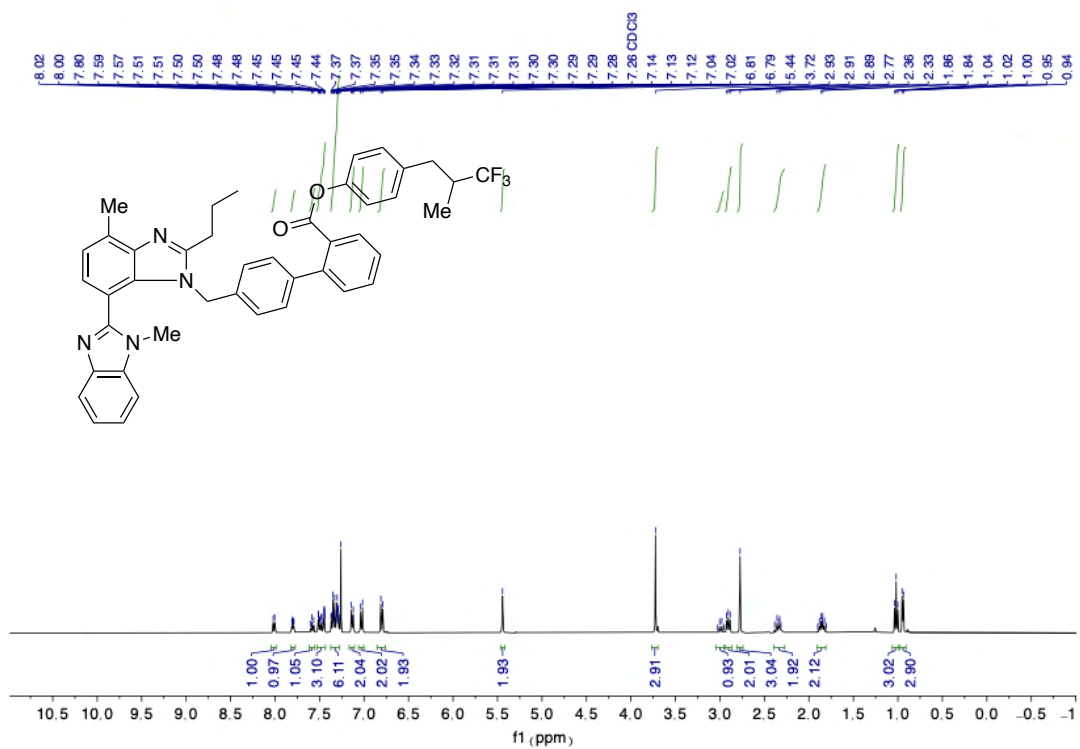




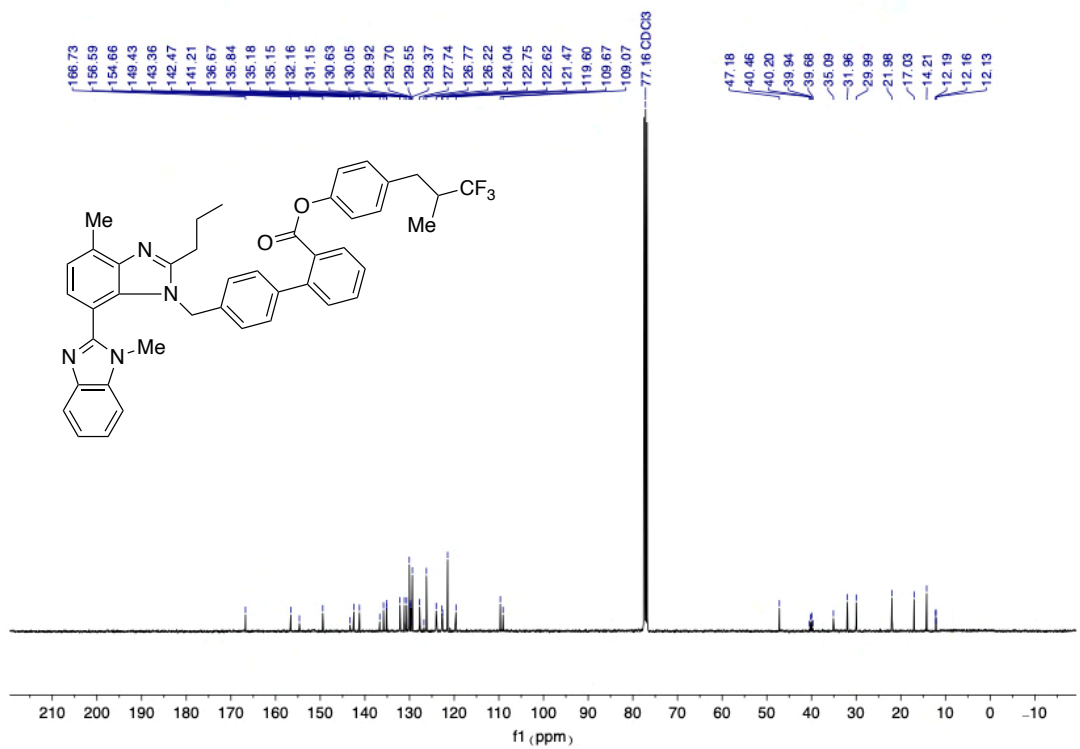
<sup>13</sup>C NMR (101 MHz, CDCl<sub>3</sub>) of **56**



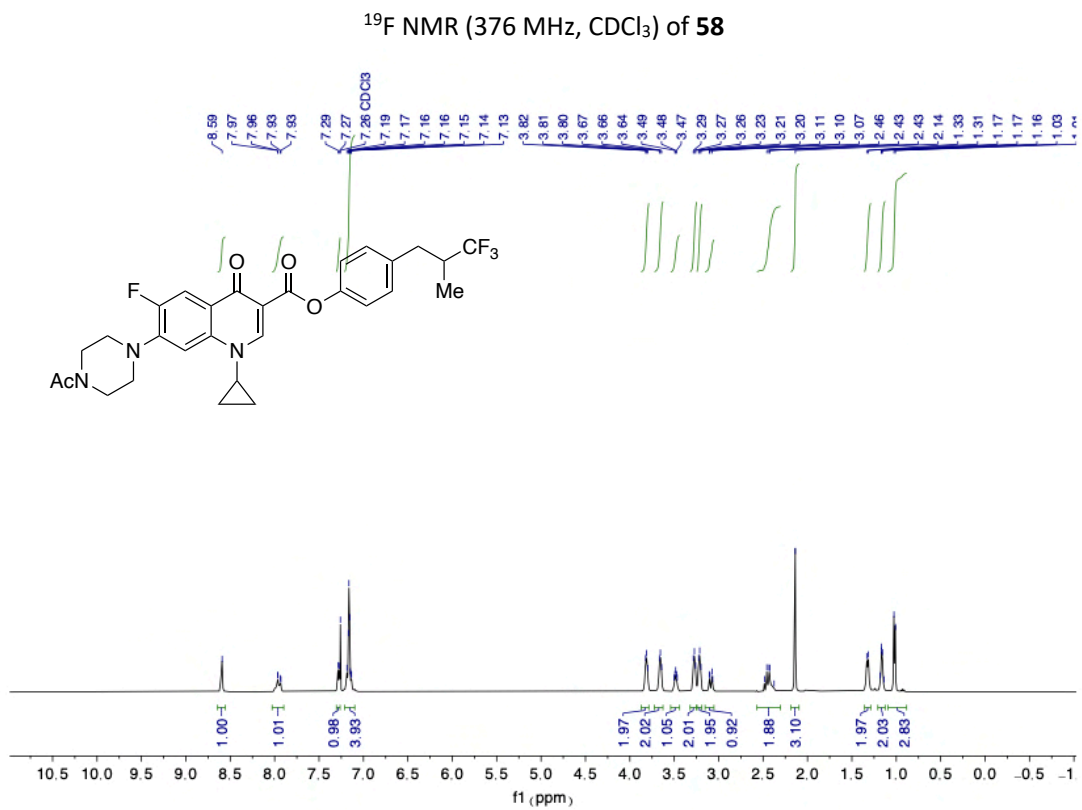
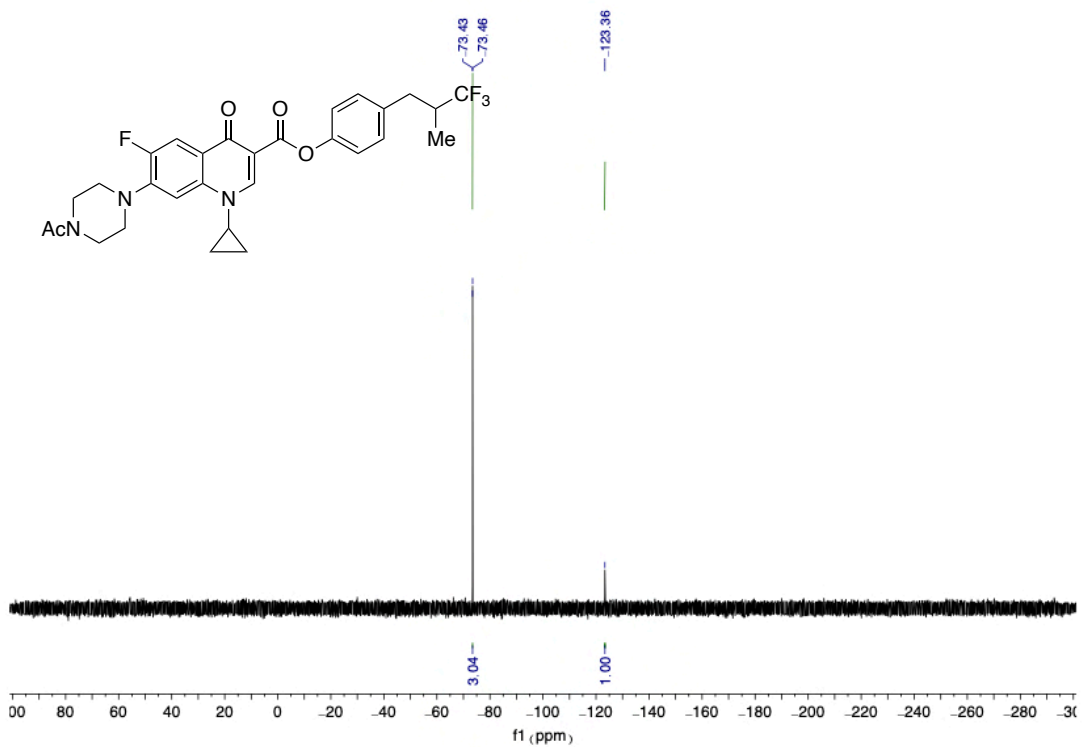
<sup>19</sup>F NMR (376 MHz, CDCl<sub>3</sub>) of **57**

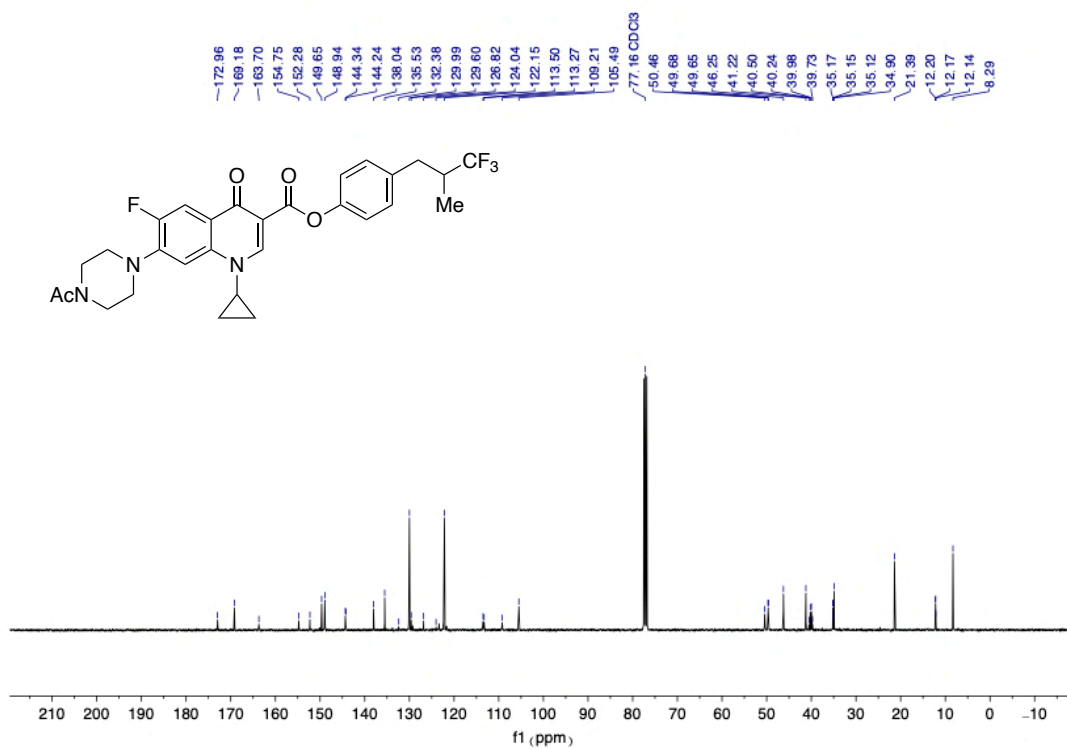


<sup>1</sup>H NMR (400 MHz, CDCl<sub>3</sub>) of **57**

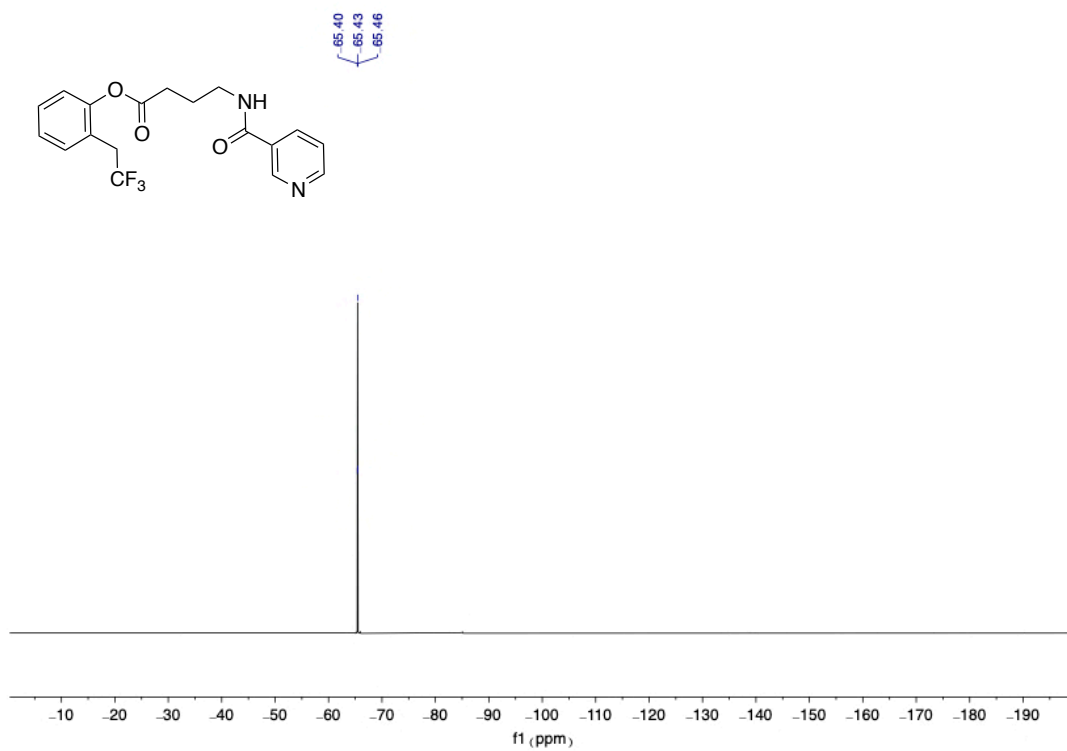


<sup>13</sup>C NMR (101 MHz, CDCl<sub>3</sub>) of **57**

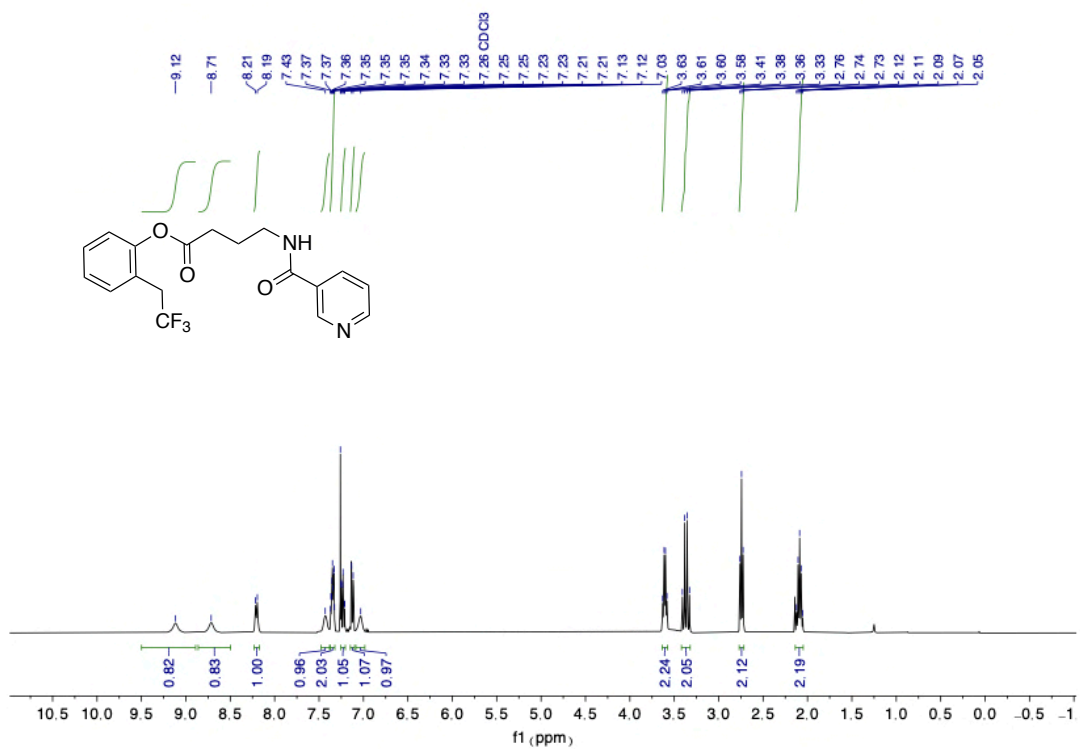




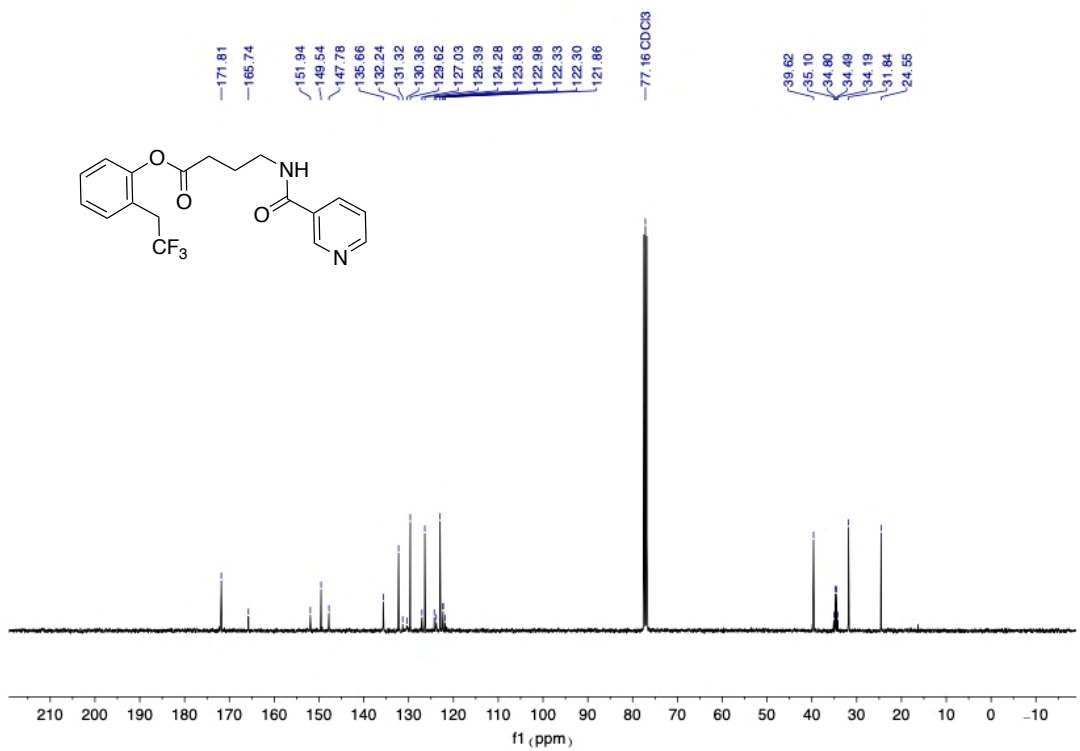
<sup>13</sup>C NMR (101 MHz, CDCl<sub>3</sub>) of **58**



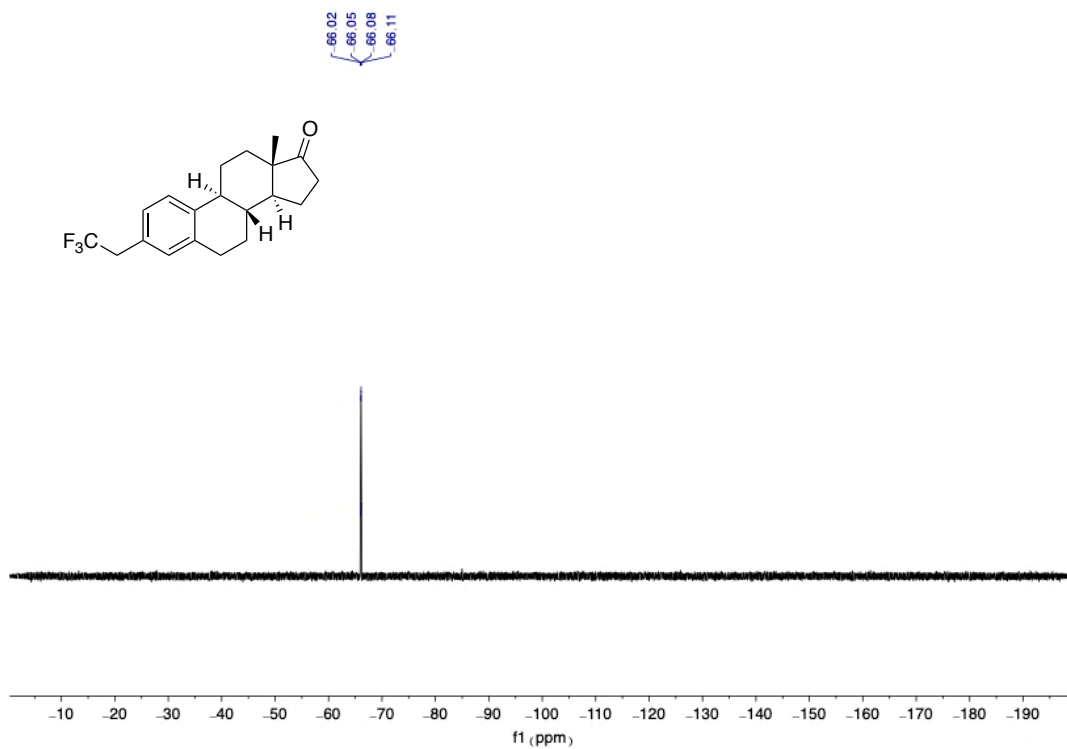
<sup>19</sup>F NMR (376 MHz, CDCl<sub>3</sub>) of **59**



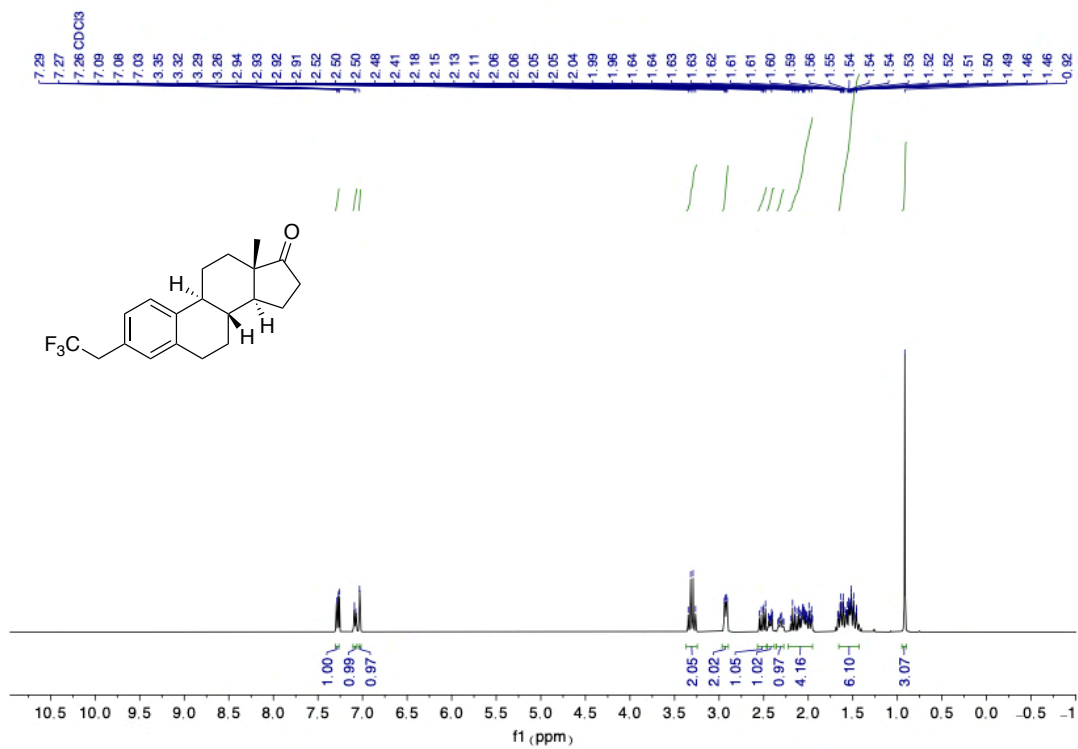
**<sup>1</sup>H NMR (400 MHz, CDCl<sub>3</sub>) of 59**



**<sup>13</sup>C NMR (101 MHz, CDCl<sub>3</sub>) of 59**

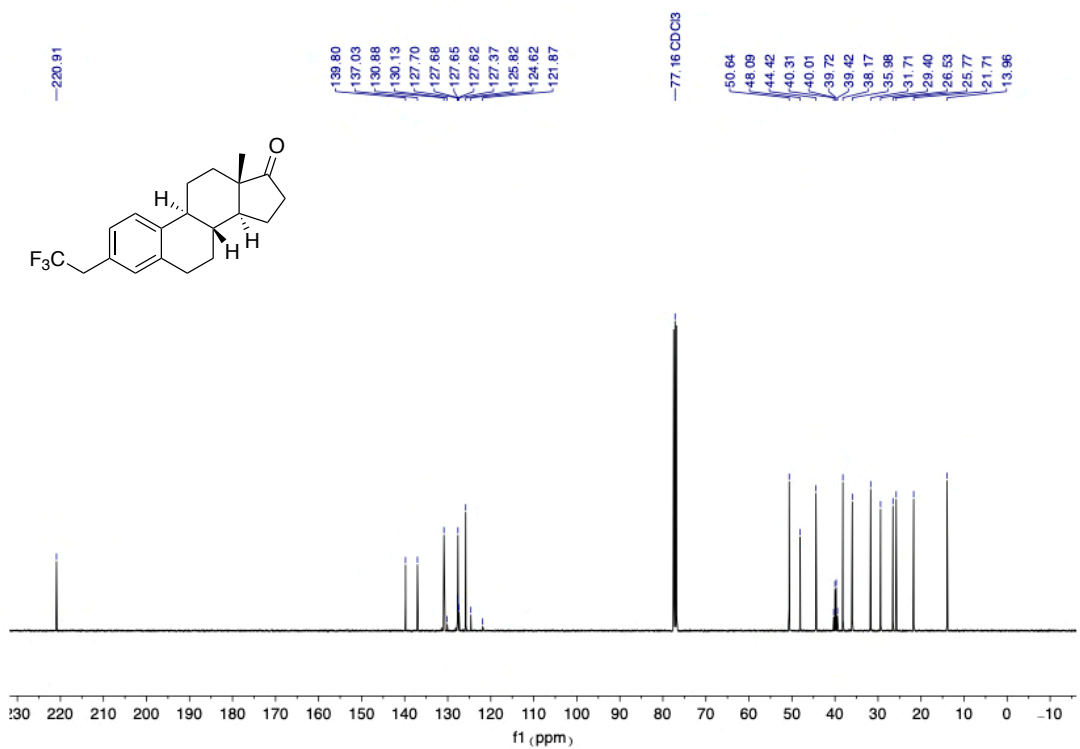


$^{19}\text{F}$  NMR (376 MHz,  $\text{CDCl}_3$ ) of **60**

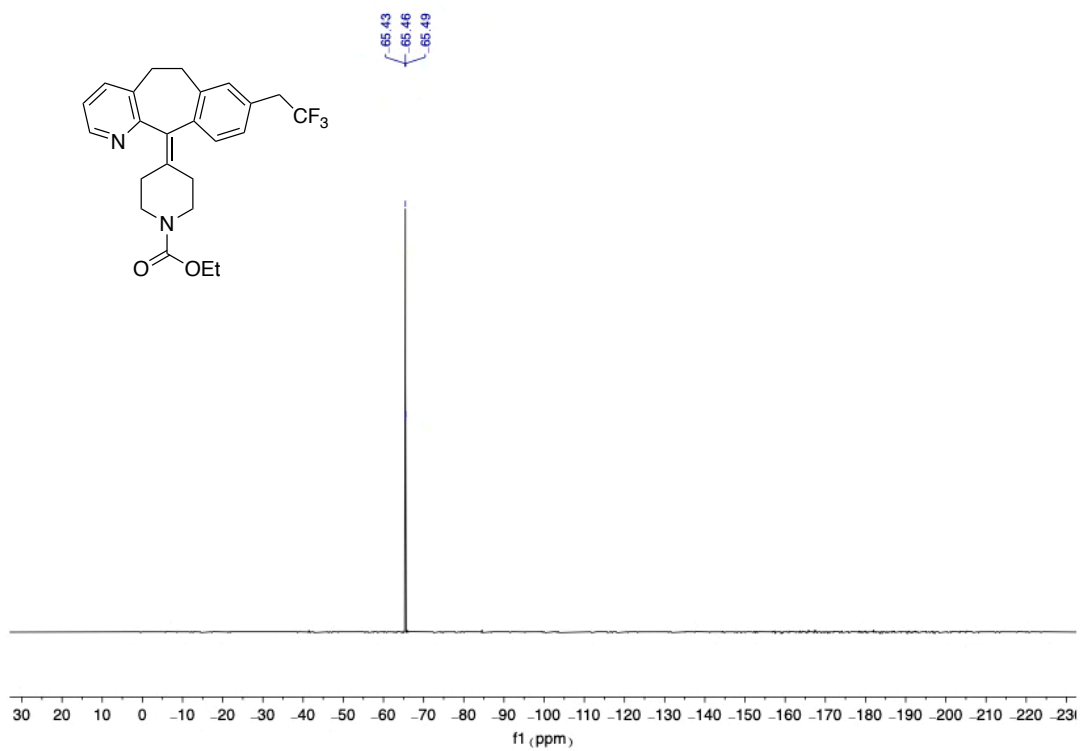


$^1\text{H}$  NMR (400 MHz,  $\text{CDCl}_3$ ) of **60**

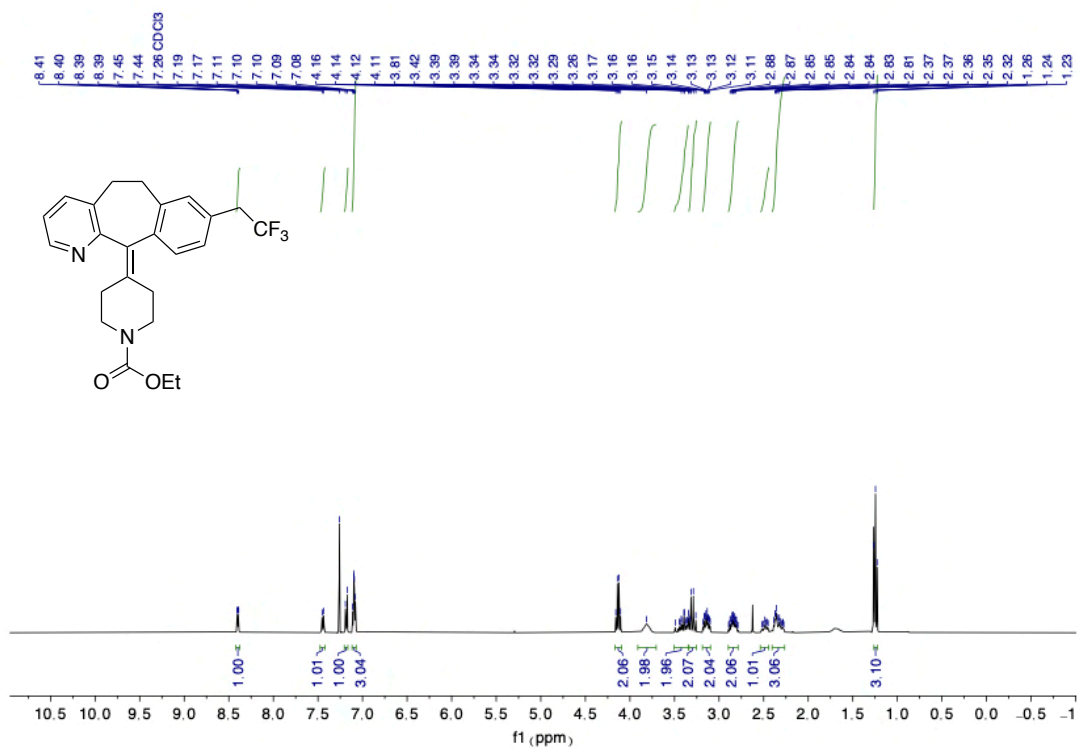




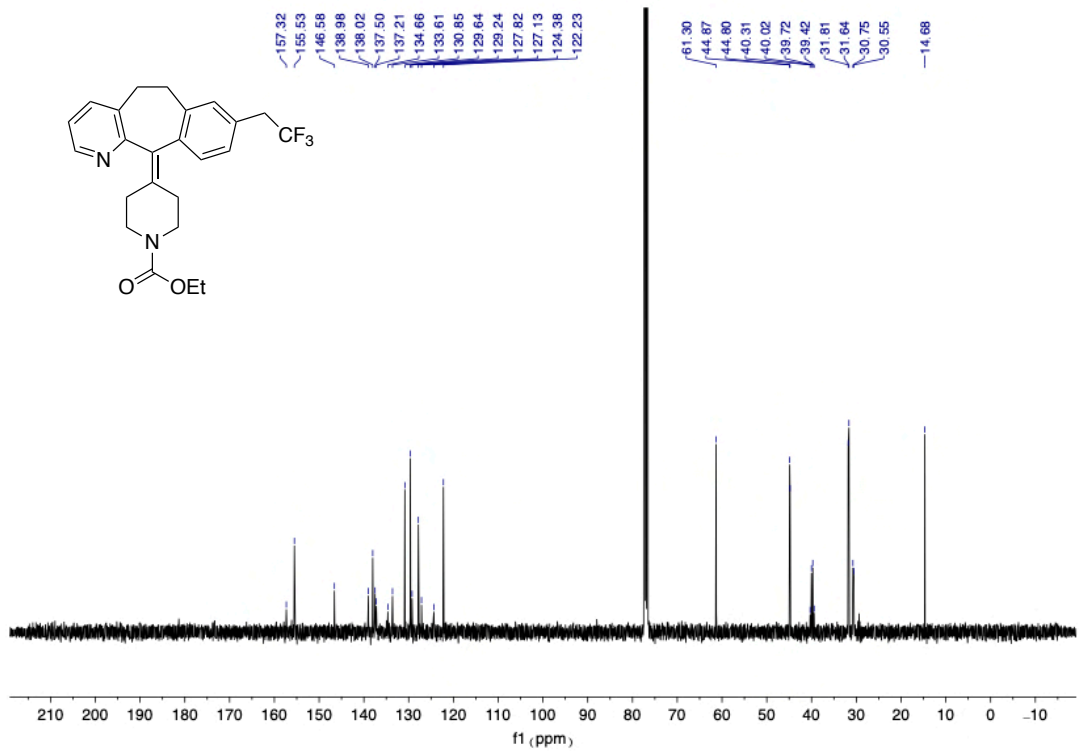
<sup>13</sup>C NMR (101 MHz, CDCl<sub>3</sub>) of **60**



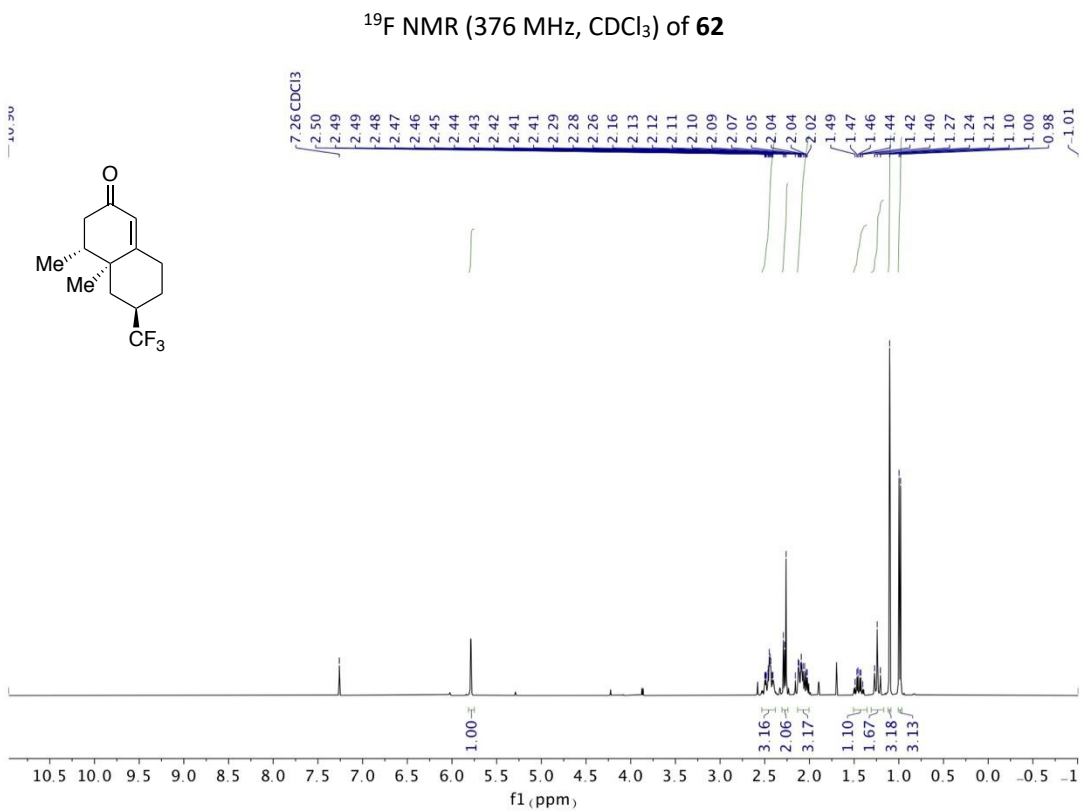
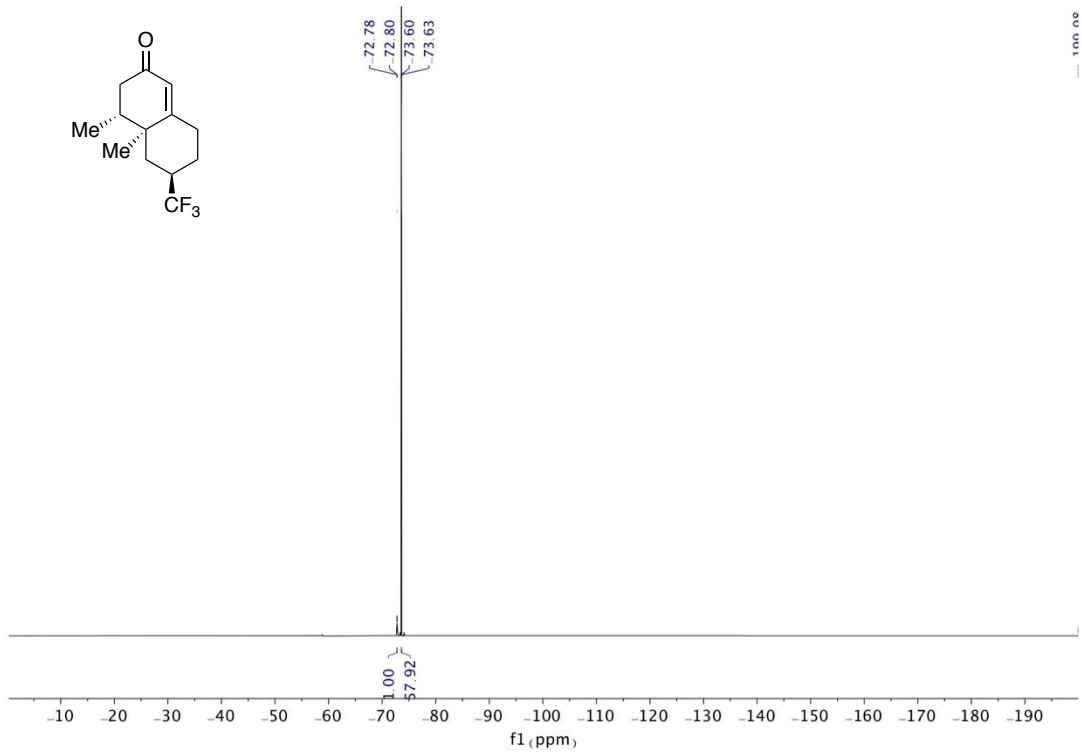
<sup>19</sup>F NMR (376 MHz, CDCl<sub>3</sub>) of **61**

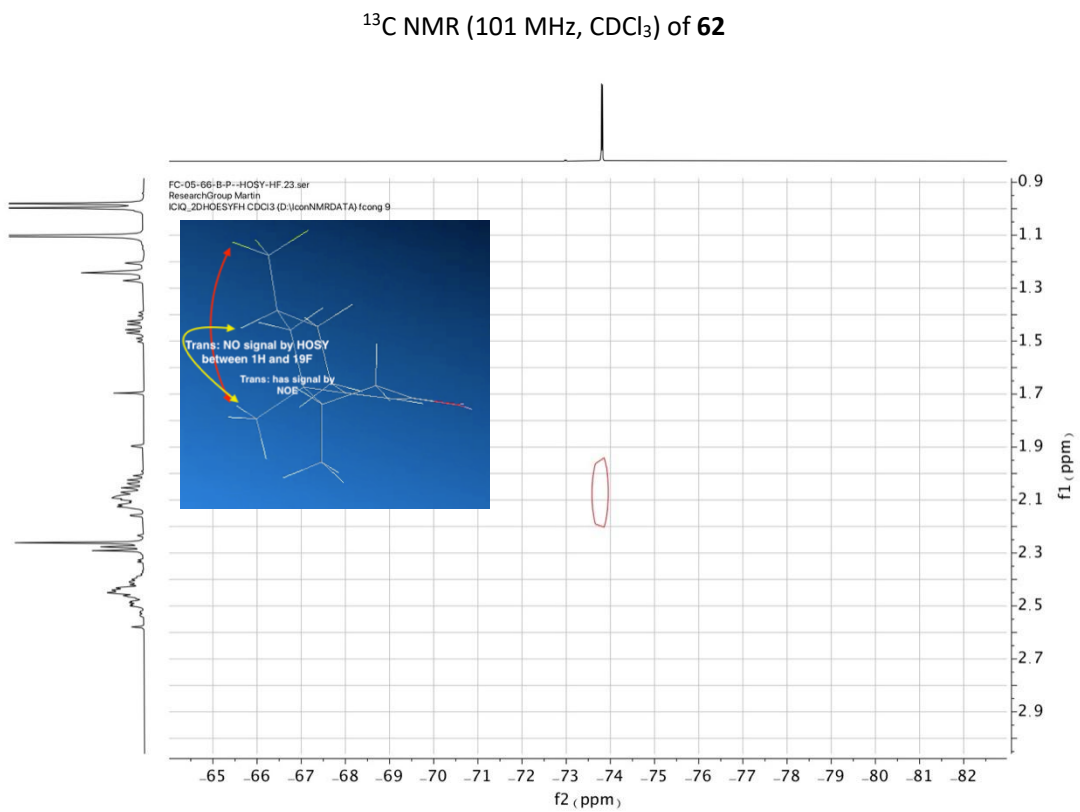
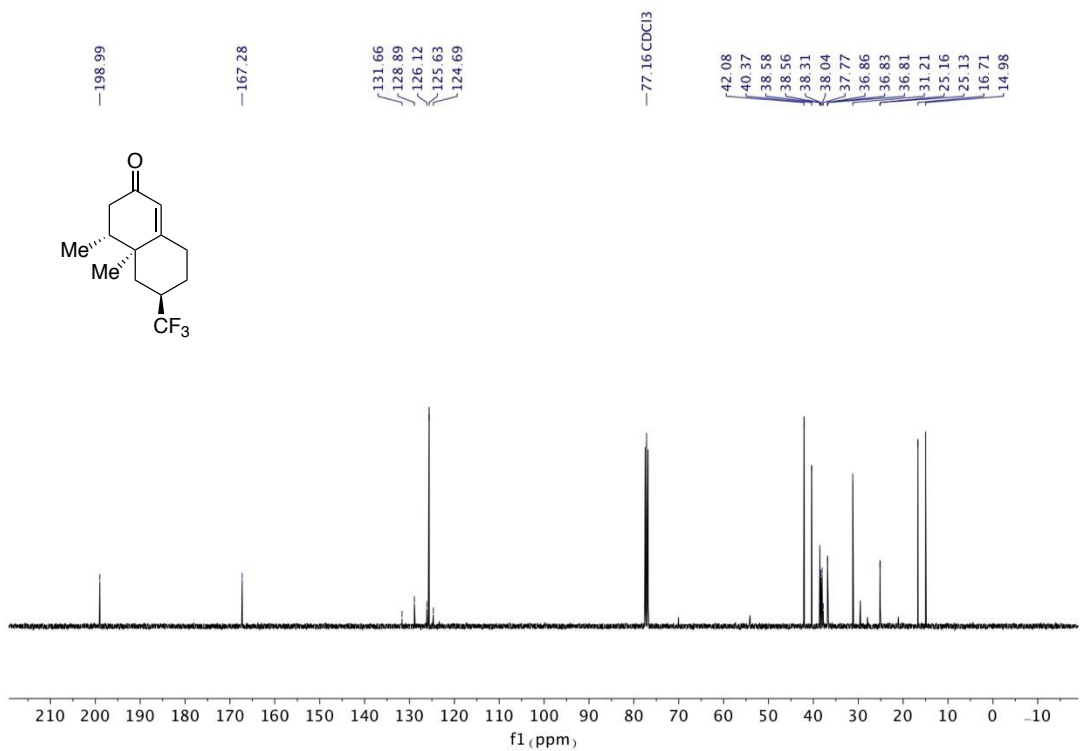


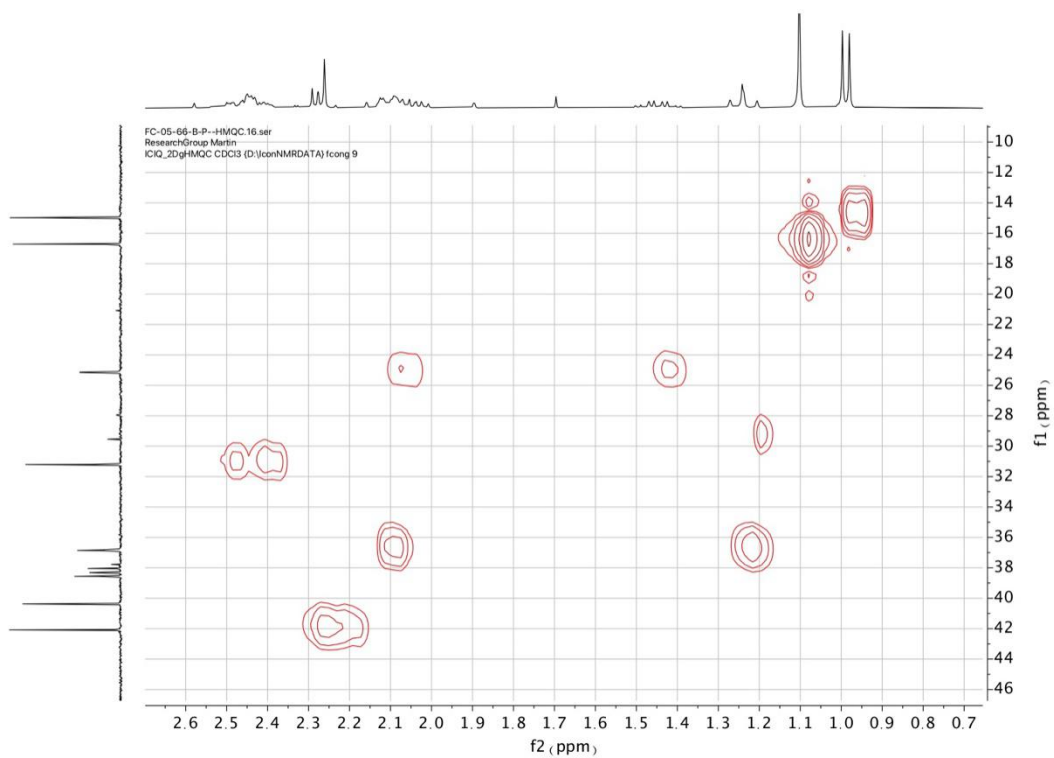
<sup>1</sup>H NMR (400 MHz, CDCl<sub>3</sub>) of **61**



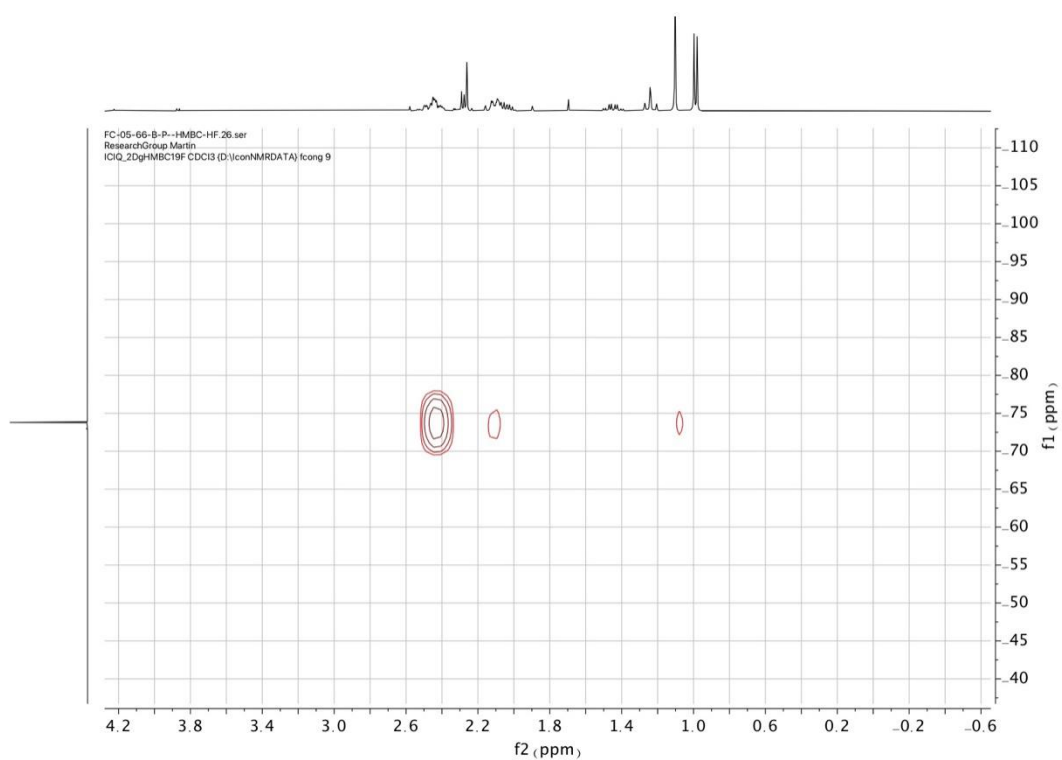
<sup>13</sup>C NMR (101 MHz, CDCl<sub>3</sub>) of **61**



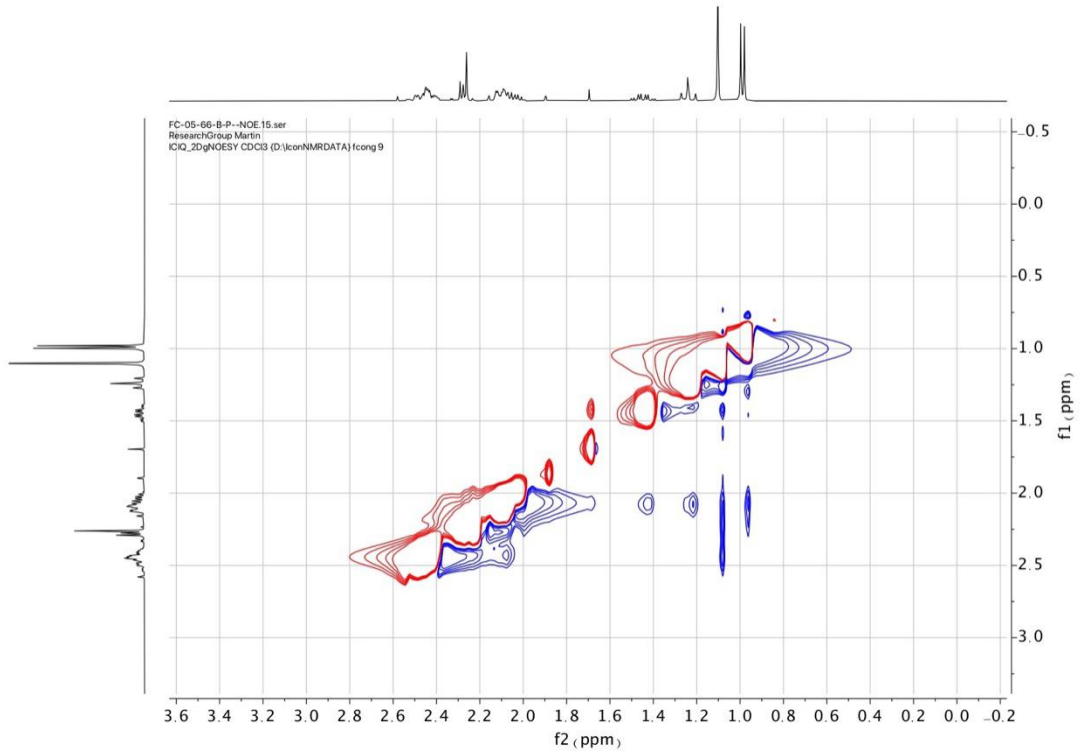




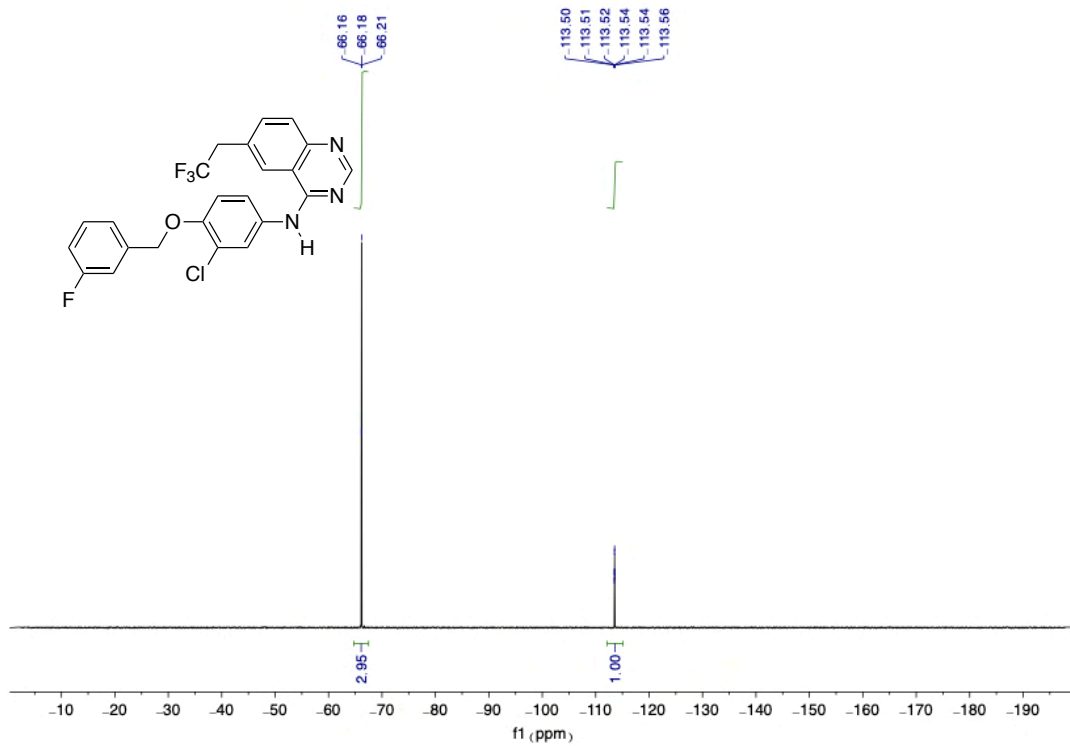
HMQC (CDCl<sub>3</sub>) of **62**



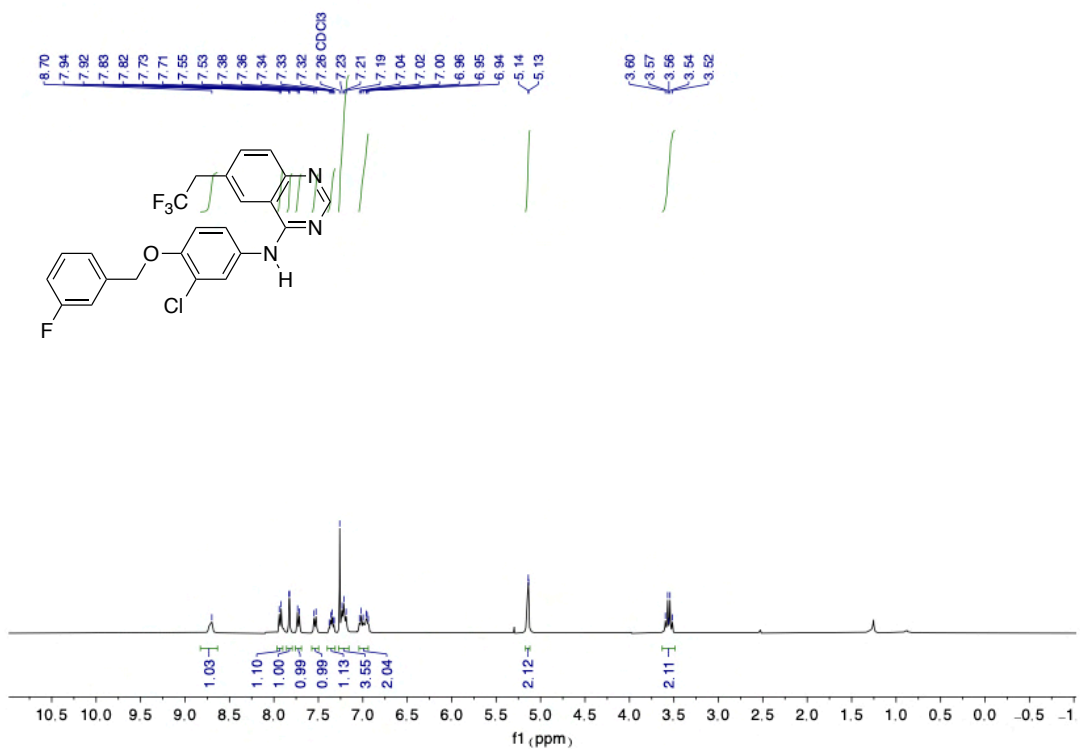
HMBC-F (CDCl<sub>3</sub>) of **62**



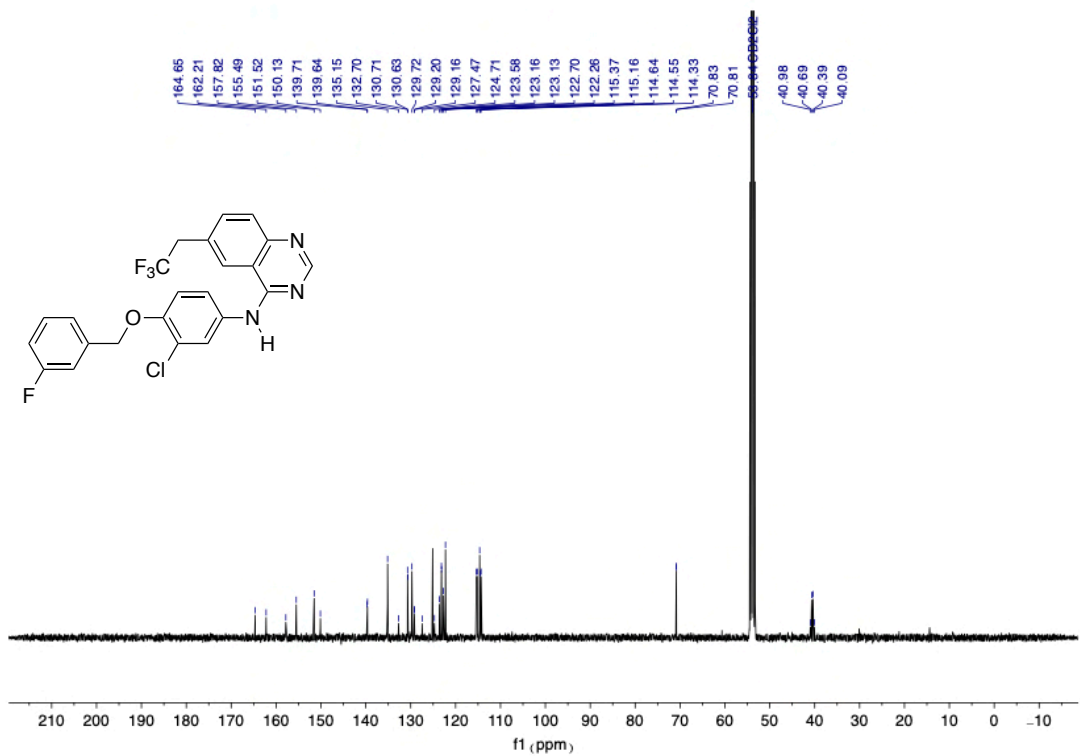
NOE (CDCl<sub>3</sub>) of **62**



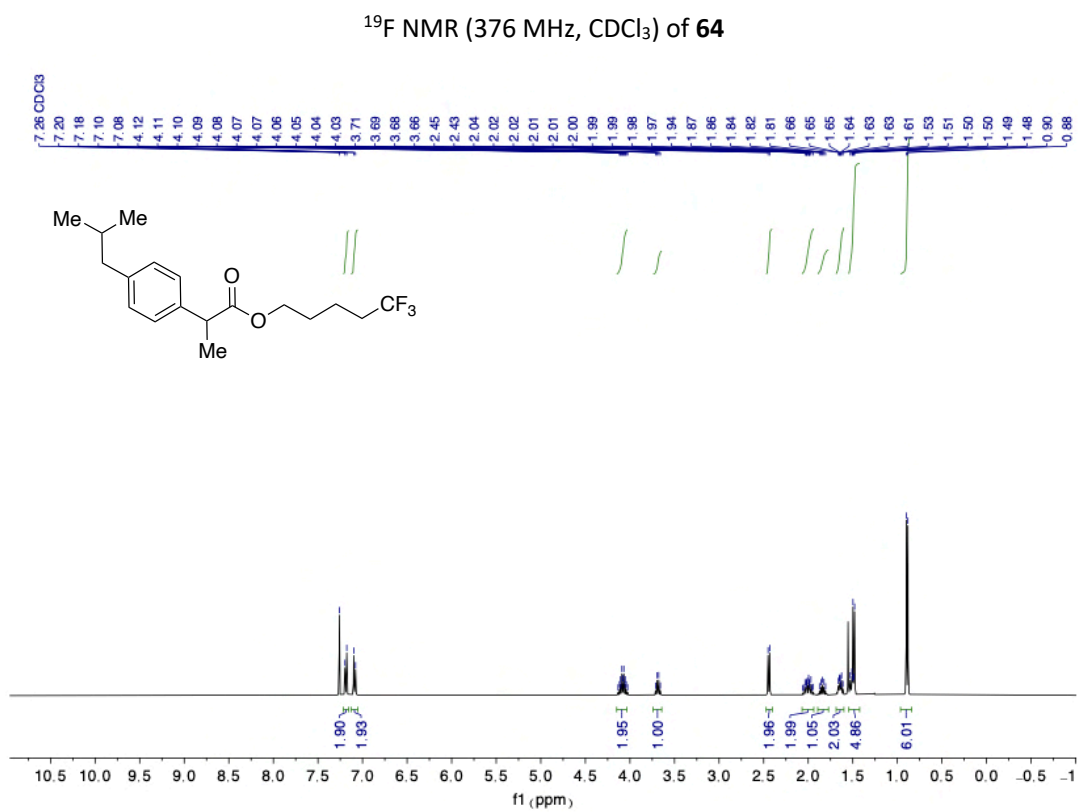
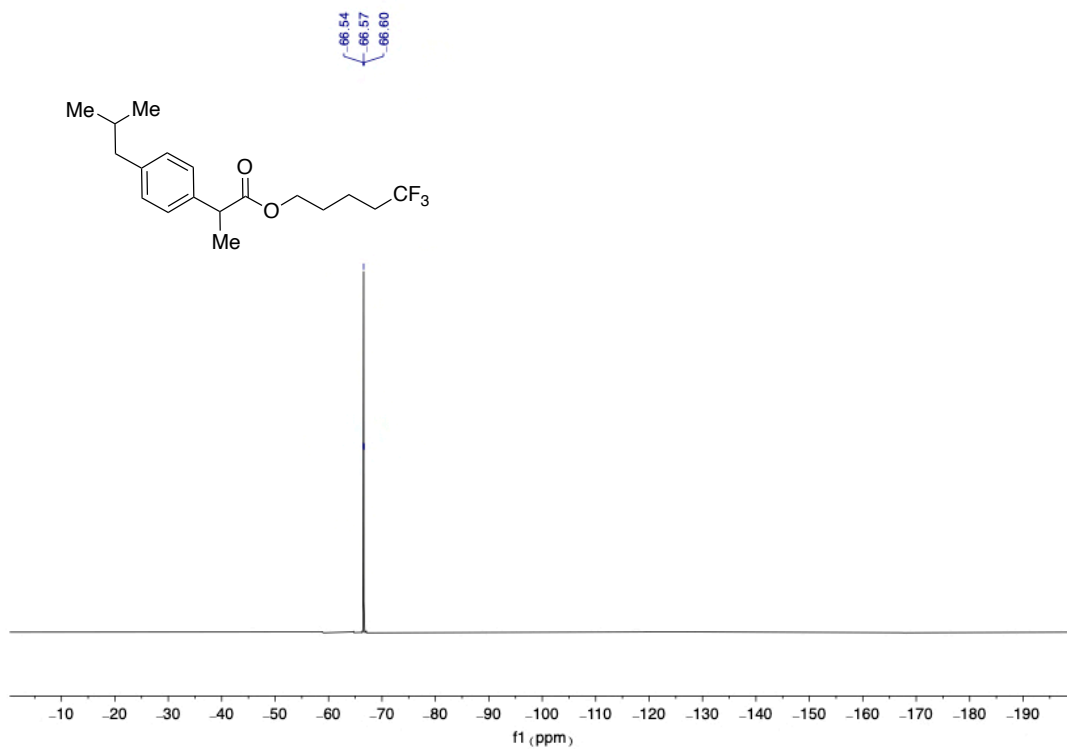
<sup>19</sup>F NMR (376 MHz, CDCl<sub>3</sub>) of **63**



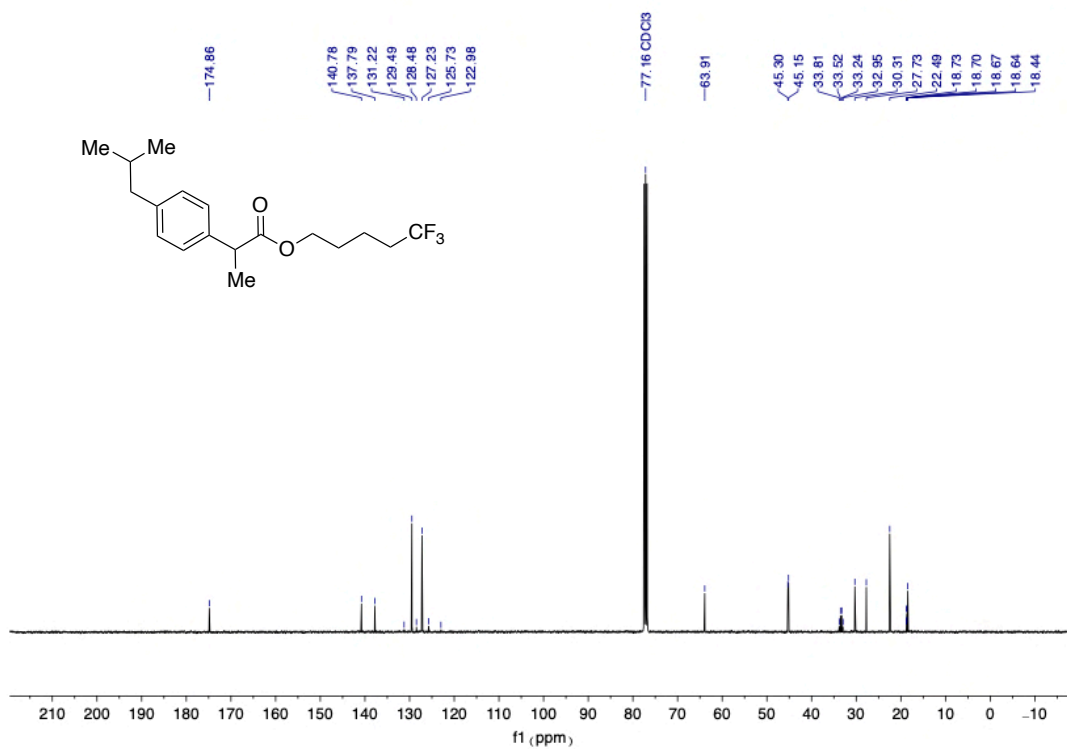
**<sup>1</sup>H NMR (400 MHz, CDCl<sub>3</sub>) of 63**



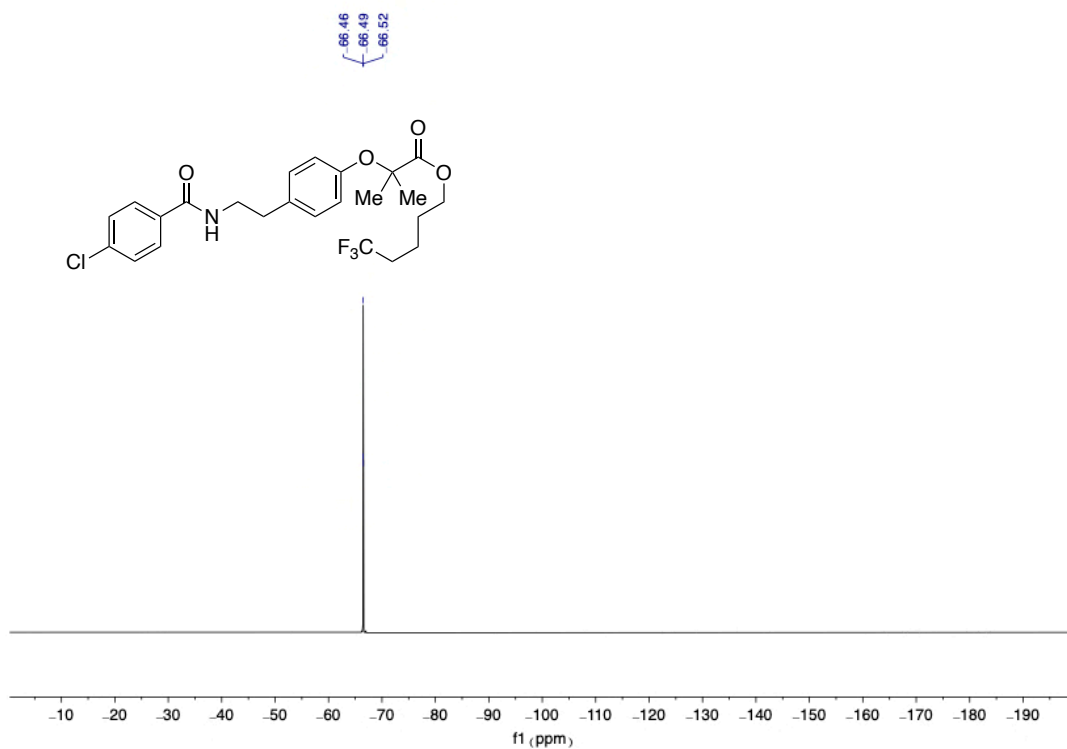
**<sup>13</sup>C NMR (101 MHz, CD<sub>2</sub>Cl<sub>2</sub>) of 63**



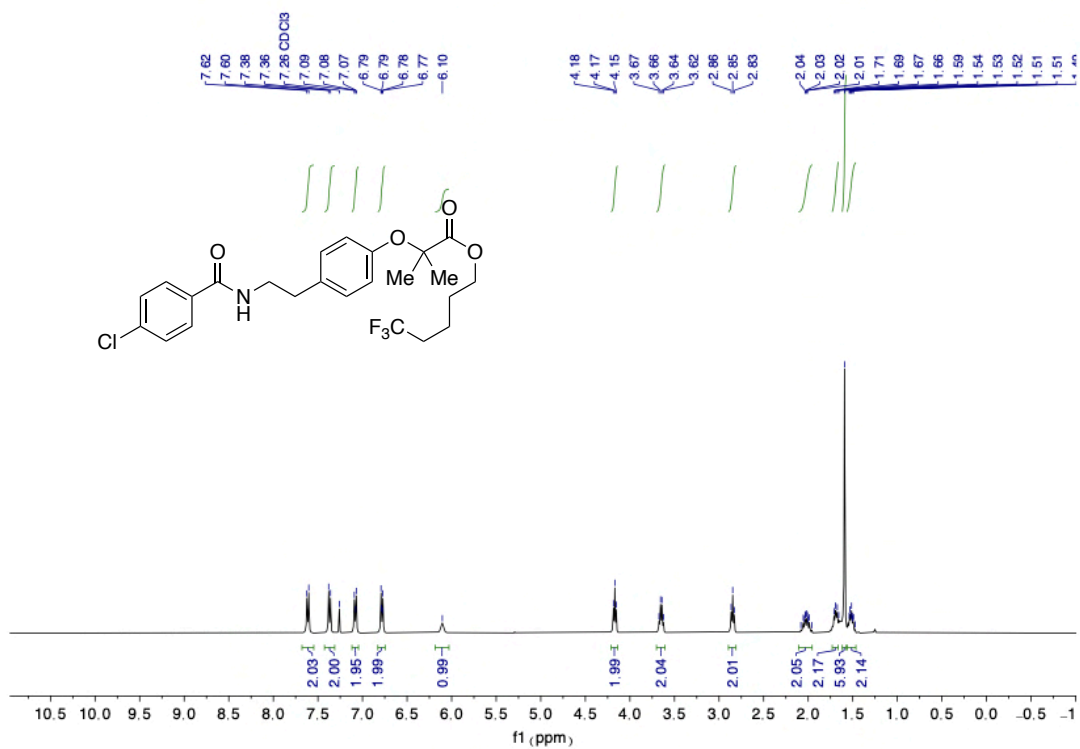




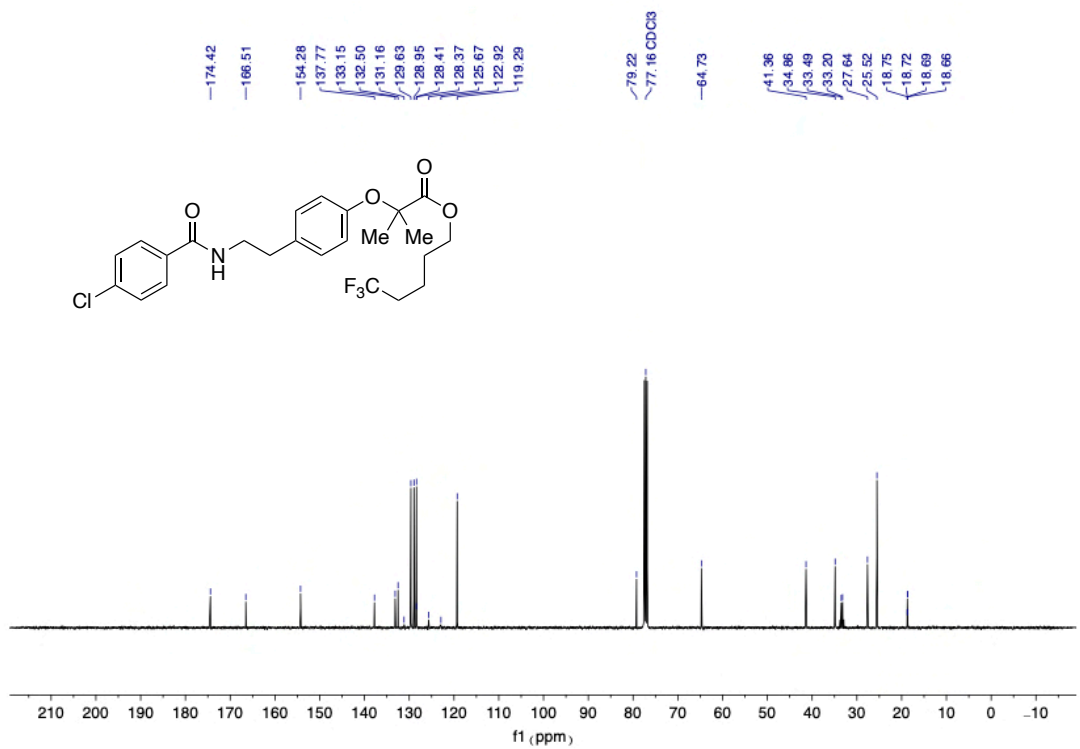
$^{13}\text{C}$  NMR (101 MHz,  $\text{CDCl}_3$ ) of **64**



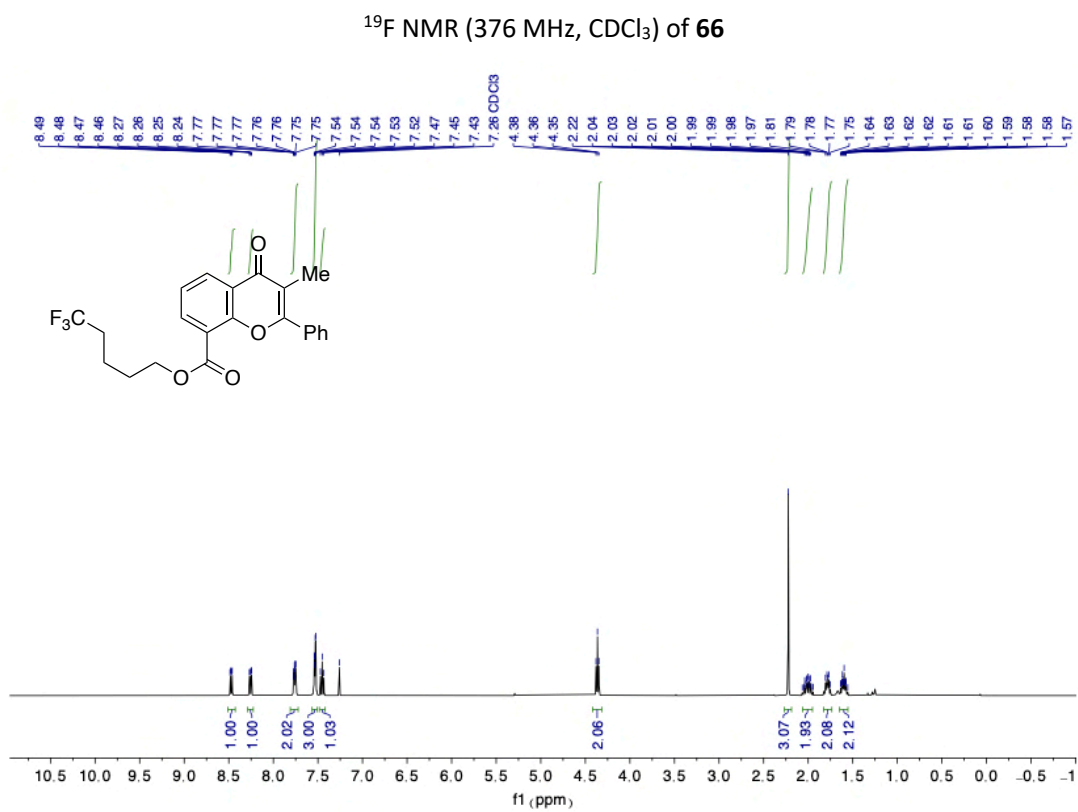
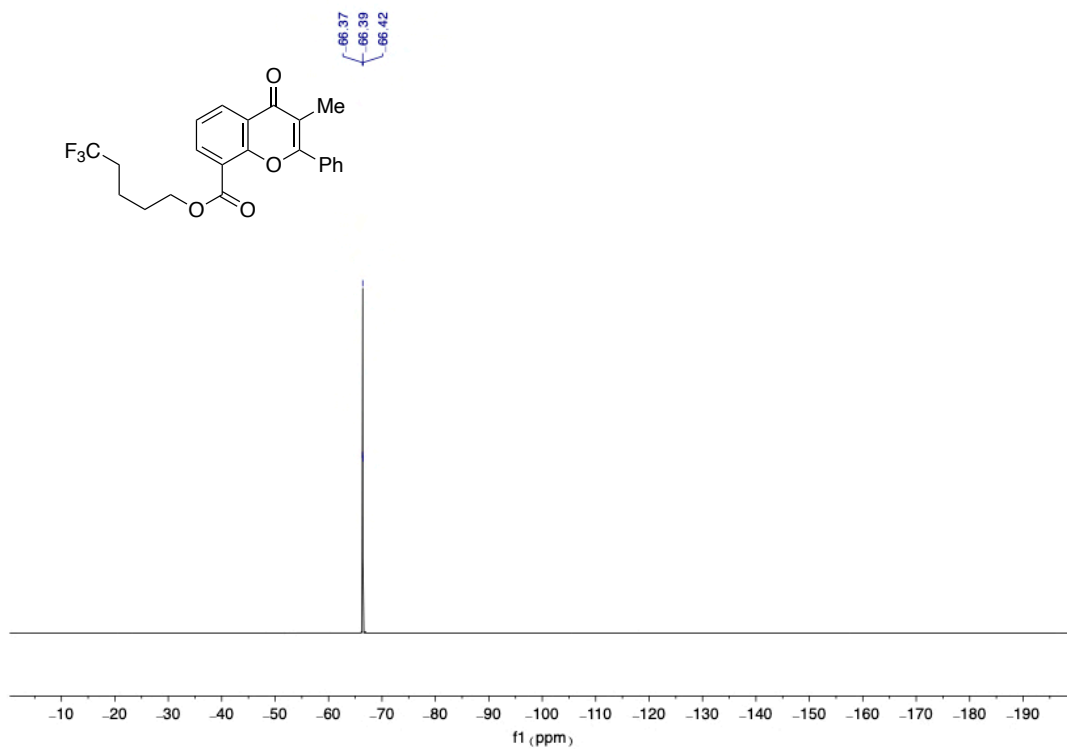
$^{19}\text{F}$  NMR (376 MHz,  $\text{CDCl}_3$ ) of **65**

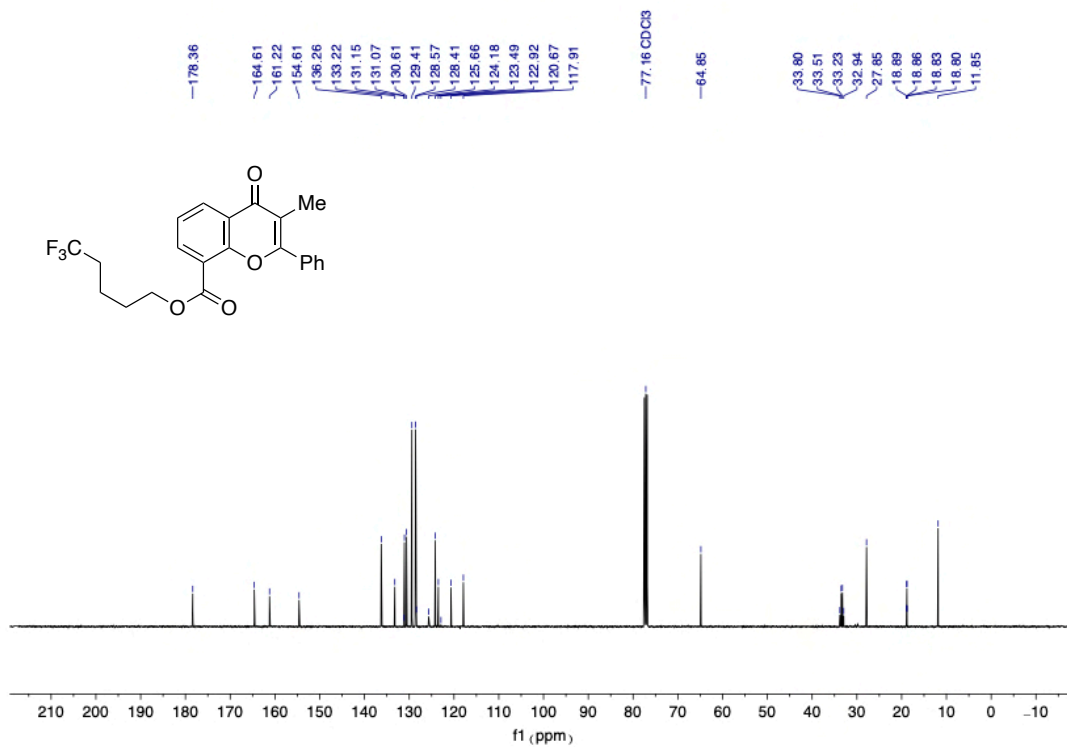


<sup>1</sup>H NMR (400 MHz, CDCl<sub>3</sub>) of **65**

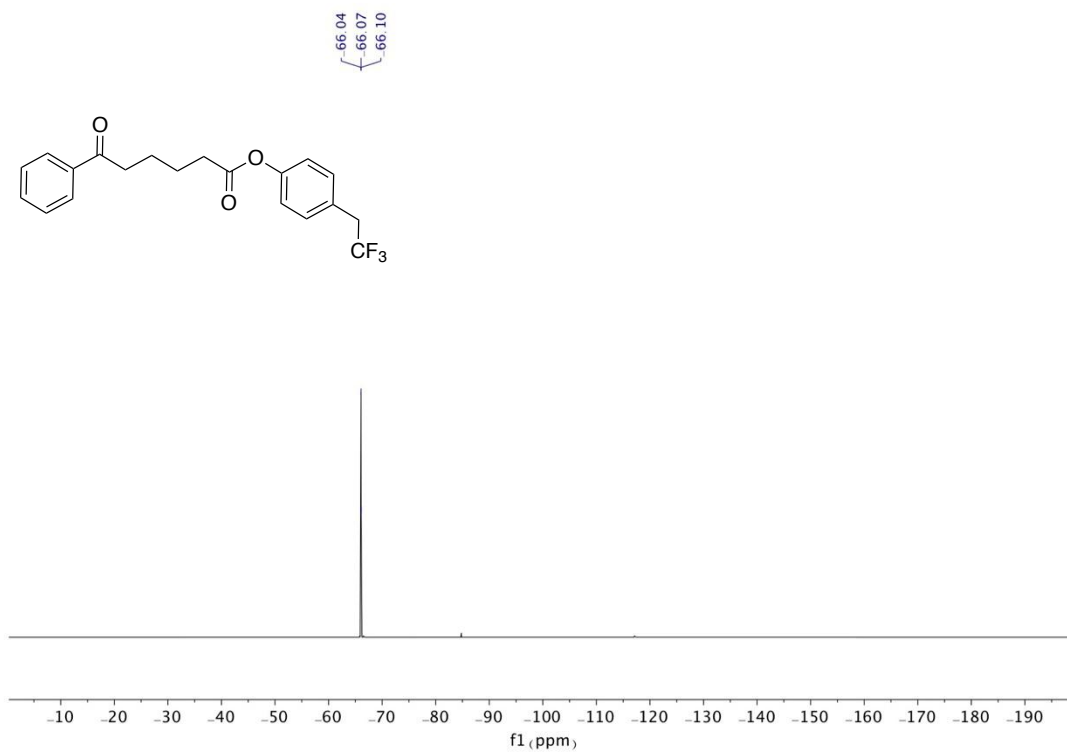


<sup>13</sup>C NMR (101 MHz, CDCl<sub>3</sub>) of **65**

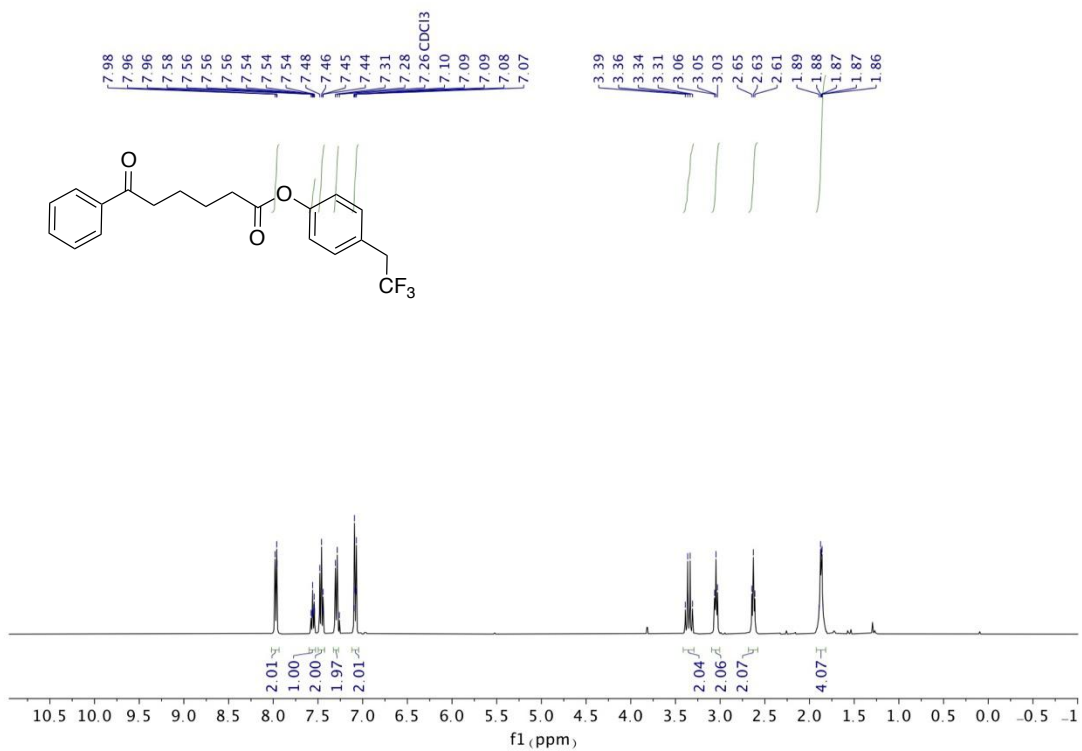




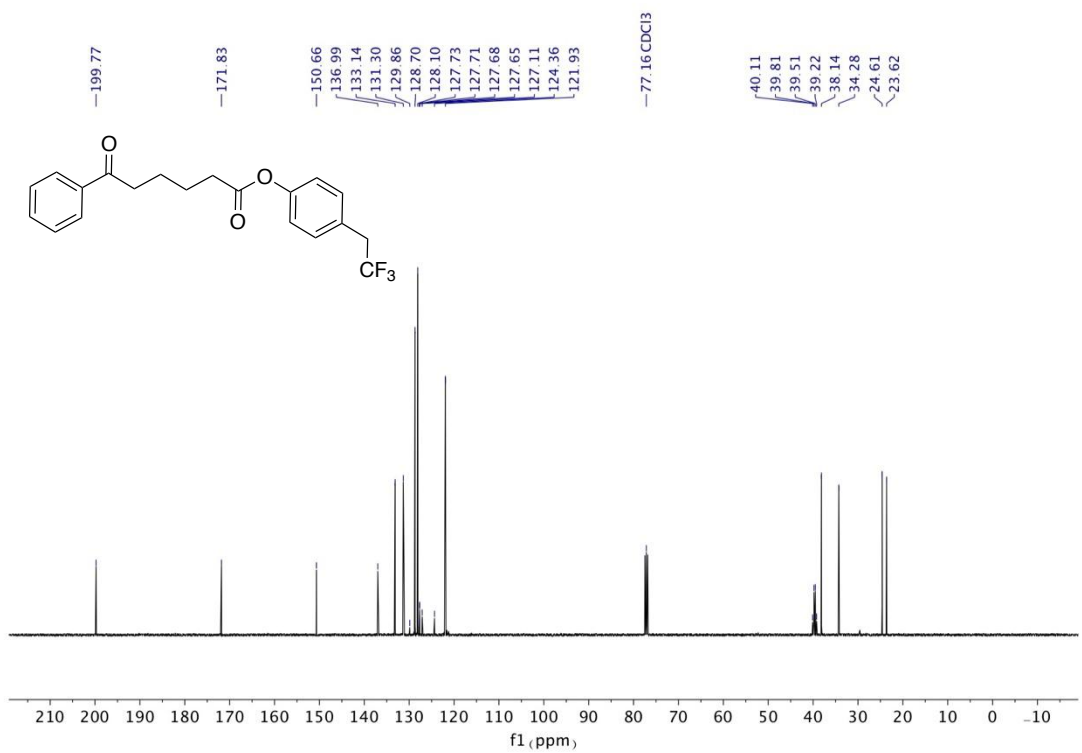
<sup>13</sup>C NMR (101 MHz, CDCl<sub>3</sub>) of **66**



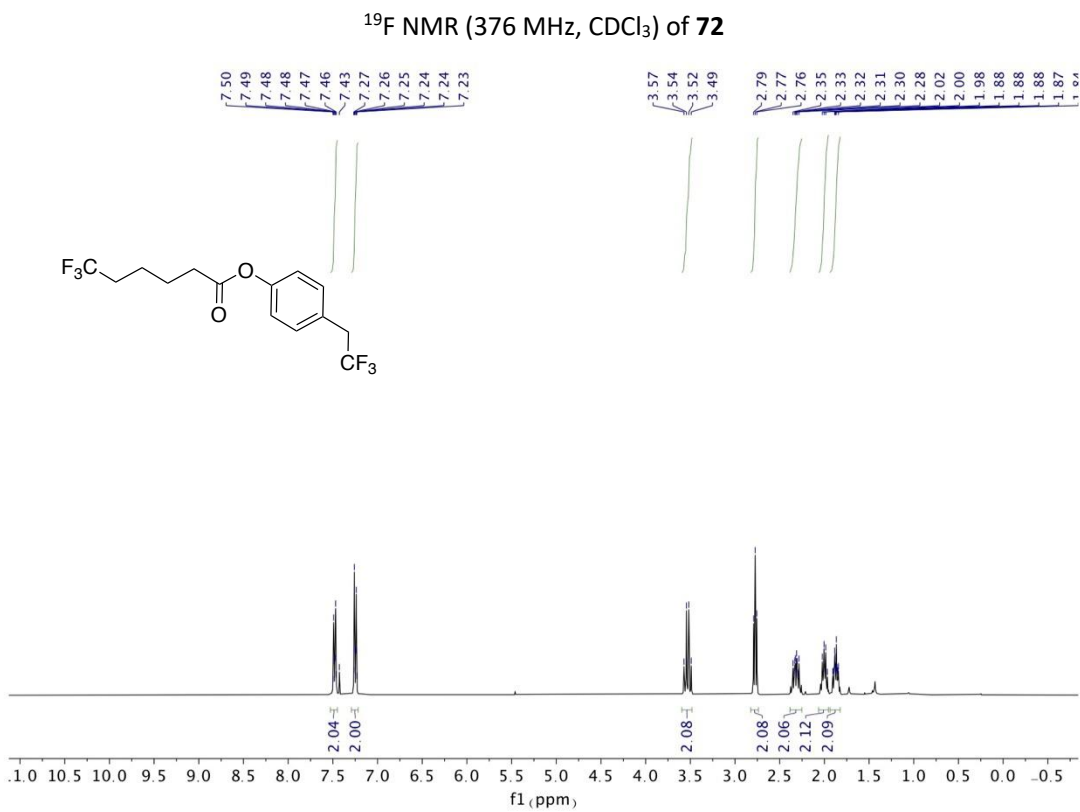
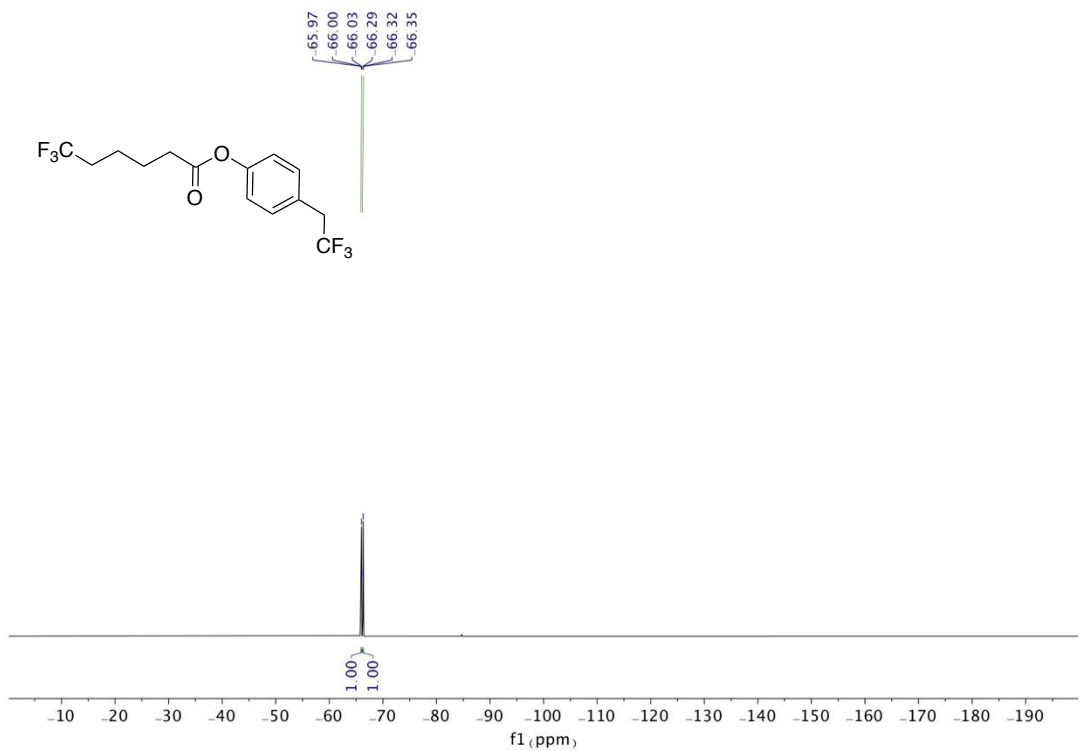
<sup>19</sup>F NMR (376 MHz, CDCl<sub>3</sub>) of **71**

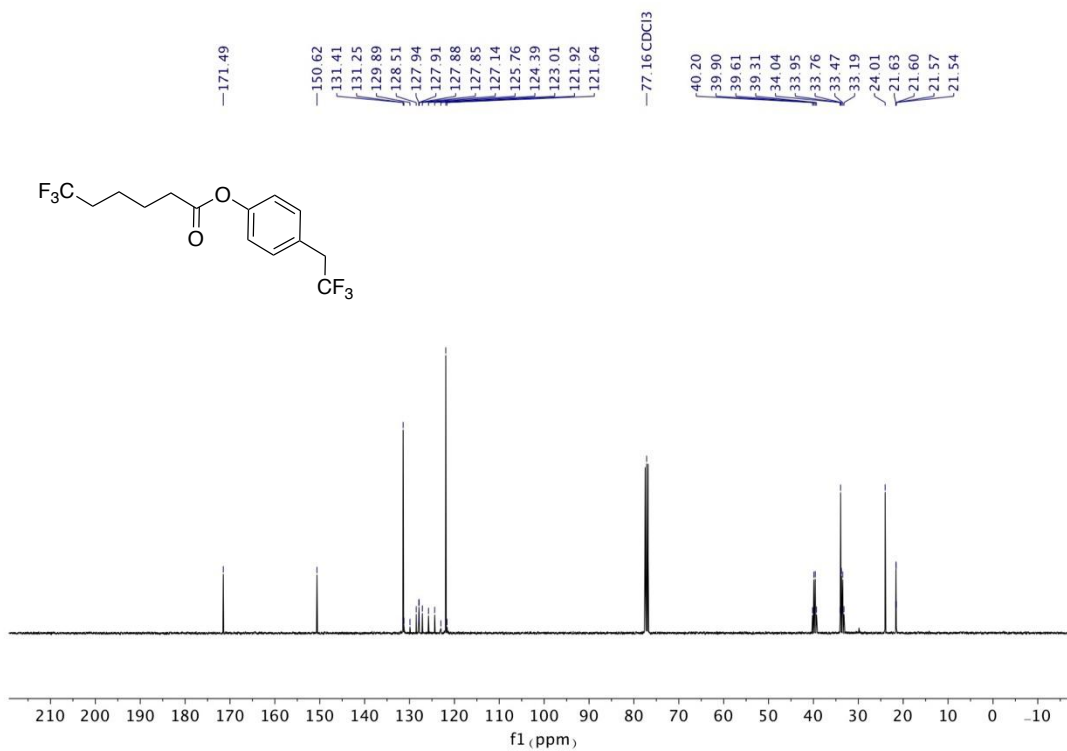


**<sup>1</sup>H NMR (400 MHz, CDCl<sub>3</sub>) of 71**



**<sup>13</sup>C NMR (101 MHz, CDCl<sub>3</sub>) of 71**





---

## Chapter 4

### *Nickel-Catalyzed Regio- and Stereoselective 1, 2-Alkylboration of Allenes*

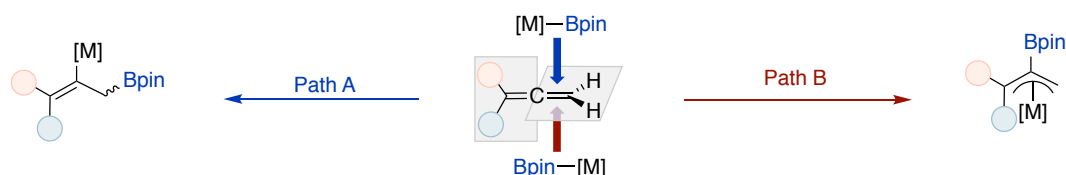




## 4.1 General Introduction

Allenes have attracted the chemical society's continuous attention due to their unique chemical structure containing two cumulative  $\pi$ -bonds with  $sp^2$ -hybridized carbons and a  $sp$ -hybridized central carbon, and the ability of the substituents to display diverse functional groups.<sup>2</sup> Although allenes belong to the same class of unsaturated compounds as alkyne and alkene analogues, their unique orthogonal geometry allows them to exhibit a distinct reactivity. Allenes are more reactive than alkenes and alkynes, allowing for milder and more atom economical transformations and access to more complex chemical structures.<sup>3</sup> In turn, the enhanced reactivity of this highly unsaturated functional group gives rise to regio-, stereo-, and enantioselective issues, which pose great challenges to the use of allenes in chemical research.<sup>4</sup>

The manipulation of allenes through transition-metal catalyzed process plays an important role and have continually offered a series of powerful strategies to create a variety of  $sp^2/sp^3$  C–C bonds.<sup>2c, 2d, 4</sup> For example, metal borylation of orthogonal cumulative  $\pi$ -bonds generates allyl or vinyl metal intermediates (Scheme 4.1), which can subsequently react with a variety of electrophilic coupling partners.<sup>5</sup> Introducing boron functional groups into unsaturated systems via transition metal-catalyzed carboboration has become a bright spot in synthetic chemistry.<sup>6,7</sup>

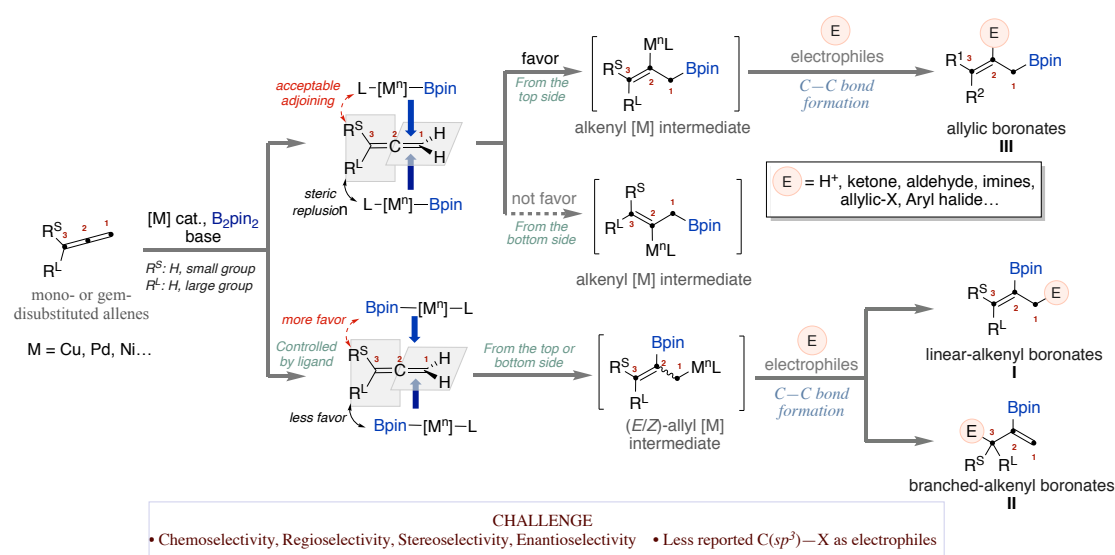


**Scheme 4.1** Metal borylation of allene with orthogonal cumulative  $\pi$ -bonds.

### 4.1.1 Copper Catalyzed 1,2-Carboration Reactions of Allenes

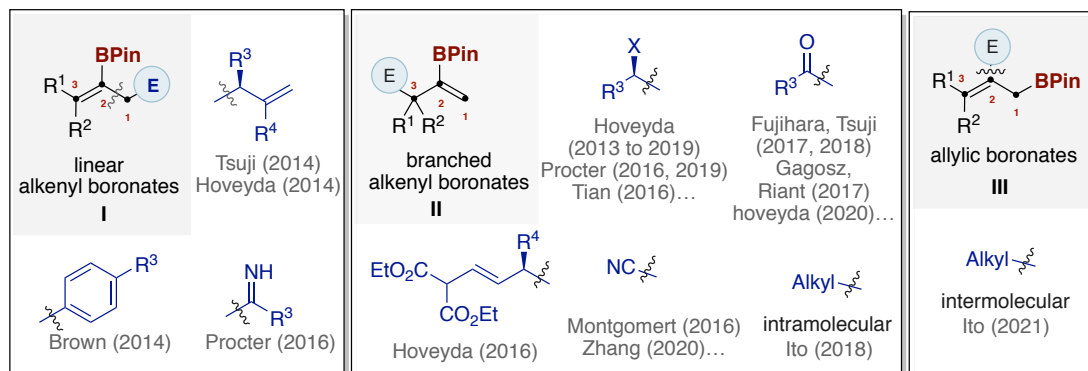
Transition metal-catalyzed three-component coupling reactions among allenes, carbon-electrophilic reagents, and boron sources can provide access to a variety of alkenyl and allyl boronic esters due to the regional and steric divergence of carbon-boration reactions of allenes.<sup>5,6</sup> Typically, the formation of  $[M]$ - $[B]$  intermediates from transition metals  $[M]$  and diboron reagents (i.e.  $B_2pin_2$ ) leads to the insertion of mono- or di-substituted alkenes to generate the associated  $\pi$ -allyl- $[M]$  or  $sp^2$  C- $[M]$  species,

where the regioselectivity present is usually controlled by both substrate and ligand. Among them, the  $\pi$ -allyl-[M] generated in situ by 2,1-boryl metalation is a key intermediate for further reactivity with electrophiles to build  $sp^3$  C–C bonds and to prepare linear chain alkenyl boronic esters **I** or branched chain alkenyl boronic esters **II** (Scheme 4.2). On the other hand, the generation of  $sp^2$  C-[M] intermediates via the 1,2-boron metalation of allenes allows for coupling reactions with the electrophilic reagents, which would be an effective complementary strategy to the synthesis of allyl boronic esters **III**. So far, despite a series of research works on electrophilic reagents for carboborylation of allene systems, the electrophilic trapping reagents for subsequent interception of  $sp^2/sp^3$  C-[M] intermediates mostly focus on the conversion of proton sources, aldehydes, ketones, imines, Michael acceptors, allyl species, aryl halides, or a cyano group.<sup>8</sup> the  $sp^3$ -hybridized alkyl electrophiles combining with C( $sp^3$ )-[M] intermediates in the intermolecular carbonborylation of allenes are still unreported.<sup>9</sup>



**Scheme 4.2** Transition metal-catalyzed 1,2-carboboration of allenes.

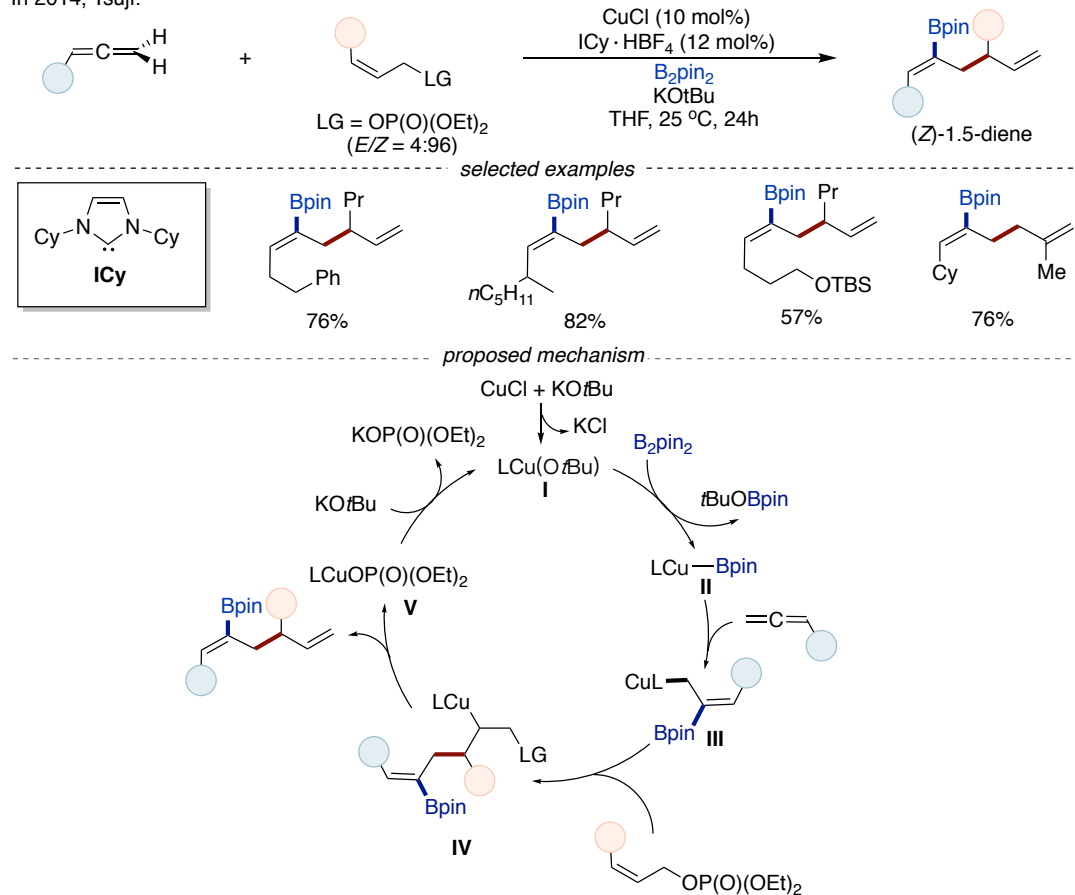
In particular, based on the fact that copper is a cheap, abundant and nontoxic metal, as well as the development of copper-derived nucleophilic intermediates, the pioneering use of organocuprates as coupling partners in organic synthesis has been widely reported (Scheme 4.3).<sup>10</sup> Therefore, Cu-catalyzed 1,2-carboboration reactions of allenes is one of the most attractive strategies for the synthesis of organoboron derivatives.<sup>6, 8, 11</sup>



**Scheme 4.3** Reported examples of copper-catalyzed 1,2-carboboration reactions of allenes.

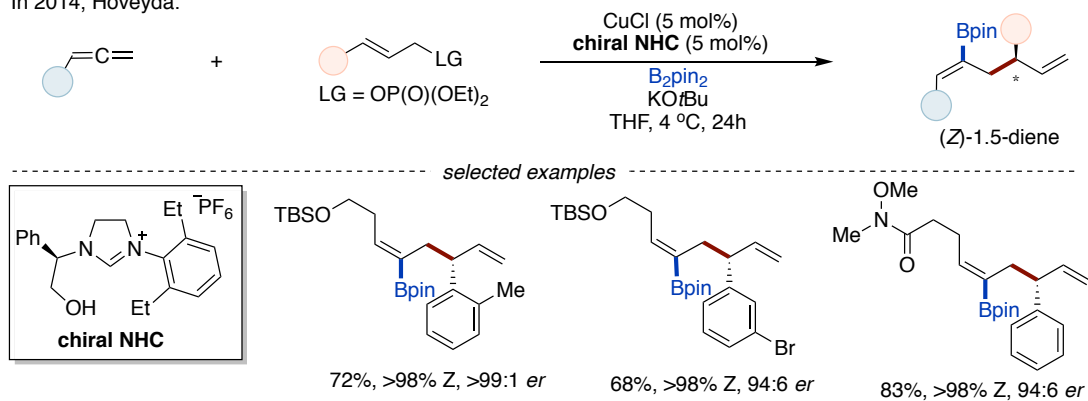
The first type of reactions to be introduced delivered linear alkenyl boronates via a copper-catalyzed 1,2-carboboration of allenes. In 2014, the Tsuji group reported the first borylative allyl-based coupling of allene using B<sub>2</sub>pin<sub>2</sub> and allyl phosphate under copper-NHC catalysis (Scheme 4.4).<sup>6c</sup> This method successfully synthesized boron-substituted 1,5-dienes with excellent stereoselectivity and regioselectivity, which were difficult to obtain by other strategies. Immediately afterwards, Hoveyda and colleagues reported a similar multicomponent catalytic process (Scheme 4.5),<sup>12</sup> but they controlled chemoselectivity, site selectivity, and stereoselectivity while also achieving enantioselectivity by using chiral NHC ligands. This reactivity mode begins with a copper-boron addition to a monosubstituted alkene, and the resulting boron-substituted organocopper intermediates then engage in similar selective allylic substitutions.

In 2014, Tsuji:



**Scheme 4.4** Borylative allyl-based coupling of allenes.

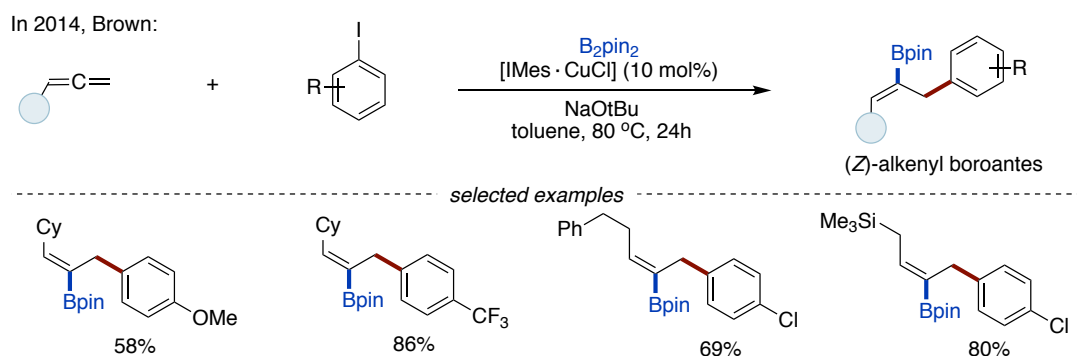
In 2014, Hoveyda:



**Scheme 4.5** Enantioselective allyl-borylation of allenes.

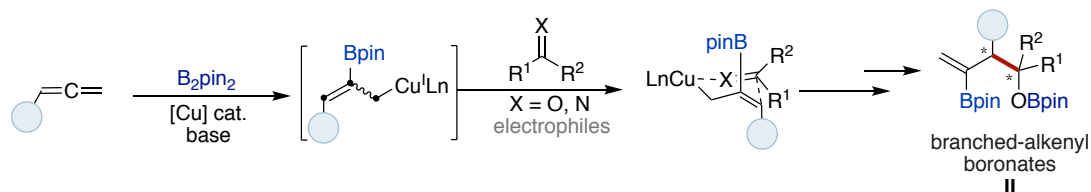
In the same year, Brown's group used [IMesCuCl] as a catalyst and aryl iodides as C(*sp*<sup>2</sup>)-electrophiles to achieve the carboborylation of allenes and the formation of vinyl boronic esters with well-defined stereoselectivity (Scheme 4.6).<sup>13</sup> In this process, the coupling of the resulting allyl copper intermediate with aryl iodide occurs at the least

substituted position, which resulted in the highly selective formation of *Z*-alkenyl borates.



**Scheme 4.6** Carboborylation of allenes by aryl iodides as  $C(sp^2)$ -electrophiles.

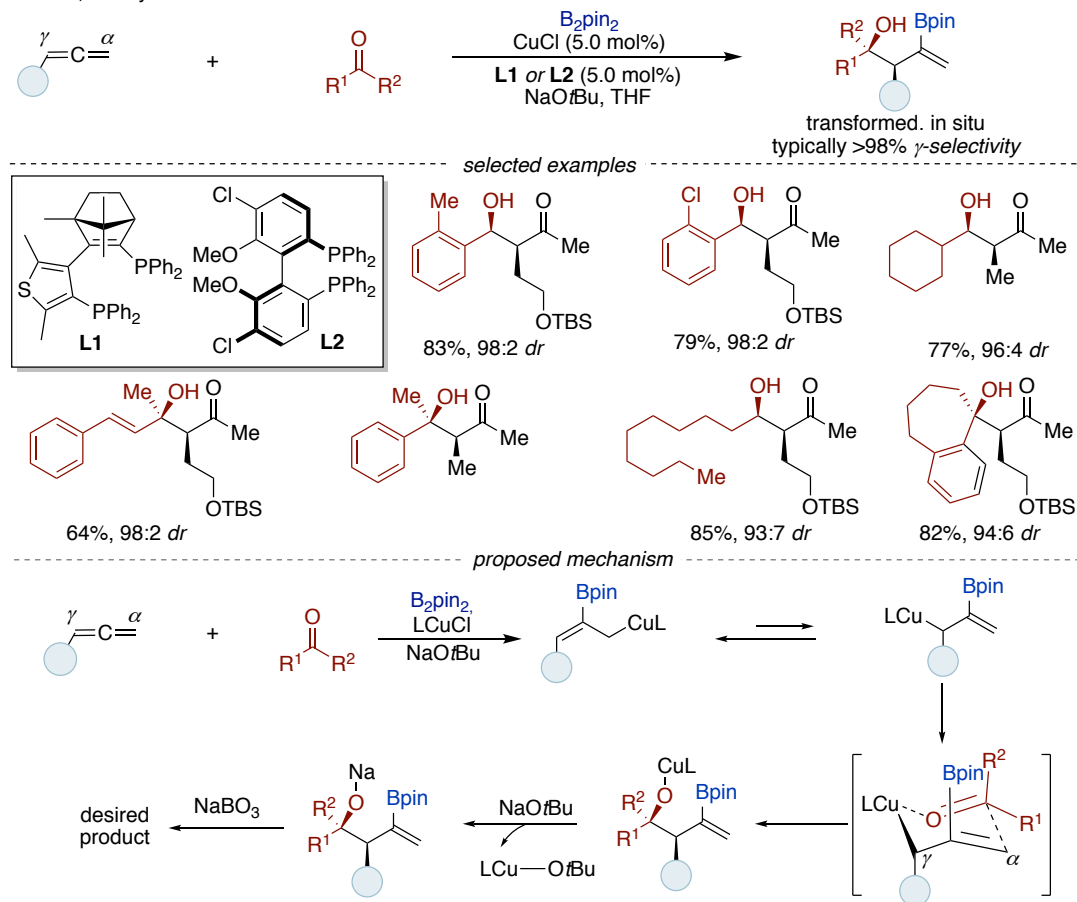
On the other hand, the isomerized allyl copper (I) intermediate can react at its  $\gamma$ -position by pro-metal rearrangement to produce branched alkenyl boronic esters II (Scheme 4.7).<sup>14</sup> Subsequent coupling with electrophiles deliver highly functionalized asymmetric products. In this process, the co-establishment of stereoselectivity and enantioselectivity may arise from the co-interaction of the original allene backbone and the prochiral electrophile with the copper chiral ligand.



**Scheme 4.7** The preparation of prochiral- and branched-alkenyl boronates.

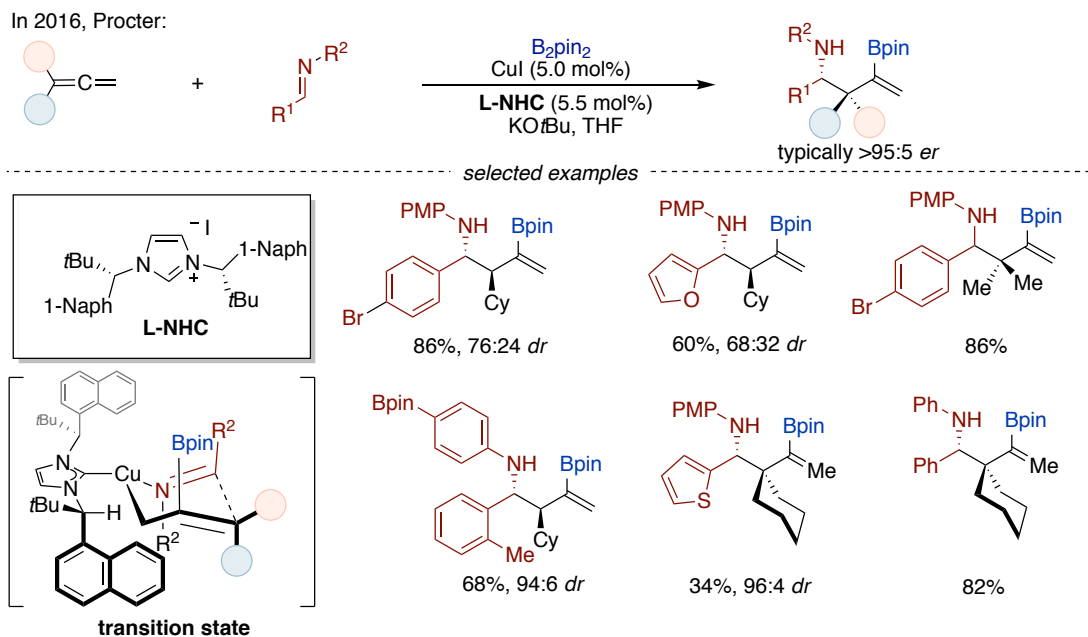
The enantioselective coupling of aldehydes or ketones with mono-substituted allenes and  $B_2pin_2$  was described by Hoveyda and coworkers (Scheme 4.8).<sup>14a</sup> Allyl copper (I) intermediate is trapped with an aldehyde or ketone to produce highly functionalized vinyl boronates, and ketones were added enantioselectively to access tertiary alcohols. Through a hypothesized six-membered transition state structure, where the substituent on the aldehyde is in a pseudoequatorial position, syn-products are generated (Scheme 4.8, *bottom*).

In 2013, Hoveyda:



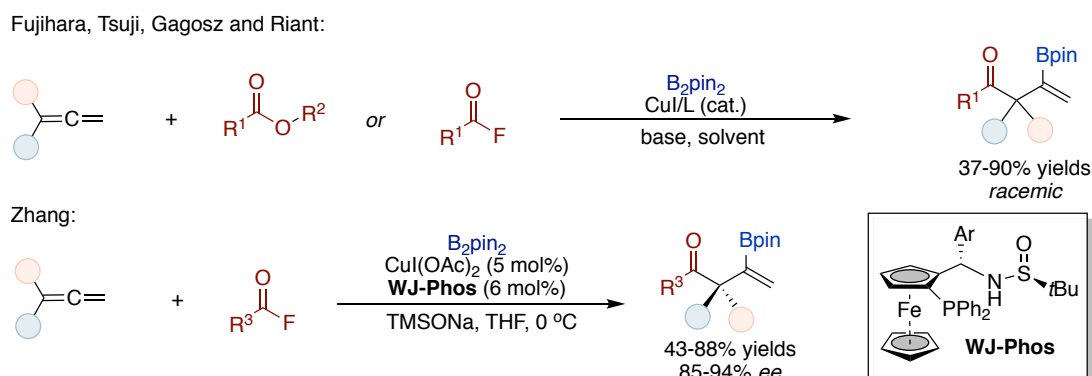
**Scheme 4.8** Cu-catalyzed enantioselective and diastereoselective coupling of allenes with carbonyls.

In 2016, Procter and co-workers reported a strategy using imines as electrophiles, Cu(I)-NHC-catalyzed enantioselective three-component coupling of allenes with excellent functional group tolerance, this reaction brought various allylic amines with adjacent stereocenters (Scheme 4.9).<sup>14b</sup> In addition, the coupling product can be further functionalized by oxidation to form branched  $\beta$ -amino ketones. Here, the branched alkenyl boronic esters produced may also proceed from the addition of allyl copper to imine through a preferred chair-like transition state, where the orientation of the substituent on the imine in a pseudoaxial position is simultaneously modulated by the chiral ligand.



**Scheme 4.9** Cu-catalyzed enantioselective and diastereoselective coupling of allenes with imines.

In recent years, several groups such as Fujihara,<sup>14g</sup> Tsuji,<sup>6g</sup> and Riant<sup>15</sup> have independently reported elegant Cu-catalyzed three-component borylations reacting with different acylation reagents on 1,1-disubstituted alkenes, which provided an accessible way to form  $\beta$ -boronyl- $\beta$ , $\alpha$ -unsaturated ketones with chiral quaternary stereocenters (Scheme 4.10). Subsequently, Cu-catalyzed enantioselective boronylation of 1,1-disubstituted malondienes was also investigated.



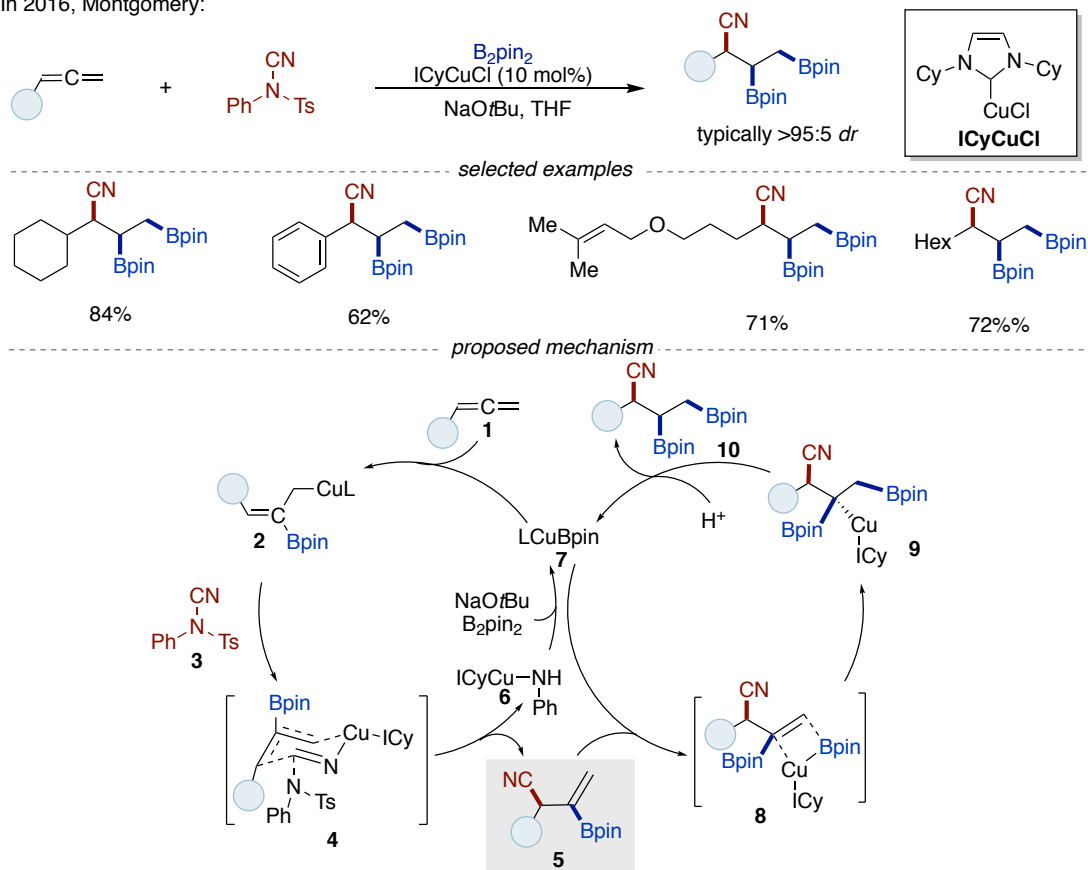
**Scheme 4.10** Copper-catalyzed boroacylation of 1,1-disubstituted allenes.

In 2016, Montgomery reported an example of diastereo- and regioselective copper-catalyzed trifunctionalization of terminal allenes using *N*-cyano-*N*-phenyl-p-tosylbenzene sulfonamide as the electrophile for cyanation (Scheme 4.11).<sup>14f</sup> In this



reaction, the initial borocupration of allene produced an allyl copper intermediate (**2**) which is subsequently cyanated to afford intermediate (**5**) capable of being borylated and protonated to give the trifunctionalized product (**10**).

In 2016, Montgomery:

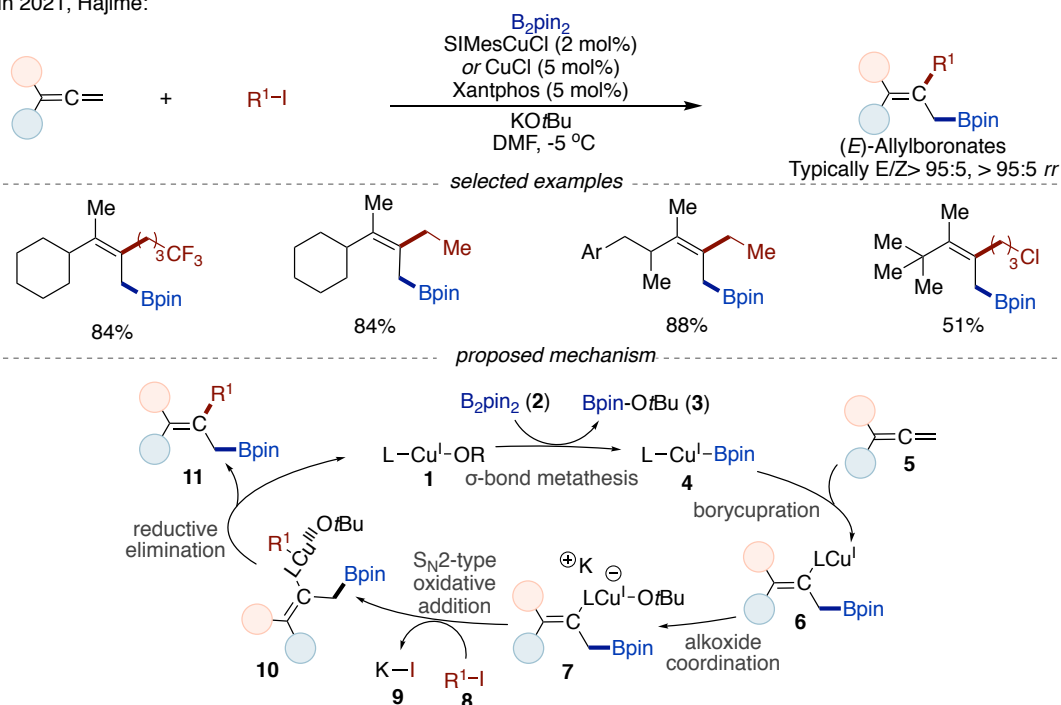


**Scheme 4.11** Copper-catalyzed trifunctionalization of using allenes *N*-cyano-*N*-phenyl-*p*-tosylbenzene sulfonamide as the electrophile.

Although these methods described above demonstrate the impressive array of allene functionalization that can occur under copper catalysis through the formation of allyl copper intermediates in combination with different electrophilic reagents, these methods are still limited to the construction of  $sp^3$  hybridized carbon sites based on allene functionalizations, particularly with alkyl halides as electrophilic reagents.<sup>16</sup> It was not until 2021 that the Hajime group reported the first copper catalyzed regioselective and stereoselective intermolecular three-component coupling reaction to synthesize spatially crowded allylboronates by using alkyl halides as electrophiles and gem-dialkylallenes as substrates (Scheme 4.12).<sup>17</sup> It is a challenging reaction, which achieves high chemoselectivity of the boryl copper (I) intermediate for the carbofunctionalization of allene rather than the alkyl-electrophiles, as well as regioselectivity

and stereoselectivity for alkylation of allenes. Mechanistically, the in situ formation of the copper(I) alkoxide (**1**) from  $\text{Cu}^{\text{I}}\text{Cl}$  and  $\text{KO}t\text{Bu}$  first undergoes a  $\sigma$ -bond metathesis with  $\text{B}_2\text{pin}_2$  to form the boronic copper (I) intermediate (**4**). Coordination and borylcupration of allene (**5**) with intermediate (**4**) provides the alkenyl copper(I) species (**6**). The copper(I) center in intermediate (**6**) coordinates with the alkoxide to generate cuprate species (**7**). The nucleophilic cuprate species (**7**) undergoes  $\text{S}_{\text{N}}2$ -type oxidative addition with alkyl iodides (**8**) to form the organocopper (III) intermediate (**10**). The final reductive elimination of the higher valent copper (III) species (**10**) produces the alkylation product (**11**), while the resulting reductive copper (I) alkoxide (**1**) completes the catalytic cycle.

In 2021, Hajime:



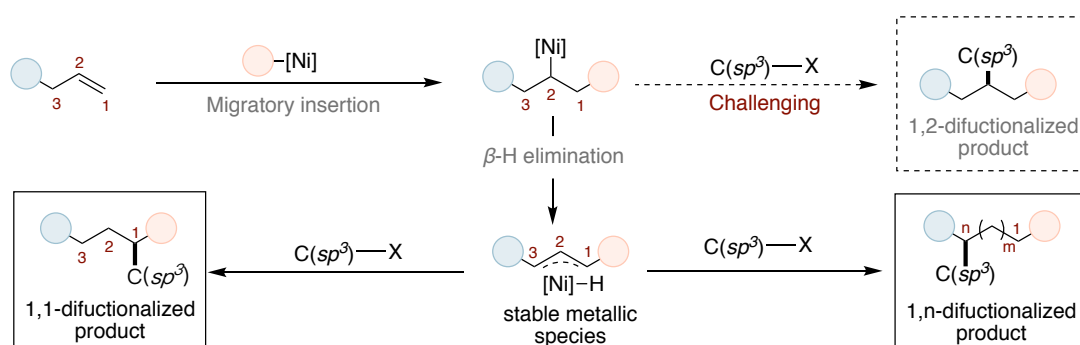
**Scheme 4.12** Copper-catalyzed regioselective and stereoselective intermolecular 1,2-alkylboronation to form allylboronates.

#### 4.1.2 Nickel-Catalyzed Alkylation of Unsaturated C–C Bond

In recent years, the study of nickel catalysis has shown new prospects in the field of cross-coupling reactions and has received much attention from chemists, not only because of its lower cost compared to other transition metals, but also because of its unique reaction mode.<sup>18</sup> Particularly, nickel catalysts have shown strong reactivity and

selectivity in the construction of more challenging bonds of  $sp^3$  hybridized carbon, making alkyl reagents suitable cross-coupling partners in nickel-catalyzed reactions.<sup>19</sup>

In the reaction of nickel-catalyzed 1,2-alkylboration of unsaturated systems, the migration and insertion of nickel-boron species into  $\pi$ -bonds to form  $\sigma$ -alkyl organometallic intermediates is a key step.<sup>20</sup> Among them, interception of organonickel intermediates and inhibition of  $\beta$ -hydride elimination are the main challenges to achieve 1,2-alkylboration of unsaturated C–C bonds. In particular, the construction of C( $sp^3$ )–C( $sp^3$ ) bonds using alkyl halides as electrophiles is still yet to be accomplished (Scheme 4.13).<sup>21</sup> Mechanistically,  $\beta$ -hydride elimination occurs more rapidly than the interception of organonickel intermediates by alkyl electrophiles, then rapid  $\beta$ -hydride elimination and migratory reinsertion will readily occur, resulting in the formation of a new stable nickel complex. Alkyl halides are then bonded to provide 1,1- or 1, $n$ -alkylboronated products.<sup>21a</sup>

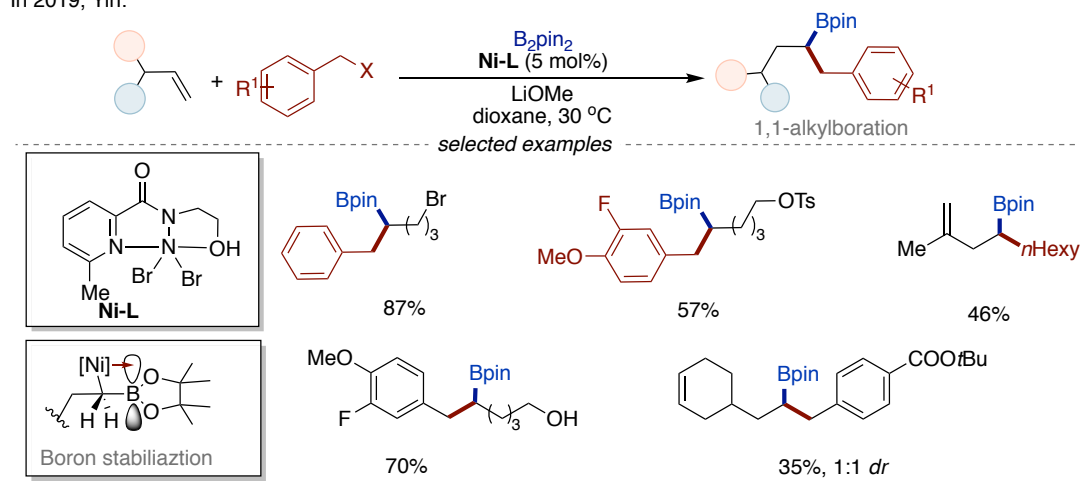


**Scheme 4.13** Nickel-catalyzed alkylation of unsaturated C–C bonds.

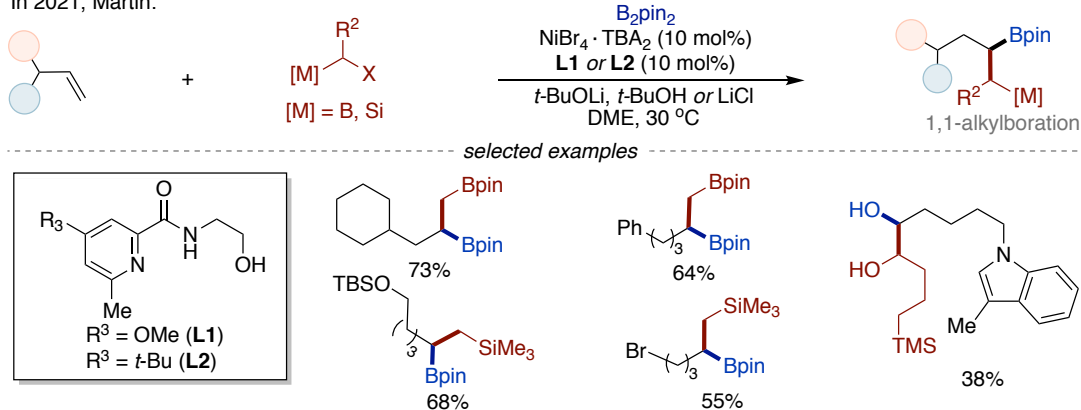
In 2019, the Yin group reported the Ni-catalyzed three-component 1,1-alkylboration of unactivated alkenes with benzyl bromides (Scheme 4.14, *top*).<sup>22</sup> The unusual selectivity of the 1,1-alkylboration reaction was found to be dependent on the use of a ligand based on the type of pyridylcarboxamide coordinated with nickel catalyst. Notably, the directing groups are not necessary for the strong regioselectivity of this work, because the final  $\alpha$ -boron alkyl-nickel species generated after migration is more stable than the secondary alkyl-nickel species in situ, due to a Lewis acid-base interaction metal-boron that the unpaired electrons in the d-orbital of nickel could leave the domain to the empty p orbitals of the adjacent boron atom.<sup>21a</sup> This method generates secondary aliphatic boronic esters from unactivated terminal alkenes and benzyl bromides. Immediately after, our group followed the Yin group to develop a nickel catalyzed 1,1-difunctionalization of unactivated olefins to generate  $sp^3$  bis-

organometallics bearing both B and Si motifs with ambiphilic  $\alpha$ -haloboranes (Scheme 4.14, *bottom*).<sup>23</sup>

In 2019, Yin:



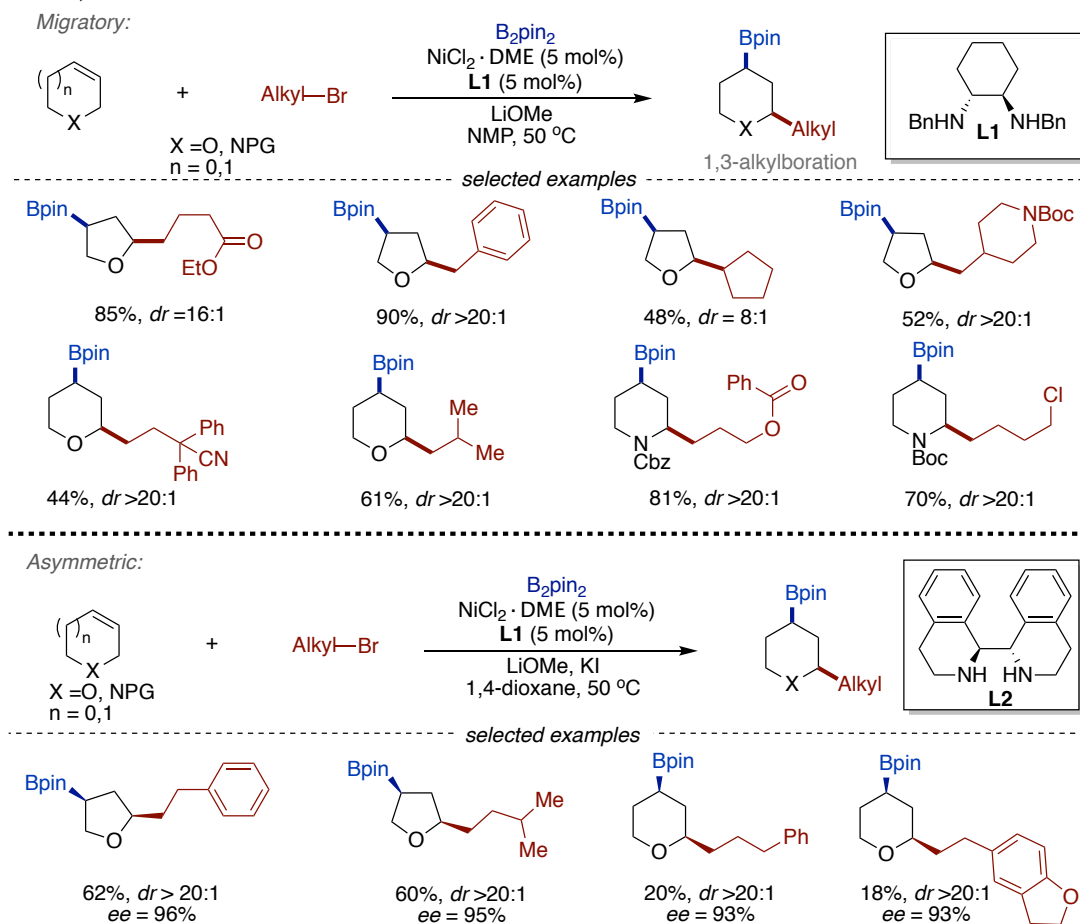
In 2021, Martin:



**Scheme 4.14** Nickel-catalyzed 1,1-alkylboration of alkenes.

In 2021, Yin's group developed a modular platform for the synthesis of 2,4-disubstituted heterocycles from readily available materials via nickel-catalyzed migrating alkylboronization in a high diastereoselectivity (Scheme 4.15, *top*).<sup>24</sup> Numerous stereospecific diversifications of the borylation product and a high functional group tolerance were described. When ligand **L2** is used instead of **L1**, the excellent enantioselectivity is expressed along with the completion of the migrating alkylborylation (Scheme 4.15, *bottom*). According to preliminary mechanistic studies, reductive elimination from the organonickel intermediate, rather than a two-electron nucleophilic substitution pathway, is essential for the stereochemistry of the C–C bond formation process.

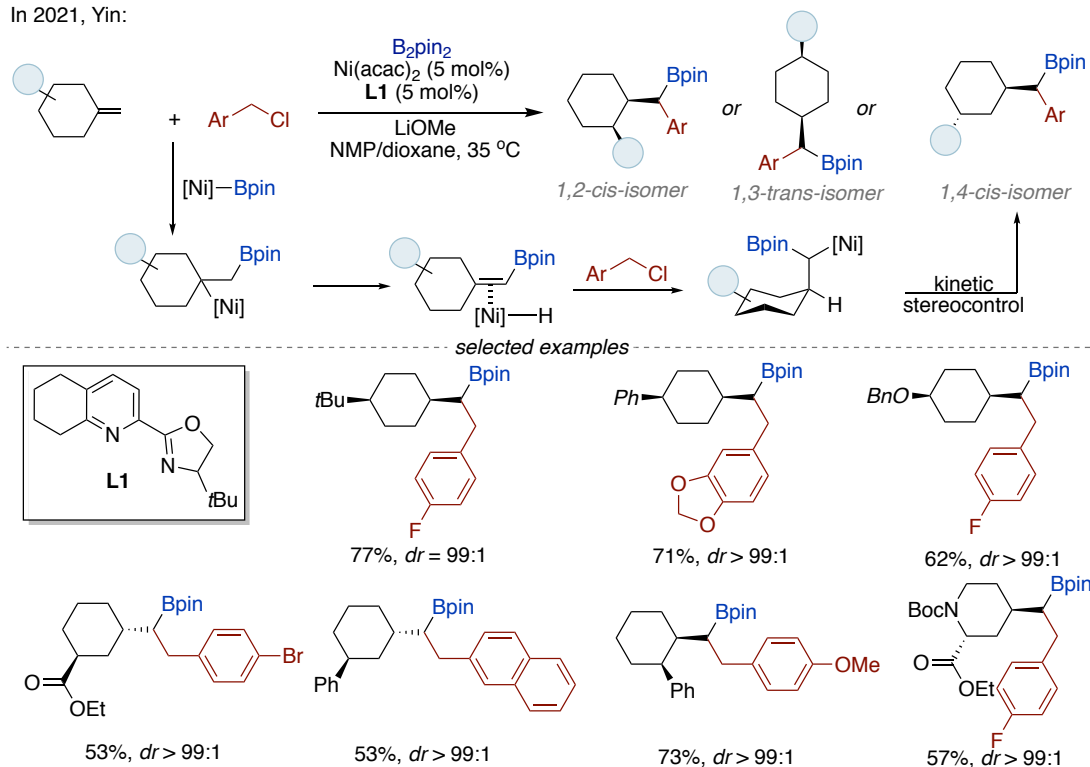
In 2021, Yin:



**Scheme 4.15** Nickel-catalyzed 1,3-alkylboration of heterocyclic alkenes.

Recently, Yin and his colleagues disclosed again a Ni-catalyzed three-component 1,1-alkylboronation reaction to synthesize thermodynamically disfavored disubstituted cyclohexanes from readily available methylene cyclohexanes,  $\text{B}_2\text{pin}_2$  and benzyl halides via a chain-walking manner (Scheme 4.16).<sup>25</sup> Conventional cross-coupling methods normally tend to synthesise thermodynamically stable stereoisomeric cyclohexyl derivatives. However, this strategy modularizes the control of stereochemistry through the boron ester group adjacent to the cyclohexane for excellent kinetic stereocontrol. At the same time, the late-stage functionalization of complex bioactive compounds demonstrates the synthetic potential of this strategy.

In 2021, Yin:



**Scheme 4.16** Nickel-catalyzed 1,1-alkylboronation of methylene cyclohexanes.

Although nickel-catalyzed 1, n ( $n = 1, 3$ ) -regioselective alkylboronations of alkenes are well developed, their difunctionalization of unsaturated systems other than olefins remains relatively unstudied. In terms of the strategies developed to control the generation of stabilized organic nickel intermediates by substrate structure is the key to alkylboronation with non-activated alkyl halides as electrophilic reagents. Taking advantage of this core and the property of nickel-catalyzed alkyl halides via single electron transfer under related ligand control, further development of new transformations is to be expected.

---

## 4.2 General Aim of the Project

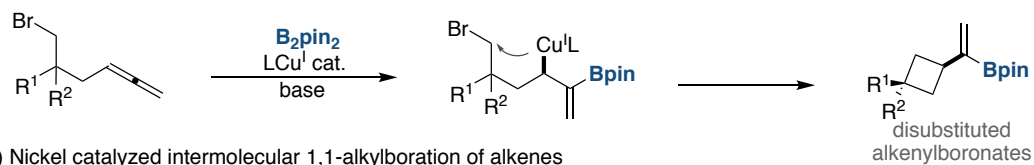
The strategy of transition metal-catalyzed difunctionalization to introduce boron functional groups into unsaturated systems has become a highlight of synthetic chemistry. In particular, metal boryl functionalization from orthogonal cumulative  $\pi$ -bonds of allene to generate alkenyl borates has been developed as well. However, the use of alkyl halides as electrophilic reagents for the construction of  $sp^3$  hybridized carbon centers to forge polysubstituted alkenyl borates has yet to be developed, where polysubstituted alkenyl borates have the potential to continue to expand the conversion of  $sp^2$  C–B bonds to a variety of other functional groups.

To create the regio- and stereoselective polysubstituted olefins is still a big challenge in the field of synthetic organic chemistry.<sup>26</sup> To date, most approaches to building alkenylborates have focused on end-shaped alkenylborates, or *E*-alkenylborates. For example, 1) transition-metal-catalyzed cross-coupling from alkenyl halides, triflates or silanes to provide end-shaped alkenylboronates;<sup>27</sup> 2) hydroboration of alkynes is the common method for the synthesis of *E*-alkenylboronates.<sup>28,29</sup> However, methods for the construction of *Z*-polysubstituted alkenyl borates have rarely been reported.<sup>30</sup>

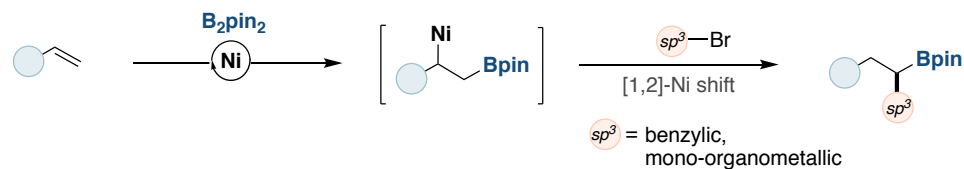
Metal-catalyzed cross-coupling reactions of  $sp^3$  mono-organometallic reagents have reached remarkable levels of sophistication as vehicles to rapidly build up  $sp^3$  architectures<sup>31</sup> Based on our group's interest in forging  $sp^3$  linkages with amphiphilic  $\alpha$ -haloborane reagents, we wondered whether it was possible to build polysubstituted alkenylborates via 1,2-alkylborylation of allenes as a platform, and  $sp^3$  mono-organometallic motifs can be simultaneously introduced into the alkenylboronates as a side chain to enrich the molecular structure (Scheme 4.17).

■ Previous work:

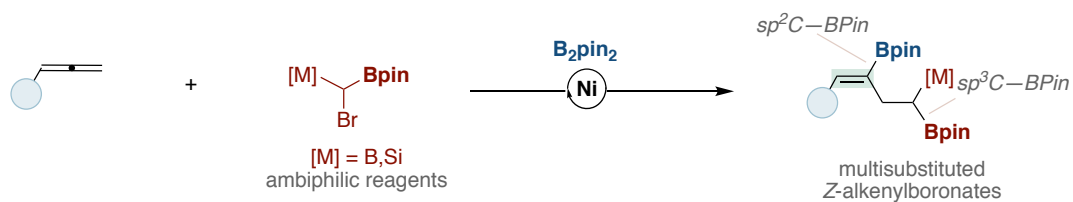
1) Intramolecular 1,2-alkylboration of allenes via allylcopper(I) isomerization



2) Nickel catalyzed intermolecular 1,1-alkylboration of alkenes



■ This chapter: Nickel catalyzed intermolecular 1,2-alkylboration of allenes



➤ highly chemo, regio-, and stereoselective carboboration

➤ 1,3-bisorganometallic compounds

**Scheme 4.17** Alkylboration of unsaturated moieties.



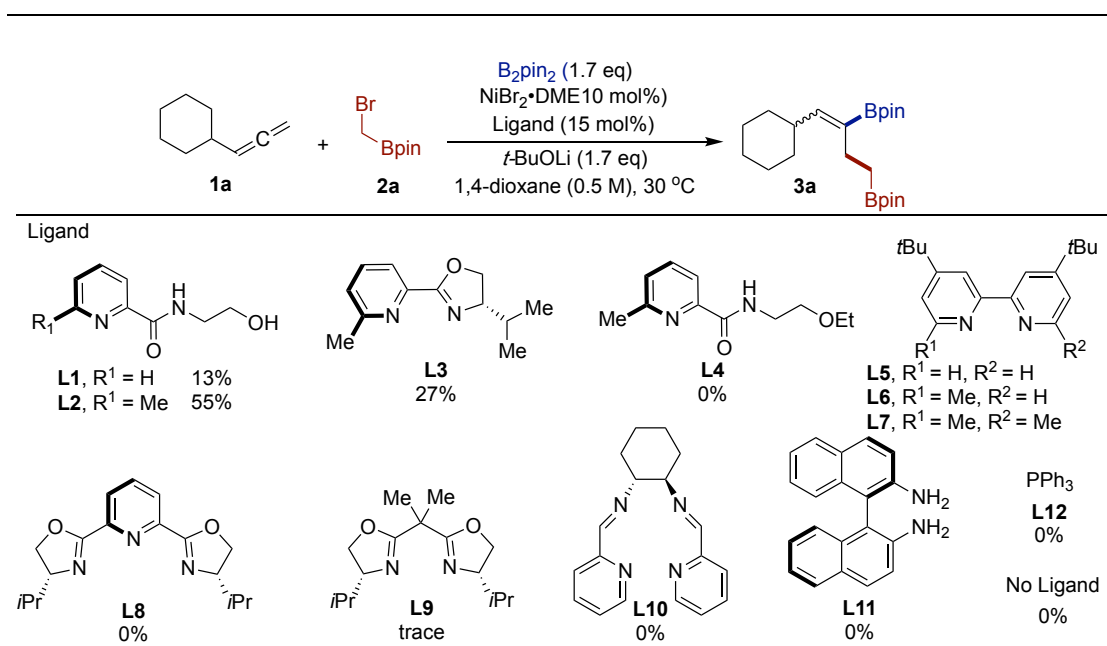
---

## 4.3 Nickel-Catalyzed Regio- and Stereoselective 1,2-Alkylboration of Allenes

### 4.3.1 Optimization of the Reaction Conditions

#### 4.3.1.1 Optimized conditions of $\alpha$ -haloborane reagents as electrophiles

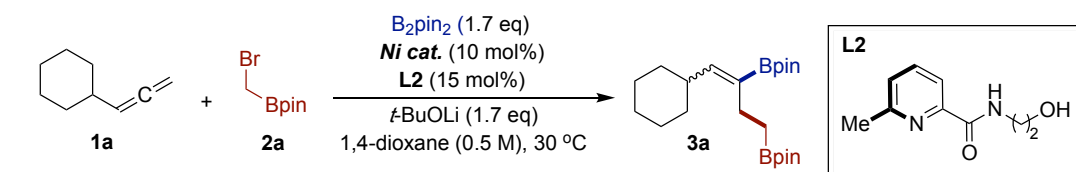
Inspired by our group's work in the catalytic 1,1-alkylboration of unactivated olefins leading to the preparation of  $sp^3$ -bis-organometallic B, B(Si) reagents,<sup>23</sup> we began our work by borrowing the catalytic mode and reaction conditions of previous studies. Initially, we investigated using the readily available propa-1,2-dien-1-ylcyclohexane (**1a**) as the model substrate, the most common Bis(pinacolato)diboron ( $B_2pin_2$ ) as a boron source, and the primary 2-(bromomethyl)-4,4,5,5-tetramethyl-1,3,2-dioxaborolane (**2a**) as an  $\alpha$ -haloborane reagent, since **2a** is readily available on a large scale through Matteson reaction. Using  $NiBr_2 \cdot DME$  as a nickel pre-catalyst, we firstly examined a large number of different types of ligands, which play a crucial role in nickel-catalyzed cross-coupling reactions. As table 4.1 shown, the use of **L1-L3** type bidentate nitrogen-ligands provided better results, while other types of ligands such as bipyridine ligands, Oxazoline ligands, PyrOx ligands and other diamine-based ligands were unsuccessful, obtaining no conversion of the starting material allene. No reactivity was obtained under reaction conditions with electron-rich phosphine ligands (**L12**) or without the addition of ligands. Notably, comparing the structures of the ligands **L1**, **L2**, and **L4**, *N*-(2-hydroxyethyl)-6-methylpicolinamide (**L2**) was identified as the best ligand for this reaction system. It can be seen that the methyl group at the 6-position and the hydroxyl functional group in the type of pyridylcarboamide ligand are very important. A gain in the stability of alkyl-Ni intermediates against  $\beta$ -hydride elimination could be a reasonable explanation for the requirement of ortho substituted-ligands. The effect of steric hindrance of the substituents distorts the geometry and hinders the co-planar rearrangement between the metals and the  $\sigma$  C-H bonds. From the result of ligand **L4**, it is presumed that the hydroxyl group would interact with the nickel center in a corresponding coordination.



Conditions: <sup>a</sup> **1a** (0.10 mmol, 1.0 equiv), **2a** (0.2 mmol, 2.0 equiv), NiBr<sub>2</sub>·DME (10 mol%), Ligand (15 mol%), *t*-BuOLi (0.17 mmol, 1.7 equiv), 1,4-dioxane (0.2 mL), 30 °C, 15 h. <sup>b</sup> Yields were determined by GC FID, using 1-decane as the internal standard.

**Table 4.1** Screening of different types of ligands.<sup>a</sup>

Subsequent investigation of the nickel pre-catalysts in combination with **L2** showed that NiBr<sub>2</sub>·DME was optimal. Zero-valent nickel (Table 4.2, entry 4) didn't give the desired product, which means the reaction was not initiated by Ni<sup>0</sup>. By separation analysis assay, we obtained a small amount of side products from the addition of two molecules of amphiphilic  $\alpha$ -haloboranes (**2a**) to allene under this condition, which is speculated that alkyl borane radicals from **2a** perform radical addition to allenes. Some of the divalent nickel pre-catalysts may also not exhibit the expected reactivity due to solubility.

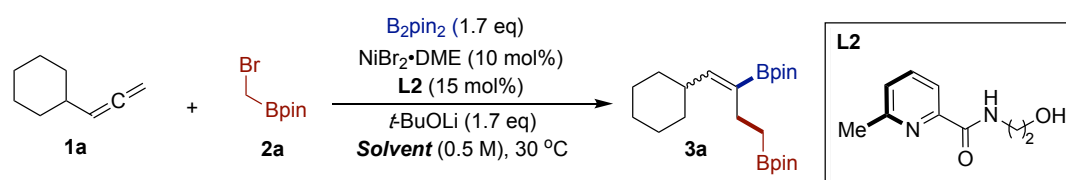


Entry	Ni cat.	Con. (%)	<b>3a</b> Yield (%) <sup>b</sup>
<b>1</b>	<b>NiBr<sub>2</sub>·DME</b>	<b>78</b>	<b>58</b>
2	NiBr <sub>2</sub> ·diglyme	74	55
3	NiCl <sub>2</sub> ·DME	78	49
4	Ni(COD) <sub>2</sub>	13	0
5	NiI <sub>2</sub>	6	0
6	Ni(acac) <sub>2</sub>	66	45
7	NiBr <sub>2</sub> (TBAB) <sub>4</sub>	11	0
8	NiCl <sub>2</sub> ·6H <sub>2</sub> O	8	0
9	NiCl <sub>2</sub> (PPh <sub>3</sub> ) <sub>2</sub>	63	44
10	No Ni cat.	0	0

Conditions: <sup>a</sup> **1a** (0.10 mmol, 1.0 equiv), **2a** (0.2 mmol, 2.0 equiv), Ni cat. (10 mol%), L2 (15 mol%), *t*BuOLi (0.17 mmol, 1.7 equiv), 1,4-dioxane 0.2 mL), 30 °C, 15 h. <sup>b</sup> Yields were determined by GC FID, using 1-decane as the internal standard.

**Table 4.2** Screening of nickel pre-catalysts.<sup>a</sup>

To assess the solubility of the nickel catalyst and other reagents, we replaced 1,4-dioxane with other solvents (Table 4.3), but 1,4-dioxane still showed relatively good results. We further tried changing the concentration of the reaction system, although the solubility state of the inorganic base and B<sub>2</sub>pin<sub>2</sub> dissolved improved under dilute conditions, the effect of reaction was still better under concentrated conditions, we proposed the high concentration is benefited to the step of transmetalation between B<sub>2</sub>pin<sub>2</sub> and Ni(L).

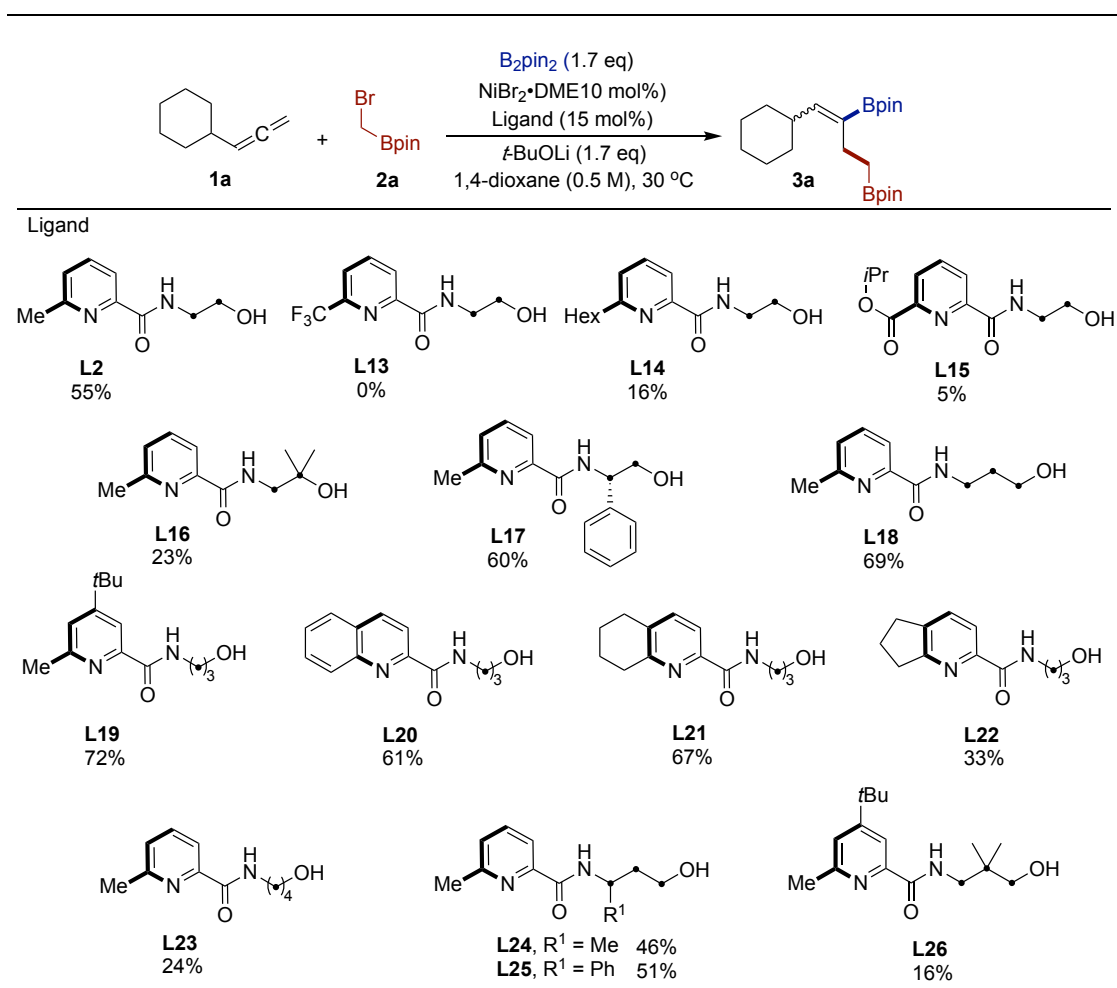


Entry	Solvent	<b>3a</b> Yield (%) <sup>b</sup>
1	<b>1,4-dioxane</b>	<b>57</b>
2	1,3-dioxane	42
3	EA	43
4	DME	10
5	THF	trace
6	DMA	0
7	CH <sub>3</sub> CN	15
8	DCM	8
9	1,4-dioxane (1.0 M)	55
10	1,4-dioxane (0.2 M)	28

Conditions: <sup>a</sup> **1a** (0.10 mmol, 1.0 equiv), **2a** (0.2 mmol, 2.0 equiv), NiBr<sub>2</sub>·DME (10 mol%), **L2** (15 mol%), *t*-BuOLi (0.17 mmol, 1.7 equiv), solvent (0.2 mL), 30 °C, 15 h. <sup>b</sup> Yields were determined by GC FID, using 1-decane as the internal standard.

**Table 4.3** Screening of solvents.<sup>a</sup>

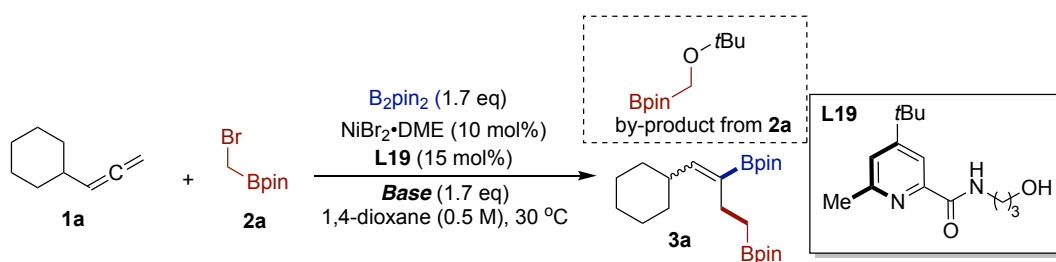
Next, we focused on modifying and tuning the structure of pyridylcarboamide based- to further improve reaction yields (Table 4.4). Based on the structure of **L2**, we first modified the structure of the hydroxyethyl group on the amide chain, with a positive correlation when increasing the length of the carbon chain (**L18**). On the other hand, the modification of the the carbon chain structure on hydroxyethyl group was found to affect the yield (**L16**, **L17**, **L24-L26**). Delightfully, a subtle change in the electrical properties of the pyridine moiety (**L19**) afforded a 72% yield.



Conditions: <sup>a</sup> **1a** (0.10 mmol, 1.0 equiv), **2a** (0.2 mmol, 2.0 equiv), NiBr<sub>2</sub>·DME (10 mol%), Ligand (15 mol%), *t*-BuOLi (0.17 mmol, 1.7 equiv), 1,4-dioxane (0.2 mL), 30 °C, 15 h. <sup>b</sup> Yields were determined by GC FID, using 1-decane as the internal standard.

**Table 4.4** Modification of the structure of pyridylcarboamide based-ligands.<sup>a</sup>

The role of bases was evaluated, we explored different types of bases and different alkalinity (Table 4.5). Lithium ions could promote the reaction well, and the yield can get 72% with the addition of LiOtBu as a strong base and weak nucleophilicity. Considering the relationship between the basicity and the nucleophilicity of the base, in order to avoid the formation of by-products of the nucleophilic attack of the base on **2a**, a weakly nucleophilic base with strong hindrance is favorable.

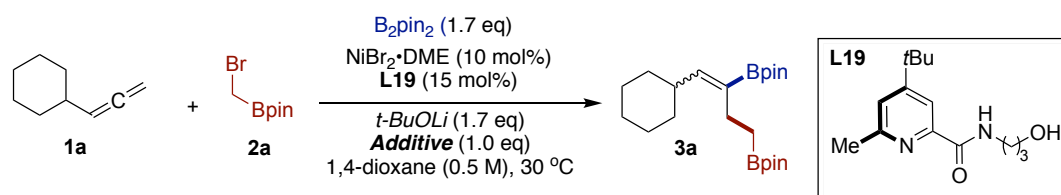


Entry	Base	Con. (%)	3a Yield (%) <sup>b</sup>
1	<i>t</i> -BuOLi	92	72
2	<i>t</i> -BuONa	23	16
3	<i>t</i> -BuOK	8	0
4	MeOLi	34	18
5	LHMDS	21	11
6	KF	5	0
7	K <sub>2</sub> CO <sub>3</sub>	0	0

Conditions: <sup>a</sup> **1a** (0.10 mmol, 1.0 equiv), **2a** (0.2 mmol, 2.0 equiv), NiBr<sub>2</sub>·DME (10 mol%), L2 (15 mol%), bases (0.17 mmol, 1.7 equiv), 1,4-dioxane (0.2 mL), 30 °C, 15 h. <sup>b</sup> Yields were determined by GC FID, using 1-decane as the internal standard. LHMDS = Lithium bis(trimethylsilyl)amide.

**Table 4.5** Screening of bases.<sup>a</sup>

The further optimize this reaction, we started to test different additives (Table 4.6). We try to weaken the nucleophilic attack of base pair **2a** and reduce the consumption of **2a**. So next we mainly choose additives from two aspects. On the one hand, we introduced several halide salts which would activate **2a** in situ and produce  $\alpha$ -haloborane with poor leaving group ability during S<sub>N</sub>2 process (entry 1-5). On the other hand, we attempted to add a certain amount of polar protic solvents in an effort to affect the nucleophilicity of Lewis base through hydrogen-bonding interactions (entry 7-9). Unfortunately, the additives had an inhibitory effect on the reaction.



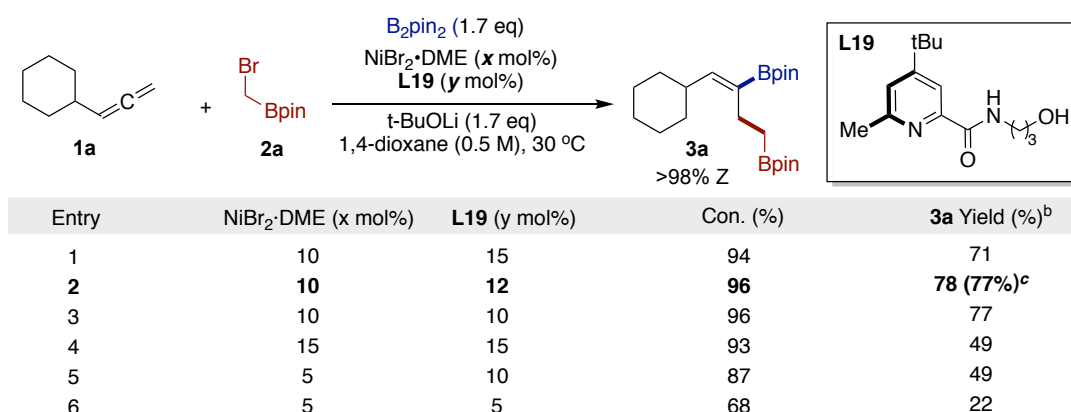
Entry	Additive	3a Yield (%) <sup>b</sup>
1	LiCl	71
2	LiBr	70
3	KF	27
4	TBAB	6
5	Mg(OEt) <sub>2</sub>	50
6	LHMDS	9
7	<i>t</i> -BuOH (4.0 eq)	71
8	<i>i</i> -PrOH (4.0 eq)	50
9	H <sub>2</sub> O (4.0 eq)	48

Conditions: <sup>a</sup> **1a** (0.10 mmol, 1.0 equiv), **2a** (0.2 mmol, 2.0 equiv), NiBr<sub>2</sub>·DME (10 mol%), Ligand (15 mol%), *t*-BuOLi (0.17 mmol, 1.7 equiv), Additive (0.1 mmol, 1.0 equiv), 1,4-dioxane (0.2 mL), 30 °C,

15 h. <sup>b</sup> Yields were determined by GC FID, using 1-decane as the internal standard. LHMDS = Lithium bis(trimethylsilyl)amide.

**Table 4.6** Screening of additives.<sup>a</sup>

Finally, we examined the effect of nickel-ligand ratio. A small increase in yield up to 78% was obtained when reducing the ligand (**L19**) loading (entry 2). Notably, as shown in entry 2 of table 4.7, allene **1a** and  $\alpha$ -haloborane **2a** as model substrates under the final optimized conditions gave alkenylboronate **3a** in 77% isolated yield with perfect regioselectivity and E/Z selectivity (*Z* selectivity through NMR spectroscopic analysis of the isolated **3a** was certified).



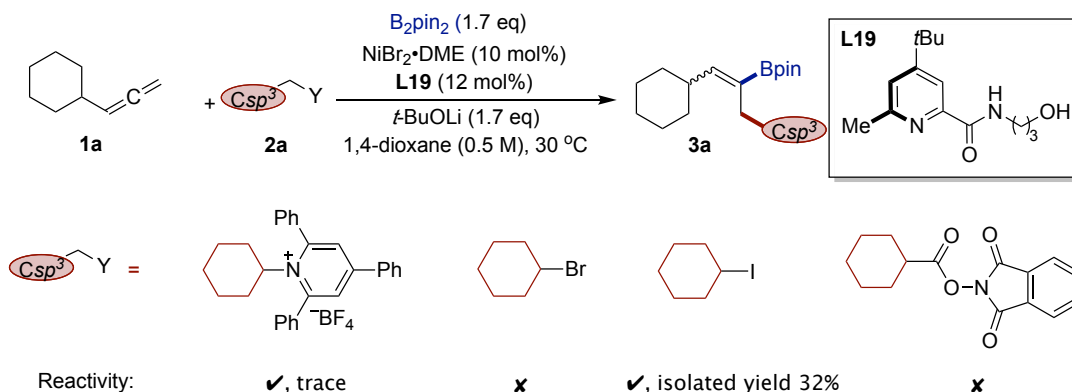
Conditions: <sup>a</sup> **1a** (0.10 mmol, 1.0 equiv), **2a** (0.2 mmol, 2.0 equiv), NiBr<sub>2</sub>·DME (10 mol%), Ligand (15 mol%), *t*-BuOLi (0.17 mmol, 1.7 equiv), Additive (0.1 mmol, 1.0 equiv), 1,4-dioxane (0.2 mL), 30 °C, 15 h. <sup>b</sup> Yields were determined by GC FID, using 1-decane as the internal standard. <sup>c</sup> isolated yield.

**Table 4.7** Screening of the ratio of Ni cat. to ligand.<sup>a</sup>

#### 4.3.1.2 Optimized conditions of alkyl iodides as electrophiles

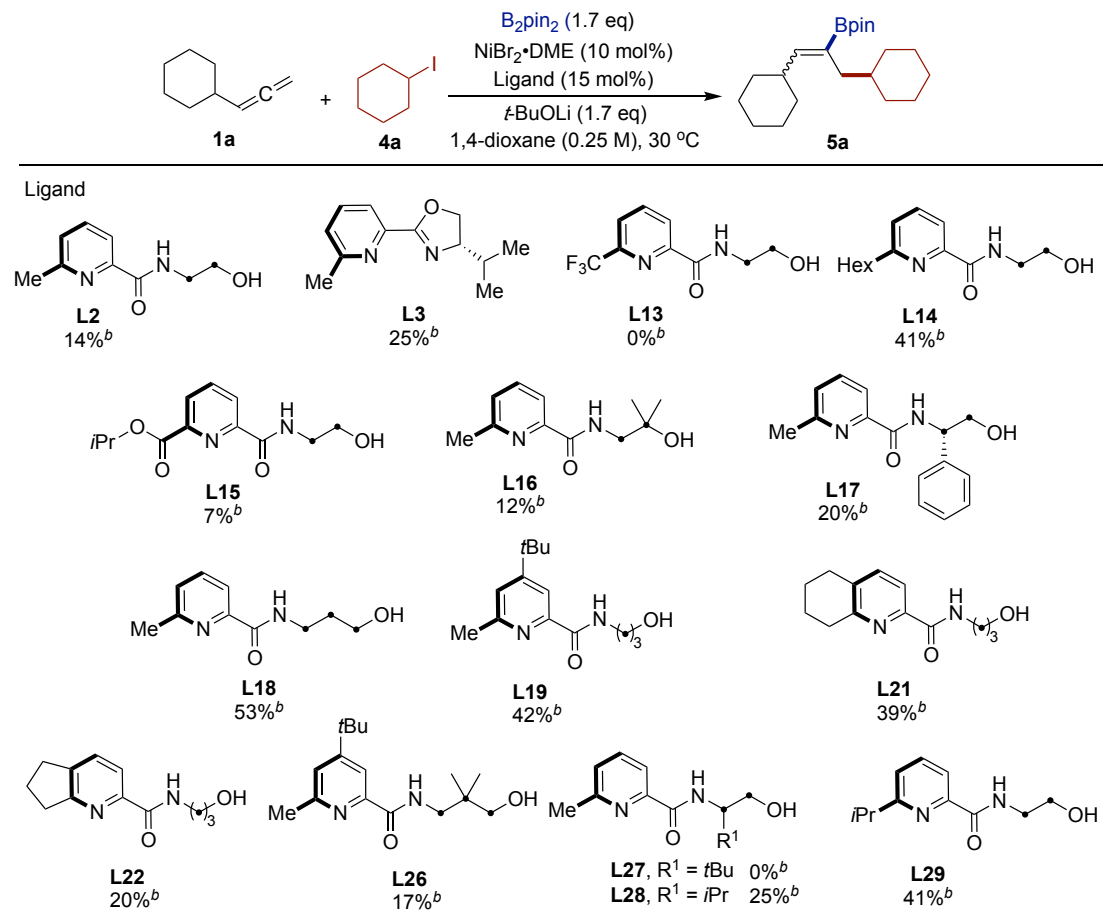
Encouraged by the previous results that we successfully established nickel-catalyzed alkylation of allene with amphiphilic  $\alpha$ -haloborane reagents, we speculated whether we could extend the haloalkylboranes to other electrophilic reagents with  $sp^3$  hybridized carbon center (Scheme 4.18), such as Katritzky salts, non-activated alkyl halides, and NHP esters derived from alkyl carboxylic acids, all of which are reported in the literature to have the potential for cross-coupling with organonickel metal centers via single electron transfer (SET). We discovered that the use of ubiquitous alkyl iodides provided the desired products. This result reflects the generality of our method, allowing modular alkylation using common alkyl halides, which in addition provides a new pathway - the formation of primary or secondary  $C(sp^3)$ - $C(sp^3)$  bonds - especially

more challenging for secondary alkyl halides because of space congestion in the product and the general difficulty of cross-coupling of secondary alkyl halides.



**Scheme 4.18** Extend the haloalkylboranes to other  $sp^3$  C-electrophiles.

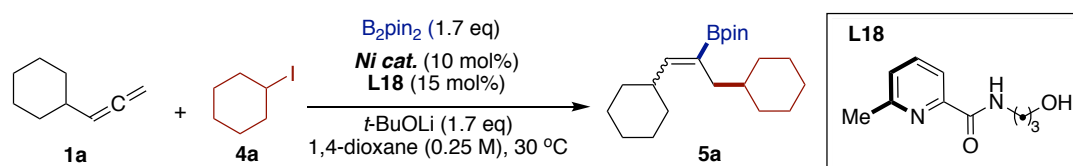
Although we obtained reactivity in the nickel-catalyzed 1,2-alkylborylation of allene using alkyl iodide instead of  $\alpha$ -haloborane, the promising yield of 32% was further optimized. At first, we focused on investigating different ligands based on the pyridylcarboamide structure. As shown in Table 4.8, **L18** without electron rich functional group (*t*-Bu) provided better yields (53%) than **L19**.



Condition s: <sup>a</sup> **1a** (0.10 mmol, 1.0 equiv), **4a** (0.2 mmol, 2.0 equiv), NiBr<sub>2</sub>·DME (10 mol%), Ligand (15 mol%), *t*-BuOLi (0.17 mmol, 1.7 equiv), 1,4-dioxane (0.4 mL), 30 °C, 15 h. <sup>b</sup> Yields were determined by GC FID, using 1-decane as the internal standard.

**Table 4.8** Screening of ligands using alkyl iodide as electrophile.<sup>a</sup>

Next, we screened various nickel pre-catalysts (Table 4.9). Although NiBr<sub>2</sub>·DME was more effective, the generality of alkyl iodide to different nickel catalysts was seen to be broader compared to the previous results of screening nickel catalysts with  $\alpha$ -haloboranes as the electrophiles.



Entry	Ni cat.	<b>5a</b> Yield (%) <sup>b</sup>
1	NiBr <sub>2</sub> ·DME	53
2	NiBr <sub>2</sub> ·diglyme	50
3	NiCl <sub>2</sub> ·DME	41
4	Ni(COD) <sub>2</sub>	0
5	Nil <sub>2</sub>	0
6	Ni(acac) <sub>2</sub>	38
7	NiBr <sub>2</sub> (TBAB) <sub>4</sub>	26
8	NiCl <sub>2</sub> ·6H <sub>2</sub> O	25
9	NiCl <sub>2</sub> (PPh <sub>3</sub> ) <sub>2</sub>	14
10	Ni(NO <sub>3</sub> ) <sub>2</sub> ·6H <sub>2</sub> O	27
11	No Ni cat.	0

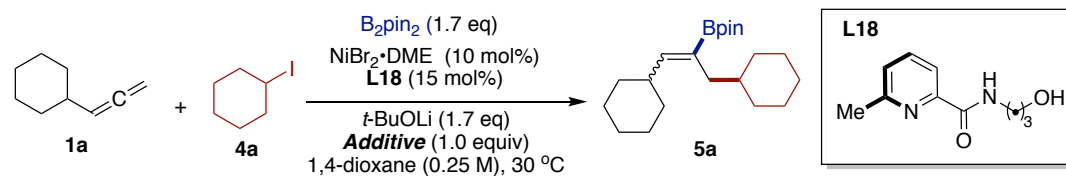
Conditions: <sup>a</sup> **1a** (0.10 mmol, 1.0 equiv), **4a** (0.2 mmol, 2.0 equiv), Ni cat. (10 mol%), **L18** (15 mol%), *t*-BuOLi (0.17 mmol, 1.7 equiv), 1,4-dioxane (0.4 mL), 30 °C, 15 h. <sup>b</sup> Yields were determined by GC FID, using 1-decane as the internal standard.

**Table 4.9** Screening of nickel pre-catalysts using alkyl iodide as electrophile.<sup>a</sup>

We subsequently investigated other parameters of the reaction, such as bases or solvents. However, a series of experiments demonstrated that the reaction remained optimal under the conditions of *t*-BuOLi as base and 1,4-dioxane as solvent. We observed that the conversion of allenes remained in the range of 80-95% during the optimization of the reaction, and we did not observe any other products that could be determined by GC-MS or NMR analysis, except for the regioselectivity. Compared to the yield of the desired product, we suspect that the lost starting material allene may have been converted to polymeric compounds. Finally, we decided to focus on the screening of additives. as shown in the table 4.10, a large number of inorganic salts or organic compounds were tried as additives, but the results were not what we expected. Interestingly, when we added copper salts, a loss in regioselectivity and large amounts



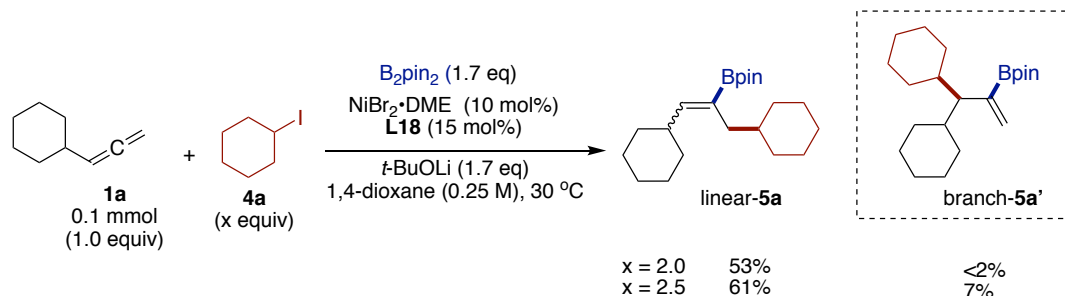
of branched-products were obtained (Table 4.10, entry 13-14). Moreover, when we tried to accelerate the conversion of the desired pathway by increasing the amount of alkyl iodide, the regioselectivity of the reaction deteriorated despite a slight increase in yield (Scheme 4.19).



Entry	Additive	Con. (%)	5a Yield (%) <sup>b</sup>
1	LiCl	76	46
2	LiBr	100	43
3	Mg(OEt) <sub>2</sub>	100	49
4	KF	83	38
5	KBr	88	54
6	NaCl	84	46
7	NaI	76	16
8	MgCl <sub>2</sub>	100	22
9	Cs <sub>2</sub> CO <sub>3</sub>	100	47
10	Na <sub>2</sub> CO <sub>3</sub>	93	52
11	K <sub>3</sub> PO <sub>4</sub>	91	45
12	TBAI	93	21
13	CuF <sub>2</sub>	100	49(23) <sup>c</sup>
14	CuI	100	21(28) <sup>c</sup>
15	Ag <sub>2</sub> CO <sub>3</sub>	100	50
16	H <sub>2</sub> O	89	41
17	<i>t</i> -BuOH (4.0 eq)	86	53
18	DMAP	76	8
19	2,6-diethylpyridine	93	56
20	PPh <sub>3</sub> (10 mol%)	—	20
21	dppf (10 mol%)	—	9

Conditions: <sup>a</sup> **1a** (0.10 mmol, 1.0 equiv), **4a** (0.2 mmol, 2.0 equiv), NiBr<sub>2</sub>·DME (10 mol%), L18 (15 mol%), *t*-BuOLi (0.17 mmol, 1.7 equiv), Additive (0.10 mmol, 1.0 equiv), 1,4-dioxane (0.4 mL), 30 °C, 15 h. <sup>b</sup> Yields were determined by GC-FID, using 1-decane as the internal standard. <sup>c</sup> Yields of branch product were determined by GC analysis of the reaction mixture.

**Table 4.10** Screening of nickel pre-catalysts using alkyl iodide as electrophile.<sup>a</sup>

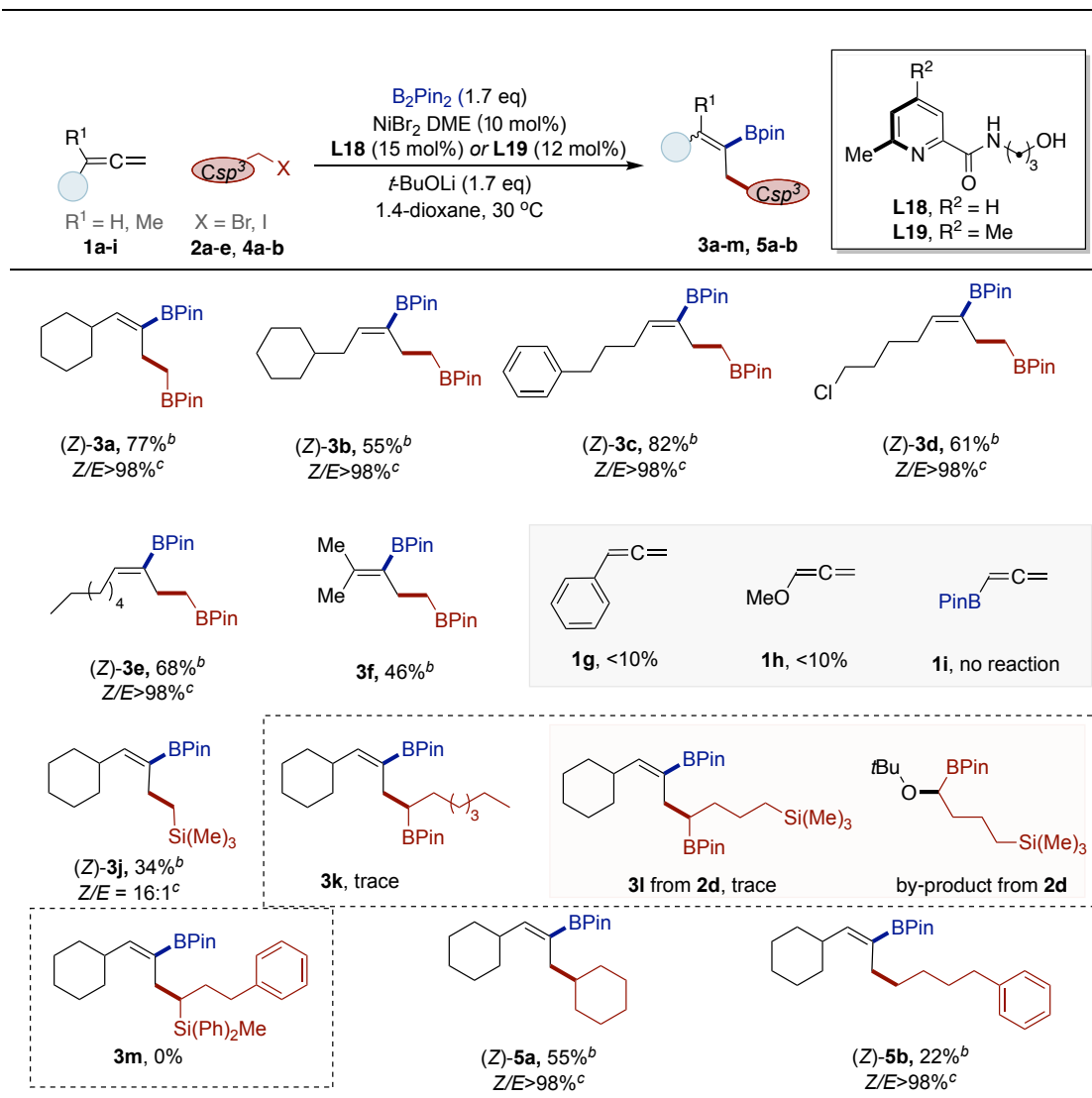


**Scheme 4.19** The regioselectivity of the reaction by changing amount of **4a**.

---

### 4.3.2 Substrate Scope

With the optimized reaction conditions in hand, we turned our attention to exploring the generality of reactivity. As shown by the results compiled in Scheme 4.20, on the one hand, we tried various allenes **1a-i**, and we obtained desired products from allene **1a-f** with primary  $\alpha$ -haloboranes (**2a**) accompanied by excellent E/Z and regioselectivity [(Z)-**3a-e**, Z/E > 98%]. We used NOESY experiments to confirm the stereochemistry of (Z) from a 1,2-alkylboronated product synthesized under reactive conditions. (see experiment for details). The reaction proceeds well when disubstituted allene (**3f**) was used. The electron-rich allenes (**1j,1h**) delivered poorer reactivity, and the detected results of the reaction systems were messy. the reaction could not proceed when the allene has bulky substituents (**1i**). Next, we plan to synthesize more alkyl allenes containing a variety of functional groups to show the functional group tolerance of our method. On the other hand, we investigated the scope and limitations of alkyl halides. The successful synthesis of 1,3-methylsilylboranes by catalytic 1,2-difunctionalization of allene using readily available (bromomethyl)trimethylsilane provided a useful entry point to forge 1,3-bis- organometallic reagents (**3j**). Disappointingly, the use of secondary  $\alpha$ -haloboranes failed under the reaction conditions (**3k, 3l**), obtaining a large number of by-products from base *t*-BuOLi nucleophilic attack on the secondary  $\alpha$ -haloboranes. It is tempting to propose that simple primary or secondary alkyl iodides (**5a, 5b**) can behave as electrophiles, albeit in low yields. In the future, the left work of this project will be continued by another member of my group.



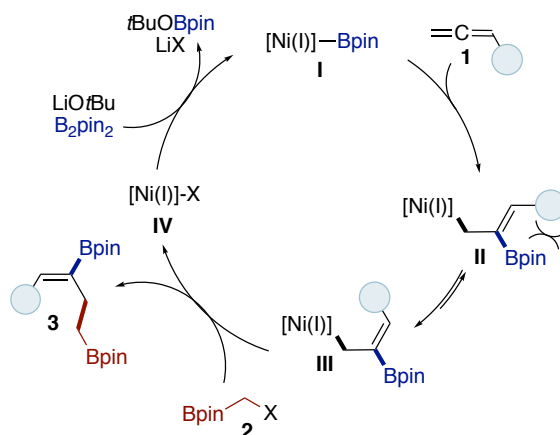
Conditions: <sup>a</sup> **1** (0.10 mmol, 1.0 equiv), **2** or **4** (0.2 mmol, 2.0 equiv),  $B_2pin_2$  (0.20 mmol, 2.0 equiv),  $NiBr_2 \cdot DME$  (10 mol%), **L18** (15 mol%) or **L19** (12 mol%),  $t-BuOLi$  (0.17 mmol, 1.7 equiv), 1,4-dioxane, 30 °C, 15 h. <sup>b</sup> Isolated yields <sup>c</sup> The ratio of E/Z was determined by GC-MS and  $^1H$  NMR spectrum analysis.

**Scheme 4.20** Substrate scope.

### 4.3.3 Mechanistic Proposal

With the related results of mechanistic studies on the nickel-catalyzed 1,1-alkylboration of non-activated alkenes by Yin's group and our group, we speculate that the reaction mechanism may be as follows (Scheme 4.21): (i) by initiating the  $Ni^I$ -Bpin species through metal transfer in the  $Ni^I$  species with  $B_2pin_2$ , (ii)  $Ni^I$ -Bpin under the effect of a special pyridylcarboamide-ligand may occur migratory insertion on the allene from the least hindered p-side, resulting in the formation of a new  $sp^3$  C- $Ni^I$  intermediate stabilized by allyl position, which is not possible to go through the  $\beta$ -H

elimination. The desired 1,2-alkylborylated product is delivered upon allyl-Ni<sup>I</sup> intermediate and  $\alpha$ -haloborane.



**Scheme 4.21** Proposed mechanism.

## 4.4 Conclusion

Although the transformation of nickel-catalyzed 1,2-alkylboration of allene has been preliminarily realized, the applicability of the substrate scope is currently limited under our optimized conditions. Next we plan to expand the substrate scope while further conditions optimization will be conducted for the substrates with poor reactivity, especially the secondary  $\alpha$ -haloboranes, which will provide a new pathway for the synthesis of 1,3-bis-metallic reagents if their efficient conversion can be achieved. In addition, further applicability of the transformation which boron groups are converted to hetero groups by cascade oxidation and Mitsunobu reaction, or to  $sp^2/sp^3$ -carbon chains by cross-coupling is to be expected.

The exceptional reactivity and selectivity of this synthetic method is noteworthy, which may have been influenced by nitrogen-based ligands. Further studies on the synthetic application of this strategy and the specific reaction mechanism will be assessed in our laboratory.

## 4.5 References

- (a) Alcaide, B.; Almendros, P. Progress in allene chemistry. *Chem. Soc. Rev.*, **2014**, 43, 2886. (b) Hoffmann-Röder, A.; Krause, N. Synthesis and properties of allenic natural products and pharmaceuticals. *Angew. Chem. Int. Ed.* **2004**, 43, 1196. (c)

- 
- Soriano, E.; Fernández, I. Allenes and computational chemistry: from bonding situations to reaction mechanisms. *Chem.Soc.Rev.*, **2014**, *43*, 3041.
2. (a) Yu, S.; Ma, S. Allenes in catalytic asymmetric synthesis and natural product syntheses. *Angew. Chem., Int. Ed.*, **2012**, *51*, 3074. (b) Neff, R. K.; Frantz, D. E. Recent advances in the catalytic syntheses of allenes: a critical assessment. *ACS Catal.*, **2014**, *4*, 519. (c) Alonso, J. M. M.; Quirós, T.; Muñoz, M. P. Chirality transfer in metal-catalysed intermolecular addition reactions involving allenes. *Org. Chem. Front.*, **2016**, *3*, 1186. (d) Lechel, T.; Pfrengle, F.; Reissig, H-U.; Zimmer, R. Three carbons for complexity: Recent developments of palladium-catalyzed reactions of allenes. *Chem CatChem*, **2013**, *5*, 2100.
3. Buckl, K.; Mieswinkel, A. Propyne. In *Ullmann's Encyclopedia of Industrial Chemistry*; Wiley-VCH: Weinheim, **2008**.
4. (a) Jeganmohan, M.; Chen, C-H. Transition metal-catalyzed three-component coupling of allenes and the related allylation reactions. *Chem. Commun.*, **2008**, 3101. (b) Eppe, G.; Didier, D.; Marek, I. Stereocontrolled formation of several carbon-carbon bonds in acyclic systems. *Chem. Rev.*, **2015**, *115*, 9175.
5. (a) Pulis, A. P.; Yeung, K.; Procter, D. J. Enantioselective copper catalysed, direct functionalisation of allenes via allyl copper intermediates. *Chem. Sci.* **2017**, *8*, 5240. (b) Fujihara, T.; Tsuji, Y. Cu-catalyzed borylative and silylative transformations of allenes: Use of  $\beta$ -functionalized allyl copper intermediates in organic synthesis. *Synthesis* **2018**, *50*, 1737. (c) Whyte, A.; Torelli, A.; Mirabi, B.; Zhang, A.; Lautens, M. Copper-catalyzed borylative difunctionalization of  $\pi$ -systems. *ACS Catal.* **2020**, *10*, 11578. (d) Talbot, F. J. T.; Dherbassy, Q.; Manna, S.; Shi, C.; Zhang, S.; Howell, G. P.; Perry, G. J. P.; Procter, D. J. Copper-catalyzed borylative couplings with C-N electrophiles. *Angew. Chem., Int. Ed.* **2020**, *59*, 20278.
6. For Cu-catalyzed three-component boro-functionalization of allenes, see: (a) Rae, J.; Yeung, K.; McDouall, J. J. W.; Procter, D. J. Copper-catalyzed borylative cross-coupling of allenes and imines: Selective three-component assembly of branched homoallyl amines. *Angew. Chem., Int. Ed.* **2016**, *55*, 1102. (b) Zhao, W-X.; Montgomery, J. Cascade copper-catalyzed 1,2,3-trifunctionalization of terminal allenes. *J. Am. Chem. Soc.* **2016**, *138*, 9763. (c) Semba, K.; Bessho, N.; Fujihara, T.; Terao, J.; Tsuji, Y. Copper-catalyzed borylative allyl-allyl coupling reaction. *Angew. Chem., Int. Ed.* **2014**, *53*, 9007. (d) Pulis, A. P.; Yeung, K.; Procter, D. J. Enantioselective copper catalysed, direct functionalisation of allenes via allyl

- 
- copper intermediates. *Chem. Sci.* **2017**, *8*, 5240. (e) Yeung, K.; Talbot, F.; Howell, G. P.; Pulis, A. P.; Procter, D. J. Copper-catalyzed borylative multicomponent synthesis of quater-nary  $\alpha$ -amino esters. *ACS Catal.* **2019**, *9*, 1655. (f) Fujihara, T.; Sawada, A.; Yamaguchi, T.; Tani, Y.; Terao, J.; Tsuji, Y. Boraformylation and silaformylation of allenes. *Angew. Chem., Int. Ed.* **2017**, *56*, 1539. (g) Tsuji, Y. Copper-catalyzed bora-acylation and bora-alkoxyoxalation of Allenes. *Adv. Synth. Catal.* **2018**, *360*, 2621.
7. (a) Wen, Y.; Deng, C.; Xie, J.; Kang, X. Recent synthesis developments of organoboron compounds via metal-free catalytic borylation of alkynes and alkenes. *Molecules* **2019**, *24*, 101. (b) Meng, F.; McGrath, K. P.; Hoveyda, A. H. Multifunctional organoboron compounds for scalable natural product synthesis. *Nature* **2014**, *513*, 367.
8. (a) Parra, A.; Trulli, L.; Tortosa, M. Copper-Catalyzed Addition of Diboron Species. *PATAI'S Chemistry of Functional Groups*; Wiley, **2020**; pp 1–82. (b) Liu, Z.; Gao, Y.; Zeng, T.; Engle, K. M. Transition-metal-catalyzed 1,2-carboboration of alkenes: strategies, mechanisms, and stereocontrol. *Isr. J. Chem.* **2020**, *60*, 219. (c) Hoveyda, A. H.; Zhou, Y.; Shi, Y.; Brown, K.; Wu, H.; Torker, S. Sulfonate N-heterocyclic carbene–copper complexes: Uniquely effective catalysts for enantioselective C–C, C–B, C–H, and C–Si bond formation. *Angew. Chem., Int. Ed.* **2020**, *59*, 21304. (c) Tsuji, Y.; Fujihara, T. Copper-catalyzed transformations using Cu–H, Cu–B, and Cu–Si as active catalyst species. *Chem. Rec.* **2016**, *16*, 2294. (d) Rivera-Chao, E.; Fra, L.; Fañanaś-Mastral, M. Synergistic bimetallic catalysis for carboboration of unsaturated hydrocarbons. *Synthesis* **2018**, *50*, 3825.
9. Ito, H.; Kubota, K. Copper(I)-catalyzed boryl substitution of unactivated alkyl halides. *Org. Lett.* **2012**, *14*, 890.
10. For recent reviews, see: (a) Müller, D. S.; Marek, I. Copper mediated carbometalation reactions. *Chem. Soc. Rev.*, **2016**, *45*, 4552. (b) Zhu, X.; Chiba, S. Copper-catalyzed oxidative carbon–heteroatom bond formation: a recent update. *Chem. Soc. Rev.*, **2016**, *45*, 4504. (c) Thapa, S.; Shrestha,; Gurung, B. S. K.; Giri, R. Copper-catalysed cross-coupling: an untapped potential. *Org. Biomol. Chem.*, **2015**, *13*, 4816. (d) Yoshikai, N.; Nakamura, E. Mechanisms of nucleophilic organocopper (I) reactions. *Chem. Rev.*, **2012**, *112*, 2339.
11. (a) Rae, J.; Hu, Y. C.; Procter, D. J. Cu (I)–NHC-catalyzed silylation of allenes: diastereoselective three-component coupling with aldehydes. *Chem. Eur. J.* **2014**,

- 
- 20, 13143. (b) Xu, Y-H.; Wu, L-H.; Wang, J.; Loh, T-P. Synthesis of multi-substituted vinylsilanes via copper (I)-catalyzed hydrosilylation reactions of allenes and propiolate derivatives with silylboronates. *Chem. Commun.* **2014**, *50*, 7195. (c) Tani, Y.; Fujihara, T.; Terao, J.; Tsuji, Y. Copper-catalyzed regiodivergent silacarboxylation of allenes with carbon dioxide and a silylborane. *J. Am. Chem. Soc.* **2014**, *136*, 17706. (d) Tani, Y.; Yamaguchi, T.; Fujihara, T.; Terao, J.; Tsuji, Y. Copper-catalyzed silylative allylation of ketones and aldehydes employing allenes and silylboranes. *Chem. Lett.* **2015**, *44*, 271. (e) Liu, R. Y.; Yang, Y.; Buchwald, S. L. Regiodivergent and diastereoselective CuH-Catalyzed allylation of imines with terminal allenes. *Angew. Chem., Int. Ed.* **2016**, *55*, 14077–14080. (f) Fujihara, T.; Yokota, K.; Terao, J.; Tsuji, Y. Copper-catalyzed hydroallylation of allenes employing hydrosilanes and allyl chlorides. *Chem. Commun.* **2017**, *53*, 7898.
12. Meng, F.; McGrath, K. P.; Hoveyda, A. H. Multifunctional organoboron compounds for scalable natural product synthesis. *Nature*, **2014**, *513*, 367.
13. Zhou, Y.; You, W.; Smith, K. B.; Brown, M. K. Copper-catalyzed cross-coupling of boronic esters with aryl iodides and application to the carboboration of alkynes and allenes. *Angew. Chem. Int. Ed.*, **2014**, *53*, 3475
14. (a) Meng, F.; Jang, H.; Jung, B.; Hoveyda, A. H. Cu-catalyzed chemoselective preparation of 2-(Pinacolato) boron-substituted allylcopper complexes and their in situ site-, diastereo-, and enantioselective. *Angew. Chem., Int. Ed.*, **2013**, *52*, 5046. (b) Rae, J.; Yeung, K.; McDouall, J. J. W.; Procter, D. J. Copper-catalyzed borylative cross-coupling of allenes and imines: Selective three-component assembly of branched homoallyl amines. *Angew. Chem., Int. Ed.* **2016**, *55*, 1102. (c) Yeung, K.; Ruscoe, R. E.; Rae, J.; Pulis, A. P.; Procter, D. J. Enantioselective generation of adjacent stereocenters in a copper-catalyzed three-component coupling of imines, allenes, and diboranes. *Angew. Chem., Int. Ed.* **2016**, *55*, 11912. (d) Meng, F.; Li, X.; Torker, S.; Shi, Y.; Shen, X.; Hoveyda, A. H. Catalytic enantioselective 1,6-conjugate additions of propargyl and allyl groups. *Nature* **2016**, *537*, 387. (e) Zhao, Y-S.; Tang, X-Q.; Tao, J-C.; Tian, P.; Lin, G-Q. Efficient access to cis-decalinol frameworks: Copper(I)-catalyzed borylative cyclization of allene cyclohexanediones. *Org. Biomol. Chem.* **2016**, *14*, 4400. (f) Zhao, W.; Montgomery, J. Cascade copper-catalyzed 1,2,3-trifunctionalization of terminal allenes. *J. Am. Chem. Soc.* **2016**, *138*, 9763. (g) Fujihara, T.; Sawada, A.; Yamaguchi, T.; Tani, Y.; Terao, J.; Tsuji, Y. Boraformylation and silaformylation of allenes. *Angew. Chem.*,

- 
- Int. Ed.* **2017**, *56*, 1539. (h) Ozawa, Y.; Iwamoto, H.; Ito, H. Copper(I)-catalysed regio- and diastereoselective intramolecular alkylboration of terminal allenes via allylcopper(I) isomerization. *Chem. Commun.* **2018**, *54*, 4991.
15. Boreux, A.; Indukuri, K.; Gagosz, F.; Riant, O. Acyl Fluorides as Efficient Electrophiles for the Copper-Catalyzed Boroacylation of Allenes. *ACS Catal.* **2017**, *7*, 8200–8204.
16. Ozawa, Y.; Iwamoto, H.; Ito, H. Copper(I)-catalysed regio- and diastereoselective intramolecular alkylboration of terminal allenes via allylcopper(I) isomerization. *Chem. Commun.*, **2018**, *54*, 4991.
17. Ozawa, Y.; Endo, K.; Ito, H. Regio- and stereoselective synthesis of multi-alkylated allylic boronates through three-component coupling reactions between allenes, alkyl halides, and a diboron reagent. *J. Am. Chem. Soc.* **2021**, *143*, 13865.
18. Reviews on nickel catalysis: (a) “Organonickel Chemistry”: J. Montgomery in *Organometallics in Synthesis*, Wiley, Hoboken, **2013**, 319. (b) Tasker, S. Z.; Standley, E. A.; Jamison, T. F. Recent advances in homogeneous nickel catalysis. *Nature* **2014**, *509*, 299. (c) Ananikov, V. P. Nickel: the “spirited horse” of transition metal catalysis. *ACS Catal.* **2015**, *5*, 1964.
19. (a) Choi, J.; Fu, G. C. Transition metal-catalyzed alkyl-alkyl bond formation: another dimension in cross-coupling chemistry. *Science* **2017**, *356*, 152. (b) Rudolph, A.; Lautens, M. Secondary alkyl halides in transition-metal-catalyzed cross-coupling reactions *Angew. Chem. Int. Ed.* **2009**, *48*, 2656.
20. (a) Vasseur, A.; Bruffaerts, J.; Marek, I. Remote functionalization through alkene isomerization. *Nat. Chem.* **2016**, *8*, 209. (b) Sommer, H.; Julià-Hernández, F.; Martin, R.; Marek, I. Walking metals for remote functionalization. *ACS Cent. Sci.* **2018**, *4*, 153. (c) Li, L.; Gong, T.; Xiao, B.; Fu, Y. Nickel-catalyzed synthesis of 1,1-diborylalkanes from terminal alkenes. *Nat. Commun.* **2017**, *8*, 345.
21. (a) Li, Y.; Wu, D.; Cheng, H-G.; Yin, G. Difunctionalization of Alkenes Involving Metal Migration. *Angew. Chem. Int. Ed.* **2020**, *132*, 8066. (b) Liu, Z.; Gao, Y.; Zeng, T.; Engle, K. M. *Isr.* Transition-metal-catalyzed 1,2-carboboration of alkenes: Strategies, mechanisms, and stereocontrol. *Isr. J. Chem.* **2020**, *60*, 219
22. Li, Y.; Pang, H.; Wu, D.; Li, Z.; Wang, W.; Wei, H.; Fu, Y.; Yin, G. Nickel-catalyzed 1,1-alkylboration of electronically unbiased terminal alkenes. *Angew. Chem. Int. Ed.* **2019**, *58*, 8872.



- 
23. Sun, S-Z.; Talavera, L.; Spieß, P.; Day, C. S.; Martin, R. *sp*<sup>3</sup> Bis-organometallic reagents via catalytic 1,1-difunctionalization of unactivated olefins. *Angew. Chem. Int. Ed.* **2021**, *60*, 11740.
24. Ding, C.; Ren, Y.; Sun, C.; Long, J.; Yin, G. Regio- and stereoselective alkylboration of endocyclic olefins enabled by nickel catalysis. *J. Am. Chem. Soc.* **2021**, *143*, 20027.
25. Li, Y.; Li, Y.; Shi, H.; Wei, H.; Li, H.; Funes-Ardoiz, I.; Yin, G. Modular access to substituted cyclohexanes with kinetic stereocontrol. *Science* **2022**, *376*, 749.
26. (a) Denmark, S. E.; Amburgey, J. A new, general, and stereoselective method for the synthesis of trisubstituted alkenes. *J. Am. Chem. Soc.* **1993**, *115*, 10386. (b) Brown, S. D.; Armstrong, R. W. Synthesis of tetrasubstituted ethylenes on solid support via resin capture. *J. Am. Chem. Soc.* **1996**, *118*, 6331. (c) Organ, M. G.; Cooper, J. T.; Rogers, L. R.; Soleymanzadeh, F.; Paul, T. Synthesis of stereodefined polysubstituted olefins. 1. Sequential intermolecular reactions involving selective, stepwise insertion of Pd(0) into allylic and vinylic halide bonds. The stereoselective synthesis of disubstituted olefins. *J. Org. Chem.* **2000**, *65*, 7959. (d) Shi, Y.; Peterson, S. M.; Haberaecker, W. W.; Blum, S. A. Alkynes as stille reaction pseudohalides: gold- and palladium-cocatalyzed synthesis of tri- and tetrasubstituted olefins. *J. Am. Chem. Soc.* **2008**, *130*, 2168.
27. (a) Brown, H. C.; Bhat, N. G. A simple conversion of [E]- into the isomeric [Z]-2-(1-substituted-1-alkenyl)-1,3,2-dioxaborinanes, providing a convenient stereospecific synthesis of both [E]- and [Z]-1,2-disubstituted vinyl bromides. *Tetrahedron Lett.* **1988**, *29*, 21. (b) Takagi, J.; Takahashi, K.; Ishiyama, T.; Miyaura, N. Palladium-catalyzed cross-coupling reaction of bis (pinacolato) diboron with 1-alkenyl halides or triflates: convenient synthesis of unsymmetrical 1, 3-dienes via the borylation-coupling sequence. *J. Am. Chem. Soc.* **2002**, *124*, 8001. (c) Itami, K.; Kamei, T.; Yoshida, J.-I. Diversity-oriented synthesis of tamoxifen-type tetrasubstituted olefins. *J. Am. Chem. Soc.* **2003**, *125*, 14670.
28. (a) Gridnev, I. D.; Miyaura, N.; Suzuki, A. Regio- and stereospecific preparation of beta-(alkylthio) alkenyl-1, 3, 2-benzodioxaboroles by nickel-catalyzed hydroboration of thioacetylenes with catecholborane. *Organometallics* **1993**, *12*, 589. (b) Lipshutz, B. H.; Boskovic, Z. V.; Aue, D. H. Synthesis of activated alkenylboronates from acetylenic esters by CuH-catalyzed 1, 2-addition/transmetalation. *Angew. Chem., Int. Ed.* **2008**, *47*, 10183. (c) Molander, G.

- 
- A.; Ellis, N. M. Highly stereoselective synthesis of cis-alkenyl pinacolboronates and potassium cis-alkenyltrifluoroborates via a hydroboration/ protodeboronation approach. *J. Org. Chem.* **2008**, *73*, 6841.
29. Pereira, S.; Srebnik, M. Hydroboration of alkynes with pinacolborane catalyzed by HZrCp<sub>2</sub>Cl. *Organometallics* **1995**, *14*, 3127. (b) Ohmura, T.; Yamamoto, Y.; Miyaura, M. [HTML] Rhodium- or Iridium-Catalyzed trans-Hydroboration of Terminal Alkynes, Giving (Z)-1-Alkenylboron Compounds. *J. Am. Chem. Soc.* **2000**, *122*, 4990. (c) Gunanathan, C.; Hölscher, M.; Pan, F.; Leitner, W. Ruthenium catalyzed hydroboration of terminal alkynes to Z- vinylboronates. *J. Am. Chem. Soc.* **2012**, *134*, 14349. (d) Lee, Y.; Jang, H.; Hoveyda, A. H. Vicinal diboronates in high enantiomeric purity through tandem site-selective NHC– Cu-catalyzed boron– copper additions to terminal alkynes. *J. Am. Chem. Soc.* **2009**, *131*, 18234.
30. (a) Brown, H. C.; Imai, T. Organoboranes. 37. Synthesis and properties of (Z)-1-alkenylboronic esters. *Organometallics* **1984**, *3*, 1392. (b) Campbell, J. B.; Molander, G. A. Organoborates in new synthetic reactions. *J. Organomet. Chem.* **1978**, *156*, 71. (c) Kiesewetter, E. T.; O'Brien, R. V.; Yu, E. C.; Meek, S. J.; Schrock, R. R.; Hoveyda, A. H. Synthesis of Z-(Pinacolato)allylboron and Z-(Pinacolato)alkenylboron Compounds through Stereoselective Catalytic Cross-Metathesis. *J. Am. Chem. Soc.* **2013**, *135*, 6026. (d) Jang, H.; Zhugralin, A. R.; Lee, Y.; Hoveyda, A. H. Highly selective methods for synthesis of internal (α-) vinylboronates through efficient NHC–Cu-catalyzed hydroboration of terminal alkynes. Utility in chemical. *J. Am. Chem. Soc.* **2011**, *133*, 7859.
31. Cheng, L.-J.; Mankad, N. P. C–C and C–X coupling reactions of unactivated alkyl electrophiles using copper catalysis. *Chem. Soc. Rev.*, **2020**, *49*, 8036.

---

## 4.6 Experimental Section

### 4.6.1 General Considerations

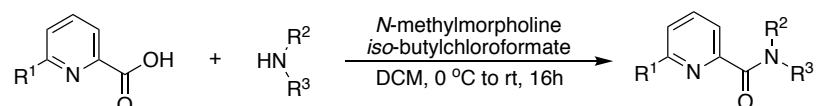
**Reagents:** Commercially available materials were used as received without further purification. (Bromomethyl)boronic acid pinacol ester, Bis(pinacolato)diboron ( $B_2Pin_2$ ) and Bis[(1R,2R,3S,5R)-pinanediolato]diboron were purchased from Fluorochem. (Bromomethyl)trimethylsilane was purchased from TCI. *t*-BuOLi was purchased from Sigma-Aldrich. Anhydrous 1,4-dioxane (99.5% purity) was purchased from Acros.

**Analytical methods:**  $^1H$  and  $^{13}C$  NMR spectra were recorded on Bruker 400 MHz and Bruker 500 MHz at 20 °C. All  $^1H$  NMR spectra are reported in parts per million (ppm) downfield of TMS and were calibrated using the residual solvent peak of  $CHCl_3$  (7.26 ppm), unless otherwise indicated. All  $^{13}C$  NMR spectra are reported in ppm relative to TMS, were calibrated using the signal of residual  $CHCl_3$  (77.16 ppm). Gas chromatographic analyses were performed on Hewlett-Packard 6890 gas chromatography instrument with FID detector. Flash chromatography was performed with EM Science silica gel 60 (230-400 mesh). Thin layer chromatography was used to monitor reaction progress and analyze fractions from column chromatography. To this purpose TLC Silica gel 60 F254 aluminium sheets from Merck were used and visualization was achieved using UV irradiation and/or staining with Cerium Molybdate solution.

### 4.6.2 Synthesis of Ligands and Starting Materials

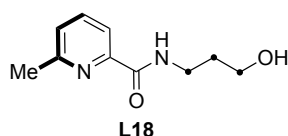
The ligands **L1-L4** (Table 4.1), **L13-L17**, **L27-L28** (Table 4.4) were prepared previously by others in our group and the preparation steps and data characterisation are reported in the literature.<sup>1</sup>

#### General Procedure for the Preparation of Ligands

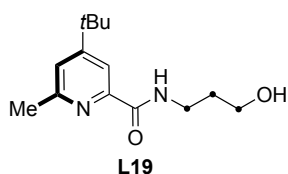


The ligands **L18-L26** were prepared according to a procedure reported in literature.<sup>2</sup> To a round-bottom flask containing a stirring bar was added the corresponding picolinic

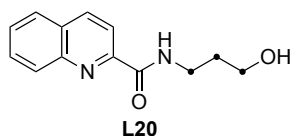
acid (10 mmol, 1.0 equiv), then dry DCM (40 mL) was added via syringe under inert atmosphere. Subsequently, N-methylmorpholine (15 mmol, 1.5 equiv) was added and the reaction mixture was cooled down to 0 °C. Subsequently, iso-butyl chloroformate was added dropwise (12 mmol, 1.2 equiv), and the mixture was stirred for further 20 min. Then the corresponding amine (12 mmol, 1.2 equiv) dissolved in DCM (10 mL) and added via syringe. After the addition, the mixture was allowed to warm to room temperature and stirred for 16 h. Afterwards, the mixture was extracted with DCM (10 mL), washed with water (10 mL), brine (10 mL), dried over MgSO<sub>4</sub> and concentrated in vacuum. The residue was purified by silica gel flash chromatography.



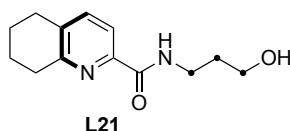
**N-(3-hydroxypropyl)-6-methylpicolinamide (L18)** Following the general procedure, using 6-methylpicolinic acid (1.15 g, 8.38 mmol) and 3-aminopropan-1-ol (0.77 mL, 10.1 mmol). The product was purified by flash chromatography (Hexane/EtOAc =2:1) to afford the compound as a colorless oil, 1.18 g (73%). <sup>1</sup>H NMR (400 MHz, CDCl<sub>3</sub>) δ 8.34 (s, 1H), 7.98 (d, *J* = 7.7 Hz, 1H), 7.71 (t, *J* = 7.7 Hz, 1H), 7.27 (d, *J* = 7.2 Hz, 1H), 3.68 – 3.61 (m, 4H), 2.55 (s, 3H), 1.84 – 1.76 (m, 2H) ppm. <sup>13</sup>C NMR (101 MHz, CDCl<sub>3</sub>) δ 165.9, 157.3, 148.8, 137.7, 126.2, 119.5, 58.9, 35.7, 32.7, 24.3 ppm.



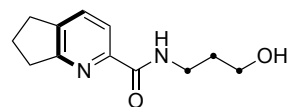
**4-(tert-butyl)-N-(3-hydroxypropyl)-6-methylpicolinamide (L19)** Following the general procedure, using 4-(tert-butyl)-6-methylpicolinic acid (0.80 g, 4.14 mmol) and 3-aminopropan-1-ol (0.33 mL, 4.9 mmol). The product was purified by flash chromatography (Hexane/EtOAc = 2:1) to afford the compound as a colorless oil, 0.81 g (78%). <sup>1</sup>H NMR (400 MHz, CDCl<sub>3</sub>) δ 8.36 (s, 1H), 8.02 (d, *J* = 2.0 Hz, 1H), 7.26 (d, *J* = 2.3 Hz, 1H), 3.76 – 3.56 (m, 4H), 2.55 (s, 3H), 1.91 – 1.68 (m, 2H), 1.32 (s, 9H), 0.91 (d, *J* = 6.7 Hz, 1H) ppm. <sup>13</sup>C NMR (101 MHz, CDCl<sub>3</sub>) δ 166.4, 162.2, 157.2, 148.7, 123.1, 116.9, 58.8, 35.6, 35.1, 32.8, 30.6, 24.5 ppm.



***N*-(3-hydroxypropyl)quinoline-2-carboxamide (L20)** Following the general procedure, using quinoline-2-carboxylic acid (0.54 g, 3.10 mmol) and 3-aminopropan-1-ol (0.28 g, 3.7 mmol). The product was purified by flash chromatography (Hexane/EtOAc =2:1) to afford the compound as a colorless oil, 0.46 g (65%). <sup>1</sup>H NMR (400 MHz, CDCl<sub>3</sub>): δ <sup>1</sup>H NMR (400 MHz, CDCl<sub>3</sub>) δ 8.52 (s, 1H), 8.36 – 8.27 (m, 2H), 8.09 (m, 1H), 7.88 (d, *J* = 8.2 Hz, 1H), 7.76 (d, *J* = 8.4 Hz, 1H), 7.62 (d, *J* = 8.2 Hz, 1H), 3.71 (m, 4H), 1.87 (m, 2H) ppm. <sup>13</sup>C NMR (101 MHz, CDCl<sub>3</sub>) δ 165.8, 149.5, 146.6, 137.7, 130.3, 129.7, 129.5, 128.1, 127.9, 119.0, 59.1, 36.0, 32.7 ppm.

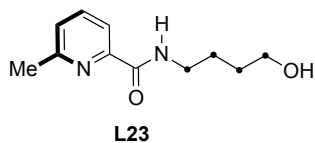


***N*-(3-hydroxypropyl)-5,6,7,8-tetrahydroquinoline-2-carboxamide (L21)** Following the general procedure, using 5,6,7,8-tetrahydroquinoline-2-carboxylic acid (0.73 g, 4.10 mmol) and 3-aminopropan-1-ol (0.33 mL, 4.9 mmol). The product was purified by flash chromatography (Hexane/EtOAc =2:1) to afford the compound as a colorless oil, 0.73 g (76%). <sup>1</sup>H NMR (400 MHz, CDCl<sub>3</sub>) δ 8.28 (s, 1H), 7.91 (d, *J* = 7.8 Hz, 1H), 7.50 (d, *J* = 7.9 Hz, 1H), 3.64 (dd, *J* = 7.2, 5.1 Hz, 4H), 3.54 (s, 1H), 2.90 (t, *J* = 6.5 Hz, 2H), 2.82 (t, *J* = 6.4 Hz, 2H), 2.01 – 1.87 (m, 2H), 1.87 – 1.72 (m, 4H) ppm. <sup>13</sup>C NMR (101 MHz, CDCl<sub>3</sub>) δ 156.3, 146.5, 138.1, 136.0, 119.7, 58.8, 35.6, 32.9, 32.5, 28.9, 23.0, 22.6 ppm.

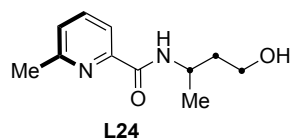


***N*-(3-hydroxypropyl)-6,7-dihydro-5H-cyclopenta[*b*]pyridine-2-carboxamide (L22)** Following the general procedure, using 6,7-dihydro-5H-cyclopenta[*b*]pyridine-2-carboxylic acid (0.67 g, 4.10 mmol) and 3-aminopropan-1-ol (0.33 mL, 4.9 mmol). The product was purified by flash chromatography (Hexane/EtOAc =2:1) to afford the compound as a colorless oil, 0.66 g (74%). <sup>1</sup>H NMR (400 MHz, CDCl<sub>3</sub>) δ 8.25 (d, *J* = 10.7 Hz, 1H), 7.95 (d, *J* = 7.8 Hz, 1H), 7.62 (dd, *J* = 7.7, 1.3 Hz, 1H), 3.64 (td, *J* = 5.6, 3.6 Hz, 4H), 2.99 (q, *J* = 7.9 Hz, 4H), 2.30 – 2.09 (m, 2H), 1.95 – 1.67 (m, 2H) ppm.

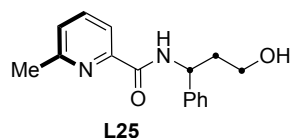
$^{13}\text{C}$  NMR (101 MHz,  $\text{CDCl}_3$ )  $\delta$  166.3, 164.9, 147.7, 140.9, 133.1, 120.4, 58.8, 35.6, 33.9, 32.8, 30.8, 23.4 ppm.



**4-(*tert*-butyl)-*N*-(4-hydroxybutyl)-6-methylpicolinamide (L23)** Following the general procedure, using 6-methylpicolinic acid (0.56 g, 4.10 mmol) and 4-aminobutan-1-ol (0.44 g, 4.90 mmol). The product was purified by flash chromatography (Hexane/EtOAc =2:1) to afford the compound as a white solid, 0.71 g (83%).  $^1\text{H}$  NMR (400 MHz,  $\text{CDCl}_3$ )  $\delta$  8.22 (s, 1H), 8.03 – 7.95 (m, 1H), 7.77 – 7.64 (m, 1H), 7.27 (d,  $J$  = 6.5 Hz, 2H), 3.76 – 3.69 (m, 2H), 3.60 – 3.47 (s, 3H), 1.81 – 1.64 (m, 4H) ppm.  $^{13}\text{C}$  NMR (101 MHz,  $\text{CDCl}_3$ )  $\delta$  164.7, 157.2, 149.3, 137.6, 125.9, 119.44, 62.7, 39.2, 30.0, 26.5, 24.3 ppm.

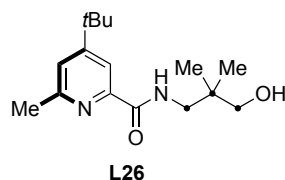


***N*-(4-hydroxybutan-2-yl)-6-methylpicolinamide (L24)** Following the general procedure, using 6-methylpicolinic acid (0.56 g, 4.10 mmol) and 3-aminobutan-1-ol (0.44 g, 4.90 mmol). The product was purified by flash chromatography (Hexane/EtOAc =2:1) to afford the compound as a colorless oil, 0.58 g (68%).  $^1\text{H}$  NMR (400 MHz,  $\text{CDCl}_3$ )  $\delta$  7.99 (m, 2H), 7.73 (t,  $J$  = 7.7 Hz, 1H), 7.29 (dd,  $J$  = 7.7, 1.1 Hz, 1H), 4.53 – 4.30 (m, 1H), 3.71 – 3.48 (m, 2H), 2.58 (s, 3H), 1.95 (dd,  $J$  = 14.1, 10.7 Hz, 1H), 1.56 – 1.44 (m, 1H), 1.38 (s, 3H) ppm.  $^{13}\text{C}$  NMR (101 MHz,  $\text{CDCl}_3$ )  $\delta$  165.30, 157.41, 148.69, 137.75, 126.27, 119.66, 58.89, 42.07, 40.66, 24.36, 21.42 ppm.



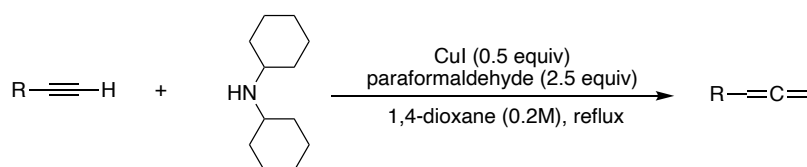
***N*-(3-hydroxy-1-phenylpropyl)-6-methylpicolinamide (L25)** Following the general procedure, using 6-methylpicolinic acid (0.56 g, 4.10 mmol) and 3-amino-3-phenylpropan-1-ol (mL, mmol). The product was purified by flash chromatography (Hexane/EtOAc =1:1) to afford the compound as a white solid, 0.62 g (56%).  $^1\text{H}$

NMR (400 MHz, CDCl<sub>3</sub>) δ 8.50 (d, *J* = 8.6 Hz, 1H), 8.01 (d, *J* = 7.5 Hz, 1H), 7.73 (td, *J* = 7.7, 2.9 Hz, 1H), 7.47 – 7.36 (m, 4H), 7.34 – 7.27 (m, 2H), 5.42 (ddd, *J* = 10.8, 9.0, 4.1 Hz, 1H), 3.71 (m, 3H), 2.56 (s, 3H), 2.32 – 2.20 (m, 1H), 1.99 (m, 1H) ppm. No signal for OH-group has been observed. <sup>13</sup>C NMR (101 MHz, CDCl<sub>3</sub>) δ 165.1, 157.4, 148.6, 141.6, 137.7, 129.0, 127.8, 126.9, 126.4, 119.7, 58.9, 50.2, 39.3, 24.3 ppm.

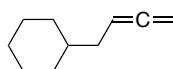


***N*-(3-hydroxy-2,2-dimethyl-2λ<sup>5</sup>-propyl)-6-methylpicolinamide (L26)** Following the general procedure, using 4-(*tert*-butyl)-6-methylpicolinic acid (0.79 g, 4.10 mmol) and 3-amino-2,2-dimethyl-2λ<sup>5</sup>-propan-1-ol (0.50 g, 4.90 mmol). The product was purified by flash chromatography (Hexane/EtOAc =2:1) to afford the compound as a yellow oil, 0.44 g (48%). <sup>1</sup>H NMR (400 MHz, CDCl<sub>3</sub>) δ 8.46 (s, 1H), 8.07 – 7.97 (m, 1H), 7.27 (d, *J* = 1.9 Hz, 1H), 3.30 (d, *J* = 7.2 Hz, 2H), 3.18 (d, *J* = 7.2 Hz, 2H), 2.56 (s, 3H), 1.33 (s, 9H), 0.95 (s, 6H) ppm. <sup>13</sup>C NMR (101 MHz, CDCl<sub>3</sub>) δ 166.7, 157.3, 148.5, 123.2, 117.1, 68.0, 46.3, 37.5, 35.1, 30.6, 24.5, 22.9 ppm.

### General procedure for the Preparation of Allenes<sup>3</sup>

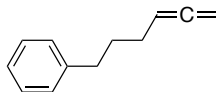


Alkyne (1.0 equiv), paraformaldehyde (2.5 equiv), copper iodide (0.5 equiv), dicyclohexylamine (1.8 equiv) and 1,4-dioxane (0.2 M) were added sequentially into a flask under a nitrogen atmosphere. The resulting mixture was stirred under reflux for 12 h. Water and diethyl ether was added and the aqueous solution was extracted with diethyl ether. The organic layer was then washed with brine and dried over anhydrous MgSO<sub>4</sub>. Evaporation and column chromatography on silica gel afforded allene as product.

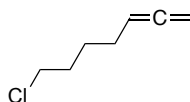


**Buta-2,3-dien-1-ylcyclohexane (1b)** Following the general procedure, using prop-2-yn-1-ylcyclohexane (0.50 g, 4.1 mmol), the crude was purified by flash column

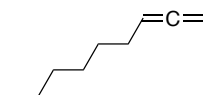
chromatography (hexane), to afford **1b** (0.25 g, 44% yield) as a colorless liquid. <sup>1</sup>H NMR (400 MHz, CDCl<sub>3</sub>) δ 5.16 – 4.96 (m, 1H), 4.62 (dt, *J* = 6.6, 2.9 Hz, 2H), 1.90 (tt, *J* = 7.5, 2.9 Hz, 2H), 1.79 – 1.56 (m, 5H), 1.36 – 1.11 (m, 4H), 1.03 – 0.71 (m, 2H) ppm. <sup>13</sup>C NMR (101 MHz, CDCl<sub>3</sub>) δ 209.1, 88.5, 73.9, 38.2, 36.5, 33.1, 26.7, 26.4 ppm.



**Hexa-4,5-dien-1-ylbenzene (1c)** Following the general procedure, using pent-4-yn-1-ylbenzene (0.59 g, 4.1 mmol), the crude was purified by flash column chromatography (hexane), to afford **1b** (0.39 g, 60% yield) as a colorless liquid. <sup>1</sup>H NMR (400 MHz, CDCl<sub>3</sub>) δ 7.35 – 7.28 (m, 2H), 7.24 – 7.18 (m, 3H), 5.17 (m, 1H), 4.72 (m, 2H), 2.72 – 2.67 (m, 2H), 2.18 – 2.02 (m, 2H), 1.85 – 1.73 (m, 2H) ppm. <sup>13</sup>C NMR (101 MHz, CDCl<sub>3</sub>) δ 208.8, 142.4, 128.6, 128.4, 125.8, 89.8, 75.0, 35.3, 30.9, 27.8 ppm.



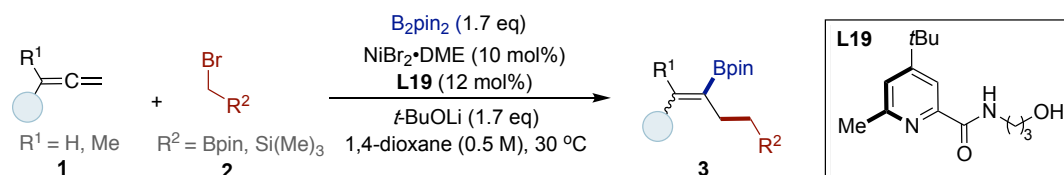
**7-chlorohepta-1,2-diene (1d)** Following the general procedure, using 6-chlorohex-1-yne (0.48 g, 4.1 mmol), the crude was purified by flash column chromatography (hexane), to afford **1b** (0.30 g, 57% yield) as a colorless liquid. <sup>1</sup>H NMR (400 MHz, CDCl<sub>3</sub>) δ 5.09 (m, 1H), 4.67 (dt, *J* = 6.6, 3.3 Hz, 2H), 3.54 (t, *J* = 6.7 Hz, 2H), 2.20 – 1.95 (m, 2H), 1.89 – 1.74 (m, 2H), 1.64 – 1.51 (m, 2H) ppm. <sup>13</sup>C NMR (101 MHz, CDCl<sub>3</sub>) δ 208.72, 89.54, 75.13, 45.00, 32.09, 27.56, 26.37 ppm.



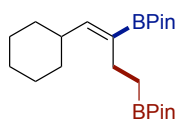
**Nona-1,2-diene (1e)** Following the general procedure, using prop-2-yn-1-ylcyclohexane (0.45 g, 4.1 mmol), the crude was purified by flash column chromatography (hexane), to afford **1b** (0.27 g, 53% yield) as a colorless liquid. <sup>1</sup>H NMR (400 MHz, CDCl<sub>3</sub>) δ 5.14 – 5.01 (m, 1H), 4.64 (dt, *J* = 6.6, 3.2 Hz, 2H), 1.99 (dq, *J* = 10.2, 3.4 Hz, 2H), 1.48 – 1.36 (m, 2H), 1.35 – 1.24 (m, 6H), 0.93 – 0.83 (m, 5H) ppm. <sup>13</sup>C NMR (101 MHz, CDCl<sub>3</sub>) δ 208.6, 90.2, 74.6, 31.8, 29.2, 28.9, 28.4, 22.8, 14.2 ppm.

### 4.6.3 General Procedure of Ni-Catalyzed 1,1-Alkylboration of Allenes with $\alpha$ -Haloboranes and B<sub>2</sub>Pin<sub>2</sub>

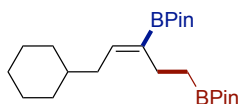




General procedure A: An oven-dried 8 mL screw-cap test tube containing a stirring bar was charged with NiBr<sub>2</sub>·DME (6.2 mg, 10 mol%), 4-(*tert*-butyl)-*N*-(3-hydroxypropyl)-6-methylpicolinamide (**L19**, 6.0 mg, 12 mol%), B<sub>2</sub>Pin<sub>2</sub> (86.3 mg, 0.34 mmol). Subsequently, the tube was put into the glove-box under N<sub>2</sub> atmosphere, and *t*-BuOLi (0.34 mmol, 27.2 mg) was added in the glove-box. Then the tube was sealed with a Teflon-lined screw cap and taken outside from the glove-box. Afterwards, the corresponding allene (**1**, 0.20 mmol, 1.0 equiv),  $\alpha$ -Bromo boronic acid pinacol ester (**2**, 0.4 mmol, 2.0 equiv) and 1,4-dioxane (0.4 mL) were added via syringe, independently. Then, the tube was stirred at 30 °C for 15 h. After the reaction was completed, the mixture was diluted with EtOAc, filtered through silica gel and concentrated under vacuum. The corresponding product **3a-3f** and **3j** were purified by flash column chromatography on silica gel.

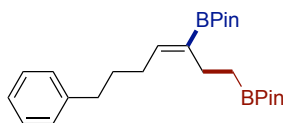


**(Z)-2,2'-(4-cyclohexylbut-3-ene-1,3-diyl)bis(4,4,5,5-tetramethyl-1,3,2-dioxaborolane) (3a)**: Following the general procedure A, using propa-1,2-dien-1-ylcyclohexane (**1a**, 30  $\mu$ L, 0.20 mmol), the crude was purified by flash column chromatography (pentane/EtOAc, gradient: 30 :1 to 15:1), to afford **3a** (60.1 mg, 77% yield) as a colorless oil. <sup>1</sup>H NMR (400 MHz, CDCl<sub>3</sub>)  $\delta$  6.00 (d, *J* = 9.2 Hz, 1H), 2.41 (m, 1H), 2.23 – 2.14 (m, 2H), 1.73 – 1.55 (m, 6H), 1.23 (s, 24H), 1.14 – 1.01 (m, 4H), 0.90 – 0.80 (m, 3H) ppm. <sup>13</sup>C NMR (101 MHz, CDCl<sub>3</sub>)  $\delta$  150.3, 82.97, 82.93, 37.2, 32.9, 26.2, 26.0, 25.01, 24.9, 24.9, 22.9 ppm.

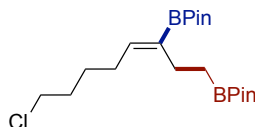


**(Z)-2,2'-(5-cyclohexylpent-3-ene-1,3-diyl)bis(4,4,5,5-tetramethyl-1,3,2-dioxaborolane) (3b)**: Following the general procedure A, using buta-2,3-dien-1-ylcyclohexane (**1b**, 27.2 mg, 0.20 mmol), the crude was purified by flash column chromatography (pentane/EtOAc, gradient: 30 :1 to 15:1), to afford **3b** (44.5 mg, 55% yield) as a colorless oil. <sup>1</sup>NMR (400 MHz, CDCl<sub>3</sub>)  $\delta$  6.21 (t, *J* = 7.2 Hz, 1H), 2.22 – 2.13 (m, 2H), 2.02 (t, *J* = 7.1 Hz, 2H), 1.75 – 1.57 (m, 6H), 1.31 (dd, *J* = 7.3, 3.8 Hz,

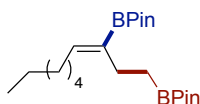
1H), 1.23 (s, 12H), 1.22 (s, 12H), 1.20 – 1.12 (m, 2H), 0.93 – 0.79 (m, 4H) ppm. <sup>13</sup>C NMR (101 MHz, CDCl<sub>3</sub>) δ 143.8, 82.9, 82.9, 38.0, 36.3, 33.5, 26.7, 26.5, 24.9, 24.9, 22.8 ppm.



**(Z)-2,2'-(7-phenylhept-3-ene-1,3-diyl)bis(4,4,5,5-tetramethyl-1,3,2-dioxaborolane) (3c):** Following the general procedure A, using hexa-4,5-dien-1-ylbenzene (**1c**, 31.6 mg, 0.20 mmol), the crude was purified by flash column chromatography (pentane/EtOAc, gradient: 30 :1 to 15:1), to afford **3c** (70.0 mg, 82% yield) as a colorless oil. <sup>1</sup>H NMR (400 MHz, CDCl<sub>3</sub>) δ 7.29 – 7.23 (m, 2H), 7.17 (dt, *J* = 8.2, 1.9 Hz, 3H), 6.24 (t, *J* = 7.1 Hz, 1H), 2.66 – 2.59 (m, 2H), 2.21 (dt, *J* = 10.5, 6.1 Hz, 4H), 1.72 (m, 2H), 1.25 (s, 12H), 1.23 (s, 12H), 0.87 (dd, *J* = 9.2, 7.5 Hz, 2H) ppm. <sup>13</sup>C NMR (101 MHz, CDCl<sub>3</sub>) δ 144.5, 142.7, 128.5, 128.4, 125.7, 83.1, 82.9, 35.8, 30.9, 28.2, 25.0, 24.9, 24.9, 22.9 ppm.

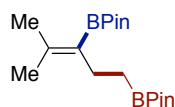


**(Z)-2,2'-(8-chlorooct-3-ene-1,3-diyl)bis(4,4,5,5-tetramethyl-1,3,2-dioxaborolane) (3d):** Following the general procedure A, using 7-chlorohepta-1,2-diene (**1d**, 26.0 mg, 0.20 mmol), the crude was purified by flash column chromatography (pentane/EtOAc, gradient: 30 :1 to 15:1), to afford **3d** (48.4 mg, 61% yield) as a colorless oil. <sup>1</sup>H NMR (400 MHz, CDCl<sub>3</sub>) δ 6.17 (t, *J* = 7.1 Hz, 1H), 3.52 (t, *J* = 6.7 Hz, 2H), 2.18 (q, *J* = 7.3 Hz, 4H), 1.84 – 1.72 (m, 2H), 1.53 (tt, *J* = 9.9, 6.3 Hz, 2H), 1.24 (s, 12H), 1.23 (s, 12H), 0.87 – 0.82 (m, 2H) ppm. <sup>13</sup>C NMR (101 MHz, CDCl<sub>3</sub>) δ 143.9, 83.1, 82.9, 45.1, 32.4, 27.6, 26.6, 25.0, 24.9, 24.8, 22.8 ppm.



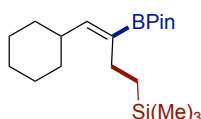
**(Z)-2,2'-(dec-3-ene-1,3-diyl)bis(4,4,5,5-tetramethyl-1,3,2-dioxaborolane) (3e):** Following the general procedure A, using nona-1,2-diene (**1e**, 24.8 mg, 0.20 mmol), the crude was purified by flash column chromatography (pentane/EtOAc, gradient: 30 :1 to 15:1), to afford **3e** (53.3 mg, 68% yield) as a colorless oil. <sup>1</sup>H NMR (400 MHz, CDCl<sub>3</sub>) δ 6.21 (t, *J* = 7.1 Hz, 1H), 2.24 – 2.16 (m, 2H), 2.14 (q, *J* = 7.1 Hz, 2H), 1.31 –

1.26 (m, 6H), 1.24 (s, 12H), 1.23 (s, 12H), 0.90 – 0.82 (m, 6H) ppm. <sup>13</sup>C NMR (101 MHz, CDCl<sub>3</sub>) δ 145.3, 83.0, 82.9, 31.9, 29.3, 28.5, 25.0, 24.9, 22.8, 22.7, 14.2 ppm.



### 2,2'-(4-methylpent-3-ene-1,3-diyl)bis(4,4,5,5-tetramethyl-1,3,2-dioxaborolane)

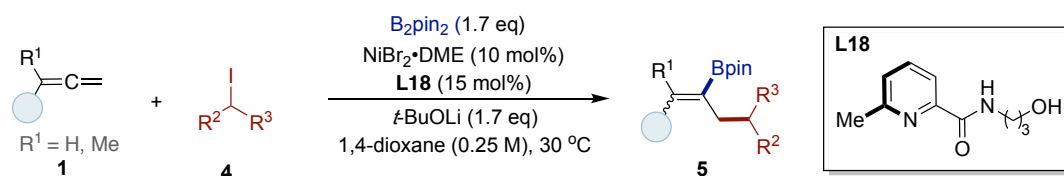
**(3f)**: Following the general procedure A, using 3-methylbuta-1,2-diene (**1f**, 13.6 mg, 0.20 mmol), the crude was purified by flash column chromatography (pentane/EtOAc, gradient: 30 :1 to 15:1), to afford **3f** (31.2 mg, 46% yield) as a colorless oil. <sup>1</sup>H NMR (400 MHz, CDCl<sub>3</sub>) δ 2.24 – 2.14 (m, 2H), 1.91 (d, *J* = 0.9 Hz, 3H), 1.73 (s, 3H), 1.26 (s, 12H), 1.23 (s, 12H), 0.83 – 0.76 (m, 2H) ppm. <sup>13</sup>C NMR (101 MHz, CDCl<sub>3</sub>) δ 145.5, 82.9, 82.8, 25.2, 24.9, 24.9, 24.8, 20.9 ppm.



### (Z)-(4-cyclohexyl-3-(4,4,5,5-tetramethyl-1,3,2-dioxaborolan-2-yl)but-3-en-1-yl)trimethylsilane

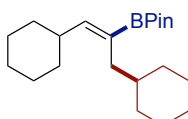
**(3j)**: Following the general procedure A, using propa-1,2-dien-1-ylcyclohexane (**1a**, 30 μL, 0.20 mmol) and (bromomethyl)trimethylsilane (**2b**, 66.8 mg, 0.40 mmol), the crude was purified by flash column chromatography (pentane/EtOAc, gradient: 50 :1 to 25:1), to afford **3j** (22.8 mg, 34% yield) as a colorless oil. <sup>1</sup>H NMR (400 MHz, CDCl<sub>3</sub>) δ 5.98 (d, *J* = 9.3 Hz, 1H), 2.39 – 2.26 (m, 1H), 2.12 – 2.03 (m, 2H), 1.71 – 1.54 (m, 6H), 1.25 (s, 12H), 1.19 – 1.05 (m, 4H), 0.58 – 0.49 (m, 2H), 0.00 (s, 9H) ppm. <sup>13</sup>C NMR (101 MHz, CDCl<sub>3</sub>) δ 149.3, 83.0, 37.5, 32.9, 26.2, 26.1, 24.9, 22.8, 18.5, -1.5 ppm.

## 4.6.4 General Procedure of Ni-Catalyzed 1,1-Alkylboration of Allenes with Alkyl iodides and B<sub>2</sub>Pin<sub>2</sub>



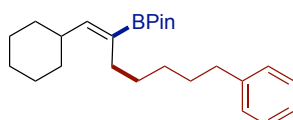
General procedure B: An oven-dried 8 mL screw-cap test tube containing a stirring bar was charged with NiBr<sub>2</sub>·DME (17.3 mg, 10 mol%), *N*-(3-hydroxypropyl)-6-methylpicolinamide (**L18**, 5.8 mg, 15 mol%), B<sub>2</sub>Pin<sub>2</sub> (86.3 mg, 0.34 mmol).

Subsequently, the tube was put into the glove-box under N<sub>2</sub> atmosphere, and *t*-BuOLi (0.34 mmol, 27.0 mg) was added in the glove-box. Then the tube was sealed with a Teflon-lined screw cap and taken outside from the glove-box. Afterwards, the corresponding allene (**1**, 0.20 mmol, 1.0 equiv), alkyl iodide (**4**, 0.40 mmol, 2.0 equiv) and 1,4-dioxane (0.8 mL) were added via syringe, independently. Then, the tube was stirred at 30 °C for 15 h. After the reaction was completed, the mixture was diluted with EtOAc, filtered through silica gel and concentrated under vacuum. The corresponding product **5a-5b** were purified by flash column chromatography on silica gel.



**(Z)-2-(1,3-dicyclohexylprop-1-en-2-yl)-4,4,5,5-tetramethyl-1,3,2-dioxaborolane**

**(5a)**: Following the general procedure B, using propa-1,2-dien-1-ylcyclohexane (**1a**, 30  $\mu$ L, 0.20 mmol) and iodocyclohexane (**4a**, 60  $\mu$ L, 0.40 mmol), the crude was purified by flash column chromatography (pentane/EtOAc, gradient: 50 :1 to 25:1), to afford **5a** (36.9 mg, 55% yield) as a colorless oil. <sup>1</sup>H NMR (400 MHz, CDCl<sub>3</sub>)  $\delta$  6.09 (d, *J* = 9.6 Hz, 1H), 2.36 – 2.28 (m, 1H), 2.02 (dd, *J* = 7.1, 1.1 Hz, 2H), 1.71 – 1.62 (m, 13H), 1.24 (s, 12H), 1.17 – 1.06 (m, 8H) ppm. <sup>13</sup>C NMR (101 MHz, CDCl<sub>3</sub>)  $\delta$  151.7, 83.1, 39.0, 36.4, 33.5, 32.7, 26.8, 26.7, 26.3, 26.1, 24.8 ppm.



**(Z)-2-(1-cyclohexyl-7-phenylhept-1-en-2-yl)-4,4,5,5-tetramethyl-1,3,2-**

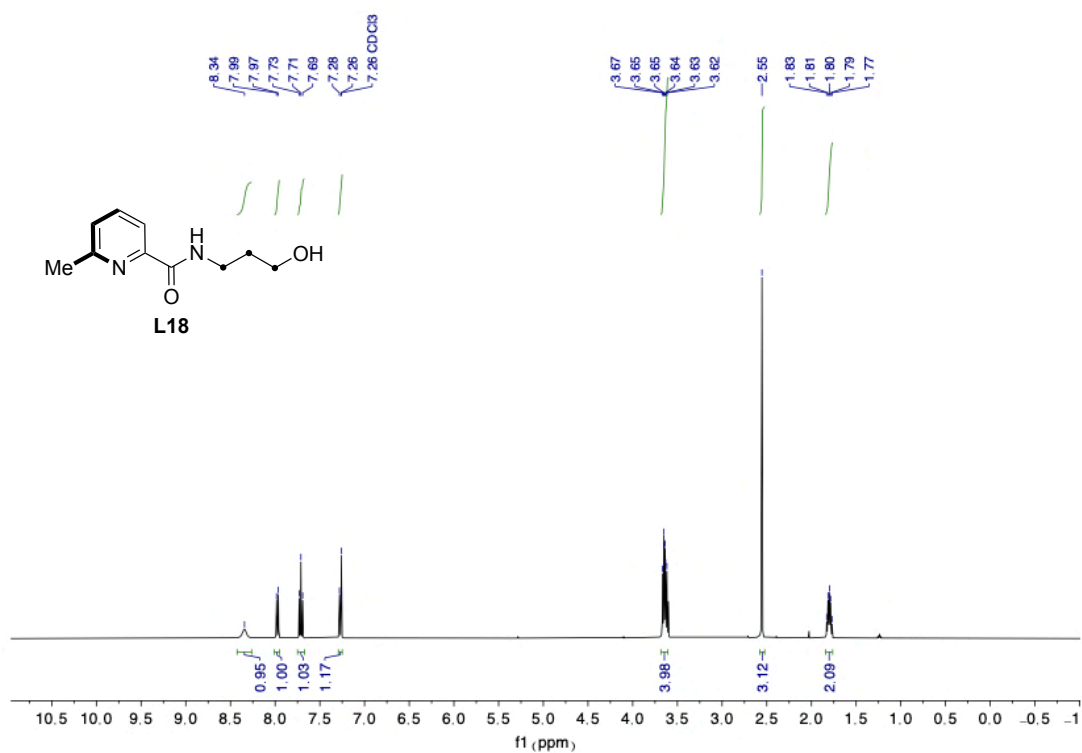
**dioxaborolane (5b)**: Following the general procedure B, using propa-1,2-dien-1-ylcyclohexane (**1a**, 30  $\mu$ L, 0.20 mmol) and (4-iodobutyl)benzene (**4b**, 70  $\mu$ L, 0.40 mmol), the crude was purified by flash column chromatography (pentane/EtOAc, gradient: 50 :1 to 25:1), to afford **5b** (16.7 mg, 22% yield) as a colorless oil. <sup>1</sup>H NMR (400 MHz, CDCl<sub>3</sub>)  $\delta$  7.38 – 7.30 (m, 2H), 7.25 (d, *J* = 8.0 Hz, 2H), 6.15 (d, *J* = 9.4 Hz, 1H), 2.71 – 2.63 (m, 2H), 2.48 – 2.35 (m, 1H), 2.19 (t, *J* = 6.9 Hz, 2H), 1.83 – 1.58 (m, 8H), 1.45 – 1.40 (m, 4H), 1.32 (s, 12H), 1.25 – 1.12 (m, 4H) ppm. <sup>13</sup>C NMR (101 MHz, CDCl<sub>3</sub>)  $\delta$  151.3, 143.2, 128.6, 128.3, 125.6, 83.1, 37.6, 36.1, 32.9, 31.6, 30.6, 29.3, 28.7, 26.2, 26.1, 24.9 ppm.

---

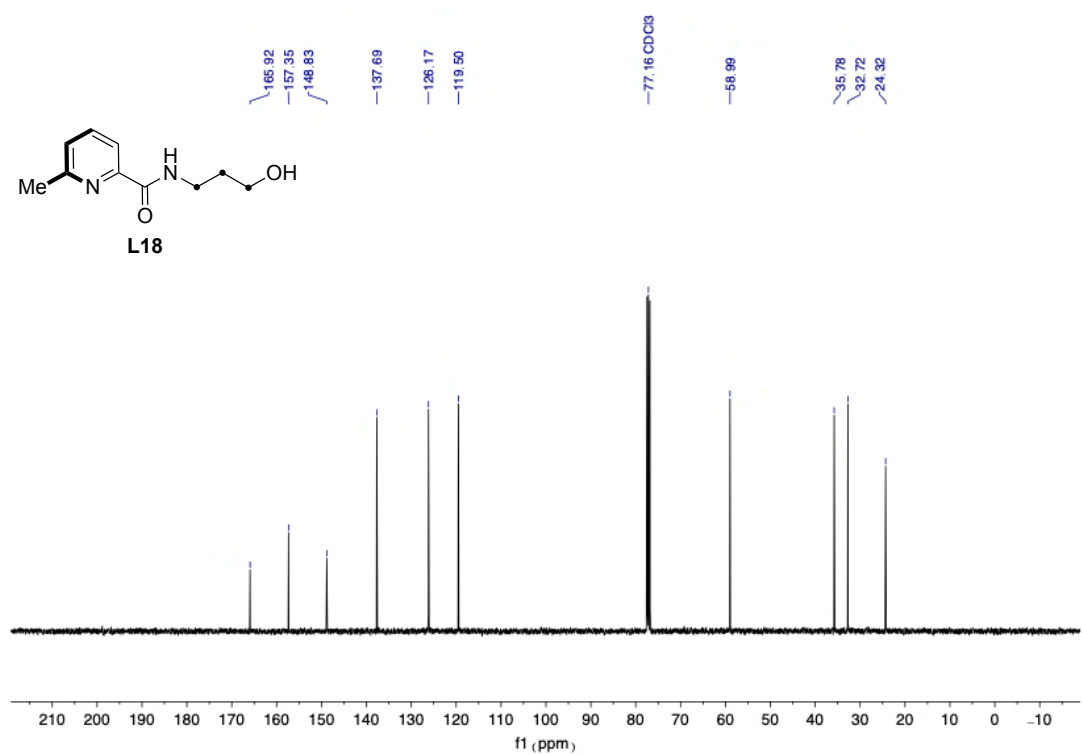
#### 4.6.5 References of Experimental Procedures

1. Sun, S-Z.; Talavera, L.; Spieß, P.; Day, C. S.; Martin, R. *sp*<sup>3</sup> Bis-organometallic reagents via catalytic 1,1-difunctionalization of unactivated olefins. *Angew. Chem. Int. Ed.* **2021**, *60*, 11740.
2. Li, Y.; Pang, H.; Wu, D.; Li, Z.; Wang, W.; Wei, H.; Fu, Y.; Yin, G. Nickel-catalyzed 1,1-alkylboration of electronically unbiased terminal alkenes. *Angew. Chem. Int. Ed.* **2019**, *58*, 8872.
3. Li, Z.; Zhang, .; Nishiura, M.; Luo, .; Luo, Y.; Hou, Z. Enantioselective cyanoborylation of allenes by *N*-heterocyclic carbene-copper catalysts. *ACS Catal.* **2020**, *10*, 11685.

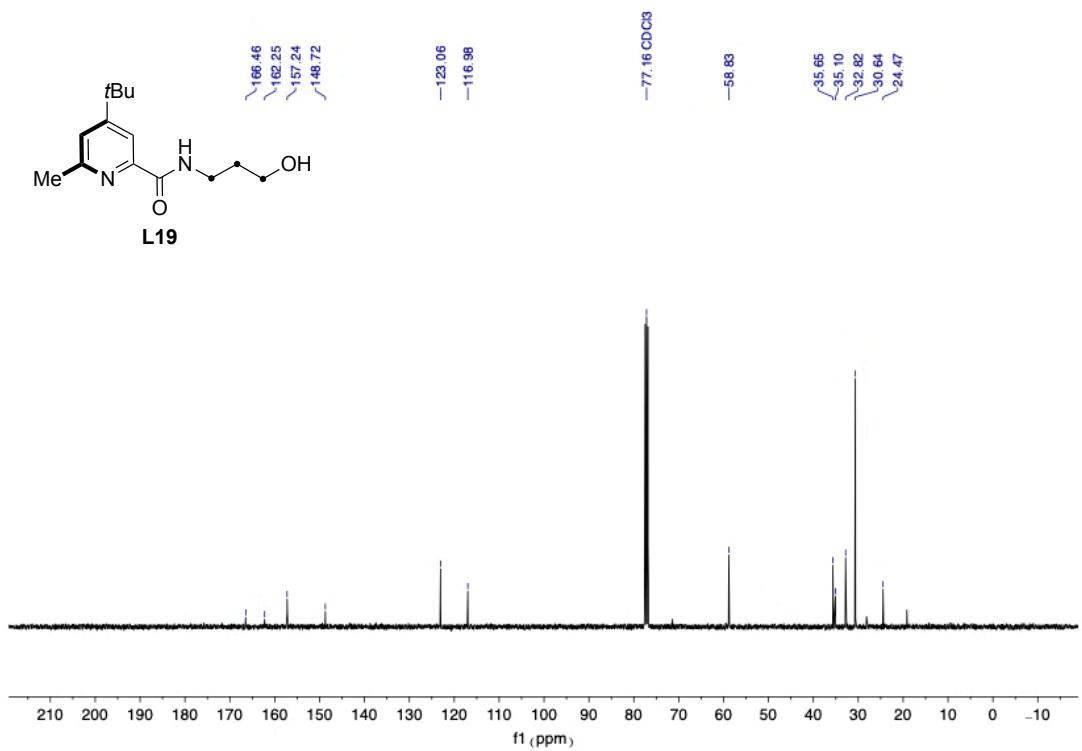
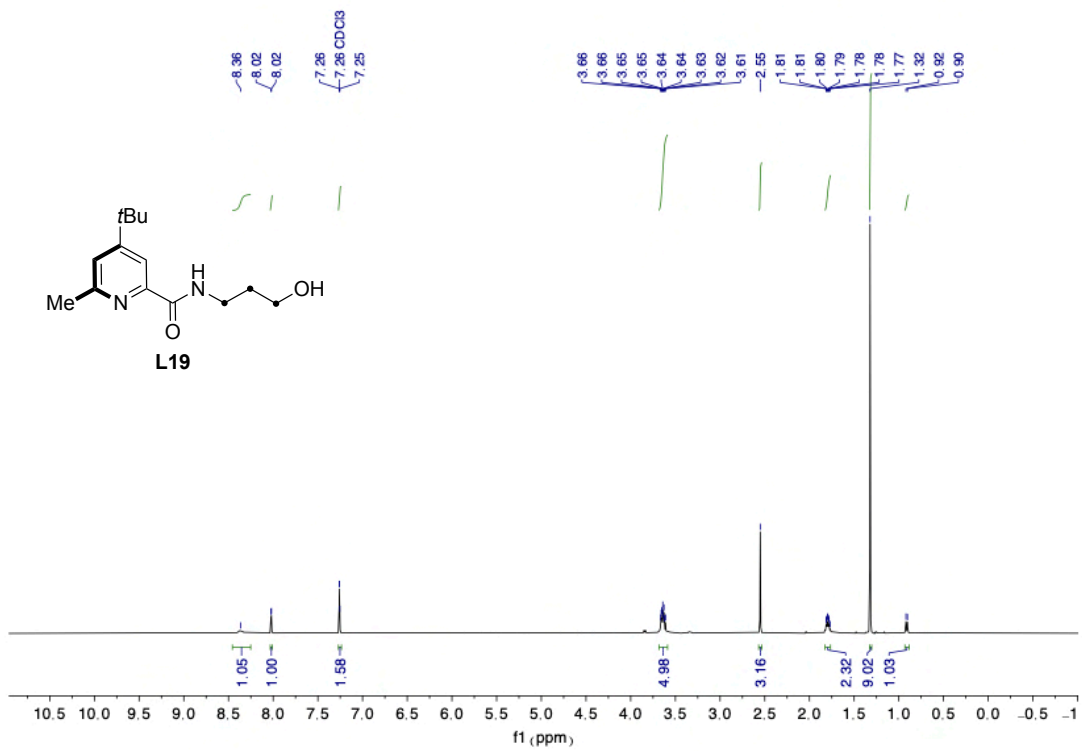
## 4.6.6 NMR Spectra

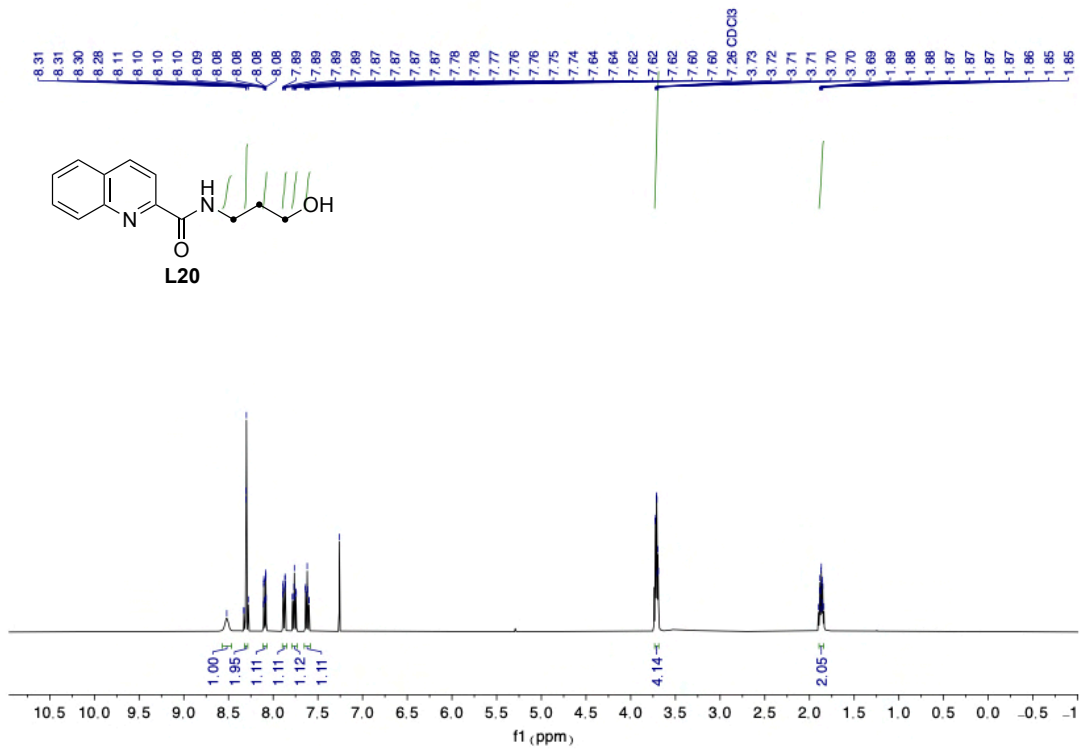


<sup>1</sup>H NMR (400 MHz, CDCl<sub>3</sub>) of **L18**

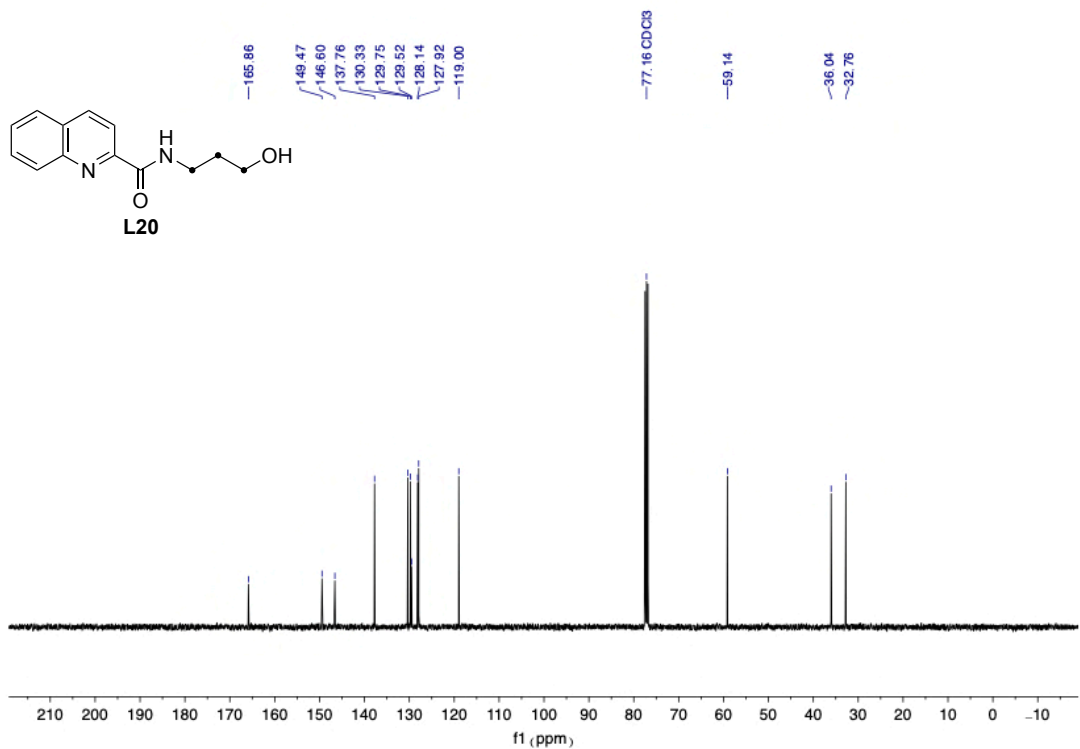


<sup>13</sup>C NMR (101 MHz, CDCl<sub>3</sub>) of **L18**



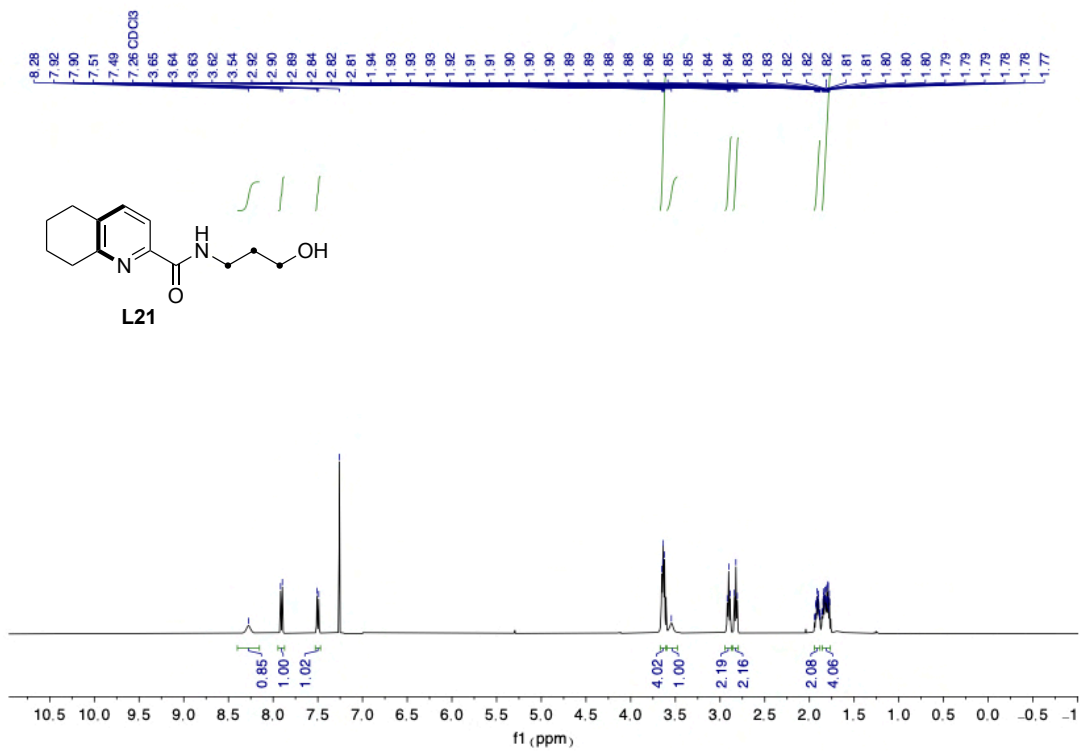


**<sup>1</sup>H NMR (400 MHz, CDCl<sub>3</sub>) of L20**

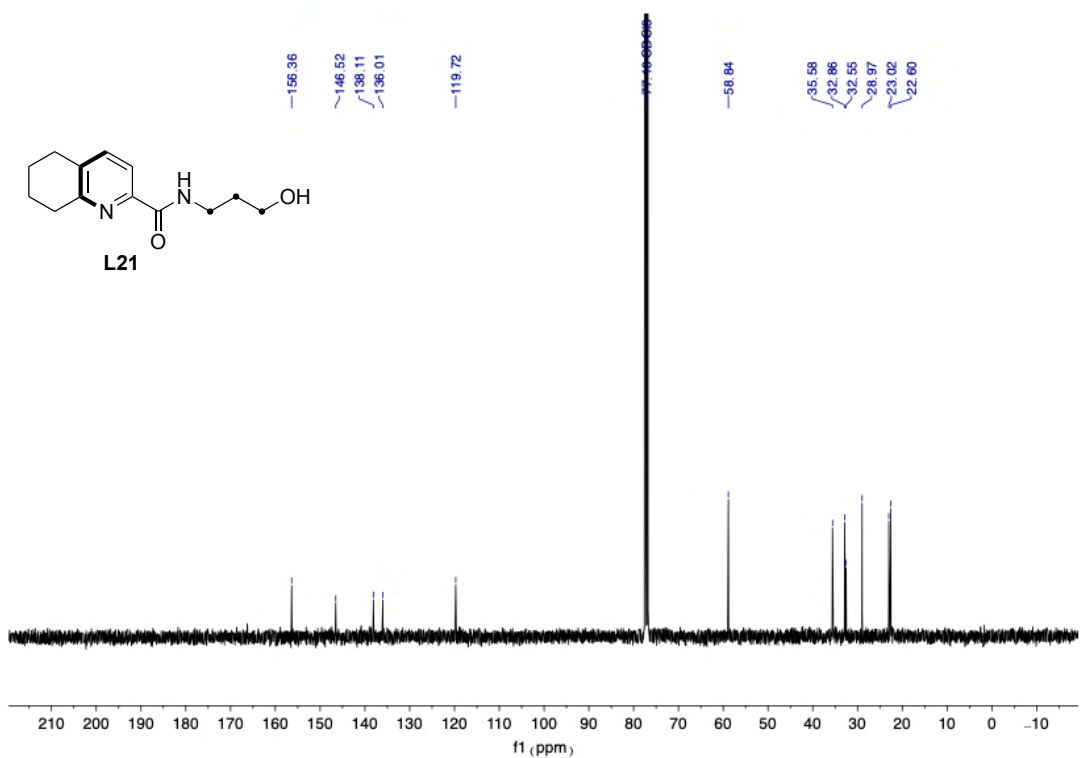


**<sup>13</sup>C NMR (101 MHz, CDCl<sub>3</sub>) of L20**

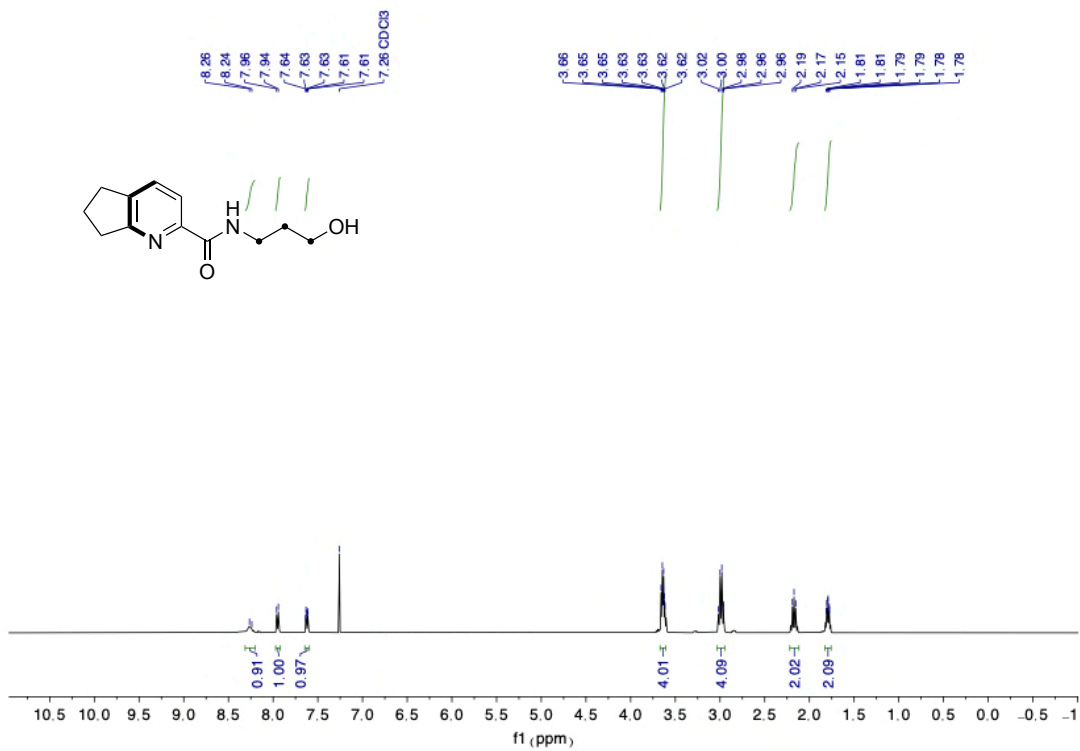




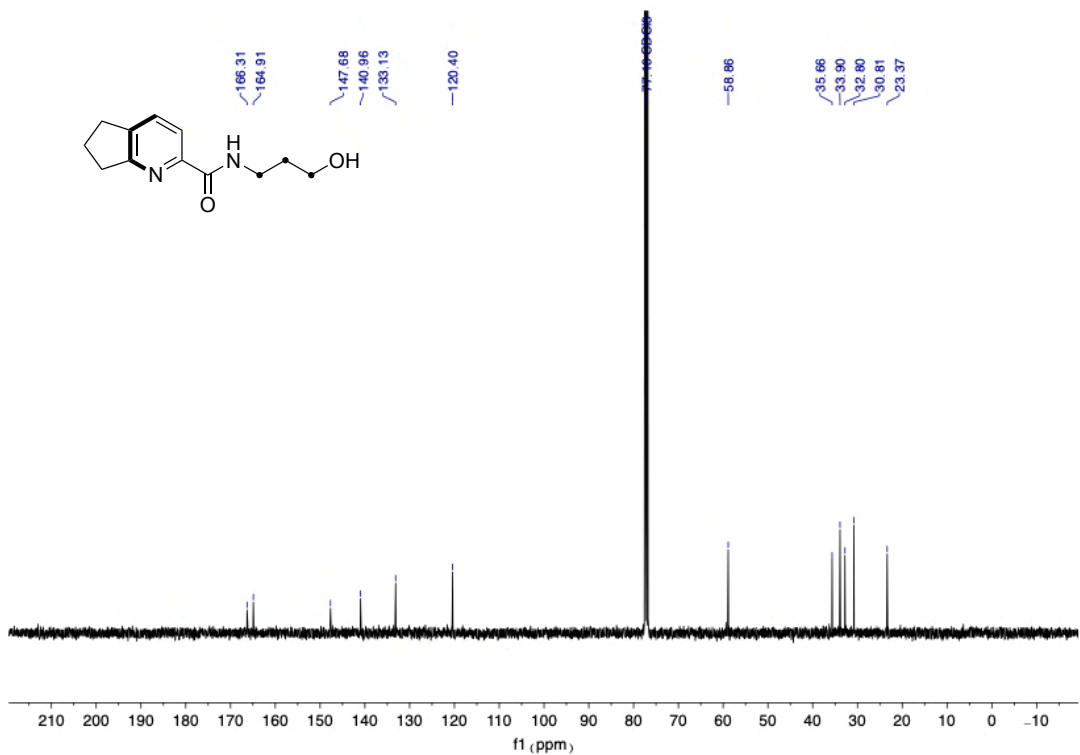
<sup>1</sup>H NMR (400 MHz, CDCl<sub>3</sub>) of L21



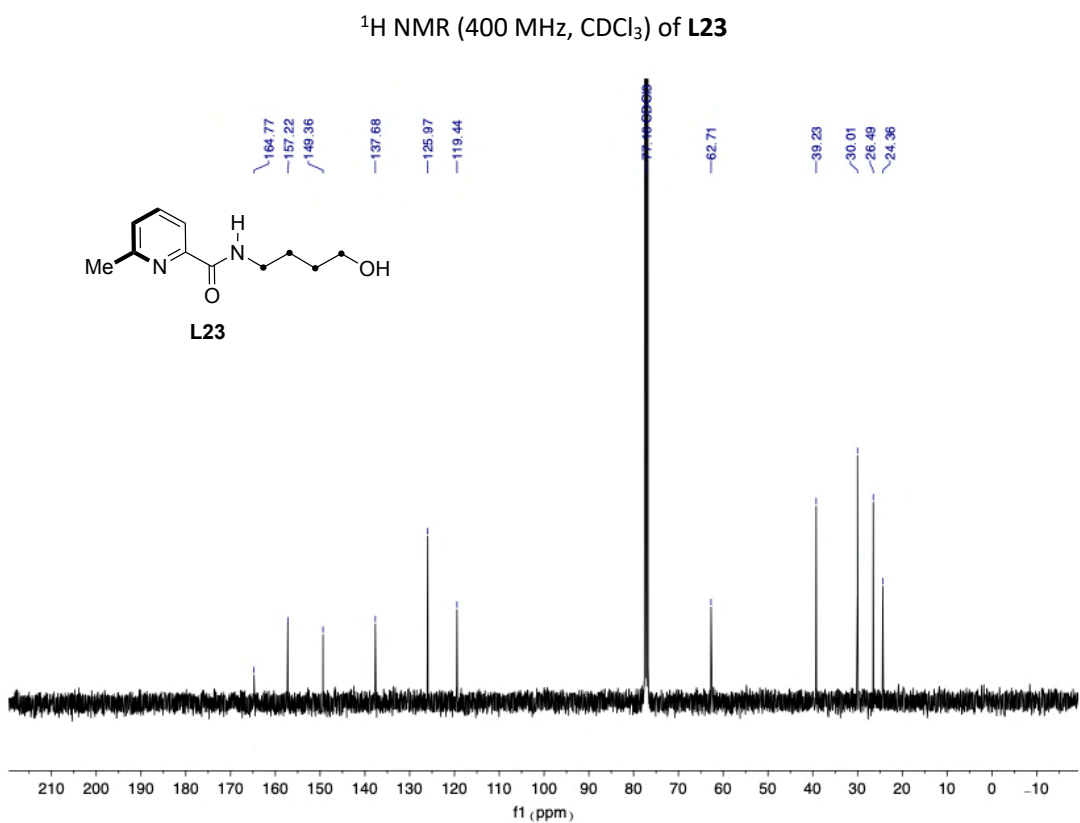
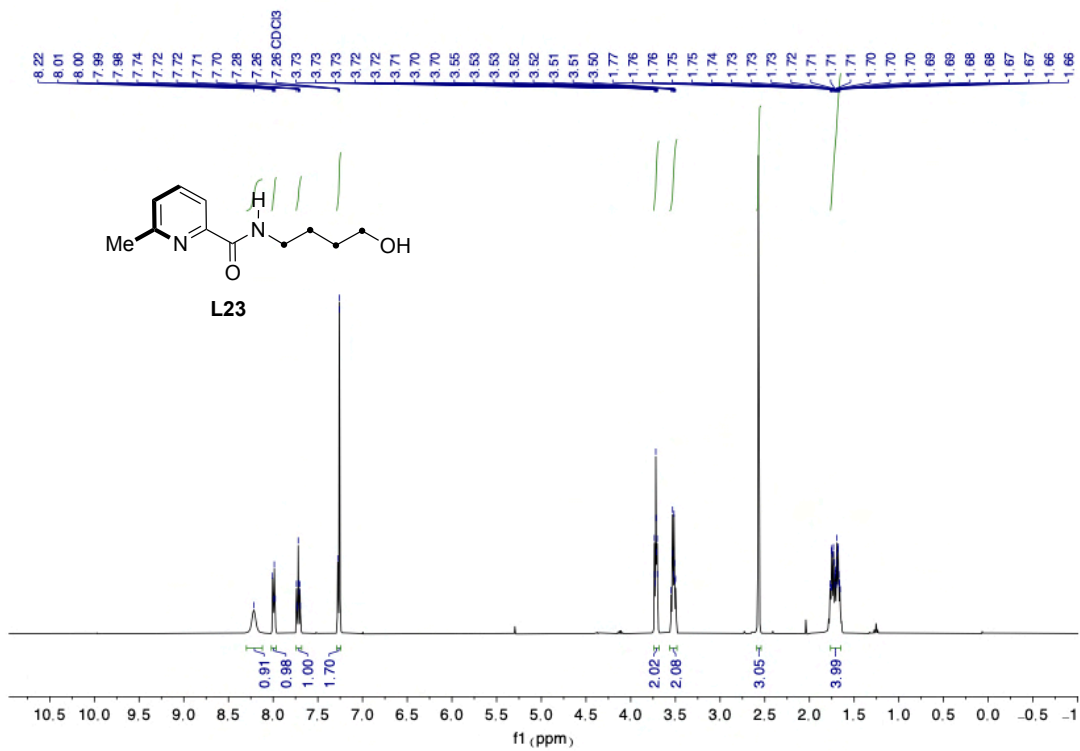
<sup>13</sup>C NMR (101 MHz, CDCl<sub>3</sub>) of L21

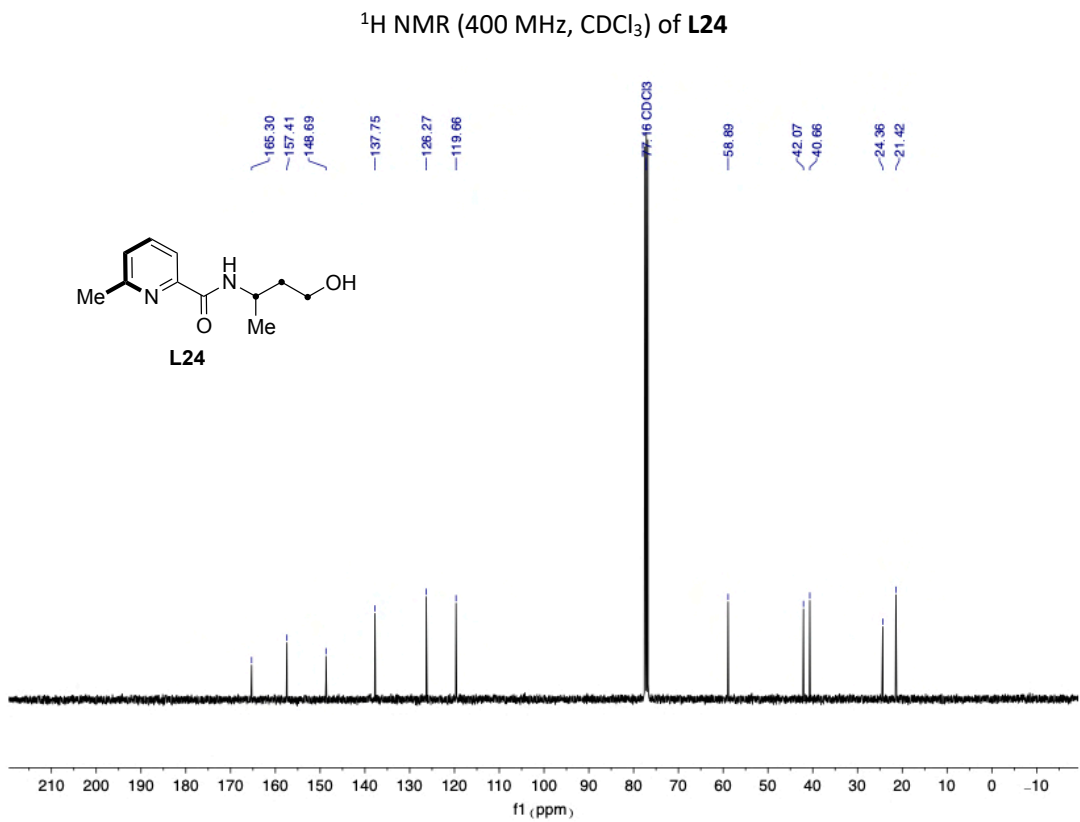
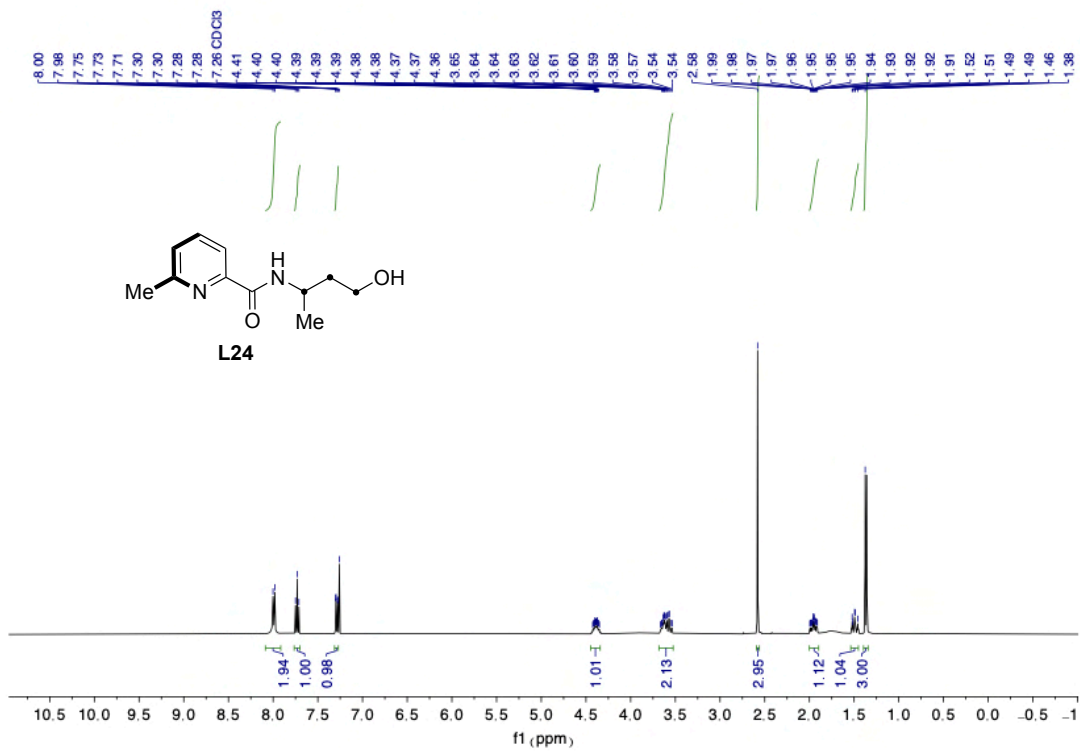


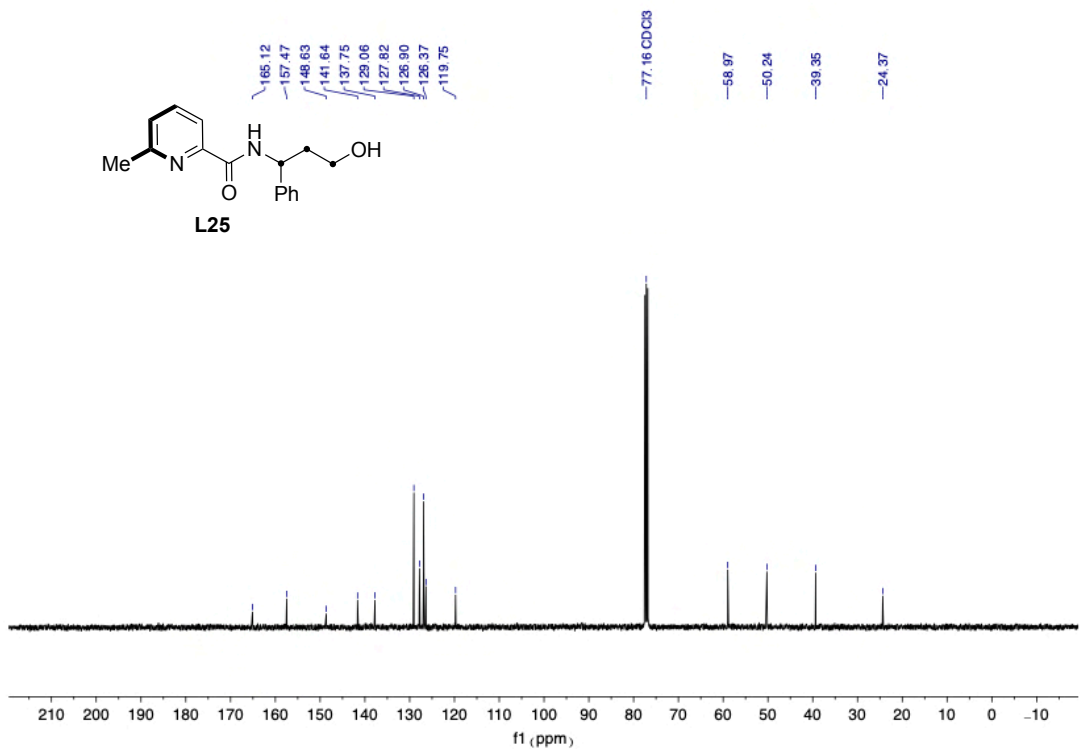
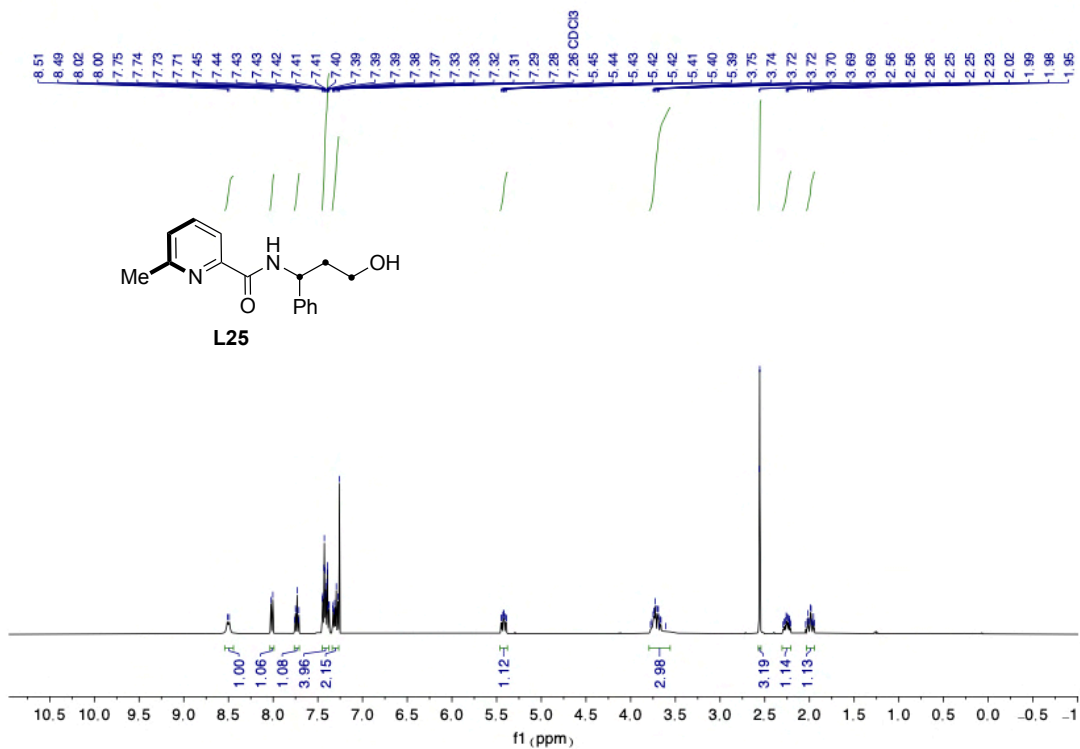
**<sup>1</sup>H NMR (400 MHz, CDCl<sub>3</sub>) of L22**

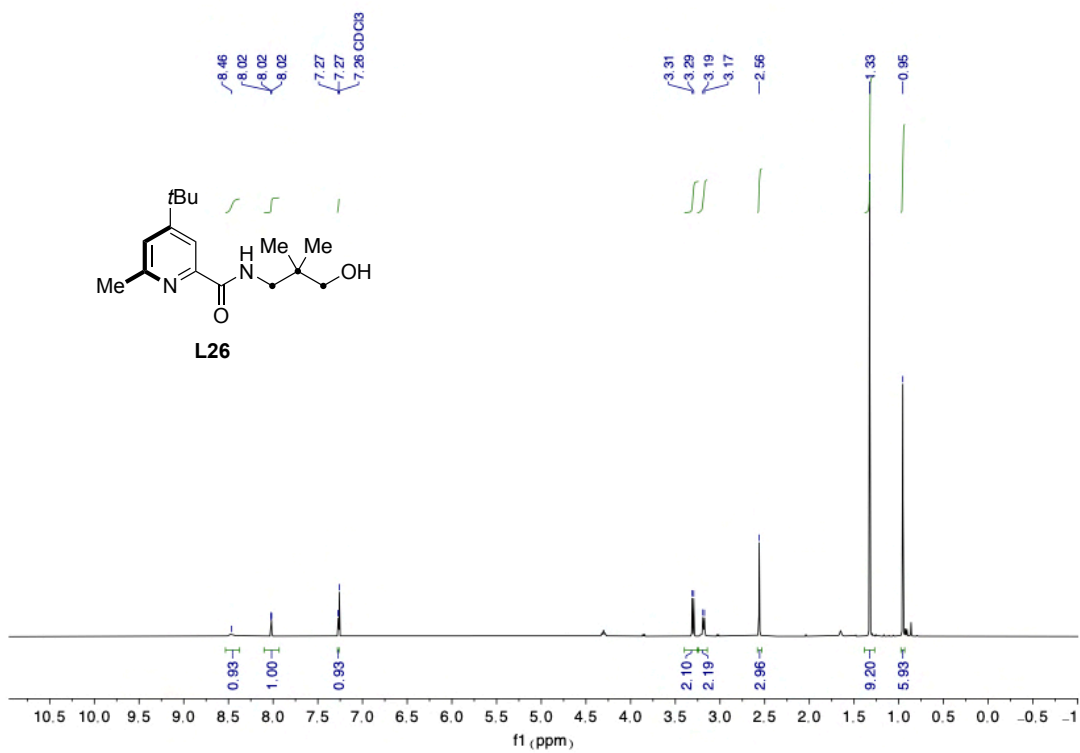


**<sup>13</sup>C NMR (101 MHz, CDCl<sub>3</sub>) of L22**

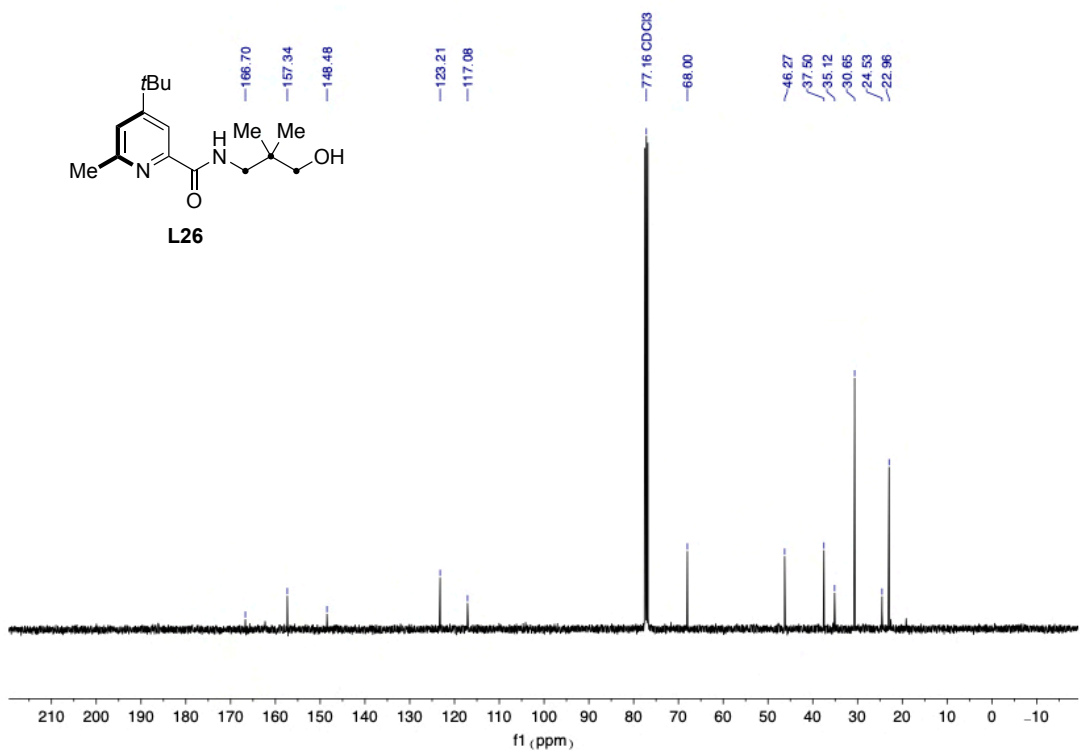




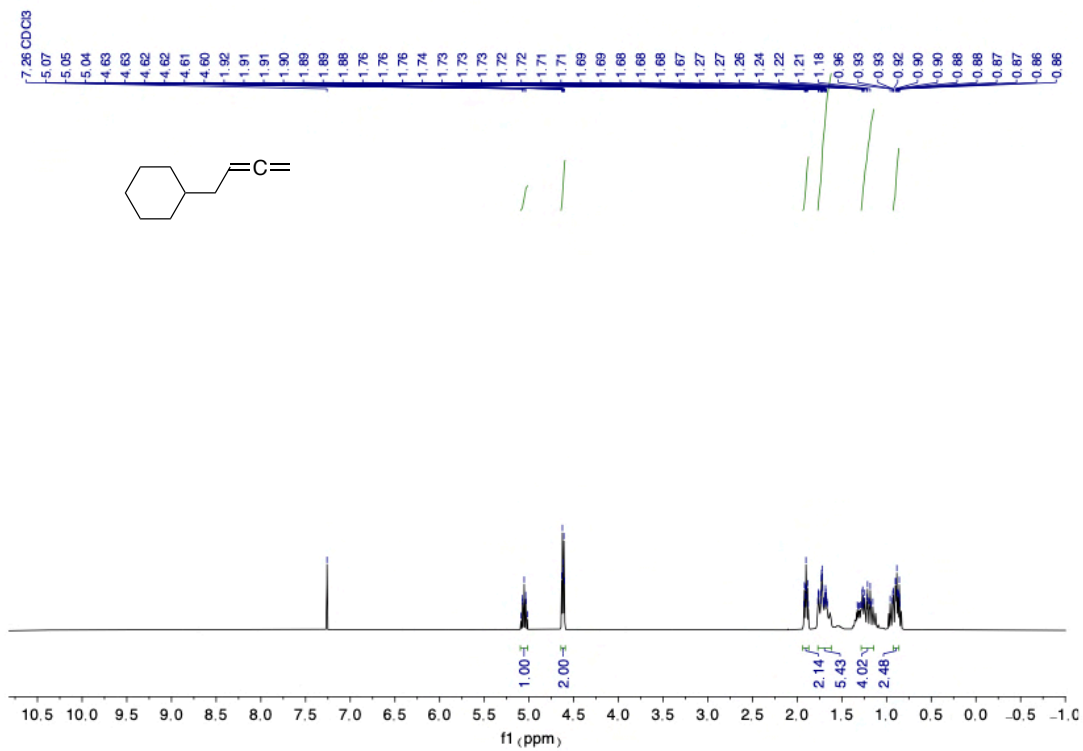




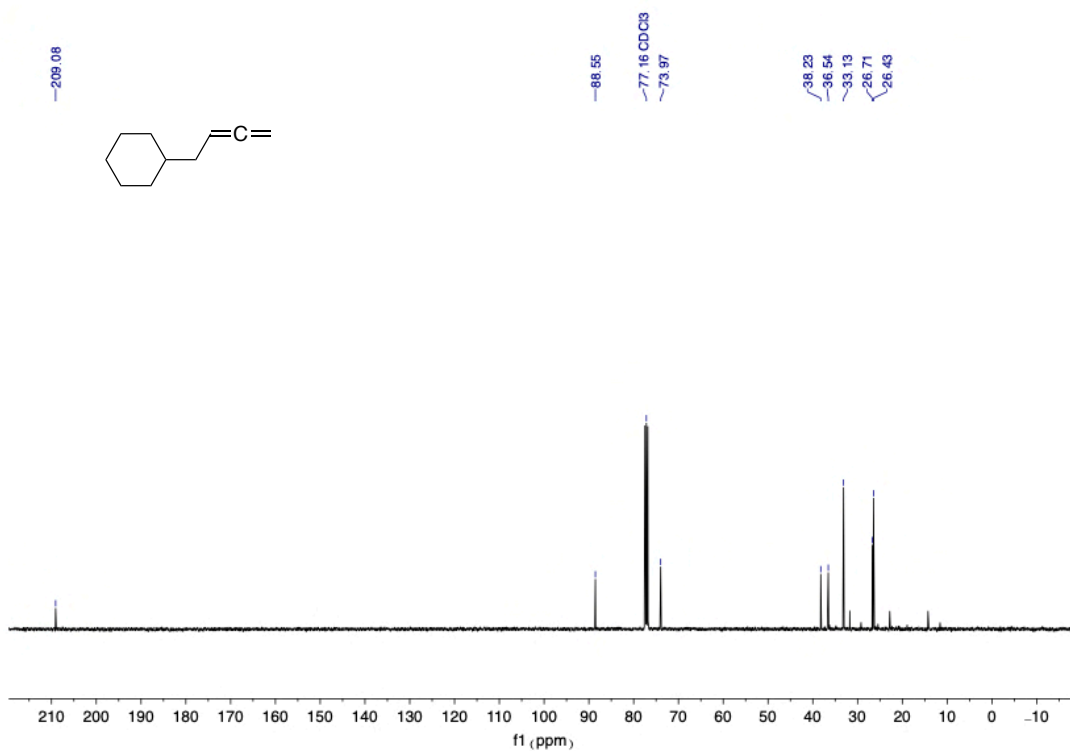
<sup>1</sup>H NMR (400 MHz, CDCl<sub>3</sub>) of L26



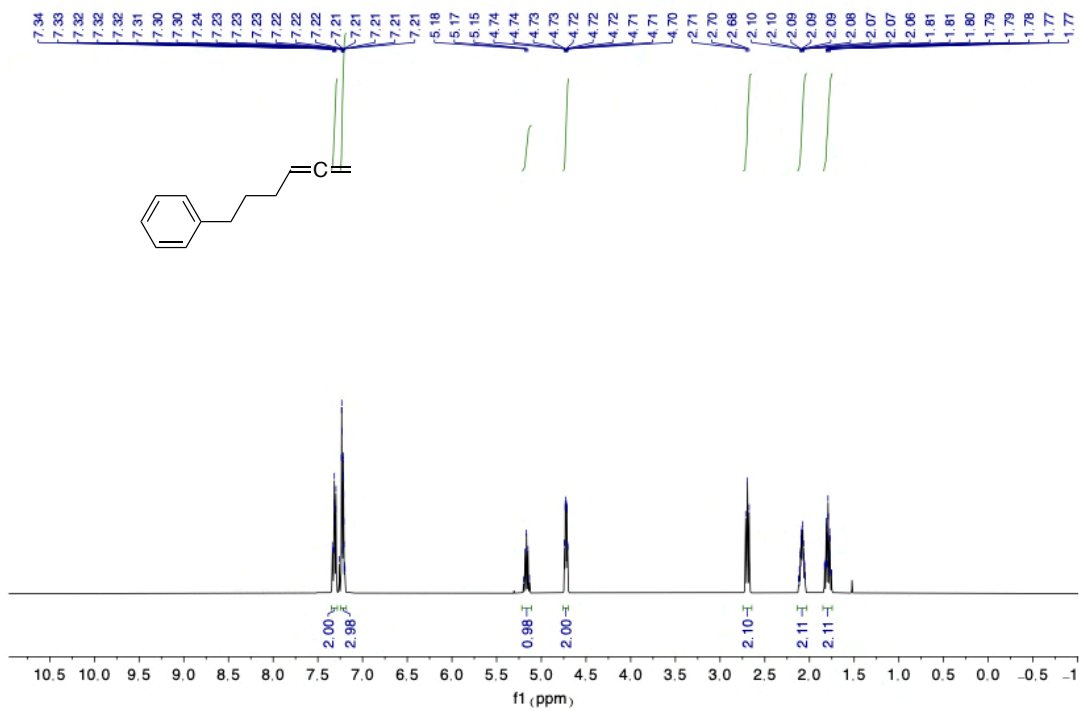
<sup>13</sup>C NMR (101 MHz, CDCl<sub>3</sub>) of L26



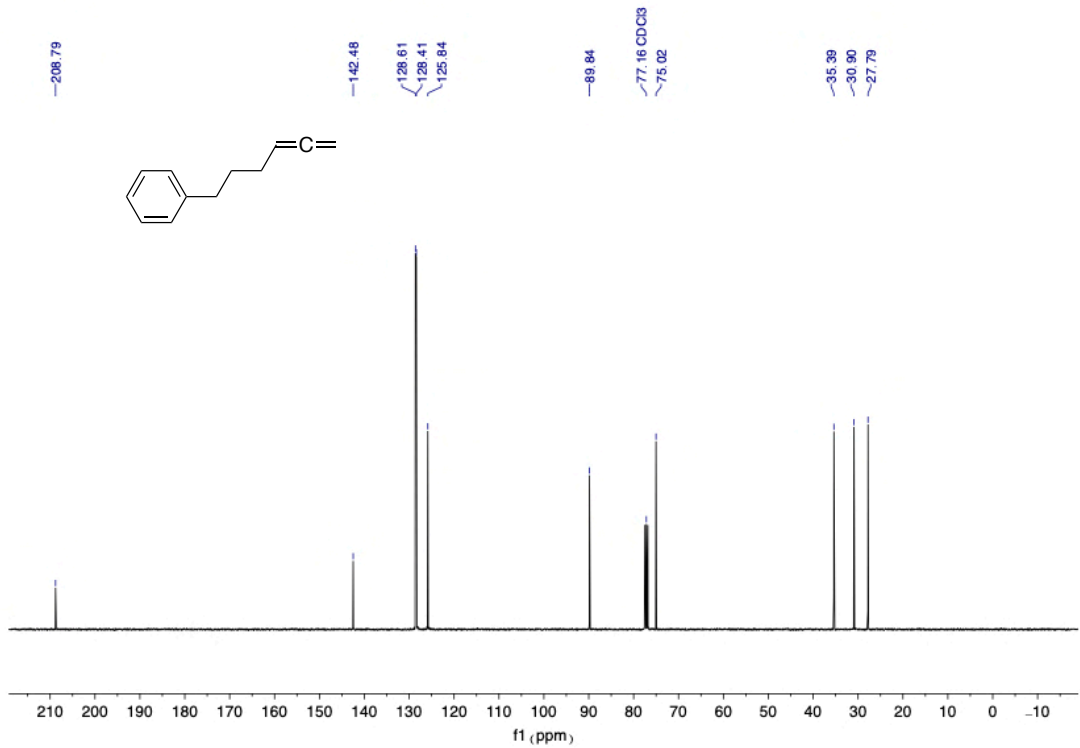
<sup>1</sup>H NMR (400 MHz, CDCl<sub>3</sub>) of **1b**



<sup>13</sup>C NMR (101 MHz, CDCl<sub>3</sub>) of **1b**

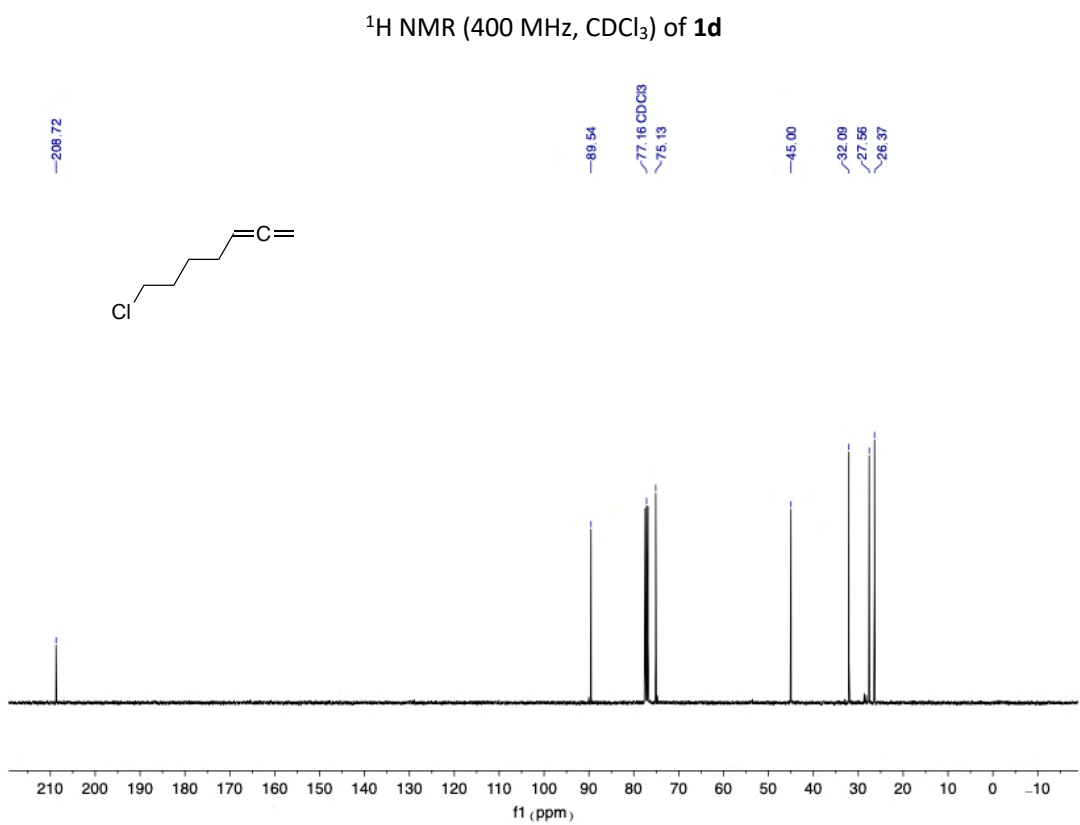
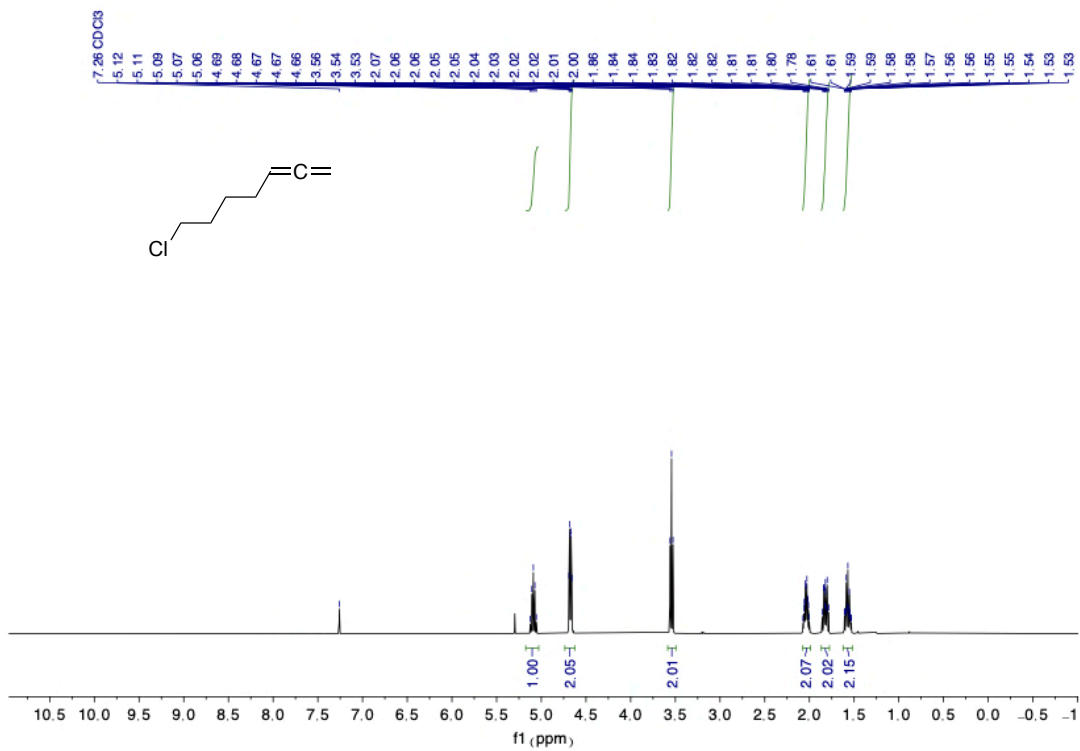


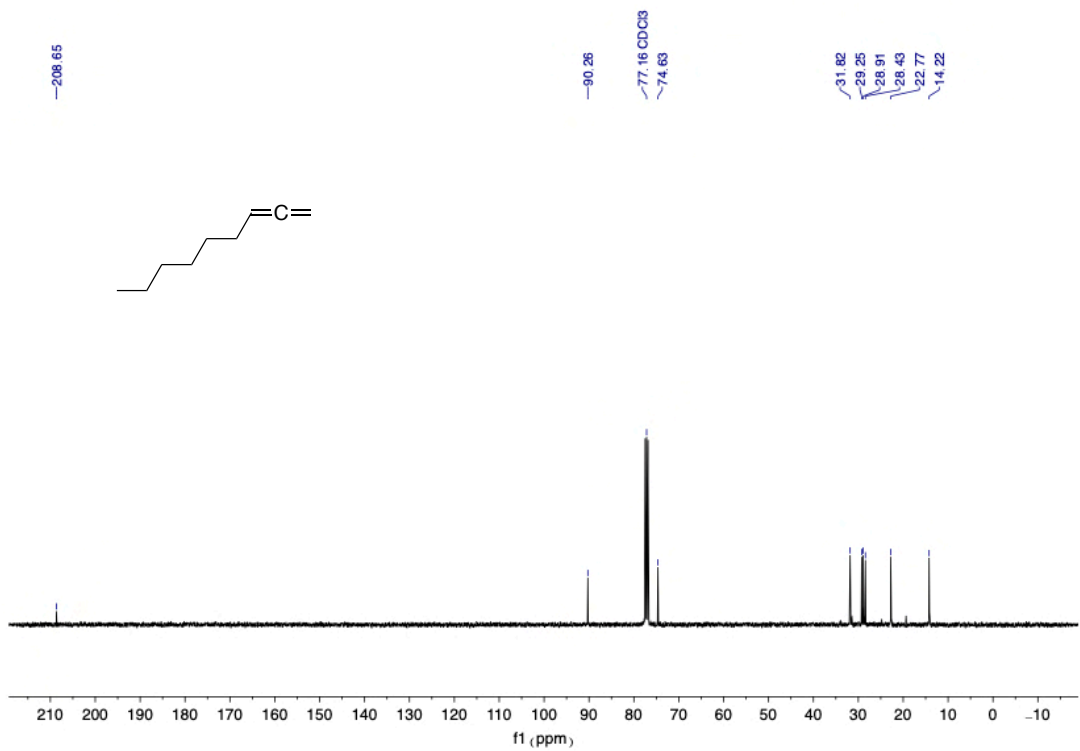
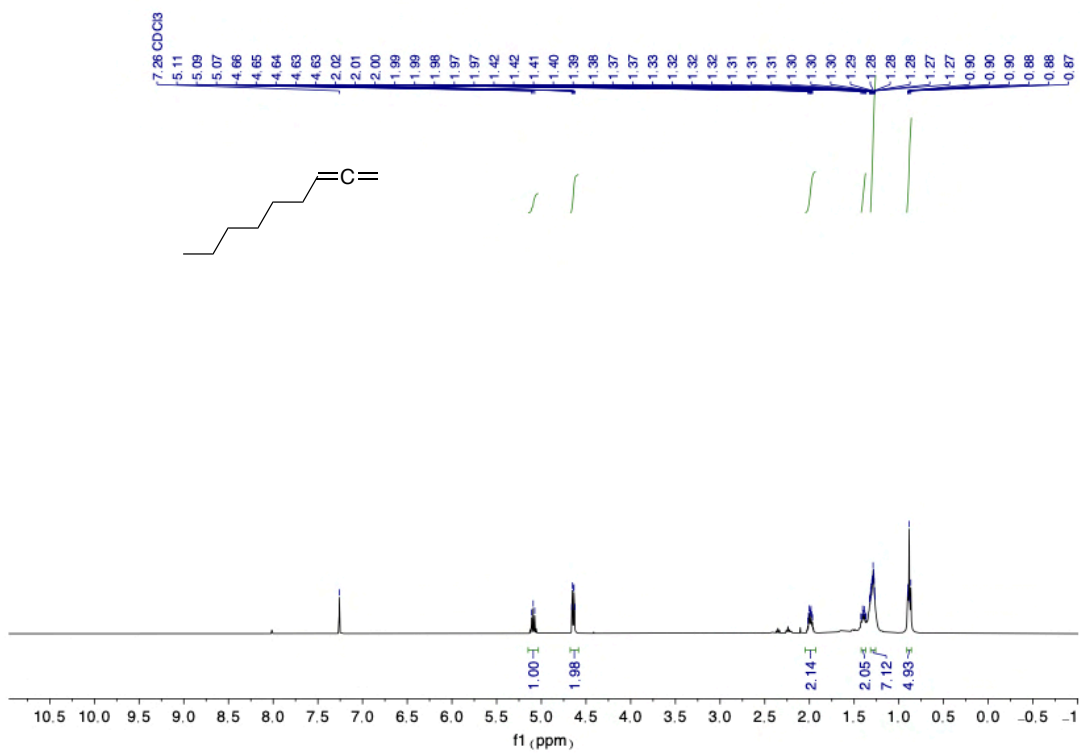
$^1\text{H}$  NMR (400 MHz,  $\text{CDCl}_3$ ) of **1c**

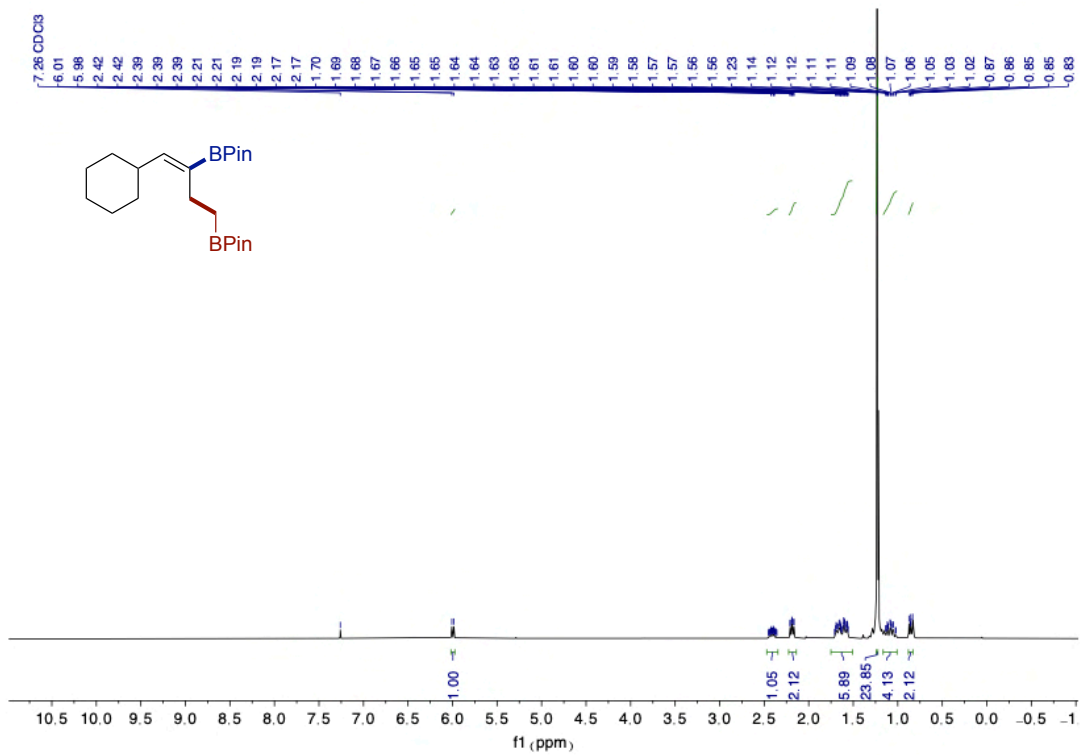


$^{13}\text{C}$  NMR (101 MHz,  $\text{CDCl}_3$ ) of **1c**

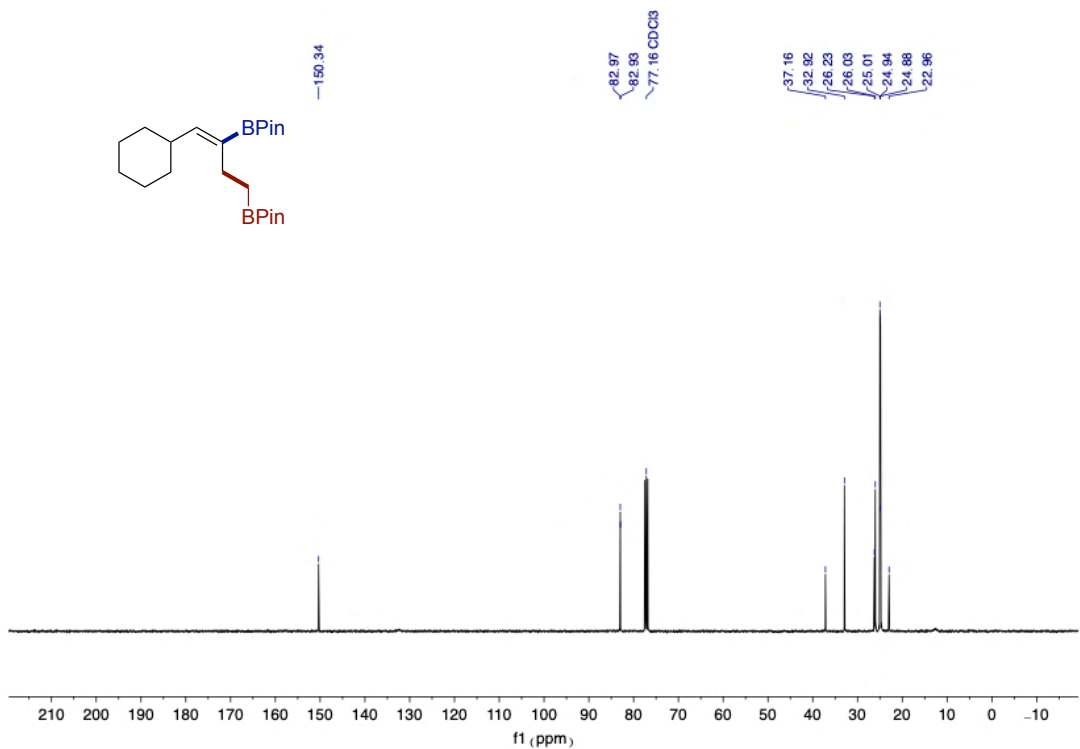




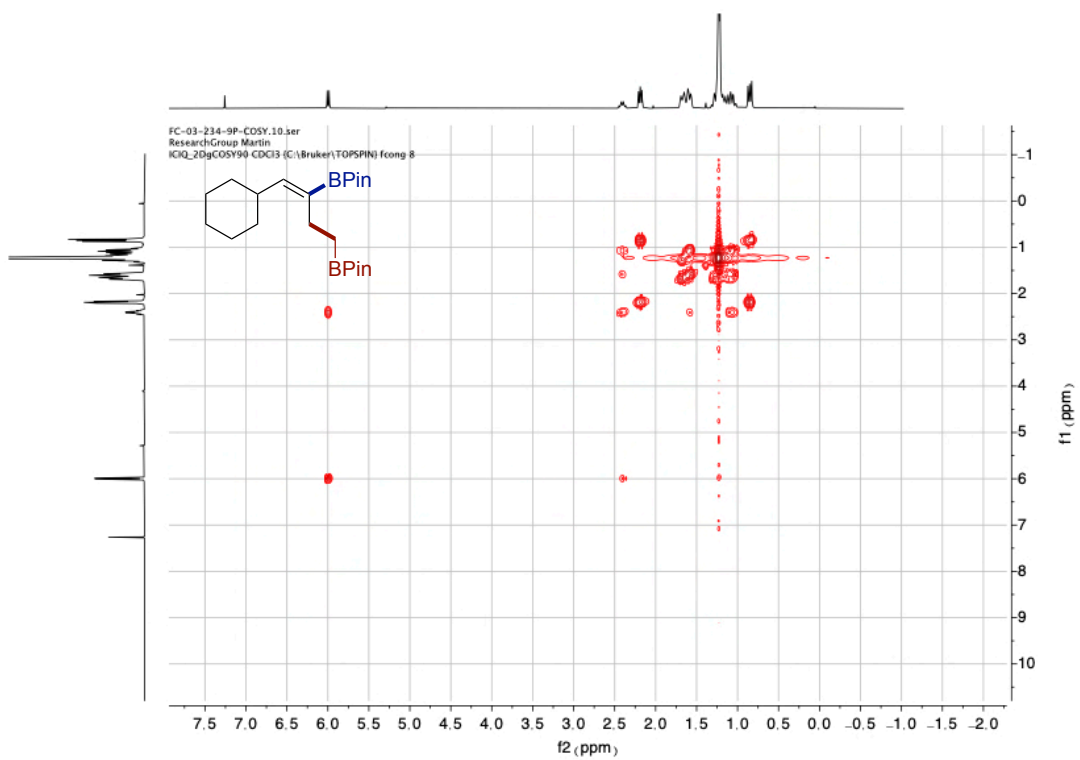




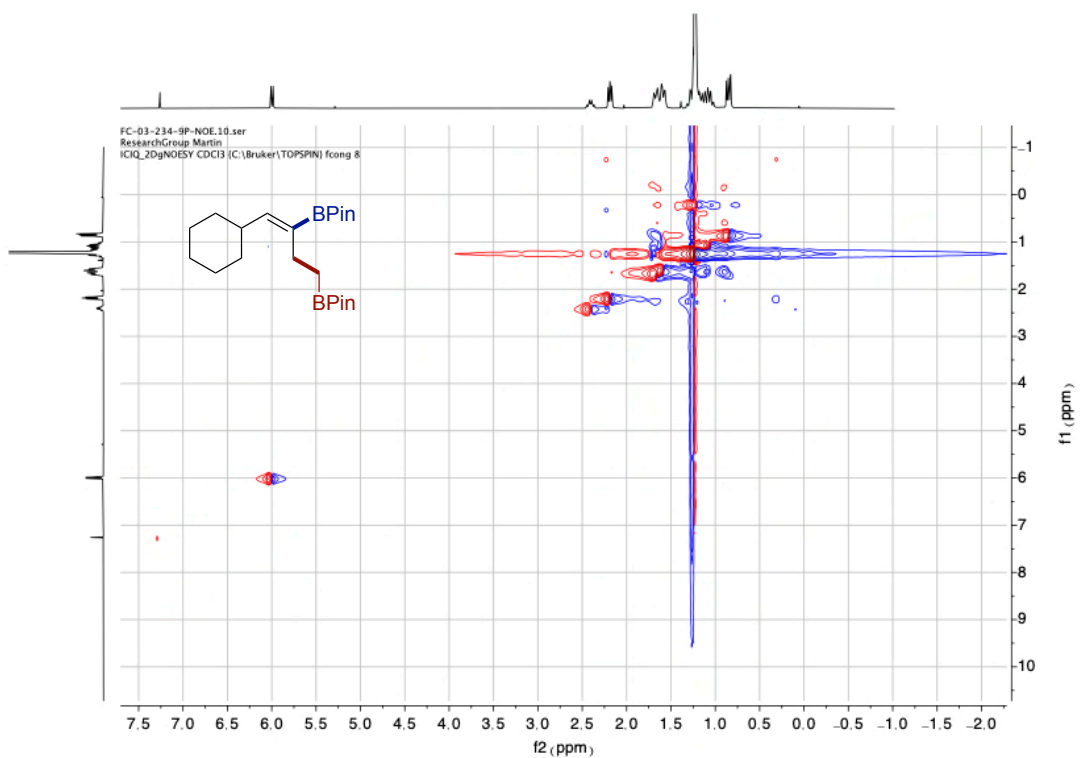
<sup>1</sup>H NMR (400 MHz, CDCl<sub>3</sub>) of **3a**



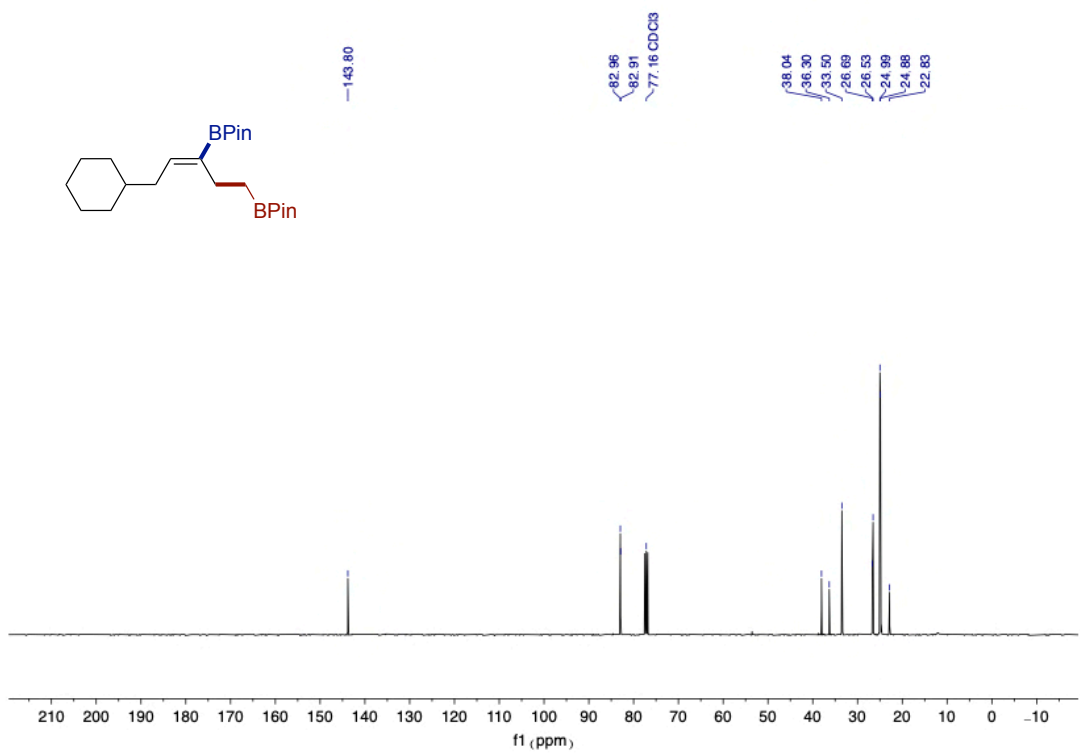
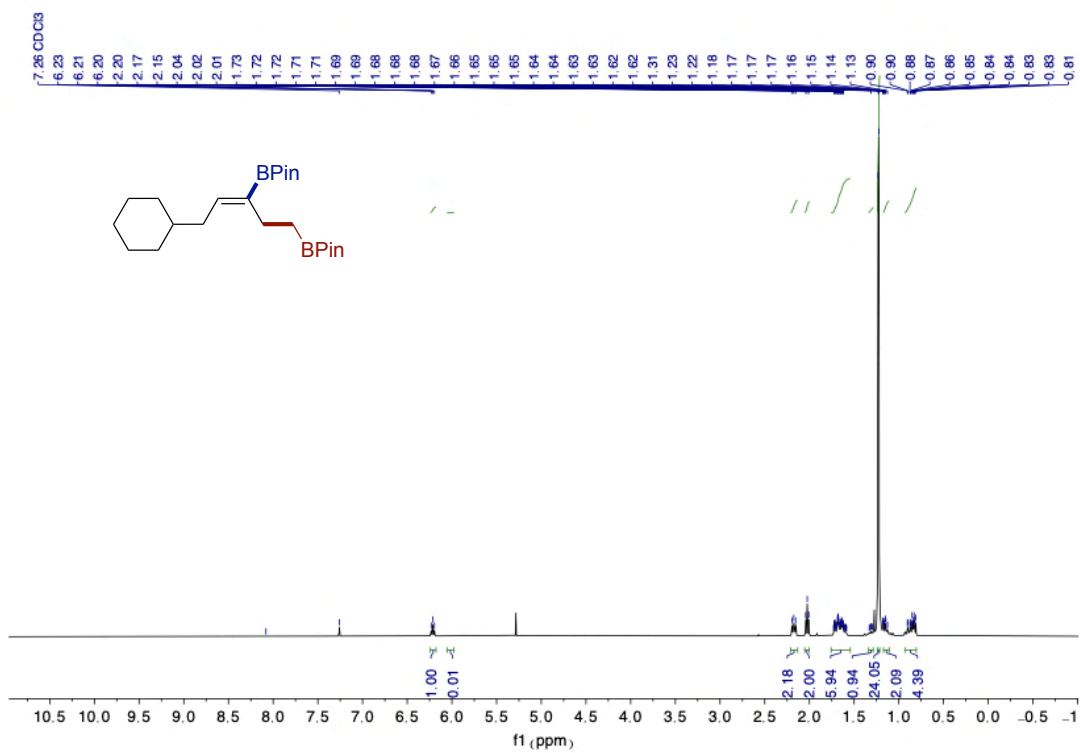
<sup>13</sup>C NMR (101 MHz, CDCl<sub>3</sub>) of **3a**

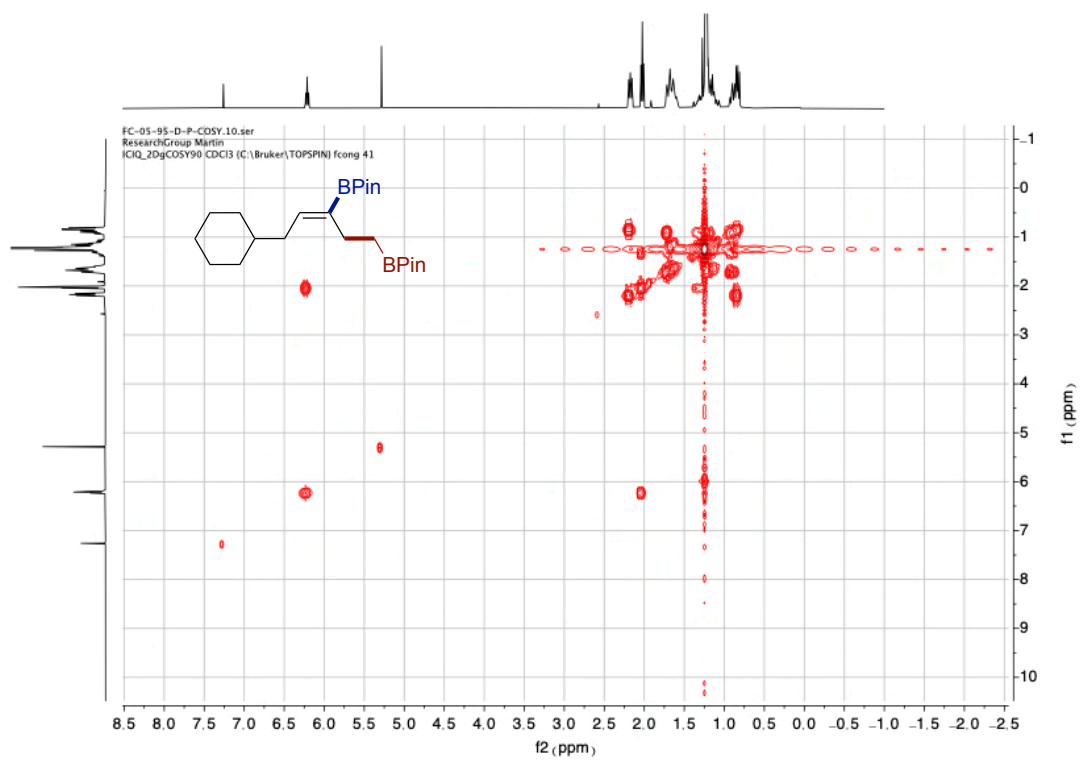


COSY of **3a**

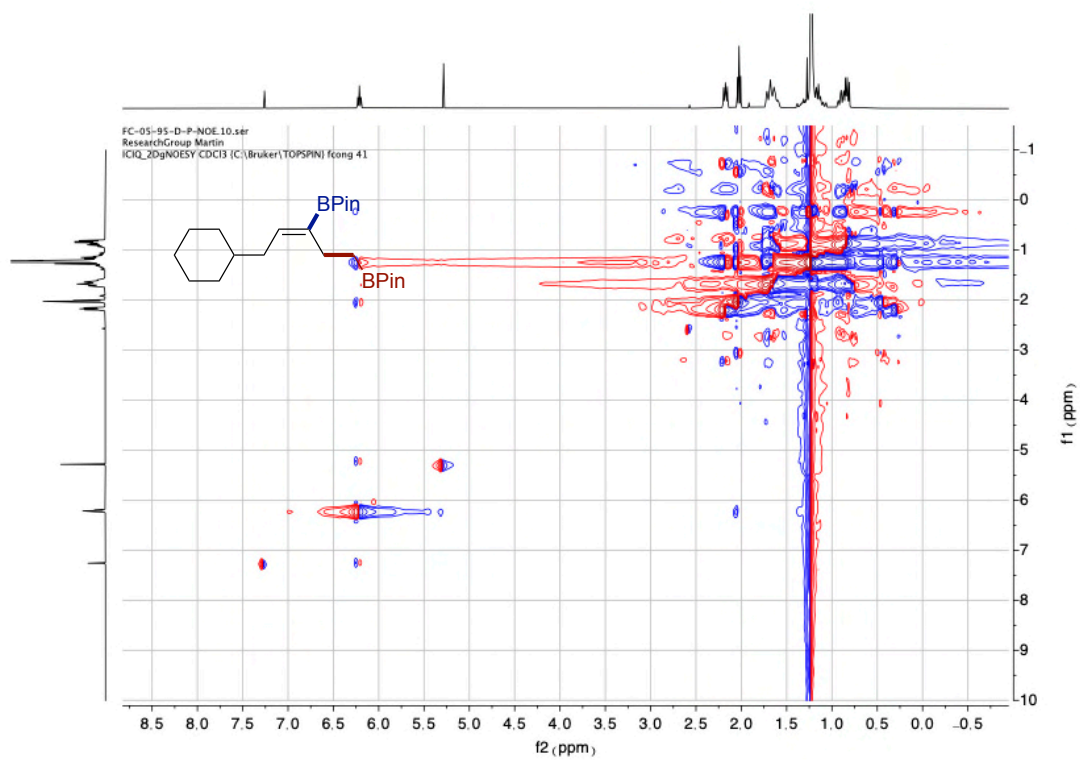


NOESY of **3a**

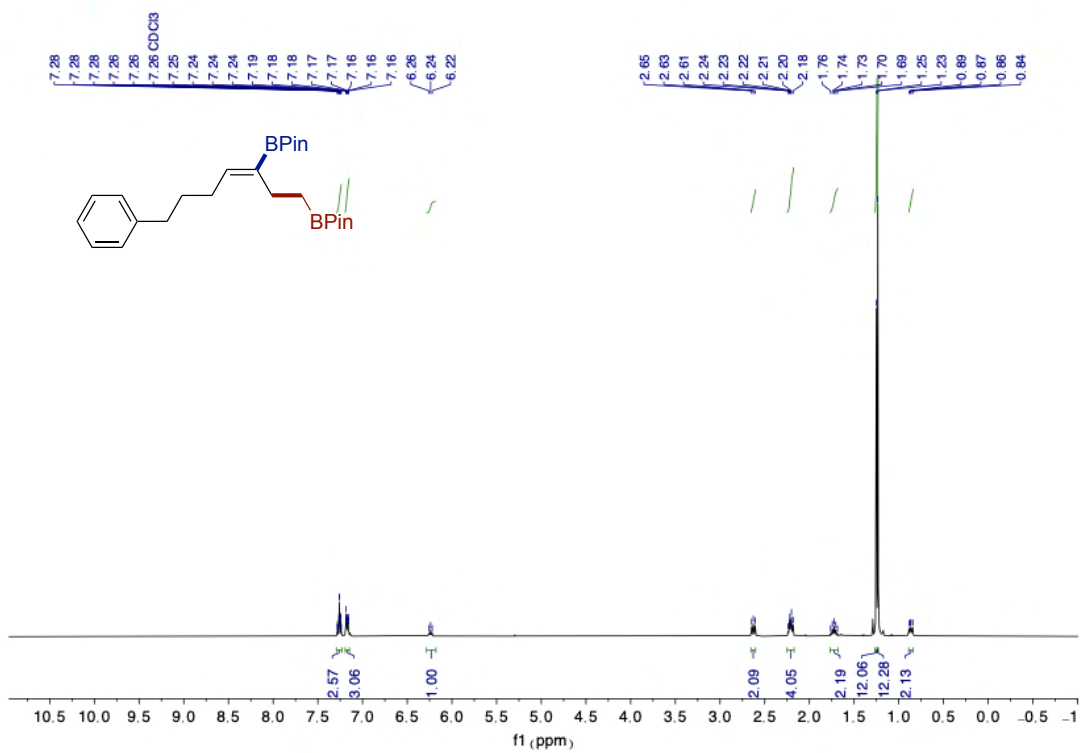




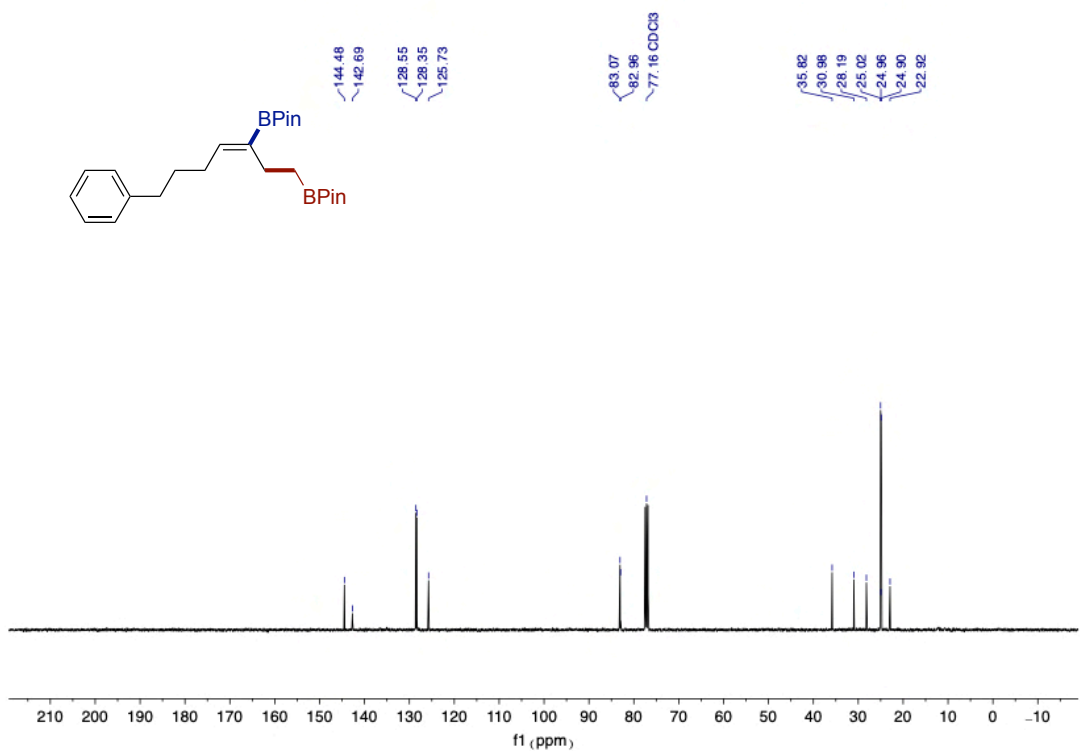
COSY of **3b**



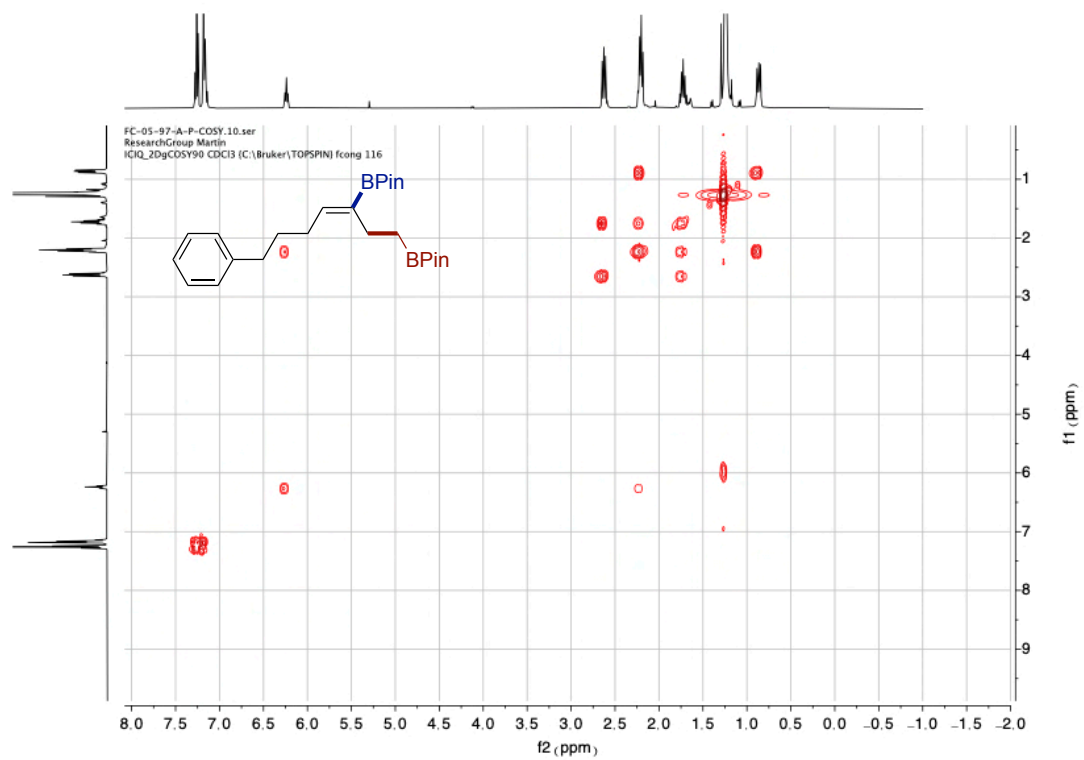
NOESY of **3b**



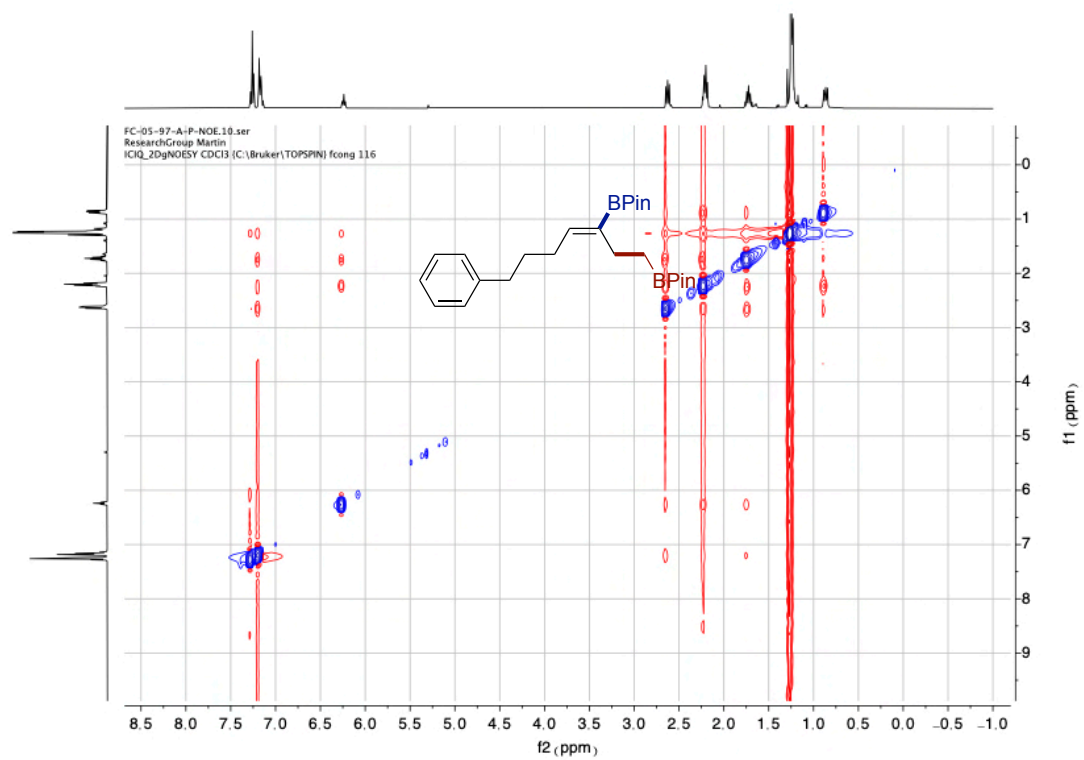
**<sup>1</sup>H NMR (400 MHz, CDCl<sub>3</sub>) of 3c**



**<sup>13</sup>C NMR (101 MHz, CDCl<sub>3</sub>) of 3c**

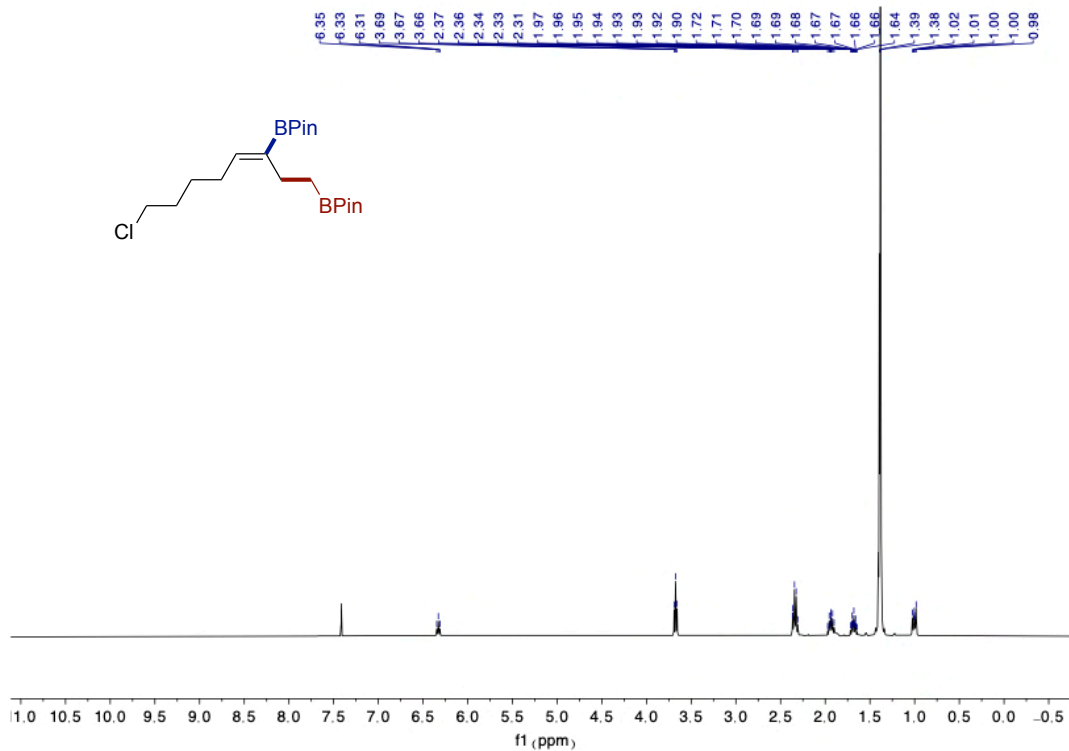


COSY of **3c**

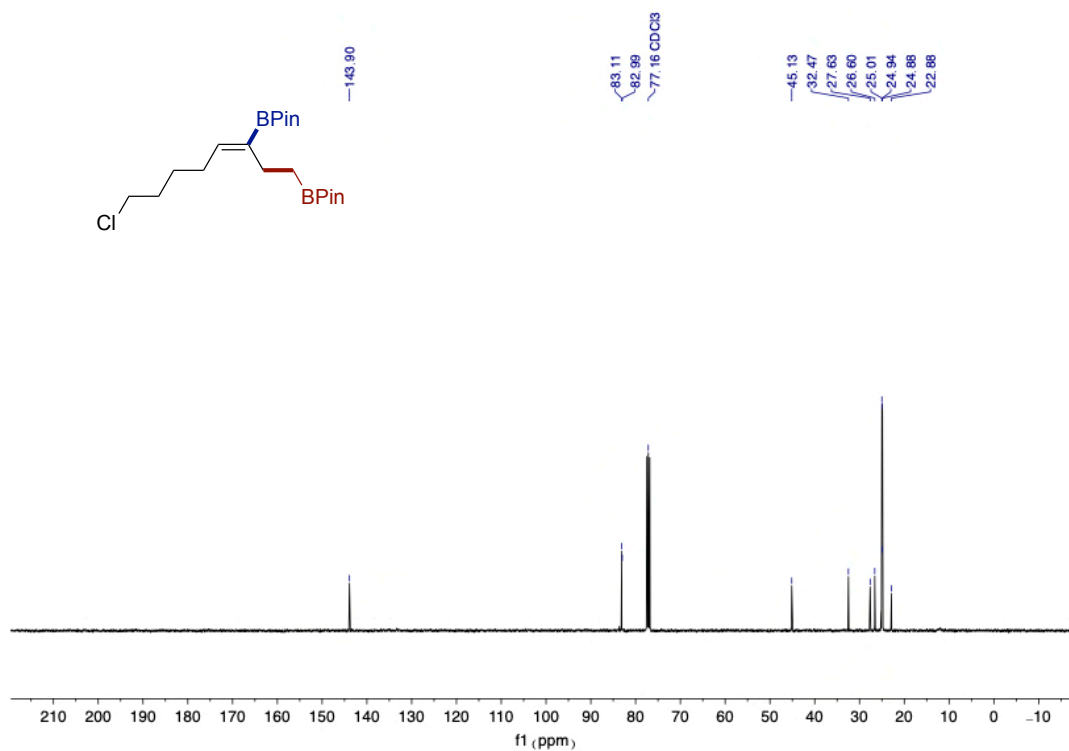


NOESY of **3c**

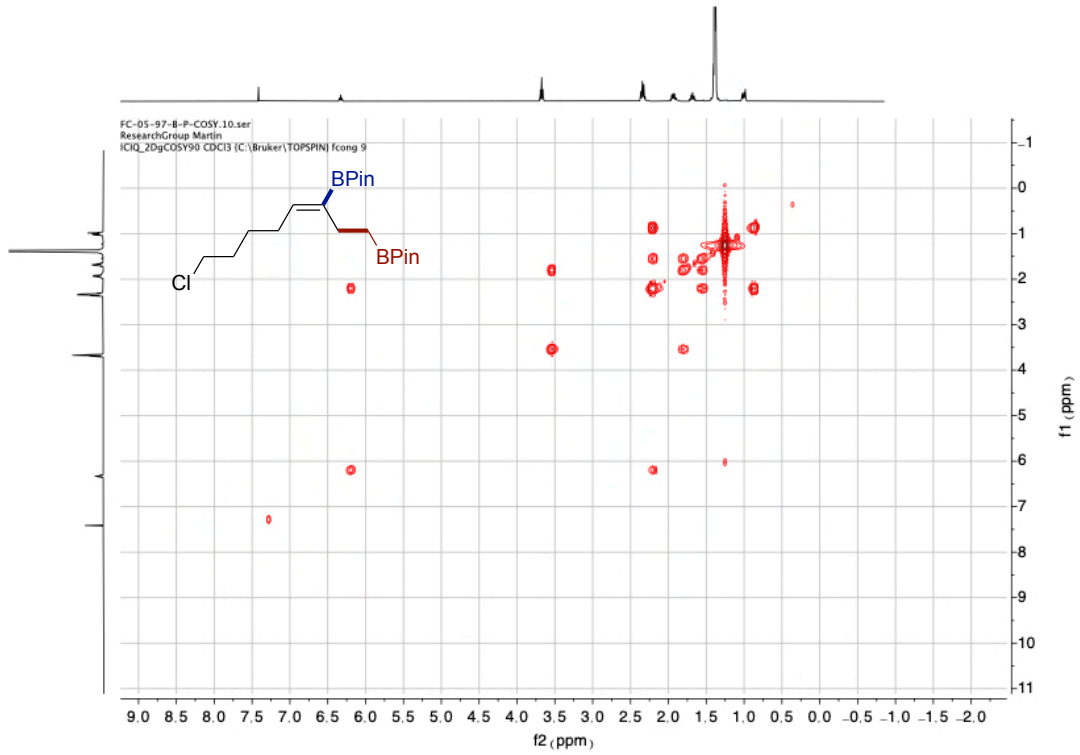




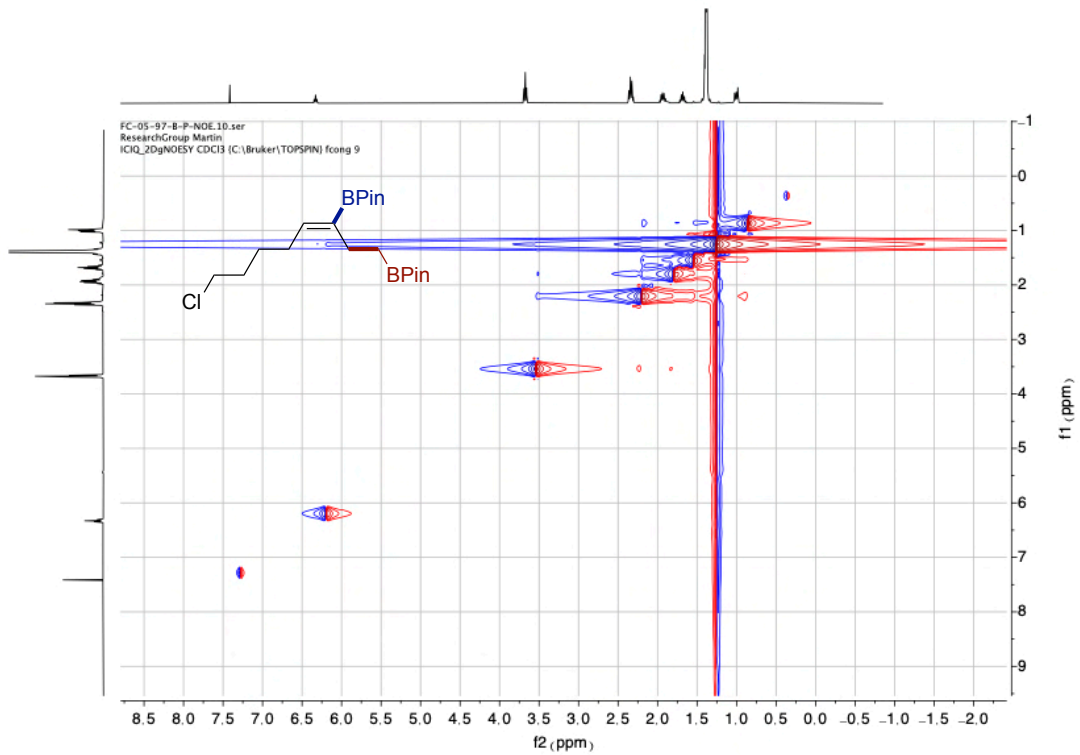
$^1\text{H NMR}$  (400 MHz,  $\text{CDCl}_3$ ) of **3d**



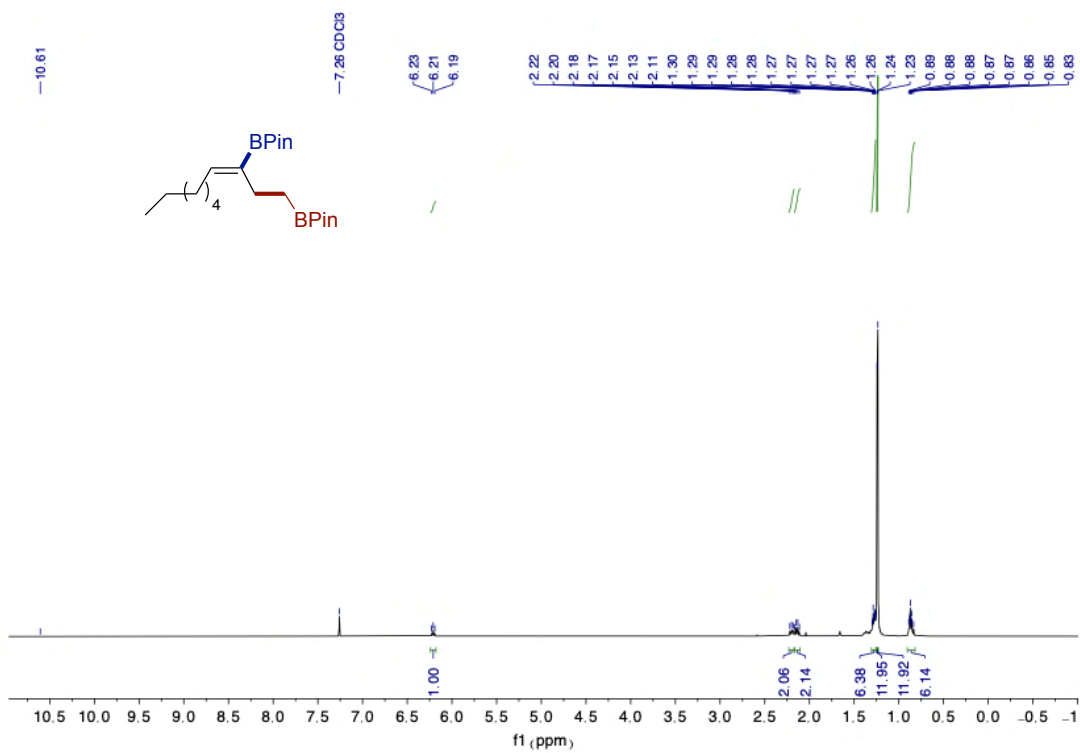
$^{13}\text{C NMR}$  (101 MHz,  $\text{CDCl}_3$ ) of **3d**



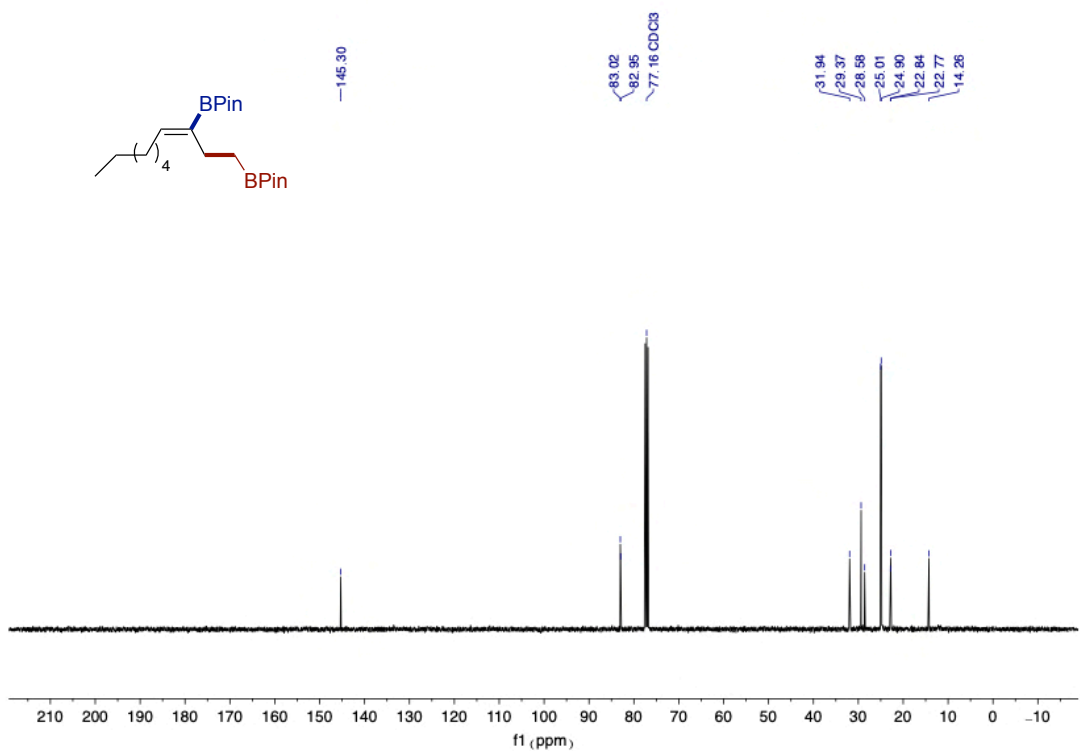
COSY of **3d**



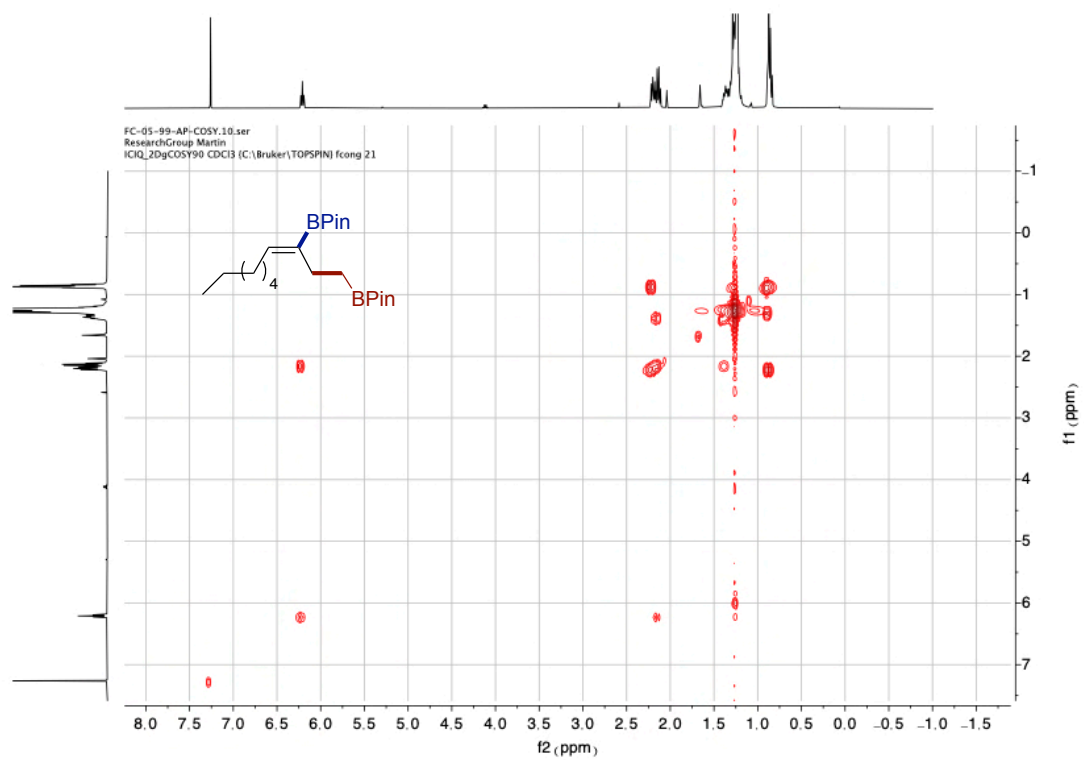
NOESY of **3d**



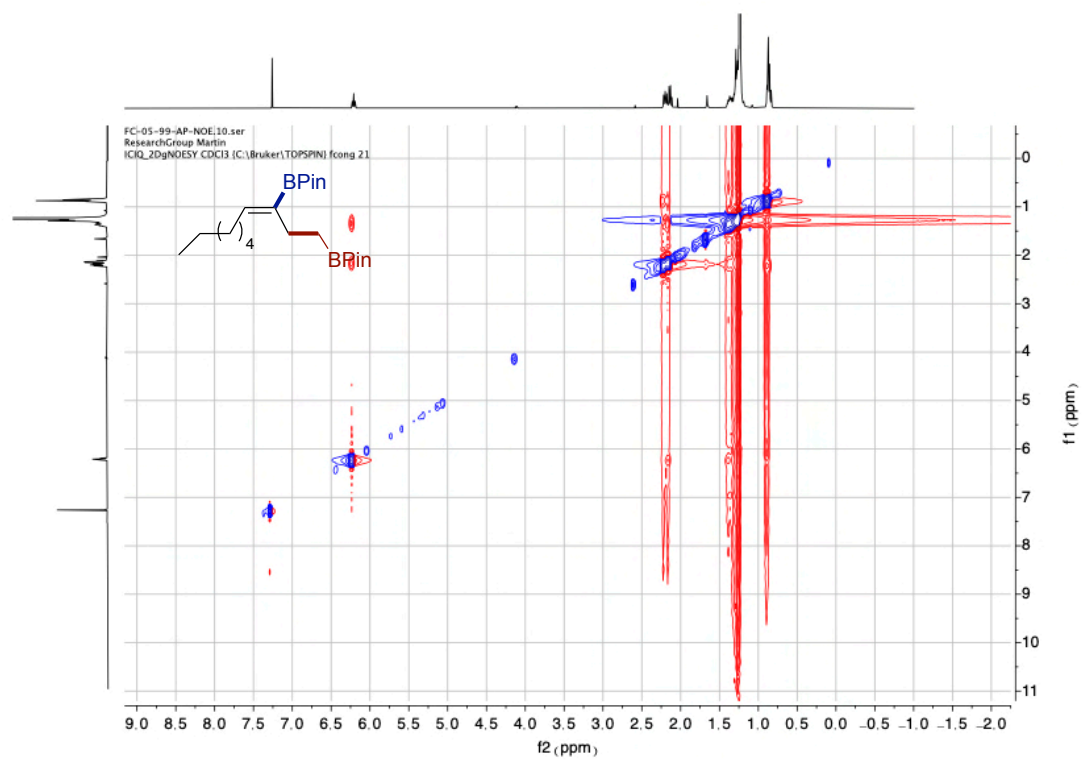
<sup>1</sup>H NMR (400 MHz, CDCl<sub>3</sub>) of **3e**



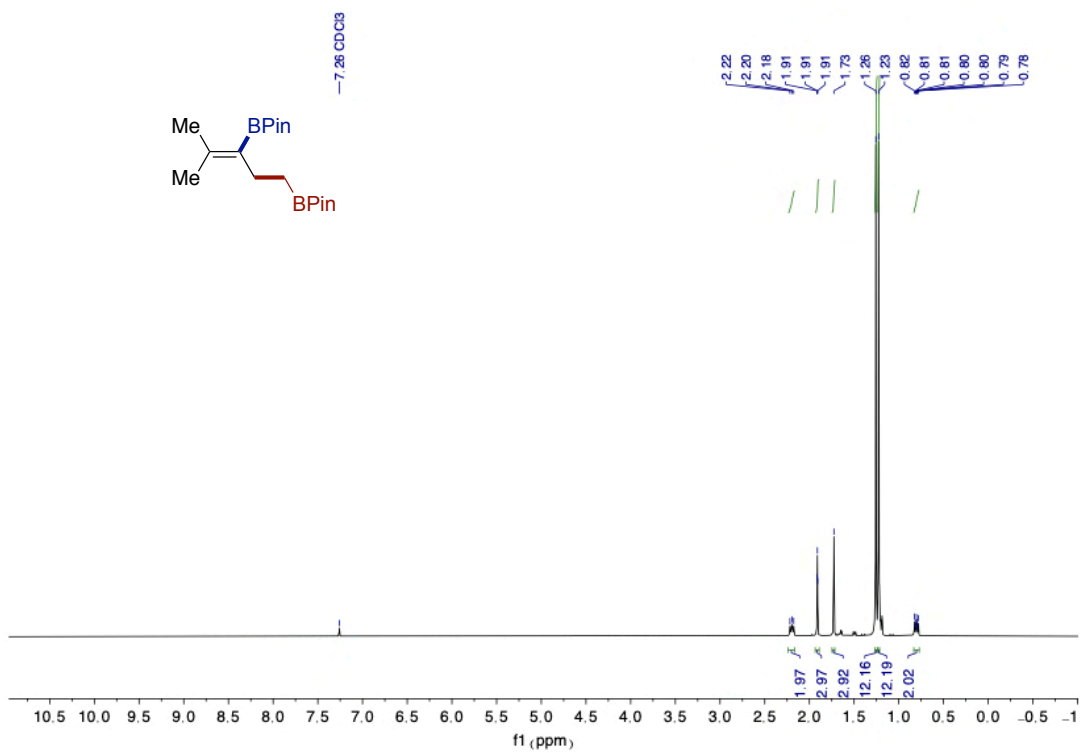
<sup>13</sup>C NMR (101 MHz, CDCl<sub>3</sub>) of **3e**



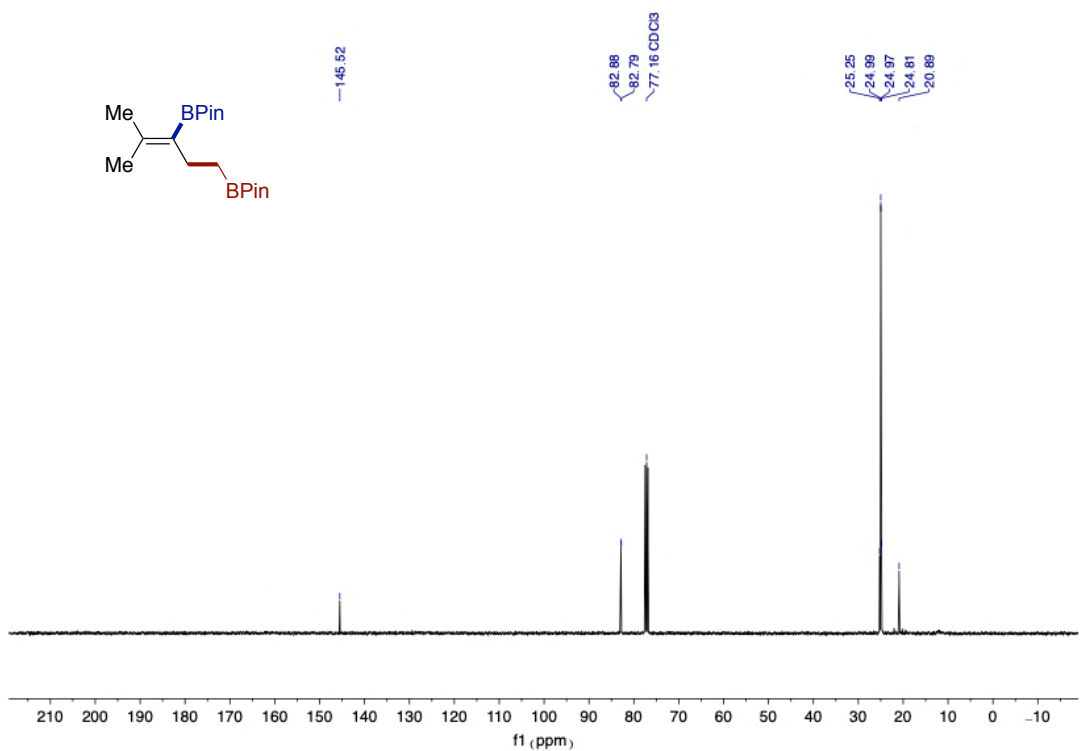
COSY of **3e**



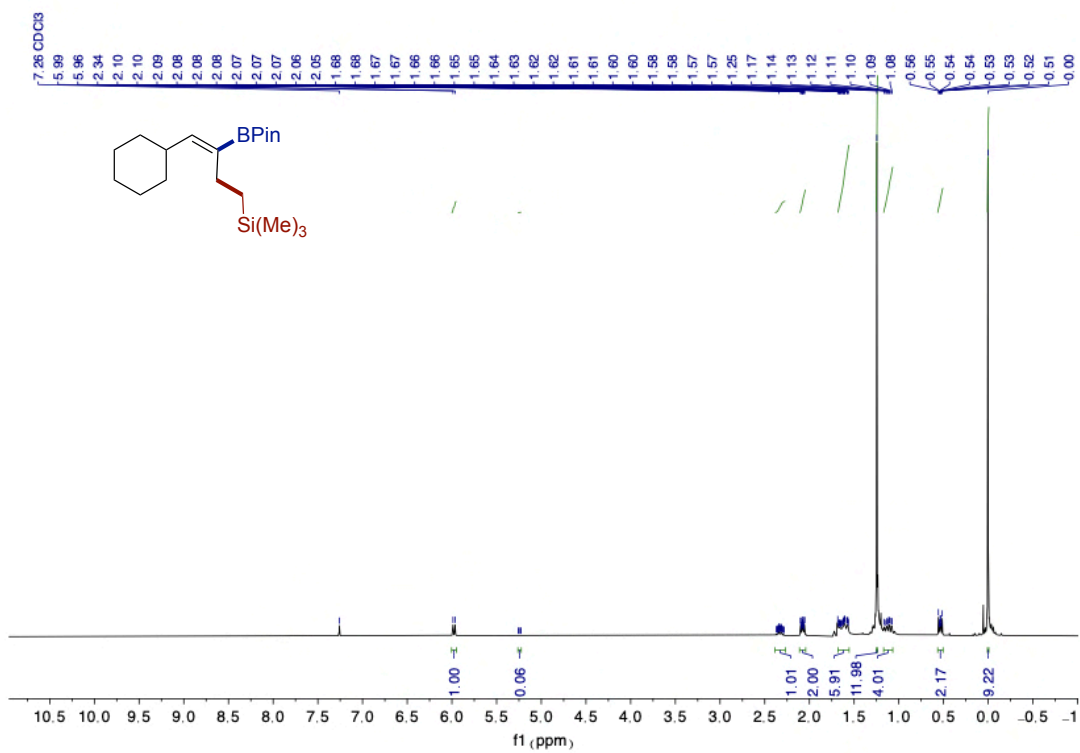
NOESY of **3e**



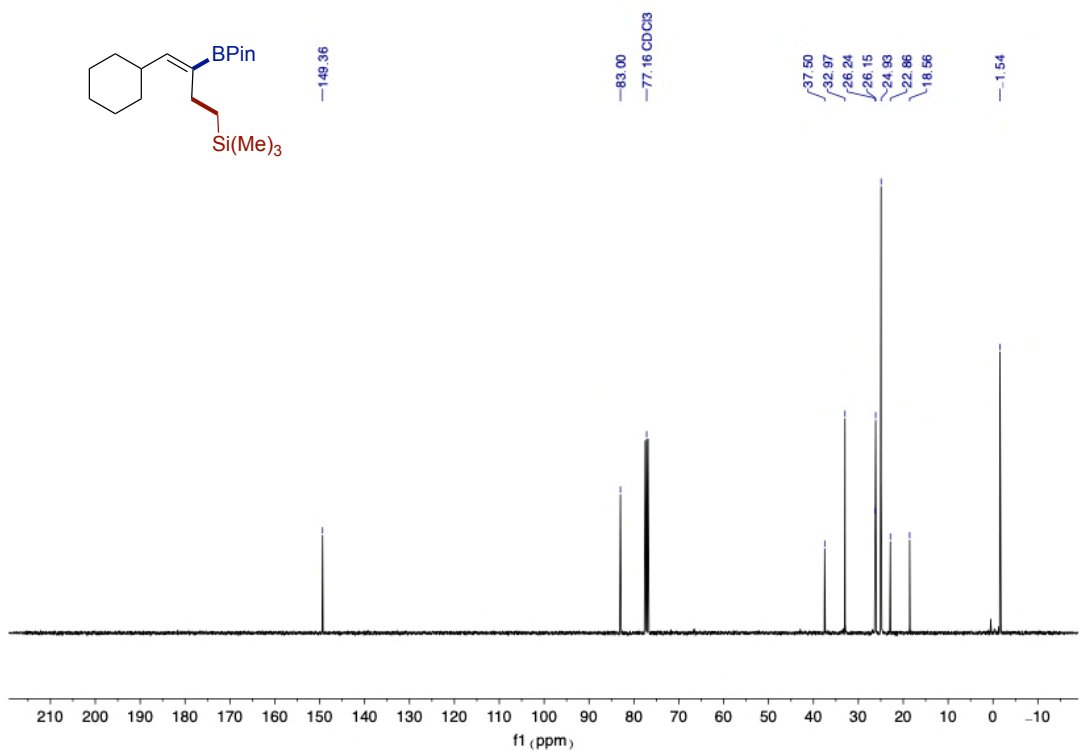
$^1\text{H}$  NMR (400 MHz,  $\text{CDCl}_3$ ) of **3f**



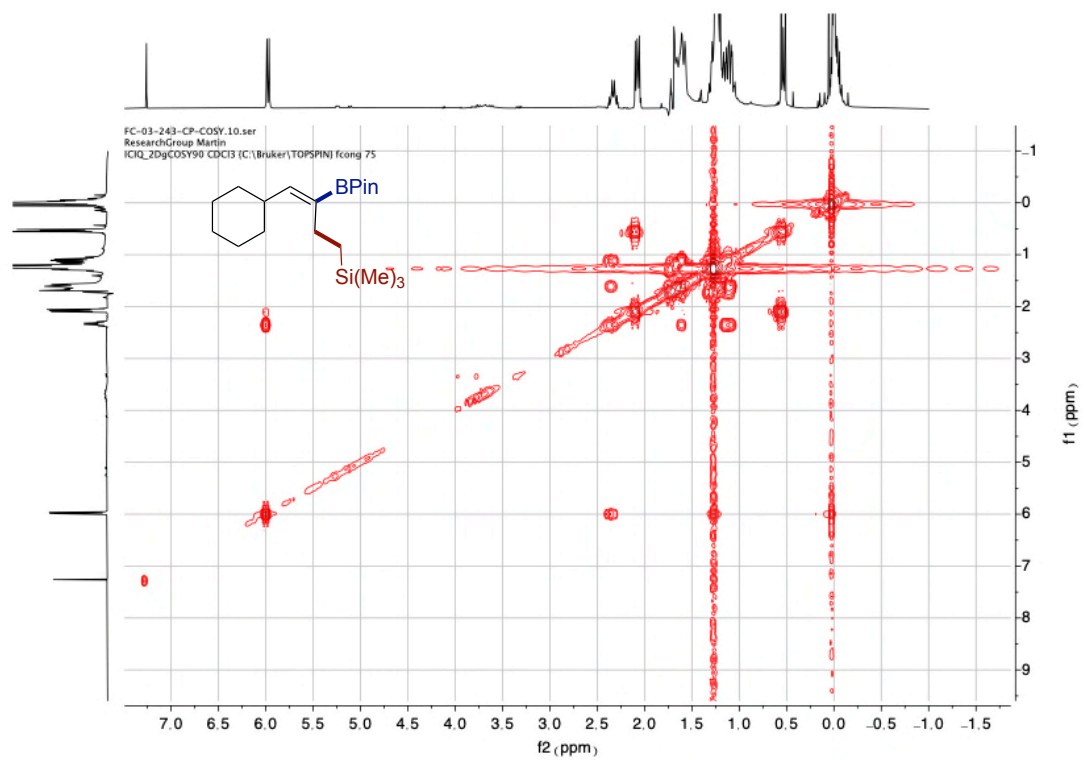
$^{13}\text{C}$  NMR (101 MHz,  $\text{CDCl}_3$ ) of **3f**



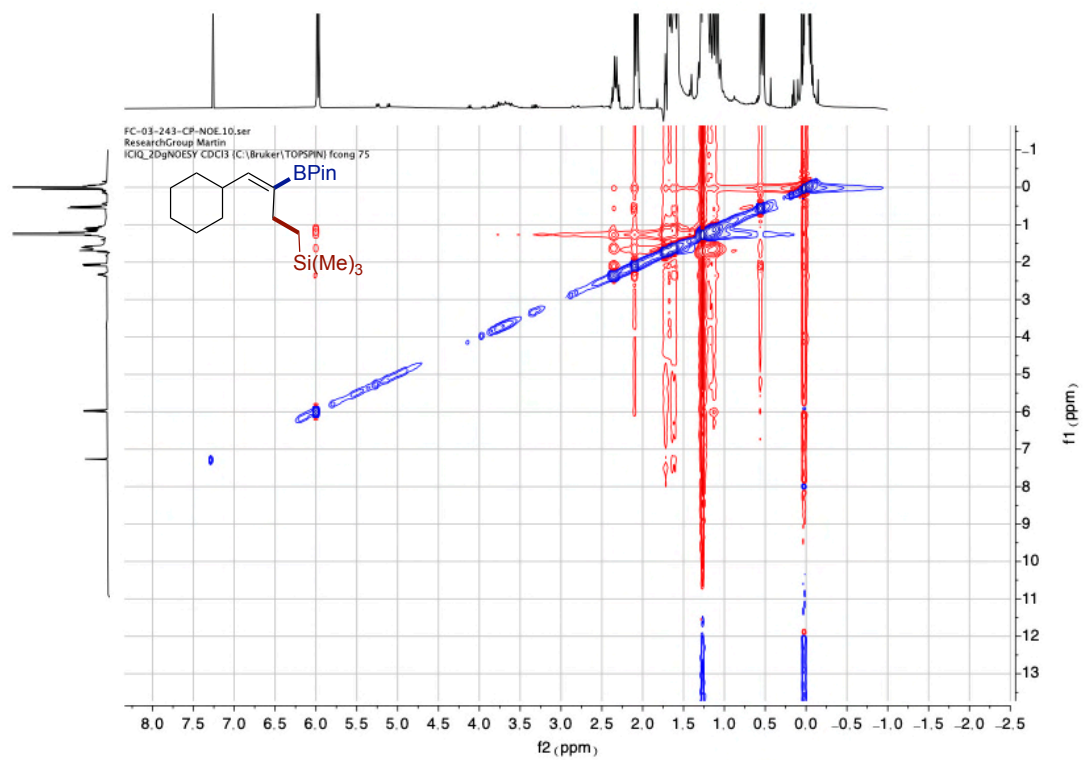
<sup>1</sup>H NMR (400 MHz, CDCl<sub>3</sub>) of **3j**



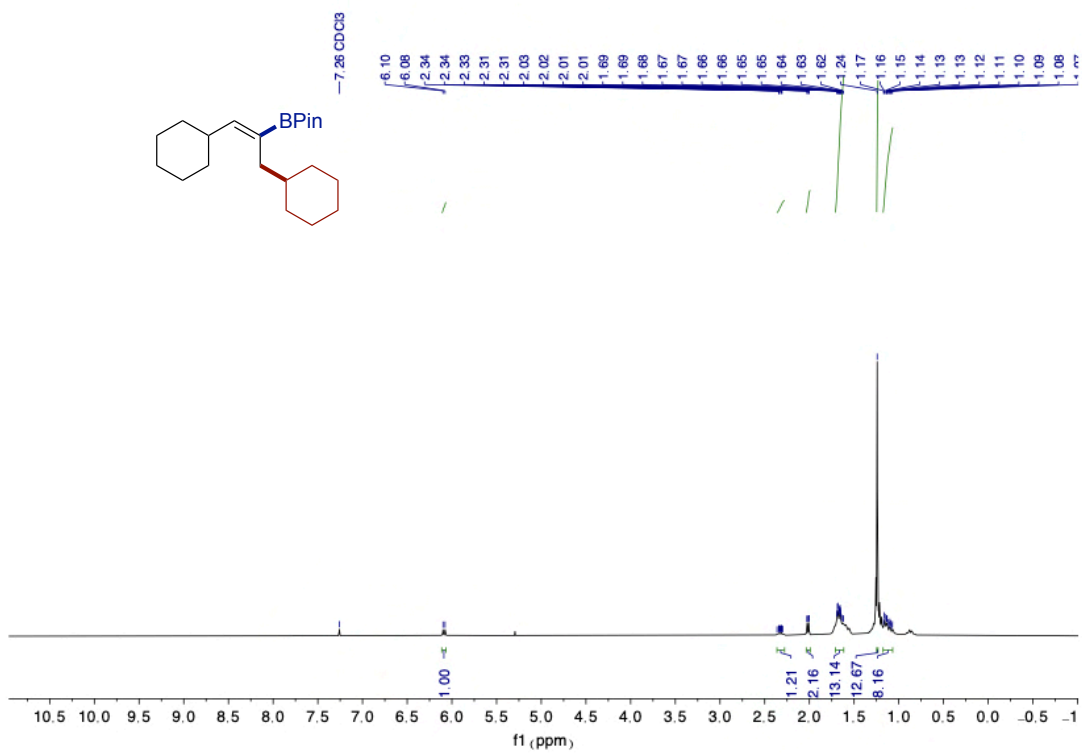
<sup>13</sup>C NMR (101 MHz, CDCl<sub>3</sub>) of **3j**



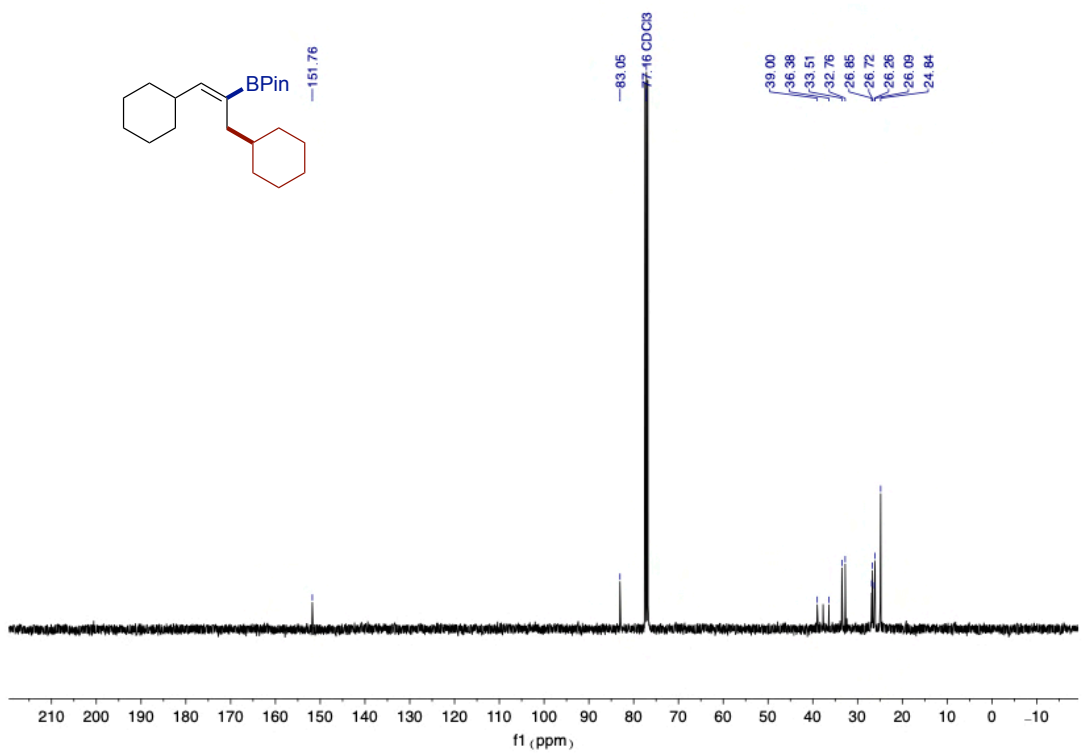
COSY of **3j**



NOESY of **3j**

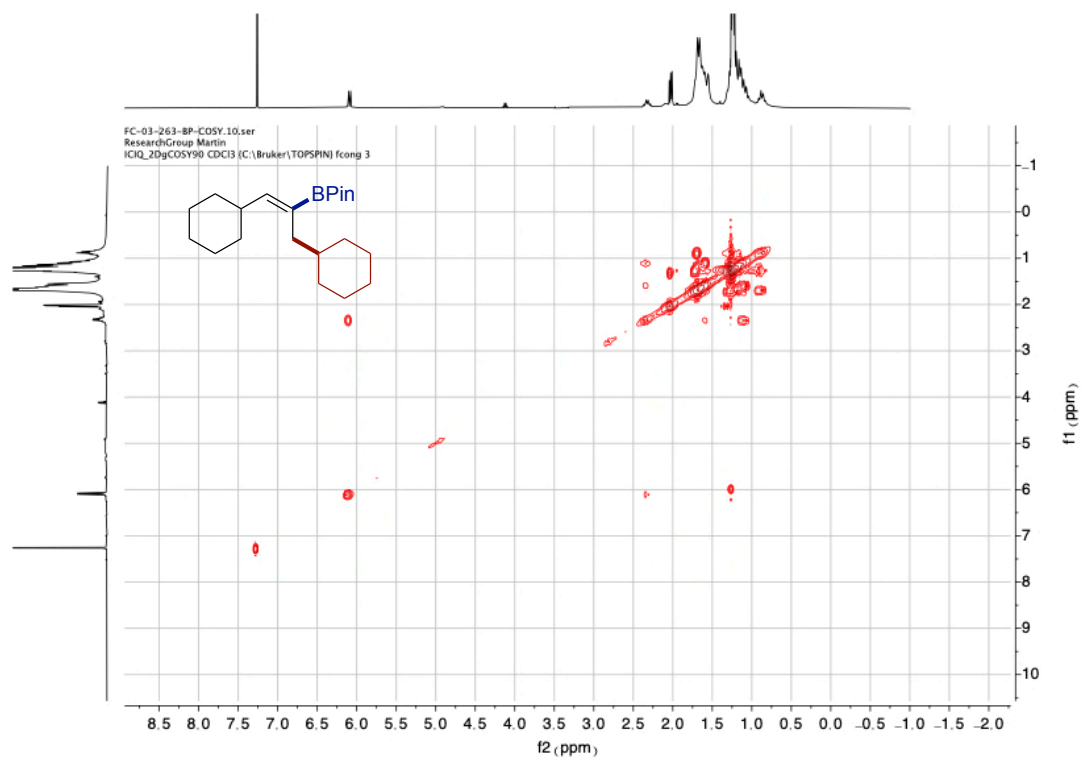


$^1\text{H NMR}$  (400 MHz,  $\text{CDCl}_3$ ) of 5a

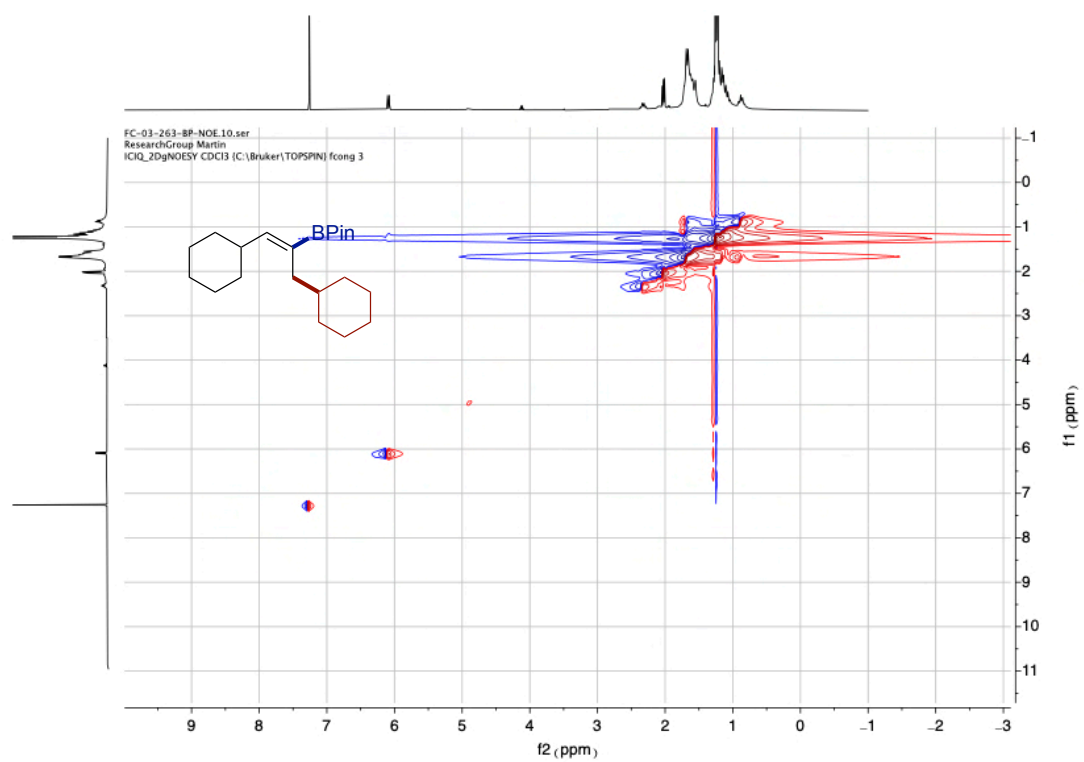


$^{13}\text{C NMR}$  (101 MHz,  $\text{CDCl}_3$ ) of 5a

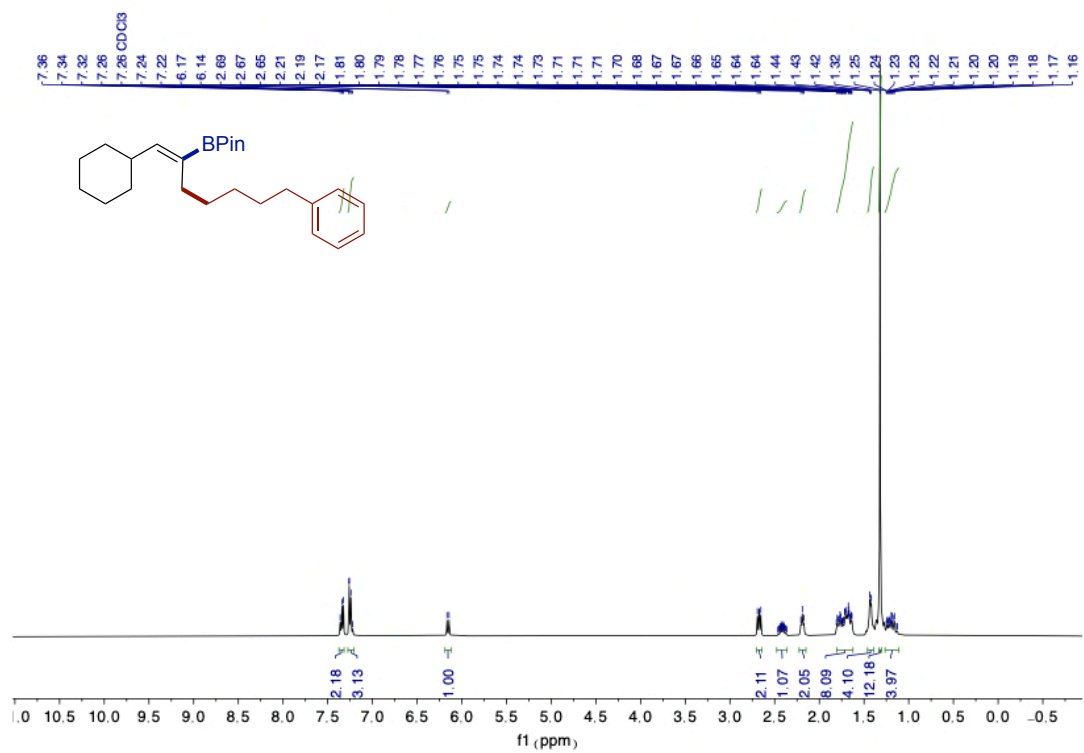




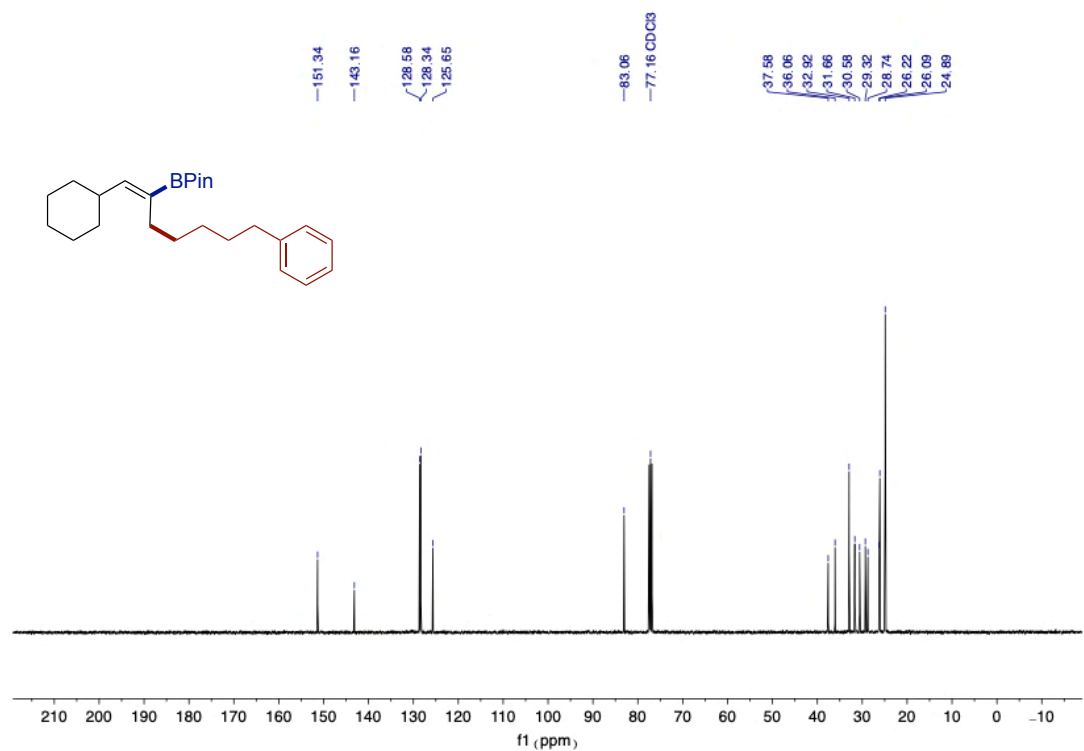
COSY of 5a



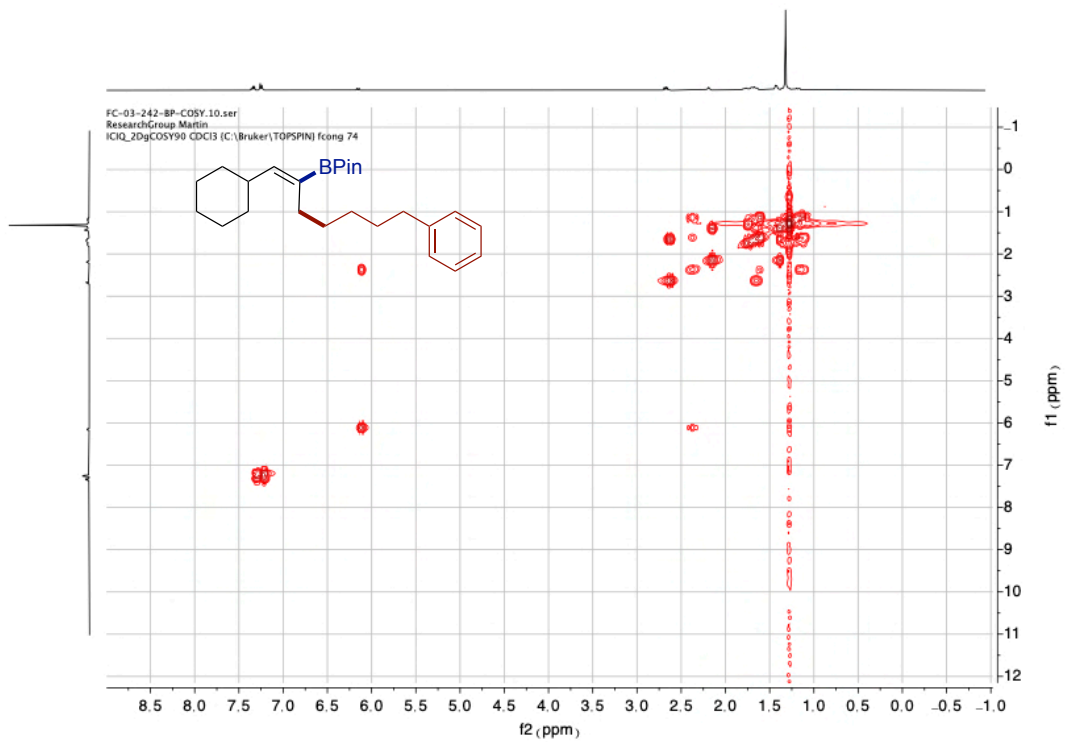
NOESY of 5a



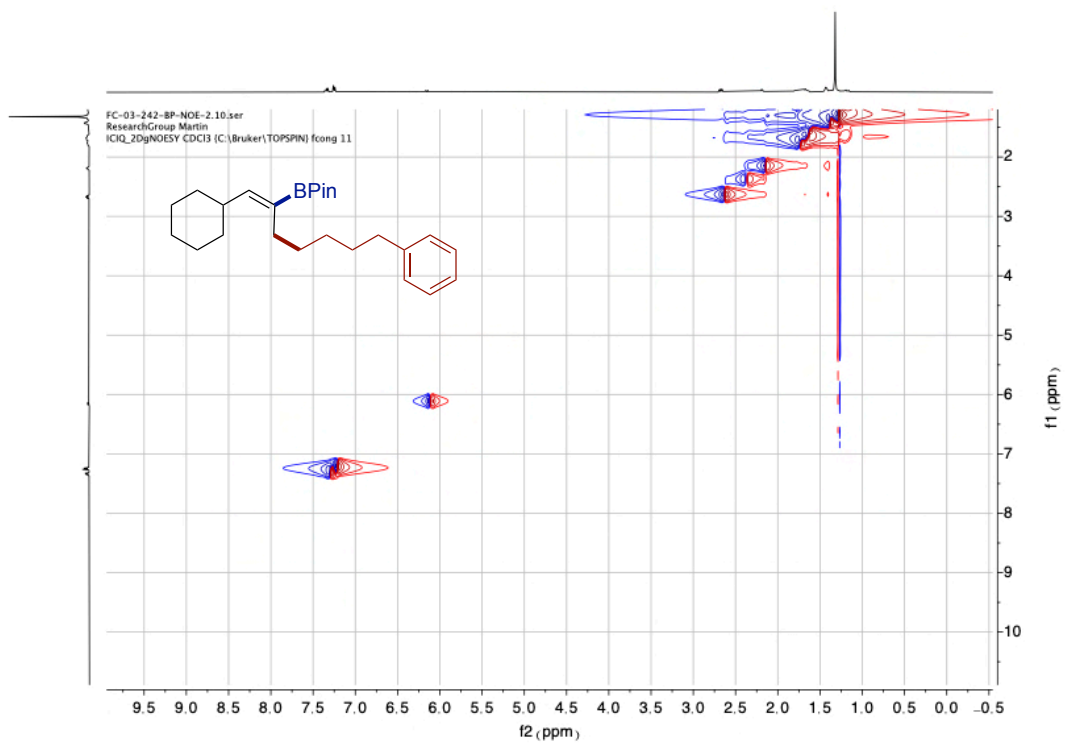
$^1\text{H NMR}$  (400 MHz,  $\text{CDCl}_3$ ) of **5b**



$^{13}\text{C NMR}$  (101 MHz,  $\text{CDCl}_3$ ) of **5b**



COSY of **5b**



NOESY of **5b**

---

## **Chapter 5**

### ***General Conclusions***

---

The organic synthesis strategy developed in this PhD thesis provide access to structurally diverse  $sp^3$ -carbon scaffolds via transition metal-catalyzed cross-coupling reactions. The main achievements of the initial program are highlighted herein:

### Chapter 2:

- A nickel/photoredox dual catalytic strategy for forging  $sp^2$ - $sp^3$  and  $sp^3$ - $sp^3$  architectures via  $\beta$ -scission of aliphatic alcohol derivatives have been developed.
- The method uses naturally abundant and commercially available aliphatic alcohols as building blocks and aryl and alkyl halides for successful  $sp^3$ -arylation and  $sp^3$ -alkylation events under nickel-catalyzed mild photocatalytic conditions via  $\beta$ -cleavage of alkoxy radicals as an unconventional manifold.
- The synthetic method demonstrates its excellent chemoselectivity and a wide range of applications. The applicability of the reaction has been extended in the context of late-stage functionalization of sugar derivatives and advanced intermediates. Notably, the  $sp^3$ -carbon synthons obtained from various aliphatic alcohols by the more challenging pathway of  $\beta$ -cleavage of alkoxy radicals have great synthetic potential as a versatile and flexible protocol for C-C bond formation.
- Preliminary mechanistic studies were used to support the presence of oxygen-centered radical intermediates and the subsequent  $\beta$ -scission of alkoxy radicals step. the formation of EDA complexes between Hantzsch esters (HE) and N-phthalimide ethers (OPht) is key to generate alkoxy radicals under photoexcitation.

### Chapter 3:

- Trifluoromethylation of structurally diverse carbonyl (ketones, aldehydes) and olefin derivatives via  $sp^3$  C-C bond cleavage have been achieved.
- This technique increases the opportunity to move from organic molecules containing simple unsaturated motifs such as ketones, aldehydes, and alkenes to provide  $sp^3$  hybridized carbon center properties through aromatization-driven  $C(sp^3)$ -C cleavage.

- 
- This new platform enables trifluoromethylation events with excellent chemoselectivity under mild conditions. This method tolerates a wide range of functional groups such as amides, halides,  $\alpha,\beta$ -unsaturated ketones, free alcohols or amines, heterocyclic motifs, sterically hindered substrates and substrates with highly sensitive C–H bonds. It is applicable to the late-stage modification of natural products and medicinal agents. Numerous synthetic examples have demonstrated the versatility and application profile of the scheme to reveal valuable C( $sp^3$ )-CF<sub>3</sub> architectures from unsaturated fractions.
  - The mechanism initially suggests that the conversion of carbonyl compounds or olefins to the former proaromatic precursors may be achieved by photoinduced single electron transfer to achieve the homogeneous cleavage of adjacent  $\alpha$ -C–C bonds and the generation of the related alkyl radicals, followed by the contact of the open-shell alkyl radicals with [Cu]-CF<sub>3</sub> substances to produce the target products through the reductive elimination of the alkyl-Cu<sup>III</sup>-CF<sub>3</sub> intermediates.

#### **Chapter 4:**

- A regio-, stereo-selective 1,2-alkylboration of allenes via a nickel-catalyzed three-component reaction using  $sp^3$  mono-organometallic reagents or alkyl iodides as electrophiles has been described.
- This strategy offers new vistas to access polysubstituted 1,3-( $sp^2$ ,  $sp^3$ )-bisorganometallic alkenes with excellent chemo- and regio-selectivity under mild conditions. The high selectivity (chemo-, regio- and stereoselectivity) controlled by nitrogen-based ligands under nickel catalysis is noteworthy. Further refinements and studies of this strategy, synthetic applications and detailed reaction mechanism experiments are being implemented.



UNIVERSITAT  
ROVIRA i VIRGILI